EXPERIMENTAL ASSESSMENT OF COUPLED PHYSICAL-BIOCHEMICAL-MECHANICAL-HYDRAULIC PROCESSES OF MUNICIPAL SOLID WASTE UNDERGOING BIODEGRADATION

by

Xunchang Fei

A dissertation submitted in partial fulfillment
of the requirements for the degree of
Doctor of Philosophy
(Environmental Engineering)
in the University of Michigan
2016

Doctoral Committee:

Associate Professor Dimitrios Zekkos, Co-Chair
Professor Lutgarde Raskin, Co-Chair
Associate Professor Adda Athanasopoulos-Zekkos
Associate Professor Gregory J. Dick
Professor Nancy G. Love

ACKNOWLEDGEMENTS

I would like to express my deepest gratitude to my advisor, Prof. Dimitrios Zekkos, for his guidance, encouragement, understanding and wholehearted helps in many aspects. He greatly influenced my career path and career goals. My co-advisor, Prof. Lutgarde Raskin, also helped me tremendously in both research and career development throughout my doctoral study and deserves my deepest gratitude. I would like to thank my doctoral dissertation committee members, Prof. Adda Athanasopoulos-Zekkos, Prof. Nancy Love, and Prof. Gregory Dick, for their invaluable advices and patience. I would like to acknowledge other professors in the geotechnical engineering and environmental engineering programs for their advices and support during my time in the University of Michigan, specifically Prof. Roman Hryciw, Prof. Richard Woods, Prof. Radoslaw Michalowski, and Prof. Terese Olson. I am also grateful to Mr. Thomas Yavaraski, Mr. Merrick Burch, Mr. Robert Fischer, and Mr. Jan Pantolin, for their help on my laboratory experiments and for sharing their experience and useful tips with me.

I really appreciate the friendship, companion and support of my friends, many of them are (or were) in the geotechnical engineering and environmental engineering programs at the University of Michigan, others I knew since high school or Tongji University, or via internet. I express my best wishes to them in their career and life.

Finally, I thank sincerely my parents, Chengkang Fei and Liqin Wang, and my wife, Yinan Tang, for everything ☺.

TABLE OF CONTENTS

LIST OF TABLES

LIST OF FIGURES

ABSTRACT

Proper management and disposal of municipal solid waste (MSW) remains an unresolved global problem. One solution to handle existing and future MSW is to move away from modern landfills that focus on containment and move towards bioreactor landfills that promote MSW biodegradation and enhance methane (CH_4) generation and its collection as an alternative energy source. Solid, liquid and gas phases of MSW coexist in different proportions within a landfill, and evolve with time due to concurring and coupled physical-biochemical-mechanical-hydraulic processes during MSW biodegradation. A fundamental understanding of the concurring processes is needed to design, monitor, and operate bioreactor landfills effectively and efficiently.

Seven large-size (d=300 mm; h=600 mm) laboratory landfill simulators were developed to degrade unprocessed MSW of variable waste composition that is representative of the MSW in a mega-scale landfill. The simulators were operated and monitored for up to four years to assess the evolution of the physical, mechanical, and hydraulic properties of MSW, the evolution of the biochemical characteristics of generated leachate and biogas, and population dynamics of MSW-degrading microorganisms. The coupled processes were found to be systematic, correlated to each other, and dependent on initial waste composition.

Testing of MSW in fresh and fully-degraded (retrieved from laboratory simulators) states was performed to assess the physical and mechanical properties of MSW using a unique 300-mm diameter simple shear apparatus. The shear strength and compressibility of MSW changed due to biodegradation and was a function of the initial waste composition and the biodegradation state.

A relationship between the shear strength and shear-wave velocity of MSW was established for fresh and degraded MSW.

Laboratory results on CH_4 generation and settlement of MSW during biodegradation generated as part of this study were supplemented by an extensive database synthesized from the literature that includes laboratory results and field measurements from numerous landfills. The database was analyzed to quantify the influence of moisture content of waste, overburden pressure, landfill monitoring and control, and temperature on MSW degradation. Based on the findings of this study, recommendations to promote MSW biodegradation include enhancing biodegradation conditions, optimizing initial waste composition, and increasing biogas collection efficiency.

PART I BACKGROUND INFORMATION

Chapter 1 Introduction on Landfill Disposal of Municipal Solid Waste

1.1 Generation and disposal of municipal solid waste

Municipal solid waste (MSW, or simply waste in this context) is defined by the United States (U.S.) Environmental Protection Agency (EPA) as "everyday items we use and then throw away, such as product packaging, grass clippings, furniture, clothing, bottles, food scraps, newspapers, appliances and paint." Approximately 250 million tons of MSW have been generated on a yearly basis during the last decade in the U.S. (EPA 2014a). Given a stable U.S. population growth of about 1% (CensusBureau 2010; van Haaren et al. 2010) and a positive correlation between population and generation quantity (Staley and Barlaz 2009; van Haaren et al. 2010), the annual generation rate of MSW is expected to increase steadily in the future. The generation mass and percentage of each MSW constituent before recycling is listed in Table 1-1 for 2012.

The recycling rate of MSW reached a historical high value of 34.5% of total generated MSW in 2012. However, only certain waste constituents are recycled due to economic interest and their recycling rates generally have limits beyond which it is neither economical nor technically feasible. The quantity of recycled MSW in U.S. reached a plateau of around 85 million tons for the last few years. Other treatment methods for MSW include incineration, composting, anaerobic digestion, and pyrolysis. 11.7% of generated MSW in 2012 was incinerated, and this proportion has remained quite stable for the last decade. Composting, anaerobic digestion and pyrolysis are primarily used to treat yard waste, organic-rich waste and

hazardous waste, respectively. Their shares among MSW treatment methods are relatively low (EPA 2014a).

In 2012, 53.8% of MSW, i.e. 135 million tons, was disposed of in landfills. The percentage of MSW managed by landfill disposal fluctuated only slightly for the last decade (EPA 2014a). Because of the limitations in recycling and other waste treatment methods, it is expected that the quantity of landfilled MSW will remain high in the foreseeable future. To accommodate for the need for MSW disposal, about 1,800 landfills are currently operated across the country, while the number of closed landfills or dumps is estimated to be on the order of a few tens of thousands (EPA 2010a).

1.2 Design of landfills

Modern landfills for MSW disposal are regulated by Subtitle D of the Resource Conservation and Recovery Act (RCRA) promulgated in 1976. Basic requirements for these landfills are hydro-geological isolation, formal engineering design, permanent control and planned waste disposal and covering (EPA 1976). Modern landfills are sophisticated engineered system and the following issues are considered during the design process: geometry and configuration, base containment, waste mass stability, biogas collection, surface water collection, leachate collection and management, groundwater monitoring, final cover and post-closure development (Figure 1-1).

Landfill construction is a standardized practice with stringent design and operating guidelines and quality assurance and quality control construction criteria. After determination of location, geometry and configuration of a landfill, its sub-grade is prepared and its liner system deployed. The leachate collection system is also installed. Subsequently, waste placement begins

and daily as well as monthly to quarterly interim soil covers are added. A landfill is divided into a series of cells and MSW is disposed of sequentially in each cell. When a cell reaches its design height and capacity, it is closed. The biogas collection system, final cover, and surface water collection system are then installed for the closed cell. Hence, the closed cell is monitored for quality and quantity of biogas and leachate generation, waste settlement, infrastructure integrity and serviceability and potential groundwater pollution. Construction and filling of new waste cells usually take place concurrently with the closure of filled cells. The typical life span of a modern landfill is on the order of decades. When the design capacity of a landfill is reached, the whole site is closed, and the owner is liable for the site for 30 years, known as post-closure care period (PCCP) (Qian et al. 2002; Tchobanoglous and Kreith 2002).

Modern Subtitle D landfills are designed to minimize moisture infiltration and degradation of waste. However, moisture eventually infiltrates into any landfill and accumulates in landfilled waste (Bengtsson et al. 1994; Abichou et al. 2013; Yochim et al. 2013). Therefore, slow and uncontrolled degradation of waste occurs in modern Subtitle D landfills and may extend beyond PCCP (Barlaz et al. 2002; Zekkos et al. 2010b).

A bioreactor landfill is a more recent type of landfill that implements moisture addition and leachate recirculation in waste cells (Figure 1-2). It aims at accelerating the biodegradation and stabilization of waste while alleviating leachate strength (Kim and Pohland 2003). With enhanced degradation of MSW, rapid generation of biogas consisting of over 50% of methane (CH_4) is expected during stable methanogenesis, and if collected properly, it can be recovered as an energy source (Themelis and Ulloa 2007; Barlaz et al. 2010b). Effective collection of CH_4 and complementary carbon dioxide (CO_2) in biogas reduces greenhouse gas (GHG) emission from landfills which are currently the second largest anthropogenic CH_4 emission source in the

U.S. (Bogner and Matthews 2003; EPA 2014b). Approximately 15-20 full-scale bioreactor landfills have been constructed and are being operated throughout U.S. (Bareither et al. 2010; EPA 2010b; Bioreactor.org 2011). They are receiving increasing interest from both government as well as waste management industry. This indicates a paradigm shift in the philosophy of MSW disposal from permanent containment with minimal degradation of waste to a combination of active degradation and energy recovery.

1.3 Geotechnical failures of landfills

Two states of failure of landfills are identified as ultimate limit state and serviceability limit state. Ultimate limit state failure indicates "a complete loss of stability or function of a landfill" which is controlled by shear strength of waste mass or interface shear strength of waste-geosynthetic or geosynthetic-geosynthetic interfaces (Koerner and Soong 2000; Jones and Dixon 2005). Ultimate failure is rarer but the aftermath is disastrous, it brings the operation of the entire landfill to halt and even costs human lives sometimes. Dona Juana landfill in Colombia (Hendron et al. 1999), Rumpke landfill in Cincinnati, Ohio (Eid et al. 2000; Stark et al. 2000), Payatas landfill in Philippines, Leuwigajah landfill in Indonesia (Koelsch et al. 2005) and Xerolakka landfill in Greece (Zekkos et al. 2013c) are several examples.

Serviceability limit state failure occurs when the function of an infrastructure is impaired. It happens more frequently and the loss due to a single failure is not as significant as that of an ultimate limit state failure. However, cumulative economic loss due to serviceability limit state failures might be well excess of those of ultimate limit state failures. For example, the integrity and impermeability of a base containment system are essential. There should be nearly no tears on geomembrane and limited cracking on clay liner so that low hydraulic conductivity of the

containment system is maintained to minimize leachate migration into adjacent environment. The integrity of a final cover system guarantees minimal moisture infiltration. Differential settlement of waste is not desired because it causes cracking and creates impoundments on final cover. The slope grade of a landfill determines its ultimate landfilling capacity and is designed based on values of waste mass and interfacial shear strength. The integrity of a slope containment system should be ensured which has similar requirements as those for a base containment system. The integrity of biogas collection pipelines and wells should be secured against differential settlement of waste. Biogas collection efficiency is another concern because accumulation of hydrogen sulfide and other volatile organic compounds induces odor problem and health hazards while CH_4 accumulation increases the risk of landfill fire and explosion. The functionality of leachate collection pipelines should be ensured against compression of overlying MSW mass and clogging due to biochemical reactions in leachate.

Incidences of both types of failures are determined by the physical, mechanical and hydrological properties of MSW, and these properties of waste evolve with time due to waste degradation. Therefore the stability of a landfill and performance of landfill components are affected by time-dependent MSW behaviors.

1.4 Research objectives

With the early-closed Subtitle D landfills being about half a century old, it is logical to expect noticeable changes of waste properties in these landfills. Whether containment system and waste mass will fail due to altered waste properties and when will the waste be stabilized remain major questions. The American Society of Civil Engineers (ASCE) graded solid waste infrastructure in U.S. a “B-”, thus suggesting large room for improvement and research on the predominant

Subtitle D landfills (ASCE 2014). On the other hand, the development of bioreactor landfill technology is still in its early stage, and its design, monitoring and operation are not optimized due to lack of fundamental understanding of MSW behaviors under enhanced biodegradation conditions.

Overall, three research questions related to MSW disposed of in landfills remain unanswered:

1. What processes take place during MSW biodegradation and how to monitor them?

2. What is the impact of biodegradation on the physical and mechanical properties of MSW?

3. What environmental and operating factors influence MSW biodegradation process?

1.5 Organization of dissertation

This dissertation aims, at least partially, to address these three research questions, and is thus divided into five parts with Part II, III and IV target specifically on each of the questions.

- PART I introduces the background information. Chapter 1 briefly summarizes the generation of MSW and state of practice landfill disposal of MSW. A comprehensive literature review is presented in Chapter 2 on processes taking place during MSW degradation in landfills, engineering properties of MSW of interest, factors influencing degradation processes and the changes in properties of MSW during degradation, and research approaches adopted in the literature.
- PART II presents the results of laboratory degradation experiments on MSW, including experimental setup and monitoring and sampling procedures for large-size laboratory bioreactor landfill simulators in Chapter 3; observed coupled physical-biochemical-

mechanical-hydraulic processes during MSW degradation in Chapter 4; and time-dependent microbial activity and populations during MSW degradation in Chapter 5.

- PART III presents the testing results of geotechnical properties of MSW with variable waste composition, overburden pressure, unit weight, and degree of degradation. The shear strength of MSW assessed using simple shear and direct shear testing and shear-wave velocity of MSW measured using bender elements and accelerometers are presented in Chapter 6. Response of MSW to mechanical compression is studied in Chapter 7.
- PART IV investigates influences of environmental and operating factors on various aspects of MSW degradation using experimental results reported in Part II and Part III as well as those synthesized from the literature. Specifically, Chapter 8 investigates impacts of initial waste composition, moisture content and overburden pressure of waste on its degradation. Chapter 9 focuses on factors influencing biogas generation during MSW degradation. Chapter 10 focuses on factors influencing long-term settlement of MSW due to mechanical compression and degradation.
- PART V summarizes the results presented in this dissertation, discusses potential engineering applications and significances, and proposes recommendations for future work.

1.6 Tables

Table 1-1 Generation mass and percentage of MSW constituents before recycling in 2012 (EPA 2014a).

Waste constituent	Generation mass (million tons)	Generation percentage (%)
Paper and paperboard	68.62	27.4
Food scraps	36.43	14.5
Yard trimmings	33.96	13.5
Plastics	31.75	12.7
Metals	22.38	8.9
Rubber, leather and textiles	21.86	8.7
Wood	15.82	6.3
Glass	11.57	4.6
Other	8.50	3.4
Total municipal solid waste	250.89	100

1.7 Figures

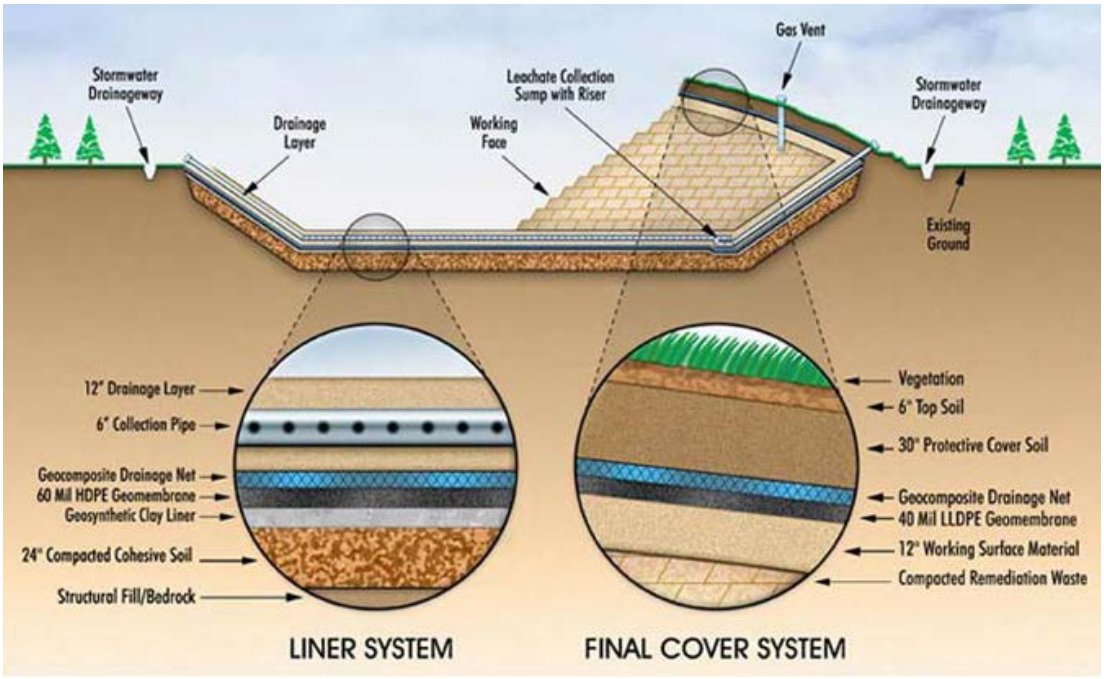

Figure 1-1 Cross-sectional view of a typical Subtitle D landfill (http://www.projectdataresearch.com/landfills.html).

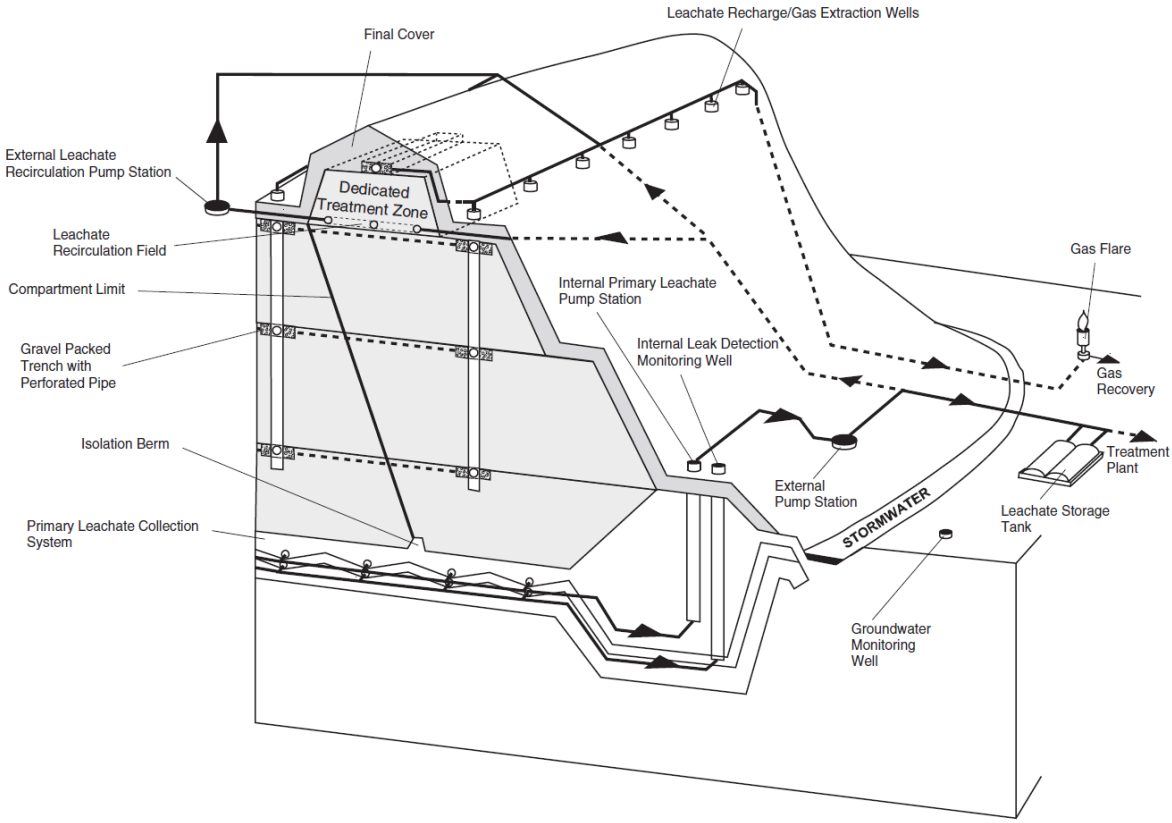

Figure 1-2 Schematic of a bioreactor landfill (Kim and Pohland 2003).

Chapter 2 Literature Review

2.1 MSW degradation in landfills

2.1.1 **Overview**

MSW degrades through a number of biochemical and physical processes in modern Subtitle D and bioreactor landfills. Biodegradation of biodegradable solid waste consists of four steps under anaerobic conditions, disintegration, hydrolysis, fermentation, and methanogenesis (Batstone 2002; Barlaz et al. 2010b). Large-size biodegradable waste particles, e.g., food, paper and yard trimmings, are first disintegrated into finer particles by physicochemical process. The finer particles have higher surface areas and the complex polymers in the particles are easily hydrolyzed by microorganisms at appropriate moisture content. The products from hydrolysis are soluble monomers in leachate including sugars and amino acids. They are converted by fermentative bacteria to volatile fatty acids (VFAs), hydrogen (H_2) and CO_2 which are eventually consumed by methanogenic archaea to produce CH_4 and CO_2 (Barlaz et al. 2010b). In addition, the properties of MSW change due to mechanical compression and long-term creep (Olivier and Gourc 2007; Bareither et al. 2012d).

The properties of solid waste and characteristics of leachate and biogas generated during MSW biodegradation change with time. The settlement of waste is contributed by immediate mechanical compression, biological settlement due to biodegradation, and long-term mechanical creep (Bjarngard and Edgers 1990; Edil et al. 1990; Gourc et al. 2010; Bareither et al. 2013a). Biodegradable solid waste particles sustaining waste matrix are broken down due to

disintegration and hydrolysis, and results in settlement and change in phase relationship in waste. The change in phase relationship in waste results in changes in total unit weight (γ_t) and volumetric water content (θ) of the waste (Stoltz et al. 2010b; Stoltz et al. 2012). Consequently, the hydraulic and mechanical properties of waste, such as hydraulic conductivity (k) and shear strength (τ), are altered (Breitmeyer 2011; Reddy et al. 2011; Bareither et al. 2012c; Woodman et al. 2014; Zekkos and Fei 2016). Meanwhile, the products of hydrolysis are generated and consumed by microorganisms in leachate with time, resulting in changes in concentrations of soluble chemical oxygen demand (sCOD) and VFAs and pH for the leachate. In response to the dynamic microbial activity in the leachate, the concentrations and generation rates of CH_4 and CO_2 in gas phase change with time (Barlaz et al. 1989b; Kim and Pohland 2003; Ivanova et al. 2008b; Bareither et al. 2013b; Fei et al. 2015a).

2.1.2 **Scales of studies**

Studies on MSW biodegradation are typically conducted in one of three scales, macro- (full- and pilot-scale landfills), meso- (large-size laboratory simulator) and micro- (laboratory batch tests and microbiological studies) scale. They all have their respective advantages and shortcomings regarding reliability, representativeness and repeatability of acquired data.

- **Meso-scale study**

MSW biodegradation has been frequently studied in laboratory simulators with reconstituted waste specimens. However, significant differences exist among studies with regards to the simulator configurations, the types of measurements collected and the sampling approaches followed. This is mostly because testing objectives among studies vary significantly. Most studies focus on one or some aspects of the biodegradation process without the intent to characterize the interdependency of the various processes as outlined in Figure 2-1.

Representative experimental setups and corresponding measurements and sampling approaches available in the literature are summarized in Table 2-1.

In MSW biodegradation tests, the size of the simulator is important. As outlined in Table 2-1, various simulator sizes ranging from 0.06m to 1m in diameter and maximum waste particle sizes ranging from 1.9 cm to 15 cm have been used. The smallest of these simulators cannot accommodate the size of waste constituents placed in landfills, and waste shredding is often performed to accommodate the need for small specimen sizes. Many studies have shredded MSW to sizes smaller than 2.5 cm, greatly reducing the size of the original fibrous waste constituents (Table 2-1). Tests have shown that shredding of waste particles increases the biodegradation rate and changes the physical, mechanical, and hydraulic properties of the specimen relative to the conditions in actual landfills (Landva and Clark 1990; Zekkos et al. 2008; Zhang and Banks 2013). Small simulators have also been used to study the microbial communities present during MSW biodegradation (Barlaz et al. 1989b; Valencia et al. 2009b; Valencia et al. 2009a; Benbelkacem et al. 2010; Gourc et al. 2010; Staley et al. 2011a). In these cases, shredding allows the reconstitution of "uniform" MSW specimens. The largest simulator size described in the literature has a diameter of 1 m (Gourc et al. 2010; Huang et al. 2012; Rafizul et al. 2012; Staub et al. 2013). At such a size, simulators can accommodate waste constituents of sizes that are more representative of those observed in actual landfills. Specimens with a minimum diameter of 0.3m that can represent unshredded waste have been recommended to reduce the biases in results associated with geotechnical laboratory testing (Zekkos et al. 2008; Bray et al. 2009; Athanasopoulos 2011b; Bareither et al. 2012b).

As indicated in Table 2-1, a wide variety of measurements have been conducted to characterize aspects of MSW biodegradation. Some studies measured waste settlement in the

simulators, but many did not. To the best of our knowledge, no study has systematically measured changes in specimen total weight (W_t) with time, even though changes in the total unit weight likely affect the mechanical behavior of MSW, including parameters such as shear strength and compressibility (Zekkos et al. 2006). Only total unit weight of the waste before and after biodegradation has been measured by a few studies (Borglin et al. 2004; Olivier and Gourc 2007; Gourc et al. 2010; Reddy et al. 2011).

Most of the simulator studies include measurement of biogas and leachate. As indicated above, biogas consists mainly of CH_4 and CO_2 and its volume and composition are indicators of the degree of biodegradation and the composition of the waste. Leachate measurements involve most commonly chemical oxygen demand (COD). pH and alkalinity (alk.) of leachate have also been measured as they are generally indicative of the growth conditions of microorganisms and the degree of biodegradation (Barlaz et al. 2010b). Occasionally, simulators are destructively sampled for chemical and microbiological analyses (Valencia et al. 2009b; Valencia et al. 2009a; Reddy et al. 2011; Staley et al. 2011a).

Durations of tests reported in the literature range from 14 days to over 1,000 days (Table 2-1). Typically, tests aiming at characterizing microbial processes have shorter durations, because intensive anaerobic biodegradation and CH_4 generation is usually completed within 100 to 200 days in the laboratory. In contrast, long-term compression of the waste is not observed until after several hundred days and thus tests with emphasis on monitoring physical and mechanical properties often last longer.

- **Macro-scale study**

Macro-scale studies are conducted in pilot- or full-scale landfill cells (El-Fadel et al. 1996a; Augenstein et al. 1997; Reinhart and Townsend 1998; Mehta et al. 2002; EPA 2006a; Benson et al. 2007; Bareither et al. 2010; Barlaz et al. 2010a; Bareither et al. 2012e; Yazdani et al. 2012;

Oonk et al. 2013; Zhao et al. 2013b). The period of time for data acquisition may last for decades, spanning from construction, operating to post-closure care period of a landfill. This makes macro-scale data scarce and sometimes incomplete. It is also subject to constraints such as high expenses, intensive labor and disturbances from surrounding environment. Field observations and measurements are often obscured by the fact that many processes and phenomena occur concurrently, thus it is almost impossible to unravel the processes and distinguish individual contribution of each mechanism. Instead, only general trends and the range for expected values are obtained. Reaction rates, coefficients and parameters obtained from macro-scale studies are usually conservative. Nevertheless, field data from these studies serve as the basis for landfill design, monitoring and operation and are used to validate the results of laboratory studies and modeling efforts.

- **Micro-scale study**

Micro-scale laboratory experiments are conducted in less than 1 L reactors and focus on biochemical and microbiological aspects. The experimental setups are generally highly idealized compared to field conditions in landfills. Waste specimen is often shredded or sieved to reduce the size of waste particles to accommodate for the small reactor volume. Recent studies suggested that selected or shredded waste may not be appropriate to represent field conditions, thus micro-scale study is not suitable for investigating the physical and mechanical properties of MSW (Bray et al. 2009; Zekkos et al. 2010a; Athanasopoulos 2011a). Nevertheless, experimental conditions can be controlled precisely in small reactors and the process under investigation can be monitored closely, thus micro-scale studies have been conducted to determine upper-bound values for the dynamics and microbial activities of MSW biodegradation (Barlaz et al. 1992; Eleazer et al. 1997; Stroot et al. 2001; Hossain et al. 2003).

2.1.3 **Temporal phases of MSW biodegradation**

Biodegradation of waste initiates after its disposal in a landfill and consists of many biochemical processes with biogas and soluble compounds in leachate as major products. Generalized temporal phases of MSW biodegradation have been studied extensively by other researchers and are briefly summarized here (Figure 2-2).

- **Phase 1: initial phase**

Oxygen (O_2) entrapped in MSW during collection, transportation and dumping is consumed by aerobic microorganisms in this phase. Since the amount of O_2 present is small compared to that needed for aerobic biodegradation of waste, most of the MSW remain undegraded (Barlaz et al. 1989a). Biogas generation is negligible due to limited aerobic biodegradation and minimal anaerobic biodegradation. Increase in the amount of soluble compounds in leachate mainly results from physicochemical reactions between waste and leachate such as washout and dissolution.

- **Phase 2: transition phase**

O_2 is depleted in phase 1 and MSW shifts from aerobic to anaerobic environment. An anaerobic microbial community starts to develop. Chemical oxygen demand (COD) in leachate increases rapidly due to hydrolysis of solid waste particles by microorganisms. Volatile fatty acids (VFAs) start to accumulate as a consequence of fermentation of large organic molecules. Biogas generation is slow and consists mainly of CO_2 as a result of fermentation.

- **Phase 3: acid formation phase**

The concentration of VFAs reaches the maximum value as a result of intensive fermentation and lack of acid-removal mechanism. This leads to low pH value around 5-6. The concentration of COD reaches the maximum value as well due to high quantity of fermentation and hydrolysis products. H_2 is also present as a fermentation product. Biogas generation is still slow and

consists of CO_2 and H_2. Methanogenesis is inhibited by low pH and high H_2 concentration, while syntrophic bacteria are still adjusting to the environment.

- **Phase 4: CH4 fermentation phase**

Syntrophic and acetogenic bacteria consume VFAs and H_2 and produce substrate for methanogenic archaea such as acetate, methanol and CO_2. pH for leachate increases to around neutral after removal of excess VFAs. In addition, low H_2 concentration also provides favorable reaction condition for continuous fermentation and subsequent methanogenesis. As a result, CH_4 generation rate increases to the maximum value shortly after the onset of methanogenesis. COD in leachate begins to decrease as organic compounds are removed steadily. Stable anaerobic biodegradation activity is maintained with hydrolysis as the rate determine step (Halvadakis et al. 1983; Barlaz et al. 1989b).

- **Phase 5: final maturation phase**

After readily biodegradable MSW is depleted, the rate of biodegradation decreases and COD in leachate remains at low value. In this phase, hydrolytic bacteria start to convert more recalcitrant substrate, hence hydrolysis is still the rate limiting step and overall reaction rate is low. Biogas generation rate and CH_4 concentration decrease gradually due to substrate limitation and suboptimal environmental conditions for methanogenesis.

2.1.4 **Biogas generated during MSW degradation**

The cumulative volume and rate of CH_4 generation are functions of waste composition (Wang et al. 1994; Eleazer et al. 1997; Wang et al. 1997; Staley and Barlaz 2009). Each waste constituent has different decay rate (k) and CH_4 generation potential (L_0) (Table 2-2). For example, food waste degrades within days to weeks (Wang et al. 1997), paper degrades within years (Eleazer et al. 1997), whereas wood (Barlaz 2006; Wang et al. 2011a) and plastic (Mersiowsky et al. 2001; Ishigaki et al. 2004) require years to decades to degrade. The CH_4 generation potential of waste

is defined as the total volume of CH_4 generated per dry mass of waste (typically L CH_4/kg dry waste) (EPA 2005). The L_0 values of different types of biodegradable waste vary widely from 300 L/kg for food waste to 25 L/g for yard waste (Eleazer et al. 1997; Wang et al. 2011b).

The ratio of the concentrations of cellulose (C) and hemicelluloses (H) over the concentration of lignin (L) (C+H/L) in solid waste is one indicator for L_0 and k. It is rationalized that C and H are the major biodegradable compounds in various types of waste, whereas L is recalcitrant to biodegradation in anaerobic environment (Wang et al. 1994). Food waste which has low C and H generally degrades rapidly, whereas paper and wood that contain plenty of C, H and L require more time to degrade (De la Cruz and Barlaz 2010). The value of L_0 of waste is correlated with the volatile solids content (VS) of the waste (Kelly et al. 2006).

Biogas generation data can be fitted using the first-order decay model described in U.S. EPA's Landfill Gas Emission Model (LandGEM) to obtain the values of k and L_0 (EPA 2005). Many other biogas generation and transport models have been established which are largely based on past experience of landfill operations and the determination of model parameters requires fitting of field measurement data (El-Fadel et al. 1996b; Hashemi et al. 2002; Copty et al. 2004; Faour et al. 2007; Garg and Achari 2010; Amini et al. 2012; Lamborn 2012).

2.1.5 **Leachate generated during MSW degradation**

Exposure of MSW to leachate induces physicochemical and biochemical reactions in both solid and liquid phases. Physicochemical reactions include dissolution, adsorption, precipitation, complexation, oxidation and reduction. Dissolution of solid waste enlarges void volume in waste matrix, whereas adsorption and precipitation of compounds reduces pore size. Complexation of ligands affects substrate and nutrient availabilities for microorganisms and can be determined by traditional aquatic chemistry approaches (Morel and Hering 1993). Oxidation and reduction of

soluble compounds in leachate are usually not characterized explicitly, rather, oxidation reduction potential (ORP) for leachate is measured. Leachate composition can be correlated to the degree of stabilization of MSW (Pohland and Alyousfi 1994).

Because of the high heterogeneity and complexity of MSW matrix, determination and prediction of transport and fate of both soluble compounds and microorganisms are extremely difficult. Leachate generation and hydrologically transport behavior in landfill have been modeled (El-Fadel et al. 1997; Fellner and Brunner 2010; Tinet et al. 2011; White et al. 2011). In practice, leachate samples are collected from accessible locations in a landfill such as leachate sump, monitoring well, and storage tank for composition measurement and microbiological study. The sampled leachate in the field is mixed liquid from different parts of a landfill at different times, and may not be representative of the leachate from a specific location.

Leachate can contaminate groundwater, if base containment system leaks. Excessive accumulation of leachate is generally the trigger mechanism for landfill failures (Koerner and Soong 2000). Therefore leachate must be removed by leachate collection system and pumped offsite frequently. Knowledge of the composition of leachate is needed to determine monitoring criteria for groundwater and to evaluate the feasibility of offsite treatment (Pohland and Kim 2000; Kjeldsen et al. 2002; Kim and Pohland 2003). High concentrations of calcium, iron, carbonate and sulfate ions may lead to mineral precipitation and clogging of pipelines which affect long-term leachate collection efficiency (Gallagher 1998; Fleming et al. 1999; Rowe et al. 2000a; Rowe et al. 2000b; Cooke et al. 2001; Rittmann et al. 2003; Fleming and Rowe 2004; VanGulck and Rowe 2004a; VanGulck and Rowe 2004b; McLsaac and Rowe 2007; McIsaac and Rowe 2008; Palmeira et al. 2008; Lozecznik et al. 2010; Rowe 2012).

2.1.6 **MSW-degrading microorganisms**

- **Microbial activities and interactions**

Aerobic biodegradation of MSW is transient and only a small fraction of biodegradable waste is consumed. Anaerobic biodegradation of MSW is carried out by a consortium of microorganisms as illustrated in Figure 2-3. Complex polymers of MSW is first disintegrated and hydrolyzed by hydrolytic, especially cellulolytic, bacteria to simpler organics like monomer sugars, amino acids and proteins. Fermentative bacteria consume these products to generate H_2, CO_2, acetate, alcohols and other VFAs such as propionate, butyrate and valerate. H_2 and CO_2 serves as substrate for homoacetogens to produce more acetate, whereas VFAs, succinate and alcohols serve as substrate for syntrophic bacteria to yield additional H_2 and acetate. H_2, acetate and simple methyl-group chemicals can be used by methanogens to produce CH_4. End products of anaerobic biodegradation are CH_4 and CO_2 which are emitted from the system.

Onset of methanogenesis is highly influenced by the growth environment for methanogens. Neutral pH, low concentrations of VFAs and H_2 are essential for the growth of methanogens (Zehnder and Stumm 1988; Zinder 1993). Syntrophic bacteria facilitate the growth of methanogens by consuming excess VFAs and H_2 to maintain neutral pH and create favorable reaction conditions for continuous fermentation. For example, propionate is oxidized by propionate-oxidizing bacteria and butyrate is oxidized by saturated-fatty-acid-beta-oxidizing syntrophs (Stams 1994; Schink and Stams 2006). Methanogenesis and overall biodegradation performance may be enhanced by retaining syntrophic juxtaposition (McMahon et al. 2001; Stroot et al. 2001; Vavilin and Angelidaki 2005) and neutral-pH microhabitats (Vavilin et al. 2006; Staley et al. 2011a) for methanogens which are influenced by the matrix structure of waste and leachate flow as suggested previously. Three pathways for methanogenesis are identified as acetoclastic, hydrogentrophic and methylotrophic methanogenesis (Thauer et al. 2008). Common

methanogens in MSW are *Methanobacteriales*, *Methanomicrobiales* and *Methanosarcinales*. All of the three genera are found in fresh MSW , whereas methanogenic population shifts to hydrogentrophic genera in *Methanobacteriales* and *Methanomicrobiales* as biodegradation proceeds (Uz et al. 2003; Nayak et al. 2009; Qu et al. 2009a; Staley et al. 2012).

- **Microbiological techniques**

Microbial communities conducting anaerobic biodegradation of MSW were first studied by culture-based method (Donnelly and Scarpino 1984; Grainger et al. 1984; Sleat et al. 1987; Barlaz et al. 1989b; Westlake et al. 1995; Pourcher et al. 2001). Microorganisms responsible for hydrolysis, fermentation and methanogenesis were isolated, identified and enumerated, respectively. However, certain microbial species are not culturable so far.

Recently, molecular biology techniques have been demonstrated as effective and efficient tools for microbial community analyses in anaerobic systems (Griffin et al. 1998; McMahon et al. 2001; McMahon et al. 2004). The typical procedure consists of biomass sampling and pretreatment, nucleic acid extraction, design of specific primers and polymerase chain reaction (PCR). When amplified nucleic acid is obtained, microbial community structure and phylogeny can be analyzed with various methods such as clone library and sequencing, pyrosequencing, denaturing gel gradient electrophoresis (DGGE), and terminal restriction fragment length polymorphism (T-RFLP) (Head et al. 1998; Forney et al. 2004; Rittmann et al. 2006).

Microbial communities in leachate and solid waste in landfills have been characterized. Leachate samples from numerous landfills were obtained and specific microorganism species or microbial communities were analyzed (Van Dyke and McCarthy 2002; Huang et al. 2004; Huang et al. 2005; Lockhart et al. 2006; McDonald et al. 2008; Nayak et al. 2009; McDonald et al. 2010; Mellendorf et al. 2010; Staley et al. 2011a), some communities were visualized by fluorescence in-situ hybridization (FISH) (Burrell et al. 2004; Calli et al. 2006; Laloui-Carpentier et al. 2006).

However, a recent study by Staley (2012) stated that microbial community in leachate is not necessarily identical to that in actual solid waste in a landfill, therefore direct referencing between microbial communities in leachate and solid waste is not warranted. Biomass was also obtained directly from MSW in full-scale landfills (Luton et al. 2002; Chen et al. 2003; Uz et al. 2003; Sawamura et al. 2010) and laboratory-scale simulators (Mellendorf et al. 2010; Staley et al. 2011a), but the heterogeneous nature of MSW and limited sample numbers may undermine the repeatability and representativeness of such results. Moreover, the results of microbial community analyses for both leachate and solid waste samples encounter problems of biased recovery due to sampling technique (Palmisano and Barlaz 1996) and nucleic acid extraction procedures (Raskin et al. 1997; Staley et al. 2011b). As a result, high uncertainty remains in the studies of microbial communities in MSW landfills.

2.2 Physical properties of MSW

2.2.1 **As-covered MSW composition**

The as-covered composition of waste varies spatially in a landfill due to changes in incoming MSW stream with time (Zekkos et al. 2010b; Wang et al. 2013) and regionally among different landfills (Staley and Barlaz 2009; van Haaren et al. 2010). Therefore estimation of waste composition always has relatively high uncertainty. Prior to laboratory testing, MSW samples are typically characterized according to the procedures described by Zekkos et al. (2010b) or Dixon (2008). The samples are first separated into <20 and >20 mm fractions. The <20 mm fraction is typically soil-like in nature, i.e., includes significant amounts of daily cover soil and inorganic debris as well as fine waste inclusions. The >20 mm material consists primarily of discarded waste, i.e., paper, plastics, wood, metal and miscellaneous objects.

The initial composition of waste influences the characteristics of leachate (Barlaz et al. 1989b; Appels et al. 2011) and biogas (Eleazer et al. 1997; Kelly et al. 2006; Fei et al. 2015b) generated during MSW degradation, and settlement and compressibility (McDougall 2011; Bareither et al. 2013a; Zekkos et al. 2016), shear strength and shear modulus (Bareither et al. 2012c; Kavazanjian et al. 2013; Sahadewa et al. 2014a; Fei and Zekkos 2015; Zekkos and Fei 2016), total and dry unit weight (Zekkos et al. 2006; Yu et al. 2011), and void ratio and hydraulic conductivity (Reddy et al. 2011; Hossain and Haque 2012; Stoltz et al. 2012; Breitmeyer and Benson 2014; Woodman et al. 2014) of fresh and degraded waste.

2.2.2 **Moisture content of MSW**

Moisture content (w_c) has been identified as the most important factor controlling the initiation, distribution and rate of biodegradation (Pohland 1975; Leckie et al. 1979; Reinhart and Townsend 1998). Leachate is the media for microbial activity, which influences substrate distributions, growth environment, migration and population distribution of microorganisms (White et al. 2011).

The moisture content (w_c) of disposed waste is greatly influenced by passive infiltration and active addition and recirculation of moisture in landfills. Moisture infiltration to waste is minimized in a modern Subtitle-D landfill, thus w_c of the waste is always below its field capacity. In contrast, a bioreactor landfill is operated with moisture addition and leachate recirculation to increase w_c of the waste, although in most cases field capacity w_c of the waste was still not achieved (Reinhart et al. 2002; Benson et al. 2007; Bareither et al. 2010; Yazdani et al. 2012). Leachate recirculation has been demonstrated to accelerate biodegradation of MSW by increasing its w_c (Wall and Zeiss 1995; Reinhart and Townsend 1998; Pohland and Kim 2000; Barlaz et al. 2010a; Fei and Zekkos 2012).

The w_c of each waste constituent varies widely and typical values are listed in Table 2-2 (Tchobanoglous and Kreith 2002), although the values appear to be representative of the waste in arid regions and are near lower-bound. The moisture content of waste also varies with overburden pressure (Zornberg et al. 1999; Stoltz et al. 2012) and depth of waste in a landfill (Zhan et al. 2008; Zhan et al. 2015).

Microorganisms require appropriate moisture content to conduct anaerobic digestion of biodegradable solid waste (Pohland and Harper 1986; Reinhart and Townsend 1998), thus the bulk w_c of waste controls the average rate of MSW biodegradation which is measured by the changes in characteristics of leachate and biogas (Reinhart et al. 2002; Barlaz et al. 2010b; Fei et al. 2015b). Waste constituent with high moisture retention ability is more likely to provide suitable environment for microorganisms and stimulate the onset of biodegradation (Vavilin and Angelidaki 2005). In addition, softening and raveling of waste particles due to moisture addition and migration contribute to settlement and changes in unit weight and void ratio of waste (McDougall 2011; Bareither et al. 2012d). The response of waste to shearing is different depending on whether existing moisture can be drained (Harris et al. 2006; Zekkos et al. 2012; Zekkos and Fei 2016).

2.2.3 **Unit weight of MSW**

The knowledge of unit weight of waste is necessary for almost all engineering calculations and analysis on landfill stability (Dixon and Jones 2005) and it varies dramatically due to many reasons. The unit weight of waste depends heavily on the composition of landfilled waste. Shortly after landfilling, the unit weight of as-covered waste is influenced by compaction effort, the composition of waste, and the quantity of daily cover soil used (Dixon and Jones 2005). In

the long-term, the burial depth and progress of degradation of waste also affect its unit weight (Powrie and Beaven 1999; Dixon and Jones 2005; Zekkos et al. 2006).

Typical total unit weight of major MSW constituents are listed in Table 2-2, while total unit weight of daily cover soil is generally between 18 and 20 kN/m^3. For a certain composition of waste, its unit weight increases with compaction effort. In addition, the unit weight of MSW exhibits low variation when highly compacted (Oweis and Khera 1986; Landva and Clark 1990). The total unit weight of waste increases with burial depth and general trends have been reported by several researchers (Figure 2-4). Since a wide range of measured total unit weight at different depths and ages are available, Zekkos et al. (2006) recommended categorizing the profiles based on compaction effort and quantity of cover soil. For MSW with low compaction effort and small quantity of cover soil, the unit weight ranges from 5 kN/m^3 at surface to 10 kN/m^3 at a depth of 60 m, whereas highly compacted MSW has unit weight around 15 kN/m^3 throughout the burial depth (Figure 2-5).

The unit weight of waste is influenced by its degradation process, as cavitation and collapsing of the matrix structure of waste occurs concurrently with time (McDougall et al. 2004; Dixon and Jones 2005). A handful of researchers have reported the total unit weight of MSW at different degrees of MSW degradation (Gourc et al. 2001; Kavazanjian 2001; Zekkos et al. 2006). However, locations for in-situ measurements and samplings for laboratory testing were often not co-located, thus the results are inconsistent and inapt to indicate a definite relationship between the degree of degradation and unit weight of waste. Kavazanjian (2006) proposed rational mechanisms for all of increasing, constant or decreasing unit weight of waste due to biodegradation.

Change in unit weight of waste is the result of simultaneous volume reduction and mass loss. Whether it will increase or decrease depends on the rates of these two counterbalancing processes. In addition, methanogenic archaea and fermentative bacteria can generate large quantities of biogas, thus potentially changing the phase relationship in MSW matrix (Merry et al. 2006). This also leads to change in unit weight. In essence, long-term change in the unit weight of waste is still largely unknown (Sharma and Reddy 2004).

2.2.4 **Matrix structure of MSW**

Biodegradable solid waste particles are broken down and solubilized by microorganisms, thus the matrix structure of waste is changed. When interwoven solid waste particles undergoing biodegradation become too weak to sustain external stress, microscopic collapse occurs in waste mass which leads to biological settlement (McDougall and Pyrah 2004). Hydrolytic and acidogenic bacteria are believed to contribute mainly to solid waste dissolution (Barlaz et al. 1989b).

A three phase system consisting of biogas, leachate and both organic and inert solid phases is used to represent MSW matrix in a landfill (Figure 2-6). It has been identified that unit weight, void ratio and gravimetric moisture content are three independent physical variables describing the system (Stoltz et al. 2010b). The change in matrix structure of waste due to mechanical compression can be calculated using traditional soil mechanics principles (Holtz and Kovacs 1981; Mitchell and Soga 2005). Biological change in waste matrix has been studied theoretically with approaches aiming at fundamental understanding and modeling of biodegradation process by several researchers (McDougall and Pyrah 2004; McDougall 2007; Elagroudy et al. 2008; Gawande et al. 2010; Gourc et al. 2010). Such models incorporate rate equations of anaerobic digestion and functions for solid structure deformation and consequent

changes in settlement and hydraulic conductivity. For example, McDougall and Pyrah (2004) hypothesized that the void ratio of waste could increase, decrease or remain unchanged based on the matrix structure of waste and environmental and operating conditions.

2.3 Mechanical properties of MSW

2.3.1 **Compressibility of MSW**

The compressibility of MSW has been a topic of significant interest in engineering practice since it affects the short- and long-term performance of landfills, and particularly, the performance of gas collection systems and landfill covers, the vertical expansion and closure of landfills, as well as the post-closure development of landfills. Nearly any post-closure development project involves an assessment of the response of the waste mass to a change in stress conditions. In many cases, the uncertainties involved in the estimation of waste compressibility increase the development risk and may adversely affect the decision to develop the closed landfill. Increased interest in vertical expansion of landfills also requires an assessment of the compression of the waste in existing landfill cells.

Thus, it is not surprising that significant amount of effort has been expended since the early work by Sowers (1973) to characterize the compressibility of MSW. Research has been directed towards the collection of laboratory experimental data (Wall and Zeiss 1995; Kavazanjian et al. 1999; Landva et al. 2000; Hossain et al. 2003; Olivier and Gourc 2007; Ivanova et al. 2008b; Stoltz et al. 2010b; Reddy et al. 2011; Bareither et al. 2012b; Fei and Zekkos 2013; Fei et al. 2014a), field measurement of settlements (Bjarngard and Edgers 1990; Stulgis et al. 1995; Spikula 1997; Zhao et al. 2001; Mehta et al. 2002; Yuen and McDougall 2003; Sharma and De 2007; Bareither et al. 2012e) and modeling of the settlement behavior

(Edil et al. 1990; Ling et al. 1998; McDougall and Pyrah 2004; Oweis 2006; Chen et al. 2010b; Gourc et al. 2010; Bareither et al. 2013a). An extensive review of the compressibility of MSW has been made by McDougall (2011).

One of the complicating factors associated with assessing the compressibility of MSW in the field, is that there are numerous mechanisms contributing nearly simultaneously to the observed settlement of MSW. These include physical and biochemical processes. Variations in the initial conditions of waste (i.e. composition, waste size, moisture content, total unit weight, compaction and amount of daily soil cover) and operations after waste placement (aeration, liquid addition and leachate recirculation) influence the observed settlement as well (Bareither et al. 2012b; Bareither et al. 2012d). Biodegradation of the organic constituents is one of the most critical, if not the key, contributor and often masks immediate and long-term compression of the waste due to load application. However, as clearly demonstrated by field and laboratory evidence, MSW is a soft material that deforms significantly when subjected to a load, and the deformation associated with mechanical compression of MSW may even reach half its original height.

- **Mechanical compression**

Since MSW is a geo-material, a large number of studies have used immediate (ε_I) and long-term vertical strain (ε_M) and the corresponding primary (C_{ce}) and secondary compression ratios ($C_{\alpha e}$) to estimate the compression characteristics of MSW due to vertical stress application, as illustrated in Figure 2-7. A synthesis of available 1D mechanical compression laboratory experiments (e.g., Sowers (1973), Landva and Clark (1990), Chen et al. (2009)) has been made by Bareither et al. (2012a) and McDougall (2011). Important recent lessons associated with the compressibility of MSW in response to a 1D compression loading are described briefly hereafter.

Case histories-based back-calculated values of $C_{\alpha e}$ are consistent with results from laboratory studies. Sharma and De (2007) presented a comprehensive review of $C_{\alpha e}$ values from a large number of case histories and concluded that the overall range of $C_{\alpha e}$ for MSW subjected to an external load generally varies between 0.01 and 0.07. A slightly narrower range (0.014-0.06) was reported for C_{ae} of MSW subjected to the self-weight of waste. From a fundamental, as well a practical perspective, the C_{ae} values are the same for self-weight vs. external loading.

Accommodating the larger particles of MSW is important in laboratory testing is important to capture the waste's field settlement behavior. Executing tests on the <25 mm fraction is not representative of field behavior (Bareither et al. 2012b). Thus, conventional size devices are not appropriate for waste testing. Experience from compressibility testing (Bareither et al. 2012b), shear strength testing (Bray et al. 2009), degradation testing (Fei and Zekkos 2013) shows that a specimen size of 300-mm is probably adequate. Milling of the coarser fraction to accommodate them in smaller devices also affects the characteristics of the MSW and its mechanical properties (Zekkos et al. 2008).

The effect of degradation on the immediate response of MSW to a compression loading, remains unknown. Hossain et al. (2003) performed small-scale testing (d=63.5 mm cells) and found that C_{ce} was a function of the state of decomposition. Waste with lower cellulose and hemicellulose to lignin ratios (C+H/L) yielded higher C_{ce} values, i.e., more degraded waste was more compressible. Bareither et al. (2012b) found a negligible effect of waste decomposition on C_{ce} of reconstituted degraded specimens. However, the authors also pointed out that the specimen undergoing degradation experienced a decrease in C_{ce} due to removal of organic content and stiffening of the waste matrix.

- **Biological compression**

The long-term settlement of MSW is caused by several mechanisms including physicochemical degradation, biodegradation creep, and raveling of waste (Sowers 1968; Bjarngard and Edgers 1990; Edil et al. 1990; Edgers et al. 1992; Sharma and De 2007; McDougall 2011). From a long-term settlement perspective, MSW is a heterogeneous medium with solid, liquid and gas phases. MSW solids can be distinguished as bio-accessible and bio-inaccessible (McDougall 2007). Both types of wastes are further identified as biodegradable and non-biodegradable. Inter-particle and intra-particle voids may be occupied by liquid and gas (Zhang et al. 2010; McDougall 2011). Inter-particle voids are voids between individual waste particles that are open to migration of moisture and microorganisms, and are termed bio-accessible voids hereafter. Intra-particle voids are encapsulated within individual waste particles and are inaccessible to moisture or microorganisms, i.e. bio-inaccessible voids. Initial and operational conditions cause volume changes to solids and voids leading to long-term settlement of waste. Long-term settlement of MSW can be divided temporally into three phases as schematically illustrated in Figure 2-8.

Phase 1 is termed as transitional phase (P_1). Upon completion of immediate compression, settlement continues due to time-dependent physical mechanisms such as particle reorientation and movement, raveling, delayed compression of deformable particles as a result of stress redistribution, as well as potential softening of waste constituents due to moisture introduction in the waste mass (Wall and Zeiss 1995; Bareither et al. 2012d). These mechanisms dominate especially if moisture content is low. Waste may remain in this phase indefinitely. If moisture introduction becomes significant, physicochemical and biological dissolution of soluble compounds from waste to leachate creates a suitable environment for microorganisms, and biodegradation emerges as a major contributor to the long-term settlement. Microorganisms start to grow in the transitional phase, but their population and activity level are still low (Barlaz et al.

2010b; Staley et al. 2011a). With continued moisture presence, MSW settlement shifts to Phase 2, active biodegradation phase (P_2).

Phase 2 occurs when most microbial species reach their maximum growth rates, and thus a robust microbial community has been established (Barlaz et al. 2010b). Biodegradable MSW is rapidly hydrolyzed, disintegrated, fermented and metabolized to final products such as CH_4, CO_2 and dissolved compounds (Barlaz et al. 1989b; Pohland and Kim 2000). Hydrolysis of solid waste causes structural change in the waste matrix and is the rate-limiting step in this phase (Barlaz et al. 1989b; McDougall and Pyrah 2004; McDougall 2011). Physical mechanisms such as creep and raveling are also ongoing, but their contributions are significantly lower compared to biodegradation (Elagroudy et al. 2008; Gourc et al. 2010; Bareither et al. 2012d).

As availability of biodegradable MSW decreases steadily during active biodegradation phase, MSW settlement transits to the residual phase (P_3) (Barlaz et al. 2010b). Settlement slows down due to retarded microbial activity. Subdued biodegradation along with creep become the two major contributors to settlement (Bjarngard and Edgers 1990; Edgers et al. 1992).

Alternatively, the total strain of waste can be divided based on contributions from different mechanisms into immediate compression strain (ε_I) as discussed previously, biological strain (ε_B) observed subsequent to ε_I until CH_4 generation stopped, and mechanical creep strain (ε_M) afterward (Gourc et al. 2010; Bareither et al. 2013a; Fei and Zekkos 2013). An example illustration demonstrating this concept is shown in Figure 2-9.

2.3.2 **Shear strength of MSW**

- **Methodologies of shear strength testing**

A significant number of studies have been conducted to assess the shear strength of MSW in the laboratory using large-size experimental devices. In this dissertation, large-size testing is defined

as tests that have specimen diameter or width that is at least 300 mm, a definition that is consistent with earlier recommendations (Bray et al. 2009; Athanasopoulos 2011b). Most commonly, large-size direct shear testing has been conducted (e.g., (Landva and Clark (1990); Bray et al. (2009); Singh et al. (2009); Zekkos et al. (2010a); Bareither et al. (2012c); Zekkos et al. (2013a))). Zekkos et al. (2010a) compiled reported shear strength of MSW in the literature in direct shear testing as shown in Figure 2-10. Large-size triaxial shear testing has also been conducted by some researchers (e.g., (Jessberger and Kockel (1993); Grisolia et al. (1995); Zekkos et al. (2012); Ramaiah et al. (2014))), whereas large-size simple shear testing of MSW has been conducted as part of two studies only (Kavazanjian et al. 1999; Pelkey et al. 2001). Only a few *in situ* direct shear tests on MSW have been reported (e.g., (Richardson and Reynolds (1991); Houston et al. (1995); Mazzucato et al. (1999); Caicedo et al. (2002))).

The overwhelming majority of tests to assess the shear strength of MSW have been conducted under "drained" conditions. Undrained triaxial shearing tests have been conducted by Karimpour-Fard et al. (2011) who used a 200-mm diameter triaxial device and Shariatmadari et al. (2009) who tested specimens that were 220-mm in diameter. For both studies the waste originated from the Metropolitan Center landfill in Salvador, Brazil. Tests were also conducted by Harris et al. (2006) and involved 152-mm diameter simple shear testing of MSW and Reddy et al. (2011) that involved tests on synthetic waste specimens that were 50-mm in diameter.

- **MSW characteristics that influence its shear strength**

Characteristics of landfilled waste often vary widely in the field due to variable environmental and operating conditions, especially the overburden pressure, waste composition, matrix structure, and degree of degradation of MSW (Dixon and Jones 2005; Zekkos et al. 2006; Kavazanjian et al. 2013). These characteristics are influential to the shear strength of MSW.

As shown in Figure 2-11, the secant friction angle of MSW obtained from direct shear testing decreases with increasing normal stress applied to waste in logarithmic scale for a variety of MSW specimens.

The respective portions and properties of <20 and >20 mm fractions of waste influence its shear strength. Waste specimens containing more fibrous waste appear to be stronger than specimens with lower content of fibrous waste in simple shear testing (Kavazanjian et al. 1999). However, Bareither et al. (2012c) concluded that, in direct shear testing when fibrous waste constituents are oriented primarily parallel to the shearing plane, higher ϕ were obtained for specimens with greater fraction of <20 mm materials and stiff constituents such as gravel and metal, whereas lower ϕ were associated with greater fraction of paper and plastic waste. Testing results in Zekkos et al. (2010a) and Zekkos et al. (2013a) suggested that, in addition to the portion of fibrous waste, the mechanical properties of different fibrous waste constituents and the orientation of fibrous waste affect the shear strength of specimens significantly in direct shear testing.

MSW has been shown to be one of the most anisotropic geomaterials due to the presence of fibrous constituents, such as paper, soft plastics and soft wood, that tend to become horizontally oriented during compaction and upon application of a vertical load. Evidence of this layering has been observed both in the field and the laboratory (Gotteland et al. 2000; Zekkos 2013). In fact it has been shown that MSW has significant similarities to fibrous peats (Zekkos 2013). In triaxial testing of the material, it is practically impossible to avoid the contribution of fibrous waste constituents on the stress-strain response. Thus, shear resistances observed in triaxial shear are high with friction angle (φ) of 48 degrees or higher (e.g., Zekkos et al. (2012)). However, as shown by Bray et al. (2009), in direct shear testing, the horizontal failure plane is

parallel to the orientation of the fibrous waste constituents and as a result the shear resistance in direct shear is the lowest.

Conflicting results have been reported on the impact of degradation of waste on its shear strength (Harris et al. 2006; Gabr et al. 2007; Hossain et al. 2009; Reddy et al. 2011; Bareither et al. 2012c; Fei and Zekkos 2015). Bareither et al. (2012c) and Harris et al. (2006) conducted direct shear and simple shear testing, respectively, on fresh and degraded waste, and reported increasing φ with decreasing cellulose plus hemicellulose to lignin ratio ((C+H)/L) which indicates an increase in degree of degradation. Similarly, Reddy et al. (2011) reported increased cohesion and decreased φ for degraded synthetic waste compared to fresh waste in both direct shear and triaxial shear tests. In contrast, a decrease in φ with decreasing (C+H)/L and volatile solids (VS) content, i.e., increasing degree of degradation, has been reported by Gabr et al. (2007) and Hossain and Gabr (2009). Fei and Zekkos (2015) showed slightly decreased shear strength and φ for a fully degraded waste specimen compared to an identical waste specimen without degradation in simple shear testing.

2.3.3 **Shear-wave velocity and small-strain shear modulus of MSW**

The shear-wave velocity (V_s) is an important engineering property of MSW and is related to the small-strain shear modulus (G_{max}) of MSW using elasticity theory (Kramer 1996). The V_s can be used to characterize the stiffness and damping of MSW (Zekkos et al. 2008) and is a critical input parameter in seismic analyses (Kramer 1996). There are three large-size laboratory studies on the V_s of MSW available in the literature using devices with specimen diameter or width between 150-305 mm. All three studies tested MSW from the Tri-Cities landfill in CA dynamically using resonant column, triaxial device, and simple shear device, respectively (Lee

2007; Zekkos et al. 2008; Yuan et al. 2011). The values of V_s of the specimens were subsequently calculated from the values of G_{max}.

The loading frequency of dynamic testing has an impact on V_s and G_{max}, where the G_{max} value increased by a factor of 1.1 per log cycle for frequencies ranging between 0.01-10 Hz (Zekkos et al. 2008). Lee (2007) independently showed similar results, and found that the G_{max} of MSW increased by the same factor per log cycle of frequency for frequencies ranging between 0.03-260 Hz. The importance of the impact of frequency is that *in situ* seismic testing with borehole methods (e.g., cross-hole and down-hole) typically entails measurements at frequencies approaching 100-300 Hz, yielding higher estimates of V_s compared to surface wave methods where frequencies are in the range of 3-50 Hz. On the other hand, the V_s of MSW measured at frequency higher than around 500 Hz (0.5 kHz) has not been reported.

Confining stress has a pronounced effect on the V_s and G_{max} of MSW. Zekkos et al. (2008) reported increases in V_s by a factor of about 1.4 as the confining stress increases from 25-75 kPa and is consistent with the V_s data in Lee (2007) from resonant column tests performed over a confining stress range between 8-276 kPa. Normal stress applied to MSW in simple shear and direct shear tests should have a similar effect.

Composition of waste also significantly affects its V_s. Zekkos et al. (2008) and Yuan et al. (2011) both reported a change in V_s from around 70 to 150 m/s at a confining stress of 75 kPa as the composition changes from waste-rich (18% of <20 mm fraction by weight) to soil-rich (100% of <20 mm fraction by weight). At confining stress up to 300 kPa, Lee (2007) found V_s to increase by a factor of 1.1-1.35 for changes in composition from 62-76 to 100% of <20 mm fraction by weight. The data from Zekkos et al. (2008) suggested a strong correlation between the V_s and γ_t for all Tri-Cities landfill waste specimens that have variable waste composition.

Thus, as suggested in Zekkos et al. (2006), the γ_t of MSW can be considered as an index of compactness as well as waste composition.

For reconstituted MSW specimens with identical waste composition, the γ_t (and the associated compaction effort) was found to have some impact on the V_s and G_{max} of waste (Zekkos et al. 2008). The values of V_s and G_{max} increased by 3-7% and 10-20%, respectively, from loosely compacted to densely compacted MSW specimens of the same composition tested at the same confining stress.

The impacts of moisture content and capillarity, structural and stress-induced anisotropy, and degree of degradation on the V_s of MSW have not been investigated. Generally, factors influencing the shear strength of MSW should affect the V_s of MSW as well.

As illustrated in Figure 2-12, Zekkos et al. (2014) developed a semi-empirical and an empirical model for V_s of MSW in landfills using 13 V_s profiles from four landfills in Michigan generated as part of the study and 36 additional V_s profiles from 15 landfills worldwide available in the literature. The models, shown in Figure 2-13, are intended to provide estimation of the V_s of MSW for preliminary design purposes and to evaluate the seismic response of landfills.

2.4 Tables

Table 2-1 Summary of representative experimental setups of MSW biodegradation studies described in this study and the literature.

	Reference(s)														
	Bareither et al. (2012b)	Bareither et al. (2013a)	Bareither et al. (2013b)	Barlaz et al. (1989)	Benbelkacem et al. (2010); Gourc et al. (2010)	Borglin et al. (2004)	Francois et al. (2006)	Hossain et al. (2003)	Ivanova et al. (2008)	Olivier et al. (2007)	Reddy et al. (2011)	Staley et al. (2011)	Valencia et al. (2009a,b)	Wall and Zeiss (1995)	This study
Simulator dimensions															
Diameter, m	0.6	0.3	0.6	0.1	0.96	0.7	0.38	0.06	0.48	1	0.13	0.25	0.7	0.57	0.3
Volume, L	100	11	190	2	800	200	120	4	650	830	6	10	710	260	40
Operations															
Temperature control, ^{0}C	–	–	35±5	41	35	–	38±2	39±2	30±2	–	36±2	–	30±4	25	40±3
Vertical stress (≤), kPa	–	400	–	–	–	–	–	1500	150	130	–	–	–	10	–
Initial and final measurements of the specimen															
Composition[a]	Y	Y	Y	N/R	Y	Y	Y	N/R	Y	Y	Y	Y	Y	Y	Y
Particle size (≤), cm[b]	Sh 10	Sh 2.5	Sh 2.5	Sh 1.9	Sh 15	Sh 5	Sh 5	Sh 2	Sh 4	Sy Sh 15	Sy N/R	Sh 6	Sh 4	Sh 4	Ex 10
w_c	√	√	√		√	√		√	√	√	√	√	√	√	√
G_s		√									√				
n															√
k						√				√	√				√
VS	√		√		√				√		√		√	√	√
BMP	√	√	√		√		√								
TOC				√	√				√					√	
CHL	√	√	√	√		√		√	√						√
Time-series measurements															
Test duration, days	1150	1067	181	110	466	400	550	70	919	668	varies N/R	14	350	230	1000
1. Physical measurements															
W_t															√
n								√							√
k															√
Temperature	√	√	√			√			√	√					√
Settlement	√	√	√		√	√		√	√	√				√	√
2. Biogas measurements															
Volume	√	√	√	√	√		√	√	√		√	√	√	√	√
Concentration	√	√	√	√	√	√	√	√	√	√	√	√	√	√	√
3. Leachate measurements															
pH	√	√	√	√	√	√	√	√	√	√	√	√	√	√	√
alk.	√						√								√
COD	√	√	√		√	√	√						√		√
BOD					√	√	√						√		
TOC									√				√	√	√
VFAs				√			√		√			√	√		√
Ions							√		√				√		√
NH_4^+						√	√		√				√		√
4. Microbial analyses[c]															
Culture				√											
DNA			√									√			√
5. Other time-series samples[d]															
Solid waste				D							D	D			C
Geotextile															√

Note: –: not applied; N/R: not reported; √: measured; blank: not measured; CHL: concentrations of cellulose, hemicellulose and lignin; G_s: specific gravity; VS: volatile solids; BMP: biological methane potential; k: hydraulic conductivity; n: porosity; W_t: total weight; alk.: alkalinity; BOD: biochemical oxygen demand; TOC: total organic carbon; VFAs: volatile fatty acids; Ions: common anions and cations; NH_4^+: ammonium concentration.

[a] characterization level, Y: sieving and manual separation of retained large particles into different categories.
[b] The largest dimension of particle. Ex: excluded oversized waste particle;
Sh: shredded oversized waste particle;
Syn: synthetic waste particles.
[c] Culture: culture-based microbial characterization, in this case most probable number method;
DNA: DNA-based microbial characterization, such as DNA concentration measurement, terminal-restriction fragment length polymorphism, DNA clone library, quantitative polymerase chain reaction, pyrosequencing.
[d] C: continuous solid waste: retrieve solid waste sample from the same simulator without destructively disassembly;
D: destructive solid waste: retrieve solid waste sample by destructively dissembling a simulator;
geotextile: retrieve geotextile sample from the same simulator without destructively disassembly.

Table 2-2 Unit weight, moisture content, CH_4 yield and decay rate of selected waste constituents

Waste component	Total unit weight[a] (γ_t, kN/m^3)	Moisture content[a] (w_c, w/w %)	CH_4 generation potential[b] (L_0, L CH_4/kg dry waste)	Laboratory waste decay rate[c] (k, 1/yr)
Paper	4.4	6	75-215	3.5
Paperboard	4.8	5	150	2.1
Plastics	2.2	2		
Yard trimmings	8.7	60	30-140	17.8-31.1
Ferrous metals	3.3	3		
Rubber	2.1	2		
Leather	2.1	10		
Textiles	2.4	10		3.1
Wood	4.9	20	0-85	1.6
Food wastes	11.6	70	150-300	15.0
Other	12.2			
Aluminum	2.2	3		
Glass	14.5	2		

Blank: value not available.
[a] from Tchobanoglous and Kreith (2002);
[b] from Eleazer et al. (1997);
[c] from De la Cruz and Barlaz (2010).

2.5 Figures

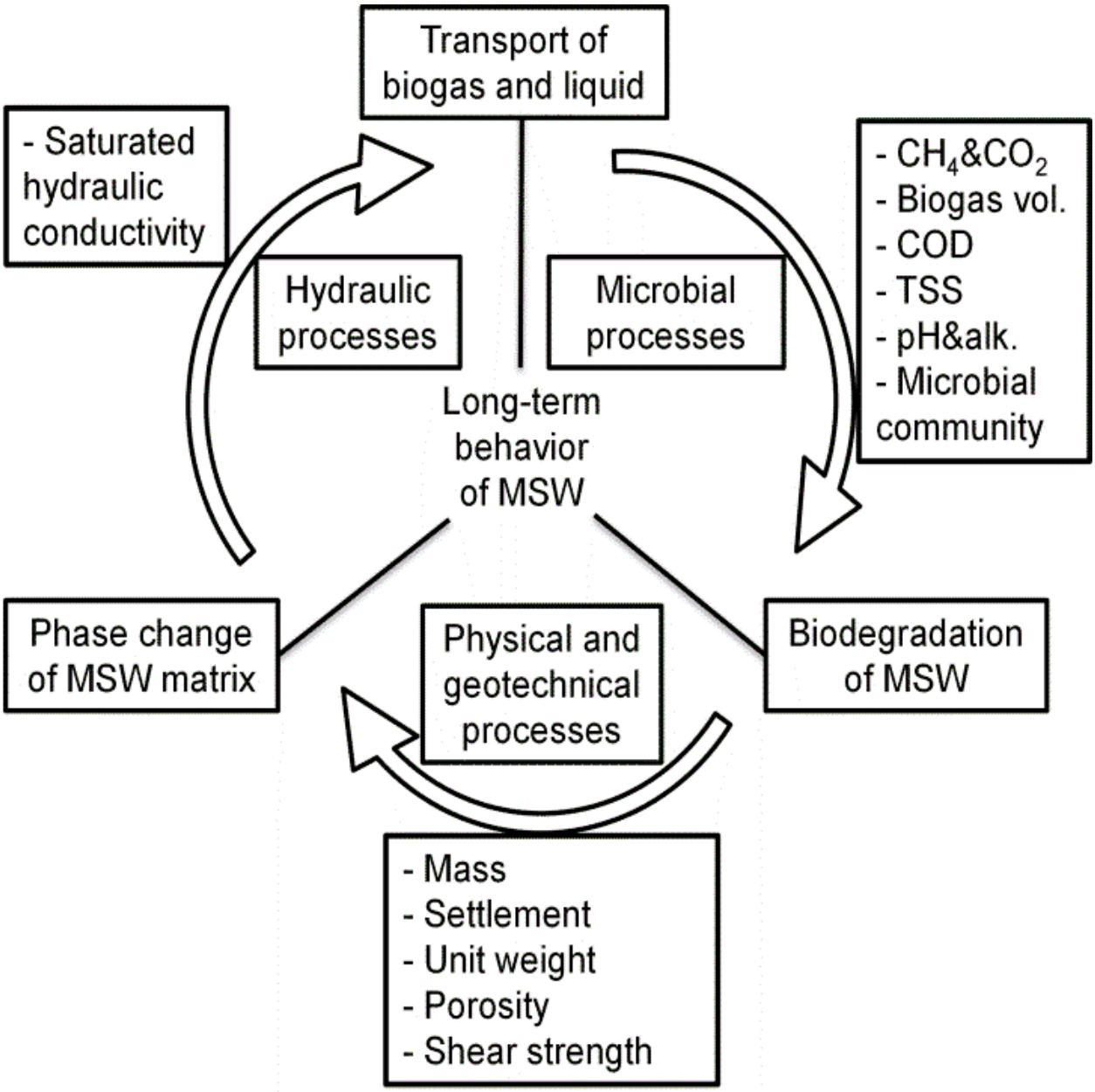

Figure 2-1 Schematic of the processes taking place during MSW biodegradation and examples of the parameters measured in the experimental setup described.

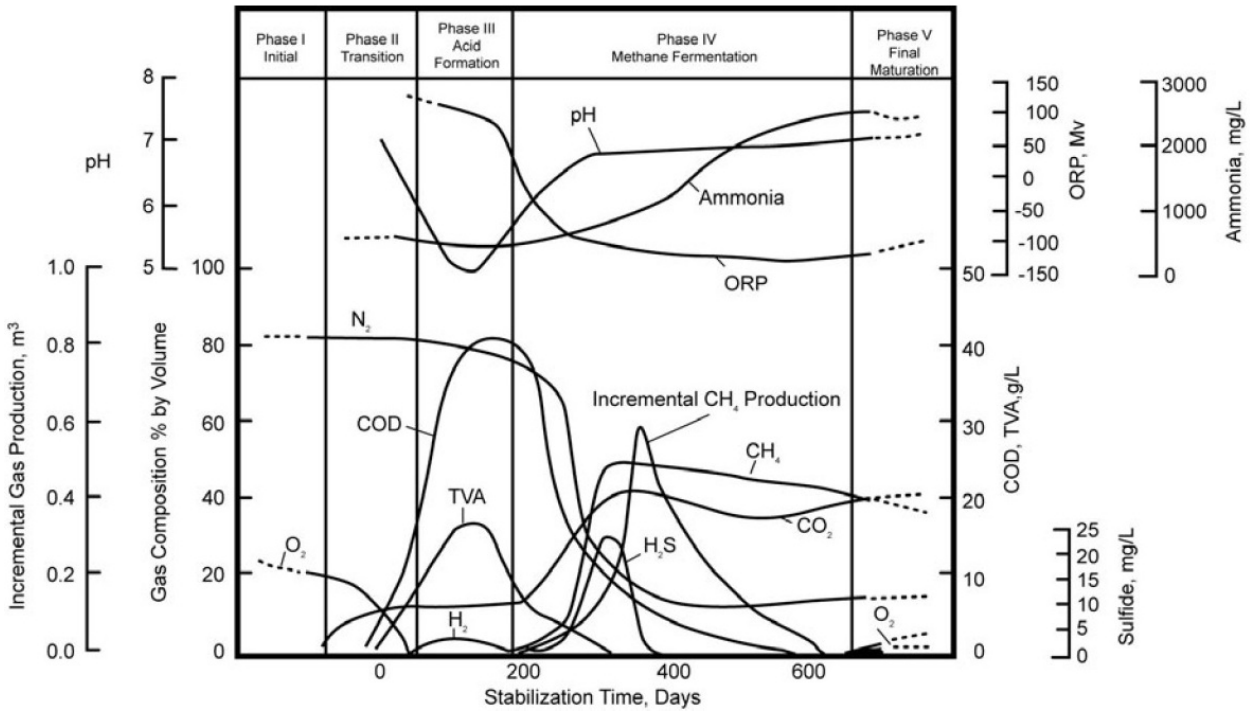

Figure 2-2 Five temporal phases of MSW biodegradation (Kim and Pohland 2003).

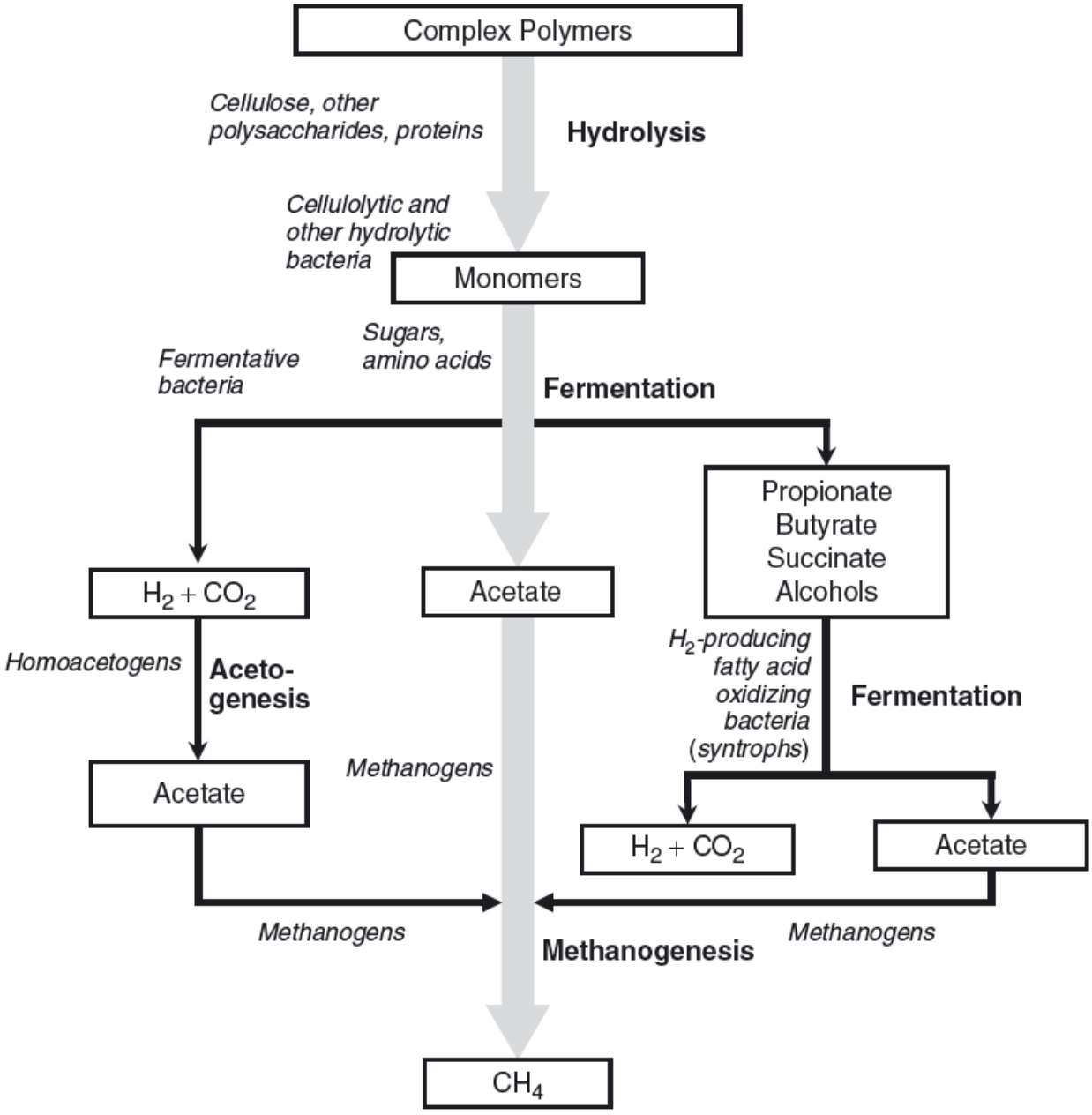

Figure 2-3 Microorganisms and pathways for MSW biodegradation (Barlaz et al. 2010b).

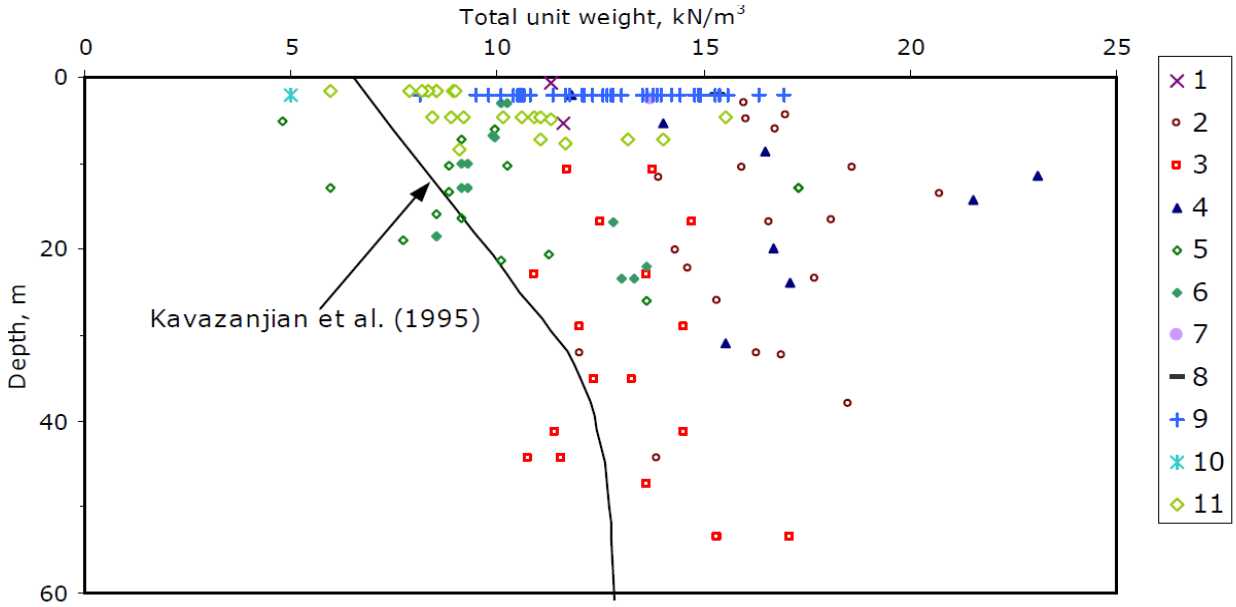

(1) Santo Tirso, Portugal (Gomes et al. 2002); (2) OII, California, USA (Matasovic and Kavazanjian, 1998); (3) Azusa, California, USA (Kavazanjian et al, 1996); (4) Tri-Cities, California, USA (this study); (5) no name older landfill (Oweis and Khera, 1998); (6) no name younger landfill (Oweis and Khera, 1998); (7) Hong Kong, China (Cowland et al. 1993); (8) Central Mayne landfill, USA (Richardson and Reynolds, 1991); (9) 11 Canadian landfills (Landva & Clark, 1986); (10) Valdemingomez, Spain (Pereira et al. 2002); (11) Cherry Island landfill, Delaware, USA (Geosyntec, 2003);

Figure 2-4 Reported total unit weight of MSW from different studies (Zekkos et al. 2006).

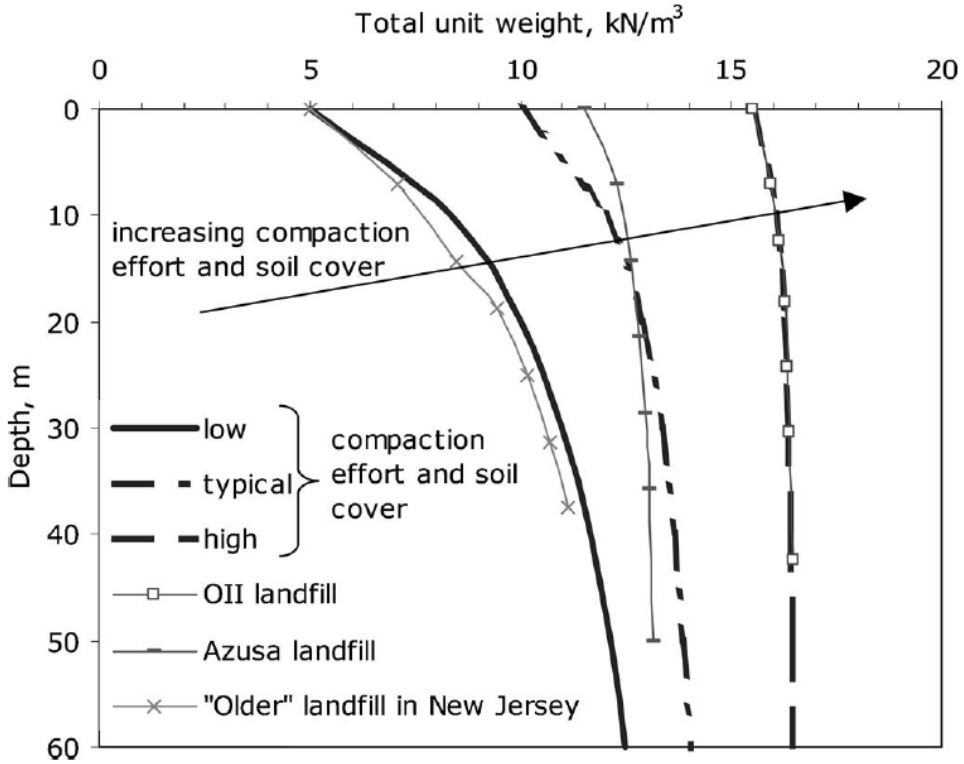

Figure 2-5 Typical MSW unit weight profiles along depth distinguished by compaction effort and soil cover (Zekkos et al. 2006).

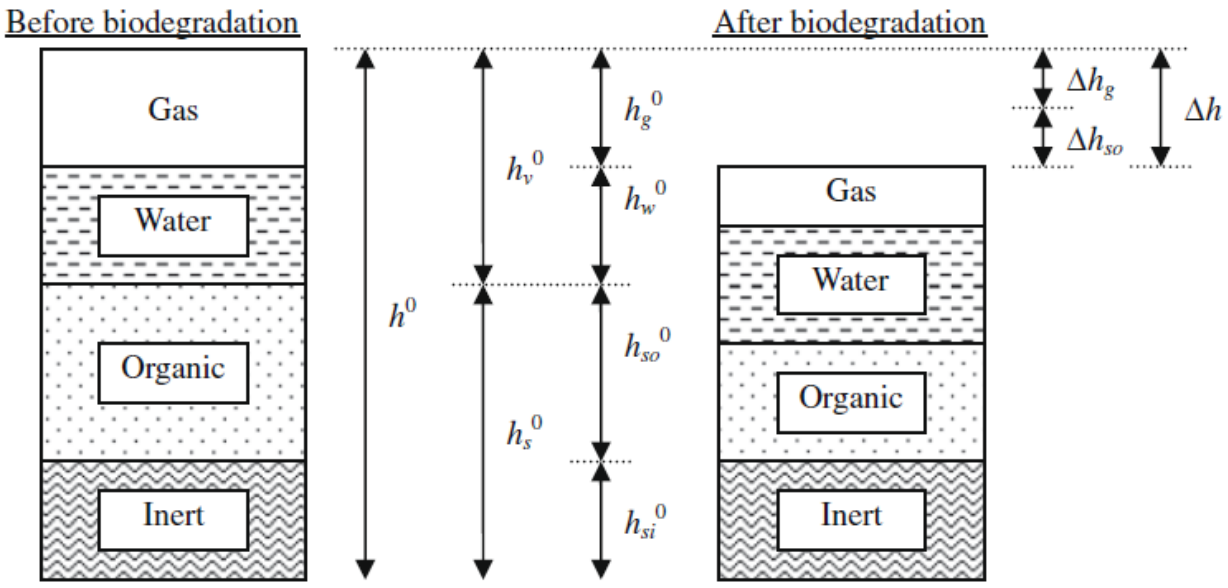

Figure 2-6 Phase diagram of MSW matrix before and after biodegradation (Gourc et al. 2010).

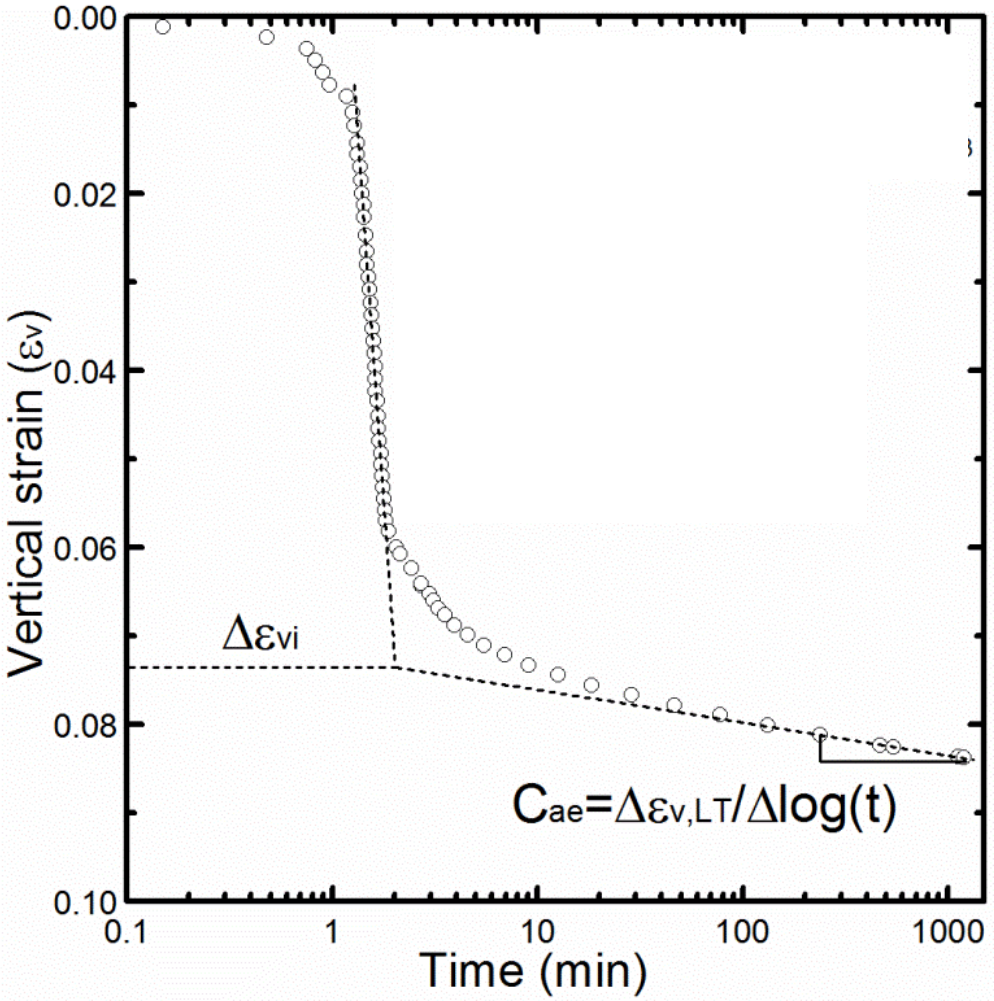

Figure 2-7 Typical response of MSW to mechanical compression.

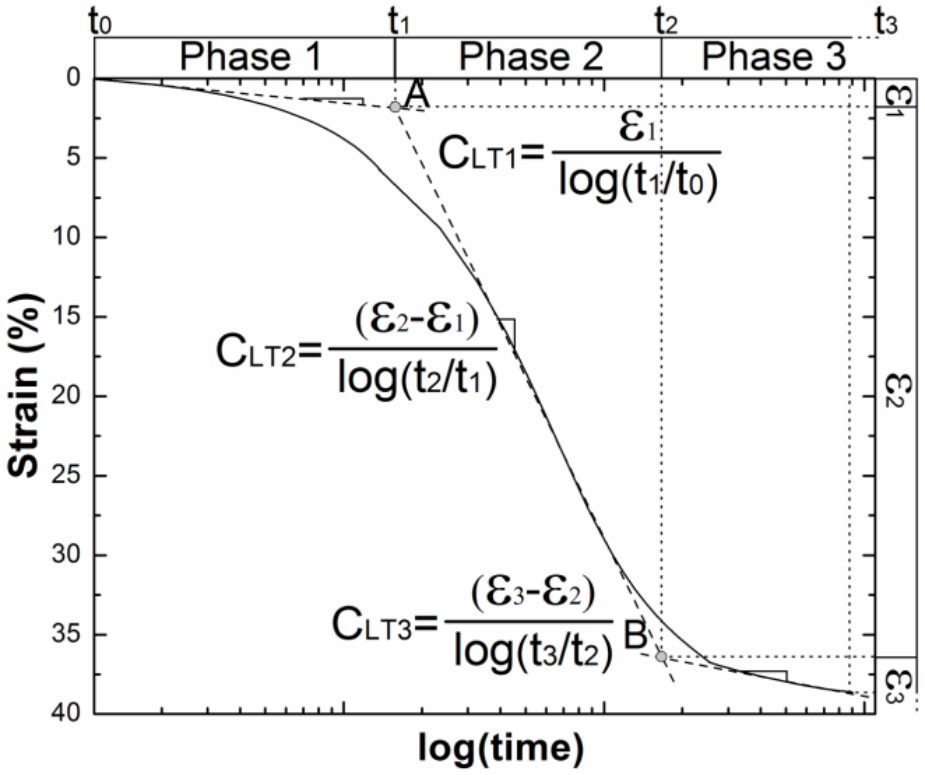

Figure 2-8 Idealized strain versus logarithmic time curve for three phases of long-term settlement of MSW.

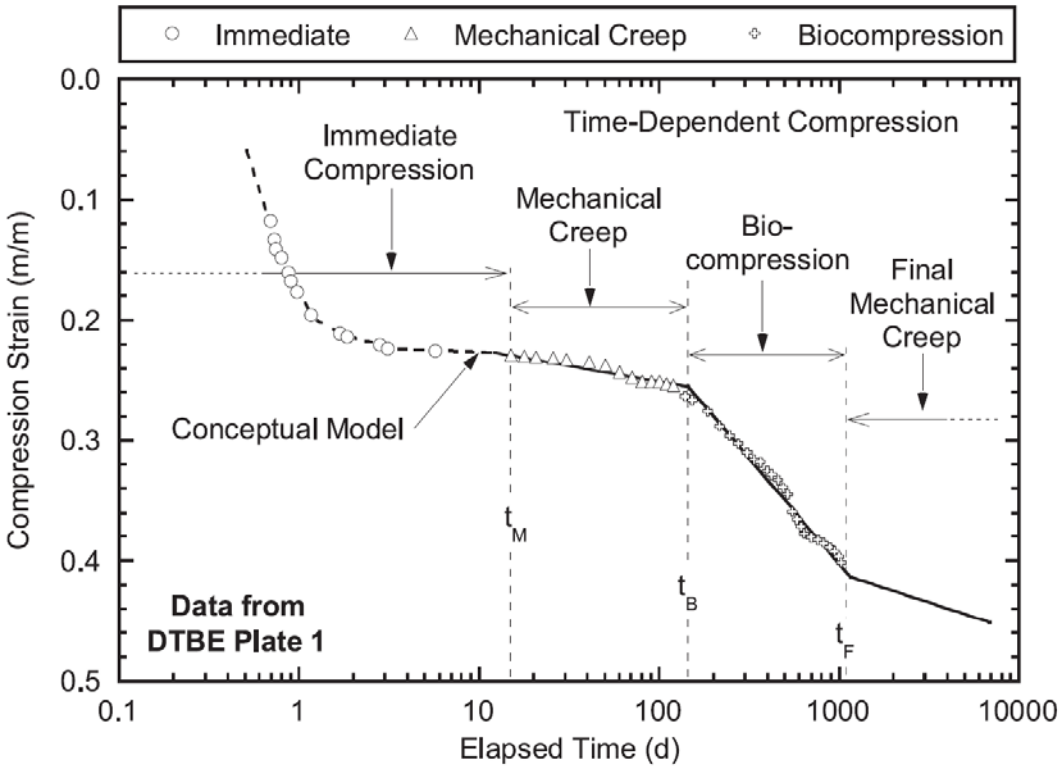

Figure 2-9 Idealized strain versus logarithmic time curve for different mechanisms contributing to long-term settlement of MSW (Bareither et al. 2013a).

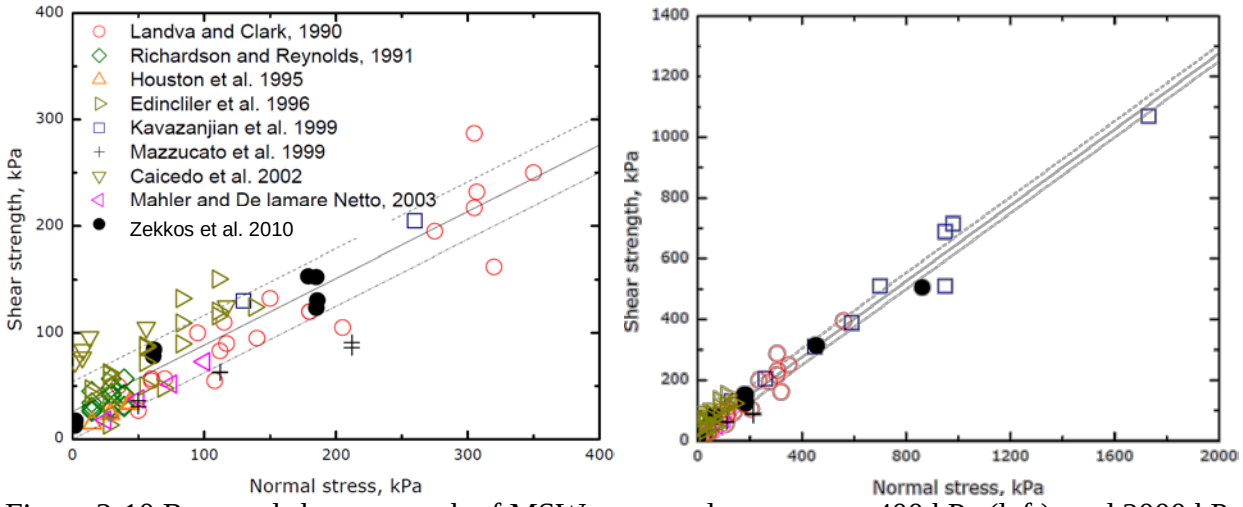

Figure 2-10 Reported shear strength of MSW at normal stress up to 400 kPa (left); and 2000 kPa (right) (Zekkos et al. 2010a).

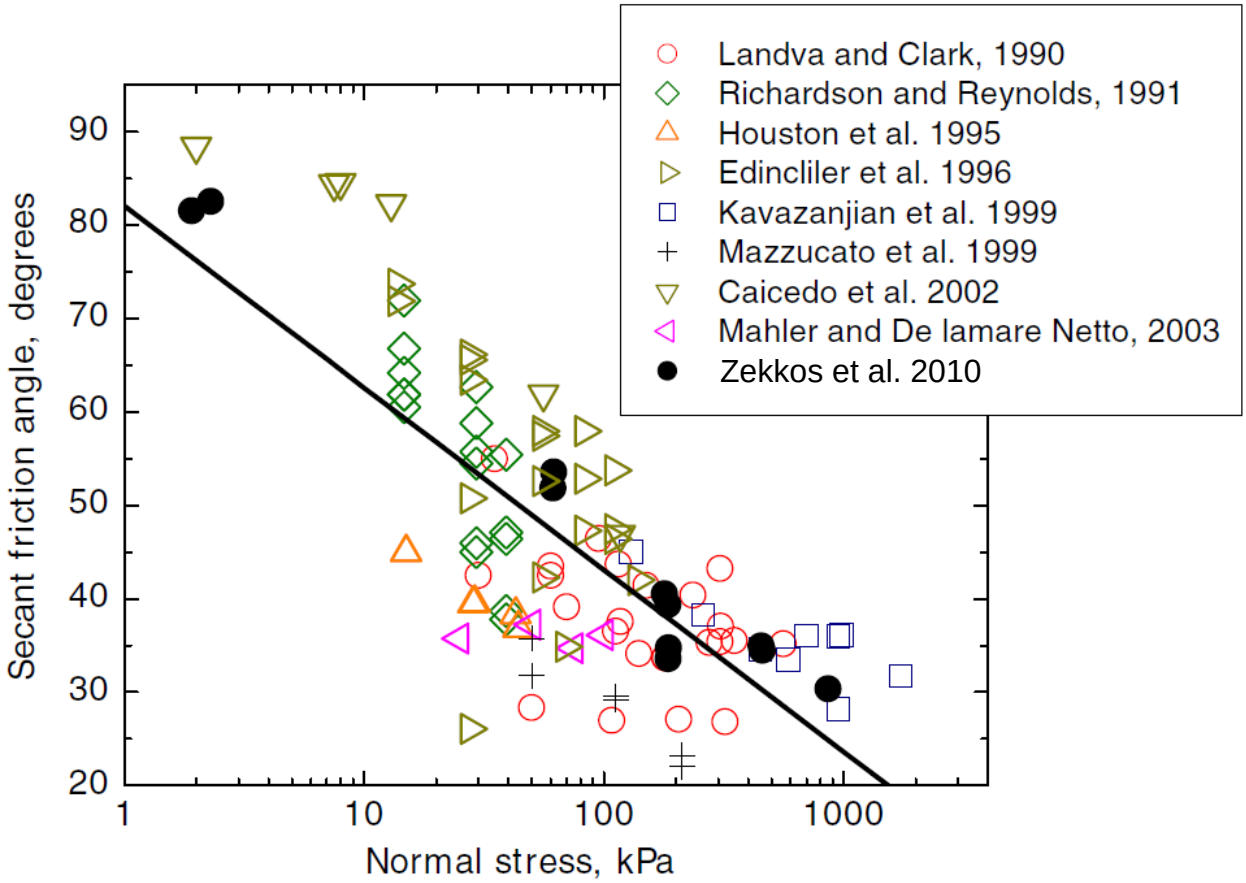

Figure 2-11 Relationship between reported section friction angle of MSW in direct shear testing and applied normal stress (Zekkos et al. 2010a).

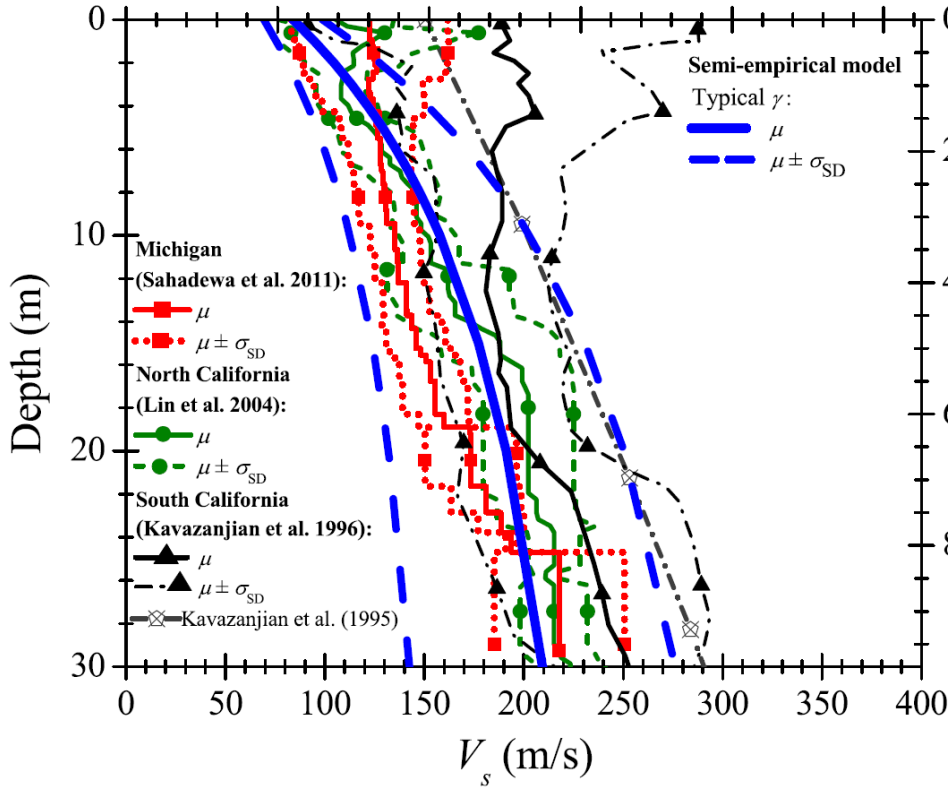

Figure 2-12 Shear-wave velocity profiles at MSW landfills and mean and upper and lower bounds of the semi-empirical model (Zekkos et al. 2014).

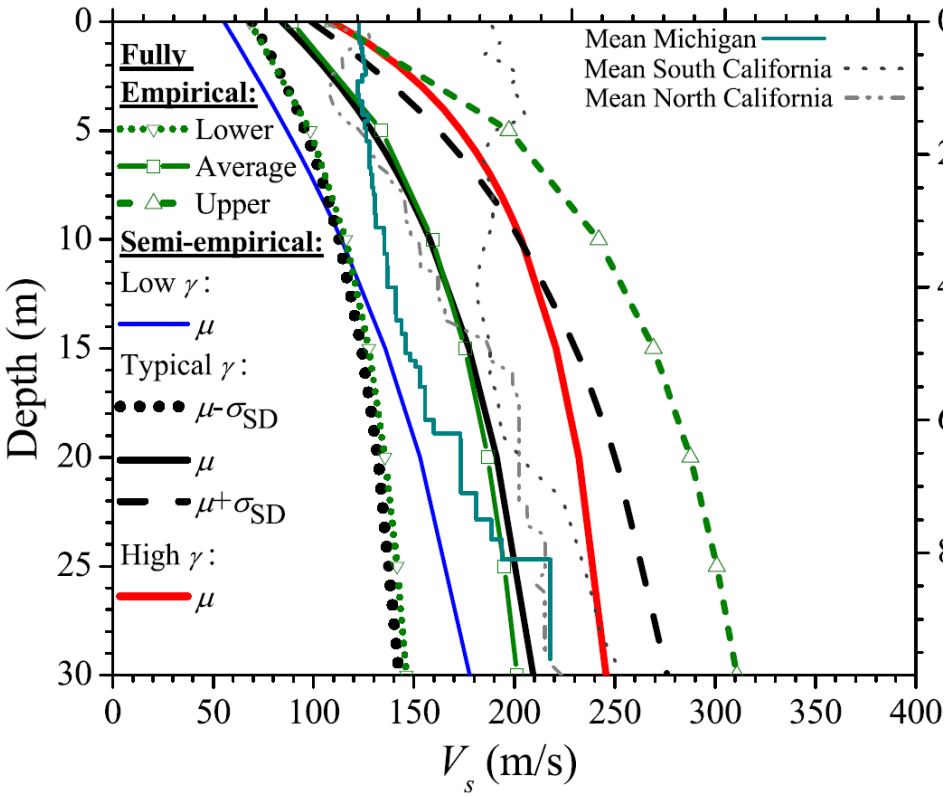

Figure 2-13 Regressed semi- and fully-empirical V_s profiles for MSW in landfills (Zekkos et al. 2014).

PART II LONG-TERM DEGRADATION EXPERIMENTS ON MUNICIPAL SOLID WASTE

Chapter 3 An Experimental Setup for Simultaneous Physical, Geotechnical, and Biochemical Characterization of Municipal Solid Waste Undergoing Biodegradation in the Laboratory

3.1 Abstract

Municipal solid waste (MSW) is biodegradable in landfills under anaerobic conditions. The biodegradation of MSW consists of physical and biochemical processes that affect the geotechnical characteristics of the waste. Laboratory landfill simulators that enable simultaneous characterization of these processes are presented. The simulator configuration, testing procedure, sampling methods, and measurement methods are described. The temporal phases of MSW biodegradation were studied using the experimental setup. Good repeatability of the measurements was demonstrated between duplicate simulators. In addition to data on biogas and leachate samples, a solid waste core sampling technique for retrieving disturbed solid waste samples for chemical and microbial analyses is presented. It was demonstrated that core sampling did not significantly affect simulator operation and measurements. The simulators and sampling methods presented in this study can be used to generate data that will be useful in the development and calibration of comprehensive models for MSW biodegradation in landfills.

Fei, X., Zekkos, D., and Raskin, L. (2014). "An experimental setup for simultaneous physical, geotechnical and biochemical characterization of municipal solid waste undergoing biodegradation in the laboratory." *Geotechnical Testing Journal*, 37(1).

3.2 Introduction

About 250 million tons of MSW are generated in the United States annually and more than half of this waste is landfilled. In 2010, 60% by wet weight of the landfilled MSW consisted of paper, food and yard wastes (EPA 2011). These organic waste fractions are biodegradable under anaerobic conditions in landfills.

Biodegradation of MSW takes place through the metabolic activity of microorganisms and results in changes in mechanical and hydraulic properties of the waste as shown in Figure 3-1 (McDougall 2007). The biodegradable organic waste fractions are degraded by a consortium of anaerobic microorganisms responsible for hydrolysis, acidogenesis, and methanogenesis (Pohland and Kim 2000; Barlaz et al. 2010b). Hydrolysis of the biodegradable organic waste leads to mass loss and void creation in the MSW matrix. As a consequence, physical properties, such as porosity (n) and total unit weight (γ_t) and, by extension, geotechnical properties, such as compressibility and shear strength, change. Hydrolysis of MSW followed by acidogenesis and methanogenesis result in the dissolution of organic compounds in the leachate and the production of biogas consisting primarily of methane (CH_4) and carbon dioxide (CO_2). As a result, the phase relationships between solid, liquid and gas phases within the MSW matrix are altered. Changes in the MSW matrix also result in changes in pneumatic and hydraulic conductivities, respectively, for biogas and leachate generated during biodegradation (Olivier and Gourc 2007; Stoltz et al. 2010b). Biogas and leachate flows distribute substrates for microorganisms and affect local environmental conditions. Microorganisms can also be transported and redistributed by leachate flow (Vavilin et al. 2003). All of the microbial, physical, mechanical, and hydraulic characteristics of MSW are interdependent. Understanding how each of these characteristics changes requires an understanding of the linkages between all of these properties.

In this study, unshredded waste was tested in large duplicate laboratory simulators (0.3 m in diameter and 0.6 m in height) to simulate the biodegradation of MSW in landfills and evaluate repeatability of measurements between the duplicate simulators. Multiple physical (weight, volume, temperature), geotechnical (settlement, total unit weight, porosity, hydraulic conductivity), and biochemical parameters in the leachate (pH, alkalinity, total COD (tCOD)) and the biogas (biogas volume and concentrations of CH_4 and CO_2) were monitored simultaneously, along with microbial analyses (such as DNA concentration measurement, quantitative polymerase chain reaction and pyrosequencing) (Fei et al. 2013) to allow for a comprehensive characterization of MSW biodegradation. The duplicate simulators have been operational for approximately one year and degradation is still ongoing. Multiple tests (porosity and hydraulic conductivity) and microbial analyses are still being carried out and the results will be presented in the future. To our knowledge, no other laboratory experimental study has measured all key physical, geotechnical, microbial, and chemical parameters that are necessary to generate a comprehensive understanding of long-term MSW biodegradation.

3.3 Experimental Apparatus

3.3.1 **Simulator Configuration**

Two laboratory simulators (simulator A and B) were designed and constructed in the Geoenvironmental Engineering Laboratory at the University of Michigan (Figure 3-1). Simulator A was made of poly-(methyl-methacrylate) (PMMA) and simulator B was made of glass to assess any potential long-term leakage through the materials. Simulator A included two temperature sensors, whereas simulator B included five sampling ports. The two simulators were identical in all other aspects.

Each simulator consisted of a waste column, a heating blanket, a weighing scale, a leachate tank, a leachate recirculation and sampling system, a biogas collection and sampling system, transducers, and a data acquisition system. The waste column had a diameter of 0.3 m, a height of 0.6 m and a volume of 42 L. Two PMMA or stainless steel (SS) caps were clamped by SS rods on both ends of the waste columns of simulator A and B, respectively. The contact surface between the column and the caps were sealed by rubber gaskets.

A heating blanket was wrapped around the waste column to maintain a specimen temperature of 40±3 ^{0}C. This temperature was selected based on the reported optimal temperature for growth of mesophilic methanogens (Zinder 1993). A narrow "window" of the waste column was not covered by the heating blanket to allow for visual inspection of the waste specimen and the leachate level during recirculation. For simulator B, five 2.5-cm (1") diameter sampling ports were installed in the "window" area along the height of the column for core sampling of solid waste. They were plugged with rubber stoppers and sealed using vacuum grease when not in use. The simulator was placed on the weighing scale (0.01 kg resolution) and the total weight was read from the scale screen.

A drainage valve was installed on the bottom cap and was connected to the leachate tank via flexible tubing. The leachate tank was assembled with a PMMA column and two PMMA caps clamped together by SS rods and sealed with rubber gaskets. A magnetic stirrer was placed at the bottom of the leachate tank to allow for complete mixing of the collected leachate. A sampling port was installed in the lower part of the leachate tank column. A peristaltic pump delivered leachate from the tank to the top of the waste column.

The pump was connected to the inlet of a SS pipe with flexible tubing. The pipe was screwed into a perforated leachate distribution plate placed on top of a 25-mm layer of gravel

above the waste specimen to uniformly distribute the recirculated leachate. The pipe went through an opening on the top cap of the waste column without contacting the cap, allowing the plate and the pipe to settle with the waste specimen in vertical direction without any side friction. The opening between the top cap and the pipe was sealed using a Neoprene membrane sleeve fixated on the pipe by O-rings. Another 25-mm layer of gravel and a non-woven geotextile were placed at the bottom of the waste specimen to prevent wash-out of large waste particles from the waste column through the drainage valve. The geotextile was obtained from a manufacturer and cut to a 5 cm by 5 cm square piece. Alternatively, a detachable chamber can be used that allows flow through geotextile over the entire diameter of the specimen. This facilitates inspection of the geotextile for physical and biological clogging during the process of degradation (results will be presented in the future).

A gas sampling port sealed with a nitrile rubber septum was installed on the top cap to allow for direct biogas sampling from the waste column headspace. Generated biogas was collected in a gas sampling bag connected to the top cap with flexible tubing. Two gas vents from the headspaces of the waste column and the leachate tank were connected to the gas sampling bag to equalize gas pressure throughout the simulator. A gas pressure gauge was connected to the waste column headspace to monitor excessive biogas accumulation.

A cable extension transducer was positioned above the simulator and the cable was fixated to the SS pipe. Continuous settlement data were recorded using a data acquisition system. A temperature transducer was placed in the MSW specimen at the center of simulator A to continuously measure the waste temperature. Another temperature transducer tracked temperature between the heating blanket and the waste column of simulator A. The heating blanket was controlled by a third independent internal temperature sensor inserted between the

blanket and the waste column A. There was no feedback control loop between the temperatures of the waste and the heating blanket. Control of the heating blanket of simulator B was based on the readings from simulator A, since simulator configurations and environmental conditions were identical for the two simulators.

3.3.2 **Solid Waste Core Sampling Apparatus**

A double-tube coring apparatus was designed and utilized to collect disturbed solid waste samples (Figure 3-2). Both tubes were made of SS and marked with length grades. The outer coring tube was 30 cm (12”) in length, 1.1 cm (7/16”) in diameter, and was serrated on one end. The inner coring tube was 45 cm (18”) in length, 0.9 cm (6/16”) in diameter, and was sharpened on one end. The diameters of the inner and outer coring tubes were selected to be close, so that the tubes can move independently from each other while minimizing the space in between. The inner coring tube was 6” longer than the outer one to provide access clearance to a hand-held power drill.

3.4 Experimental Procedure

3.4.1 **Specimen Preparation**

Three month old MSW was excavated from a landfill in Austin, Texas, and was shipped to the laboratory in sealed drums. A total of 600 kg of waste was characterized according to the characterization procedures recommended by Zekkos et al. (2010b). Briefly, waste was segregated to coarser and finer fractions using a 20-mm sieve. The coarser fraction (>20 mm material) was manually separated into different waste categories. On the basis of this characterization, two piles of approximately 35-kg waste were prepared separately with 74.5% by weight <20 mm material, 15.0% paper, 5.5% soft plastic and 5.0% wood and mixed

manually. Average moisture content of the <20 mm material was 26.5% (dry basis) and volatile solid content was 7% (APHA 2005). The waste particles were not milled or in any other way processed, although oversized waste constituents, i.e., constituents larger than 1/3 of the waste column diameter (0.1 m), were not included. Paper and plastic with largest dimensions as high as 1/3 of the simulator diameter were included, because these constituents were flat, soft and flexible. Each pile of waste was placed into a simulator manually with minimal compaction. The initial waste specimen heights (H_0) were 0.525 m and 0.517 m for simulators A and B without the gravel layers, respectively. The corresponding initial specimen weights were 30.0 kg and 29.3 kg, and the initial total unit weights were both 7.9 kN/m^3. No external vertical load was applied to the specimen except for the overlying 25-mm gravel layer, the leachate distribution plate and the SS pipe. The total weight of these items was about 5 kg, equivalent to an applied vertical stress that was less than 1 kPa.

3.4.2 **MSW Biodegradation Test**

The simulators were sealed after the waste specimens were loaded on day 1. On day 12, additional moisture and external heating were applied to maintain a waste temperature of 40±3 □C and accelerate MSW biodegradation. 20.5 L of deionized water was added to each leachate tank. Before each recirculation, the total weight, settlement, and temperature of waste were recorded. The leachate drainage valve below the specimen was closed and deionized water or leachate was pumped to the inlet of the SS pipe at a rate of about 350 ml/min (21 L/h). The pump was stopped when the leachate level reached the bottom of the leachate distribution plate (i.e., top of the upper gravel layer) based on visual inspection. The specimen was allowed to be submerged in leachate for 10 minutes so that trapped gas bubbles could escape from the waste matrix. More leachate was recirculated as necessary until the leachate level reached the bottom

of the top plate again. Generally, up to 0.3 L of additional leachate was needed to fill the voids of expelled gas to “saturate” the specimen. Note that the term “saturated” is used loosely since back-pressure saturation was not feasible and the B-value was not measured. Total weight, settlement, and temperature at the saturation state were recorded, and then leachate was drained. These readings were recorded several more times between recirculations. Collected leachate was thoroughly mixed for 10 minutes using the magnetic stirrer each time before recirculation and was recirculated three times a week throughout the test period. Data from the operation of the duplicate simulators for a year are presented.

3.4.3 **Sampling of Biogas, Leachate and Solid Waste**

Triplicate biogas samples from the waste column headspace were taken immediately before leachate recirculation using a gas tight syringe. Gas composition was measured three times a week until day 100, and once per week thereafter.

A completely mixed leachate sample was collected from the leachate tank about 1 hour after the leachate started draining from the waste column. Leachate was sampled three times a week until day 100, and once per week thereafter.

Solid waste was cored seven times from simulator B on day 47, 82, 111, 142, 179, 211 and 310. The core sampling technique is illustrated in Figure 3-2a. Both coring tubes were sterilized by histological grade ethanol before coring. The outer coring tube was inserted through the sampling port first and was aligned with the inside perimeter of the waste column. The inner coring tube was attached to the hand-held power drill and was slid through the outer coring tube (Figure 3-2a-1). The inner coring tube was driven into the waste specimen by power drill for about 2 to 3 cm (Figure 3-2a-2). Then the outer coring tube was manually pushed into the waste specimen for about the same distance while keeping the inner coring tube in place (Figure 3-2a-

3). Subsequently, the inner coring tube was pulled out from the specimen slowly while keeping the outer coring tube in place (Figure 3-2a-4). The cored solid waste inside the inner coring tube was retrieved by a sterilized spatula and stored in a sterile tube (Figure 3-2b and Figure 3-2c). The process was repeated until inner coring tube penetrated approximately 4/5 of the waste column diameter (0.24 m). Both coring tubes and the spatula were sterilized by ethanol again before sampling from the next port. Solid wastes sampled from different ports were stored in separate tubes at -80 ˚C. The samples were subsequently subjected to DNA extraction and microbial ecology analysis.

3.4.4 **Measurements and Calculations**

The biogas composition was measured by a gas chromatograph equipped with Thermal Conductivity Detector using nitrogen as carrier gas. Means and standard deviations of the CH_4 and CO_2 concentrations of triplicate samples were calculated. The volume of generated biogas was measured by a mass flow meter and was adjusted to standard temperature and pressure. The volume of generated CH_4 (V_{CH4}) was calculated as the product of the CH_4 concentration and the volume of biogas. Leachate samples were analyzed for pH, alkalinity and total chemical oxygen demand (tCOD) according to standard methods (APHA 2005).

The total weight readings of the simulators were tracked between recirculations. Total weights of the specimen at saturation state ($W_{t,sat}$) and after gravity drainage, i.e., at field capacity state ($W_{t,fc}$), as shown in Figure 3-3, were calculated by subtracting the weight of the simulator and gravel from the total weight of the simulator. The height of the specimen (H_t) was calculated by subtracting the settlement from H_0. There was no difference in the speicmen height at the field capacity state immediately before recirculation and at the subsequent saturation state. The total volume and total unit weights at the two states ($\gamma_{t,sat}$ and $\gamma_{t,fc}$) were calculated

accordingly. The recorded waste temperatures were averaged every 5 days and the standard deviations were calculated.

The strain of the specimen, in percent, was defined as the specimen settlement divided by H_0:

$$\varepsilon = \frac{settlement}{H_0} \times 100\% \tag{3-1}$$

The long-term compression ratio (C_{LT}) was calculated according to Eqn. 3-2 :

$$C_{LT} = \frac{\frac{H_{t2}-H_{t1}}{H_0}}{\log(t_2)-\log(t_1)} \tag{3-2}$$

where H_{t1}, H_{t2} are the specimen heights for two measurements over a period of time between t_1 and t_2. The period was selected as one day to calculate daily $C_{LT,i}$ with i being the elapsed time in days (i=1, 2, 3…). A simple moving average (SMA) of $C_{LT,i}$'s was calculated for a period of 15 days ($C_{LT15,j}$) per Eqn. 3-3:

$$C_{LT15,j} = \frac{C_{LT,i}+C_{LT,i+1}+\cdots+C_{LT,i+13}+C_{LT,i+14}}{15} \tag{3-3}$$

where j=i+7. The first $C_{LT15,j}$ value was plotted on day 8, which was halfway of the first 15-day period (j=8, 9, 10…) .

3.5 Experimental Results

3.5.1 **Total Weights**

Initial total weights of the specimens were 30.0 kg and 29.3 kg for simulator A and B, respectively. Initial saturation by deionized water on day 12 increased the total weights to 47.4 and 45.5 kg, respectively. The total weights at subsequent saturation states decreased to 41.4 kg and 39.4 kg by day 50, and 38.9 kg and 37.7 kg by day 350, respectively. When the leachate was drained after initial saturation, total weights at field capacity were 36.0 kg and 35.5 kg. The values decreased slightly to 35.3 and 34.7 kg by day 350 (Figure 3-4).

3.5.2 **Strain**

After initial moisture addition and leachate drainage on day 12, strains of both specimens increased linearly with logarithmic time. By day 350, 14.0% and 12.4% strains were observed in simulators A and B, respectively. Core sampling of MSW did not appear to affect strains in simulator B (coring times indicated by squares in Figure 3-5).

3.5.3 **Total Unit Weight**

Initial total unit weights of both specimens at field w_c were 7.9 kN/m^3. The first $\gamma_{t,sat}$ were 12.6 kN/m^3 and 12.1 kN/m^3, respectively. The values decreased to the minimum of 11.7 kN/m^3 and 11.1 kN/m^3 by day 40, then increased to 12.0 kN/m^3 and 11.5 kN/m^3 by day 350. After initial moisture saturation and leachate drainage, $\gamma_{t,fc}$ of both specimens were 9.3 kN/m^3. They increased to 10.8 kN/m^3 and 10.5 kN/m^3 by day 350 (Figure 3-6). Although both weight and volume of the specimens decreased over time, volume reduction was faster than weight reduction. As a result, total unit weights at both states increased.

3.5.4 **Long-Term Compression Ratio**

Initial C_{LT} values prior to recirculation (day 1 through day 12) were 0.023 and 0.046 for simulators A and B, respectively. They both increased significantly to 0.13 around day 50 and remained above 0.08 until day 80. The values decreased to 0.071 and 0.065 by day 200. Between day 205 and day 225, the maximum C_{LT15} values of 0.175 and 0.166 were observed, in response to an increase of $T_{blanket}$ to maintain a constant waste temperature. C_{LT15} values on day 343 were 0.049 and 0.035 for the last 15-day period (Figure 3-7).

3.5.5 **Biogas Composition**

Time-series biogas compositions of both simulators followed similar trends as illustrated in Figure 3-8. CO_2 concentrations decreased from 65% and 73% at the start of operation to around 45% by day 30. During the same time period, CH_4 concentrations rose from nearly 0% to 60% by day 30. The compositions of both CH_4 and CO_2 showed a gradual change until around day 250 and a more abrupt change afterward. This suggested low biogas generation rate and intrusion of air due to occasional simulators maintenance and tubing changes after day 250.

3.5.6 **Cumulative volume of CH_4**

A total of 483 L and 475 L of CH_4 were generated by simulators A and B by day 350, which were equivalent to 16.1 L and 16.2 L CH_4 per kg of initial total waste mass, respectively (Figure 3-9). V_{CH4} increased rapidly from the start of operation to around day 50. CH_4 generation slowed down between day 50 and day 100 and the V_{CH4} curves approached the final values gradually afterward.

3.5.7 **pH of Leachate**

The leachate was not buffered by chemical addition throughout the test period. The initial leachate pH was 6.0 for both simulators. Maximum pH values between 6.8 and 7.0 were

measured between day 40 and day 70. The values fluctuated between 6.5 and 6.7 after day 100 (Figure 3-10).

3.5.8 **Alkalinity of Leachate**

The alkalinity of leachate increased from about 1,000 mg/L $CaCO_3$ to the maximum of 2,000 mg/L $CaCO_3$ and 3,000 mg/L $CaCO_3$ for simulators A and B, respectively, shortly after leachate recirculation started on day 12. Stable leachate alkalinity concentrations between 1,000 and 1,200 mg/L $CaCO_3$ were observed for both simulators after day 50 (Figure 3-11).

3.5.9 **Total Chemical Oxygen Demand**

The maximum tCOD values were measured on day 18 and day 25 at 5,543 mg/L and 5,673 mg/L for simulators A and B, respectively, as shown in Figure 3-12. Both tCOD concentrations decreased to less than 2,000 mg/L by day 50. Stable residual concentrations of less than 1,000 mg/L were reached by day 150.

3.6 Discussion of the Data

3.6.1 **Phases of MSW Biodegradation**

Three consecutive phases of MSW biodegradation were identified based on the trends of physical and chemical measurements of the current duplicate simulators. Briefly, the microorganisms were adapting to anaerobic conditions in the first phase, they were the most active in the second phase, and exhibited significantly lower activity in the last phase.

The first phase took place between the initial leachate recirculation on day 12 and the initiation of active methanogenesis around day 20 and 30. In this phase, around 2.5% strain of the specimen was observed, mainly due to physical mechanisms such as waste particle softening and particle raveling. C_{LT15} values during that period were low (Bjarngard and Edgers 1990; Edil et al. 1990; McDougall 2011). $W_{t,sat}$ decreased due to the reduction of available voids volume for

leachate in the specimen. On the other hand, $W_{t,fc}$ only decreased slightly, because the mass loss of hydrolyzed solid waste was largely compensated by the leachate retained in the specimen at field capacity state. Due to these volume changes, $\gamma_{t,sat}$ decreased while $\gamma_{t,fc}$ increased. All leachate properties, i.e., pH, alkalinity and tCOD, increased from their initial values. Because of the high alkalinity, the pH of the leachate was above 6 at all times. Initial acidification of the leachate, as reported in other studies (Wang et al. 1994; Bareither et al. 2012d), did not occur. Although the pH was sub-optimal for methanogens, the microorganisms were able to sustain MSW biodegradation without observable inhibition. Increases in tCOD concentration indicated hydrolysis and wash-out of the waste.

Active methanogenesis of the specimen initiated in the beginning of the second phase between day 20 and day 30, when the dominant biogas component shifted from CO_2 to CH_4 and the biogas composition remained stable afterward. The phase was also characterized by rapid accumulation and removal of tCOD in the leachate until around day 100, indicating rapid hydrolysis and consumption of biodegradable MSW by microorganisms. Similar to the trend of tCOD, pH and alkalinity of leachate reached maximum and dropped to stable residual values. As a result, $W_{t,fc}$ and $W_{t,sat}$ decreased and strain increased. Total unit weights appeared to increase, indicating that the specimen volumes reduced faster than specimen total weights. C_{LT15} exceeded 0.1, which is a typical value observed in the long-term compression of MSW undergoing biodegradation (Fei and Zekkos 2013), and started to decline.

The last phase of MSW biodegradation took place after approximately day 100 when intensive biodegradation was largely completed. tCOD concentration decreased at much slower rates, and stable residual concentrations were reached around day 200. C_{LT15} decreased gradually while $\gamma_{t,sat}$ and $\gamma_{t,fc}$ kept increasing, indicating densification of the specimens.

3.6.2 **Repeatability of Simulator Results**

High repeatability between physical, geotechnical and chemical measurements of the duplicate simulators was observed. The relatively small variations in $W_{t,fc}$, $W_{t,sat}$, $\gamma_{t,fc}$, $\gamma_{t,sat}$ and ε values between simulators were likely caused by small variations in initial waste conditions introduced during specimen preparation. The almost identical trends in measurements of biogas and leachate properties, and C_{LT15} between simulators indicated similar progress of long-term MSW biodegradation in the duplicate simulators. Overall, the experimental setup appeared to yield repeatable results under the same initial and operational conditions.

3.6.3 **Influence of Core Sampling on Measurements**

Variations between ε and C_{LT15} of the duplicate specimens were not influenced by core sampling. The fourth core sampling on day 142 was carried out less carefully, possibly contributing to C_{LT15} around day 150 being elevated. Except for this core sampling, other core samplings did not result in a significant increase of C_{LT15} in simulator B, although localized disturbance of the specimen may be introduced. Total mass loss due to core sampling of solid waste from all sampling ports was less than 50 g each time, so the measurement of total specimen weight was not affected. No abrupt change of strain was observed after core sampling, thus the total unit weights were not affected either. Measurements of biogas and leachate properties were not disturbed following core sampling.

Some high C_{LT15} values measured after the active biodegradation phase were introduced by other disturbance events. For example, high C_{LT15} of simulator B around day 180 was due to the repeated raising and lowering of the SS pipe when the Neoprene membrane fixated on it was replaced. A series of high C_{LT15} values of both simulators after day 200 were due to the increase of $T_{blanket}$ and possible waste column expansion. Temperature changes have been shown to affect

MSW biodegradation (Meima et al. 2008; Bareither et al. 2012d). However the duplicate specimens had been largely biodegraded when $T_{blanket}$ was raised. Therefore besides short-term increases of strain and C_{LT15}, other measurements were not affected.

3.6.4 **Implication of Measurements to Modeling**

Several mechanistic models describing MSW biodegradation processes have been developed (Vavilin et al. 2003; Beaven 2008; Gawande et al. 2010; McDougall 2011). However, there is a lack of comprehensive datasets to validate and calibrate such models. Datasets of Barlaz et al. (1989) and Ivanova et al. (2008b), among a few others, have been used. This study generated a unique dataset comprising of simultaneous and repeatable physical, geotechnical and chemical measurements of MSW biodegradation tests in laboratory simulators. The dataset can be valuable to parameterizations and validations of existing models and developments of new models.

3.7 Conclusions

An experimental setup was developed to study MSW biodegradation under anaerobic landfill conditions. Simultaneous measurements of physical, geotechnical, and chemical characteristics were collected and time-series sampling of biogas, leachate and solid waste were conducted.

Three sequential MSW biodegradation phases were observed during the test and were characterized by measurements in the solid, gas and liquid characteristics. Changes of leachate and biogas properties occurred mostly in the transition and the active biodegradation phases. Changes of physical and geotechnical properties were observed throughout these phases and continued in the last phase.

The current simulator configuration yielded repeatable results. The solid waste core sampling technique was applied and observable disturbance was avoided, probably due to the small volume of the core samples. The technique enabled time-series solid waste sampling from the same simulator for microbial analyses undergoing long-term biodegradation. There was no obvious difference between the performance of PMMA and glass as waste column materials.

3.8 Figures

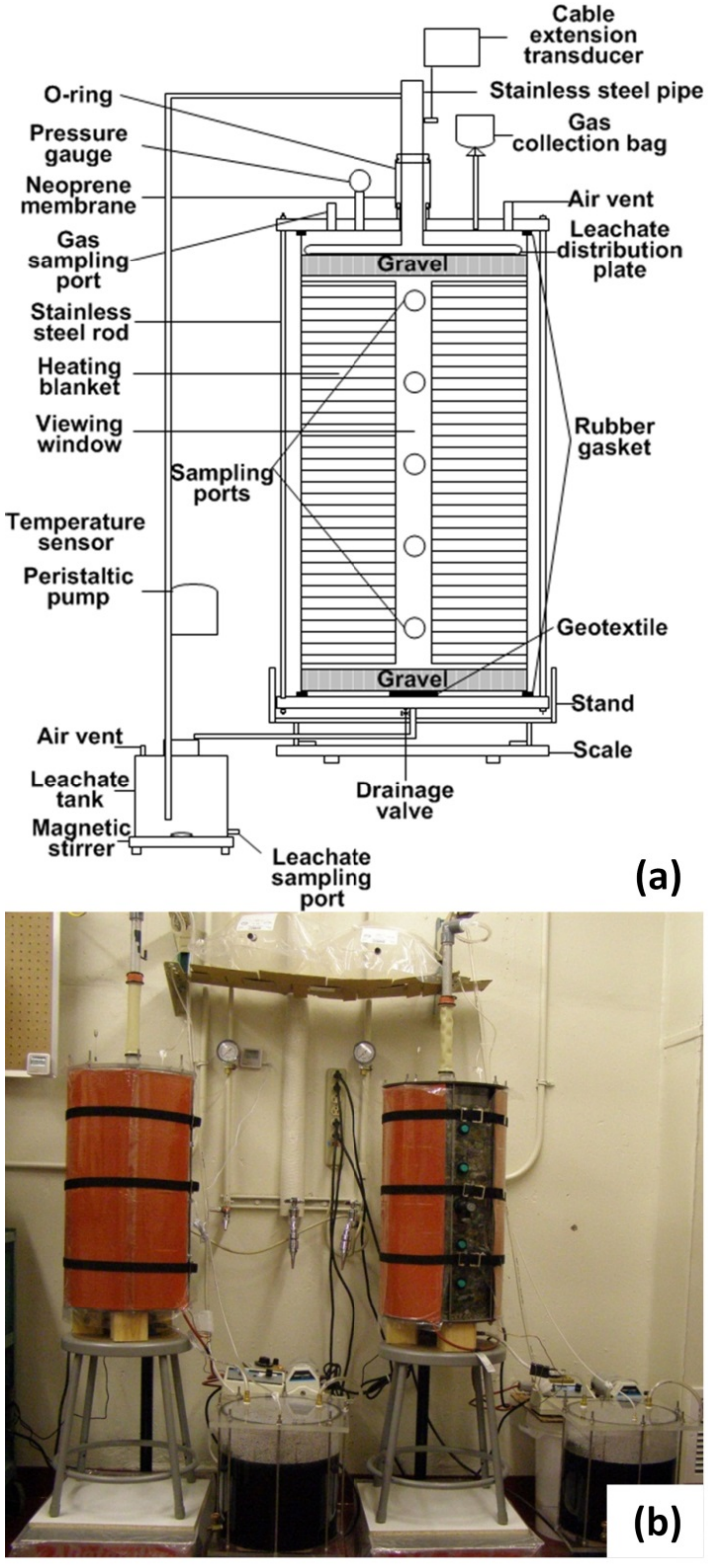

Figure 3-1 (a) Schematic of simulator B and (b) photo of the duplicate simulators (simulator A on the left, simulator B on the right).

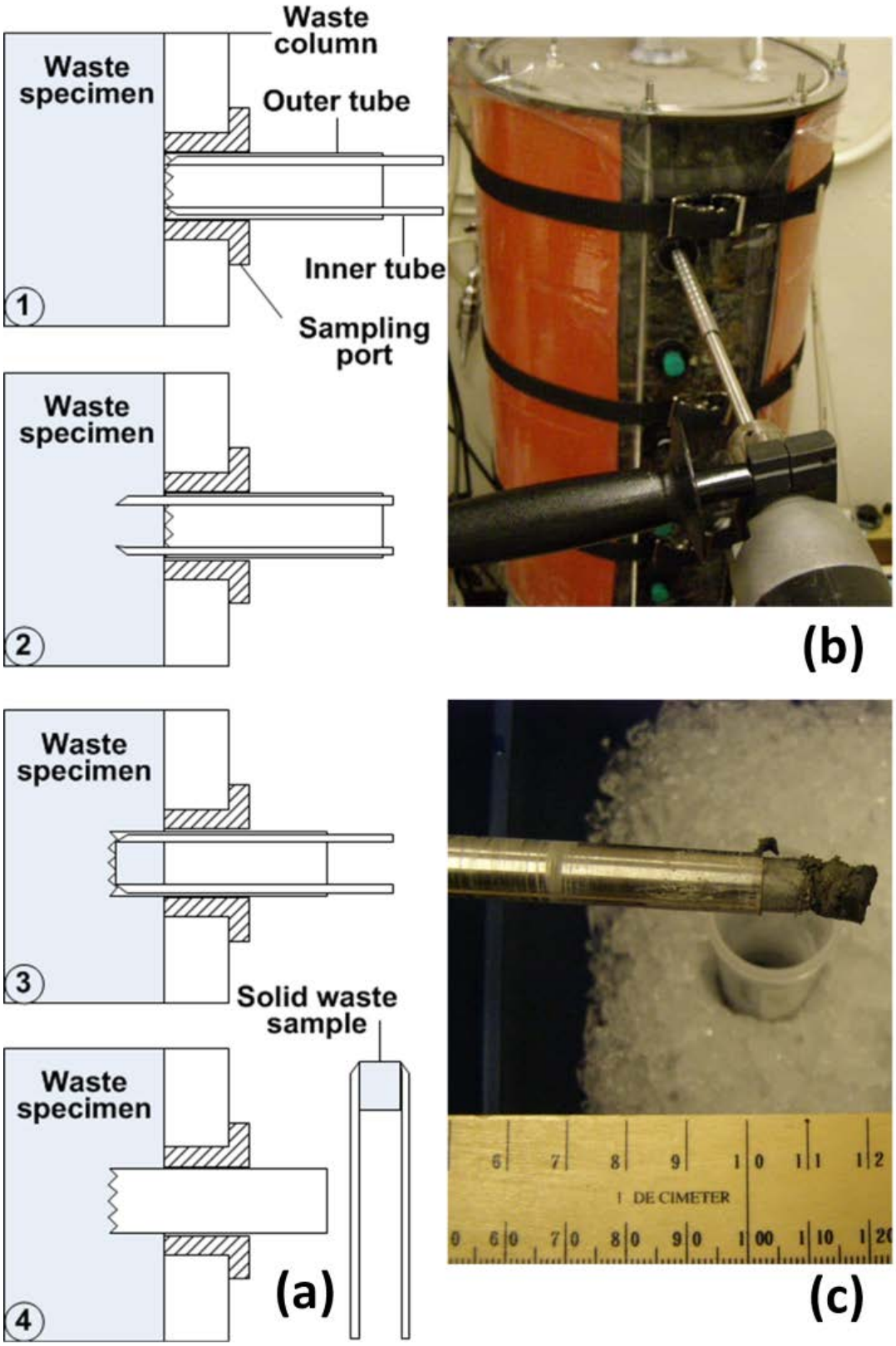

Figure 3-2 Solid waste core sampling technique (a): step-by-step illustrations; (b): photo of core sampling; and (c): cored solid waste sample.

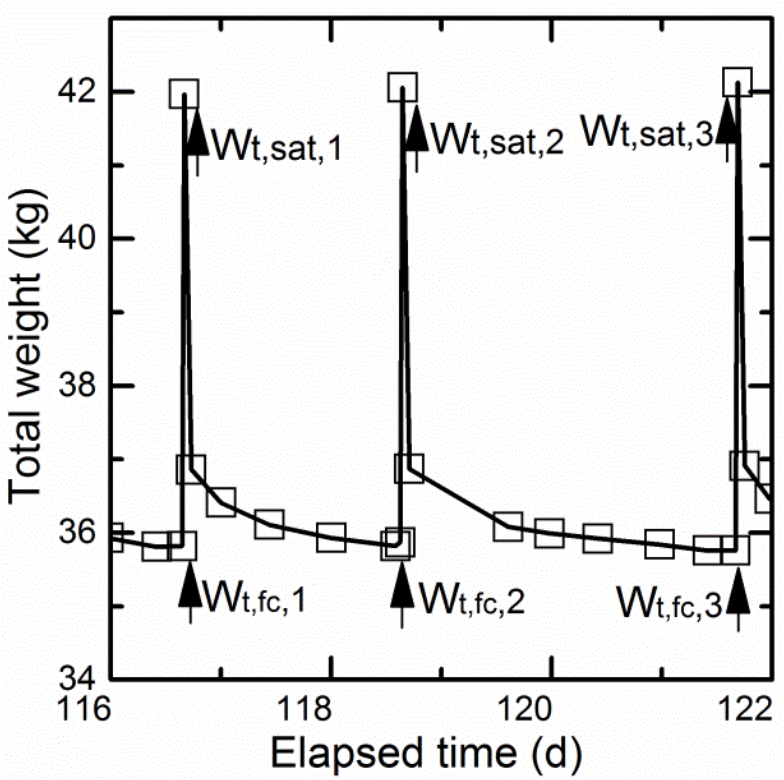

Figure 3-3 Excerpt of specimen total weight profile at saturation and field-capacity states.

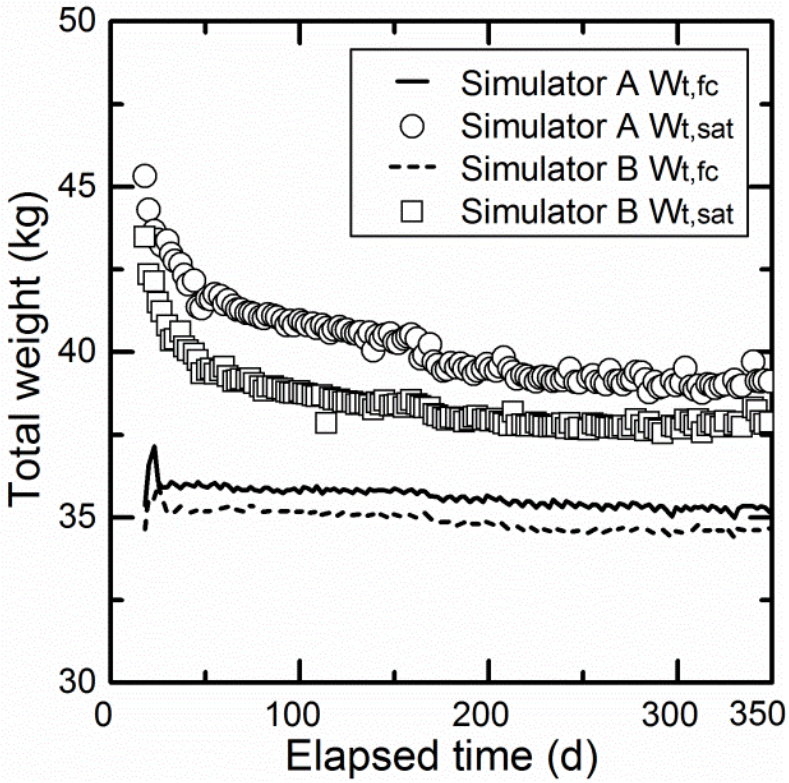

Figure 3-4 Total weights (W_t) of the specimens at saturation and field capacity states.

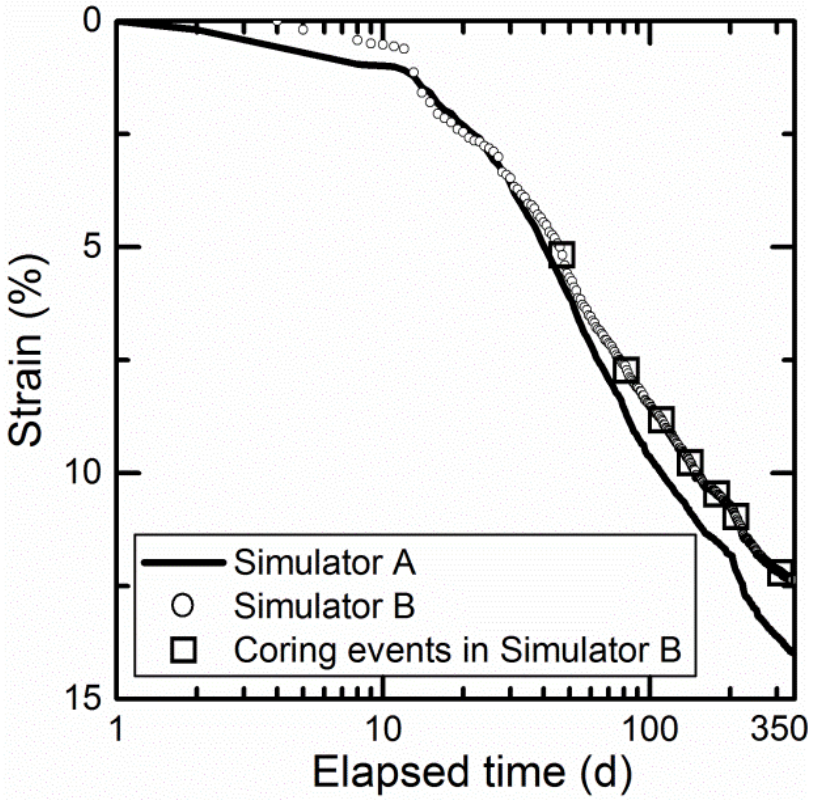

Figure 3-5 Semi-logarithmic plot of the specimen strains (ε).

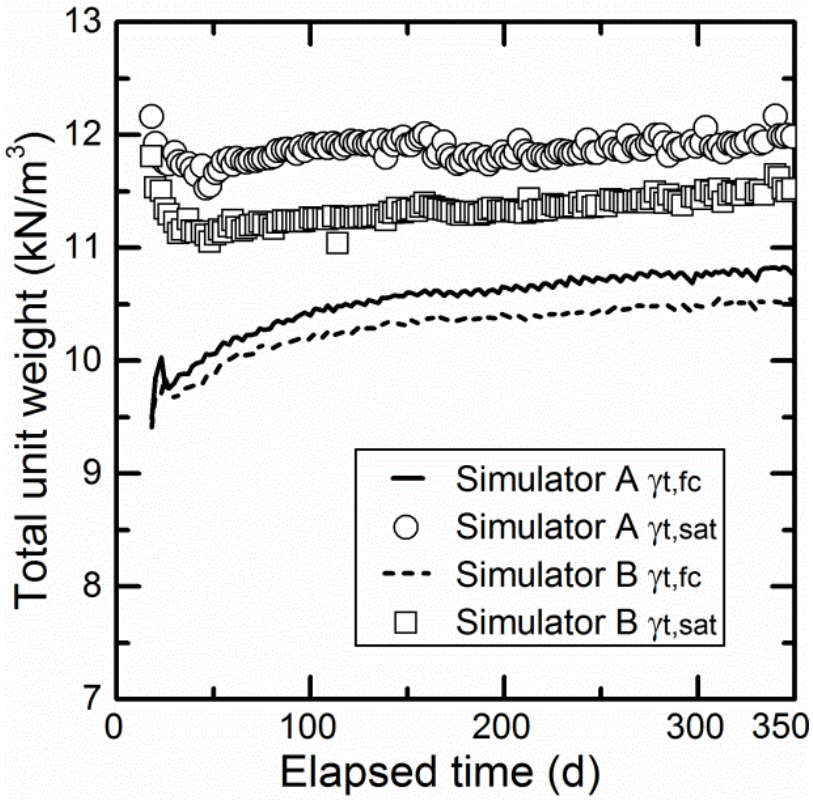

Figure 3-6 Total unit weights (γ_t) of the specimens at saturation and field capacity states.

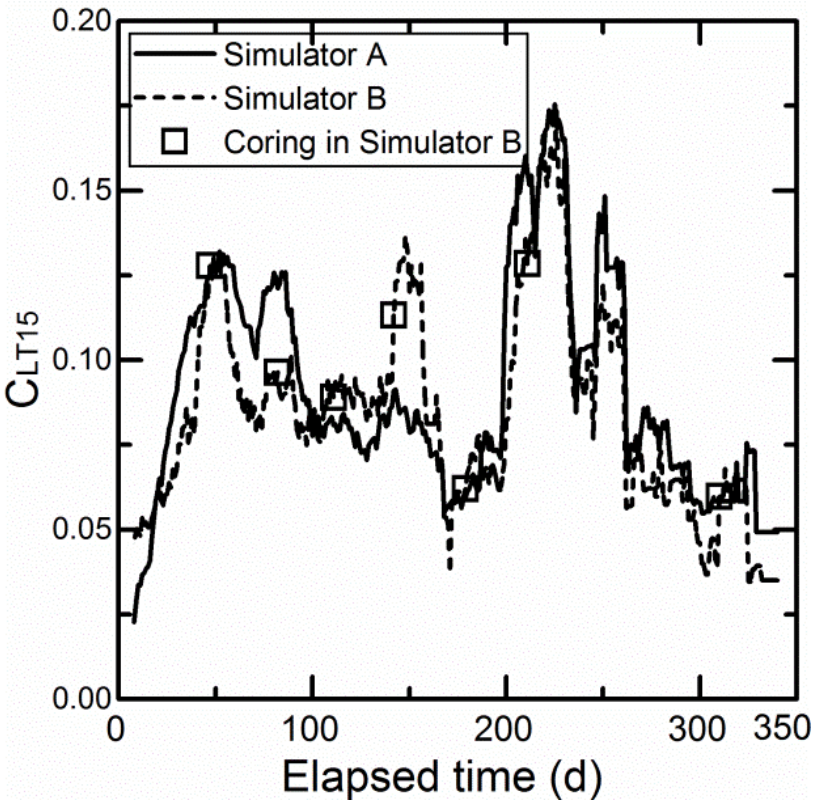

Figure 3-7 Fifteen-day simple moving average long-term compression ratios of the specimens.

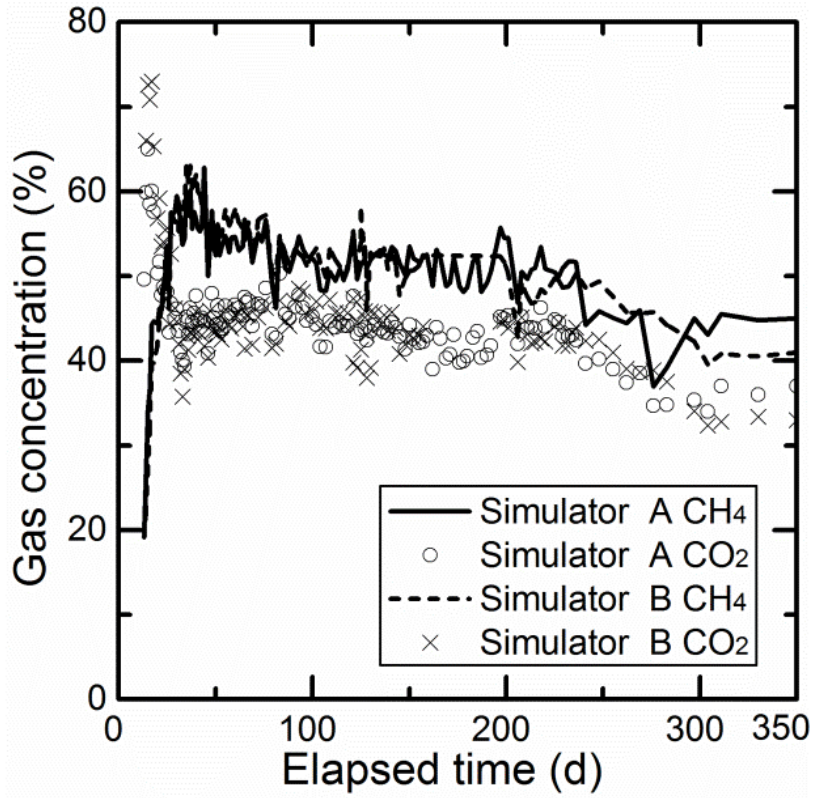

Figure 3-8 CO_2 and CH_4 concentrations in biogas of simulators A and B.

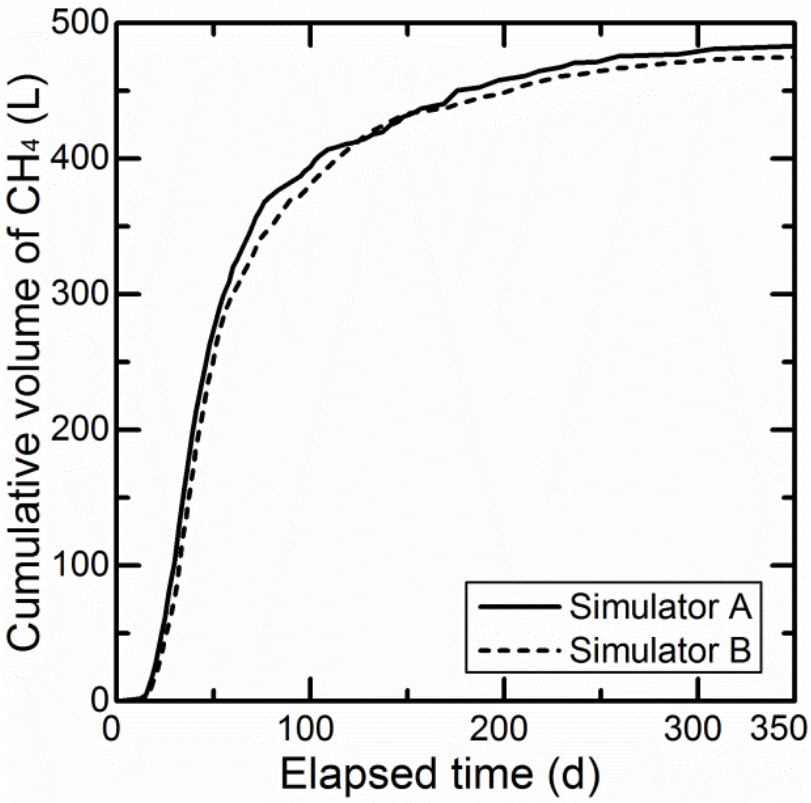

Figure 3-9 Cumulative volume of CH_4 (ΣV_{CH4}) produced by simulators A and B.

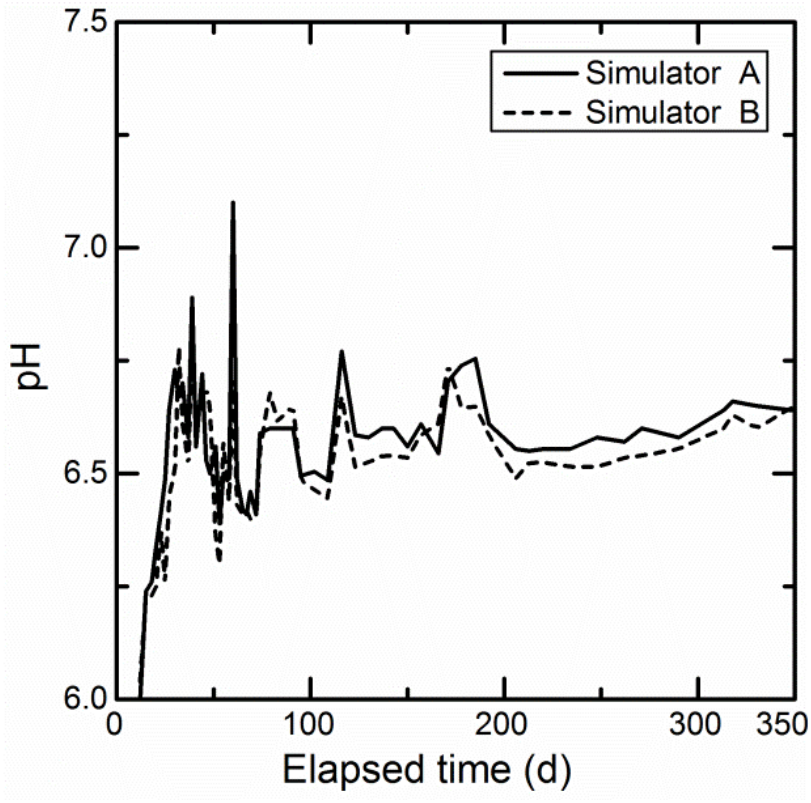

Figure 3-10 pH of leachate for simulators A and B.

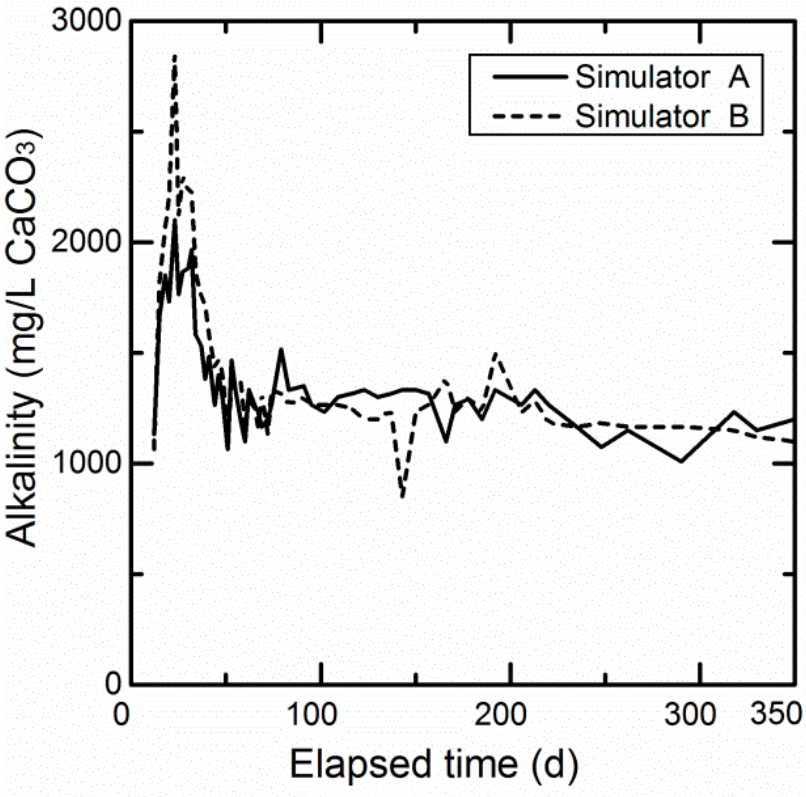

Figure 3-11 Alkalinity of leachate for simulators A and B.

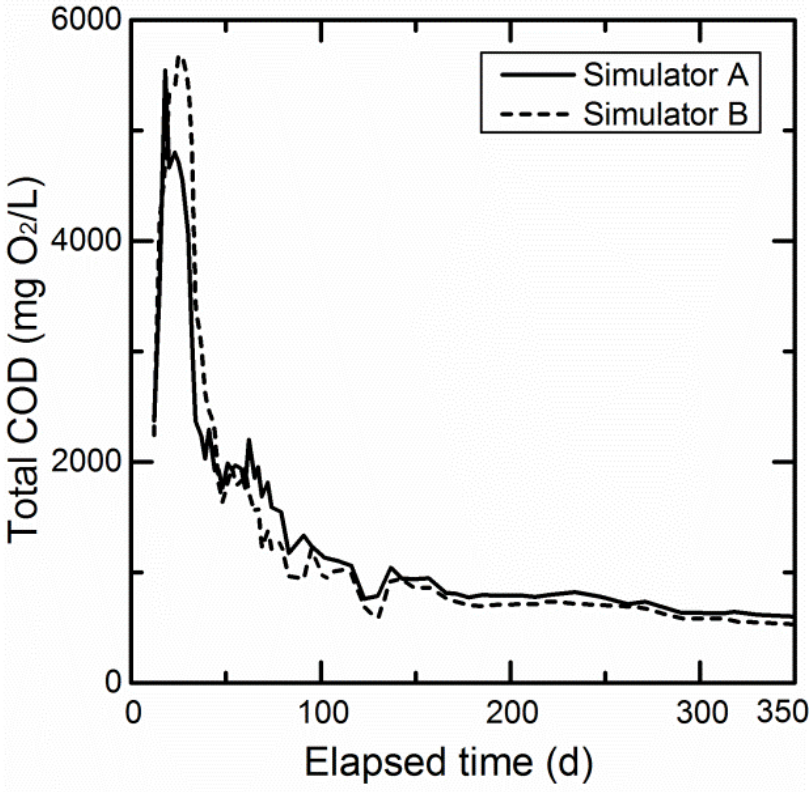

Figure 3-12 Total chemical oxygen demand (tCOD) of leachate for simulators A and B.

Chapter 4 Experimental Assessment of Biochemical-Physico-Hydro-Mechanical Characteristics of Municipal Solid Waste Undergoing Degradation

4.1 Abstract

Seven large-size municipal solid waste (MSW) specimens having variable initial waste compositions were degraded in laboratory simulators under enhanced biodegradation conditions to investigate changes in the biochemical-physico-hydro-mechanical characteristics of solid waste, leachate and biogas during degradation. The trends with time among various characteristics were systematic and inter-related. Removal of soluble compounds in leachate and methane (CH_4) generation from waste stopped after around 300 days. Changes in vertical strain, total unit weight and volumetric moisture content of waste continued in decreasing rates even after 1,000 days. CH_4 generation potential (L_0) of the waste is dependent on the percentage of biodegradable waste prior to degradation (B_0). Maximum CH_4 generation rate ($_{rCH4,max}$) increases with increasing L_0 and maximum soluble chemical oxygen demand in leachate. Final strain of waste due to biodegradation ($\varepsilon_{B,f}$) increases with increasing B_0 and L_0. Maximum long-term compression ratio increases with increasing $\varepsilon_{B,f}$ and $_{rCH4,max}$. The submerged and field capacity total unit weight and volumetric moisture content of waste are also dependent on the initial composition and strain of waste. The hydraulic conductivity of the specimens decreased

Fei, X., Zekkos, D., and Raskin, L. (2016). "Experimental assessment of physico-biochemical-hydro-mechanical characteristics of municipal solid waste undergoing degradation." *Journal of Geotechnical and Geoenvironmental Engineering*, (under review).

during waste degradation. The trends and correlations presented in this study improve the understanding of coupled processes during MSW degradation under enhanced conditions.

4.2 Introduction

Municipal solid waste (MSW) disposed of in modern Subtitle D and bioreactor landfills degrade with time due to biochemical-physico-hydro-mechanical processes. Biochemically, anaerobic biodegradation of biodegradable solid waste consists of four steps, disintegration, hydrolysis, fermentation, and methanogenesis (Batstone 2002). Large-size biodegradable waste particles, e.g., food, paper and yard trimmings, are first disintegrated into finer particles by physicochemical processes. The finer particles have higher surface area and the complex polymers in the particles are hydrolyzed by microorganisms at appropriate moisture content and environmental conditions. The hydrolytic products in leachate are soluble monomers and include sugars and amino acids which are then fermented to volatile fatty acids (VFAs), hydrogen and carbon dioxide (CO_2). The VFAs, hydrogen and CO_2 are eventually consumed by methanogenic archaea to produce biogas consisting primarily of methane (CH_4) and CO_2 (Barlaz et al. 2010b). The characteristics of the solid phase of waste also change with time due to mechanical compression, creep and leachate submersion and drainage (Olivier and Gourc 2007; Bareither et al. 2012d).

The characteristics of solid (solid waste), liquid (leachate) and gas (biogas) phases of MSW change continually during degradation and the changes in the characteristics are inter-related. Biodegradable solid waste particles that are part of the solid skeleton of waste are broken down due to disintegration and hydrolysis, resulting in settlement and a change in the volume and mass of the three phases of the waste. Settlement of waste occurs due to immediate

mechanical compression, biodegradation-induced settlement, and mechanical creep. The vertical strain of waste (ε) caused by settlement can be consequently divided into immediate strain (ε_I), biodegradation strain (ε_B) and mechanical creep strain (ε_M) based on the progress of waste degradation (Bjarngard and Edgers 1990; Gourc et al. 2010; McDougall 2011; Bareither et al. 2013a; Fei and Zekkos 2013). The biodegradation strain of MSW can be related to the mass of generated biogas which also reflects the progress of MSW biodegradation (McDougall 2007; Gourc et al. 2010). The change in the relationship between the three phases of waste results in changes in total unit weight (γ_t), porosity and volumetric moisture content (θ) of the waste (Stoltz et al. 2010b). The changes in ε, γ_t and θ of waste are related to each other (McDougall 2007; White et al. 2014; Woodman et al. 2014). The hydraulic conductivity (k) of waste which is dependent of the θ of waste is also altered during MSW degradation (Reddy et al. 2009a; Breitmeyer 2011; Reddy et al. 2011; Bareither et al. 2012c; Woodman et al. 2014).

Meanwhile, the hydrolytic products produced from degradation of biodegradable waste particles are consumed by microorganisms in leachate with time, resulting in changes in pH and the concentrations of soluble chemical oxygen demand (sCOD) and VFAs. Due to the evolving microbial activities in leachate, the concentrations and generation rates of CH_4 and CO_2 in biogas change with time (Barlaz et al. 1989b; Bareither et al. 2013b; Fei et al. 2015a). Solid waste degradation is conducted by a consortium of interacting microorganisms, therefore the dynamics of generation, conversion and consumption of soluble compounds and generation of biogas are related (Staley et al. 2011a; Fei et al. 2015a).

In this study, the results of a comprehensive laboratory experimental investigation on the biochemical-physico-hydro-mechanical characteristics of MSW undergoing degradation are presented. Seven large-size specimens reconstituted using MSW from four landfills across the

United States (U.S.) were degraded under enhanced biodegradation conditions in landfill simulators. The trends of the characteristics of the three phases during degradation were studied. Correlations were established between the initial composition of the specimens and the time-dependent characteristics of solid waste, biogas and leachate during degradation. The results of this study improve our ability to achieve more effective degradation of landfilled MSW and efficient energy generation via biogas collection with appropriate monitoring techniques.

4.3 Methodology

4.3.1 **Waste sampling and characterization**

MSW was collected from pits excavated at the surface from four landfills in U.S., i.e., Los Reales Landfill in Arizona (AZ), Lamb Canyon Landfill in California (CA), Sauk Trail Hills Landfill in Michigan (MI), and Austin Community Landfill in Texas (TX) (Sahadewa et al. 2014b; Zekkos et al. 2014). Waste was collected from two locations in the CA landfill and one location in the AZ, TX and MI landfills, and the samples were shipped in sealed drums to the Geoenvironmental Engineering Laboratory at the University of Michigan. The field composition for each waste sample was characterized according to the procedures described by Zekkos et al. (2010b). The waste was first separated into a finer fraction of soil-like material that passed through a 20-mm sieve (<20 mm particles) and a coarser fraction. The coarser fraction was subsequently manually segregated based on the type of waste constituents. The three primary constituents of the coarser fraction by weight for all samples were paper, soft plastic and wood, and other minor constituents include hard plastic, metal, rubber, textile, rock and miscellaneous objects. No distinguishable food waste was found in any sample, likely because they had already been scavenged or composted prior to excavation and sampling. The ages of the waste samples

varied between six and fifteen months according to landfill records and the degree of anaerobic biodegradation of waste was considered minimal based on visual inspection of the segregated paper waste.

The segregated waste constituents from each sample were weighted and the corresponding percentages on a wet weight basis were calculated. Moisture content of the four constituents from each sample was measured by heating the waste at 75 ˚C to avoid vaporizing organic compounds in the waste. The content of volatile solids (VS) of each dried waste constituent was evaluated by heating the waste at 550 ˚C.

4.3.2 **Waste specimen preparation**

A modified waste composition was calculated for each sample by increasing the percentages of the four major constituents, <20 mm fraction, paper, soft plastic and wood, to 100%, as other constituents were not considered significant by volume or mass. Seven MSW specimens were reconstituted and the percentages of the major constituents by mass (%) and average moisture content ($w_{c,ave}$) of the specimens were calculated on a dry weight basis (Table 4-1). The average moisture content of the sample waste and prepared specimens were below field capacity. Two replicate specimens with identical waste composition and total unit weight were prepared using the sample from TX (TX1 and TX2), two specimens with different composition were prepared using the sample from MI (MI1 and MI2), and one specimen was prepared using each sample from the other three locations (AZ, CA1 and CA2). The amount of biodegradable waste in each specimen is assessed by two parameters. The percentage of biodegradable waste prior to degradation (B_0, dry mass/dry mass %) is defined as the proportion by mass of food, yard waste and paper plus the mass of VS in <20 mm fraction of the entire dry waste mass (Fei et al. 2015a). Similarly, the percentage of volatile solids in biodegradable waste prior to degradation (VS_{B0},

dry mass/dry mass %) is calculated as the portion by mass of VS in food, yard waste, paper and <20 mm fraction of the entire dry waste mass, while the VS in plastic is excluded (Table 4-2).

4.3.3 **Simulators operation**

Detailed descriptions of the laboratory landfill simulators and operating procedures are presented by Fei et al. (2014a; 2015a). In summary, each specimen was manually loaded into a 42-L simulator with a diameter of 0.3 m and a height of 0.6 m (Figure 4-1) on day 1 and the as-prepared total and dry unit weight of the specimens ($\gamma_{t,0}$ and $\gamma_{d,0}$) were calculated (Table 4-2). The material was generally placed at a loose state, i.e., without significant compaction. Besides the vertical load from a plastic leachate distribution plate and a stainless steel rod for settlement measurement that impose <1 kPa vertical stress, no additional vertical stress was applied to the specimens. Thus the effect of mechanical compression due to vertical stress application on MSW biodegradation process and properties of the specimens is eliminated. No moisture was added to AZ, CA1, CA2 and MI2 until day 7, and to MI1, TX1 and TX2 until day 12.

On day 7 or day 12, the temperature of the simulators was raised from laboratory temperature to 40±3 ^{0}C using heating blankets. On the same day, drainage valves at the bottom of the simulators were closed and deionized water was added to the simulators from the top to completely submerge the specimens. The specimens remained submerged for 10 minutes before the drainage valves were opened and the leachate drained by gravity. The leachate was collected in leachate tanks and recirculated to submerge the specimens three times a week. Thus, the specimens were maintained at field capacity moisture content in-between leachate submersion. The generated biogas was collected in gas sampling bags.

Different than the other six simulators, the simulator for MI1 was maintained at laboratory temperature (22±3 ^{0}C) until day 450, whereas the leachate recirculation and drainage

procedure was identical to the other simulators. Only some of the leachate and solid waste measurements and no biogas measurement were performed for the simulator.

4.3.4 **Leachate measurements**

The leachate was sampled after each recirculation event and pH and concentrations of sCOD (g O_2/L) and VFAs (converted to equivalent COD, g O_2/L) in the leachate were measured (Fei et al. 2015a). The mass of sCOD and VFAs present in the leachate (g O_2) were calculated by multiplying the respective concentration by the total volume of liquid in contact with the specimen (the sum of the added deionized water and moisture retained in the specimen on day 1). The maximum masses of sCOD and VFAs ($sCOD_{max}$ and VFA_{max}) were normalized by the initial dry mass of the specimen ($W_{s,0}$) to obtain $sCOD_{max}/W_{s,0}$ and $VFA_{max}/W_{s,0}$. The time until the $sCOD_{max}$ and rise of pH ($t_{sCODmax}$ and $t_{pH,rise}$) was recorded starting with the day of first submersion (day 7 or day 12).

4.3.5 **Biogas measurements**

The volume of generated biogas was measured with time using a gas mass flow meter and the concentrations of gas species were measured using Gas Chromatography with a Thermal Conductivity Detector. The cumulative volume (V_{CH4}) and generation rate (r_{CH4}) of CH_4 were then calculated. The cumulative volume of V_{CH4} when CH_4 generation stopped was divided by $W_{s,0}$ to obtain the CH_4 generation potential of the specimen (L_0, L CH_4/kg dry waste). The time until the initiation of CH_4 generation and maximum r_{CH4} ($r_{CH4,max}$) was measured ($t_{rCH4,0}$ and $t_{rCH4,max}$) was recorded starting with the day of first submersion (day 7 or day 12).

4.3.6 **Solid waste measurements**

The settlement of each specimen was recorded with time using a linear cable extension transducer and vertical strain was calculated using the initial height of the specimen. The

settlement of the specimen from the time it was loaded until one day after the first leachate drainage event was used to calculate immediate strain (ε_I). The settlement observed subsequently until CH_4 generation stopped was calculated as biodegradation strain (ε_B). Additional subsequent strain was attributed to mechanical creep (ε_M) (Gourc et al. 2010; Bareither et al. 2013a). Long-term strain (ε_{LT}) of the specimen is the sum of ε_B and ε_M. Long-term compression ratio (C_{LT}) was calculated for each 10-day period according to Fei et al. (2013).

The total weight of the specimen when submerged by leachate or at field capacity moisture content after leachate drainage was measured using a floor scale, and the corresponding total unit weight was calculated ($\gamma_{t,sub}$ and $\gamma_{t,fc}$). The drainable volumetric water content (θ_{drain}, v/v %) of the specimen was calculated by dividing the volume of recirculated leachate needed to submerge the specimen by the total volume of the specimen.

Falling head permeability tests were performed on submerged AZ, CA1, CA2 and MI2 by recirculating additional leachate to establish a free liquid level above the top of the specimen. The leachate was then allowed to drain until its level dropped to the top of the specimen, and the elapsed time was recorded. The tests were repeated four times on each specimen and an average "saturated" hydraulic conductivity was calculated for that elapsed time. The tests were conducted five times in the first three months and once every two to three months afterward. The k values for TX1 and TX2 were tested following the same procedure only once during the experiments due to different configuration of the simulators.

4.4 Results and discussion

The changes in the evolving characteristics of solid waste, leachate and biogas with time for the seven specimens are illustrated in Figure 4-2. TX1 and TX2 were degraded for 1,136 and 1,300

days, respectively, and AZ, CA1, CA2 and MI2 were degraded for 800 days. MI1 was degraded for 1,460 days, but only the data for the first 450 days was shown before the temperature was raised from laboratory temperature to 40 ˚C.

The trends in each characteristic for all specimens were similar, suggesting that the observed behaviors of MSW under enhanced biodegradation conditions are similar. The differences in the values of each measured characteristic between specimens are primarily caused by the differences in the initial composition and unit weight of the specimens since all other operation conditions are identical.

4.4.1 **Chemical characteristics of leachate**

The concentrations of VFAs and sCOD in leachate increased since leachate was first recirculated through the waste mass and reached their maximum values, VFA_{max} and $sCOD_{max}$ respectively, within 40 days. They then decreased to residual values after around 100 days (Figure 4-2a and Figure 4-2b). The changes in the concentrations are attributed to generation and consumption of soluble organic compounds in the leachate by microorganisms (Barlaz et al. 1989b; Fei et al. 2015a). Volatile fatty acids are the microbial fermentative products from hydrolyzed solid waste particles and serve as the soluble substrates for subsequent acetogenesis and methanogenesis, while sCOD measures other inorganic oxidizable compounds in leachate in addition to VFAs. Therefore the concentration of sCOD was also higher than the concentration of VFAs at any given time. The values of $VFA_{max}/W_{s,0}$ are approximately 70% of the $sCOD_{max}/W_{s,0}$ (Figure 4-3a, Eqn. 4-1, R^2=0.99), suggesting that sCOD, a more readily measurable variable and often regulated for leachate monitoring (Barlaz et al. 2002), is a good indicator for the concentration of soluble substrates for methanogenesis in leachate.

$$\frac{VFA_{max}}{W_{s,0}}\left(\frac{g\ O_2}{kg}\right) = 0.70 \times \frac{sCOD_{max}}{W_{s,0}}\left(\frac{g\ O_2}{kg}\right) \quad (4\text{-}1)$$

The pH for leachate dropped to between 5.5-6.5 within 10 days after the initial leachate recirculation event and increased to stable values between 6.5-7 after 10-40 days (Figure 4-2c). Therefore the initial inhibition of MSW biodegradation due to acidic environment in leachate and solid waste caused by accumulation of VFAs was temporary and the pH recovered without external intervention. The time until $sCOD_{max}$ ($t_{sCODmax}$) is proportional to the time until rise of pH in leachate ($t_{pH,rise}$) (Figure 4-3b), and according to Eqn. 4-2 (R^2=0.94), if t_{pHrise} is longer than 17 days, then $t_{sCODmax}$ is expected to occur prior to t_{pHrise} which suggests possible initial inhibition. The $t_{sCODmax}$ for AZ was lower than its t_{pHrise}, indicating prolonged inhibition period in AZ compared to other specimens which was a consequence of the very high concentrations of sCOD and VFAs in the leachate (Figure 4-2a and Figure 4-2b) and the highest B_0 among the specimens. The correlation is useful in assessing the duration of initial inhibition in MSW under enhanced biodegradation conditions.

$$t_{sCOD,max}\ (day) = 0.43 \times t_{pH,rise}\ (day) + 9.7 \quad (4\text{-}2)$$

4.4.2 **Physicochemical characteristics of biogas**

The CH_4 concentration in generated biogas increased to between 50-55% shortly after the specimens were first submerged and the value remained stable afterward with CO_2 being the predominant complementary gas species (Fei et al. 2014a). The cumulative volume of generated CH_4 increased following a sigmoidal trend and approached the final value asymptotically which is typical for CH_4 generation from MSW (Figure 4-2d) (Eleazer et al. 1997; Fei et al. 2015b).

CH_4 generation from the specimens was completed after 250-300 days by which time anaerobic biodegradation of MSW was considered complete.

The value of CH_4 generation potential (L_0) is controlled by the initial composition of waste. As illustrated in Figure 4-4a, L_0 increases with increasing B_0 of the specimens, with 1% of biodegradable constituent in 1 kg of dry waste roughly yields 1.50 L of CH_4 (Eqn. 4-3a, R^2=0.94). AZ and MI have different B_0 but comparable L_0, because they consisted of different percentage of <20 mm fraction and paper (Table 4-1) which have different individual CH_4 generation potential (Eleazer et al. 1997). The biodegradable waste constituents included in the specimens in this study (paper and biodegradable particles in <20 mm fraction) tend to yield low CH_4 than other biodegradable waste constituents (paper and yard waste), thus the L_0 reported in this study are near the lower-bound values compared to other L_0 reported in the literature (Eleazer et al. 1997; Fei et al. 2015b). The correlation between the L_0 and VS_{B0} of the specimens gives a higher coefficient of determination (Eqn. 4-3b, R^2=0.97), showing that 1% of VS_{B0} in 1 kg of dry waste yields about 2.43 L of CH_4 (Figure 4-4b). However, determining VS_{B0} for waste in the field may be more difficult, whereas B_0 can be more easily estimated using available information from waste characterization studies (Staley and Barlaz 2009; Zekkos et al. 2010b; EPA 2014a).

$$L_0 \left(\frac{L\ CH_4}{kg}\right) = 1.50 \times B_0\ (\%) \tag{4-3a}$$

$$L_0 \left(\frac{L\ CH_4}{kg}\right) = 2.43 \times VS_{B0}\ \left(\frac{kg}{L}\right) \tag{4-3b}$$

CH_4 generation did not start immediately until a few days after leachate recirculation started ($t_{rCH4,0}$). Once started, r_{CH4} increased to $r_{CH4,max}$ within the following 30 days. The peak

r_{CH4} was maintained for a few days and decreased to practically zero after 250-300 days (Figure 4-2e). The normalized $r_{CH4,max}$ ($r_{CH4,max}/W_{s,0}$) is proportional to L_0, demonstrating that CH_4 generation from waste is a first-order decay process (De la Cruz and Barlaz 2010). Under these enhanced biodegradation conditions, the $r_{CH4,max}/W_{s,0}$ is equal to 2% of the corresponding L_0 per day(Figure 4-5a, Eqn. 4-4, R^2=0.99). The $t_{rCH4,max}$ increases with increasing $t_{rCH4,0}$ (Figure 4-5b), and $t_{rCH4,max}$ equals 18 days when $t_{rCH4,0}$ is zero, suggesting that 18 days is likely the shortest delay time between the initiation and maximum rate of CH_4 generation for these conditions (Eqn. 4-5, R^2=0.87).

$$\frac{r_{CH4,max}}{W_{s,0}}\left(\frac{L\ CH_4}{day-kg}\right) = \frac{0.020\times L_0\left(\frac{L\ CH_4}{kg}\right)}{1\ day} \quad (4\text{-}4)$$

$$t_{rCH4,max}\ (day) = 0.70 \times t_{rCH4,0}\ (day) + 18.2 \quad (4\text{-}5)$$

4.4.3 **Settlement of degrading MSW**

The biodegradation strain of the specimens (ε_B) increased rapidly in the first 100 days and asymptotically approached the final biodegradation strain ($\varepsilon_{B,f}$) by about 300 days (Figure 4-2f), whereas mechanical creep strain (ε_M) increased until beyond 1,000 days (Figure 4-2g). Since the increment of ε after 700 days was minimal compared to the total ε, the last measured ε of each specimen was defined as the final total ε (ε_f).

The trends of the strain of the specimens were divided into ε_I, ε_B, and ε_M, as shown in Figure 4-6. The final values of ε_I range between 1.5-9.6%, and the final values of ε_M range between 1.1-2.7%. The range of $\varepsilon_{B,f}$ is between 5.6-20.9% and constituted 35-79% of the total strain (ε_f). As shown in Figure 4-7a, $\varepsilon_{B,f}$ increases with increasing B_0, indicating that removal of

biodegradable solid waste particles is the cause for biodegradation settlement of waste as shown in Eqn. 4-6 (R^2=0.96). In contrast, higher variability is observed in the correlation between ε_f and B (Figure 4-7b), because ε_I and ε_M which are included in ε_f are not directly influenced by B. Therefore, it is recommended that the settlement of waste undergoing degradation should be evaluated separately for the ε_I, ε_B, and ε_M to achieve a more accurate estimation.

$$\varepsilon_{B,f}\ (\%) = 0.55 \times B_0\ (\%) \tag{4-6}$$

As shown in Figure 4-2h, the initial long-term compression ratio (C_{LT}) values observed in the first 10 days were between 0.01-0.34 and are associated with physical processes. Except for the high initial C_{LT} values, the maximum values of C_{LT} ($C_{LT,max}$) were between 0.04-0.32 and were measured between day 40-80 when MSW biodegradation was intensive. The C_{LT} decreased to between 0.02-0.04 after around 500 days which were 2-10 times lower than the $C_{LT,max}$ and are equivalent to reported secondary compression ratio (C_α) of waste (McDougall 2011). As shown in Figure 4-7c, the $C_{LT,max}$ is higher for higher $\varepsilon_{B,f}$, therefore waste showing higher $C_{LT,max}$ during degradation is expected to have higher biodegradation strain and vice versa. These observations highlight that C_{LT} for degrading MSW is both time- and composition-dependent and is much higher than the calculated C_α for the same waste.

4.4.4 **Unit weight, volumetric moisture content and hydraulic conductivity of MSW**

The moisture content of the specimens was increased to field capacity after the specimens were submerged and the leachate was drained for the first time. Subsequently, the $\gamma_{t,fc}$ increased with time due to settlement and densification of waste and possible increase of field capacity moisture content with time (Figure 4-2i). The $\gamma_{t,sub}$ decreased until between 10-50 days and increased

afterward (Figure 4-2j). Since CH_4 generation had already stopped and ε increased minimally after 700 days, the $\gamma_{t,fc}$ and $\gamma_{t,sub}$ are not expected to change significantly beyond that time, thus the last $\gamma_{t,fc}$ and $\gamma_{t,sub}$ measurements were considered as the final values ($\gamma_{t,fc,f}$ and $\gamma_{t,sub,f}$). It is noted that the $\gamma_{t,sub,f}$ were always lower than or equal to the initial $\gamma_{t,sub}$. As shown in Figure 4-8a and 8b and Eqn. 4-7 (R^2=0.94) and Eqn. 4-8 (R^2=0.86), higher initial $\gamma_{t,fc}$ ($\gamma_{t,fc,0}$) is correlated with higher $\gamma_{t,fc,f}$ and $\gamma_{t,sub,f}$, therefore $\gamma_{t,fc,0}$ is informative for estimating the $\gamma_{t,fc}$ and $\gamma_{t,sub}$ of waste after degradation.

$$\gamma_{t,fc,f}\ \left(\frac{kN}{m^3}\right) = 1.05 \times \gamma_{t,fc,0}\ \left(\frac{kN}{m^3}\right) + 1.14 \quad (4\text{-}7)$$

$$\gamma_{t,sub,f}\ \left(\frac{kN}{m^3}\right) = 0.69 \times \gamma_{t,fc,0}\ \left(\frac{kN}{m^3}\right) + 5.45 \quad (4\text{-}8)$$

The value of θ_{drain} equals the difference between the maximum (saturated) and residual (field capacity) volumetric water content of a specimen (Woodman et al. 2014). The initial values of θ_{drain} were calculated after the specimens were submerged for the first time, and were between 150-250% for AZ, CA1, CA2 and MI2, and around 50% for TX1 and TX2. The <20 mm fraction in TX1 and TX2 contained mostly soil that was classified as high plasticity silt, thus their initial θ_{drain} were much lower than the other specimens. The θ_{drain} of the specimens decreased sharply afterward, indicating that much less leachate was needed to submerge the specimens and they were maintained at field capacity moisture content between recirculation events. About 10-20 days after leachate recirculation started, the change in θ_{drain} slowed down. The θ_{drain} of AZ, CA2, TX1 and TX2 decreased eventually to between 10-50%, whereas the θ_{drain} of MI and CA1 increased to around 100% by the end of the experiments (Figure 4-2k).

As shown in Figure 4-2l, the initial values of k (k_0) for the specimens were on the order of 10^{-1} cm/s, k decreased in the next 100 days during intensive biodegradation. The final values of k (k_f) are dependent on MSW biodegradation process, the % of <20 mm fraction, and the soil type in <20 mm fraction. The values of $sCOD_{max}/W_{s,0}$, $rCH_{4,max}/W_{s,0}$ and L_0 of AZ were all higher than the other specimens which indicate the most intensive microbial activity and its k_f was more than 20 times lower than the k_0. In comparison, the k_f values for MI2, CA1 and CA2 were 1/3 to half of the k_0. The k for TX1 and TX2 were on the order of 10^{-3} cm/s which are typical for high plasticity silt under minimal vertical stress (Mitchell and Soga 2005).

4.4.5 **Coupling soluble compounds in leachate with CH_4 generation**

The biochemical characteristics in leachate and biogas and physical characteristics of waste mass are found to be interrelated. As shown in Figure 4-9a, normalized maximum r_{CH4} ($r_{CH4,max}/W_{s,0}$) increases with increasing normalized maximum mass of sCOD ($sCOD_{max}/W_{s,0}$) of the specimens. Therefore, monitoring and comparing sCOD in leachate during waste degradation is informative for estimating the rate of CH_4 generation (Fei et al. 2015a). It is important to note that, the $sCOD_{max}/W_{s,0}$ of AZ was about two times higher than that of MI, whereas the corresponding $r_{CH4,max}/W_{s,0}$ were similar. This is because methanogenesis is the rate limiting step during active MSW biodegradation (Barlaz et al. 2010b), and a upper-bound $r_{CH4,max}/W_{s,0}$ may exist under a specific biodegradation condition (Fei et al. 2015a). Therefore accumulation of excess soluble compounds in leachate beyond a certain value may not further contribute to proportional increase of r_{CH4}.

A linear relationship is also found between the time until the initiation of CH_4 generation and rise of pH ($t_{rCH4,0}$ and $t_{pH,rise}$, respectively) (Figure 4-9b). Therefore monitoring pH in leachate is informative to estimate the initiation of CH_4 generation. For all the specimens, the

time until the $sCOD_{max}$ was measured ($t_{sCODmax}$) always precedes the time until the $r_{CH4,max}$ was measured ($t_{rCH4,max}$) (Figure 4-9c), suggesting that intensive hydrolysis, indicated by the measured $sCOD_{max}$, precedes intensive methanogenesis. The observation agrees with the statement that hydrolysis is the initial rate limiting step of MSW biodegradation prior to methanogenesis (Barlaz et al. 2010b).

4.4.6 **Coupling CH_4 generation with biodegradation strain of MSW**

CH_4 generation and settlement due to biodegradation of waste are also coupled. The final biodegradation strain ($\varepsilon_{B,f}$) increases with increasing CH_4 generation potential (L_0) of the specimens, highlighting that conversion of biodegradable solid waste to CH_4 (and CO_2) is directly coupled with biodegradation strain (Figure 4-10a). The correlation can be used to link CH_4 generation with the accompanying settlement of waste in bioreactor landfills of low overburden pressure (Eqn. 4-9, R^2=0.95). The $C_{LT,max}$ value increases with increasing $r_{CH4,max/Ws,0}$. Thus C_{LT} measured in the field can be used to inform biogas generation rate and vice versa (Figure 4-10b). However, it is important to highlight that as discussed earlier, field settlement may also be affected by mechanisms causing immediate settlement and creep.

$$\varepsilon_{B,f} = 0.35 \times L_0 \tag{4-9}$$

4.4.7 **Coupling settlement, unit weight, volumetric moisture content and hydraulic conductivity of MSW**

The normalized $\gamma_{t,fc}$ ($\gamma_{t,fc}/\gamma_{t,fc,0}$, %) increases with ε_{LT} and a generic trend is observed independent of waste composition and initial unit weight (Figure 4-11a). The final values of $\gamma_{t,fc}/\gamma_{t,fc,0}$ were between 1.15 and 1.25 for the specimens. The normalized θ_{drain} ($\theta_{drain}/\theta_{drain,0}$, %)

also decreases with increasing ε_{LT} and remains relatively constant when ε_{LT} is higher than 10% (Figure 4-11b). The final $\theta_{drain}/\theta_{drain,0}$ values for MI and CA1 were around 0.4 which are significantly higher than for the remaining specimens. This is because the $\gamma_{d,I}$ for MI and CA1 were lower than 4 kN/m^3 and the % of <20 mm fraction were below 50%. Such specimens had a loose matrix structure supported by high numbers of large-size and elongated waste particles, therefore the moisture retention capacity of them are low and the θ_{drain} remained relatively high in the long term (Agostini et al. 2012; White et al. 2014). In contrast, the $\gamma_{d,I}$ and % of <20 mm fraction for AZ, CA2, TX1 and TX2 are significantly higher than those for MI and CA1, therefore pore sizes in the prior specimens are likely smaller and more suitable for moisture retention, leading to lower $\theta_{drain}/\theta_{drain,0}$ in the long-term. As shown in Figure 4-12, the value of k increases with increasing θ_{drain}. When θ_{drain} is higher than 30%, the corresponding k value remains on the order of 10^{-1} cm/s, whereas k changes significantly when θ_{drain} is lower than 30%.

4.5 Conclusions

A comprehensive experimental investigation on long-term degradation of MSW specimens of different initial compositions under enhanced biodegradation conditions in 0.3 m diameter laboratory landfill simulators has been conducted. Biochemical-physico-hydro-mechanical characteristics in liquid, gas and solid phases of MSW were measured with time and systematic and repeatable trends were observed. Soluble compounds in leachate were depleted after 100 days and CH_4 generation and biodegradation of waste was largely completed after around 300 days. The hydraulic conductivity (k) of the specimens decreased due to waste degradation. Changes in vertical strain (ε), total unit weight at field capacity and when submerged ($\gamma_{t,fc}$, $\gamma_{t,sub}$)

and drainable volumetric moisture content (θ_{drain}) of waste continued in decreasing rates even after 1,000 days.

The concentration of VFAs in leachate is proportional to the concentration of sCOD. L_0 is dependent on the amount of biodegradable waste that can be quantified by B_0 and VS_{B0}. The normalized maximum CH_4 generation rate ($r_{CH4,max}/W_{s,0}$) is correlated with CH_4 generation potential (L_0), normalized maximum mass of sCOD ($sCOD_{max}/W_{s,0}$) and maximum long-term compression ratio ($C_{LT,max}$). The time for pH rise, initiation and maximum rate of CH_4 generation, and maximum sCOD in leachate are correlated. The settlement of waste in terms of strain can be separated into ε_I, ε_B and ε_M. The final ε_B ($\varepsilon_{B,f}$) is dependent on B_0 and correlates well with L_0. $C_{LT,max}$ increases with increasing $\varepsilon_{B,f}$. The changes in $\gamma_{t,fc}$ and θ_{drain} are also dependent of long-term strain (ε_{LT}). The k of waste can be estimated from the θ_{drain}.

4.6 Tables

Table 4-1 Test time, composition, moisture content and volatile solids for six MSW specimens.

Specimen	Test time (day)	<20 mm particles (%)	paper (%)	soft plastic (%)	wood (%)	$W_{t,0}$ (kg)	$w_{c,ave}$ (%)	$W_{s,0}$ (kg)	VS in <20 mm fraction (g/g)	VS in paper (g/g)
TX1	1136	79.1	10.6	6.0	4.3	30.02	34.6	22.31	0.070	0.610
TX2	1300	79.1	10.7	5.9	4.3	29.31	37.7	21.75	0.070	0.610
AZ	800	67.9	21.4	8.5	2.1	21.69	32.7	16.75	0.128	0.806
CA2	800	68.3	4.6	3.9	5.8	29.02[a]	28.1	23.03	0.086	0.436
CA1	800	50.8	17.0	11.9	20.2	19.88	39.5	14.38	0.089	0.436
MI1	1460[b]	80.0	10.0	5.7	4.3	21.36	43.6	14.80	0.218	0.398
MI2	800	22.8	33.7	19.8	23.7	13.52	53.0	8.77	0.252	0.398

[a] included 4.2 kg of hard plastic, metal and cobbles.
[b] the temperature of MI1 was increased from 22 ˚C to 40 ˚C after 450 days of degradation, and the data after 450 days was not shown.

Table 4-2 Percentage of biodegradable waste, percentage of biodegradable volatile solids, and dry and total unit weight for six MSW specimens.

Specimen	B_0 (%)	VS_{B0} (%)	$\gamma_{t,0}$ (kN/m^3)	$\gamma_{t,fc,0}$ (kN/m^3)	$\gamma_{t,sat,0}$ (kN/m^3)	$\gamma_{d,0}$ (kN/m^3)	$\gamma_{d,I}$ (kN/m^3)
TX1	16.1	12.0	7.90	9.35	12.62	5.87	5.93
TX2	16.4	12.2	7.83	9.35	12.22	5.81	5.85
AZ	30.6	26.4	5.38	7.28	11.54	4.16	4.57
CA2	10.3	7.7	7.20	9.52	12.26	5.72	6.26
CA1	21.7	12.0	4.96	6.97	10.58	3.59	3.86
MI1	27.4	17.4	5.77	n. a.	n. a.	4.02	4.12
MI2	48.1	22.4	3.52	4.69	9.67	2.28	2.35

n. a.: not available.

4.7 Figures

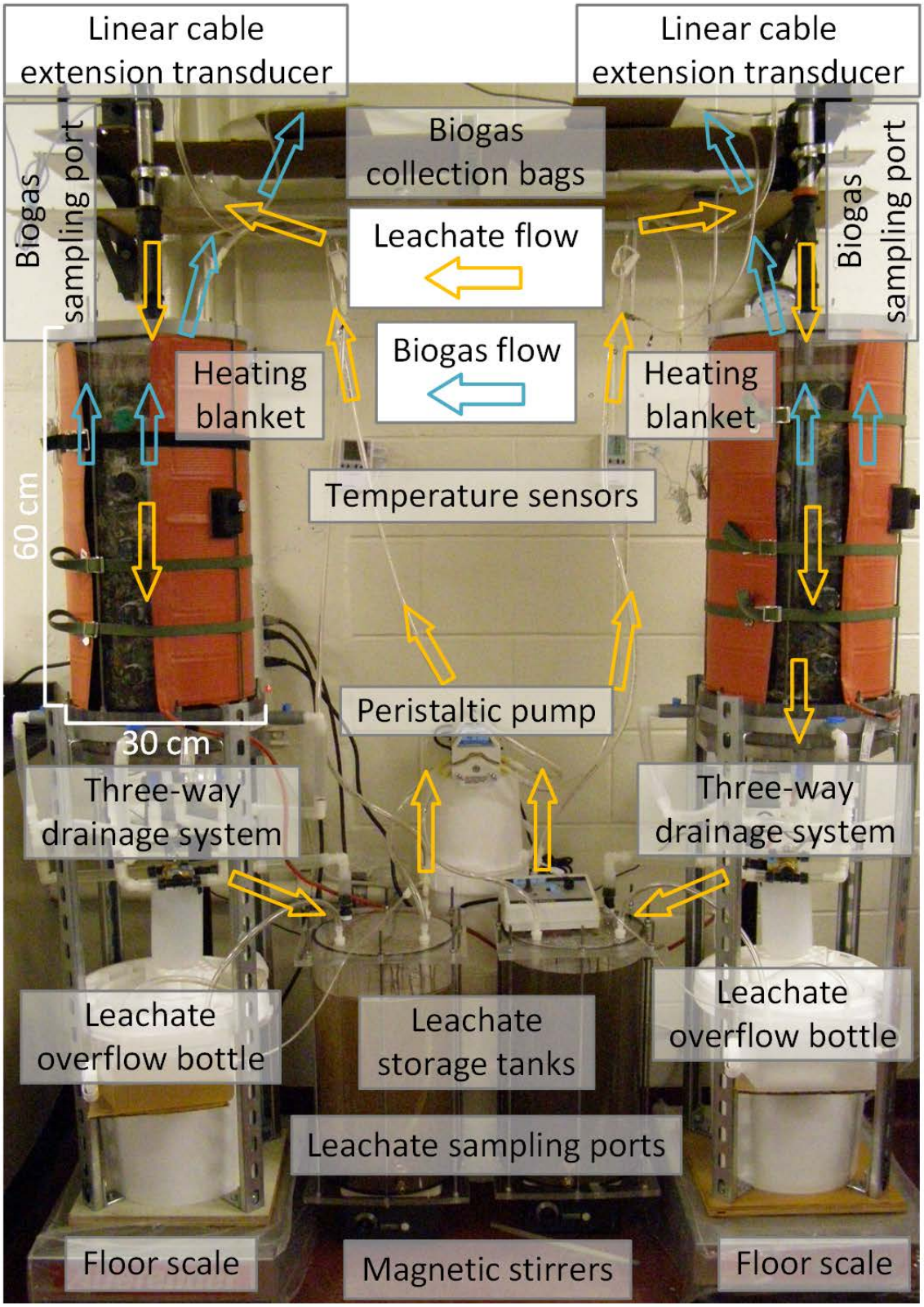

Figure 4-1 Schematic of two parallel laboratory landfill simulators.

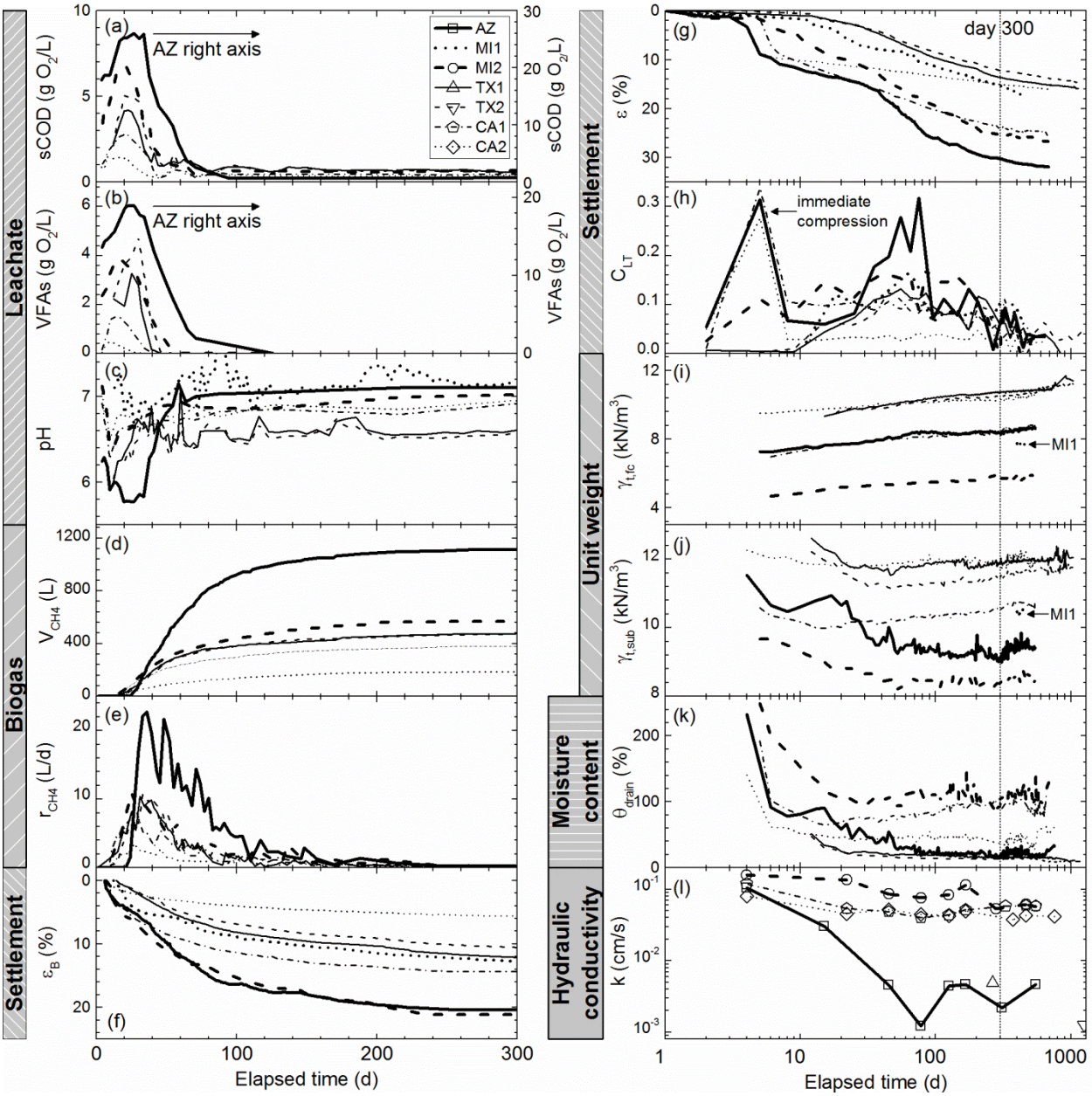

Figure 4-2 Changes of characteristics during MSW degradation: (a) concentration of soluble chemical oxygen demand (sCOD); (b) total concentration of volatile fatty acids (VFAs); (c) pH for leachate; (d) cumulative volume of generated CH_4 (V_{CH4}); (e) generation rate of CH_4 (r_{CH4}); (f) biodegradation strain (ε_B); (g) total strain (ε); (h) long-term compression ratio (C_{LT}); (i) total unit weight at field capacity moisture content ($\gamma_{t,fc}$); (j) saturated total unit weight ($\gamma_{t,sat}$); (k) drainable volumetric moisture content (θ_{drain}); (l) "saturated" hydraulic conductivity (k).

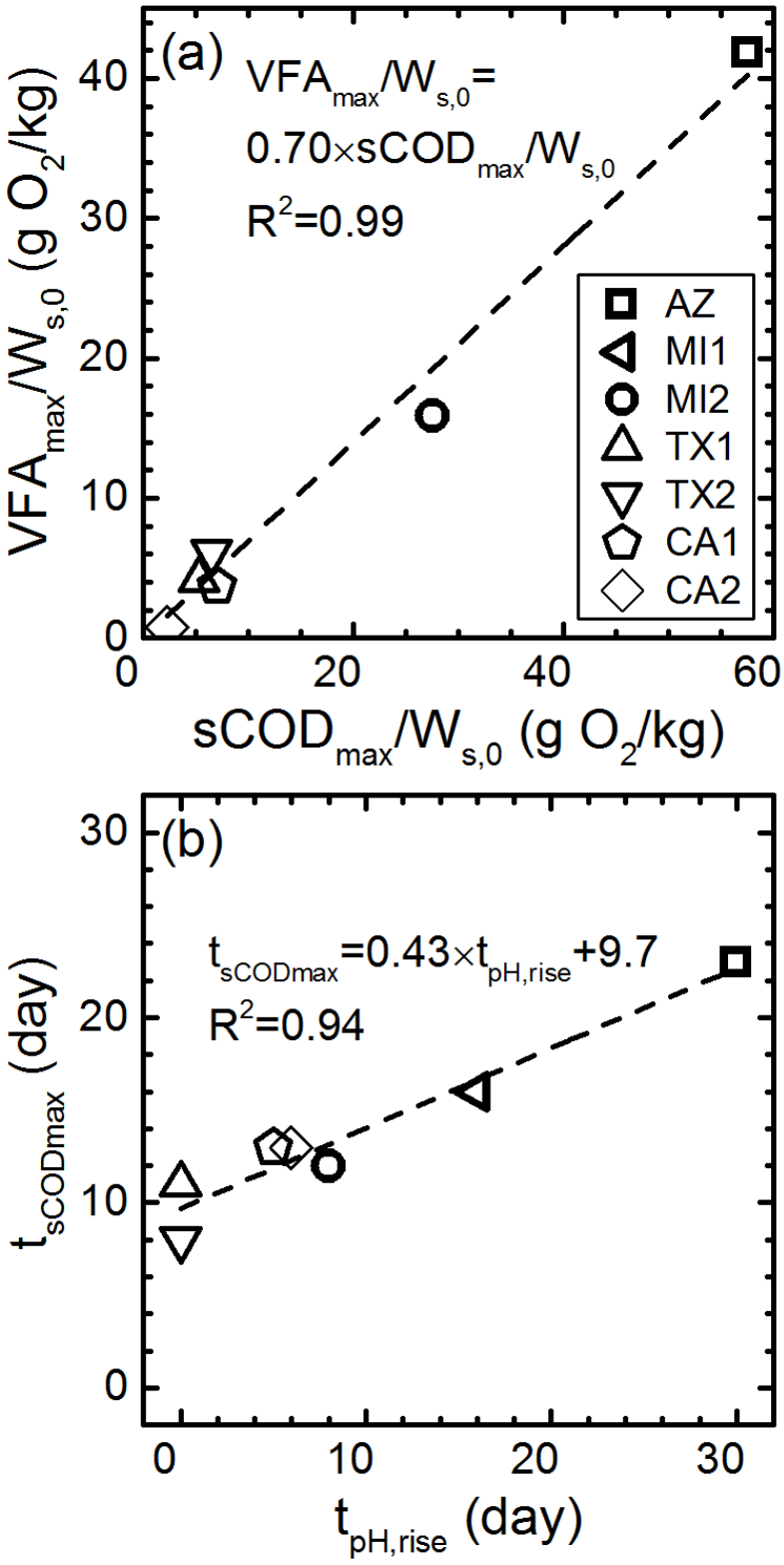

Figure 4-3 Correlations between biochemical characteristics of leachate: (a) normalized maximum VFAs ($VFA_{max}/W_{s,0}$) and normalized maximum sCOD ($sCOD_{max}/W_{s,0}$); and (b) time until $sCOD_{max}/W_{s,0}$ ($t_{sCODmax}$) and time until pH increase (t_{pHrise}).

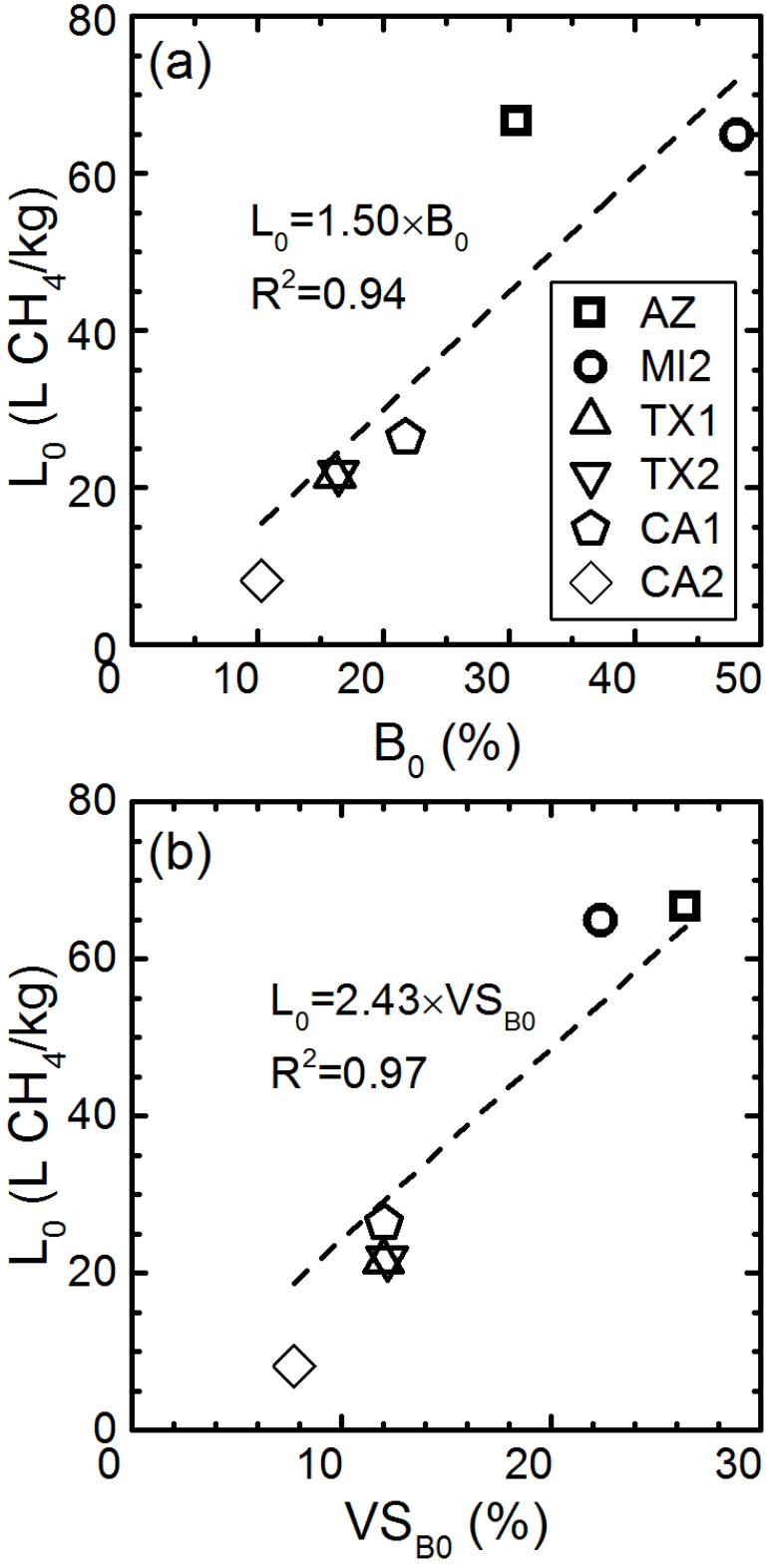

Figure 4-4 Relationship between CH_4 generation potential (L_0) and initial composition of the specimens: (a) percentage of biodegradable waste (B_0); and (b) percentage of biodegradable volatile solids (VS_{B0}).

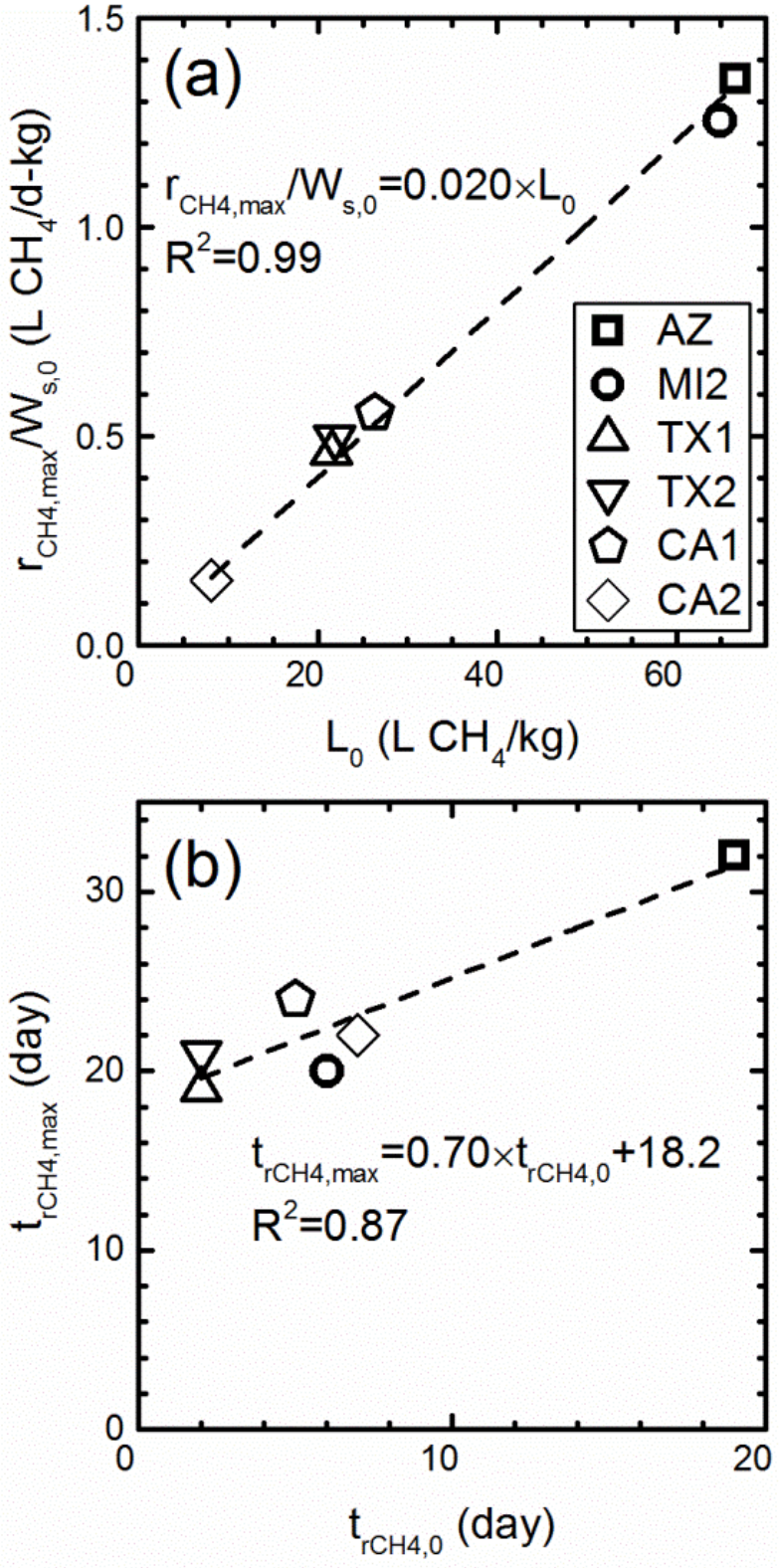

Figure 4-5 Correlations between physico-chemical characteristics of biogas: (a) normalized maximum CH4 generation rate ($r_{CH4,max}/W_{s,0}$) and CH_4 generation potential (L_0); and (b) time until $r_{CH4,max}/W_{s,0}$ ($t_{rCH4,max}$) and time until initiation of CH_4 generation ($t_{rCH4,0}$).

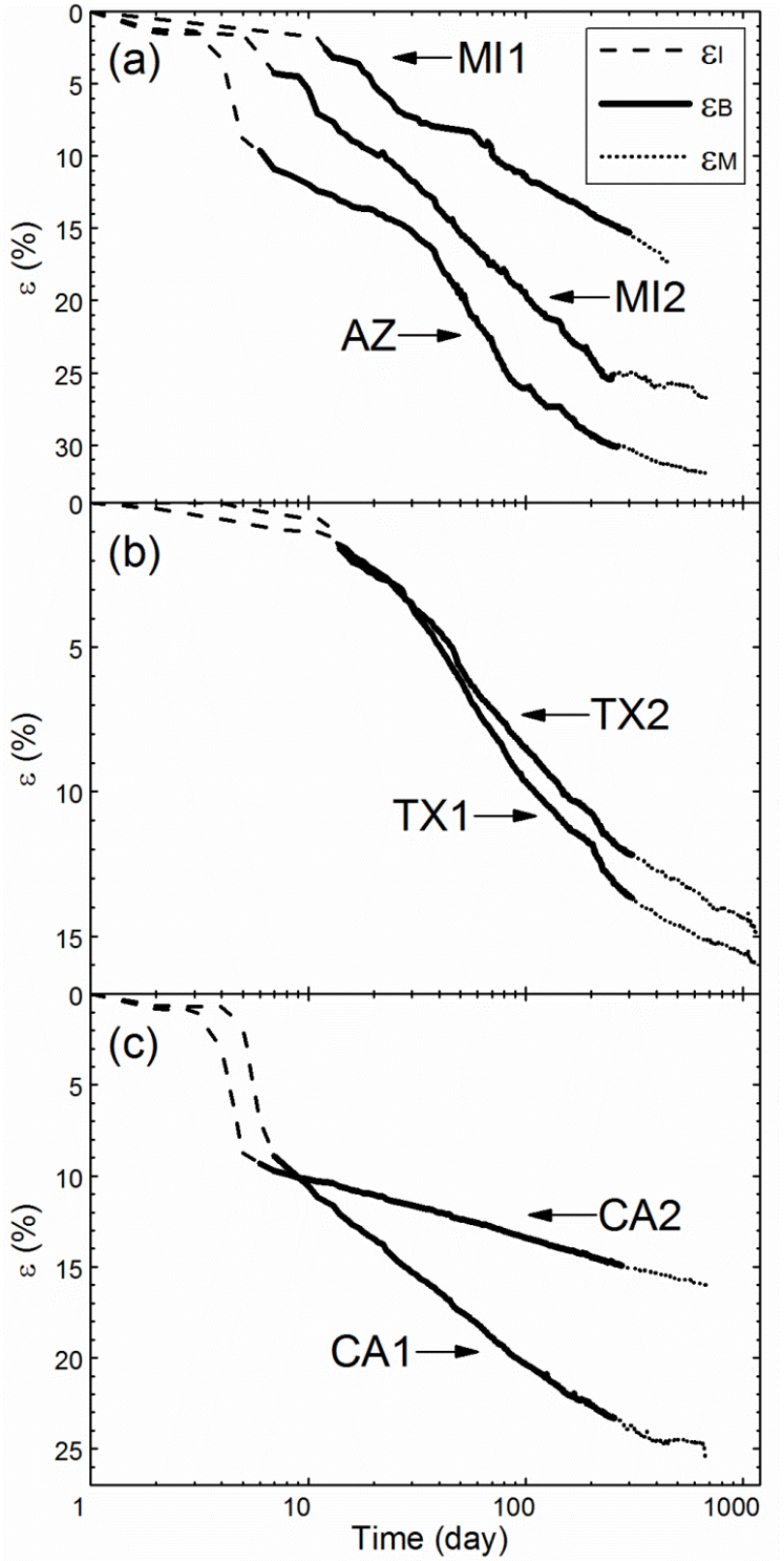

Figure 4-6 Contributions of immediate strain (ε_I), biodegradation strain (ε_B) and creep strain (ε_M) to total strain (ε) for (a) AZ and MI; (b) TX1 and TX2; and (c) CA1 and CA2.

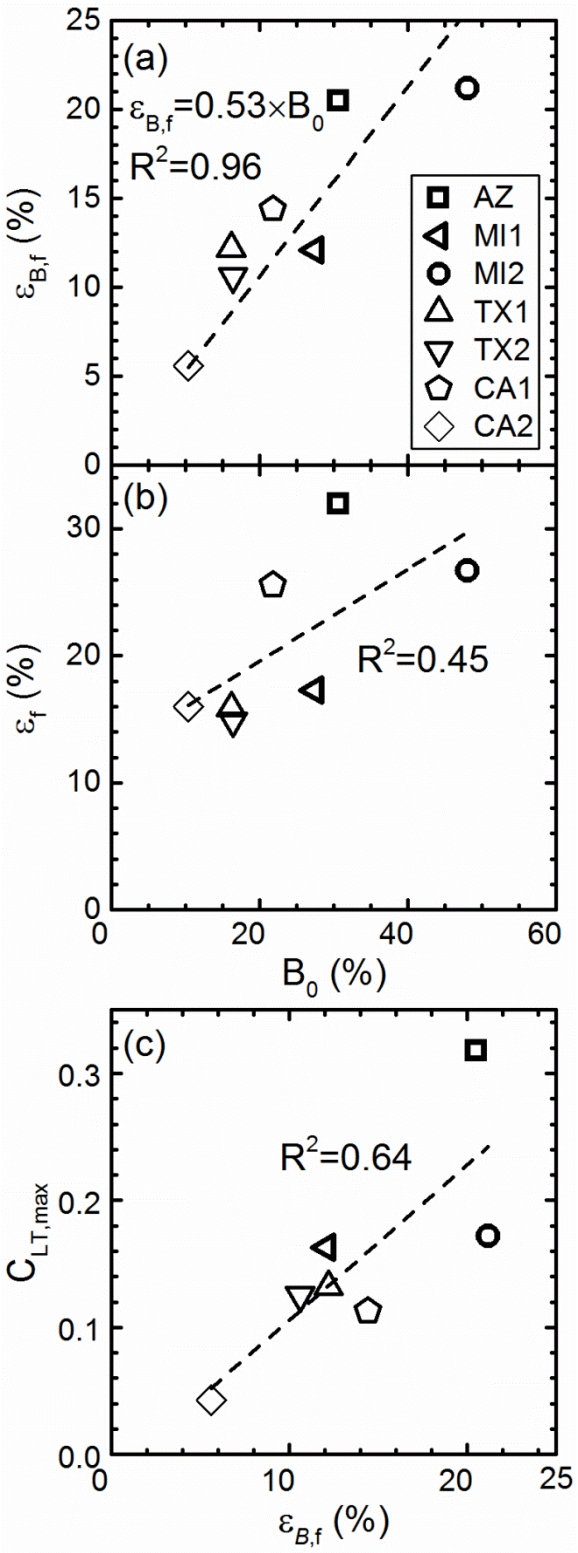

Figure 4-7 Relationships between percentage of biodegradable waste (B_0) and (a) final biodegradation strain ($\varepsilon_{B,f}$); (b) final total strain (ε_f); and (c) between maximum long-term compression ratio ($C_{LT,max}$) and $\varepsilon_{B,f}$.

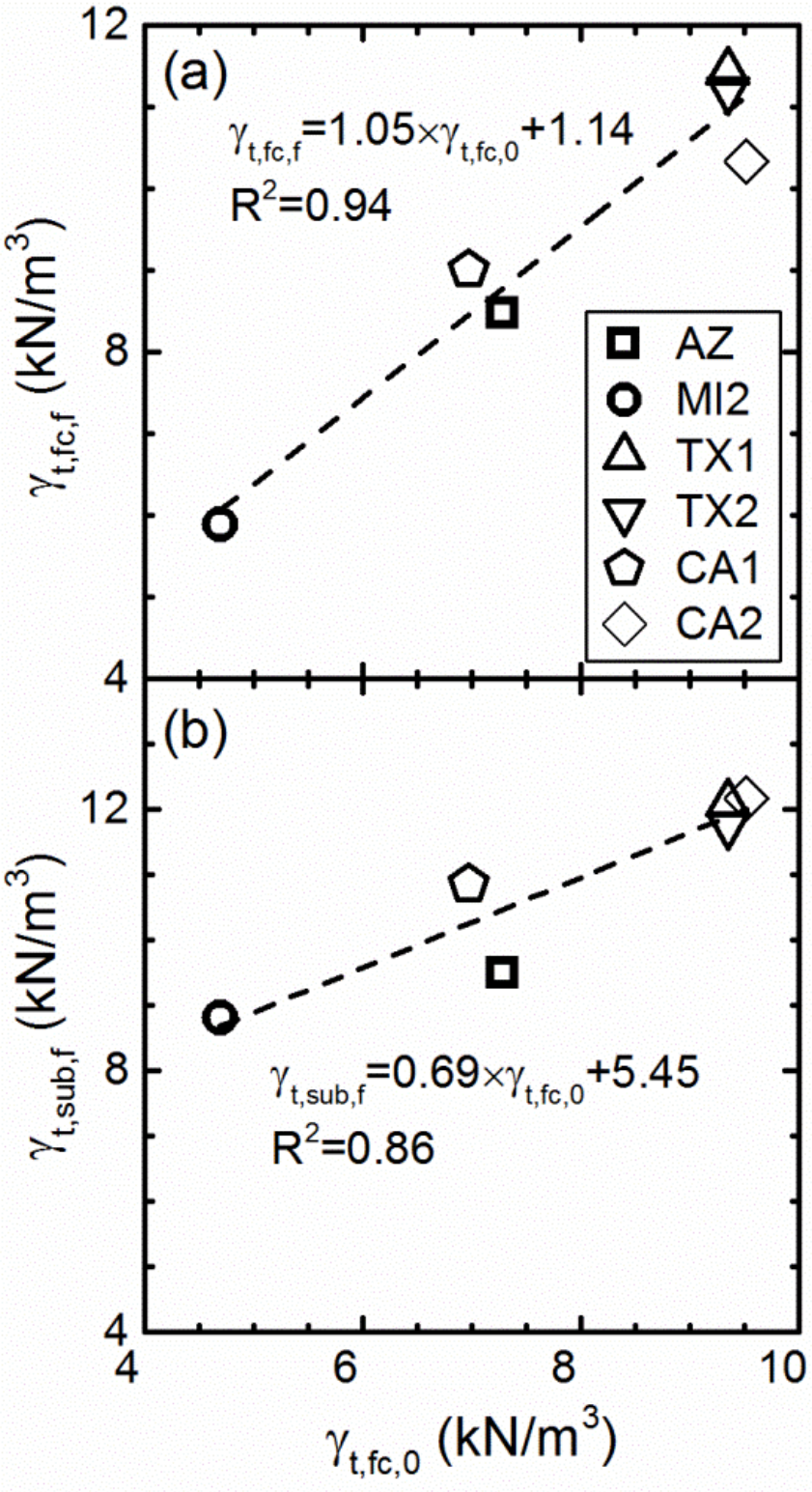

Figure 4-8 Correlations between initial total unit weight at field capacity moisture content ($\gamma_{t,fc,0}$) and (a) final total unit weight at field capacity moisture content ($\gamma_{t,fc,f}$); and (b) final total unit weight at saturation ($\gamma_{t,sat,f}$).

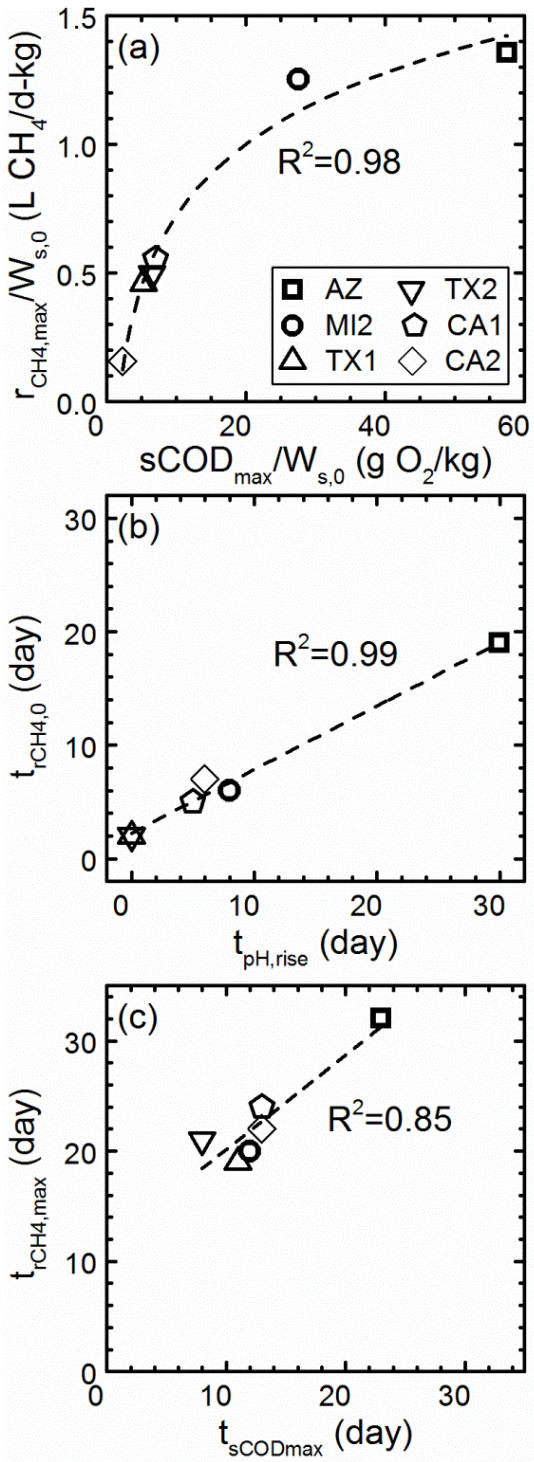

Figure 4-9 Correlations between characteristics of leachate and biogas: (a) normalized maximum CH_4 generation rate in biogas ($r_{CH4,max}/W_{s,0}$) and normalized maximum sCOD in leachate ($sCOD_{max}/W_{s,0}$); (b) time until initiation of CH_4 generation in biogas ($t_{rCH4,0}$) and time until pH rise in leachate ($t_{pH,rise}$); and (c) time until $r_{CH4,max}/W_{s,0}$ in biogas ($t_{rCH4,max}$) and time until $sCOD_{max}/W_{s,0}$ in leachate ($t_{sCODmax}$).

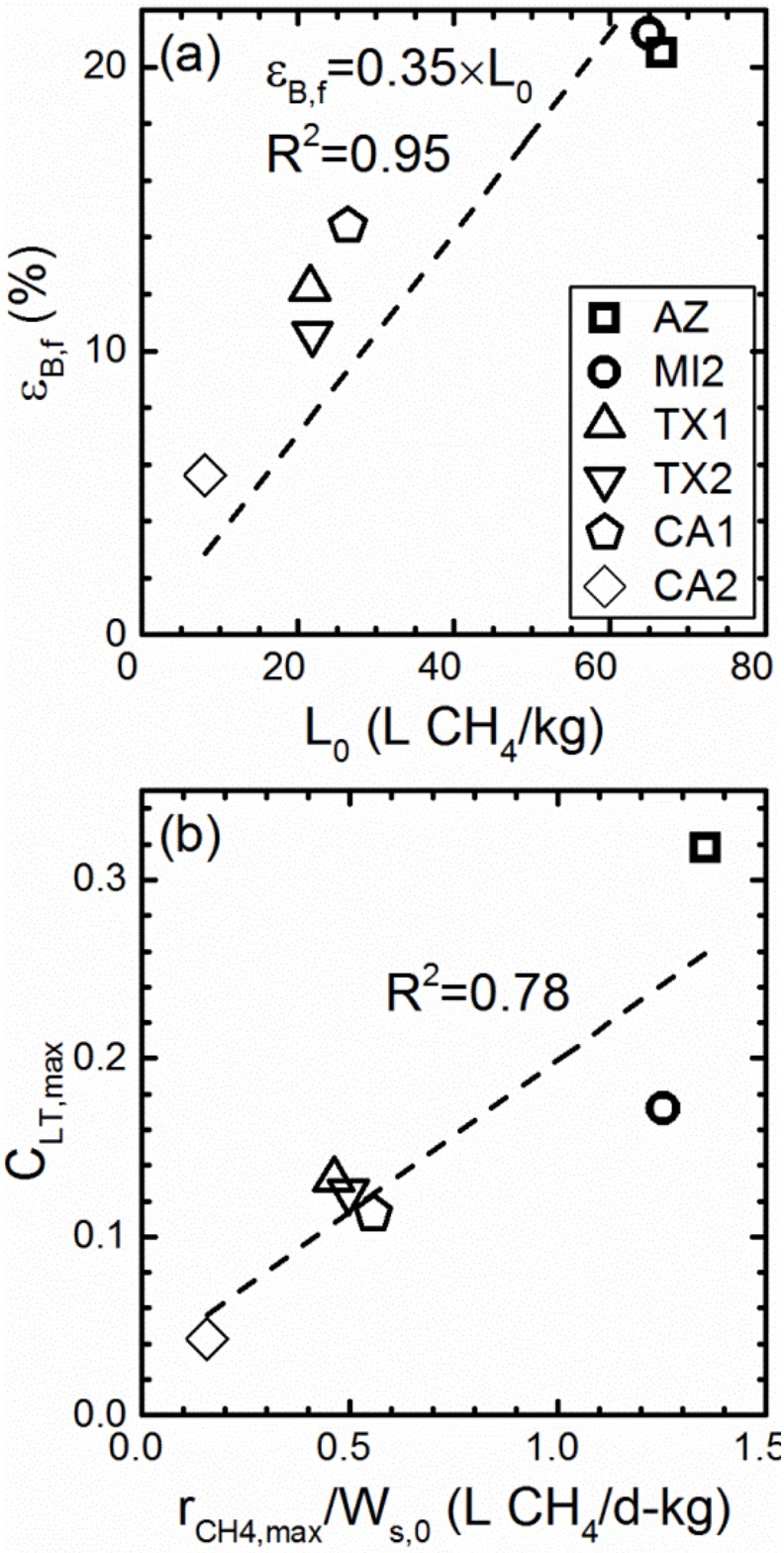

Figure 4-10 Correlations between CH_4 generation and settlement of the specimens: (a) final biodegradation strain ($\varepsilon_{B,f}$) and CH_4 generation potential (L_0); (b) maximum long-term compression ratio ($C_{LT,max}$) and normalized maximum CH_4 generation rate ($r_{CH4,max}/W_{s,0}$).

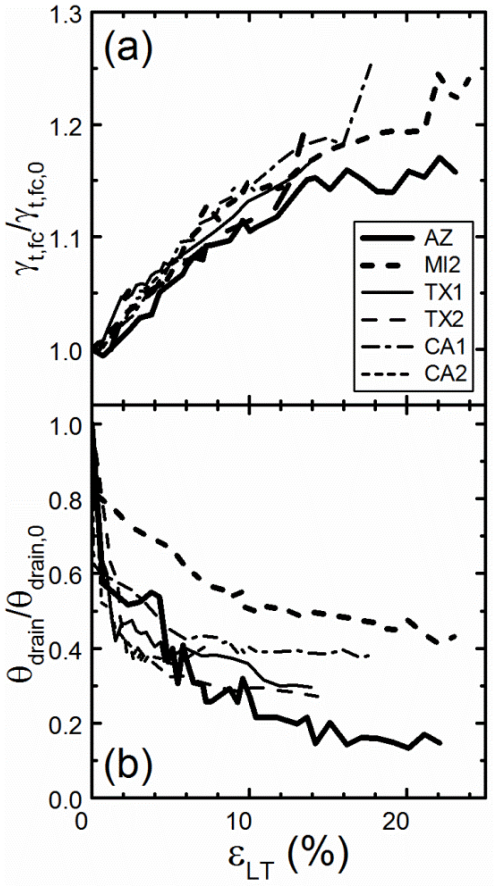

Figure 4-11 Relationships between long-term settlement (ε_{LT}) and (a) normalized $\gamma_{t,fc}$ ($\gamma_{t,fc}/\gamma_{t,fc,0}$); and (b) normalized θ_{drain} ($\theta_{drain}/\theta_{drain,0}$).

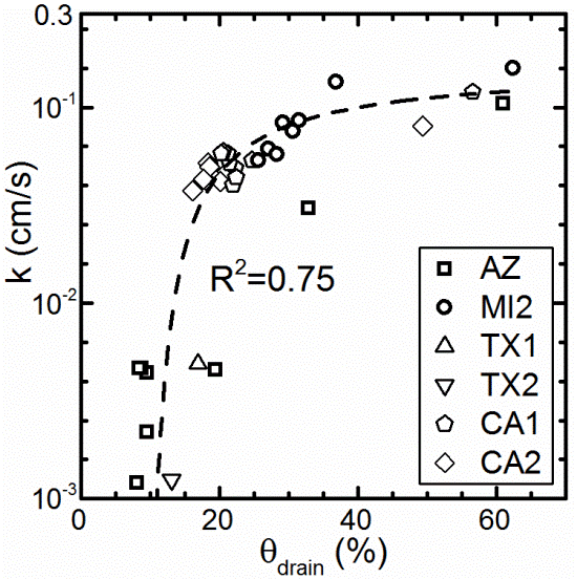

Figure 4-12 Correlation between "saturated" hydraulic conductivity in logarithmic scale (log(k)) and drainable volumetric moisture content (θ_{drain}).

Chapter 5 Archaeal Community Structure in Leachate and Municipal Solid Waste during Biodegradation of Municipal Solid Waste

5.1 Abstract

Duplicate carefully-characterized municipal solid waste (MSW) specimens were reconstituted with waste constituents obtained from a MSW landfill and biodegraded in large-scale landfill simulators for about a year. Repeatability and relationships between changes in physical, chemical, and microbial characteristics taking place during the biodegradation process were evaluated. Parameters such as rate of change of soluble chemical oxygen demand in the leachate (r_{sCOD}), rate of methane generation (r_{CH4}), rate of specimen volume reduction (r_{Vt}), DNA concentration in the leachate, and archaeal community structures in the leachate and solid waste were monitored during operation. The DNA concentration in the leachate was correlated to r_{CH4} and r_{Vt}. The r_{CH4} was related to r_{sCOD} and r_{Vt} when waste biodegradation was intensive. The structures of archaeal communities in the leachate and solid waste of both simulators were very similar and *Methanobacteriaceae* were the dominant archaeal family throughout the testing period. Monitoring the chemical and microbial characteristics of the leachate was informative of the biodegradation process and volume reduction in the simulators, suggesting that leachate monitoring could be informative of the extent of biodegradation in a full-scale landfill.

Fei, X., Zekkos, D., and Raskin, L. (2015). "Archaeal community structure in leachate and municipal solid waste is correlated to the methane generation and volume reduction during biodegradation of municipal solid waste." *Waste Management*, 36, 184-190.

5.2 Introduction

Approximately 150 million tons of municipal solid waste (MSW) are annually disposed of in landfills in the United States. More than 50% of the landfilled waste consists of paper, food and yard waste (EPA 2011), which are biodegradable under anaerobic conditions (Barlaz et al. 2010b). MSW biodegradation and CH_4 generation are greatly accelerated in bioreactor landfills compared to Subtitle D landfills, and generated CH_4 is collected efficiently via landfill gas pipelines deployed for active biogas extraction.

Significant challenges associated with the monitoring and operation of bioreactor landfills remain (Reinhart et al. 2002). Specifically, high variability in landfill monitoring data makes them hard to interpret (Wang et al. 2013) and guide decisions on landfill operations. The heterogeneity of landfilled waste often contributes to the variability in the parameters monitored during MSW biodegradation in bioreactor landfills (Staley et al. 2011a). Because studies to evaluate the repeatability of the biodegradation process under the same conditions are rare (Fei et al. 2014b), the expected differences in degradation characteristics in bioreactor landfills are not well established, impacting the optimization of MSW biodegradation and CH_4 collection.

Physical, chemical, and microbial processes take place simultaneously during MSW biodegradation altering the chemical, physical and mechanical properties of the solid, liquid and gas phases of MSW (McDougall 2007; Gawande et al. 2010; Fei et al. 2014a). While the evolution of biodegradation process parameters during MSW biodegradation has been studied, relationships among the many interdependent parameters have only been explored in a few studies (Reddy et al. 2011; Bareither et al. 2013b). It, thus, remains unclear which parameters are most characteristic of each process and most appropriate for monitoring MSW biodegradation in bioreactor landfills.

Physical and chemical processes taking place during MSW biodegradation are mostly driven by microbial processes conducted by a complex consortium of microorganisms. These microorganisms are present as biofilms attached to the solid waste particles and suspended in the leachate that percolates through the waste (Barlaz et al. 2010b). To the authors' knowledge, retrieval of solid waste and leachate samples from the same landfill simulator at different times during the biodegradation process, as presented herein, has not been attempted to date (see Fei et al. (2014a)). Thus, direct comparisons between the microbial communities in the solid waste and leachate during MSW biodegradation have not yet been established.

In the current study, MSW specimens of well-defined waste composition were prepared and degraded in duplicate laboratory landfill simulators using MSW excavated from a landfill with the intent to evaluate the repeatability of the MSW biodegradation process. Changes in the volume of waste, chemical properties of leachate, and microbial parameters in both leachate and solid waste were monitored for about a year to characterize their respective dynamics and investigate the relationships among them.

5.3 Material and methods

5.3.1 **Specimen preparation and experimental setup**

The MSW used in this study was excavated from a landfill in Austin, Texas, after two to three years of disposal and shipped in sealed drums to the University of Michigan. The waste composition was characterized according to the procedures described by Zekkos et al. (2010b). The waste was first separated into a finer fraction of soil-like material that passed through a 20-mm sieve and a coarser fraction. The coarser fraction was subsequently segregated based on the type of waste constituents (i.e., paper, soft plastic, and wood). Two MSW specimens were

reconstituted using these waste fractions based on the field waste composition on a wet weight basis. Each specimen weighed approximately 30 kg and consisted of 74.5% by weight soil-like material, 15.0% various types of paper, 5.5% soft plastic, and 5.0% wood. The gravimetric average moisture content of each specimen was 23% on dry basis.

Detailed descriptions of the simulators and operating procedures are presented by Fei et al. (2014a). In summary, each 42-L simulator (diameter = 0.3 m, height = 0.6 m) was filled manually with MSW on day 1. Initial volumes of the specimens were 37.1 L (simulator A) and 36.6 L (simulator B), and initial total unit weight was 7.9 and 7.8 kN/m^3, respectively. No moisture was added and there was no leachate recirculation in the first 12 days of the experiment. On day 12, the temperature of the simulators was raised from room temperature to 40±3 ^{0}C using a heating blanket. On the same day, drainage valves at the bottom of the simulators were closed and deionized water was added to the simulators to completely submerge the specimens. The specimens remained submerged for 10 minutes before the valves were opened and the leachate drained by gravity. Thus, the specimens were maintained at field capacity (the maximum moisture content of the specimen under gravitational drainage condition) in between saturations. The leachate was collected in a leachate tank and recirculated three times a week, resulting in a leachate recirculation rate of 20 L, on average, per week. The simulators were operated for about a year.

5.3.2 **Sampling and measurements of biogas, leachate and solid waste**

The biogas was collected in a gas sampling bag (SKC Inc., Eighty Four, PA) and triplicate biogas samples were taken from the headspace of each simulator immediately before leachate recirculation. Leachate was mixed using a magnetic stir plate and a sample was collected one

hour after specimen drainage started. Biogas and leachate were sampled three times a week until day 100, and once per week thereafter.

The biogas composition was measured by a gas chromatograph equipped with a thermal conductivity detector (HP5890, Agilent, Santa Clara, CA). The biogas volume was measured by a gas mass flow meter (XFM series, Aalborg, Orangeburg, NY) and adjusted to standard temperature and pressure conditions. The rate of CH_4 generation (r_{CH4}, L/day) was calculated by multiplying the daily biogas generation volume by its corresponding CH_4 concentration. The cumulative volume of generated CH_4 (ΣV_{CH4}) was calculated over time.

Leachate samples were centrifuged at 10,000 g for 15 minutes and the precipitates were stored at -80 ^{0}C for the extraction of biomass DNA. The supernatants were filtered through 0.45 μm nylon membrane filters and filtrates were analyzed for soluble chemical oxygen demand (sCOD) (APHA 2005). The change rate of sCOD (r_{sCOD}, mg/L-day) was calculated between each pair of measurements. The concentrations of volatile fatty acids (VFAs), i.e., acetic acid, propionic acid, butyric acid and valeric acid, in the filtrates were analyzed using an ion chromatography system (Dionex, Sunnyvale, CA) and converted to equivalent COD values (Smith et al. 2013). The detection limits were 5.0, 3.5, 5.5, and 3.6 mg COD/L for the respective VFAs.

The height of the MSW specimen in the simulators was measured continuously using a cable extension transducer (PT1 series, Celesco, Chatsworth, CA). The volume reduction (ΣV_t) of the specimens was calculated, and the rate of specimen volume reduction (r_{Vt}, L/day) between two consecutive r_{CH4} values was averaged to facilitate pair-wise data analysis. Solid waste samples were collected using a core sampling technique from three sampling ports located along the height of simulator B (Fei et al. 2014a). Each sample was retrieved by augering a piece of

sterilized thin-wall stainless steel tubing attached to a power drill into the waste (Fei et al. 2014a) and was stored at -80 ^{0}C for the extraction of biomass DNA. The total mass of each waste specimen was measured over time and the total unit weight was calculated. The total unit weight of the specimens in simulators A and B increased to 9.8 and 9.7 kN/m^3 by day 20 and changed to 10.8 and 10.6 kN/m^3 by day 350, respectively.

5.3.3 **DNA extraction, PCR amplification and pyrosequencing**

Total DNA was extracted from the pellets obtained by centrifuging the leachate samples of the duplicate simulators collected on days 23, 34, 46, 83, 109, and 178. A 2xTENS-C buffer was prepared with 100 mM Tris-HCl, 40 mM Ethylenediaminetetraacetic acid (EDTA), 200 mM NaCl, and 2% sodium dodecyl sulfate (SDS) mixed with 1% hexadecyltrimethyl ammonium bromide (CTAB). The biomass of each leachate sample was re-suspended with 0.4 ml of 2xTENS-C buffer and 15 µl of 10 mg/ml Proteinase K (Promega Corporation, Madison, Wisconsin) was added. Solid waste samples collected on days 47, 82, 111, and 179 were thawed on ice for about 1 hour and 0.4 g of each sample was weighed and transferred to a screw cap tube with a sterile spatula. 0.4 ml of 2xTENS-C buffer and 15 µl of 10 mg/ml Proteinase K was added. Duplicates were prepared for DNA extraction of each leachate and solid waste sample. Following this, a standard bead-beating and phenol-chloroform extraction protocol, as described in Urakawa et al. (2010), was performed.

DNA concentrations were measured using a spectrophotometer (NanoDrop 1000, Thermo Scientific, Wilmington, DE). The mass of DNA recovered from the leachate samples was normalized using the original volume of the collected leachate sample (ng DNA/ml leachate). The DNA extracted from the solid waste taken from the three sampling ports at each sampling time was pooled. Six leachate samples of each simulator (12 in total) and four solid

waste samples of simulator B were processed. The leachate and solid waste samples were not retrieved on the same day, but were collected one to two days apart only.

PCR amplification of the 16S rRNA gene was performed using the protocol of Pinto and Raskin (2012) except that archaeal pyrosequencing primers Univ-519F/Arch-915R were used (Klindworth et al. 2013). Quantification, purification and pooling of the amplicons were performed according to Smith et al. (2013) and the pooled amplicons were submitted to the Keck Center of the University of Illinois at Urbana-Champaign in Urbana, IL, for pyrosequencing (Genome Sequencer FLX+, 454 Life Sciences, Branford, CT).

5.3.4 **Processing and analyses of pyrosequencing data**

Pyrosequencing data were processed using Mothur (Schloss et al. 2009) as described by Pinto et al. (2012). A total of 152,555 quality-filtered and chimera free sequences were obtained for the 12 leachate samples and 3,203 sequences were obtained for the four solid waste samples. The sequences were clustered using the average neighbor approach to form operational taxonomic units (OTUs) at 95% sequence similarity cutoff (5% sequence divergence). The OTUs were classified using the RDP training set provided through Mothur at a confidence level cutoff of 80%. The Basic Local Alignment Search Tool was used to identify possible phylogenic placement of unclassified OTUs (Altschul et al. 1990). All of the 16 leachate and solid waste communities were sub-sampled *in silico* to 351 sequences per sample (1,000 iterations) for further analyses. The α-diversity of each community was calculated using the Inverse-Simpson diversity index (Legendre and Legendre 2012). The DNA sequences were submitted to NCBI BioProject (ID PRJNA242946).

5.4 Results and discussion

5.4.1 Duplicate landfill bioreactor simulators provided repeatable patterns in changes of leachate properties and CH_4 generation

The rate of CH_4 generation (r_{CH4}), the cumulative volume of generated CH_4 (ΣV_{CH4}), and the sCOD and VFA concentrations in the leachate are common parameters measured when monitoring MSW biodegradation (Pohland and Kim 2000; Barlaz et al. 2010b; Fei et al. 2014a). The change rate of sCOD (r_{sCOD}) reflects the production and consumption of sCOD by microorganisms. As shown in Figure 5-1, the leachate and biogas measurements for the duplicate simulators were very similar throughout the one year testing period highlighting their repeatability in a well-controlled laboratory study.

The evolution of the leachate properties is also characteristic of the MSW biodegradation process. Initial moisture addition on day 12 and subsequent leachate recirculation facilitated hydrolysis of biodegradable waste and transport of hydrolysis products, which serve as microbial substrates. The sCOD values in the leachate of simulators A and B were 2,285 and 2,133 mg/L, respectively, on day 12. The maximum r_{sCOD} values were observed at the same time in both simulators (day 20) when sCOD values were 4,187 and 5,048 mg/L, respectively (Figure 5-1a and b). The maximum propionate concentrations were 3,069 mg COD/L on day 25 in the leachate of simulator A and 4,220 mg COD/L on day 30 in the leachate of simulator B. The maximum acetate concentrations in the leachates of both simulators were measured on day 20 and were much lower than the corresponding propionate concentrations (Figure 5-1c). The high concentrations of sCOD, propionate, and acetate measured around days 20 to 25 indicated that by then soluble substrates had accumulated in the leachate and that syntrophic propionate

oxidation and methanogenesis were the rate-limiting steps of the MSW biodegradation process (Barlaz et al. 1989b; McMahon et al. 2004).

The sCOD concentrations in the leachate decreased to around 900 mg/L by day 70, fluctuated between 700 and 900 mg/L until day 150, and remained stable thereafter, resulting in r_{sCOD} values close to zero (Figure 5-1a). The propionate and acetate concentrations decreased to below the detection limit by day 50 (Figure 5-1c). These leachate characteristics indicated that the soluble substrates were depleted and hydrolysis of biodegradable waste had become the rate-limiting step (Barlaz et al. 1989b; McMahon et al. 2004).

CH_4 generation initiated promptly after initial moisture saturation of the specimens on day 12. The maximum r_{CH4} of 10.5 L/day was measured on day 32 following the measured maximum concentrations of sCOD, propionate, and acetate, indicating active microbial conversion of the soluble substrates to CH_4. The value of r_{CH4} decreased to around 3.0 L/d by day 60 and to less than 0.5 L/d by day 150 (Figure 5-1d). About 50% of the ΣV_{CH4} measured by day 350 was generated between days 20 and 50, indicating that MSW biodegradation was most intensive during this period. Approximately 90% of the ΣV_{CH4} measured by day 350 had been collected by day 150, suggesting that MSW biodegradation was largely completed by day 150. CH_4 was generated at low rates afterwards.

A total of 483 L and 475 L of CH_4 had been collected by day 350 from simulators A and B, respectively (Figure 5-1d). The CH_4 generation potential of the waste specimens was approximately 20 L CH_4 per kilogram of dry waste. This value is much lower than the reference value of 100 L/kg for general MSW used by United States Environmental Protection Agency (EPA 2005). However, the observed low CH_4 generation potential is reasonable taking into account the high percentage of soil-like material in the specimens (Fei et al. 2014b).

5.4.2 **Volume reduction of waste was mainly driven by microbial activity during active biodegradation**

Volume reduction of waste is not often reported in biochemical studies of MSW biodegradation. Despite the heterogeneity of the solid waste specimens, volume reduction measured during MSW biodegradation was in good agreement between the duplicate simulators. The rates of specimen volume reduction (r_{Vt}) increased from 0 to around 0.07 L/day by day 16 and decreased to less than 0.01 L/day by day 150. The initial volume reduction, i.e., 15±1% of the ΣV_t of simulators A and B measured by day 15, was primarily the result of physical compression mechanisms such as particle movement, particle reorientation, particularly associated with leachate flow as well as material creep, particle lubrication and softening of paper immediately after specimen placement and moisture addition. The physical compression, with the exception of creep, was largely completed by day 20 (Fei and Zekkos 2013). The maximum r_{Vt} for simulators A and B were observed on day 17, and the volume reduction at that time was caused by both physical and microbial-induced compressions. The r_{Vt} remained high until around day 50, by which time the most intensive MSW biodegradation had been completed and hydrolysis had become the rate-limiting step of MSW biodegradation as discussed earlier. By day 50, 45±1% of the total observed ΣV_t was achieved (Figure 5-1e).

The r_{Vt} decreased to lower than 10% of the maximum rate by day 150, and 80±1% of the ΣV_t was achieved at that time. The specimen volumes decreased at much lower rates after day 150 and the cumulative specimen volume reductions reached 5.2 L (14.0% of initial volume) and 4.5 L (12.3% of initial volume) by day 350 for simulators A and B, respectively (Figure 5-1e). Overall, a significant portion of the long term volume reduction occurred during the most

intensive biodegradation period, indicating that the specimen volume reduction was mainly driven by microbial activity.

5.4.3 **Relationships among the r_{CH4}, r_{sCOD} and r_{Vt} were characteristic of MSW biodegradation**

Similar relationships among the r_{sCOD}, r_{CH4} and r_{Vt} were observed for the duplicate simulators. As shown in Figure 5-2a, a positive r_{sCOD} was concurrent with a low r_{CH4}, which suggested that accumulation of soluble substrates in the leachate produced by hydrolysis preceded intensive methanogenesis. A negative r_{sCOD} and a high r_{CH4} were measured before day 50, consistent with the observation that an increase in CH_4 generation paralleled a decrease in sCOD concentration. These data suggest that tracking the sCOD concentration in the leachate is informative of the r_{CH4} during intensive MSW biodegradation in laboratory. The r_{sCOD} remained close to zero after approximately day 50 regardless of the change in the r_{CH4} (Figure 5-2b).

The r_{Vt} was related to the r_{CH4} after day 17 when contribution of physical compression mechanisms to the r_{Vt} diminished (Figure 5-2c). The r_{CH4} and the r_{Vt} increased proportionally until the rates approached 7 L/d and 0.06 L/d, respectively. The strong relationship supports the conclusion that the observed volume reduction was primarily associated with biodegradation, which is expressed by the r_{CH4}. The maximum r_{Vt} did not exceed 0.06 L/d, whereas the r_{CH4} increased further to a maximum of around 10 L/d (Figure 5-2c). This analysis suggests that in laboratory experiments the volume reduction of MSW and CH_4 generation due to biodegradation are correlated.

5.4.4 **The concentration of DNA in leachate correlated well with r_{sCOD}, r_{CH4} and r_{Vt}**

The concentration of DNA in the leachate was used as a proxy of the quantity of microbial biomass in the leachate and was comparable between the duplicate simulators. On days 23, 34,

and 46, the DNA concentrations in the leachate of both simulators were higher than 6,000 ng/ml. The concentrations decreased by day 83 to less than 4,000 and 2,000 ng/ml in the leachate of simulators A and B, respectively, and to less than 1,000 ng/ml by day 178 (Figure 5-1f). Before day 23, the sCOD, propionate, and acetate concentrations increased rapidly, thus the high DNA concentration likely indicated that rapid growth of hydrolytic and fermentative *Bacteria* took place before this time point. Between days 23 and 46, the high r_{CH4} and negative r_{sCOD} suggested that an increase in methanogenic biomass took place, which was consistent with an increase in DNA concentration in the leachate of simulator A (Figure 5-1b, d and f). The DNA concentration in the leachate of simulator B did not change substantially during this time period (Figure 5-1f).

It should be noted that the DNA associated with dead or inactive microbial cells and extracellular DNA were not distinguished from DNA associated with active cells since only total DNA was measured in this study. Therefore, this approach would be suitable to monitor an increase in microbial biomass as a result of growth, but would not necessarily be suitable to monitor a decrease in activity or microbial biomass as DNA is relatively stable in most environments (Pietramellara et al. 2009; Chiao et al. 2014). However, a significant decrease of the DNA concentrations between days 46 and 178 corresponded well with the decreasing r_{CH4} and the low r_{sCOD} during the same period (Figure 5-1b and f). This decrease in leachate DNA concentration may suggest that DNA not associated with active microbial cells was removed from the leachate and was retained in the solid waste during leachate recirculation. Regardless of the exact reason for this decrease, DNA concentrations in the leachate correlated well with microbial activity measured using chemical data and thus with the MSW biodegradation process. The DNA concentration in the leachate was positively correlated to the r_{CH4} and the r_{Vt},

indicating biomass levels in the leachate were linked to the rate of CH_4 generation (Figure 5-3a) and the rate of volume reduction of waste (Figure 5-3b). Overall, direct relationships were identified among the four parameters, r_{CH4}, r_{sCOD}, r_{Vt} and DNA concentration in the leachate that describe changes taking place during MSW biodegradation.

5.4.5 **Archaeal communities in the leachate are indicative of those in the solid waste**

The dominant OTU in all leachate archaeal communities was a member of the family *Methanobacteriaceae,* and accounted for 88% to 95% of the archaeal abundance by day 46 and around 99% between days 83 and 179. The second to the fourth most abundant OTUs represented members of the *Methanosarcinaceae, Desulfurococcaceae,* and *Methanomicrobiaceae,* and accounted for 1% to 9% of the archaeal abundance. The relative abundance of *Methanosarcinaceae* in the leachate communities decreased from more than 5% to less than 0.5% between days 23 and 83 (Figure 5-4a and b). The archaeal communities in the solid waste were dominated by *Methanobacteriaceae* as well; their relative abundance increased from 78% to 92% between days 47 and 179. The relative abundance of *Methanosarcinaceae* in the solid waste communities decreased from 12% to 2% between days 47 and 179 (Figure 5-4c). The Inverse-Simpson diversity index of the leachate and solid waste communities generally decreased with time indicating a decrease in archaeal diversity when biodegradation was more complete (as shown in Table 5-1).

The five most abundant OTUs that were classified as methanogens represented more than 99.5% of all detected methanogenic OTUs (Figure 5-4a, b and c). They were categorized into two groups based on their (in)ability to use acetate as a substrate. The aceticlastic methanogens include the families *Methanosarcinaceae* and *Methanosaetaceae,* whereas the hydrogenotrophic methanogens consisted of families *Methanobacteriaceae, Methanomicrobiaceae,* and an

uncultured *Methanomicrobia*. The abundance of each group of methanogenic OTUs was normalized to the total abundance of all methanogenic OTUs (%). The relative abundance of hydrogenotrophic methanogens in the leachate increased from 95% to higher than 99% between days 23 and 178. The corresponding value in the solid waste increased from 88% to 97% (Figure 5-4d). The relative abundances of aceticlastic methanogens in the leachate and solid waste decreased from 5% to 0.5% and from 12% to 3%, respectively (Figure 5-4e). The aceticlastic methanogens were more abundant when soluble substrate concentrations were high and MSW biodegradation was intensive. In contrast, hydrogenotrophic methanogens became more abundant when soluble substrate concentrations were low and hydrolysis was the rate limiting step. These observations agree with and provide explanations for observations reported in previous studies on methanogens in solid waste and leachate of laboratory- and full-scale landfills (Nayak et al. 2009; Staley et al. 2011a; Staley et al. 2012; Bareither et al. 2013b)

The relative abundances of hydrogenotrophic and aceticlastic methanogens in the leachate of both simulators were in good agreement during the biodegradation process. Given the similar DNA concentrations in the leachate, as shown in Figure 5-1f, it was concluded that the absolute abundances of the different microbial populations were also similar in both simulators. Moreover, the relative levels of hydrogenotrophic and aceticlastic methanogens in the solid waste over time increased and decreased respectively and paralleled those in the leachate (Figure 5-4d and e), suggesting that methanogenic pathways in the solid waste and leachate were similar during MSW biodegradation. As a result, the status of methanogenesis in a waste specimen undergoing biodegradation can be informed by analyzing the archaeal community in the leachate.

Differences between the relative abundances of hydrogenotrophic and aceticlastic methanogens in the solid waste versus in the leachate likely resulted from different growth conditions in solid and liquid phases. Leachate was recirculated to saturate the waste specimens three times a week in this study. The recirculated leachate was either adsorbed to waste particles or drained by gravity to the leachate tank afterward. Hydrolysis of biodegradable waste is a surface reaction catalyzed by hydrolytic *Bacteria* adjacent to or attached to the waste particles, so hydrolytic products are released to the adsorbed leachate first (Vavilin et al. 2004). Leachate recirculation and drainage enabled mixing of the waste-adsorbed leachate and the gravity-drained leachate periodically, thus facilitating transport of the soluble substrates to the entire waste specimen and to the drained leachate.

Hydrolysis of biodegradable waste became rate-limiting after around day 50, therefore the r_{sCOD} for the leachate fluctuated around zero. Meanwhile, the r_{CH4} and r_{Vt} remained substantial between days 50 and 150, suggesting that MSW biodegradation continued (Section 3.1 and 3.2, Figure 5-1b, d and e). The data suggests that the soluble substrates were continually generated and consumed in the waste-adsorbed leachate before being transported to the drained leachate by recirculation after day 50. Therefore, differences between the relative abundances of the two groups of methanogens in the solid waste and leachate were likely influenced by the different availability of soluble substrates in the solid and liquid phases (Figure 5-4d and e).

5.4.6 **Lessons learned about monitoring the physical, chemical and microbial parameters during MSW biodegradation in bioreactor landfills**

Chemical and microbial characterization of leachate, specifically determining the r_{sCOD} and DNA concentration, is informative to monitor the overall MSW biodegradation process including volume change of waste and CH_4 generation. Frequent leachate recirculation facilitates mixing

of waste-adsorbed and drained leachate. Therefore, leachate characterization is an effective and efficient approach to monitor the general performance of a bioreactor landfill.

The high sCOD, VFAs, and DNA concentrations in the leachate observed between days 12 and 50 suggested that CH_4 was generated at considerable rates from the drained leachate as well. Therefore leachate drained from actively biodegrading waste in landfills should be properly managed to increase the effectiveness of CH_4 collection and reduce CH_4 emission (Spokas et al. 2006; Lozecznik et al. 2010). We also demonstrated that methanogenesis in the solid waste continued after dissolved organics (as indicated by the sCOD concentration) in the drained leachate were depleted. This observation suggests that improved MSW biodegradation may be achieved by extending the period of leachate recirculation and drainage even after the sCOD in the leachate reaches low values. On the other hand, it may not be necessary to maintain the same frequency of leachate recirculation. As a result, the leachate recirculation strategy should remain flexible and be optimized based on site-specific conditions and the degree of MSW biodegradation.

A lag time of up to several hundred days has been observed before the initiation of active methanogenesis in previous laboratory landfill simulators degrading MSW with low moisture content and under occasional leachate recirculation conditions (e.g., Bareither et al. 2013 and Gourc et al.). Frequent leachate recirculation dilutes and redistributes high levels of VFAs in waste-adsorbed leachate, thus preventing acidification and inhibition of methanogenesis (Vavilin et al. 2003). In this study, saturation of the MSW specimens and leachate recirculation resulted in an expedited initiation of active methanogenesis (within 10 days of the start of leachate recirculation). Therefore, moisture addition and leachate recirculation are effective strategies to achieve rapid MSW biodegradation and CH_4 generation.

5.5 Conclusions

Two MSW specimens were degraded in duplicate laboratory bioreactor landfill simulators. The changes of sCOD of leachate, CH_4 generation, and volume reduction of waste of the duplicate simulators were repeatable and characteristic of the MSW biodegradation process. The r_{CH4} was strongly correlated to the r_{sCOD} and r_{Vt} when MSW biodegradation was intensive. The DNA concentration in the leachate was indicative of the quantity of microbial biomass and positively related to the r_{CH4} and r_{Vt}. Similar archaeal community structures in the leachate and solid waste were observed throughout the biodegradation process with *Methanobacteriaceae* being dominant. Therefore, monitoring chemical and microbial properties of the leachate was informative of the MSW biodegradation process and volume reduction of waste, suggesting that timely and detailed leachate monitoring has the potential to effectively evaluate the extent of biodegradation in full-scale bioreactor landfills.

5.6 Tables

Table 5-1 Summary of Mothur-processed pyrosequencing results of each sample at 95% sequence similarity cutoff, as well as the calculated Inverse-Simpson diversity indices.

Sample name and elapsed time (d)	Number of sequences[a]	Number of observed OTUs	Inverse-Simpson diversity index
Leachate-A 23	5961	20	1.15
Leachate-A 34	4184	26	1.24
Leachate-A 46	5828	27	1.32
Leachate-A 83	8523	19	1.09
Leachate-A 109	6290	27	1.09
Leachate-A 178	16080	30	1.05
Leachate-B 23	2232	12	1.19
Leachate-B 34	11635	31	1.09
Leachate-B 46	11564	33	1.11
Leachate-B 83	32143	28	1.02
Leachate-B 109	12858	21	1.02
Leachate-B 178	35257	38	1.02
Solid-B 47	675	7	1.58
Solid-B 82	909	9	1.28
Solid-B 111	351	8	1.61
Solid-B 179	1268	7	1.16

[a] quality-filtered and chimera free pyrosequencing reads.

5.7 Figures

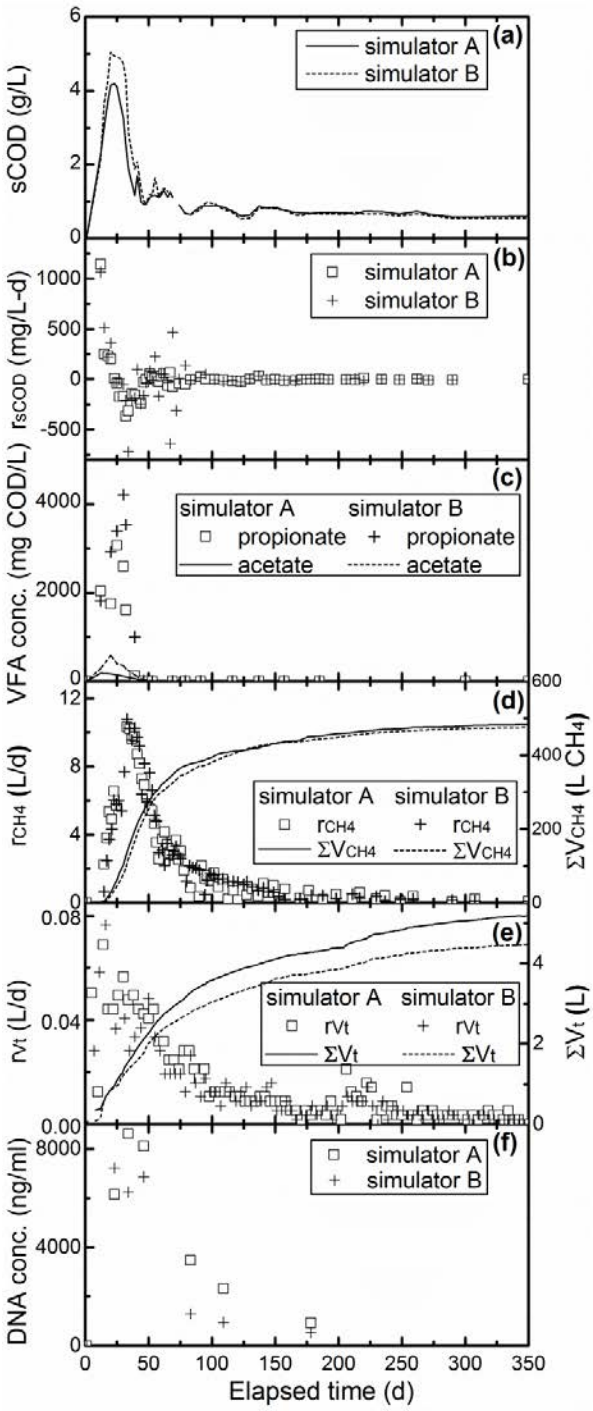

Figure 5-1 Measurements obtained for simulators A (hollow symbols and solid lines) and B (cross symbols and dash lines) during MSW biodegradation: (a) soluble chemical oxygen demand (sCOD) in the leachate; (b) change rate of sCOD in the leachate (r_{sCOD}); (c) concentrations of propionate and acetate in the leachate; (d) cumulative volume of generated CH_4 (ΣV_{CH4}) and rate of CH_4 generation (r_{CH4}); (e) cumulative specimen volume reduction (ΣVt) and rate of specimen volume reduction (r_{Vt}); (f) DNA concentration in the leachate.

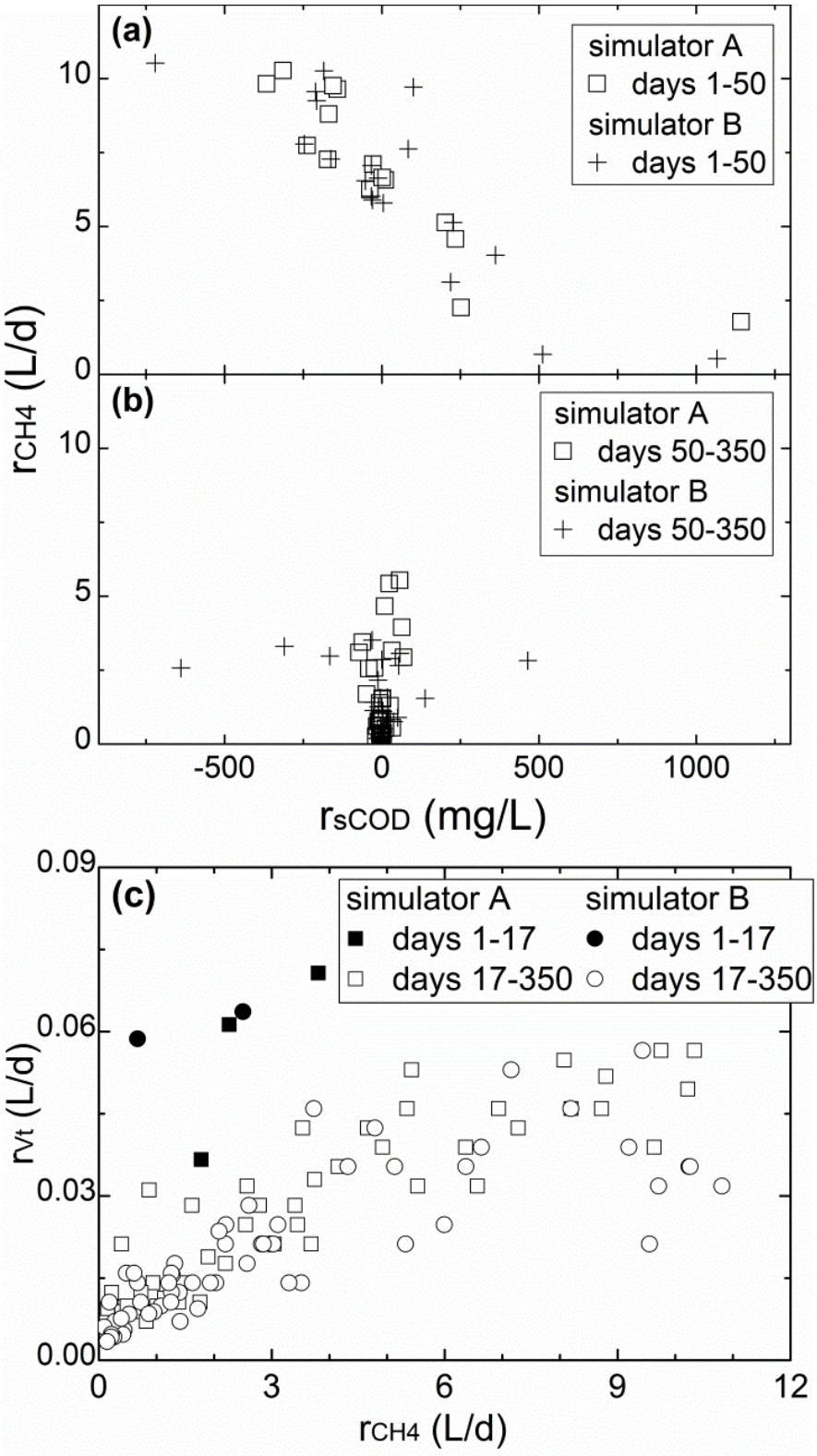

Figure 5-2 Relationships between physical and chemical parameters during MSW biodegradation of simulators A (hollow symbols) and B (cross symbols): (a) change rate of sCOD (r_{sCOD}) and rate of CH_4 generation (r_{CH4}) between days 1 and 48, and (b) between days 48 and 350; (c) rate of CH_4 generation (r_{CH4}) and rate of specimen volume reduction (r_{Vt}).

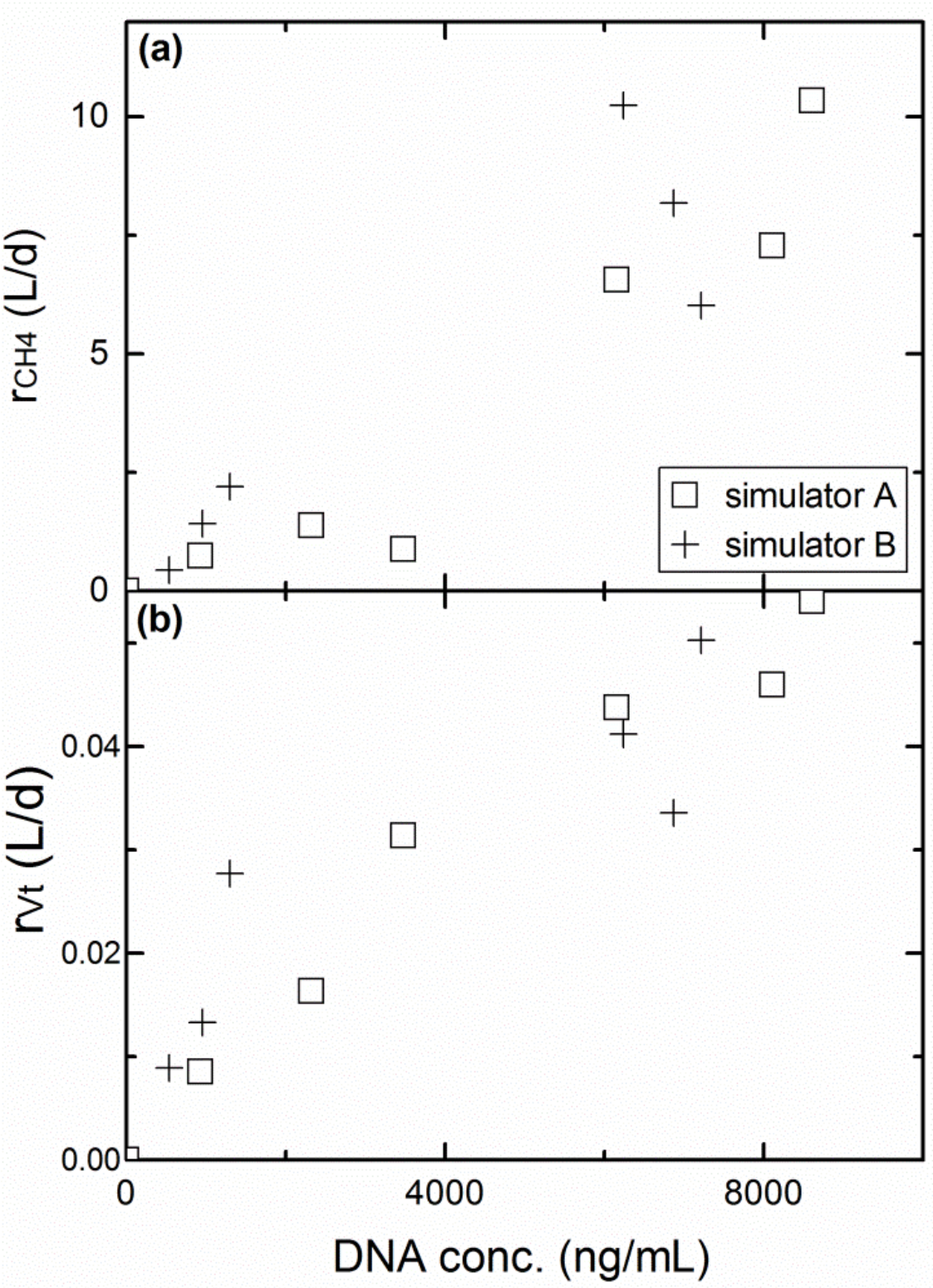

Figure 5-3 Relationships between physical, chemical and microbial parameters during MSW biodegradation of simulators A (hollow symbols) and B (cross symbols): (a) DNA concentration in the leachate and rate of CH_4 generation (r_{CH4}), and (b) DNA concentration in the leachate and rate of specimen volume reduction (r_{Vt}).

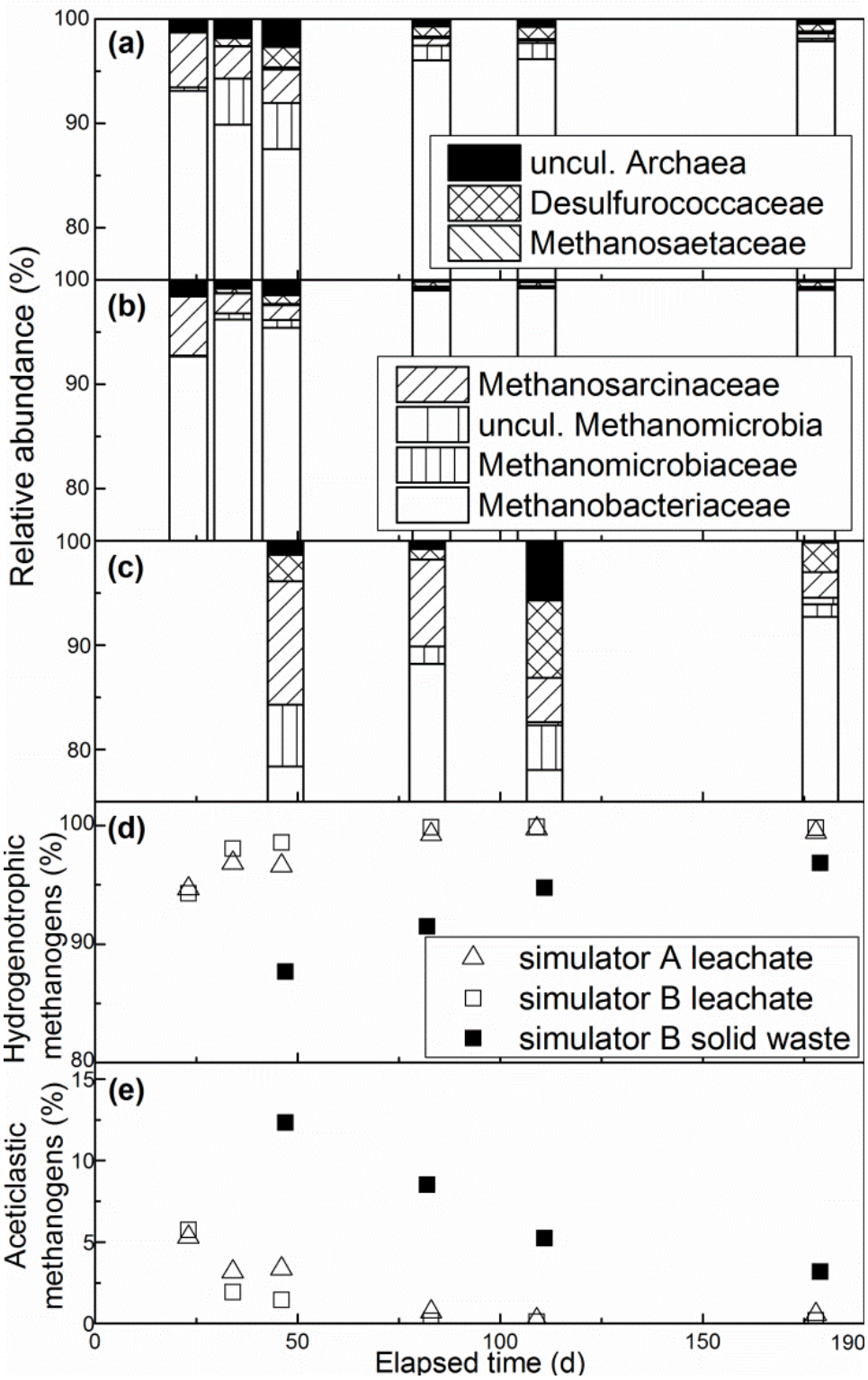

Figure 5-4 Temporal change of archaeal community structures in the leachate and solid waste of simulators A and B: (a) relative abundances of OTUs in the leachate of simulator A; (b) relative abundances of OTUs in the leachate of simulator B; (c) relative abundances of OTUs in the solid waste of simulator B; (d) relative abundances of hydrogenotrophic methanogens among all methanogens; (e) relative abundances of aceticlastic methanogens among all methanogens.

PART III IMPACTS OF DEGRADATION ON MECHANICAL PROPERTIES OF MUNICIPAL SOLID WASTE

Chapter 6 Shear Strength and Shear-wave Velocity of Fresh and Degraded Municipal Solid Waste

6.1 Introduction

6.1.1 Shear strength of municipal solid waste and testing methods

Modern municipal solid waste (MSW) landfills are steadily increasing in size to accommodate the growing amounts of generated MSW and to maximize waste containment capacity. Thus, it is becoming more common for many landfills to reach heights of 100 m or more. The slopes of these mega-size facilities need to remain stable under static and dynamic loads. Unfortunately, landfill slope instabilities continue to occur (Eid et al. 2000; Huvaj-Sarihan and Stark 2008; Jafari et al. 2013; Zekkos et al. 2013c).

Probably the most critical input parameter in assessing the stability of landfill slopes is the shear strength of MSW. A significant number of studies have been conducted to assess the shear strength of MSW in the laboratory using large-size experimental devices. In this paper, large-size testing is defined as tests that have specimen diameter or width that is at least 300 mm, a definition that is consistent with earlier recommendations (Bray et al. 2009; Athanasopoulos 2011b). Most commonly, large-size direct shear testing has been conducted (e.g., Landva and Clark 1990; Bray et al. 2009; Singh et al. 2009; Zekkos et al. 2010a; Bareither et al. 2012c;

Partially submitted as Fei, X., and Zekkos, D. (2016). "Comparison of constant load and constant volume simple shear testing of municipal solid waste." *Canadian Geotechnical Journal*, (under review).

Zekkos et al. 2013a). Large-size triaxial shear testing has also been conducted by some researchers (e.g., Jessberger and Kockel 1993; Grisolia et al. 1995; Zekkos et al. 2012; Ramaiah et al. 2014), whereas large-size simple shear testing of MSW has been conducted as part of two studies only (Kavazanjian et al. 1999; Pelkey et al. 2001).

The simple shear test was originally developed to evaluate the shear response of soils under simple shear strain conditions (Kjellman 1951; Roscoe 1953; Bjerrum and Landva 1966). Following 1-D compression of a specimen (or consolidation for a saturated specimen), horizontal shear stress is applied and the major principal shear stress axis rotates. Simple shear testing has been executed on a large range of natural soils (e.g., Bjerrum and Landva 1966; Sivathayalan 1994) and is presently a common test in engineering practice. It does, however, have several limitations (e.g., La Rochelle 1981). Among the most important limitations is the non-uniformity of normal and shear stress on the specimen boundaries due to the lack of complementary shear stresses on the sides of the specimen (Duncan and Dunlop 1969; Prevost and Høeg 1976; Budhu 1984; DeGroot et al. 1992).

Despite the significantly smaller testing database in simple shear for MSW, simple shear testing has important advantages over triaxial testing and direct shear testing of MSW. MSW has been shown to be one of the most anisotropic geomaterials due to the presence of fibrous constituents, such as paper, soft plastics and wood, that tend to become horizontally oriented during compaction and upon application of a vertical load. Evidence of this layering has been observed both in the field and the laboratory (Gotteland et al. 2000; Zekkos 2013). In fact, it has been shown that MSW has significant similarities to fibrous peats (Zekkos 2013). In triaxial testing of the material, it is practically impossible to avoid the contribution of fibrous waste constituents on the stress-strain response. Thus, shear resistances observed in triaxial shear are

high with friction angles (φ) of 48 degrees or higher (e.g., Zekkos et al. 2012). However, as shown by Bray et al. (2009), in direct shear testing, the horizontal failure plane is parallel to the orientation of the fibrous waste constituents and as a result the shear resistance in direct shear is the lowest. Still, direct shear testing essentially forces the failure plane. Given the variability in the constituents of a waste specimen, the predefined horizontal failure plane may not necessarily be the weakest, and a weaker plane may exist that is not tested. Such plane, if present, would be the failure plane in simple shear testing. However, no experimental results on the comparison in shear response of MSW between simple shear and direct shear testing has been reported so far.

In addition, the overwhelming majority of tests to assess the shear strength of MSW have been conducted under "drained" conditions. These testing conditions are appropriate for conventional "dry tomb" landfills where the waste has low moisture content, typically well below field capacity. However, in old, or abandoned, landfills without a properly operating leachate collection and removal system or a final cover system, as well as in recirculation and bioreactor landfills, the moisture content of MSW may be significantly higher. The waste may even, in some occasions, become submerged in leachate and, in the absence of gas generation, approach saturation. In addition, there have been field evidences of trapped leachate and gas pressures within layers of waste that are "encapsulated" between daily cover soil layers of lower permeability (e.g., Jiang et al. 2010; Zhan et al. 2015). In these cases the stress-strain response of MSW in "undrained" conditions is of interest. There are no large-size (>300-mm diameter) specimen studies that have investigated the response of MSW in "undrained" shearing conditions. Undrained triaxial shearing tests have been conducted by Karimpour-Fard et al. (2011) who used a 200-mm diameter triaxial device and Shariatmadari et al. (2009) who tested specimens that were 220-mm in diameter. For both studies the waste originated from the Metropolitan Center

landfill in Salvador, Brazil. Triaxial tests were also conducted by (Ramaiah et al. 2014) using 150-mm diameter specimens and Reddy et al. (2011) that involved tests on synthetic waste specimens that were 50-mm in diameter. Harris et al. (2006) tested 152-mm diameter MSW specimens in simple shear testing.

6.1.2 **Characteristics of MSW that influence its shear strength**

Characteristics of landfilled waste often vary widely in the field due to variable operating and environmental conditions, especially the composition, unit weight and degree of degradation of waste (Dixon and Jones 2005; Zekkos et al. 2006; Kavazanjian et al. 2013). These characteristics are influential to the shear strength of MSW and their impacts need systematic evaluation.

Most of the shear strength tests of MSW have been conducted in the laboratory, whereas only a few *in situ* tests have been reported (e.g., Richardson and Reynolds 1991; Houston et al. 1995; Mazzucato et al. (1999); Caicedo et al. 2002). Prior to laboratory testing, MSW samples are ni some cases characterized according to the procedures described by Zekkos et al. (2010b) or Dixon (2008). The samples were first separated into <20 and >20 mm fractions. The <20 mm fraction is typically soil-like in nature, i.e., includes significant amounts of daily cover soil and inorganic debris as well as fine waste inclusions. The >20 mm material consists primarily of discarded waste, i.e., paper, plastics, wood, metal and miscellaneous objects.

The respective proportions and properties of <20 and >20 mm fractions of waste influence its shear strength. Waste specimens containing more fibrous waste appear to be stronger than specimens with lower content of fibrous waste in simple shear testing (Kavazanjian et al. 1999). Testing results in Zekkos et al. (2010a) and Zekkos et al. (2013a) suggested that, in addition to the portion of fibrous waste, the mechanical properties of different fibrous waste constituents and the orientation of fibrous waste compared to the shearing plane, affect the shear

strength of specimens significantly in direct shear testing. Specimens of variable waste composition prepared with the same compaction effort in these two studies had similar shear strength. However, Bareither et al. (2012c) concluded that, in direct shear testing when fibrous waste constituents were oriented primarily parallel to the shearing plane, higher ϕ were obtained for specimens with greater fraction of <20 mm materials and stiff constituents such as gravel and metal, whereas lower ϕ were associated with greater fraction of paper and plastic waste.

The total unit weight of MSW increases with increasing disposal depth and compaction effort of waste (Zekkos et al. 2006). Elevated moisture content of waste, frequently encountered in open dumps, landfills with failing final covers and bioreactor landfills, results in higher total unit weight of waste. However, Reddy et al. (2009b) suggested that neither cohesion nor φ were correlated with the dry moisture content of waste ranging between 44-100% in direct shear testing.

Conflicting results have been reported on the impact of degradation of waste on its shear strength (Harris et al. 2006; Gabr et al. 2007; Hossain et al. 2009; Reddy et al. 2011; Bareither et al. 2012c; Fei and Zekkos 2015). Bareither et al. (2012c) and Harris et al. (2006) conducted direct shear and simple shear testing, respectively, on fresh and degraded waste, and reported increasing φ with decreasing cellulose plus hemicellulose to lignin ratio ((C+H)/L) which indicates an increase in degree of degradation. Similarly, Reddy et al. (2011) reported increased cohesion and decreased φ for degraded synthetic waste compared to fresh waste in both direct shear and triaxial shear tests. In contrast, a decrease in φ with decreasing (C+H)/L and volatile solids (VS) content, i.e., increasing degree of degradation, has been reported by Gabr et al. (2007) and Hossain and Gabr (2009).

Briefly, biodegradable waste constituents, including food waste, yard waste and different types of paper, are consumed by microorganisms and converted to biogas which consists primarily of methane (CH_4) and carbon dioxide (CO_2). Thus, the composition, unit weight and matrix structure of MSW change during degradation (McDougall 2007; Gawande et al. 2010; Fei et al. 2016). MSW degrades at variable rates and may be interrupted at different stages before being fully degraded in modern landfills due to widely varying and time-dependent environmental and operating conditions (Reinhart et al. 2002; Benson et al. 2007; Barlaz et al. 2010a; Fei and Zekkos 2016). The measured shear strength of degrading MSW likely depends on the specific characteristics of the waste at the time of testing. Mechanisms by which the shear strength of MSW may increase, reduce or remain the same can all be postulated. The matrix structure of waste may be loosened due to removal of biodegradable solid waste particles, resulting in reduced unit weight and consequently lower shear strength of waste after biodegradation. Alternatively, formation of excess voids in the matrix structure of waste could cause collapse of weakened waste structure, thus leading to densification of waste and increasing of its shear strength after biodegradation. The two counteracting processes may occur in waste simultaneously and results in negligible change in its shear strength.

6.1.3 **Shear-wave velocity of MSW**

The shear-wave velocity (V_s) is an important engineering property of MSW and is related to the small-strain shear modulus (G_{max}) of MSW using elasticity theory (Kramer 1996). The V_s can be used to characterize the stiffness of MSW (Zekkos et al. 2008) and is a critical input parameter in seismic analyses (Kramer 1996). Zekkos et al. (2014) analyzed testing results from three large-size laboratory studies on the V_s of MSW available in the literature using devices with specimen diameter or width between 150-305 mm. All three studies tested MSW from the Tri-Cities

landfill in CA using the resonant column device, cyclic triaxial device, and cyclic simple shear device, respectively (Lee 2007; Zekkos et al. 2008; Yuan et al. 2011). The values of V_s of the specimens were subsequently calculated from the values of G_{max}. An empirical and a semi-empirical model were then developed to correlate the V_s and G_{max} of waste with its unit weight and confining stress.

Zekkos et al. (2014) also summarized the influences of various factors on the V_s and G_{max} of MSW. Briefly, the loading frequency of dynamic testing has an impact on V_s and G_{max}. The three laboratory studies used frequencies ranging between 0.03-260 Hz, similar to *in situ* seismic testing with borehole methods (e.g., cross-hole and down-hole) typically entailing measurement frequencies approaching 100-300 Hz, whereas the frequencies for surface wave methods are in the range of 3-50 Hz. On the other hand, the V_s of MSW measured at frequencies higher than around 500 Hz (0.5 kHz) has not been reported. Confining stress, waste composition, γ_t and compaction effort were found to influence the V_s and G_{max} of MSW to different extents. The three aforementioned studies tested both loosely and densely compacted MSW specimens consisting of 18-100% of <20 mm fraction of waste at up to 300 kPa confining stress.

6.1.4 **Objectives of this study**

In this study, a 300 mm-diameter simple shear device was used to test the shear strength of waste specimens prepared using waste sampled from five locations in four landfills across the United States (U.S.). A unique extensive large-size experimental dataset of 53 constant load and 45 constant volume simple shear tests and 8 direct shear tests on fresh and fully degraded waste specimens and the corresponding V_s for 66 specimens is presented. Fresh waste specimens identical to the specimens tested at fresh state were degraded in 300 mm-diameter laboratory landfill simulators and the degradation processes were closely monitored. Fully degraded

specimens were tested to assess the impact of degradation on the shear strength of waste. Influences of other characteristics of waste, including composition, compaction effort, total and dry unit weight, and shearing mode (constant load, constant volume and direct shear) on the shear strength and V_s of waste were also investigated. Finally, the shear strength and V_s of waste were correlated.

6.2 Methodology

6.2.1 **Sampling and characterization of MSW**

MSW samples were collected from pits excavated at the surface from four landfills in U.S., Los Reales landfill in Arizona (AZ), Lamb Canyon landfill in California (two locations, CA3 and CAF), Sauk Trail Hills landfill in Michigan (MI), and Austin Community landfill in Texas (TX), and were shipped in sealed drums to the Geoenvironmental Engineering Laboratory at the University of Michigan (Sahadewa et al. 2014b; Zekkos et al. 2014). The field composition for each waste sample was characterized according to the procedures described by Zekkos et al. (2010b). The waste was first separated into a finer fraction of soil-like material that passed through a 20 mm sieve (<20 mm fraction) and a coarser >20 mm fraction. The >20 mm fraction was subsequently manually segregated based on the type of waste constituents. Three primary constituents of the >20 mm fraction by weight for all samples were paper, soft plastic and wood, and other minor constituents included hard plastic, metal, rubber, textile, rock and miscellaneous objects. No distinguishable food waste was found in any sample, likely because they had already been composted prior to excavation and sampling. The ages of the waste samples varied between six and fifteen months according to landfill records and the degree of anaerobic biodegradation

of waste was considered minimal based on visual inspection of the segregated paper and yard waste.

The segregated waste constituents from each sample were weighed and the corresponding percentages on a wet weight basis were calculated. A modified waste composition was calculated for each sample by increasing the percentages of the four major constituents, <20 mm fraction, paper, soft plastic and wood, to 100%, as other constituents were not considered significant by volume or mass. The only exception is the CAF waste sample in which stiff >20 mm particles (hard plastic, metal and rock) was included as an additional constituent in addition to the four major constituents. Moisture content on a dry weight basis (w_c) of the four major constituents from each sample was measured by heating the waste at 75 ˚C to avoid vaporizing organic compounds in the waste. The percentages of the major constituents by mass (%) and average moisture content ($w_{c,ave}$) for the modified waste composition were calculated on a dry weight basis. The volatile solids (VS) content of each dried waste constituent was evaluated by heating the waste at 550 ˚C. The measured properties of waste constituents in the fresh samples were tabulated in Table 6-1.

6.2.2 **Degradation experiment of MSW**

The experimental setup of waste degradation experiments and methodology for monitoring, sampling and measurements during the experiments are described in details in Fei et al. (2016) and Chapter 4. Briefly, MSW specimens were reconstituted using the modified waste composition, as shown in Table 6-1, and were manually loaded into five 42-L simulators each with a diameter of 300 mm and a height of 600 mm on day 1. The material was generally placed at a loose state, i.e., without significant compaction. Besides the vertical load from a plastic leachate distribution plate and a stainless steel rod for settlement measurement that impose <1

kPa vertical stress, no additional vertical stress was applied to the specimens. Thus the effect of mechanical compression due to vertical stress application on MSW biodegradation process and properties of the specimens is eliminated. The as-prepared total and dry unit weight of the specimens ($\gamma_{t,0}$ and $\gamma_{d,0}$) were calculated (Table 6-2).

After around 10 days, the temperature of the simulators was raised from laboratory temperature to 40±3 ^{0}C using heating blankets. The specimens were completely submerged by adding deionized water or recirculating leachate from the leachate distribution plate on top of the specimens for 10 minutes before the drainage valves were opened and the leachate drained by gravity. The leachate was collected in leachate tanks and recirculated to submerge the specimens three times a week. Thus, the specimens were maintained at field capacity w_c in-between leachate submersion and biodegradation conditions were enhanced. The cumulative volume of CH_4 generated from biodegradation of waste and the settlement of each specimen were measured with time to determine the progress of waste degradation.

The specimens were considered fully biodegraded after CH_4 generation stopped and the observed settlement of waste was attributed mostly to mechanical creep (Gourc et al. 2010; Bareither et al. 2013a; Fei et al. 2016). The degradation experiments were stopped after between 900-1500 days for the five specimens and the total strain (%), CH_4 generation potential (final cumulative volume of CH4 divided by initial dry weight of waste in L CH_4/kg), and final total and dry unit weight ($\gamma_{t,f}$ and $\gamma_{d,f}$) of the specimens were calculated (Table 6-2).

6.2.3 **Simple shear testing of MSW at the University of Michigan**

A prototype 300 mm-diameter simple shear device has been developed and used in this study. The device, shown in Figure 6-1, allows the performance of simple shear tests with a cylindrical specimen that has a nominal diameter of 300 mm and a maximum height of 138 mm. Two micro

stepper motors are used to apply the vertical and horizontal loads and two 4.4 kN (equivalent to around 600 kPa for a 300 mm diameter specimen) load cells are used to measure the loads. Two displacement transducers are used to measure the vertical and horizontal displacements and calculate the mean volumetric strain and the average distortion of the specimen during shearing. The specimen is prepared within a stack of 6.35 mm thick, Teflon-coated circular aluminum shear rings that have minimal friction between one another instead of reinforced membranes of this size which are not generally available and are very expensive to manufacture. An unreinforced specimen membrane is used as a cushion to protect the stacked shear rings.

Once a specimen was prepared, it was first compressed in a compression device at a target stress in the vertical direction (σ'_{v0}, one-dimensional compression) for 23±1 hours (1,380±60 minutes). The specimen was then unloaded and placed in the simple shear device, and consolidated for 1 hour at the same target σ'_{v0}. The as-consolidated total ($\gamma_{t,con}$) and dry unit weight ($\gamma_{d,con}$) of the specimen prior to shearing were calculated.

A simple shear test can be conducted either by maintaining a constant vertical stress, or constant height during shearing. When vertical stress is maintained constant, the specimen may compress or dilate (with movement in the vertical direction). This is typically referred to as a constant load (CL) test and is equivalent to a drained test. When constant height is maintained during shearing, the specimen volume remains the same and the test is known as a constant volume (CV) test. To maintain CV conditions, the vertical stress changes during shearing. For contractive material response, vertical stress reduction is needed to maintain CV conditions. The reduction in vertical stress is considered equal to the amount of pore pressure that would be generated if the specimen was saturated, as shown by Dyvik et al. (1987) for a clayey soil. Thus, the CV test is considered equivalent to an undrained test. Simple shear CV tests were conducted

according to ASTM D6528-07 (2007) for simple shear testing of soils. While no dedicated ASTM standard is available for simple shear CL tests, both ASTM D3080-11 (2011) for direct shear testing and ASTM D6528-07 (2007) are used as references.

During each test, horizontal and vertical applied force and displacement were recorded with time. Subsequently, the shear stress (τ) and effective vertical stress (σ'_v) are calculated as the horizontal and vertical load divided by the cross-sectional area of the specimen, and shear strain (ε) and vertical strain (ε_v) are calculated as the horizontal and vertical displacements during shearing divided by the specimen height prior to shearing. The specimens were sheared at constant and slow shearing strain rate of between 0.34-0.5% per minute. Selected specimens prepared using MI waste were subjected to 1-D compression for shorter or longer durations, or sheared at lower or higher shearing strain rates to investigate the effects of vertical stress duration and shearing rate on the shearing response of MSW, respectively.

6.2.4 **Determination of effective friction angle**

Tests in this study were conducted on unsaturated MSW specimens. Although definitive data is presently unavailable, negative pore pressures are not expected to be significant at the macroscopic level (specimen size) due to the waste's high porosity and the range of constituents involved. Lee (2007) showed that there was no significant difference in the shear stiffness of MSW for specimens below field capacity to fully submerged specimens, an indication that negative pore pressure does not play a significant role in the stress-strain relationship of MSW. Note also that Dyvik et al. (1987) tested moist clays at their natural moisture content in constant volume, although the clays were likely to be saturated in the first place. Tests between these clays in truly undrained and constant volume conditions were equivalent for all practical

purposes. Similarly, Daliri and Basu (2013) showed that the monotonic response of dry, partially saturated and saturated silt subjected to constant volume simple shear was identical.

The simple shear test results are most commonly presented in terms of shear stress vs. shear strain. The maximum shear stress (τ_{max}), or the mobilized shear stress at a certain level of strain, is defined in the literature as the shear strength. Interpretation of the simple shear results becomes more complex, if the objective is to estimate the effective friction angle of the tested material. This is because only a single stress point (σ_v', τ) on the Mohr circle is measured during the test and thus, the Mohr circle (i.e., the specimen's stress state) is poorly defined. An extensive discussion of these issues has been made by others, particularly DeGroot et al. (1992), and is beyond the scope of this paper.

An assumption for the stress state at failure of the specimen needs to be made in order to estimate the friction angle of the material. DeGroot et al. (1992) discussed seven alternative assumptions. Of these assumptions, two of the most commonly used ones that also provide a reasonable range for the friction angle were used in this study, and are shown in Figure 6-2. One assumption is that the horizontal plane is the failure plane, i.e., the plane of maximum obliquity. In that case, the friction angle of the soil is given by Eqn. 6-1:

$$\varphi_{tan} = \beta = \tan^{-1}\frac{\tau_{hf}}{\sigma_{vf}'} \tag{6-1}$$

where τ_{hf} is the measured horizontal shear stress at failure, and σ_{vf}' is the measured vertical effective stress at failure. This assumption is generally considered incorrect (Roscoe 1953; Airey et al. 1985; DeGroot et al. 1992), but is widely used in practice because it yields a low, and thus conservative, friction angle. The second theory assumes that the horizontal plane is the plane of

maximum shear stress. Roscoe et al. (1967) suggested that this theory was valid for drained tests on medium-loose sand, but not for tests on dense sand and was also reasonable for undrained tests on sands regardless of void ratio. In this case, the friction angle of the soil is given by Eqn. 6-2:

$$\varphi_{sin} = \alpha = \sin^{-1}\frac{\tau_{hf}}{\sigma_{vf}'} \quad (6\text{-}2)$$

6.2.5 **Specimen preparation using fresh and degraded MSW**

After the degradation experiments were completed, the simulators were disassembled. Caution was taken to minimize disturbance to the degraded waste specimen during disassembly of each simulator. As illustrated in Figure 6-3, the Plexiglas column of a simulator containing a fully degraded waste specimen was moved onto the specimen pedestal of the simple shear device. A 300-mm diameter latex membrane was wrapped around the column and the column was carefully pulled out to the desired initial height of a specimen. Extra waste left in the column was separated from the specimen using a wood saw and used later to prepare another specimen. One or two "undisturbed" degraded MSW specimens were retrieved from each simulator for simple shear testing. The composition of the degraded waste specimen was characterized after shear testing following the same procedure described previously and % of the major constituents, $w_{c,ave}$, and VS of each dried waste constituent were measured and listed in Table 6-3.

Fresh waste specimens of identical waste composition and as-prepared unit weight as those loaded in the landfill simulators were reconstituted for simple shear testing. After testing the "undisturbed" degraded waste specimens retrieved directly from the landfill simulators, degraded waste specimens were reconstituted using the same composition and unit weight as the

"undisturbed" specimens. Fresh and reconstituted degraded specimens were prepared under either minimal or high compaction effort to different dry unit weight. Specimens subject to minimal compaction effort were prepared by simply placing the waste carefully within the stacked shear rings without any compaction. The other specimens were compacted in three to four layers by dropping a 98 N hammer from a height of 0.9 m for 30 times per layer to achieve a dry unit weight close to its maximum possible value at the current w_c following the procedure described in Zekkos et al (2012).

Waste constituents were not modified in size for the specimens used in degradation experiments and simple shear tests, as this process has been shown to result in degradation (Pommier et al. 2010; Zhang and Banks 2013) and shear responses (Bray et al. 2009; Athanasopoulos 2011b) that may not be representative of field conditions. Instead, over-sized waste constituents were not used in specimen preparation. To accommodate the fixed specimen diameter of 300 mm, the largest particle size of >20 mm waste constituents was 1/6 of the diameter of the specimen (50 mm). However, for fibrous waste constituents such as paper, soft plastics and branch, a maximum size of 1/4 the specimen diameter (75 mm) was allowed, consistent with previous recommendations (Bray et al. 2009; Athanasopoulos 2011b). Note that ASTM D6528-07 (2007) only requires that the largest grain size is not larger than 1/10 of the specimen height, a requirement satisfied for the <20 mm fraction of waste. The >20 mm particles were also expected to be horizontally oriented (i.e., the larger constituent dimension is along the horizontal direction), so this also satisfied this requirement.

6.2.6 **Direct shear testing of MSW at the University of Michigan**

The configuration of the large-size simple shear device was modified to perform direct shear testing on MSW. A rectangular specimen box with internal dimensions of 300- x 400- mm is

used to contain the lower part of a specimen, and a stack of shear rings supported by an interface plate contains the upper part of the specimen. The 300 mm-diameter shear rings are locked to the interface plate and no lateral movement is allowed. There is a 300 mm-diameter opening on the interface plate as well, so that the cross-sectional area of a specimen on the predefined shearing plane in direct shear is identical to the horizontal area of a specimen in simple shear. The extra length of a specimen in the lower specimen box provides continuous shearing surface along the direction of the predefined shearing plane. The heights of the upper and lower parts of a specimen for direct shear testing are both approximately 50 mm. A schematic of the direct shear testing setup is illustrated in Figure 6-4.

Specimens reconstituted using TX and CAF wastes were tested in direct shear. Direct shear testing was conducted while maintaining a constant σ'_v that is equal to the target σ'_{v0} in accordance with ASTM D3080-11 (2011). The horizontal displacement of each specimen was recorded with time and τ and ε_v were calculated from recorded data.

6.2.7 **Shear-wave velocity measurement of MSW in the lab at the University of Michigan**

A pair of bender elements is used to measure the V_s of MSW specimens. The bender elements were manufactured in the Geoenvironmental Engineering Lab at the University of Michigan. As illustrated in Figure 6-5, the bender element in the specimen pedestal serves as a shear-wave transmitter and the other in the top platen serves as a receiver. The transmitter is excited with a supply voltage to generate waves that are sensed by the receiver. A function generator (Agilent Inc.) is used to excite the transmitter using one cycle of sinusoidal wave at frequencies between 1-8 kHz.

In addition, a pair of identical accelerometers attached to the side of the top platen and specimen pedestal is used to measure the Vs of MSW specimens. For this setup, a source wave is

generated by hitting the base plate of the simple shear device using either a rubber or plastic mallet in the horizontal direction. The accelerometer on the specimen pedestal senses the source wave and the accelerometer on the top platen senses the wave traveled through the specimen.

An oscilloscope is used to collect data from the bender elements and accelerometers. The V_s of a specimen was measured after immediate compression was completed and prior to shearing. By measuring the travel time of shear wave through the specimen (Δt_s), the shear-wave velocity of the specimen (V_s) can be calculated using Eqn. 6-3:

$$V_s = \frac{L}{\Delta t_s} \tag{6-3}$$

where L (m) is the tip-to-tip distance between the bender elements or the edge-to-edge distance between the accelerometers. The determination of Δt_s for geomaterials has been studied extensively by multiple researchers (e.g., Viggiani and Atkinson 1995; Lee and Santamarina 2005) and is not the focus of this paper. The approach described by Sahadewa et al. (2014b) which is commonly used in the literature is adopted here. The V_s of each specimen is normalized to V_{s1} according to Eqn. 6-4 (Kayen et al. 2013):

$$V_{s1} = V_s \times \left(\frac{P_a}{\sigma'_{v0}}\right)^{0.25} \tag{6-4}$$

6.3 Experimental results and discussion

All specimens tested in this study are listed in Table 6-4 along with information on the testing modes, target σ'_{v0}, as-consolidated unit weight ($\gamma_{t,con}$ and $\gamma_{d,con}$), shear strength and V_s values. In the subsequent sections, the interpretation of simple shear testing results is first discussed,

followed by the comparison between constant load and constant volume shearing response of MSW. Effects of vertical stress duration, shearing strain rate, compaction effort, waste composition, and degradation on the shear strength of MSW are evaluated. In addition, results of constant load simple shear testing and direct shear testing of MSW are compared. Factors influencing the V_s of MSW, including source wave frequency, compaction effort, waste degradation, and total and dry unit weight, are discussed. Finally, correlations are established between the shear strength in CL and CV testing and V_s of MSW.

6.3.1 **Interpretation of simple shear testing results**

- **Influence of shear strength definition on shear strength of MSW**

Figure 6-6 presents the stress-strain relationship of the simple shear tests conducted on MI and TX specimens prepared at the same waste composition in CL (Figure 6-6a) and CV (Figure 6-6b) modes. The shear resistance of MI and TX waste increases significantly with ε and the τ_{max} is reached at large shear strains, mostly exceeding 15-20%. This level of strain may be too large for many engineering applications, and thus, it is common to define the shear strength at a threshold shear strain value. For example, Kavazanjian et al. (1999) defined shear strength as the shear resistance at 10% of shear strain ($\tau_{\varepsilon=10\%}$). On the other hand, Pelkey et al. (2001) used τ_{max} as the shear strength. In this study, the shear resistance using both definitions was first evaluated using the results of MI and TX waste.

When all waste specimens using MI, TX, AZ, CA3 and CAF waste are considered in Figure 6-7, $\tau_{\varepsilon=10\%}$ equals on average 88.3±7.6% of the τ_{max}. Specifically, on average 83.3% (Figure 6-7a) and 95.1% (Figure 6-7b) of the τ_{max} is mobilized in CL and CV tests, respectively. The differences between shear strength normalized by initial vertical stress (τ/σ'_{v0}) and effective friction angles (φ_{tan} and φ_{sin}) estimated from maximum and 10%-strain shear strength are shown

in Figure 6-8 for CL tests and Figure 6-9 for CV tests. In CL tests, the differences between τ/σ'_{v0}, φ_{tan} and φ_{sin} estimated from maximum and 10%-strain shear strength are not affected by the vertical stress for most of the specimens. The differences are on average 0.075±0.031 for τ/σ'_{v0} (Figure 6-8a), 3.6˚ ±1.4˚ for φ_{tan} (Figure 6-8b) and 4.7˚ ±2.0˚ for φ_{sin} (Figure 6-8c), respectively. The differences between τ/σ'_{v0}, τ/σ'_{v}, φ_{tan} and φ_{sin} estimated from maximum and 10%-strain shear strength are not dependent on vertical stress in CV tests. The differences are on average 0.017±0.015 for τ/σ'_{v0} (Figure 6-9a), 0.069±0.033 for shear strength normalized by effective vertical stress (τ/σ'_{v}) (Figure 6-9b), 3.2˚ ±1.5˚ for φ_{tan} (Figure 6-9c) and 4.6˚ ±2.2˚ for φ_{sin} (Figure 6-9d), respectively.

Therefore, in the subsequent discussion, the shear strain at "failure" is assumed to be 10%, a conservative assumption that is also consistent with previous studies (Kavazanjian et al. 1999), and τ_{hf} equals $\tau_{\varepsilon=10\%}$, unless noticed otherwise.

- **Determination of effective friction angle**

As shown in Figure 6-10, when $\tau_{\varepsilon=10\%}$ is considered, φ_{tan} is on average 1.5˚±1.2˚ lower than φ_{sin} in CL tests and the difference appears to be mostly independent of the vertical stress, except for one test with a difference as high as 8˚ (Figure 6-10a). The difference between φ_{tan} and φ_{sin} decreases with increasing σ'_{v0} and ranges between 1-8˚ and mostly in between 2-4˚ in CV tests (Figure 6-10b). Because the estimation of effective friction angle based on φ_{tan} interpretation is more conservative, and may be more appropriate given that MSW is anisotropic and the horizontal plane is expected to be the weakest plane, it is used in the subsequent discussion.

6.3.2 **Constant load and constant volume response of MSW in simple shear**

- **Constant load shear strength of MSW in simple shear**

The shear strength of all MSW specimens in CL tests are shown in Figure 6-11a and is summarized in Table 6-4. The values of $\tau_{\varepsilon=10\%}/\sigma'_{v0}$ range between 0.30-0.66 at σ'_{v0} of 50 kPa and between 0.21-0.42 at σ'_{v0} of 400 kPa (Figure 6-11b). Consequently, φ_{tan} between 12-33˚ and mostly between 16-24˚ is calculated as shown in Figure 6-11c.

Figure 6-12 compares the results of MSW tested in this study to the other two studies (Kavazanjian et al. 1999; Pelkey et al. 2001) that conducted large-size simple shear CL testing. Note that Pelkey et al. (2001) reported τ_{max} for MSW from Canadian landfills. Kavazanjian et al. (1999) used $\tau_{\varepsilon=10\%}$ for waste from the OII landfill in CA which is the criterion used in this study as well. The results for specimens with minimal compaction effort from this study are lower than the data reported by Pelkey et al. (2001) and Kavazanjian et al. (1999). However, the shear strength of highly compacted specimens from this study are similar to or slightly lower than the shear strength of the OII waste at σ'_{v0} up to 200 kPa.

These shear strength values are lower than reported earlier in triaxial (Bray et al. 2009; Zekkos et al. 2012) and direct shear tests (Zekkos et al. 2010a; Reddy et al. 2011; Bareither et al. 2012c). This may be attributed to a number of factors: first, it is well established that the shearing mode in simple shear results in lower shear strength parameters than triaxial shear. Second, the assumed shear strength was based on a failure strain of 10% which is a conservative assumption. A third reason is that 73 out of 88 specimens listed in Table 6-4 were prepared without compaction. This is because MSW is commonly placed in bioreactor landfills more loosely to allow for liquids to percolate through the waste mass compared to conventional “dry-tomb” landfills where recirculation of liquids is not an issue and waste is densified to maximize waste burial capacity. Finally, potential anisotropy of waste specimens resulted from the

inclusion of >20 mm fibrous waste particles which tend to become oriented horizontally during specimen preparation and compaction may affect the shear strength as well.

- **Constant volume shear strength of MSW in simple shear**

The shear strength of MSW in CV tests is shown in Figure 6-13 and is also summarized in Table 6-4. The effective φ_{tan} ranges between 15-34˚ and is mostly between 22-28˚ (Figure 6-13b). The values of $\tau_{\varepsilon=10\%}/\sigma'_{v0}$ (Figure 6-13c) and $\tau_{\varepsilon=10\%}/\sigma'_{v}$ (Figure 6-13d) decrease with increasing σ'_{v0}. Most of the specimens under minimal compaction effort exhibit a $\tau_{\varepsilon=10\%}/\sigma'_{v0}$ ratio of 0.3-0.35, while specimens subject to high compaction effort has a $\tau_{\varepsilon=10\%}/\sigma'_{v0}$ ratio of 0.3-0.45 (Figure 6-13c). These values are significantly higher than the τ_{hf}/σ'_{v0} ratio reported for clays, silts and organic soils, even though $\tau_{\varepsilon=10\%}$ was used instead of τ_{hf} for MSW. DeGroot et al. (1992) reported an average value of 0.23 for a variety of low and high plasticity soils, 0.20 for Boston Blue Clay and 0.22 for San Francisco Bay Mud. They also reported a value of 0.26 for silts and organics soils below the A-line, a value that is closer to, but still lower than, the values observed for MSW. This highlights the significant constant volume shear strength of MSW at both loose and dense states.

- **Comparison of constant load and constant volume response of MSW in simple shear**

For two identical specimens at the same σ'_{v0}, the shear strength in CL (τ_{CL}) is always higher than the shear strength in CV (τ_{CV}). As shown in Figure 6-14a, the ratio of τ_{CL}/τ_{CV} is between 1-1.34 with an average value of 1.16, i.e., τ_{CL} is on average 16% higher than the corresponding τ_{CV}. The value of $\tau_{\varepsilon=10\%}/\sigma'_{v}$ is between 0-0.27 lower in CL than in CV, since CV tests are considered to be representative of “undrained” conditions and the effective vertical stress of specimens decreased during shearing (Figure 6-14b). For the same reason, the φ_{tan} of specimens in CL tests are between 0-12˚ lower than those in CV tests (Figure 6-14c). In addition, the differences in τ_{CL},

$\tau_{\varepsilon=10\%}/\sigma'_{v0}$ and φ_{tan} in CL (Figure 6-11a, b and c) are always higher than those in CV for the same σ'_{v0} (Figure 6-13a, b and c).

6.3.3 **Effects of specimen preparation and testing conditions on shear strength of MSW**

- **Effect of vertical stress duration**

The influence of vertical stress duration on stress-strain response of MSW has not been investigated in the literature, although previous studies have shown that confining stress duration affects significantly the small-strain shear modulus and shear-wave velocity of MSW (Zekkos et al. 2008; Zekkos et al. 2013b). The influence of vertical stress duration was investigated in this study by subjecting MI waste specimens of identical composition to variable vertical stress durations prior to shearing. Specifically, CL tests were conducted after 170, 1500 and 8520 min under vertical stress and at shearing strain rate of 0.4±0.05 %/min, and CV tests were conducted after 170, 1440 and 8465 min under vertical stress and at shearing strain rate of 4.7±0.4 %/min.

Vertical stress duration does not appear to significantly affect the CL shear response beyond the first few hours and the shear strength after 24 hours of vertical stress application and beyond are practically the same (Figure 6-15a and c). The situation is different for CV testing, vertical stress duration affects the stress-strain response (Figure 6-15a) and the pore pressure generation pattern as expressed by the stress path (Figure 6-15b). As shown in Figure 6-15b, increasing time under vertical stress beyond 24 hours results in an increasingly dilational response in CV testing that is reflected as decreasing pore pressure. Increasing vertical stress duration resulted in significantly higher $\tau_{\varepsilon=10\%}/\sigma'_{v0}$ in CV testing (Figure 6-15c). On the basis of these results, it appears that CV testing within a couple of hours after application of σ'_{v0} may result in too low shear resistances. On the other hand, testing after about 24 hours provides a more appropriate and practical estimate of the long-term shear resistance of MSW. Thus, in this

study the baseline of vertical stress duration is 24±1 hours, which is consistent with testing approaches used in earlier studies (Bray et al. 2009; Zekkos et al. 2010a; Athanasopoulos 2011b).

Note that all specimens were prepared at the same w_c and target γ_t of 5.6 kN/m^3 and compressed about the same amount, i.e., 33.5-35.6%, when subjected to the target σ'_{v0}. The $\gamma_{t,con}$ of the specimens were between 8.4-8.6 kN/m^3. It can be observed that the increased dilation observed is not associated with the $\gamma_{t,con}$, but with the duration of vertical stress as the specimen that was subjected to the longest vertical stress duration exhibited the most pronounced dilation (Figure 6-15b).

- **Effect of shearing strain rate**

Tests were performed on MI waste specimens using strain rates that varied from 0.25-2.24 %/min and the results are shown in Figure 6-16. The strain rate appears to affect the mobilized shear resistance in both CV and CL testing (Figure 6-16a) as well as shearing response in CV testing (Figure 6-16b). The averaged effect of strain rate on the shear strength in CL and CV tests is characterized by the following relationship (Figure 6-16c, R^2=0.94):

$$\left(\frac{\tau}{\tau_{rate=0.5\ \%/min}}\right)_{\varepsilon=10\%} = 0.11 \times \log\left(strain\ rate\ \left(\frac{\%}{min}\right)\right) + 1.0 \qquad (6\text{-}5)$$

Figure 6-17a compares the effect of strain rate on the shear strength of MSW in CL tests from this study to the drained shear strength of specimens of variable waste composition from Tri-Cities landfill in triaxial and direct shear testing (Zekkos et al. 2012). It appears that, for the limited available data, the effect of strain rate in simple shear is significantly lower than the effect of strain rate in triaxial shear and slightly lower than in direct shear when shearing takes place parallel to the fibrous constituents. The difference may be attributed to the anisotropic

nature of MSW and the shearing mode, although, direct comparisons are difficult since the tested MSW specimens are different. Figure 6-17b shows the effect of strain rate on the undrained shear strength of MSW in CV tests. Data by Kulhawy and Mayne (1990) on clayey soils are also shown since data from other MSW specimens are not available. The limited data available appears to indicate that the effect of strain rate on the undrained shear strength of MSW is on the upper bound of the data observed for clays.

- **Effect of compaction effort**

Specimens prepared using MI and fresh and degraded CAF waste were subjected to either minimal or high compaction effort and the shearing response were compared in Figure 6-18 and Figure 6-19, respectively. In CL testing, highly compacted specimens were stiffer than minimally compacted specimens, i.e., higher shear resistance was mobilized at the same shear strain (Figure 6-18a and Figure 6-19a) and the specimens were less contractive (Figure 6-18c and Figure 6-19c). Similar difference is observed between highly and minimally compacted specimens in CV testing, as the highly compacted specimens showed higher shear strength (Figure 6-18b and Figure 6-19b) and were less contractive (Figure 6-18d and Figure 6-19d). The compacted MI specimen became dilative at large shear strain as shown in Figure 6-19d.

As shown in Figure 6-20a and Figure 6-20b, highly compacted specimens have 5-15 kPa and 0-10 kPa higher shear strength in CL and CV testing, respectively, at σ'_{v0} between 50-400 kPa. The $\tau_{\varepsilon=10\%}/\sigma'_{v0}$ of highly compacted specimen showed a larger decrease with increasing σ'_{v0} compared to minimally compacted specimens (Figure 6-20c and Figure 6-20d). The φ_{tan} of highly compacted specimens also decreases more with increasing σ'_{v0} compared minimally compacted specimens and is 1-7˚ higher at σ'_{v0} between 50-400 kPa (Figure 6-20e and Figure

6-20f). The φ_{tan} of a highly compacted CAF specimen is lower than the counterpart specimen prepared under minimally compaction effort at σ'_{v0} of 400 kPa (Figure 6-20f).

6.3.4 **Effects of waste composition on shear strength of MSW**

- **Effect of amount and type of <20 mm material**

The <20 mm fraction of excavated waste samples consisted of locally used daily soil cover as well as any other inclusions of fine waste particles. The behavior of the MSW matrix are affected by the characteristics of <20 mm fraction. The percentages of <20 mm fraction of waste used in this study range between 50-80% by weight for the five waste samples (Table 6-1) and are typical of MSW in modern landfills. Zekkos et al. (2010b) reported 60-75 % of <20 mm material in Tri-Cities landfill and values overall above 75% was reported for the OII landfill by Kavazanjian et al. (2013). The <20 mm material in the MI, AZ and CA landfills is essentially well-graded sand (SW) with less than 5% non-plastic fines (<#200 sieve). In the TX landfill, the <20 mm material is silty sand (SM) with 33% organic fines of high plasticity (liquid limit=65%, plastic limit=46%, plasticity index=19%). The VS content of the <20 mm material was 21.8%, 12.8%, 9.0% and 7.0% for MI, AZ, CA and TX waste, respectively. Grain size distributions for the <20 mm fraction are shown in Figure 6-21.

A comparison between stress-strain relationship of MI and TX waste in CL and CV tests is shown in Figure 6-6. In CL tests, a hyperbolic stress-strain relationship is observed where a τ_{max} is reached at a strain larger than 20% and is maintained at increasing strains (Figure 6-6a). In CV tests, a hyperbolic relationship is observed for MI waste, however, a strain softening response is observed for some TX waste specimens (Figure 6-6b). Since all other testing parameters (waste composition, unit weight, σ_{v0}') were identical, this difference can only be

attributed to the daily soil cover that is used in TX that included significantly more fines and of high plasticity.

Testing results of specimens prepared using the respective waste composition for fresh CAF and TX waste and degraded TX waste were compared with the results of specimens prepared using only <20 mm fraction from the same waste (Figure 6-22 and Figure 6-23). In both CL and CV tests, the <20 mm material of CAF waste which is well-graded sand showed higher shear strength than the mixed waste at each σ'_{v0} (Figure 6-22a and Figure 6-22b). The <20 mm fraction only specimens were less contractive compared to the mixed waste, and, for one <20 mm fraction only specimen in CV testing, the shearing response was dilational (Figure 6-22c and Figure 6-22d). The <20 mm fraction of fresh TX waste was only slightly stronger than the mixed waste specimens in CL and CV tests, and was less contractive in CL testing but slightly more contractive in CV testing (Figure 6-23). Two specimens consisting of only <20 mm fraction of degraded TX waste appeared to have lower shear strength than the mixed waste at σ'_{v0} of 100 kPa which is attributed to the degradation of waste material (Figure 6-23).

The shear strength of all the specimens shown in Figure 6-22 and Figure 6-23 are plotted in Figure 6-24. Specimens consisting of <20 mm fraction of CA waste show the highest shear strength, while <20 mm fraction of fresh TX waste is stronger than that of <20 mm fraction of degraded TX waste. In both CL and CV tests, the specimens containing only <20 mm fraction of fresh TX waste were still weaker than the specimens of mixed CA waste (Figure 6-24a and Figure 6-24b), indicating that the % of <20 mm fraction is only one factor influencing the shear strength of waste. As shown in Figure 6-24e and Figure 6-24f, the φ_{tan} of <20 mm fraction only specimens are equal to or higher compared to those of mixed specimens in CL and CV tests. Overall, testing only <20 mm fraction of waste results in practically equal or higher shear

strength than the mixed waste, thus exclusion or shredding of >20 mm particles may lead to overestimation of the shear strength of soil-waste mixture.

- **Effect of amount of >20 mm particles**

Particles in >20 mm fraction of waste are mostly fibrous, elongated and easily deformable, although wood waste found in the waste samples used in this study was predominantly wood. Therefore the % of paper and soft plastic in waste are summed as the % of flexible fibrous waste in >20 mm fraction. The $\gamma_{d,con}/\gamma_w$ of waste specimens generally increases with increasing % of <20 mm (Figure 6-25a), and decreases with increasing % of flexible fibrous waste (Figure 6-25b). Therefore inclusion of more fibrous waste reduces the $\gamma_{d,con}$ of waste specimens.

Testing results of the specimens prepared using fresh waste samples under minimal compaction effort are compared to investigate the effect of amount of flexible fibrous waste on the shear strength of MSW. In both CL and CV tests, the shear strength of waste consisting of 0-30% of fibrous waste is similar at σ'_{v0} of 50 and 100 kPa, but the shear strength is 30-60 kPa different at σ'_{v0} of 200 and 400 kPa (Figure 6-26a and Figure 6-26b). The differences in the $\tau_{\varepsilon=10\%}/\sigma'_{v0}$ and φ_{tan} of specimens is between 0.05-0.15 (Figure 6-26c and Figure 6-26d) and 3-10˚ (Figure 6-26e and Figure 6-26f), respectively.

- **Effect of waste degradation on its composition and shear strength**

Paper in the >20 mm fraction of waste was broken down to finer particles by anaerobic microorganisms via biochemical processes and then converted to biogas containing CH_4 and CO_2 (Barlaz et al. 2010b). Broken down paper particles increased the mass of <20 mm fraction and the mass of VS in it. As a result, % of paper in specimens decreased after degradation, while % of <20 mm fraction increased. A portion of the VS in <20 mm fraction of waste was biodegraded, and the residual VS was recalcitrant or highly-resistant to biodegradation, e.g., lignin and humic

substances (Barlaz 2006; Barlaz et al. 2010b; Wang et al. 2011b). Therefore the VS content of the <20 mm fraction of waste could either increase or decrease after degradation. The masses of soft plastic, hardened wood and other >20 mm particles in specimens remained essentially unchanged, but % of these constituents in specimens changed accordingly.

Fresh waste samples collected from the landfills in this study have natural w_c between 28-44% which is typical for waste disposed of in conventional Subtitle D landfills where moisture infiltration is minimized (Table 6-1). The w_c of degraded waste specimens are close to their field capacity, between 80-100%, due to frequent leachate recirculation during degradation experiments. Because of the significantly higher w_c of degraded waste, the $\gamma_{t,con}$ of degraded waste specimens were much higher than those of fresh waste specimens, although the specimens may have similar $\gamma_{d,con}$ as shown in Figure 6-27. In the subsequent sections, when the unit weight of waste is involved in analysis, both $\gamma_{t,con}$ and $\gamma_{d,con}$ are used to capture any potential effect of increased w_c after degradation. A comparison of the total and dry unit weight of the specimens before and after degradation is shown in Table 6-2, while the composition, $w_{c,ave}$, and VS content of <20 mm fraction of the degraded specimens are shown in Table 6-3.

Figure 6-28 to Figure 6-32 show comparisons in CL and CV shear responses between fresh and degraded MI, TX, CAF and AZ waste and <20 mm fraction only of TX waste. The degraded MI and TX specimens showed lower shear strength than the corresponding fresh specimens. The degraded MI waste was more contractive in both CL and CV tests (Figure 6-28c), whereas the degraded TX waste and its <20 mm fraction were less contractive than the fresh specimens in CL testing but more contractive in CV testing (Figure 6-29c, Figure 6-29d, Figure 6-30c and Figure 6-30d). In contrast, the degraded CAF waste was stronger than the fresh waste

(Figure 6-31a) whereas the degraded AZ waste showed practically the same shear strength as the fresh waste (Figure 6-32a).

The shear strength of fresh, "undisturbed" degraded and reconstituted degraded waste specimens are compared in Figure 6-33. The "undisturbed" degraded specimens retrieved directly from laboratory simulators showed about 5-10% lower shear strength than the corresponding reconstituted degraded specimens, thus the shear strength of carefully reconstituted degraded specimens is reasonably representative of the shear strength of waste after degradation (Figure 6-33a). The values of $\tau_{\varepsilon=10\%}/\sigma'_{v0}$ of degraded waste specimens were between 0.05 higher to 0.11 lower than the corresponding fresh waste specimens in CL and CV tests (Figure 6-33c and Figure 6-33d). The φ_{tan} of degraded waste is between 1˚ higher to 9˚ lower than the corresponding fresh waste specimens in CL and CV tests (Figure 6-33e and Figure 6-33f).

Waste degradation process altered the composition, unit weight and characteristics of the <20 mm material of the waste to variable degrees and each of the factors has different effect on the shear strength of waste as discussed previously. Therefore the observed changes in the shear strength of waste due to degradation in this study depend on both the characteristics of waste before degradation as well as the biodegradation conditions. The results presented herein highlight the necessity of site-specific waste characterization and clear understanding of waste degradation process in landfills to account for long-term change in the shear strength of disposed waste.

6.3.5 **Comparison of constant load simple shear and direct shear response of MSW**

The results of direct shear testing are compared with the results of simple shear CL testing on identical TX and CAF waste specimens as shown in Figure 6-34. The stress-displacement

responses of waste in simple shear tests followed hyperbolic trends and the τ_{max} is obviously reached at large shear displacement. In contrast, shear resistance in direct shear testing increased with displacement in parallel to simple shear testing until about 5-10 mm of displacement, the shear resistance then increased approximately linearly with increasing shear displacement. In most cases the τ_{max} is not clearly reached even at displacement larger than 40 mm.

The shear strength of waste obtained from simple shear (τ_{SS}) and direct shear (τ_{DS}) testing are compared at the same shear displacement of 12 mm which is equivalent to approximately 10% of shear strain in simple shear testing. As shown in Figure 6-35a, the steepness of the τ_{DS}-σ'_{v0} curves for TX and CAF waste decrease with increasing σ'_{v0}, i.e., the calculated secant friction angle decreases with increasing σ'_{v0}, a typical response of waste in direct shear testing (Bray et al. 2009; Zekkos et al. 2010a). Decrease in τ_{SS} with increasing σ'_{v0} from 50 to 500 kPa is not as significant as that in direct shear. The $\tau_{\varepsilon=10\%}/\sigma'_{v0}$ of waste in simple shear testing decreases less with increasing σ'_{v0} compared to the $\tau_{\varepsilon=10\%}/\sigma'_{v0}$ in direct shear testing (Figure 6-35b).

The ratio between the τ_{SS} and τ_{DS} of a pair of two identical specimens (τ_{SS}/τ_{DS}) ranges between 0.8-1.4 for TX and CAF waste at σ'_{v0} between 100-500 kPa, highlighting that the τ_{SS} of waste may not always be lower than the corresponding τ_{DS}. It is observed that the ratio for TX specimen containing 16.6% of fibrous waste becomes higher than 1 at σ'_{v0} of 200-400 kPa. The ratio for CAF specimen would also become higher than unity at σ'_{v0} higher than 400 kPa if it follows the same trend. The τ_{SS} of the specimens consisting of only <20 mm fraction of CAF waste remain at around 90% of the τ_{DS} at σ'_{v0} between 100-400 kPa. Therefore the inclusion of >20 mm fibrous waste appears to be one cause for the higher τ_{SS} compared to τ_{DS} at high σ'_{v0}.

Pelkey et al. (2001) reported the only study in the literature testing the shear strength of identical MSW specimens using both large-size simple shear and direct shear devices. Artificial refuse containing 18% of >12.5 mm paper, soft plastic and rubber was tested in that study and the τ_{SS}/τ_{DS} at shear displacement of around 12 mm is calculated by the writers to be around 1.1 and increases slightly with increasing σ'_{v0}.

6.3.6 **Shear wave velocity measurement of MSW**

- **Effect of input shear wave frequency on Vs measurement**

In this study, the V_s measured at input frequencies of 1.5-2 kHz ($V_{s\ 1.5\text{-}2\ kHz}$) is used as baseline because most of the measured V_s are available in this frequency range. V_s of specimens measured at frequencies outside the 1.5-2 kHz range are corrected to $V_{s\ 1.5\text{-}2\ kHz}$. Based on test results from this study, the ratio of $V_s/V_{s\ 1.5\text{-}2\ kHz}$ for each specimen increases with increasing frequency of input shear wave, according to Eqn. 6-6 (Figure 6-36, R^2=0.66):

$$\frac{V_s}{V_{s\ 1.5-2\ kHz}} = 0.136 \times \log(frequency) + 0.918 \qquad (6\text{-}6)$$

The observed variability is expected and is mostly caused by differences in σ'_{v0}, waste composition and unit weight of waste specimens. The $V_{s\ 1.5\text{-}2\ kHz}$ for 13 specimens are not available, thus the V_s measured at other frequencies are adjusted to the corresponding $V_{s\ 1.5\text{-}2\ kHz}$ according to Eqn. 6-6 (noted in Table 6-4). The values of $V_{s\ 1.5\text{-}2\ kHz}$ are used in the subsequent sections and are referred to as V_s for simplicity.

- **Effect of compaction on Vs of MSW**

The effect of compaction effort on the V_s of waste is investigated using MI and CAF specimens. The V_s of waste consolidated at σ'_{v0} of 50-200 kPa was increased by increasing compaction effort (Figure 6-37). Similar effect of increased compaction effort on the shear strength of waste

has been shown previously in this study with the shear strength of specimens consolidated at σ'_{v0} of 400 kPa are similar regardless of different compaction effort.

- **Effect of amount of <20 mm fraction on Vs of MSW**

Both $\gamma_{t,con}$ and $\gamma_{d,con}$ of waste increase with increasing % of <20 mm. As shown in Figure 6-38, the V_s of specimens consisting of only <20 mm material is higher than the mixed waste. The V_s of <20 mm material of CAF waste is significantly higher than the V_s of <20 mm material of degraded TX waste due to different soil classifications, however the $\gamma_{t,con}/\gamma_w$ of the specimens are similar (Figure 6-38a). Also, the V_s of the specimens generally increase with increasing $\gamma_{d,con}/\gamma_w$ (Figure 6-38b). This highlights the importance of using both $\gamma_{t,con}/\gamma_w$ and $\gamma_{d,con}/\gamma_w$ in investigating the V_s of waste specimens having variable w_c. Overall, a change in V_s is expected during degradation of MSW.

- **Effect of degradation on Vs of MSW**

Multiple processes occurred during MSW degradation and many characteristics of MSW changed as discussed previously, thus the V_s of waste did not always increase after degradation. As can be seen in Figure 6-39a, b and c, the V_s of degraded specimens is higher than the corresponding fresh specimens for TX waste, but the opposite trend is observed for MI and CAF waste. The relationship between the ratio of V_s of degraded and fresh specimens prepared using MI, TX and CAF waste and σ'_{v0} is shown in Figure 6-39d. The ratio of V_s appears to be dependent on waste composition and increases with increasing σ'_{v0}. Therefore V_s measurement combined with an estimation of overburden pressure of waste may be used to characterize the degree of degradation of waste with time.

6.3.7 **Correlation between shear-wave velocity and shear strength of MSW**

Higher shear strength of waste in both CL and CV testing are generally correlated with higher V_s of waste (Figure 6-40a and Figure 6-40b). The values of shear strength and V_s of waste are both increased, but not by the same amount, by increasing σ'_{v0} applied to waste (Figure 6-40c and Figure 6-40d). Consequently, shear strength was normalized by the initial vertical effective stress ($\tau_{\varepsilon=10\%}/\sigma'_{v0}$) and V_s was stress corrected using Eqn. 6-4 (Kayen et al. 2013) and the results as shown in Figure 6-41. The $\tau_{\varepsilon=10\%}/\sigma'_{v0}$ of waste under minimal compaction effort is on average 0.331±0.054 and 0.291±0.034 in CL and CV testing, respectively, for the corresponding range of V_{s1} between 110-240 m/s. Increasing compaction effort results in higher $\tau_{\varepsilon=10\%}/\sigma'_{v0}$ and V_{s1} of waste.

6.4 Conclusions

A 300 mm-diameter simple shear device was used to test the shear strength of waste specimens prepared using fresh waste sampled from five locations in four landfills across U.S. Fresh waste specimens identical to the specimens tested at fresh state were degraded in a series of 300 mm-diameter laboratory landfill simulators and the degradation processes were closely monitored. Fully degraded specimens were tested in simple shear testing also to assess the impact of degradation on the shear strength and V_s of waste. A unique extensive large-size experimental dataset of 53 constant load and 45 constant volume simple shear tests and 8 direct shear tests on fresh and fully degraded waste specimens and the corresponding shear-wave velocity (V_s) for 66 specimens is presented. Main conclusions are summarized in the following bullets:

- Shear resistance at 10% of shear strain is used as the shear strength of waste specimens in this study. Tangent interpretation of effective friction angle of waste is shown to be conservative and used throughout this study.
- The shear strength of waste in constant load testing is on average 15% higher than in constant volume testing.
- Longer vertical stress duration and higher shearing strain rate in simple shear testing results in higher shear strength of identical waste specimens.
- Increasing compaction effort results in higher unit weight, shear strength and V_s of waste.
- The shear strength and V_s both increased when the amount of <20 mm material in a specimen is increased.
- The soil type of <20 mm material influences the shear strength of waste.
- Higher percentage of >20 mm flexible fibrous waste results in lower shear strength in simple shear testing and V_s of waste.
- In addition to compaction effort and waste composition, the V_s of MSW increases with increasing frequency of the input shear wave.
- Since multiple processes occurred during MSW degradation and many characteristics of MSW were changed, the shear strength and V_s of waste could either increase, remain about the same, or decrease after degradation. V_s measurement and estimation of overburden pressure can be used to characterize the degree of degradation of waste with time.
- The shear strength and V_s of waste and their normalized values, τ/σ'_{v0} and V_{s1}, are correlated with each other.

6.5 Tables

Table 6-1 List of composition, w_c and VS content of fresh MSW specimens.

Waste	<20 mm particles (%dry)	paper (%dry)	soft plastic (%dry)	wood (%dry)	$w_{c,ave}$ (%dry)	$VS_{<20\ mm}$ (g/g)	Grain size distribution (C_u, C_c)	<0.075 mm particles (%dry)	Atterberg limits (LL, PL, PI)
TX	79.1	10.6	6.0	4.3	34.6	0.070	4.2, 3. 6	29.8	65, 46, 19
AZ	67.9	21.4	8.5	2.1	32.7	0.128	2.9, 1.0	3.5	39, 25, 14
CAF [a]	68.3	4.6	3.9	5.8	28.1	0.087	5.6, 0.5	10.0	44, 29, 15
CA3	50.8	17.0	11.9	20.2	39.5				
MI	80.0	10.0	5.7	4.3	43.6	0.218	4.0, 1.0	4.6	

blank: data pending.

[a] include 17.4% of hard plastic, metal and rocks.

Table 6-2 Results of degradation experiments and comparison between the unit weight of fresh and degraded specimens.

Specimen	CH_4 generation potential (L CH4/kg)	Total strain (%)	$\gamma_{t,0}$ (kN/m^3)	$\gamma_{d,0}$ (kN/m^3)	$\gamma_{t,f}$ (kN/m^3)	$\gamma_{d,f}$ (kN/m^3)
TX	21.5	15.9	7.90	5.87	11.48	6.34
AZ	66.6		5.38	4.16		
CAF [a]	8.1	16.0	7.20	5.72	10.22	6.28
CA3	26.4		4.96	3.59		
MI	n. a.	26.1	5.77	4.02	8.68	4.27

blank: data pending.

Table 6-3 List of composition, w_c and VS content of degraded MSW specimens.

Specimen	<20 mm particles (%dry)	paper (%dry)	soft plastic (%dry)	wood (%dry)	$w_{c,ave}$ (%dry)	$VS_{<20\ mm}$ (g/g)
TX	92.9	0.1	4.3	2.7	81.1	0.085
AZ						
CAF [a]	71.6	1.0	3.1	5.4	62.7	0.105
CA3						
MI	83.7	3.7	7.3	5.3	103.3	0.246

blank: data pending.

[a] include 18.9% of hard plastic, metal and rocks.

Table 6-4 List of testing mode, specimen preparation, σ'_{v0}, unit weight, shear strength and V_s of specimens for simple shear testing at vertical stress duration of 24±1 hours and shearing strain rate of 0.4±0.05 %/min.

#test	Testing mode and specimen preparation	σ'_{v0} (kPa)	$\gamma_{t,con}$ (kg/m^3)	$\gamma_{d,con}$ (kg/m^3)	$\tau_{\varepsilon=10\%}$ (kPa)	$\tau_{\varepsilon=10\%}/\sigma'_{v0}$	$\tau_{\varepsilon=10\%}/\sigma'_{v}$ [a]	φ_{tan} (°)	τ_{peak} (kPa)	$V_{s\ 1.5\text{-}2\ kHz}$ (m/s)	V_{s1} (m/s)
MI25	CL	48	881	653	17.2	0.35		19.4	22.9		
MI28	CL	96	963	713	37.1	0.38		20.8	46.9		
MI20	CL	196	981	727	82.9	0.42		22.8	97.2	128 [b]	109
MI23	CL	393	1169	866	162.5	0.41		22.3	194.1		
MI24	CV	49	898	665	16.6	0.32	0.45	24.2	18.8		
MI26	CV	99	962	713	32.3	0.32	0.43	23.1	35.0	138	139
MI33	CV	197	1062	787	62.3	0.32	0.43	23.3	67.6	231	196
MI37	CV	395	1139	843	124.9	0.31	0.42	23.0	137.4	235	167
MI38	CV	394	1160	859	121.1	0.31	0.42	22.7	129.0	211 [b]	150
MI39	CV	394	1144	847	121.1	0.31	0.44	23.7	127.8	225	160
MI36	CL comp.	97	1031	764	41.2	0.43		23.1	48.9		
MI35	CV comp.	97	1018	754	39.4	0.41	0.53	27.7	46.5	157	159
MID1	CL undis.	197	1321	790	62.9	0.32		17.7	77.1	185	157
MID2	CL	48	1199	731	17.2	0.36		19.9	21.8		
MID3	CL	97	1309	811	34.3	0.35		19.6		170	172
MID6	CL	196	1392	886	67.9	0.35		19.1	83.0	210	178
MID9	CL	394	1484	1005	140.8	0.36		19.7	176.6		
MID4	CV	47	1214	742	15.8	0.34	0.53	27.7	16.5		
MID5	CV	97	1316	810	28.0	0.29	0.45	24.4	28.5		
MID7	CV	197	1432	909	61.3	0.31	0.47	25.3	65.4	195	165
MID8	CV	394	1494	986	114.0	0.29	0.43	23.2	116.6	212 [b]	151
TX1	CL	46	1136	859	17.0	0.36		19.6	22.0	103	126
TX2	CL	96	1303	991	37.1	0.38		20.9	43.3	157 [b]	160
TX3	CL	197	1356	1026	63.5	0.32		17.8	77.4	189	160
TX7	CL	394	1673	1272	121.7	0.31		17.2	141.1	224	160
TX4	CV	48	1122	850	16.5	0.34	0.55	28.7	17.1	119	143
TX5	CV	97	1305	988	33.6	0.35	0.53	28.1	34.0		
TX6	CV	196	1513	1149	59.0	0.30	0.51	26.9	59.1	210	178
TX18	CV	398	1712	1307	101.3	0.25	0.42	22.9	107.4	218	155
TX11	CL <20	96	1514	1236	37.3	0.39		21.3	50.5		
TX12	CL <20	197	1701	1297	76.7	0.39		21.4	83.2		
TX13	CL <20	496	1918	1460	128	0.26		14.5	140.4		
TX9	CV <20	97	1500	1224	32.3	0.33	0.66	33.4	32.3		
TX10	CV <20	198	1751	1430	58.8	0.30	0.62	32.0	62.5		
TX14	CV <20	499	1926	1468	118.7	0.24	0.39	21.1	124.0		
TXD1	CL undis.	100	1507	1022	27.1	0.28		15.3	30.0		
TXD2	CL undis.	200	1636	1123	40.8	0.20		11.6	41.5	192 [b]	162
TXD4	CL	97	1545	1048	29.2	0.30		16.9	31.9	145	147
TXD5	CL	96	1600	1085	30.4	0.32		17.6	33.5		
TXD6	CL	196	1675	1153	40.8	0.21		11.8	41.5	243	206
TXD9	CL	397	1733	1229	85.0	0.21		12.1	97.7	280	199
TXD3	CV	97	1576	1069	29.1	0.29	0.45	24.0	29.2	160	162
TXD8	CV	397	1742	1238	66.9	0.17	0.25	14.2	66.9	299	212
TXD11	CL <20	98	1703	1192	29.2	0.30		16.7	30.5	216	218
TXD10	CV <20	98	1711	1196	26.3	0.27	0.51	26.8	26.8	214	215
CAF2	CL	49	1019	825	18.7	0.38		20.8	24.0	144	173
CAF4	CL	98	1147	929	36.4	0.37		20.4	45.8	197	199
CAF6	CL	194	1300	1053	67.9	0.35		19.2	87.1	218	185

CAF1	CL	395	1400	1134	130.9	0.33		18.3	168.9	314 [b]	223
CAF3	CV	48	1030	834	15.2	0.32	0.51	26.8	15.7	157	190
CAF5	CV	94	1170	948	31.5	0.32	0.50	26.5	33.5	202	206
CAF7	CV	196	1287	1042	54.8	0.28	0.46	24.7	57.0	210	178
CAF8	CV	395	1459	1182	106.4	0.27	0.44	23.8	110.7	280 [b]	199
CAF9	CL comp.	47	1249	1013	23.9	0.51		27.4	27.9	161 [b]	195
CAF11	CL comp.	98	1342	1087	47.5	0.49		26.1	54.6	254	256
CAF12	CL comp.	198	1440	1166	80.8	0.41		22.3	97.6	247	209
CAF13	CL comp.	394	1555	1258	141.5	0.36		19.8	166.4	297	212
CAF14	CV comp.	97	1392	1127	41.5	0.43	0.54	28.7	42.0		
CAF15	CV comp.	198	1437	1164	61.6	0.31	0.49	26.1	62.7		
CAF16	CV comp.	399	1502	1216	106.3	0.27	0.38	20.8	108.1		
CAF18	CL <20 comp.	99	1633	1325	64.9	0.66		33.0	74.3		
CAF20	CL <20 comp.	199	1637	1335	95.2	0.48		25.6	112.6	269	227
CAF23	CL <20 comp.	497	1794	1464	182.3	0.37		20.2	233.8	331	222
CAF21	CV <20 comp.	197	1676	1367	87.9	0.45	0.63	32.4	97.2	323	274
CAF22	CV <20 comp.	500	1770	1443	143.3	0.29	0.54	28.4	150.0	375	252
CAFD1	CL undis.	200	1373	937	69.7	0.35		19.4	92.2	174	147
CAFD2	CL undis.	399	1555	1063	137.6	0.34		19.0	161.5	308	219
CAFD4	CL	96	1480	1000	39.9	0.42		22.7	49.5	178	151
CAFD3	CL	199	1391	956	77.5	0.39		21.5	98.0	169 [b]	171
CAFD5	CL	395	1487	1063	143.6	0.36		19.9	177.9	308	219
CAFD6	CL comp.	197	1506	1062	92.0	0.47		25.0	113.8		
CA32	CL	48	850	616	17.4	0.36		20.0	20.0	86 [b]	104
CA34	CL	97	969	701	34.5	0.36		19.6	43.2	127	128
CA36	CL	197	1097	795	67.3	0.34		18.9	84.0	144	122
CA31	CL	395	1191	862	121.5	0.31		17.1	151.1		
CA33	CV	48	841	609	15.5	0.32	0.49	26.1	16.3	121	146
CA35	CV	97	960	695	28.4	0.29	0.43	23.3	29.5	111	112
CA37	CV	197	1084	785	58.1	0.30	0.43	23.3	61.2	168	142
CA38	CV	395	1207	874	109.1	0.28	0.41	22.1	112.9	211	150
AZ2	CL	49	899	684	15.9	0.33		18.4	19.6	150 [b]	181
AZ4	CL	98	968	736	28.0	0.31		17.2	35.2	193 [b]	195
AZ6	CL	194	1282	975	61.6	0.32		17.6	77.0	219	186
AZ1	CL	393	1237	940	104.8	0.27		14.9	128.9	287 [b]	205
AZ3	CV	50	902	686	14.7	0.30	0.42	22.7	16.0	180	215
AZ5	CV	96	1028	781	28.0	0.29	0.43	23.1	30.4		
AZ7	CV	194	1170	889	54.0	0.28	0.40	22.0	57.9	238	202
AZ8	CV	394	1364	1038	98.7	0.25	0.38	20.8	109.3	267	190
AZD1	CL	397	1670	1282	111.0	0.28		15.7	137.8		

Note: fresh waste specimens: MI, TX, CAF, CA3 and AZ; degraded waste specimens: MID, TXD, CAFD, CA3D and AZD; comp.: high compaction effort; undis.: "undisturbed" degraded specimen; <20: 100% of <20 mm material; n. a.: V_s measurement not available.

[a] value of $\tau_{\varepsilon=10\%}/\sigma'_v$ only shown for CV tests;

[b] V_s adjusted to $V_{s\ 1.5\text{-}2\ kHz}$ according to Eqn. 6-6.

Table 6-5 List of testing mode, unit weight and shear strength of specimens for simple shear testing at σ'_{v0} of 105±5 kPa and variable vertical stress durations and shearing strain rates.

#test	Testing mode	σ'_{v0} duration (min)	Strain rate (%/min)	$\gamma_{t,con}$ (kg/m^3)	$\gamma_{d,con}$ (kg/m^3)	$\tau_{\varepsilon=10\%}$ (kPa)	$\tau_{\varepsilon=10\%}/\sigma'_{v0}$	$\tau_{\varepsilon=10\%}/\sigma'_{v}$	φ_{tan} (˚)	τ_{peak} (kPa)
MI15	CV	170	4.58	858	636	43.0	0.36	0.45	24.0	50.9
MI40	CV	1440	4.24	864	629	33.4	0.34	0.47	25.4	37.6
MI16	CV	8465	5.15	900	667	58.8	0.49	0.52	27.7	69.7
MI30	CL	170	0.36	904	670	30.5	0.37	0.37	20.1	39.3
MI31	CL	8520	0.36	902	668	37.1	0.39	0.39	21.3	43.7
MI28	CL	1500	0.48	963	713	37.1	0.38	0.38	20.8	46.9
MI32	CL	1440	2.24	909	673	39.0	0.41	0.41	22.1	48.7
MI29	CV	1560	0.25	959	710	30.6	0.31	0.45	24.3	33.7
MI26	CV	1500	0.50	962	713	32.3	0.32	0.43	23.1	35.0
MI41	CV	1440	2.23	915	634	34.8	0.35	0.47	25.4	39.4

Table 6-6 List of testing mode, specimen preparation, σ'_{v0}, unit weight and shear strength of specimens for direct shear testing at vertical stress duration of 24±1 hours and shearing displacement rate of 5±0.1 mm/min.

#test	Testing mode and specimen preparation	σ'_{v0} (kPa)	$\gamma_{t,con}$ (kg/m^3)	$\gamma_{d,con}$ (kg/m^3)	$\tau_{disp=12\ mm}$ (kPa)	$\tau_{disp=12\ mm}/\sigma'_{v0}$
TX15	DS	97	1255	1016	40.5	0.42
TX16	DS	197	1424	1153	57.5	0.29
TX17	DS	397	1568	1270	86.5	0.22
CAF26	DS comp.	99	1329	1077	59.5	0.60
CAF28	DS comp.	196	1382	1119	95.6	0.49
CAF27	DS comp.	497	1480	1198	160.6	0.32
CAF24	DS <20 comp.	99	1630	1328	73.2	0.74
CAF25	DS <20 comp.	498	1754	1432	196.6	0.39

Note: comp.: high compaction effort; <20: 100% of <20 mm material.

6.6 Figures

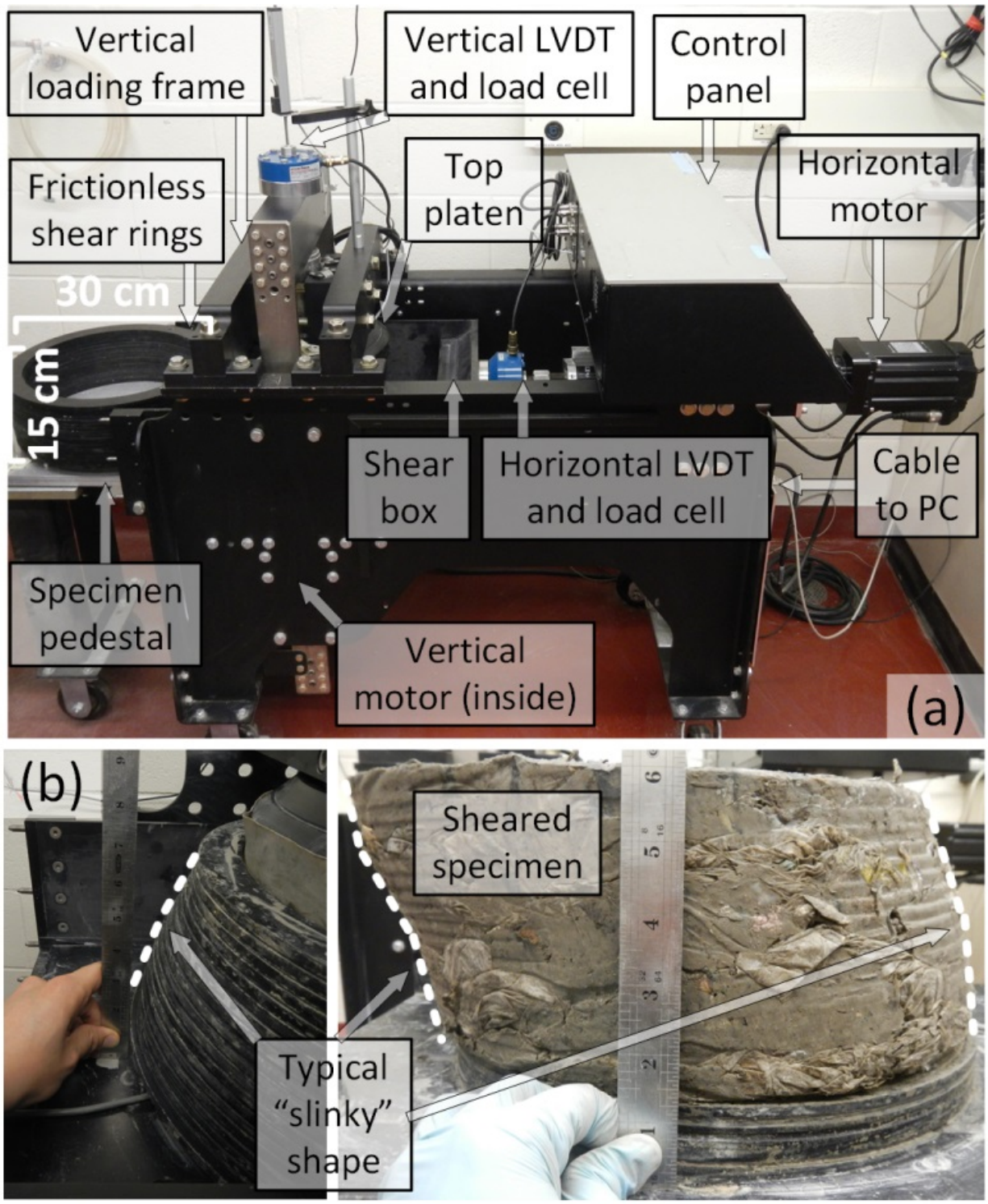

Figure 6-1 Schematic of (a) the large-size simple shear testing apparatus; and (b) a typical specimen after simple shear testing.

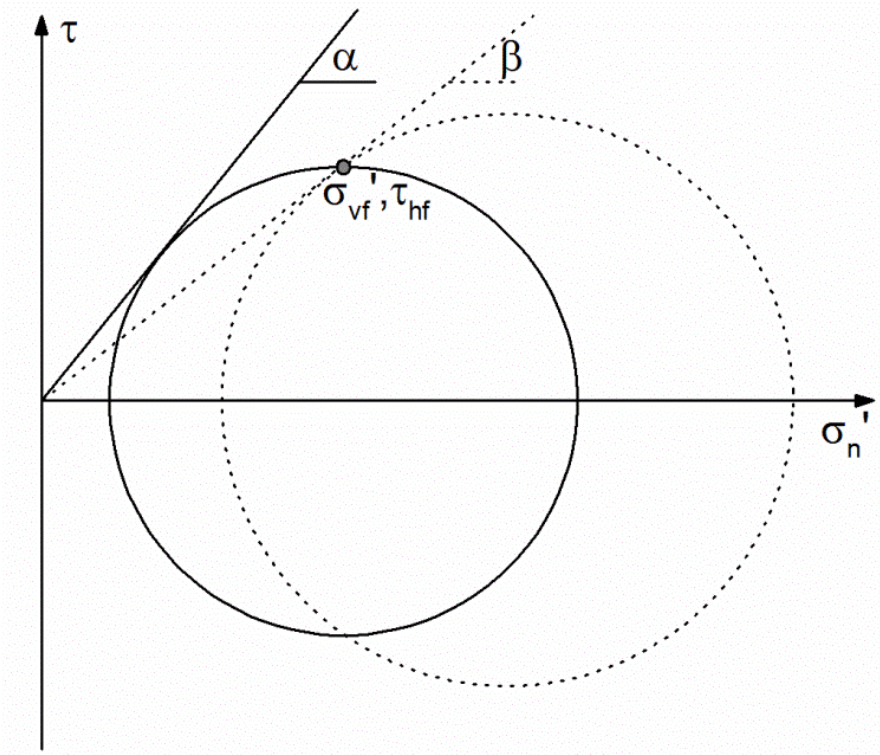

Figure 6-2 Alternative interpretations of the specimen's stress state at failure using the data collected during simple shear.

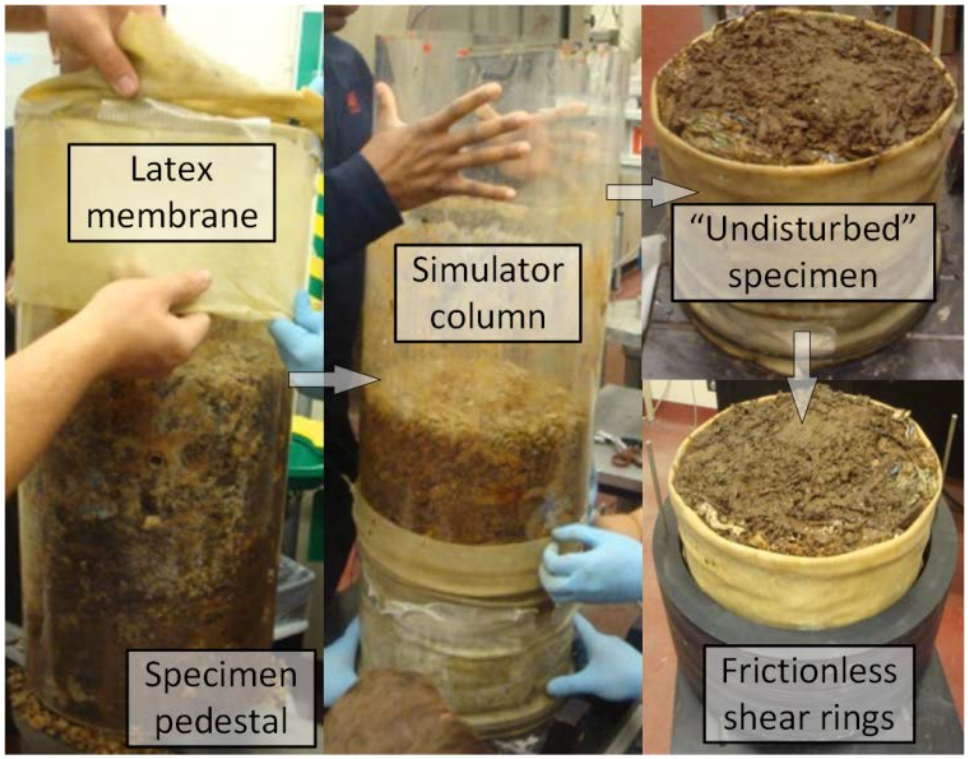

Figure 6-3 Procedure for disassembly of a large-size laboratory landfill simulator and preparation of a "undisturbed" specimen for simple shear testing.

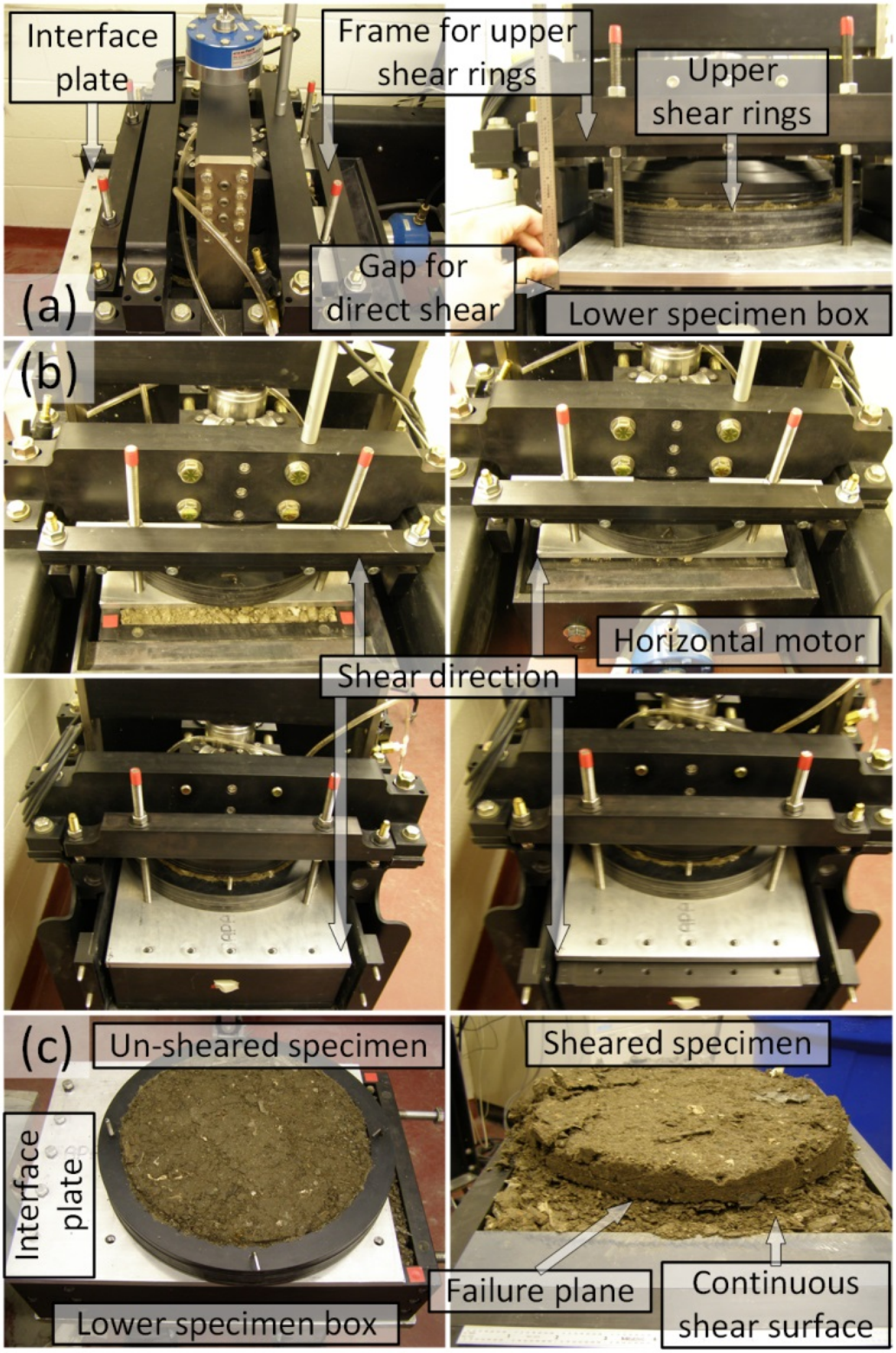

Figure 6-4 Schematic of (a) the large-size direct shear testing setup using the simple shear testing apparatus; (b) a comparison of the apparatus before and after direct shear testing; and (c) a comparison of a specimen before and after direct shear testing.

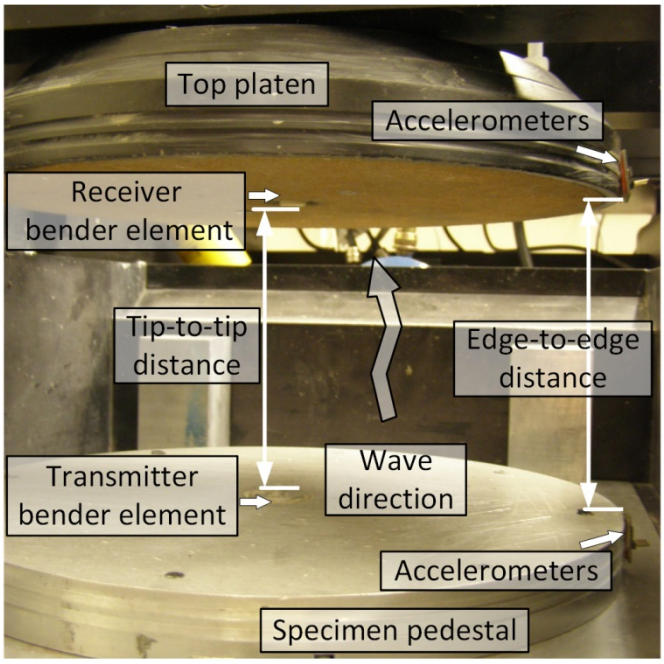

Figure 6-5 Schematic of the setups for shear-wave velocity measurements using bender elements and accelerometers.

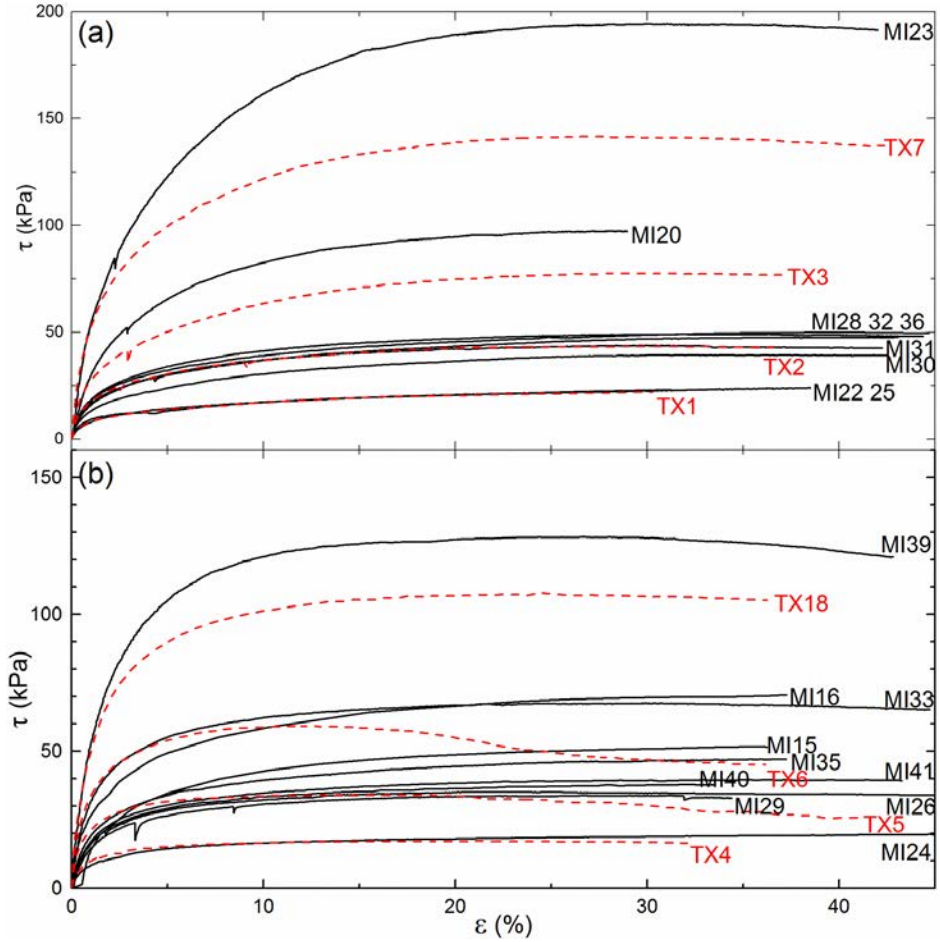

Figure 6-6 Shear stress (τ) - shear strain (ε) relationship for MI and TX fresh waste in (a) constant load; and (b) constant volume simple shear tests.

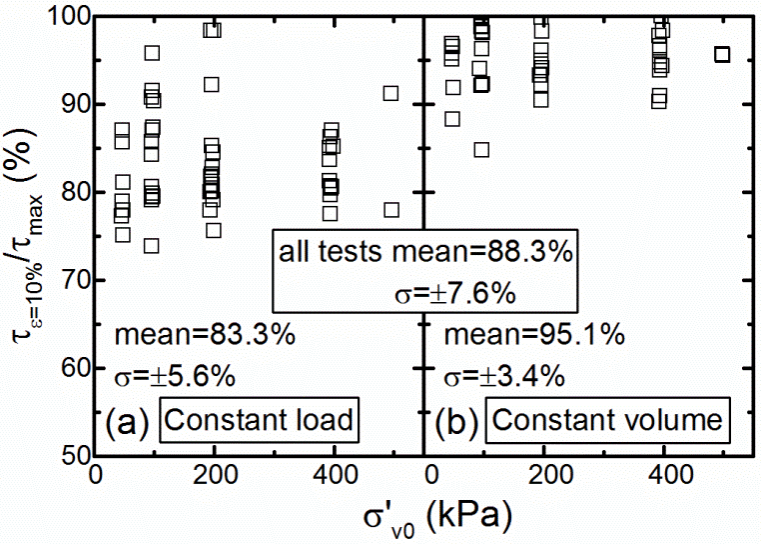

Figure 6-7 Comparison between ratio of shear resistance at (a) 10% shear strain; and (b) 20% shear strain and maximum shear resistance (τ/τ_{max}).

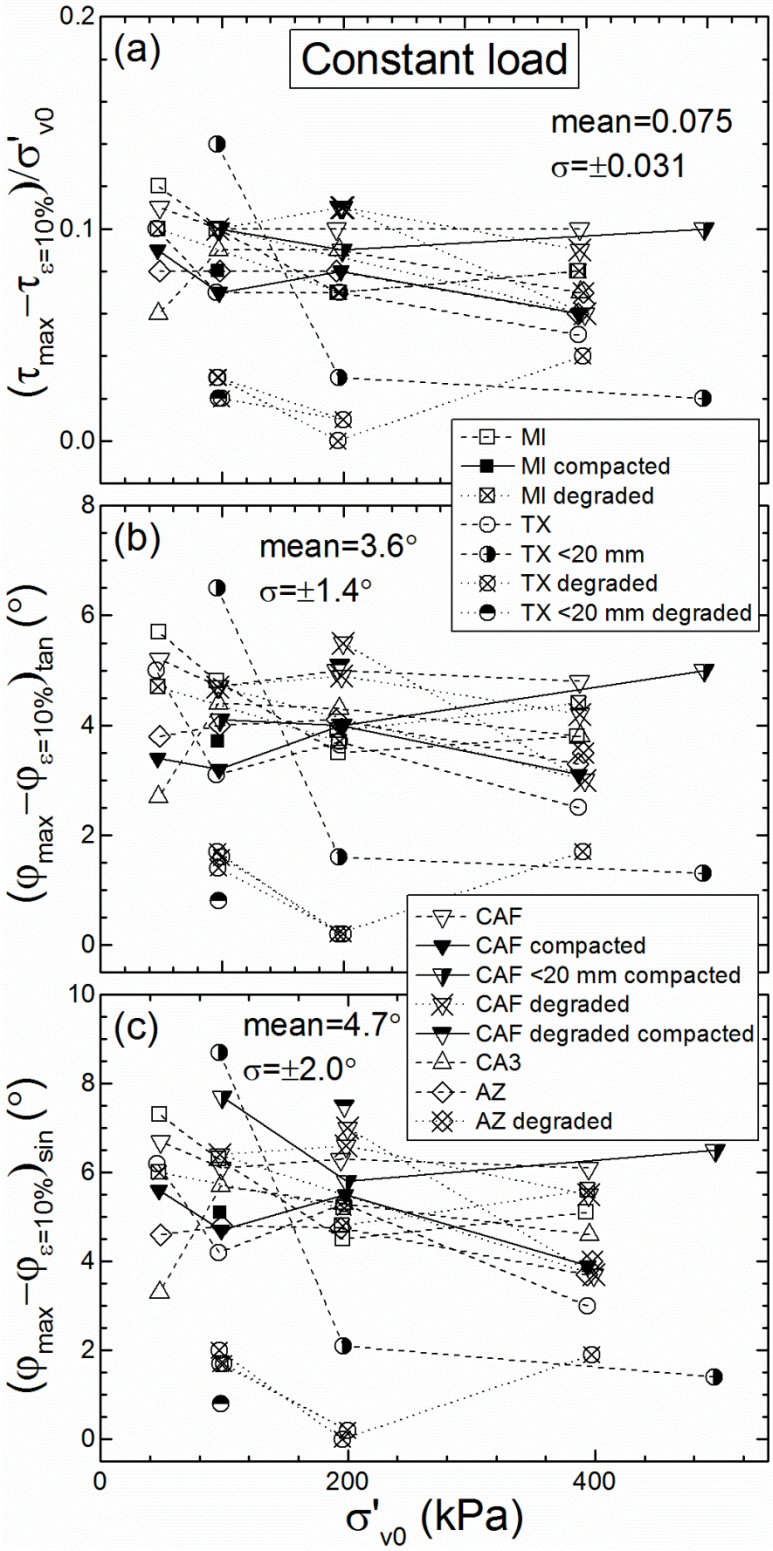

Figure 6-8 Difference between (a) shear strength normalized by initial vertical stress ($(\tau_{max}$-$\tau_{\varepsilon=10\%})/\sigma'_{v0}$); (b) tan friction angle interpretation ($(\varphi_{max}$-$\varphi_{\varepsilon=10\%})_{tan}$); and (c) sin friction angle interpretation ($(\varphi_{max}$-$\varphi_{\varepsilon=10\%})_{sin}$) using maximum shear strength compared to shear strength at 10% shear strain in constant load tests.

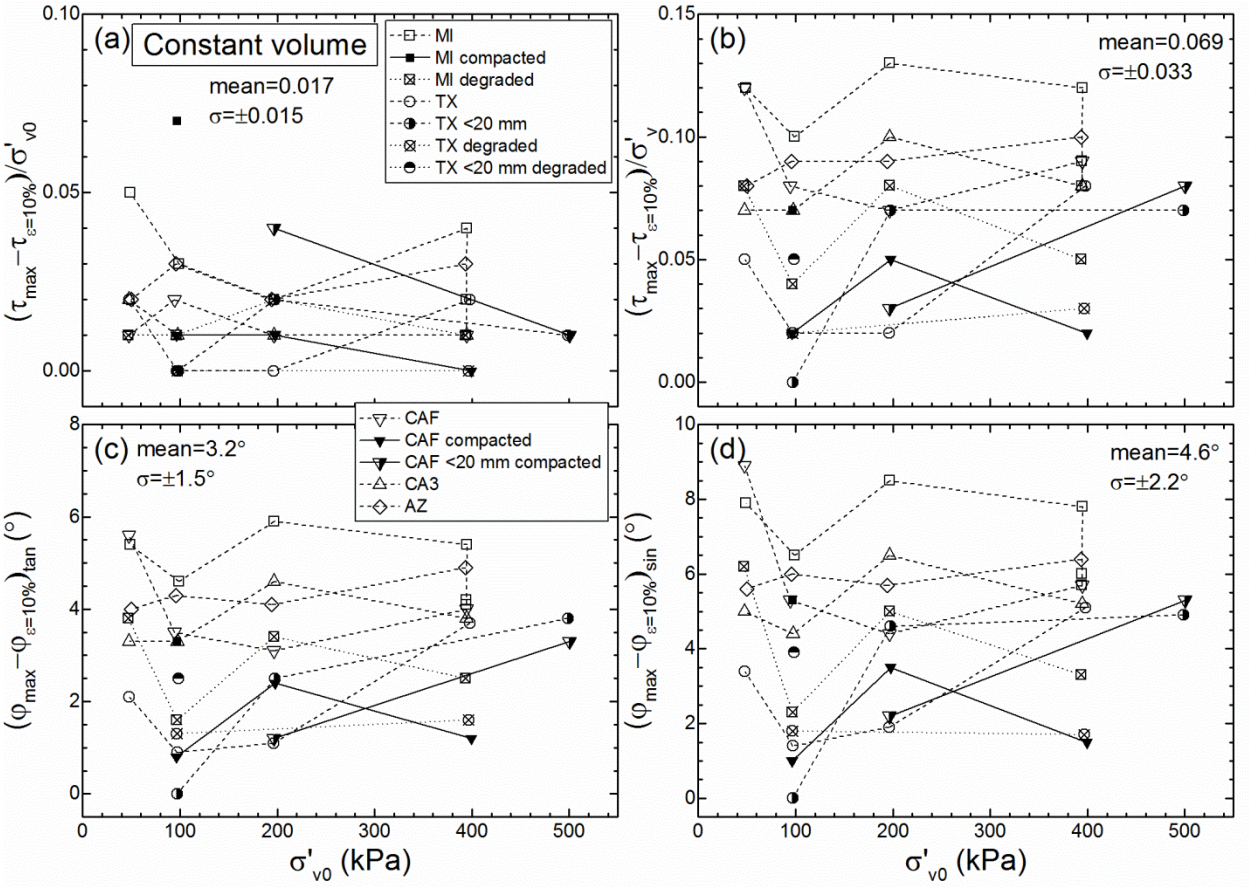

Figure 6-9 Difference between (a) shear strength normalized by initial vertical stress ($(\tau_{max}-\tau_{\varepsilon=10\%})/\sigma'_{v0}$); (b) shear strength normalized by effective vertical stress ($(\tau_{max}-\tau_{\varepsilon=10\%})/\sigma'_{v0}$); (c) tan friction angle interpretation ($(\varphi_{max}-\varphi_{\varepsilon=10\%})_{tan}$); and (d) sin friction angle interpretation ($(\varphi_{max}-\varphi_{\varepsilon=10\%})_{sin}$) using maximum shear strength compared to shear strength at 10% shear strain in constant volume tests.

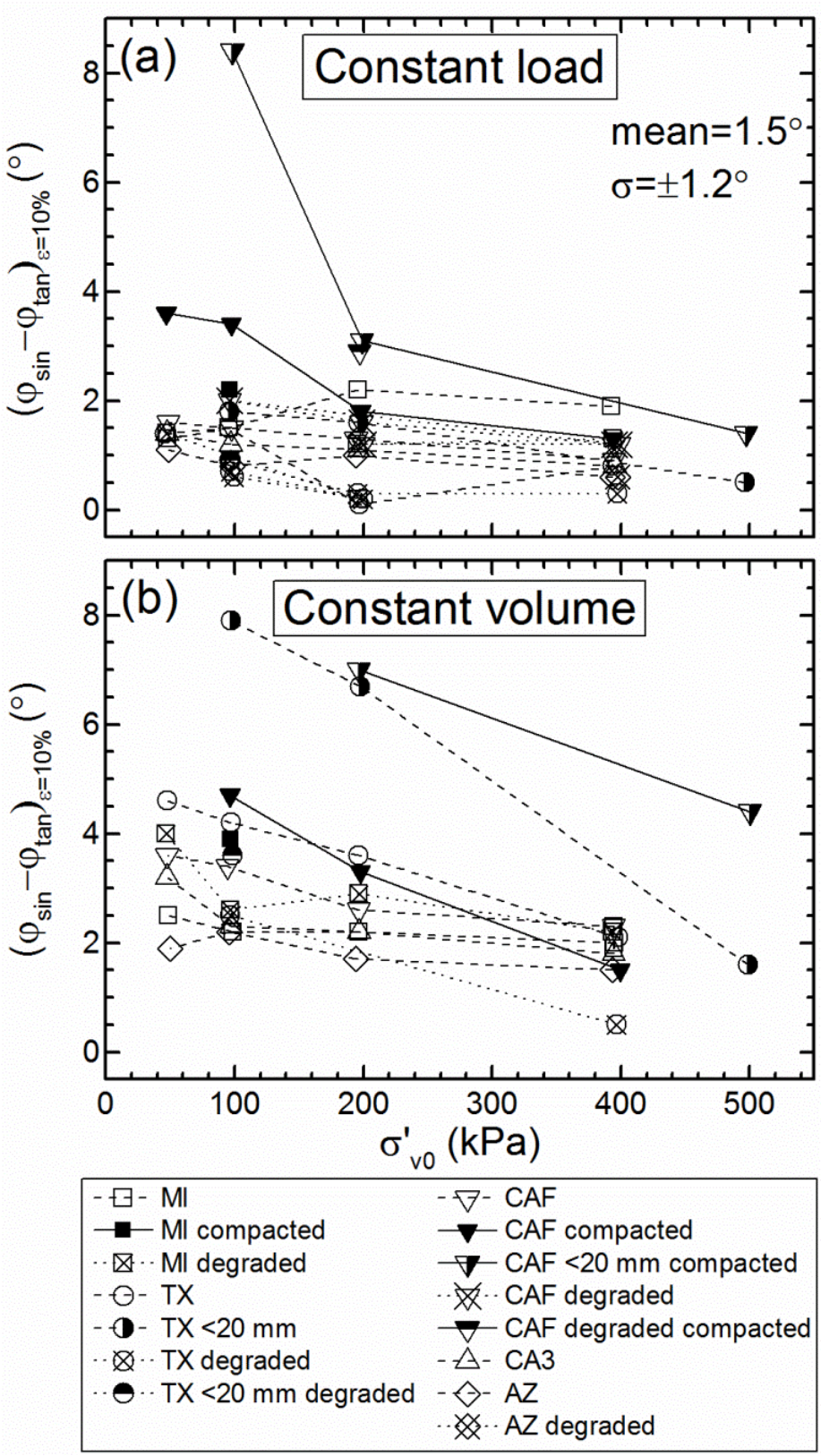

Figure 6-10 Difference in calculated friction angle (Δφ) at 10% shear strain for different failure criteria considered (φ_{sin} and φ_{tan}) for (a) constant load and (b) constant volume tests.

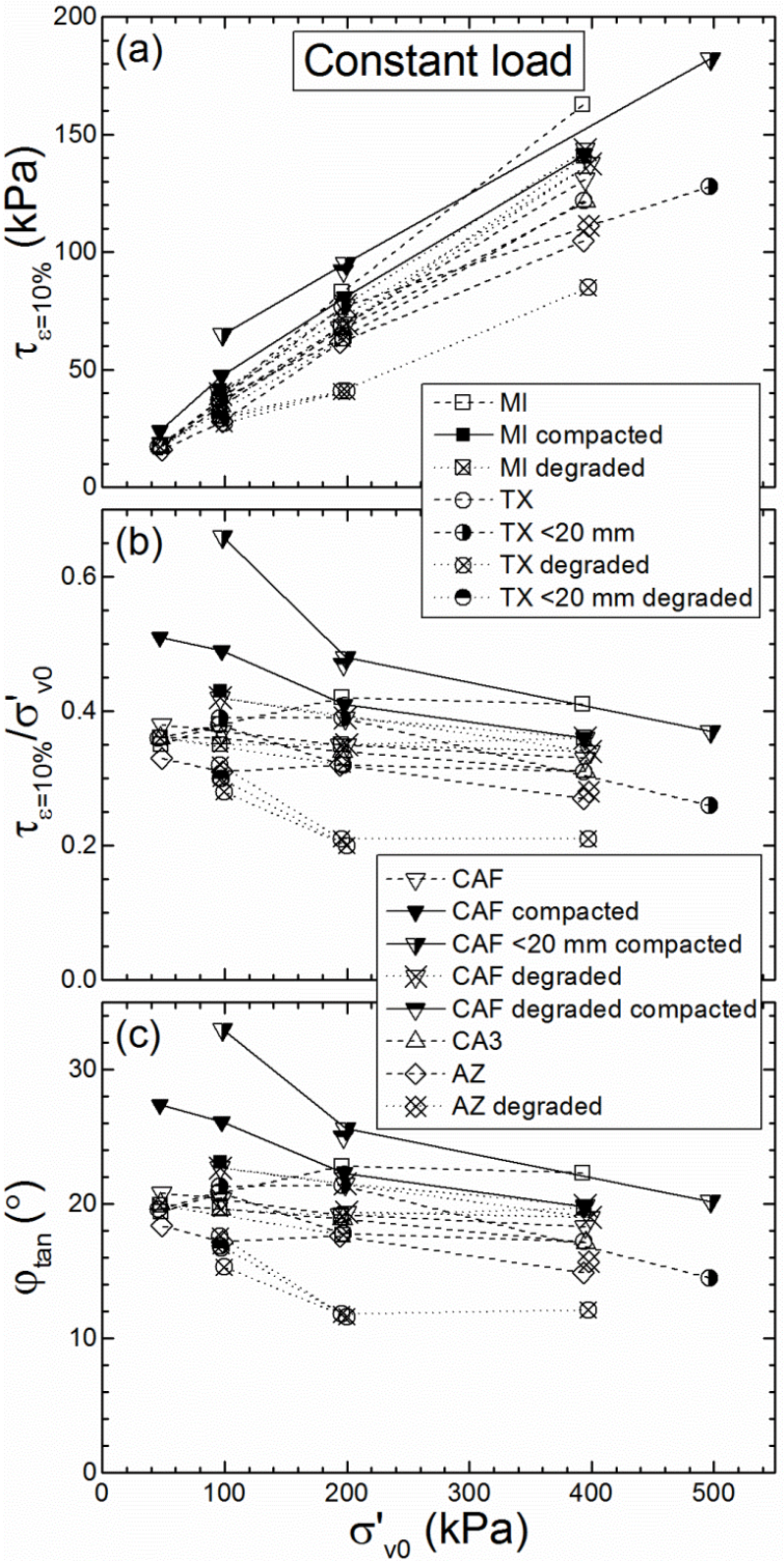

Figure 6-11 Relationship between vertical stress (σ'_{v0}) and (a) shear strength ($\tau_{\varepsilon=10\%}$); (b) normalized shear strength by σ'_{v0} ($\tau_{\varepsilon=10\%}/\sigma'_{v0}$); and (c) tangent friction angle (φ_{tan}) in constant load tests.

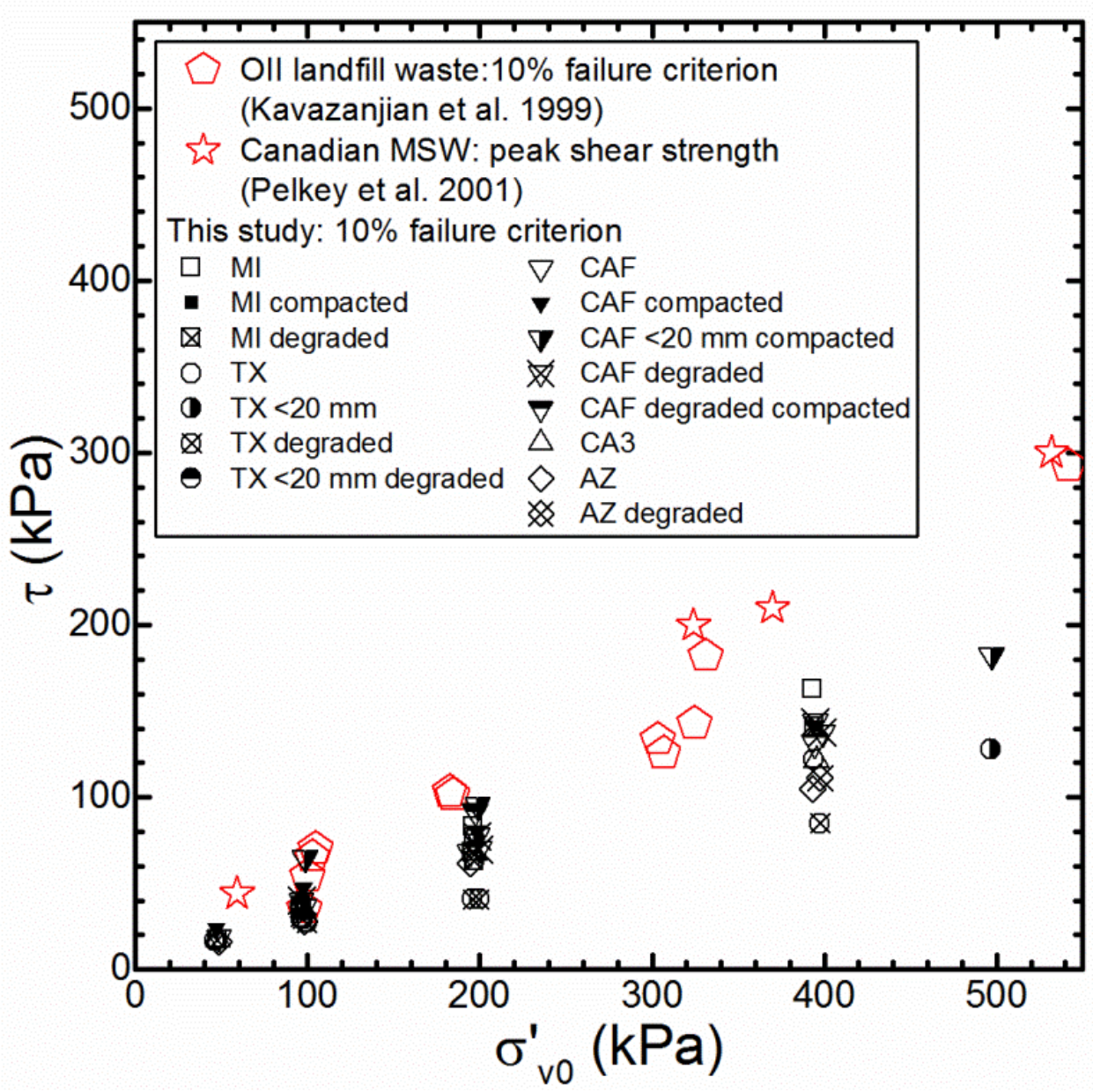

Figure 6-12 Comparison between constant load (drained) shear strength (τ) of MSW in simple shear testing from this study and the literature.

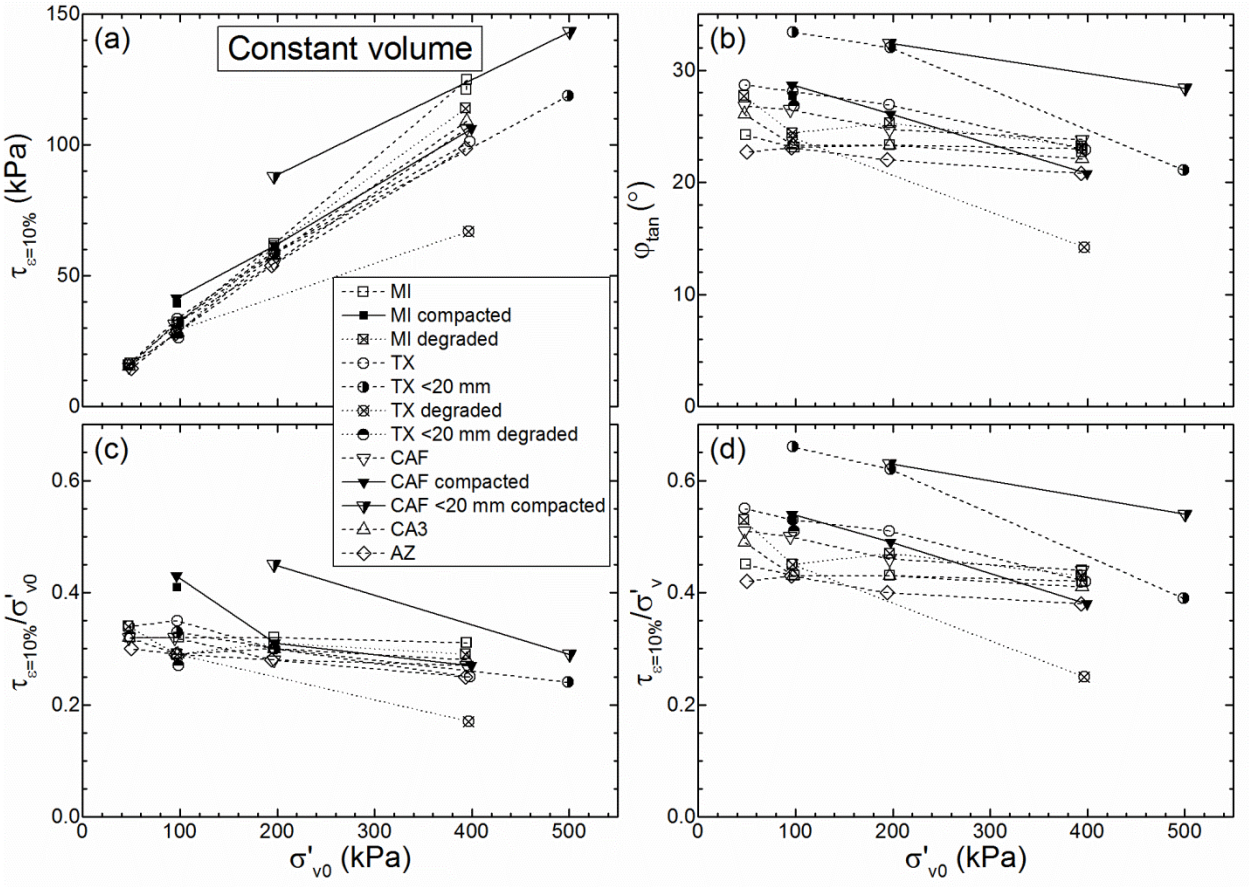

Figure 6-13 Relationship between vertical stress (σ'_{v0}) and (a) shear strength ($\tau_{\varepsilon=10\%}$); (b) tangent friction angle (φ_{tan}); (c) normalized shear strength by σ'_{v0} ($\tau_{\varepsilon=10\%}/\sigma'_{v0}$); and (d) normalized shear strength by σ'_{v} ($\tau_{\varepsilon=10\%}/\sigma'_{v}$) in constant volume tests.

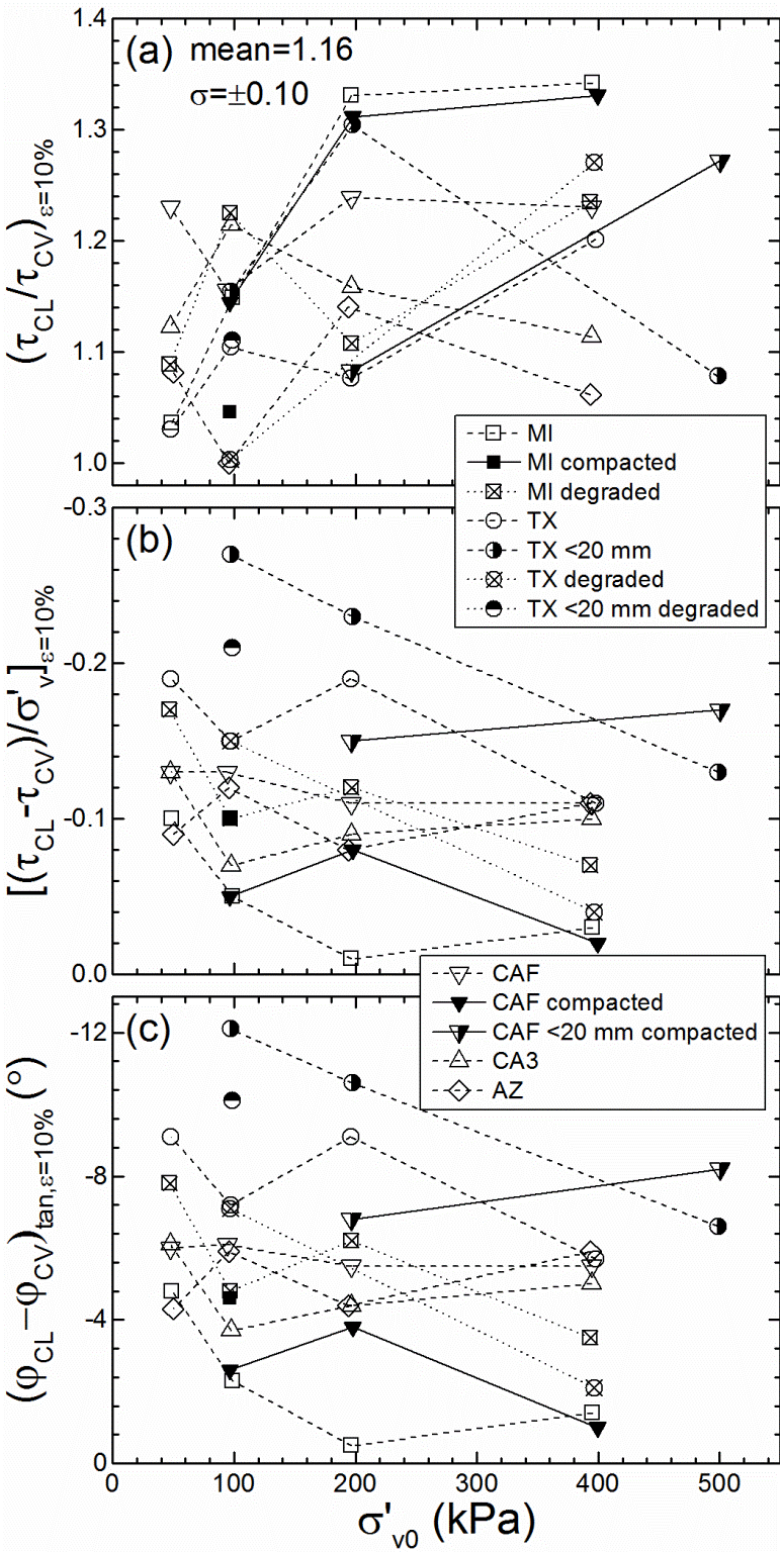

Figure 6-14 Comparison between shear response in constant load and constant volume tests at different vertical stress (σ'_{v0}) in terms of (a) ratio of shear strength ($(\tau_{CL}/\tau_{CV})_{\varepsilon=10\%}$); (b) difference between shear strength normalized by effective vertical stress ($[(\tau_{CL}-\tau_{CV})/\sigma'_v]_{\varepsilon=10\%}$); and (c) difference between φ_{tan} ($(\varphi_{CL}-\varphi_{CV})_{tan,\varepsilon=10\%}$).

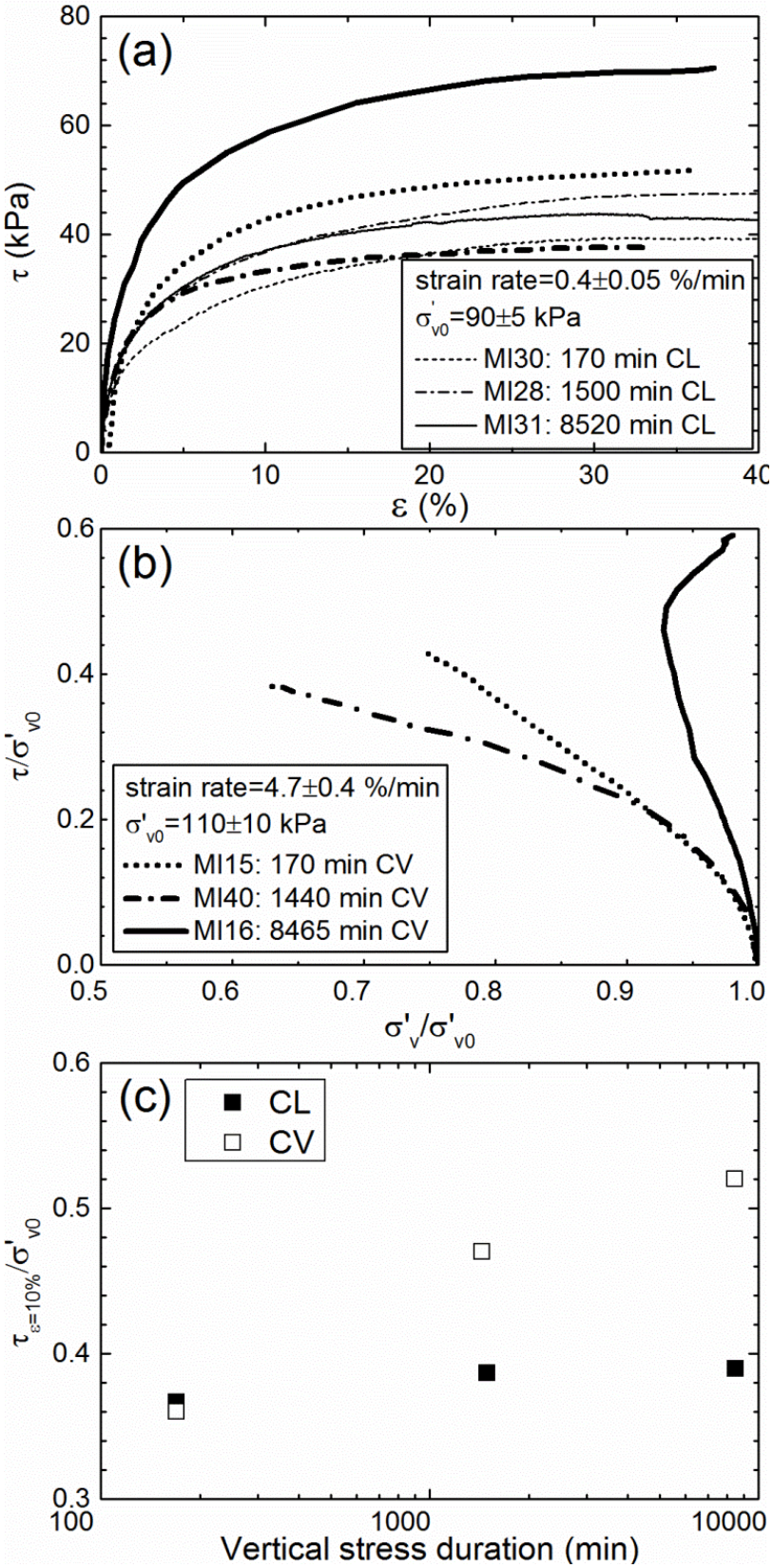

Figure 6-15 Impact of vertical stress duration on (a) stress-strain relationship; (b) stress path; and (c) normalized shear strength ($\tau_{\varepsilon=10\%}/\sigma'_{v0}$) in constant load and constant volume tests.

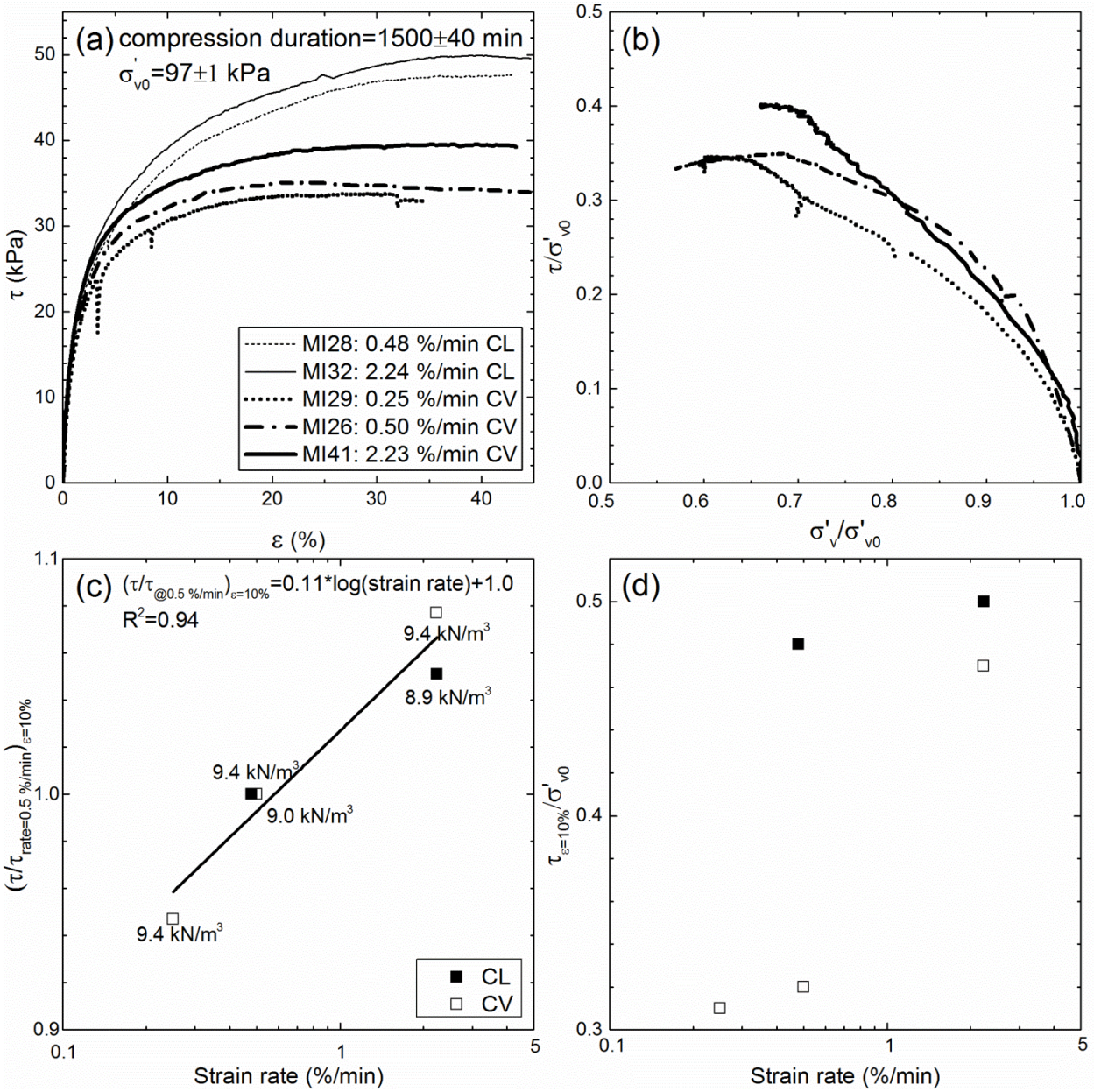

Figure 6-16 Impact of shearing strain rate on (a) stress-strain relationship; (b) stress path; (c) ratio of shear strength to shear strength obtained at 0.5 %/min ($(\tau/\tau_{rate=0.5\ \%/min})_{\varepsilon=10\%}$); and (d) normalized shear strength ($\tau_{\varepsilon=10\%}/\sigma'_{v0}$).

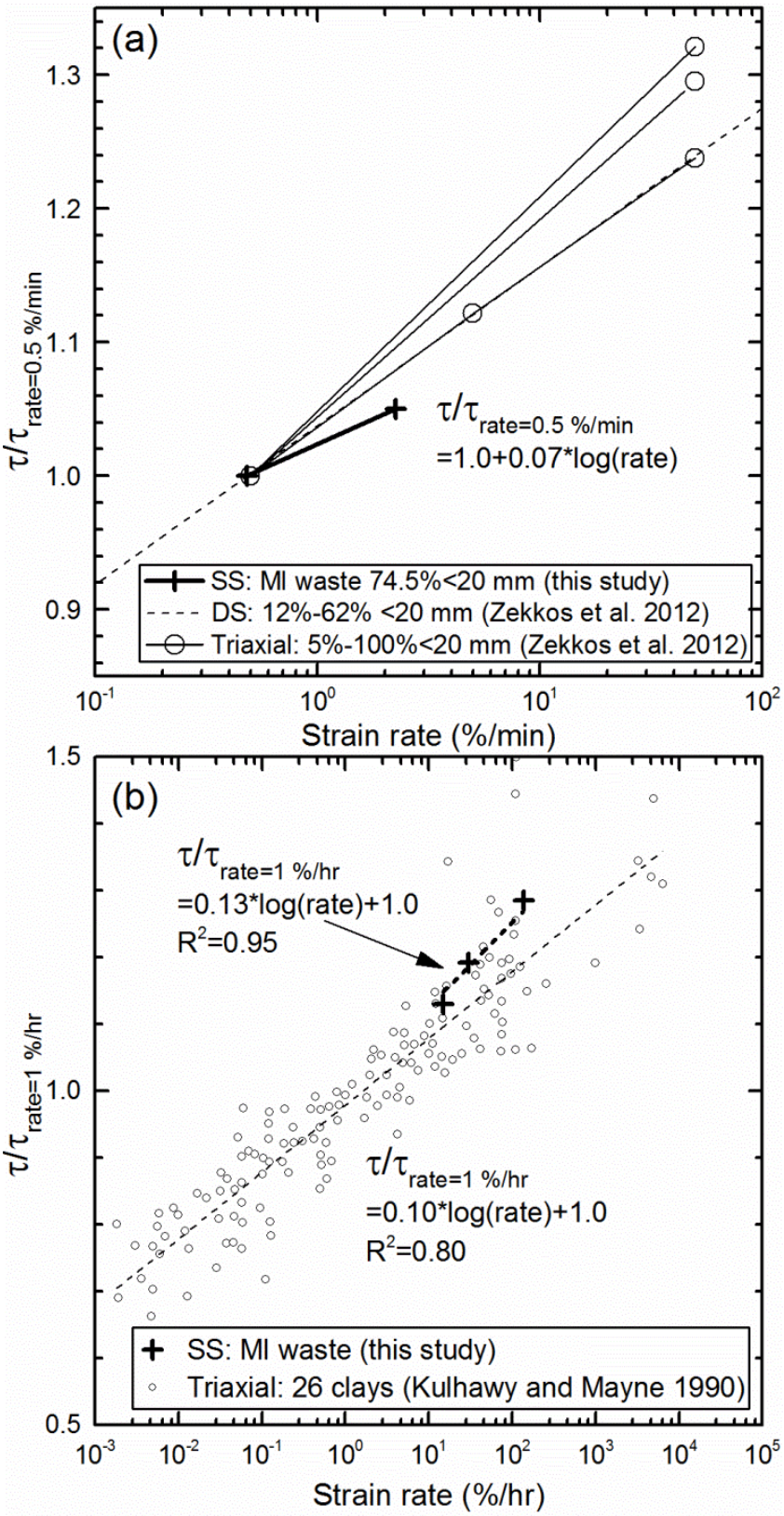

Figure 6-17 Comparison of strain rate effects on (a) drained ($\tau/\tau_{rate=0.5\ \%/min}$); and (b) undrained shear strength ($\tau/\tau_{rate=1\ \%/hr}$) of waste between this study and previous data in the literature.

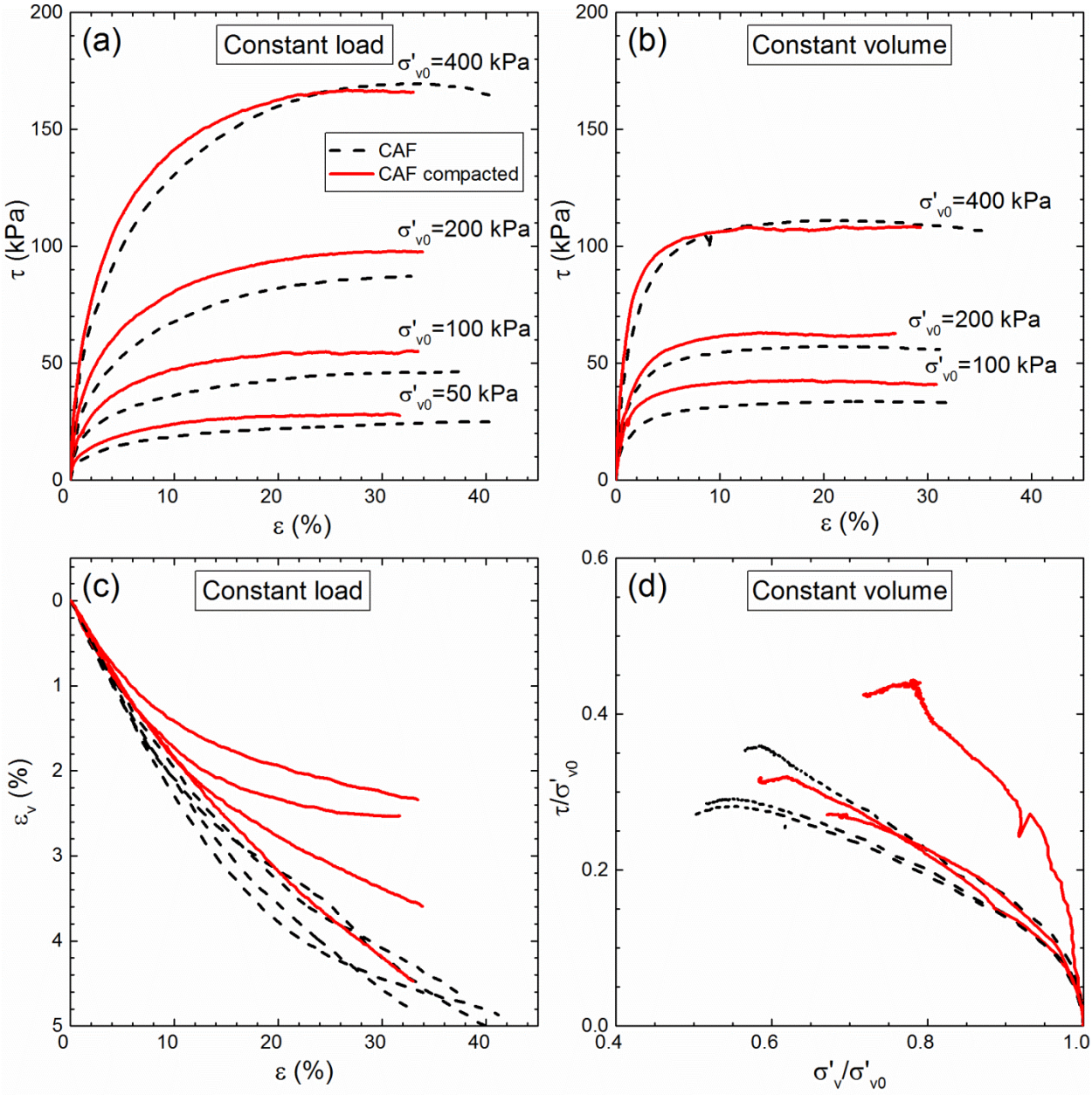

Figure 6-18 Stress-strain relationship in (a) constant load; and (b) constant volume tests; and (c) vertical strain (ε_v) - shear strain (ε_h) relationship in constant load tests; and (d) stress path in constant volume tests for highly and minimally compacted CAF waste at different vertical stress (σ'_{v0}).

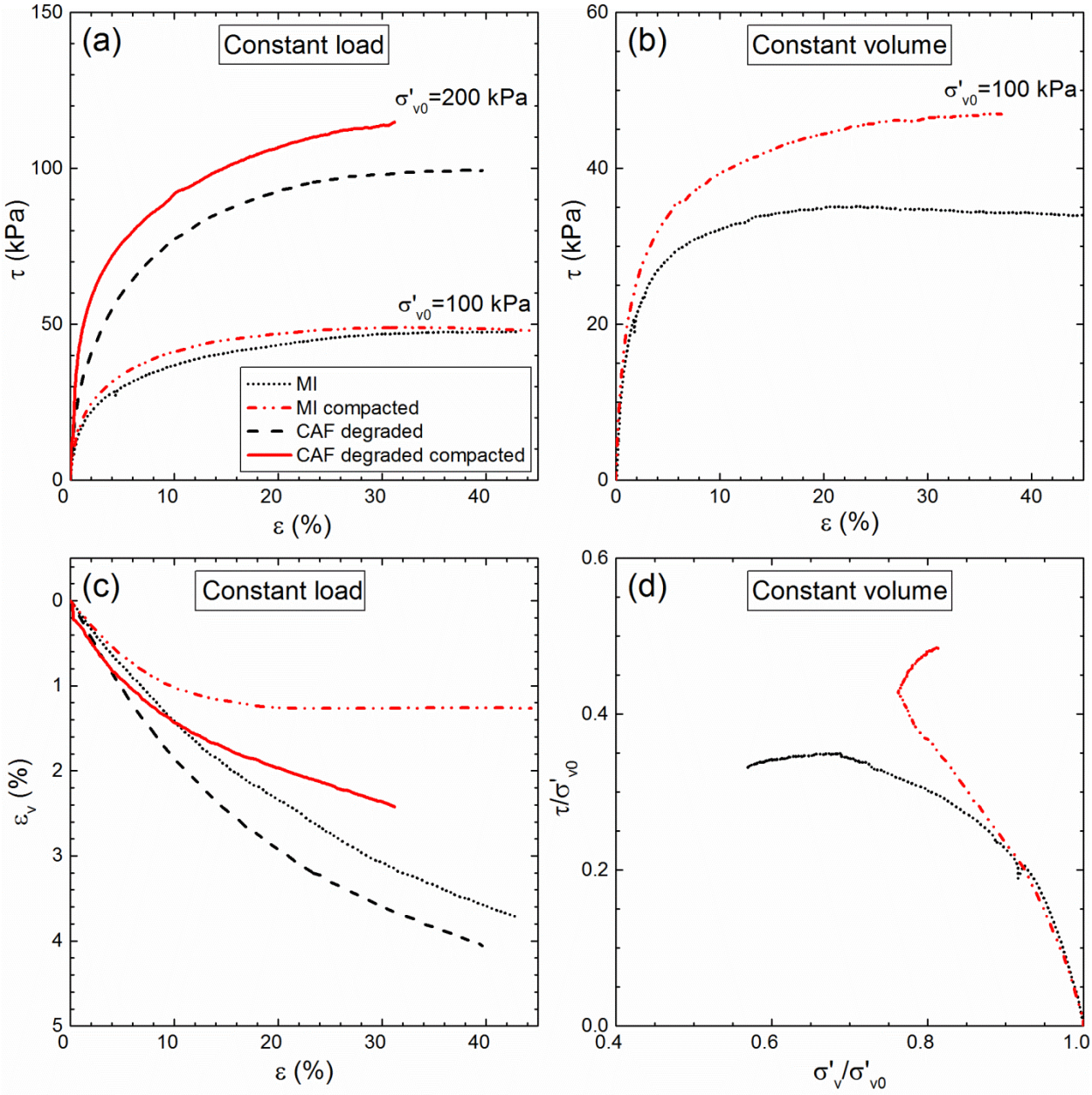

Figure 6-19 Stress-strain relationship in (a) constant load; and (b) constant volume tests; and (c) vertical strain (ε_v) - shear strain (ε_h) relationship in constant load tests; and (d) stress path in constant volume tests for highly and minimally compacted MI and degraded CAF waste at different vertical stress (σ'_{v0}).

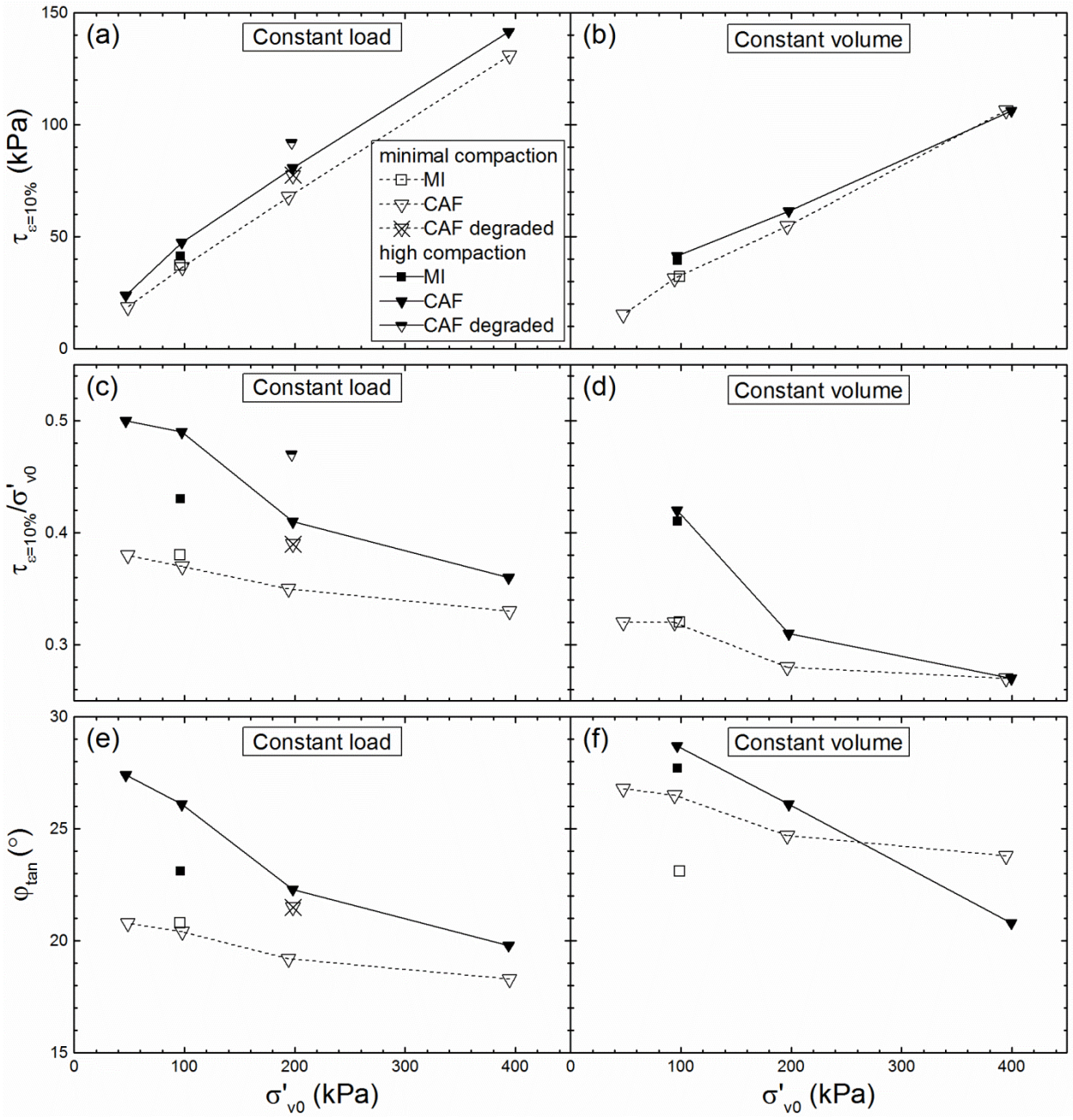

Figure 6-20 Relationships between shear strength ($\tau_{\varepsilon=10\%}$) and vertical stress (σ'_{v0}) of highly and minimally compacted waste in (a) constant load; and (b) constant volume tests; and between normalized shear strength ($\tau_{\varepsilon=10\%}/\sigma'_{v0}$) and σ'_{v0} in (c) constant load; and (d) constant volume tests; and between tangent friction angle (φ_{tan}) and σ'_{v0} in (e) constant load; and (f) constant volume tests.

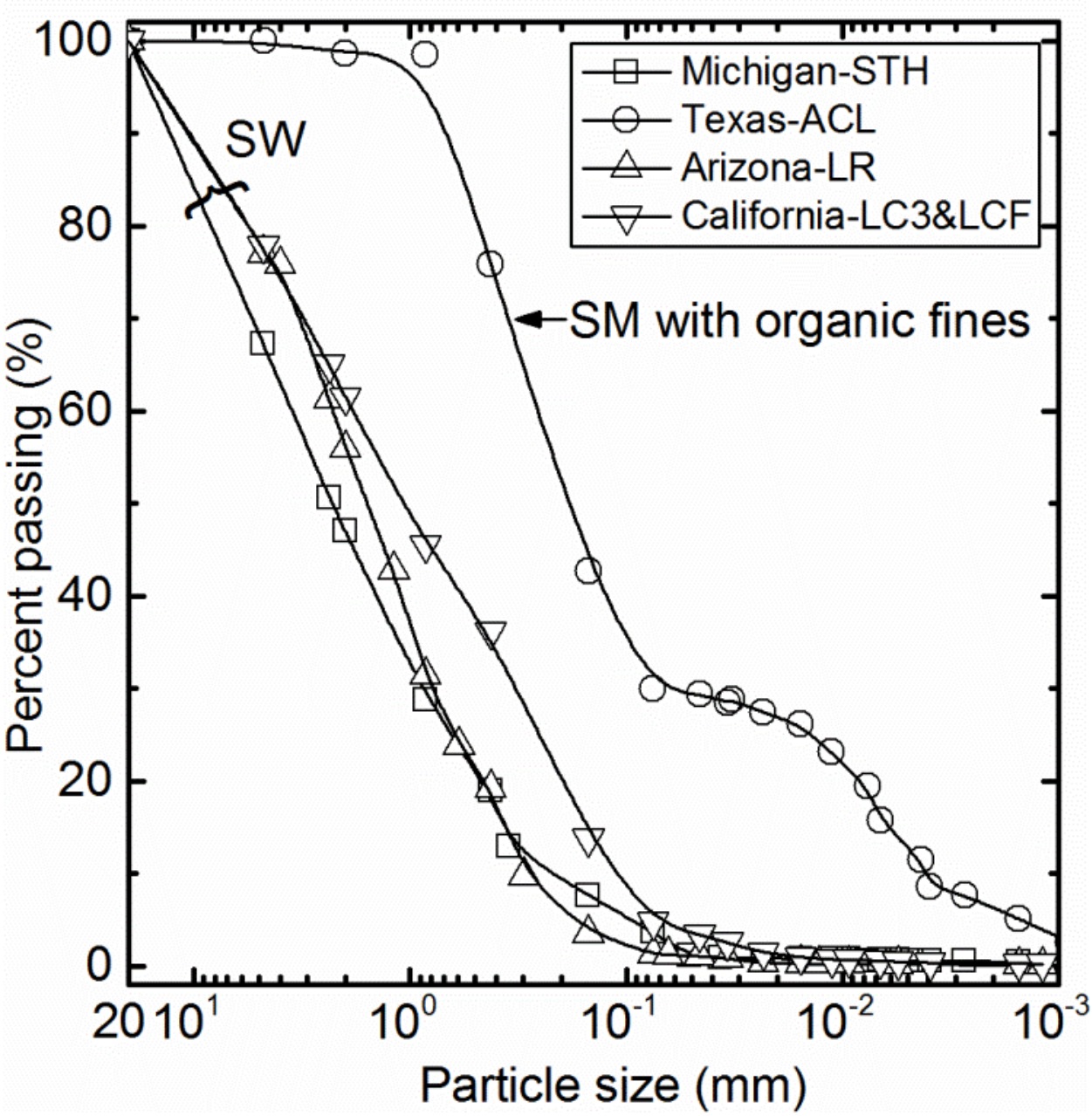

Figure 6-21 Grain size distribution for <20 mm fraction of MI, TX, AZ and CA waste and corresponding soil classification.

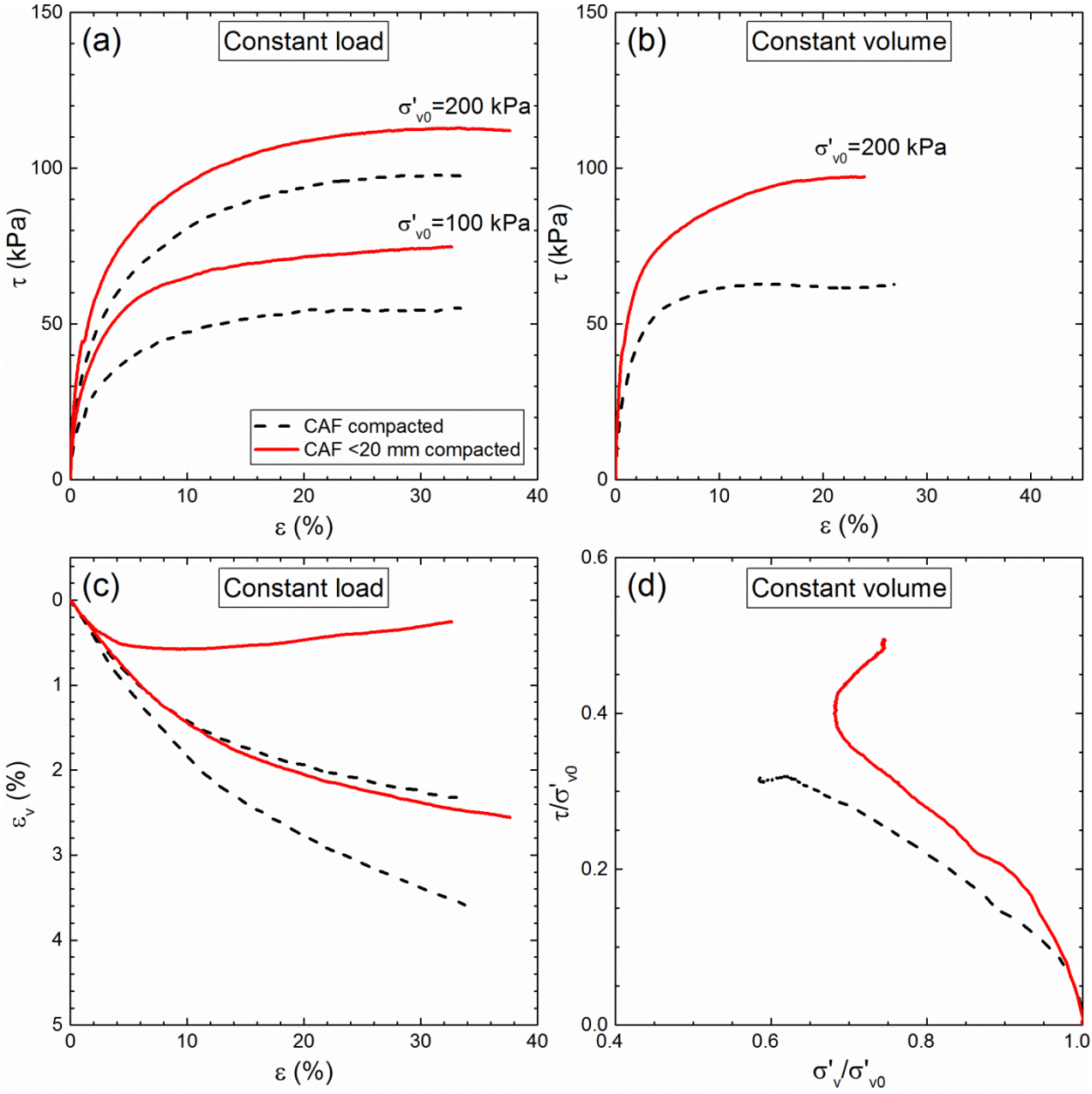

Figure 6-22 Stress-strain relationship in (a) constant load; and (b) constant volume tests; and (c) vertical strain (ε_v) - shear strain (ε_h) relationship in constant load tests; and (d) stress path in constant volume tests for <20 mm fraction only and mixed CAF waste at different vertical stress (σ'_{v0}).

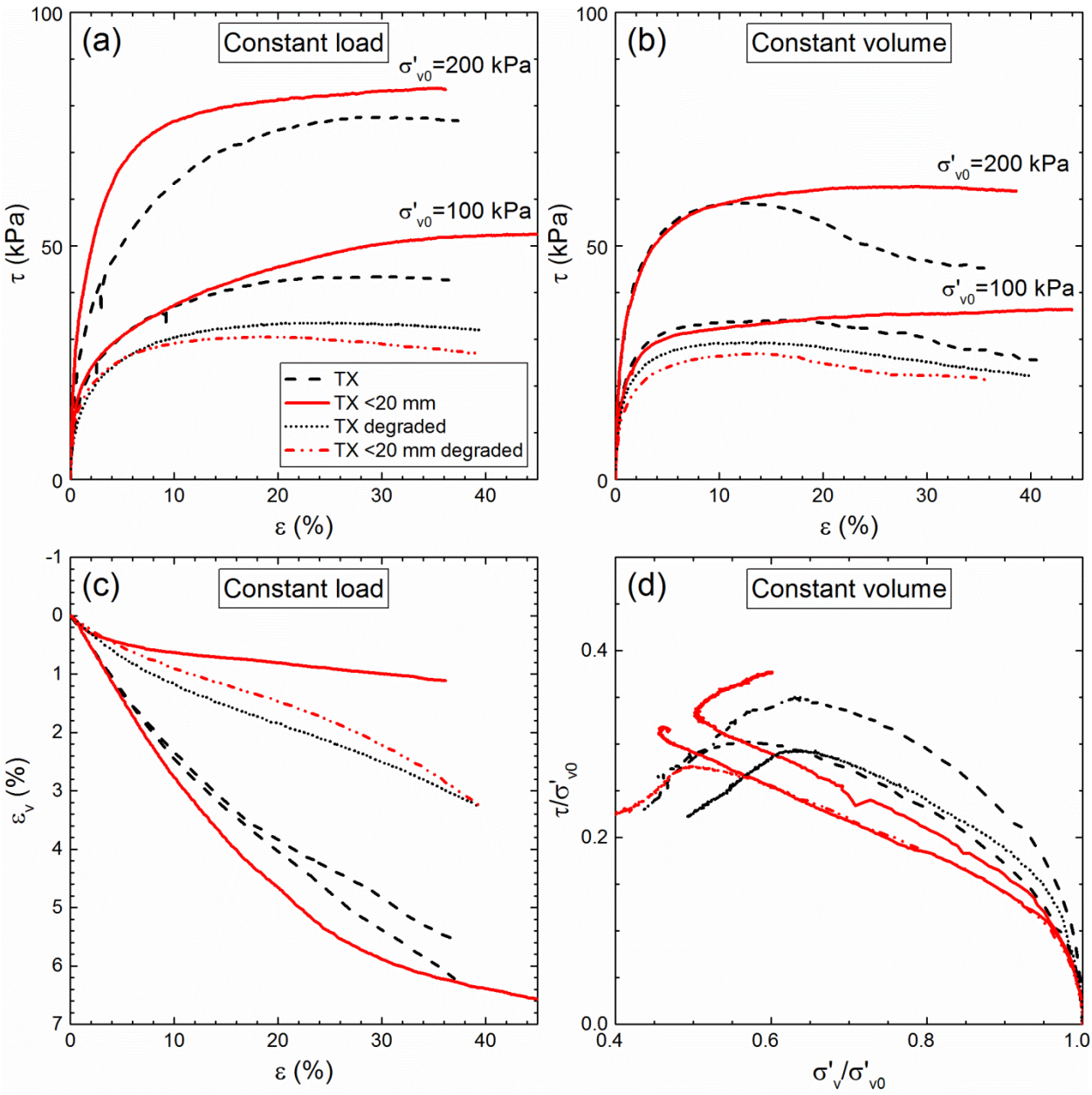

Figure 6-23 Stress-strain relationship in (a) constant load; and (b) constant volume tests; and (c) vertical strain (ε_v) - shear strain (ε_h) relationship in constant load tests; and (d) stress path in constant volume tests for <20 mm fraction only and mixed fresh and degraded TX waste at different vertical stress (σ'_{v0}).

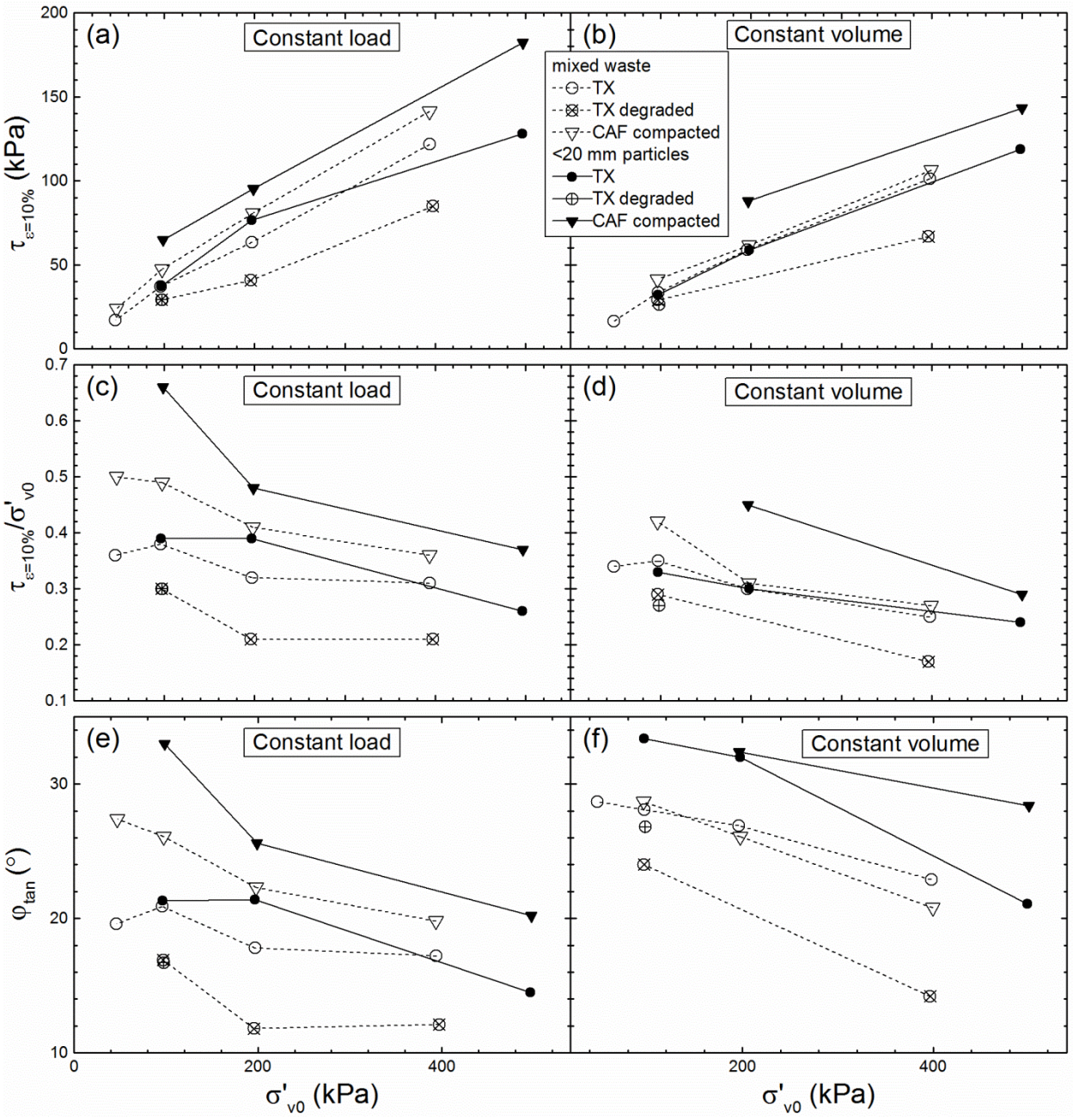

Figure 6-24 Relationships between shear strength ($\tau_{\varepsilon=10\%}$) and vertical stress (σ'_{v0}) of <20 mm fraction only and mixed waste in (a) constant load; and (b) constant volume tests; and between normalized shear strength ($\tau_{\varepsilon=10\%}/\sigma'_{v0}$) and σ'_{v0} in (c) constant load; and (d) constant volume tests; and between tangent friction angle (φ_{tan}) and σ'_{v0} in (e) constant load; and (f) constant volume tests.

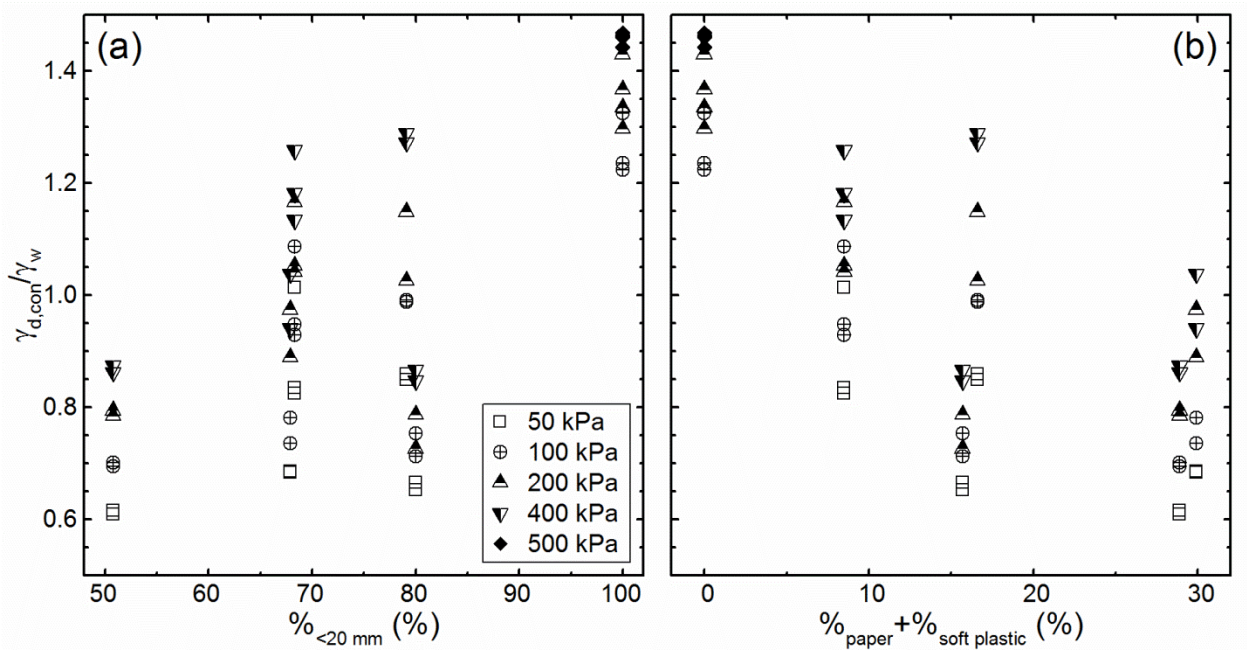

Figure 6-25 Relationship between normalized dry unit weight ($\gamma_{d,con}/\gamma_w$) and (a) % of <20 mm fraction; and (b) % of paper and soft plastic of waste specimens.

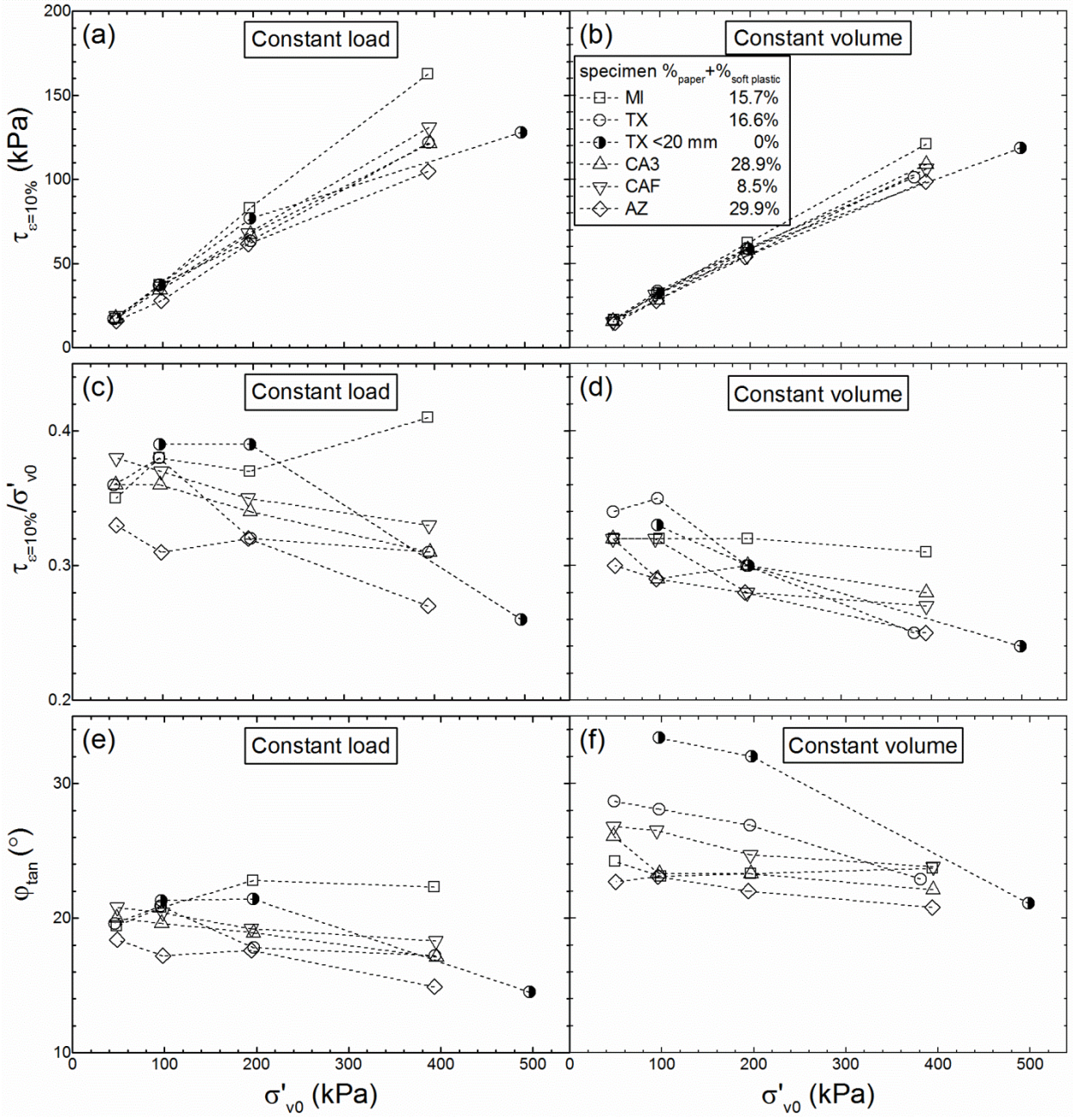

Figure 6-26 Relationship between shear strength ($\tau_{\varepsilon=10\%}$) and vertical stress (σ'_{v0}) of waste of different % of paper and soft plastic in (a) constant load; and (b) constant volume tests; and between normalized shear strength ($\tau_{\varepsilon=10\%}/\sigma'_{v0}$) and σ'_{v0} in (c) constant load; and (d) constant volume tests; and between tangent friction angle (φ_{tan}) and σ'_{v0} in (e) constant load; and (f) constant volume tests.

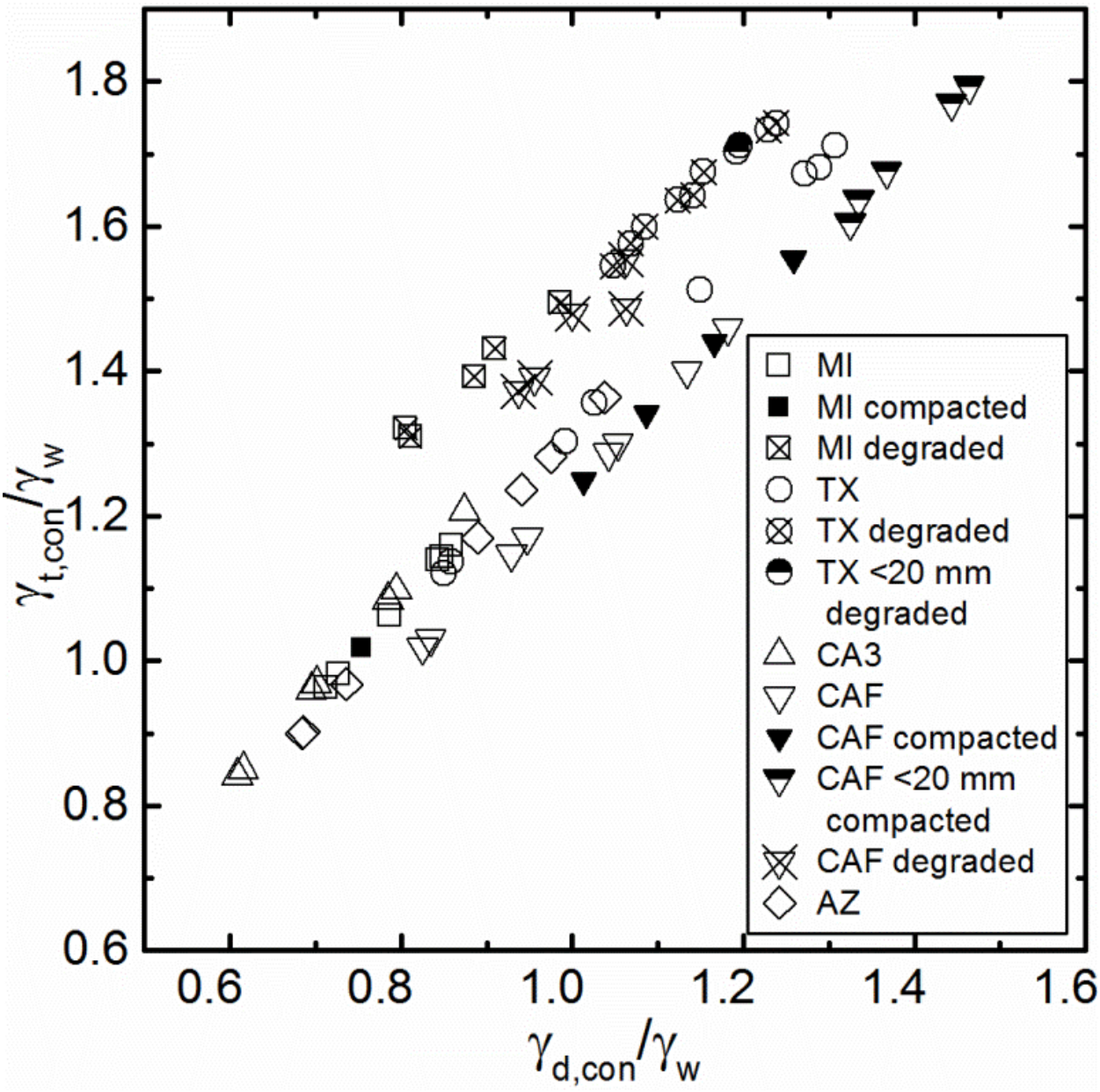

Figure 6-27 Relationship between normalized total ($\gamma_{t,con}/\gamma_w$) and dry unit weight ($\gamma_{d,con}/\gamma_w$) of waste specimens.

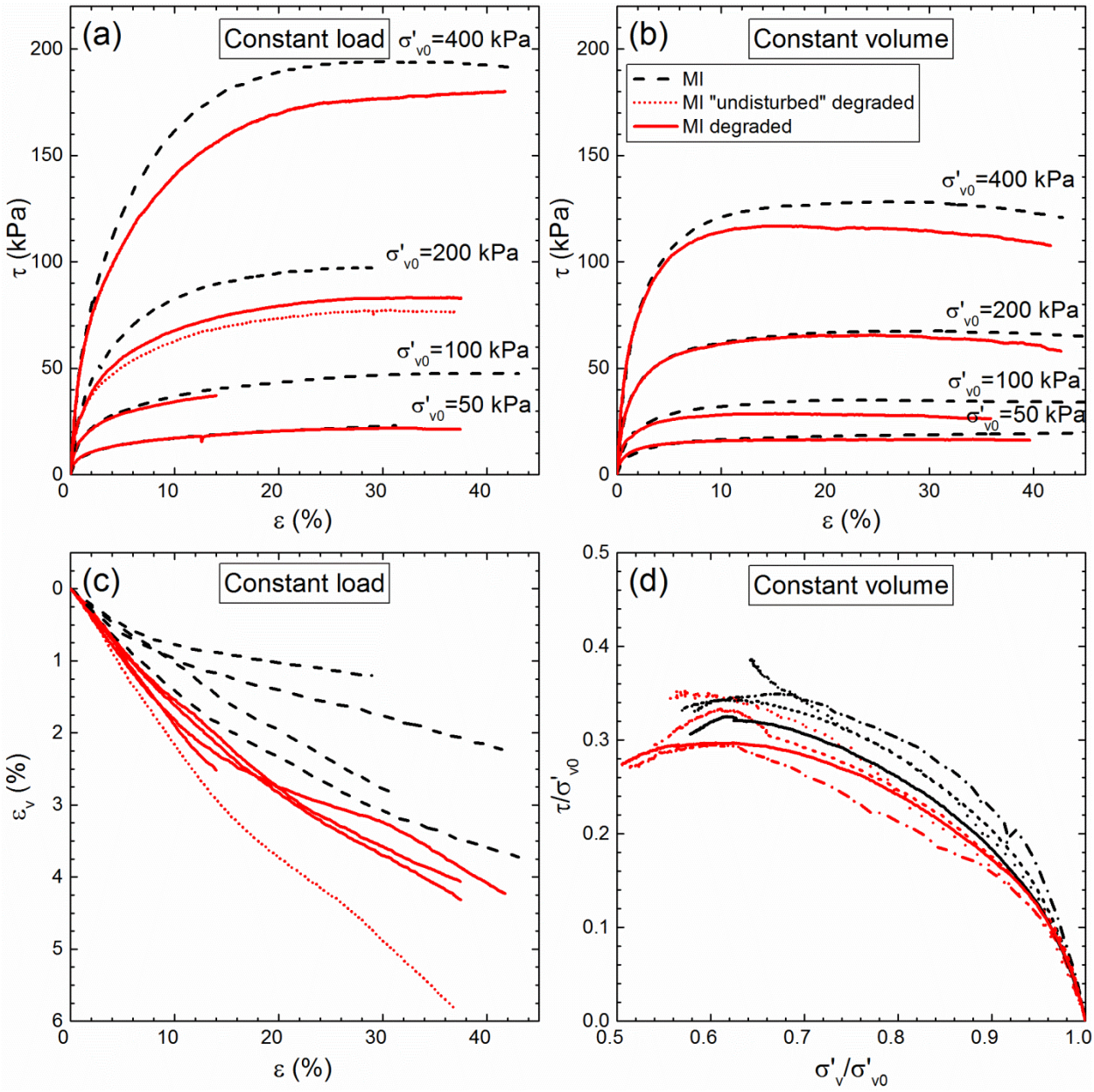

Figure 6-28 Stress-strain relationship in (a) constant load; and (b) constant volume tests; and (c) vertical strain (ε_v) - shear strain (ε_h) relationship in constant load tests; and (d) stress path in constant volume tests for fresh and degraded MI waste at different vertical stress (σ'_{v0}).

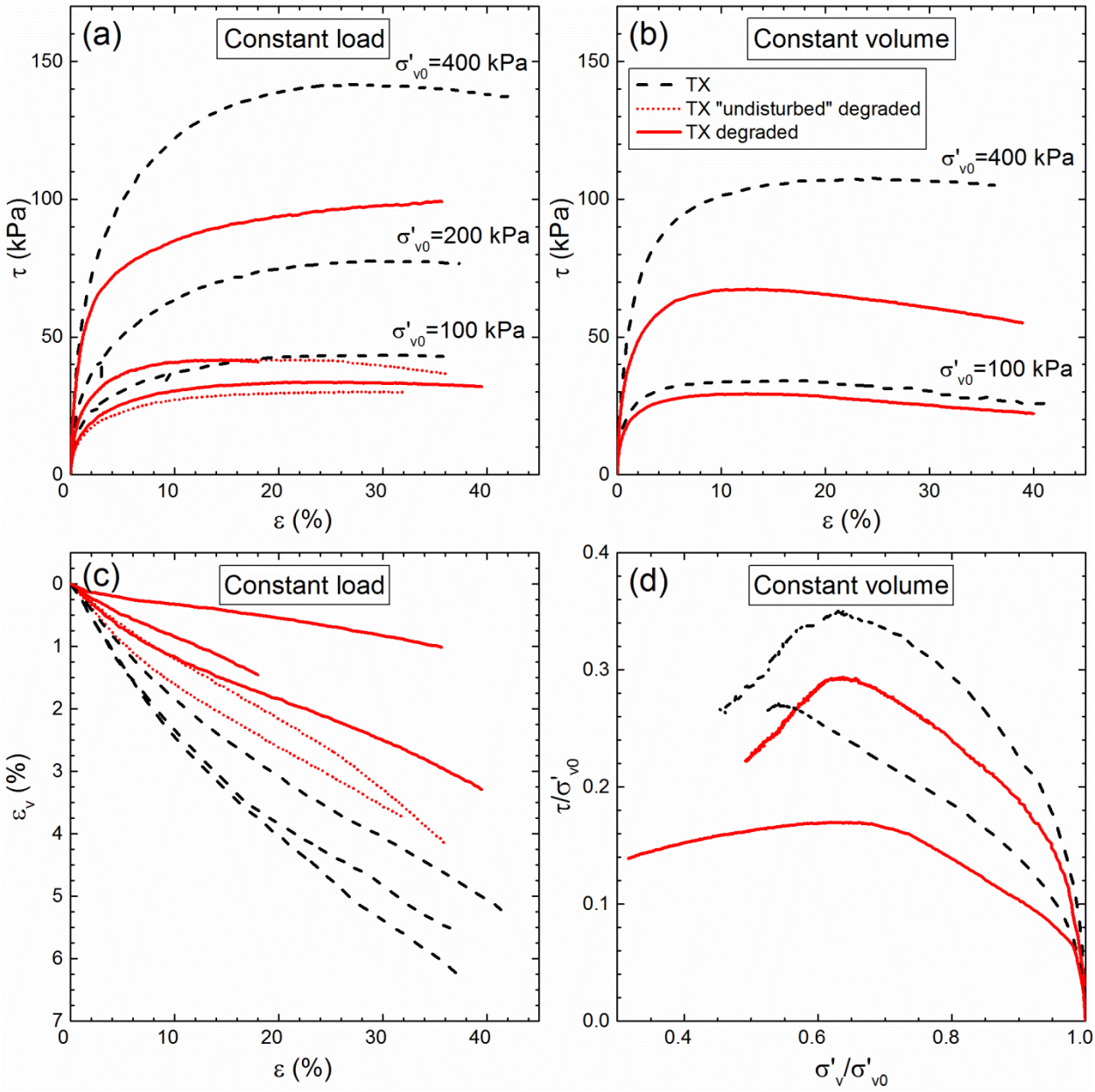

Figure 6-29 Stress-strain relationship in (a) constant load; and (b) constant volume tests; and (c) vertical strain (ε_v) - shear strain (ε_h) relationship in constant load tests; and (d) stress path in constant volume tests for fresh and degraded TX waste at different vertical stress (σ'_{v0}).

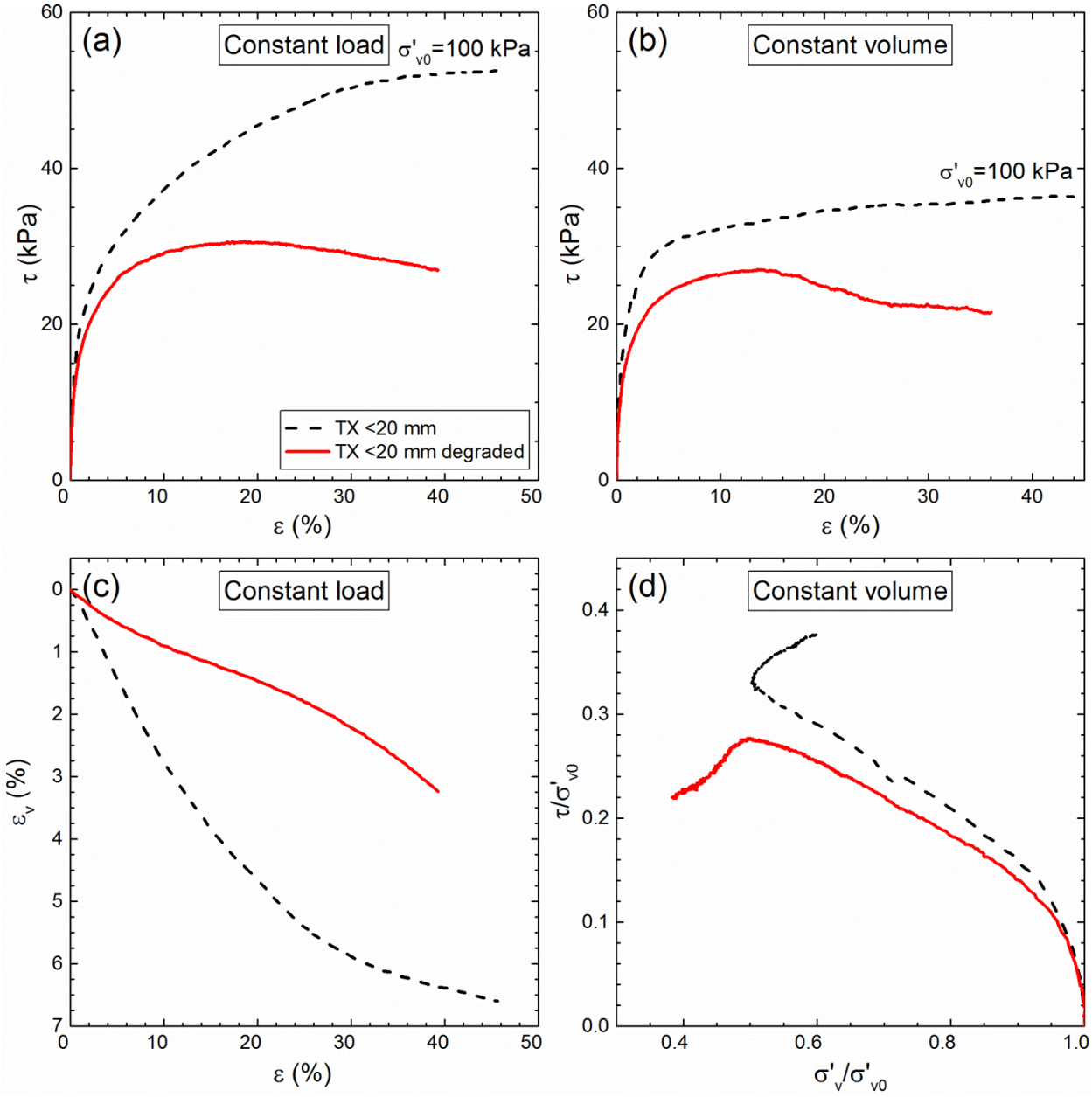

Figure 6-30 Stress-strain relationship in (a) constant load; and (b) constant volume tests; and (c) vertical strain (ε_v) - shear strain (ε_h) relationship in constant load tests; and (d) stress path in constant volume tests for fresh and degraded <20 mm fraction only TX waste at different vertical stress (σ'_{v0}).

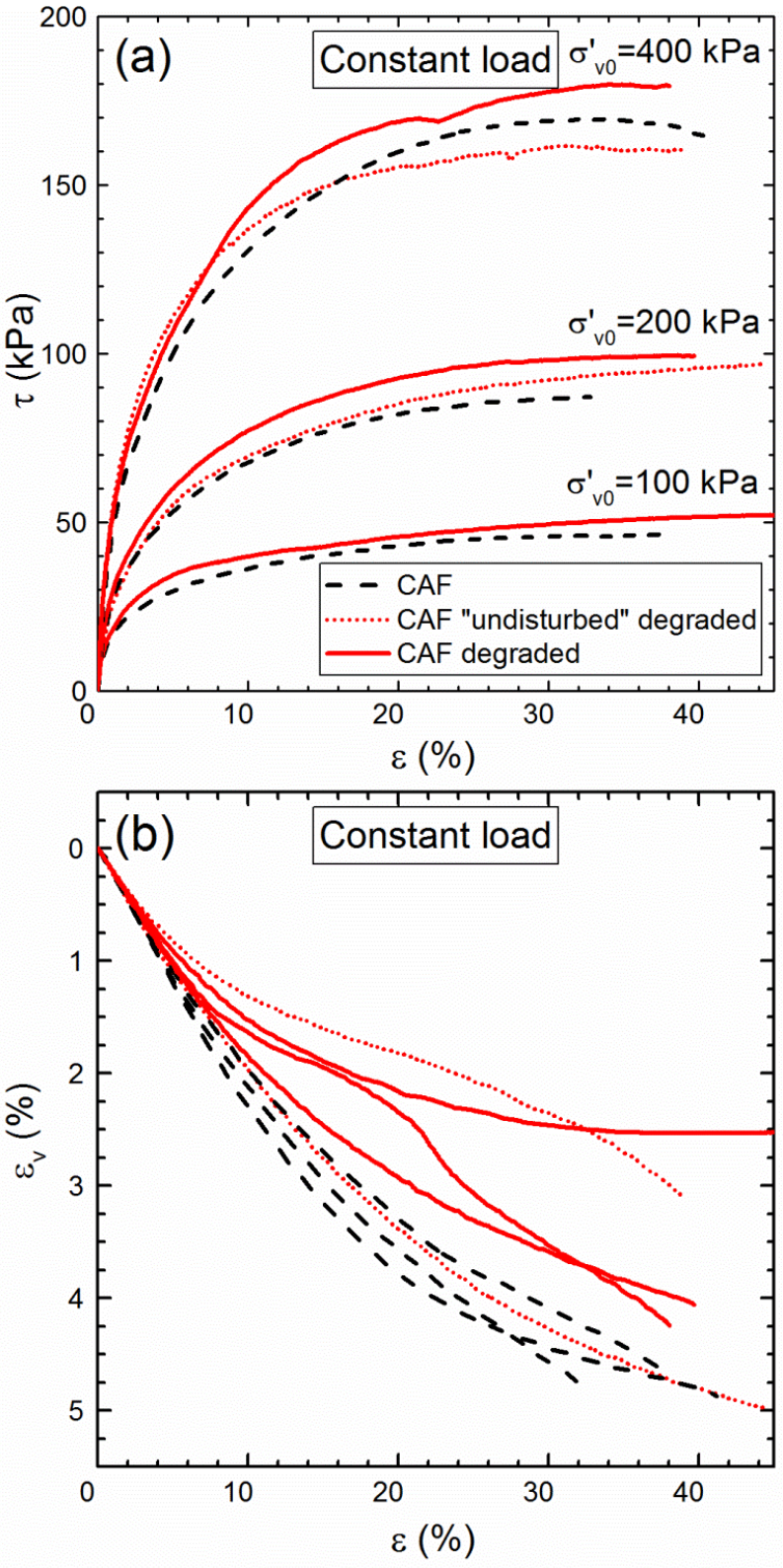

Figure 6-31 (a) Stress-strain relationship; and (b) vertical strain (ε_v) - shear strain (ε_h) relationship in constant load tests for fresh and degraded CAF waste at different vertical stress (σ'_{v0}).

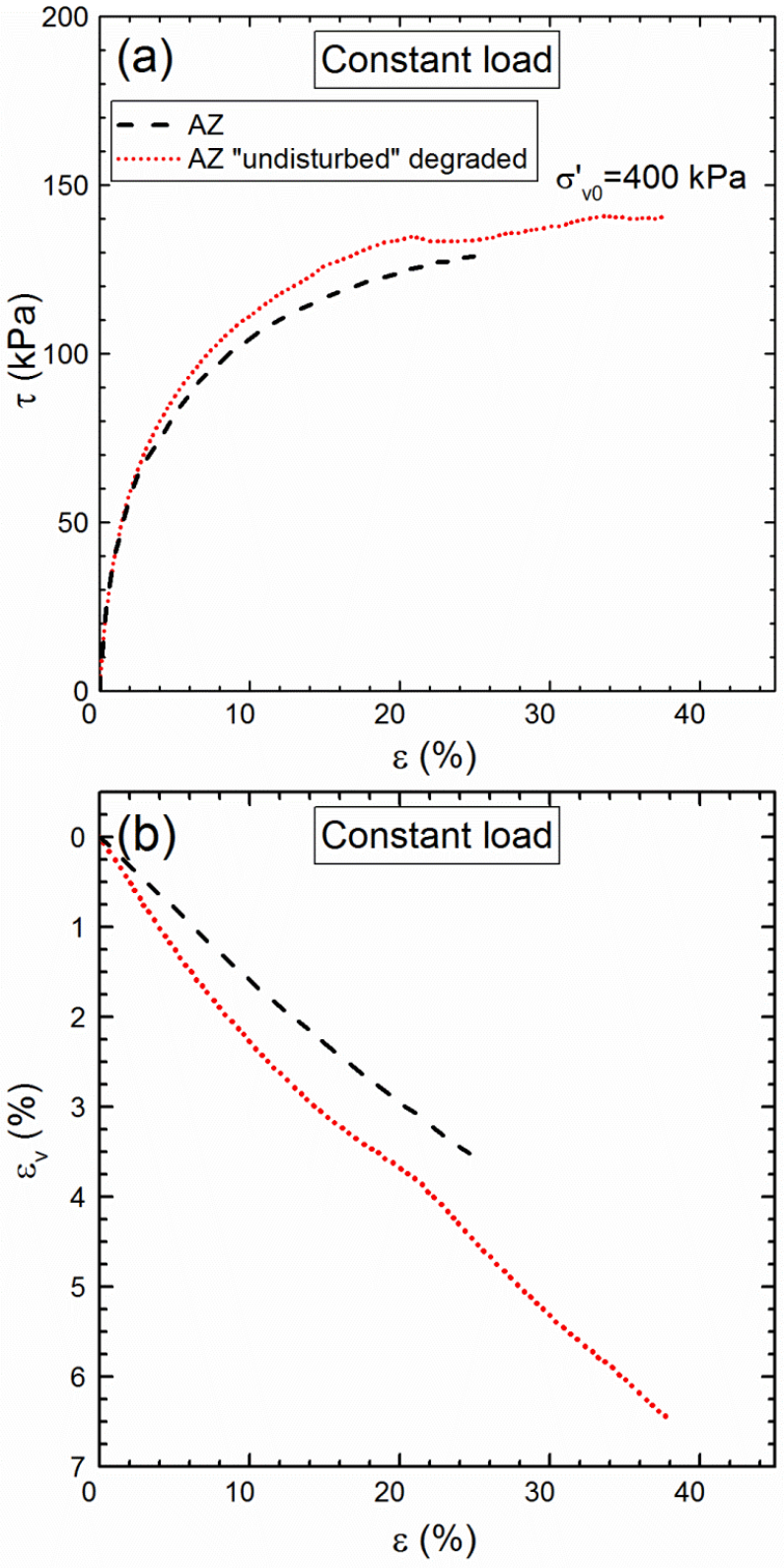

Figure 6-32 (a) Stress-strain relationship; and (b) vertical strain (ε_v) - shear strain (ε_h) relationship in constant load tests for fresh and degraded AZ waste at different vertical stress (σ'_{v0}).

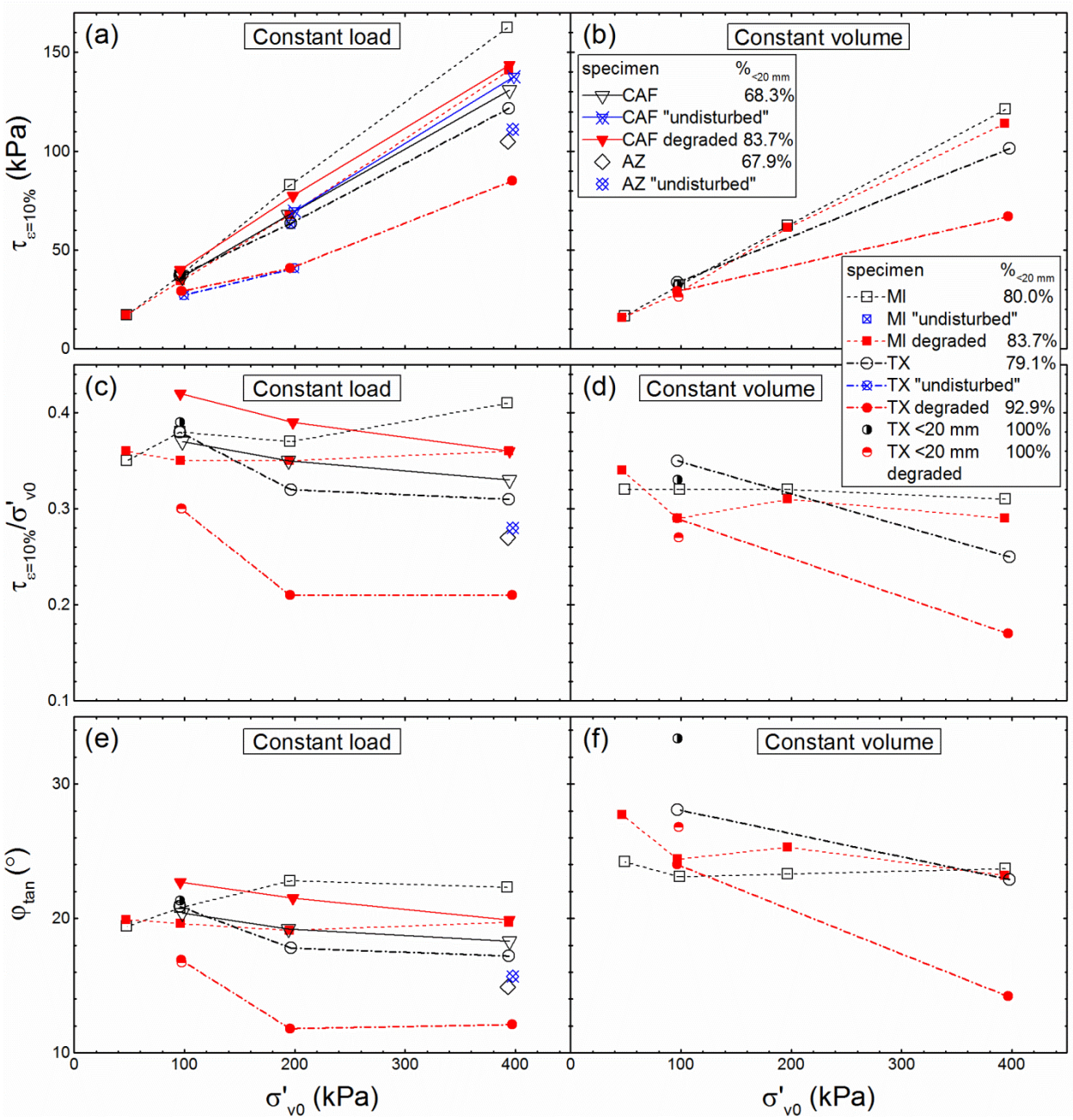

Figure 6-33 Relationships between shear strength ($\tau_{\varepsilon=10\%}$) and vertical stress (σ'_{v0}) of fresh and degraded waste in (a) constant load; and (b) constant volume tests; and between normalized shear strength ($\tau_{\varepsilon=10\%}/\sigma'_{v0}$) and σ'_{v0} in (c) constant load; and (d) constant volume tests; and between tangent friction angle (φ_{tan}) and σ'_{v0} in (e) constant load; and (f) constant volume tests.

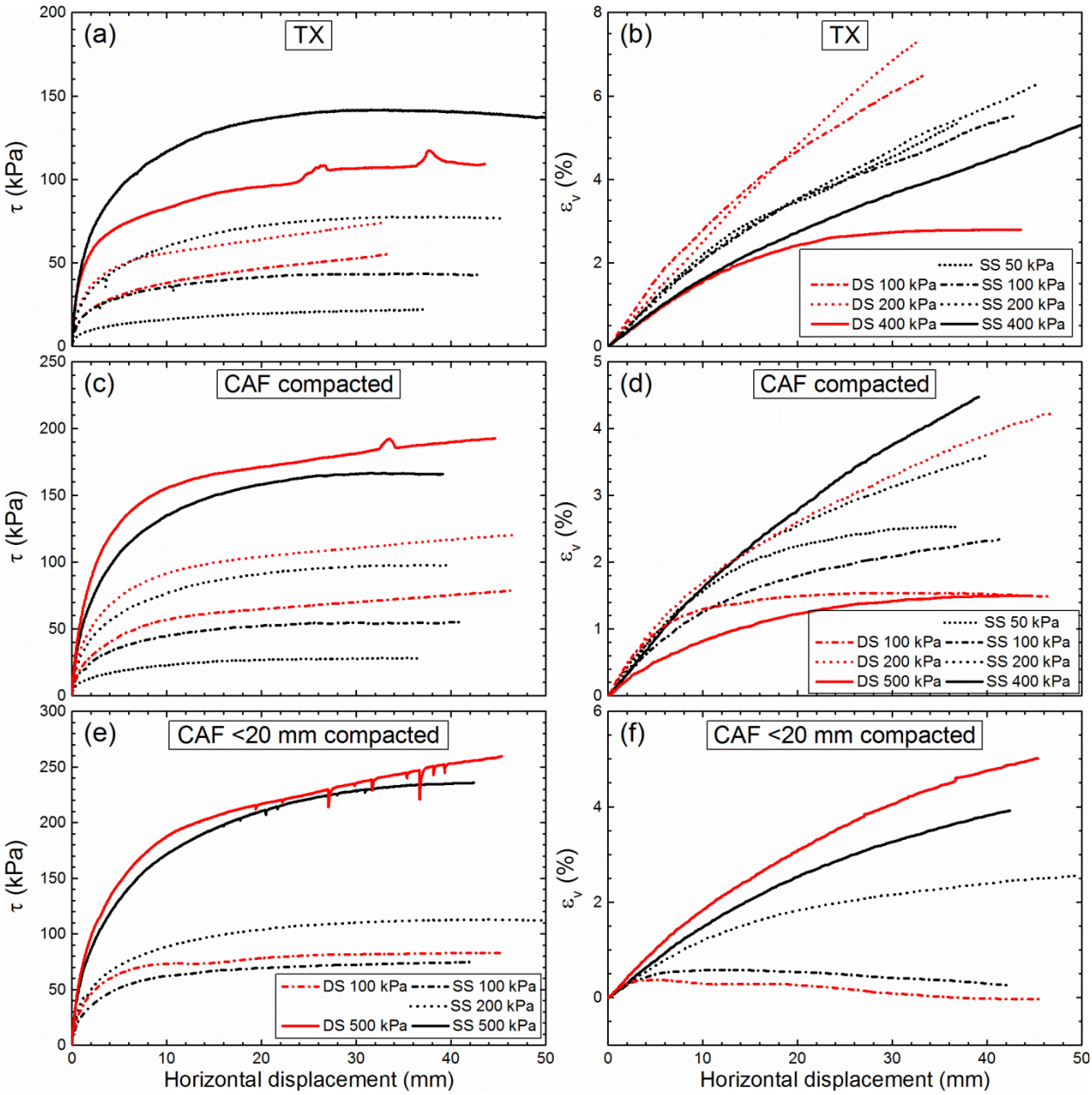

Figure 6-34 Comparison between direct shear and simple shear response of TX waste: (a) stress (τ)-displacement relationship; and (b) vertical strain (ε_v)-displacement relationship; highly compacted CAF waste: (c) τ-displacement relationship; and (d) ε_v-displacement relationship; highly compacted <20 mm fraction of CAF waste: (e) τ-displacement relationship; and (f) ε_v-displacement relationship.

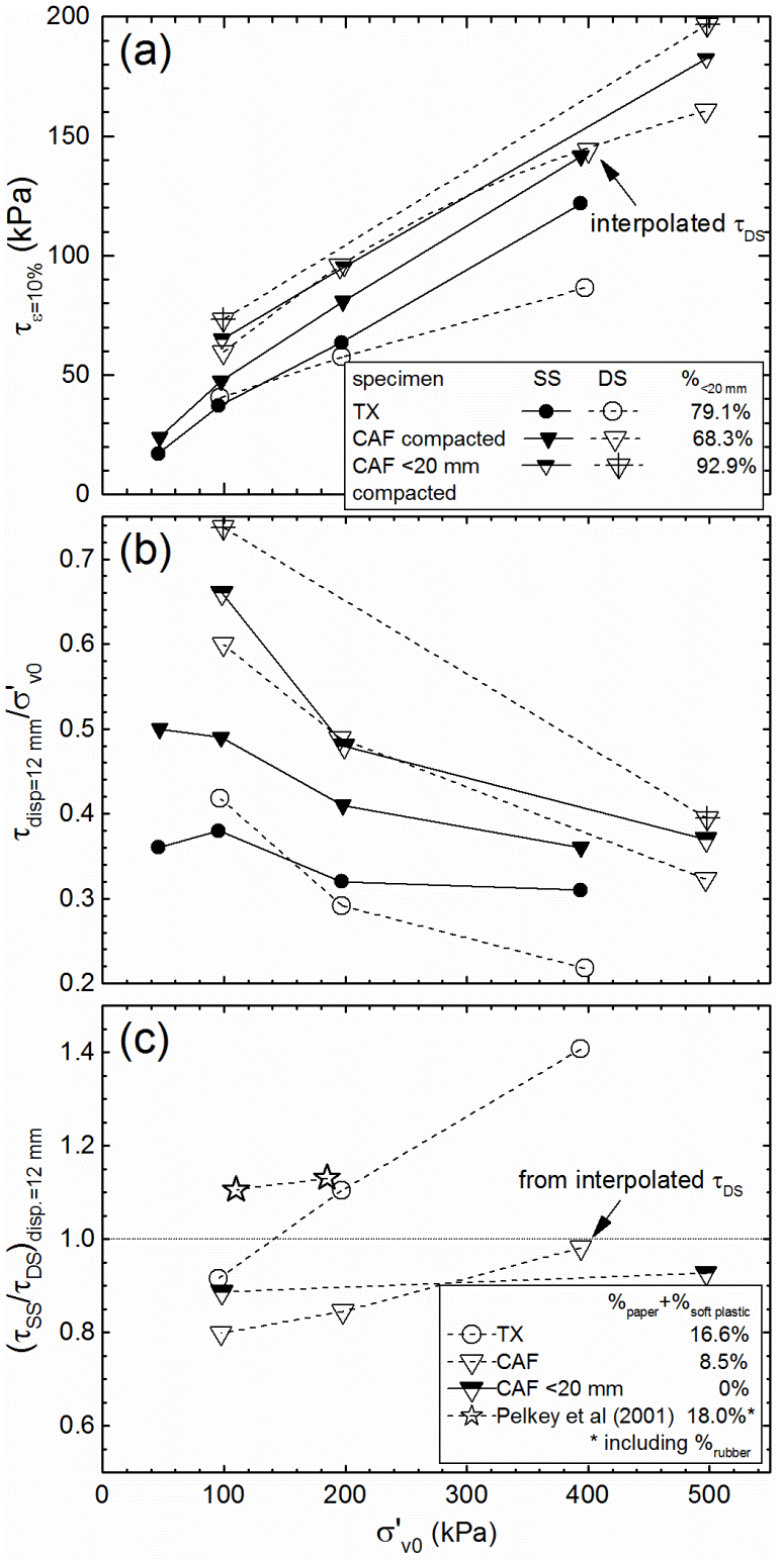

Figure 6-35 Comparison between direct shear and simple shear response of waste at different vertical stress (σ'_{v0}) in terms of (a) shear strength ($\tau_{disp=12\ mm}$); (b) normalized shear strength ($\tau_{disp=12\ mm}/\sigma'_{v0}$); and (c) ratio of shear strength from simple shear and direct shear testing ($(\tau_{SS}/\tau_{DS})_{disp=12\ mm}$).

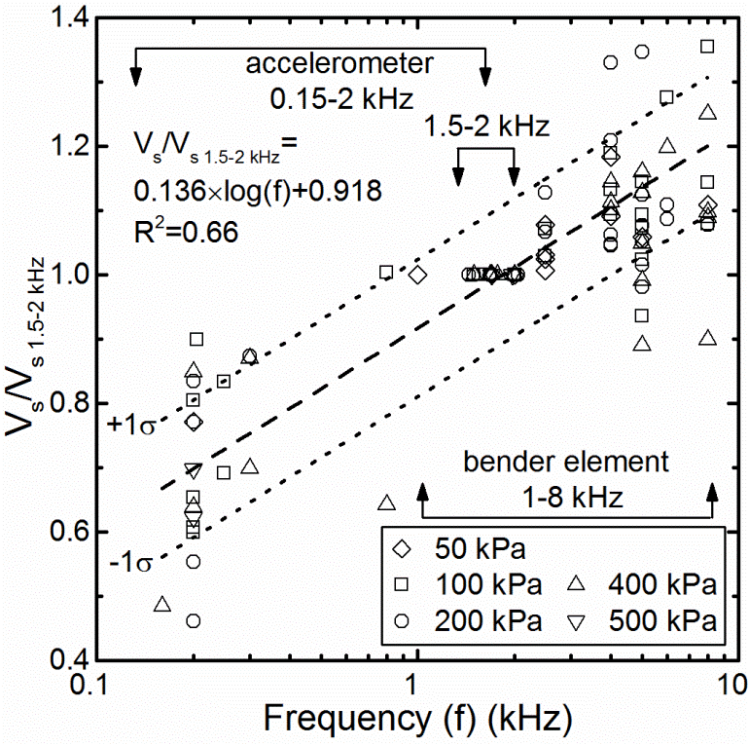

Figure 6-36 Ratio of shear-wave velocity (V_s) and V_s measured at source wave frequency between 1.5-2 kHz of waste ($V_s/V_{s\ 1.5\text{-}2\ kHz}$) at different source wave frequencies.

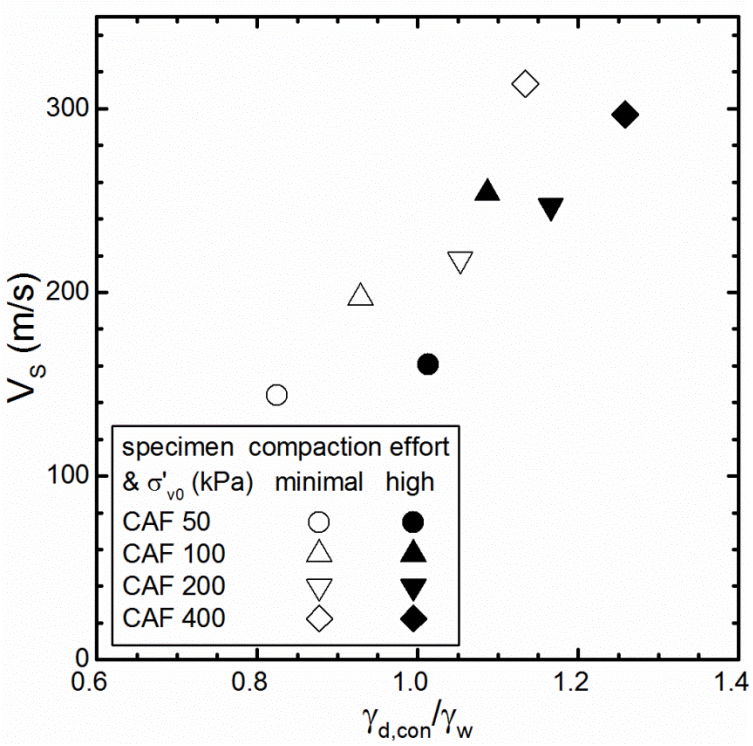

Figure 6-37 Relationship between shear-wave velocity (V_s) and normalized dry unit weight ($\gamma_{d,con}/\gamma_w$) of minimally and highly compacted MI and CAF waste at different vertical stress (σ'_{v0}).

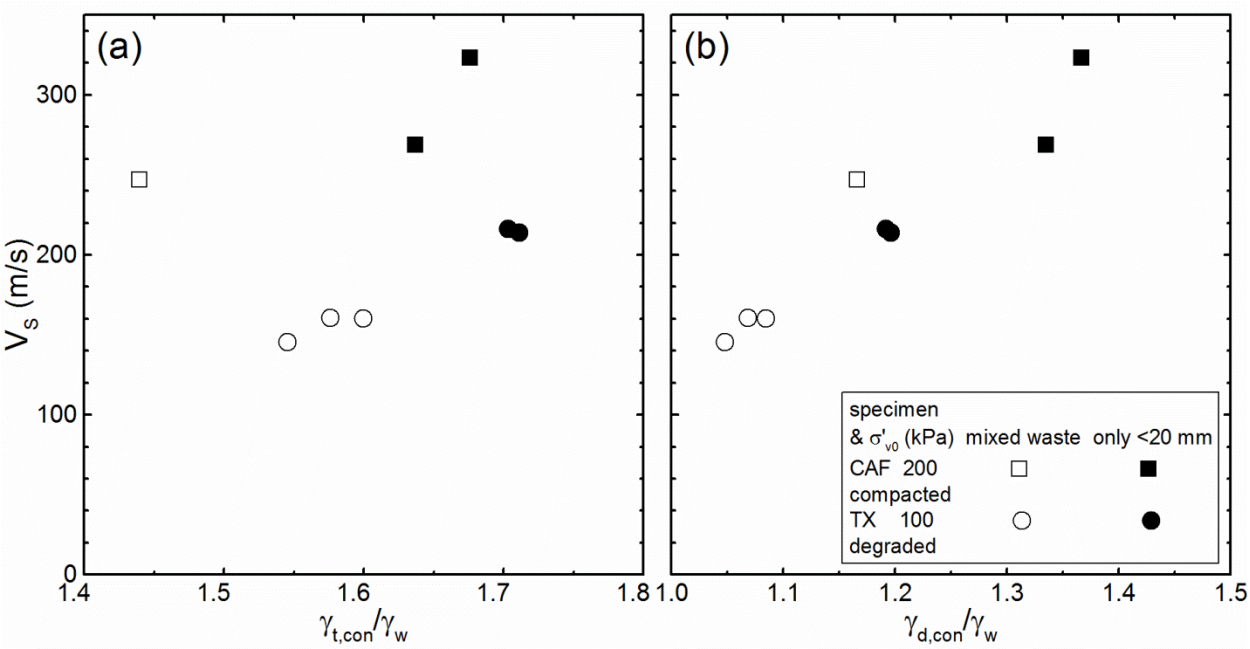

Figure 6-38 Relationship between shear-wave velocity (V_s) and (a) normalized total unit weight ($\gamma_{t,con}/\gamma_w$); and (b) normalized dry unit weight ($\gamma_{d,con}/\gamma_w$) of minimally and highly compacted MI and CAF waste at different vertical stress (σ'_{v0}).

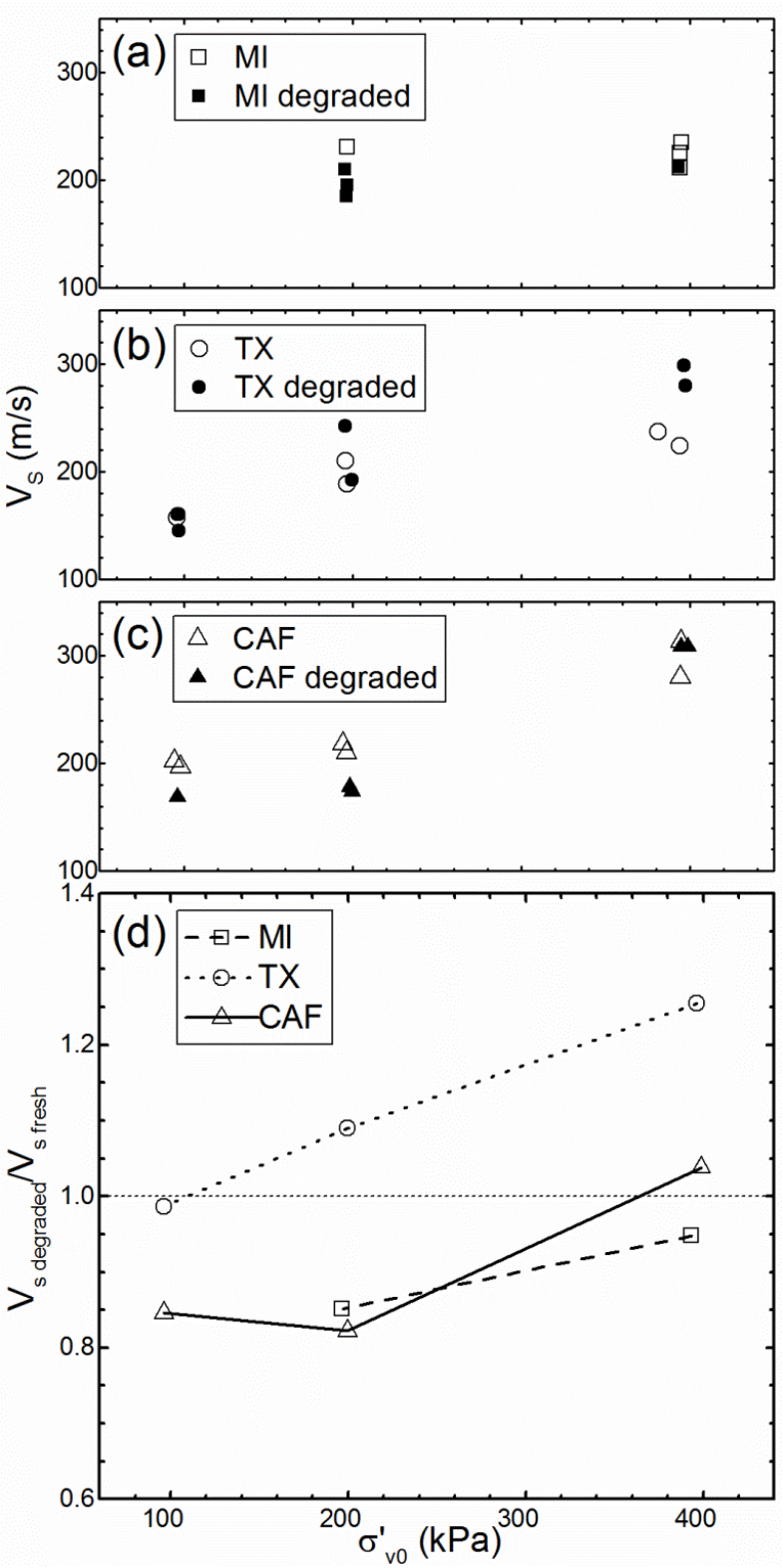

Figure 6-39 Relationship between shear-wave velocity (V_s) and vertical stress (σ'_{v0}) of fresh and degraded specimens from (a) MI waste; (b) TX waste; and (c) CAF waste; and (d) relationship between the ratio of V_s of degraded and fresh specimens ($V_{s\ degraded}/V_{s\ fresh}$) prepared using MI, TX and CAF waste and σ'_{v0}.

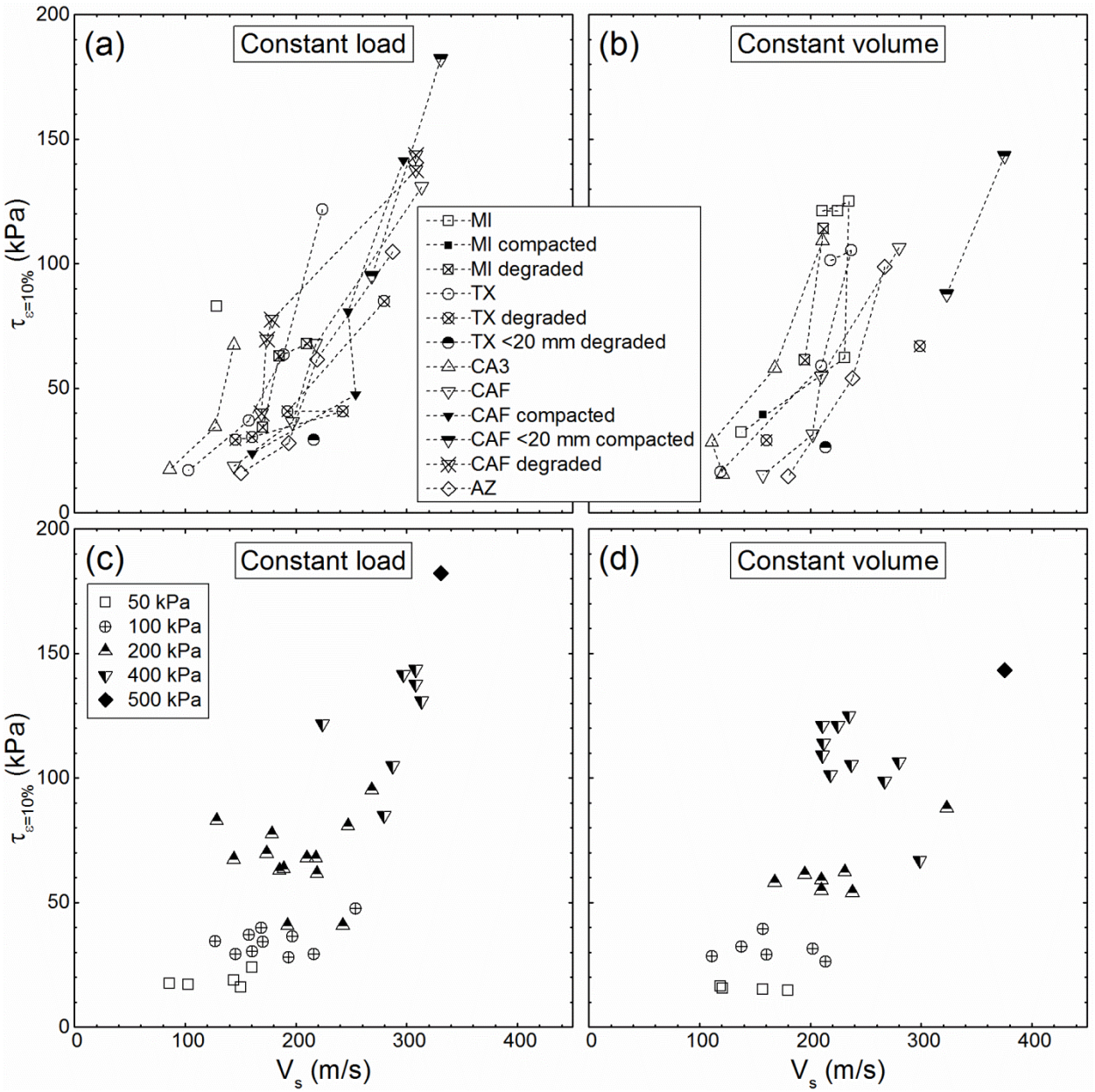

Figure 6-40 Relationship between shear strength ($\tau_{\varepsilon=10\%}$) and shear-wave velocity (V_s) of all waste specimens in (a) constant load; and (b) constant volume tests; and relationship between $\tau_{\varepsilon=10\%}$ and V_s at σ'_{v0} between 50-500 kPa in (c) constant load; and (d) constant volume tests.

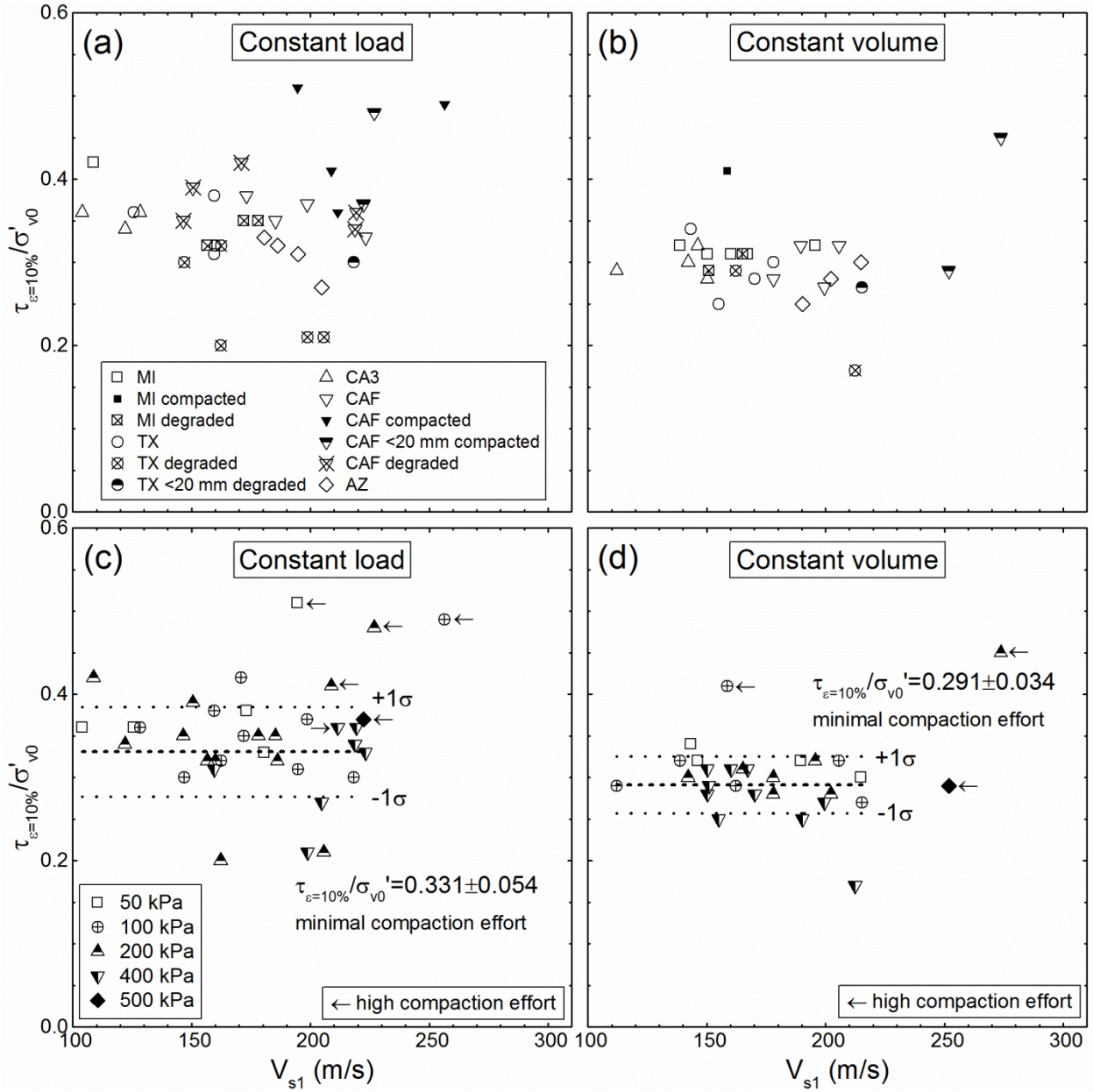

Figure 6-41 Relationship between normalized shear strength ($\tau_{\varepsilon=10\%}/\sigma'_{v0}$) and normalized shear-wave velocity (V_{s1}) of all waste specimens in (a) constant load; and (b) constant volume tests; and relationship between $\tau_{\varepsilon=10\%}/\sigma'_{v0}$ and V_{s1} at σ'_{v0} between 50-500 kPa in (c) constant load; and (d) constant volume tests.

Chapter 7 Response of Municipal Solid Waste to Mechanical Compression

7.1 Abstract

The compressibility of Municipal Solid Waste is of interest as it affects the short and long-term performance of landfills, as well as their expansion, closure and post-closure development. An assessment of the field settlement behavior of MSW can be reliably executed only when the various mechanisms contributing to the settlement are properly accounted for. A comprehensive large-size experimental testing program that involved a total of 128 compression tests from five landfills, in Michigan, California, Texas, Arizona of the US and Greece was executed to systematically assess the compressibility characteristics of MSW that is subjected to a compressive load. Emphasis is given on the influence of waste structure, waste composition, density and confining stress on compressibility parameters that are used in engineering practice, such as the constrained modulus and compression ratio, as well as long term compression ratio due to mechanical creep only. The effect of waste composition and density on the compressibility parameter is quantified. It is also found that the type of waste constituent (i.e., paper, plastic or wood), as well as the waste's anisotropic structure can have a significant effect on the compressibility characteristics of the soil-waste mixture. The proposed relationships shown can be used for MSW of any degradation state as long as the waste composition and density are known.

Zekkos, D., Fei, X., Grizi, A., and Athanasopoulos, G. (2016). "Response of municipal solid waste to mechanical compression." *Journal of Geotechnical and Geoenvironmental Engineering*, (under review).

7.2 Introduction

The compressibility of Municipal Solid Waste (MSW) has been a topic of significant interest in engineering practice since it affects the short- and long-term performance of landfills, and particularly, the performance of gas collection systems and landfill covers, the vertical expansion and closure of landfills, as well as the post-closure development of landfills. Nearly any post-closure development project involves an assessment of the response of the waste mass to a change in stress conditions. In many cases, the uncertainties involved in the estimation of waste compressibility increase the development risk and may adversely affect the decision to develop the closed landfill. Increased interest in vertical expansion of landfills also requires an assessment of the compression of the waste in existing landfill cells.

Thus, it is not surprising that significant amount of effort has been expended since the early work by Sowers (1973) to characterize the compressibility of MSW. Research has been directed towards the collection of laboratory experimental data (Wall and Zeiss 1995; Kavazanjian et al. 1999; Landva et al. 2000; Hossain et al. 2003; Olivier and Gourc 2007; Ivanova et al. 2008b; Stoltz et al. 2010b; Reddy et al. 2011; Bareither et al. 2012b; Fei and Zekkos 2013; Fei et al. 2014a), field measurement of settlements (Bjarngard and Edgers 1990; Stulgis et al. 1995; Spikula 1997; Zhao et al. 2001; Mehta et al. 2002; Yuen and McDougall 2003; Sharma and De 2007; Bareither et al. 2012e) and modeling of the settlement behavior (Edil et al. 1990; Ling et al. 1998; McDougall and Pyrah 2004; Oweis 2006; Chen et al. 2010b; Gourc et al. 2010; Bareither et al. 2013a). An extensive review of the compressibility of MSW has been made by McDougall (2011).

One of the complicating factors associated with assessing the compressibility of MSW in the field, is that there are numerous mechanisms contributing nearly simultaneously to the

observed settlement of MSW. These include physical and biochemical processes. Biodegradation of the organic constituents is one of the most critical, if not the key, contributor and often masks immediate and long-term compression of the waste due to load application. However, as clearly demonstrated by field and laboratory evidence, MSW is a soft material that deforms significantly when subjected to a load, and the deformation associated with mechanical compression of MSW may even reach half its original height.

Understanding the various compression mechanisms of MSW and the ability to separate their contribution to the observed total settlement is key to reliably predict settlement behavior during waste filling, post-closure development, or even vertical expansion of a landfill. A fundamental understanding of the factors that affect the mechanical compression of MSW will allow its separation from other mechanisms associated with the biodegradation process of MSW. The mechanisms causing mechanical compression of MSW are physical, whereas in the case of biodegradation, are primarily biochemical.

The objective of this study is to systematically assess the compressibility characteristics of MSW that is subjected to a compressive load. Emphasis is given on the influence of waste structure, waste composition, density and confining stress on compressibility parameters that are used in engineering practice, such as the constrained modulus and compression ratio, as well as long term compression ratio due to mechanical creep only. Settlement associated with biodegradation is beyond the scope of this paper.

7.3 Compression theory

Similarly to soils, when a vertical load is applied on MSW, either due to overburden layers of waste, or another external load (e.g., a structure), there will be deformation of the waste mass.

This deformation is associated with a reduction of pore volume between the particles, particle slippage, particle movement and re-orientation, and especially for MSW, particle bending, folding and compression or extension of waste constituents that can be soft and thin, as well as raveling of finer particles into large voids within the waste structure (Bjarngard and Edgers 1990). Thus, it is not surprising that waste compresses significantly more than inorganic soils. A portion of that deformation is recoverable upon unloading (i.e., elastic), and another portion is irrecoverable (i.e., plastic). If water is present within the voids, it will squeeze out, typically at high rates, due to the relatively high hydraulic conductivity of MSW.

In 1D-compression, in response to an increment of vertical stress, $\Delta\sigma_v$, there is an immediate vertical strain increment $\Delta\varepsilon_{vi}$ that is given by:

$$\Delta\varepsilon_{vi} = \frac{\Delta\sigma_v}{D} \tag{7-1}$$

where D is the constrained modulus and has units of stress. Since MSW behavior is confining stress dependent, D is a function of the initial vertical stress σ_{v0}. Also, because the stress-strain response of MSW to a load is never linear, D is also not a constant during a compression sequence, but is dependent on the stress or strain increment.

A common alternative to the use of the constrained modulus D that is also customarily used in consolidation analysis is to use Eqn. 7-2 when calculating the immediate vertical strain in response to a new stress increment:

$$\Delta\varepsilon_{vi} = C_{ce} \times log\left(\frac{\sigma_{v0}+\Delta\sigma_v}{\sigma_{v0}}\right) \tag{7-2}$$

where C_{ce} is the modified compression coefficient assuming that the material has never experienced that stress increment before. If the material has previously experienced that load increment, C_{ce} can be replaced by the modified recompression coefficient C_{re}. It is commonly considered that C_{ce}, and C_{re} are confining stress independent and constant for a specific ground material.

Thus, from Eqn. 7-1 and Eqn. 7-2, it can be deduced that:

$$D = \frac{\Delta\sigma_v}{C_{ce}\times\log\left(1+\frac{\Delta\sigma_v}{\sigma_{v0}}\right)} \tag{7-3}$$

when subjected to sustained compression loading, waste will continue to deform due to the physical mechanisms described earlier that result in stress redistribution and changes in particle-to-particle stress contacts. Presence of moisture and liquid flow may also cause particle lubrication and particle slippage or even raveling. Occasionally, this progressive stress readjustment, and the material loss due to biodegradation, may lead to "unexpected" waste structure collapse that may be reflected at the landfill surface as localized, and highly irregular, differential settlements. This long-term deformation, commonly referred to as secondary compression, can be calculated as follows:

$$\Delta\varepsilon_{v,LT} = C_{ae} \times log\left(\frac{t}{t_0}\right) \tag{7-4}$$

where $C_{\alpha e}$ is the modified secondary compression ratio; and t_0 is commonly assumed to be the duration of time until the material first experiences the sustained constant loading (for clays this is considered the near-completion of consolidation). Typical ratios of $C_{\alpha e}/C_{ce}$ for natural soils are

overall between 0.03-0.06 with amorphous and fibrous peats being around 0.035-0.085, and organic silts 0.035-0.06 (Holtz and Kovacs 1981).

Since MSW is a geo-material, these fundamental principles are also applicable. A large number of studies have used Eqn. 7-1, Eqn. 7-2 and Eqn. 7-4 to estimate the compression characteristics of MSW.

7.4 Methodology

A total of 128 large-diameter one dimensional compression tests were conducted on MSW from landfills in California, Texas, Arizona, Michigan and Greece. Specifically, 23 tests on reconstituted MSW from Tri-Cities landfill in north California, 40 on soil-waste mixtures from Xerolakka landfill in Greece, 31 from Sauk Trail Hills landfill in Michigan, 17 from the Austin Community landfill in Texas, 8 from Los Reales landfill in Arizona and 24 from Lamb Canyon landfill in south California.

The Tri-Cities landfill tests were conducted first to systematically evaluate the effect of waste composition on the mechanical characteristics of MSW. Subsequent tests on soil-waste mixtures from Xerolakka landfill were performed to assess the impact of waste structure anisotropy and waste constituent type on the compressibility of the waste mixtures. Finally, a large number of tests were also conducted on specimens from Texas, Arizona, and California at a fresh and degraded state to assess whether the trends observed in these earlier test programs were generally applicable. All 1D-compression tests were conducted prior to shearing and had a duration of approximately 24 hrs (1440 min). Shearing results have been reported elsewhere for Tri-Cities and Xerolakka landfill waste (Zekkos et al. 2010a; Zekkos et al. 2013a), Michigan and Texas waste (Fei and Zekkos 2015; Zekkos and Fei 2016).

An example of data collected during 1D-compression of a specimen from Tri-Cities landfill, CA, is shown in Figure 7-1, along with the relevant compressibility parameters. For each test, ε_{vi}, C_{ce}, D, and $C_{\alpha e}$ are derived.

Waste composition was well defined for each specimen prepared. The characterization procedures proposed by Zekkos et al. (2010b) were used for all specimens. The amount and type of waste constituents is known, and a detailed characterization (grain size distribution, Atterberg limits, moisture and organic content) of the finer, soil-like (i.e., <20 mm fraction) is performed. Specimens were compacted through a variety of techniques. Repeated drops of a mass on subsequent layers of waste to achieve a target compaction energy input or target density, moist-compaction in layers using a tamper, and, in some cases, placement of the material without any compaction effort. It was generally found that for specimens with the same waste composition and density, the specimen preparation technique was not as important.

A significant differentiation among specimens relates to the manner by which waste was placed in the specimen preparation mold. With the exception of the Xerolakka landfill waste, all other specimens were prepared in layers of mixed waste material, i.e., all constituents were mixed together and placed in layers in the specimen mold and compacted. Observations during compaction showed that, similarly to field conditions, the fibrous waste constituents (>20 mm fraction) tend to become aligned in the horizontal direction, resulting in an anisotropic waste structure (Zekkos 2013). To investigate this issue further, specimens from Xerolakka landfill were prepared and included only the <20 mm material and a specific waste constituent (i.e., plastic, paper or wood). The material was placed in distinct successive layers of <20 mm material and waste constituent. This specimen preparation technique resulted in a well-defined waste structure that allowed an improved assessment of the impact of waste structure and waste

type on the compressibility of soil-waste mixtures. Extensive description of this specimen preparation technique is included in Zekkos et al. (2013a). Note that all Xerolakka landfill and Tri-Cities landfill specimens are tested at moisture contents below field capacity, conditions that are typical of Subtitle D, dry tomb, landfills. Specimens from Sauk Trail Hills landfill in MI and Austin Community landfill in TX were tested at similar moisture contents, as well as nearly saturated levels of moisture.

7.5 Results

7.5.1 **Impact of waste composition and unit weight on compressibility of MSW**

As mentioned earlier, the impact of waste composition and unit weight on the compressibility of MSW was systematically assessed on waste from Tri-Cities landfill. As shown in Figure 7-2a, C_{ce} is significantly affected by the amount of <20 mm material. As the percentage by weight of <20 mm material increases, C_{ce} reduces, i.e, MSW becomes stiffer. Waste-rich MSW has C_{ce} values that may vary by a factor of two or more compared to specimens with 100% of <20 mm.

$C_{\alpha e}$ is also significantly affected by the amount of <20 mm material, as shown in Figure 7-2b. As the <20 mm material increases, $C_{\alpha e}$ reduces, i.e., the long term settlement is lower. Waste-rich MSW has $C_{\alpha e}$ that may vary by a factor of two or more compared to 100% of <20 mm material.

The scatter observed in the data is largely attributed to the variable compaction efforts involved in preparing the specimens with highly compacted, denser specimens plotting below the shown regressed line and looser specimens plotting above. Confining stress does not appear to play a significant role on the C_{ce} and $C_{\alpha e}$ values.

Similarly, as shown in Figure 7-3, unit weight affects significantly both C_{ce} and $C_{\alpha e}$. In Figure 7-3, total unit weight prior to immediate compression (γ_{t0}) is shown. All specimens had moisture contents that are significantly lower than field capacity. The observed impact of unit weight on compressibility, can be attributed to two main factors: (a) for the same waste composition, specimens that are compacted with more energy input are denser and tend to have lower C_{ce} and $C_{\alpha e}$; (b) unit weight and composition are highly correlated with waste-rich MSW having lower unit weight values (3-8 kN/m^3) and soil-rich MSW having higher unit weight values (12-17 kN/m^3) for the same confining stress and the same compaction effort (Zekkos et al. 2006). Thus, total unit weight variations from 5-15 kN/m^3 can essentially be considered an index of waste composition.

Note that in Figure 7-3b the total unit weight upon compaction γ_{to} is shown. A similar relationship was also observed when the data were plotted against the total unit weight upon completion of the immediate compression, i.e., the density state of the MSW during long-term compression. However, the regression results were similar and so that trend is not shown. Regression of the data indicates the following approximate relationship (R2=0.37 and 0.64, respectively):

$$C_{ce} = 0.15 - 0.0079 \times \gamma_{t0} \quad (7\text{-}5a)$$

$$C_{ae} = 0.016 - 0.00078 \times \gamma_{t0} \quad (7\text{-}5b)$$

7.5.2 **Impact of waste structure & waste constituent type on compressibility of MSW**

A series of tests were also conducted on soil-waste mixtures from Xerolakka landfill. As mentioned earlier, these specimens were prepared in carefully placed successive layers of soil

and waste with the intent to assess the impact of waste structure, as well as the impact of specific common waste constituents on compressibility of a soil-waste mixture.

The type of waste constituent (i.e., paper, plastic or wood) was found to affect the stiffness of the soil-waste mixture. Soil-waste mixtures that were compacted with the same compaction effort, and have soil-paper only, soil-plastic only, or soil-wood only, have different C_{ce} and $C_{\alpha e}$. Figure 7-4 shows test results on specimens that include variable amounts of <20 mm material subjected to compression from 0-50 kPa. As shown in Figure 7-4, specimens with soft plastic or paper have significantly higher C_{ce} and $C_{\alpha e}$ than specimens with wood, or specimens that consisted entirely of <20 mm material. The change in C_{ce} and $C_{\alpha e}$ due to inclusion of wood constituents compared to specimens with 100% of <20 mm is not comparatively significant.

The amount of waste constituent was also found to affect the stiffness of the mixture, but its influence on C_{ce} and $C_{\alpha e}$ was also dependent on the type of fibrous waste constituent. As shown in Figure 7-4, for specimens compressed in the direction parallel to the waste constituent orientation ($i=90^{o}$), as the amount of paper and plastic increases, C_{ce} and $C_{\alpha e}$ increase significantly. C_{ce} is highest for plastic, followed by paper, and practically unaffected by the percentage of wood. $C_{\alpha e}$ is highest for paper, followed by plastic, and then wood.

Previous studies have highlighted the pronounced effect of waste anisotropy on hydraulic conductivity (Landva et al. 1998; Hudson et al. 2009), the shear strength of MSW (Bray et al. 2009; Zekkos et al. 2010a) and seismic wave propagation (Zekkos 2013; Sahadewa et al. 2014a; Sahadewa et al. 2014b). The influence of structure of the soil-waste specimens on the stiffness was also assessed by preparing specimens of soil and waste in layers at different angles compared to the horizontal, with the orientation of the fibrous constituents being well defined.

As shown in Figure 7-5, the stiffness of the specimens is significantly dependent on the relative orientation of the waste fibrous constituent's long axis and the direction of compression loading. Overall, as shown in Figure 7-5b, C_{ce} varies as much as 2.5 times for specimens of soil-plastic mixtures as a function of the orientation of the waste constituent, but less for soil-paper (factor of 1.7 difference for different waste constituent orientations) and soil-wood mixtures (factor of 1.25). Soil-paper and soil-wood mixtures are found to be the softest (have the highest C_{ce}) when the particles are oriented perpendicular to the load ($i=0^o$), but the opposite trend is observed for specimens that include soil-plastic only. These specimens appear to be stiffer when plastic particles are oriented perpendicular to the compression load ($i=0^o$). The results shown point to the significant anisotropy of soil-waste mixtures. This finding is also supported by testing on specimens from Tri-Cities landfill, as shown in Figure 7-6, that had intermediate waste composition (Bray et al. 2009) and were found to be stiffer (not more than 20%) when the particle orientation was oriented parallel to the compression loading, rather than perpendicular to the compression loading. The results of this study point to the importance of the orientation of loading compared to the waste structure, in assessing the compressibility characteristics of the MSW.

7.5.3 **Synthesis & Recommendations for Compressibility of MSW**

Tests were also executed on specimens from four additional landfills in the United States in Michigan, California, Texas, and Arizona. A summary figure of the 128 test data is shown in Figure 7-7. In this figure, hollow symbols are used for specimens that are uncompacted, whereas full symbols are used for specimens that have intermediate to high compaction efforts. As shown in Figure 7-7a immediate strain can reach 60% of the specimen initial height, C_{ce} ranges from 0.01-0.26 and $C_{\alpha e}$ ranges from 0.001-0.014. Specimens that are soil-rich (100% of <20 mm)

and/or compacted, tend to have lower immediate strains (up to approximately 30%), and lower C_{ce} values (up to 0.15), but generally similar $C_{\alpha e}$ values. As discussed earlier, no effect of vertical stress on C_{ce} and $C_{\alpha e}$ is observed.

Figure 7-8 shows the relationship of C_{ce} with waste composition and dry unit weight prior to compression (γ_{d0}). Note that the dry unit weight is used instead of the total unit weight, because some of the specimens in the dataset, are in nearly saturated conditions. C_{ce} is better correlated with γd0 instead of the percentage of <20 mm material. There is some scatter in the data, which is not surprising given the variable waste sources, compositions and testing conditions. Looser and waste-rich specimens have distinctly higher C_{ce} than dense and soil-rich specimens. A relationship between C_{ce} and γ_{d0} was derived with an R^2=0.73:

$$C_{ce} = 0.48 * e^{-0.20*\gamma_{d0}} \tag{7-6}$$

Figure 7-9 shows the variation of $C_{\alpha e}$ with waste composition and γ_{d0}. There is significant scatter in the data. For the entire dataset there is a stronger relationship between $C_{\alpha e}$ and the amount of <20 mm material rather than with dry density. This may not be surprising given the established importance of organics on the long-term compressibility of earth materials.

Similar results are observed for the constrained modulus D. However, as shown in Figure 7-10, D is increasing with vertical stress. At a given vertical stress, soil-rich specimens (100% of <20 mm) and denser MSW specimens have higher D values. Figure 7-10b illustrates the normalized constrained modulus D' with final vertical stress σ_{vf} defined as follows:

$$D' = \frac{D}{\sigma_m} \tag{7-7}$$

where $\sigma_m = \frac{\sigma_{vf}+\sigma_{vo}}{2}$, is the mean stress over the stress increment.

As shown in Figure 7-10b, initially, it appears that D' reduces with normal stress. This may also be an initial assessment for the relationship of C_{ce} with normal stress shown in Figure 7-2a. Similar observations were made by Bareither et al. (2012b) in terms of C_{ce}. However, this apparent trend is merely a reflection of the effect of compaction effort and densification. Compacted (overconsolidated) specimens, especially at lower normal stresses, (e.g., 50 kPa) appear to have higher D' (or lower equivalent C_{ce}) i.e., the compacted specimens appear stiffer than the uncompacted ones for stress increments that are below the compacted stress. However as the stress increment increases to levels significantly higher than the compaction stress levels, they approach a relatively "constant" value. This "overconsolidation" observation has also been made in terms of shear wave and p-wave velocity in the field by Sahadewa et al. (2014b). Overall, in the normally consolidated regime, D' has essentially a constant value that ranges between 4 and 8, a range that can be used as a first-order estimate of the constrained modulus of MSW.

Tests on fresh and fully biodegraded specimens were executed on specimens from Michigan and Texas landfills. Biodegradation was executed using large-size laboratory simulators as described in Fei et al. (2014a) for extended periods of time (>1000 days). The biodegraded specimens are also included in the data and are no different than the fresh specimens in their general trend. However, the composition and total unit weight of the degraded specimen is different than that of the fresh specimen because during biodegradation the % of <20 mm material increases and dry unit weight increases and so the absolute values of the various compressibility parameters are different than the same specimen at a fresh state. This observation

indicates that the relationships shown in this study should be valid regardless of the state of degradation of the specimen, as long as the waste composition and density of the material is known.

Figure 7-11 illustrates the relationship between C_{ce} and D' (in kPa). Each of the values shown for the specimens has been derived from the experimental data independently. The two parameters are expected to be closely correlated, as shown in Eqn. 7-3. For the data presented, the following simple relationship can be used:

$$C_{ce} = \frac{0.90}{D'} \tag{7-8}$$

Of interest is also the ratio of $C_{\alpha e}$ to C_{ce}. Typical ratios of $C_{\alpha e}/C_{ce}$ for natural soils are between 0.03-0.06 with amorphous and fibrous peats being around 0.035-0.085, and organic silts 0.035-0.06 (Holtz and Kovacs 1981). The experimental data from this study indicates that the typical ratios are 0.01-0.04 for normally consolidated MSW. However, this ratio is representative of $C_{\alpha e}$ values that are representative of mechanical compression (creep) only, and do not include the biodegradation component of the long-term settlement.

7.6 Conclusions

The response of MSW to a compression loading has been experimentally investigated by executing a total of 128 1D-compression testing on solid waste from five landfills. The results of this study indicate that the compressibility characteristics of MSW, as expressed by C_{ce}, D' and $C_{\alpha e}$ are largely confining stress independent. They are also impacted primarily by waste composition and density. Waste composition is a critical factor. The % of <20 mm material and

the density of the material can be used to provide a reasonable estimate of the compressibility parameters. However, the type of waste constituent (i.e., paper, plastic or wood) can have a significant effect on the compressibility characteristics of the soil-waste mixture. Also, because of the anisotropic structure of the MSW, the direction of compression load compared to the fibrous constituent orientation is important. Relationships of C_{ce}, (or D'), $C_{\alpha e}$ as a function of waste composition and unit weight were derived. Finally, the relationships shown can be used for specimens of any degradation state, as long as the waste composition and density are known. Typical ratios of $C_{\alpha e}/C_{ce}$ for MSW are between 0.01-0.04.

7.7 Figures

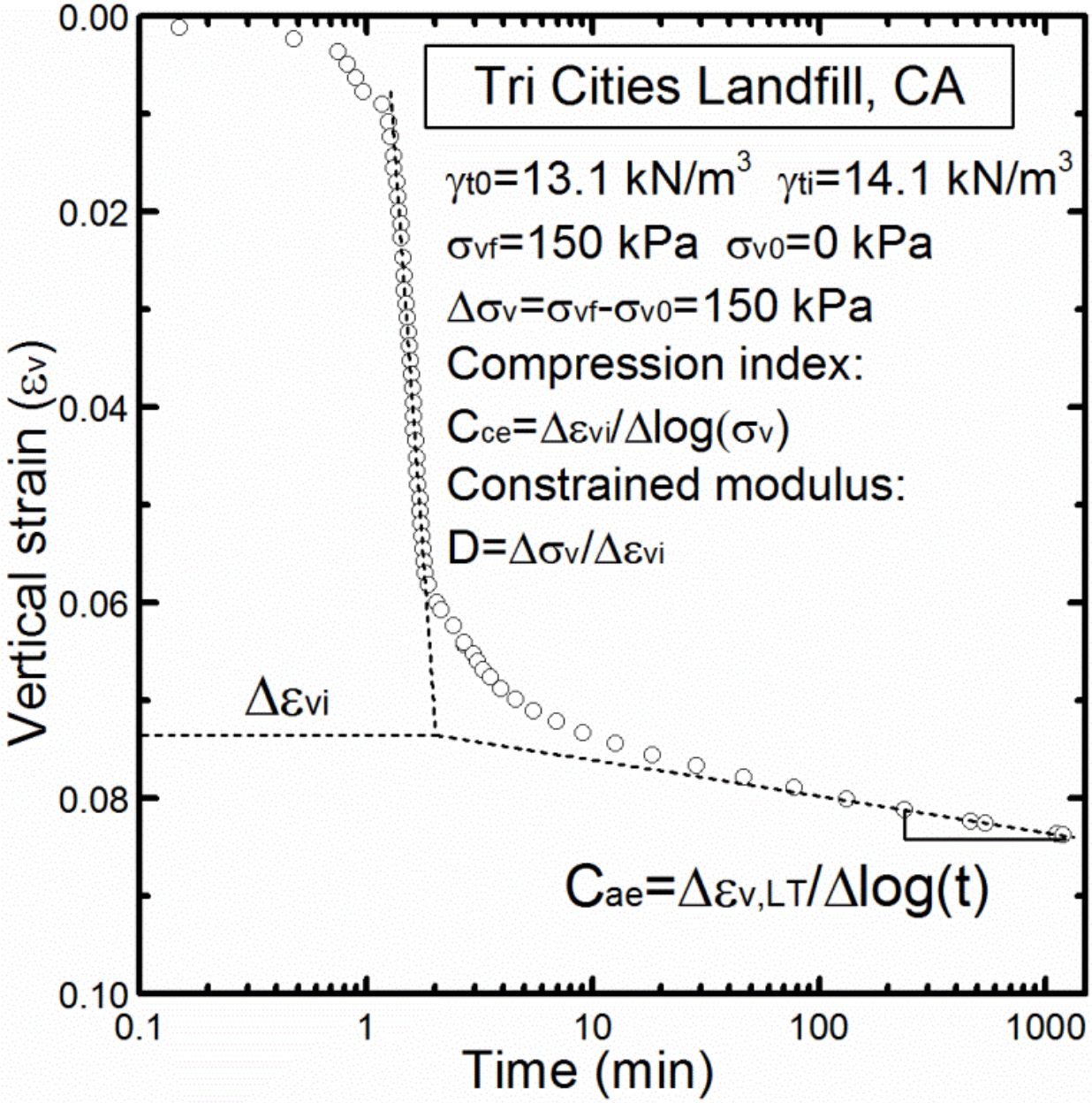

Figure 7-1 Example compressibility data for a specimen from Tri-Cities landfill, and associated compressibility parameters.

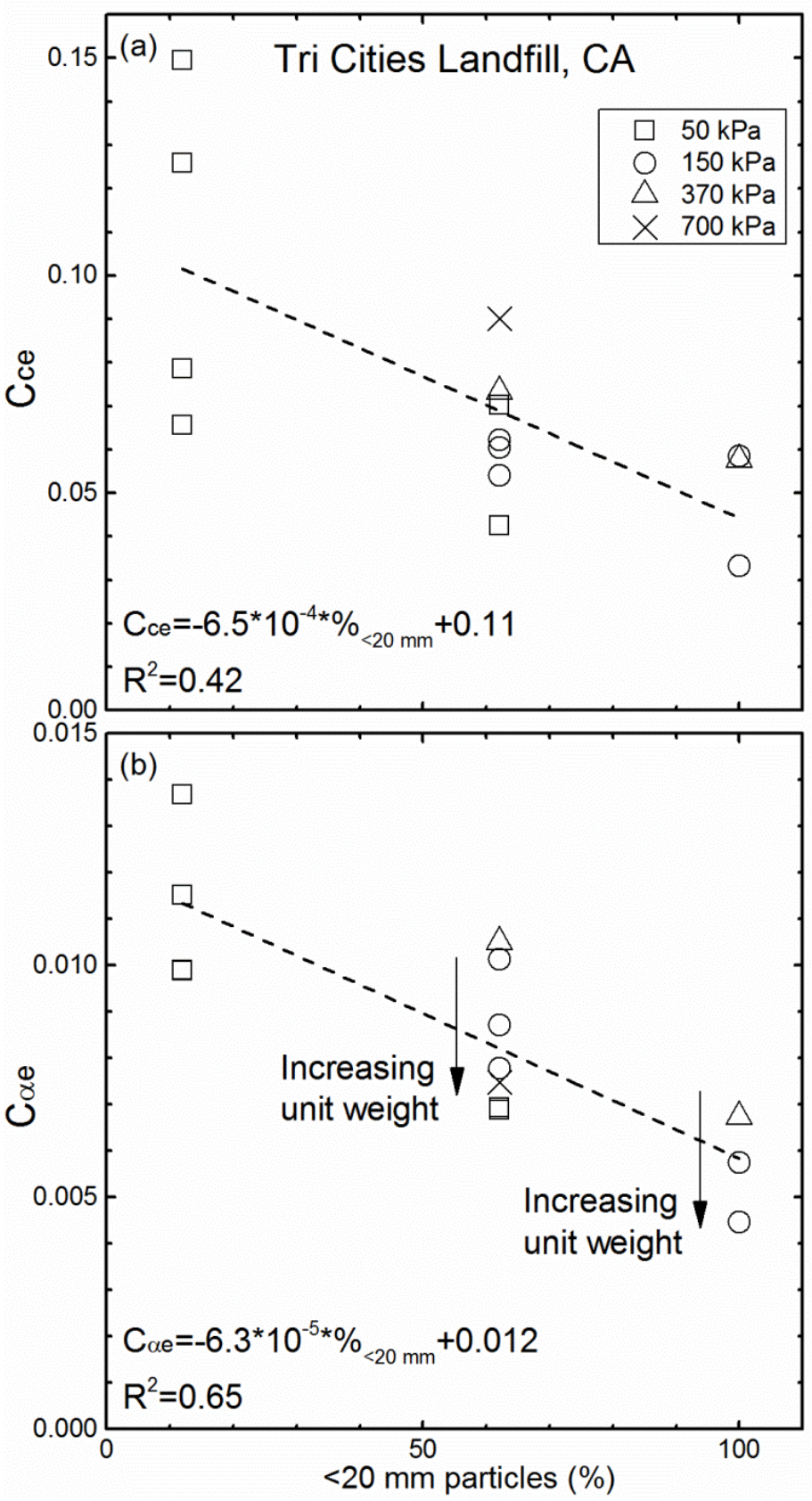

Figure 7-2 Impact of amount of <20 mm material on C_{ce} and C_{ae}.

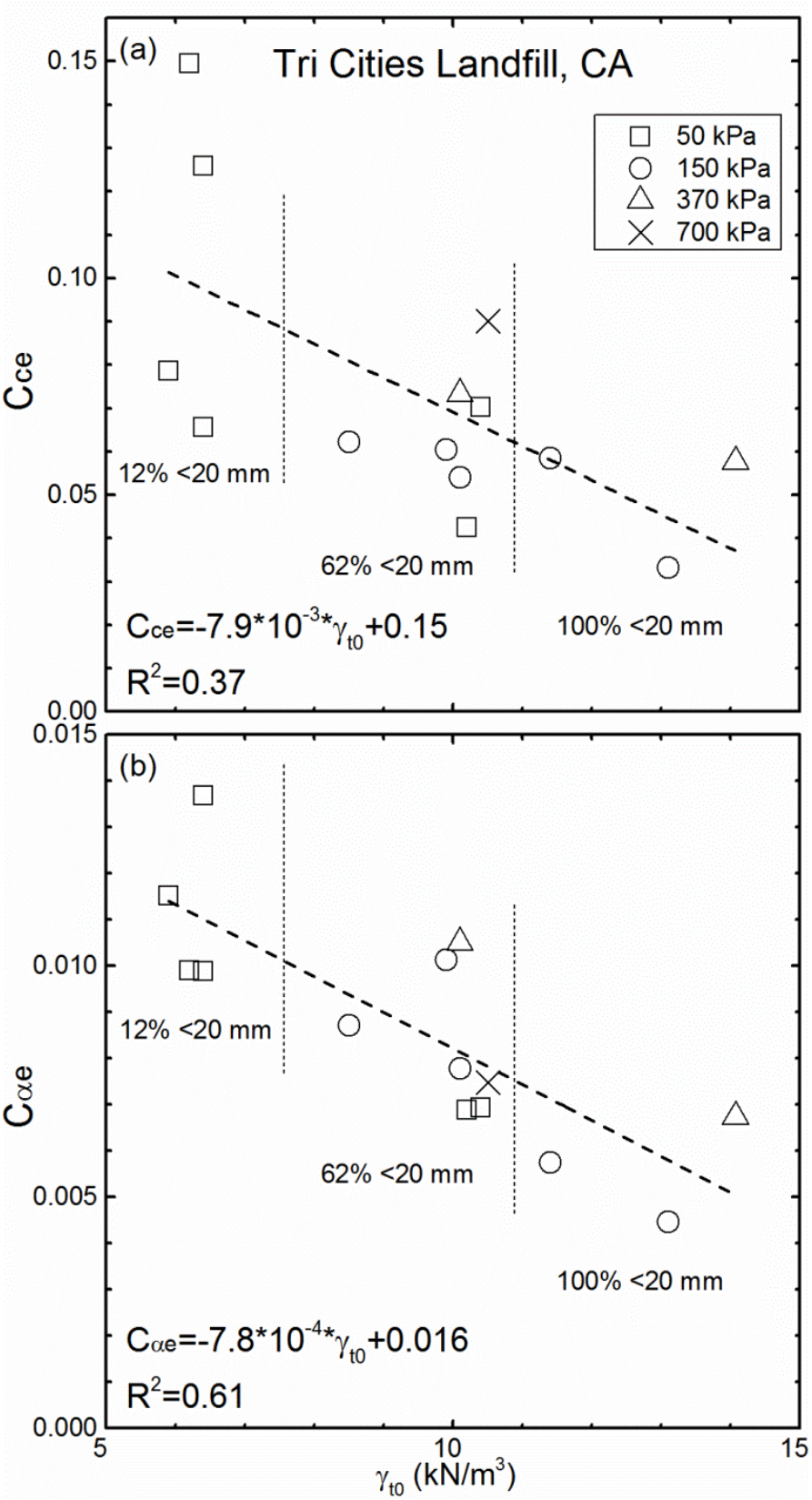

Figure 7-3 Relationship between (a) C_{ce} or (b) C_{ae} and total unit weight prior to immediate compression (γ_{t0}).

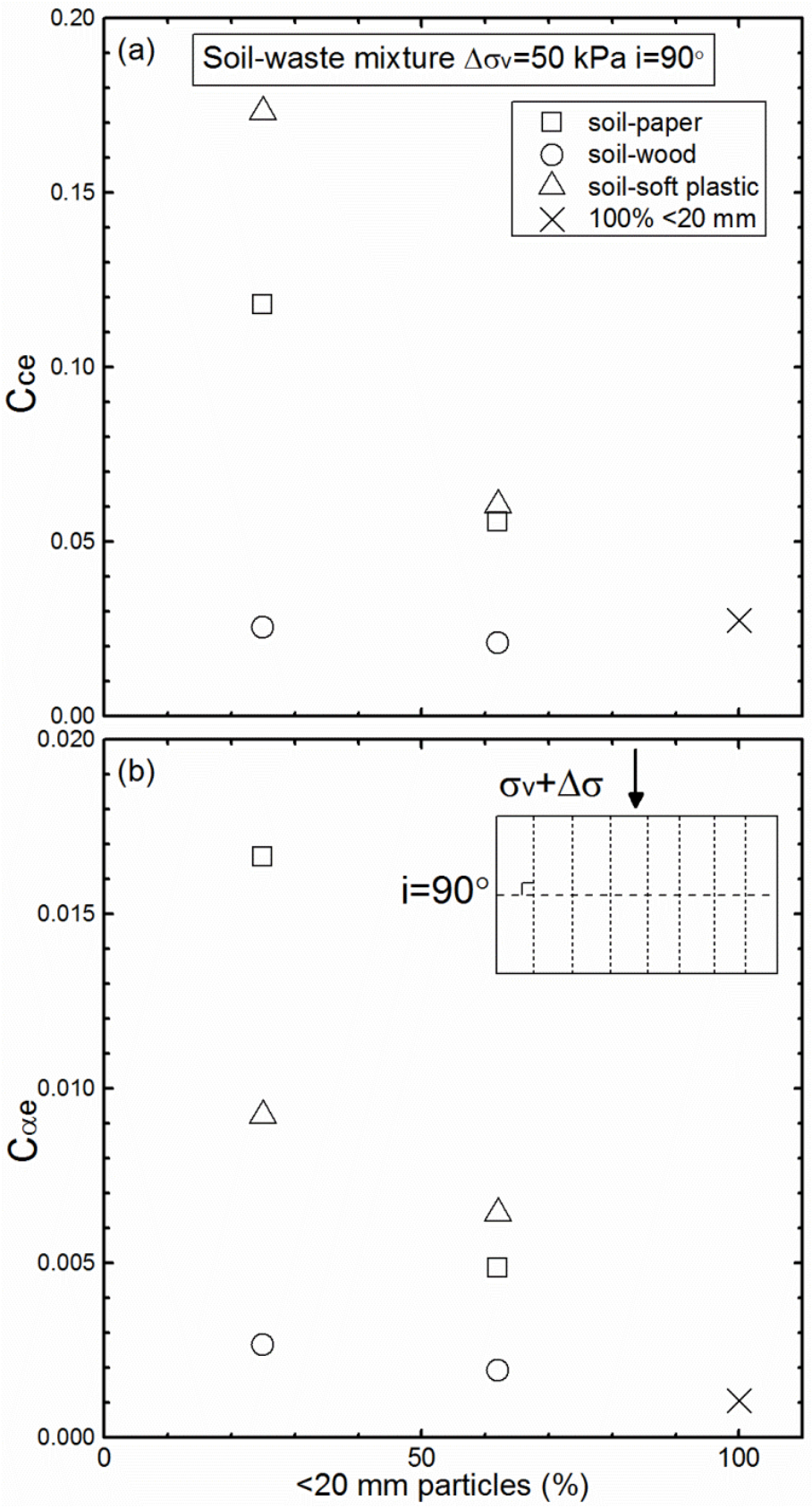

Figure 7-4 The impact of waste composition and waste type on (a) C_{ce} and (b) C_{ae}.

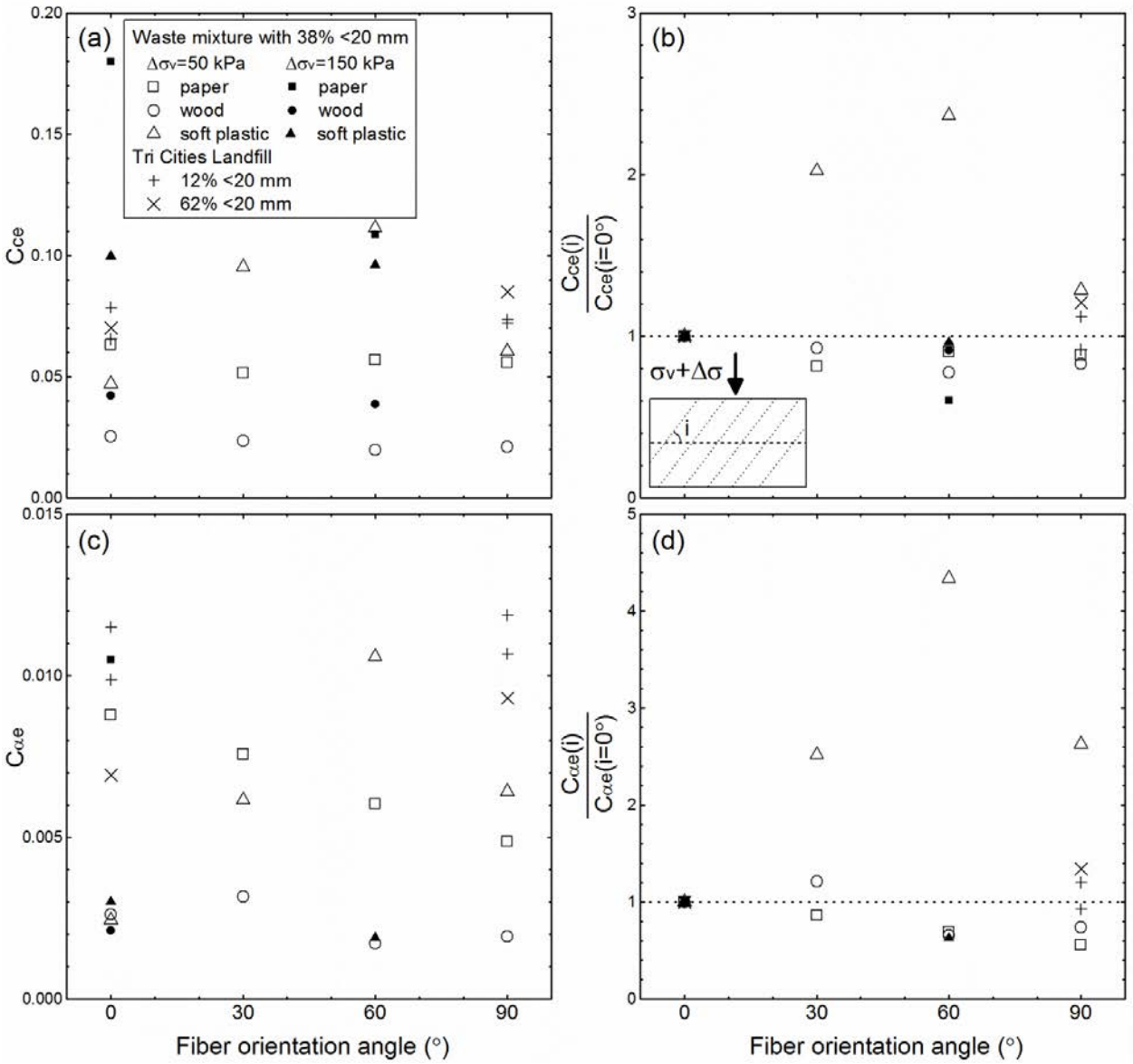

Figure 7-5 The impact of fiber orientation angle on (a-b) C_{ce} and (c-d) C_{ae}.

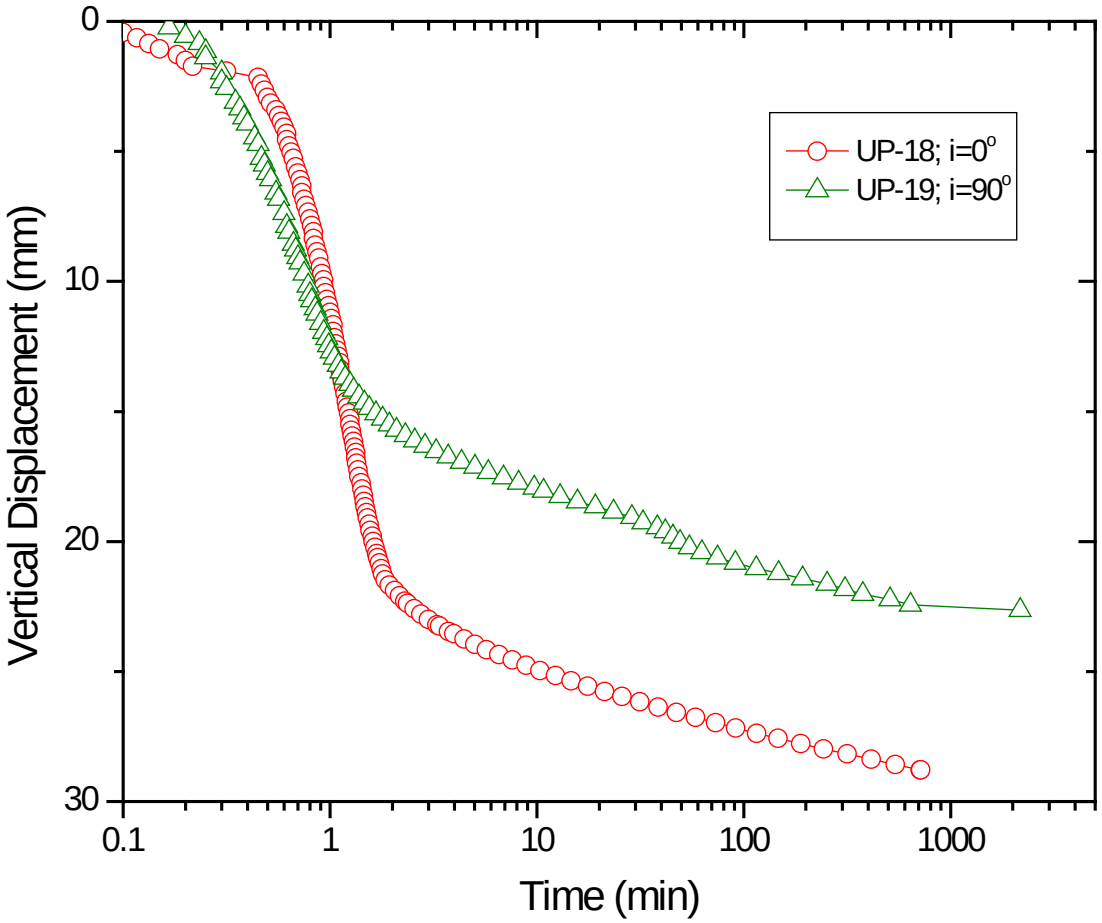

Figure 7-6 Effect of fibrous waste orientation on the compressibility of practically identical MSW from Tri-Cities landfill.

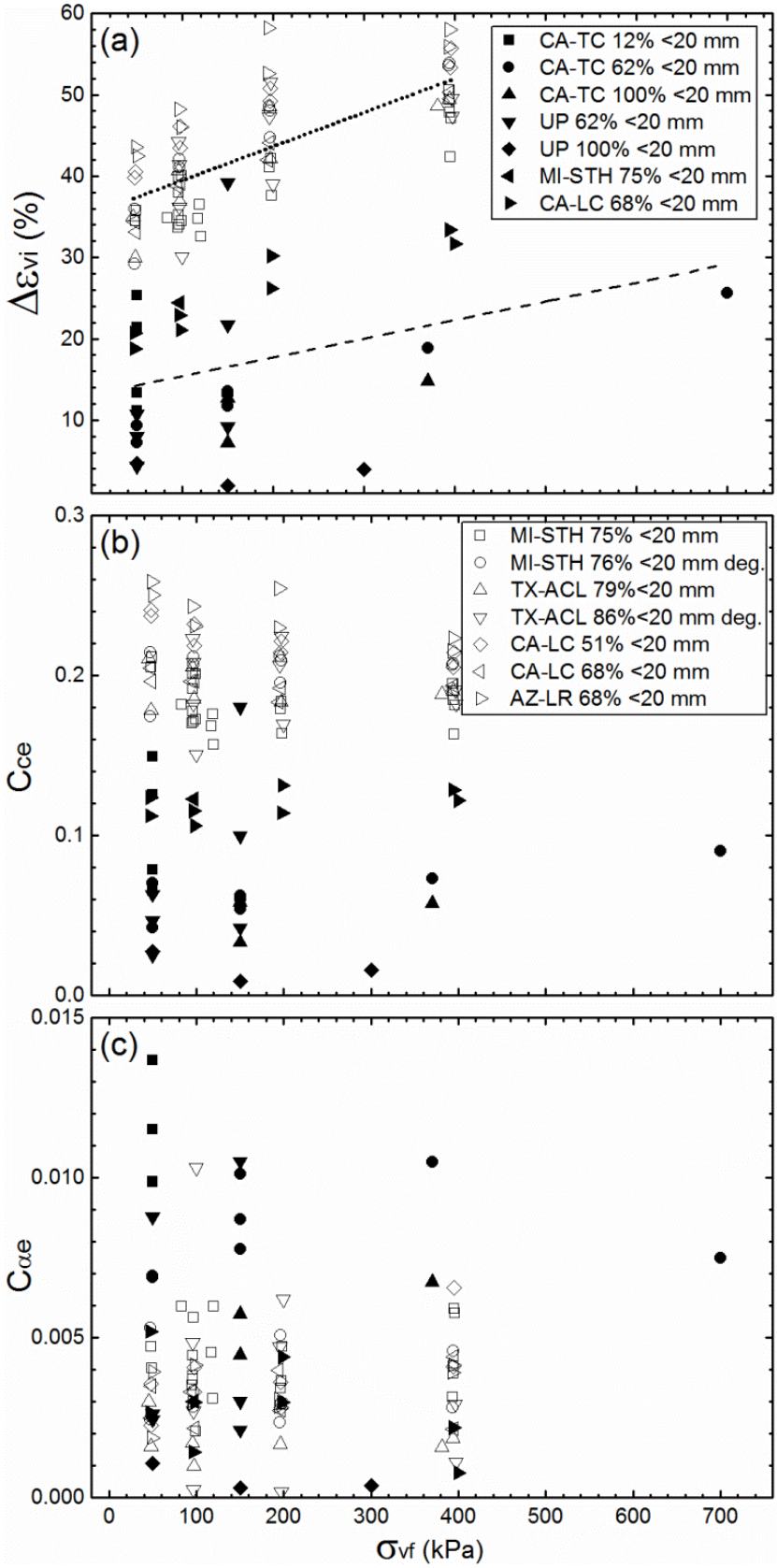

Figure 7-7 Experimental results in terms of (a) immediate strain; (b) C_{ce}, and (c) $C_{\alpha e}$.

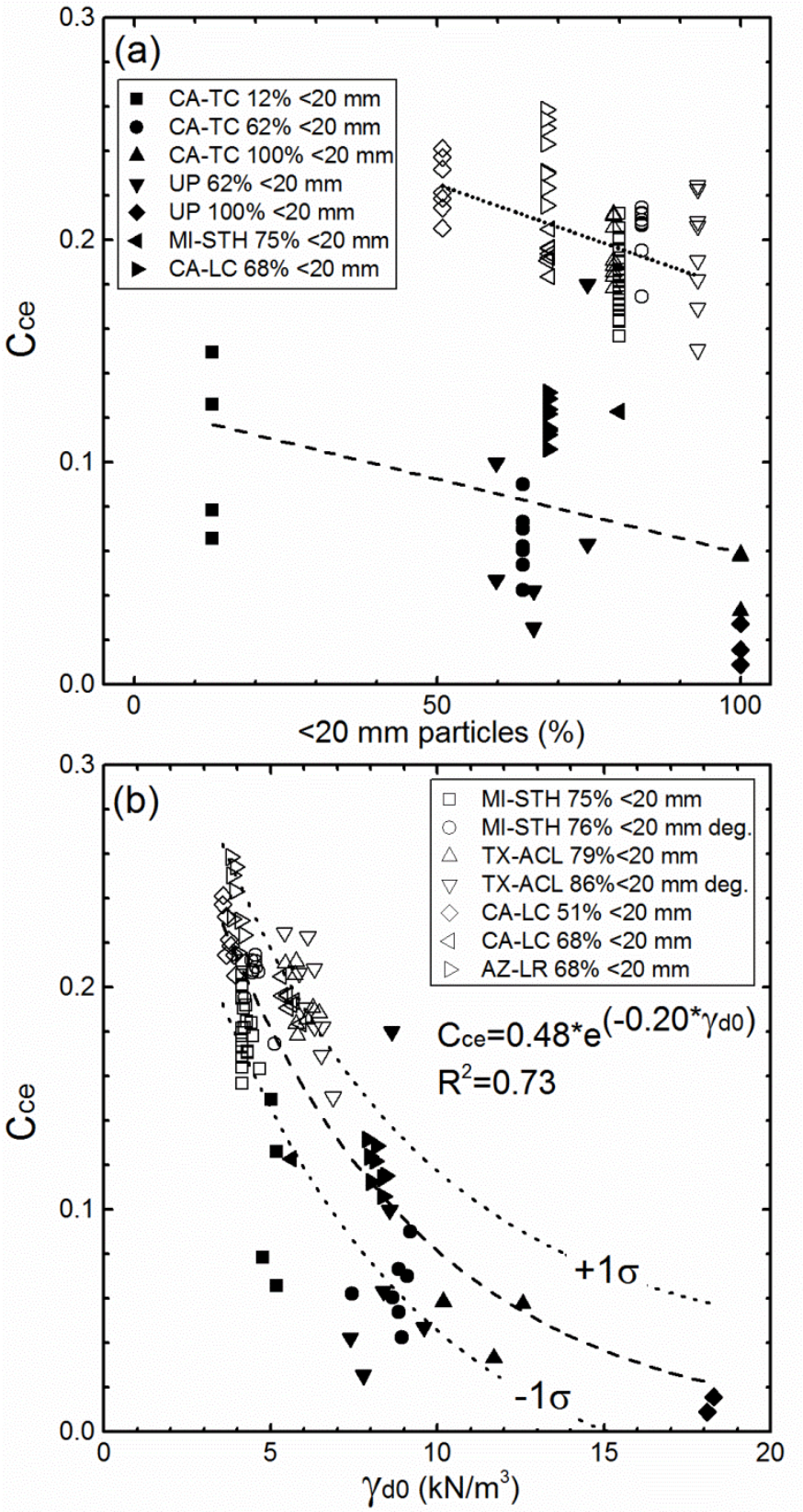

Figure 7-8 Relationship between C_{ce} and (a) percentage of <20 mm material, and (b) dry unit weight prior to compression (γ_{d0}).

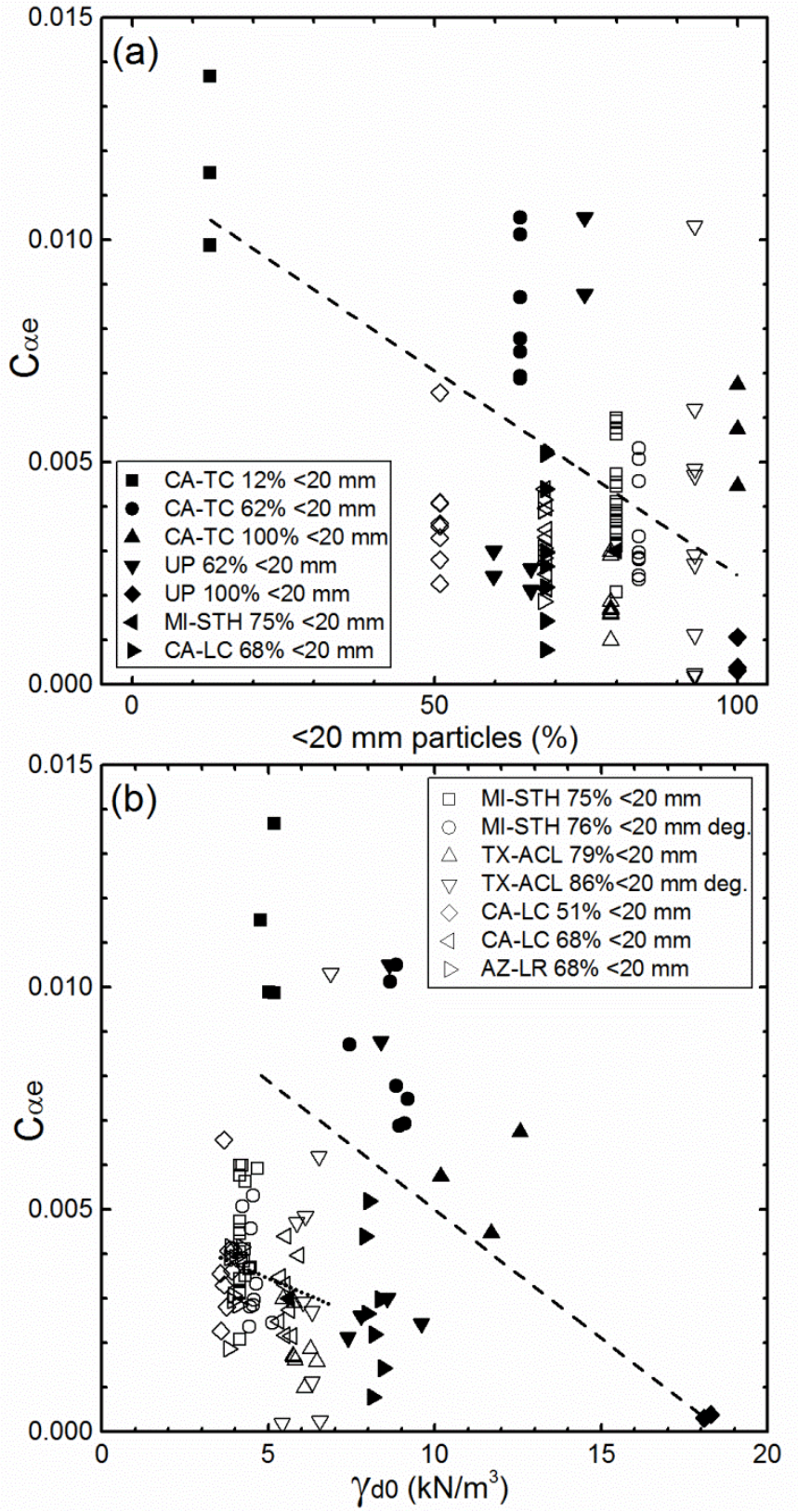

Figure 7-9 Relationship between $C_{\alpha e}$ and (a) percentage of <20 mm material, and (b) dry unit weight prior to compression (γ_{d0}).

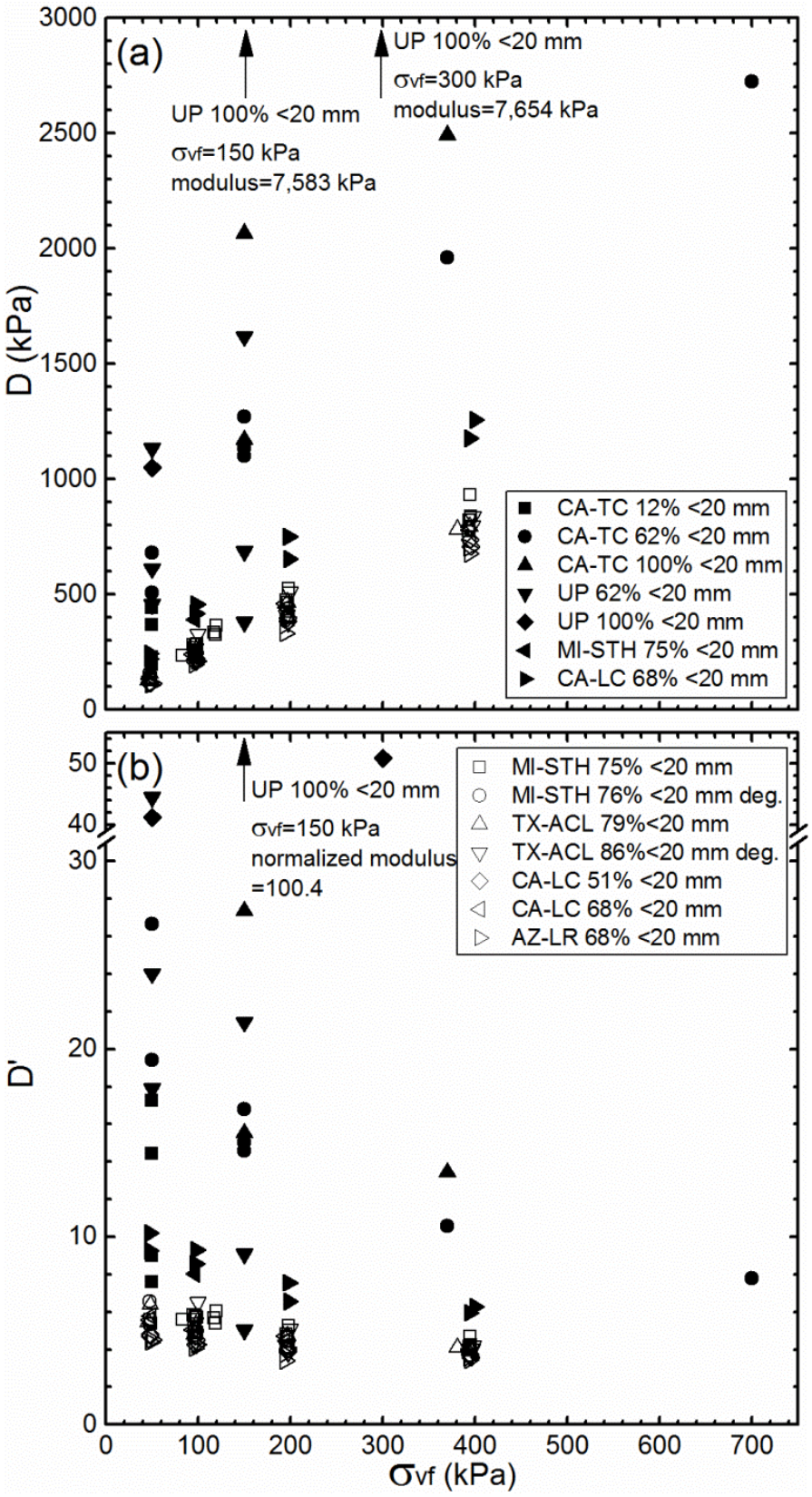

Figure 7-10 Relationship between final vertical stress (σ_{vf}) and (a) constrained modulus (D), and (b) normalized constrained modulus (D').

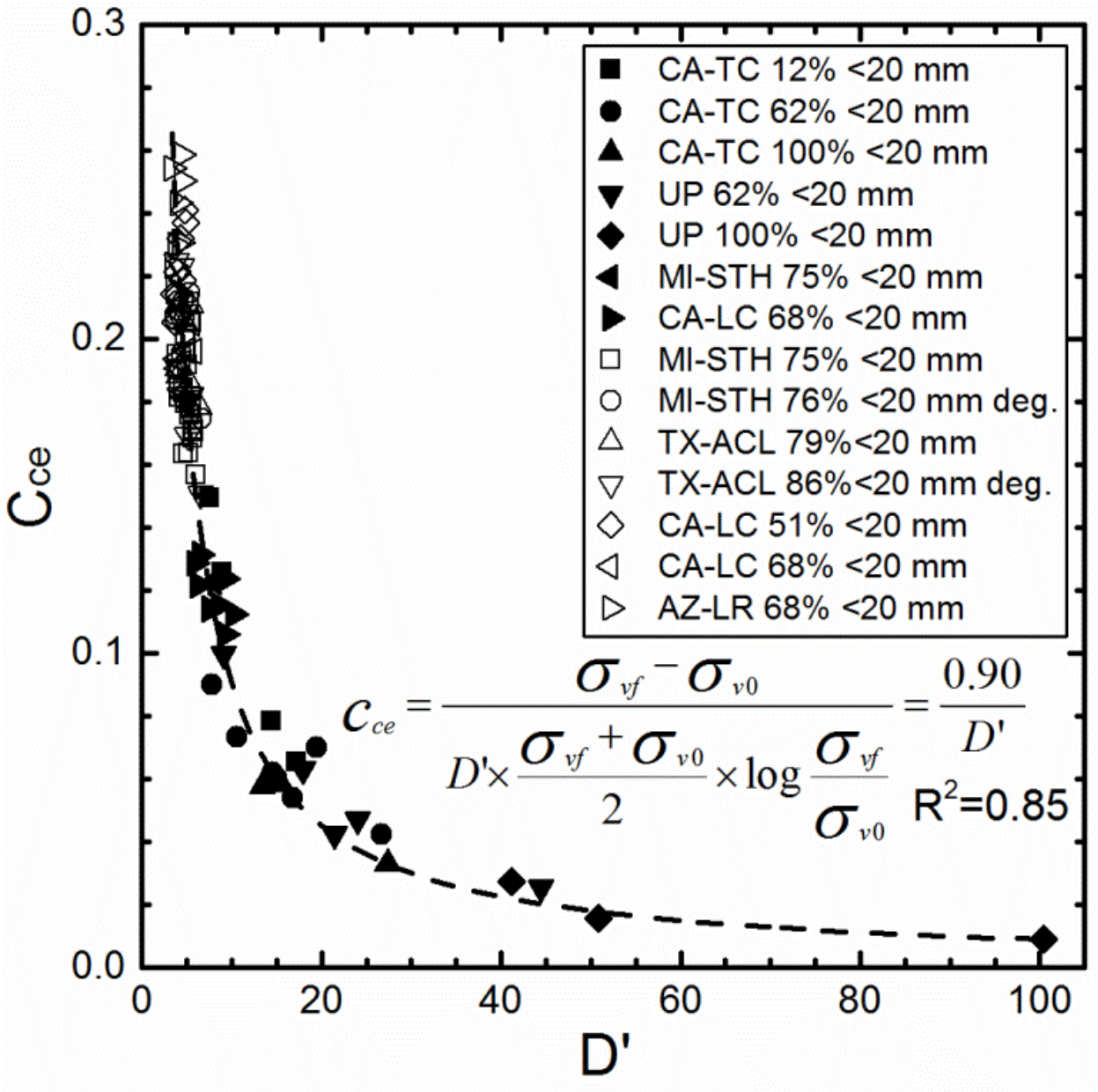

Figure 7-11 Correlation between C_{ce} and D'.

PART IV ENVIRONMENTAL AND OPERATING FACTORS INFLUENCING DEGRADATION OF MUNICIPAL SOLID WASTE

Chapter 8 Impacts of Initial Composition, Moisture Content and Overburden Pressure of Landfilled Municipal Solid Waste on Its Degradation Process

8.1 Abstract

The initial composition, moisture content and overburden pressure of municipal solid waste (MSW) are critical to the degradation process. Their impact on the evolving characteristics of waste during degradation are evaluated by synthesizing the results of degradation experiments and testing on MSW conducted by the writers and in the literature. The percentage of biodegradable waste of a specimen prior to degradation (B_0) largely determines its methane (CH_4) generation potential (L_0=2.19*B_0). Higher density of as-compressed biodegradable waste ($\gamma_{B,I}$) leads to higher maximum CH_4 generation rate per initial dry weight ($r_{CH4,max}/W_{s,0}$) and maximum long-term compression ratio ($C_{LT,max}$), but prolongs the delays before the initiation and maximum rate of CH_4 generation and $C_{LT,max}$ are measured. Changes in dry unit weight ($\gamma_{d,f}/\gamma_{d,I}$) and hydraulic conductivity due to waste degradation become larger with increasing $\gamma_{B,I}$. Maintaining field capacity moisture content of waste during its degradation increases the $r_{CH4,max}/W_{s,0}$ to 1.8% of the L_0 per day. For specimens with similar compositions, higher overburden pressure reduces the $\varepsilon_{B,f}$, $C_{LT,max}$ and k of waste, but increases the $\gamma_{d,f}/\gamma_{d,I}$. The $\varepsilon_{B,f}$ of

Fei, X., and Zekkos, D. (2016). "Impacts of initial composition, moisture content and overburden pressure of landfilled municipal solid waste on its degradation process." *Journal of Geotechnical and Geoenvironmental Engineering*, (under review).

waste can be estimated from $C_{LT,max}$ using a hyperbolic function. The impacts of the factors and correlations between the characteristics of waste provide estimation tools and guidance for the operation and monitoring of landfills receiving MSW of highly variable initial composition and moisture content and subject to varying vertical stress.

8.2 Introduction

Municipal solid waste (MSW) disposed of in modern Subtitle D and bioreactor landfills degrades with time. Biodegradable waste particles are converted by microorganisms to soluble compounds in leachate and biogas consisting of methane (CH_4) and carbon dioxide (CO_2). Characteristics of leachate and biogas and solid waste are changed during the degradation process (Pohland and Kim 2000; Barlaz et al. 2010b; Bareither et al. 2012d; Fei et al. 2016). The characteristics of solid waste are also changed by physical processes such as compression, creep, moisture softening and raveling of waste particles (McDougall 2007; Gourc et al. 2010; Bareither et al. 2012d; Fei et al. 2016). Multiple biochemical and physical processes take place simultaneously during MSW degradation and are influenced by operating conditions in landfills, among which the initial composition, moisture content (w_c), and overburden pressure (σ_v) of waste have been identified as three critical factors (Reinhart et al. 2002; Bareither et al. 2010; Barlaz et al. 2010a; Barlaz et al. 2010b; Fei et al. 2014a; Fei et al. 2015b). Since wide ranges of initial composition, w_c and σ_v of waste are encountered in the field, their impacts on MSW degradation needs to be quantified to inform efficient operation and effective monitoring of landfills.

The composition of as-placed MSW varies spatially in a landfill due to changes in incoming MSW stream with time (Zekkos et al. 2010b; Wang et al. 2013) and among different landfills because of different regional socioeconomic conditions and regulations (Staley and

Barlaz 2009; van Haaren et al. 2010). The as-placed composition of waste has been shown to affect biochemical characteristics of leachate (Barlaz et al. 1989b) and biogas (Eleazer et al. 1997; Kelly et al. 2006; Fei et al. 2015b) generated during MSW degradation, and physical, mechanical and hydraulics characteristics of solid waste including compressibility (McDougall 2011; Bareither et al. 2013a; Zekkos et al. 2016), shear strength and shear modulus (Bareither et al. 2012c; Kavazanjian et al. 2013; Sahadewa et al. 2014a; Fei and Zekkos 2015; Zekkos and Fei 2016), total and dry unit weight (Zekkos et al. 2006; Yu et al. 2011), and void ratio and hydraulic conductivity (Reddy et al. 2011; Hossain and Haque 2012; Stoltz et al. 2012; Breitmeyer and Benson 2014; Woodman et al. 2014). Nevertheless, the influence of waste composition on the trends of evolving characteristics during MSW degradation and changes in the characteristics before and after MSW degradation has not been evaluated quantitatively.

The moisture content of waste is greatly influenced by moisture management practice for landfills. Moisture infiltration to waste is minimized in modern Subtitle-D landfills, thus the w_c of waste is close to its as-placed value and almost always well below the field capacity. In contrast, moisture addition and leachate recirculation are actively implemented in bioreactor landfills to increase the w_c of waste and enhance biodegradation. However, in most available case studies on bioreactor landfills, the w_c of waste was still below field capacity (Reinhart et al. 2002; Benson et al. 2007; Bareither et al. 2010; Yazdani et al. 2012). The average w_c of waste also varies with waste composition (Tchobanoglous et al. 2002; Fei et al. 2016), overburden pressure (Zornberg et al. 1999; Stoltz et al. 2012), and the depth of waste in a landfill (Zhan et al. 2008; Zhan et al. 2015). Biodegradation of MSW only occurs in niches in waste mass where moisture and other environmental conditions, e.g., temperature and pH, are appropriate (Staley et al. 2011a). Therefore the w_c of waste greatly influences the number of potential niches (Vavilin

et al. 2003; Pommier et al. 2007) and thus the rate of biodegradation (Reinhart et al. 2002; Barlaz et al. 2010b; Fei et al. 2015b). Softening and raveling of waste particles due to moisture migration through waste mass also contributes to settlement and changes in unit weight and void ratio of waste (McDougall 2011; Bareither et al. 2012d). Although the general influence of w_c on MSW degradation are understood, differences in evolving characteristics of degrading waste specimens have not been related to the difference in w_c of waste yet.

Overburden pressure of waste increases with the depth of waste and depends on the total unit weight of overlaying waste which is related to the composition and w_c of the waste (Zekkos et al. 2006). Waste is compressed when subject to vertical stress, thus the matrix structure of waste is altered (Landva et al. 2000; Dixon et al. 2006; McDougall 2011; Bareither et al. 2012b; Zekkos et al. 2016). Consequently, the total and dry unit weight (Zekkos et al. 2006; Bareither et al. 2012e), shear strength and shear modulus (Zekkos et al. 2008; Bray et al. 2009), and void ratio and hydraulic conductivity (Hossain et al. 2003; Stoltz et al. 2010b; Woodman et al. 2014) of waste are changed. However, the impacts of σ_v of waste on its biodegradation process have not been explored.

A large number of laboratory degradation experiments and testing on MSW have been conducted using wide ranges of waste composition, moisture content and overburden pressure of waste to simulate diverse field conditions. Because of that, large discrepancies in experimental setups and degradation and testing conditions for MSW exist, leading to highly variable, and sometimes contradictory, results. Therefore available studies in the literature are frequently neither readily comparable to each other nor directly applicable to general monitoring and operation of landfills without specific assumptions and extrapolations. In this study, the monitoring results of laboratory degradation experiments on MSW by the writers and other

researchers and testing data focusing on physical and hydraulic characteristics of waste are synthesized. Consequently, impacts of the three critical factors on characteristics of waste during degradation are evaluated systematically. Engineering applications of established correlations between the factors and characteristics of waste are discussed subsequently.

8.3 Methodology

8.3.1 **Synthesis of experimental and testing results**

Around 100 available studies on laboratory degradation experiments and testing of MSW were reviewed. Studies using large-size simulators with the minimum dimeter of 30 cm were considered adequate of containing waste constituents of realistic and representative sizes (Athanasopoulos 2011b; Bareither et al. 2013a; Fei et al. 2014a) and were selected for further analysis. The selected studies were then screened for the availability of information on the initial composition, moisture content and overburden pressure of waste and the completeness and resolution of monitoring data with time during MSW degradation. The results of six experiments reported by the writers (Fei et al. 2016) and 45 experiments in 18 studies in the literature were considered satisfactory and compiled into a database as shown in Table 8-1. A few exceptions to the minimum size of simulators were made, Chen et al. (2010b) and Xu et al. (2015) used simulators with 19 cm diameter which was considered an acceptable size for the specimens they tested. Kim (2005) used two simulators with 15 cm diameter and only the final unit weight of MSW after biodegradation was included in analysis. Xie et al. (2006) used a 10-cm diameter simulator and only the hydraulic conductivity measurements were used in analysis.

8.3.2 **Estimation of waste composition parameters**

The specimens tabulated in Table 8-1 were reconstituted using selected waste constituents from the corresponding field waste samples. The composition of the waste samples used in the studies were all characterized by separating and weighing different waste constituents, and two generic and similar procedures are described by Zekkos et al. (2010b) and Dixon et al. (2008). Major waste constituents by weight were particles passing a 20-mm sieve (<20 mm fraction) and larger than 20-mm particles including paper, soft plastic, wood, yard waste, food, and miscellaneous non-biodegradable waste constituents. The waste composition of each specimen was evaluated by the writers using two parameters, percentage and density of biodegradable waste.

The percentage of biodegradable waste before waste degradation started (B_0, dry mass/dry mass %) is defined as the proportion by mass of food, yard waste and paper plus the mass of volatile solids (VS) in <20 mm fraction of the entire dry waste mass ($W_{s,0}$) (Fei et al. 2015a). Immediate compression of waste occurred immediately after a specimen was loaded into a simulator and stopped after a few days, by that time waste degradation had not started (McDougall 2011; Fei and Zekkos 2013). Therefore the density of biodegradable waste after immediate compression stopped and before degradation started ($\gamma_{B,I}$, kg/m^3) is defined using Eqn. 8-1:

$$\gamma_{B,I}\left(\frac{kg}{m^3}\right) = \frac{B_0\,(\%)}{100} \times \gamma_{d,I}\left(\frac{kg}{m^3}\right) \tag{8-1}$$

where $\gamma_{d,I}$ (kg/m^3) is the dry unit weight of a specimen when immediate compression of waste was practically completed (Bareither et al. 2012b). The $\gamma_{B,I}$ of waste is a volumetric parameter, whereas the B_0 of waste is calculated on a gravimetric basis.

8.3.3 **Characteristics of biogas, leachate and solid waste during waste degradation**

Changes in characteristics of leachate, biogas and solid waste with time were re-analyzed using the data reported in the respective studies to assure consistency in interpretation and calculation. The values of characteristics were obtained whenever available, but not every characteristic was available in all the studies. The mass of soluble chemical oxygen demand in leachate (sCOD, g O_2) was first calculated using reported concentration of sCOD and total volume of leachate in contact with each MSW specimen. The maximum value of sCOD was then normalized by the initial dry mass of waste ($W_{s,0}$, kg) to obtain $sCOD_{max}/W_{s,0}$ (g O_2/kg). The maximum CH_4 generation rate ($r_{CH4,max}$, L CH_4/d) and final volume of generated CH_4 were normalized by $W_{s,0}$, respectively, to obtain $r_{CH4,max}/W_{s,0}$ (L CH_4/kg-d) and CH_4 generation potential (L_0, L CH_4/kg). The time until initiation of CH_4 generation ($t_{rCH4,0}$, d) and $r_{CH4,max}$ was observed ($t_{rCH4,max}$, d) were identified using the CH_4 generation data with time for each specimen. From the time-dependent settlement measurements of each specimen, total strain due to biodegradation ($\varepsilon_{B,f}$, %) (Gourc et al. 2010), maximum long-term compression ratio ($C_{LT,max}$, d^{-1}) (Fei and Zekkos 2013), and the corresponding time for $C_{LT,max}$ ($t_{CLT,max}$, d) were calculated. The dry unit weight of waste after primary compression was practically completed ($\gamma_{d,I}$, kN/m^3) and after degradation stopped ($\gamma_{d,f}$, kN/m^3) were calculated. Reported hydraulic conductivity values (k, cm/s) of waste were recorded and the change in k due to degradation (k_f/k_I) was calculated.

8.3.4 **Categorization of moisture content and overburden pressure of waste**

The environmental and operating conditions in each study were recorded. Subsequently, the w_c of waste specimens in degradation experiments is categorized into two types based on the respective liquid management procedures and available w_c measurements. The w_c of a specimen was maintained at or beyond its field capacity ($w_c \geq$ f.c.) if water (sometimes seeded with leachate

or sludge) was added to the specimen at the beginning of the experiment and drained leachate was recirculated frequently (more frequent than weekly) and in sufficient amount (all of the drained leachate or more than 10% of the $W_{s,0}$). In contrast, the w_c of a specimen was considered to be below its field capacity (w_c<f.c.) when no moisture was added to the specimen initially or leachate recirculation was sporadic (between weekly to monthly) and in small amount (typically less than 5% of the $W_{s,0}$).

The values of vertical stress applied to waste specimens are divided into three groups, lower than 10 kPa (<10 kPa), 10-150 kPa, and 150-400 kPa, which roughly represent the σ_v of waste disposed of near the surface and at intermediate and high depth (Zekkos et al. 2006).

8.4 Results and discussion

8.4.1 Initial composition, moisture content and overburden pressure of analyzed waste specimens

The percentage of biodegradable waste prior to degradation (B_0) of the specimens listed in Table 8-1 range between 4.0-100% and $\gamma_{B,I}$ range between 43-648 kg/m^3. The average B_0 for discarded waste in the United States after recycling and composting and prior to landfilling is 45% (EPA 2014a), and the average B_0 of as-placed waste should be lower due to inclusion of cover soil and well-bounded by the range of B_0 investigated in this study. The values of $\gamma_{d,I}$ range between 1.25-13.48 kN/m^3.

As shown in Table 8-1, the w_c and σ_v of each specimen in degradation experiment is categorized. The operating conditions of the specimens are then divided into five types: 11 tests have w_c≥f.c. and σ_v<10 kPa (Valencia et al. 2009b; Gourc et al. 2010; Mali et al. 2012; Fei et al. 2016); 3 tests have w_c≥f.c. and σ_v=10-150 kPa (Ivanova et al. 2008b; Woodman et al. 2013); 5

tests have w_c<f.c. and σ_v<10 kPa (Erses et al. 2008; Gourc et al. 2010; Bareither et al. 2012d); 10 tests have w_c<f.c. and σ_v=10-150 kPa (Kim 2005; Olivier and Gourc 2007; Chen et al. 2010b; Bareither et al. 2013a; Staub et al. 2013; Xu et al. 2015); and 5 tests have w_c<f.c. and σ_v=150-400 kPa (Bareither et al. 2013a; Xu et al. 2015). The five operating types represent typical conditions of MSW disposed of at different depths in modern Subtitle D and bioreactor landfills and are used to distinguish the impacts of w_c and σ_v of waste on its degradation process in the subsequent sections.

8.4.2 **Impact of initial waste composition on biochemical characteristics of leachate and biogas**

As shown in Figure 8-1, normalized maximum mass of soluble chemical oxygen demand in leachate ($sCOD_{max}/W_{s,0}$) increases with increasing $\gamma_{B,I}$ of specimens. Higher $\gamma_{B,I}$ of a specimen provides more biodegradation niches for microorganisms (Vavilin and Angelidaki 2005; Vavilin et al. 2006), thus more widely distributed microbial activities concur. As a result, higher mass of sCOD is produced and accumulated in leachate for a given period of time. Measuring sCOD in leachate with time is informative for estimating the amount of biodegradable waste within a waste mass from which the leachate is drained.

CH_4 generation potential (L_0) of waste increases with increasing B_0 of specimens (Figure 8-2a). As shown in Eqn. 8-2, 1% increment of B_0 results in approximately 2.2 L increment of L_0 per kg of dry waste (R^2=0.77). The variability in the L_0 values is at least partially due to different CH_4 yield of individual waste constituents (e.g., paper, yard waste and food waste) in the specimens which is not captured by the value of B_0 (Eleazer et al. 1997; Fei et al. 2015b). There is no evidence indicating that L_0 is affected by the w_c or σ_v of waste during degradation. Correlations between L_0 (equivalent to biological methane potential, BMP) and VS content

(Kelly et al. 2006) and cellulose and hemi-cellulose content (Eleazer et al. 1997) of waste have been demonstrated and higher R^2 values have been reported for the correlations. Nevertheless, the B_0 of waste is influential to multiple processes during waste degradation in addition to methanogenesis, as will be demonstrated in the subsequent sections. Therefore B_0 is a practical parameter for assessing the initial composition and degradation process of MSW.

$$L_0\ (\frac{L}{kg}) = 2.19 \times B_0\ (\%) \tag{8-2}$$

Normalized maximum CH_4 generation rate ($r_{CH4}/W_{s,0}$) increases with increasing $\gamma_{B,I}$ of specimens at $w_c \geq$f.c. (Figure 8-2b), suggesting that $r_{CH4,max}/W_{s,0}$ and $\gamma_{B,I}$ of waste are correlated when w_c is sufficient for microbial activity. Since the $r_{CH4,max}/W_{s,0}$ of waste at $w_c \geq$f.c. can be readily estimated from its $\gamma_{B,I}$, biogas collection systems in landfill cells containing wet waste can be designed based on the characterization of incoming waste stream.

Higher $\gamma_{B,I}$ of waste results in accumulation of excess sCOD in leachate (Figure 8-1) which has been related to longer period of inhibition before methanogenesis initiates (Vavilin et al. 2003; Barlaz et al. 2010b; Fei et al. 2016). Therefore both the time until the initiation and maximum rate of CH_4 generation ($t_{rCH4,0}$ and $t_{rCH4,max}$, respectively) roughly increase with increasing $\gamma_{B,I}$ of waste, as shown in Figure 8-3a and Figure 8-3b.

8.4.3 **Impact of initial waste composition on physical and hydraulic characteristics of solid waste**

Final biodegradation strain ($\varepsilon_{B,f}$) of waste increases with increasing $\gamma_{B,I}$ within each σ_v group, indicating that higher amount of biodegradable waste is related to larger settlement of waste during biodegradation (Gawande et al. 2010; Gourc et al. 2010; Fei et al. 2016) (Figure 8-4a).

Maximum long-term compression ratio ($C_{LT,max}$) of waste increases with increasing $\gamma_{B,I}$ within each σ_v group as well, because higher $\gamma_{B,I}$ leads to higher biodegradation rate of waste (Figure 8-4b). The values of $C_{LT,max}$ during MSW biodegradation are on the same order of magnitude as the primary compression ratios of MSW subject to vertical stress application reported by other researchers (Bjarngard and Edgers 1990; Landva and Clark 1990; Zekkos et al. 2016).

As shown in Figure 8-5, $\gamma_{d,f}/\gamma_{d,I}$ increases with increasing $\gamma_{d,I}$ of specimens, and higher σ_v of waste also results in higher $\gamma_{d,f}/\gamma_{d,I}$. Overall, specimens consisting of more biodegradable waste tend to have lower $\gamma_{d,f}$ after degradation, while the value of $\gamma_{d,f}/\gamma_{d,I}$ also depends on the $\gamma_{d,I}$ and σ_v of waste.

The hydraulic conductivity (k) of waste decreases with increasing γ_d of the tested specimen, because specimen having higher γ_d typically has higher % of <20 mm fraction which reduces the value of k (Reddy et al. 2011; Woodman et al. 2014) (Figure 8-6a). Since <20 mm fraction of waste typically contains lower % of biodegradable waste than the same mass of >20 mm waste particles which consists of significant amount of paper, the k of waste should increase with increasing B_0 and $\gamma_{B,I}$ representing higher % of biodegradable waste. The change in k due to degradation (k_f/k_I) was calculated using the hydraulic conductivity of as-compressed waste (k_I) and hydraulic conductivity of degraded waste (k_f) for specimens degraded in simulators at constant σ_v and not destructively sampled or reconstituted (Xie et al. 2006; Fei et al. 2016). The values of k_f/k_I decrease with increasing $\gamma_{B,I}$, suggesting that the reduction of k due to waste degradation is dependent on the initial waste composition (Figure 8-6b).

8.4.4 **Impact of moisture content on waste degradation**

As shown in Figure 8-2b, the values of $r_{CH4,max}/W_{s,0}$ are proportional to $\gamma_{B,I}$ of waste when $w_c \geq$f.c., but are not clearly correlated with $\gamma_{B,I}$ when waste has $w_c <$f.c., thus $r_{CH4,max}$ of waste is

heavily influenced by the w_c of waste. As shown in Figure 8-7, linear relationships are established between the L_0 and $r_{CH4,max}/W_{s,0}$ of specimens, and the $r_{CH4,max}/W_{s,0}$ of waste being degraded at $w_c \geq$f.c. can be estimated as 1.8% of the corresponding L_0 per day (Eqn. 8-3a, R^2=0.93), whereas the value is 0.6% of the L_0 per day when waste has $w_c <$f.c. (Eqn. 8-3b, R^2=0.91). Therefore maintaining MSW at $w_c \geq$f.c. is essential to accelerate CH_4 generation, possibly as high as three times faster, and consequently achieving more efficient and economical energy generation from biogas recovery.

$$\frac{r_{CH4,max}\,(\frac{L}{d})}{W_{s,0}\,(kg)} = 0.018 \times L_0\,(\frac{L}{kg}) \text{ when } w_c \geq \text{f.c.} \quad (8\text{-}3a)$$

$$\frac{r_{CH4,max}\,(\frac{L}{d})}{W_{s,0}\,(kg)} = 0.0060 \times L_0\,(\frac{L}{kg}) \text{ when } w_c < \text{f.c.} \quad (8\text{-}3b)$$

Both $t_{rCH4,0}$ and $t_{rCH4,max}$ are generally longer for specimens having $w_c <$f.c. in Figure 8-3a and 3b. This is because moisture migration through waste is limited when the w_c of waste is low, thus microorganisms and soluble substrates and nutrients for them are less likely to be redistributed to potential niches and volatile fatty acids inhibiting methanogenesis cannot be diluted rapidly (Vavilin et al. 2006; Barlaz et al. 2010b). As the result, the initiation and maximum rate of CH_4 generation from the whole waste mass appear to be delayed.

8.4.5 **Impact of overburden pressure on physical and hydraulic characteristics of solid waste**

Vertical stress application to waste induces immediate compression, and reduces the amount of additional settlement observed during biodegradation (Bareither et al. 2012b; Fei and Zekkos 2013; Zekkos et al. 2016). As shown in Figure 8-4a, as the σ_v of waste increases from <10 kPa

to 10-150 kPa and 150-400 kPa, the values of $\varepsilon_{B,f}$ decrease for specimens having similar $\gamma_{B,I}$. Similarly, the values of $C_{LT,max}$ for specimens having similar $\gamma_{B,I}$ decrease with increasing σ_v of waste (Figure 8-4b). The maximum and minimum values of $\varepsilon_{B,f}$ and $C_{LT,max}$ could be more than 10 times different due to the change in σ_v. The values of $\gamma_{d,f}/\gamma_{d,I}$ for specimens at σ_v=10-150 kPa are mostly higher than unity which indicates densification of waste after degradation, whereas the $\gamma_{d,f}$ of specimens at lower σ_v were generally lower than the $\gamma_{d,I}$ (Figure 8-5). Higher σ_v of waste typically results in higher γ_d, thus the k of waste is reduced (Woodman et al. 2014).

8.4.6 **Correlations between characteristics of leachate, biogas and solid waste and their engineering applications**

The impacts of initial composition, moisture content, and overburden pressure of waste on the changes in characteristics of leachate, biogas and solid waste during degradation are summarized in Table 8-2. The generalized trends and regression equations shown previously can be used to estimate the behavior of MSW undergoing degradation under various operating conditions in landfills. Generally speaking, B_0 of waste largely impacts the values of characteristics before and after MSW degradation, including L_0, $\gamma_{d,I}$, e_{drain}, e_{total}, and k, whereas $\gamma_{d,I}$ of waste influences the characteristics related to the rate of MSW degradation, such as $sCOD_{max}/W_{s,0}$, $r_{CH4,max}/W_{s,0}$, $t_{rCH4,0}$, $t_{rCH4,max}$, $C_{LT,max}$, $t_{CLT,max}$. In addition, $\gamma_{d,I}$ of waste affects the changes in strain ($\varepsilon_{B,f}$), dry unit weight ($\gamma_{d,f}/\gamma_{d,I}$) and hydraulic conductivity (k_f/k_I) due to degradation. Increasing w_c of waste contributes to accelerating CH_4 generation and initiation of MSW degradation. Increasing σ_v of waste reduces $\varepsilon_{B,f}$, $C_{LT,max}$ and k of waste, and results in densification during biodegradation.

In addition to estimating the characteristics during MSW degradation using initial composition, w_c and σ_v of waste, the progress of MSW degradation can be assessed by

correlating characteristics measured during waste degradation. The time until the initiation and maximum rate of CH_4 generation and $C_{LT,max}$ are measured are correlated with each other and always occur consecutively as shown in Figure 8-8. Therefore both $t_{rCH4,max}$ and $t_{CLT,max}$ can be estimated once $t_{rCH4,0}$ is observed using Eqn. 8-4a (R^2=0.64) and 4b (R^2=0.59). Additionally, $t_{CLT,max}$ and $t_{rCH4,max}$ can be reliably estimated from each other using Eqn. 8-4c with a higher R^2 of 0.92:

$$\log\left(t_{rCH4,max}\ (d)\right) = 0.66 \times \log\left(t_{rCH4,0}\ (d)\right) + 1.28 \quad (8\text{-}4a)$$

$$\log\left(t_{CLT,max}\ (d)\right) = 0.48 \times \log\left(t_{rCH4,0}\ (d)\right) + 1.60 \quad (8\text{-}4b)$$

$$\log\left(t_{CLT,max}\ (d)\right) = 0.74 \times \log\left(t_{rCH4max}\ (d)\right) + 0.72 \quad (8\text{-}4c)$$

The $\varepsilon_{B,f}$ of waste can be roughly estimated based on measured $C_{LT,max}$ and a hyperbolic function appears to be the best fit for the correlation, as shown in Figure 8-9 and Eqn. 8-5 (R^2=0.59):

$$\varepsilon_{B,f}\ (\%) = \frac{23.5 \times C_{LT,max}\ (d^{-1})}{0.11 + C_{LT,max}\ (d^{-1})} \quad (8\text{-}5)$$

8.5 Conclusions

The impacts of initial composition, moisture content and overburden pressure of waste on the evolving characteristics of leachate, biogas and solid waste during degradation are evaluated using the results of degradation experiments on waste specimens by the writers and in the literature. The waste composition of each specimen is evaluated by the writers using two parameters, percentage and density of biodegradable waste prior to biodegradation and after

immediate compression (B_0 and $\gamma_{B,I}$, respectively). The moisture content (w_c) of specimens is categorized into two types ($w_c \geq$ f.c. and $w_c <$ f.c.) based on the respective liquid management procedures and available w_c measurements. The values of vertical stress (σ_v) applied to waste specimens are divided into four groups, lower than 10 kPa (<10 kPa), 10-150 kPa, and 150-400 kPa.

The impacts of initial composition of waste on its biodegradation process are:

- Normalized maximum mass of soluble chemical oxygen demand in leachate ($sCOD_{max}/W_{s,0}$) increases with increasing $\gamma_{B,I}$ of specimens;
- CH_4 generation potential of waste (L_0) increases with increasing B_0, and 1% increment of B_0 results in approximately 2.2 L/kg increment of L_0 (R^2=0.80). Maximum CH_4 generation rate ($r_{CH4,max}$) is normalized by the initial dry weight of waste ($W_{s,0}$) and the value increases with increasing $\gamma_{B,I}$ when $w_c \geq$ f.c. (R^2=0.63);
- Time until initiation of CH_4 generation ($t_{rCH4,0}$) and $r_{CH4,max}$ was observed ($t_{rCH4,max}$) are generally longer for waste having higher $\gamma_{B,I}$;
- Both final biodegradation strain ($\varepsilon_{B,f}$) and maximum long-term compression ratio of waste ($C_{LT,max}$) increase with increasing $\gamma_{B,I}$ and the maximum reported values are 30% and 0.7 d^{-1}, respectively.
- Specimens of higher $\gamma_{B,I}$ and lower dry unit weight after immediate compression ($\gamma_{d,I}$) tend to have lower final dry unit weight after degradation ($\gamma_{d,f}$);
- Hydraulic conductivity of waste (k) decreases with increasing dry unit weight of tested specimen. Higher $\gamma_{B,I}$ of waste results in larger reduction of k due to biodegradation compared to its initial value.

Difference in moisture content between waste specimens results in differences in evolving characteristics during degradation:

- Although $r_{CH4,max}/W_{s,0}$ increases with increasing $\gamma_{B,I}$ of waste when $w_c \geq$ f.c., no clear correlation is observed between them when w_c of waste is <f.c.;
- The $r_{CH4,max}/W_{s,0}$ of waste being degraded at $w_c \geq$ f.c. is approximately 1.8% of the corresponding L_0 per day (R^2=0.93), whereas the value is 0.6% of the L_0 per day when waste is degraded at $w_c <$ f.c. (R^2=0.91);
- Both $t_{rCH4,0}$ and $t_{rCH4,max}$ are generally longer for specimens having lower w_c.

Vertical stress application to waste prior to and during its degradation process has the following impacts:

- For a given $\gamma_{B,I}$, the values of $\varepsilon_{B,f}$ and $C_{LT,max}$ decrease with increasing σ_v between 10-400 kPa, and the difference between the maximum and minimum values could be more than 10 times;
- Waste at higher σ_v tends to have higher $\gamma_{d,f}/\gamma_{d,I}$ compared to waste at lower σ_v;
- The γ_d of waste is typically increased by increasing σ_v, and the k of waste is reduced consequently.

In addition, correlations are established between the evolving characteristics measured during MSW degradation to facilitate effective and efficient monitoring and operation of landfills. Correlations are established among the values of $t_{rCH4,0}$, $t_{rCH4,max}$ and time until $C_{LT,max}$ is observed ($t_{CLT,max}$), the three time points always occur consecutively. Higher $r_{CH4,max}/W_{s,0}$ indicates higher L_0, while higher $C_{LT,max}$ indicates higher $\varepsilon_{B,f}$.

8.6 Tables

Table 8-1 Initial composition, moisture content and overburden pressure of the specimens used in degradation experiments and available measurements for each study.

Reference and specimen description	Specimen size (cm) diameter x height	Initial composition			Moisture content	Overburden pressure (kPa)	Measurements	
		B_0 (%)	$\gamma_{B,I}$ (kg/m^3)	$\gamma_{d,I}$ (kN/m^3)			Biochemical characteristics	Physical and hydrological properties
(Bareither et al. 2012d)								
Wisconsin fresh waste	61x34	69.6	191	2.69	<f.c.	8	$sCOD_{max}$ L_0 [a] $r_{CH4,max}$	$\varepsilon_{B,f}$ $C_{LT,max}$ $\gamma_{d,I}$
(Bareither et al. 2013a)								
Wisconsin fresh waste	30x15	33.1	226	7.01	<f.c.	64	L_0 [c]	$\varepsilon_{B,f}$ $C_{LT,max}$ $\gamma_{d,I}$ [d]
<25 mm particles of fresh waste		20.2	231	9.91		64		
>25 mm particles of fresh waste		46.4	380	6.05		64		
low degradation waste		6.0 [b]	43	6.97		64		
high degradation waste		16.8 [b]	122	7.14		64		
Wisconsin fresh waste		33.1	314	7.38		400		
low degradation		6.0 [b]	45	7.41		400		
high degradation		16.8 [b]	122	6.98		400		
(Chen and Chynoweth 1995)								
8 specimens synthetic paper waste		100	160-480	1.57-4.71	n. a.	1	n. a.	k
(Chen et al. 2010b)								
China fresh waste	19x30	59.4	391	6.46	<f.c.	150	n. a.	$\varepsilon_{B,f}$ $C_{LT,max}$
(Erses et al. 2008)								
Turkey fresh waste	35x100	59.5	446	n. a.	<f.c.	1	$sCOD_{max}$ L_0 $r_{CH4,max}$	n. a.
(Fei et al. 2016)								
Texas fresh waste #1	30x55	16.1	98	5.93	≥f.c.	1	$sCOD_{max}$ L_0 $r_{CH4,max}$	$\varepsilon_{B,f}$ $C_{LT,max}$ $\gamma_{d,I}$ $\gamma_{d,f}$ k_I k_f
Texas fresh waste #2		16.4	98	5.85				
Arizona fresh waste		30.6	143	4.57				
California fresh waste #1		10.3	66	6.26				
California fresh waste #2		21.8	86	3.86				
Michigan fresh waste		48.1	115	2.35				
(Valencia et al. 2009b)								
Netherlands fresh waste leachate seeding	70x174	40.8	173	4.21	≥f.c.	1	$sCOD_{max}$ L_0 $r_{CH4,max}$	$\gamma_{d,I}$
(Gourc et al. 2010)								
France fresh waste #A2 leachate seeding	96x110	37.9	147	3.81	≥f.c.	1	L_0 $r_{CH4,max}$	$\varepsilon_{B,f}$ $C_{LT,max}$
France fresh waste #B2 leachate seeding		37.8	150	3.89	≥f.c.			
France fresh waste #A1 leachate seeding		37.9	147	3.81	<f.c.			
France fresh waste #B1 leachate seeding		37.8	140	3.63	<f.c.			

France fresh waste #C1 leachate seeding	22 m^3	36.1	159	4.33	<f.c.			
				(Han et al. 2011)				
3 specimens synthetic paper waste	29x12	100	127-210	1.25-2.06	n. a.	30-45	n. a.	k
				(Ivanova et al. 2008b)				
U.K. fresh waste #1 sludge seeding	48x65	53.2	234	4.31	≥f.c.	150	$sCOD_{max}$ L_0 $r_{CH4,max}$	$\varepsilon_{B,f}$ $C_{LT,max}$ $\gamma_{d,I}$ $\gamma_{d,f}$ k_f [e]
U.K. fresh waste #2 sludge seeding		53.2	190	3.51		50		
				(Kim 2005)				
2 specimens Florida degrading waste	15x140	64.0	335	5.16	<f.c.	98	n. a.	$\gamma_{d,f}$
				(Mali et al. 2012)				
India fresh waste #2 sludge seeding	30x100	37.2 [f]	127	3.33	≥f.c.	1	$sCOD_{max}$ L_0 $r_{CH4,max}$	$\varepsilon_{B,f}$ $C_{LT,max}$ $\gamma_{d,I}$ $\gamma_{d,f}$
India fresh waste #4 sludge seeding		48.8 [f]	182	3.66				
				(Olivier and Gourc 2007)				
France degrading waste	100x85	55.0	322	5.74	<f.c.	130	n. a.	k_f
				(Rosqvist and Bendz 1999)				
Sweden excavated waste	193x120	43.9	259	5.79	n. a.	1	n. a.	k
				(Staub et al. 2013)				
France fresh waste leachate seeding	100x120	45.5	280	6.04	<f.c.	140	L_0 $r_{CH4,max}$	$\varepsilon_{B,f}$ $C_{LT,max}$ $\gamma_{d,I}$ $\gamma_{d,f}$ [g]
France fresh waste leachate seeding		45.5	309	6.65	<f.c.	140		
				(Tinet et al. 2011)				
France fresh waste	96x90	26.4	119	4.41	n. a.	1	n. a.	k
				(Woodman et al. 2013)				
U.K. degrading mechanically-biologically treated waste	48x35	14.3	85	5.83	≥f.c.	50	L_0 $r_{CH4,max}$	$\varepsilon_{B,f}$ $C_{LT,max}$ $\gamma_{d,I}$ k_I k_f [h]
U.K. bio-inhibition mechanically-biologically treated waste		14.3	85	5.83	≥f.c.	50		
				(Xie et al. 2006)				
Germany degrading mechanical-biological treated waste	10x11	4.0	44	10.89	<f.c.	1	n. a.	k_I k_f
				(Xu et al. 2015)				
China fresh waste #1	19x55	47.2 [f]	501	10.42	<f.c.	100	L_0 $r_{CH4,max}$	$\varepsilon_{B,f}$ $C_{LT,max}$ $\gamma_{d,I}$
China fresh waste #2		47.2 [f]	565	11.76		200		
China fresh waste #3		47.2 [f]	648	13.48		400		

n. a.: not available;

[a]: reported biogas leakage from the simulator, not included in the regression for L_0.

[b]: calculated from cellulose and hemi-cellulose content of waste.

[c]: L_0 measurements available for the first five specimens.

[d]: $\gamma_{d,I}$ measurements available for the first one and last three specimens.

[e]: k_f measurement available for U.K. fresh waste #2 specimen.

[f]: contained >50% wet food waste, but only reported average w_c, thus B_0 was reduced slightly because food waste typically has very high w_c.
[g]: $\gamma_{d,f}$ measurement available for the second specimen.
[h]: k_f measured at σ_v of 150 kPa.

Table 8-2 Summary of the impacts of initial composition, moisture addition, and overburden pressure of MSW on the changes in characteristics of leachate, biogas and solid waste during degradation.

Process during MSW degradation	Characteristics and properties	Initial composition B_0 and $\gamma_{B,I}$	Moisture content	Overburden pressure
Hydrolysis from solid waste and acidogenesis in leachate	$sCOD_{max}/W_{s,0}$	↑	?	?
Methanogenesis from soluble compounds to biogas	L_0	↑	--	--
	$r_{CH4,max}/W_{s,0}$	↑	↑	?
	$t_{rCH4,0}$ and $t_{rCH4,max}$	↑	↓	?
Biodegradation settlement of waste	$\varepsilon_{B,f}$	↑	--	↓
	$C_{LT,max}$	↑	--	↓
	$t_{CLT,max}$	↑	↓	?
Change in dry unit weight of waste	$\gamma_{d,f}/\gamma_{d,I}$	↓	?	↑
Change in hydraulic conductivity of waste	k	↑	?	↓
	k_f/k_I	↓	?	?

blank: not applicable;
↑: increases with increasing value of the factor;
↓: decreases with increasing value of the factor;
--: not affected by the factor;
?: insufficient evidence.

8.7 Figures

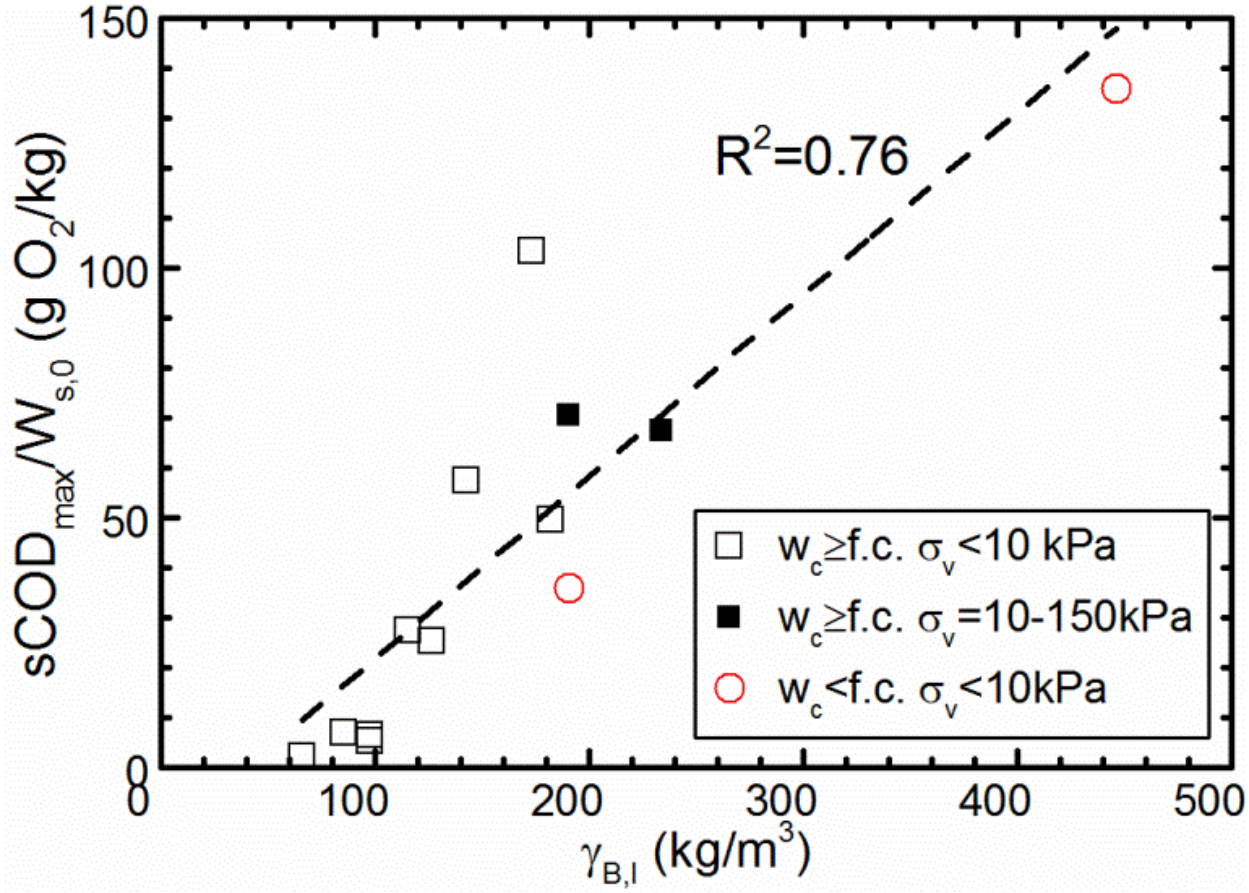

Figure 8-1 Correlation between normalized maximum mass of soluble oxygen demand in leachate ($sCOD_{max}/W_{s,0}$) and density of biodegradable waste ($\gamma_{B,I}$).

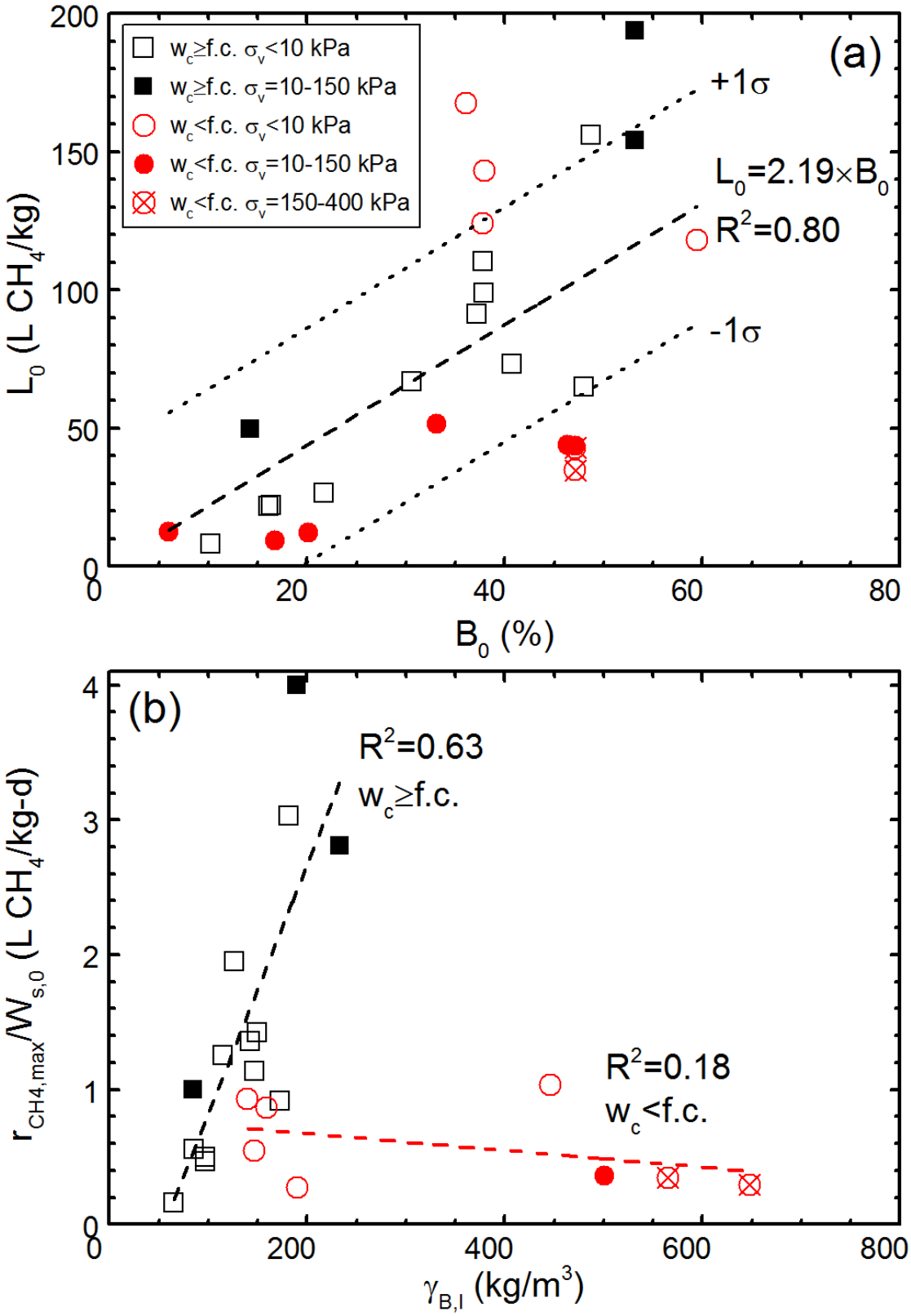

Figure 8-2 Correlations between initial composition of waste and biogas generation: (a) CH_4 generation potential (L_0) and percentage of biodegradable waste (B_0); and (b) normalized maximum CH4 generation rate ($r_{CH4,max}/W_{s,0}$) and density of biodegradable waste ($\gamma_{B,I}$).

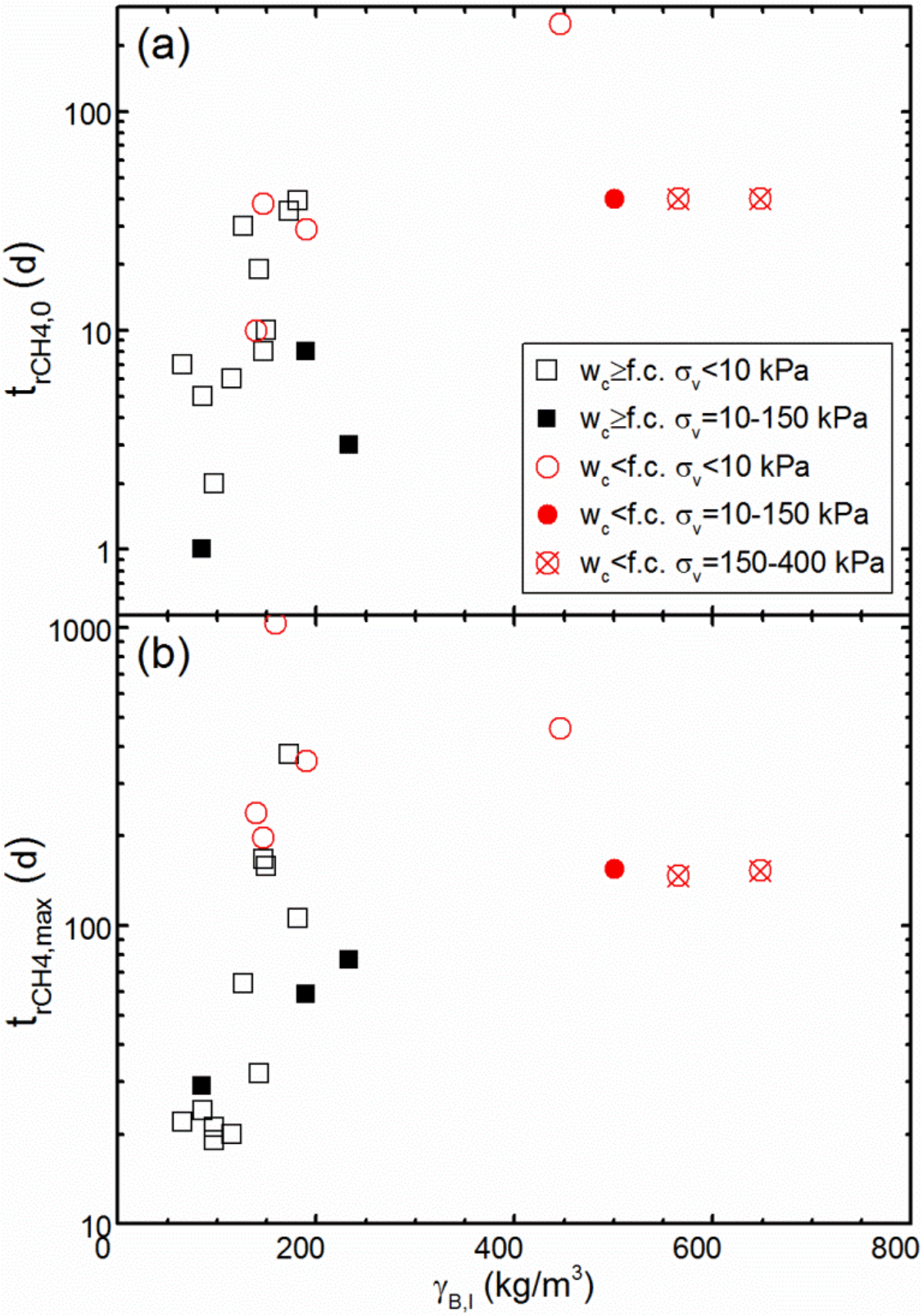

Figure 8-3 Correlations between density of biodegradable waste ($\gamma_{B,I}$) and (a) the time until the initiation of CH_4 generation ($t_{rCH4,0}$); and (b) the time until the maximum generation rate of CH_4 ($t_{rCH4,max}$).

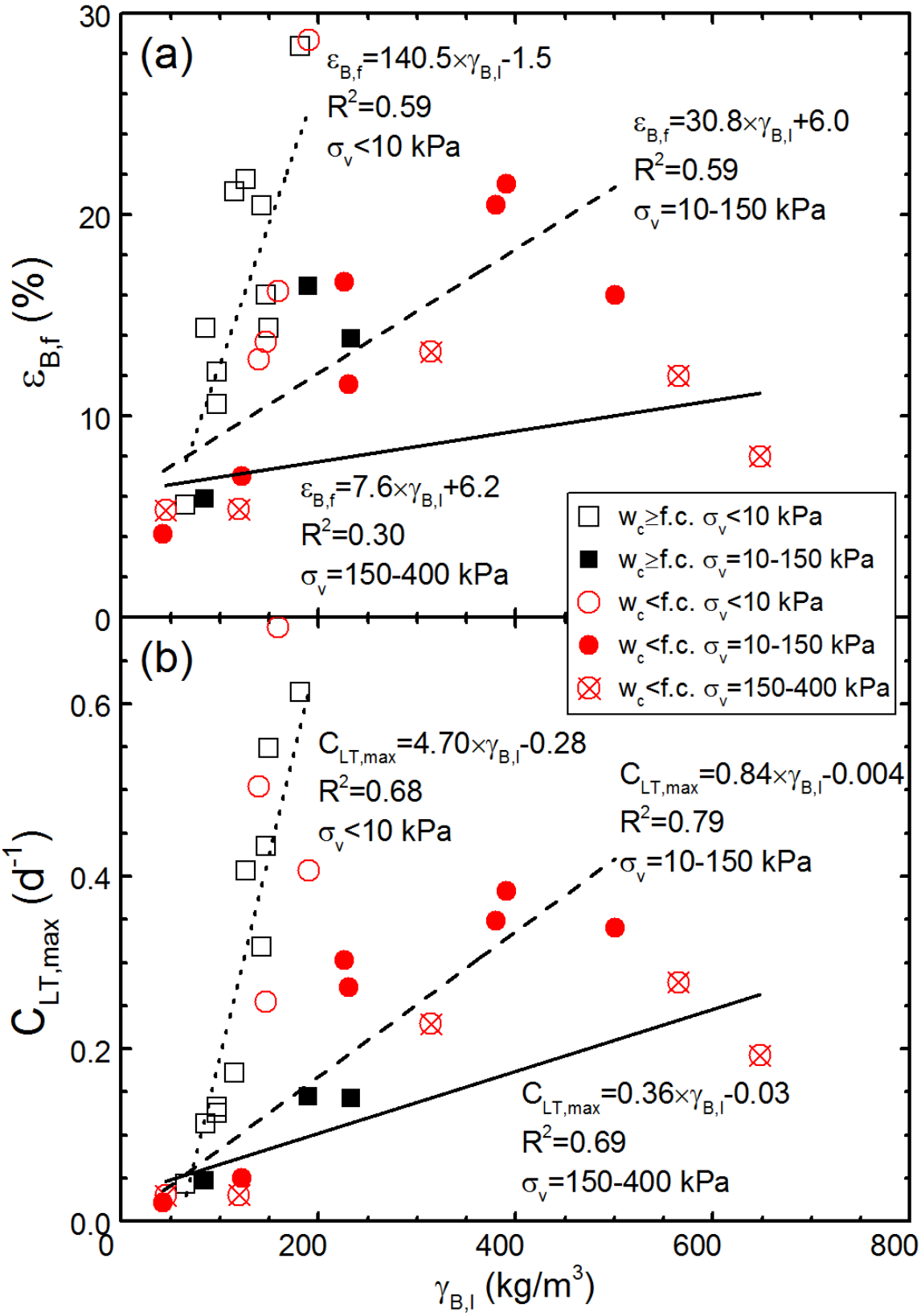

Figure 8-4 Correlations between density of biodegradable waste ($\gamma_{B,I}$) and (a) biodegradation strain ($\varepsilon_{B,f}$); and (b) maximum long-term compression ratio ($C_{LT,max}$).

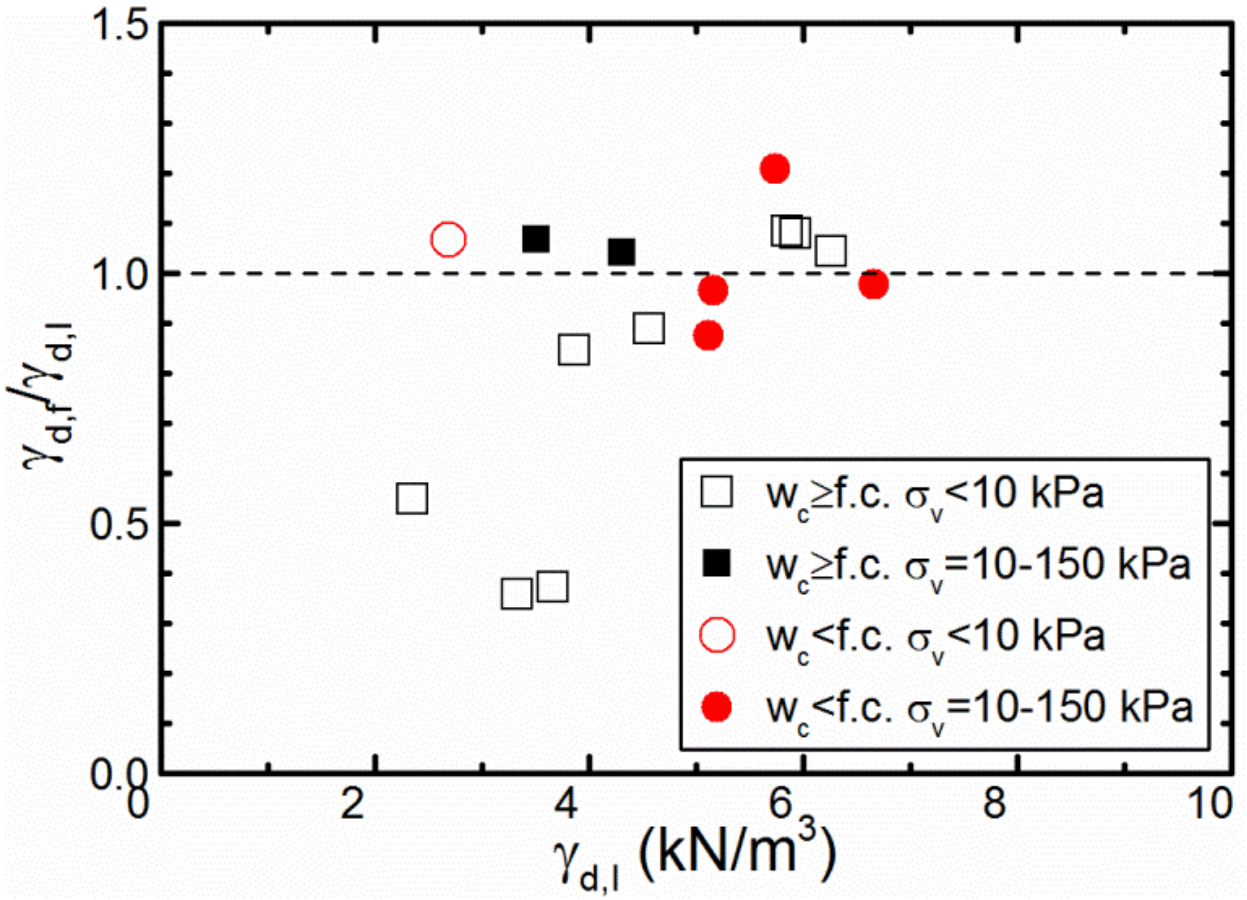

Figure 8-5 Relationships between change in dry unit weight of waste due to degradation ($\gamma_{d,f}/\gamma_{d,I}$) and as-compressed dry unit weight of waste after ($\gamma_{d,I}$).

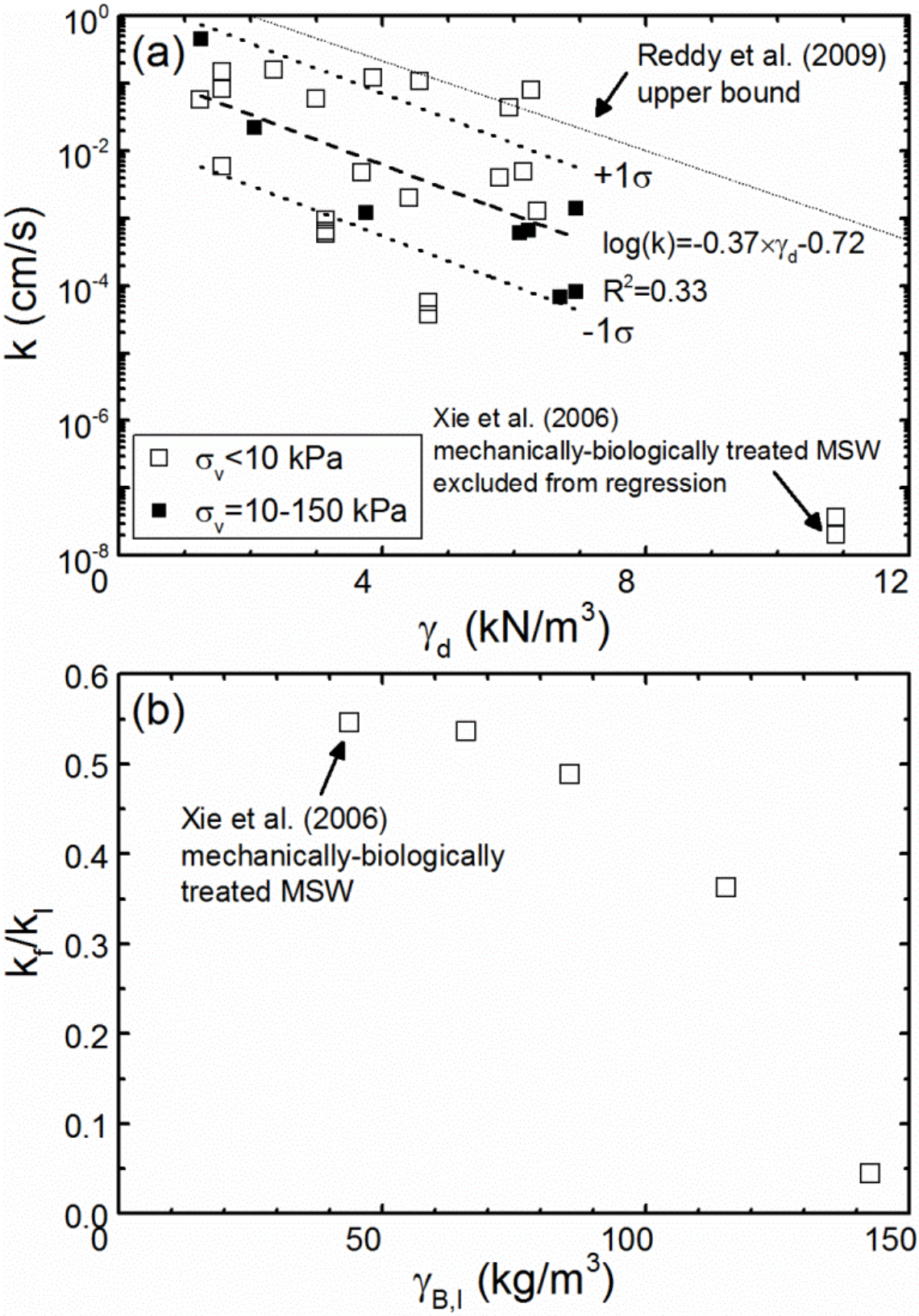

Figure 8-6 Relationship between (a) hydraulic conductivity (k) and dry unit weight (γ_d) of waste; (b) change in k of waste due to degradation (k_f/k_I) and density of biodegradable waste ($\gamma_{B,I}$).

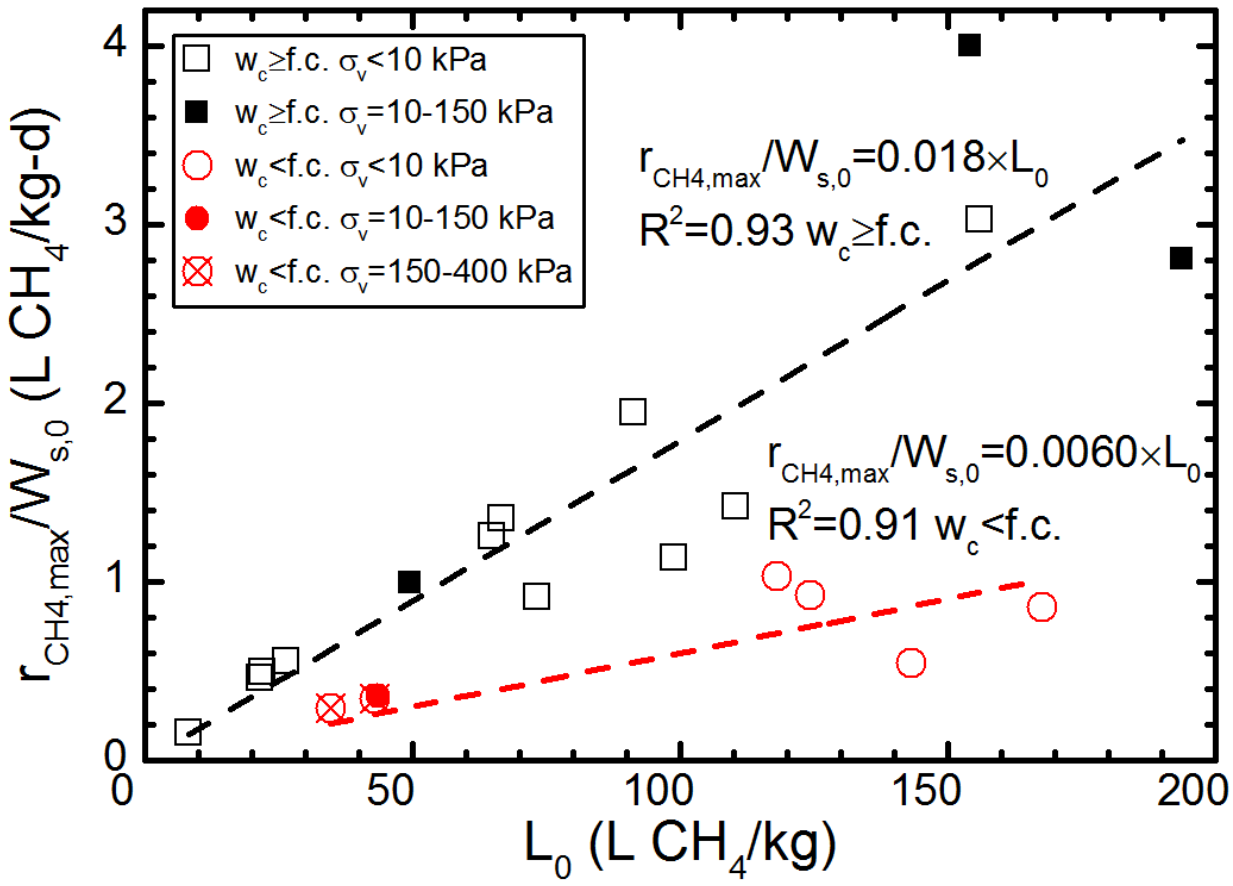

Figure 8-7 Correlation between normalized maximum CH_4 generation rate ($r_{CH4,max}/W_{s,0}$) and CH_4 generation potential (L_0) of waste.

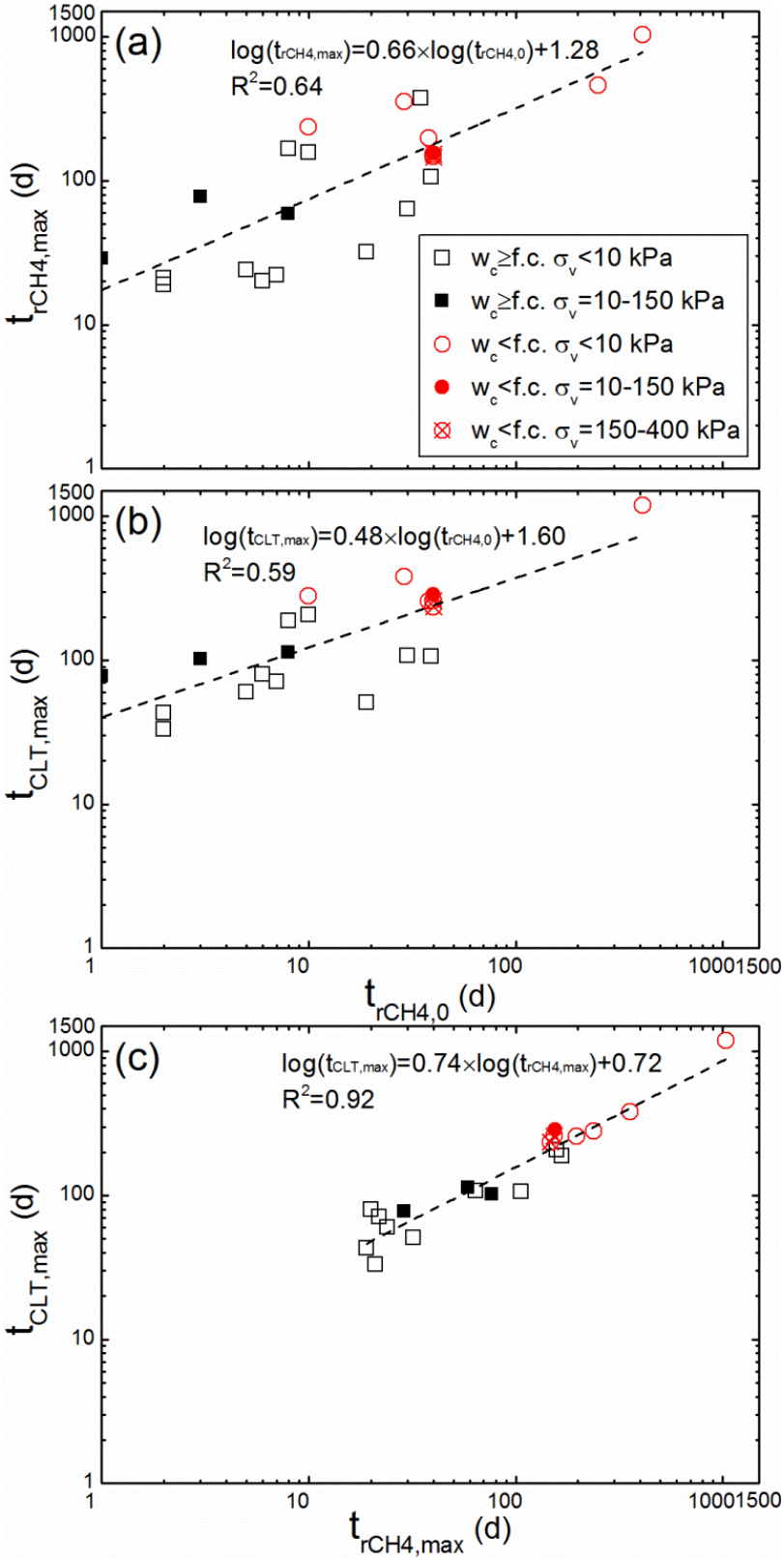

Figure 8-8 Correlations between characteristic time points: (a) the time until maximum CH_4 generation rate ($t_{rCH4,max}$) and until initiation of CH_4 generation ($t_{rCH4,0}$); (b) the time until maximum long-term compression ratio ($t_{CLT,max}$) and $t_{rCH4,0}$; and (c) $t_{CLT,max}$ and $t_{rCH4,max}$.

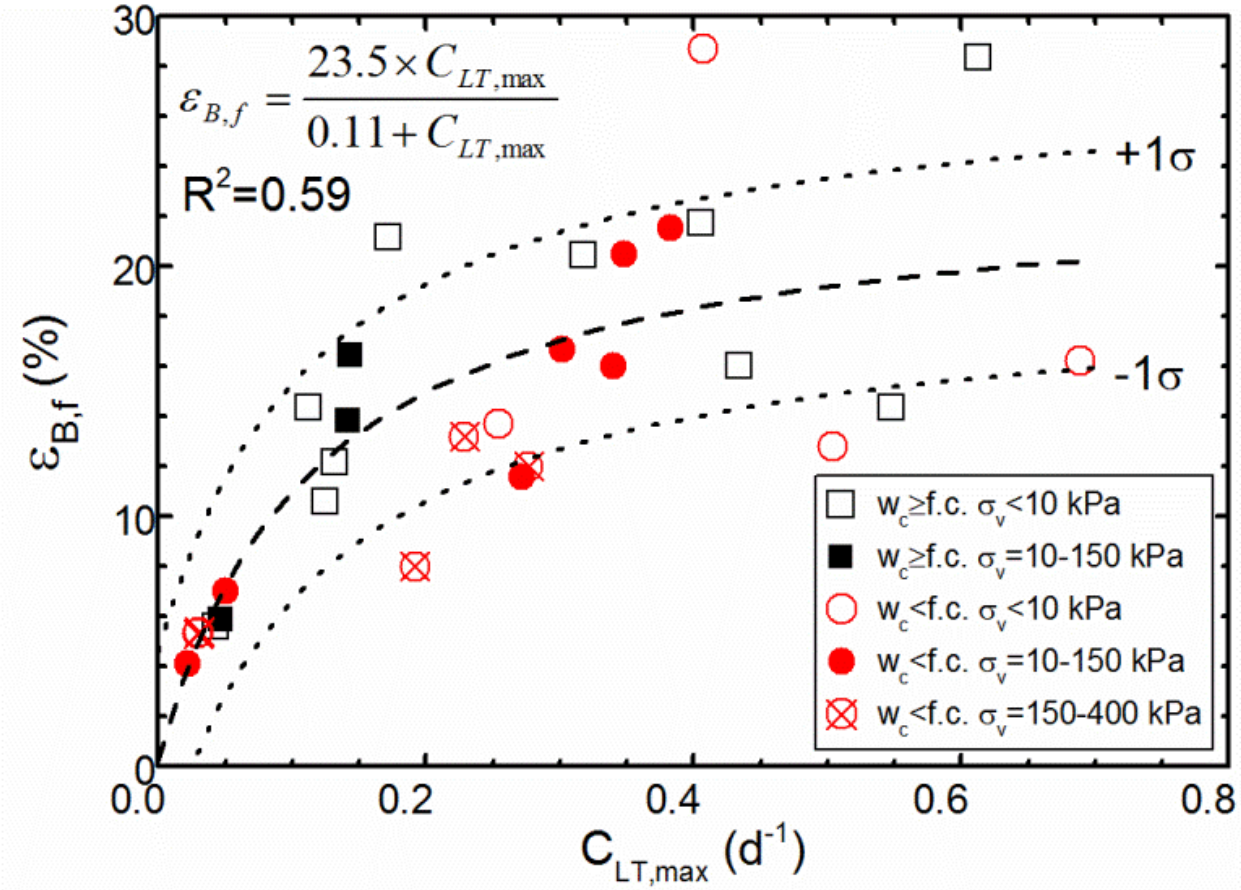

Figure 8-9 Correlation between biodegradation strain of waste ($\varepsilon_{B,f}$) and maximum long-term compression ratio ($C_{LT,max}$).

Chapter 9 Quantification of Parameters Influencing Methane Generation due to Biodegradation of Municipal Solid Waste in Landfills and Laboratory Experiments

9.1 Abstract

The energy conversion potential of municipal solid waste (MSW) disposed of in landfills remains largely untapped because of the slow and variable rate of biogas generation, delayed and inefficient biogas collection, leakage of biogas, and landfill practices and infrastructure that are not geared toward energy recovery. A database consisting of methane (CH_4) generation data, the major constituent of biogas, from 49 laboratory experiments and field monitoring data from 57 landfills was developed. Three CH_4 generation parameters, i.e., waste decay rate (k), CH_4 generation potential (L_0), and time until maximum CH_4 generation rate (t_{max}), were calculated for each dataset using U.S. EPA's Landfill Gas Emission Model (LandGEM). Factors influencing the derived parameters in laboratory experiments and landfills were investigated using multi-linear regression analysis. Total weight of waste (W) was correlated with biodegradation conditions through a ranked classification scheme. k increased with increasing percentage of readily biodegradable waste (B_{r0} (%)) and waste temperature, and reduced with increasing W, an indicator of less favorable biodegradation conditions. The values of k obtained in the laboratory were commonly significantly higher than those in landfills and those recommended by LandGEM. The mean value of L_0 was 98 and 88 L CH_4/kg waste for laboratory and field studies, respectively, but was significantly affected by waste composition

Fei, X., Zekkos, D., and Raskin, L. (2016). "Quantification of parameters influencing methane generation from biodegradation of municipal solid waste in landfills and laboratory experiments." *Waste Management*, (in press).

with ranges from 10 to 300 L CH_4/kg. t_{max} increased with increasing percentage of biodegradable waste (B_0) and W. The values of t_{max} in landfills were higher than those in laboratory experiments or those based on LandGEM's recommended parameters. Enhancing biodegradation conditions in landfill cells has a greater impact on improving k and t_{max} than increasing B_0. Optimizing the B_0 and B_{r0} values of landfilled waste increases L_0 and reduces t_{max}.

9.2 Introduction

The generation rate and disposal demand of municipal solid waste (MSW) continue to increase whereas suitable sites for landfills are limited worldwide. Out of the 251 million tons of MSW generated in 2012 in the United States (U. S.), 54% was disposed of in landfills, 34% was recycled and 12% was incinerated (EPA 2014a). Since the 1960s, more than 9 billion tons of MSW are estimated to have been generated and 6.7 billion tons have been disposed of in dumps or landfills. Although efforts are made to divert MSW from landfilling, the amount of MSW disposed of in landfills continues to increase (Figure 9-1a). Since each alternative waste management options, i.e., recycling, incineration, anaerobic co-digestion with other waste streams, and composting, have their own technological and economic limitations, landfilling is expected to remain a major management option for MSW in the near future.

Under the prevailing anaerobic conditions in most landfills, biogas is produced during biodegradation of MSW. Landfill gas consists of approximately 40-60% methane (CH_4), 40-60% carbon dioxide (CO_2), and trace amounts of other gases (Barlaz et al. 1989a; Pohland and Alyousfi 1994). Modern landfills in the U.S. are regulated by Subtitle D of the Resource Conservation and Recovery Act, and are operated as "dry tombs" where the moisture content of waste is intended to remain low due to minimization of moisture infiltration (EPA 2006b). Even

in bioreactor landfills or wet landfills that allow infiltration through permeable covers, moisture addition is often insufficient to allow for optimal biodegradation of the total weight of landfilled waste and moisture is often added intermittently and distributed unevenly (Benson et al. 2007; Bareither et al. 2010). As a result, MSW biodegradation and biogas generation are much slower than under optimal conditions (Pohland and Kim 2000; Reinhart et al. 2002). The rate of MSW biodegradation in landfills and the factors that influence the biodegradation process are significantly different from those in common anaerobic digestion systems, primarily because waste is a heterogeneous and porous material, and is under predominantly unsaturated conditions in landfills (Barlaz et al. 2010b).

The low biogas generation rate in landfills is a major barrier toward economical active collection of biogas and its conversion to usable energy, while the fluctuation in price of natural gas significantly affects commercial biogas recovery (EPA 2010c). In many landfills, biogas is collected passively through natural pressure gradient from degrading MSW and is flared for decades until MSW biodegradation and biogas generation stops (EPA 2014b). Since energy recovery in landfills is currently not an explicit design objective, gas collection systems are not geared toward maximizing energy generation, but focus on regulation conformity which emphasizes emission minimization. The collection efficiency of biogas in modern landfills, with a gas collection system in place, is estimated to range between 35% and 90%. The remaining portion of biogas is either oxidized by methane-oxidizing bacteria present in cover soil or is leaked and emitted to the atmosphere (Spokas et al. 2006). In addition, gas collection systems are most commonly installed with some delay after waste placement. Thus, any CH_4 generated before a gas collection system is installed is lost.

Currently, out of 1,754 landfills in the U.S., only 558 (32%) collect methane (EPA 2010c). Even in landfills where energy is recovered, design and management procedures are largely empirical leading to sub-optimal energy recovery and production. Although energy generation from landfill biogas has increased more than five times from 1989 to 2012 (Figure 9-1b), MSW remains a largely untapped energy source. In 2012, the annual CH_4 generation from landfills in the U.S. was estimated to be 18.7×10^9 Nm^3, of which only approximately 35% (6.5×10^9 Nm^3 of CH_4) was converted into energy through combustion, another 30% (5.7×10^9 Nm^3 of CH_4) was flared and released to the atmosphere as CO_2, and 35% remained uncaptured and was emitted to the atmosphere. The emitted CH_4 is estimated to be equivalent to 102.8×10^{12} g of CO_2 (CH_4 is considered to be at least 20 times more potent than CO_2 in terms of global warming potential (Solomon et al. 2007)) and responsible for approximately 21% of total anthropogenic CH_4 emissions in the U.S. (EPA 2014b).

Besides the loss of potential energy and significant greenhouse gas emission due to slow MSW biodegradation in landfills, undegraded waste occupies more landfill space compared to biodegraded waste. Therefore, slow MSW biodegradation reduces the total waste disposal capacity of a landfill. The slowly biodegrading MSW also poses a long-term environmental threat as failure of the engineered containment systems of landfills will occur eventually exposing undegraded waste. For these reasons, the design philosophy and practices of modern landfills are not sustainable.

MSW biodegradation and biogas generation processes have been studied extensively in the laboratory and are commonly monitored in landfills. However, the availability, reliability and completeness of field monitoring data of landfills is often limited by labor, equipment, duration requirements, and cost (Wang et al. 2013). Biodegradation experiments of MSW conducted in

the laboratory are better controlled and employ operating procedures to enhance microbial activity. Because of these reasons, laboratory experiments produce more reliable and predictable results compared to field monitoring studies.

This study presents a review of available MSW biodegradation data from laboratory experiments and field studies. The available data are synthesized with the intent to systematically identify similarities and differences between them. The CH_4 generation data of each dataset were fit using the U.S. EPA Landfill Gas Emission Model (LandGEM) (EPA 2005). Three characteristic CH_4 generation parameters were obtained: waste decay rate (k, 1/yr), CH_4 generation potential of waste (L_0, L CH_4/kg), and time between waste placement and the maximum CH_4 generation rate (t_{max}, d). Relationships between initial waste composition, biodegradation conditions, and the CH_4 generation parameters were investigated and quantified based on the results of more than 100 laboratory experiments and field studies. Recommendations to improve operating practices that enhance energy harvesting from disposed waste in landfills are presented.

9.3 Methods and calculations

9.3.1 **Literature review and classification of biodegradation conditions**

Results of laboratory MSW biodegradation experiments and field monitoring data from landfills in the literature were reviewed. Around 200 available studies were first screened for completeness and resolution of time-dependent biogas generation data. From these, 45 studies were considered sufficiently comprehensive and were selected for further analysis. A database consisting of 49 laboratory experiments (Eleazer et al. 1997; Borglin et al. 2004; He et al. 2005; Francois et al. 2006; Dearman and Bentham 2007; Faour et al. 2007; Zheng et al. 2007; Erses et

al. 2008; Ivanova et al. 2008a; Ivanova et al. 2008b; Qu et al. 2009b; Valencia et al. 2009a; Gourc et al. 2010; Abbassi-Guendouz et al. 2012; Cho et al. 2012; Huang et al. 2012; Mali et al. 2012; Bareither et al. 2013b; Staub et al. 2013; Fei et al. 2014a; Fei et al. 2015a) and field monitoring data from 57 landfills was compiled (El-Fadel et al. 1996b; Morris et al. 2003; Bentley et al. 2005; Budka et al. 2007; Faour et al. 2007; Willumsen 2007; Machado et al. 2009; Thompson et al. 2009; Barlaz et al. 2010a; Tolaymat et al. 2010; Amini et al. 2012; Lamborn 2012; Yazdani et al. 2012; Amini et al. 2013; Oonk et al. 2013; Sormunen et al. 2013; Wang et al. 2013; Zhao et al. 2013a). The source and composition of waste, and operating and environmental conditions for biodegradation of each study were recorded. The values of L_0 and k for 57 landfills were directly obtained from the same studies since detailed CH_4 generation data were not available. All other parameters presented were calculated in the current study using data reported in the respective studies to assure consistency in interpretation and calculation.

Significant differences exist between the conditions in the laboratory experiments and the landfills. These differences greatly influence biogas generation. It was also difficult to accurately quantify the influence of some conditions on biogas generation, specifically, moisture and seed (inoculum) addition to waste. Therefore, biodegradation classes were defined, as shown in Table 9-1, and each dataset in the database was assigned a class to distinguish their differences in operation conditions (e.g., moisture content, seeding, biogas collection efficiency, and completeness and reliability of monitoring data collected, etc.). As the class number increases from 0 to 6, operation conditions, biogas collection efficiency and monitoring improves, thus creating more favorable and controlled biodegradation conditions

Laboratory experiments conducted in nine countries were included in the analysis. Most of the studies used mixed MSW obtained directly from landfills whereas two studies (Eleazer et

al. 1997; Qu et al. 2009b) investigated biodegradation processes of individual biodegradable waste constituents, i.e., various types of paper, yard waste and food. The database includes field studies from eleven countries. Only field monitoring data available in the published literature were analyzed; no specific effort was made to obtain monitoring data from individual landfills that have not been published.

9.3.2 **Parameter calculation**

The percentage of biodegradable waste (B_0 (%)) is defined as the proportion by mass of food, yard, and paper waste of the entire waste mass (W) including all landfilled waste and daily cover soils (Eqn. 9-1):

$$B_0 = \frac{mass\ of\ biodegradable\ waste}{total\ mass\ of\ waste} \tag{9-1}$$

The proportion by mass of food and yard waste by weight of all biodegradable waste is defined as the percentage of readily biodegradable waste (B_{r0} (%)) (Eqn. 9-2):

$$B_{r0} = \frac{mass\ of\ food\ and\ yard\ waste}{mass\ of\ biodegradable\ waste} \tag{9-2}$$

Note that branches are usually characterized as yard waste but are not readily biodegradable (De la Cruz and Barlaz 2010). However, yard waste is rarely separated into grasses, leaves and branches in the studies, and the percentage of branches by weight is always low, thus the reported weight and percentage of yard waste in the literature is used in this study.

The values of B_0 (%) and B_{r0} (%) were calculated for each laboratory experiment since their waste composition was known. The values of B_0 (%) for 13 landfills were obtained from

the same studies, and the values for the 44 remaining landfills in the database were assumed based on the landfill locations and the corresponding waste composition from regional survey data (Staley and Barlaz 2009; Thompson et al. 2009). The volatile solid content (VS) of waste indicating the amount of organic waste, including both biodegradable waste and non-biodegradable waste (plastic, textile and rubber), was also available for 43 laboratory experiments. The values of B_{r0} (%), VS and waste temperature (T) were unavailable for landfills.

9.3.3 **CH_4 generation analyses using LandGEM**

Biogas generation data were fitted using the first-order decay model described in LandGEM to obtain values of k, L_0 and t_{max} (EPA 2005). Measured concentrations of CH_4 and CO_2 reported in each study were used in the calculations. If the concentrations were unknown, both CH_4 and CO_2 concentrations were assumed to be equal to 50% of generated biogas, an assumption consistent with industry practices and the recommended default values of U.S. EPA's Landfill Methane Outreach Program (EPA 2010c). The cumulative volumes of generated CH_4 and CO_2 were converted to equivalent masses of biodegradable carbon (C, assuming standard temperature of 273 K and pressure conditions of 1 atmospheric pressure), $m_{C,CH4}$ and $m_{C,CO2}$. The initial mass of C ($m_{C,0}$) was the sum of the maximum $m_{C,CH4}$ and $m_{C,CO2}$. A single waste decay rate, k (1/yr), was derived by applying linear regression as shown in Eqn. 9-3 (EPA 2005; De la Cruz and Barlaz 2010):

$$\ln\left(m_{C,0} - m_{C,CH4} - m_{C,CO2}\right) = -k \times (t - t_{lag}) + \ln(m_{C,0}) \quad (9\text{-}3)$$

where t is the time of biogas generation data, and t_{lag} is the delay time before the initiation of biogas generation.

Although all datasets analyzed appeared to have reached their maximum biogas generation volume, the time required to achieve the maximum biogas generation volume is very long and it is likely that some studies were not conducted long enough to measure this value. To account for this possible underestimation of biogas generation volume and to obtain accurate L_0 values, $m_{C,0}$ was varied between 100% and 160% of its initially calculated value for each study to obtain the highest squared correlation coefficient (R^2) of the linear regression of Eqn. 9-3. Among the values of $m_{C,0}$ in the 49 laboratory experiments, 35 did not or only minimally increased (≤110%) compared to the initially calculated $m_{C,0}$, eight $m_{C,0}$ values increased between 110% and 130%, whereas six $m_{C,0}$ values increased from 130% to 160% (Table 9-2). The maximum $m_{C,CH4}$ and $m_{C,CO2}$ were recalculated using the value of best-fit $m_{C,0}$ corresponding to the highest R^2. L_0 (L CH_4/kg waste) was calculated using stoichiometry from the recalculated maximum $m_{C,CH4}$ using Eqn. 9-4:

$$L_0 = \frac{\frac{m_{C,CH4}}{12} \times 22.4}{W} \tag{9-4}$$

The time to maximum CH_4 generation rate (t_{max}, d) was obtained from the time-series curve of CH_4 generation rate. An example of biogas generation data and its analysis is shown in Figure 9-2 using test results reported by Fei et al. (2015a).

The values of k and L_0 of all laboratory experiments and three landfills and the values of t_{max} for all laboratory experiments and 24 landfills were calculated in this study. Since complete CH_4 generation data of 54 landfills were unavailable, the k and L_0 values reported in the same studies were used. It should be noted that the reported values of L_0 for landfills only account for collected CH_4 which leads to underestimation of the true L_0 of waste. Nevertheless, the as-

observed L_0 is considered the best-estimation value which reflects the state-of-practice CH_4 collection practice, and is informative in assessing the parameters influencing CH_4 generation in landfills.

9.3.4 **Multi-linear regression analysis of factors influencing CH_4 generation parameters**

Correlations between CH_4 generation model parameters (dependent variables k, L_0 and t_{max}) and initial waste composition (expressed by variables B_0 (%), B_{r0} (%) and VS) and biodegradation conditions (expressed by variables W, T, and biodegradation class) were analyzed using multip-linear regression (MLR). k, t_{max} and W were logarithmically transformed to log(k), log(t_{max}), and log (W). Each variable in the database was standardized to a mean value of 0 and a standard deviation of 1 prior to MLR (indicated by a subscript "std"). The adjusted coefficient of determination (R^2_{adj}) was calculated for each MLR equation. Variables for waste composition and biodegradation conditions were evaluated for collinearity and, when found to be highly correlated, one of the two variables was expressed by the other (Legendre and Legendre 2012).

9.4 Results and discussion

9.4.1 **Differences in waste composition and biodegradation conditions between laboratory experiments and field studies**

A summary of the literature information and calculated parameters for each study is provided in Table 9-2 and Table 9-3. The values of B_0 (%) and B_{r0} (%) in the database range between 6-100% and 0-100%, respectively, indicating that the datasets under investigation are representative of a wide range of waste compositions.

Broad differences in waste composition and biodegradation conditions between laboratory experiments and field monitoring data of landfills are summarized in Table 9-4.

Specifically, differences in moisture and seeding conditions and biogas collection efficiency are represented by the biodegradation classes described in Table 9-1 as discussed subsequently. Waste specimens degraded in the laboratory have relatively small amounts that range from 10^{-1} to 10^{3} kg. The waste composition is typically well characterized. Waste specimens are in some cases seeded with microorganisms and nutrients to accelerate the biodegradation process. Large-size waste particles are often shredded, especially in smaller-size experimental setups, thus reducing waste heterogeneity and accelerating biodegradation (Pommier et al. 2010; Fei and Zekkos 2013). Waste tested in these laboratory setups is easily saturated and drained to field capacity. In larger laboratory-scale simulators, moisture content may be lower and moisture distribution within the specimen may become uneven (Capelo and de Castro 2007; Staub et al. 2010). In all cases, the collection efficiency of CH_4 in sealed laboratory simulators is 100%.

Because of the difficulties in characterizing massive amounts of incoming waste typically exceeding 10^{7} kg (10,000 ton), the waste composition in landfills used in this study is not always site-specific, but often estimated based on regional waste generation surveys (Staley and Barlaz 2009; van Haaren et al. 2010), and in some cases may be inaccurate (Wang et al. 2013). Due to regulations, the amount of moisture in waste mass is limited and recirculation is not commonly employed. The moisture content of waste in conventional (Subtitle D) landfills is typically lower than its field capacity (Reinhart et al. 2002; Reddy et al. 2009b), and varies greatly depending on the climate and precipitation patterns at the landfill's location. Moisture addition and leachate recirculation are implemented in most pilot-scale cells and full-scale wet landfill cells, and are intended to be operated differently than conventional dry landfill cells. However, the distribution of moisture is difficult to control and monitor in the field, and the moisture content of waste may be in places below its field capacity, following recirculation.

Waste in landfills is highly heterogeneous due to varying particle sizes, stratification of waste, variable disposal times and placement procedures. Waste heterogeneity retards migration and distribution of added moisture and the microorganisms, substrates and nutrients carried by it (Zacharof and Butler 2004; Staley et al. 2011a; Bareither et al. 2013a; Fei et al. 2015a). The temperature of waste from near the surface to higher depths in landfills is influenced by ambient temperature and fluctuates seasonally (Bareither et al. 2010; Hanson et al. 2010). In general, the larger the size of a landfill, the more difficult and costly it is to maintain uniform and favorable biodegradation conditions in the waste mass.

As summarized in Table 9-1, pilot and single landfill cells are differentiated from multiple landfill cells by operating duration and configuration of the CH_4 collection system. The operating duration of landfill cells increases from pilot to single and multiple cells, whereas the collection efficiency of CH_4 typically decreases. The collection efficiency of CH_4 in landfills varies during their operation and after closure, but is estimated to be lower than 90% even after closure (Spokas et al. 2006). No gas is collected during waste placement, an operation that may last months to years. For example, in a landfill containing more than 2.5 million tons of waste, gas collection and control system is regulated to be installed within five years of waste placement or two years of final cover installation (EPA 1996). The influence of the significant differences between the laboratory experiments and monitoring data of landfills on CH_4 generation model parameters is explored in the following sections.

9.4.2 **Collinearity between initial waste composition and biodegradation conditions**

As shown in Figure 9-3 and summarized in Table 9-1 and Table 9-4, the biodegradation class was found to be strongly correlated to the total weight of waste in laboratory experiments and field studies for a range of weight between 10^{-2} and 10^{10} kg (R^2=0.91). The strong correlation

suggests that the favorability of biodegradation conditions reduces as the amount of waste increases, and is associated with limitations in control of the biodegradation process and waste heterogeneity. This also indicates that, under current practices, the control of biodegradation conditions and measurements for landfills containing large amount of waste are significantly limited by practical and economic considerations. In contrast, specimens containing small amount of waste (e.g., in laboratory experiments) are mostly subject to enhanced biodegradation conditions. Therefore, the total weight of the waste can be used in MLR analyses as a proxy of biodegradation class and, consequently, of biodegradation conditions. In addition, as shown in Figure 9-4, the amount of biodegradable waste (B_0 (%)) is correlated to the VS of MSW in laboratory experiments (R^2=0.63) (Kelly et al. 2006). However, because data is more readily available about B_0 (%) as opposed to VS, B_0 (%) was used in subsequent regression analyses.

9.4.3 **Statistical analyses of CH_4 generation parameters for laboratory experiments and field studies**

The results of statistical analyses of CH_4 generation parameters, waste composition and biodegradation conditions variables are shown in Table 9-5. The mean values of *k*, L_0 and t_{max} are 5.66 1/yr, 98 L/kg and 138 d, respectively, for the laboratory experiments. The corresponding mean values for landfills are 0.18 1/yr, 88 L/kg and 1,751 d. Overall, the mean L_0 value is similar for the laboratory and the field data. The mean *k* value for landfills including pilot-scale and full-scale cells is higher than those reported previously for full-scale cells (El-Fadel et al. 1996b; Morris et al. 2003; Bentley et al. 2005; Willumsen 2007; Thompson et al. 2009; Barlaz et al. 2010a; Tolaymat et al. 2010; Amini et al. 2012; Amini et al. 2013). Furthermore, the mean *k* value for the laboratory studies is significantly higher compared to the measured *k* based on field data. Also, mean t_{max} is significantly shorter in the laboratory studies compared to the field data.

These trends are attributed to the systematic recirculation of liquids and well-controlled operations in the laboratory experiments which results in more favorable biodegradation conditions. The range of waste compositions in the laboratory experiments, as expressed by B_0 (%) and B_{r0} (%), is much greater than those for landfills, resulting in higher variability of each variable for the laboratory studies compared to the field data.

9.4.4 **Multi-linear regression analysis on waste decay rate**

The waste decay rate is influenced primarily by B_0 (%), B_{r0} (%), W and T based on regression analyses of the laboratory experiments only (Figure 9-5a). As indicated by the statistically significant MLR coefficients (Table 9-6), *k* increased with decreasing B_0 (%) (Figure 9-5b) and increasing B_{r0} (%) (Figure 9-5c). As the B_0 (%) of waste specimens increased, generally both amounts of readily and slowly biodegradable waste increased. The readily biodegradable waste was on average 38% of B_0 (%) for the analyzed laboratory experiments. Since high amount of slowly biodegradable waste tends to lower the value of *k* (Lobo et al. 2002), *k* appeared to decrease with increasing B_0 (%). In contrast, higher B_{r0} (%) resulted in higher *k* (Vavilin et al. 2008; Fei et al. 2014b). *k* also decreased with increasing W highlighting the influence of the total weight of waste and biodegradation conditions on the rate of MSW biodegradation (Figure 9-5d) (Zacharof and Butler 2004; Bareither et al. 2013a). *k* was also increasing with increasing T, an observation that agrees with the results of previous laboratory studies (Figure 9-5e) (Meima et al. 2008; Vavilin et al. 2008).

The four variables used in MLR of the data from laboratory studies resulted in a R^2_{adj} value of 0.52 (Figure 9-5a), indicating that the regression did not capture all aspects of the biodegradation process. Additional variables not considered herein, and partially responsible for the observed variability, likely include the cellulose and hemicellulose content of waste (Eleazer

et al. 1997; Kelly et al. 2006), the use of B_0 (%) instead of the preferable parameter of VS, the frequency and quantity of moisture and seed addition (Mehta et al. 2002; Kim and Pohland 2003; Pommier et al. 2007), and the influence of anisotropy and preferential flow pathways in waste that affects recirculation of leachate (Rosqvist et al. 2005; White et al. 2011; Zekkos 2013).

Regression was also performed by combining data from laboratory and field studies and the results are shown in Figure 9-6a. Only B_0 (%) and W were used in this analysis because the other two variables (B_{r0} and T) were not known for landfills. The resulting regression has an R^2_{adj} of 0.88 and is expressed in Eqn. 9-5:

$$\log(k_{std}) = -0.16 \times B_{0,std} - 0.99 \times \log(W_{std}) \quad (9\text{-}5)$$

The discrepancies between measured and modeled k_{std} values for multiple wet landfill cells are lower than those for single landfill cell and multiple dry landfill cells, suggesting that the values of *k* in multiple wet landfill cells can be estimated using B_0 and W formulated in Eqn. 9-5. Unaccounted factors that may influence the values of *k* for single landfill cells include the frequency of addition of leachate or septage containing high amounts of microorganisms and nutrients for microbial activity (El-Fadel et al. 1996b; Budka et al. 2007; Faour et al. 2007; Barlaz et al. 2010a; Yazdani et al. 2012; Oonk et al. 2013; Zhao et al. 2013a). Because of the low amount and uneven distribution of moisture in relatively dry landfill cells, the values of B_0 and W do not necessarily represent the amount of waste undergoing active biodegradation.

The influence of W on *k* was dominant (MLR coefficient=-0.99, Table 9-6, Figure 9-6b). The influence of B_0 (%) on *k* was also statistically significant, but less critical as demonstrated by its lower MLR coefficient (-0.16) (Figure 9-6c). The rate of MSW biodegradation can be

limited at each step of the anaerobic biodegradation process, such as hydrolysis, acidogenesis and methanogenesis (Barlaz et al. 2010b). In laboratory experiments where a wide range of compositions have been tested, the amount and availability of biodegradable waste was usually the dominant limiting factor on *k*, while other factors (e.g., amount of liquid recirculated, moisture accessibility and temperature) are less critical. In contrast, in landfills, numerous inefficiencies associated with the large waste mass and unfavorable biodegradation conditions exist, resulting in lower *k*. Measurement errors, incomplete data and other uncertainties, particularly from the field studies, are also contributing to the variability (Wang et al. 2013; Wang et al. 2015).

9.4.5 **Multi-linear regression analysis on CH_4 generation potential of MSW**

The values of L_0 from the laboratory experiments and field studies were on average 98±70 and 88±23 L/kg, respectively (Table 9-5), and increased generally with increasing B_0 (%) (Figure 9-7a) (Eleazer et al. 1997; Kelly et al. 2006; Fei et al. 2014b). L_0 values varied between 30 and 300 L/kg when B_0 (%) equaled 100%. In this case, lower values of L_0 were observed in experiments biodegrading yard waste which has low cellulose and hemi-cellulose content, whereas higher values of L_0 were obtained from biodegradation of food and office paper (Eleazer et al. 1997). Low collection efficiency (Spokas et al. 2006; Wang et al. 2013) of CH_4 in landfills has been reported to negatively affect the volume of collected CH_4 in the field, thus likely resulting in lower reported L_0 values in the field compared to laboratory experiments under similar conditions. L_0 correlates better with VS as shown in Figure 9-7b, because VS is a more accurate indicator of the amount of biodegradable waste than B_0.

A low R^2_{adj} value of 0.20 was obtained from MLR on L_0 from the laboratory experiments when the four variables are considered (Figure 9-8). This is attributed to waste composition and

biodegradation conditions variables not considered in the MLR analysis. A previous study by the writers found a strong correlation between VS and L_0 in laboratory experiments that were operated under identical conditions for enhanced biodegradation (W=10^1 to 10^3 kg) (Fei et al. 2014b). Therefore VS is likely a better parameter than B_0 (%) in estimating L_0 (Kelly et al. 2006). The content of cellulose and hemi-cellulose of waste is an alternative variable that is also well correlated with L_0 (Eleazer et al. 1997; Kelly et al. 2006). Correlations between total CH_4 generation and VS and cellulose and hemi-cellulose content of waste are likely more accurate and reliable, and lead to higher CH_4 yield per mass of VS and cellulose and hemi-cellulose. Unfortunately, these values are not typically available in laboratory experiments and landfill studies, and are more time consuming and expensive to measure than the amount of biodegradable waste.

9.4.6 **Comparisons of *k* and L_0 between landfills, laboratory experiments and LandGEM recommended model parameters**

A diagram of *k* and L_0 from laboratory experiments and field monitoring data of landfills is shown in Figure 9-9. The recommended ranges of *k* and L_0 in LandGEM are 0.04-0.20 1/yr and 100-170 L/kg, respectively, although the upper-bound values of *k* and L_0 are often considered unrealistic for conventional landfills (EPA 2005). These have been obtained from the results of a series of field monitoring data of "dry tomb" landfills, particularly in the early 1990s, and laboratory experiments conducted under sub-optimal biodegradation conditions (EPA 2005). For organic-rich specimens, L_0 values from laboratory experiments were significantly higher than L_0 values from landfills and LandGEM recommended values, which was attributed to higher amounts of food and yard waste included in the laboratory specimens. These constituents typically degrade fast in the field, thus their CH_4 yield is collected by gas collection systems that

are likely constructed after their degradation. The B_0 (%) of incoming waste is critical and is influenced by various socio-economical, regulatory, regional and temporal factors. Daily soil cover for disposed MSW is a regulated practice in modern landfills but has no gas generation potential. A reduction in the amount of daily soil cover will increase B_0 (%) in the entire waste mass and positively affect the biogas yield per total mass of material disposed of in landfills.

The decay rate *k* in the laboratory experiments was orders of magnitudes higher than in landfills or *k* recommended by LandGEM for waste of similar initial waste composition and L_0. In addition, it is shown that for MSW having similar L_0 values, the multiple wet landfill cells and single cells operated under enhanced conditions for MSW biodegradation resulted in *k* values that were more than 10 times higher than those for landfills operated conventionally as "dry tombs". These differences highlight the sub-optimal CH_4 generation process in modern landfills and point to strategies that can be implemented to achieve rapid generation and efficient collection of CH_4 in landfills. These include reduction of waste heterogeneity, improvements on the addition, distribution, and migration of moisture in waste, and increased gas collection efficiencies. Some of the potential improvements mentioned previously have been implemented in a few studies and demonstrated very promising increases in *k* values, which approached those achieved in laboratory experiments (Budka et al. 2007; Yazdani et al. 2012; Oonk et al. 2013). As suggested by Eqn. 9-5 and Figure 9-6a, changing B_0 (%) in landfilled waste appears to have lower impact on improving *k* than reducing W, for landfill cells, where W represents the biodegradation conditions. Therefore it is suggested that priority be given to upgrading infrastructure and improving planning and management of leachate recirculation, waste covering, and energy recovery for each cell in landfills (Figure 9-3).

9.4.7 **Multi-linear regression analysis on time until maximum CH_4 generation rate**

Measured t_{max} in laboratory studies was regressed using the four variables (R^2_{adj}=0.49, Figure 9-10a). The value of t_{max} increased with increasing B_0 (%), suggesting that increasing amount of biodegradable waste could inhibit prompt initiation of methanogenesis (Figure 9-10b). For example, it has been shown that initial accumulation of volatile fatty acids in degrading waste due to rapid hydrolysis of biodegradable waste may inhibit the growth of methanogens and thus result in increases in t_{max} (Zehnder and Stumm 1988; Vavilin et al. 2006). The low values of t_{max} for waste having 90-100% B_0 were heavily influenced by the low W of waste and initial inoculation in the experiments (Eleazer et al. 1997; He et al. 2005; Qu et al. 2009b; Abbassi-Guendouz et al. 2012). The influence of B_{r0} (%) on t_{max} was not statistically significant (Table 9-6), indicating that B_0 (%) is a more appropriate descriptor of waste composition in estimating t_{max} (Figure 9-10c). High W is correlated with high t_{max}, highlighting that unfavorable biodegradation conditions prolong the adaptation period of microorganisms before the initiation of methanogenesis (Figure 9-10d). High T, up to 40 ^{0}C, accelerated microbial growth and activity and resulted in reduced t_{max} (Figure 9-10e) (Meima et al. 2008; Vavilin et al. 2008).

Eqn. 9-6 describes the relationship of t_{max} in days as a function of B_0 (%) and W (kg) in both laboratory and field studies with a R^2_{adj} of 0.75 (Figure 9-11a):

$$\log(t_{max,std}) = 0.08 \times B_{0,std} + 0.99 \times \log(W_{std}) + 0.43 \quad (9\text{-}6)$$

The influence of W on t_{max} is again dominant (MLR coefficient=0.99, Table 9-6, Figure 9-11b). t_{max} increased systematically from laboratory-size experiments to single landfill cells and further to multiple landfill cells, confirming that smaller W, and thus more favorable biodegradation

conditions, facilitated rapid initiation of methanogenesis. The influence of B_0 (%) on t_{max} was comparatively low (MLR coefficient=0.08, Table 9-6, Figure 9-11c). The low value of t_{max} for the single landfill cell containing 100% biodegradable waste is due to waste inoculated with manure (Yazdani et al. 2012).

The value of t_{max} should also be a function of the amount and type of seed, and the moisture content of waste (Staley et al. 2011a), factors not directly included in the regression, but indirectly considered through the correlation of W with the biodegradation classes.

9.4.8 **Comparison of t_{max} between landfills, laboratory experiments and LandGEM recommended model parameters**

The measured values of k and t_{max} in laboratory and field studies are plotted in Figure 9-12. The LandGEM recommended values are also shown. The maximum CH_4 generation rate for waste placed within each time step in LandGEM is assumed to occur instantaneously. Thus, t_{max} is dependent on the input time step interval value which typically varies between 0.1 and 1 year in LandGEM. This study demonstrates that for landfills with k values similar to those recommended by LandGEM, t_{max} can be much longer than assumed in LandGEM. Therefore LandGEM may overestimate the CH_4 generation rate at early stages of waste disposal.

A relationship between t_{max} and k from laboratory and field studies is shown in Eqn. 9-7 (R^2=0.74):

$$t_{max} = 256.2 \times k^{-0.78} \quad (9\text{-}7)$$

This equation provides improved estimates of t_{max} as a function of k which are both critical parameters when estimating CH_4 generation (and leakage) in landfills. As indicated by Eqn. 9-6,

t_{max} is also affected by changes in waste composition and biodegradation conditions in landfills. The closure plan of landfills and the design and operation of gas collection system can be optimized based on site-specific waste composition and biodegradation conditions. For example, increasing the number of individually operated and controlled landfill cells and consequently reducing W in each cell would lower t_{max} and accelerate k in the cell. Similar to the discussion in Section 3.6, a few studies have demonstrated effective reduction in t_{max} values, which approached those achieved in laboratory experiments (Budka et al. 2007; Yazdani et al. 2012; Oonk et al. 2013). In addition, changing B_0 (%) in landfilled waste appears to have a lower impact than reducing W on reducing t_{max} for landfill cells.

9.5 Conclusions

A database consisting of CH_4 generation data from 49 laboratory experiments and field monitoring data from 57 landfills was developed. Three CH_4 generation parameters, i.e., waste decay rate (k, 1/yr), CH_4 generation potential of waste (L_0, L CH_4/kg), and time between waste placement and the maximum CH_4 generation rate (t_{max}, d), were calculated for each dataset according to the model in U.S. EPA's LandGEM. Factors influencing the derived parameters in laboratory experiments and landfills were investigated using MLR analysis. W was correlated with biodegradation conditions through biodegradation class. k increased with increasing B_{r0} (%) and waste temperature T, and reduced with increasing W. The values of k obtained in the laboratory were significantly higher than in landfills and recommended by LandGEM. The mean value of L_0 was 98 and 88 L CH_4/kg waste for laboratory and field studies, respectively, but is significantly affected by waste composition. t_{max} increased with increasing B_0 (%) and W. The

values of t_{max} in landfills were much higher than those in laboratory experiments or those based on LandGEM's recommended parameters.

9.6 Tables

Table 9-1 Definition of biodegradation classes.

Class number	CH_4 collection	Control of moisture content	Monitoring
0	Collection efficiency varied temporally and spatially, and was typically below 100%.	Moisture addition was minimal and the moisture content of waste was well below field capacity.	Annual to monthly monitoring and measurements for a few variables.
1	Collection efficiency varied temporally and spatially, and was typically below 100%.	Moisture addition was not well controlled and the moisture content of waste was below field capacity.	Annual to monthly monitoring and measurements for a few variables.
2	Collection efficiency varied temporally and was typically below 100%.	Moisture addition was not well controlled and the moisture content of waste was below field capacity.	Weekly to daily monitoring and measurements for multiple variables.
3	Collection efficiency was 100%.	Moisture addition was controlled, but insufficient to maintain the field capacity of waste.	Daily monitoring and measurements for multiple variables.
4	Collection efficiency was 100%.	Moisture addition was controlled, but insufficient to maintain the field capacity of waste; Biomass and/or nutrients for microorganisms were added to waste.	Daily monitoring and measurements for multiple variables.
5	Collection efficiency was 100%.	Sufficient moisture was added to maintain the field capacity of waste.	Daily monitoring and measurements for multiple variables.
6	Collection efficiency was 100%.	Sufficient moisture was added to maintain the field capacity of waste; Biomass and/or nutrients for microorganisms were added to waste.	Daily monitoring and measurements for multiple variables.

Table 9-2 Summary of data obtained from laboratory experiments included in this study.

Ref.	Waste type and source	biodeg. class	B_0 (%)	B_{r0} (%)	log(W) (kg)	T (°C)	k (yr^{-1})	log(k)	L_0 (L/kg)	log(t_{max})
(Abbassi-Guendouz et al. 2012)	Mixed France	6	100	0	-1.82	35	4.20	0.62	187	1.93
		6	100	0	-1.70	35	4.71	0.67	174	1.79
		6	100	0	-1.60	35	3.91	0.59	175	1.78
(Eleazer et al. 1997)	Office paper	6	100	0	-0.22	40	3.08	0.49	217	1.57
	Grass	6	100	100	-0.22	40	31.13	1.49	144	1.11
	Branches	6	100	0	-0.22	40	1.56	0.19	63	1.18
	Newspaper	6	100	0	-0.22	40	3.45	0.54	74	1.58
	Corrugated container	6	100	0	-0.22	40	2.05	0.31	152	1.52
	Food	6	100	100	-0.22	40	15.02	1.18	301	1.69
	Leaves	6	100	100	-0.22	40	17.82	1.25	31	1.15
	Coated paper	6	100	0	-0.22	40	12.68	1.10	84	1.20
	N. Carolina									
(Ivanova et al. 2008a)	Mixed U.K.	6	48	43	-1.00	30	7.45	0.87	188	1.59
(Qu et al. 2009b)	Cardboard	6	100	0	-2.00	35	9.60	0.98	164	1.51
	Office paper	6	100	0	-2.00	35	4.82	0.68	258 [a]	1.92
	France									
(Zheng et al. 2007)	Mixed U.K.	6	35	7	-1.00	30	4.42	0.65	59 [a]	1.85
(Fei et al. 2015a)	Mixed Texas	5	15	0	1.48	35	5.55	0.74	20	1.51
		5	15	0	1.47	35	5.44	0.74	20	1.52
(Fei et al. 2014a; Fei et al. 2015a)	Mixed Arizona	5	28	0	1.34	40	8.36	0.92	59	1.67
	Mixed California	5	6	0	1.46	40	5.15	0.71	8	1.41
	Mixed California	5	21	0	1.30	40	6.75	0.83	21	1.61
	Mixed Michigan	5	43	0	1.13	40	5.95	0.77	49	1.36
(Bareither et al. 2013b)	Mixed Wisconsin	4	20	7	2.17	35	4.78	0.68	6 [a]	1.81
		4	20	7	2.17	35	4.96	0.70	17 [a]	1.88
		4	20	7	2.17	35	8.32	0.92	20	1.72
(Cho et al. 2012)	Mixed Korea	4	55	47	1.32	30	1.90	0.28	73	2.32
(Dearman and Bentham 2007)	Mixed Australia	4	65	100	1.54	37	9.27	0.97	62 [a]	1.61
(Francois et al. 2006)	Mixed France	4	59	54	1.30	38	7.77	0.89	15	2.26
		4	59	54	1.30	38	7.19	0.86	32	2.14

(Gourc et al. 2010)	Mixed France	4	34	21	2.61	35	1.68	0.23	143 [a]	2.29
		4	34	21	2.62	35	5.69	0.76	99	2.22
		4	34	20	2.61	35	5.00	0.70	124	2.38
		4	34	20	2.61	35	5.26	0.72	110	2.20
(He et al. 2005)	Mixed China	4	92	92	-0.71	35	4.64	0.67	42 [b]	1.93
		4	92	92	-0.71	35	2.85	0.45	60 [b]	1.96
		4	92	92	-0.71	35	3.32	0.52	70 [b]	1.93
		4	92	92	-0.71	35	6.50	0.81	98 [a]	1.96
(Ivanova et al. 2008b)	Mixed U.K.	4	51	47	1.81	30	2.56	0.41	194	1.92
		4	51	47	1.86	30	2.96	0.47	154	1.77
(Mali et al. 2012)	Mixed India	4	55	91	1.56	30	8.10	0.91	91	1.62
		4	75	91	1.60	30	4.78	0.68	156	2.03
(Staub et al. 2013)	Mixed France	4	53	75	2.86	30	2.92	0.47	11	2.56
(Borglin et al. 2004)	Mixed California	3	40	53	1.30	20	2.99	0.48	58	2.18
(Erses et al. 2008)	Mixed Turkey	3	60	76	1.29	32	3.29	0.52	118	2.66
(Valencia et al. 2009a)	Mixed Netherlands	3	51	71	2.52	30	1.46	0.16	98 [a]	2.38
		3	51	71	2.54	30	1.10	0.04	125 [b]	2.31
(Faour et al. 2007)	Mixed Georgia	3	58	22	2.3	25	1.7	0.23	85	2.95
(Gourc et al. 2010)	Mixed France	3	53	55	3.90	30	1.72	0.23	168	3.01
(Huang et al. 2012)	Mixed China	3	85	46	3.54	25	0.80	-0.10	55 [b]	2.31
		3	85	46	3.54	25	0.80	-0.10	61 [b]	2.31

Note: biodeg. class: biodegradation class defined per Table 9-1; B_0: percentage of biodegradable waste; B_{r0}: percentage of readily biodegradable waste of B_0; W: total weight of waste; T: temperature of waste; *k*: waste decay rate; L_0: CH_4 generation potential of waste; t_{max}: time until maximum CH_4 generation rate.

[a] $m_{c,0}$ and L_0 values were increased between 110% and 130% from the initially calculated values.

[b] $m_{c,0}$ and L_0 values were increased between 130% and 160% from the initially calculated values.

Table 9-3 Summary of data obtained from landfills included in this study.

Ref.	Landfill location [a]	biodeg. class	B_0 (%)	log(W) (kg)	k (yr^{-1})	log(k)	L_0 [c] (L/kg)	log(t_{max}) [c]
(Barlaz et al. 2010a)	California	2	51 [a]	8.25	0.09	-1.05	n.a.	2.98
		2	51 [a]	7.84	0.15	-0.82		2.90
(Budka et al. 2007)	France	2	60	7.69	0.24	-0.62	50	2.96
	France	2	59	7.66	1.36	0.13	53	2.96
(El-Fadel et al. 1996b)	California	2	55 [a]	7.50	0.11	-0.96	35	2.65
(Faour et al. 2007)	U.K.	2	54	7.15	0.39	-0.41	73	3.23
	California	2	61 [a]	6.89	0.23	-0.64	88	2.42
(Oonk et al. 2013)	Netherlands	2	15	7.40	1.37	0.14	36	2.30
(Yazdani et al. 2012)	California	2	100	6.26	1.02	0.01	52	2.22
(Zhao et al. 2013b)	Michigan	2	25 [a]	8.35	0.30	-0.53	n.a.	2.98
	Michigan	2	25 [a]	8.10	0.08	-1.09		2.84
(Amini et al. 2013)	Confidential	1	65 [a]	9.88	0.09	-1.05	74	3.52
(Barlaz et al. 2010a)	Delaware	1	47 [a]	10.23	0.16	-0.80	n.a.	3.22
	New England	1	48 [a]	9.84	0.09	-1.05		3.16
(Faour et al. 2007)	Delaware	1	54 [a]	7.20	0.21	-0.68	115	3.04
	Florida	1	57 [a]	9.20	0.11	-0.96	95	n.a.
	Delaware	1	54 [a]	7.90	0.12	-0.92	87	
(Morris et al. 2003)	Delaware	1	54 [a]	8.81	0.05	-1.30	n.a.	n.a.
(Sormunen et al. 2013)	Finland	1	20 [a]	9.95	0.18	-0.74	120	3.82
(Tolaymat et al. 2010)	Kentuky	1	44 [a]	8.75	0.11	-0.96	56	2.94
	Kentuky	1	44 [a]	8.90	0.11	-0.96	41	2.86
(Wang et al. 2013)	North Carolina	1	38 [a]	9.15 [b]	0.12	-0.92	n.a.	n.a.
	Wisconsin	1	33 [a]	9.65 [b]	0.10	-1.00		
	Wisconsin	1	16 [a]	9.30 [b]	0.15	-0.82		
	Pennsylvania	1	51 [a]	10.46 [b]	0.06	-1.22		
	Virginia	1	52 [a]	9.79 [b]	0.17	-0.77		
(Amini et al. 2012)	Florida	0	45 [a]	10.15	0.13	-0.89	63	3.04
	Florida	0	57 [a]	10.15	0.08	-1.10	62	n.a.

	Florida	0	57 [a]	9.84	0.08	-1.10	77	
	Florida	0	57 [a]	9.34	0.04	-1.40	70	
	Florida	0	57 [a]	9.93	0.13	-0.89	61	
(Amini et al. 2013)	Confidential	0	63	9.34	0.06	-1.22	140	3.60
	Confidential	0	68	9.89	0.04	-1.40	93	3.79
(Bentley et al. 2005)	Tennessee	0	58 [a]	9.89	0.08	-1.11	103	n.a.
	Georgia	0	58 [a]	8.68	0.09	-1.07	108	
	Georgia	0	58 [a]	8.99	0.18	-0.75	115	
	Louisiana	0	58 [a]	9.03	0.20	-0.70	111	
	Louisiana	0	58 [a]	9.57	0.24	-0.62	110	
	Georgia	0	58 [a]	8.86	0.15	-0.83	102	
(Lamborn 2012)	Australia	0	60	9.66	0.02	-1.64	n.a.	3.32
(Machado et al. 2009)	Brazil	0	38	9.77 [b]	0.20	-0.70	67	3.37
(Thompson et al. 2009)	British Columbia	0	70 [a]	9.27 [b]	0.05	-1.32	109	n.a.
	Alberta	0	58 [a]	10.05 [b]	0.02	-1.64	100	
	Ontario	0	65 [a]	9.49 [b]	0.04	-1.43	90	
	Quebec	0	62 [a]	9.91 [b]	0.04	-1.38	128	
	Nova Scotia	0	68 [a]	8.88 [b]	0.06	-1.25	90	
(Tolaymat et al. 2010)	Kentuky	0	46 [a]	8.71	0.06	-1.22	45	3.42
(Wang et al. 2013)	New York	0	45 [a]	9.72 [b]	0.17	-0.77	n.a.	n.a.
	North Carolina	0	50 [a]	9.63 [b]	0.04	-1.40		
	Illinois	0	23 [a]	9.23 [b]	0.13	-0.89		
	Michigan	0	23 [a]	9.45 [b]	0.15	-0.82		
	Missouri	0	48 [a]	9.71 [b]	0.09	-1.05		
	North Carolina	0	50 [a]	9.74 [b]	0.11	-0.96		
(Willumsen 2007)	Brazil	0	60	10.30	0.11	-0.98	77	n.a.
	Mexico	0	67	9.94	0.07	-1.18	94	
	Uruguay	0	70	8.55	0.28	-0.55	68	
	Argentina	0	19	8.26	0.10	-1.00	102	

[a] % of biodegradable waste (B_0) is estimated based on landfill location using survey data of Staley and Barlaz (2009);
[b] Total weight of disposed waste (W) is calculated using disposal capacity reported in literature;
[c] n.a.: the values of L_0 and t_{max} are not available due to incomplete CH_4 generation data.

Table 9-4 Summary of information included in the database developed in this study highlighting the differences between laboratory experiments operated to simulate anaerobic biodegradation of MSW and landfills.

Comparison	Laboratory experiments	Landfills
Waste stream	Total weight 10^{-1} to 10^{3} kg; Waste often shredded, blended, or homogenized.	Total weight 10^{7} to more than 10^{10} kg; Waste rarely shredded.
Waste composition	Well characterized; Characteristic variables: B_0: 6-100% B_{r0}: 0-100% VS[a]: 0.17-0.99 g/g	Bulk estimation or based on survey data; Characteristic variables: B_0[b]: 15-100%
Biodegradation conditions	Frequent moisture addition; Well quantified moisture content; Often seeded with microorganisms and nutrients; Controlled temperature; Characteristic variables: W, biodegradation class, T	Limited moisture addition; Poorly quantified moisture content; Rarely seeded with microorganisms and nutrients; Uncontrolled and unmonitored temperature; Characteristic variables: W, biodegradation class
Measurements	Biogas collection begins immediately after startup; 100% biogas collection efficiency; Accurate and frequent measurements; Numerous types of collected measurements	Biogas collection begins at variable times; 30% to 90% biogas collection efficiency; Inaccurate and sparse measurements; Few types of collected measurements
Number of datasets (studies)	49 experiments (21 studies)	57 landfills (18 studies)
CH_4 generation parameters	k, L_0, t_{max}[c]	k[d], L_0[d], t_{max}[e]

Note: B_0: percentage of biodegradable waste; B_{r0}: percentage of readily biodegradable waste; VS: volatile solids content of waste (g/g); W: total weight of waste (kg); T: temperature of waste (˚C); k: waste decay rate (1/yr); L_0: CH_4 generation potential of waste (L/kg); t_{max}: delay time until the maximum CH_4 generation rate (d).

[a] volatile solids (VS) content of waste was available for 43 laboratory experiments;

[b] B_0 was estimated based on landfill location using survey data of Staley and Barlaz (2009) for 44 landfills;
[c] t_{max} was calculated for 41 laboratory experiments;
[d] k and L_0 values were calculated for three landfills and obtained directly from the literature for 54 landfills;
[e] t_{max} was calculated for 24 landfills.

Table 9-5 Means, standard deviations and regression coefficients of the waste composition, biodegradation conditions, and CH_4 generation variables based on laboratory experiments and field monitoring data of landfills.

	Waste composition variables		Biodegradation conditions variables		CH_4 generation variables				
	B_0 (%)	B_{r0} [c] (%)	log(W) (kg)	T [c] (ºC)	k (1/yr)	log(k)	L_0 (L/kg)	t_{max} (d)	log(t_{max})
Laboratory experiments									
mean	63	38	0.93	34	5.66	0.63	98	138	1.90
stdev [a]	31	38	1.59	5	5.09	0.33	70	196	0.44
c.v. [b]	0.49	0.99	1.71	0.14	0.90	0.52	0.71	1.42	0.23
95%	100	100	3.54	40	15.02	1.18	217	459	2.66
5%	15	0	-1.82	25	1.10	0.04	11	32	1.51
Landfills									
mean	51		9.05		0.18	-0.93	88	1751	3.06
stdev	16		0.98		0.27	0.36	23	1720	0.42
c.v.	0.31	n.a.	0.11	n.a.	1.46	0.39	0.26	0.98	0.14
95%	70		10.23		1.02	0.01	120	6205	3.79
5%	19		7.15		0.04	-1.43	41	201	2.30
Laboratory experiments and landfills									
mean	57		5.30		2.71	-0.21	93	668	2.28
stdev	24		4.27		4.41	0.86	50	1246	0.70
c.v.	0.43	n.a.	0.81	n.a.	1.62	4.07	0.54	1.86	0.31
95%	100		10.05		9.27	0.97	187	3285	3.52
5%	19		-1.00		0.04	-1.40	20	32	1.51

[a] stdev: standard deviation;
[b] c.v.: coefficient of variation;
[c] n.a.: the values of B_{r0} and T are not available for landfills.

Table 9-6 Summary of the results of multi-linear regression and significance test for laboratory experiments and field monitoring data of landfills.

	R^2_{adj}	Intercept (P) [a]	B_0 (P)	log(W) (P)	B_{r0} (P)	T (P)
			Laboratory experiments			
log(*k*)	0.52	0 (0)	-0.52 (6×10^{-4})	-0.55 (4×10^{-4})	0.42 (6×10^{-4})	0.53 (2×10^{-5})
L_0	0.20	0 (0)	0.44 (0.02)	-0.15 (0.43)	-0.10 (0.48)	-0.16 (0.27)
log(t_{max})	0.49	0 (0)	0.15 (0.29)	0.43 (5×10^{-3})	0.01 (0.91)	-0.50 (9×10^{-5})
			Landfills			
log(*k*)	0.34	0 (0)	-0.18 (0.11)	-0.59 (1×10^{-6})		
L_0	0.06	0 (0)	-0.05 (0.70)	0.30 (0.02)	n.a.[b]	
log(t_{max})	0.53	0.33 (0.04)	0.09 (0.49)	0.64 (3×10^{-5})		
			Laboratory experiments and landfills			
log(*k*)	0.88	0 (0)	-0.16 (4×10^{-5})	-0.99 (0)		
L_0	0.14	0 (0)	0.39 (1×10^{-4})	-0.02 (0.87)	n.a.	
log(t_{max})	0.75	0.43 (8×10^{-9})	0.08 (0.16)	0.99 (0)		

[a] P: p-value of significance test; P<0.05 is considered statistically significant, 0.05<P<0.1 is considered marginally significant, and P>0.1 is considered statistically insignificant;
[b] n.a.: data not available.

9.7 Figures

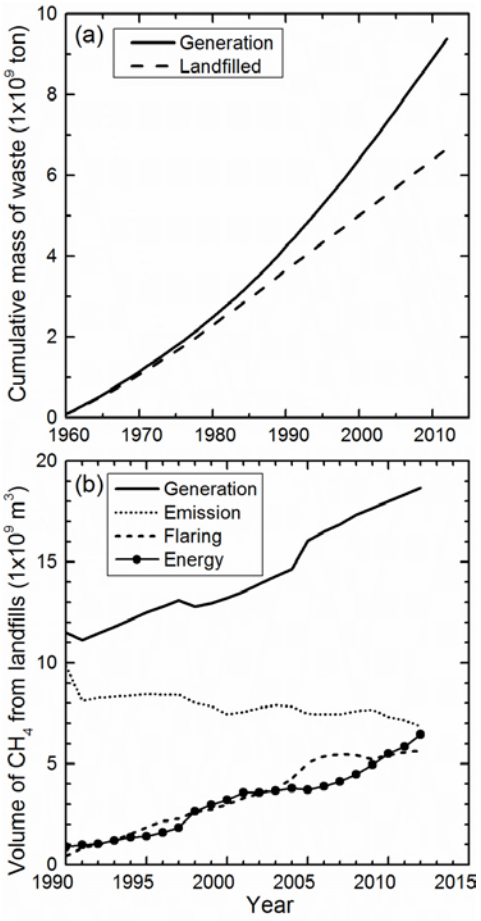

Figure 9-1 (a) Cumulative mass of generated and landfilled waste with time; and (b) volume of CH_4 generated, emitted, flared and converted to energy in landfills with time (based on U.S. EPA's survey data (2014a)).

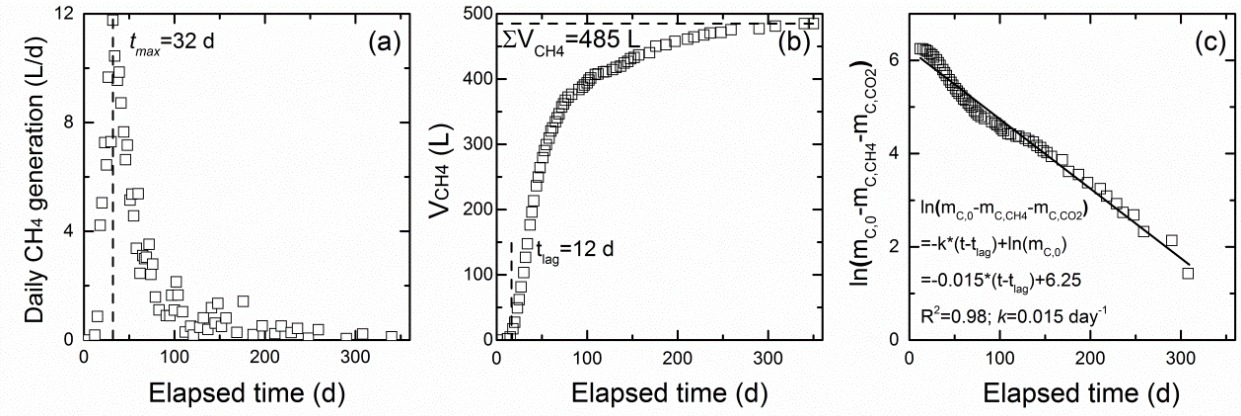

Figure 9-2 An example dataset illustrating the calculations of waste decay rate (k), cumulative volume of generated CH_4 (ΣV_{CH4}) and time until the maximum CH_4 generation rate (t_{max}) using LandGEM for experimental data reported by Fei et al. (2014a).

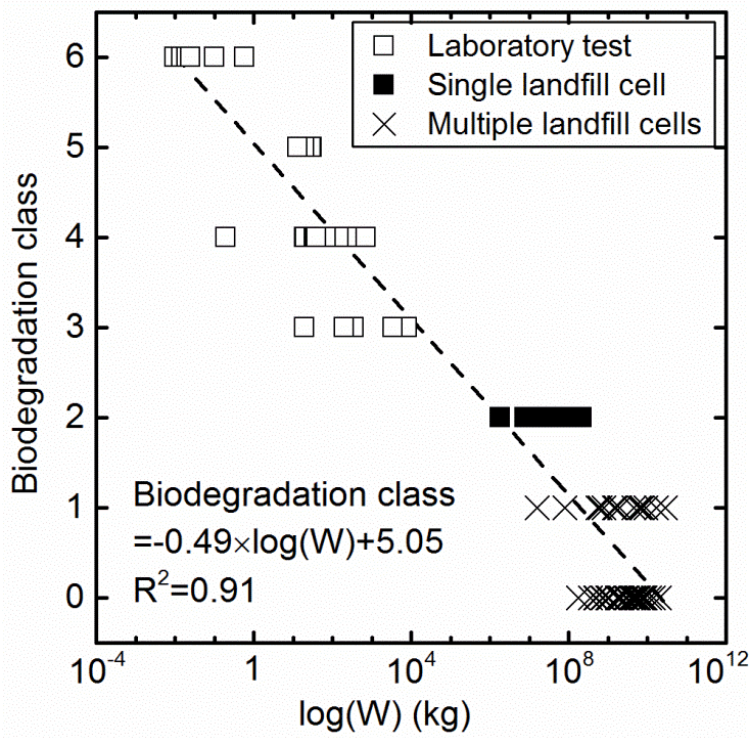

Figure 9-3 Correlation between total weight of waste (log(W)) and biodegradation class (Table 9-1) of laboratory and field studies included in Table 9-2 and Table 9-3.

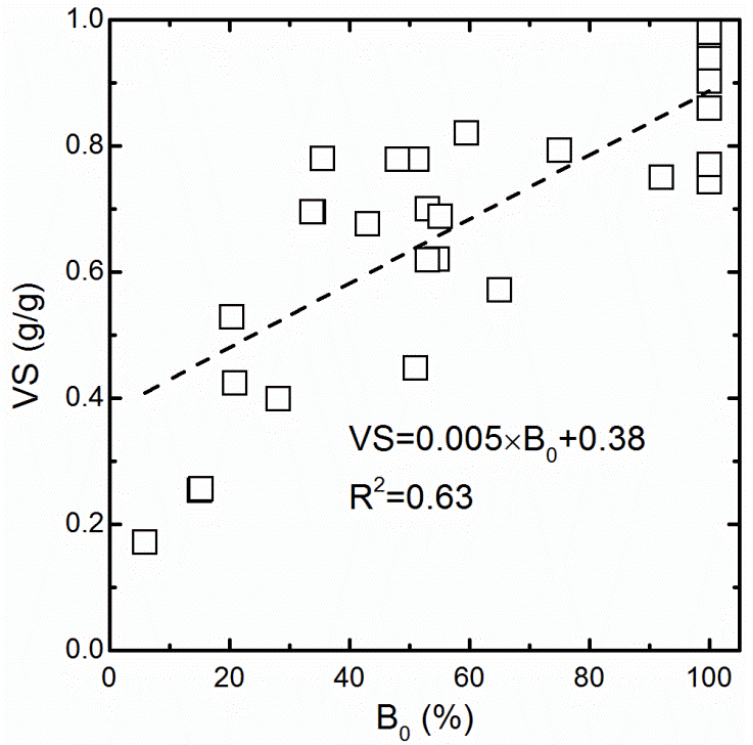

Figure 9-4 Correlation between the percentage of biodegradable waste (B_0) and the content of volatile solid (VS) of MSW of laboratory experiments.

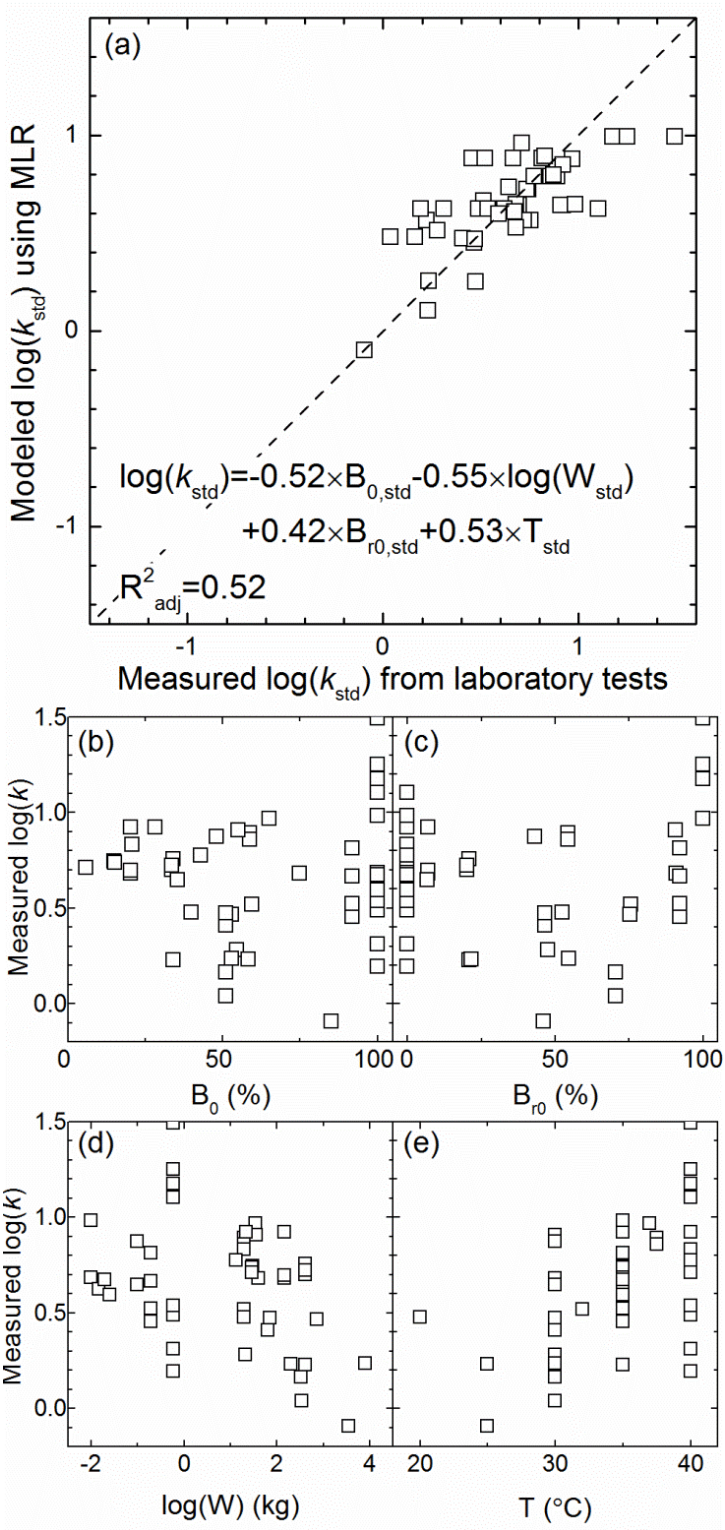

Figure 9-5 Relationships between waste decay rate (k) and waste composition and biodegradation conditions variables of laboratory experiments: (a) measured and modeled log(k_{std}); (b) measured log(k) and percentage of biodegradable waste (B_0); (c) measured log(k) and percentage of readily biodegradable waste of B_0 (B_{r0}); (d) measured log(k) and total weight of waste (log(W)); and (e) measured log(k) and waste temperature (T).

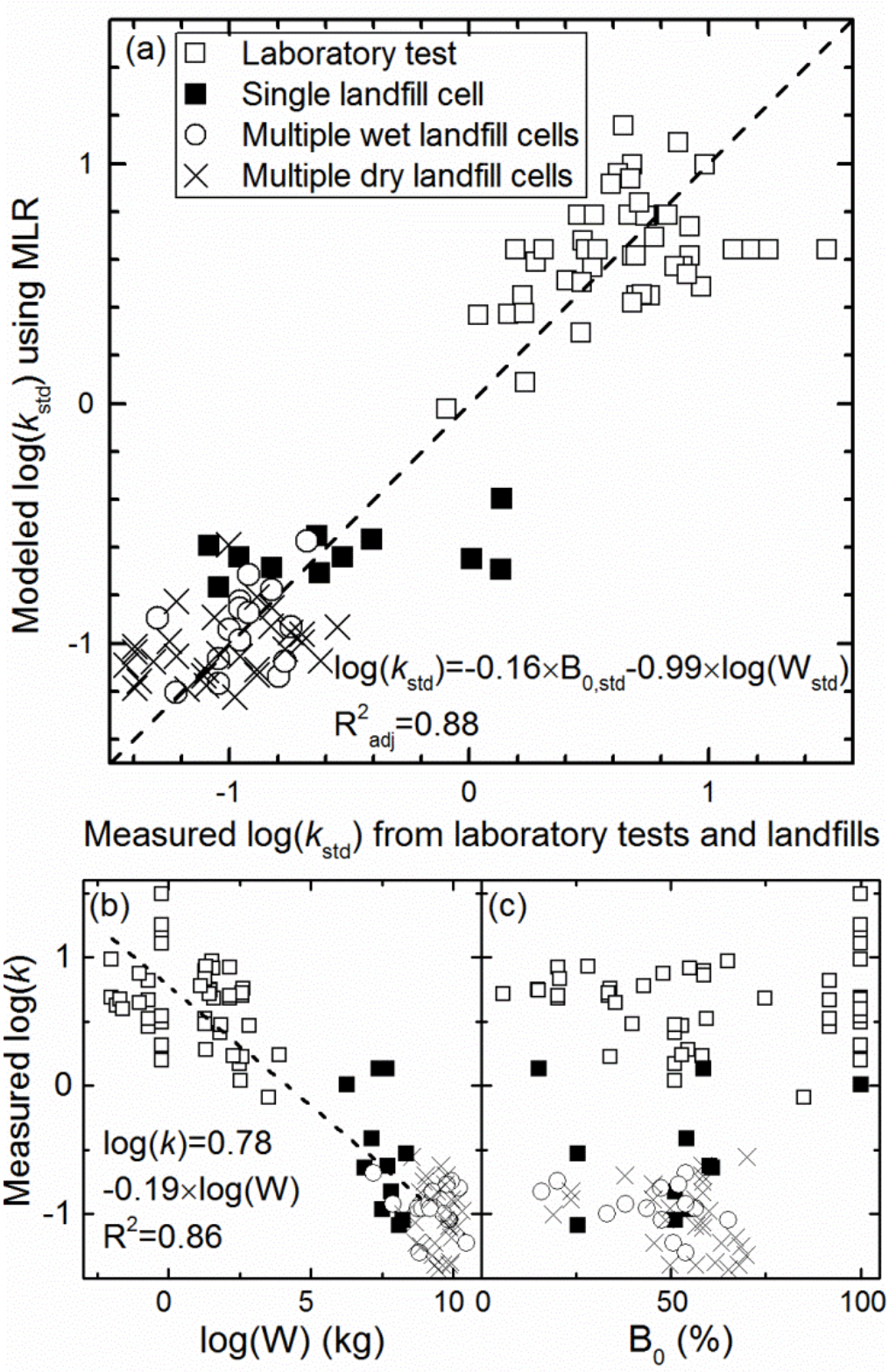

Figure 9-6 Relationships between waste decay rate (k) and waste composition and biodegradation conditions variables of laboratory and field studies: (a) measured and modeled log(k_{std}); (b) measured log(k) and total weight of waste (log(W)); and (c) measured log(k) and percentage of biodegradable waste (B_0).

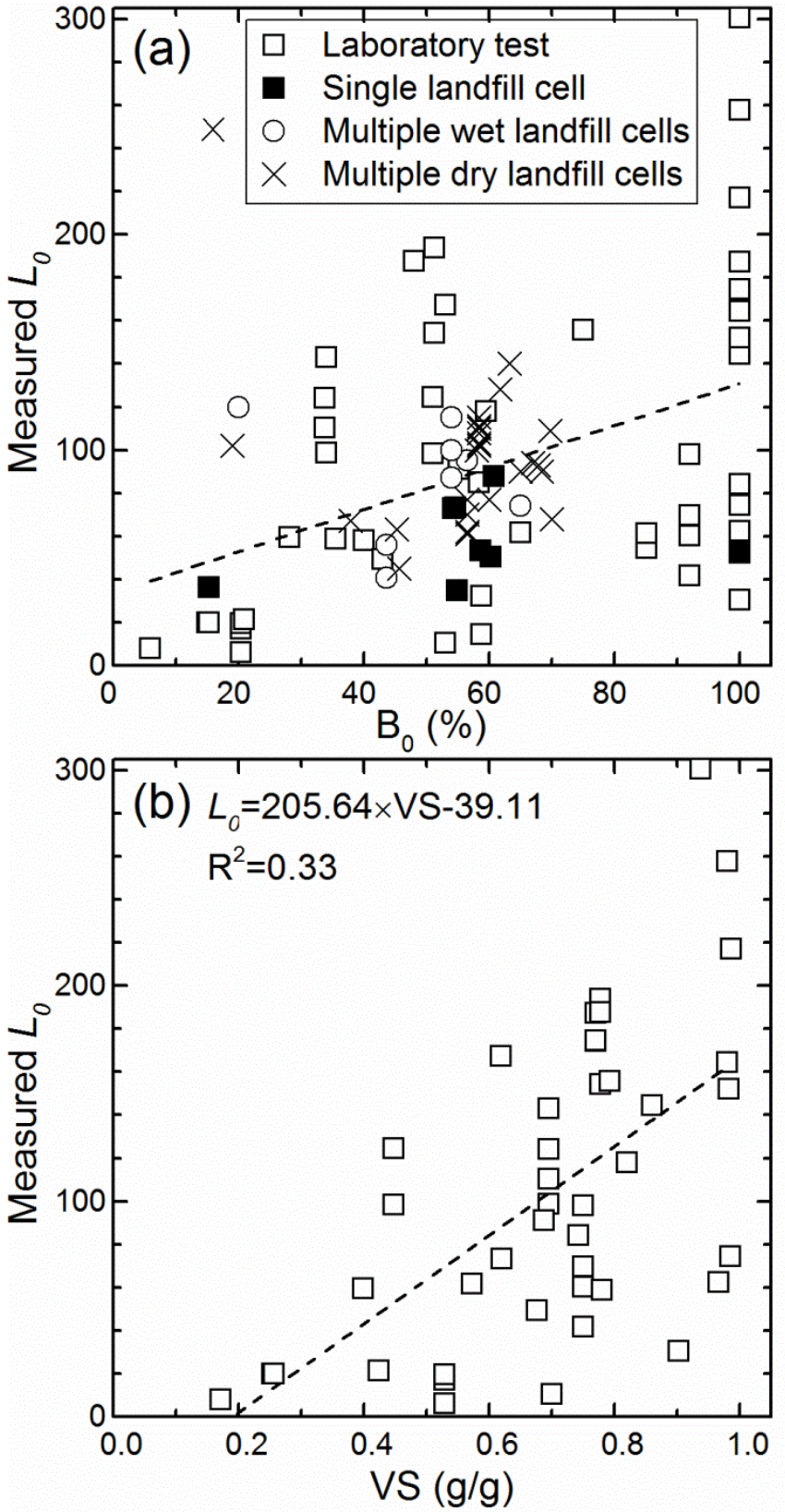

Figure 9-7 Relationships between measured L_0 of laboratory experiments and landfills and (a) the percentage of biodegradable waste (B_0), and (b) the volatile solid (VS) content of MSW.

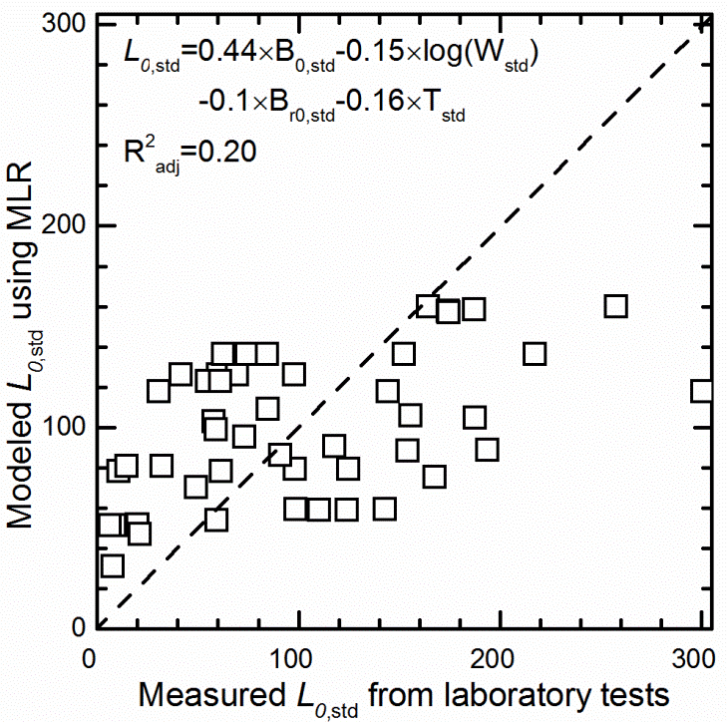

Figure 9-8 Relationship between measured and modeled standardized CH_4 generation potential ($L_{0,std}$) of laboratory experiments.

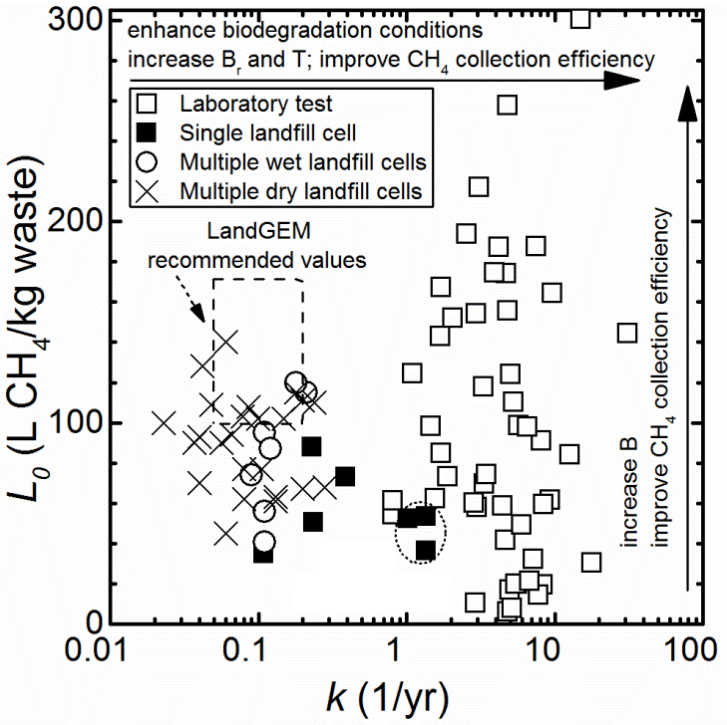

Figure 9-9 Diagram of waste decay rate (k) and CH_4 generation potential (L_0) of laboratory experiments and landfills, and ranges of recommended values of LandGEM. Potential approaches to increase the values of k and L_0 of landfills are marked with arrows.

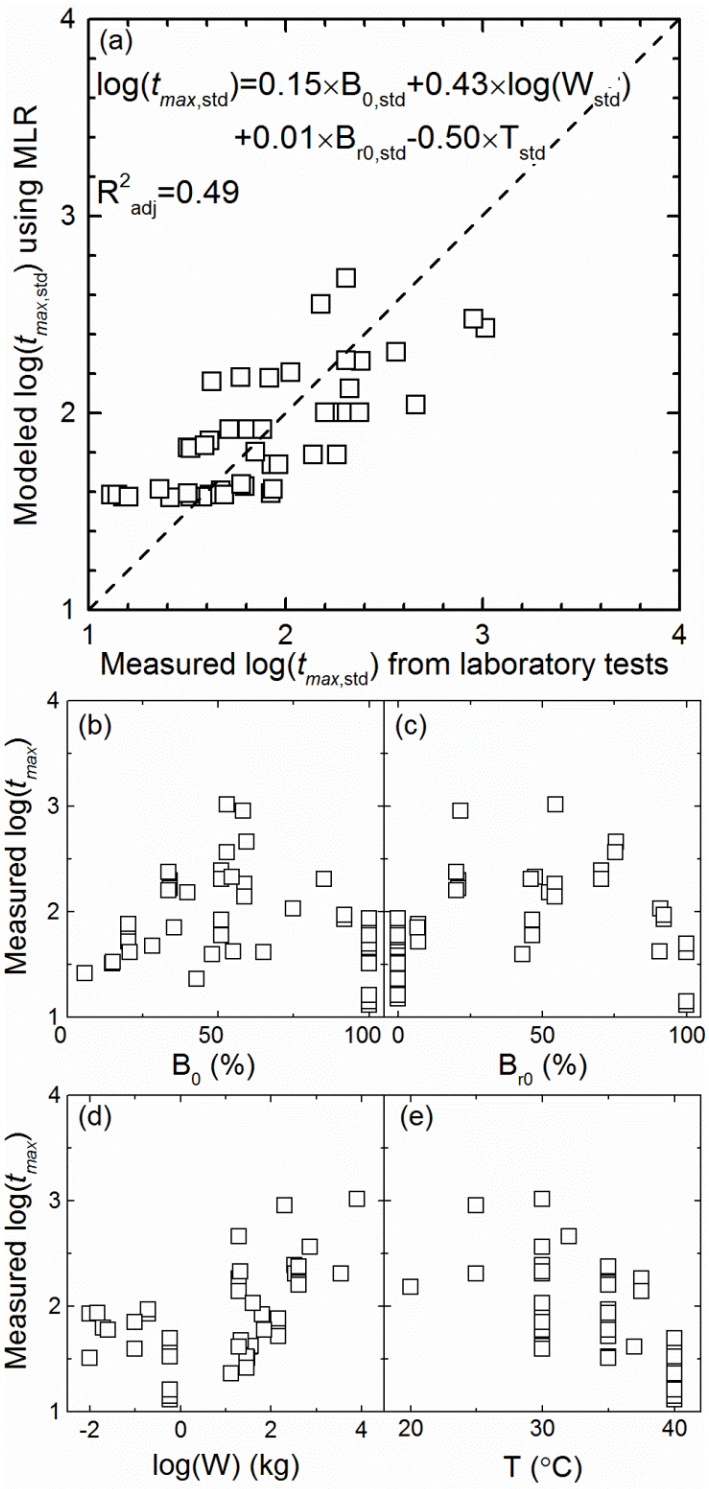

Figure 9-10 Relationships between time until maximum CH_4 generation rate (t_{max}) and waste composition and biodegradation conditions variables of laboratory experiments: (a) measured and modeled log($t_{max,std}$); (b) measured log(t_{max}) and percentage of biodegradable waste (B_0); (c) measured log(t_{max}) and percentage of readily biodegradable waste of B_0 (B_{r0}); (d) measured log(t_{max}) and total weight of waste (log(W)); and (e) measured log(t_{max}) and waste temperature (T).

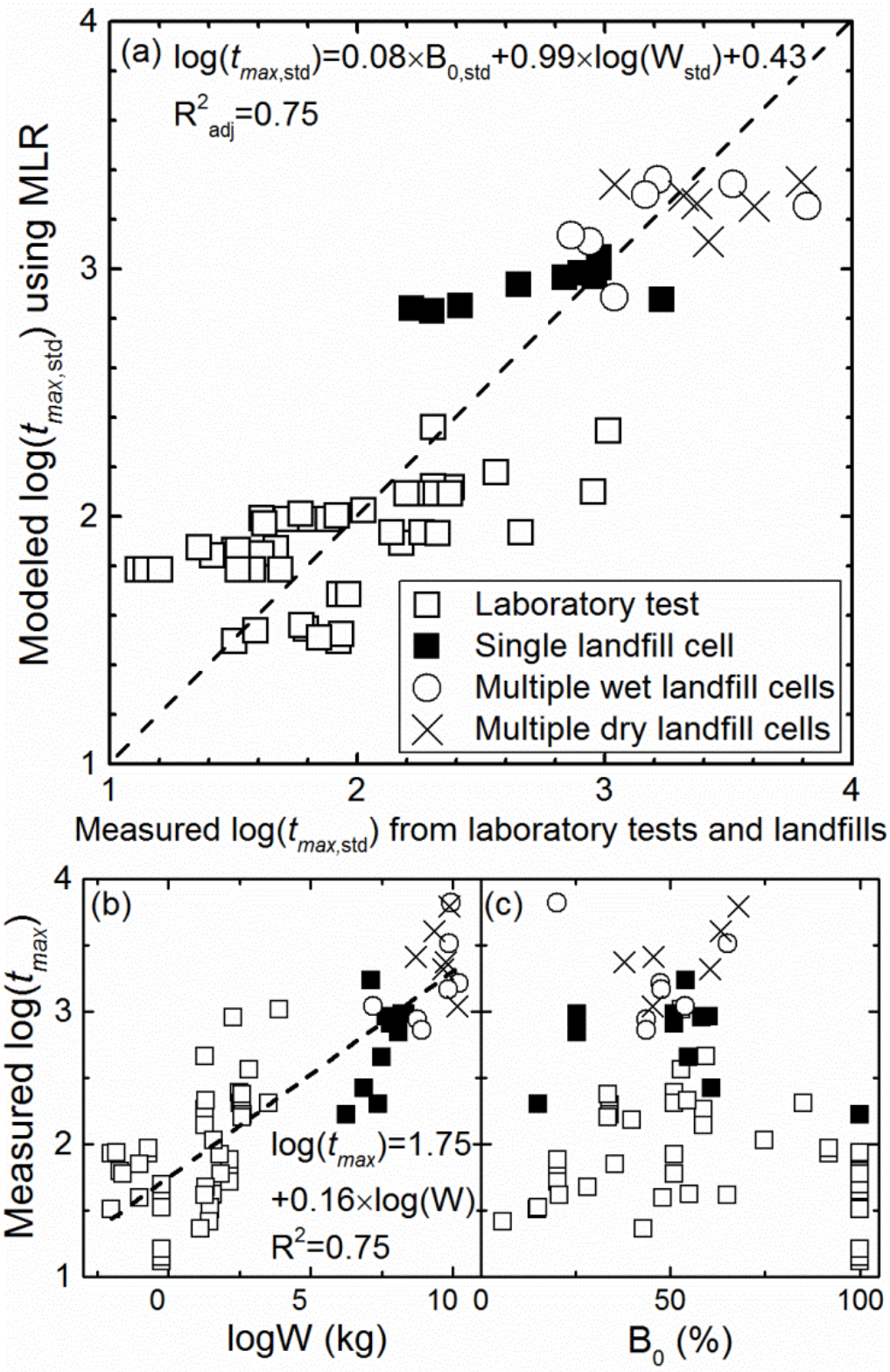

Figure 9-11 Relationships between time until maximum CH_4 generation rate (t_{max}) and waste composition and biodegradation conditions variables of laboratory and field studies: (a) measured and modeled log(t_{max}); (b) measured log(t_{max}) and total weight of waste (log(W)); and (c) measured log(t_{max}) and percentage of biodegradable waste (B_0).

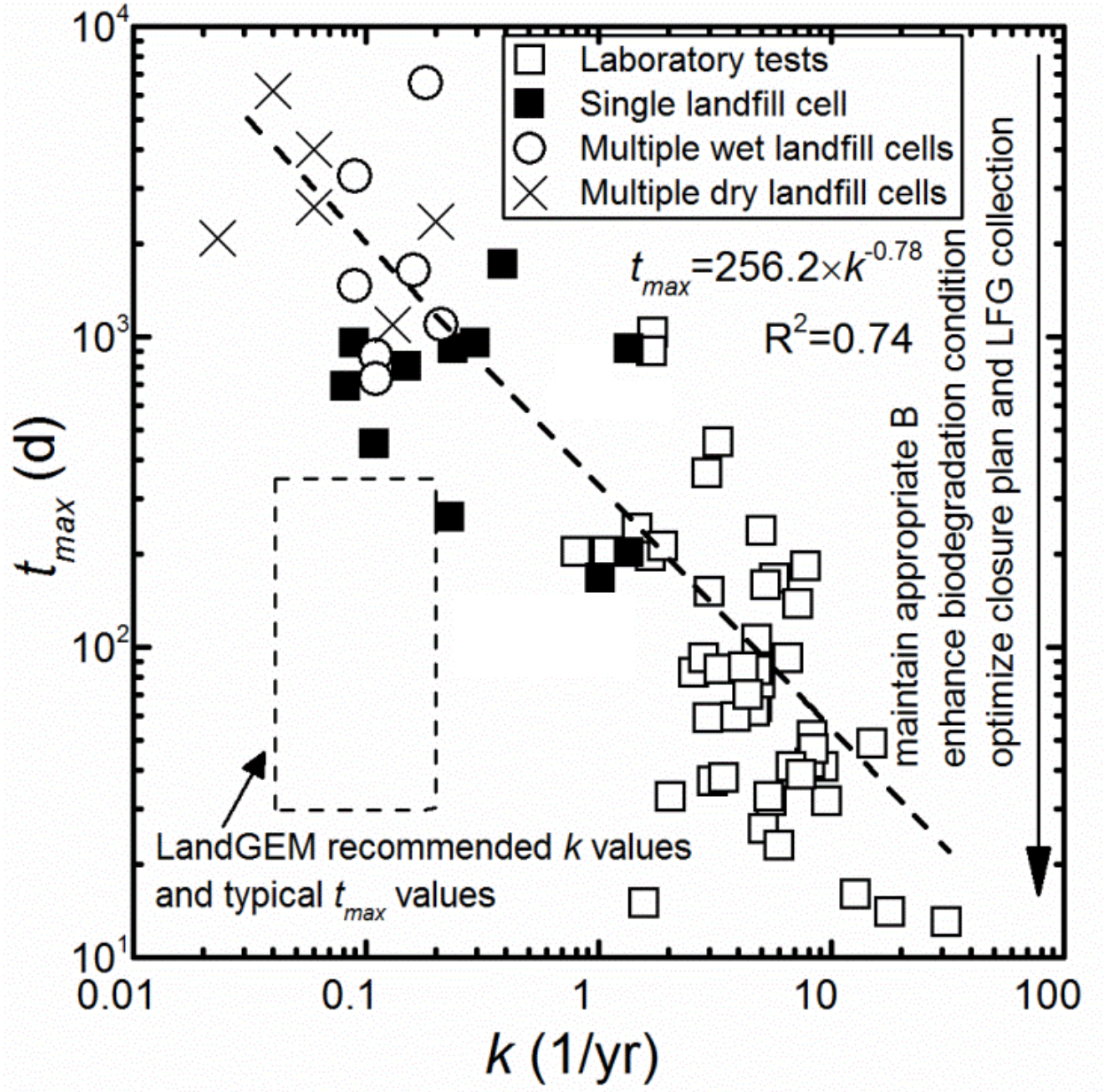

Figure 9-12 Diagram of waste decay rate (k) and time until maximum CH_4 generation rate (t_{max}) of laboratory experiments and landfills, and ranges of recommended values of LandGEM. Potential approaches to decrease the value of t_{max} of landfills are marked with an arrow.

Chapter 10 Factors Influencing Long Term Settlement of Municipal Solid Waste in Meso-Scale Laboratory Bioreactor Landfill Simulators

10.1 Abstract

Long-term settlement of municipal solid waste (MSW) in bioreactor and conventional landfills is caused by a number of mechanisms. Laboratory tests in bioreactor landfill simulators allow for a careful assessment of each mechanism and of the factors that affect it. A systematic review and synthesis of 98 tests from 29 meso-scale simulator studies available in the literature is presented. Long-term settlement is divided into three phases: transitional phase, active biodegradation phase and residual phase. Duration, strain and long-term compression ratio (equal to the ratio of strain to duration) is calculated for each phase. Statistical analysis of the data is conducted. The majority of the long-term settlement occurs during the active biodegradation phase (9.5% strain on average) and the mean compression ratio is 0.168. The other two phases contribute significantly less to the total long-term settlement. The effects of initial and operational conditions of simulators on magnitude and rate of long-term settlement of MSW are explored. External vertical stress application prior to long-term testing is found to reduce the amount and rate of long-term settlement. Aeration of waste during long-term testing increases the settlement rate by promoting aerobic biodegradation. MSW long-term settlement is also affected by waste composition, total unit weight and simulator size.

Fei, X., and Zekkos, D. (2013). "Factors influencing long-term settlement of municipal solid waste in laboratory bioreactor landfill simulators." *Journal of Hazardous, Toxic, and Radioactive Waste*, 17(4), 25-271.

10.2 Introduction

Over 200 million tons of MSW is generated in the United States each year and more than 50% is disposed of in landfills. Of the 1,754 landfills that were operated across the country in 2010, only 29 were bioreactor landfills, the remaining being operated as conventional “dry-tomb” landfills regulated by Subtitle D of Resource Conservation and Recovery Act (EPA 2010a).

Moisture migration is minimized in conventional Subtitle D landfills, especially in dry areas of the country, thus biodegradation is taking place in sub-optimal conditions (EPA 1976). As a result, MSW may remain largely undegraded even after decades. Bioreactor landfills represent a sustainable alternative to conventional landfills. In bioreactor landfills, biodegradation of MSW is accelerated via active leachate recirculation and/or liquid addition that increases moisture content and transports nutrients to microorganisms (Pohland and Kim 2000; Mehta et al. 2002; Kim and Pohland 2003; Soong et al. 2009). Degradation of MSW leads to landfill gas generation, a sustainable energy source, waste volume reduction and settlement. Moisture content is the most important factor controlling the degree and rate of MSW biodegradation (Reinhart and Townsend 1998; EPA 2006a; Barlaz et al. 2010b).

Mechanisms for long-term settlement of MSW in landfills include a variety of physical, chemical and biological processes (Bjarngard and Edgers 1990; Edil et al. 1990; McDougall 2011). They take place concurrently in the field, and thus are very hard to be studied separately. Variations in the initial conditions of waste (i.e. composition, waste size, moisture content, total unit weight, compaction and amount of daily soil cover) and operations after waste placement (aeration, liquid addition and leachate recirculation) influence the observed settlement (Bareither et al. 2012b; Bareither et al. 2012d).

Meso-scale laboratory simulators, defined in this study as diameter from 0.1 m to 1.3 m, are valuable in isolating the contribution of each settlement mechanism and elucidating the effects of initial and operation conditions, since they can be better controlled and the degradation process monitored closely. Liquid addition and/or leachate recirculation is adopted by most simulators to promote MSW biodegradation and shorten test duration. This paper systematically reviews and synthesizes results from studies in the literature that utilize laboratory simulators to stimulate MSW biodegradation in an effort to better understand the long-term settlement behavior of MSW.

10.3 Settlement mechanisms and temporal phases

Similar to soils, settlement of MSW is typically divided into immediate compression, primary consolidation and long-term settlement (Bjarngard and Edgers 1990; Grisolia et al. 1992). Immediate compression is caused by the self-weight of overlying MSW and the application of additional loads on waste during landfilling. It is completed within hours, and results in significant strain (Bjarngard and Edgers 1990; Wall and Zeiss 1995; Bareither et al. 2012b; Bareither et al. 2012e). Primary consolidation strictly occurs when soil is saturated (Holtz and Kovacs 1981), but this condition is rarely true of MSW due to its very high hydraulic conductivity and unsaturated state after placement (Bjarngard and Edgers 1990; Edil et al. 1990; Edgers et al. 1992). Therefore primary consolidation is not considered hereafter.

The focus of this paper is exclusively on the long-term settlement of MSW which is caused by several mechanisms including creep, raveling, physicochemical degradation and biodegradation (Sowers 1968; Bjarngard and Edgers 1990; Edil et al. 1990; Edgers et al. 1992; Sharma and De 2007; McDougall 2011). From a long-term settlement perspective, MSW is a

heterogeneous medium with solid, liquid and gas phases. MSW solids can be distinguished as bio-accessible and bio-inaccessible (McDougall 2007). Both types of wastes are further identified as biodegradable and non-biodegradable. Inter-particle and intra-particle voids may be occupied by liquid and gas (Zhang et al. 2010; McDougall 2011). Inter-particle voids are voids between individual waste particles that are open to migration of moisture and microorganisms, and are termed bio-accessible voids hereafter. Intra-particle voids are encapsulated within individual waste particles and are inaccessible to moisture or microorganisms, i.e. bio-inaccessible voids. Initial and operation conditions cause volume changes to solids and voids leading to long-term settlement of waste.

Long-term settlement of MSW can be divided into three phases as schematically illustrated in Figure 10-1 (Bjarngard and Edgers 1990; Edgers et al. 1992; Grisolia et al. 1992; McDougall 2011; Fei and Zekkos 2012).

10.4 Methodology

Settlement of MSW is represented by vertical strain, ε, as shown in Eqn. 10-1. Initial height of MSW is measured after settlement due to immediate compression has occurred.

$$\varepsilon = \frac{settlement\ of\ MSW\ in\ simulator}{initial\ height\ of\ MSW\ in\ simulator} \times 100\% \quad (10\text{-}1)$$

The total long-term settlement is the sum of strains caused by the three phases defined above (El-Fadel and Khoury 2000; Hossain and Gabr 2005):

$$\varepsilon_{total} = \varepsilon_1 + \varepsilon_2 + \varepsilon_3 \quad (10\text{-}2)$$

where ε_{total} is total long-term strain of MSW, ε_1, ε_2 and ε_3 are strains in Phase 1, Phase 2 and Phase 3 of long-term settlement.

Long-term settlement curves of 98 tests from 29 studies are identified and analyzed. Each experimental curve is digitized and strain is plotted against the logarithm of time for each test. The parameters derived by original authors are not adopted directly, but strains, durations and long-term compression ratios of all tests are recalculated for consistency according to the approach shown in Figure 10-1. Thus the reported strain, duration and compression ratios in this study for each test may not be identical to those reported by the original authors.

This approach essentially linearizes the three sections of the settlement curve. A straight line is fitted to each section of the curve. Intersection points of the three straight lines are defined (points A and B in Figure 10-1) and three phases are identified accordingly. Durations and strains of P_1 (t_1 and ε_1) and P_2 (t_2 and ε_2) are calculated using points A and B, whereas duration and strain of P_3 (t_3 and ε_3) are calculated by subtracting t_1, t_2 and ε_1, ε_2 from total testing duration and strain. The slope of each straight line is the long-term compression ratio, C_{LT}, of that phase, per Eqn. 10-3:

$$C_{LT} = \frac{\Delta\varepsilon}{\Delta\log(time)} \tag{10-3}$$

In tests where an external vertical stress (σ) is applied, the strain from immediate compression is identified as a near-vertical drop of settlement vs. time curve in semi-logarithmic diagram and is not included in the calculations of long-term settlement (Bareither et al. 2012b). The long-term settlement curve is then set to start at an initial time t_0=1 day and ε_0=0%.

Alternate approaches can be used to separate the short- and long-term settlement (Handy 2002; Bareither et al. 2012b).

The duration, strain and long-term compression ratio of each phase from all tests are analyzed statistically to calculate the mean, standard deviation (δ) and coefficient of variation (COV, defined as the ratio of the standard deviation to the mean). The database includes tests in laboratory simulators with diameters from 0.1 to 1.3 m and heights from 0.1 to 2.4 m. Waste composition varied from mostly inorganic (soil rich) to entirely organic (paper and food). Moisture addition methods also varied. Tests were performed by a single water addition at the beginning of the test to achieve field capacity (S). In other tests, the specimen was flushed with only fresh water (F). In a third set of tests, leachate recirculation (R) was performed. External vertical stress varied from negligible (i.e., self-weight of the waste) to 500 kPa. The majority of the tests were performed under anaerobic conditions (i.e., specimens were sealed leading to oxygen depletion). A smaller subset of the database involves tests under aerobic conditions. Aerated tests included either passive aeration (by exposing waste to atmosphere) or active aeration (using an air blower). As a consequence of all these differences in initial and operation conditions, significant variability is observed in the results. However some systematic trends can be discerned. In order to better analyze the results, data bins are used for variables with a wide range of values, and means and standard deviations for data within each bin are calculated (i.e., vertical stress, percentage of >20 mm waste, diameter and height).

The database of tests is divided into four datasets with the objective to assess the impacts of external vertical stress application and aeration on the long-term settlement: anaerobic tests with external vertical stress application (52 tests, Table 10-1) (Wall and Zeiss 1995; de Abreu 2003; Sheridan 2003; Peng 2004; de Abreu et al. 2005; Kim 2005; Liu et al. 2005; Kong et al.

2006; Liao 2006; Liao 2007; Olivier and Gourc 2007; Sun 2007; Ivanova et al. 2008b; Swati and Joseph 2008; Liu et al. 2009; Bareither 2010; Chen et al. 2010b; Liu 2010; Kim et al. 2011; Bareither et al. 2012e); aerobic tests with external vertical stress application (4 tests, Table 10-2) (Sheridan 2003; Kim 2005; Kim et al. 2011); anaerobic tests without external vertical stress application (26 tests, Table 10-3) (Stessel and Murphy 1992; Fang 2005; Jin 2005; Boni et al. 2006; Wang 2007; Chen et al. 2008; Elagroudy et al. 2008; Swati and Joseph 2008; Chen 2009; Feng 2009; Feng et al. 2009; Chen et al. 2010a; Gourc et al. 2010; Sun et al. 2011); and aerobic tests without external vertical stress application (16 tests, Table 10-4) (Stessel and Murphy 1992; Jin 2005; Wang 2007; Elagroudy et al. 2008; Tang et al. 2008; Mahar et al. 2009; Sun et al. 2011).

10.5 Analysis of long-term settlement behavior

The entire database is first analyzed to quantify the long-term settlement behavior in all laboratory simulators. Subsequently, analyses of the four datasets (Table 10-1 through Table 10-4) are performed to assess systematic differences in the results. A summary of means and standard deviations are tabulated in Table 10-5. The high standard deviations and COVs for durations, strains and long-term compression ratios indicate high variability among tests. Such variability is expected given the significant differences in initial and operation conditions among all tests.

For the entire database, the mean durations, t_1 and t_2 for P_1 and P_2, are 53 days and 162 days, respectively. Since long-term settlement in residual phase (P_3) continues indefinitely, t_3 is not reported. The mean total duration of t_1 and t_2 is 215 days (COV=0.78) (Figure 10-2a). Mean duration of P_1 represents only 24% of the total duration, P_2 represents the remaining 76%. Note

that 83 out of 98 tests were interrupted prior to reaching P_3, leading also to some underestimation of t_2. Thus, the duration of P_2 represents the majority of experimental degradation time.

Total long-term strain, ε_{total}, is on average 11.0% of initial specimen height. Mean strains of P_1, P_2 and P_3 are 1.2%, 9.5% and 0.3%, respectively (Figure 10-2b). Thus, strain of P_1 is responsible on average for 10.9% of ε_{total}, ε_2 for 86.4% of ε_{total} and ε_3 approximately 2.7% of ε_{total}. For each test, strain of P_1 never exceeds that of P_2. Overall, P_2 is responsible for the majority of long-term strain. Although ε_3 is very variable (has the highest COV), it has a minor contribution to the total strain.

Mean long-term compression ratios for each phase are C_{LT1}=0.009, C_{LT2}=0.168 and C_{LT3}=0.011 (for the 15 out of 98 tests that reached P_3) (Figure 10-2c). Mean C_{LT2} is more than 15 times higher than C_{LT1} and C_{LT3} or even typical secondary compression ratios of organic clays ($C_\alpha \approx 0.01$) (Holtz and Kovacs 1981). C_{LT1} and C_{LT3} are comparable to secondary compression ratio of organic clay.

Mean strain and long-term compression ratio derived herein also agree well with previously reported field data by Bareither *et al.* (2012c) (ε_{total}=6-25%, C_{LT2} ($C_{\alpha,bio}$)=0.048-0.35), Bjarngard and Edgers (1990) (ε_{total}=1-30%, C_{LT2} ($C_{\alpha,max}$)=0.02-0.51) and Park and Lee (2002) (ε_{total}=5-20%). Durations in laboratory tests are significantly shortened compared to field conditions due to optimized biodegradation conditions and better control and monitoring of the biodegradation process (Hossain et al. 2003; Bareither et al. 2012d). Interestingly, long-term strains of MSW observed in simulators are of the same order as strains due to immediate compression, which vary between 3% and 20% (Bjarngard and Edgers 1990; Bareither et al. 2012b), but are not significantly higher as it has been commonly postulated (Edgers et al. 1992;

Wall and Zeiss 1995; El-Fadel and Khoury 2000; McDougall 2011). This observation may be partially attributed to the fact that a significant number of experiments (83 out of 98 tests) were interrupted before long-term settlement reached Phase 3, leading to an underestimation of total settlement.

10.5.1 **Effect of external vertical stress**

External vertical stress (σ_v) is applied to waste in landfills by overlying MSW and daily soil cover layers. Compaction during landfilling also introduces immediate compression to the waste. Typical *in situ* vertical stress reaches 400 to 600 kPa at a depth of 40 m for typical MSW unit weight (Zekkos et al. 2006). The effect of external vertical stress is evaluated by analyzing the datasets of anaerobic tests with and without vertical stress application (Table 10-1 and Table 10-3, Figure 10-3a and Figure 10-3b). Specimens subjected to the tests in Table 10-3 are only subjected to the self-weight of the waste specimen (with an average stress of less than 5 kPa typically) and are listed as 0 kPa for simplicity.

Mean duration of P_1 averages 57 days and does not appear to be affected by vertical stress (Figure 10-3c). Mean duration of P_2 decreases from 184 days under negligible vertical stress to 131 days when 500 kPa stress is applied (29% decrease) (Figure 10-3d). Overall, mean durations of P_2 represent 75-82% of total duration for all vertical stresses.

Mean strain of P_1 decreases on average by 86% from 1.4% at zero external stress to 0.2% at 500 kPa vertical stress (Figure 10-3e). Similarly, mean strain of P_2 decreases on average by 80% from 8.9% to 1.8% (Figure 10-3f). As a result, total long-term strain is reduced significantly. On average by 80%, under 500 kPa vertical stress compared to no external vertical stress. Strain of P_1 and P_2 represent on average 13% and 87% of total long-term strain respectively regardless of vertical stress level.

Because duration of P_1 is not affected by vertical stress, but strain decreases considerably with increasing vertical stress, mean C_{LT1} decreases from 0.009 at zero vertical stress to 0.001 at 500 kPa vertical stress (89% reduction) (Figure 10-3g). Similarly, mean C_{LT2} decreases from 0.146 to 0.036 (75% reduction) (Figure 10-3h). The mean C_{LT2}/C_{LT1} ratios remain constant at around 13 at all vertical stress increments.

These trends are reasonable. Waste matrix is densified due to the application of external vertical stress. As a result, the densified MSW has lower settlement potential during long-term settlement compared to MSW that has not been subjected to the higher vertical stress. In addition, in denser waste, smaller voids provide bio-accessible substrate to microorganisms. During P_1, microbial population is low while biodegradable waste is abundant (Barlaz et al. 2010b). As a result, duration of P_1 is not affected by high vertical stress application, because even when bio-accessibility of biodegradable waste is reduced, the availability is still high enough for a growing microbial population. During P_2, the microbial growth rates are at maximum and are affected by available biodegradable MSW (Barlaz et al. 2010b). However, waste bio-accessibility is limited by smaller voids due to external stress application. External vertical stress also reduces hydraulic conductivity of waste matrix, restricting transportation of moisture and nutrients (Olivier and Gourc 2007; Reddy et al. 2009a; Stoltz et al. 2010b; Stoltz et al. 2010a; Breitmeyer and Benson 2011). As shown previously for soils and gravel drainage layers, a reduction in hydraulic conductivity impedes migration of microorganisms by reducing throat and void sizes (Abuashour et al. 1994; Cooke et al. 2005; VanGulck and Rowe 2008). Therefore it is reasonable to expect that microbial migration in MSW matrix is also slowed down. Overall, less biodegradable MSW is bio-accessible and is depleted sooner. Duration of P_2 is shortened and a transition into P_3 occurs earlier.

10.5.2 **Effect of aeration**

Oxygen entrapped in waste matrix is depleted rapidly after landfilling. Therefore anaerobic conditions are common in conventional and bioreactor landfills (Reinhart and Townsend 1998; EPA 2006a; Barlaz et al. 2010a; Barlaz et al. 2010b). Aeration does not alter the volume of voids within waste, but accelerates the macroscopic biodegradation rate of MSW and increases waste biodegradability (Reinhart and Townsend 1998; EPA 2000; Rich et al. 2008; Yazdani et al. 2010). Organic waste and papers can be consumed at higher rate and to larger extent aerobically than anaerobically due to higher energy generation from oxic respiration (Zinder 1993; Meima et al. 2008; Barlaz et al. 2010b; Madigan et al. 2010). Biodegradation of wood is highly unfavorable and incomplete in the absence of oxygen, but is facilitated under aerobic conditions (Colberg 1988; Barlaz 2006; Wang et al. 2011b). Permeation and distribution of air are influenced by numerous factors such as aeration method, void ratio and connectivity of voids, hydraulic conductivity and simulator configurations (Stoltz et al. 2010a; Yazdani et al. 2010; Han et al. 2011).

Aerobic (Table 10-4) and anaerobic (Table 10-3) tests without external vertical stress application are analyzed and illustrated in Figure 10-4a and Figure 10-4b, respectively. When waste is aerated, mean t_1 and t_2 are 29 days and 74 days, respectively. For comparison, t_1 and t_2 in anaerobic tests without external vertical stress averages 58 days and 185 days (Figure 10-4c). Thus, aeration reduces t_1 by 50% and t_2 by 60%. The contribution of t_1 and t_2 to the total duration remain relatively unchanged under aerobic or anaerobic conditions.

Aeration appears to increase MSW settlement in both P_1 and P_2. Strain of P_1 is raised to 1.9% from 1.4% (36% increase) and ε_2 is increased to 13.8% from 8.9% (55% increase) (Figure

10-4d). For both aerobic and anaerobic tests, ε_1 represents 13% (COV=0.94 and 0.88) and ε_2 87% (COV=0.13 and 0.13) of total strain, respectively.

Mean C_{LT1} and C_{LT2} in aeration tests are 0.015 and 0.259, in comparison to 0.009 and 0.147 in anaerobic tests (Figure 10-4e, Table 10-5). Mean C_{LT1} is increased by 67% and C_{LT2} by 76% under aerobic conditions compared to anaerobic, confirming the expedited biodegradation. Mean C_{LT2}/C_{LT1} ratio is raised from 12.5 to 15.8 when waste is aerated.

Aeration reduces t_1 and increases ε_1 by accelerating microbial growth. Thus transition to active biodegradation phase occurs earlier (Madigan et al. 2010). Higher C_{LT1} under aeration conditions suggests faster settlement due to faster initiation of biodegradation. In P_2, more bio-accessible MSW is biodegradable in the presence of oxygen, thus ε_2 is enhanced. Hydrolysis of solid waste is often the rate limiting step in P_2, but metabolisms of hydrolytic microorganisms are boosted under aerobic condition, resulting in reduced t_2 and increased C_{LT2} (Barlaz et al. 2010b).

10.5.3 **Effect of waste composition**

MSW composition in landfills differs regionally, temporally and spatially (Grellier et al. 2007; Staley and Barlaz 2009; Zekkos et al. 2010b). Waste constituents have been categorized into different groups based on size and type for geotechnical purposes (Dixon et al. 2008). In laboratory experiments, waste particles are often shredded to accommodate smaller simulator sizes. Among the database of 98 tests, 59 tests included size reduction of large waste particles. Of those, 16 tests included shredded waste without providing information about the maximum particle size, 15 tests had maximum waste sizes between 100 to 200 mm, 18 tests had maximum waste sizes between 20 to 50 mm, and the remaining 10 tests had maximum particle size of 20 mm. In the following analysis, 20 mm is adopted as size criterion to separate waste particles into

different fractions (Zekkos et al. 2010b). The >20 mm fraction of waste typically includes organics, paper, plastic, textile, wood, rubber and gravel pieces. The <20 mm fraction includes primarily soil due to the presence of daily soil cover as well as contaminated soils and debris, and shredded fine size waste. Since there is no consistent approach for the classification of waste size and composition, some inconsistencies in reported quantity of various waste constituents are observed making interpretation of results more difficult.

The anaerobic datasets are analyzed to study the impact of waste composition on the long-term settlement. Figure 5 shows the relationships of strain and compression ratio as a function of percentage of >20 mm fraction of waste. Mean strain of P_2 increases from 2.7% to 8.6% and C_{LT2} from 0.039 to 0.156 with increasing percentage of >20 mm fraction of waste (Figure 10-5a and Figure 10-5b).

<20 mm fraction of MSW consisting mainly of soil has relatively low compressibility due to long-term biodegradation compared to the >20 mm fraction. In contrary, >20 mm fraction such as paper and plastic containers is deformable and undergoes compressions of both bio-accessible and bio-inaccessible voids. Many particles with size larger than 20 mm are also subject to continuous biodegradation and their volume is reduced due to immediate compression and long-term settlement. As a result, higher and faster settlement is observed for specimen with more >20 mm fraction of waste. This conclusion is in accordance with previous observations that MSW compressibility increases with the amount of >20 mm fraction (Kavazanjian et al. 1999; Reddy et al. 2011).

10.5.4 **Effect of total unit weight**

For the data available in the literature, the weight, height and total unit weight (γ_t) of each MSW specimen after immediate compression and initial moisture addition to field capacity are

calculated. As discussed, external vertical stress application causes immediate compression and higher γ_t prior to long-term settlement (Kavazanjian 2001; Zekkos et al. 2006), whereas aeration evaporates moisture and lowers γ_t (EPA 2000; Yazdani et al. 2010). To isolate the influence of these two important factors, and study the effect of initial unit weight on long-term settlement of MSW, the 26 anaerobic tests without external vertical stress (Table 10-3) are analyzed. The anaerobic data generally indicates that strain of Phase 2 reduces with increasing γ_t (Figure 10-6a). Similarly, higher long-term compression ratios are observed when γ_t is lower than 6 kN/m^3 (Figure 10-6b).

The observed trends are justified. The >20 mm fraction of waste includes biodegradable waste (food, yard waste, and paper) with γ_t between 5 and 11 kN/m^3 or non-biodegradable large particles (plastic, hollow metal containers, rubber, leather, textile and etc.) with γ_t from 2 to 4 kN/m^3 (Tchobanoglous and Kreith 2002). The <20 mm fraction of waste has similar γ_t as organic soils, in the order of 15 kN/m^3 or possibly higher (Zekkos et al. 2006). Thus the γ_t of MSW will depend on its composition with typical field γ_t commonly varying from 5 to 15 kN/m^3 (Kavazanjian 2001; Zekkos et al. 2006). When a mixture of waste has low γ_t, one can expect significant amount of >20 mm fraction of waste. When γ_t is higher than 10 kN/m^3 at no vertical stress, a considerable portion of <20 mm fraction should be expected (Zekkos et al. 2006). The <20 mm fraction reduces hydraulic conductivity and secludes biodegradable waste from microorganisms (Olivier and Gourc 2007; Breitmeyer and Benson 2011; Reddy et al. 2011).

10.5.5 **Effect of simulator size**

The size of the specimen is a critical consideration in MSW testing. Small size simulators have been used to include uniform and milled waste specimens for MSW biodegradation studies. These specimens are not representative of the waste disposed of in landfills where typical MSW

is not processed. Size reduction of biodegradable particles to accommodate small simulator sizes has been shown in the laboratory to increase bio-accessibility and consequently biodegradation rate (Hartmann et al. 2000; Hansen et al. 2003), leading to increased strains and compression ratios (Hossain et al. 2003; Mahar et al. 2009; De la Cruz and Barlaz 2010). Larger size simulators are constructed in an effort to better represent field conditions. A minimum diameter of 0.3 m has been suggested by Zekkos et al. (2008) and Bray et al. (2009) for triaxial testing, Athanasopoulos (2011a) for direct shear testing, and Bareither et al. (2012b) for landfill simulators.

The anaerobic dataset (Table 10-1 and Table 10-2) is used to study the effect of simulator size. Figure 7 shows the relationships of strain and compression ratio of P_2 as a function of simulator diameter (m) and specimen height (m). Mean strains of P_2 increase with simulator diameters from 0.1 to 1.3 m. Larger and faster settlement is observed when specimen diameter is larger than 1.0 m, whereas no obvious difference is observed for diameters between 0.1 to 1.0 m (Figure 10-7a and Figure 10-7b). Specimen height does not have obvious influence on ε_2 and C_{LT2} for a range between 0.1 m and 2.4 m (Figure 10-7c and Figure 10-7d). This is probably because of the influence of other factors (e.g. composition, unit weight, operation conditions) on the settlement behavior. Therefore available data is inconclusive to provide recommendation for simulator size.

10.6 Discussion and limitations

Table 10-5 summarizes the mean and standard deviations for the strains, durations and long-term compression ratios for each phase as calculated from the statistical analyses. These results can be

used with equation 4 to generate different long-term settlement scenarios for these simulators (El-Fadel and Khoury 2000; Hossain and Gabr 2005; McDougall 2011):

$$\varepsilon_{total} = \varepsilon_1 + \varepsilon_2 + \varepsilon_3 = C_{LT1} \times log\frac{t_{P1}}{t_0} + C_{LT2} \times log\frac{t_{P2}}{t_{P1}} + C_{LT3} \times log\frac{t_{P3}}{t_{P2}} \qquad (10\text{-}4)$$

where t_{P1}, t_{P2} and t_{P3} are final times of the three phases, and t_0 is assumed to be 1 day.

A long-term compression ratio, C_{LT}, for each phase is adopted in this study. This is a deviation from using a constant secondary compression ratio, C_α, as an average value derived from initial and final testing time and strain of long-term settlement of MSW that has been commonly used by previous researchers (Wall and Zeiss 1995; El-Fadel et al. 1999; Hossain et al. 2003; Olivier and Gourc 2007; Bareither et al. 2012d). C_{LT} differs from C_α in that it represents the rate of settlement calculated for each of the three phases defined previously. This approach is deemed to be more appropriate to characterize long-term settlement because the fundamental mechanisms that are responsible for the long-term settlement are changing in each phase.

Figure 10-8 shows the relationship between strain and time using Eqn. 10-4 for three scenarios: Anaerobic tests with external vertical stress application (as listed in Table 10-1), anaerobic tests without external vertical stress application (as listed in Table 10-3), and aerobic tests without external vertical stress application (as listed in Table 10-4). The relationship is linearized as explained earlier, although a curvature could be added to make a more realistic transition from one phase to the next.

The data in Table 10-5 and Figure 10-8 highlight the significant difference in long-term settlement between the aerobic conditions and the anaerobic conditions, with aerobic conditions leading to higher settlements in shorter durations and, as a consequence, to higher long term

compression ratios. The data also indicates the impact of the application of external vertical stress, which on average, is found to lead to lower strain and compression ratios. Note that the relationship shown in Figure 10-8 is based on average values for all tests with external vertical stress application, but the effect of stress on long-term settlement behavior becomes more pronounced at increasing vertical stresses.

Significant variability is also observed in the data, as expressed by the standard deviations and coefficient of variations. That variability is expected since a number of factors affect the long-term settlement of MSW in these simulators. Some of these factors (i.e. impact of external vertical stress application, aeration, waste composition, total unit weight and the size of simulator) have been investigated on the basis of the statistical analyses of the nearly 100 tests, yielding systematic trends. Some other factors that are expected to influence degradation rates have not been studied, for example the method and frequency of recirculation is known to have an impact on long-term settlement (Reinhart and Townsend 1998; Vavilin et al. 2003; Bareither et al. 2010), but has not been investigated in this study and represents a limitation.

One critical issue that is not addressed in this study, but should affect long-term settlement is the size reduction of large waste particles of the tested waste specimens. No definitive conclusion could be made as part of this study on the impact of waste processing, although it is recognized that any shredding of waste alters the particle size compared to that in the field. Hossain et al. (2003) did not observed an effect of shredding on compressibility of MSW, whereas other researchers suggested increased compressibility (Landva and Clark 1990) after particle size reduction.

Another limitation of this study is that a significant number of the tests approach, but do not reach, Phase 3 (residual phase). As a consequence, there is more limited data on the long-

term behavior of MSW in Phase 3 and the duration and strain of P_2 may be underestimated. However, the available data indicates that the contribution of Phase 3 to the long-term settlement is small.

10.7 Conclusion

Three phases of long-term settlement of MSW are identified. Phase 1 is transitional phase from immediate compression to long-term settlement before the onset of active biodegradation. Active biodegradation (Phase 2) dominates the long-term settlement and is responsible for high strains and high long-term compression ratio of MSW. Long-term settlement continues indefinitely in residual phase (Phase 3), but low strain is observed as biodegradable waste becomes depleted and less available. A systematic method to calculate duration, strain and long-term compression ratio of each phase is implemented and 98 tests in laboratory simulators from 29 studies are reviewed and analyzed. For the entire dataset, duration, strain and long-term compression ratio of P_1 are 53 days, 1.2% and 0.009, and that of P_2 are 162 days, 9.5% and 0.168. Strain and long-term compression ratio of P_3 are on average 0.3% and 0.011. The active biodegradation phase (P_2) dominates the long-term settlement of MSW.

The effects of external vertical stress application and aeration on long-term settlement of MSW are investigated. External vertical stress reduces long-term settlement. Application of vertical stress of 500 kPa reduces duration of P_2 by 29%, strains of P_1 by 86% and P_2 by 80%, and long-term compression ratios of P_1 by 89% and P_2 by 75% compared to tests at no external vertical stress. Aeration has a significant impact on the long-term settlement. Aeration accelerates biochemical reactions and increases strains of P_1 by 36% and P_2 by 55%, while

reducing durations of P_1 by 50% and P_2 by 60% compared to anaerobic cases. As a result, in aerobic case long-term compression ratios of P_1 is increased by 67% and P_2 by 76%.

The impact of waste composition, total unit weight and simulator size on the long-term settlement behavior are also statistically investigated. Increasing >20 mm fraction of waste results in higher strain and long-term compression ratio in P_2. Higher total unit weights of specimens result in lower ε_2 and C_{LT2}. The data indicates differences in settlement between simulators that are smaller than 1.0 m compared to simulators that are larger than 1.0 m in diameter, but the specimen height does not seem to influence the results. As a consequence no final conclusion can be drawn presently from the statistical analysis on the impact of the simulator size on the long-term settlement of MSW.

10.8 Tables

Table 10-1 Data of anaerobic tests with external vertical stress application.

Reference	σ_v (kPa)	Mois-ture[a]	W_c (%)	Biod. (%)[b]	t_{LT1} (d)	t_{LT2} (d)	ε_0[c]	ε_{LT1}	ε_{LT2}	C_{LT1}	C_{LT2}
Bareither et al. (2012c)	8	R	56	69	60	237	0.251	0.009	0.112	0.005	0.161
	8	R	56	69	18	110	0.266	0.007	0.085	0.005	0.101
	8	S	56	69	16	179	0.266	0.006	0.065	0.005	0.059
Bareither (2010)	68	R	31	23	28	32	0.203	0.009	0.087	0.007	0.262
	400	R	31	23	45	141	0.432	0.011	0.146	0.007	0.282
	64	R	31	23	51	230	0.218	0.010	0.141	0.006	0.271
	68	R	31	23	83	64	0.126	0.025	0.044	0.013	0.175
	64	R	31	23	78	75	0.047	0.044	0.070	0.023	0.159
	64	R	60	23	29	194	0.238	0.008	0.037	0.005	0.042
	400	R	40	23	41	63	0.447	0.006	0.017	0.004	0.041
	64	R	46	23	8	118	0.220	0.002	0.010	0.002	0.008
	400	R	53	23	26	194	0.458	0.009	0.050	0.006	0.054
	64	R	54	23	27	191	0.214	0.005	0.038	0.003	0.042
	68	R	29	0	13	45	0.199	0.002	0.032	0.002	0.048
	400	R	28	0	48	45	0.427	0.007	0.031	0.004	0.109
	64	R	28	0	55	100	0.291	0.006	0.110	0.004	0.243
	68	R	29	45	24	46	0.228	0.038	0.140	0.027	0.299
	400	R	29	45	47	39	0.529	0.007	0.062	0.004	0.232
	64	R	29	45	62	174	0.273	0.016	0.155	0.009	0.349
Chen et al. (2010)	150	R	50	59	48	156	0.337	0.014	0.193	0.009	0.350
de Abreu (2003) de Abreu et al. (2005)	14	R	57	61	25	339	0.379	0.012	0.086	0.009	0.074
	14	R	21	61	22	342	0.358	0.017	0.087	0.013	0.071
	14	F	36	61	98	283	0.361	0.032	0.072	0.016	0.121
Ivanova et al. (2008)	150	R	139	51	61	345	0.541	0.017	0.187	0.009	0.227
	50	R	166	51	24	212	0.353	0.023	0.172	0.017	0.173
	50	R	152	51	179	751	0.432	0.013	0.120	0.006	0.179
Kim (2005) Kim et al. (2011)	98	S	149	70	202	519	0.016	0.008	0.085	0.003	0.153
	98	S	149	70	265	452	0.015	0.004	0.179	0.001	0.414
Liao (2006) Liao (2007)	58	F	50	45	26	167	0.045	0.021	0.106	0.015	0.121
Liu (2010) Liu et al. (2009)	100	R	159	76	104	261	0.468	0.009	0.152	0.004	0.307
	200	R	159	76	122	244	0.526	0.027	0.097	0.013	0.233
	400	R	159	76	117	250	0.590	0.016	0.071	0.008	0.158
Olivier and Gourc (2007)	130	R	59	55	218	430	0.323	0.005	0.165	0.002	0.348
Peng (2004) Liu et al. (2005)	10	F	49	63	29	126	0.032	0.024	0.181	0.017	0.250
	10	S	49	63	11	46	0.022	0.006	0.026	0.006	0.035
	10	F	49	63	13	75	0.021	0.006	0.086	0.005	0.103
	10	S	49	63	19	55	0.028	0.009	0.031	0.007	0.053

Sheridan (2003)	500	R	57	68	65	122	0.006	0.003	0.020	0.002	0.044
	500	R	56	68	49	140	0.006	0.001	0.017	0.001	0.029
Sun (2007) Kong et al. (2006)	50	R	84	20	17	55	0.057	0.001	0.038	0.001	0.060
	100	R	84	20	11	65	0.096	0.001	0.016	0.001	0.019
	25	R	121	53	9	42	0.138	0.003	0.023	0.003	0.031
	200	R	121	53	20	89	0.379	0.007	0.068	0.005	0.091
	25	R	150	53	19	104	0.310	0.021	0.074	0.017	0.091
	100	R	150	53	6	58	0.541	0.002	0.022	0.002	0.021
	25	R	94	80	8	49	0.062	0.004	0.030	0.004	0.036
	50	R	94	80	12	75	0.131	0.000	0.024	0.000	0.029
Swati and Joseph (2008)	9	S	163	NR[d]	156	238	0.186	0.045	0.154	0.021	0.383
	9	R	138	NR	161	236	0.112	0.060	0.199	0.027	0.508
Wall and Zeiss (1995)	10	R	128	63	19	157	0.338	0.008	0.032	0.006	0.033
	10	R	126	63	15	195	0.367	0.004	0.043	0.003	0.037
	10	R	134	63	15	200	0.340	0.005	0.064	0.004	0.055

Note: tests without plotted settlement curve but reported discrete results are not tabulated but included in corresponding analysis in the following sections.

[a] Moisture addition method: S: initial saturation; F: flushing with fresh water; R: leachate recirculation.

[b] Percentage of biodegradable waste.

[c] Immediate compression strain.

[d] NR: not reported.

Table 10-2 Data of aerobic tests with external vertical stress application.

Reference	σ_v (kPa)	Aeration[b] (m^3/d)	Moisture	W_c (%)	Biod. (%)	t_{LT1} (d)	t_{LT2} (d)	ε_0	ε_{LT1}	ε_{LT2}	C_{LT1}	C_{LT2}
Kim (2005)	98	0.1	S	149	70	69	289	0.022	0.011	0.152	0.006	0.213
Kim et al. (2011)	98	0.1	S	149	70	46	308	0.020	0.009	0.175	0.005	0.199
Sheridan (2003)	500	0.7	R	57	68	89	84	0.011	0.001	0.042	0.000	0.145
	500	0.7	R	56	68	104	84	0.007	0.002	0.043	0.001	0.166

Note: tests without plotted settlement curve but reported discrete results are not tabulated but included in corresponding analysis in the following sections.

[a] Moisture addition method: S: initial saturation; F: flushing with fresh water; R: leachate recirculation.

[b] Percentage of biodegradable waste.

[c] Immediate compression strain.

Table 10-3 Data of anaerobic tests without external vertical stress application.

Reference	Mois-ture	W_c (%)	Biod. (%)	t_{LT1} (d)	t_{LT2} (d)	ε_0	ε_{LT1}	ε_{LT2}	C_{LT1}	C_{LT2}
Boni et al. (2006)	R	NR	97	222	334	NR	0.002	0.098	0.001	0.262
	R	NR	87	65	125	NR	0.009	0.102	0.005	0.218
	R	NR	70	60	138	NR	0.000	0.007	0.000	0.020
Chen et al. (2008)	F	50	45	18	112	0.156	0.037	0.132	0.029	0.155
Chen (2009) Chen et al. (2010)	R	47	49	29	350	0.150	0.028	0.195	0.019	0.175
Elagroudy et al. (2008)	R	NR	60	8	42	0.177	0.020	0.074	0.022	0.095
	R	NR	100	6	31	0.073	0.003	0.016	0.003	0.021
Fang (2005)	S	83	45	18	173	0.193	0.008	0.077	0.006	0.074
	R	83	45	23	169	0.191	0.015	0.157	0.011	0.172
Feng (2009) Feng et al. (2009)	F	65	63	22	271	NR	0.008	0.080	0.006	0.073
	F	65	63	30	174	NR	0.009	0.051	0.006	0.062
	S	52	63	12	169	NR	0.002	0.055	0.002	0.046
	S	52	63	12	169	NR	0.001	0.070	0.001	0.059
Gourc et al. (2010)	F	97	34	96	328	0.046	0.005	0.123	0.002	0.190
	F	36	34	107	359	0.023	0.016	0.152	0.008	0.306
	F	97	34	103	334	0.008	0.008	0.121	0.004	0.243
	F	36	34	104	332	0.015	0.003	0.136	0.002	0.389
Jin (2005) Elagroudy et al. (2008)	R	203	87	12	80	0.110	0.022	0.119	0.020	0.136
Stessel and Murphy (1992)	R	NR	NR	14	21	0.127	0.015	0.068	0.013	0.172
Sun et al. (2011)	R	77	77	61	194	0.240	0.049	0.046	0.027	0.074
Swati and Joseph (2008)	S	39	NR	161	234	0.029	0.031	0.087	0.014	0.223
	R	37	NR	116	278	0.021	0.035	0.106	0.017	0.199
	F	39	NR	139	245	0.024	0.036	0.086	0.017	0.193
Wang (2007)	R	5	3	37	41	0.045	0.005	0.017	0.003	0.054
	R	13	30	16	49	0.080	0.002	0.077	0.001	0.126
	R	13	30	15	52	0.013	0.002	0.057	0.002	0.087

Note: tests without plotted settlement curve but reported discrete results are not tabulated but included in corresponding analysis in the following sections.

[a] Moisture addition method: S: initial saturation; F: flushing with fresh water; R: leachate recirculation.

[b] Percentage of biodegradable waste.

[c] Immediate compression strain.

[d] NR: not reported.

Table 10-4 Data of aerobic tests without external vertical stress application.

Reference	Aeration (m^3/d)[e]	Moisture	W_c (%)	Biod. (%)	t_{LT1} (d)	t_{LT2} (d)	ε_0	ε_{LT1}	ε_{LT2}	C_{LT1}	C_{LT2}
Elagroudy et al. (2008)	Pass.	R	NR	100	27	138	0.030	0.003	0.079	0.002	0.100
	Pass.	R	NR	100	27	138	0.048	0.007	0.085	0.005	0.110
	Pass.	R	NR	100	27	135	0.069	0.001	0.072	0.001	0.098
Jin (2005)	21.6	S	187	87	16	68	0.093	0.003	0.174	0.003	0.244
Elagroudy et al. (2008)	21.6	R	229	87	16	84	0.089	0.008	0.124	0.007	0.156
	21.6	S	240	71	18	77	0.172	0.020	0.076	0.016	0.105
Mahar et al. (2009)	Pass.	F	55	75	15	39	0.161	0.114	0.187	0.096	0.399
Stessel and Murphy (1992)	12.1	R	NR	NR	15	35	0.129	0.001	0.068	0.000	0.131
	203.9	R	NR	NR	7	51	0.184	0.019	0.122	0.022	0.254
	611.7	R	NR	NR	12	41	0.158	0.034	0.162	0.032	0.249
Sun et al. (2011)	Pass.	R	77	77	189	118	0.076	0.025	0.079	0.011	0.373
Tang et al. (2008)	Pass.	R	105	29	17	47	0.329	0.008	0.278	0.007	0.486
	Pass.	R	105	29	18	46	0.362	0.011	0.301	0.009	0.542
	Pass.	R	105	29	18	47	0.373	0.012	0.284	0.009	0.513
Wang (2007)	Pass.	R	27	30	22	56	0.119	0.023	0.065	0.017	0.264
	Pass.	R	27	30	17	61	0.114	0.020	0.059	0.016	0.114

Note: tests without plotted settlement curve but reported discrete results are not tabulated but included in corresponding analysis in the following sections.

[a] Moisture addition method: S: initial saturation; F: flushing with fresh water; R: leachate recirculation.

[b] Percentage of biodegradable waste.

[c] Immediate compression strain.

[d] NR: not reported.

[e] Aeration modes: Pass.: passive.

Table 10-5 Means and standard deviations of t_1, t_2, ε_1, ε_2 and ε_{total} for four long-term settlement scenarios.

Scenario	All inclusive	Anaerobic with external stress	Anaerobic without external stress	Aerobic without external stress
# of tests	98[a]	52	26	16
$t_1 \pm \delta$ (day)	53 ±56	56 ±60	58 ±57	29 ±43
$t_2 \pm \delta$ (day)	162 ±126	176 ±140	185 ±112	74 ±37
$\varepsilon_1 \pm \delta$ (%)	1.2 ±1.6	1.3 ±1.3	1.4 ±1.4	1.9 ±2.7
$\varepsilon_2 \pm \delta$ (%)	9.5 ±6.2	8.4 ±5.6	8.9 ±4.5	13.8 ±8.4
$\varepsilon_{total} \pm \delta$ (%)[b]	11.0 ±7.0	9.7 ±6.5	10.3 ±5.1	15.9 ±9.3
C_{LT1}	0.009 ±0.012	0.008 ±0.007	0.009 ±0.009	0.015 ±0.023
C_{LT2}	0.168 ±0.126	0.150 ±0.124	0.147 ±0.093	0.259 ±0.158
C_{LT3}	0.011±0.018[c]	-	-	-

[a] Included 4 tests with both aeration and external vertical stress application listed in Table 10-2 and all other tests.

[b] As-observed total strain, not ultimate total strain of MSW.

[c] Data from 15 tests that reached P_3.

10.9 Figures

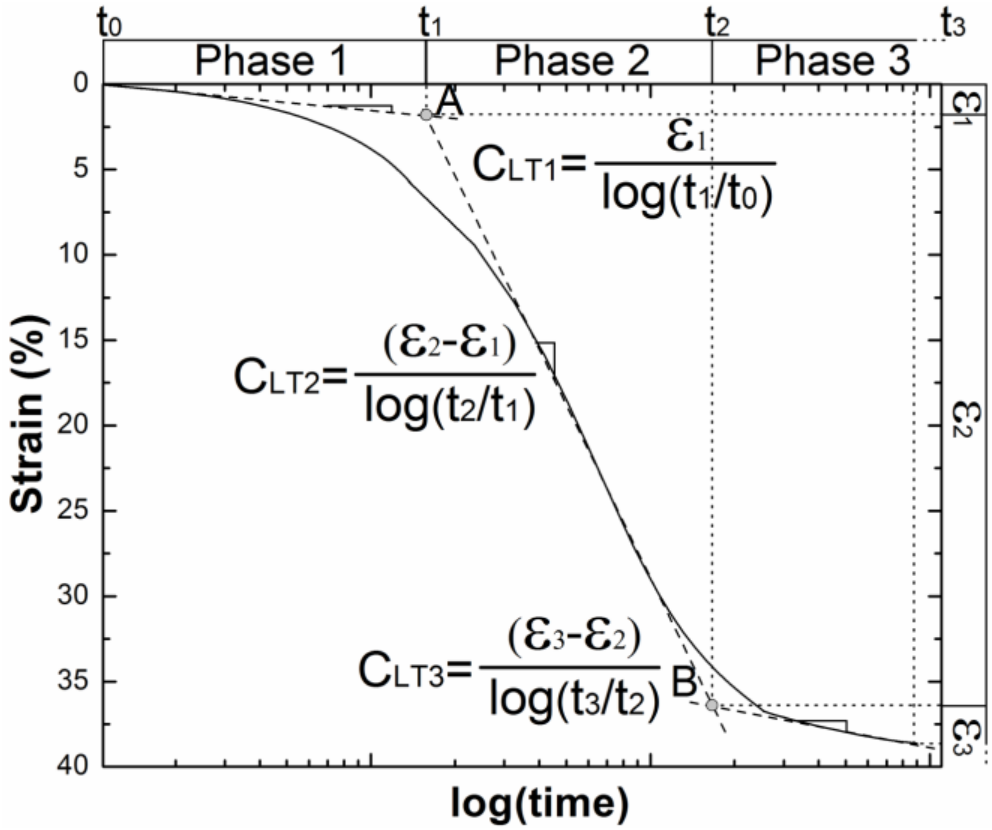

Figure 10-1 Idealized strain versus logarithmic time curve for long-term settlement of MSW.

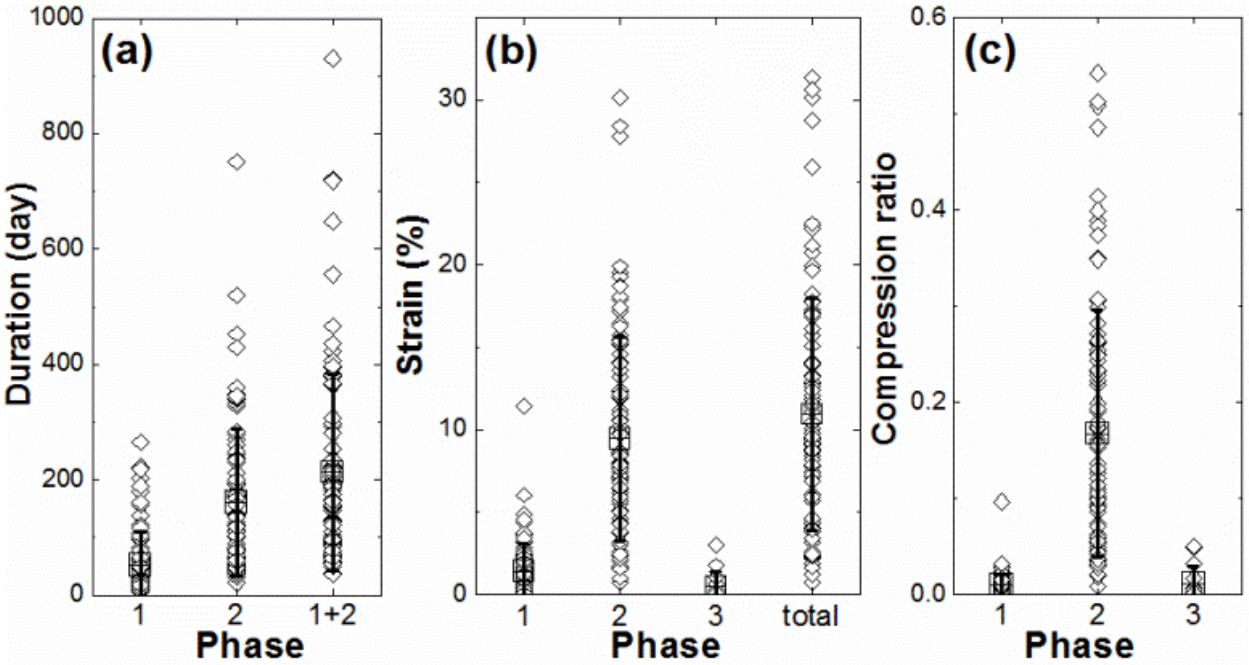

Figure 10-2 Mean values, standard deviations and individual values of (a) t_1, t_2 and t_{1+2}; (b) ε_1, ε_2, ε_3 and ε_{total}; (c) C_{LT1}, C_{LT2} and C_{LT3}.

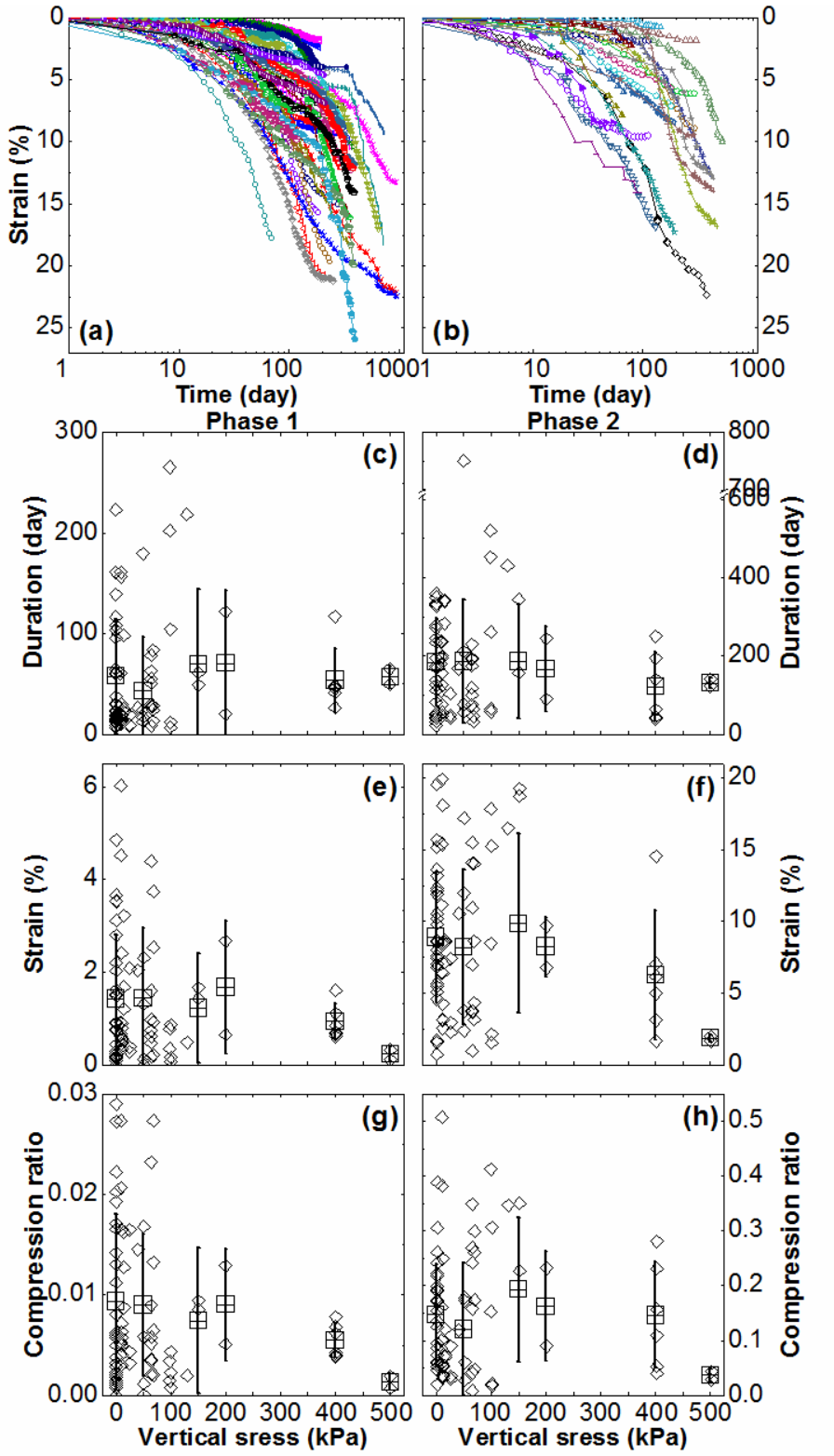

Figure 10-3 Waste settlement curves (a) with external vertical stress application and (b) without external vertical stress application; effects of vertical stress on Phase 1: (c) t_1, (e) ε_1 and (g) C_{LT1} and Phase 2: (d) t_2, (f) ε_2 and (h) C_{LT2}; square symbol and bar: mean values and standard deviations at increment of 50 kPa, ◊: individual test data.

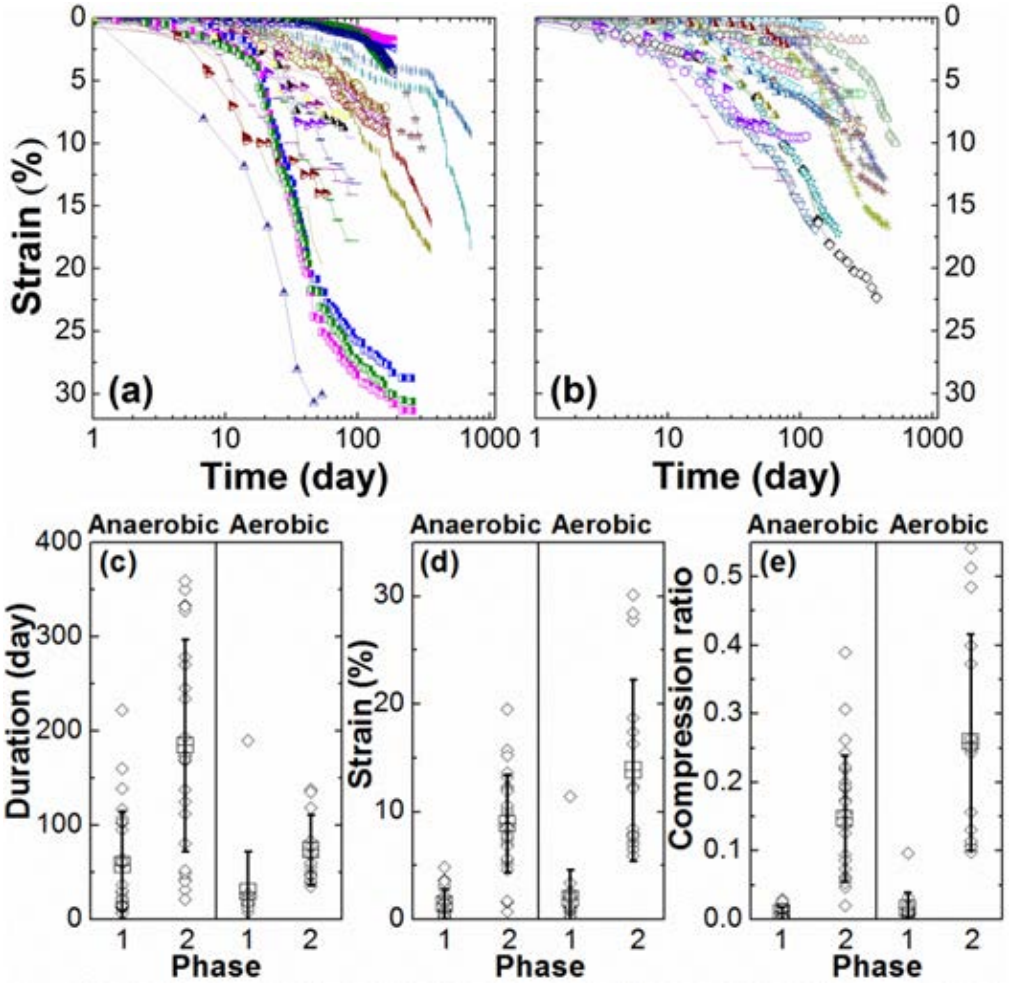

Figure 10-4 Settlement curves (a) with aeration and (b) without aeration (anaerobic); effects of aeration on (c) t_1 and t_2; (d) ε_1 and ε_2; (e) C_{LT1} and C_{LT2}.

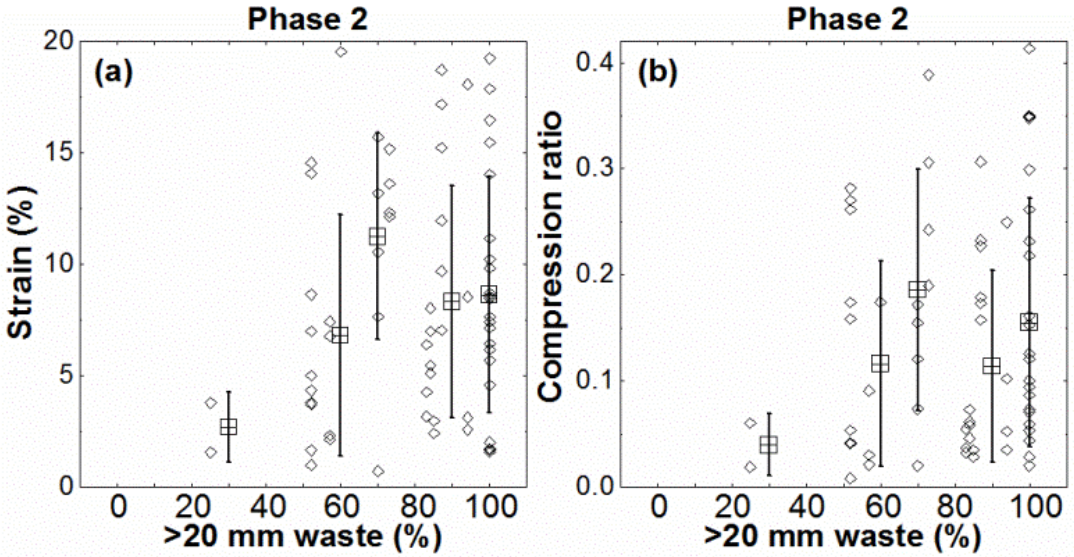

Figure 10-5 Effects of >20 mm fraction of waste on ε_2 (a) and C_{LT2} (b); square symbol and bar: mean values and standard deviations at increment of 10% of total weight, ◊: individual test data.

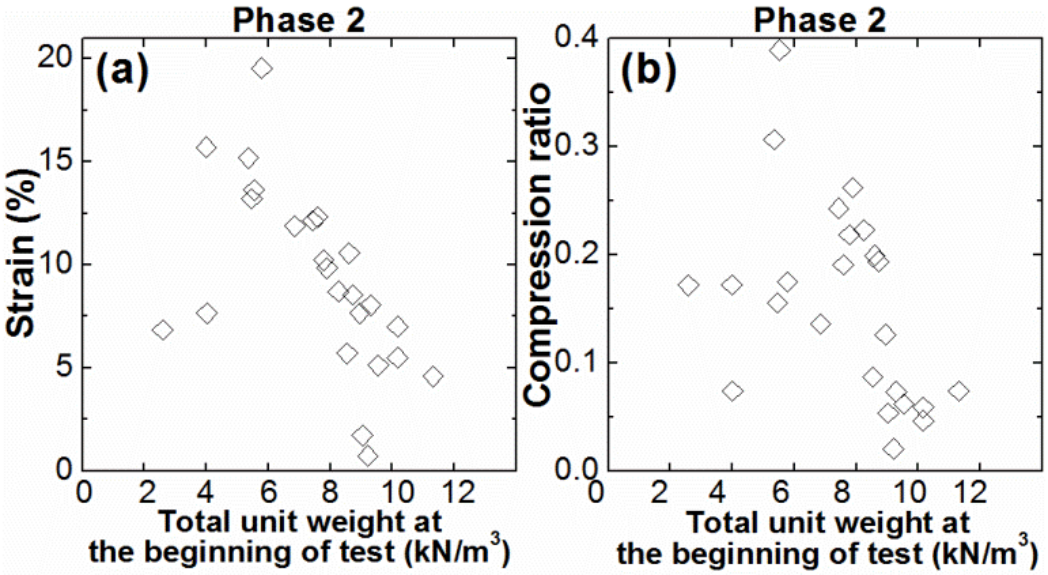

Figure 10-6 Effects of total unit weight on (a) ε_2 and (b) C_{LT2}. ◊: individual test data.

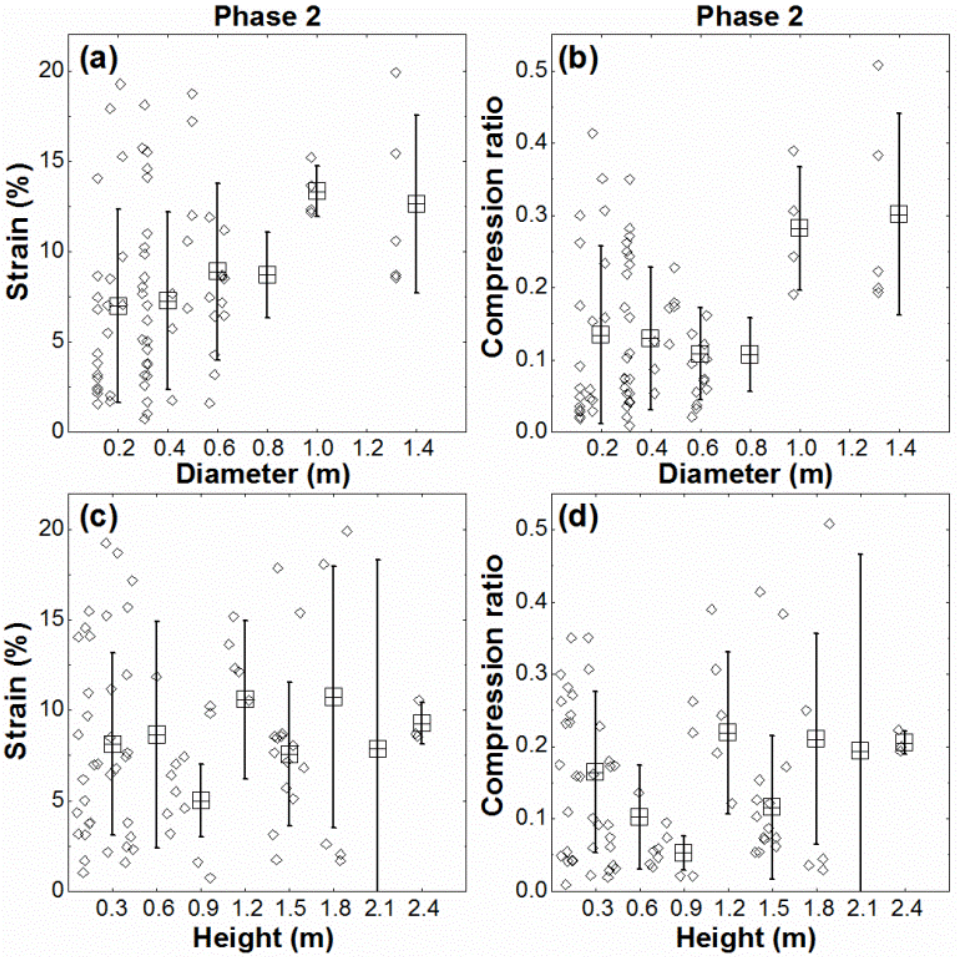

Figure 10-7 Changes of ε_2 and C_{LT2} with (a) and (b) diameter; (c) and (d) height; square symbol and bar: mean values and standard deviations at increment of 0.2 m for diameter and 0.3 m for height, ◊: individual test data.

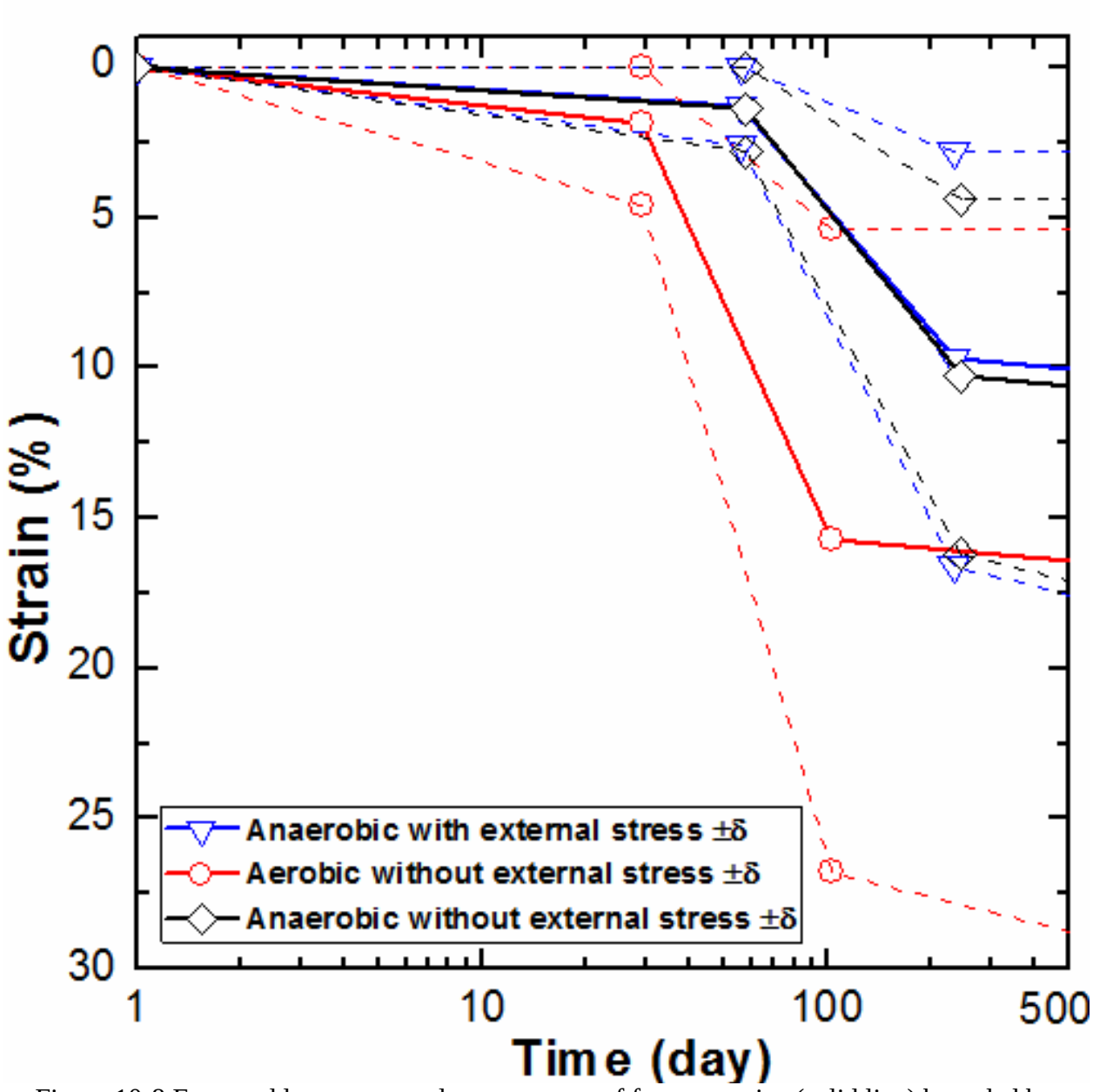

Figure 10-8 Expected long-term settlement curves of four scenarios (solid line) bounded by standard deviations (dash lines).

PART V SUMMARY

Chapter 11 Engineering Significance, Conclusions, Limitations, and Recommendations for Future Work

11.1 Engineering significance

This dissertation contributes to answer three outstanding research questions related to landfilled MSW.

To investigate "***what processes take place during MSW biodegradation and how to monitor them***", a unique versatile large-size laboratory simulator setup for biodegradation of MSW is developed and a series of experiments on MSW sampled from multiple landfills across the U.S. is conducted. The presented long-term experimental results improve the fundamental understanding of the concurring and interdependent biochemical-physical-mechanical-hydraulic processes taking place during MSW biodegradation in a realistic time-scale. The trends of a group of characteristics in leachate, biogas, solid waste and microbial community are found to be informative of the respective processes and very systematic during MSW biodegradation despite of varying initial waste composition of the specimens. As a result, the observed behavior of biodegrading MSW in landfills can be better explained. In addition, the identified time-dependent characteristics are relatively easy to measure or test not only in the laboratory, but also in the field. Therefore, the findings contribute to our ability to achieve more reliable and efficient monitoring of biodegradation process of landfilled MSW. Finally, established relationships

between studied characteristics are helpful for estimating the behavior of biodegrading MSW based on a few types of readily available in-situ measurements.

Through a unique and comprehensive experimental dataset on large-size laboratory simple shear and direct shear testing of MSW "***the impact of biodegradation on the physical and mechanical properties of MSW***" is addressed. The laboratory testing results provide realistic estimates of the shear strength and compressibility of fresh and fully-biodegraded landfilled MSW, improving the design of landfills containing continuously-degrading MSW, and specifically, long-term stability and integrity of landfill components. Measurement of shear-wave velocity (V_s) of MSW, a rapid, surface-based and non-intrusive technique, is also used to evaluate the differences between multiple physical and mechanical properties of MSW of similar composition. Specifically, a relationship between V_s and shear strength (τ) of MSW is established based on the results of laboratory testing. As a result, in-situ τ of MSW in landfills can be estimated by combining V_s measurements and estimates of moisture content, dry unit weight and overburden pressure. The evaluation of in-situ V_s and τ of MSW could further ensure the long-term resiliency of landfills against static and dynamic loading.

A database is created using data from the literature on MSW biodegradation processes observed in large-size laboratory experiments and field monitoring of landfills. Subsequently, multiple "***environmental and operating factors that influence MSW biodegradation process***" are identified and their impacts are quantified. The observations suggest that enhancing biodegradation conditions in landfill cells, e.g., by means of controlling additions of moisture, nutrients and microorganisms and maintaining appropriate temperature, would have the highest impact on increasing the first-order generation rate of CH_4 (k) and reducing the delay before the maximum CH_4 generation rate is observed (t_{max}). Optimizing initial percentages of

biodegradable and readily biodegradable waste would increase CH_4 generation potential (L_0) and reduce t_{max} as well, but this is a less critical consideration. For example, one practical approach to accomplish this would be to reduce the amount of daily soil cover mixed with waste. Increasing biogas collection efficiency contributes to higher measured L_0 and k and lower t_{max}, and can be achieved by early placement of gas collection systems, improved sealing of cover, e.g., by using resilient geosynthetic materials as covers, optimizing the closure plans of landfills and the design and operation of biogas collection systems based on site-specific waste composition and biodegradation conditions. Based on the conclusions of this study, guidance is provided on the design, monitoring and operation of landfills to optimize energy generation via controlled biodegradation of landfilled MSW coupled with well-planned biogas collection in landfills.

11.2 Summary of findings

PART I (Chapters 1 and 2) introduces background information for modern Subtitle-D landfills and summarizes state-of-art knowledge on changes of the properties of landfilled MSW during its biodegradation process.

PART II (Chapters 3, 4 and 5) presents the setup and results of a comprehensive experimental investigation on long-term degradation of MSW specimens of different initial waste composition under enhanced biodegradation conditions in a series of seven 0.3 m-diameter laboratory landfill simulators. The main conclusions are:

- Biochemical-physical-hydraulic-mechanical characteristics in liquid, gas and solid phases of MSW were measured with time and MSW degradation process can be divided into three sequential phases, transition phase, active biodegradation phase and residual phase.

- Changes of leachate and biogas properties occurred mostly in the transition and active biodegradation phases. Soluble compounds in leachate were depleted after 100 days and CH_4 generation and biodegradation of waste was largely completed after around 300 days. The hydraulic conductivity (k) of the specimens decreased due to waste degradation.
- The concentration of volatile fatty acids in leachate is proportional to the concentration of soluble chemical oxygen demand (sCOD). CH_4 generation potential (L_0) is dependent on the percentage of biodegradable waste by weight prior to biodegradation (B_0, %), which is defined as the dry weight of paper and volatile solids in soil-like particles divided by the dry weight of a specimen. The maximum CH_4 generation rate ($r_{CH4,max}$) normalized by initial dry weight of waste ($r_{CH4,max}/W_{s,0}$) is correlated to L_0, normalized maximum mass of sCOD and maximum long-term compression ratio ($C_{LT,max}$). The time for pH rise, initiation and maximum rate of CH_4 generation ($t_{rCH4,0}$ and $t_{rCH4,max}$, respectively), and maximum sCOD in leachate are also correlated.
- The DNA concentration in the leachate was indicative of the quantity of microbial biomass and positively related to the CH_4 generation rate. Similar archaeal community structures in the leachate and solid waste were observed throughout the biodegradation process with *Methanobacteriaceae* being dominant.
- Changes of physical and mechanical properties of MSW were observed throughout the transition and active biodegradation phases and continued in the residual phase. Changes in vertical strain (ε), total unit weight at field capacity and when in-submergence ($\gamma_{t,fc}$ and $\gamma_{t,sub}$, respectively) as well as drainable volumetric moisture content (θ_{drain}) of waste continued in decreasing rates even after 1,000 days.

- The settlement of waste in terms of ε can be separated into immediate strain, biodegradation strain and mechanical creep strain corresponding to the three sequential phases of MSW biodegradation. The final biodegradation strain ($\varepsilon_{B,f}$) is dependent on B_0 and correlates well with L_0. $C_{LT,max}$ increases with increasing $\varepsilon_{B,f}$. The changes in $\gamma_{t,fc}$ and θ_{drain} are also dependent of ε_{LT}. The k of waste can be estimated from the θ_{drain}.

PART III (Chapters 6 and 7) assesses the shear strength (τ) of more than 100 MSW specimens representing variable waste composition, overburden pressure (σ_v), compaction effort, and degree of degradation encountered in landfills using a unique 0.3 m-diameter simple shear testing device. The shear-wave velocity (V_s) of MSW, a property that can be measured non-invasively and rapidly *in situ*, was measured for each waste specimen prior to shear testing. The compressibility characteristics of MSW specimens are assessed prior to shear testing as well. The main conclusions are:

- Shear resistance at 10% of shear strain is used as the τ of waste specimens. The τ of waste in constant load tests is on average 15% higher than in constant volume tests. Longer vertical stress duration and higher shearing strain rate in simple shear testing results in higher τ of identical waste specimens.
- Increasing compaction effort results in higher total and dry unit weight (γ_t and γ_d, respectively), τ and V_s of waste. The τ and V_s both increased when the amount of <20 mm material in a specimen is increased. The soil type of <20 mm material influences the τ of waste. Higher percentage of >20 mm flexible fibrous waste results in lower τ in simple shear testing and V_s of waste. The V_s of MSW also increases with increasing frequency of the input shear wave. The τ and V_s of waste and their stress-corrected values, τ/σ'_{v0} and V_{s1}, are correlated with each other.

- During MSW degradation, multiple processes occur and many characteristics of MSW are changed. The τ and V_s of waste could either increase or decrease after degradation.
- The modified compression coefficient (C_{ce}), normalized constrained modulus (D') and modified secondary compression ratio ($C_{\alpha e}$) of MSW are largely confining stress independent. They are also impacted primarily by waste composition and γ_t with waste composition being a critical factor. The % of <20 mm material and the γ_t of the material can be used to provide a reasonable estimate of the compressibility parameters.
- The type of waste constituent (i.e., paper, plastic or wood) can have a significant effect on the compressibility characteristics of the MSW. Also, because of the anisotropic structure of the MSW, the direction of compression load compared to the fibrous constituent orientation is important.
- Relationships of C_{ce}, (or D'), $C_{\alpha e}$ as a function of waste composition and γ were derived. The relationships shown can be used for specimens at any degradation state, as long as the waste composition and γ_t are known. Typical ratios of $C_{\alpha e}/C_{ce}$ for MSW are between 0.01-0.04.

PART IV (Chapters 8, 9 and 10) quantifies the impacts of various environmental and operating conditions on MSW biodegradation using the results presented in the previous chapters and supplementary data synthesized from the literature. Specifically, processes of CH_4 generation, long-term settlement, and change in waste structure are investigated. The main conclusions are:

- Both B_0 and the density of biodegradable waste prior to biodegradation and after immediate compression ($\gamma_{B,I}$, B_0 multiplies γ_d of a specimen after immediate compression) are identified as characteristic parameters of waste composition. For practical purposes, the moisture

content (w_c) of specimens is categorized into two types ($w_c \geq$ f.c. and $w_c <$ f.c.) based on the respective liquid management procedures and available w_c measurements.

- Normalized maximum mass of sCOD increases with increasing $\gamma_{B,I}$ of specimens. L_0 of waste increases with increasing B_0, and 1% increment of B_0 results in approximately 2.2 L/kg increment of L_0. $r_{CH4,max}/W_{s,0}$ increases with increasing $\gamma_{B,I}$ when $w_c \geq$ f.c. $t_{rCH4,0}$ and $t_{rCH4,max}$ are generally longer for waste having higher $\gamma_{B,I}$.
- Both $\varepsilon_{B,f}$ and $C_{LT,max}$ of waste increase with increasing $\gamma_{B,I}$. Specimens of higher $\gamma_{B,I}$ and lower dry unit weight (γ_d) after immediate compression tend to have lower final γ_d after degradation. k of waste decreases with increasing γ_d of tested specimen. Higher $\gamma_{B,I}$ of waste results in larger reduction of k due to biodegradation compared to its initial value.
- Although $r_{CH4,max}/W_{s,0}$ increases with increasing $\gamma_{B,I}$ of waste when $w_c \geq$ f.c., no clear correlation is observed between $r_{CH4,max}/W_{s,0}$ and $\gamma_{B,I}$ when w_c of waste is < f.c. Both $t_{rCH4,0}$ and $t_{rCH4,max}$ are generally longer for specimens having lower w_c.
- For a given $\gamma_{B,I}$, the values of $\varepsilon_{B,f}$ and $C_{LT,max}$ decrease with increasing σ_v between 10-400 kPa, and the difference between the maximum and minimum values could be more than a factor of 10. Waste at higher σ_v tends to have higher change in final γ_d compared to waste at lower σ_v. The γ_d of waste is typically increased by increasing σ_v, and the k of waste is reduced consequently.
- Correlations are established among the values of $t_{rCH4,0}$ and $t_{rCH4,max}$ and time until maximum long-term compression ratio is observed, with the three time points always occurring consecutively.
- Weight of waste under investigation (W) is correlated with biodegradation conditions of MSW in laboratory experiments and monitoring of full-scale landfills. Waste decay rate (*k*)

increased with increasing percentage of readily biodegradable waste of B_0 and waste temperature, and reduced with increasing W. The values of *k* obtained in the laboratory were significantly higher than in landfills and recommended by EPA's LandGEM model.

- The mean value of L_0 was 98 and 88 L CH_4/kg waste for laboratory and field studies, respectively, but is significantly affected by waste composition. The $t_{rCH4,max}$ increased with increasing B_0 and W. The values of $t_{rCH4,max}$ in landfills were much higher than those in laboratory experiments or those based on LandGEM's recommended parameters.
- The active biodegradation phase dominates the long-term settlement of MSW. Long-term settlement continues indefinitely in residual phase, but low ε is observed as biodegradable waste becomes depleted and less available.

11.3 Limitations of current findings

The laboratory large-size MSW biodegradation experiments are conducted under enhanced biodegradation conditions, minimal overburden pressure and are closely monitored. The obtained results and associated conclusions have the following limitations:

- The experiments are conducted under enhanced biodegradation conditions and minimal overburden pressure, thus the reported accumulation and removal rates of sCOD in leachate, CH_4 generation rate, long-term compression ratio during biodegradation, and change rates of other characteristics in solid waste, leachate and biogas are representative of the testing conditions and are likely upper-bound values of field conditions. Quantitative impacts of sub-optimal biodegradation conditions and high overburden pressure that are frequently encountered in landfills on MSW biodegradation processes are not studied experimentally, but an effort is made to quantify their impact by synthesizing available literature results.

- Each MSW specimen is biodegraded uniformly in a simulator, thus, at a given time point, a single rate value for each of the coupled processes is calculated. Rates of the processes for landfilled MSW varied by depth and location in landfills and are not considered in the dissertation.
- The laboratory experiments are monitored continually and errors of measurements are minimized. The impact of comparatively low availability and accuracy of field measurements on applying the trends and correlations established in this dissertation are not considered.

Laboratory simple shear and direct shear tests are conducted primarily on MSW specimens prepared under minimal compaction effort. MSW in conventional landfills is typically subjected to much higher compaction effort compared to the majority of specimens tested in the dissertation, thus the experimental results on shear strength of MSW are biased low and compressibility of MSW may be biased high. Additional testing is ongoing to address this deficiency. The V_s values of MSW specimens are measured using bender element and/or accelerometer at frequencies higher than 100 Hz and strains lower than 10^{-4}%.

For the literature-based data synthesis and analysis, the observations and conclusions made are limited by the accuracy and sampling and measurement frequency of the data in the studies considered. Variability between the reported results in the literature due to different experimental setups and research methodologies are not accounted for either.

11.4 Recommendations for future work

Given the scope of the dissertation which focuses primarily on laboratory experiments and the limitations discussed previously, several directions for future work are envisioned:

- Additional laboratory experiments degrading MSW under variable biodegradation conditions, e.g., different schemes of addition of moisture, nutrients and microorganisms, different temperature and overburden pressure.
- Assessments of the structure and dynamic of microbial communities in the field which are influenced by multiple varying environmental factors likely provide new insights into MSW biodegradation processes which are microbially-induced.
- More testing on physical and mechanical properties of MSW retrieved from well-monitored laboratory biodegradation experiments at different biodegradation phases are suggested to gain further insight into the evolution of the properties of MSW during biodegradation.
- Closely-monitored and well-understood coupled processes taking place during MSW biodegradation described in the dissertation should be modeled numerically and validated using field monitoring data.
- Established process models of MSW biodegradation in landfills should be applied to improve the effectiveness and efficiency of monitoring and operation of conventional and bioreactor landfills.
- Techniques of accurate, localized and rapid in-situ measurements of the characteristics of biogas, leachate and solid waste should be explored to enhance landfill monitoring, e.g., moisture content, biogas composition, temperature, settlement, and pneumatic and hydrostatic pressure in landfilled MSW.

APPENDIX

Results for Simple Shear and Direct Shear Tests on MSW Specimens and Corresponding Shear-wave Velocity Measurements

CSS Monotonic Shear Test Report

10/28/2013_Version 8.0

Geotechnical Engineering Laboratory

General Test Info and Sample Preparation

Device:	CSS	**Relative Density (%):**	
Specimen ID:	MI-STH	**Void Ratio:**	
Test ID:	MI15	**Height (mm):**	136.5
Date of Test:	10/28/2013	**Soil-Only Specimen Diameter (mm):**	306.2
Test Performed:	Monotonic Shear	**Weight (kg):**	6.96
Test Material:	MSW	**Density (kg/m^3):**	692
Sample Preparation:	Prepared using the same initial composition and unit weight as Sim. 1. Pre-compress for 1 hours.	**Membrane Thickness (mm):**	0.635
		Moisture Content (%):	~20%
		Saturated (Y/N):	N
		Prepared by:	Fei
		Checked by:	Fei

Consolidation Stage		**Shear Stage**	
Vertical Stress (kPa):	120	**Type of Test:**	Constant Volume
Time to Compression (min):	41.8	**Stress or Strain Controlled:**	Strain
Relative Density (%):		**Shear Strain Rate (%/min):**	4.56
Void Ratio:		**Peak Shear Strength (kPa):**	51.8
Height (mm):	109.91	**Comments**	
Diameter (mm):	306.2	Consolidate to 100 kPa in 40 min, stop test to measure Vs, consolidate to 100 kPa in 5 min, monotonic shear	
Weight (kg):	6.96		
Density (kg/m^3):	860		

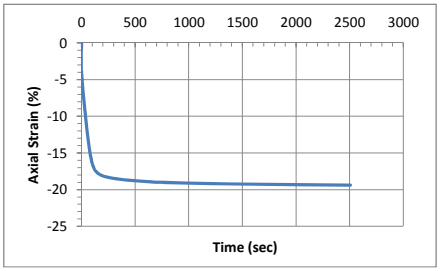

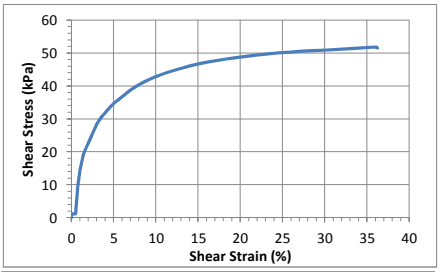

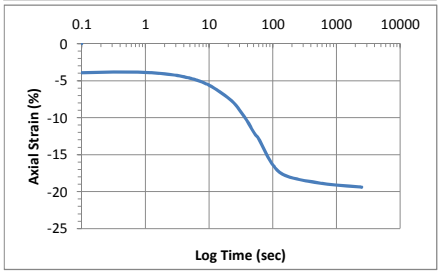

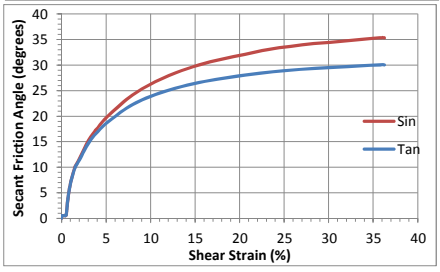

Shear

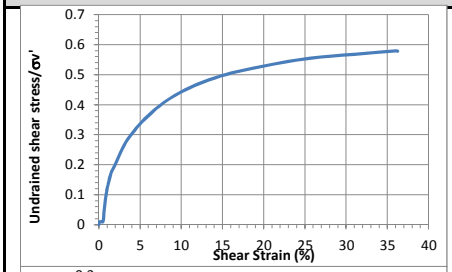

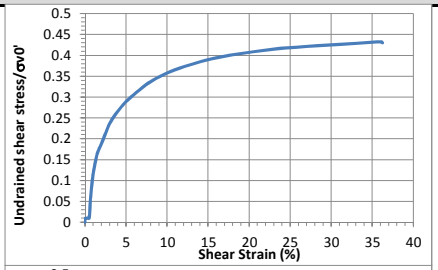

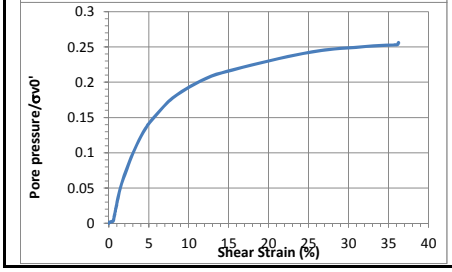

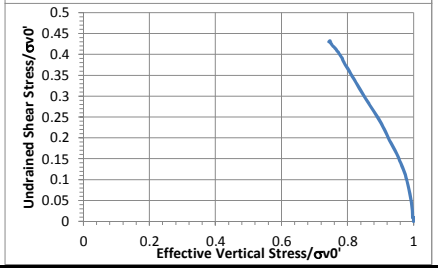

CSS Monotonic Shear Test Report

10/28/2013_Version 8.0

Geotechnical Engineering Laboratory

General Test Info and Sample Preparation

Device:	CSS	**Relative Density (%):**	
Specimen ID:	MI-STH	**Void Ratio:**	
Test ID:	MI16	**Height (mm):**	131.2
Date of Test:	11/4/2013	**Soil-Only Specimen Diameter (mm):**	306.2
Test Performed:	Monotonic Shear	**Weight (kg):**	6.96
Test Material:	MSW	**Density (kg/m^3):**	720
Sample Preparation:	Prepared using the same initial composition and unit weight as Sim. 1. Pre-compress for 140 hours.	**Membrane Thickness (mm):**	0.635
		Moisture Content (%):	~20%
		Saturated (Y/N):	N
		Prepared by:	Fei
		Checked by:	Fei

Consolidation Stage		Shear Stage	
Vertical Stress (kPa):	119	**Type of Test:**	Constant Volume
Time to Compression (min):	61.8	**Stress or Strain Controlled:**	Strain
Relative Density (%):		**Shear Strain Rate (%/min):**	5.09
Void Ratio:		**Peak Shear Strength (kPa):**	69.8
Height (mm):	108.61	**Comments**	
Diameter (mm):	306.2	Consolidate to 100 kPa in 60 min, stop test to measure Vs, consolidate to 100 kPa in 5 min, monotonic shear	
Weight (kg):	6.96		
Density (kg/m^3):	870		

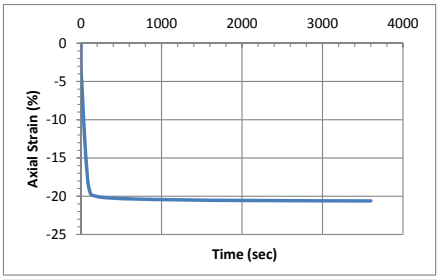

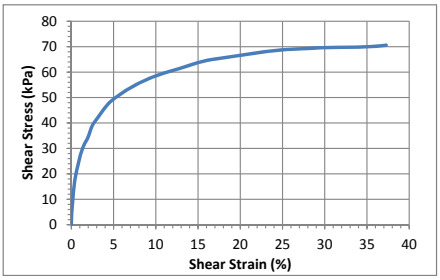

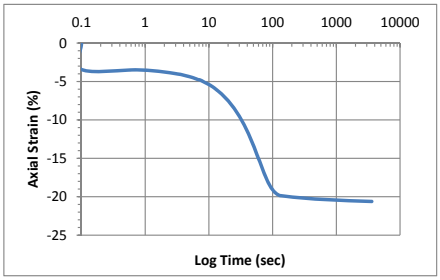

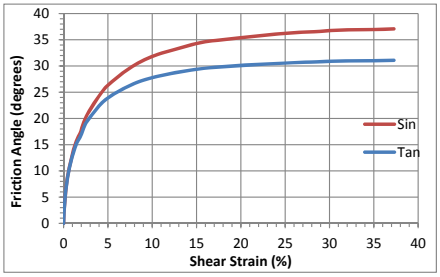

Shear

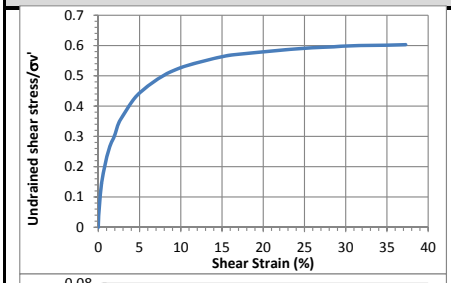

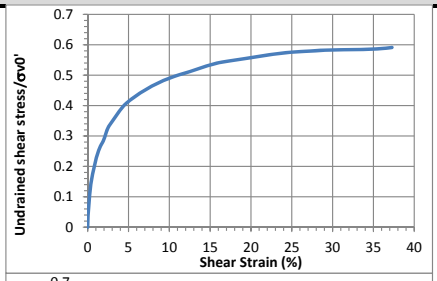

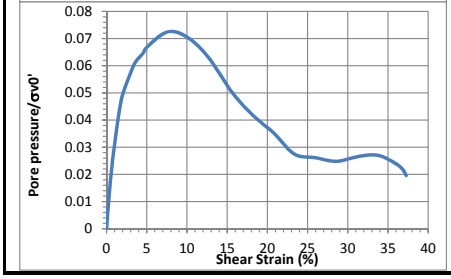

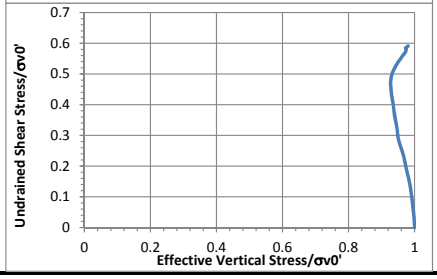

CSS Monotonic Shear Test Report

10/28/2013_Version 8.0

Geotechnical Engineering Laboratory

General Test Info and Sample Preparation

Device:	CSS	**Relative Density (%):**	
Specimen ID:	MI-STH	**Void Ratio:**	
Test ID:	MI20	**Height (mm):**	130.9
Date of Test:	11/26/2013	**Soil-Only Specimen Diameter (mm):**	306.2
Test Performed:	Monotonic Shear	**Weight (kg):**	7.49
Test Material:	MSW	**Density (kg/m^3):**	777
Sample Preparation:	Prepared using the same initial composition and unit weight as Sim. 1. Pre-compress for 26 hours.	**Membrane Thickness (mm):**	0.635
		Moisture Content (%):	~20%
		Saturated (Y/N):	N
		Prepared by:	Alex
		Checked by:	Fei

Consolidation Stage		**Shear Stage**	
Vertical Stress (kPa):	196	**Type of Test:**	Constant Load
Time to Compression (min):	120.8	**Stress or Strain Controlled:**	Strain
Relative Density (%):		**Shear Strain Rate (%/min):**	0.48
Void Ratio:		**Peak Shear Strength (kPa):**	96.9
Height (mm):	103.63	**Comments**	
Diameter (mm):	306.2	Consolidate to 100 kPa in 2 hours, monotonic shear	
Weight (kg):	7.49		
Density (kg/m^3):	981.36		

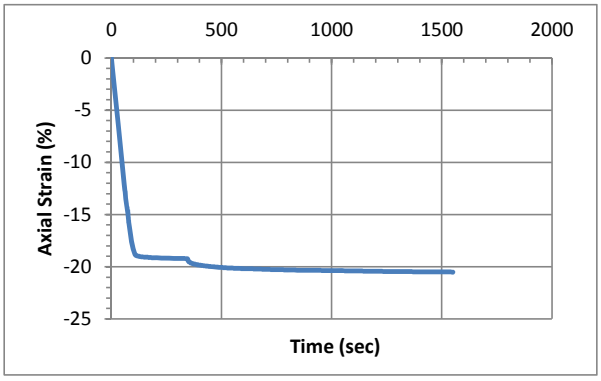

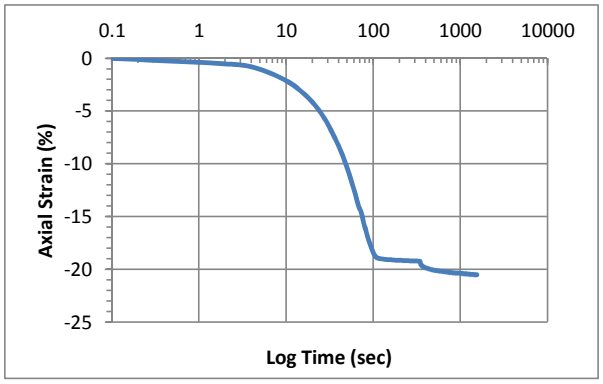

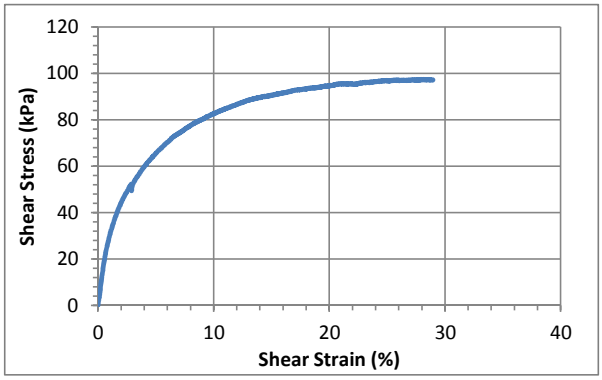

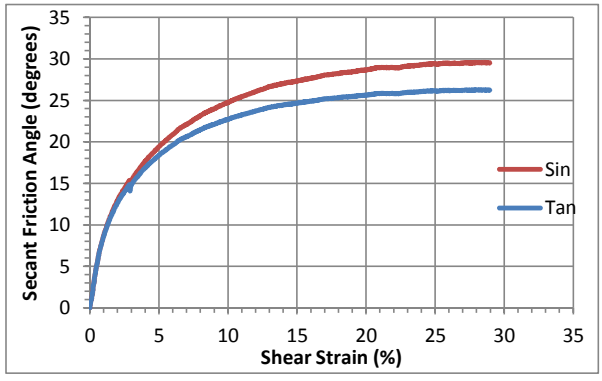

Shear

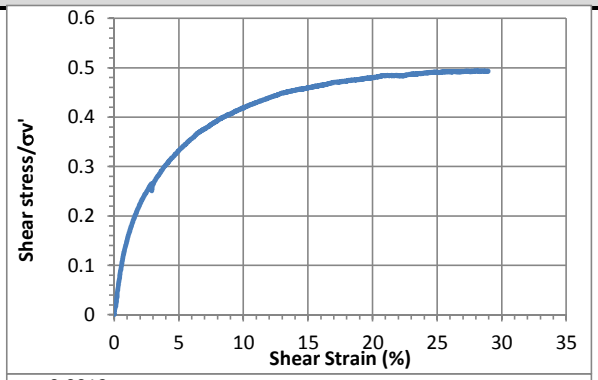

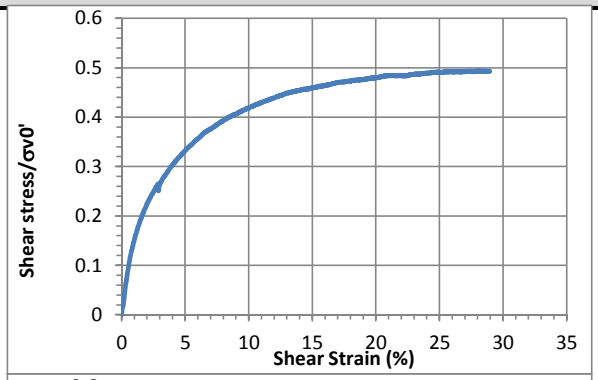

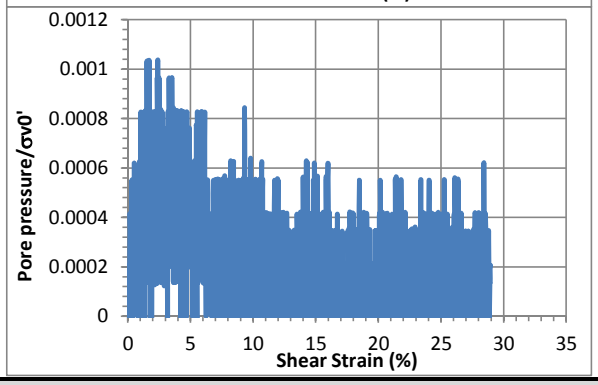

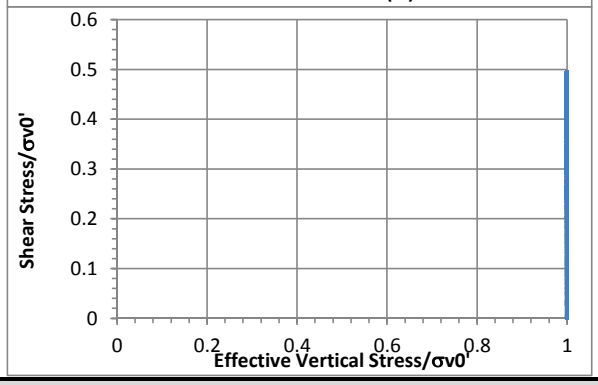

Shear wave velocity

Signal type	Sinusoidal	**First rise**	**initiation time (ms)**	-0.0154
Signal amplitude (Vpp)	90		**arrival time (ms)**	0.6093
Signal frequency (kHz)	5		**Vs (m/s)**	175
Sensor spacing (mm)	109.37	**First peak**	**initiation time (ms)**	0.0410
R+P average Vs (m/s)	171		**arrival time (ms)**	0.6963
Stdev. (m/s)	6		**Vs (m/s)**	167
P+V average Vs (m/s)	166	**First valley**	**initiation time (ms)**	0.1434
Stdev. (m/s)	1		**arrival time (ms)**	0.8038
Wavelength (m)	0.033		**Vs (m/s)**	166
Spacing/wavelength	3.3			

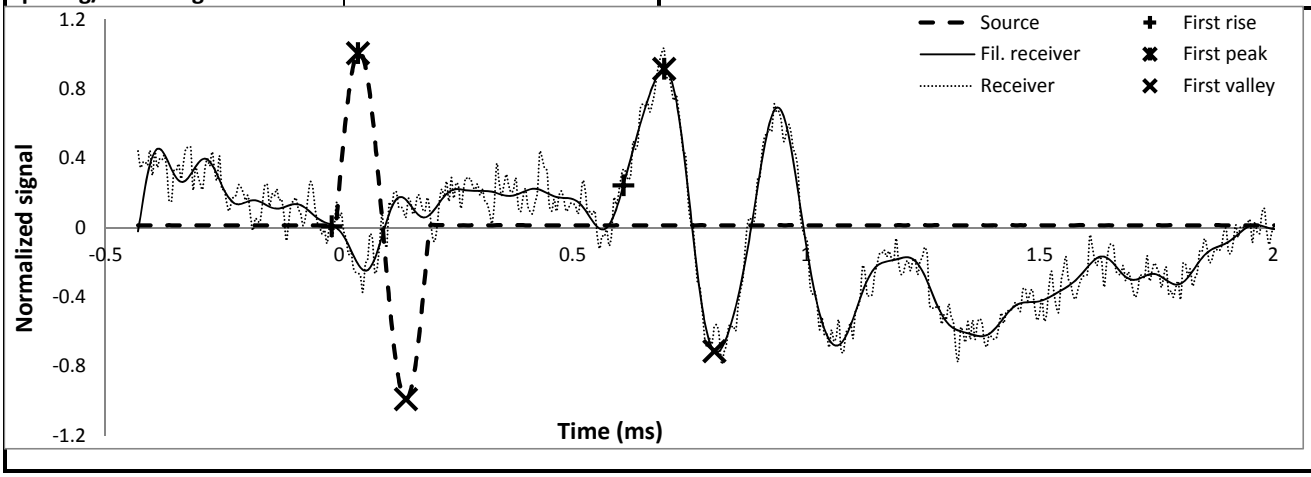

CSS Monotonic Shear Test Report

10/28/2013_Version 8.0

Geotechnical Engineering Laboratory

General Test Info and Sample Preparation			
Device:	CSS	**Relative Density (%):**	
Specimen ID:	MI-STH	**Void Ratio:**	
Test ID:	MI23	**Height (mm):**	130.9
Date of Test:	12/3/2013	**Soil-Only Specimen Diameter (mm):**	306.2
Test Performed:	Monotonic Shear	**Weight (kg):**	9.09
Test Material:	MSW	**Density (kg/m^3):**	943
Sample Preparation:	Prepared using the same initial composition and unit weight as Sim. 1. Used fresh FP with higher Wc in the top layers. Pre-compress for 24 hours.	**Membrane Thickness (mm):**	0.635
		Moisture Content (%):	~22%
		Saturated (Y/N):	N
		Prepared by:	Alex
		Checked by:	Fei

Consolidation Stage		Shear Stage	
Vertical Stress (kPa):	393	**Type of Test:**	Constant Load
Time to Compression (min):	61.8	**Stress or Strain Controlled:**	Strain
Relative Density (%):		**Shear Strain Rate (%/min):**	0.48
Void Ratio:		**Peak Shear Strength (kPa):**	195.8
Height (mm):	105.6	**Comments**	
Diameter (mm):	306.2	Consolidate to 400 kPa in 60 min, monotonic shear	
Weight (kg):	9.09		
Density (kg/m^3):	1168		

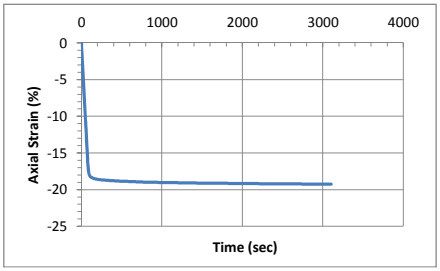

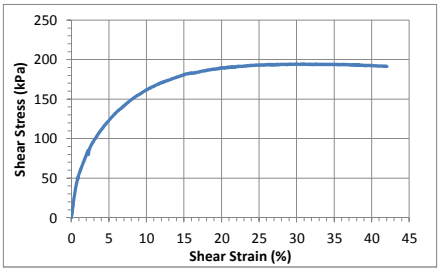

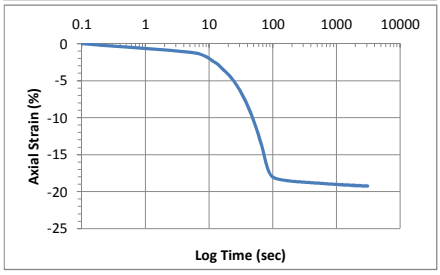

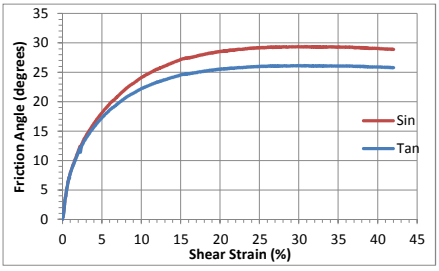

Shear

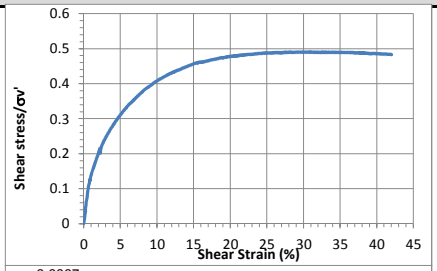

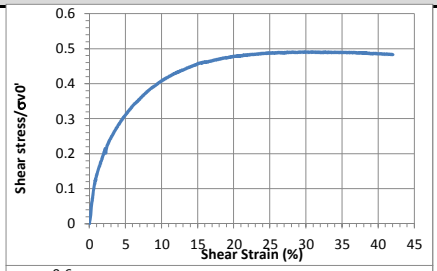

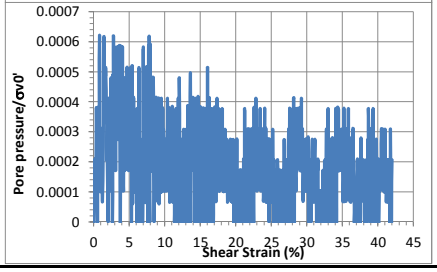

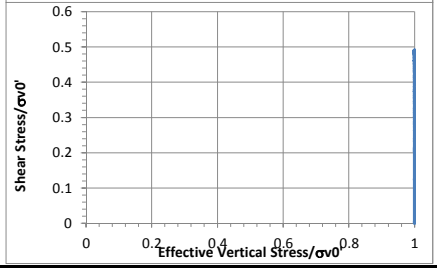

CSS Monotonic Shear Test Report

10/28/2013_Version 8.0

Geotechnical Engineering Laboratory

General Test Info and Sample Preparation			
Device:	CSS	**Relative Density (%):**	
Specimen ID:	MI-STH	**Void Ratio:**	
Test ID:	MI24	**Height (mm):**	119.6
Date of Test:	12/23/2013	**Soil-Only Specimen Diameter (mm):**	306.2
Test Performed:	Monotonic Shear	**Weight (kg):**	6.42
Test Material:	MSW	**Density (kg/m^3):**	729
Sample Preparation:	Prepared using the same initial composition and unit weight as Sim. 1. Pre-compress for 24 hours.	**Membrane Thickness (mm):**	0.635
		Moisture Content (%):	~20%
		Saturated (Y/N):	N
		Prepared by:	Fei
		Checked by:	Fei

Consolidation Stage		Shear Stage	
Vertical Stress (kPa):	49	**Type of Test:**	Constant Volume
Time to Compression (min):	64.4	**Stress or Strain Controlled:**	Strain
Relative Density (%):		**Shear Strain Rate (%/min):**	0.52
Void Ratio:		**Peak Shear Strength (kPa):**	19.5
Height (mm):	97.04	**Comments**	
Diameter (mm):	306.2	Consolidate to 100 kPa in 60 min, monotonic shear	
Weight (kg):	6.42		
Density (kg/m^3):	898		

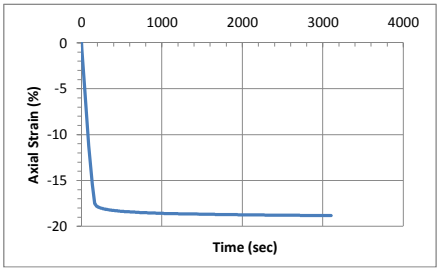

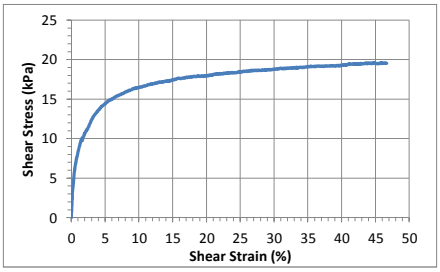

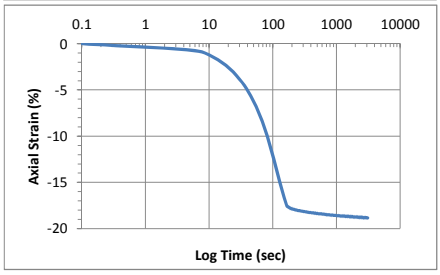

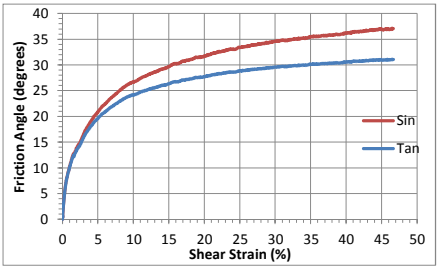

Shear

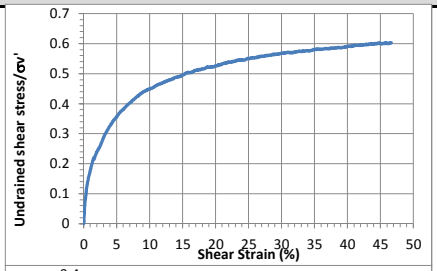

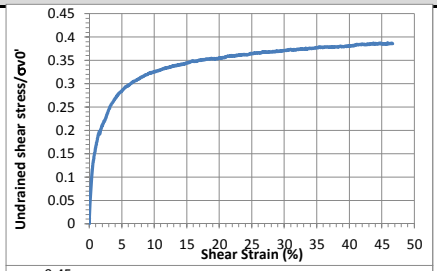

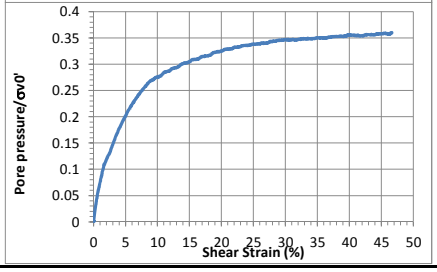

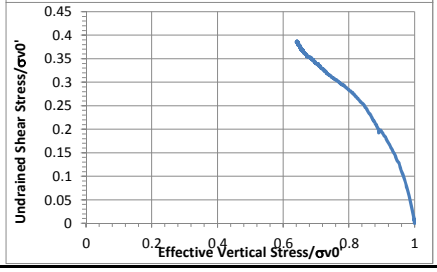

CSS Monotonic Shear Test Report

10/28/2013_Version 8.0

Geotechnical Engineering Laboratory

General Test Info and Sample Preparation			
Device:	CSS	**Relative Density (%):**	
Specimen ID:	MI-STH	**Void Ratio:**	
Test ID:	MI25	**Height (mm):**	127.0
Date of Test:	1/10/2014	**Soil-Only Specimen Diameter (mm):**	306.2
Test Performed:	Monotonic Shear	**Weight (kg):**	6.42
Test Material:	MSW	**Density (kg/m^3):**	687
Sample Preparation:	Prepared using the same initial composition and unit weight as Sim. 1. Pre-compress for 24 hours.	**Membrane Thickness (mm):**	0.635
		Moisture Content (%):	~20%
		Saturated (Y/N):	N
		Prepared by:	Fei
		Checked by:	Fei

Consolidation Stage		Shear Stage	
Vertical Stress (kPa):	48.8	**Type of Test:**	Constant Load
Time to Compression (min):	64.3	**Stress or Strain Controlled:**	Strain
Relative Density (%):		**Shear Strain Rate (%/min):**	0.51
Void Ratio:		**Peak Shear Strength (kPa):**	30.2
Height (mm):	98.90	**Comments**	
Diameter (mm):	306.2	Consolidate to 50 kPa in 60 min, monotonic shear	
Weight (kg):	6.42		
Density (kg/m^3):	881.40		

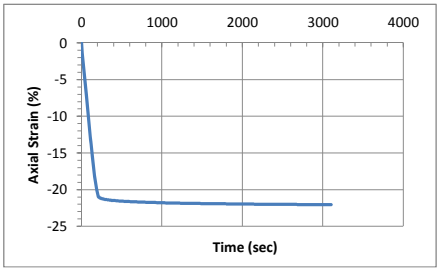

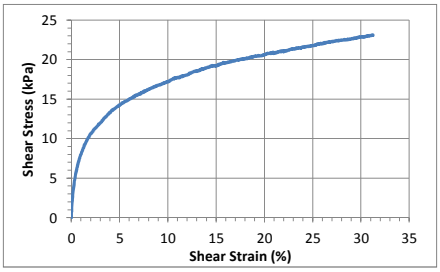

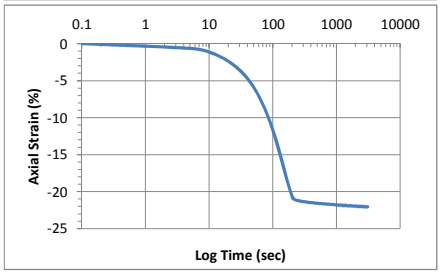

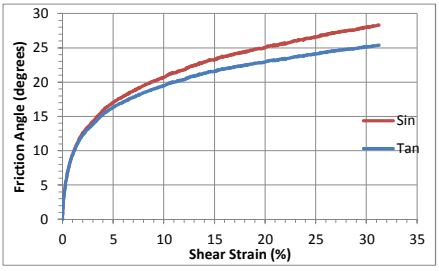

Shear

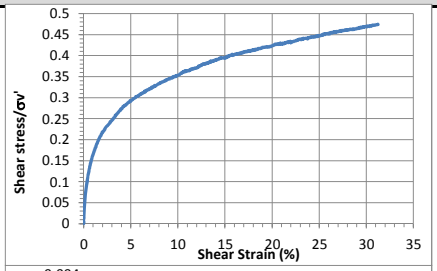

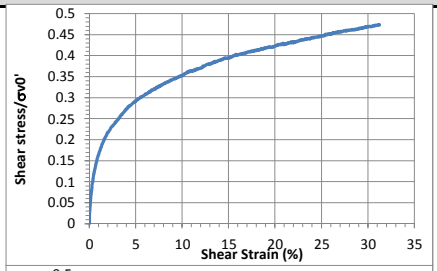

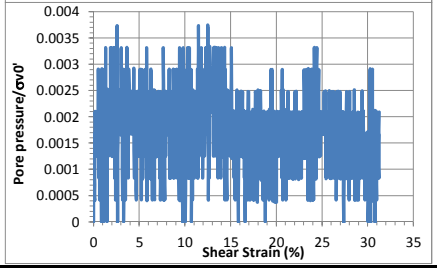

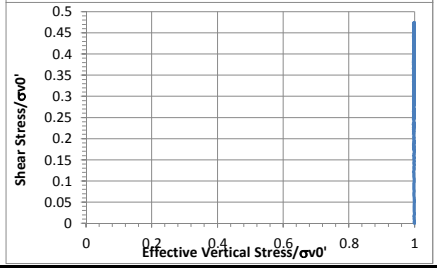

CSS Monotonic Shear Test Report

10/28/2013_Version 8.0

Geotechnical Engineering Laboratory

General Test Info and Sample Preparation			
Device:	CSS	**Relative Density (%):**	
Specimen ID:	MI-STH	**Void Ratio:**	
Test ID:	MI26	**Height (mm):**	123.6
Date of Test:	1/24/2014	**Soil-Only Specimen Diameter (mm):**	306.2
Test Performed:	Monotonic Shear	**Weight (kg):**	6.96
Test Material:	MSW	**Density (kg/m^3):**	765
Sample Preparation:	Prepared using the same initial composition and unit weight as Sim. 1. Pre-compress for 22 hours.	**Membrane Thickness (mm):**	0.635
		Moisture Content (%):	~20%
		Saturated (Y/N):	N
		Prepared by:	Alex
		Checked by:	Fei

Consolidation Stage		Shear Stage	
Vertical Stress (kPa):	99	**Type of Test:**	Constant Volume
Time to Compression (min):	182.3	**Stress or Strain Controlled:**	Strain
Relative Density (%):		**Shear Strain Rate (%/min):**	0.51
Void Ratio:		**Peak Shear Strength (kPa):**	35.6
Height (mm):	98.12	**Comments**	
Diameter (mm):	306.2	Consolidate to 100 kPa in 180 min, monotonic shear	
Weight (kg):	6.96		
Density (kg/m^3):	963		

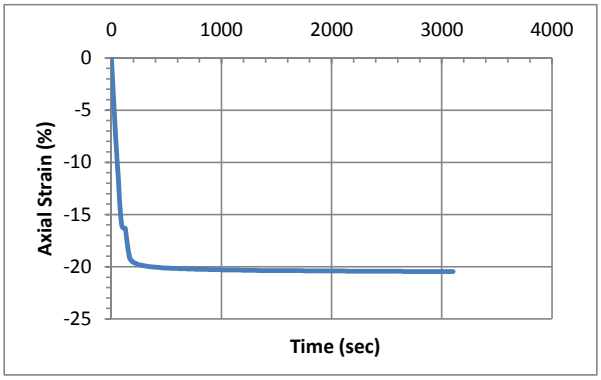

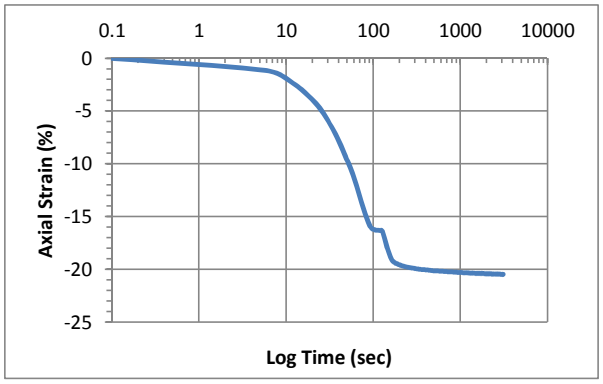

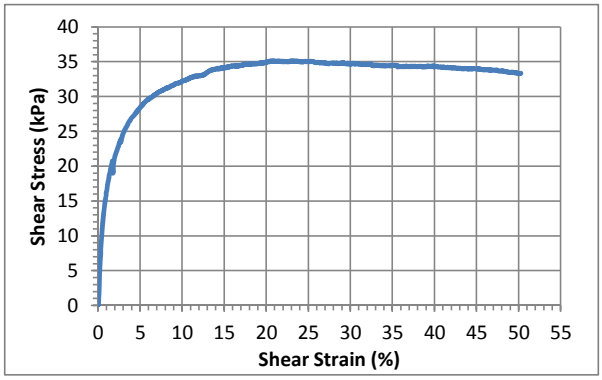

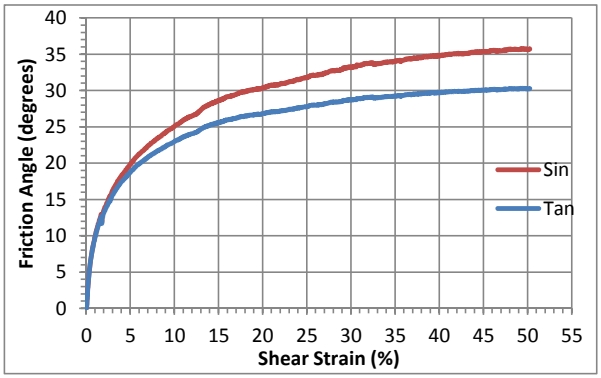

Shear

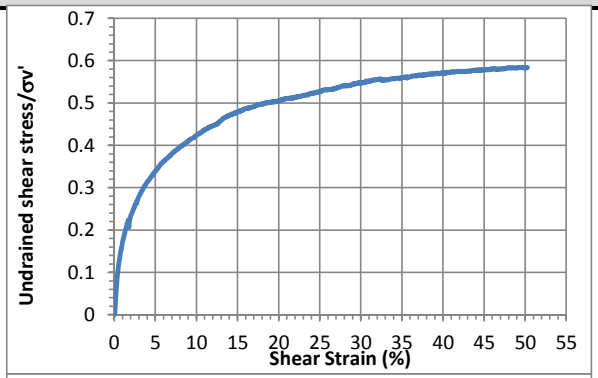

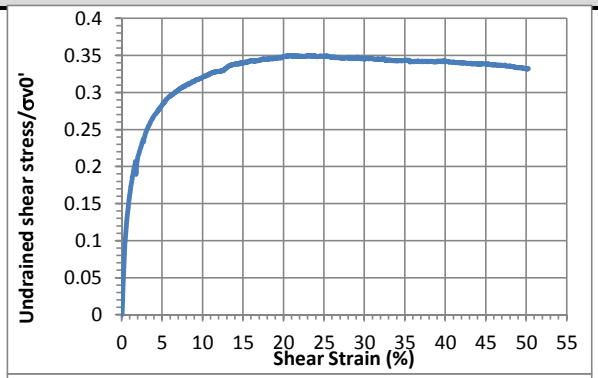

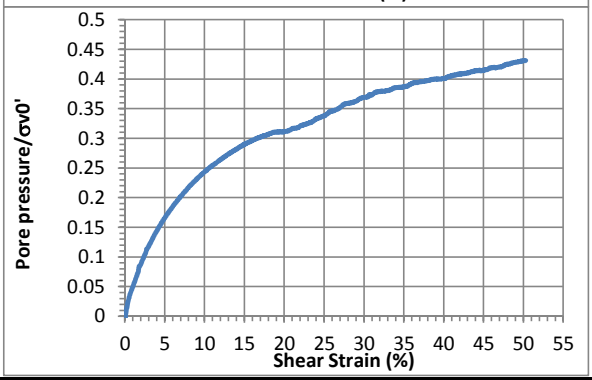

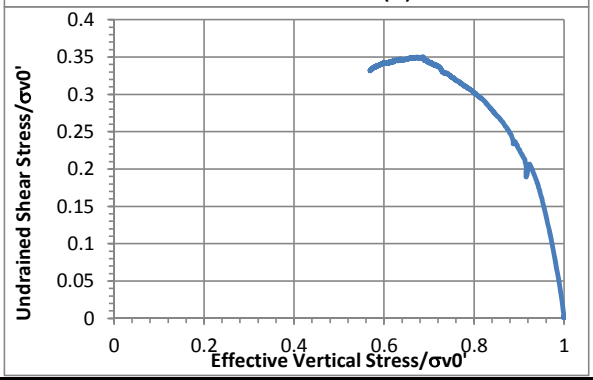

Shear wave velocity

Signal type	Sinusoidal	**First rise**	**initiation time (ms)**	-0.0102
Signal amplitude (Vpp)	90		**arrival time (ms)**	0.7936
Signal frequency (kHz)	5		**Vs (m/s)**	112
Sensor spacing (mm)	89.77	**First peak**	**initiation time (ms)**	0.0410
R+P average Vs (m/s)	109		**arrival time (ms)**	0.8909
Stdev. (m/s)	4		**Vs (m/s)**	106
P+V average Vs (m/s)	104	**First valley**	**initiation time (ms)**	0.1434
Stdev. (m/s)	2		**arrival time (ms)**	1.0138
Wavelength (m)	0.021		**Vs (m/s)**	103
Spacing/wavelength	4.3			

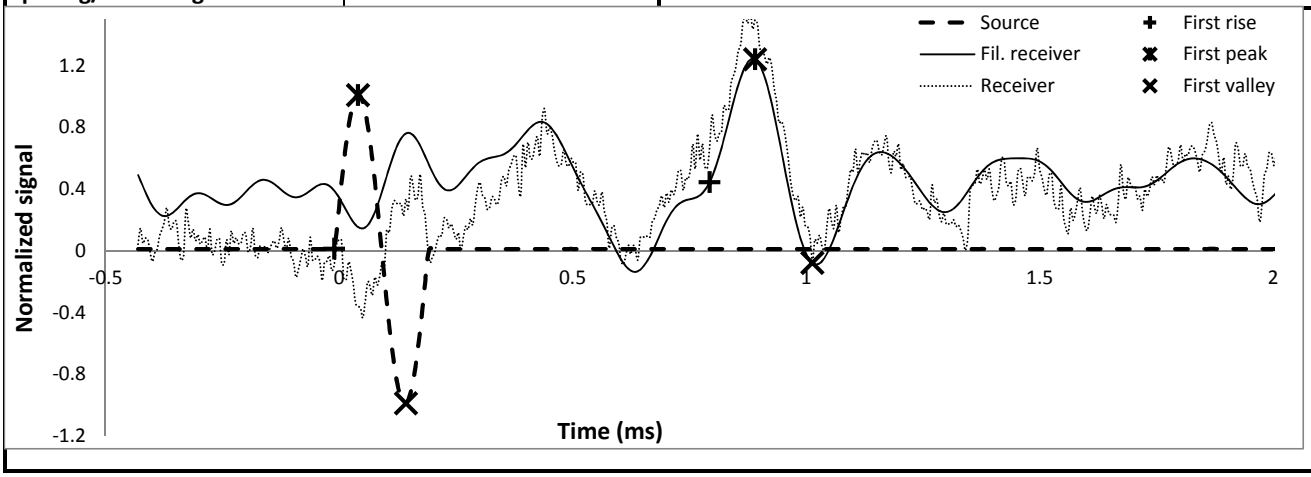

CSS Monotonic Shear Test Report

10/28/2013_Version 8.0

Geotechnical Engineering Laboratory

General Test Info and Sample Preparation			
Device:	CSS	**Relative Density (%):**	
Specimen ID:	MI-STH	**Void Ratio:**	
Test ID:	MI28	**Height (mm):**	125.3
Date of Test:	2/2/2014	**Soil-Only Specimen Diameter (mm):**	306.2
Test Performed:	Monotonic Shear	**Weight (kg):**	7.22
Test Material:	MSW	**Density (kg/m^3):**	783
Sample Preparation:	Prepared using the same initial composition and unit weight as Sim. 1. Pre-compress for 24 hours.	**Membrane Thickness (mm):**	0.635
		Moisture Content (%):	~20%
		Saturated (Y/N):	N
		Prepared by:	Fei
		Checked by:	Fei

Consolidation Stage		Shear Stage	
Vertical Stress (kPa):	96	**Type of Test:**	Constant Load
Time to Compression (min):	62.6	**Stress or Strain Controlled:**	Strain
Relative Density (%):		**Shear Strain Rate (%/min):**	0.49
Void Ratio:		**Peak Shear Strength (kPa):**	49.4
Height (mm):	101.88	**Comments**	
Diameter (mm):	306.2	Consolidate to 100 kPa in 60 min, monotonic shear	
Weight (kg):	7.22		
Density (kg/m^3):	962.15		

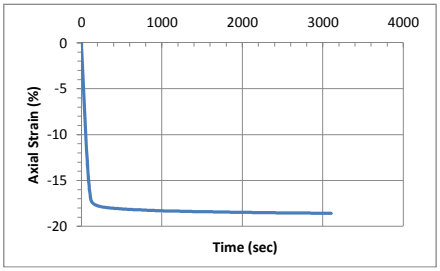

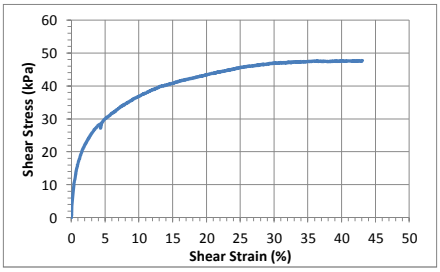

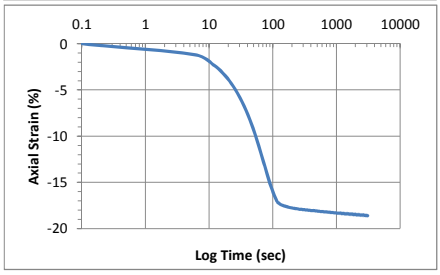

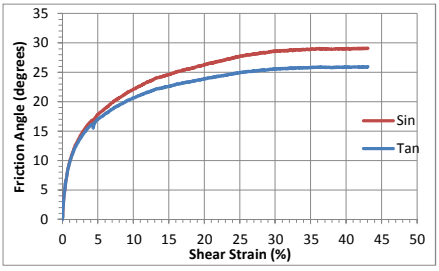

Shear

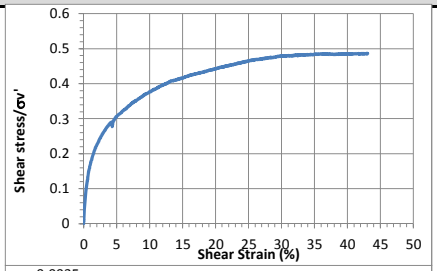

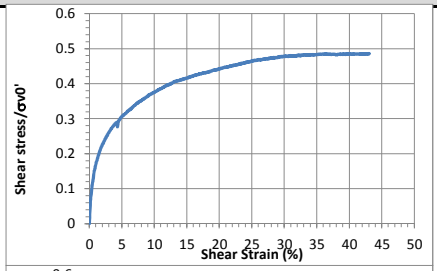

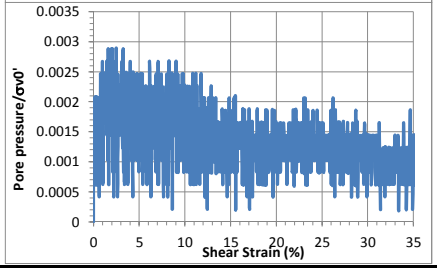

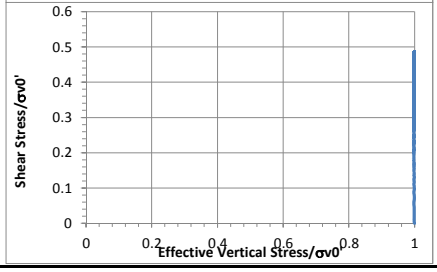

CSS Monotonic Shear Test Report

10/28/2013_Version 8.0

Geotechnical Engineering Laboratory

General Test Info and Sample Preparation			
Device:	CSS	**Relative Density (%):**	
Specimen ID:	MI-STH	**Void Ratio:**	
Test ID:	MI29	**Height (mm):**	123.2
Date of Test:	3/20/2014	**Soil-Only Specimen Diameter (mm):**	306.2
Test Performed:	Monotonic Shear	**Weight (kg):**	7.22
Test Material:	MSW	**Density (kg/m^3):**	796
Sample Preparation:	The same initial composition and unit weight as Sim. 1. Pre-compress to 100 kPa for 25 hours. New LVDT.	**Membrane Thickness (mm):**	0.635
		Moisture Content (%):	~20%
		Saturated (Y/N):	N
		Prepared by:	Fei
		Checked by:	Fei

Consolidation Stage		Shear Stage	
Vertical Stress (kPa):	96.3	**Type of Test:**	Constant Volume
Time to Compression (min):	62.6	**Stress or Strain Controlled:**	Strain
Relative Density (%):		**Shear Strain Rate (%/min):**	0.24
Secondary compression ratio		**Peak Shear Strength (kPa):**	33.6
Height (mm):	102.30	**Comments**	
Diameter (mm):	306.2	Consolidate to 100 kPa in 60 min, monotonic shear. Wrong horizontal LVDT.	
Weight (kg):	7.22		
Density (kg/m^3):	958		

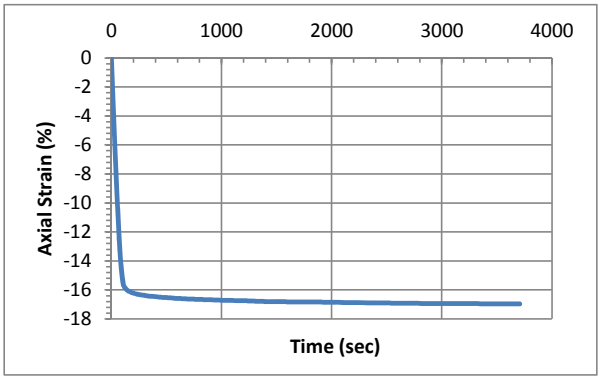

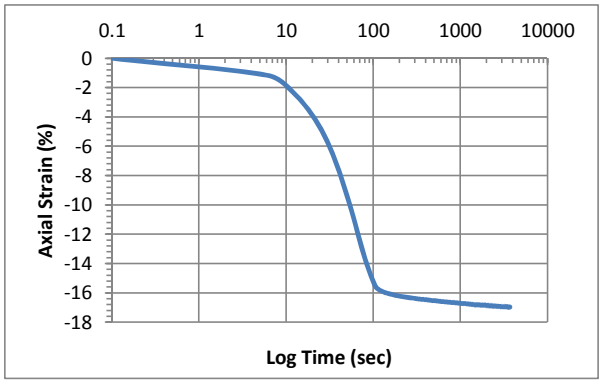

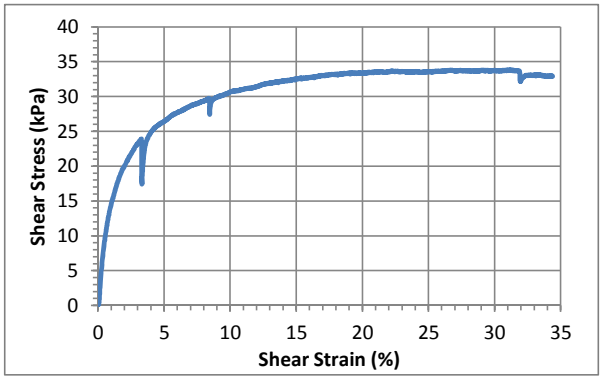

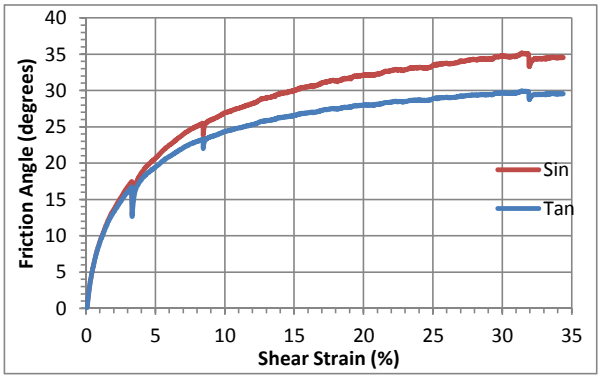

Shear

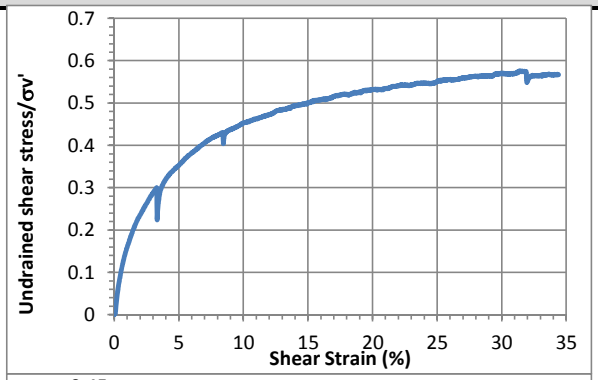

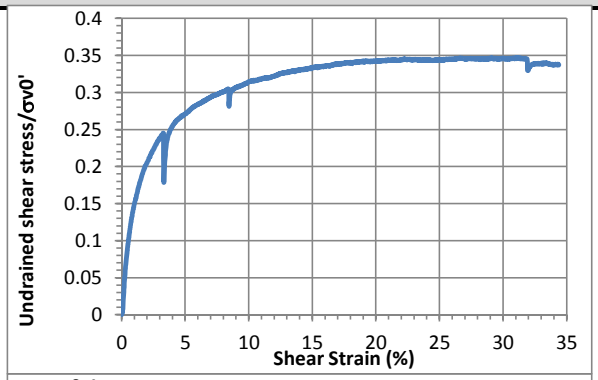

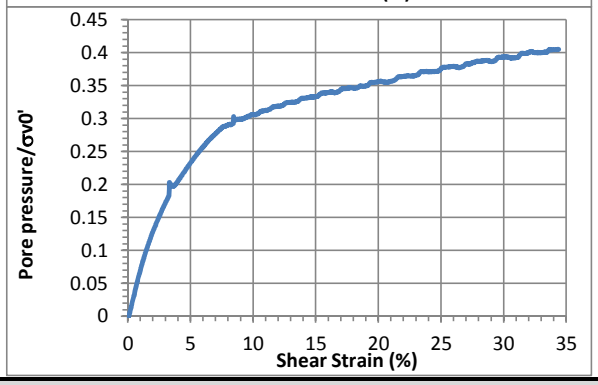

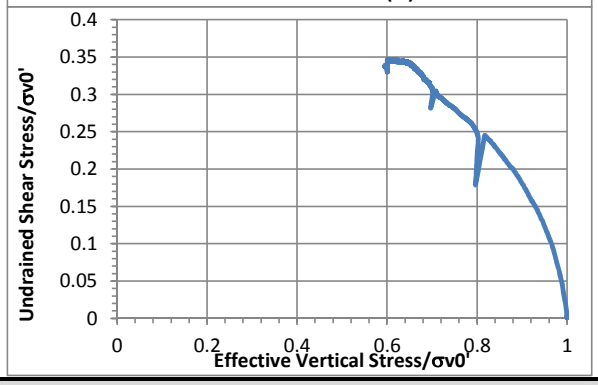

Shear wave velocity

Signal type	Sinusoidal	**First rise**	**initiation time (ms)**	-0.0102
Signal amplitude (Vpp)	90		**arrival time (ms)**	0.4762
Signal frequency (kHz)	5		**Vs (m/s)**	192
Sensor spacing (mm)	93.54	**First peak**	**initiation time (ms)**	0.0410
R+P average Vs (m/s)	184		**arrival time (ms)**	0.5734
Stdev. (m/s)	12		**Vs (m/s)**	176
P+V average Vs (m/s)	170	**First valley**	**initiation time (ms)**	0.1382
Stdev. (m/s)	8		**arrival time (ms)**	0.7066
Wavelength (m)	0.034		**Vs (m/s)**	165
Spacing/wavelength	2.7			

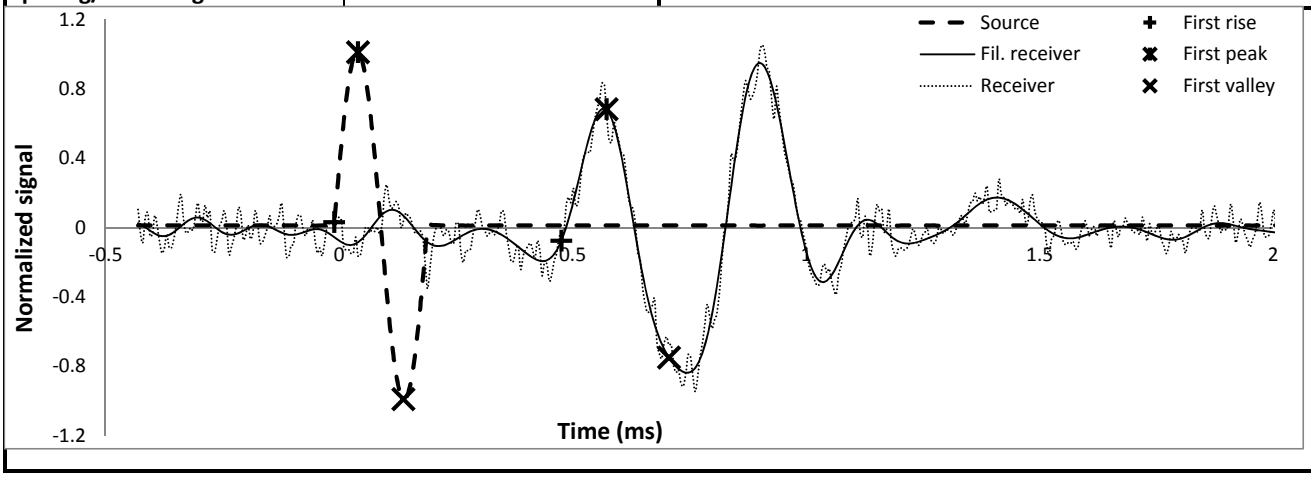

CSS Monotonic Shear Test Report

10/28/2013_Version 8.0

Geotechnical Engineering Laboratory

General Test Information and Sample Preparation			
Device:	CSS	**Layers:**	7.0
Specimen ID:	MI-STH	**Weight/layer (kg):**	1.07
Test ID:	MI30	**Height/layer (mm):**	25.4
Date of Test:	6/25/2014	**Total height (mm):**	177.8
Test Performed:	Monotonic Shear	**Soil-Only Specimen Diameter (mm):**	306.2
Test Material:	MSW	**Total weight (kg):**	7.49
Sample Preparation:	The same initial composition and unit weight as Sim. #1. Pre-compress for 2 hours, consolidate for 1 hour.	**Density (kg/m^3):**	572
		Membrane Thickness (mm):	0.000635
		Moisture Content (%):	
		Saturated (Y/N):	N
		Prepared by:	Fei

Pre-compression Stage			
Pre-compression strain:	0.35		
Height (mm):	114.1	**Density (kg/m3):**	891

Consolidation Stage		Shear Stage		
Initial height (mm):	134.2	**Type of Test:**		CD-strain
Initial density (kg/m3):	758	**Shear Strain Rate (%/min):**		0.36
Vertical Stress (kPa):	83.2	**10% strain**	**Shear stress (kPa)**	30.5
Immediate strain (εimm, %)	34.9		**Tan friction angle (°)**	20.1
Consolidated Height (mm):	112.5		**Sin friction angle (°)**	21.5
Compression index (Cc ε)	0.182	**30% strain**	**Shear stress (kPa)**	39.3
Constrained modulus	5.7		**Tan friction angle (°)**	25.3
Consolidated density (kg/m^3):	904		**Sin friction angle (°)**	28.2

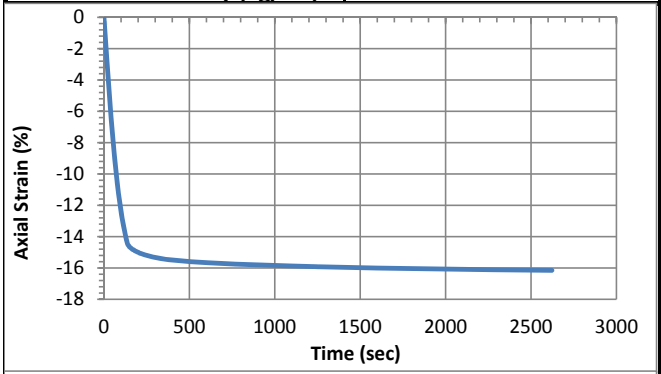

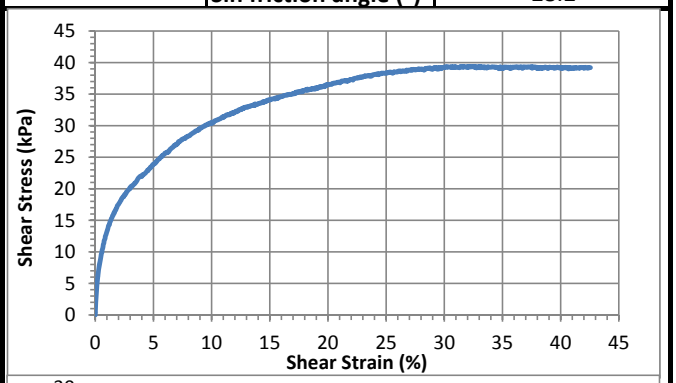

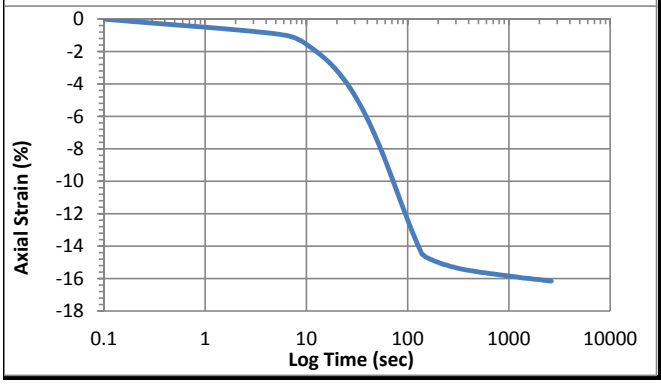

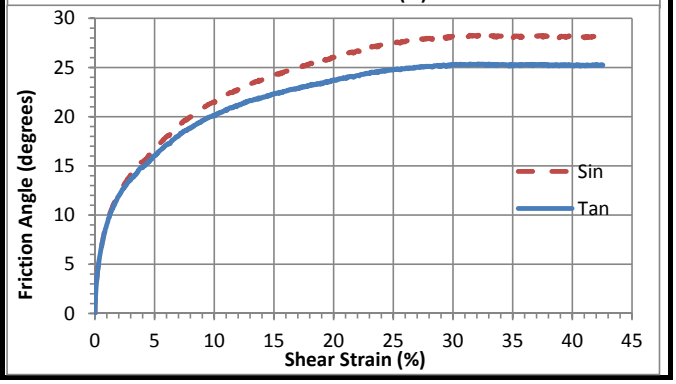

Strength			
τ/σv' at 10% strain	0.37	τ/σv0' at 10% strain	0.37
τ/σv' at 30% strain	0.47	τ/σv0' at 30% strain	0.47

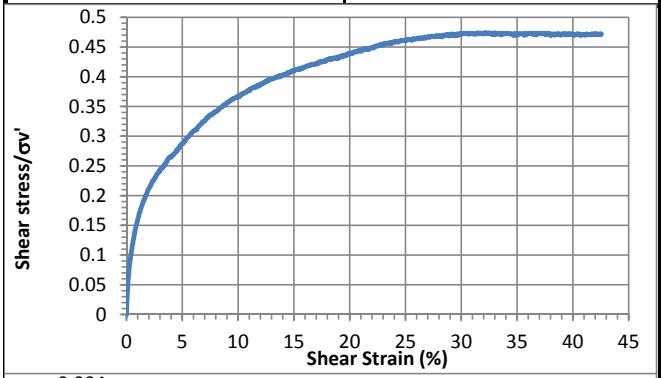

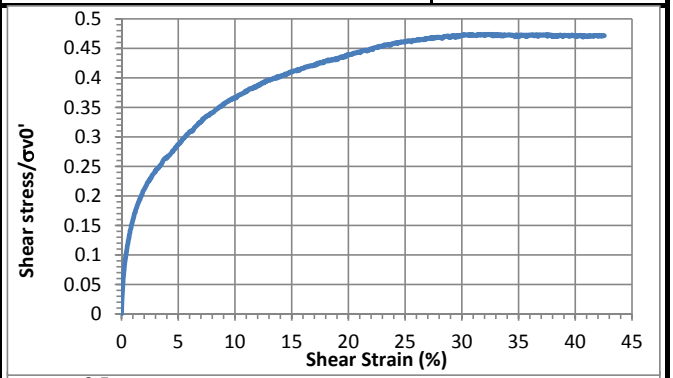

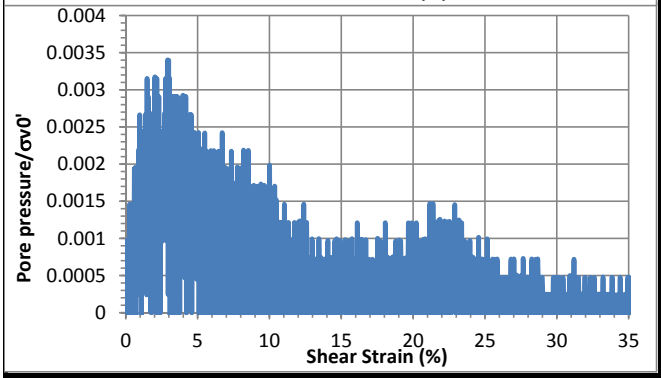

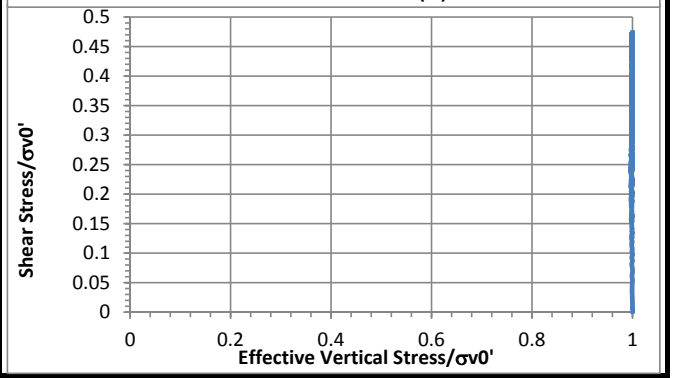

Shear wave velocity				
Signal type	Sinusoidal	First rise	initiation time (ms)	-0.0102
Signal amplitude (Vpp)	90		arrival time (ms)	0.7270
Signal frequency (kHz)	5		Vs (m/s)	146
Sensor spacing (mm)	107.96	First peak	initiation time (ms)	0.0410
R+P average Vs (m/s)	143		arrival time (ms)	0.8192
Stdev. (m/s)	5		Vs (m/s)	139
P+V average Vs (m/s)	136	First valley	initiation time (ms)	0.1434
Stdev. (m/s)	4		arrival time (ms)	0.9523
Wavelength (m)	0.027		Vs (m/s)	133
Spacing/wavelength	4.0			

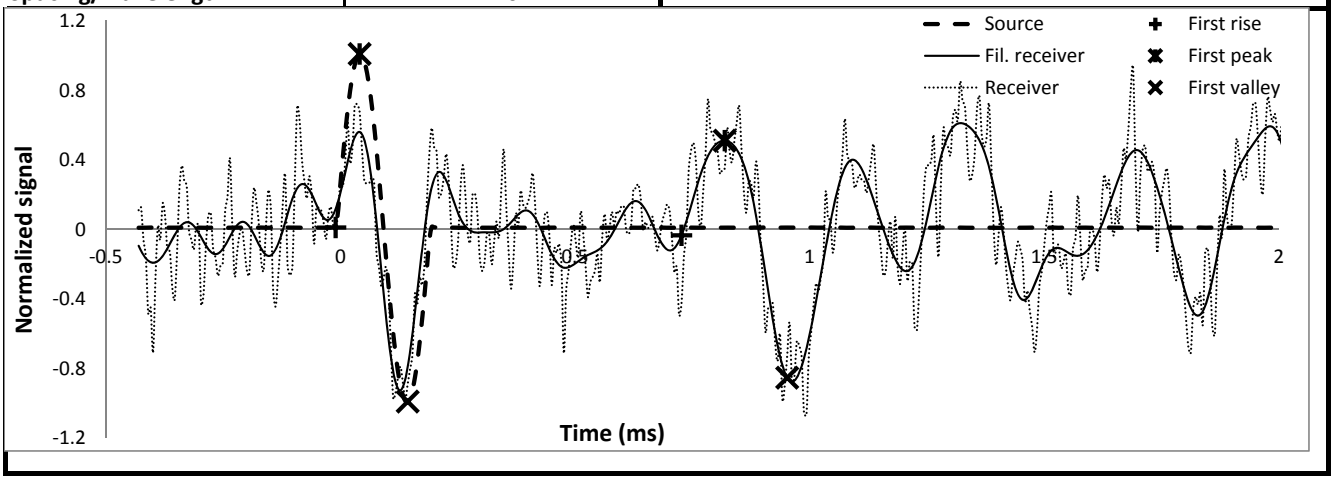

CSS Monotonic Shear Test Report

10/28/2013_Version 8.0

Geotechnical Engineering Laboratory

General Test Information and Sample Preparation			
Device:	CSS	**Layers:**	7.0
Specimen ID:	MI-STH	**Weight/layer (kg):**	1.07
Test ID:	MI31	**Height/layer (mm):**	25.4
Date of Test:	7/3/2014	**Total height (mm):**	177.8
Test Performed:	Monotonic Shear	**Soil-Only Specimen Diameter (mm):**	306.2
Test Material:	MSW	**Total weight (kg):**	7.49
Sample Preparation:	The same initial composition and unit weight as Sim. #1. Pre-compress for 141.5 hours, consolidate for 1 hour.	**Density (kg/m^3):**	572
		Membrane Thickness (mm):	0.000635
		Moisture Content (%):	
		Saturated (Y/N):	N
		Prepared by:	Fei

Pre-compression Stage			
Pre-compression strain:	0.33	**Secondary compression ratio:**	0.00351
Height (mm):	115.4	**Density (kg/m3):**	881

Consolidation Stage		Shear Stage		
Initial height (mm):	135.0	**Type of Test:**		CD-strain
Initial density (kg/m3):	753	**Shear Strain Rate (%/min):**		0.36
Vertical Stress (kPa):	95.2	**10% strain**	**Shear stress (kPa)**	37.1
Immediate strain (εimm, %)	33.7		**Tan friction angle (°)**	21.3
Consolidated Height (mm):	112.7		**Sin friction angle (°)**	23.0
Compression index (Cεc)	0.170	**30% strain**	**Shear stress (kPa)**	43.7
Constrained modulus	5.9		**Tan friction angle (°)**	24.7
Consolidated density (kg/m^3):	902		**Sin friction angle (°)**	27.4

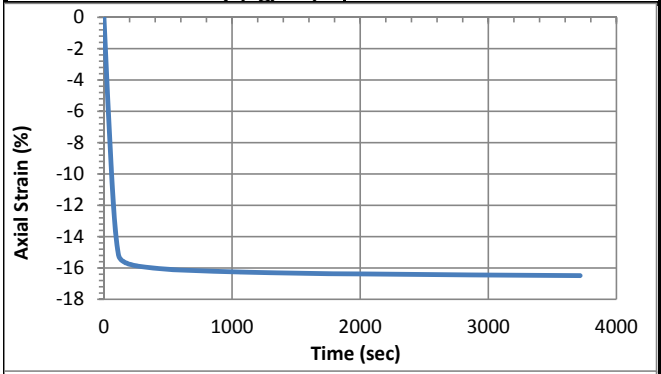

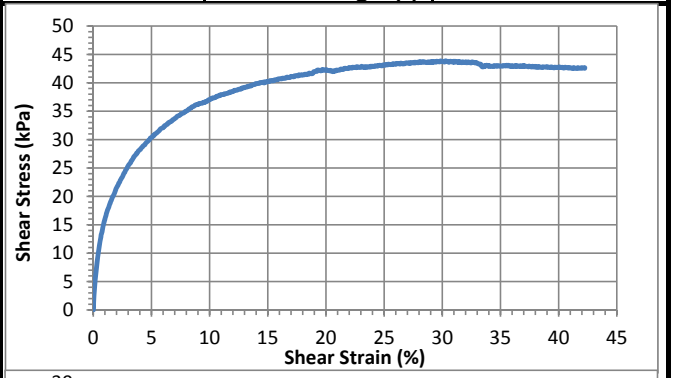

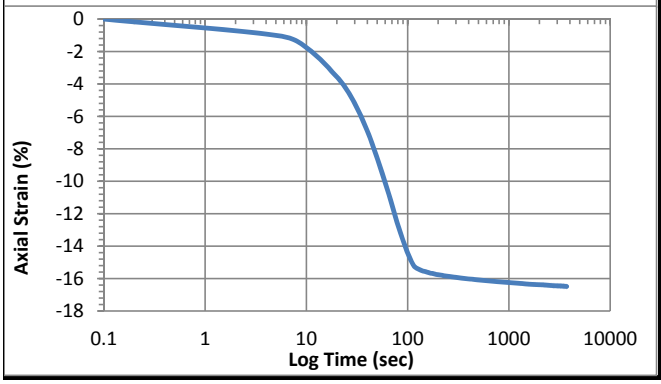

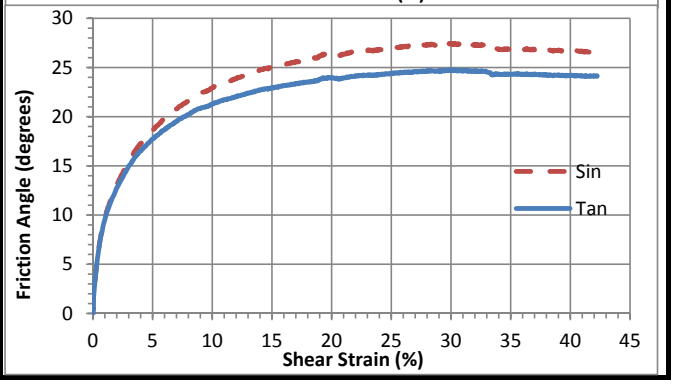

Strength			
τ/σv' at 10% strain	0.39	τ/σv0' at 10% strain	0.39
τ/σv' at 30% strain	0.46	τ/σv0' at 30% strain	0.46

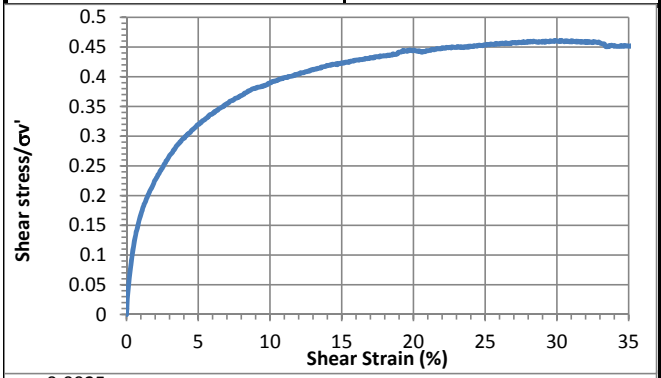

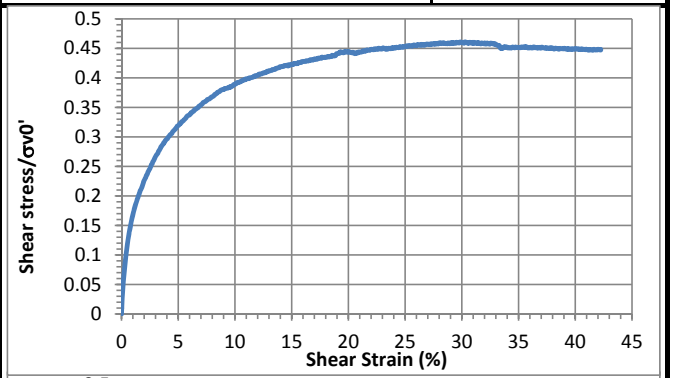

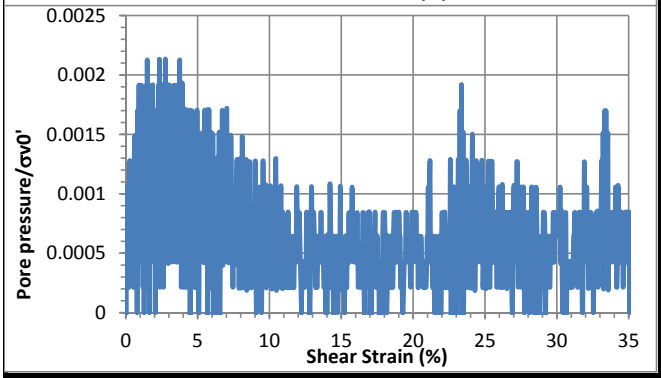

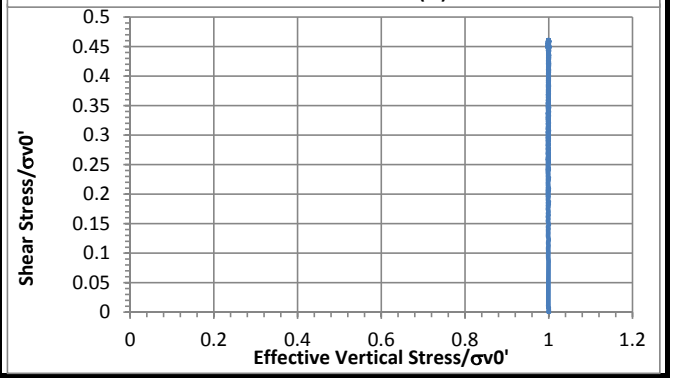

Shear wave velocity				
Signal type	Sinusoidal	First rise	initiation time (ms)	-0.0256
Signal amplitude (Vpp)	90		arrival time (ms)	0.7322
Signal frequency (kHz)	2		Vs (m/s)	137
Sensor spacing (mm)	103.97	First peak	initiation time (ms)	0.1024
R+P average Vs (m/s)	135		arrival time (ms)	0.8858
Stdev. (m/s)	3		Vs (m/s)	133
P+V average Vs (m/s)	137	First valley	initiation time (ms)	0.3533
Stdev. (m/s)	6		arrival time (ms)	1.0906
Wavelength (m)	0.068		Vs (m/s)	141
Spacing/wavelength	1.5			

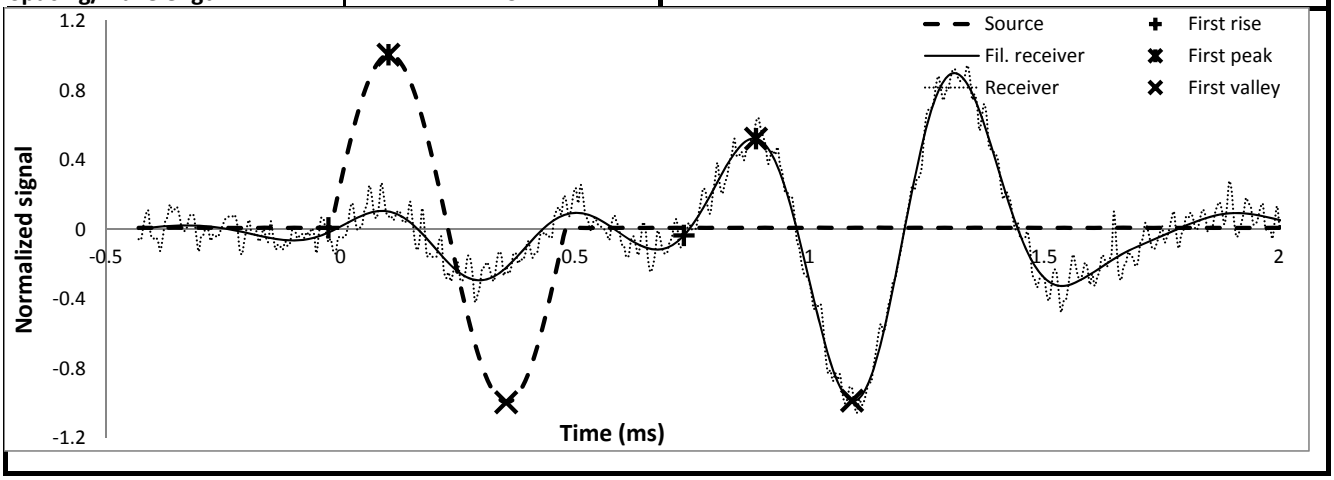

CSS Monotonic Shear Test Report

10/28/2013_Version 8.0

Geotechnical Engineering Laboratory

General Test Information and Sample Preparation			
Device:	CSS	**Layers:**	7.00
Specimen ID:	MI-STH	**Weight/layer (kg):**	1.07
Test ID:	MI32	**Height/layer (mm):**	25.4
Date of Test:	7/4/2014	**Total height (mm):**	177.8
Test Performed:	Monotonic Shear	**Soil-Only Specimen Diameter (mm):**	306.2
Test Material:	MSW	**Total weight (kg):**	7.49
Sample Preparation:	The same initial composition and unit weight as Sim. #1. Pre-compress for 23 hours, consolidate for 1 hour.	**Density (kg/m^3):**	572
		Membrane Thickness (mm):	0.000635
		Moisture Content (%):	30.4
		Saturated (Y/N):	N
		Prepared by:	Fei

Pre-compression Stage			
Pre-compression strain:	0.29	**Secondary compression ratio**	0.00709
Height (mm):	121.8	**Density (kg/m3):**	835

Consolidation Stage		Shear Stage		
Initial height (mm):	137.4	**Type of Test:**		CD-strain
Initial density (kg/m3):	740	**Shear Strain Rate (%/min):**		2.24
Vertical Stress (kPa):	96.9	**10% strain**	**Shear stress (kPa)**	39.0
Immediate strain (εimm, %)	32.9		**Tan friction angle (°)**	22.1
Consolidated Height (mm):	111.9		**Sin friction angle (°)**	23.9
Compression index (Cc̄ε)	0.171	**30% strain**	**Shear stress (kPa)**	48.7
Constrained modulus	5.9		**Tan friction angle (°)**	26.7
Consolidated density (kg/m^3):	909		**Sin friction angle (°)**	30.2

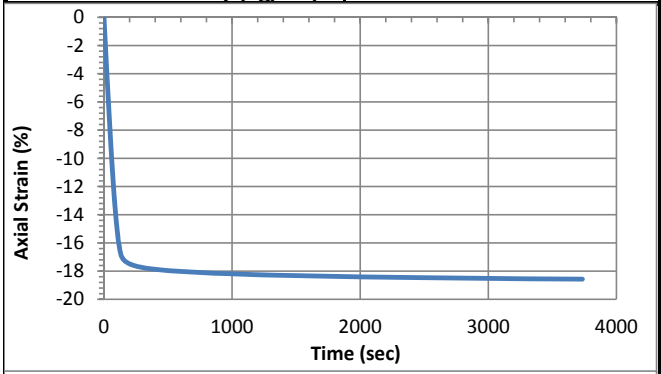

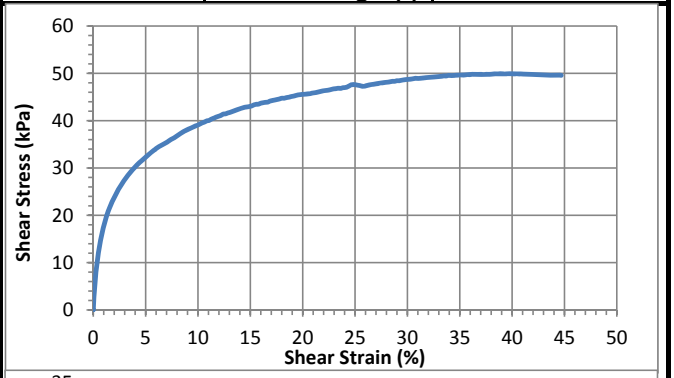

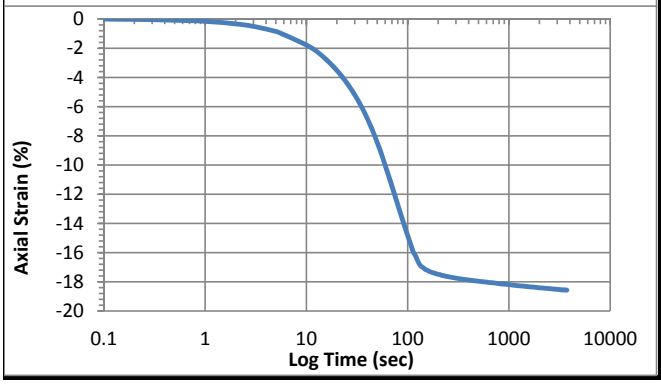

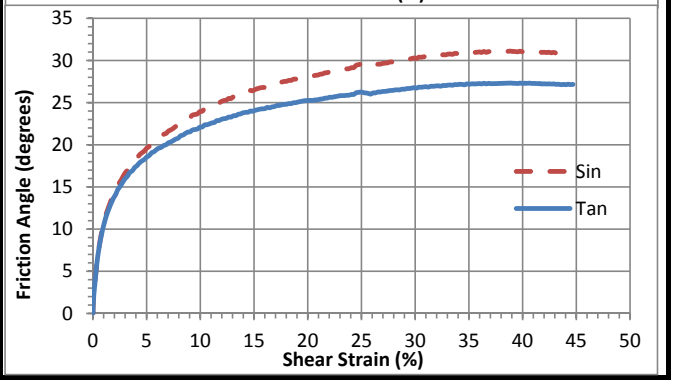

Strength			
τ/σv' at 10% strain	0.41	τ/σv0' at 10% strain	0.41
τ/σv' at 30% strain	0.50	τ/σv0' at 30% strain	0.50

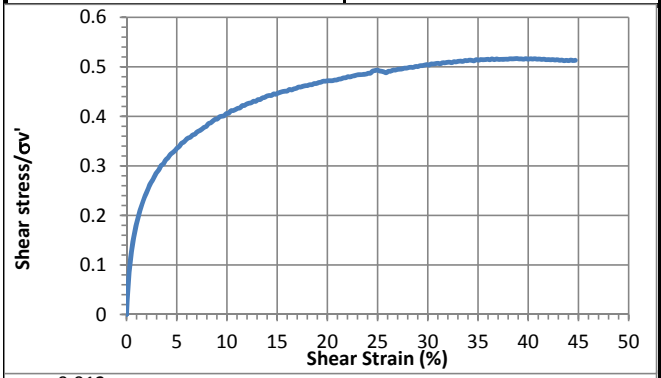

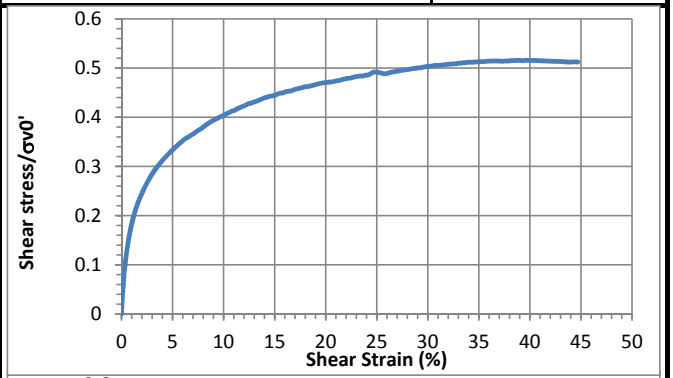

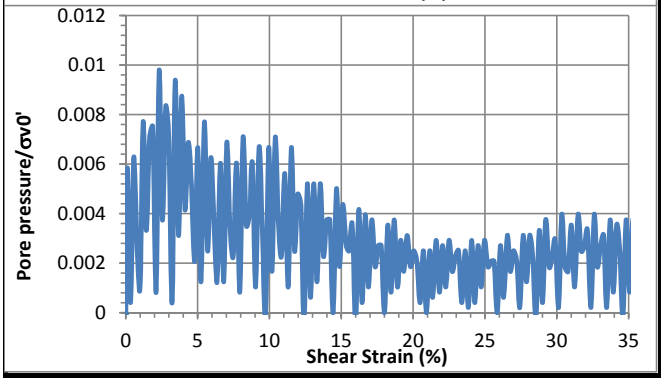

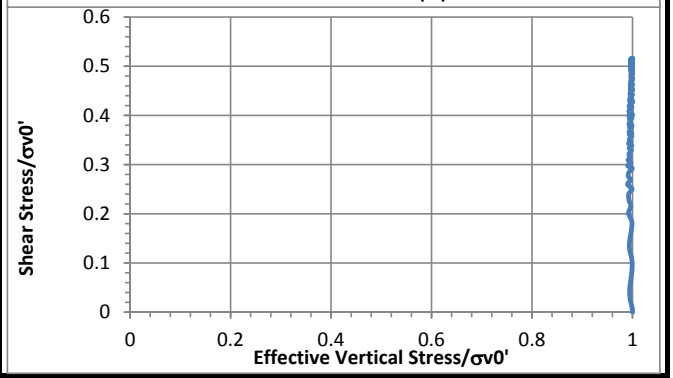

Shear wave velocity				
Signal type	Sinusoidal	First rise	initiation time (ms)	-0.0154
Signal amplitude (Vpp)	90		arrival time (ms)	0.5939
Signal frequency (kHz)	5		Vs (m/s)	169
Sensor spacing (mm)	103.11	First peak	initiation time (ms)	0.0410
R+P average Vs (m/s)	167		arrival time (ms)	0.6656
Stdev. (m/s)	3		Vs (m/s)	165
P+V average Vs (m/s)	168	First valley	initiation time (ms)	0.1382
Stdev. (m/s)	4		arrival time (ms)	0.7424
Wavelength (m)	0.034		Vs (m/s)	171
Spacing/wavelength	3.1			

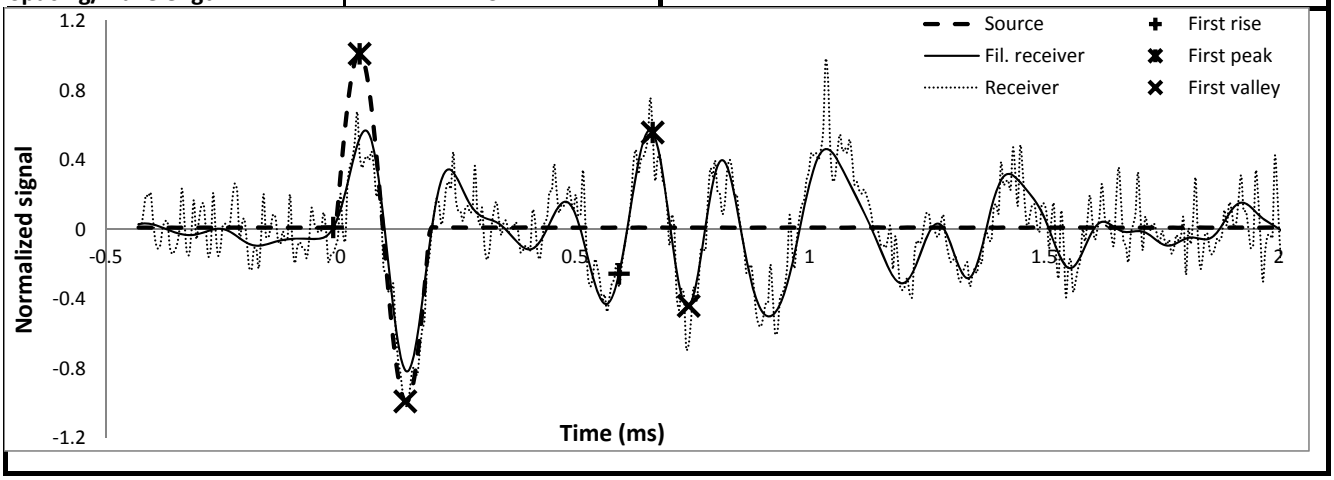

CSS Monotonic Shear Test Report

10/28/2013_Version 8.0

Geotechnical Engineering Laboratory

General Test Information and Sample Preparation			
Device:	CSS	**Layers:**	8.00
Specimen ID:	MI-STH	**Weight/layer (kg):**	1.07
Test ID:	MI33	**Height/layer (mm):**	25.4
Date of Test:	7/5/2014	**Total height (mm):**	203.2
Test Performed:	Monotonic Shear	**Soil-Only Specimen Diameter (mm):**	306.2
Test Material:	MSW	**Total weight (kg):**	8.56
Sample Preparation:	The same initial composition and unit weight as Sim. #1. Pre-compress for 23 hours, consolidate for 1 hour.	**Density (kg/m^3):**	572
		Membrane Thickness (mm):	0.000635
		Moisture Content (%):	30.4
		Saturated (Y/N):	N
		Prepared by:	Fei

Pre-compression Stage			
Pre-compression strain:	0.37	**Secondary compression ratio:**	0.00769
Height (mm):	107.5	**Density (kg/m3):**	980

Consolidation Stage		Shear Stage		
Initial height (mm):	137.5	**Type of Test:**		CU-strain
Initial density (kg/m3):	845	**Shear Strain Rate (%/min):**		0.46
Vertical Stress (kPa):	196.9	**10% strain**	**Shear stress (kPa)**	62.3
Immediate strain (εimm, %)	40.7		**Tan friction angle (°)**	23.3
Consolidated Height (mm):	109.4		**Sin friction angle (°)**	25.5
Compression index (Cc̄ε)	0.184	**30% strain**	**Shear stress (kPa)**	67.6
Constrained modulus	4.7		**Tan friction angle (°)**	29.2
Consolidated density (kg/m^3):	1062		**Sin friction angle (°)**	34.0

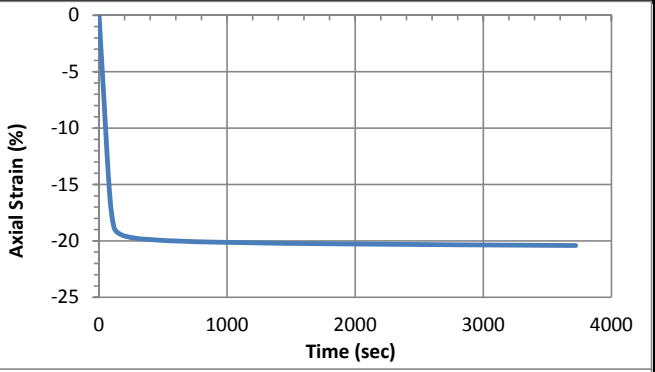

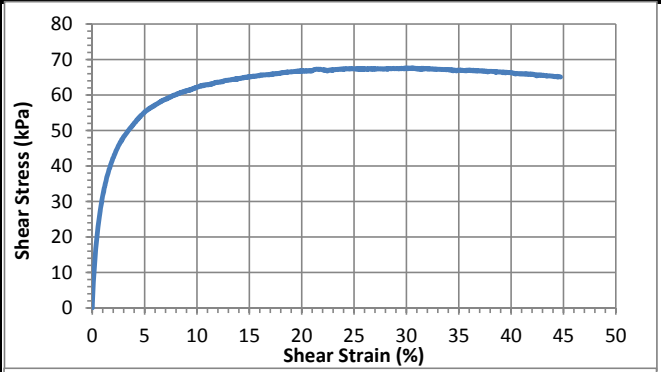

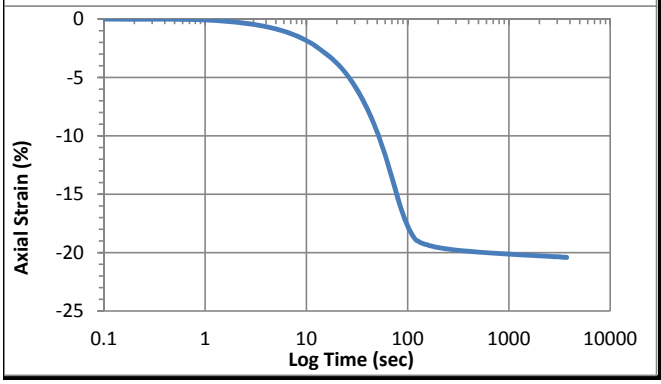

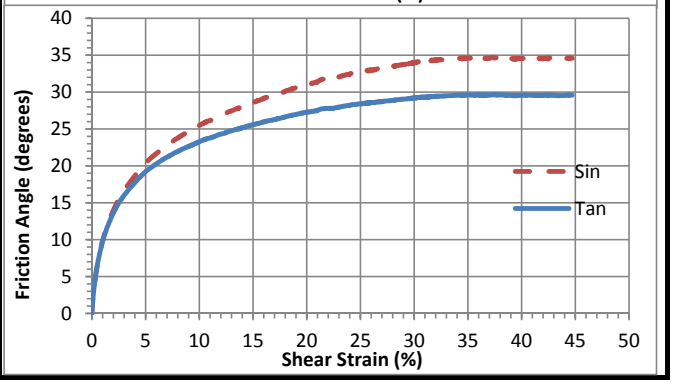

Strength			
Su/σv' at 10% strain	0.43	Su/σv0' at 10% strain	0.32
Su/σv' at 30% strain	0.56	Su/σv0' at 30% strain	0.34

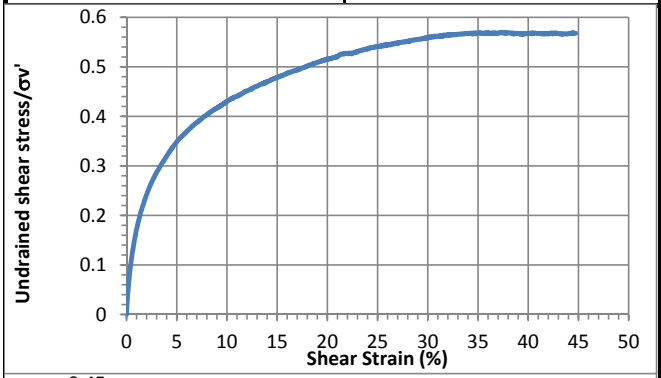

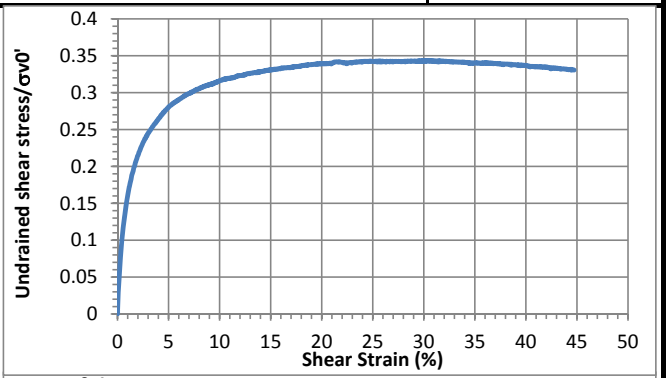

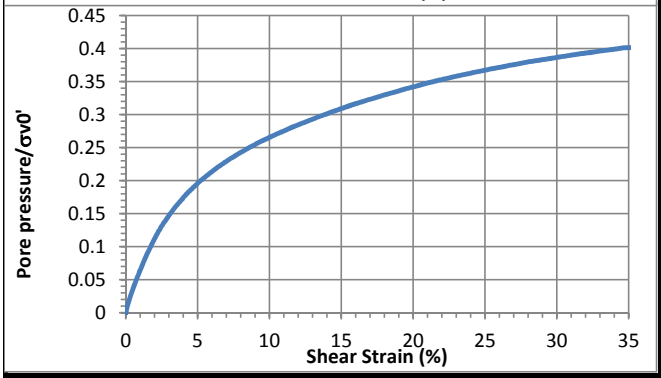

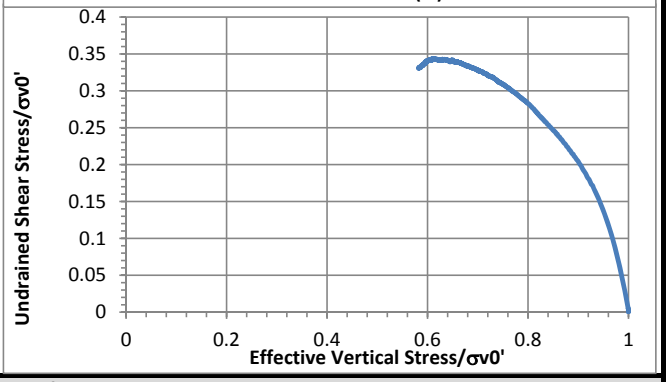

Shear wave velocity				
Signal type	Sinusoidal	First rise	initiation time (ms)	-0.0154
Signal amplitude (Vpp)	90		arrival time (ms)	0.3840
Signal frequency (kHz)	5		Vs (m/s)	252
Sensor spacing (mm)	100.64	First peak	initiation time (ms)	0.0410
R+P average Vs (m/s)	247		arrival time (ms)	0.4557
Stdev. (m/s)	7		Vs (m/s)	243
P+V average Vs (m/s)	232	First valley	initiation time (ms)	0.1382
Stdev. (m/s)	15		arrival time (ms)	0.5939
Wavelength (m)	0.046		Vs (m/s)	221
Spacing/wavelength	2.2			

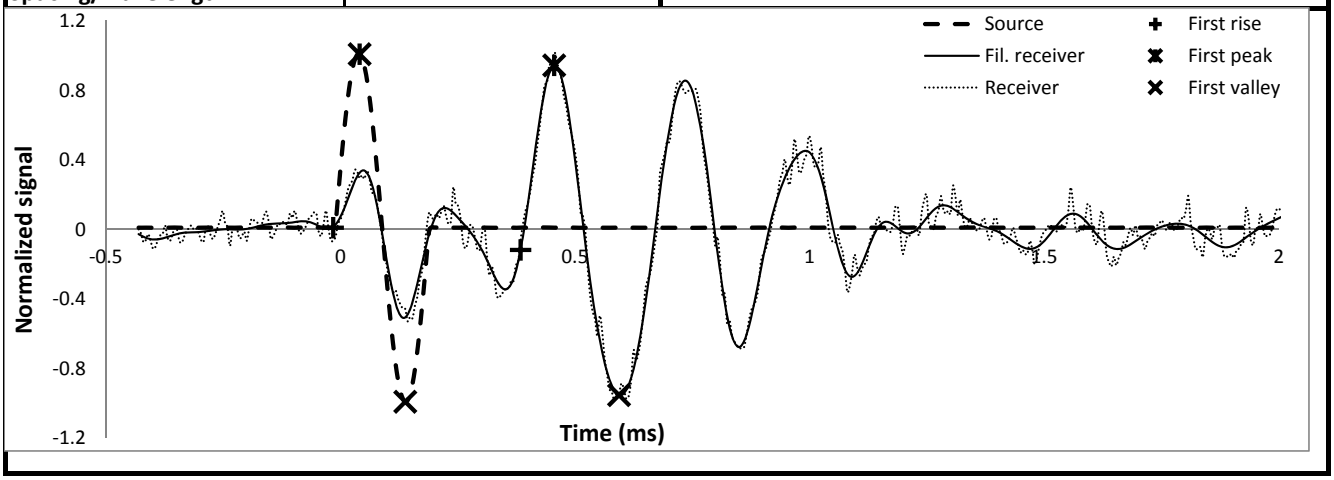

CSS Monotonic Shear Test Report

10/28/2013_Version 8.0

Geotechnical Engineering Laboratory

General Test Information and Sample Preparation			
Device:	CSS	**Layers:**	8.00
Specimen ID:	MI-STH	**Weight/layer (kg):**	1.07
Test ID:	MI35	**Height/layer (mm):**	25.4
Date of Test:	7/9/2014	**Total height (mm):**	203.2
Test Performed:	Monotonic Shear	**Soil-Only Specimen Diameter (mm):**	306.2
Test Material:	MSW	**Total weight (kg):**	8.56
Sample Preparation:	The same initial composition as Sim. #1. Compacted. Pre-compress for 23 hours, consolidate for 1 hour.	**Density (kg/m^3):**	572
		Membrane Thickness (mm):	0.000635
		Moisture Content (%):	30.4
		Saturated (Y/N):	N
		Prepared by:	Fei

Pre-compression Stage			
Pre-compression strain:	0.25	**Pre-compression ratio:**	0.00638
Height (mm):	120.6	**Density (kg/m3):**	964

Consolidation Stage		Shear Stage		
Initial height (mm):	134.9	**Type of Test:**		CU-strain
Initial density (kg/m3):	861	**Shear Strain Rate (%/min):**		0.44
Vertical Stress (kPa):	96.9	**10% strain**	**Shear stress (kPa)**	39.4
Immediate strain (εimm, %)	27.1		**Tan friction angle (°)**	27.7
Consolidated Height (mm):	114.2		**Sin friction angle (°)**	31.6
Compression index (Cc ε)	0.143	**30% strain**	**Shear stress (kPa)**	46.4
Constrained modulus	7.1		**Tan friction angle (°)**	31.0
Consolidated density (kg/m^3):	1017		**Sin friction angle (°)**	36.9

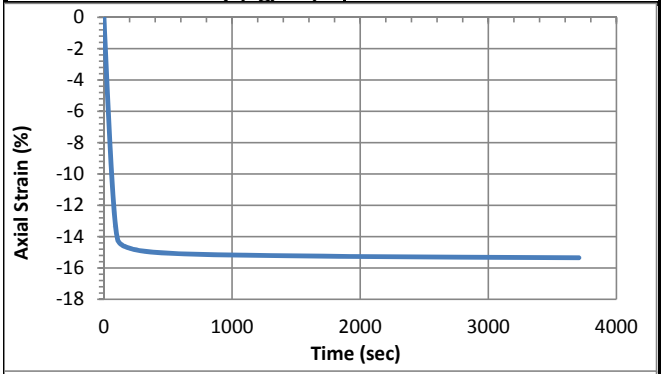

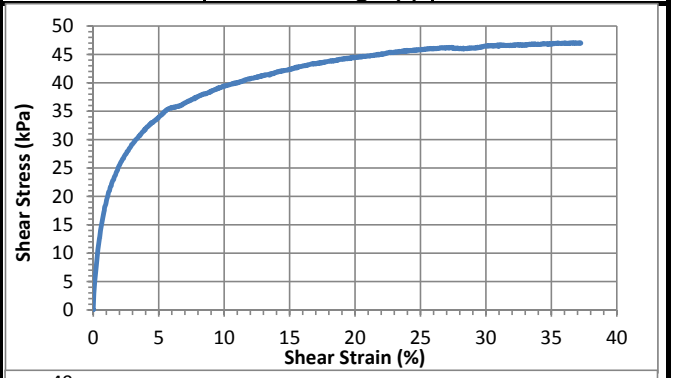

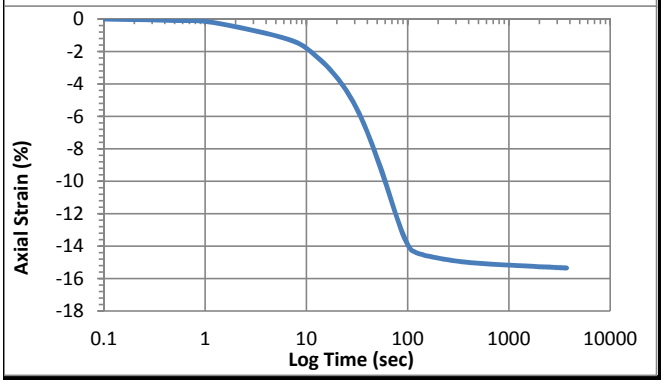

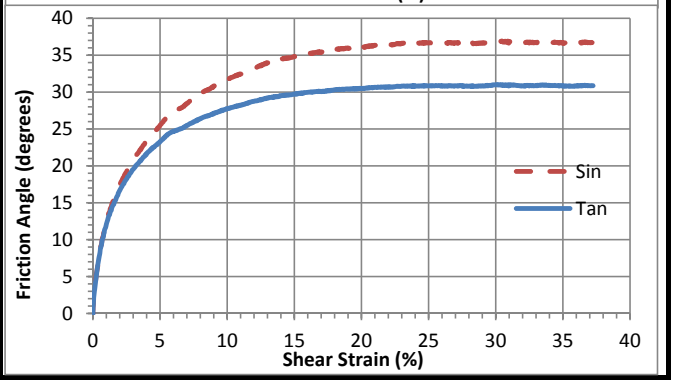

Strength			
Su/σv' at 10% strain	0.53	Su/σv0' at 10% strain	0.41
Su/σv' at 30% strain	0.60	Su/σv0' at 30% strain	0.48

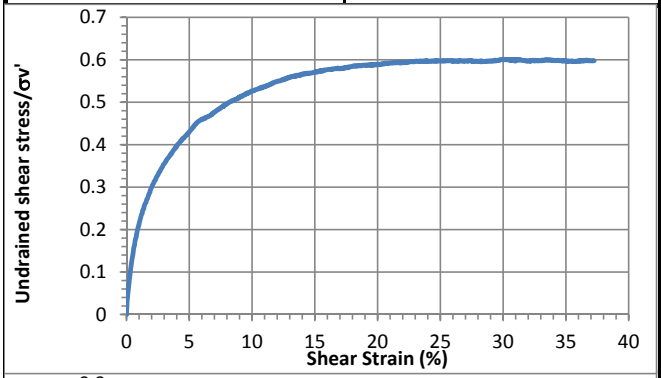

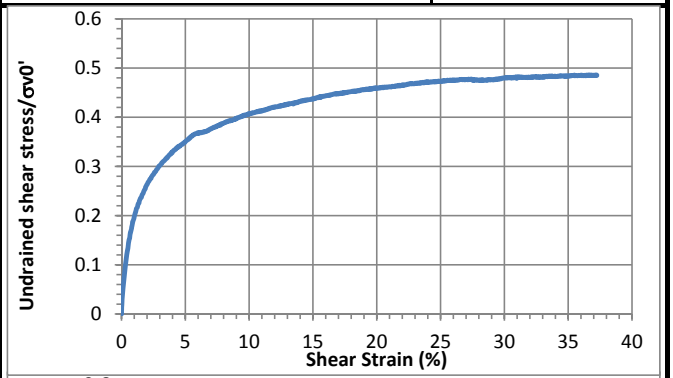

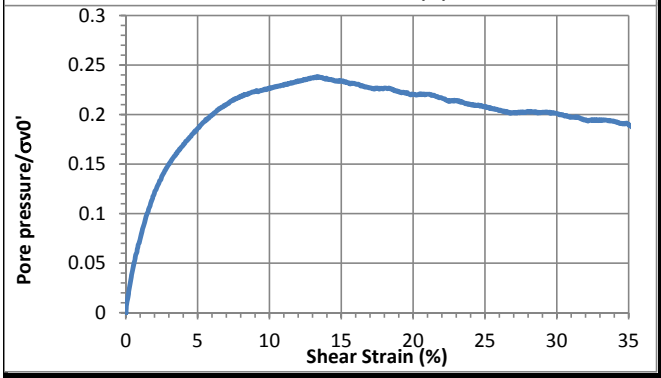

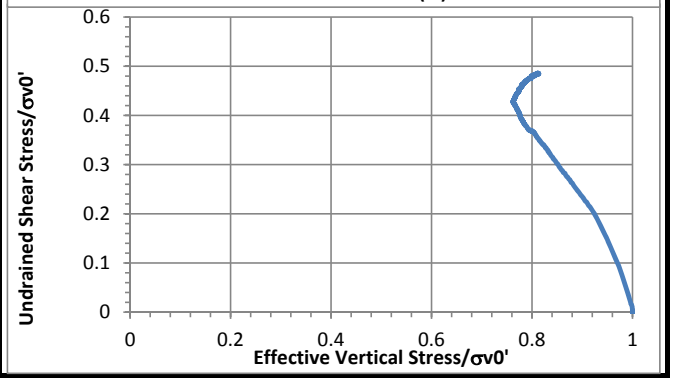

Shear wave velocity				
Signal type	Sinusoidal	First rise	initiation time (ms)	-0.0154
Signal amplitude (Vpp)	90		arrival time (ms)	0.6810
Signal frequency (kHz)	5		Vs (m/s)	151
Sensor spacing (mm)	105.39	First peak	initiation time (ms)	0.0410
R+P average Vs (m/s)	149		arrival time (ms)	0.7578
Stdev. (m/s)	3		Vs (m/s)	147
P+V average Vs (m/s)	147	First valley	initiation time (ms)	0.1434
Stdev. (m/s)	0		arrival time (ms)	0.8602
Wavelength (m)	0.029		Vs (m/s)	147
Spacing/wavelength	3.6			

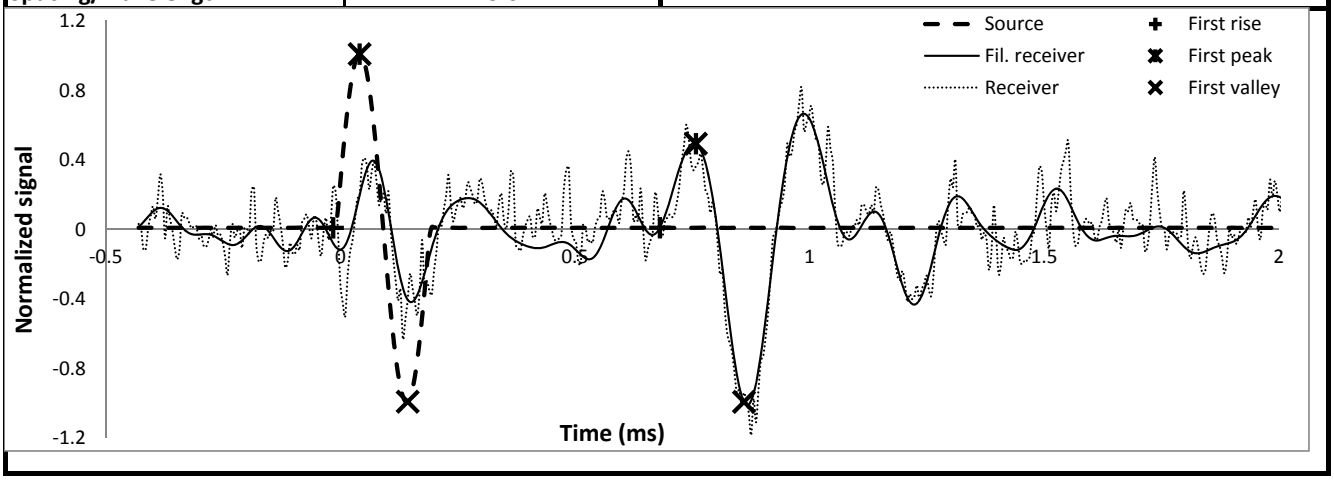

CSS Monotonic Shear Test Report

10/28/2013_Version 8.0

Geotechnical Engineering Laboratory

General Test Information and Sample Preparation

Device:	CSS	**Layers:**	8.00
Specimen ID:	MI-STH	**Weight/layer (kg):**	1.07
Test ID:	MI36	**Height/layer (mm):**	25.4
Date of Test:	7/9/2014	**Total height (mm):**	203.2
Test Performed:	Monotonic Shear	**Soil-Only Specimen Diameter (mm):**	306.2
Test Material:	MSW	**Total weight (kg):**	8.56
Sample Preparation:	The same initial composition as Sim. #1. Compacted. Pre-compress for 23 hours, consolidate for 1 hour.	**Density (kg/m^3):**	572
		Membrane Thickness (mm):	0.000635
		Moisture Content (%):	
		Saturated (Y/N):	N
		Prepared by:	Fei

Pre-compression Stage

Pre-compression strain:	0.22	**Secondary compression ratio**	0.00806
Height (mm):	119.1	**Density (kg/m3):**	976

Consolidation Stage

Initial height (mm):	128.8
Initial density (kg/m3):	903
Vertical Stress (kPa):	96.7
Immediate strain (εimm, %)	22.7
Consolidated Height (mm):	112.7
Compression index (Ccε)	0.123
Constrained modulus	8.2
Consolidated density (kg/m^3):	1031

Shear Stage

Type of Test:		CD-strain
Shear Strain Rate (%/min):		0.45
10% strain	**Shear stress (kPa)**	41.2
	Tan friction angle (°)	23.1
	Sin friction angle (°)	25.3
30% strain	**Shear stress (kPa)**	48.9
	Tan friction angle (°)	26.8
	Sin friction angle (°)	30.4

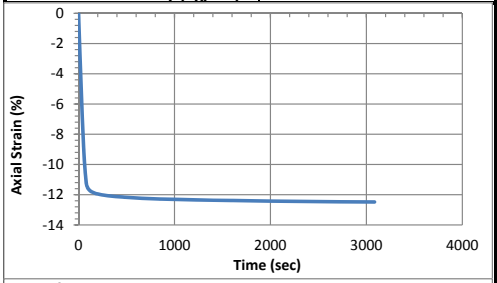

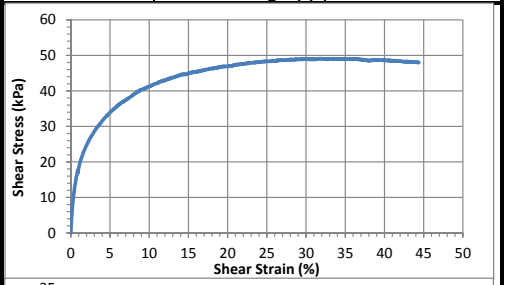

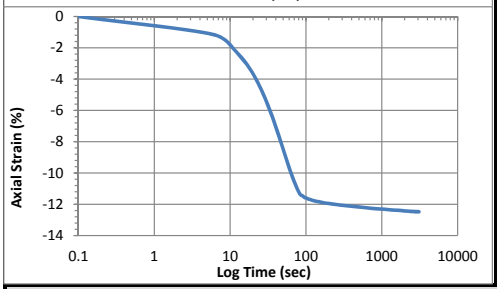

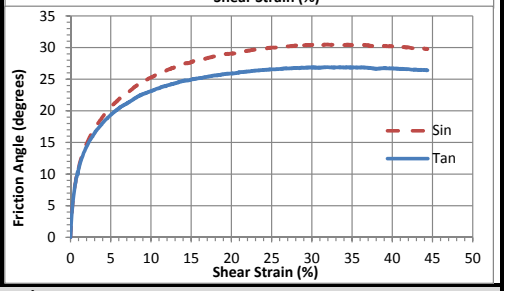

Strength

τ/σv' at 10% strain	0.43	**τ/σv0' at 10% strain**	0.43
τ/σv' at 30% strain	0.51	**τ/σv0' at 30% strain**	0.51

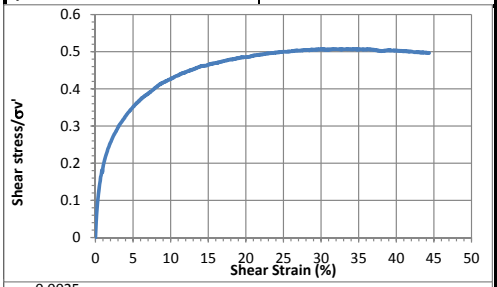

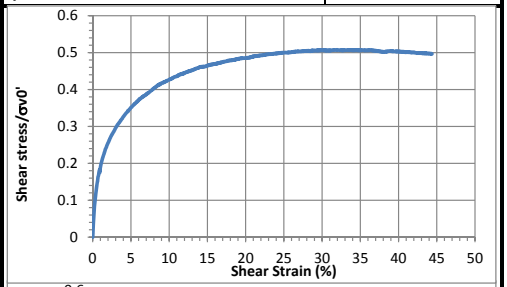

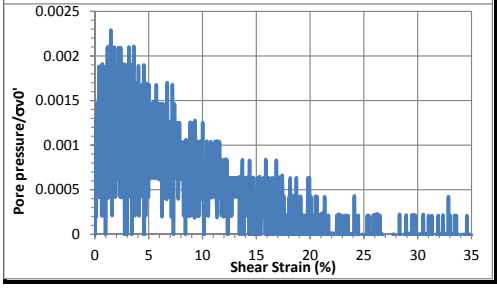

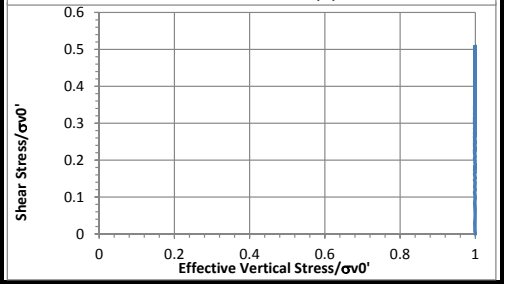

CSS Monotonic Shear Test Report

10/28/2013_Version 8.0

Geotechnical Engineering Laboratory

General Test Information and Sample Preparation			
Device:	CSS	**Layers:**	8.34
Specimen ID:	STH	**Weight/layer (kg):**	1.07
Test ID:	MI37	**Height/layer (mm):**	25.4
Date of Test:	7/11/2014	**Total height (mm):**	211.836
Test Performed:	Monotonic Shear	**Soil-Only Specimen Diameter (mm):**	306.2
Test Material:	MSW	**Total weight (kg):**	8.9238
Sample Preparation:	The same initial composition and unit weight as Sim. #1. Pre-compress for 24 hours, consolidate for 1 hour.	**Density (kg/m^3):**	572
		Membrane Thickness (mm):	0.000635
		Moisture Content (%):	
		Saturated (Y/N):	N
		Prepared by:	Fei

Pre-compression Stage			
Pre-compression strain:	0.41	**Secondary compression ratio:**	0.01054
Height (mm):	123.2	**Density (kg/m3):**	1058

Consolidation Stage		Shear Stage		
Initial height (mm):	137.5	**Type of Test:**		CU-strain
Initial density (kg/m3):	881	**Shear Strain Rate (%/min):**		0.47
Vertical Stress (kPa):	395.0	**10% strain**	**Shear stress (kPa)**	124.9
Immediate strain (εimm, %)	40.5		**Tan friction angle (°)**	23.0
Consolidated Height (mm):	106.4		**Sin friction angle (°)**	25.0
Compression index (Cc ε)	0.163	**30% strain**	**Shear stress (kPa)**	137.4
Consolidation modulus	4.7		**Tan friction angle (°)**	28.4
Consolidated density (kg/m^3):	1139		**Sin friction angle (°)**	32.8

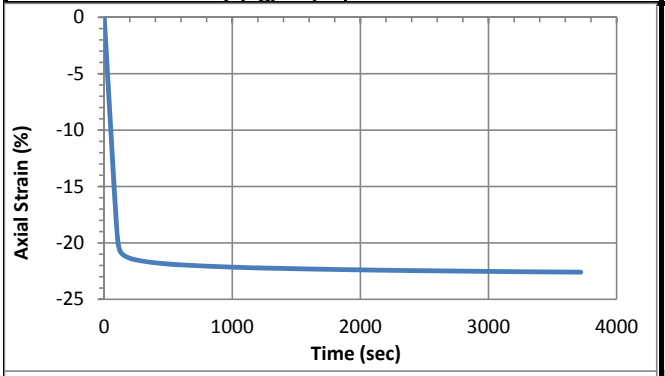

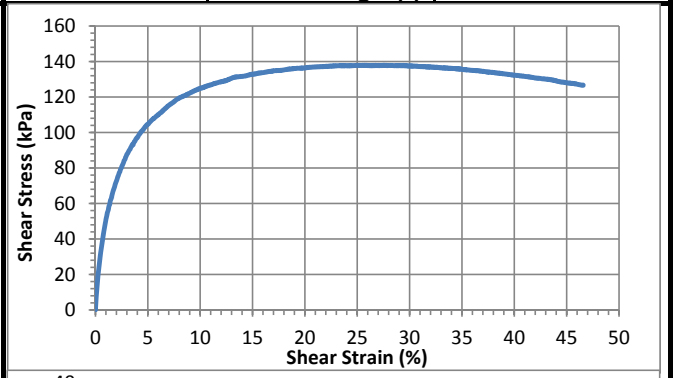

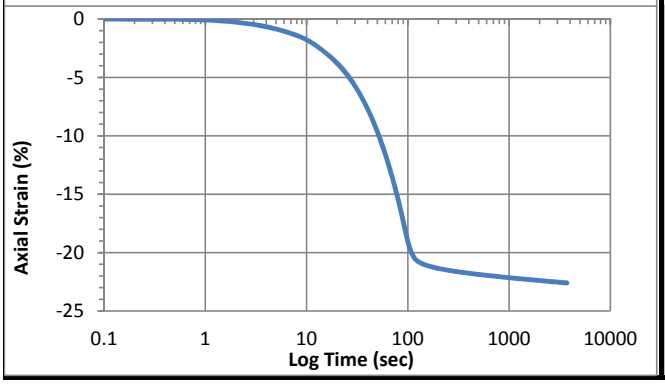

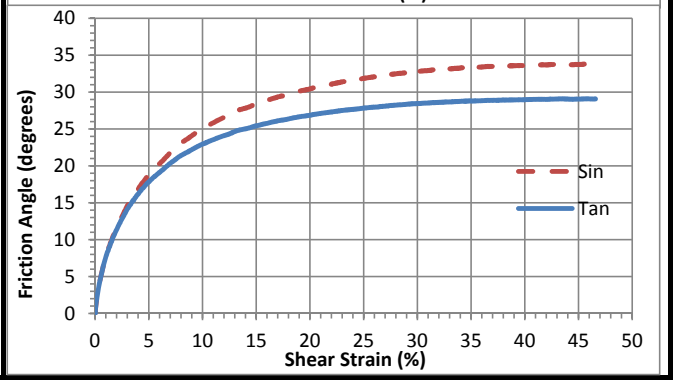

Undrained Strength			
Su/σv' at 10% strain	0.42	Su/σvc' at 10% strain	0.31
Su/σv' at 30% strain	0.54	Su/σvc' at 30% strain	0.35

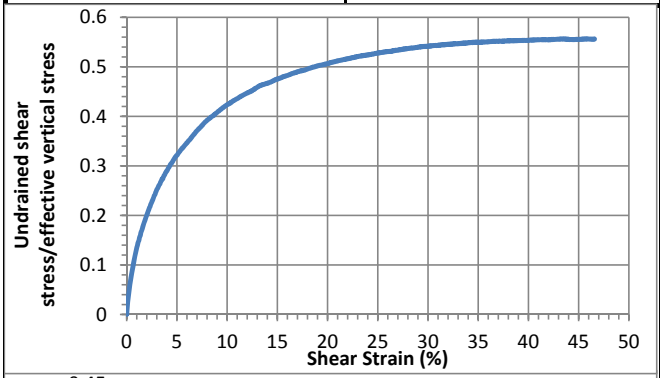

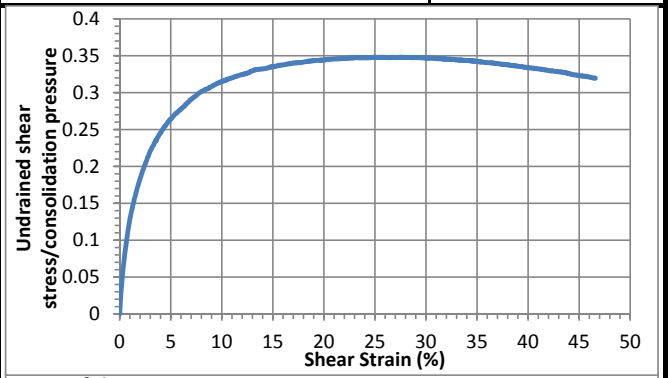

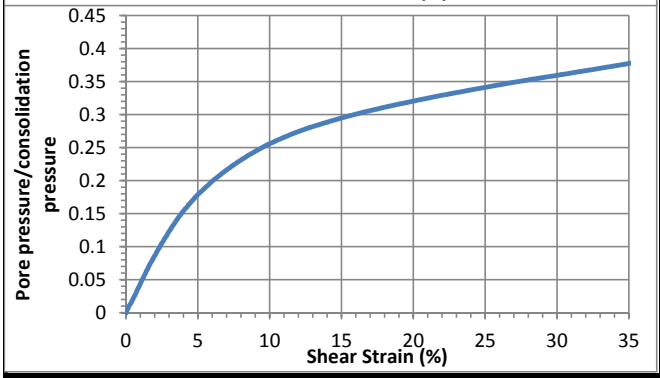

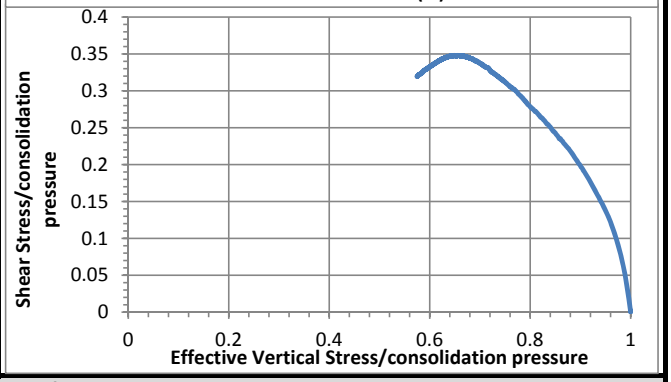

Shear wave velocity				
Signal type	Sinusoidal	First rise	initiation time (ms)	-0.0102
Signal amplitude (Vpp)	90		arrival time (ms)	0.3738
Signal frequency (kHz)	5		Vs (m/s)	254
Sensor spacing (mm)	97.64	First peak	initiation time (ms)	0.0410
R+P average Vs (m/s)	243		arrival time (ms)	0.4608
Stdev. (m/s)	15		Vs (m/s)	233
P+V average Vs (m/s)	227	First valley	initiation time (ms)	0.1382
Stdev. (m/s)	8		arrival time (ms)	0.5786
Wavelength (m)	0.045		Vs (m/s)	222
Spacing/wavelength	2.1			

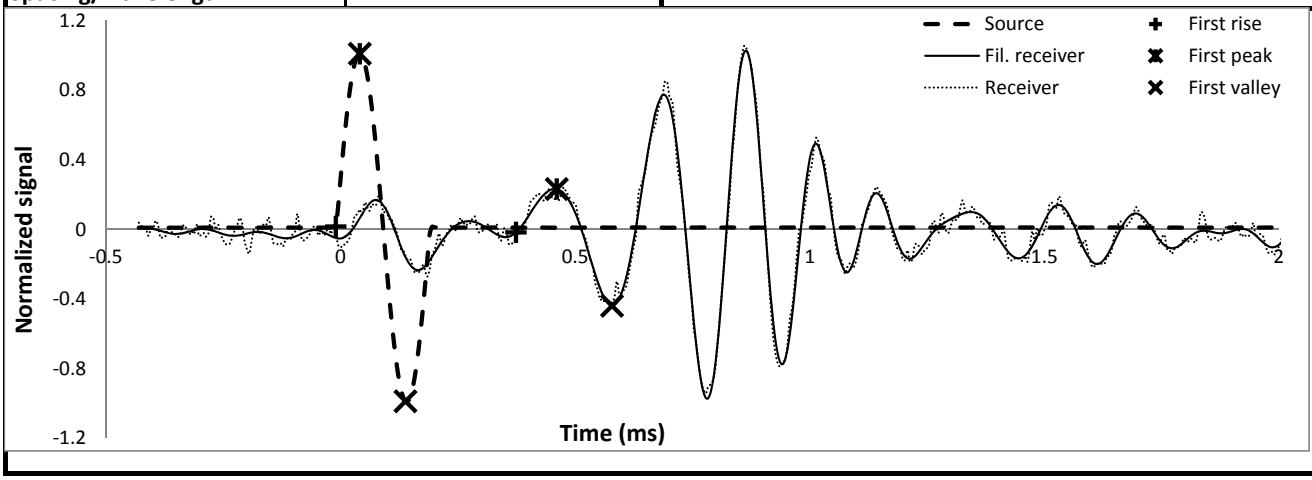

CSS Monotonic Shear Test Report

10/28/2013_Version 8.0

Geotechnical Engineering Laboratory

General Test Information and Sample Preparation			
Device:	CSS	**Layers:**	8.34
Specimen ID:	STH	**Weight/layer (kg):**	1.07
Test ID:	MI38	**Height/layer (mm):**	25.4
Date of Test:	7/13/2014	**Total height (mm):**	211.836
Test Performed:	Monotonic Shear	**Soil-Only Specimen Diameter (mm):**	306.2
Test Material:	MSW	**Total weight (kg):**	8.9238
Sample Preparation:	The same initial composition and unit weight as Sim. #1. Pre-compress for 23 hours, consolidate for 1 hour. Vertical P=4, I=0.5.	**Density (kg/m^3):**	572
		Membrane Thickness (mm):	0.000635
		Moisture Content (%):	
		Saturated (Y/N):	N
		Prepared by:	Fei

Pre-compression Stage			
Pre-compression strain:	0.48	**Secondary compression ratio:**	0.00960
Height (mm):	110.5	**Density (kg/m3):**	1085

Consolidation Stage		Shear Stage		
Initial height (mm):	134.9	**Type of Test:**		CU-strain
Initial density (kg/m3):	898	**Shear Strain Rate (%/min):**		0.48
Vertical Stress (kPa):	394.4	**10% strain**	**Shear stress (kPa)**	121.1
Immediate strain (εimm, %)	47.4		**Tan friction angle (°)**	22.7
Consolidated Height (mm):	103.3		**Sin friction angle (°)**	24.6
Compression index (Cc ε)	0.190	**30% strain**	**Shear stress (kPa)**	126.4
Consolidation modulus	4.0		**Tan friction angle (°)**	28.7
Consolidated density (kg/m^3):	1172		**Sin friction angle (°)**	33.1

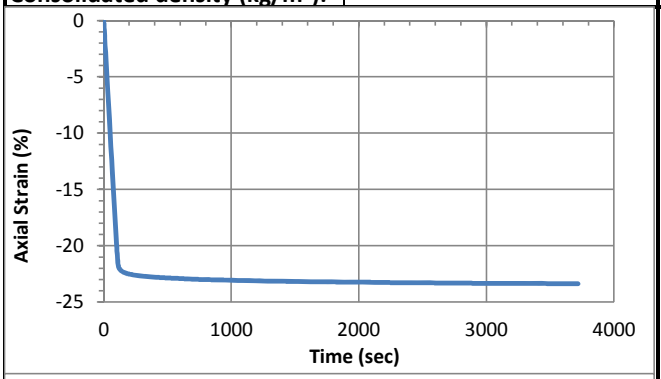

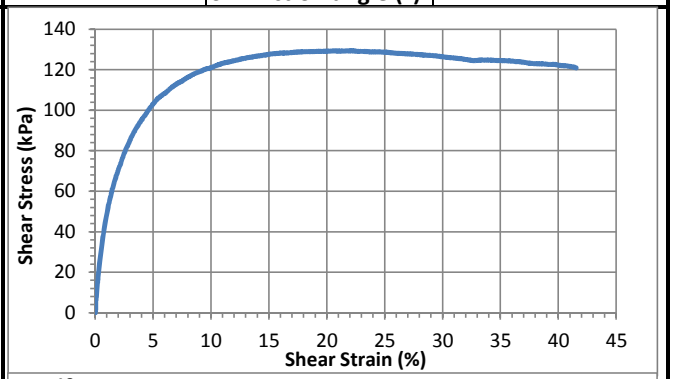

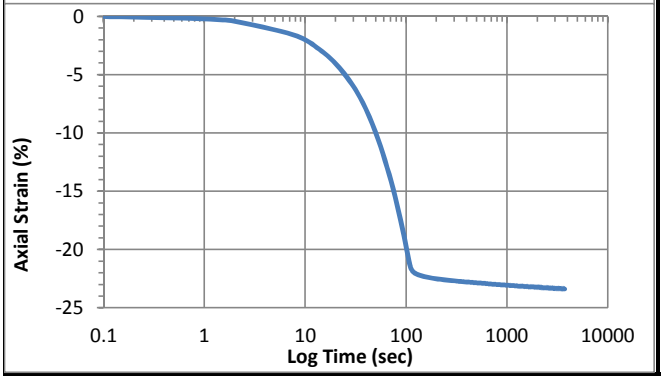

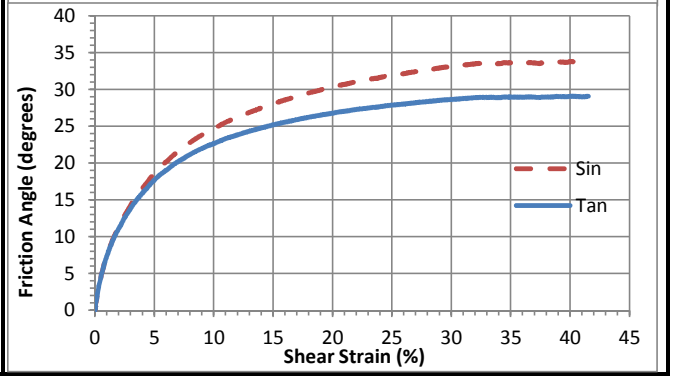

Undrained Strength			
Su/σv' at 10% strain	0.42	Su/σvc' at 10% strain	0.31
Su/σv' at 30% strain	0.55	Su/σvc' at 30% strain	0.32

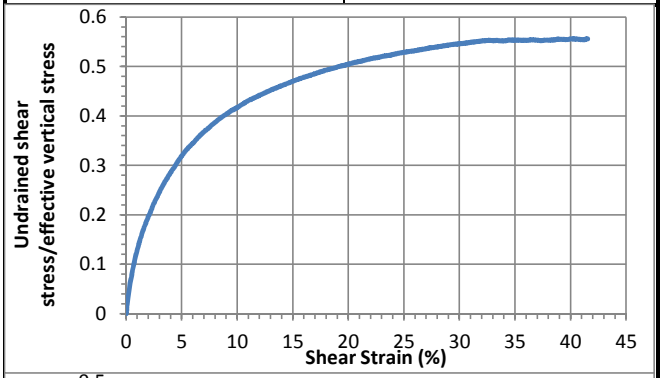

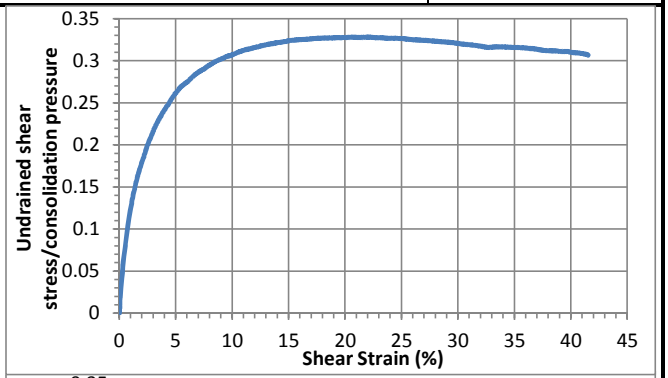

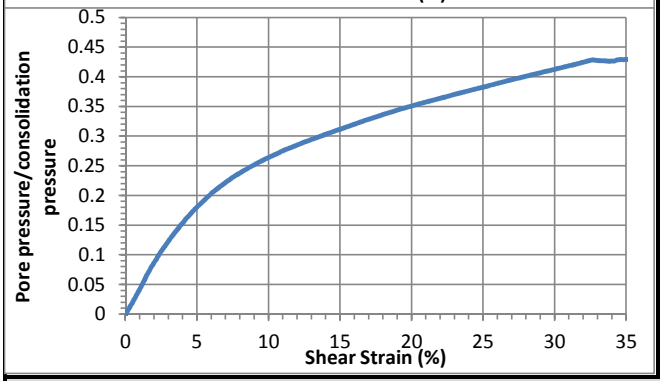

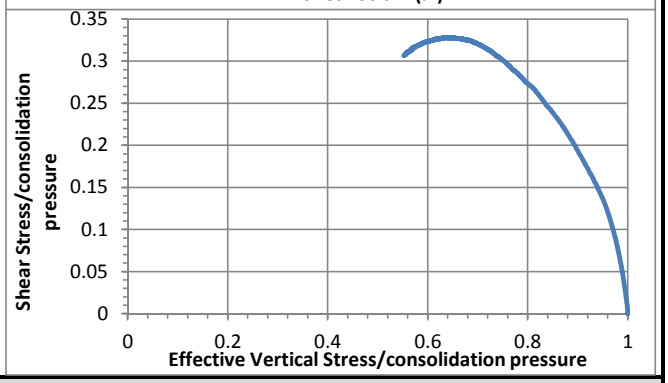

Shear wave velocity				
Signal type	Sinusoidal	First rise	initiation time (ms)	-0.0102
Signal amplitude (Vpp)	90		arrival time (ms)	0.3891
Signal frequency (kHz)	5		Vs (m/s)	237
Sensor spacing (mm)	94.57	First peak	initiation time (ms)	0.0410
R+P average Vs (m/s)	238		arrival time (ms)	0.4352
Stdev. (m/s)	2		Vs (m/s)	240
P+V average Vs (m/s)	238	First valley	initiation time (ms)	0.1382
Stdev. (m/s)	2		arrival time (ms)	0.5376
Wavelength (m)	0.048		Vs (m/s)	237
Spacing/wavelength	2.0			

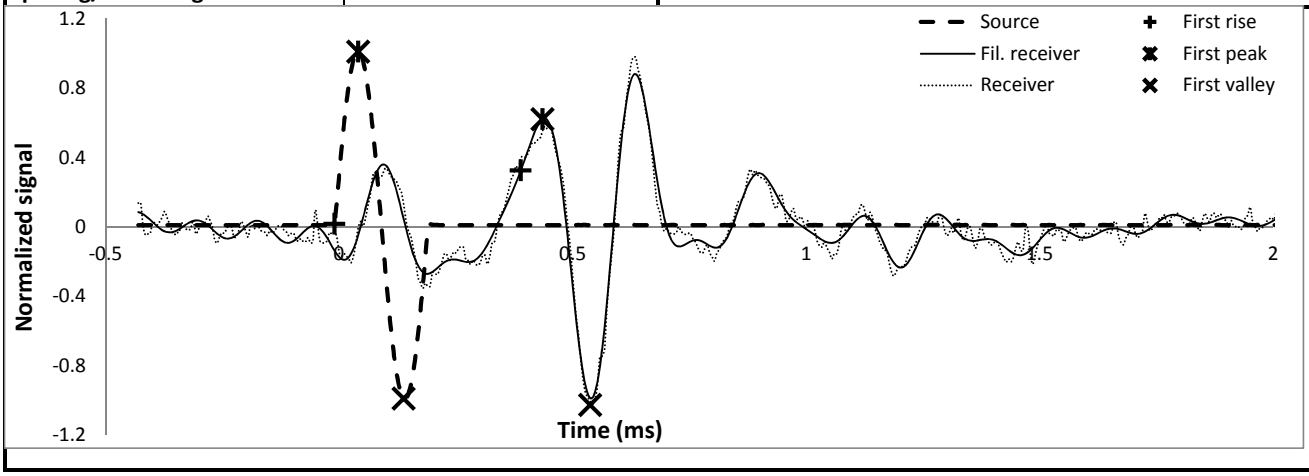

CSS Monotonic Shear Test Report

10/28/2013_Version 8.0

Geotechnical Engineering Laboratory

General Test Information and Sample Preparation			
Device:	CSS	**Layers:**	8.30
Specimen ID:	MI-STH	**Weight/layer (kg):**	1.07
Test ID:	MI39	**Height/layer (mm):**	25.4
Date of Test:	7/20/2014	**Total height (mm):**	210.82
Test Performed:	Monotonic Shear	**Soil-Only Specimen Diameter (mm):**	306.2
Test Material:	MSW	**Total weight (kg):**	8.881
Sample Preparation:	The same initial composition and unit weight as Sim. #1. Pre-compress for 23 hours, consolidate for 1 hour. Vertical P=20, I=0.5.	**Density (kg/m^3):**	572
		Membrane Thickness (mm):	0.000635
		Moisture Content (%):	
		Saturated (Y/N):	N
		Prepared by:	Fei

Pre-compression Stage			
Pre-compression strain:	0.46	**Secondary compression ratio:**	0.00919
Height (mm):	112.6	**Density (kg/m3):**	1071

Consolidation Stage		Shear Stage		
Initial height (mm):	135.2	**Type of Test:**		CU-strain
Initial density (kg/m3):	892	**Shear Strain Rate (%/min):**		0.48
Vertical Stress (kPa):	394.4	**10% strain**	**Shear stress (kPa)**	121.1
Immediate strain (εimm, %)	46.1		**Tan friction angle (°)**	23.7
Consolidated Height (mm):	105.4		**Sin friction angle (°)**	26.0
Compression index (Cc ε)	0.185	**30% strain**	**Shear stress (kPa)**	127.8
Constrained modulus	4.2		**Tan friction angle (°)**	27.9
Consolidated density (kg/m^3):	1144		**Sin friction angle (°)**	32.0

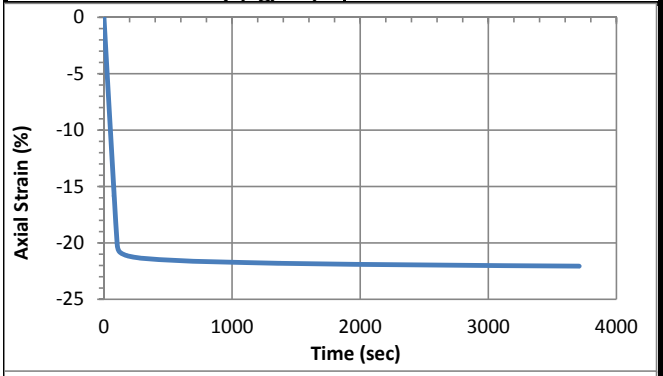

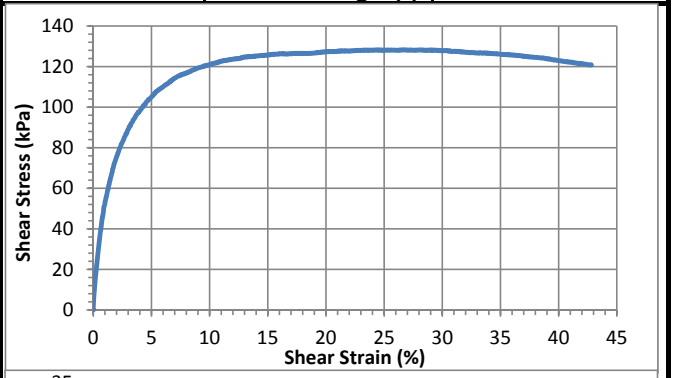

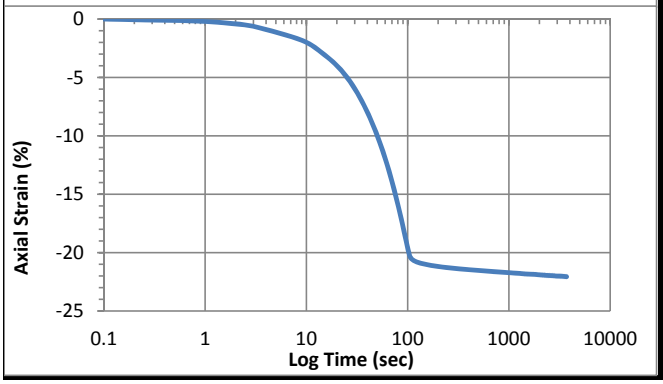

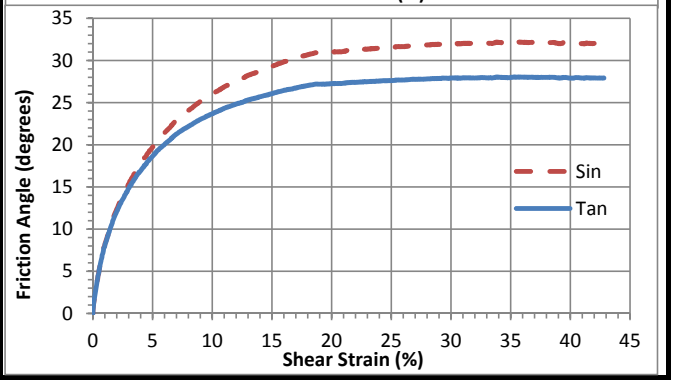

Strength			
Su/σv' at 10% strain	0.44	Su/σv0' at 10% strain	0.31
Su/σv' at 30% strain	0.53	Su/σv0' at 30% strain	0.32

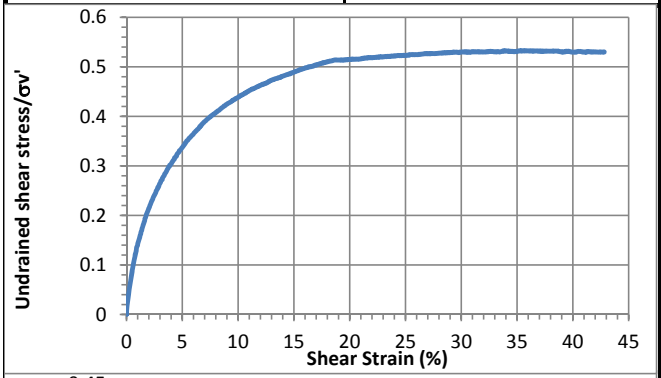

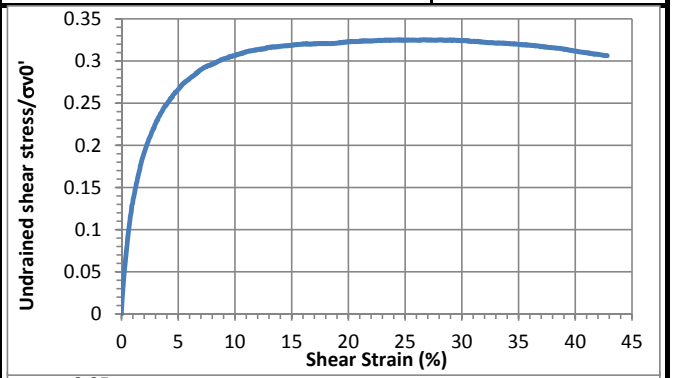

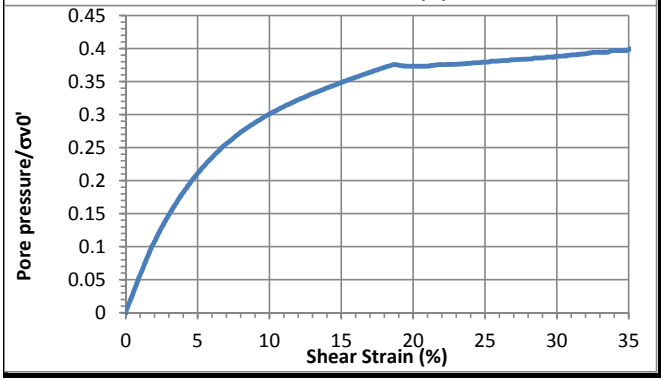

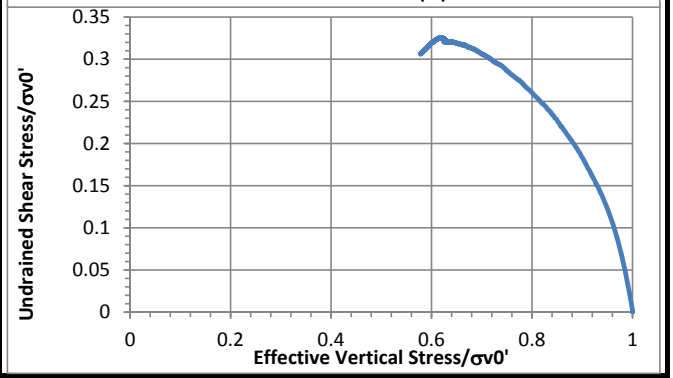

Shear wave velocity				
Signal type	Sinusoidal	First rise	initiation time (ms)	-0.0154
Signal amplitude (Vpp)	90		arrival time (ms)	0.3840
Signal frequency (kHz)	5		Vs (m/s)	242
Sensor spacing (mm)	96.57	First peak	initiation time (ms)	0.0410
R+P average Vs (m/s)	239		arrival time (ms)	0.4506
Stdev. (m/s)	4		Vs (m/s)	236
P+V average Vs (m/s)	232	First valley	initiation time (ms)	0.1382
Stdev. (m/s)	6		arrival time (ms)	0.5632
Wavelength (m)	0.046		Vs (m/s)	227
Spacing/wavelength	2.1			

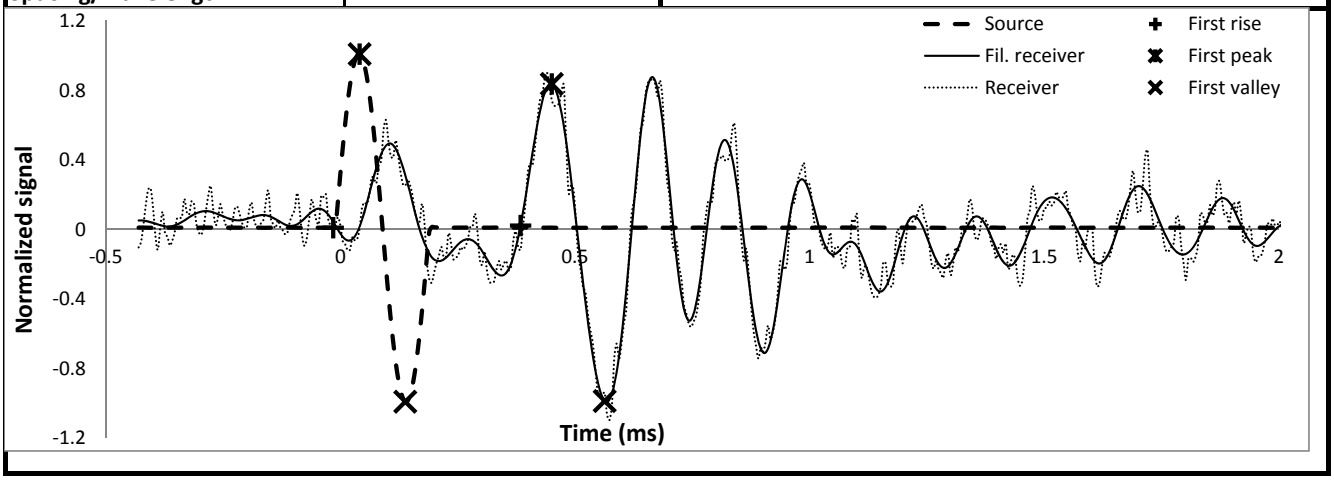

CSS Monotonic Shear Test Report

10/28/2013_Version 8.0

Geotechnical Engineering Laboratory

General Test Information		Sample Preparation	
Device:	CSS	Prepared total weight (kg):	7.490
Specimen ID:	MI-STH	Prepared dry weight (kg):	5.548
Test ID:	MI40	Prepared height (mm):	196.6
Date of test:	9/15/2015	Prepared total density (kg/m3):	517
Test performed:	Monotonic Shear	Prepared dry density (kg/m3):	383
Test material:	MSW	**Pre-compression Stage**	
Sample preparation:	MI-STH fresh. Repeat MI-STH18.	Pre-compressed strain (%):	38.3
		Compressed total density (kg/m3):	838
		Compressed dry density (kg/m3):	621
		Secondary compression ratio:	0.00607
		Total weight before shearing (kg):	7.447
		Dry weight before shearing (kg):	5.420

Consolidation Stage		Shear Stage		
Consolidated height (mm):	116.99	Type of test:		CV-strain
Vertical stress (kPa):	98.4	Shear strain rate (%/min):		4.24
Immediate strain (εimm, %)	39.70	10% strain	Shear stress (kPa)	33.4
Strain before shearing (εall, %)	40.5		Tan friction angle (°)	25.4
Compression index (Cεε)	0.199		Sin friction angle (°)	28.3
Constrained modulus	5.04	peak	Shear stress (kPa)	37.6
Consolidated total density	864		Tan friction angle (°)	31.3
Consolidated dry density	629		Sin friction angle (°)	37.7

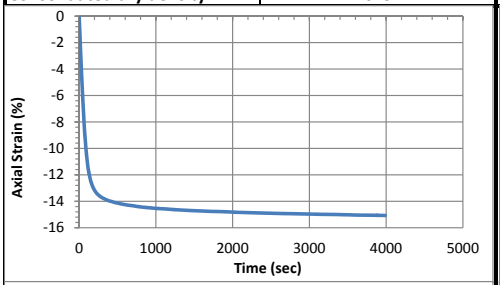

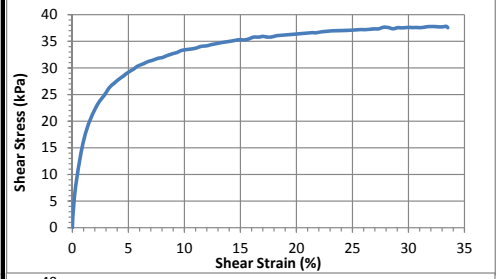

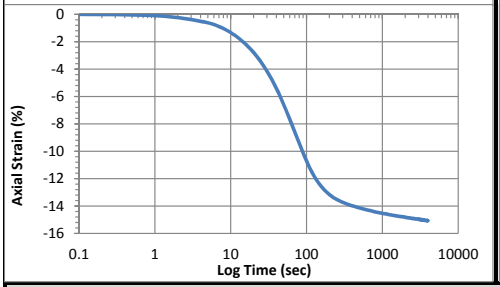

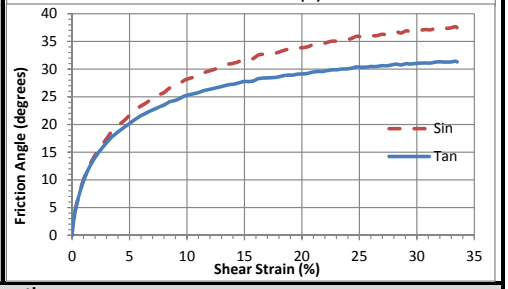

Strength			
τ/σv' at 10% strain	0.47	τ/σv0' at 10% strain	0.34
τ/σv' at peak	0.61	τ/σv0' at peak	0.38

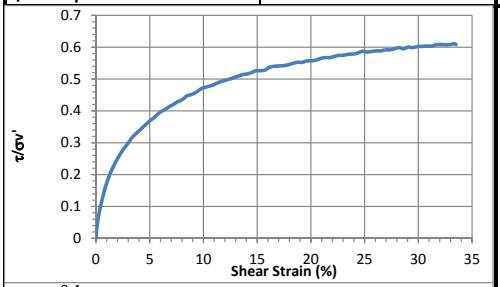

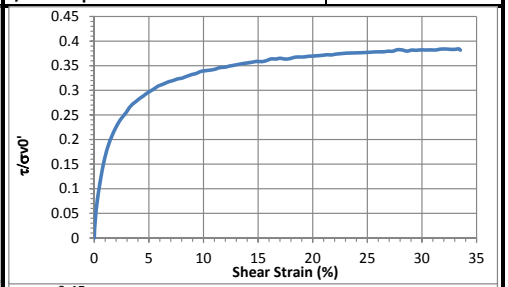

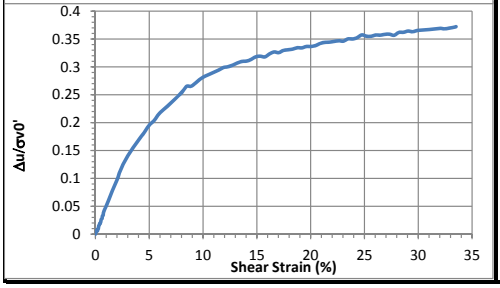

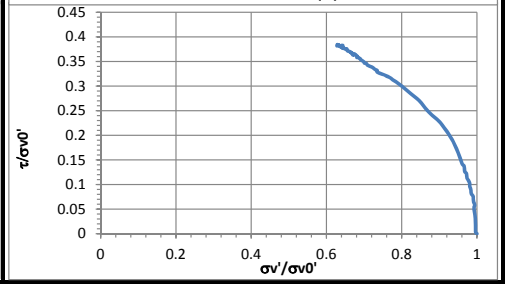

Accelerometer-Based Shear Wave Velocity Datasheet

Specimen ID: 091515-STH40-100-X-4
Test Material: STH40
Date: 091515
Test Performed by: Fei
Filename: 091515-STH40-100-X-4

Vertical Stress: 100kPa
Sensor Spacing: 0.11706 m
V_s(rise) = 138 m/s

Data Record

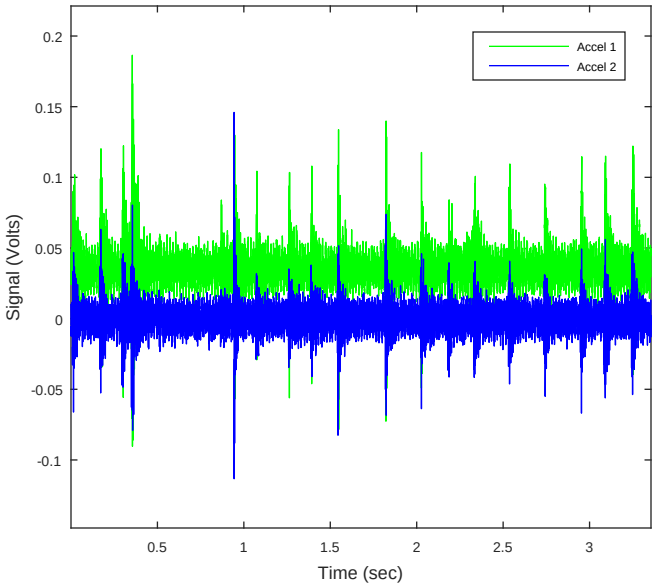

FFT of Accel 1

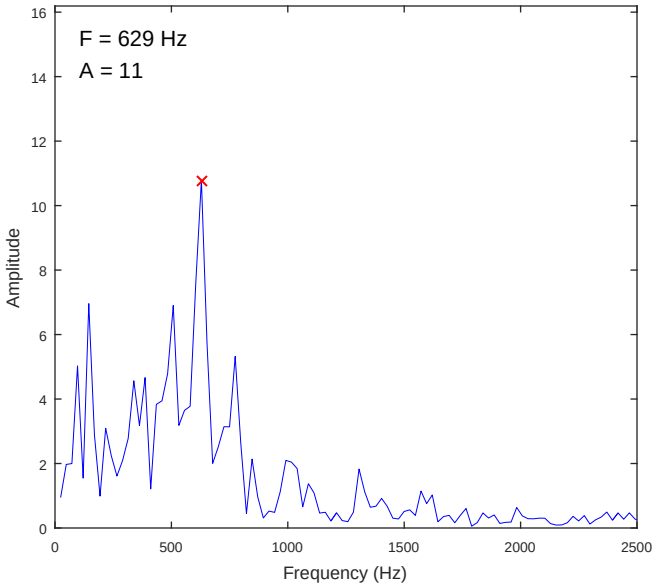

FFT of Accel 2

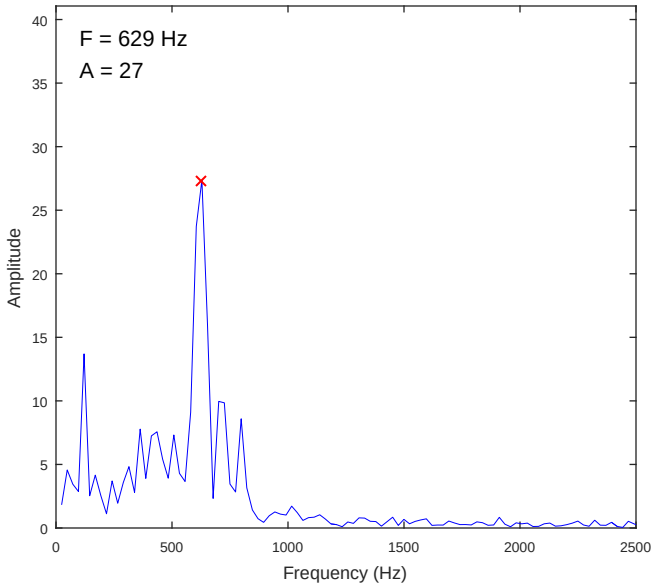

Travel Time Selection - View 1

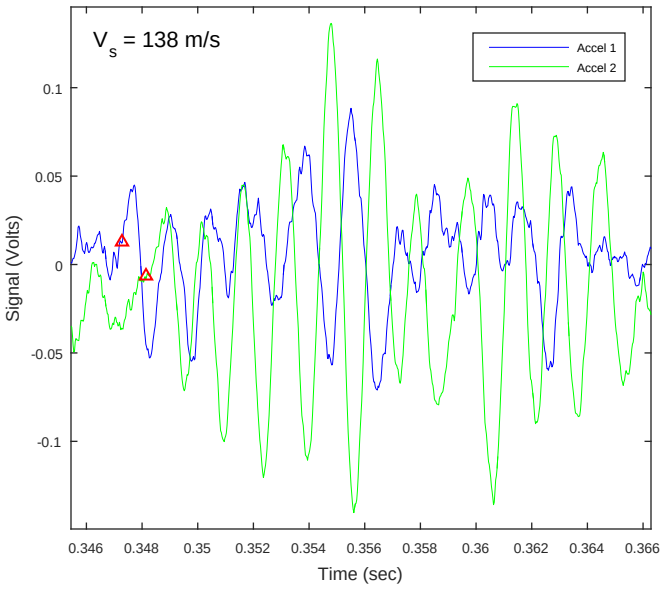

Travel Time Selection - View 2

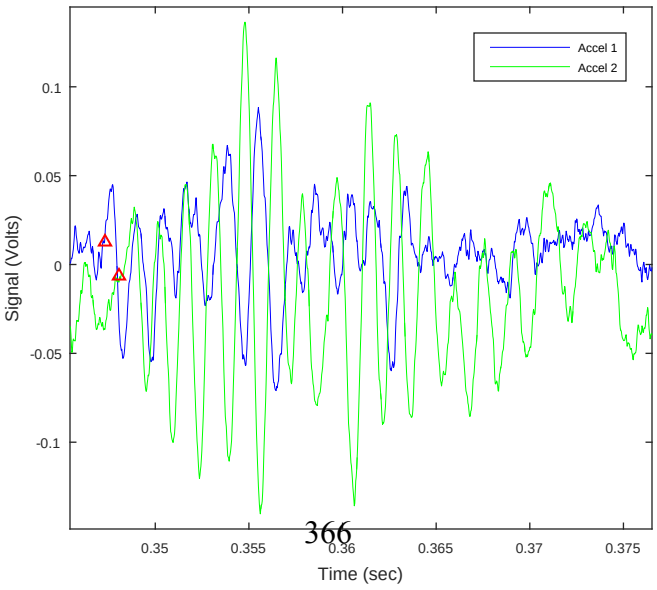

Travel Time Selection - View 3

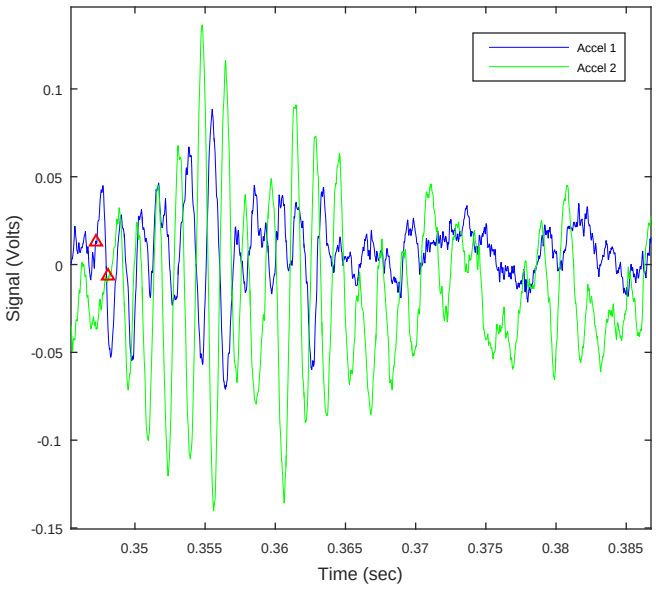

CSS Monotonic Shear Test Report

10/28/2013_Version 8.0

Geotechnical Engineering Laboratory

General Test Information	
Device:	CSS
Specimen ID:	MI-STH
Test ID:	MI41
Date of test:	9/17/2015
Test performed:	Monotonic Shear
Test material:	MSW
Sample preparation:	MI-STH fresh. Repeat MI-STH34. Constant volume gain=10000 kPa. Removed 0.355 kg before shearing.

Sample Preparation	
Prepared total weight (kg):	7.490
Prepared dry weight (kg):	5.548
Prepared height (mm):	193.0
Prepared total density (kg/m3):	527
Prepared dry density (kg/m3):	390
Pre-compression Stage	
Pre-compressed strain (%):	36.7
Compressed total density (kg/m3):	833
Compressed dry density (kg/m3):	617
Secondary compression ratio:	0.00603
Total weight before shearing (kg):	7.490
Dry weight before shearing (kg):	5.193

Consolidation Stage	
Consolidated height (mm):	111.19
Vertical stress (kPa):	99.0
Immediate strain (εimm, %)	41.65
Strain before shearing (εall, %)	42.4
Compression index (Cεε)	0.209
Constrained modulus	4.80
Consolidated total density	915
Consolidated dry density	634

Shear Stage		
Type of test:		CV-strain
Shear strain rate (%/min):		2.23
10% strain	Shear stress (kPa)	34.8
	Tan friction angle (°)	25.4
	Sin friction angle (°)	28.3
peak	Shear stress (kPa)	39.4
	Tan friction angle (°)	31.2
	Sin friction angle (°)	37.4

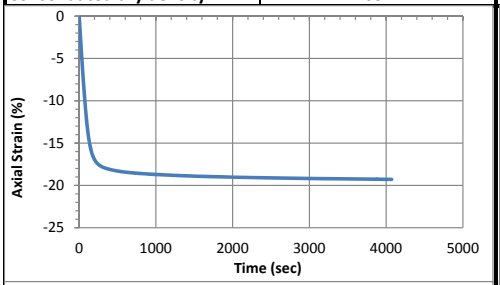

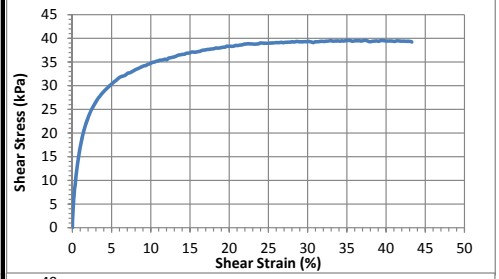

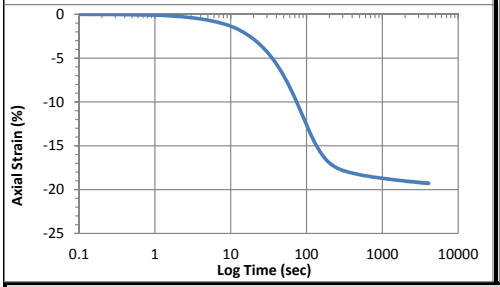

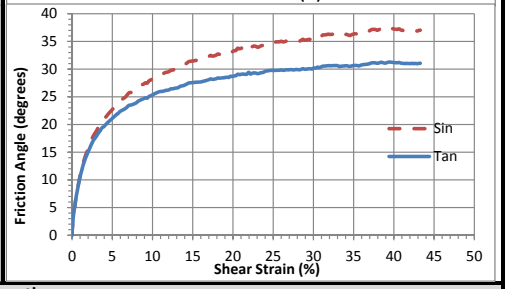

Strength

τ/σv' at 10% strain	0.47	τ/σv0' at 10% strain	0.35
τ/σv' at peak	0.61	τ/σv0' at peak	0.40

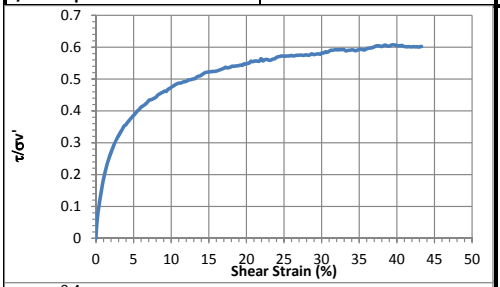

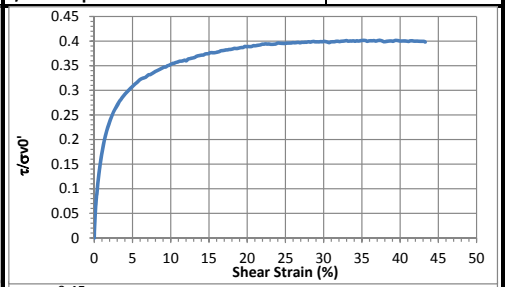

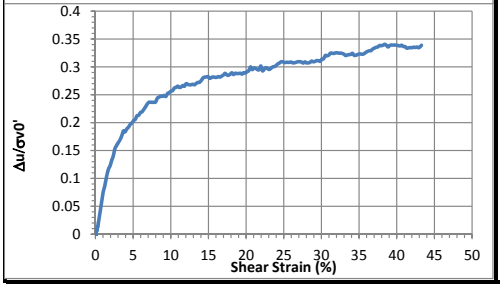

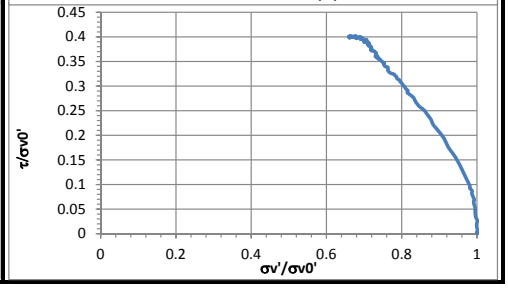

Accelerometer-Based Shear Wave Velocity Datasheet

Specimen ID: 091715-STH41-100-X-4
Test Material: STH41
Date: 091715
Test Performed by: Fei
Filename: 091715-STH41-100-X-4

Vertical Stress: 100kPa
Sensor Spacing: 0.1113 m
V_s(rise) = 128 m/s

Data Record

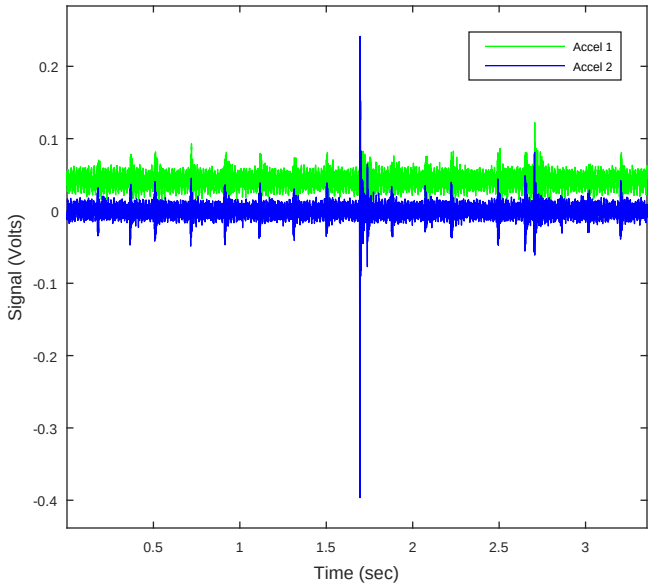

FFT of Accel 1

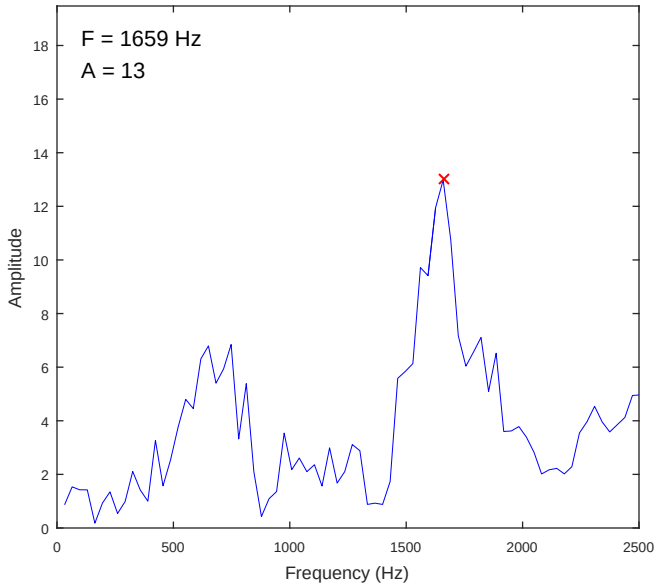

FFT of Accel 2

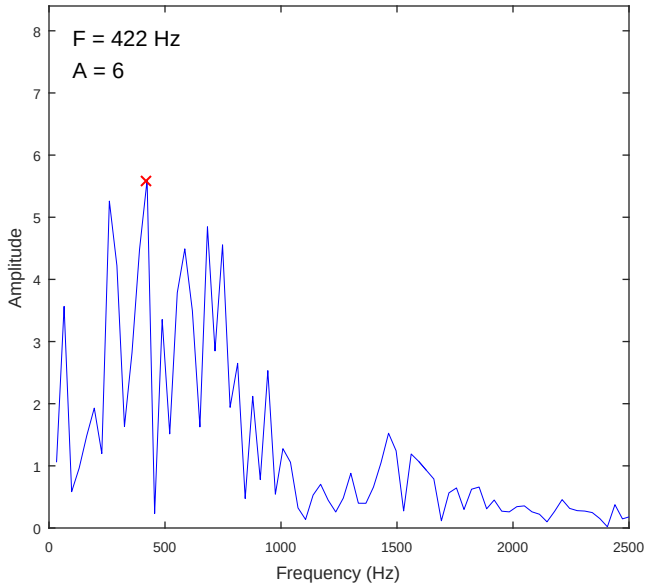

Travel Time Selection - View 1

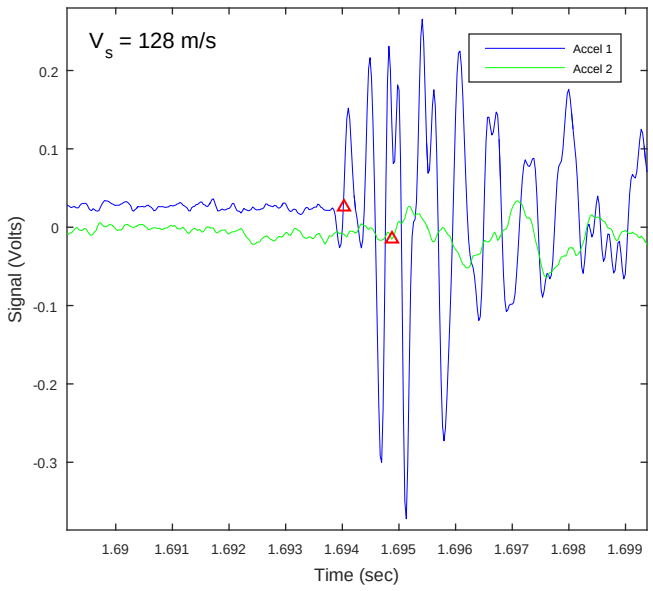

Travel Time Selection - View 2

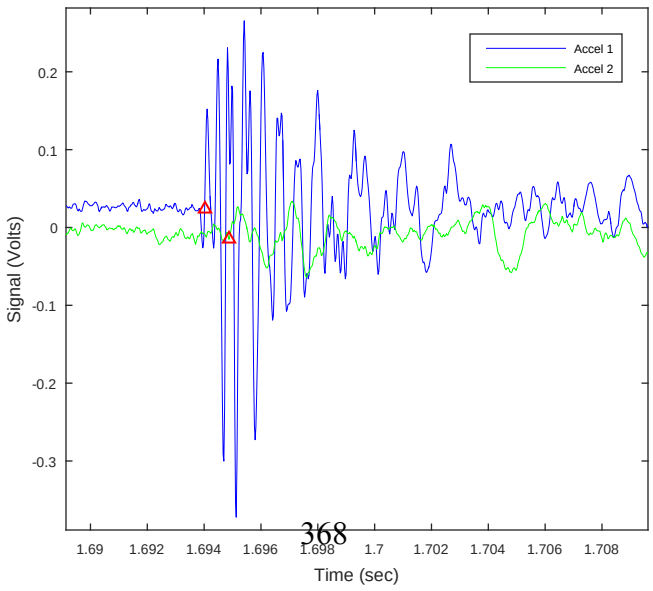

Travel Time Selection - View 3

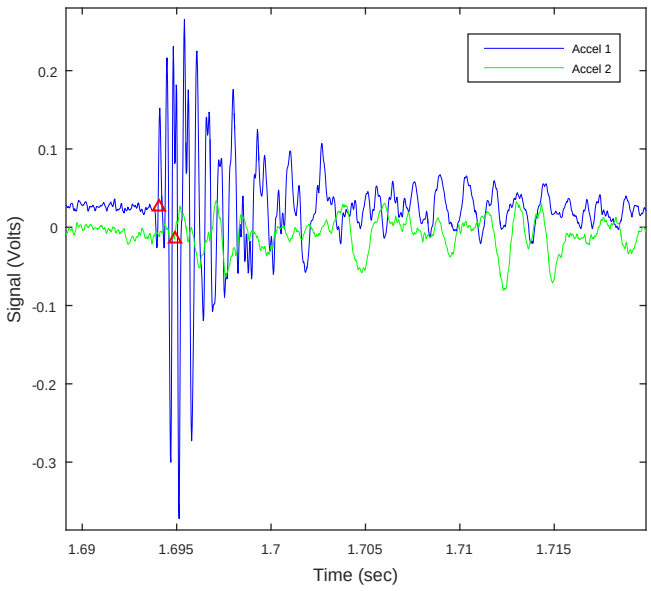

CSS Monotonic Shear Test Report

10/28/2013_Version 8.0

Geotechnical Engineering Laboratory

General Test Information and Sample Preparation			
Device:	CSS	**Layers:**	7.93
Specimen ID:	STHD	**Weight/layer (kg):**	1.35
Test ID:	MID1	**Height/layer (mm):**	25.4
Date of Test:	7/6/2014	**Total height (mm):**	201.422
Test Performed:	Monotonic Shear	**Soil-Only Specimen Diameter (mm):**	306.2
Test Material:	MSW	**Total weight (kg):**	10.7055
Sample Preparation:	Undisturbed. The same final composition and unit weight as Sim. #1. Pre-compress for 23 hours, consolidate for 1 hour. After consolidation and	**Density (kg/m^3):**	722
		Membrane Thickness (mm):	0.000635
		Moisture Content (%):	65.0
		Saturated (Y/N):	N
		Prepared by:	Fei

Pre-compression Stage			
Pre-compression strain:	0.42	**Secondary compression ratio:**	0.01031
Height (mm):	127.5	**Density (kg/m3):**	1466

Consolidation Stage		Shear Stage		
Initial height (mm):	137.4	**Type of Test:**		CD-strain
Initial density (kg/m3):	1058	**Shear Strain Rate (%/min):**		0.46
Vertical Stress (kPa):	196.7	**10% strain**	**Shear stress (kPa)**	62.9
Immediate strain (εimm, %)	42.9		**Tan friction angle (°)**	17.7
Consolidated Height (mm):	110.1		**Sin friction angle (°)**	17.9
Compression index (Ccε)	0.195	**30% strain**	**Shear stress (kPa)**	77.1
Consolidation modulus	4.5		**Tan friction angle (°)**	21.5
Consolidated density (kg/m^3):	1321		**Sin friction angle (°)**	23.2

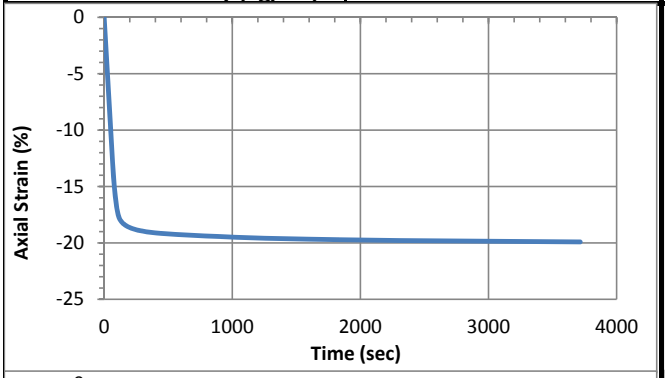

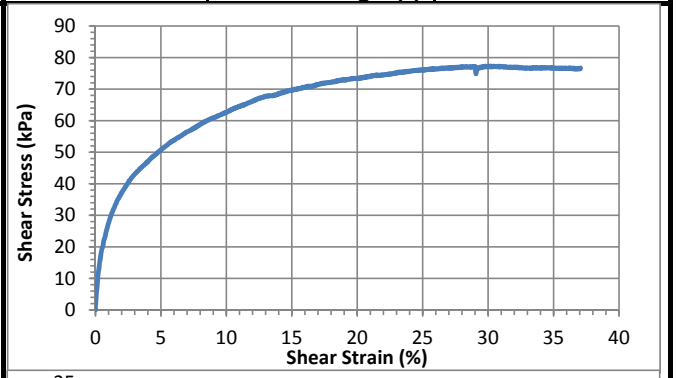

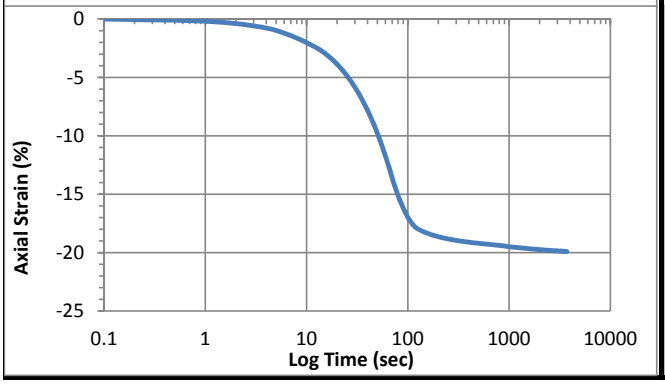

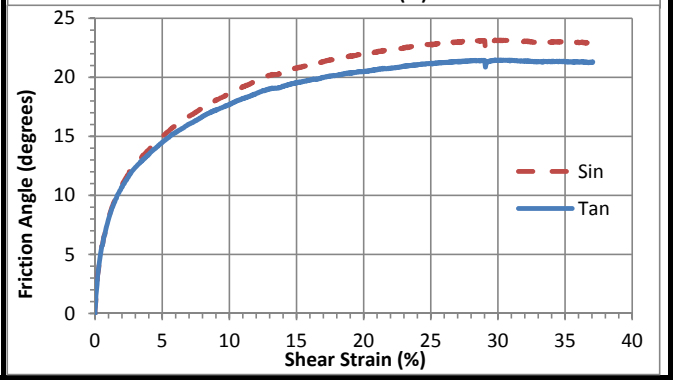

Undrained Strength			
Su/σv' at 10% strain	0.32	Su/σvc' at 10% strain	0.32
Su/σv' at 30% strain	0.39	Su/σvc' at 30% strain	0.39

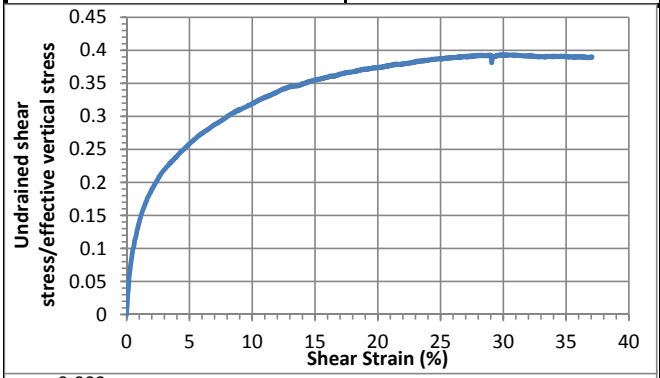

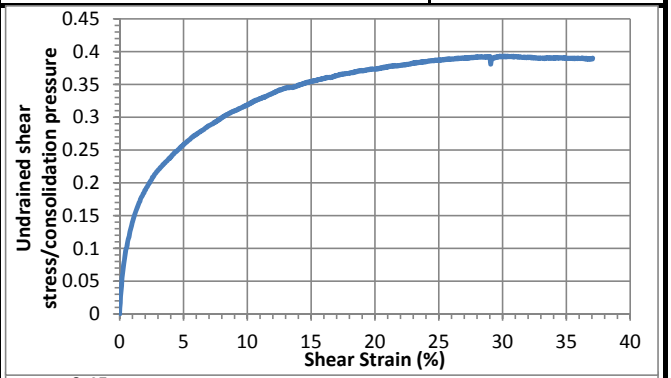

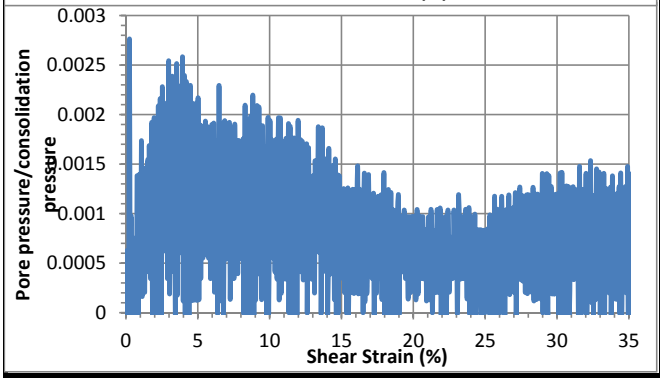

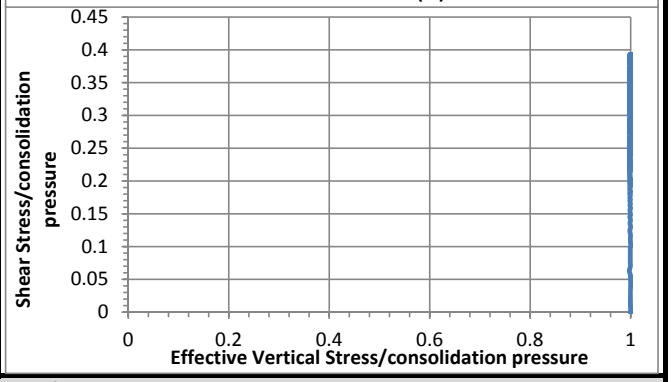

Shear wave velocity				
Signal type	Sinusoidal	First rise	initiation time (ms)	-0.0205
Signal amplitude (Vpp)	90		arrival time (ms)	0.5222
Signal frequency (kHz)	2		Vs (m/s)	187
Sensor spacing (mm)	101.27	First peak	initiation time (ms)	0.1075
R+P average Vs (m/s)	186		arrival time (ms)	0.6554
Stdev. (m/s)	1		Vs (m/s)	185
P+V average Vs (m/s)	188	First valley	initiation time (ms)	0.3584
Stdev. (m/s)	4		arrival time (ms)	0.8909
Wavelength (m)	0.094		Vs (m/s)	190
Spacing/wavelength	1.1			

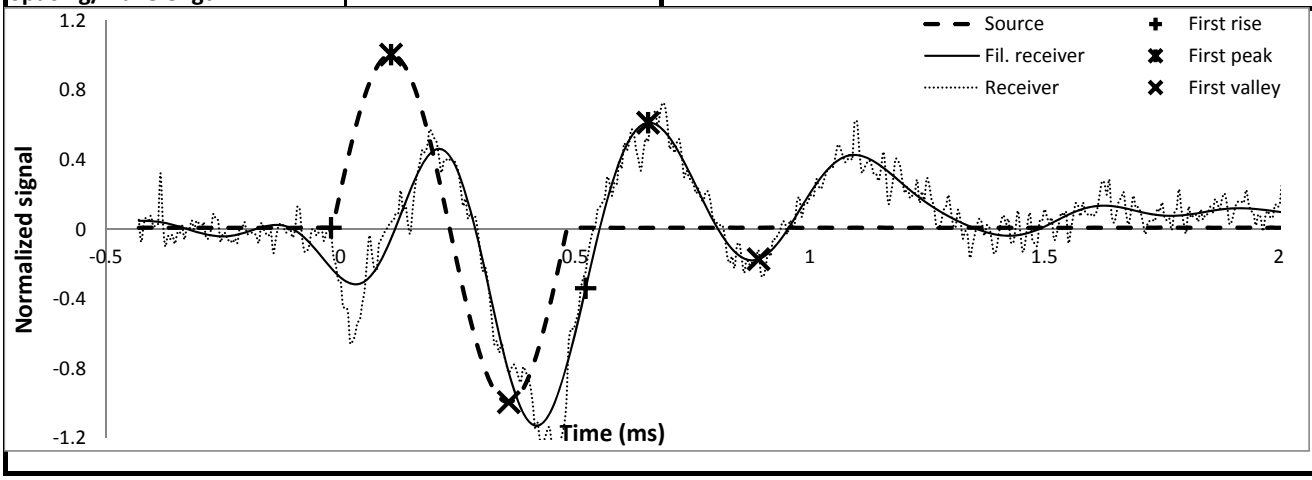

CSS Monotonic Shear Test Report

10/28/2013_Version 8.0

Geotechnical Engineering Laboratory

General Test Information and Sample Preparation

Device:	CSS	**Layers:**	7.50
Specimen ID:	STHD	**Weight/layer (kg):**	1.35
Test ID:	MID2	**Height/layer (mm):**	25.4
Date of Test:	7/18/2014	**Total height (mm):**	190.5
Test Performed:	Monotonic Shear	**Soil-Only Specimen Diameter (mm):**	306.2
Test Material:	MSW	**Total weight (kg):**	10.125
Sample Preparation:	The same final composition and unit weight as Sim. #1. Pre-compress for 23 hours, consolidate for 1 hour.	**Density (kg/m^3):**	722
		Membrane Thickness (mm):	0.000635
		Moisture Content (%):	60.0
		Saturated (Y/N):	N
		Prepared by:	Fei

Pre-compression Stage

Pre-compression strain:	0.33	**Secondary compression ratio:**	0.00910
Height (mm):	106.4	**Density (kg/m3):**	1120

Consolidation Stage

Initial height (mm):	137.2
Initial density (kg/m3):	1002
Vertical Stress (kPa):	47.5
Immediate strain (εimm, %)	34.4
Consolidated Height (mm):	114.7
Compression index (Ccε)	0.215
Weight (kg):	10.125
Consolidated density (kg/m^3):	1199

Shear Stage

Type of Test:		CU-strain
Shear Strain Rate (%/min):		0.44
10% strain	**Shear stress (kPa)**	17.2
	Tan friction angle (°)	19.9
	Sin friction angle (°)	21.3
30% strain	**Shear stress (kPa)**	21.8
	Tan friction angle (°)	24.6
	Sin friction angle (°)	27.3

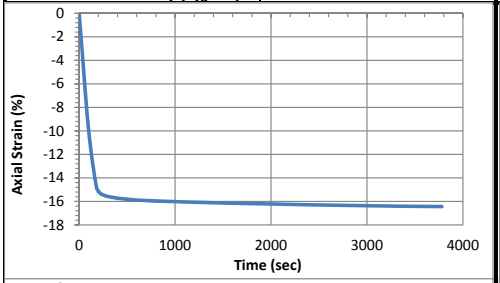

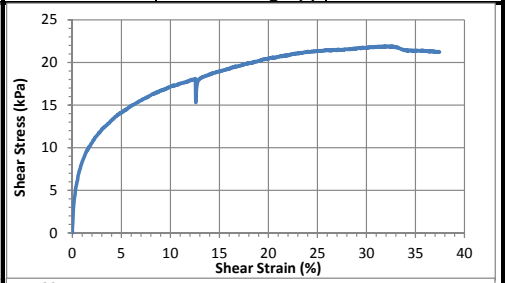

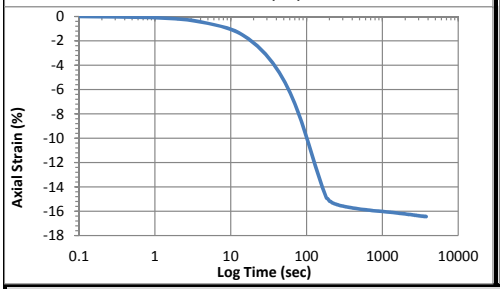

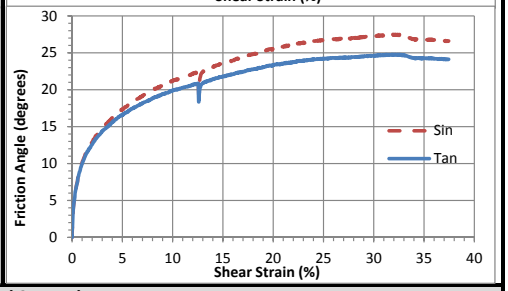

Undrained Strength

Su/σv' at 10% strain	0.36	**Su/σvc' at 10% strain**	0.36
Su/σv' at 30% strain	0.46	**Su/σvc' at 30% strain**	0.46

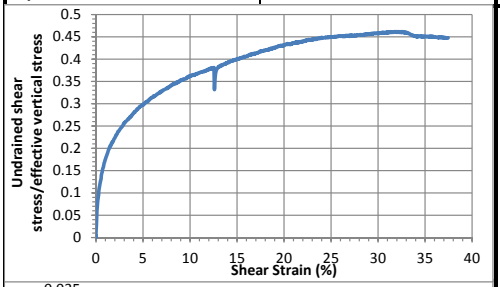

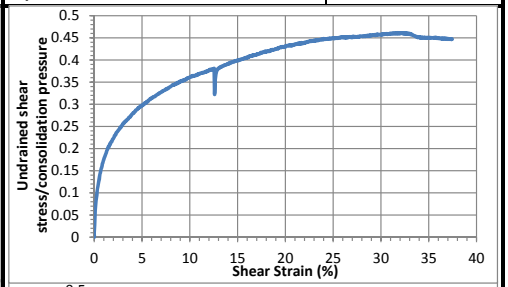

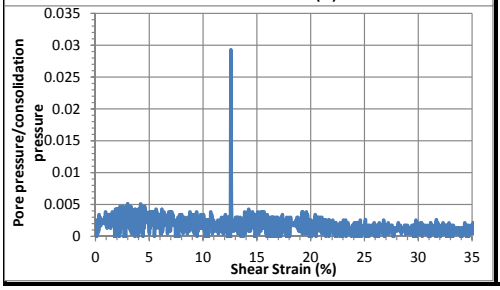

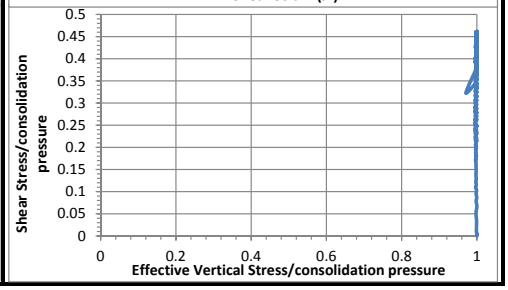

CSS Monotonic Shear Test Report

10/28/2013_Version 8.0

Geotechnical Engineering Laboratory

General Test Information and Sample Preparation			
Device:	CSS	**Layers:**	7.50
Specimen ID:	STHD	**Weight/layer (kg):**	1.35
Test ID:	MID3	**Height/layer (mm):**	25.4
Date of Test:	7/21/2014	**Total height (mm):**	190.5
Test Performed:	Monotonic Shear	**Soil-Only Specimen Diameter (mm):**	306.2
Test Material:	MSW	**Total weight (kg):**	10.125
Sample Preparation:	The same final composition and unit weight as Sim. #1. Pre-compress for 23 hours, consolidate for 1 hour.Wc=65%, Ws,0=6.136 kg.	**Density (kg/m^3):**	722
		Membrane Thickness (mm):	0.000635
		Moisture Content (%):	
		Saturated (Y/N):	N
		Prepared by:	Fei

Pre-compression Stage			
Pre-compression strain:	0.39	**Secondary compression ratio:**	0.00787
Height (mm):	110.3	**Density (kg/m3):**	1246

Consolidation Stage		Shear Stage		
Initial height (mm):	117.0	**Type of Test:**		CU-strain
Initial density (kg/m3):	1175	**Shear Strain Rate (%/min):**		0.49
Vertical Stress (kPa):	96.5	**10% strain**	**Shear stress (kPa)**	34.3
Immediate strain (εimm, %)	39.4		**Tan friction angle (°)**	19.6
Consolidated Height (mm):	103.3		**Sin friction angle (°)**	20.9
Compression index (Ccε)	0.207	**20% strain**	**Shear stress (kPa)**	
Weight (kg):	10.125		**Tan friction angle (°)**	
Consolidated density (kg/m^3):	1309		**Sin friction angle (°)**	

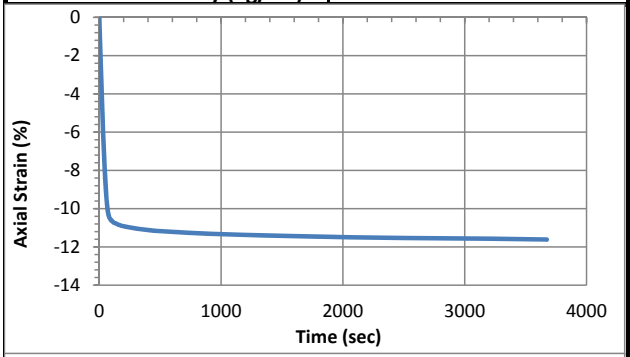

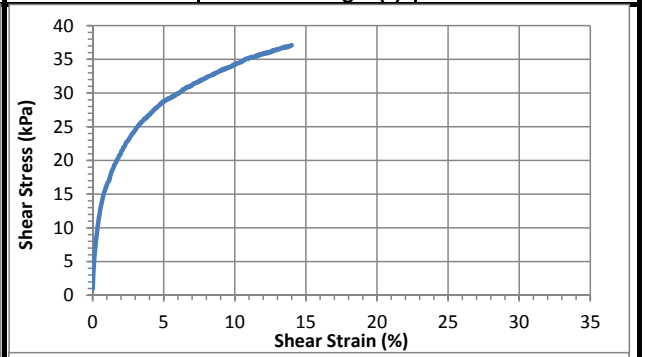

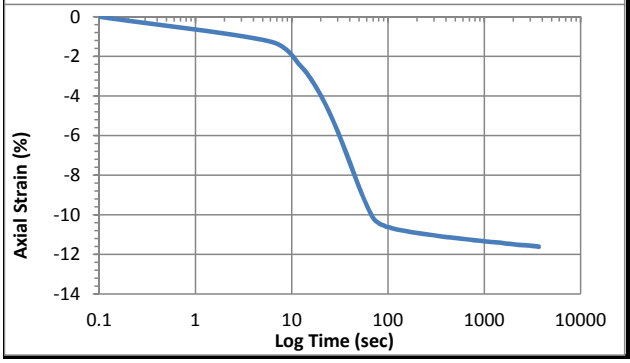

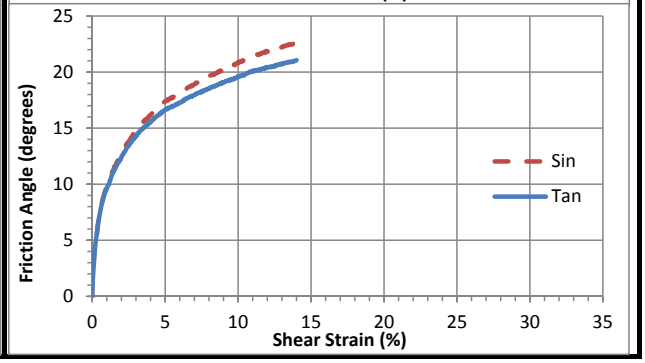

Undrained Strength			
Su/σv' at 10% strain	0.35	Su/σvc' at 10% strain	0.35
Su/σv' at 20% strain		Su/σvc' at 20% strain	

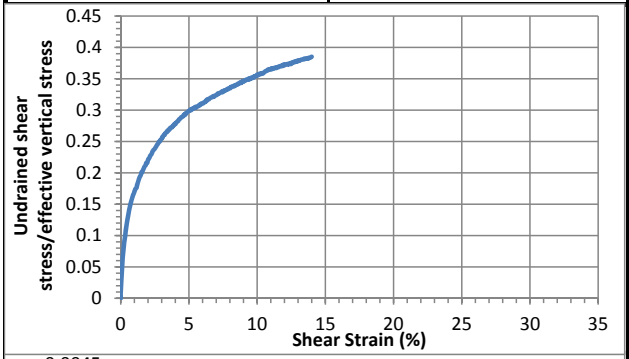

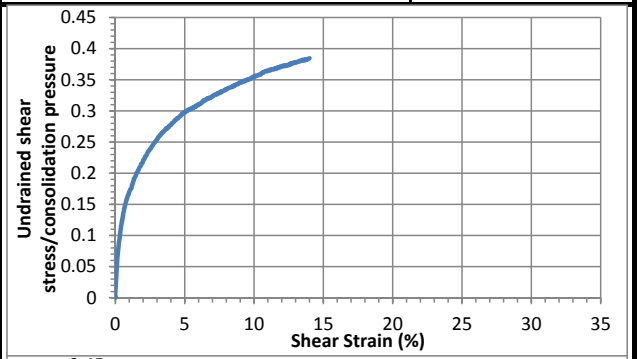

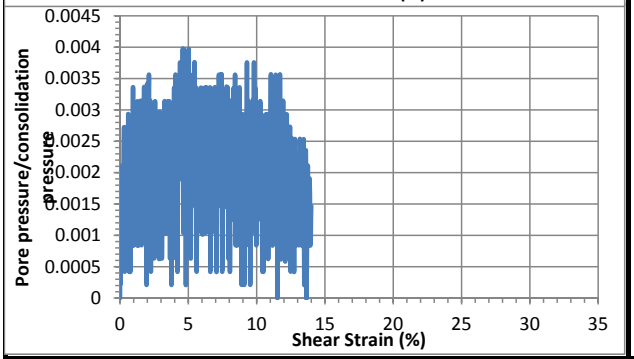

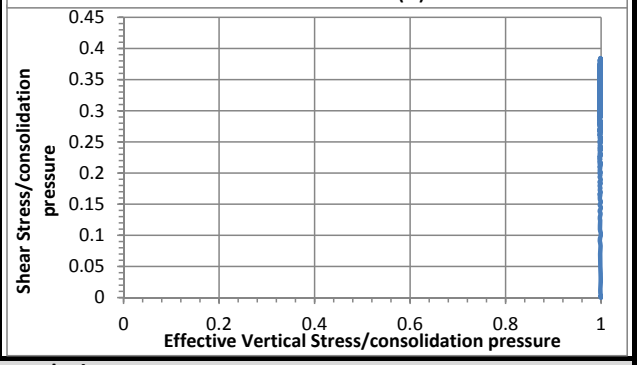

Shear wave velocity				
Signal type	Sinusoidal	First rise	initiation time (ms)	-0.0102
Signal amplitude (Vpp)	90		arrival time (ms)	0.5120
Signal frequency (kHz)	5		Vs (m/s)	193
Sensor spacing (mm)	100.69	First peak	initiation time (ms)	0.0410
R+P average Vs (m/s)	189		arrival time (ms)	0.5837
Stdev. (m/s)	5		Vs (m/s)	186
P+V average Vs (m/s)	179	First valley	initiation time (ms)	0.1434
Stdev. (m/s)	9		arrival time (ms)	0.7270
Wavelength (m)	0.036		Vs (m/s)	173
Spacing/wavelength	2.8			

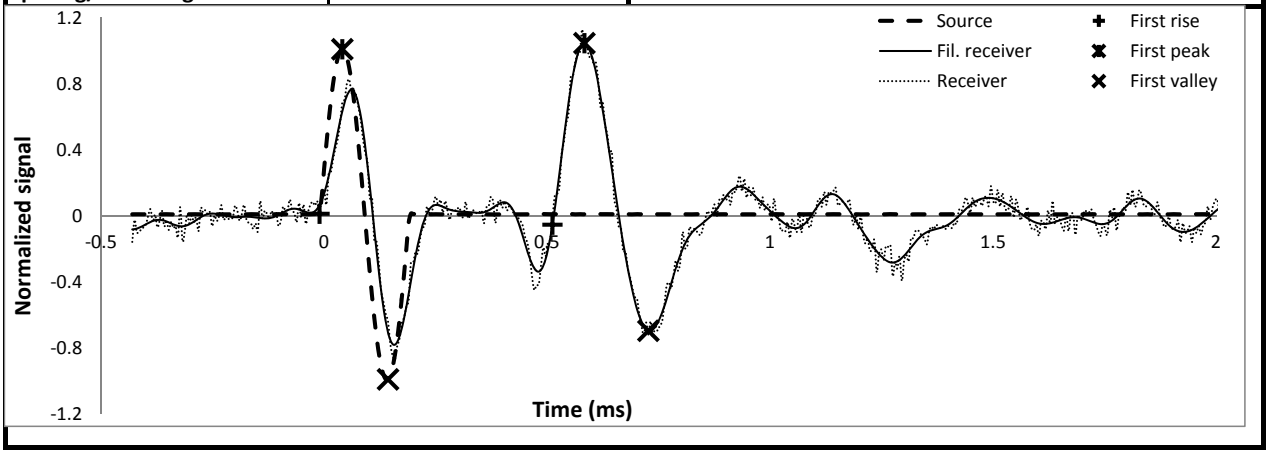

CSS Monotonic Shear Test Report

10/28/2013_Version 8.0

Geotechnical Engineering Laboratory

General Test Information and Sample Preparation			
Device:	CSS	**Layers:**	7.50
Specimen ID:	STHD	**Weight/layer (kg):**	1.35
Test ID:	MID4	**Height/layer (mm):**	25.4
Date of Test:	7/23/2014	**Total height (mm):**	190.5
Test Performed:	Monotonic Shear	**Soil-Only Specimen Diameter (mm):**	306.2
Test Material:	MSW	**Total weight (kg):**	10.125
Sample Preparation:	The same final composition and unit weight as Sim. #1. Pre-compress for 23 hours, consolidate for 1 hour. Vertical P=10, I=0.5.	**Density (kg/m^3):**	722
		Membrane Thickness (mm):	0.000635
		Moisture Content (%):	60.0
		Saturated (Y/N):	N
		Prepared by:	Fei

Pre-compression Stage			
Pre-compression strain:	0.26	**Secondary compression ratio:**	0.00659
Height (mm):	119.9	**Density (kg/m3):**	1147

Consolidation Stage		Shear Stage		
Initial height (mm):	122.9	**Type of Test:**		CU-strain
Initial density (kg/m3):	1118	**Shear Strain Rate (%/min):**		0.44
Vertical Stress (kPa):	47.0	**10% strain**	**Shear stress (kPa)**	15.8
Immediate strain (εimm, %)	27.7		**Tan friction angle (°)**	27.7
Consolidated Height (mm):	113.0		**Sin friction angle (°)**	31.7
Compression index (Ccε)	0.175	**30% strain**	**Shear stress (kPa)**	16.5
Weight (kg):	10.125		**Tan friction angle (°)**	31.5
Consolidated density (kg/m^3):	1214		**Sin friction angle (°)**	37.9

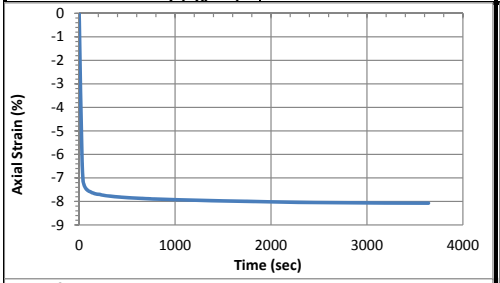

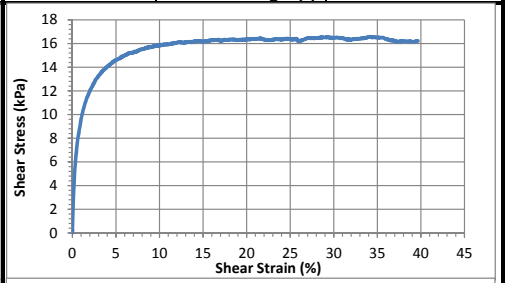

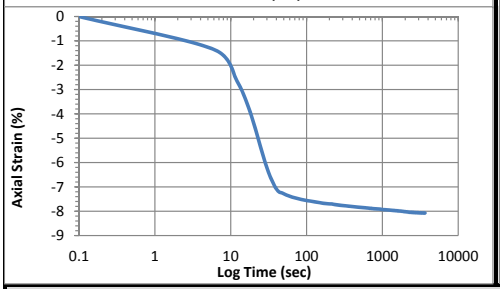

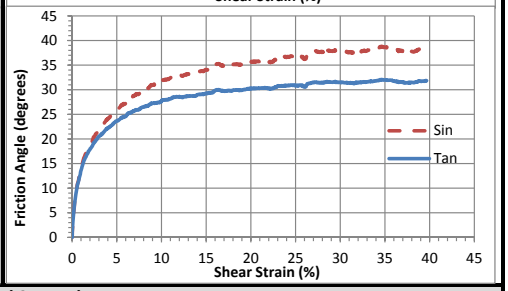

Undrained Strength			
Su/σv' at 10% strain	0.53	**Su/σvc' at 10% strain**	0.34
Su/σv' at 30% strain	0.61	**Su/σvc' at 30% strain**	0.35

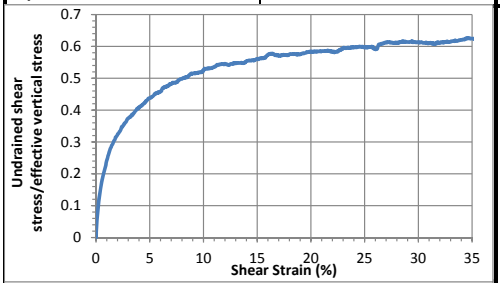

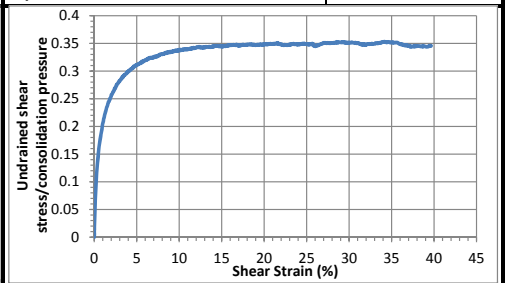

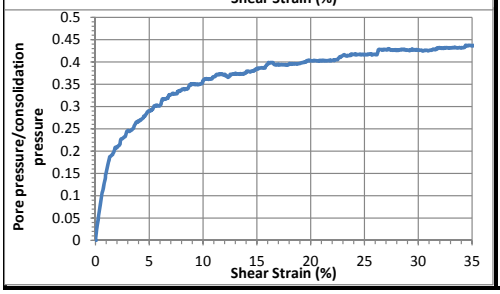

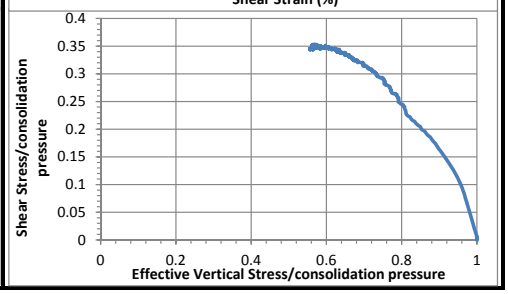

CSS Monotonic Shear Test Report

10/28/2013_Version 8.0

Geotechnical Engineering Laboratory

General Test Information and Sample Preparation			
Device:	CSS	**Layers:**	8.50
Specimen ID:	STHD	**Weight/layer (kg):**	1.35
Test ID:	MID4	**Height/layer (mm):**	25.4
Date of Test:	7/24/2014	**Total height (mm):**	215.9
Test Performed:	Monotonic Shear	**Soil-Only Specimen Diameter (mm):**	306.2
Test Material:	MSW	**Total weight (kg):**	11.475
Sample Preparation:	The same final composition and unit weight as Sim. #1. Pre-compress for 23 hours, consolidate for 1 hour. Vertical P=15, I=0.5.	**Density (kg/m^3):**	722
		Membrane Thickness (mm):	0.000635
		Moisture Content (%):	60.0
		Saturated (Y/N):	N
		Prepared by:	Fei

Pre-compression Stage			
Pre-compression strain:	0.40	**Secondary compression ratio:**	0.00711
Height (mm):	123.5	**Density (kg/m3):**	1262

Consolidation Stage		Shear Stage		
Initial height (mm):	132.7	**Type of Test:**		CU-strain
Initial density (kg/m3):	1174	**Shear Strain Rate (%/min):**		0.43
Vertical Stress (kPa):	96.9	**10% strain**	**Shear stress (kPa)**	28.0
Immediate strain (εimm, %)	40.6		**Tan friction angle (°)**	24.4
Consolidated Height (mm):	117.4		**Sin friction angle (°)**	27.0
Compression index (Ccε)	0.212	**30% strain**	**Shear stress (kPa)**	27.3
Consolidation modulus	4.7		**Tan friction angle (°)**	27.5
Consolidated density (kg/m^3):	1316		**Sin friction angle (°)**	31.4

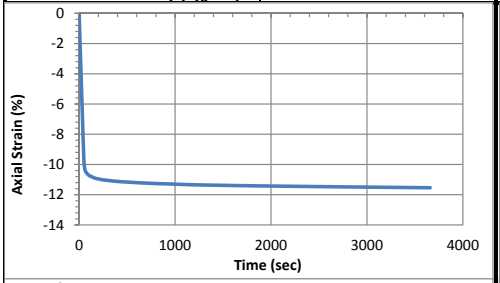

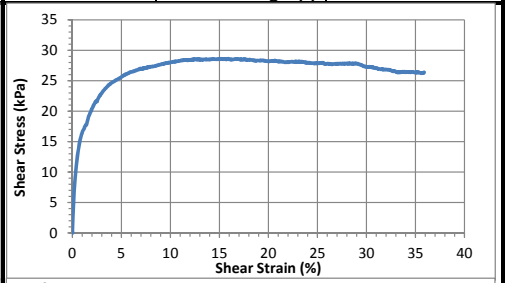

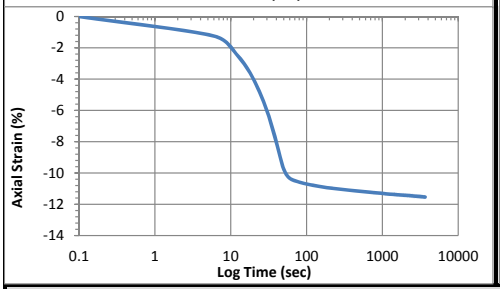

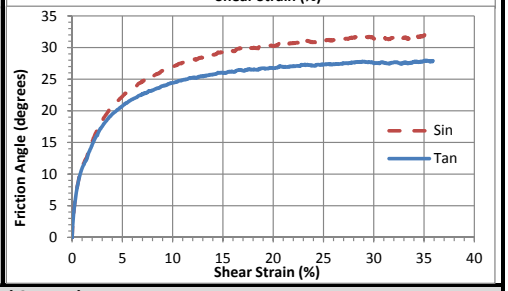

Undrained Strength			
Su/σv' at 10% strain	0.45	**Su/σvc' at 10% strain**	0.29
Su/σv' at 30% strain	0.52	**Su/σvc' at 30% strain**	0.28

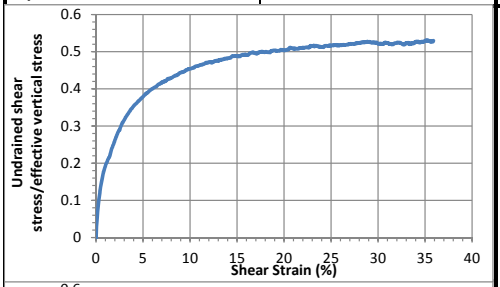

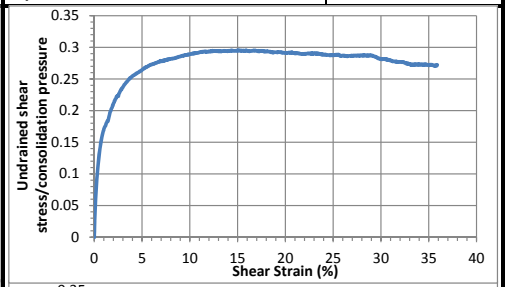

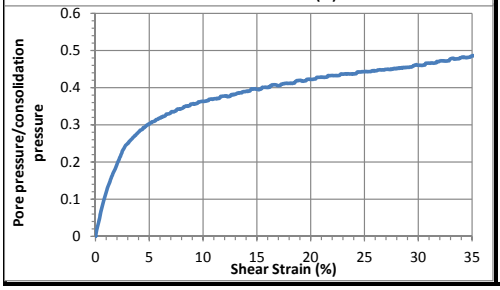

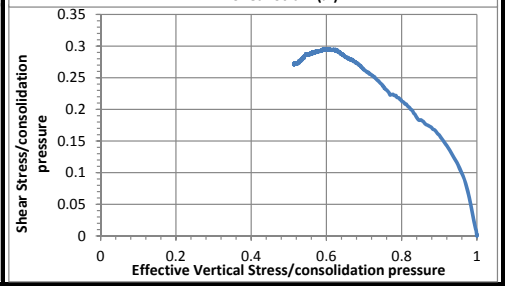

CSS Monotonic Shear Test Report

10/28/2013_Version 8.0

Geotechnical Engineering Laboratory

General Test Information and Sample Preparation			
Device:	CSS	**Layers:**	8.75
Specimen ID:	STHD	**Weight/layer (kg):**	1.35
Test ID:	MID6	**Height/layer (mm):**	25.4
Date of Test:	7/29/2014	**Total height (mm):**	222.25
Test Performed:	Monotonic Shear	**Soil-Only Specimen Diameter (mm):**	306.2
Test Material:	MSW	**Total weight (kg):**	11.8125
Sample Preparation:	The same final composition and unit weight as Sim. #1. Pre-compress for 23 hours, consolidate for 1 hour. Wc=65%, Ws,0=7.159 kg.	**Density (kg/m^3):**	722
		Membrane Thickness (mm):	0.000635
		Moisture Content (%):	60.0
		Saturated (Y/N):	N
		Prepared by:	Fei

Pre-compression Stage			
Pre-compression strain:	0.47	**Secondary compression ratio:**	0.00858
Height (mm):	117.7	**Density (kg/m3):**	1363

Consolidation Stage		Shear Stage		
Initial height (mm):	127.8	**Type of Test:**		CD-strain
Initial density (kg/m3):	1255	**Shear Strain Rate (%/min):**		0.46
Vertical Stress (kPa):	195.6	**10% strain**	**Shear stress (kPa)**	67.9
Immediate strain (εimm, %)	46.6		**Tan friction angle (°)**	19.1
Consolidated Height (mm):	109.7		**Sin friction angle (°)**	20.3
Compression index (Ccε)	0.212	**30% strain**	**Shear stress (kPa)**	82.7
Consolidation modulus	4.1		**Tan friction angle (°)**	23.0
Consolidated density (kg/m^3):	1392		**Sin friction angle (°)**	25.1

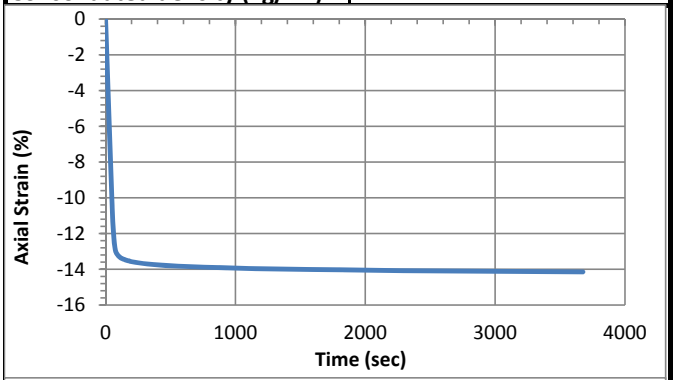

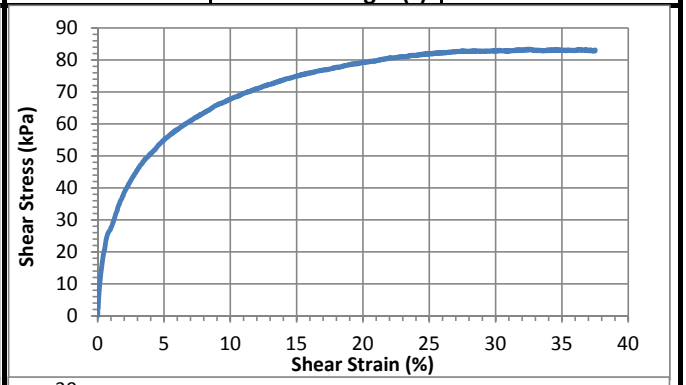

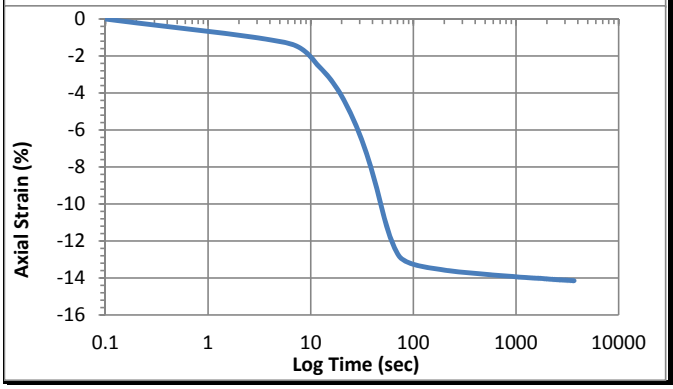

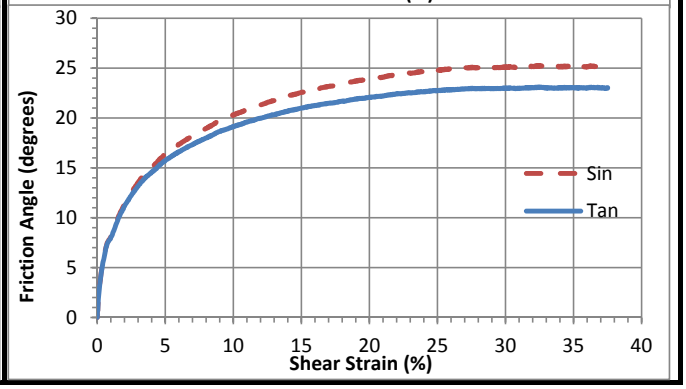

Undrained Strength

Su/σv' at 10% strain	0.35	Su/σvc' at 10% strain	0.35
Su/σv' at 30% strain	0.42	Su/σvc' at 30% strain	0.42

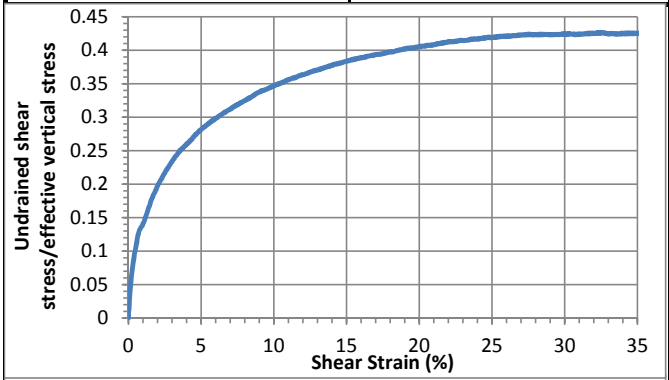

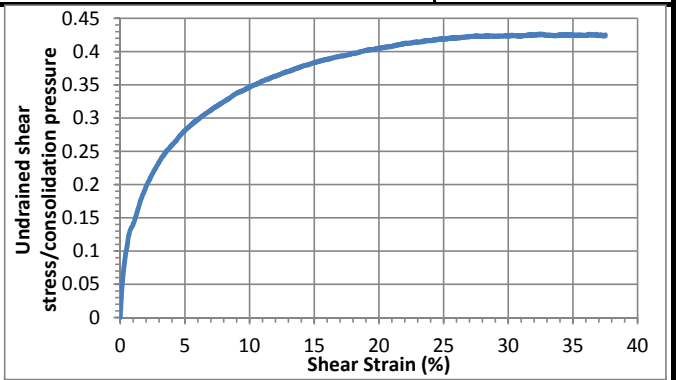

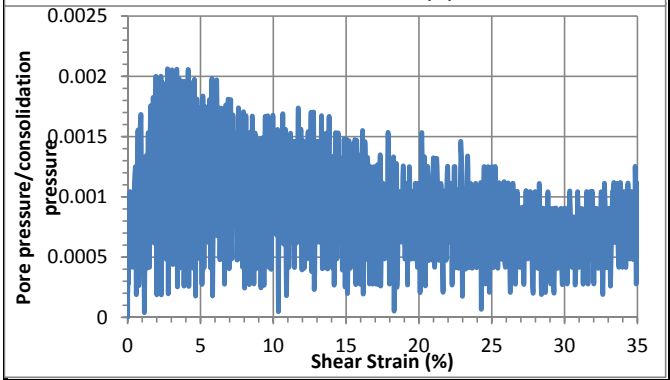

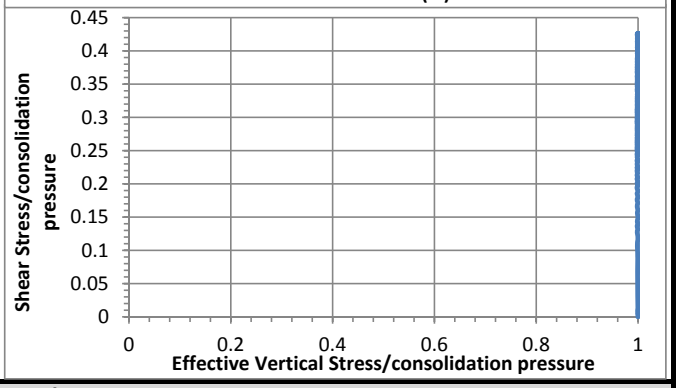

Shear wave velocity

Signal type	Sinusoidal	First rise	initiation time (ms)	-0.0154
Signal amplitude (Vpp)	90		arrival time (ms)	0.4096
Signal frequency (kHz)	2		Vs (m/s)	237
Sensor spacing (mm)	100.92	First peak	initiation time (ms)	0.0410
R+P average Vs (m/s)	231		arrival time (ms)	0.4915
Stdev. (m/s)	10		Vs (m/s)	224
P+V average Vs (m/s)	212	First valley	initiation time (ms)	0.1382
Stdev. (m/s)	18		arrival time (ms)	0.6451
Wavelength (m)	0.106		Vs (m/s)	199
Spacing/wavelength	1.0			

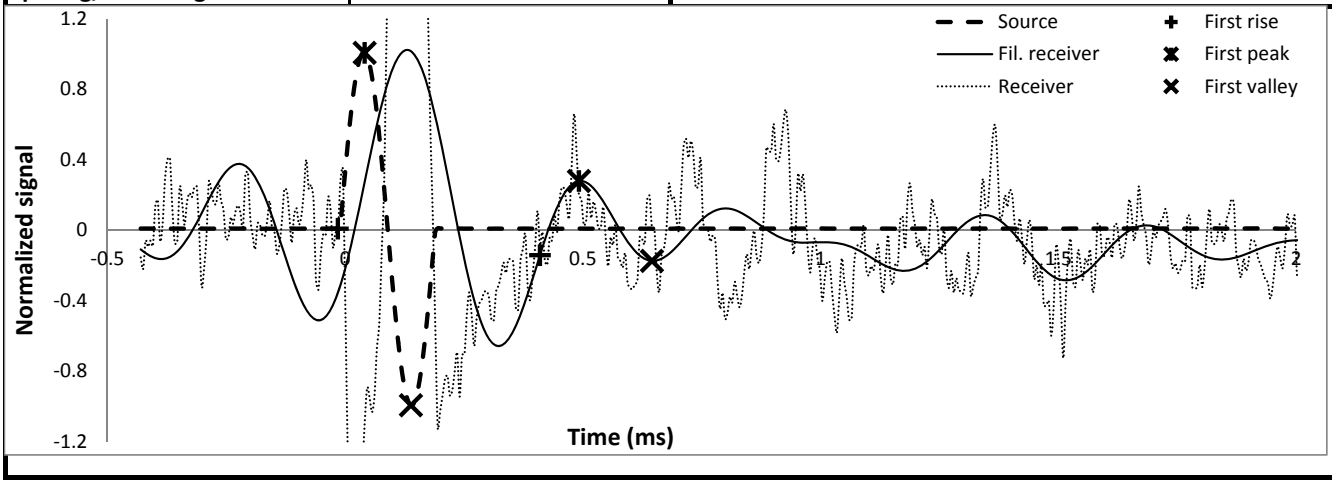

CSS Monotonic Shear Test Report

10/28/2013_Version 8.0

Geotechnical Engineering Laboratory

General Test Information and Sample Preparation			
Device:	CSS	**Layers:**	8.75
Specimen ID:	STHD	**Weight/layer (kg):**	1.35
Test ID:	MID7	**Height/layer (mm):**	25.4
Date of Test:	8/7/2014	**Total height (mm):**	222.25
Test Performed:	Monotonic Shear	**Soil-Only Specimen Diameter (mm):**	306.2
Test Material:	MSW	**Total weight (kg):**	11.8125
Sample Preparation:	The same final composition and unit weight as Sim. #1. Pre-compress for 25 hours, consolidate for 1 hour. Vertical P=20, I=0.5. Wc=65%,	**Density (kg/m^3):**	722
		Membrane Thickness (mm):	0.000635
		Moisture Content (%):	60.0
		Saturated (Y/N):	N
		Prepared by:	Fei

Pre-compression Stage			
Pre-compression strain:	0.46	**Secondary compression ratio:**	0.00906
Height (mm):	115.1	**Density (kg/m3):**	1394

Consolidation Stage		Shear Stage		
Initial height (mm):	118.0	**Type of Test:**		CU-strain
Initial density (kg/m3):	1359	**Shear Strain Rate (%/min):**		0.47
Vertical Stress (kPa):	196.9	**10% strain**	**Shear stress (kPa)**	61.3
Immediate strain (εimm, %)	45.8		**Tan friction angle (°)**	25.3
Consolidated Height (mm):	106.9		**Sin friction angle (°)**	28.2
Compression index (Ccε)	0.209	**30% strain**	**Shear stress (kPa)**	64.2
Consolidation modulus	4.2		**Tan friction angle (°)**	28.8
Consolidated density (kg/m^3):	1432		**Sin friction angle (°)**	33.4

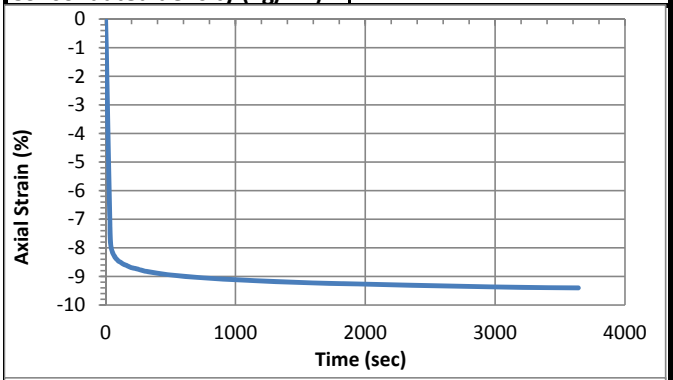

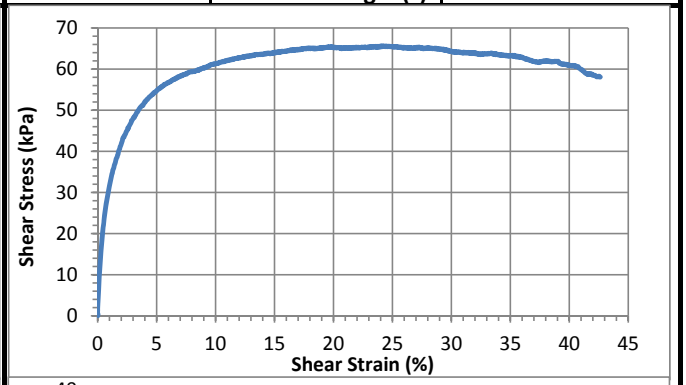

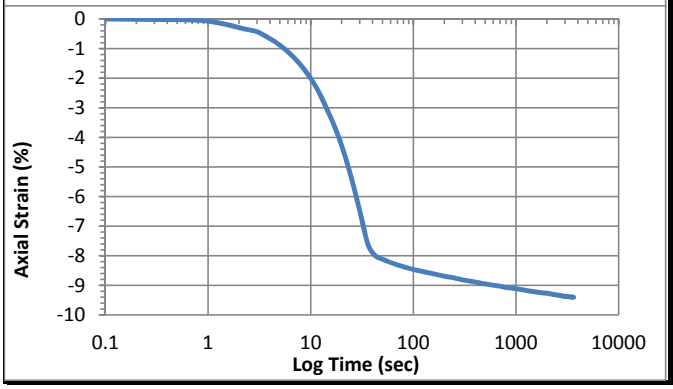

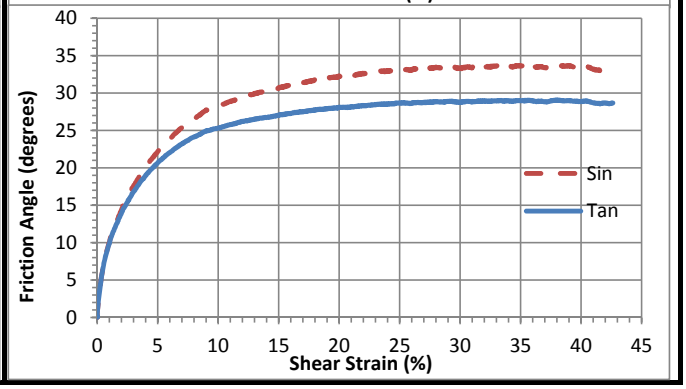

Undrained Strength			
Su/σv' at 10% strain	0.47	Su/σvc' at 10% strain	0.31
Su/σv' at 30% strain	0.55	Su/σvc' at 30% strain	0.33

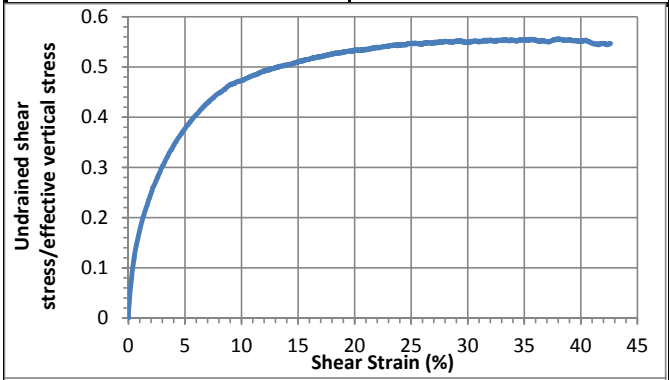

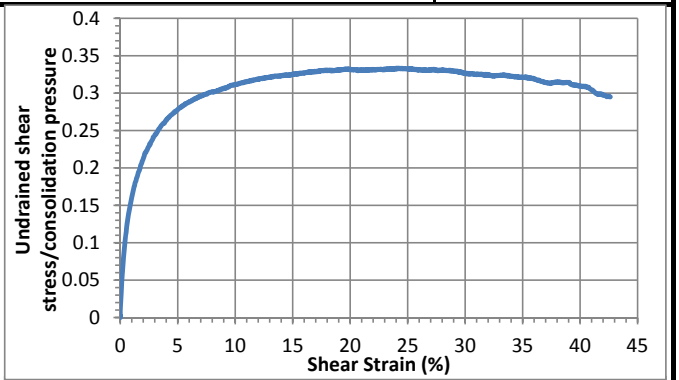

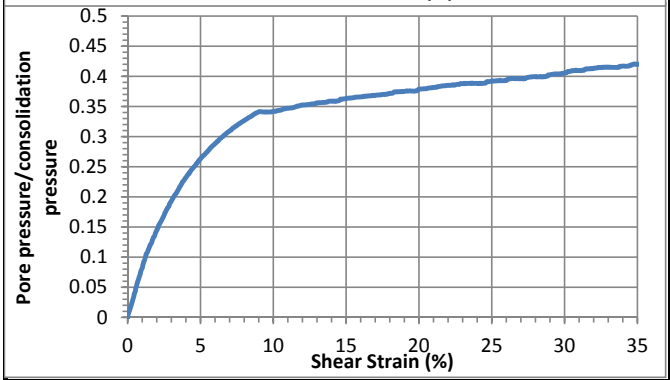

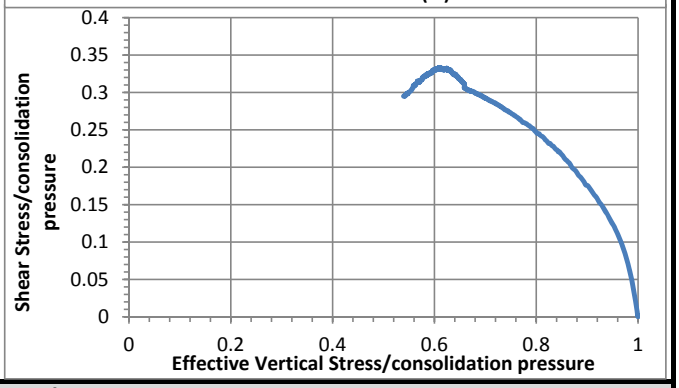

Shear wave velocity				
Signal type	Sinusoidal	First rise	initiation time (ms)	-0.0205
Signal amplitude (Vpp)	90		arrival time (ms)	0.5274
Signal frequency (kHz)	2		Vs (m/s)	179
Sensor spacing (mm)	98.09	First peak	initiation time (ms)	0.1075
R+P average Vs (m/s)	187		arrival time (ms)	0.6093
Stdev. (m/s)	12		Vs (m/s)	195
P+V average Vs (m/s)	207	First valley	initiation time (ms)	0.3584
Stdev. (m/s)	16		arrival time (ms)	0.8090
Wavelength (m)	0.103		Vs (m/s)	218
Spacing/wavelength	0.9			

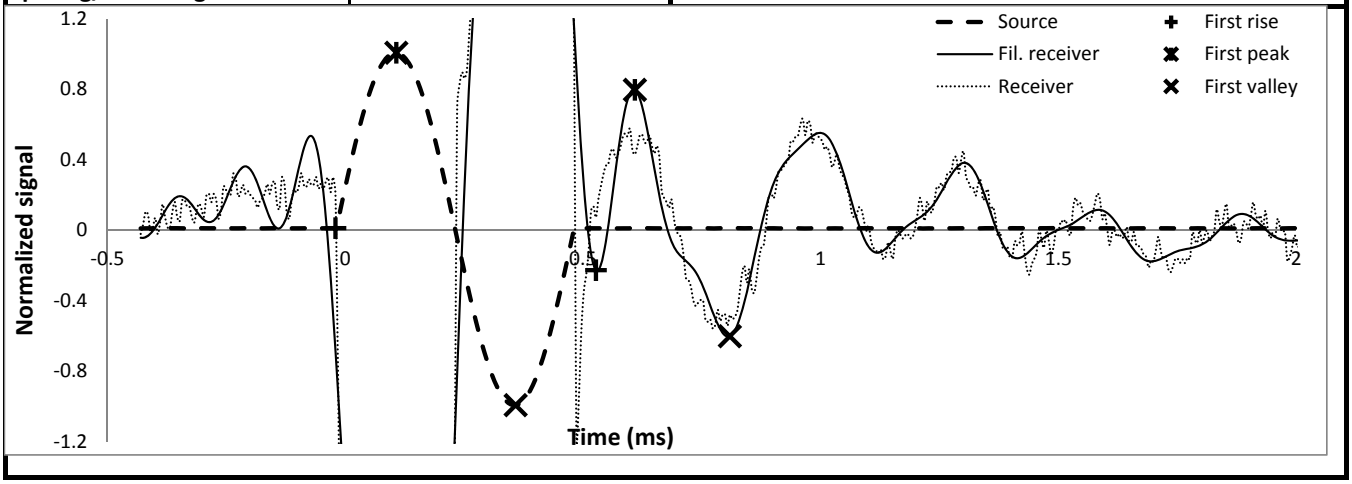

CSS Monotonic Shear Test Report

10/28/2013_Version 8.0

Geotechnical Engineering Laboratory

General Test Information and Sample Preparation			
Device:	CSS	**Layers:**	9.12
Specimen ID:	STHD	**Weight/layer (kg):**	1.35
Test ID:	MID8	**Height/layer (mm):**	25.4
Date of Test:	8/9/2014	**Total height (mm):**	231.648
Test Performed:	Monotonic Shear	**Soil-Only Specimen Diameter (mm):**	306.2
Test Material:	MSW	**Total weight (kg):**	12.312
Sample Preparation:	The same final composition and unit weight as Sim. #1. Pre-compress for 23 hours, consolidate for 1 hour. Vertical P=25, I=0.5. Wc=65%,	**Density (kg/m^3):**	722
		Membrane Thickness (mm):	0.000635
		Moisture Content (%):	60.0
		Saturated (Y/N):	N
		Prepared by:	Fei

Pre-compression Stage			
Pre-compression strain:	0.52	**Secondary compression ratio:**	0.00829
Height (mm):	109.6	**Density (kg/m3):**	1526

Consolidation Stage		Shear Stage		
Initial height (mm):	127.8	**Type of Test:**		CU-strain
Initial density (kg/m3):	1308	**Shear Strain Rate (%/min):**		0.49
Vertical Stress (kPa):	393.6	**10% strain**	**Shear stress (kPa)**	114.0
Immediate strain (εimm, %)	51.8		**Tan friction angle (°)**	23.2
Consolidated Height (mm):	102.7		**Sin friction angle (°)**	25.4
Compression index (Ccε)	0.207	**30% strain**	**Shear stress (kPa)**	114.4
Consolidation modulus	3.7		**Tan friction angle (°)**	28.2
Consolidated density (kg/m^3):	1495		**Sin friction angle (°)**	32.4

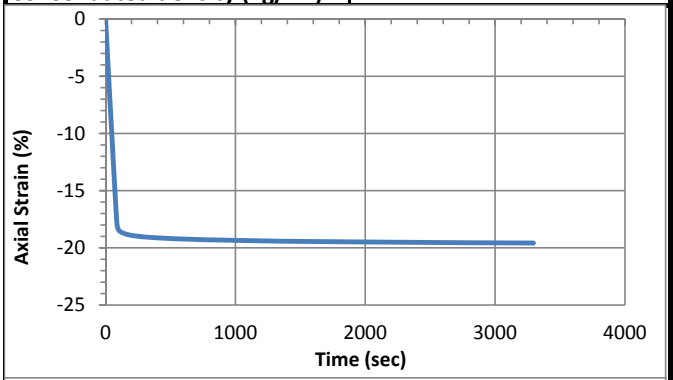

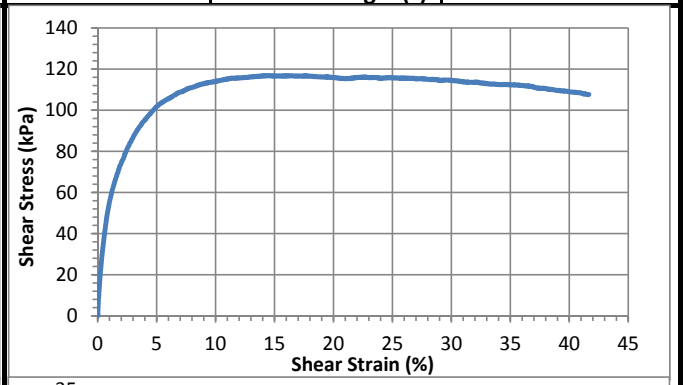

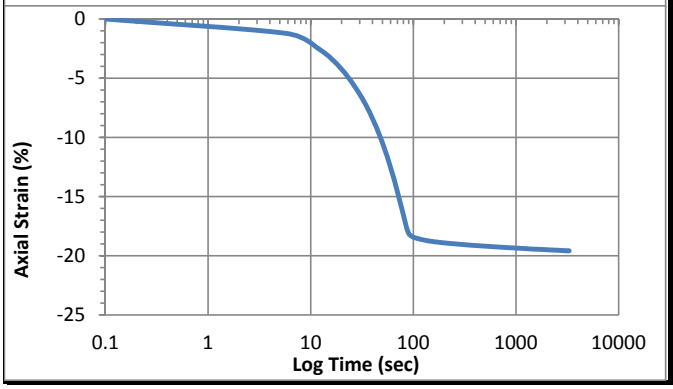

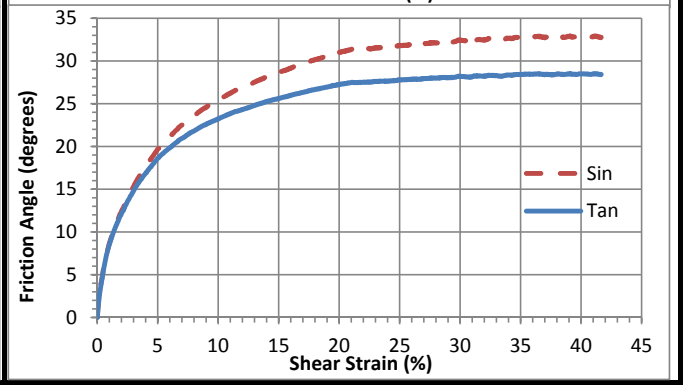

Undrained Strength			
Su/σv' at 10% strain	0.43	Su/σvc' at 10% strain	0.29
Su/σv' at 30% strain	0.54	Su/σvc' at 30% strain	0.29

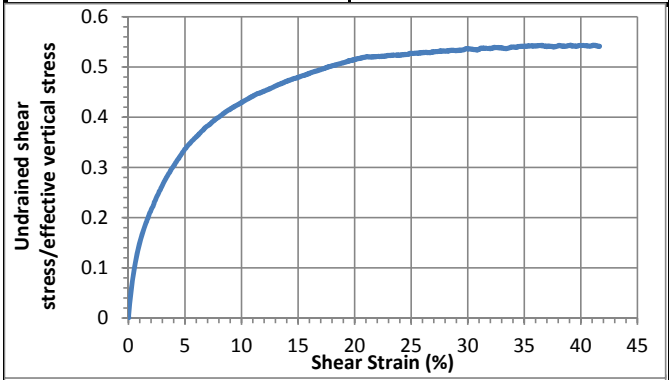

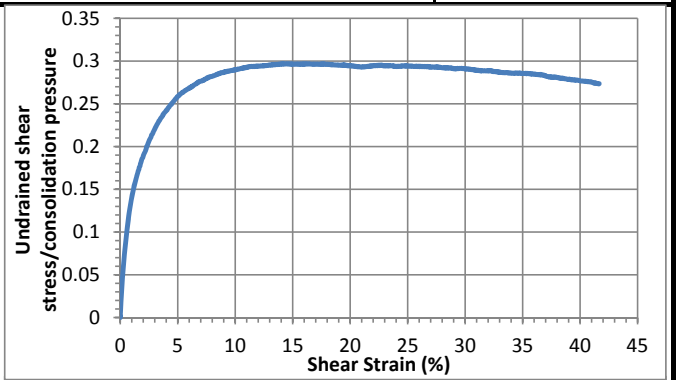

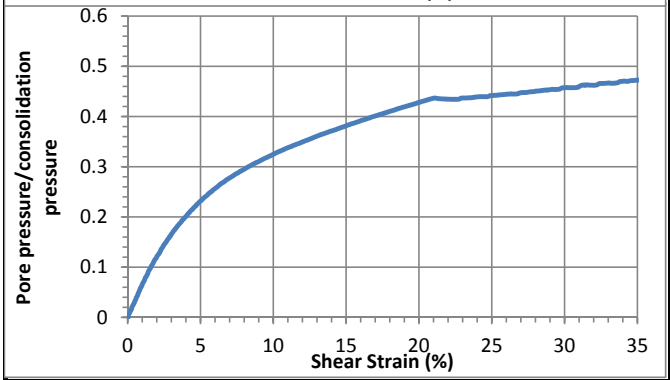

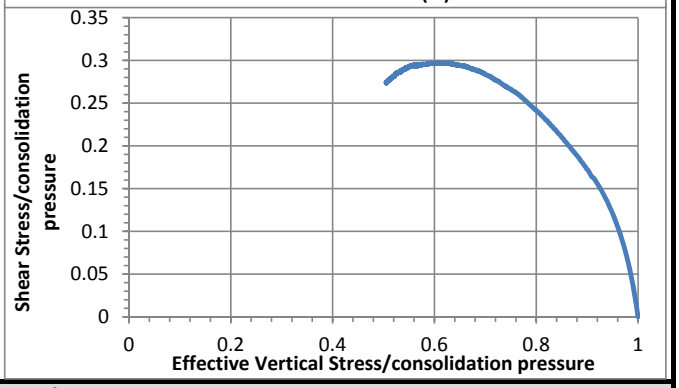

Shear wave velocity				
Signal type	Sinusoidal	First rise	initiation time (ms)	-0.0102
Signal amplitude (Vpp)	90		arrival time (ms)	0.3584
Signal frequency (kHz)	5		Vs (m/s)	255
Sensor spacing (mm)	93.97	First peak	initiation time (ms)	0.0410
R+P average Vs (m/s)	248		arrival time (ms)	0.4301
Stdev. (m/s)	9		Vs (m/s)	241
P+V average Vs (m/s)	252	First valley	initiation time (ms)	0.1434
Stdev. (m/s)	15		arrival time (ms)	0.5018
Wavelength (m)	0.050		Vs (m/s)	262
Spacing/wavelength	1.9			

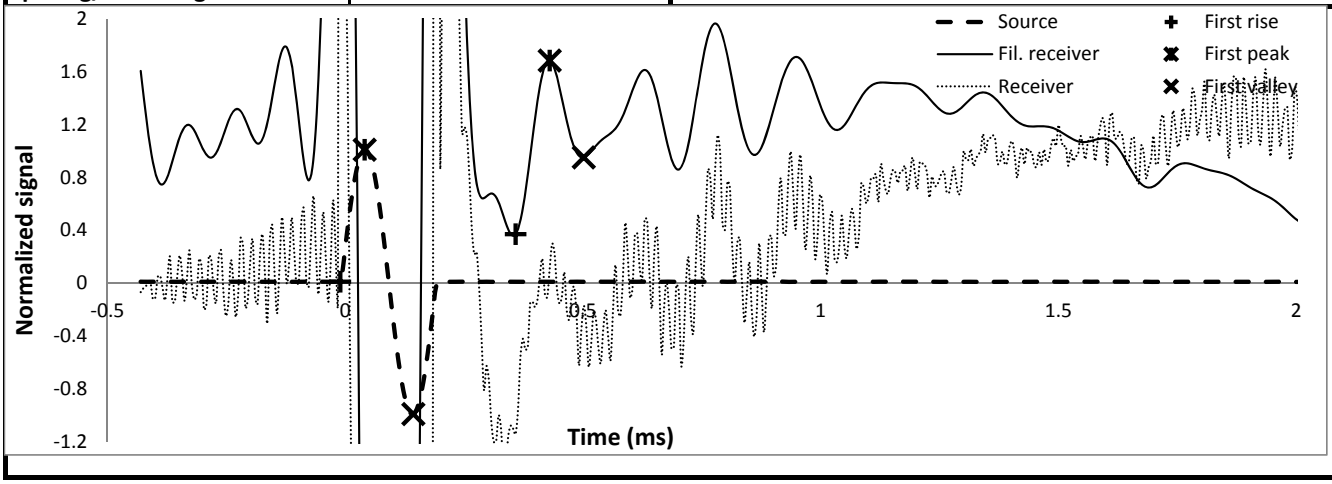

CSS Monotonic Shear Test Report

10/28/2013_Version 8.0

Geotechnical Engineering Laboratory

General Test Information and Sample Preparation			
Device:	CSS	**Layers:**	9.57
Specimen ID:	STHD	**Weight/layer (kg):**	1.35
Test ID:	MID9	**Height/layer (mm):**	25.4
Date of Test:	8/11/2014	**Total height (mm):**	243.078
Test Performed:	Monotonic Shear	**Soil-Only Specimen Diameter (mm):**	306.2
Test Material:	MSW	**Total weight (kg):**	12.9195
Sample Preparation:	The same final composition and unit weight as Sim. #1. Pre-compress for 23 hours, consolidate for 1 hour.	**Density (kg/m^3):**	722
		Membrane Thickness (mm):	0.000635
		Moisture Content (%):	60.0
		Saturated (Y/N):	N
		Prepared by:	Fei

Pre-compression Stage			
Pre-compression strain:	0.54	**Secondary compression ratio:**	0.00911
Height (mm):	104.4	**Density (kg/m3):**	1593

Consolidation Stage		Shear Stage		
Initial height (mm):	137.3	**Type of Test:**		CD-strain
Initial density (kg/m3):	1277	**Shear Strain Rate (%/min):**		0.47
Vertical Stress (kPa):	394.1	**10% strain**	**Shear stress (kPa)**	140.8
Immediate strain (εimm, %)	52.2		**Tan friction angle (°)**	19.7
Consolidated Height (mm):	105.9		**Sin friction angle (°)**	21.0
Compression index (Cc ε)	0.208	**30% strain**	**Shear stress (kPa)**	176.7
Consolidation modulus	3.7		**Tan friction angle (°)**	24.1
Consolidated density (kg/m^3):	1485		**Sin friction angle (°)**	26.6

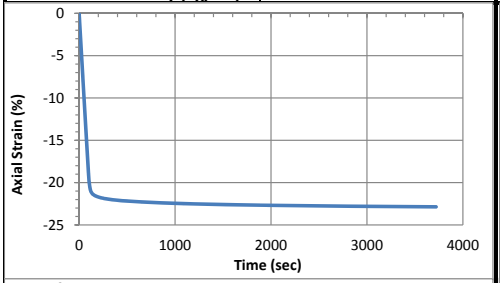

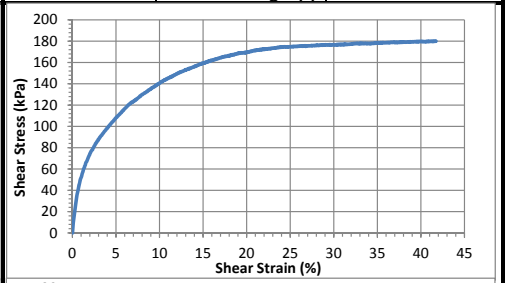

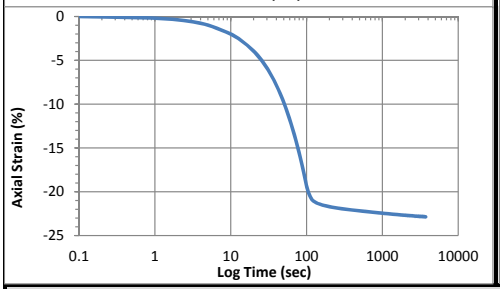

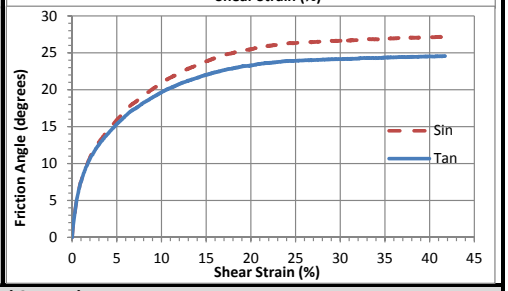

Undrained Strength			
Su/σv' at 10% strain	0.36	**Su/σvc' at 10% strain**	0.36
Su/σv' at 30% strain	0.45	**Su/σvc' at 30% strain**	0.45

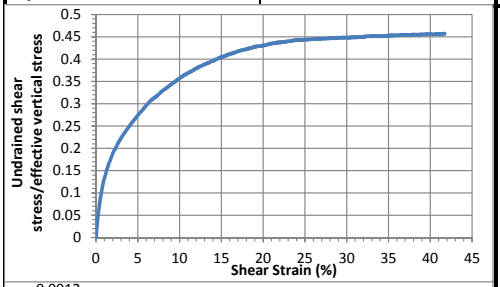

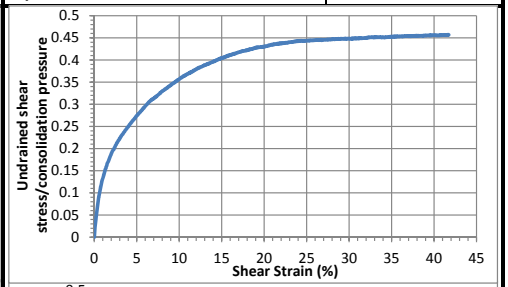

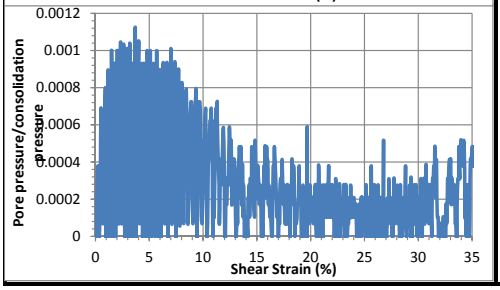

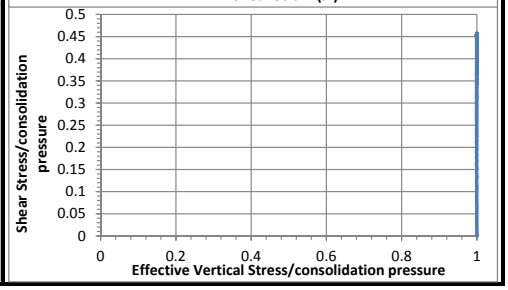

CSS Monotonic Shear Test Report

10/28/2013_Version 8.0

Geotechnical Engineering Laboratory

General Test Information and Sample Preparation			
Device:	CSS	**Layers:**	6.85
Specimen ID:	TX-ACL	**Weight/layer (kg):**	1.494
Test ID:	TX1	**Height/layer (mm):**	25.4
Date of Test:	5/11/2014	**Total height (mm):**	174.0
Test Performed:	Monotonic Shear	**Soil-Only Specimen Diameter (mm):**	306.2
Test Material:	MSW	**Total weight (kg):**	10.234
Sample Preparation:	The same initial composition and unit weight as #Sim. 2. Pre-compression under 50 kPa for 23 hours, consolidate under 50 kPa for 1 hour.	**Density (kg/m^3):**	799
		Membrane Thickness (mm):	0.000635
		Moisture Content (%):	32.3
		Saturated (Y/N):	N
		Prepared by:	Fei

Pre-compression Stage			
Pre-compression strain:	0.34	**Secondary compression ratio**	0.00710
Height (mm):	137.5	**Density (kg/m3):**	1106

Consolidation Stage		Shear Stage		
Initial height (mm):	135.9	**Type of Test:**		CD-strain
Initial density (kg/m3):	1022	**Shear Strain Rate (%/min):**		0.32
Vertical Stress (kPa):	45.8	**10% strain**	**Shear stress (kPa)**	17.0
Immediate strain (εimm, %)	33.8		**Tan friction angle (°)**	19.6
Consolidated Height (mm):	122.5		**Sin friction angle (°)**	21.0
Compression index (Cc ε)	0.211	**30% strain**	**Shear stress (kPa)**	22.0
Constrained modulus	5.71		**Tan friction angle (°)**	24.6
Consolidated density (kg/m3):	1134		**Sin friction angle (°)**	27.2

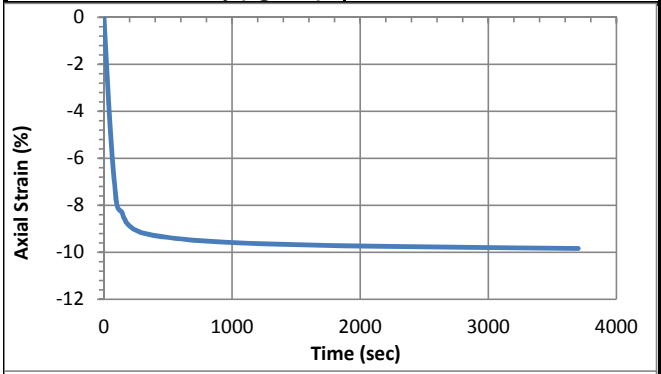

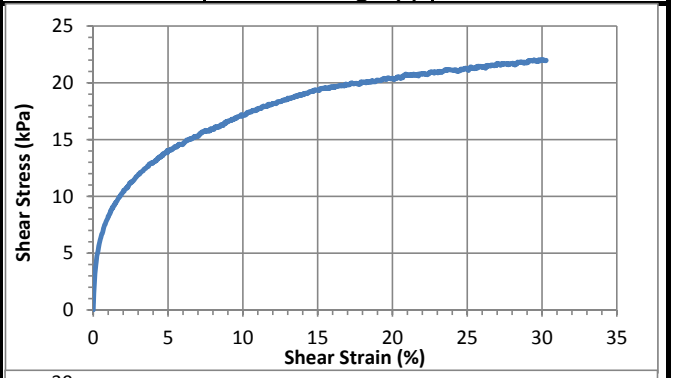

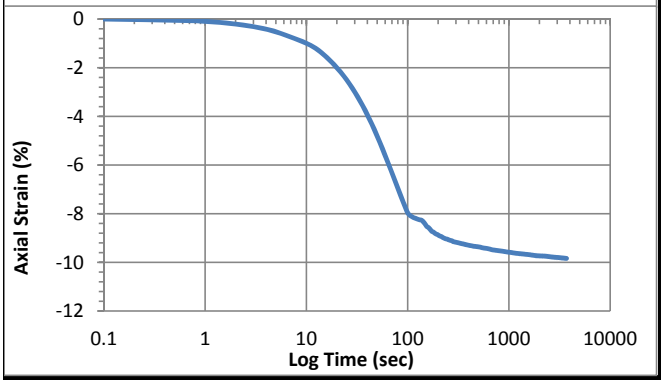

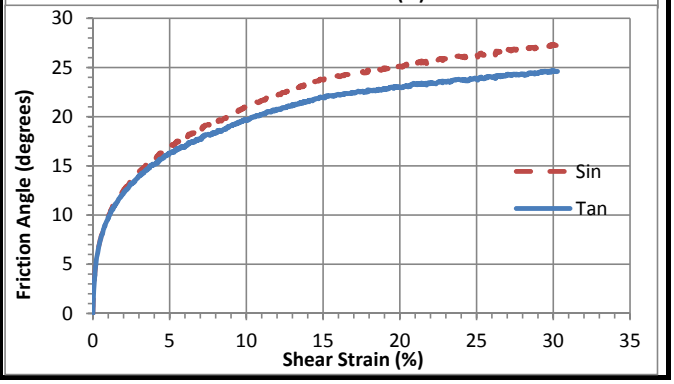

Strength			
τ/σv' at 10% strain	0.36	τ/σv0' at 10% strain	0.36
τ/σv' at 30% strain	0.46	τ/σv0' at 30% strain	0.46

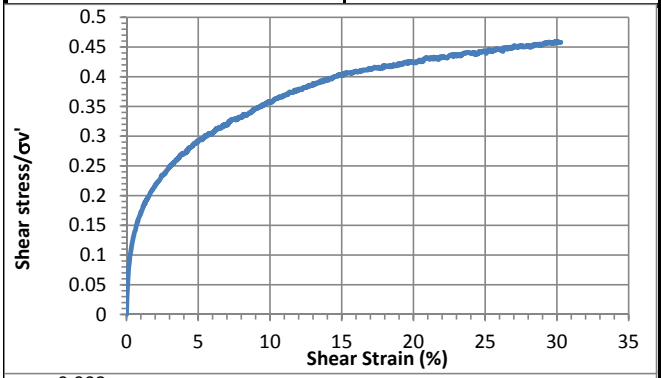

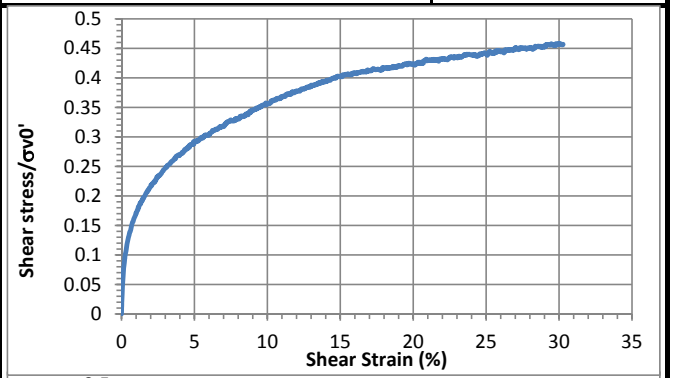

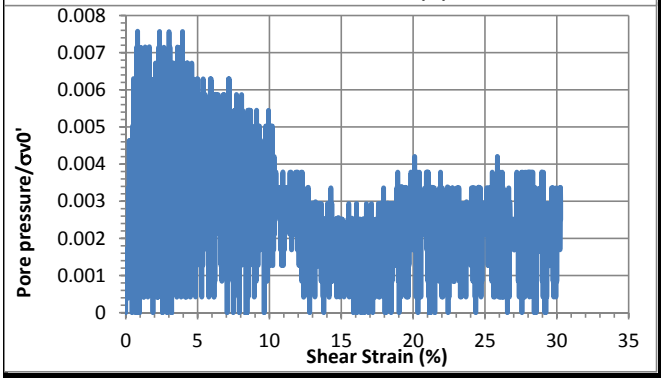

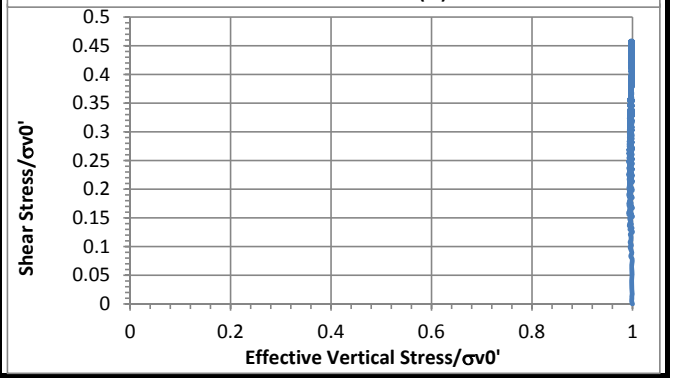

Shear wave velocity				
Signal type	Sinusoidal	First rise	initiation time (ms)	-0.0205
Signal amplitude (Vpp)	90		arrival time (ms)	1.0291
Signal frequency (kHz)	2		Vs (m/s)	108
Sensor spacing (mm)	113.74	First peak	initiation time (ms)	0.1075
R+P average Vs (m/s)	106		arrival time (ms)	1.2134
Stdev. (m/s)	3.9		Vs (m/s)	103
R+P+V average Vs (m/s)	105	First valley	initiation time (ms)	0.3584
Stdev. (m/s)	3.3		arrival time (ms)	1.4694
Wavelength (m)	0.052		Vs (m/s)	102
Spacing/wavelength	2.2			

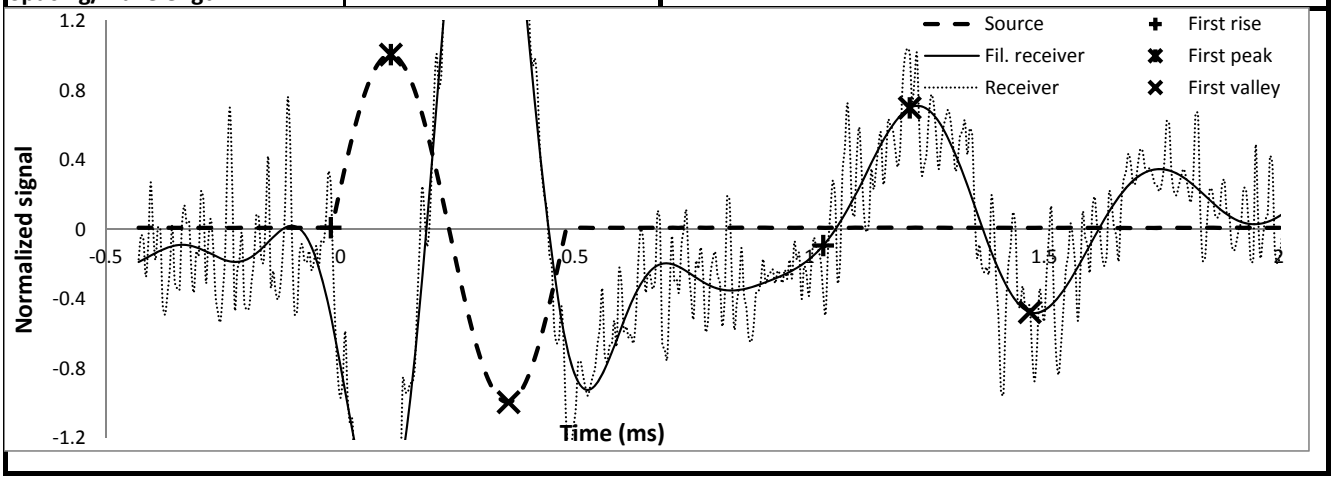

CSS Monotonic Shear Test Report

10/28/2013_Version 8.0

Geotechnical Engineering Laboratory

General Test Information and Sample Preparation			
Device:	CSS	**Layers:**	7.5
Specimen ID:	TX-ACL	**Weight/layer (kg):**	1.494
Test ID:	TX2	**Height/layer (mm):**	25.4
Date of Test:	5/14/2014	**Total height (mm):**	190.5
Test Performed:	Monotonic Shear	**Soil-Only Specimen Diameter (mm):**	306.2
Test Material:	MSW	**Total weight (kg):**	11.205
Sample Preparation:	The same initial composition and unit weight as Sim. #2. Pre-compress for 24 hours, consolidate for 1 hour.	**Density (kg/m^3):**	799
		Membrane Thickness (mm):	0.000635
		Moisture Content (%):	31.4
		Saturated (Y/N):	N
		Prepared by:	Fei

Pre-compression Stage			
Pre-compression strain:	1.00	**Secondary compression ratio**	0.00400
Height (mm):	104.4	**Density (kg/m3):**	1457

Consolidation Stage		Shear Stage		
Initial height (mm):	131.7	**Type of Test:**		CD-strain
Initial density (kg/m3):	1155	**Shear Strain Rate (%/min):**		0.34
Vertical Stress (kPa):	97.3	**10% strain**	**Shear stress (kPa)**	37.1
Immediate strain (εimm, %)	39.9		**Tan friction angle (°)**	20.9
Consolidated Height (mm):	116.8		**Sin friction angle (°)**	22.4
Compression index (Cc ε)	0.205	**30% strain**	**Shear stress (kPa)**	43.3
Constrained modulus	4.91		**Tan friction angle (°)**	24.0
Consolidated density (kg/m3):	1303		**Sin friction angle (°)**	26.6

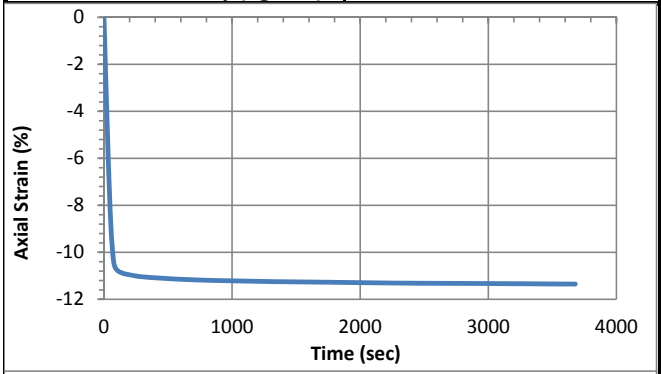

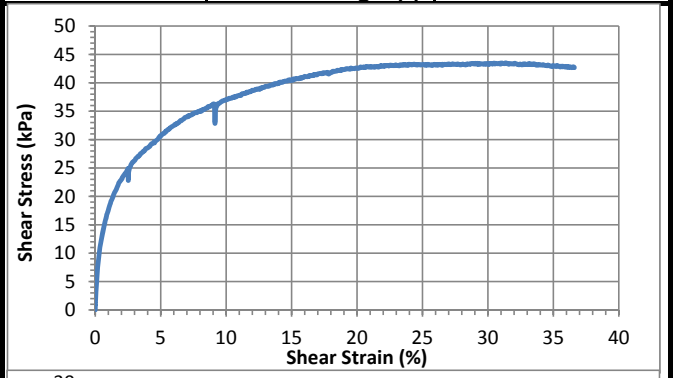

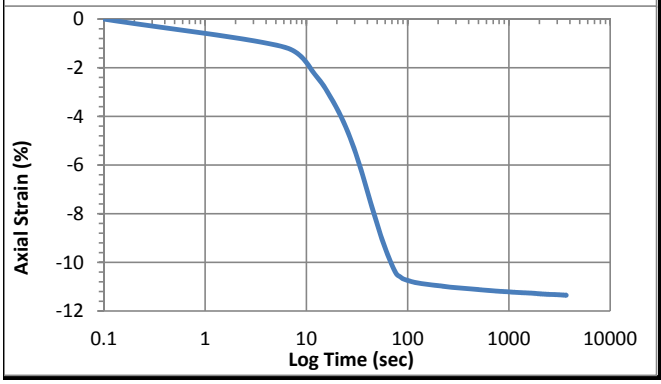

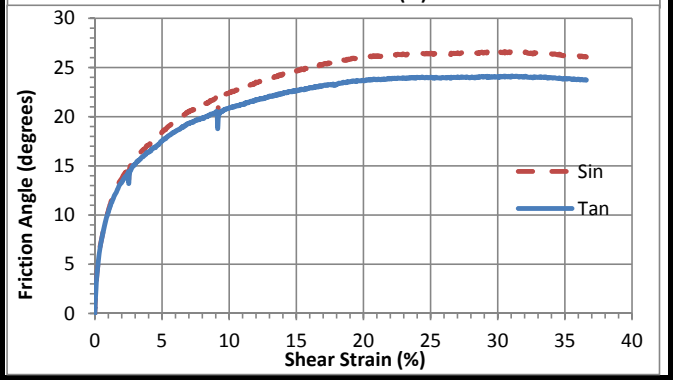

Strength			
τ/σv' at 10% strain	0.38	τ/σv0' at 10% strain	0.38
τ/σv' at 30% strain	0.45	τ/σv0' at 30% strain	0.45

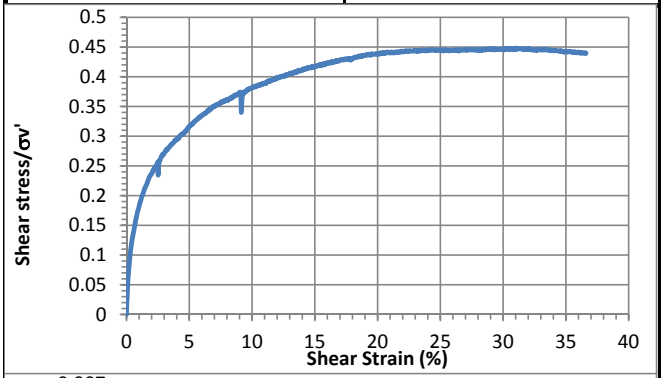

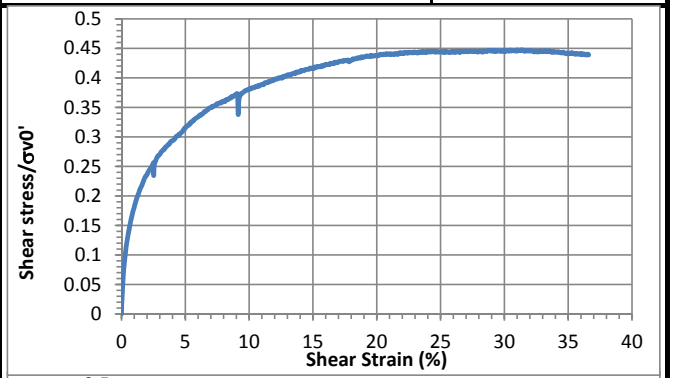

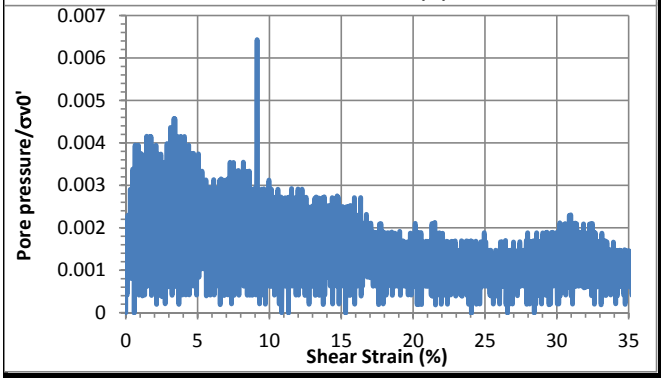

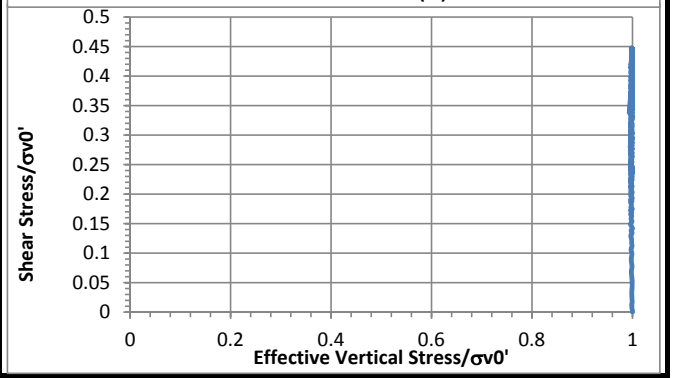

Shear wave velocity				
Signal type	Sinusoidal	First rise	initiation time (ms)	-0.1126
Signal amplitude (Vpp)	90		arrival time (ms)	0.4403
Signal frequency (kHz)	5		Vs (m/s)	195
Sensor spacing (mm)	107.98	First peak	initiation time (ms)	-0.0563
R+P average Vs (m/s)	187		arrival time (ms)	0.5478
Stdev. (m/s)	12		Vs (m/s)	179
R+P+V average Vs (m/s)	184	First valley	initiation time (ms)	0.0410
Stdev. (m/s)	10		arrival time (ms)	0.6451
Wavelength (m)	0.037		Vs (m/s)	179
Spacing/wavelength	2.9			

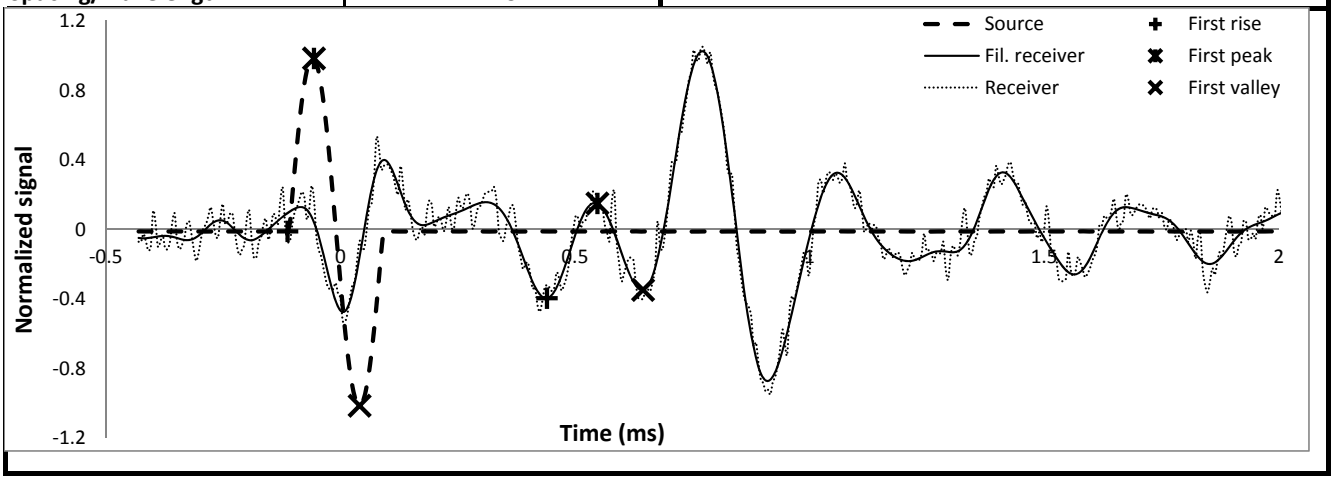

CSS Monotonic Shear Test Report

10/28/2013_Version 8.0

Geotechnical Engineering Laboratory

General Test Information and Sample Preparation			
Device:	CSS	**Layers:**	8.09
Specimen ID:	TX-ACL	**Weight/layer (kg):**	1.494
Test ID:	TX3	**Height/layer (mm):**	25.4
Date of Test:	5/16/2014	**Total height (mm):**	205.4
Test Performed:	Monotonic Shear	**Soil-Only Specimen Diameter (mm):**	306.2
Test Material:	MSW	**Total weight (kg):**	12.08
Sample Preparation:	The same initial composition and unit weight as #Sim. 2. Pre-compression under 200 kPa for 23 hours, consolidate under 200 kPa for 1 hour.	**Density (kg/m^3):**	799
		Membrane Thickness (m):	0.000635
		Moisture Content (%):	32.2
		Saturated (Y/N):	N
		Prepared by:	Drew and Fei

Pre-compression Stage			
Pre-compression strain:	0.42	**Secondary compression ratio**	0.00700
Height (mm):	137.42	**Density (kg/m3):**	1306

Consolidation Stage		Shear Stage		
Initial height (mm):	135.8	**Type of Test:**		CD-strain
Initial density (kg/m3):	1207.7	**Shear Strain Rate (%/min):**		0.33
Vertical Stress (kPa):	196.8	**10% strain**	**Shear stress (kPa)**	63.5
Immediate strain (εimm, %)	40.6		**Tan friction angle (°)**	17.8
Consolidated Height (mm):	120.92		**Sin friction angle (°)**	17.9
Compression index (Cc ε)	0.183	**30% strain**	**Shear stress (kPa)**	77.4
Constrained modulus	4.75		**Tan friction angle (°)**	21.5
Consolidated density (kg/m^3):	1356		**Sin friction angle (°)**	23.2

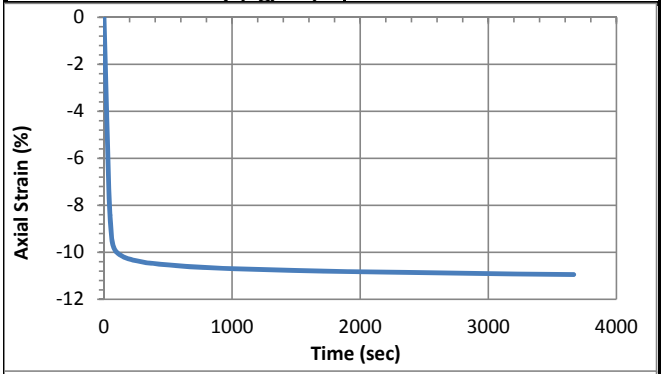

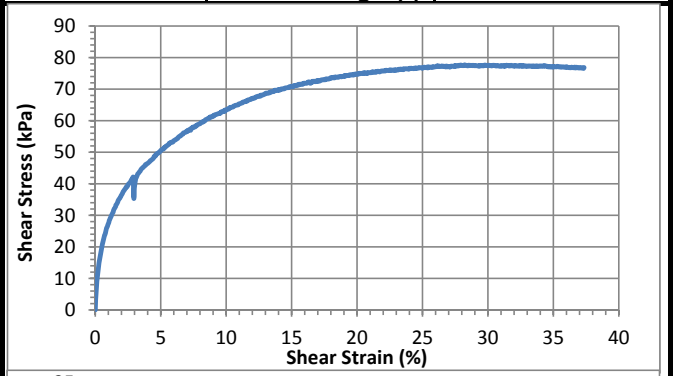

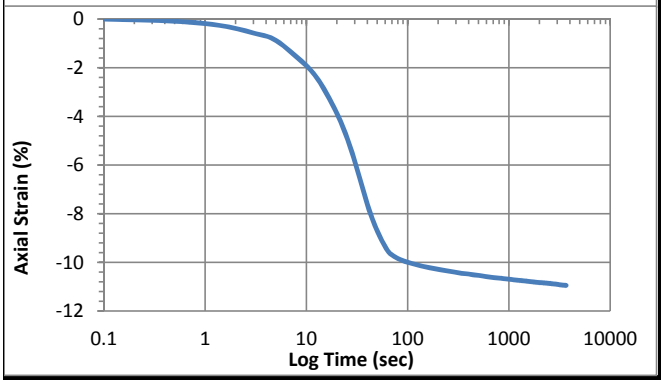

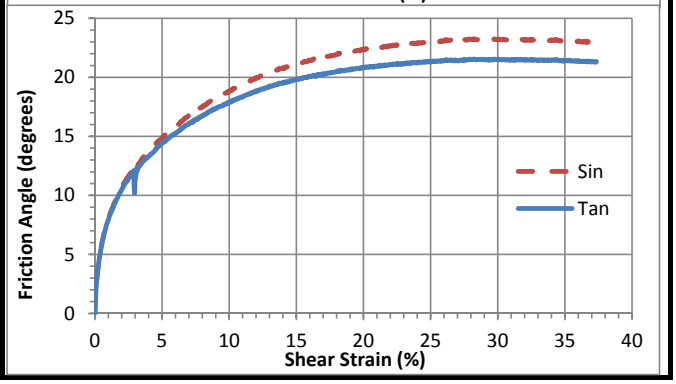

Strength			
τ/σv' at 10% strain	0.32	τ/σv0' at 10% strain	0.32
τ/σv' at 30% strain	0.39	τ/σv0' at 30% strain	0.39

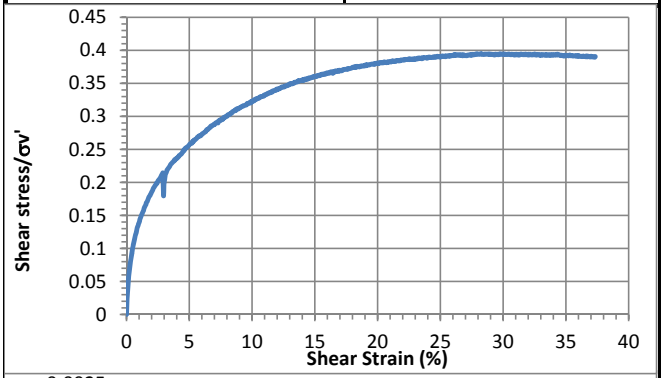

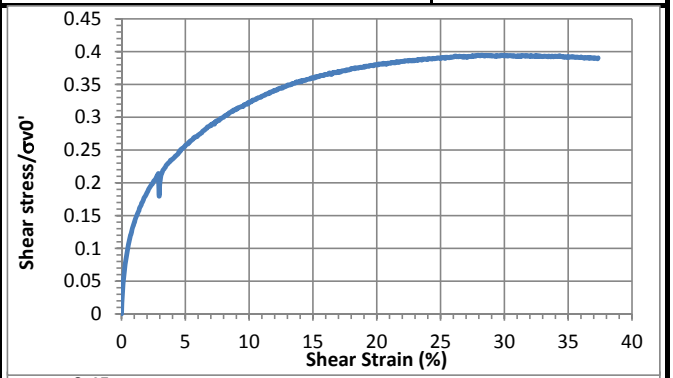

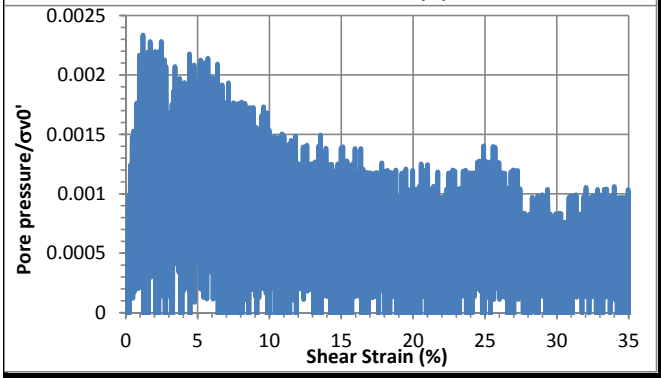

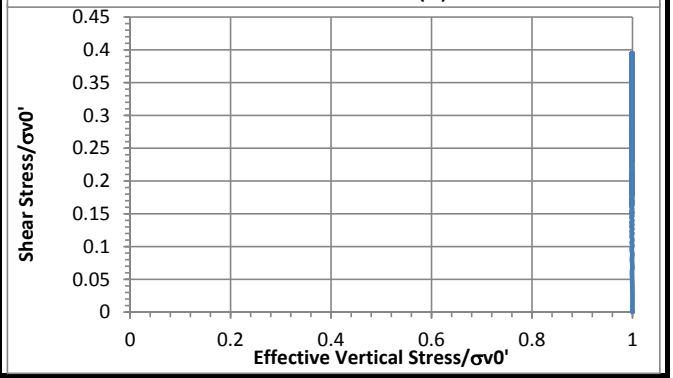

Shear wave velocity				
Signal type	Sinusoidal	First rise	initiation time (ms)	-0.0154
Signal amplitude (Vpp)	90		arrival time (ms)	0.5530
Signal frequency (kHz)	5		Vs (m/s)	197
Sensor spacing (mm)	112.13	First peak	initiation time (ms)	0.0410
R+P average Vs (m/s)	195		arrival time (ms)	0.6246
Stdev. (m/s)	4		Vs (m/s)	192
R+P+V average Vs (m/s)	192.7	First peak	initiation time (ms)	0.1382
Stdev. (m/s)	4		arrival time (ms)	0.7322
Wavelength (m)	0.039		Vs (m/s)	189
Spacing/wavelength	2.9			

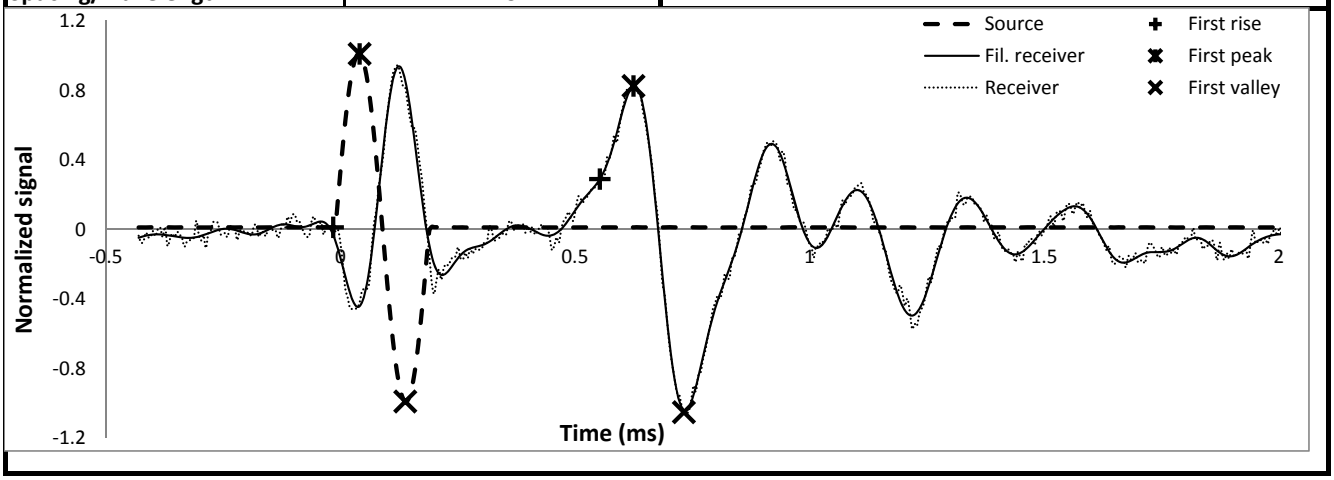

CSS Monotonic Shear Test Report

10/28/2013_Version 8.0

Geotechnical Engineering Laboratory

General Test Information and Sample Preparation			
Device:	CSS	**Layers:**	7
Specimen ID:	TX-ACL	**Weight/layer (kg):**	1.494
Test ID:	TX4	**Height/layer (mm):**	25.4
Date of Test:	5/17/2014	**Total height (mm):**	177.8
Test Performed:	Monotonic Shear	**Soil-Only Specimen Diameter (mm):**	306.2
Test Material:	MSW	**Total weight (kg):**	10.458
Sample Preparation:	The same initial composition and unit weight as Sim. #2. Pre-compress for 23 hours, consolidate for 1 hour.	**Density (kg/m^3):**	799
		Membrane Thickness (mm):	0.000635
		Moisture Content (%):	32.0
		Saturated (Y/N):	N
		Prepared by:	Fei

Pre-compression Stage			
Pre-compression strain:	0.29	**Secondary compression ratio**	0.00365
Height (mm):	129.0	**Density (kg/m3):**	1101

Consolidation Stage		Shear Stage		
Initial height (mm):	135.8	**Type of Test:**		CU-strain
Initial density (kg/m3):	1046	**Shear Strain Rate (%/min):**		0.32
Vertical Stress (kPa):	48.1	**10% strain**	**Shear stress (kPa)**	16.5
Immediate strain (εimm, %)	29.3		**Tan friction angle (°)**	28.7
Consolidated Height (mm):	126.6		**Sin friction angle (°)**	33.3
Compression index (Cc ε)	0.178	**30% strain**	**Shear stress (kPa)**	16.7
Constrained modulus	6.67		**Tan friction angle (°)**	31.3
Consolidated density (kg/m^3):	1121		**Sin friction angle (°)**	37.5

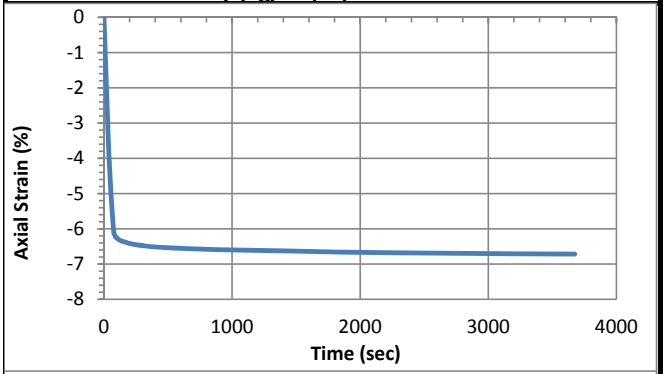

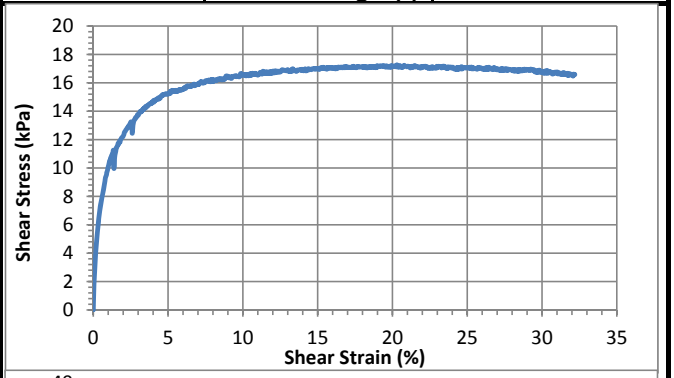

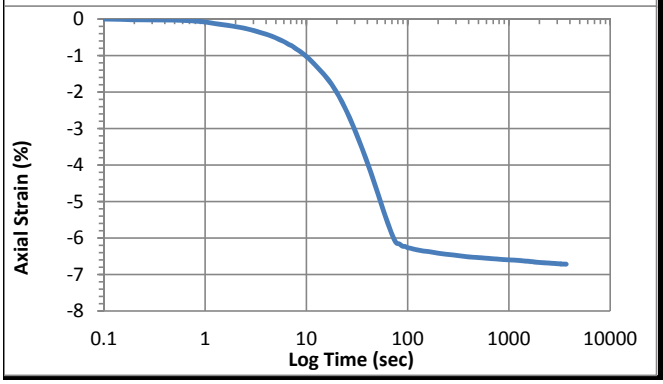

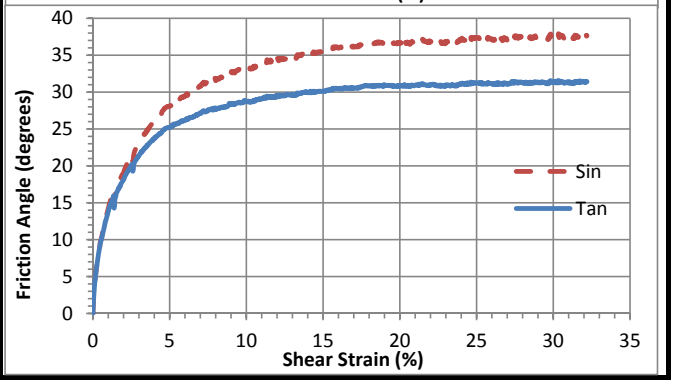

Strength			
Su/σv' at 10% strain	0.55	Su/σv0' at 10% strain	0.34
Su/σv' at 30% strain	0.61	Su/σv0' at 30% strain	0.35

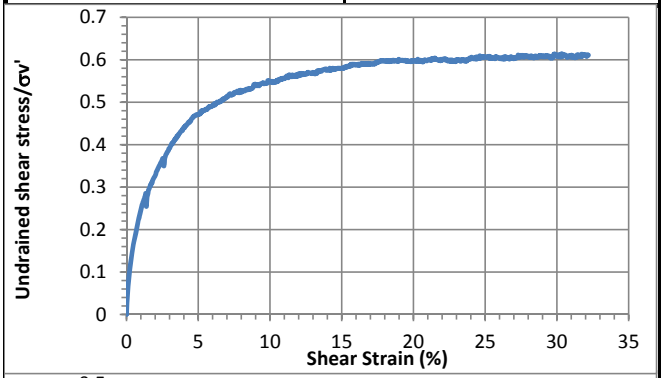

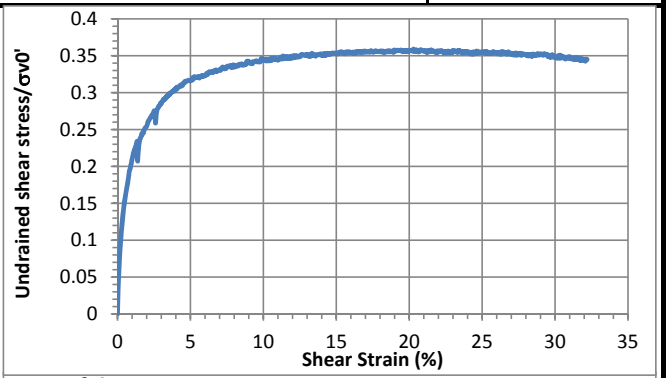

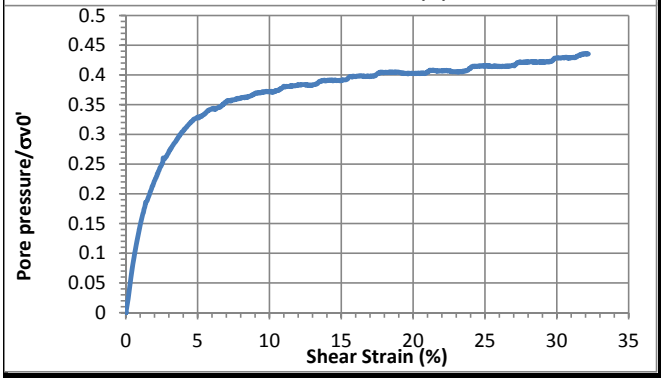

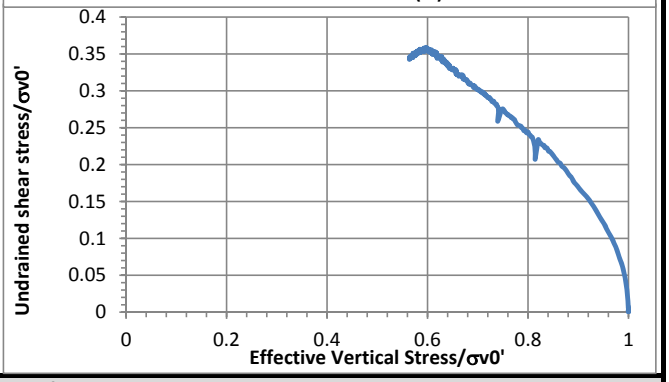

Shear wave velocity				
Signal type	Sinusoidal	First rise	initiation time (ms)	-0.0205
Signal amplitude (Vpp)	90		arrival time (ms)	0.9216
Signal frequency (kHz)	2		Vs (m/s)	125
Sensor spacing (mm)	117.85	First peak	initiation time (ms)	0.1075
R+P average Vs (m/s)	122		arrival time (ms)	1.1008
Stdev. (m/s)	5		Vs (m/s)	119
R+P+V average Vs (m/s)	120	First valley	initiation time (ms)	0.3584
Stdev. (m/s)	4		arrival time (ms)	1.3619
Wavelength (m)	0.060		Vs (m/s)	117
Spacing/wavelength	2.0			

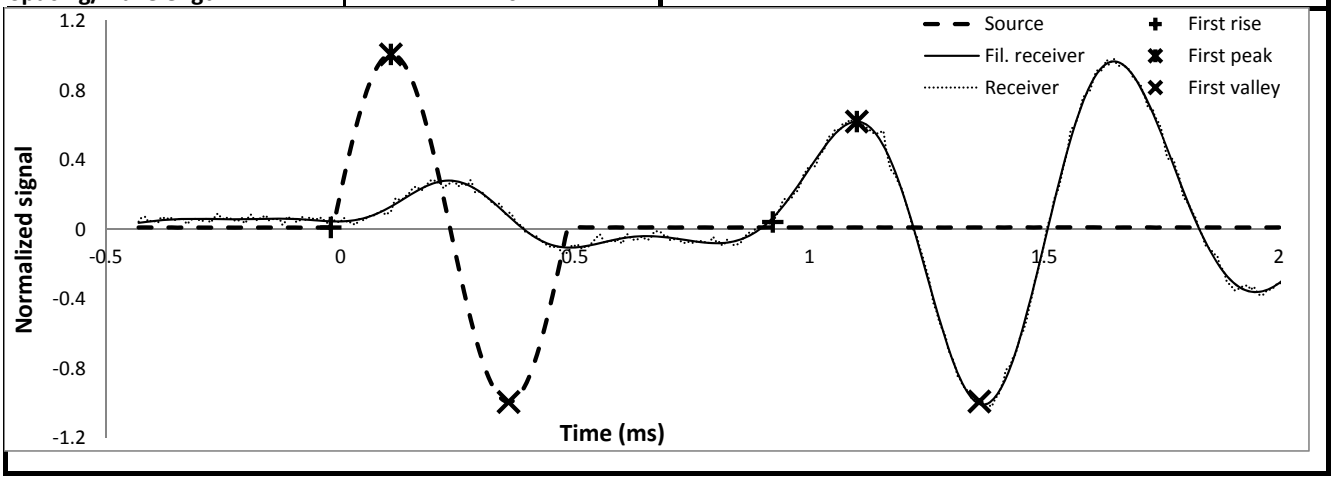

CSS Monotonic Shear Test Report

10/28/2013_Version 8.0

Geotechnical Engineering Laboratory

General Test Information and Sample Preparation

Device:	CSS	**Layers:**	7.5
Specimen ID:	TX-ACL	**Weight/layer (kg):**	1.494
Test ID:	TX5	**Height/layer (mm):**	25.4
Date of Test:	6/14/2014	**Total height (mm):**	190.5
Test Performed:	Monotonic Shear	**Soil-Only Specimen Diameter (mm):**	306.2
Test Material:	MSW	**Total weight (kg):**	11.205
		Density (kg/m^3):	799
Sample Preparation:	The same initial composition and unit weight as Sim. #2. Pre-compress for 23 hours, consolidate for 1 hour.	**Membrane Thickness (mm):**	0.000635
		Moisture Content (%):	32.0
		Saturated (Y/N):	N
		Prepared by:	Fei

Pre-compression Stage

Pre-compression strain:	0.36	**Secondary compression ratio**	0.00283
Height (mm):	118.9	**Density (kg/m3):**	1280

Consolidation Stage

Initial height (mm):	127.5
Initial density (kg/m3):	1193
Vertical Stress (kPa):	97.1
Immediate strain (εimm, %)	36.3
Consolidated Height (mm):	116.6
Compression index (Ccε)	0.186
Constrained modulus	5.42
Consolidated density (kg/m^3):	1304

Shear Stage

Type of Test:		CU-strain
Shear Strain Rate (%/min):		0.34
10% strain	**Shear stress (kPa)**	33.6
	Tan friction angle (°)	28.1
	Sin friction angle (°)	32.3
30% strain	**Shear stress (kPa)**	30.3
	Tan friction angle (°)	30.2
	Sin friction angle (°)	35.5

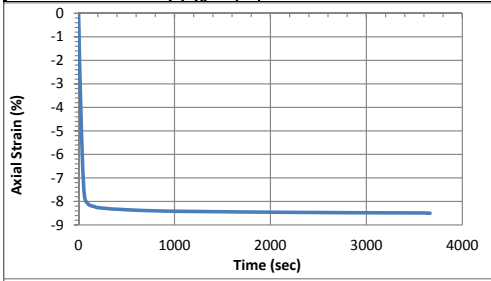

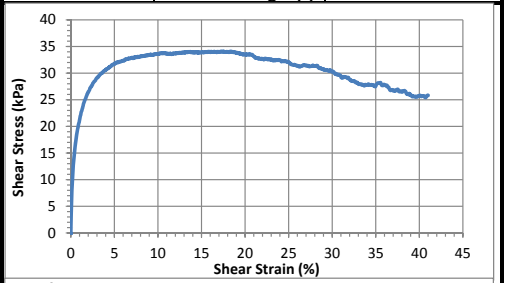

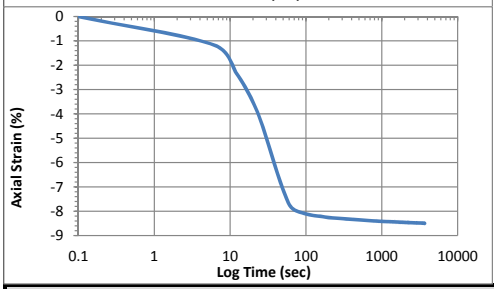

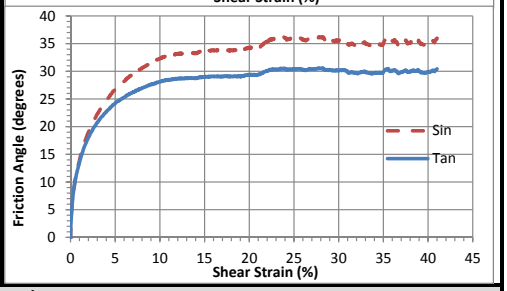

Strength

Su/σv' at 10% strain	0.53	**Su/σv0' at 10% strain**	0.35
Su/σv' at 30% strain	0.58	**Su/σv0' at 30% strain**	0.31

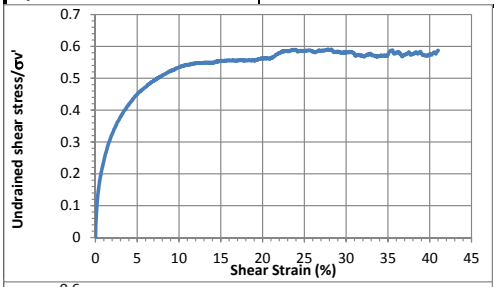

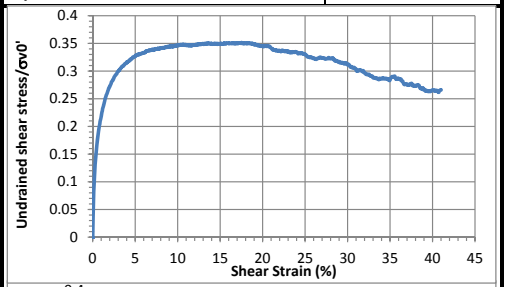

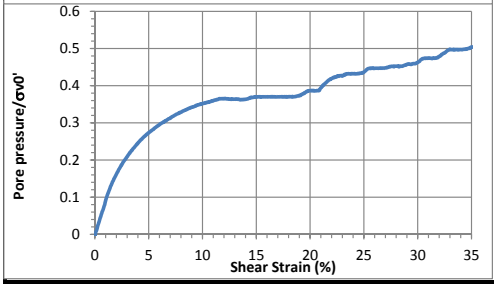

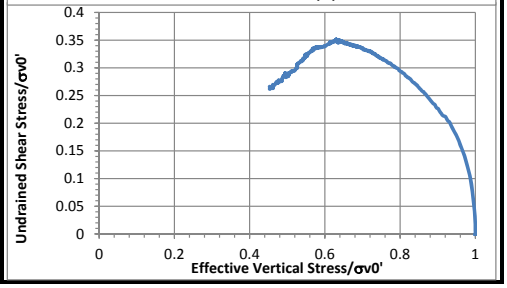

CSS Monotonic Shear Test Report

10/28/2013_Version 8.0

Geotechnical Engineering Laboratory

General Test Information and Sample Preparation			
Device:	CSS	**Layers:**	8.75
Specimen ID:	TX-ACL	**Weight/layer (kg):**	1.494
Test ID:	TX6	**Height/layer (mm):**	25.4
Date of Test:	6/16/2014	**Total height (mm):**	222.25
Test Performed:	Monotonic Shear	**Soil-Only Specimen Diameter (mm):**	306.2
Test Material:	MSW	**Total weight (kg):**	13.07
Sample Preparation:	The same initial composition and unit weight as Sim. #2. Pre-compress for 24 hours, consolidate for 1 hour. Ignore strain >25%	**Density (kg/m^3):**	799
		Membrane Thickness (m\m):	0.000635
		Moisture Content (%):	31.7
		Saturated (Y/N):	N
		Prepared by:	Fei

Pre-compression Stage			
Pre-compression strain:	0.48	**Secondary compression ratio**	0.00396
Height (mm):	120.0	**Density (kg/m3):**	1479

Consolidation Stage		Shear Stage		
Initial height (mm):	133.1	**Type of Test:**		CU-strain
Initial density (kg/m3):	1333	**Shear Strain Rate (%/min):**		0.34
Vertical Stress (kPa):	196.1	**10% strain**	**Shear stress (kPa)**	59.0
Immediate strain (εimm, %)	47.7		**Tan friction angle (°)**	26.9
Consolidated Height (mm):	117.3		**Sin friction angle (°)**	30.5
Compression index (Cc ε)	0.211	**30% strain**	**Shear stress (kPa)**	46.7
Constrained modulus	4.13		**Tan friction angle (°)**	28.0
Consolidated density (kg/m^3):	1513		**Sin friction angle (°)**	32.0

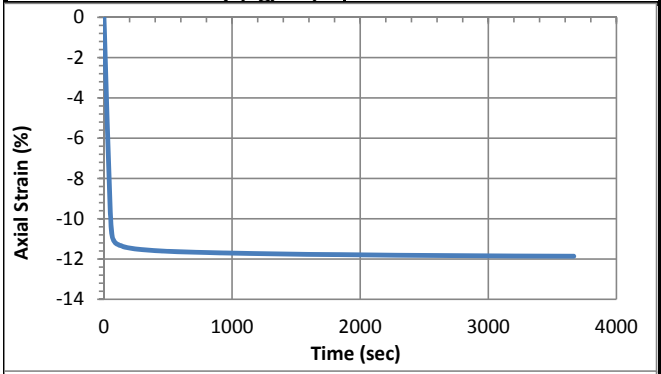

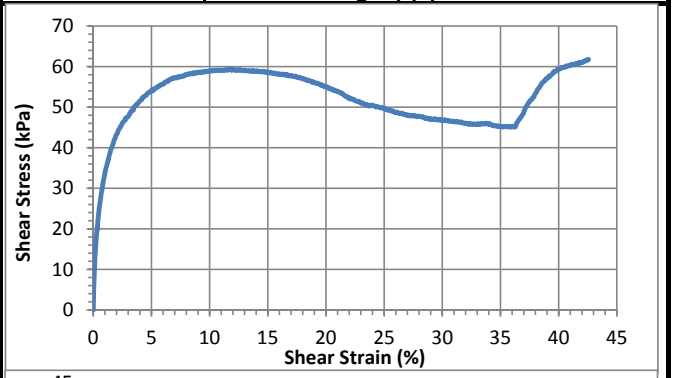

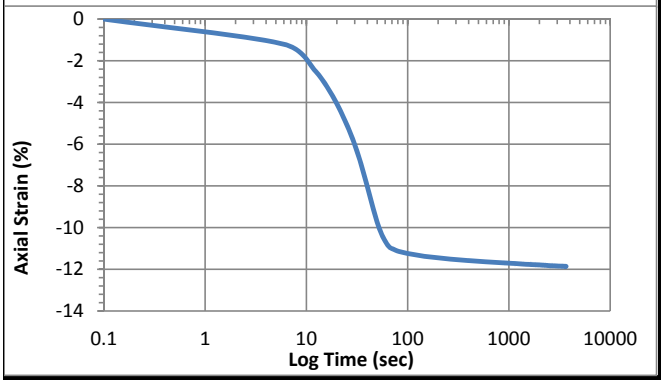

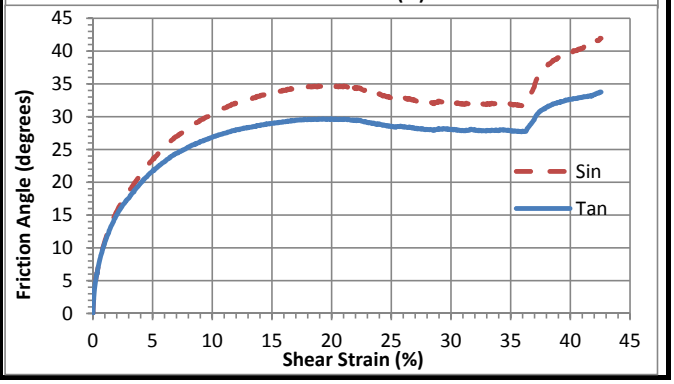

Undrained Strength			
Su/σv' at 10% strain	0.51	Su/σv0' at 10% strain	0.30
Su/σv' at 30% strain	0.53	Su/σv0' at 30% strain	0.24

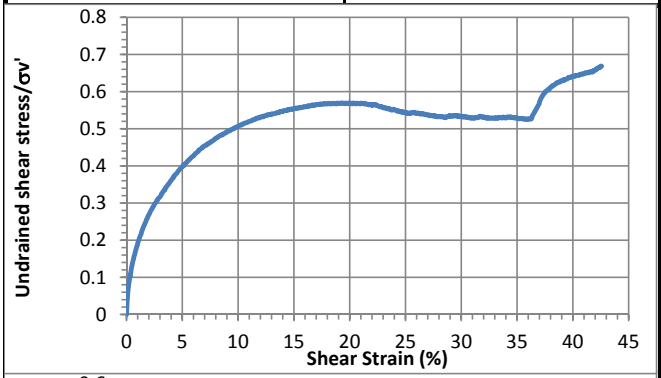

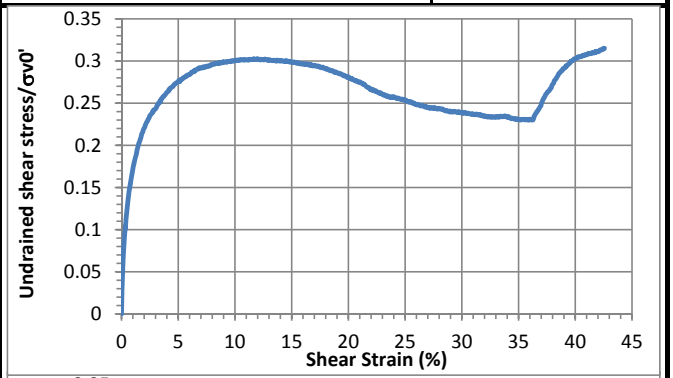

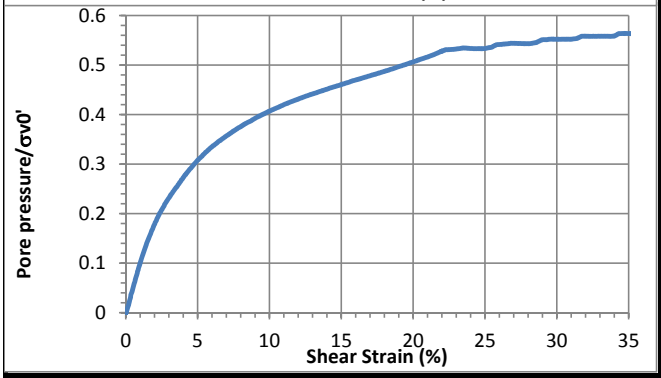

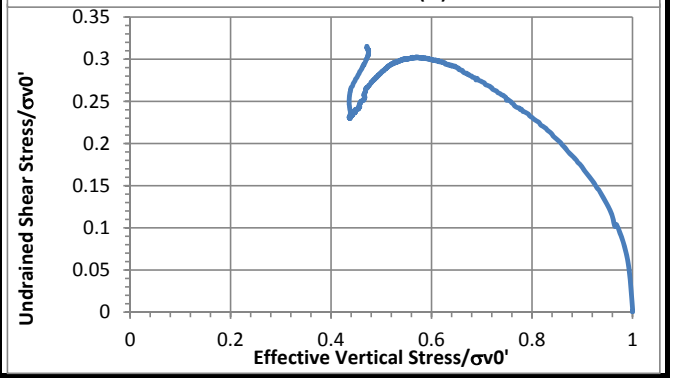

Shear wave velocity				
Signal type	Sinusoidal	First rise	initiation time (ms)	-0.0154
Signal amplitude (Vpp)	90		arrival time (ms)	0.5427
Signal frequency (kHz)	5		Vs (m/s)	194
Sensor spacing (mm)	108.48	First peak	initiation time (ms)	0.0410
R+P average Vs (m/s)	200		arrival time (ms)	0.5683
Stdev. (m/s)	8		Vs (m/s)	206
R+P+V average Vs (m/s)	197	First valley	initiation time (ms)	0.1382
Stdev. (m/s)	8		arrival time (ms)	0.7066
Wavelength (m)	0.039		Vs (m/s)	191
Spacing/wavelength	2.8			

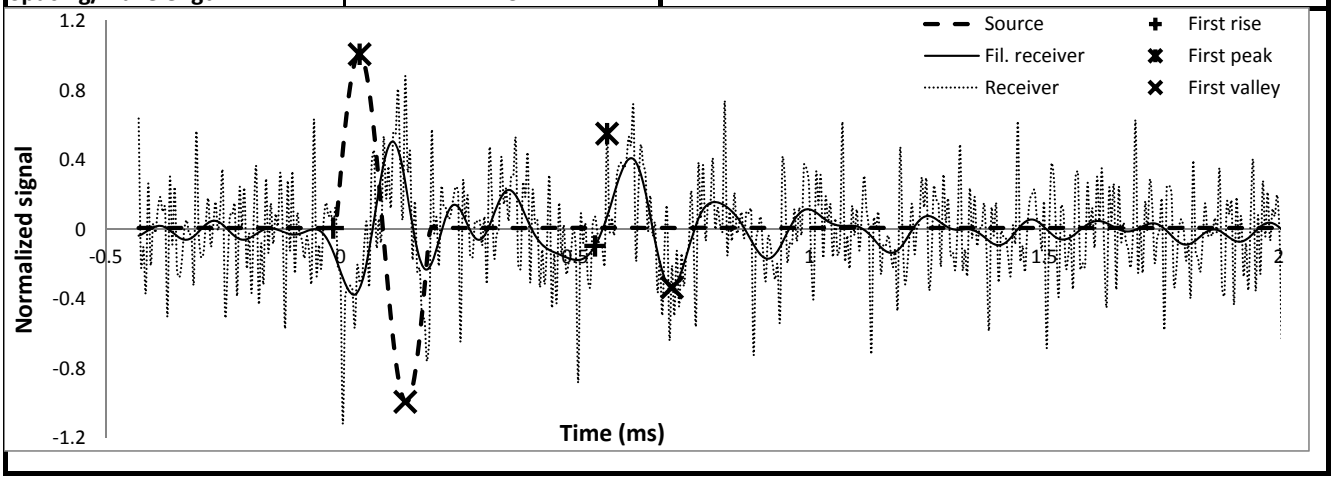

CSS Monotonic Shear Test Report

10/28/2013_Version 8.0

Geotechnical Engineering Laboratory

General Test Information and Sample Preparation			
Device:	CSS	**Layers:**	9.73
Specimen ID:	ACL	**Weight/layer (kg):**	1.494
Test ID:	TX7	**Height/layer (mm):**	25.4
Date of Test:	6/18/2014	**Total height (mm):**	247.10
Test Performed:	Monotonic Shear	**Soil-Only Specimen Diameter (mm):**	306.2
Test Material:	MSW	**Total weight (kg):**	14.53
Sample Preparation:	The same initial composition and unit weight as Sim. #2. Pre-compress for 24 hours, consolidate for 1 hour.	**Density (kg/m^3):**	799
		Membrane Thickness (m):	0.000635
		Moisture Content (%):	32.0
		Saturated (Y/N):	N
		Prepared by:	Fei

Pre-compression Stage			
Pre-compression strain:	0.45	**Secondary compression ratio**	0.00433
Height (mm):	129.8	**Density (kg/m3):**	1520

Consolidation Stage		Shear Stage		
Initial height (mm):	134.8	**Type of Test:**		CD-strain
Initial density (kg/m3):	1464	**Shear Strain Rate (%/min):**		0.34
Vertical Stress (kPa):	394.0	**10% strain**	**Shear stress (kPa)**	121.7
Immediate strain (εimm, %)	48.6		**Tan friction angle (°)**	17.2
Consolidated Height (mm):	118.0		**Sin friction angle (°)**	18.0
Compression index (Cc ε)	0.191	**30% strain**	**Shear stress (kPa)**	141.1
Constrained modulus	4.04		**Tan friction angle (°)**	19.7
Consolidated density (kg/m^3):	1673		**Sin friction angle (°)**	21.0

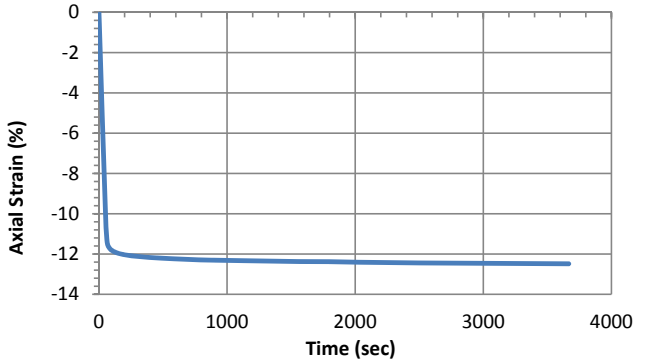

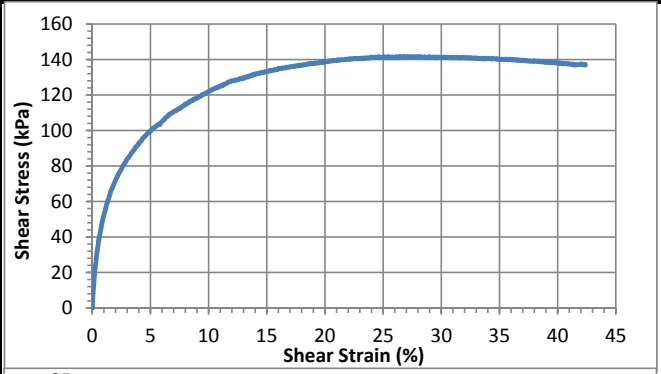

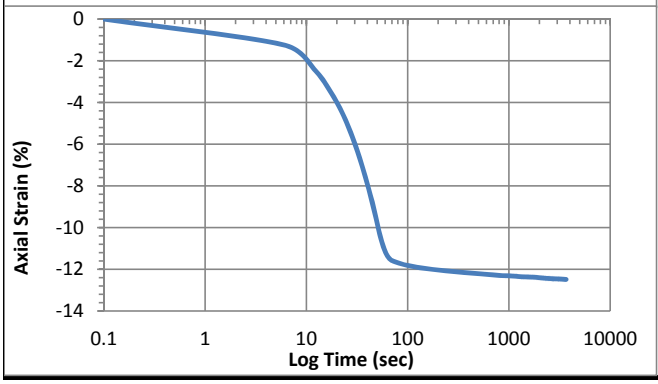

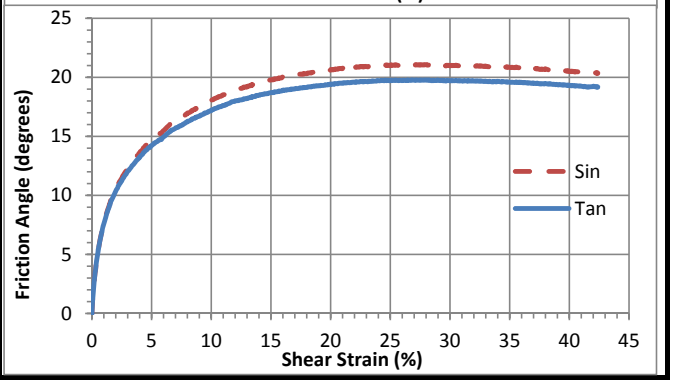

Strength			
τ/σv' at 10% strain	0.31	τ/σv0' at 10% strain	0.31
τ/σv' at 30% strain	0.36	τ/σv0' at 30% strain	0.36

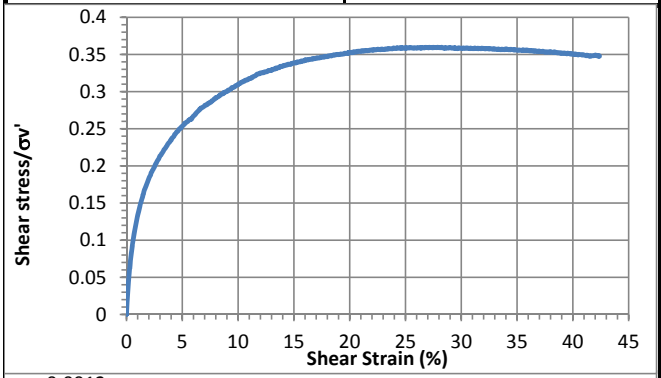

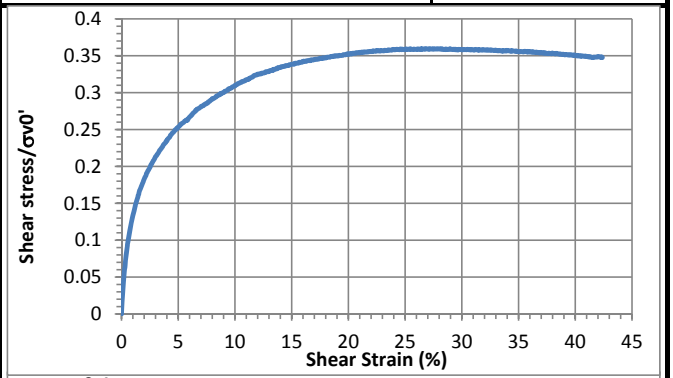

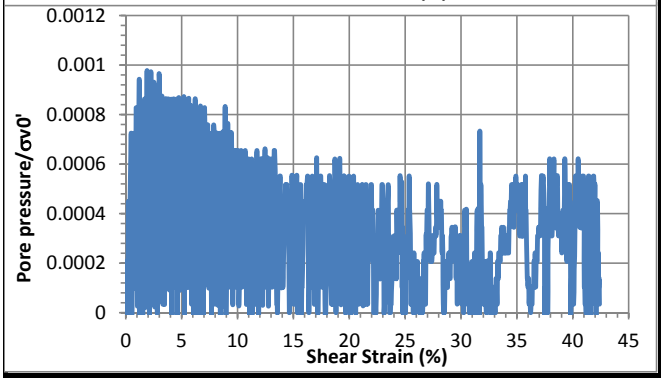

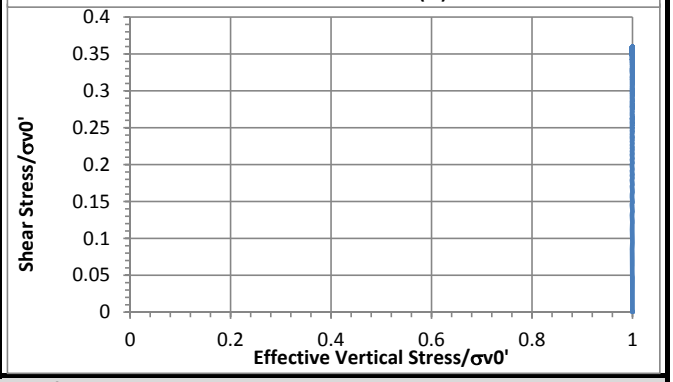

Shear wave velocity				
Signal type	Sinusoidal	First rise	initiation time (ms)	-0.0102
Signal amplitude (Vpp)	90		arrival time (ms)	0.3840
Signal frequency (kHz)	5		Vs (m/s)	277
Sensor spacing (mm)	109.16	First peak	initiation time (ms)	0.0410
R+P average Vs (m/s)	268		arrival time (ms)	0.4608
Stdev. (m/s)	12		Vs (m/s)	260
P+V average Vs (m/s)	267	First valley	initiation time (ms)	0.1434
Stdev. (m/s)	9		arrival time (ms)	0.5427
Wavelength (m)	0.053		Vs (m/s)	273
Spacing/wavelength	2.0			

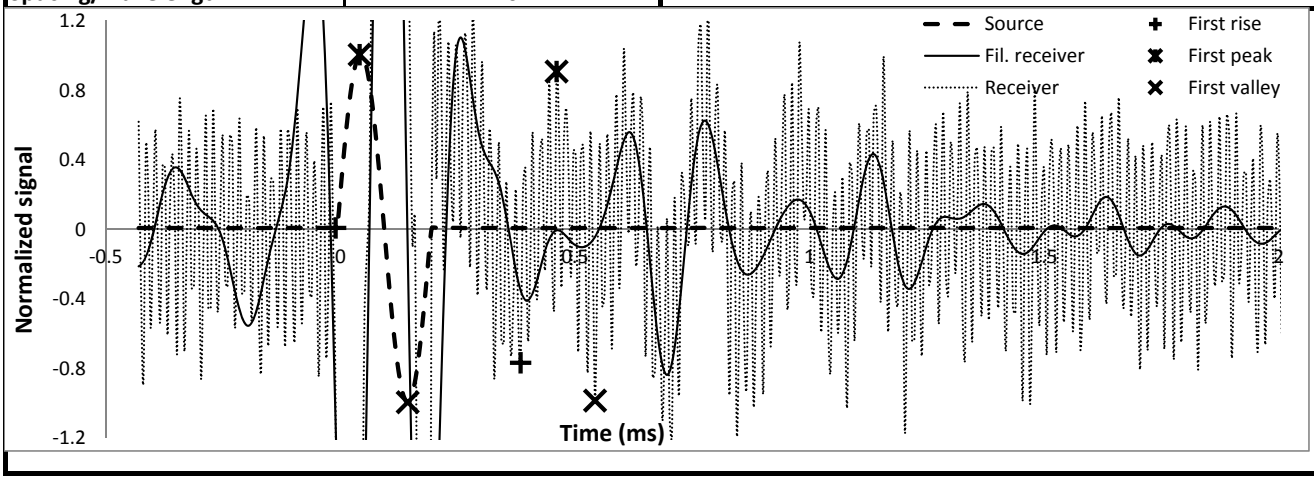

CSS Monotonic Shear Test Report

10/28/2013_Version 8.0

Geotechnical Engineering Laboratory

General Test Information		Sample Preparation	
Device:	CSS	Prepared total weight (kg):	11.952
Specimen ID:	TX-ACL	Prepared dry weight (kg):	9.124
Test ID:	TX9	Prepared height (mm):	181.5
Date of test:	6/5/2015	Prepared total density (kg/m3):	894
Test performed:	Monotonic Shear	Prepared dry density (kg/m3):	683
Test material:	MSW	**Pre-compression Stage**	
Sample preparation:	TX-ACL fresh FP. Bottom ring tilted near the end.	Pre-compressed strain (%):	41.0
		Compressed total density (kg/m3):	1517
		Compressed dry density (kg/m3):	1158
		Secondary compression ratio:	0.00101
		Total weight before shearing (kg):	11.914
		Dry weight before shearing (kg):	9.086

Consolidation Stage		Shear Stage		
Consolidated height (mm):	107.82	Type of test:		CV-strain
Vertical stress (kPa):	97.1	Shear strain rate (%/min):		0.37
Immediate strain (εimm, %)	40.39	10% strain	Shear stress (kPa)	32.3
Strain before shearing (εall, %)	40.6		Tan friction angle (°)	33.4
Compression index (Cεε)	0.203		Sin friction angle (°)	41.3
Constrained modulus	4.95	30% strain	Shear stress (kPa)	35.4
Consolidated total density	1500		Tan friction angle (°)	32.8
Consolidated dry density	1144		Sin friction angle (°)	40.2

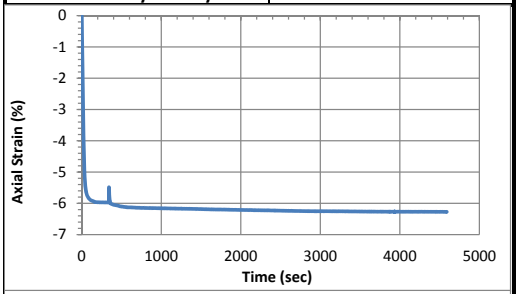

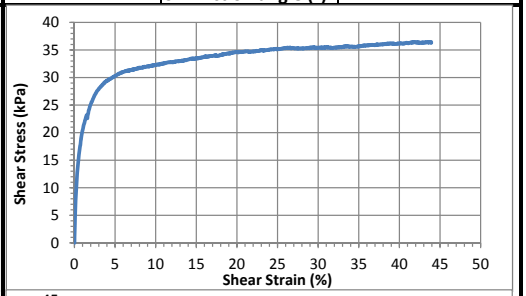

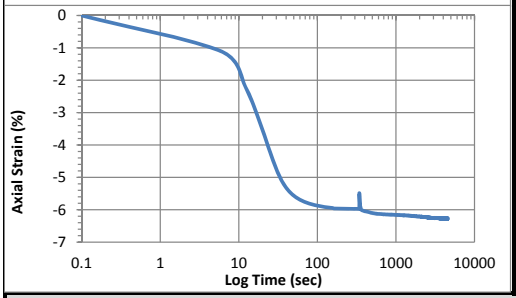

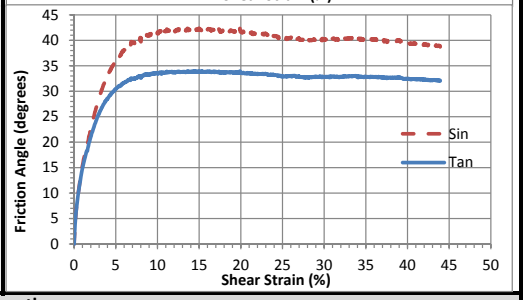

Strength			
τ/σv' at 10% strain	0.66	τ/σv0' at 10% strain	0.33
τ/σv' at 30% strain	0.64	τ/σv0' at 30% strain	0.37

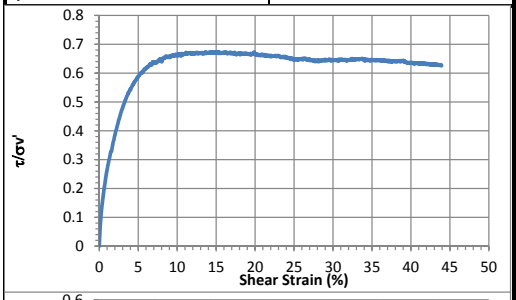

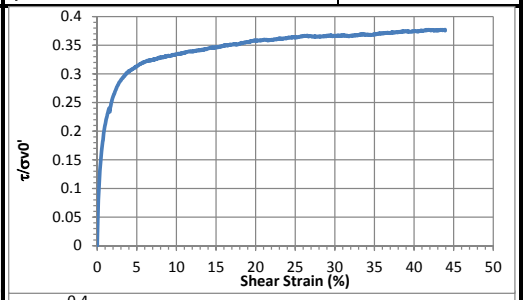

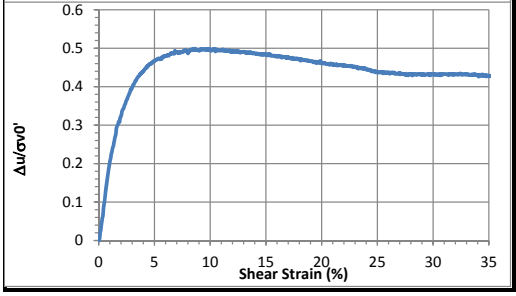

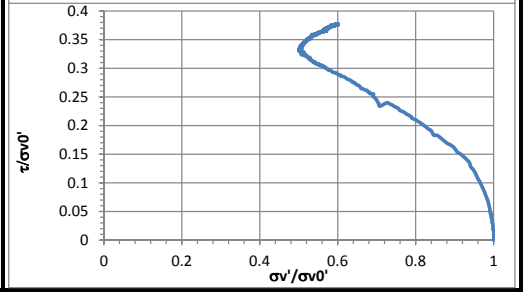

CSS Monotonic Shear Test Report

10/28/2013_Version 8.0

Geotechnical Engineering Laboratory

General Test Information	
Device:	CSS
Specimen ID:	TX-ACL
Test ID:	TX10
Date of test:	6/9/2015
Test performed:	Monotonic Shear
Test material:	MSW
Sample preparation:	TX-ACL fresh FP. Bottom ring tilted near the end.

Sample Preparation	
Prepared total weight (kg):	14.940
Prepared dry weight (kg):	11.405
Prepared height (mm):	213.1
Prepared total density (kg/m3):	952
Prepared dry density (kg/m3):	727
Pre-compression Stage	
Pre-compressed strain (%):	45.6
Compressed total density (kg/m3):	1751
Compressed dry density (kg/m3):	1336
Secondary compression ratio:	0.00143
Total weight before shearing (kg):	14.836
Dry weight before shearing (kg):	11.300

Consolidation Stage	
Consolidated height (mm):	115.81
Vertical stress (kPa):	197.8
Immediate strain (εimm, %)	45.36
Strain before shearing (εall, %)	45.6
Compression index (Cεε)	0.198
Constrained modulus	4.41
Consolidated total density	1739
Consolidated dry density	1325

Shear Stage		
Type of test:		CV-strain
Shear strain rate (%/min):		0.34
10% strain	Shear stress (kPa)	58.8
	Tan friction angle (°)	32.0
	Sin friction angle (°)	38.7
30% strain	Shear stress (kPa)	62.5
	Tan friction angle (°)	34.5
	Sin friction angle (°)	43.3

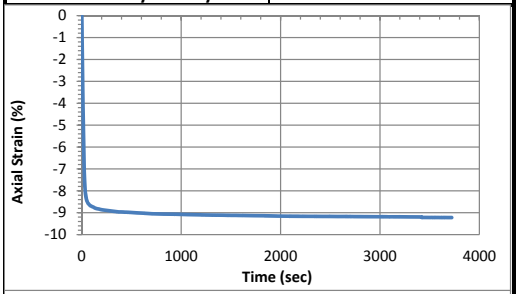

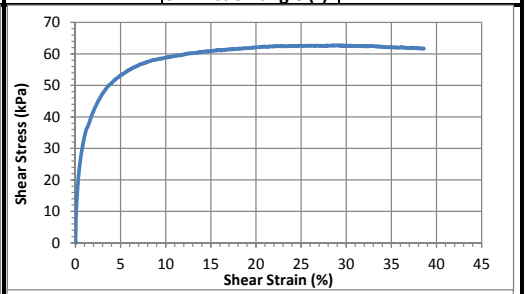

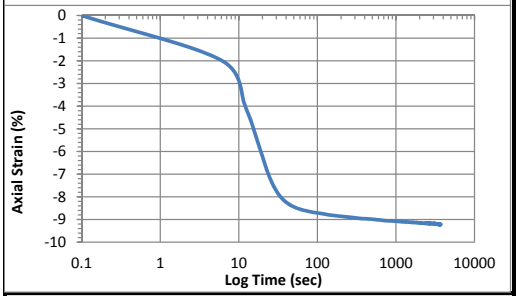

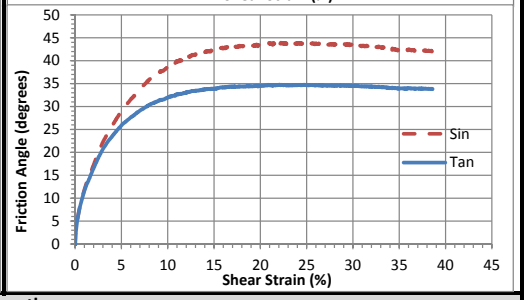

Strength

τ/σv' at 10% strain	0.62	τ/σv0' at 10% strain	0.30
τ/σv' at 30% strain	0.69	τ/σv0' at 30% strain	0.32

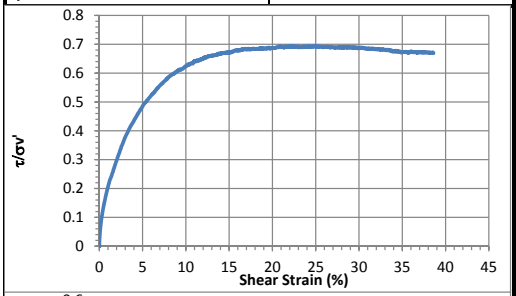

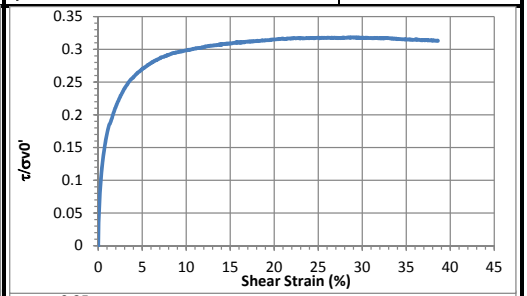

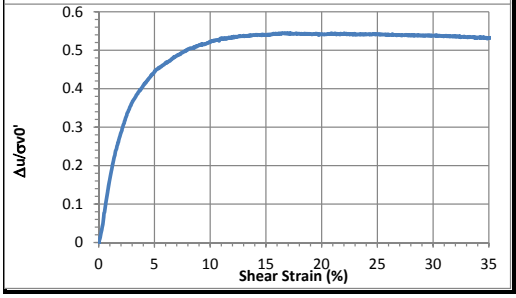

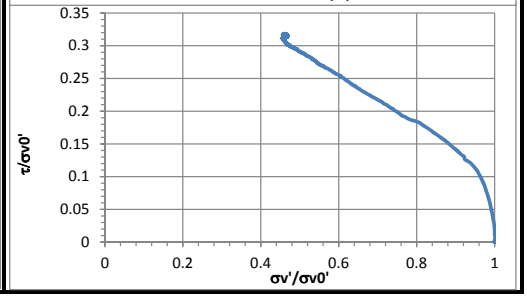

CSS Monotonic Shear Test Report

10/28/2013_Version 8.0

Geotechnical Engineering Laboratory

General Test Information		Sample Preparation	
Device:	CSS	Prepared total weight (kg):	11.952
Specimen ID:	TX-ACL	Prepared dry weight (kg):	9.124
Test ID:	TX11	Prepared height (mm):	185.7
Date of test:	6/11/2015	Prepared total density (kg/m3):	874
Test performed:	Monotonic Shear	Prepared dry density (kg/m3):	667
Test material:	MSW	**Pre-compression Stage**	
Sample preparation:	TX-ACL fresh FP. Bottom ring tilted near the end.	Pre-compressed strain (%):	41.6
		Compressed total density (kg/m3):	1496
		Compressed dry density (kg/m3):	1142
		Secondary compression ratio:	0.00090
		Total weight before shearing (kg):	11.916
		Dry weight before shearing (kg):	9.088

Consolidation Stage		Shear Stage		
Consolidated height (mm):	107.22	Type of test:		CV-strain
Vertical stress (kPa):	96.4	Shear strain rate (%/min):		0.37
Immediate strain (εimm, %)	42.09	10% strain	Shear stress (kPa)	37.3
Strain before shearing (εall, %)	42.3		Tan friction angle (°)	21.3
Compression index (Cεε)	0.212		Sin friction angle (°)	23.1
Constrained modulus	4.75	30% strain	Shear stress (kPa)	50.3
Consolidated total density	1509		Tan friction angle (°)	27.7
Consolidated dry density	1151		Sin friction angle (°)	31.7

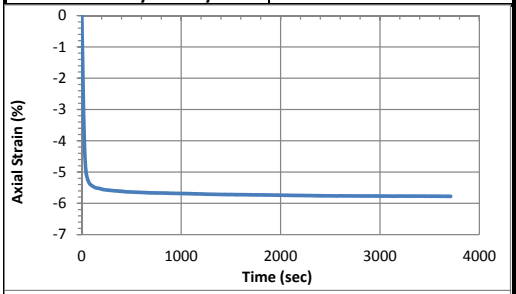

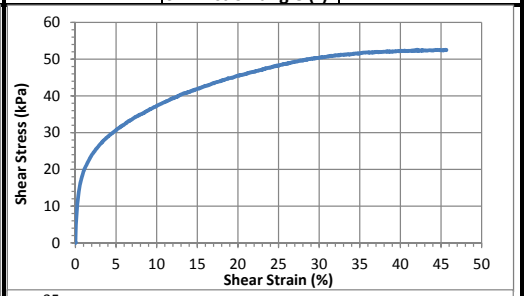

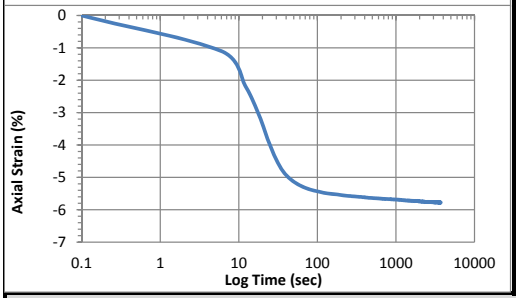

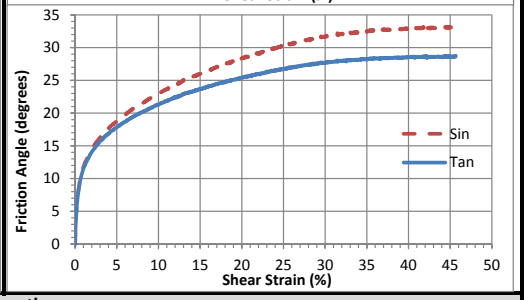

Strength			
τ/σv' at 10% strain	0.39	τ/σv0' at 10% strain	0.39
τ/σv' at 30% strain	0.53	τ/σv0' at 30% strain	0.53

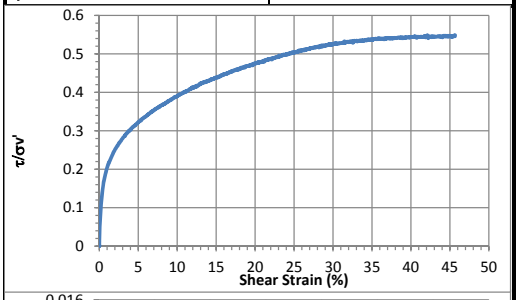

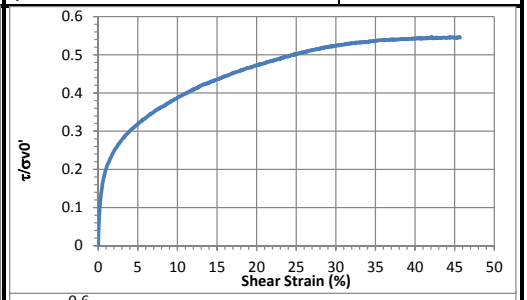

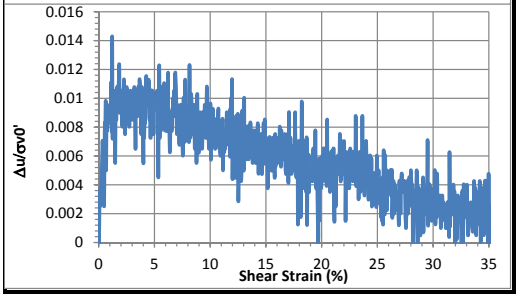

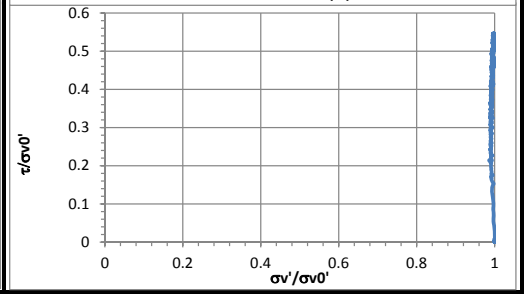

CSS Monotonic Shear Test Report

10/28/2013_Version 8.0

Geotechnical Engineering Laboratory

General Test Information		Sample Preparation	
Device:	CSS	**Prepared total weight (kg):**	14.940
Specimen ID:	TX-ACL	**Prepared dry weight (kg):**	11.405
Test ID:	TX12	**Prepared height (mm):**	221.2
Date of test:	6/13/2015	**Prepared total density (kg/m3):**	917
Test performed:	Monotonic Shear	**Prepared dry density (kg/m3):**	700
Test material:	MSW	**Pre-compression Stage**	
Sample preparation:	TX-ACL fresh FP. Bottom ring tilted near the end.	**Pre-compressed strain (%):**	46.3
		Compressed total density (kg/m3):	1709
		Compressed dry density (kg/m3):	1305
		Secondary compression ratio:	0.00052
		Total weight before shearing (kg):	14.888
		Dry weight before shearing (kg):	11.352

Consolidation Stage		Shear Stage		
Consolidated height (mm):	118.84	**Type of test:**		CL-strain
Vertical stress (kPa):	196.6	**Shear strain rate (%/min):**		0.34
Immediate strain (εimm, %)	46.19	**10% strain**	**Shear stress (kPa)**	76.7
Strain before shearing (εall, %)	46.3		**Tan friction angle (°)**	21.4
Compression index (Cεε)	0.201		**Sin friction angle (°)**	23.0
Constrained modulus	4.33	**30% strain**	**Shear stress (kPa)**	83.2
Consolidated total density	1701		**Tan friction angle (°)**	23.0
Consolidated dry density	1297		**Sin friction angle (°)**	25.1

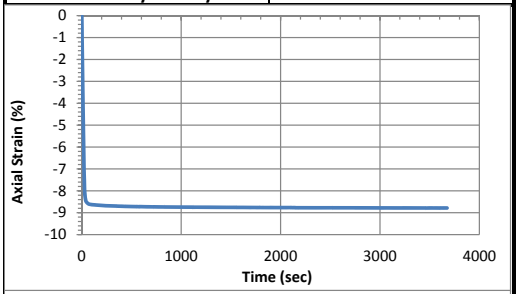

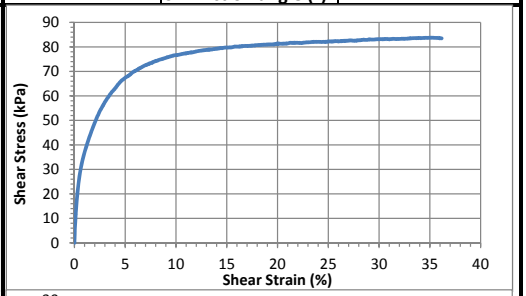

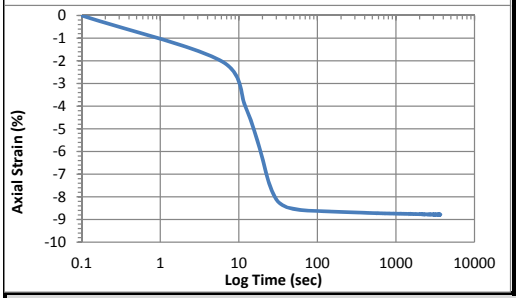

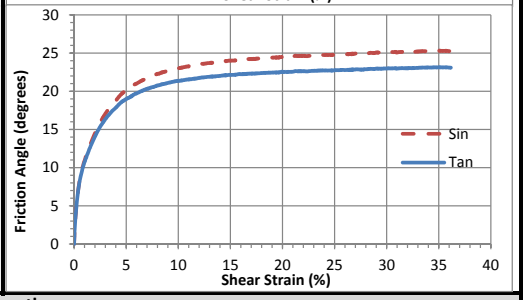

Strength			
τ/σv' at 10% strain	0.39	**τ/σv0' at 10% strain**	0.39
τ/σv' at 30% strain	0.42	**τ/σv0' at 30% strain**	0.42

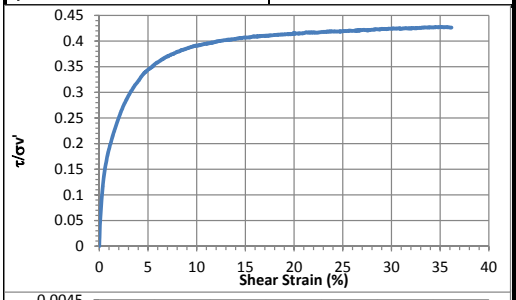

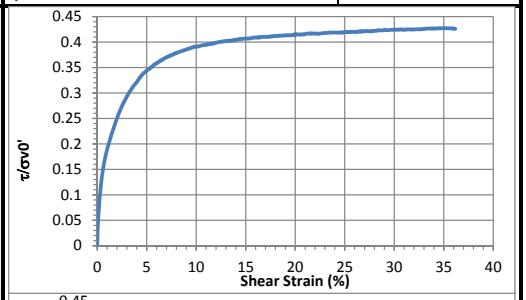

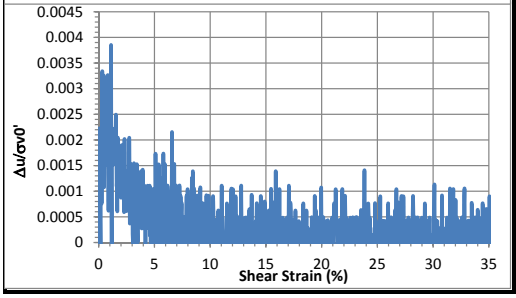

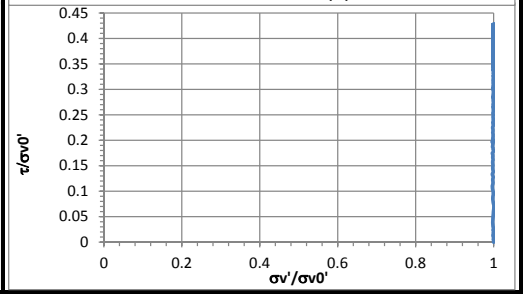

CSS Monotonic Shear Test Report

10/28/2013_Version 8.0

Geotechnical Engineering Laboratory

General Test Information	
Device:	CSS
Specimen ID:	TX-ACL
Test ID:	TX13
Date of test:	6/15/2015
Test performed:	Monotonic Shear
Test material:	MSW
Sample preparation:	TX-ACL fresh FP.

Sample Preparation	
Prepared total weight (kg):	17.928
Prepared dry weight (kg):	13.685
Prepared height (mm):	243.0
Prepared total density (kg/m3):	1002
Prepared dry density (kg/m3):	765
Pre-compression Stage	
Pre-compressed strain (%):	47.2
Compressed total density (kg/m3):	1899
Compressed dry density (kg/m3):	1449
Secondary compression ratio:	0.00084
Total weight before shearing (kg):	17.786
Dry weight before shearing (kg):	13.543

Consolidation Stage	
Consolidated height (mm):	125.92
Vertical stress (kPa):	496.4
Immediate strain (εimm, %)	48.10
Strain before shearing (εall, %)	48.2
Compression index (Cεc)	0.178
Constrained modulus	4.16
Consolidated total density	1918
Consolidated dry density	1460

Shear Stage		
Type of test:		CL-strain
Shear strain rate (%/min):		0.32
10% strain	Shear stress (kPa)	128.0
	Tan friction angle (°)	14.5
	Sin friction angle (°)	15.0
30% strain	Shear stress (kPa)	140.0
	Tan friction angle (°)	15.8
	Sin friction angle (°)	16.4

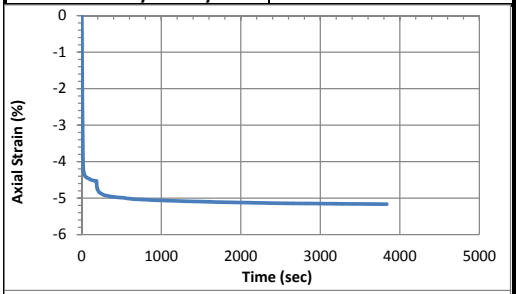

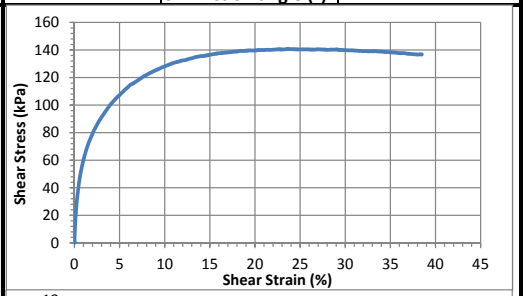

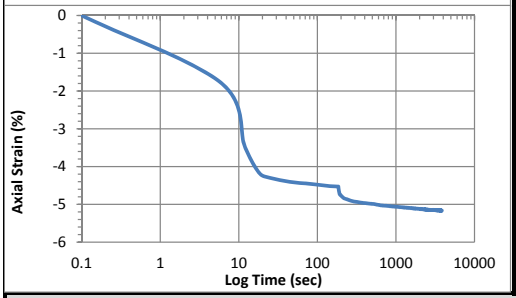

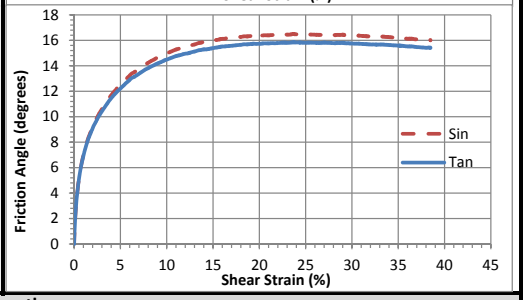

Strength

τ/σv' at 10% strain	0.26	τ/σv0' at 10% strain	0.26
τ/σv' at 30% strain	0.28	τ/σv0' at 30% strain	0.28

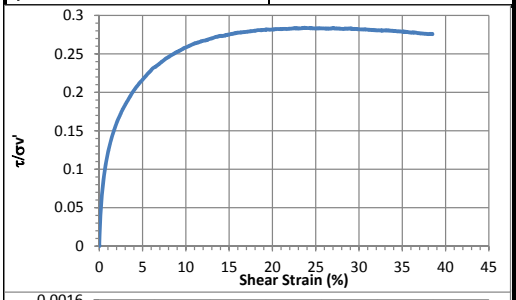

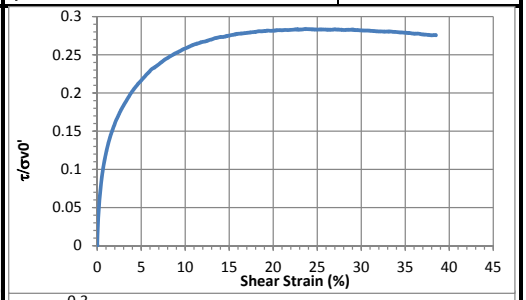

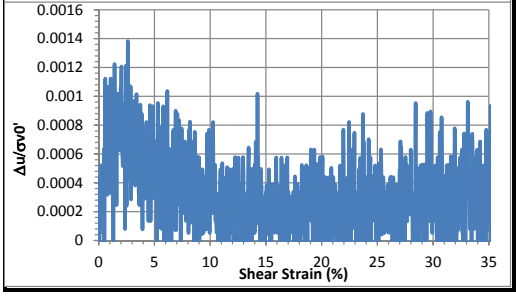

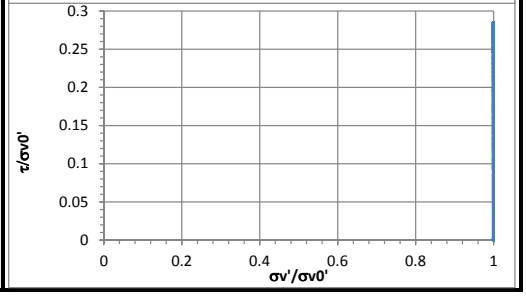

CSS Monotonic Shear Test Report

10/28/2013_Version 8.0

Geotechnical Engineering Laboratory

General Test Information	
Device:	CSS
Specimen ID:	TX-ACL
Test ID:	TX14
Date of test:	6/17/2015
Test performed:	Monotonic Shear
Test material:	MSW
Sample preparation:	TX-ACL fresh FP. The whole specimen was pulled up with top platen during unloading in the precompression device. Bottom ring tilted near the end.

Sample Preparation	
Prepared total weight (kg):	17.928
Prepared dry weight (kg):	13.685
Prepared height (mm):	233.1
Prepared total density (kg/m3):	1045
Prepared dry density (kg/m3):	797
Pre-compression Stage	
Pre-compressed strain (%):	46.7
Compressed total density (kg/m3):	1961
Compressed dry density (kg/m3):	1497
Secondary compression ratio:	0.00131
Total weight before shearing (kg):	17.837
Dry weight before shearing (kg):	13.594

Consolidation Stage	
Consolidated height (mm):	125.76
Vertical stress (kPa):	498.6
Immediate strain (εimm, %)	45.88
Strain before shearing (εall, %)	46.0
Compression index (Cεε)	0.170
Constrained modulus	4.36
Consolidated total density	1926
Consolidated dry density	1468

Shear Stage		
Type of test:		CV-strain
Shear strain rate (%/min):		0.32
10% strain	Shear stress (kPa)	118.7
	Tan friction angle (°)	21.1
	Sin friction angle (°)	22.7
30% strain	Shear stress (kPa)	119.9
	Tan friction angle (°)	27.0
	Sin friction angle (°)	30.7

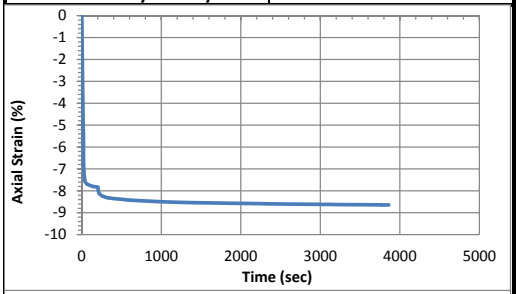

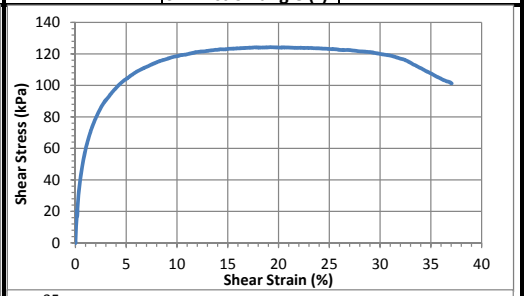

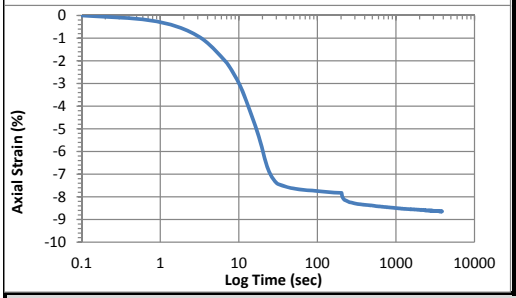

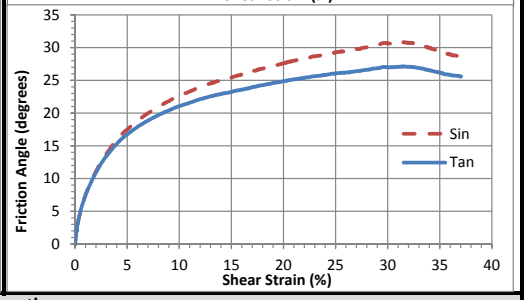

Strength

τ/σv' at 10% strain	0.39	τ/σv0' at 10% strain	0.24
τ/σv' at 30% strain	0.51	τ/σv0' at 30% strain	0.24

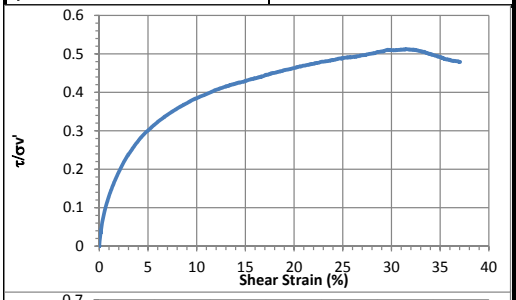

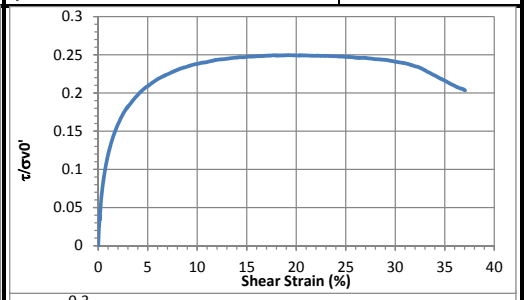

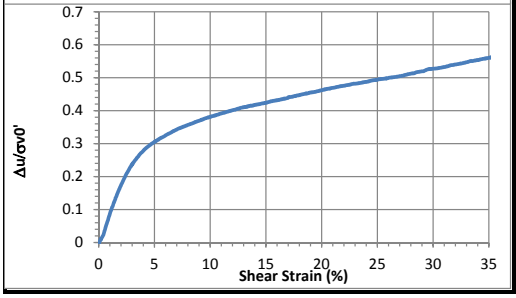

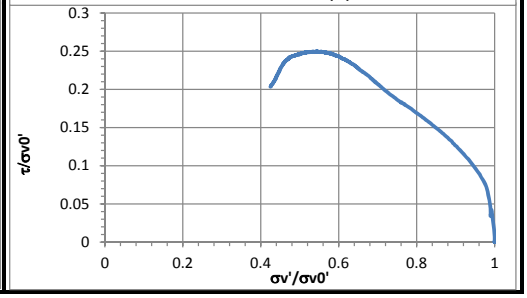

CSS Monotonic Shear Test Report

10/28/2013_Version 8.0

Geotechnical Engineering Laboratory

General Test Information		Sample Preparation	
Device:	CSS	Prepared total weight (kg):	10.458
Specimen ID:	TX-ACL	Prepared dry weight (kg):	7.983
Test ID:	TX15	Prepared height (mm):	156.2
Date of test:	6/19/2015	Prepared total density (kg/m3):	
Test performed:	Monotonic Direct Shear	Prepared dry density (kg/m3):	
Test material:	MSW	**Pre-compression Stage**	
Sample preparation:	TX-ACL fresh MSW. Direct shear. CL mode. Opening=0.2 in. Hit a pin near the end of shearing.	Pre-compressed strain (%):	44.1
		Compressed total density (kg/m3):	
		Compressed dry density (kg/m3):	
		Secondary compression ratio:	0.00169
		Total weight before shearing (kg):	10.298
		Dry weight before shearing (kg):	8.339

Consolidation Stage		Shear Stage		
Consolidated height (mm):	88.94	Type of test:		CL-direct shear
Vertical stress (kPa):	96.8	Shear strain rate (%/min):		
Immediate strain (εimm, %)	42.59	12 mm	Shear stress (kPa)	40.5
Strain before shearing (εall, %)	43.1		Tan friction angle (°)	22.8
Compression index (Cεε)	0.214		Sin friction angle (°)	
Constrained modulus	4.70	35 mm	Shear stress (kPa)	55.6
Consolidated total density	1255		Tan friction angle (°)	30.1
Consolidated dry density	1016		Sin friction angle (°)	

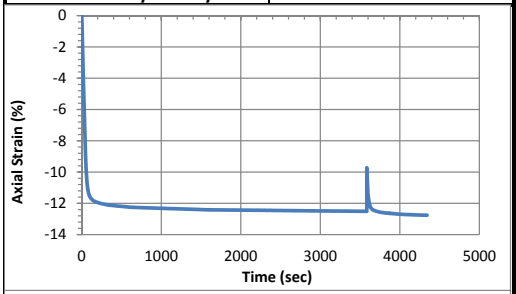

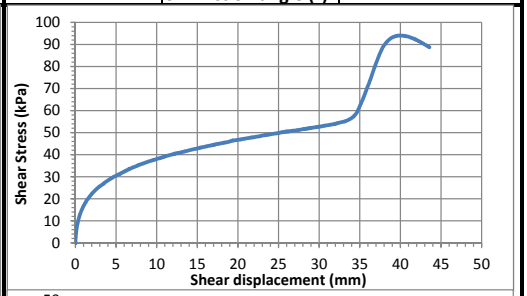

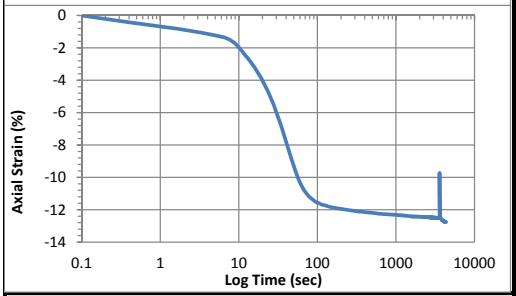

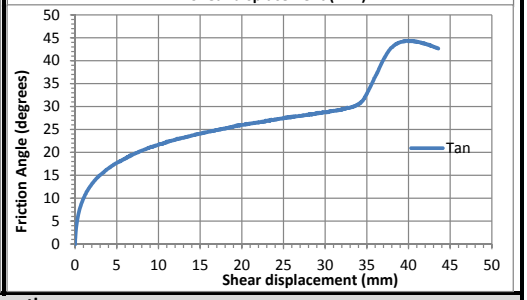

Strength			
τ/σv' at 10% strain		τ/σv0' at 10% strain	
τ/σv' at 30% strain		τ/σv0' at 30% strain	

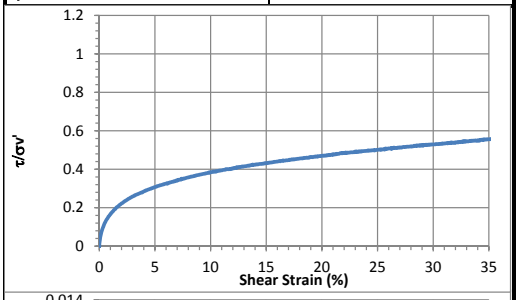

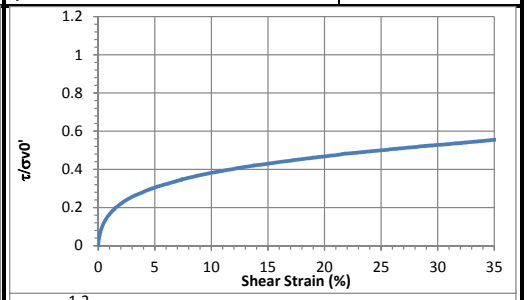

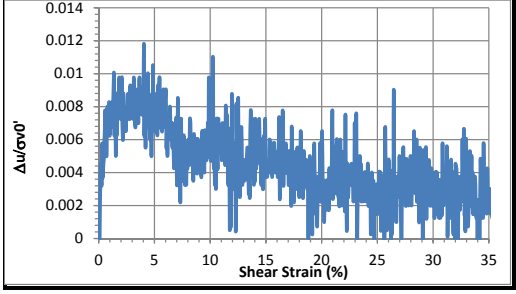

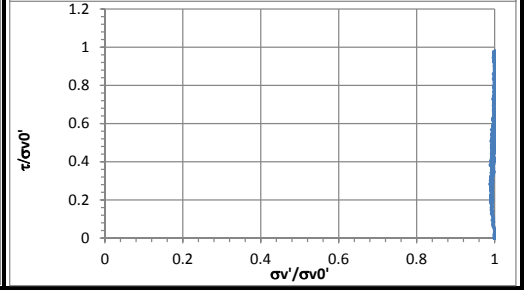

CSS Monotonic Shear Test Report

10/28/2013_Version 8.0

Geotechnical Engineering Laboratory

General Test Information		Sample Preparation	
Device:	CSS	Prepared total weight (kg):	11.952
Specimen ID:	TX-ACL	Prepared dry weight (kg):	9.124
Test ID:	TX16	Prepared height (mm):	184.9
Date of test:	6/23/2015	Prepared total density (kg/m3):	
Test performed:	Monotonic Direct Shear	Prepared dry density (kg/m3):	
Test material:	MSW	**Pre-compression Stage**	
Sample preparation:	TX-ACL fresh MSW. Direct shear. CL mode. Opening=0.2 in. Hit a rod near the end of shearing.	Pre-compressed strain (%):	51.0
		Compressed total density (kg/m3):	
		Compressed dry density (kg/m3):	
		Secondary compression ratio:	0.00184
		Total weight before shearing (kg):	11.780
		Dry weight before shearing (kg):	9.539

Consolidation Stage		Shear Stage		
Consolidated height (mm):	89.82	Type of test:		CL-direct shear
Vertical stress (kPa):	197.0	Shear strain rate (%/min):		
Immediate strain (εimm, %)	50.93	12 mm	Shear stress (kPa)	57.5
Strain before shearing (εall, %)	51.4		Tan friction angle (°)	16.4
Compression index (Cεε)	0.222		Sin friction angle (°)	
Constrained modulus	3.93	35 mm	Shear stress (kPa)	75.1
Consolidated total density	1424		Tan friction angle (°)	20.9
Consolidated dry density	1153		Sin friction angle (°)	

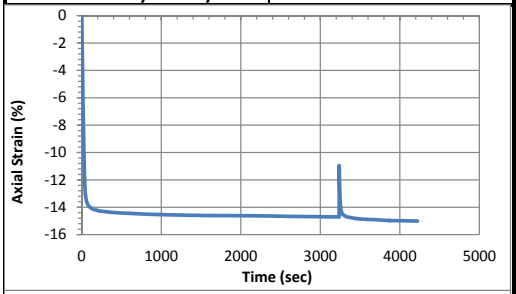

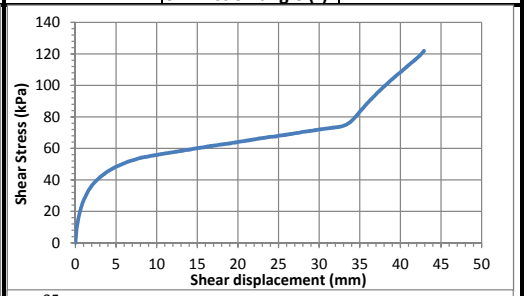

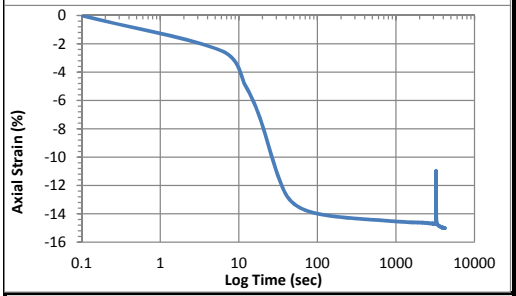

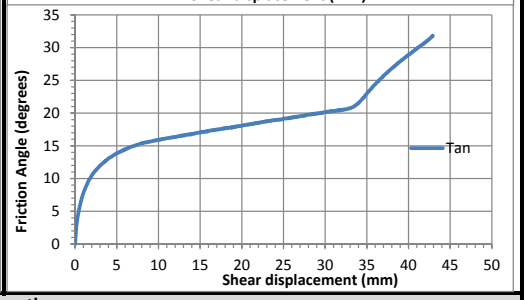

Strength

τ/σv' at 10% strain		τ/σv0' at 10% strain	
τ/σv' at 30% strain		τ/σv0' at 30% strain	

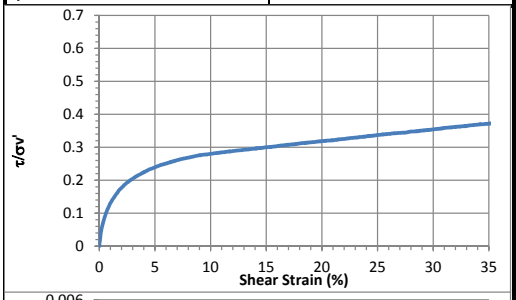

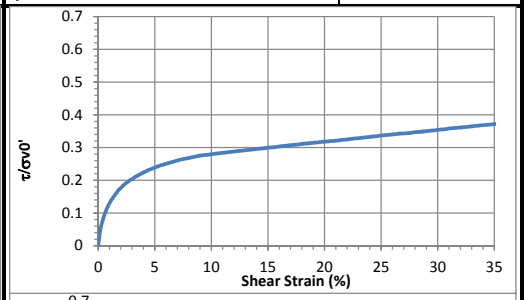

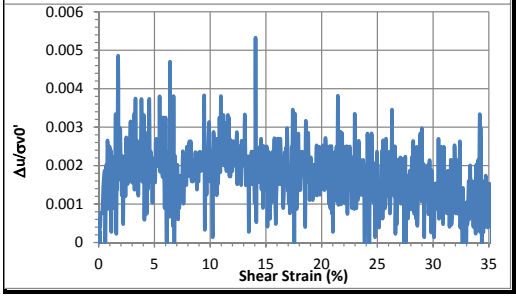

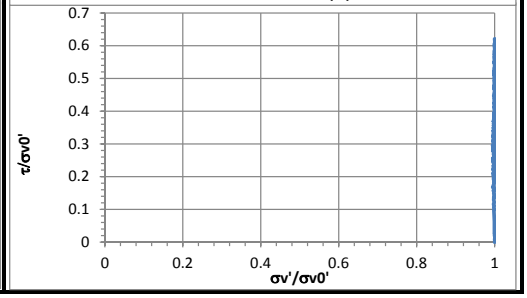

CSS Monotonic Shear Test Report

10/28/2013_Version 8.0

Geotechnical Engineering Laboratory

General Test Information		Sample Preparation	
Device:	CSS	**Prepared total weight (kg):**	13.446
Specimen ID:	TX-ACL	**Prepared dry weight (kg):**	10.264
Test ID:	TX17	**Prepared height (mm):**	201.2
Date of test:	6/25/2015	**Prepared total density (kg/m3):**	
Test performed:	Monotonic Direct Shear	**Prepared dry density (kg/m3):**	
Test material:	MSW	**Pre-compression Stage**	
Sample preparation:	TX-ACL fresh MSW. Direct shear. CL mode. Opening=0.2 in.	**Pre-compressed strain (%):**	57.4
		Compressed total density (kg/m3):	
		Compressed dry density (kg/m3):	
		Secondary compression ratio:	0.00197
		Total weight before shearing (kg):	13.180
		Dry weight before shearing (kg):	10.672

Consolidation Stage		Shear Stage		
Consolidated height (mm):	91.65	**Type of test:**		CL-direct shear
Vertical stress (kPa):	397.3	**Shear strain rate (%/min):**		
Immediate strain (εimm, %)	54.09	**12 mm**	**Shear stress (kPa)**	86.5
Strain before shearing (εall, %)	54.5		**Tan friction angle (°)**	12.3
Compression index (Cεc)	0.208		**Sin friction angle (°)**	
Constrained modulus	3.70	**35 mm**	**Shear stress (kPa)**	107.5
Consolidated total density	1568		**Tan friction angle (°)**	15.1
Consolidated dry density	1270		**Sin friction angle (°)**	

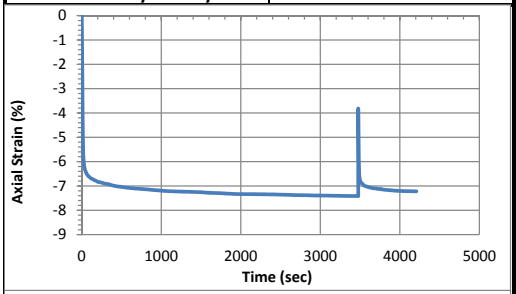

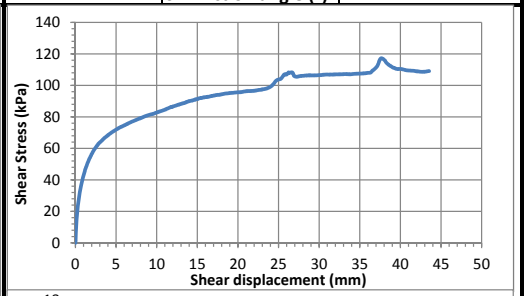

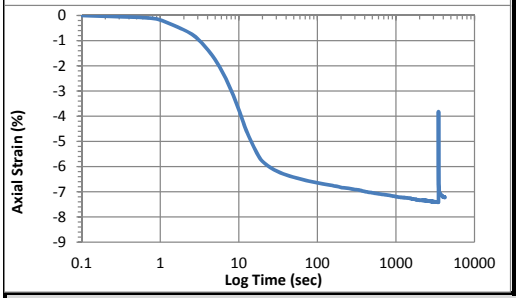

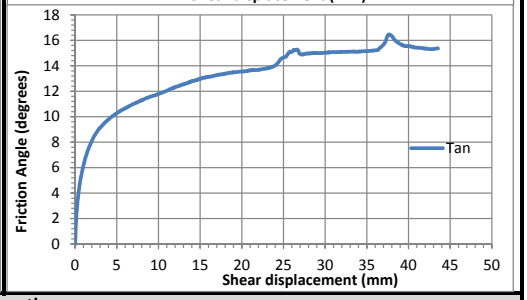

Strength

τ/σv' at 10% strain		**τ/σv0' at 10% strain**	
τ/σv' at 30% strain		**τ/σv0' at 30% strain**	

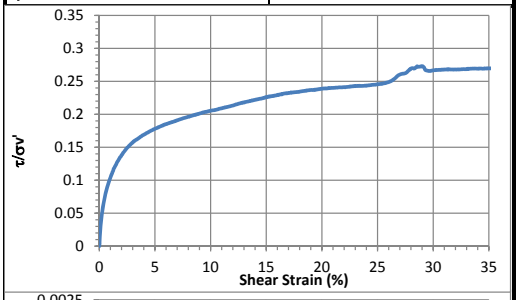

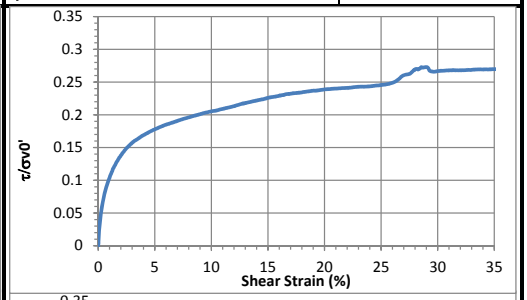

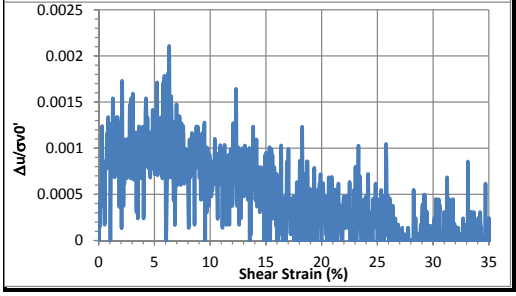

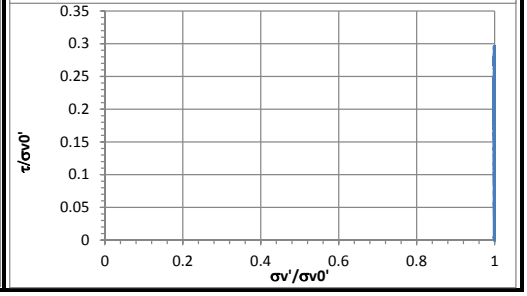

CSS Monotonic Shear Test Report

10/28/2013_Version 8.0

Geotechnical Engineering Laboratory

General Test Information	
Device:	CSS
Specimen ID:	TX-ACL
Test ID:	TX18
Date of test:	9/9/2015
Test performed:	Monotonic Shear
Test material:	MSW
Sample preparation:	TX-ACL fresh. Repeat ACL8.

Sample Preparation	
Prepared total weight (kg):	14.044
Prepared dry weight (kg):	10.720
Prepared height (mm):	235.0
Prepared total density (kg/m3):	812
Prepared dry density (kg/m3):	620
Pre-compression Stage	
Pre-compressed strain (%):	52.8
Compressed total density (kg/m3):	1721
Compressed dry density (kg/m3):	1314
Secondary compression ratio:	0.00181
Total weight before shearing (kg):	14.044
Dry weight before shearing (kg):	10.720

Consolidation Stage	
Consolidated height (mm):	111.39
Vertical stress (kPa):	397.9
Immediate strain (εimm, %)	52.26
Strain before shearing (εall, %)	52.6
Compression index (Cc ε)	0.201
Constrained modulus	3.83
Consolidated total density	1712
Consolidated dry density	1307

Shear Stage		
Type of test:		CV-strain
Shear strain rate (%/min):		0.36
10% strain	Shear stress (kPa)	101.3
	Tan friction angle (°)	22.9
	Sin friction angle (°)	25.0
peak	Shear stress (kPa)	107.4
	Tan friction angle (°)	26.6
	Sin friction angle (°)	30.1

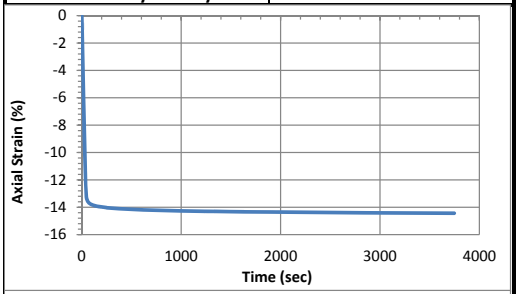

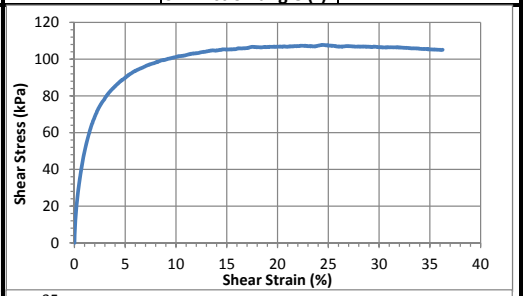

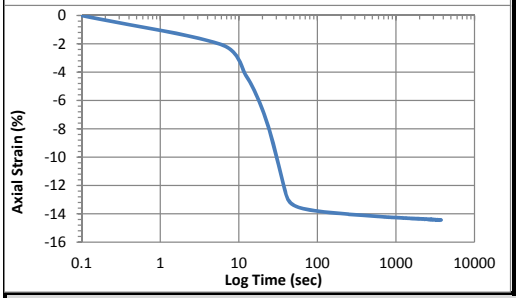

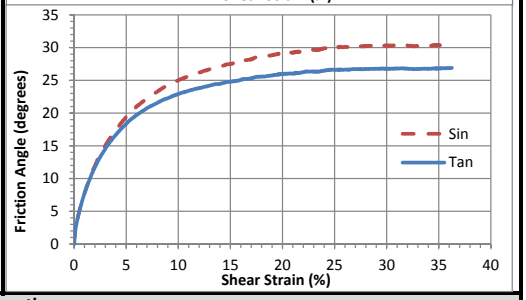

Strength

τ/σv' at 10% strain	0.42	τ/σv0' at 10% strain	0.25
τ/σv' at peak	0.50	τ/σv0' at peak	0.27

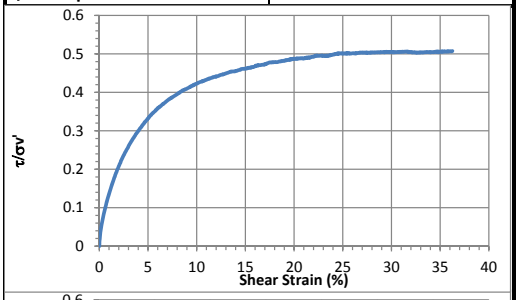

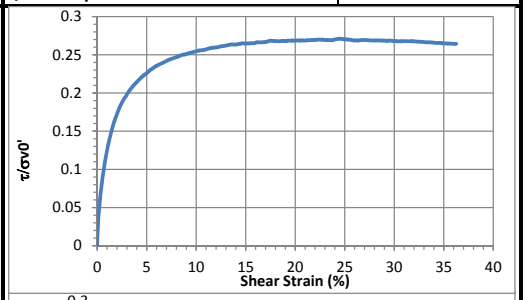

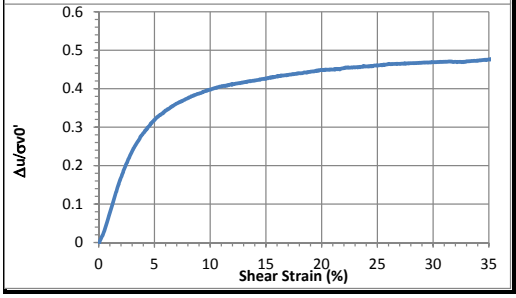

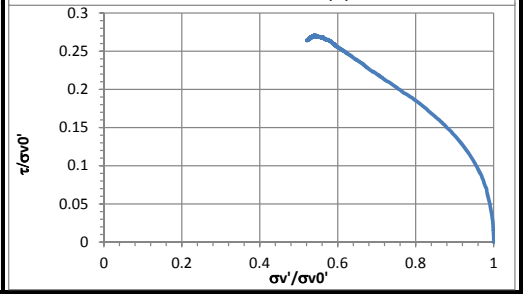

Accelerometer-Based Shear Wave Velocity Datasheet

Specimen ID: 090915-ACL18-400-X-3
Test Material: ACL18
Date: 090915
Test Performed by: Fei
Filename: 090915-ACL18-400-X-3

Vertical Stress: 400kPa
Sensor Spacing: 0.1114 m
V_s(rise) = 214 m/s

Data Record

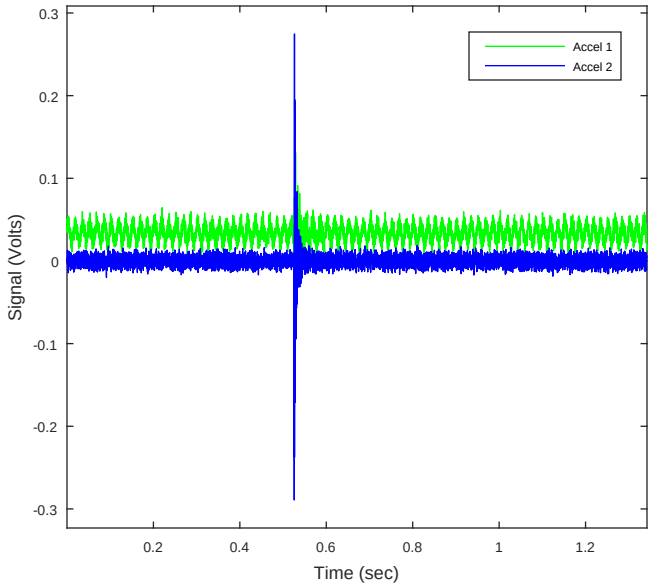

FFT of Accel 1

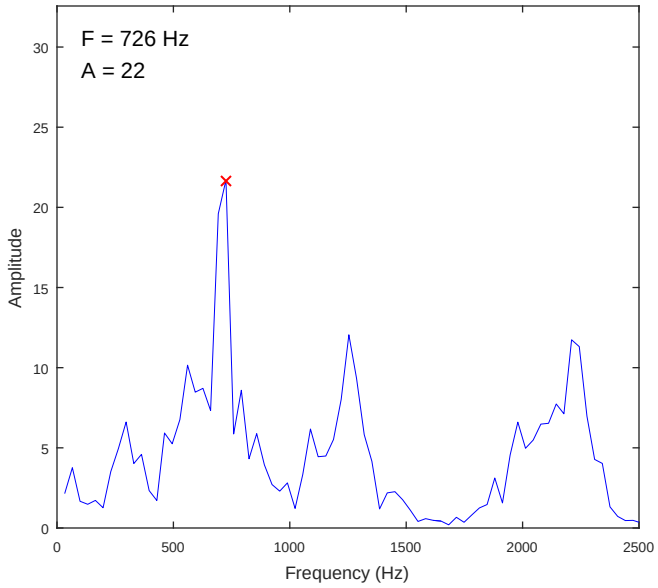

FFT of Accel 2

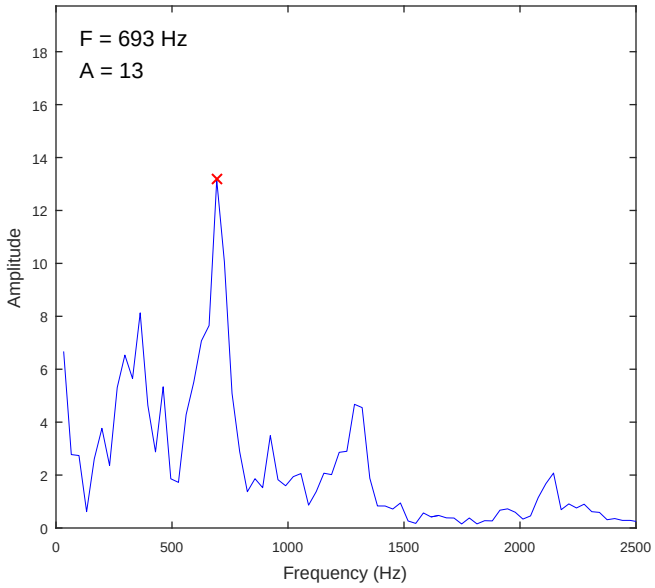

Travel Time Selection - View 1

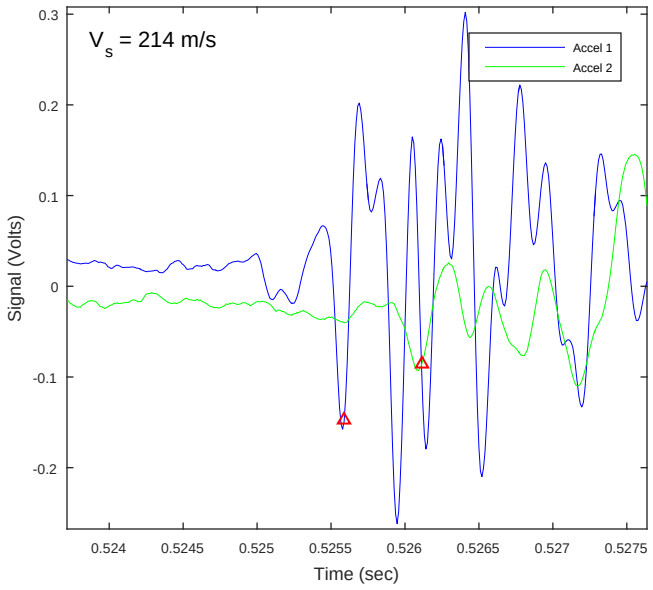

Travel Time Selection - View 2

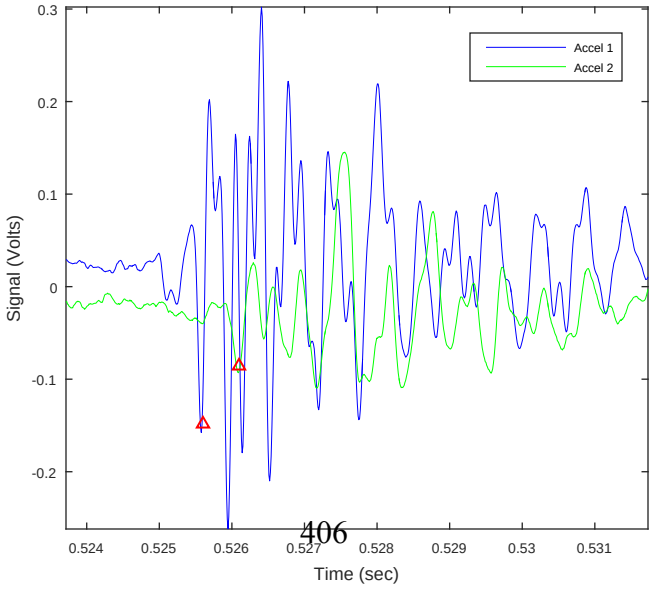

Travel Time Selection - View 3

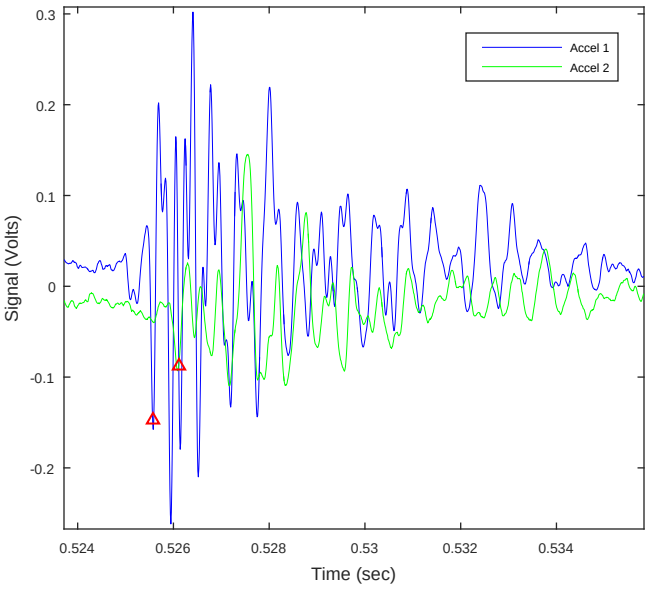

CSS Monotonic Shear Test Report

10/28/2013_Version 8.0

Geotechnical Engineering Laboratory

General Test Information and Sample Preparation

Device:	CSS	**Layers prior to shear**	6.81
Specimen ID:	TX-ACLD	**Weight/layer (kg):**	2.27
Test ID:	TXD1	**Height/layer (mm):**	25.4
Date of Test:	3/4/2015	**As-prepared height (mm):**	196.6
Test Performed:	Monotonic Shear	**Soil-only specimen diameter (mm):**	306.2
Test Material:	MSW	**Total weight (kg):**	13.0
Sample Preparation:	Bottom undisturbed specimen from #2. Removed 2112 g before consolidation. ΔWw=2627 g, assume 95% drained during pre-compression.	**As-prepared density (kg/m^3):**	1215
		Membrane thickness (mm):	0.000635
		Moisture content (%):	47.5
		Saturated (Y/N):	N
		Prepared by:	Fei

Pre-compression Stage

Pre-compressed strain (%):	30.1	**Secondary compression ratio:**	0.03344
Pre-compressed height (mm):	137.4	**Pre-compressed density (kg/m3):**	1492

Consolidation Stage

Initial height (mm):	137.7
Initial density (kg/m3):	1280
Vertical Stress (kPa):	99.6
Immediate strain (εimm, %)	30.1
Strain before shear (εall, %)	31.5
Compression index (Cεε)	0.151
Constrained modulus	6.6
Consolidated density (kg/m^3):	1507

Shear Stage

Type of test:		CL-strain
Shear strain rate (%/min):		0.34
10% strain	**Shear stress (kPa)**	27.1
	Tan friction angle (°)	15.3
	Sin friction angle (°)	15.9
30% strain	**Shear stress (kPa)**	30.0
	Tan friction angle (°)	16.9
	Sin friction angle (°)	17.6

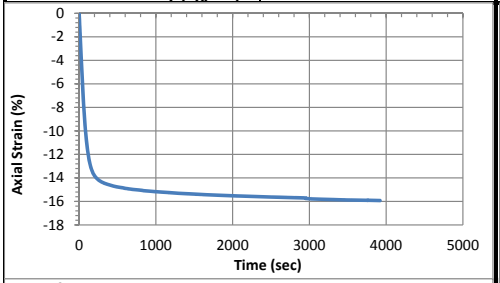

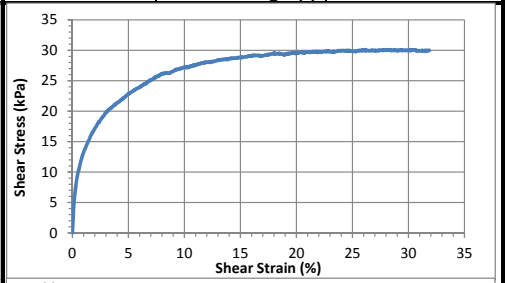

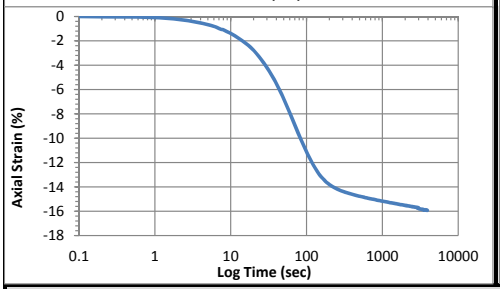

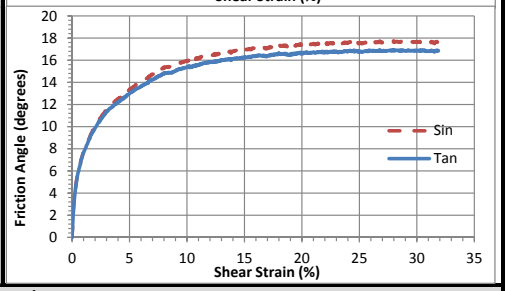

Strength

τ/σv' at 10% strain	0.28	**τ/σv0' at 10% strain**	0.28
τ/σv' at 30% strain	0.30	**τ/σv0' at 30% strain**	0.30

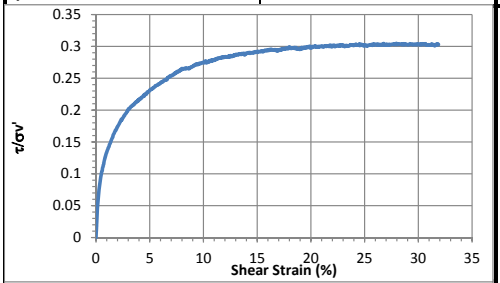

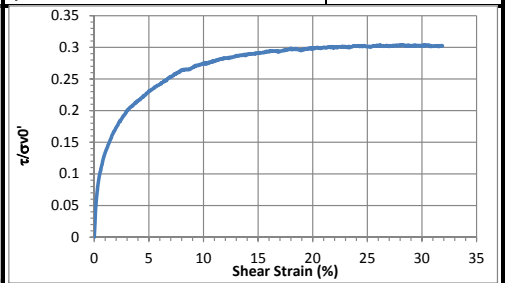

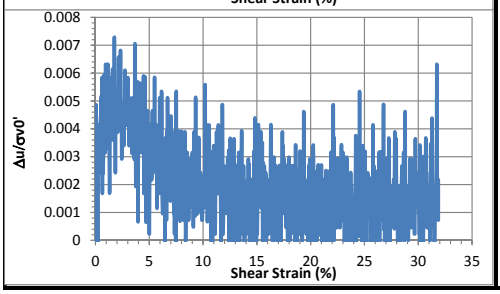

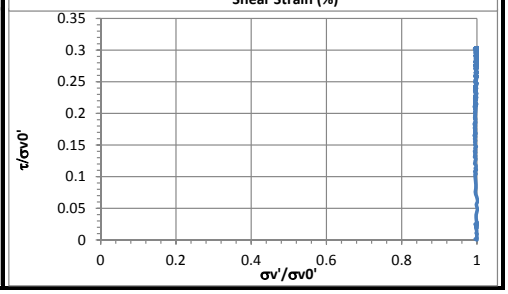

CSS Monotonic Shear Test Report

10/28/2013_Version 8.0

Geotechnical Engineering Laboratory

General Test Information	
Device:	CSS
Specimen ID:	TX-ACLD
Test ID:	TXD2
Date of test:	3/6/2015
Test performed:	Monotonic Shear
Test material:	MSW
Sample preparation:	Top undisturbed specimen from #2. Removed 2680 g before consolidation. ΔWw=2256 g, assume 95% drained during pre-compression. Vs=176 m/s using accelerometer

Sample Preparation	
Prepared layers:	8.68
Weight/layer (kg):	2.07
Prepared height (mm):	220.48
Prepared density (kg/m3):	1108
Moisture content (%):	45.7
Pre-compression Stage	
Pre-compressed height (mm):	137.6
Pre-compressed strain (%):	37.6
Pre-compressed density (kg/m3):	1565
Secondary compression ratio:	0.03802
Total weight before shearing (kg):	13.18

Consolidation Stage	
Initial height (mm):	137.7
Initial density (kg/m3):	1299
Vertical stress (kPa):	199.7
Immediate strain (εimm, %)	39.0
Strain before shearing (εall, %)	40.8
Compression index (Cc ε)	0.170
Constrained modulus	5.1
Consolidated density (kg/m^3):	1636

Shear Stage		
Type of test:		CL-strain
Shear strain rate (%/min):		0.37
10% strain	Shear stress (kPa)	40.8
	Tan friction angle (°)	11.6
	Sin friction angle (°)	11.8
30% strain	Shear stress (kPa)	39.6
	Tan friction angle (°)	11.2
	Sin friction angle (°)	11.5

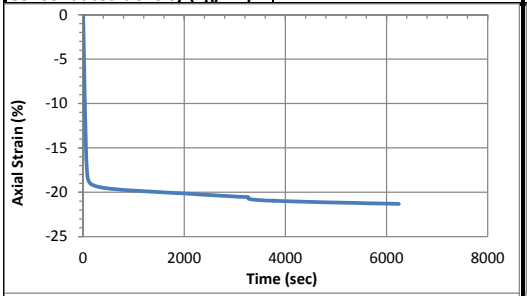

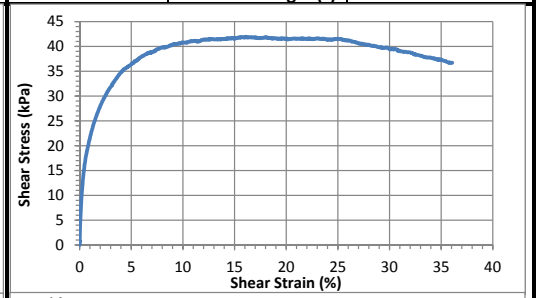

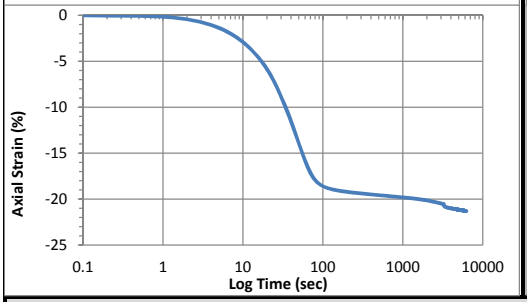

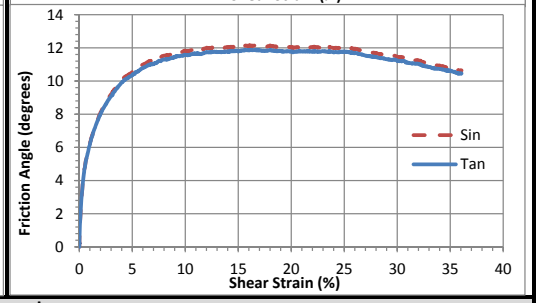

Strength			
τ/σv' at 10% strain	0.20	τ/σv0' at 10% strain	0.20
τ/σv' at 30% strain	0.20	τ/σv0' at 30% strain	0.20

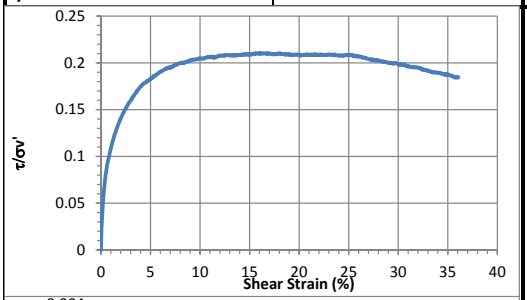

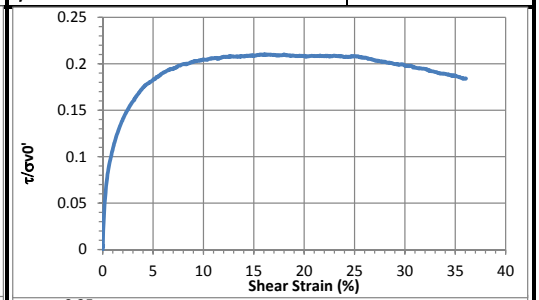

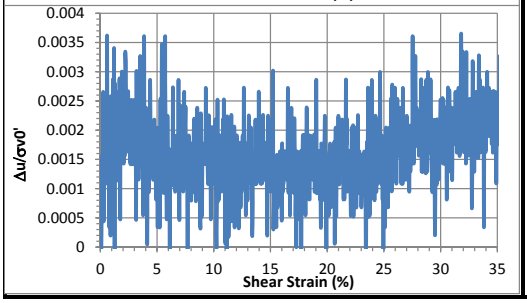

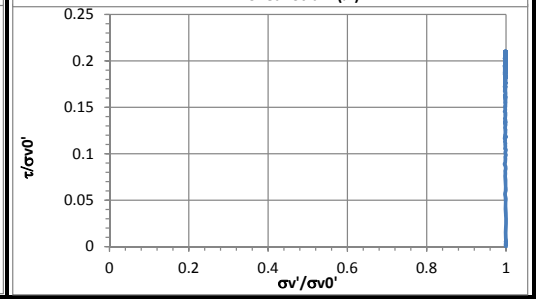

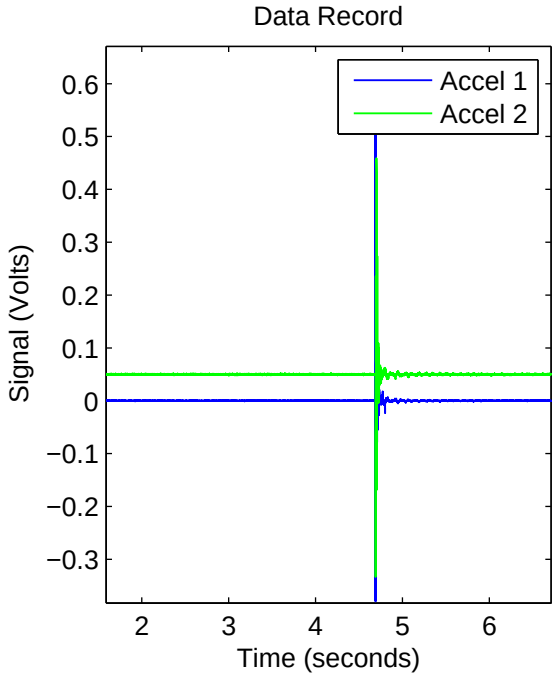
Data Record
Accel 1
Accel 2
Signal (Volts)
Time (seconds)

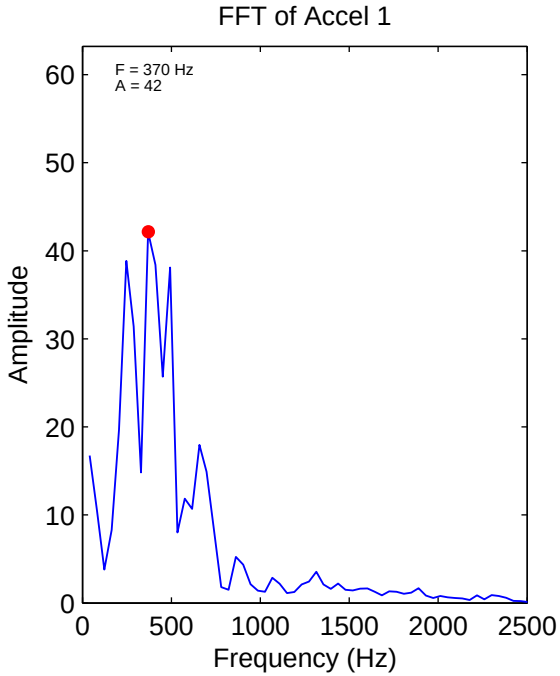
FFT of Accel 1
F = 370 Hz
A = 42
Amplitude
Frequency (Hz)

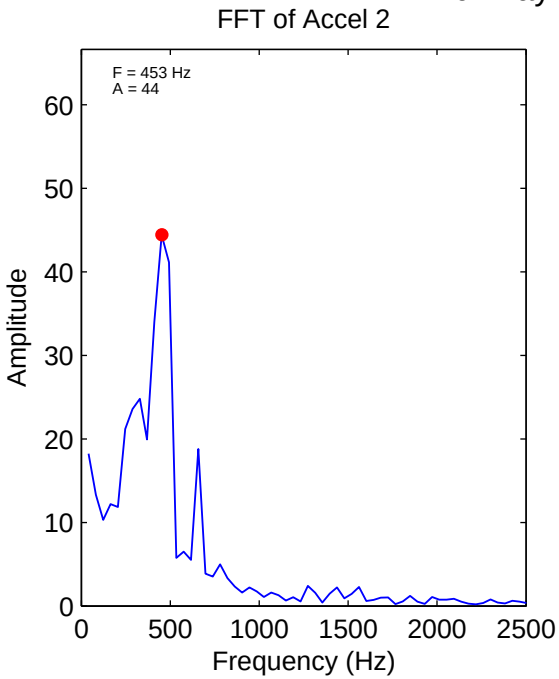
FFT of Accel 2
F = 453 Hz
A = 44
Amplitude
Frequency (Hz)

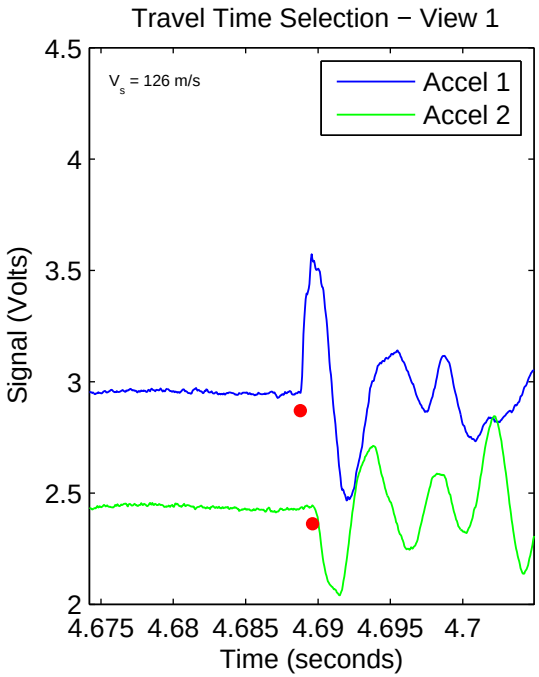
Travel Time Selection − View 1
V_s = 126 m/s
Accel 1
Accel 2
Signal (Volts)
Time (seconds)

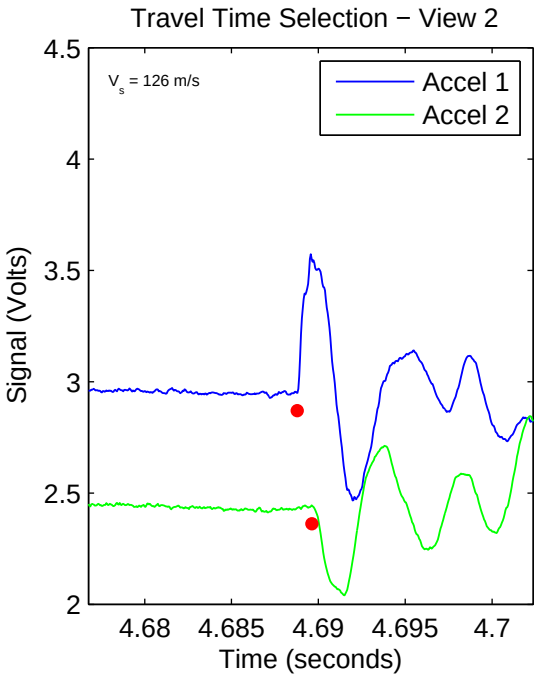
Travel Time Selection − View 2
V_s = 126 m/s
Accel 1
Accel 2
Signal (Volts)
Time (seconds)

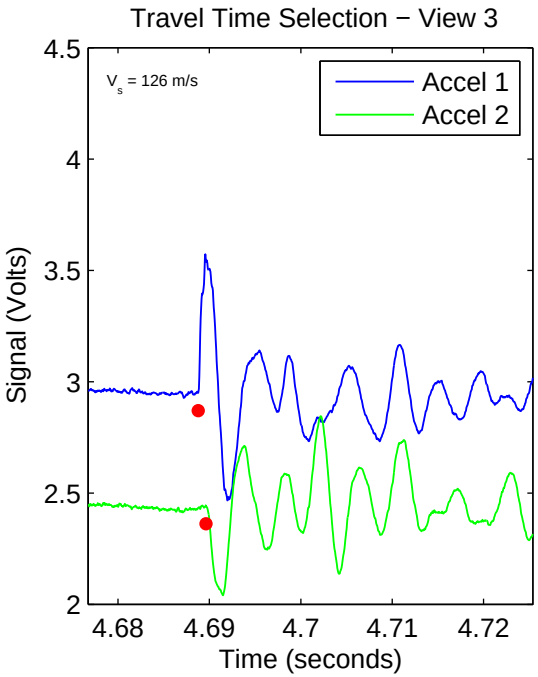
Travel Time Selection − View 3
V_s = 126 m/s
Accel 1
Accel 2
Signal (Volts)
Time (seconds)

CSS Monotonic Shear Test Report

10/28/2013_Version 8.0

Geotechnical Engineering Laboratory

General Test Information	
Device:	CSS
Specimen ID:	TX-ACLD
Test ID:	TXD3
Date of test:	3/11/2015
Test performed:	Monotonic Shear
Test material:	MSW
Sample preparation:	Reconstituted specimen with similar pre-compressed density as ACLD1.

Sample Preparation	
Prepared layers:	6.50
Weight/layer (kg):	1.953
Prepared height (mm):	181.61
Prepared density (kg/m3):	949
Moisture content (%):	47.5
Pre-compression Stage	
Pre-compressed height (mm):	106.2
Pre-compressed strain (%):	41.5
Pre-compressed density (kg/m3):	1566
Secondary compression ratio:	0.01093
Total weight before shearing (kg):	12.25

Consolidation Stage	
Initial height (mm):	115.1
Initial density (kg/m3):	1446
Vertical stress (kPa):	96.8
Immediate strain (εimm, %)	41.4
Strain before shearing (εall, %)	41.9
Compression index (Cc ε)	0.209
Constrained modulus	4.8
Consolidated density (kg/m^3):	1577

Shear Stage		
Type of test:		CV-strain
Shear strain rate (%/min):		0.38
10% strain	Shear stress (kPa)	29.1
	Tan friction angle (°)	24.0
	Sin friction angle (°)	26.5
30% strain	Shear stress (kPa)	25.2
	Tan friction angle (°)	24.7
	Sin friction angle (°)	27.5

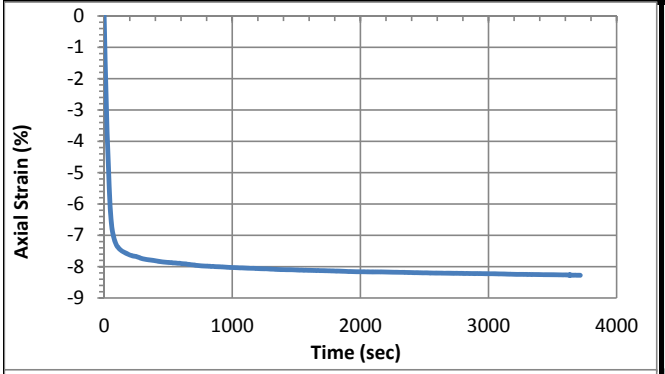

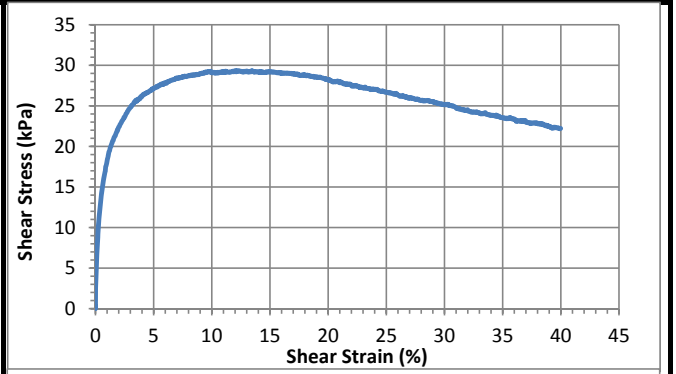

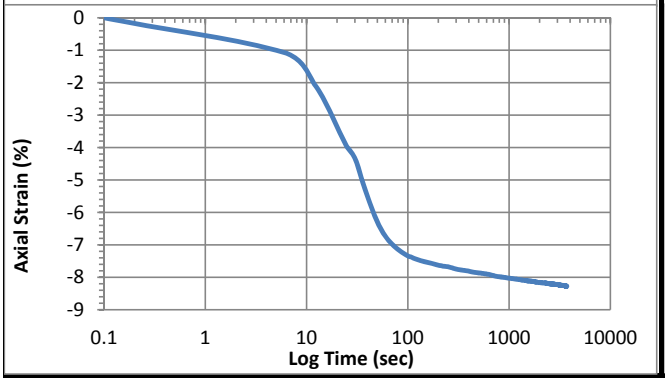

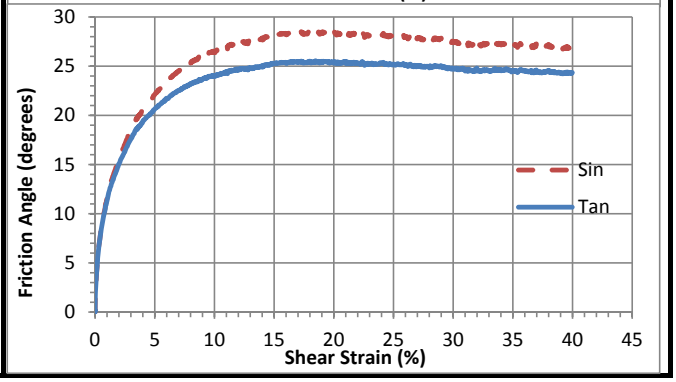

Strength			
τ/σv' at 10% strain	0.45	τ/σv0' at 10% strain	0.29
τ/σv' at 30% strain	0.46	τ/σv0' at 30% strain	0.25

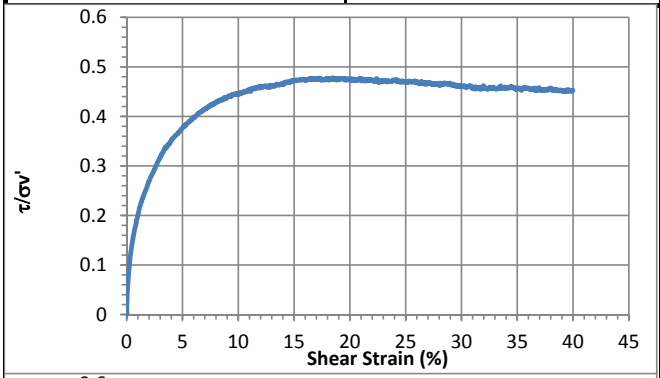

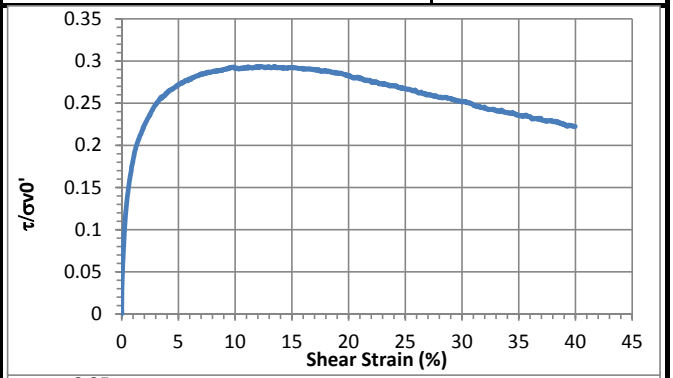

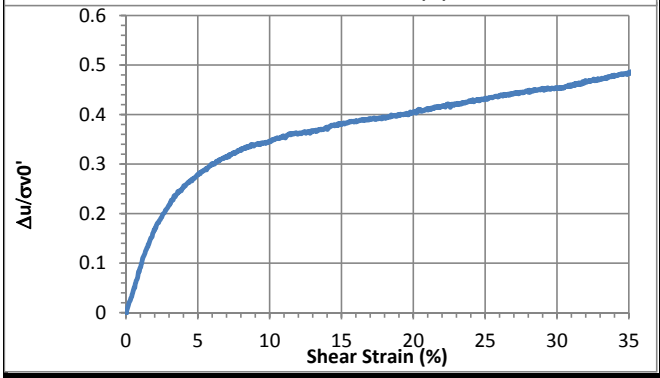

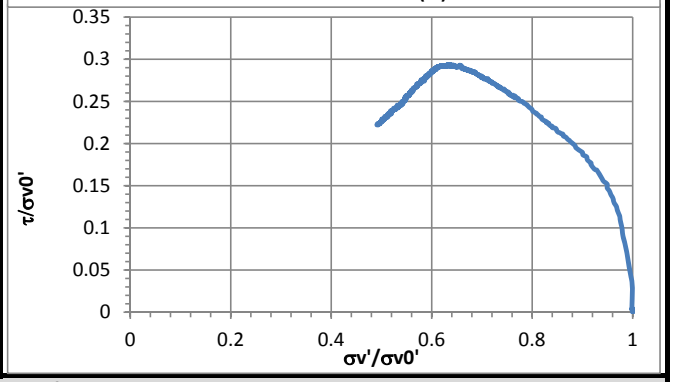

Shear wave velocity				
Signal type	Mallet low frequency	First rise	initiation time (s)	1.4039
Signal amplitude (Vpp)			arrival time (s)	1.4051
Signal frequency (kHz)			Vs (m/s)	90
Sensor spacing (mm)	105.59	First peak	initiation time (s)	1.4059
R+P average Vs (m/s)	87		arrival time (s)	1.4059
Stdev. (m/s)	4		Vs (m/s)	84
P+V average Vs (m/s)	86	First valley	initiation time (s)	1.4068
Stdev. (m/s)	3		arrival time (s)	1.4080
Wavelength (m)			Vs (m/s)	88
Spacing/wavelength				

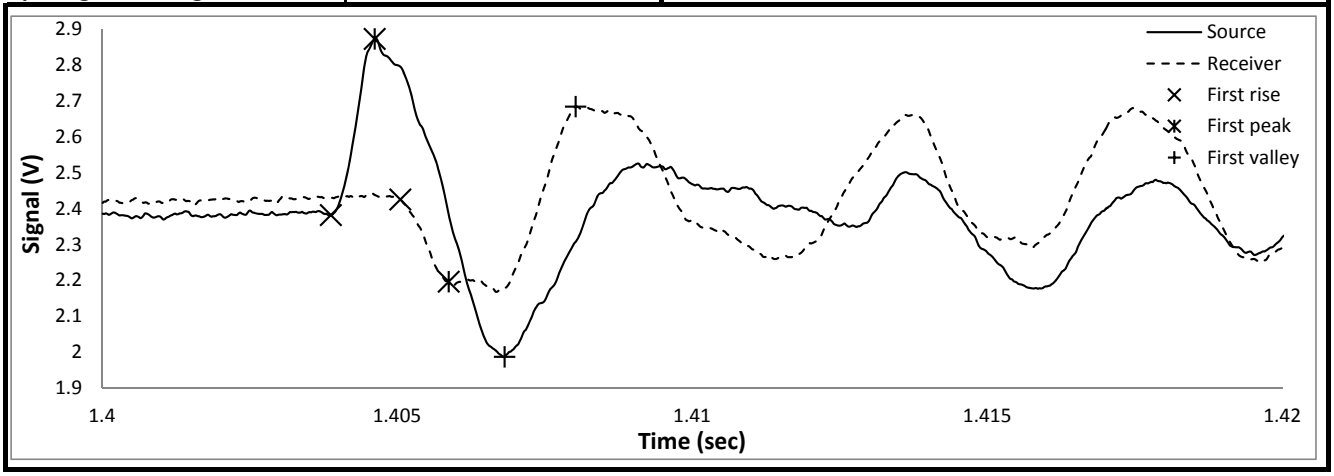

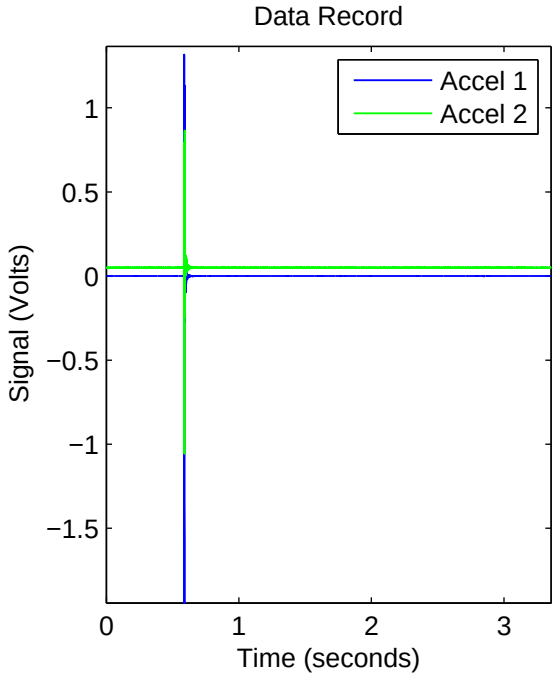
Data Record
Accel 1
Accel 2
Signal (Volts)
Time (seconds)

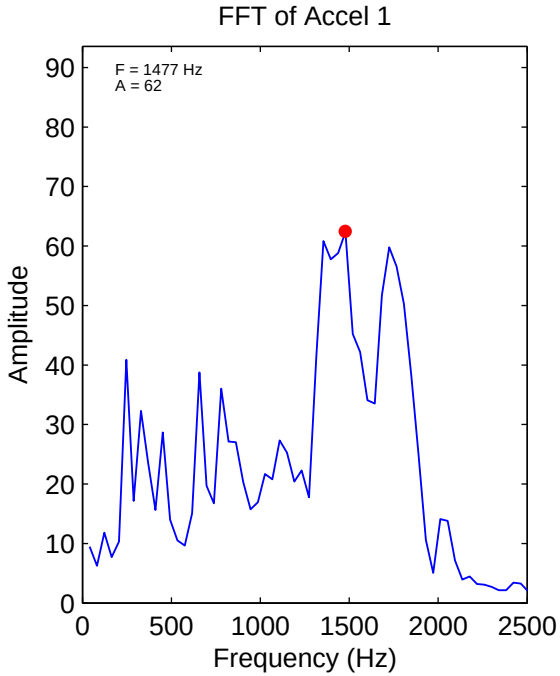
FFT of Accel 1
F = 1477 Hz
A = 62
Amplitude
Frequency (Hz)

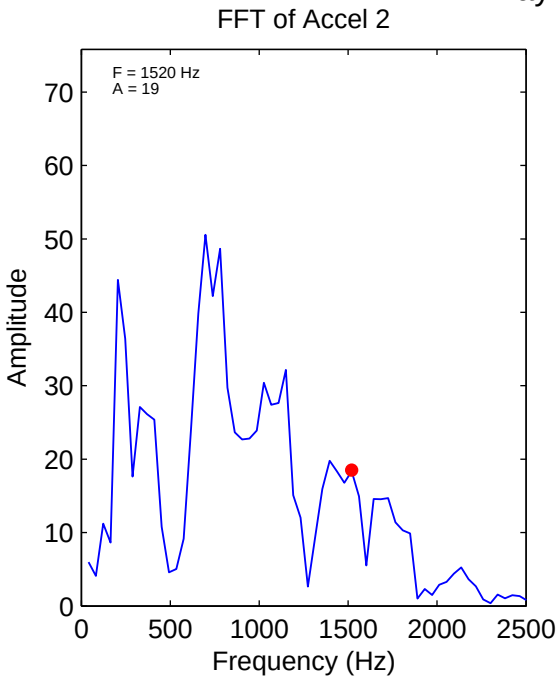
FFT of Accel 2
F = 1520 Hz
A = 19
Amplitude
Frequency (Hz)

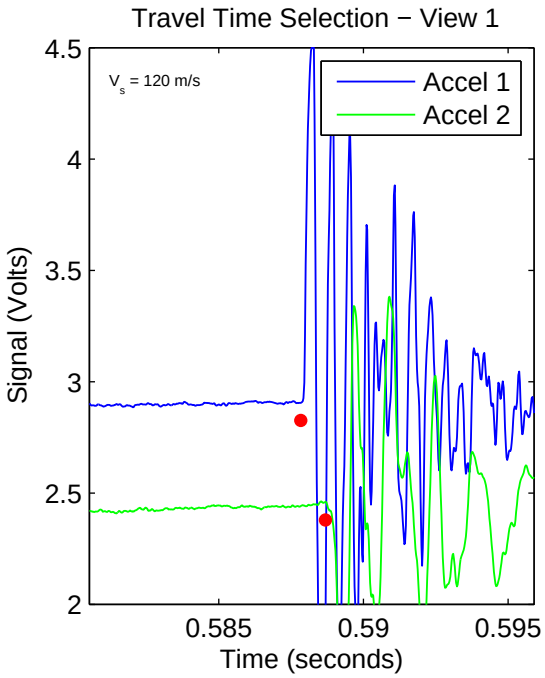
Travel Time Selection − View 1
V_s = 120 m/s
Accel 1
Accel 2
Signal (Volts)
Time (seconds)

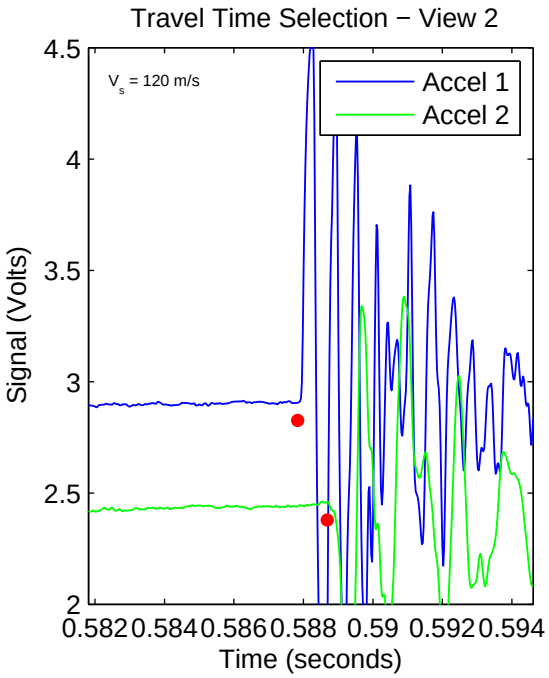
Travel Time Selection − View 2
V_s = 120 m/s
Accel 1
Accel 2
Signal (Volts)
Time (seconds)

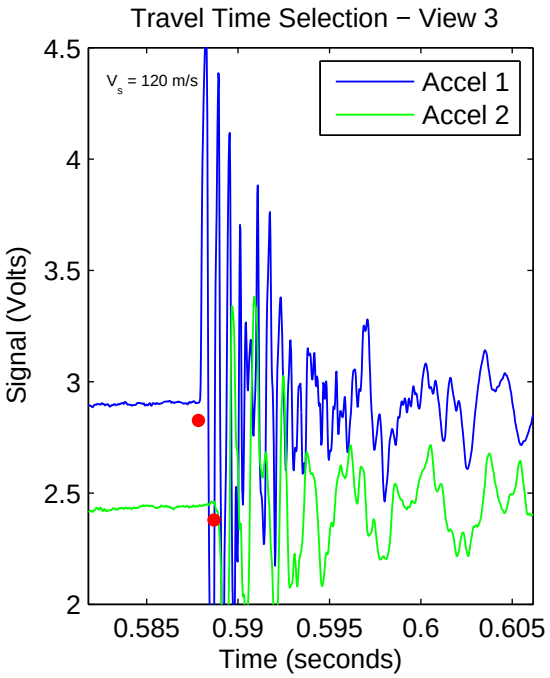
Travel Time Selection − View 3
V_s = 120 m/s
Accel 1
Accel 2
Signal (Volts)
Time (seconds)

CSS Monotonic Shear Test Report

10/28/2013_Version 8.0

Geotechnical Engineering Laboratory

General Test Information	
Device:	CSS
Specimen ID:	TX-ACLD
Test ID:	TXD4
Date of test:	3/25/2015
Test performed:	Monotonic Shear
Test material:	MSW
Sample preparation:	Reconstituted specimen with similar pre-compressed density and wc as ACLD1.

Sample Preparation	
Prepared layers:	6.50
Weight/layer (kg):	2.27
Prepared height (mm):	173.01
Prepared density (kg/m3):	1158
Moisture content (%):	47.5
Pre-compression Stage	
Pre-compressed height (mm):	109.6
Pre-compressed strain (%):	36.6
Pre-compressed density (kg/m3):	1554
Secondary compression ratio:	0.03194
Total weight before shearing (kg):	12.54

Consolidation Stage	
Initial height (mm):	122.8
Initial density (kg/m3):	1387
Vertical stress (kPa):	96.9
Immediate strain (εimm, %)	36.2
Strain before shearing (εall, %)	36.3
Compression index (Cc ε)	0.182
Constrained modulus	5.5
Consolidated density (kg/m^3):	1546

Shear Stage		
Type of test:		CL-strain
Shear strain rate (%/min):		0.36
10% strain	Shear stress (kPa)	29.2
	Tan friction angle (°)	16.9
	Sin friction angle (°)	17.6
30% strain	Shear stress (kPa)	31.9
	Tan friction angle (°)	18.3
	Sin friction angle (°)	19.3

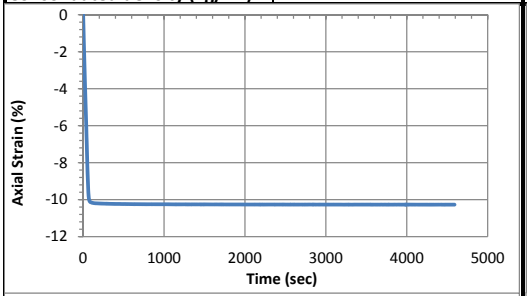

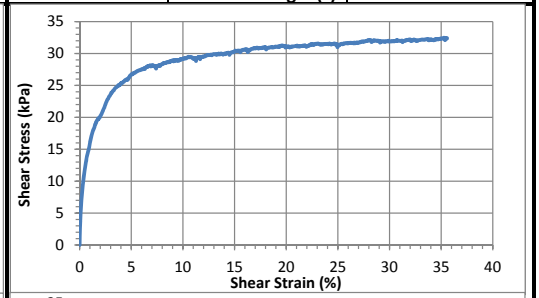

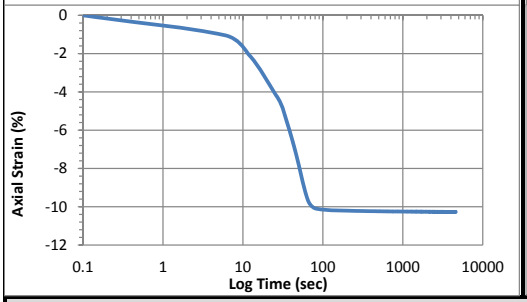

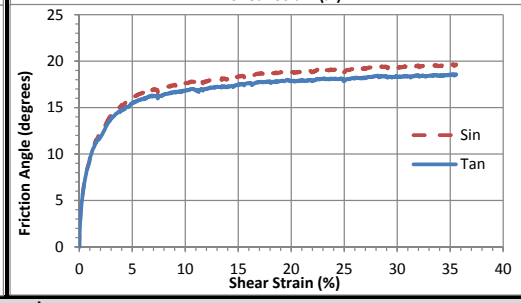

Strength			
τ/σv' at 10% strain	0.30	τ/σv0' at 10% strain	0.30
τ/σv' at 30% strain	0.33	τ/σv0' at 30% strain	0.33

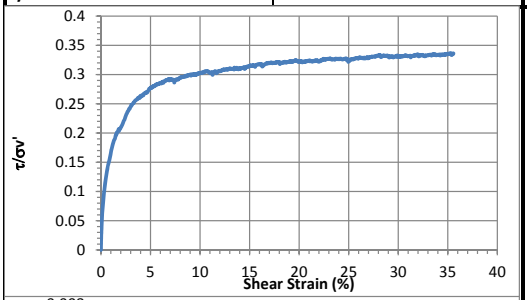

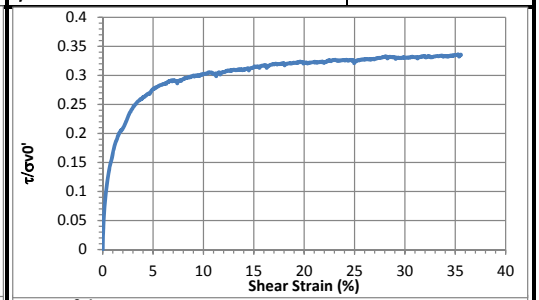

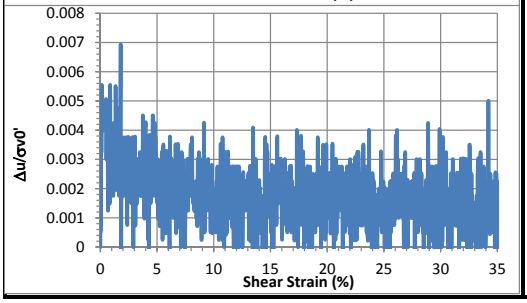

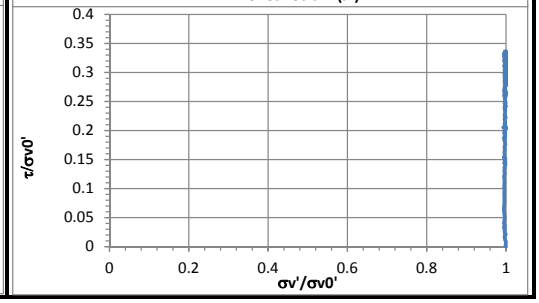

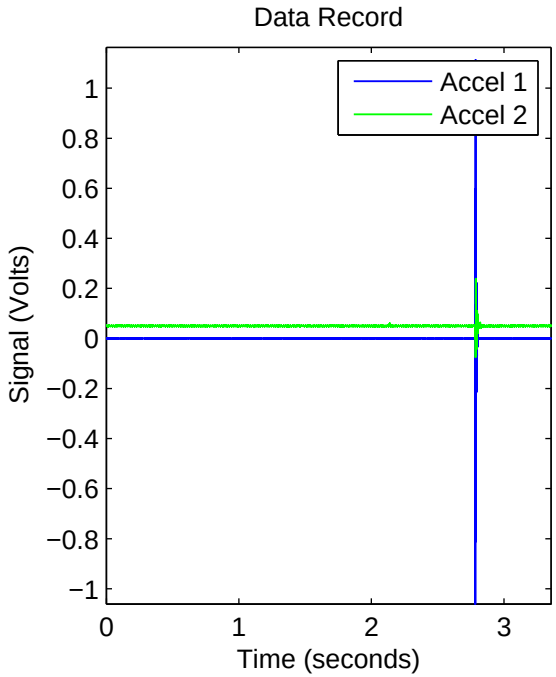
Data Record
Accel 1
Accel 2
Signal (Volts)
Time (seconds)

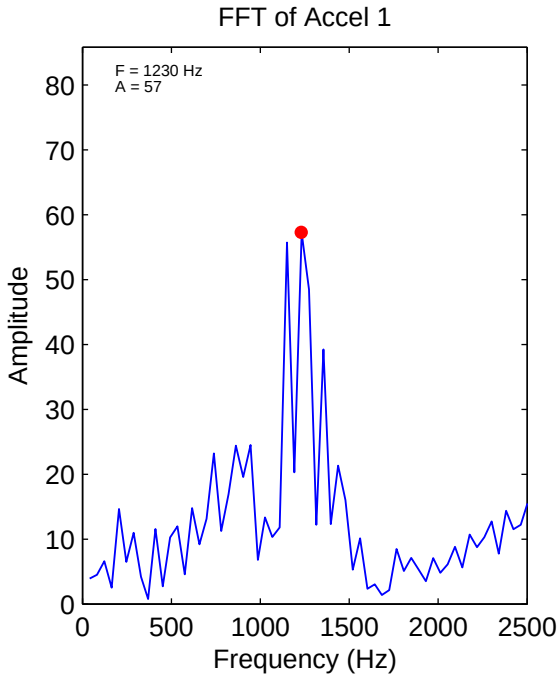
FFT of Accel 1
F = 1230 Hz
A = 57
Amplitude
Frequency (Hz)

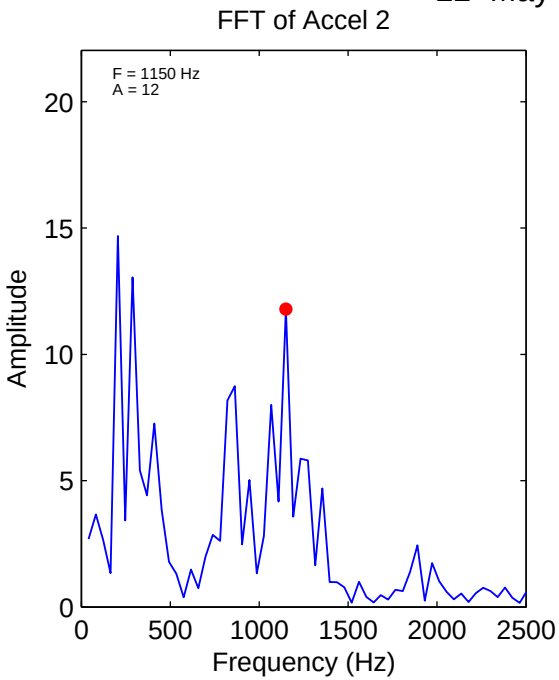
FFT of Accel 2
F = 1150 Hz
A = 12
Amplitude
Frequency (Hz)

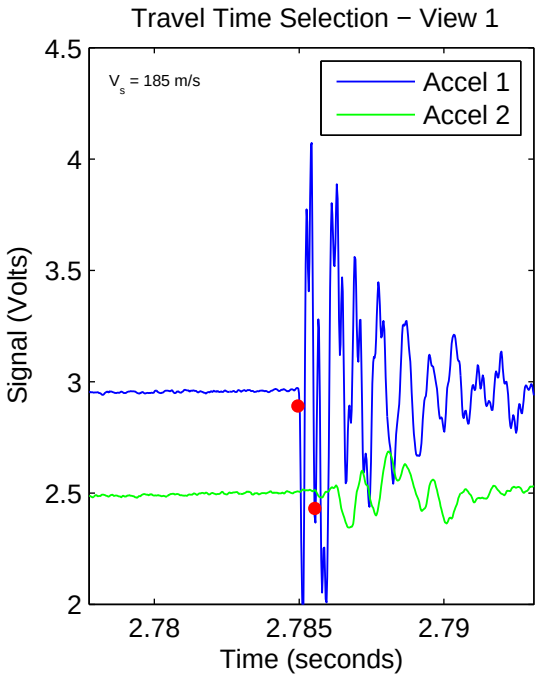
Travel Time Selection − View 1
V_s = 185 m/s
Accel 1
Accel 2
Signal (Volts)
Time (seconds)

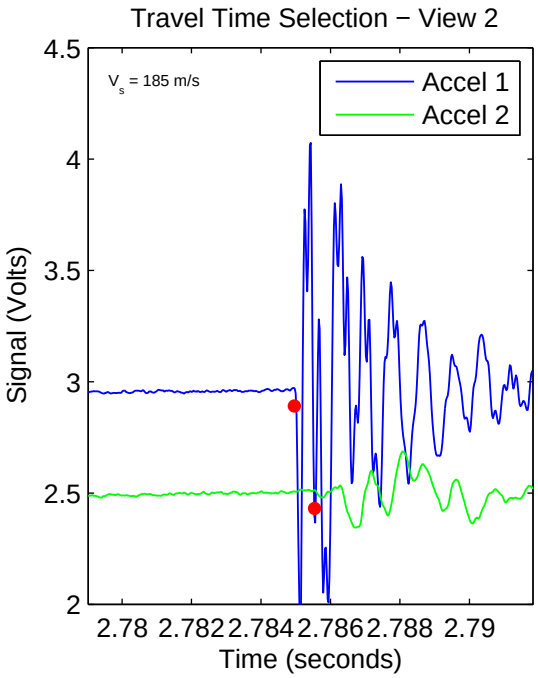
Travel Time Selection − View 2
V_s = 185 m/s
Accel 1
Accel 2
Signal (Volts)
Time (seconds)

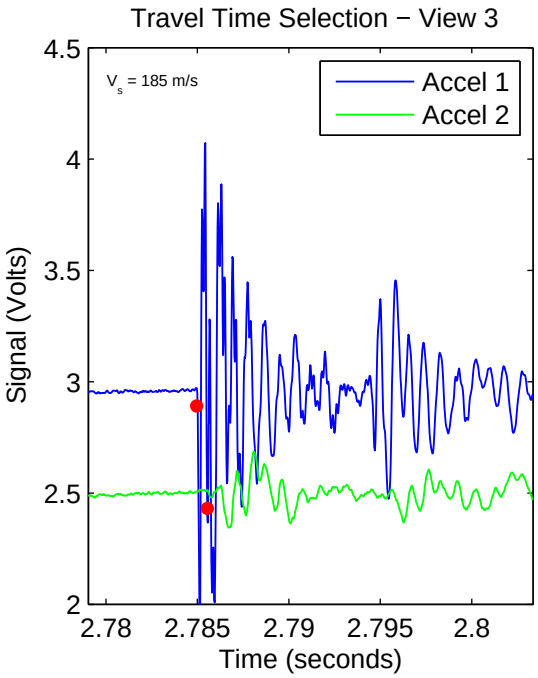
Travel Time Selection − View 3
V_s = 185 m/s
Accel 1
Accel 2
Signal (Volts)
Time (seconds)

CSS Monotonic Shear Test Report

10/28/2013_Version 8.0

Geotechnical Engineering Laboratory

General Test Information		Sample Preparation	
Device:	CSS	Moisture content (%):	47.5
Specimen ID:	TX-ACLD	Prepared total weight (kg):	12.220
Test ID:	TXD5	Prepared height (mm):	181.6
Date of test:	3/27/2015	Prepared total density (kg/m3):	914
Test performed:	Monotonic Shear	Prepared dry density (kg/m3):	619
Test material:	MSW	**Pre-compression Stage**	
Sample preparation:	Reconstituted specimen with similar pre-compressed density as ACLD1.	Pre-compressed strain (%):	44.7
		Compressed total density (kg/m3):	1584
		Compressed dry density (kg/m3):	1652
		Secondary compression ratio:	0.01295
		Total weight before shearing (kg):	12.655
		Dry weight before shearing (kg):	8.922

Consolidation Stage		Shear Stage		
Consolidated height (mm):	107.40	Type of test:		CL-strain
Vertical stress (kPa):	96.1	Shear strain rate (%/min):		0.37
Immediate strain (εimm, %)	44.2	10% strain	Shear stress (kPa)	30.4
Strain before shearing (εall, %)	44.7		Tan friction angle (°)	17.6
Compression index (Cc ε)	0.223		Sin friction angle (°)	18.5
Constrained modulus	4.52	30% strain	Shear stress (kPa)	33.1
Consolidated total density	1600		Tan friction angle (°)	19.1
Consolidated dry density	1128		Sin friction angle (°)	20.2

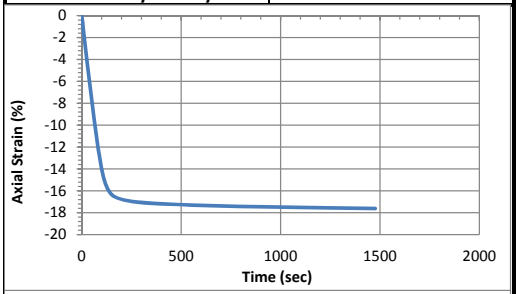

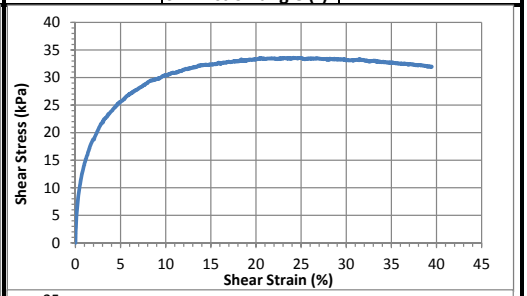

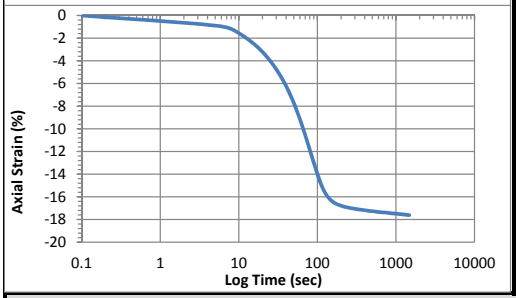

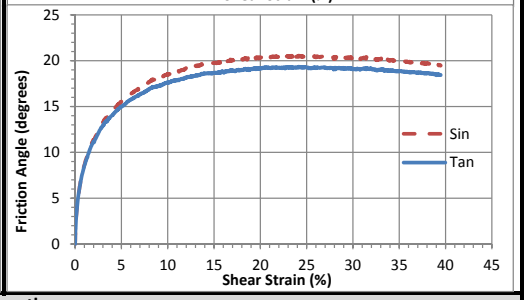

Strength			
τ/σv' at 10% strain	0.32	τ/σv0' at 10% strain	0.32
τ/σv' at 30% strain	0.35	τ/σv0' at 30% strain	0.35

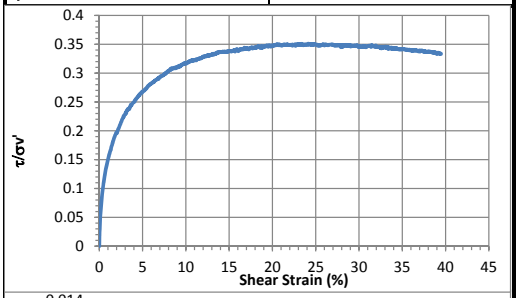

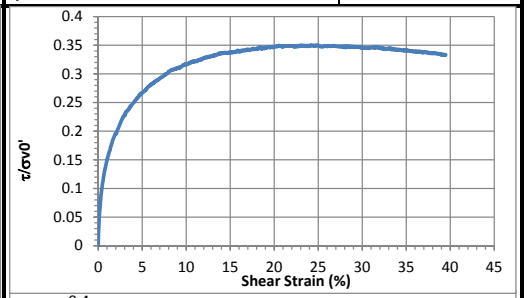

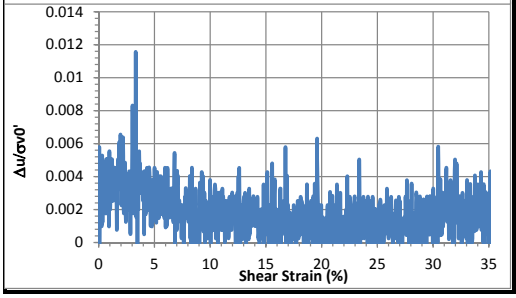

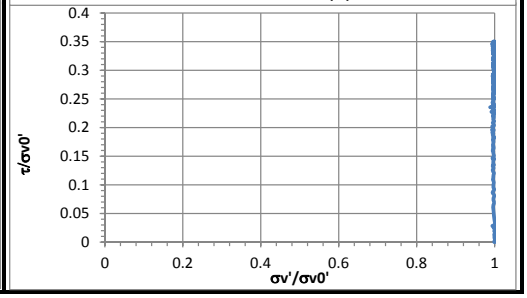

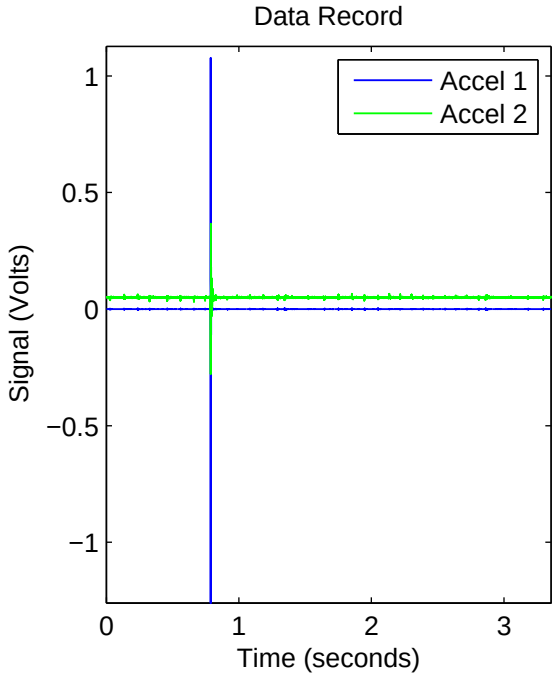
Data Record
Accel 1
Accel 2
Signal (Volts)
Time (seconds)

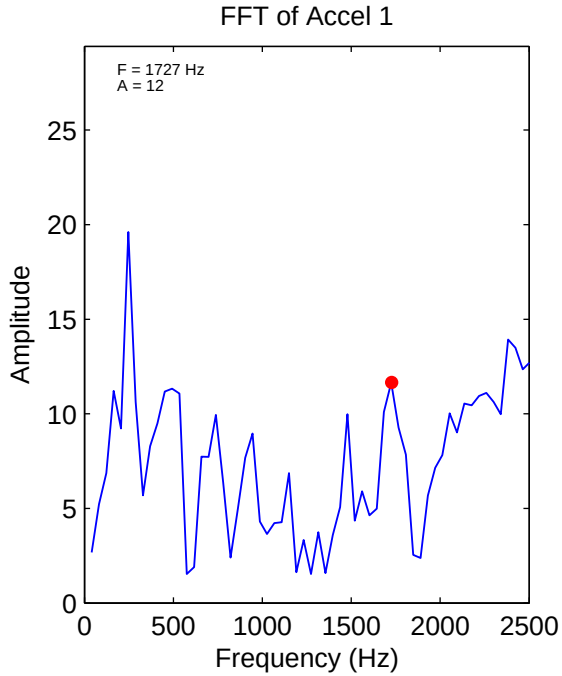
FFT of Accel 1
F = 1727 Hz
A = 12
Amplitude
Frequency (Hz)

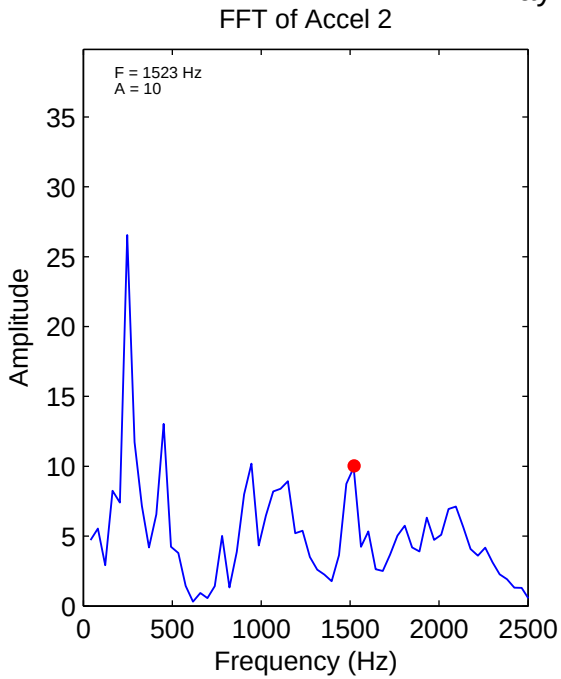
FFT of Accel 2
F = 1523 Hz
A = 10
Amplitude
Frequency (Hz)

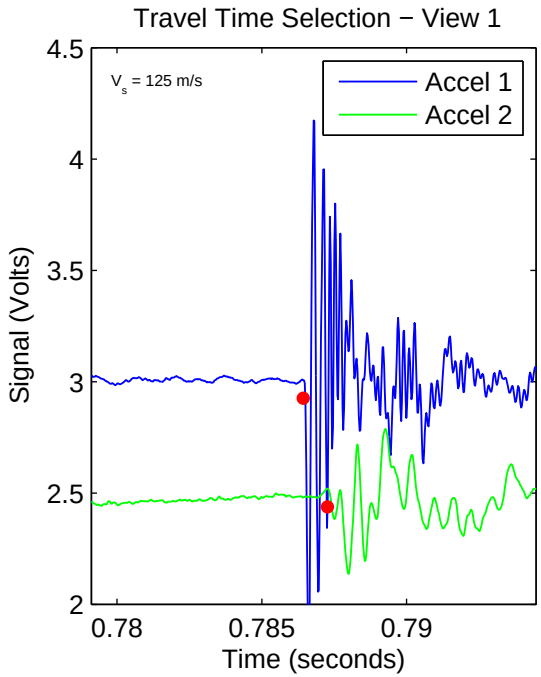
Travel Time Selection − View 1
V_s = 125 m/s
Accel 1
Accel 2
Signal (Volts)
Time (seconds)

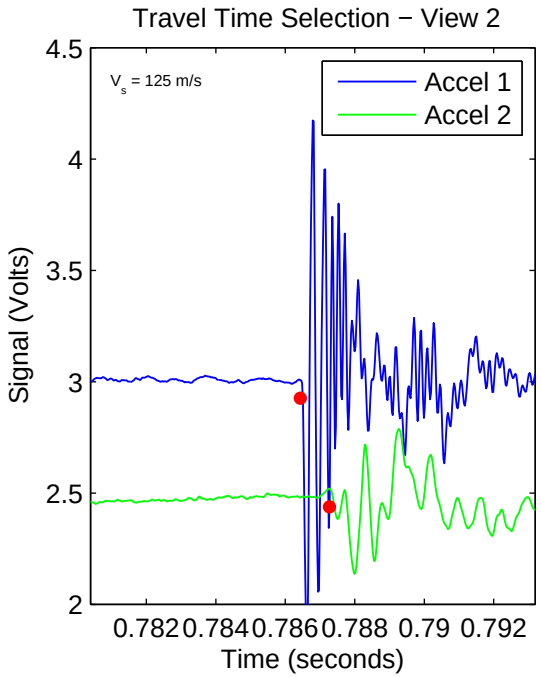
Travel Time Selection − View 2
V_s = 125 m/s
Accel 1
Accel 2
Signal (Volts)
Time (seconds)

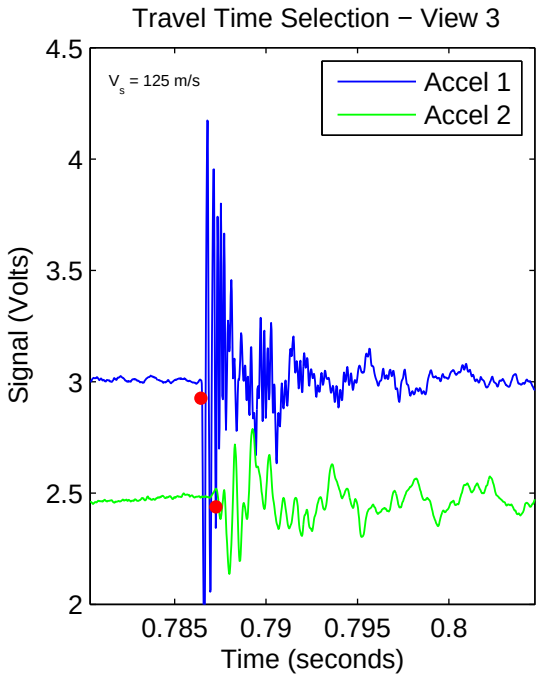
Travel Time Selection − View 3
V_s = 125 m/s
Accel 1
Accel 2
Signal (Volts)
Time (seconds)

CSS Monotonic Shear Test Report

10/28/2013_Version 8.0

Geotechnical Engineering Laboratory

General Test Information	
Device:	CSS
Specimen ID:	TX-ACLD
Test ID:	TXD6
Date of test:	4/1/2015
Test performed:	Monotonic Shear
Test material:	MSW
Sample preparation:	Reconstituted specimen with similar water content and pre-compressed density as ACLD2. Shear rings were uplifted near the end of shearing.

Sample Preparation	
Prepared total weight (kg):	15.653
Prepared dry weight (kg):	9.375
Prepared height (mm):	213.4
Prepared total density (kg/m3):	996
Prepared dry density (kg/m3):	597
Pre-compression Stage	
Pre-compressed strain (%):	47.8
Compressed total density (kg/m3):	1658
Compressed dry density (kg/m3):	1142
Secondary compression ratio:	0.02909
Total weight before shearing (kg):	13.614
Dry weight before shearing (kg):	9.375

Consolidation Stage	
Consolidated height (mm):	110.35
Vertical stress (kPa):	195.7
Immediate strain (εimm, %)	47.3
Strain before shearing (εall, %)	48.3
Compression index (Cc ε)	0.206
Constrained modulus	4.23
Consolidated total density	1675
Consolidated dry density	1153

Shear Stage		
Type of test:		CL-strain
Shear strain rate (%/min):		0.36
10% strain	Shear stress (kPa)	40.8
	Tan friction angle (°)	11.8
	Sin friction angle (°)	12.1
30% strain	Shear stress (kPa)	40.9
	Tan friction angle (°)	11.9
	Sin friction angle (°)	12.1

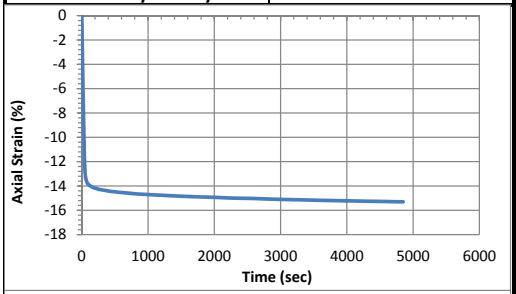

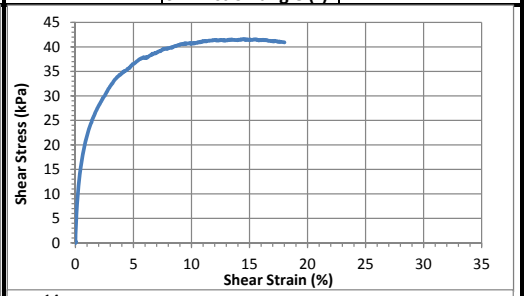

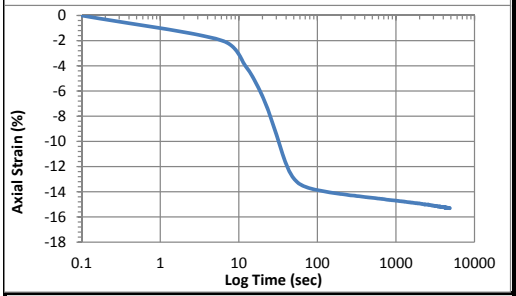

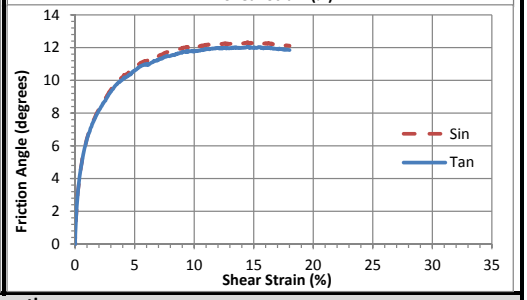

Strength			
τ/σv' at 10% strain	0.21	τ/σv0' at 10% strain	0.21
τ/σv' at 30% strain	0.21	τ/σv0' at 30% strain	0.21

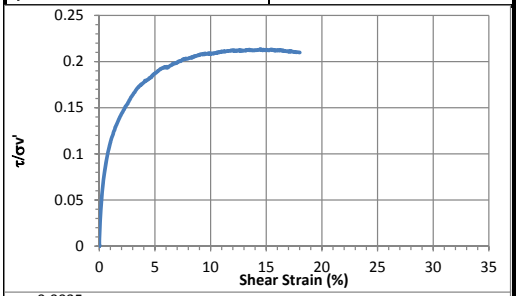

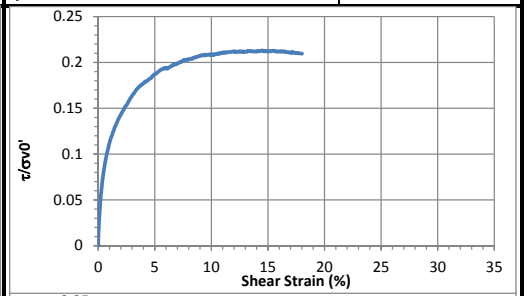

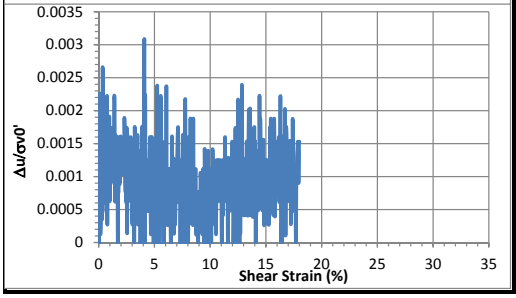

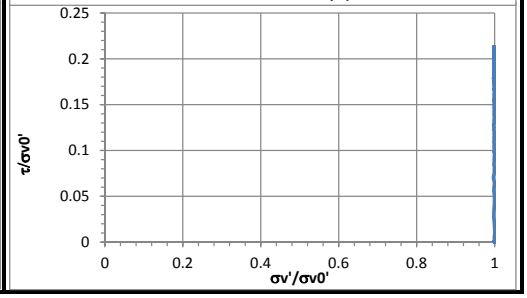

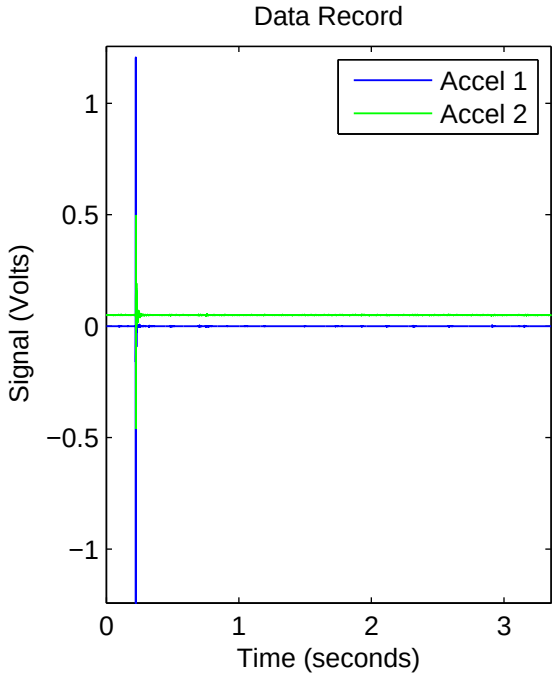
Data Record
Accel 1
Accel 2
Signal (Volts)
Time (seconds)

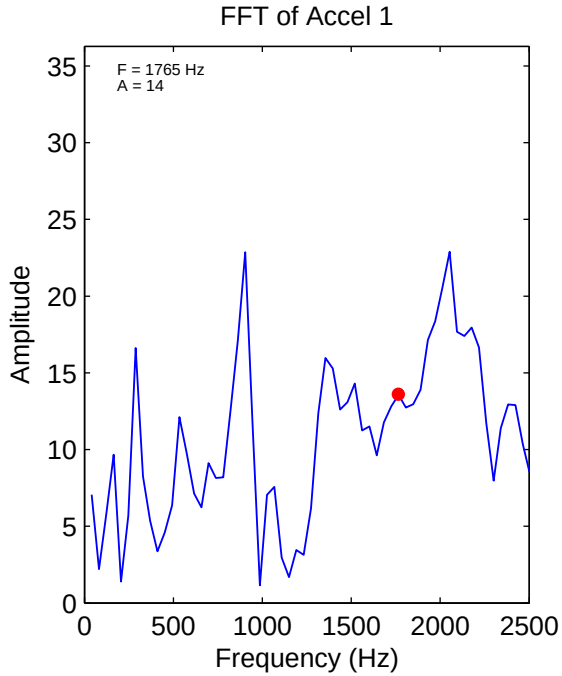
FFT of Accel 1
F = 1765 Hz
A = 14
Amplitude
Frequency (Hz)

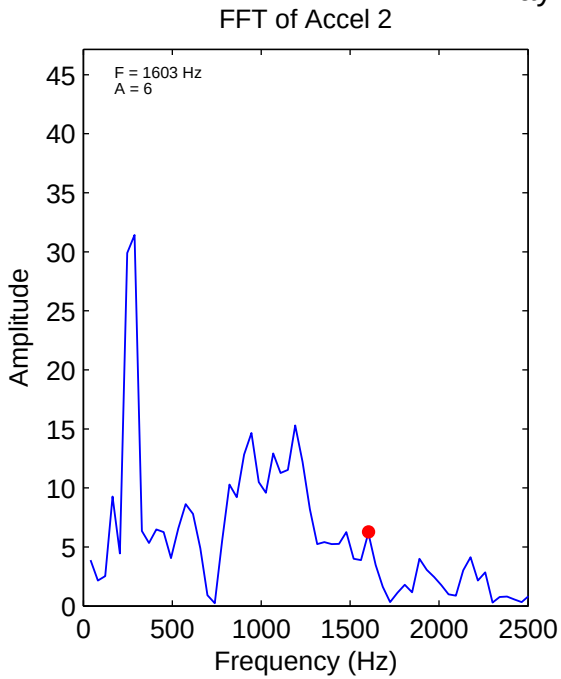
FFT of Accel 2
F = 1603 Hz
A = 6
Amplitude
Frequency (Hz)

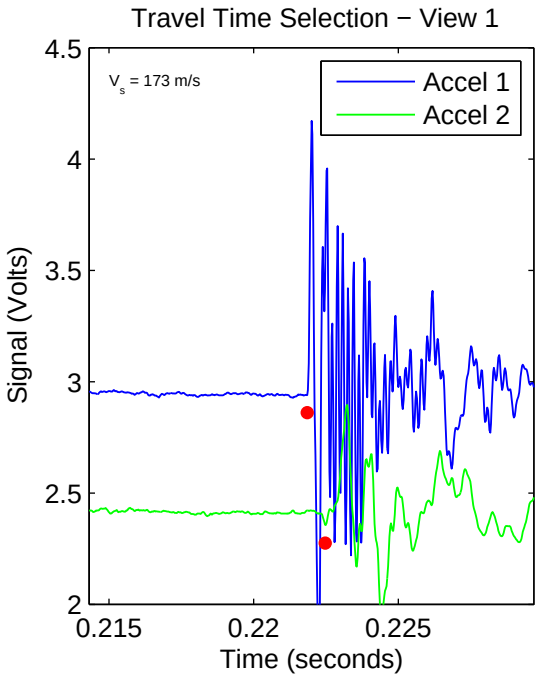
Travel Time Selection − View 1
V_s = 173 m/s
Accel 1
Accel 2
Signal (Volts)
Time (seconds)

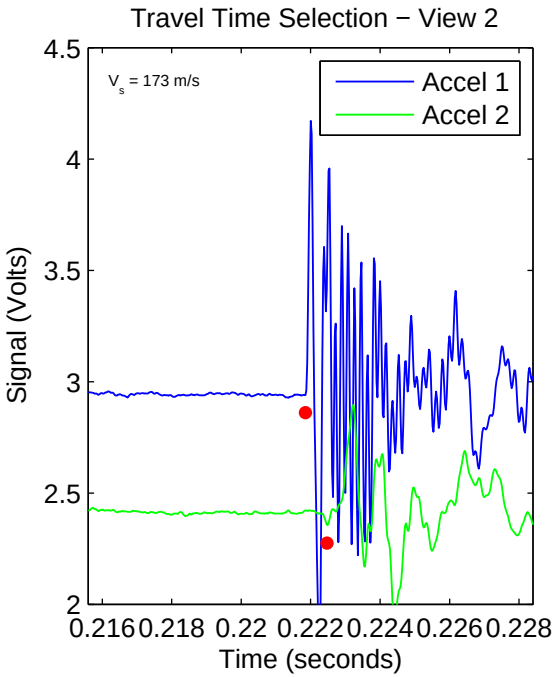
Travel Time Selection − View 2
V_s = 173 m/s
Accel 1
Accel 2
Signal (Volts)
Time (seconds)

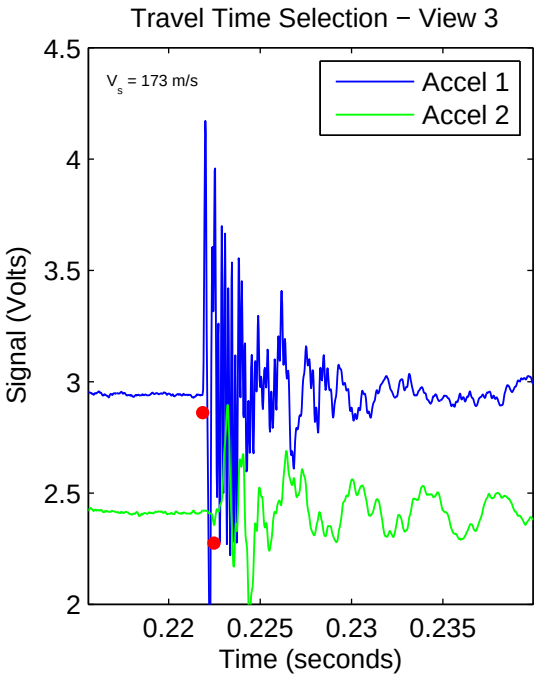
Travel Time Selection − View 3
V_s = 173 m/s
Accel 1
Accel 2
Signal (Volts)
Time (seconds)

CSS Monotonic Shear Test Report

10/28/2013_Version 8.0

Geotechnical Engineering Laboratory

General Test Information		Sample Preparation	
Device:	CSS	Prepared total weight (kg):	16.200
Specimen ID:	TX-ACLD	Prepared dry weight (kg):	11.119
Test ID:	TXD8	Prepared height (mm):	245.0
Date of test:	4/9/2015	Prepared total density (kg/m3):	898
Test performed:	Monotonic Shear	Prepared dry density (kg/m3):	616
Test material:	MSW	**Pre-compression Stage**	
Sample preparation:	Combine ACLD1 and ACLD2. Reconstituted specimen with similar pre-compressed density as ACLD2. Slid and uplifted slightly near the end.	Pre-compressed strain (%):	50.6
		Compressed total density (kg/m3):	1754
		Compressed dry density (kg/m3):	1247
		Secondary compression ratio:	0.01383
		Total weight before shearing (kg):	15.644
		Dry weight before shearing (kg):	11.119

Consolidation Stage		Shear Stage		
Consolidated height (mm):	121.92	Type of test:		CL-strain
Vertical stress (kPa):	396.6	Shear strain rate (%/min):		0.33
Immediate strain (εimm, %)	49.59	10% strain	Shear stress (kPa)	66.9
Strain before shearing (εall, %)	50.2		Tan friction angle (°)	14.2
Compression index (Cεε)	0.191		Sin friction angle (°)	14.7
Constrained modulus	4.03	30% strain	Shear stress (kPa)	60.6
Consolidated total density	1742		Tan friction angle (°)	20.7
Consolidated dry density	1238		Sin friction angle (°)	22.2

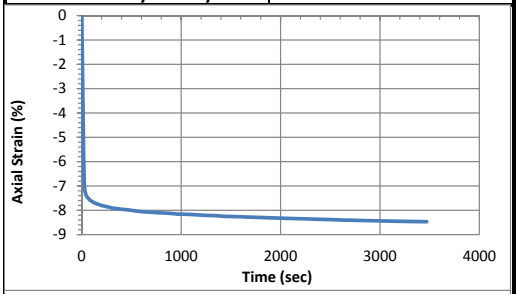

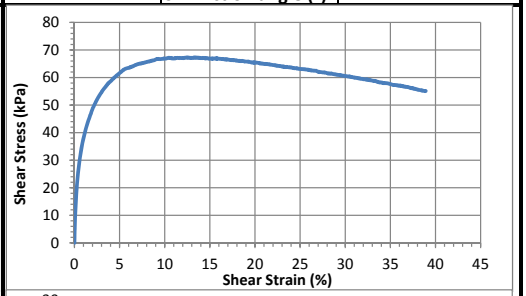

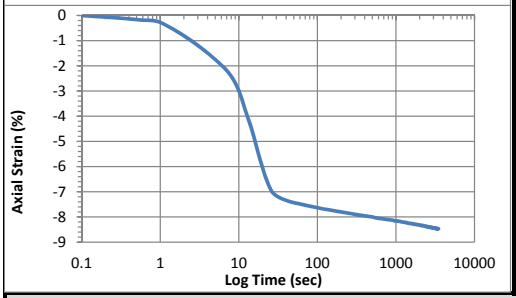

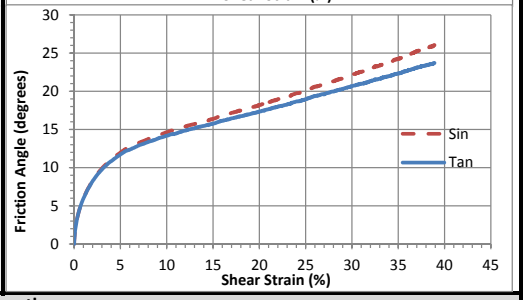

Strength			
τ/σv' at 10% strain	0.25	τ/σv0' at 10% strain	0.17
τ/σv' at 30% strain	0.38	τ/σv0' at 30% strain	0.15

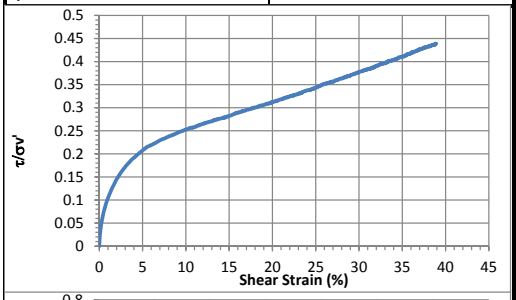

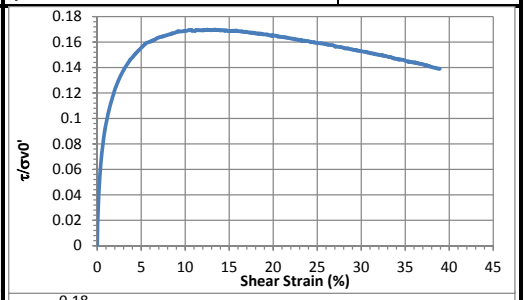

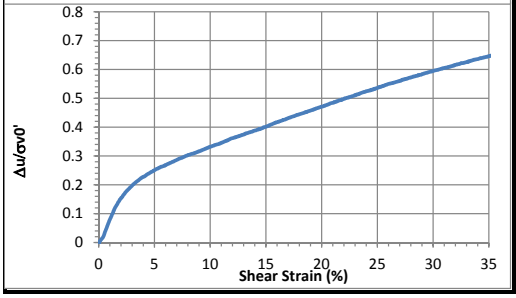

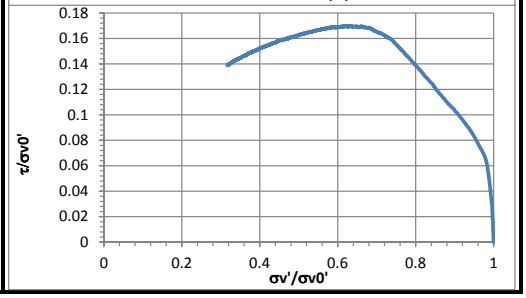

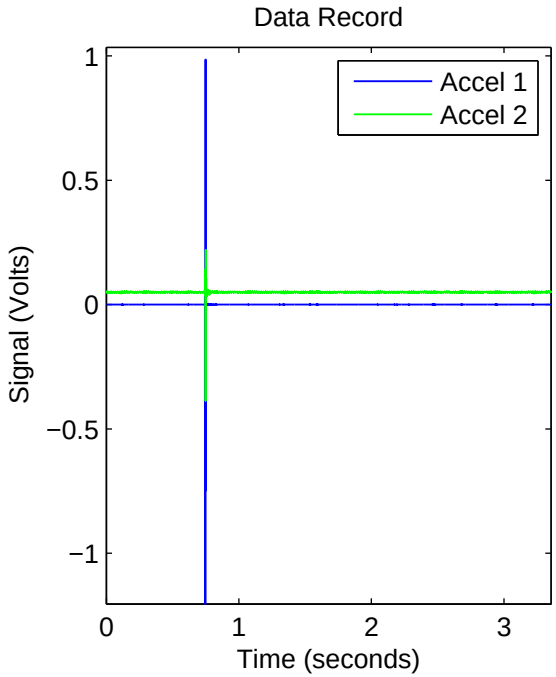
Data Record
Accel 1
Accel 2
Signal (Volts)
Time (seconds)

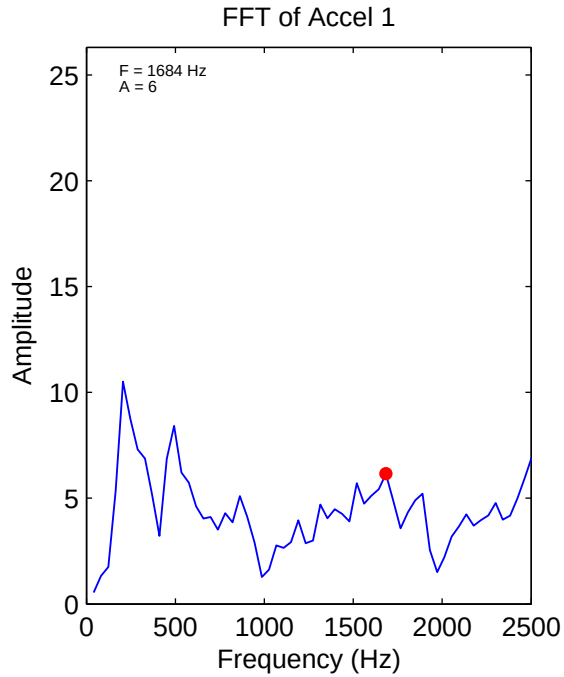
FFT of Accel 1
F = 1684 Hz
A = 6
Amplitude
Frequency (Hz)

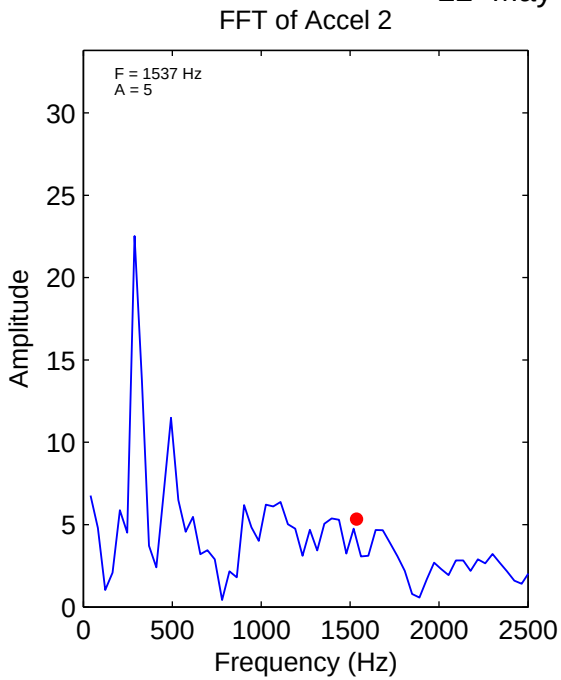
FFT of Accel 2
F = 1537 Hz
A = 5
Amplitude
Frequency (Hz)

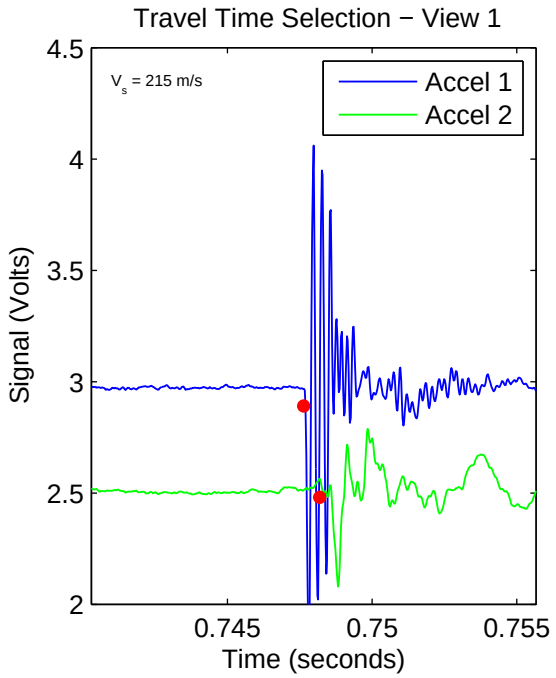
Travel Time Selection − View 1
V_s = 215 m/s
Accel 1
Accel 2
Signal (Volts)
Time (seconds)

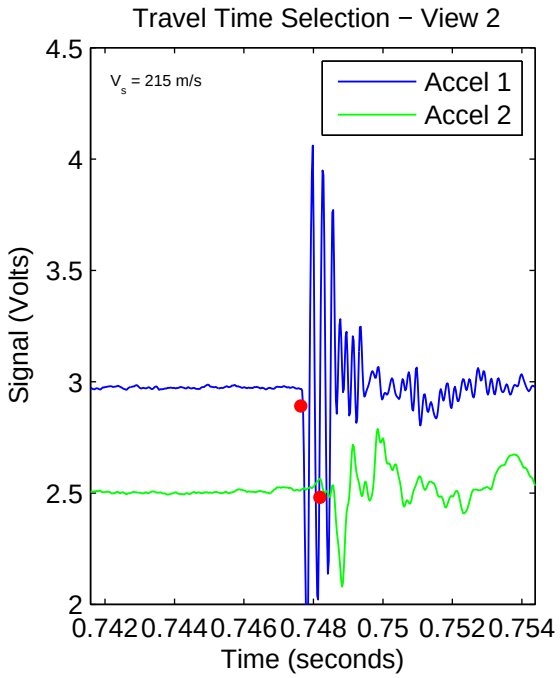
Travel Time Selection − View 2
V_s = 215 m/s
Accel 1
Accel 2
Signal (Volts)
Time (seconds)

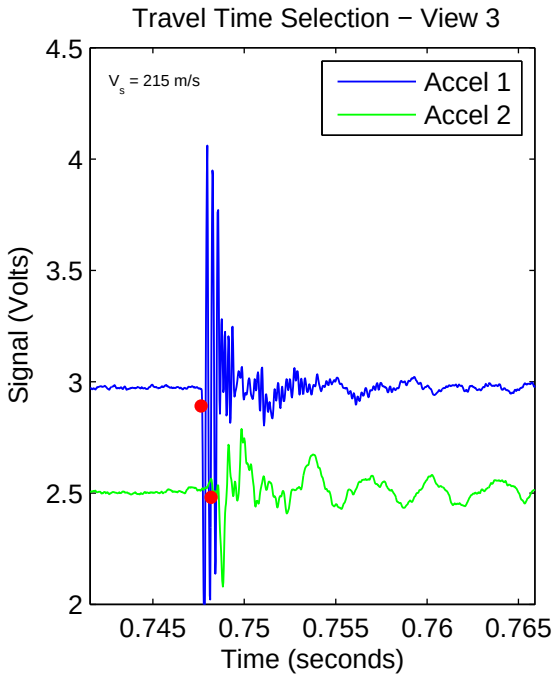
Travel Time Selection − View 3
V_s = 215 m/s
Accel 1
Accel 2
Signal (Volts)
Time (seconds)

CSS Monotonic Shear Test Report

10/28/2013_Version 8.0

Geotechnical Engineering Laboratory

General Test Information	
Device:	CSS
Specimen ID:	TX-ACLD
Test ID:	TXD9
Date of test:	4/11/2015
Test performed:	Monotonic Shear
Test material:	MSW
Sample preparation:	Combine ACLD1 and ACLD2. Reconstituted specimen with similar pre-compressed density as ACLD2.

Sample Preparation	
Prepared total weight (kg):	16.200
Prepared dry weight (kg):	11.119
Prepared height (mm):	234.5
Prepared total density (kg/m3):	938
Prepared dry density (kg/m3):	644
Pre-compression Stage	
Pre-compressed strain (%):	48.2
Compressed total density (kg/m3):	1754
Compressed dry density (kg/m3):	1244
Secondary compression ratio:	0.01085
Total weight before shearing (kg):	15.680
Dry weight before shearing (kg):	11.119

Consolidation Stage	
Consolidated height (mm):	122.84
Vertical stress (kPa):	397.3
Immediate strain (εimm, %)	47.36
Strain before shearing (εall, %)	47.6
Compression index (Cεε)	0.182
Constrained modulus	4.22
Consolidated total density	1733
Consolidated dry density	1229

Shear Stage		
Type of test:		CL-strain
Shear strain rate (%/min):		0.32
10% strain	Shear stress (kPa)	85.0
	Tan friction angle (°)	12.1
	Sin friction angle (°)	12.4
30% strain	Shear stress (kPa)	97.7
	Tan friction angle (°)	13.8
	Sin friction angle (°)	14.3

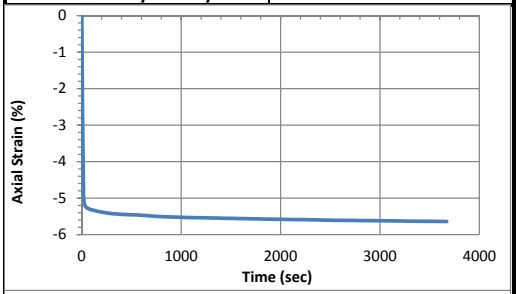

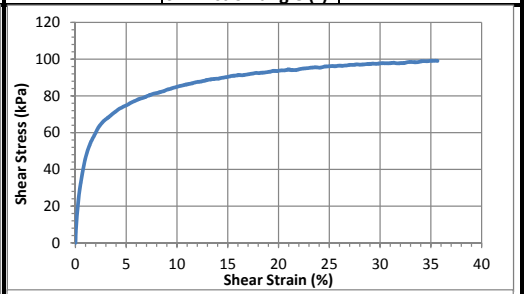

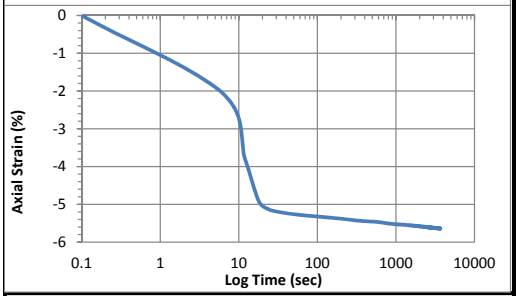

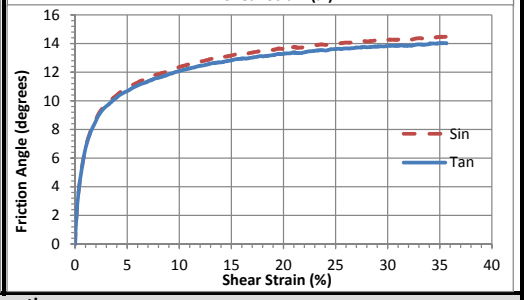

Strength

τ/σv' at 10% strain	0.21	τ/σv0' at 10% strain	0.21
τ/σv' at 30% strain	0.25	τ/σv0' at 30% strain	0.25

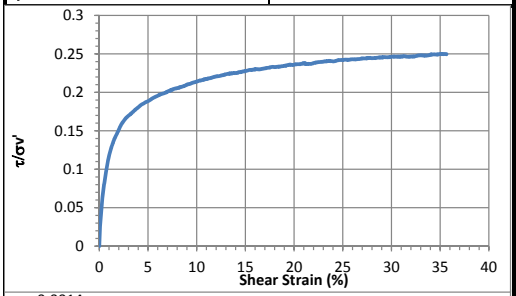

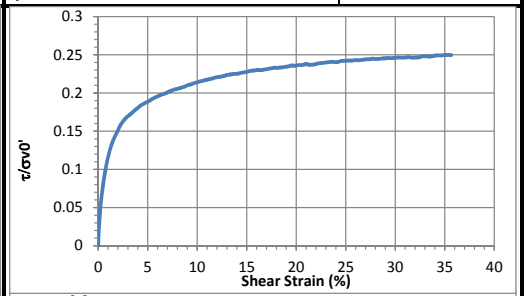

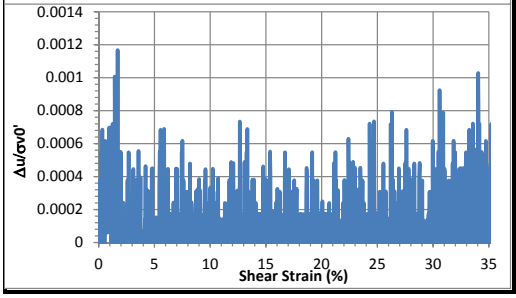

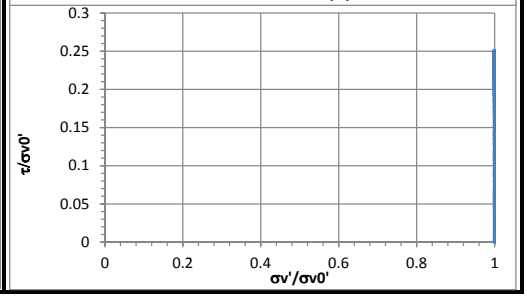

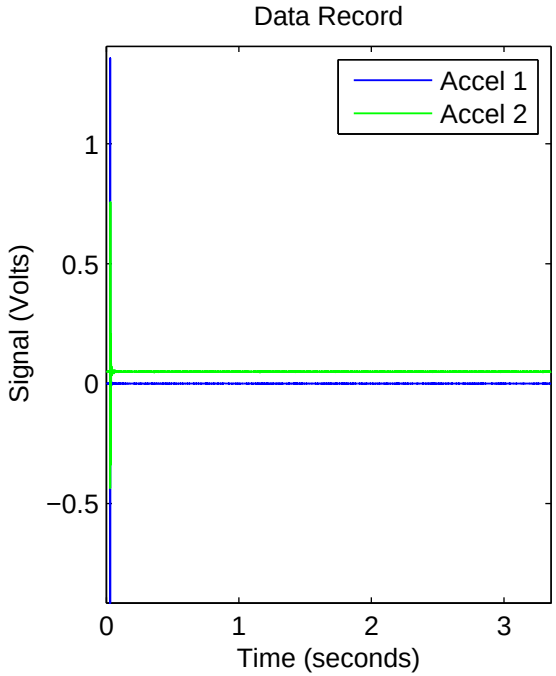
Data Record
Accel 1
Accel 2
Signal (Volts)
Time (seconds)

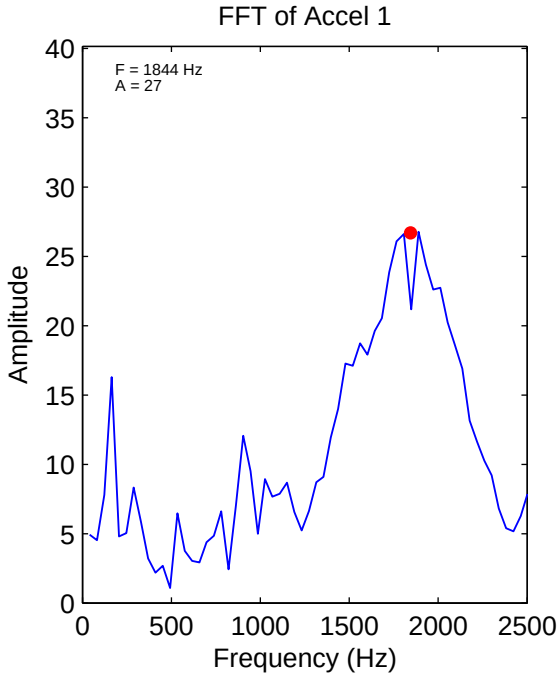
FFT of Accel 1
F = 1844 Hz
A = 27
Amplitude
Frequency (Hz)

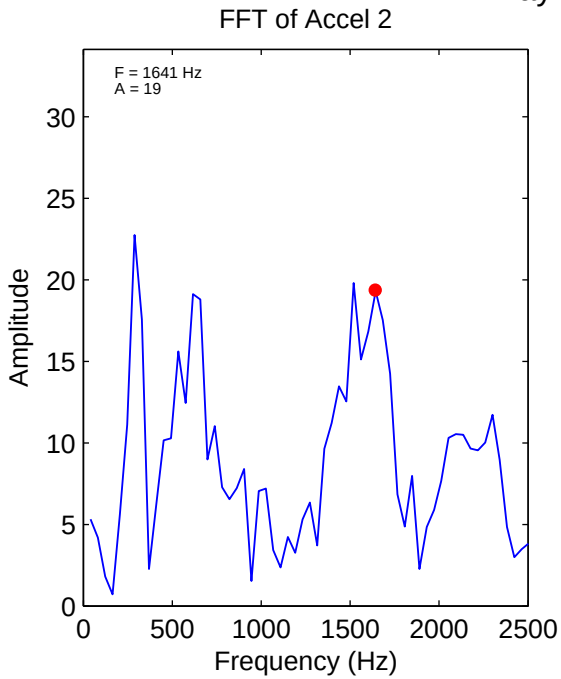
FFT of Accel 2
F = 1641 Hz
A = 19
Amplitude
Frequency (Hz)

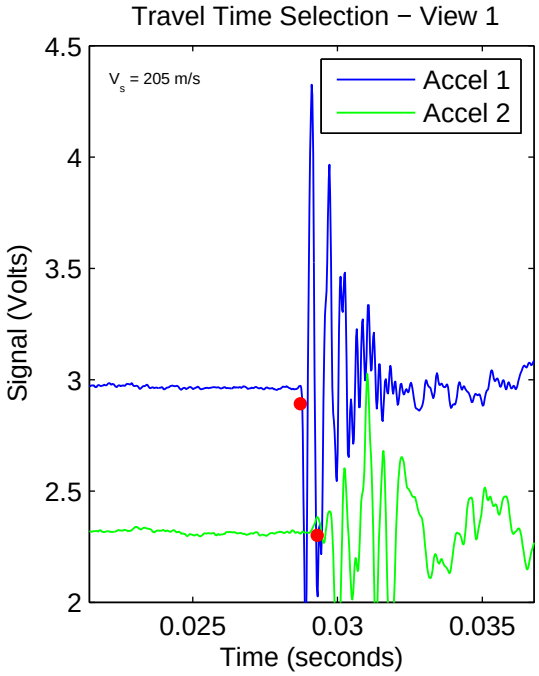
Travel Time Selection − View 1
V_s = 205 m/s
Accel 1
Accel 2
Signal (Volts)
Time (seconds)

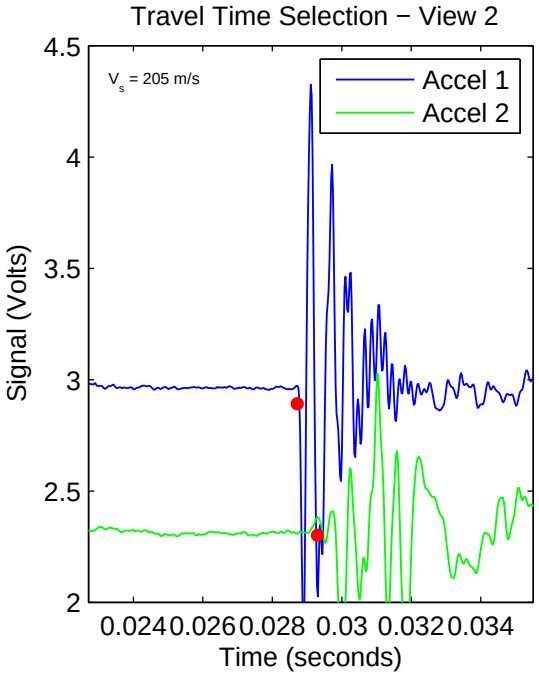
Travel Time Selection − View 2
V_s = 205 m/s
Accel 1
Accel 2
Signal (Volts)
Time (seconds)

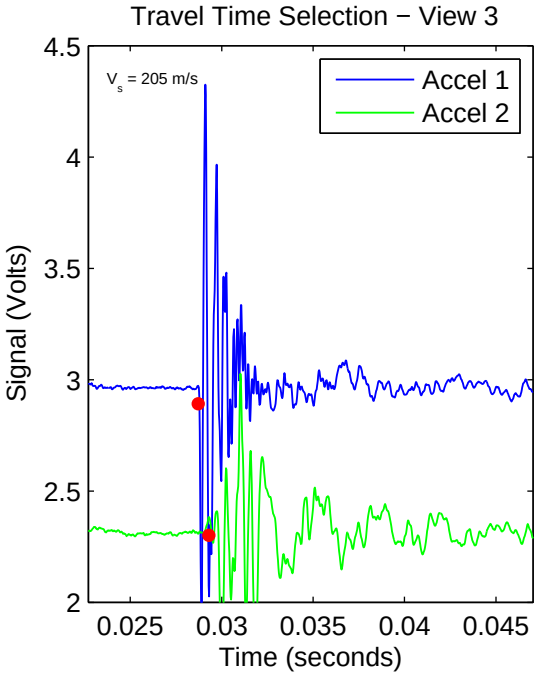
Travel Time Selection − View 3
V_s = 205 m/s
Accel 1
Accel 2
Signal (Volts)
Time (seconds)

CSS Monotonic Shear Test Report

10/28/2013_Version 8.0

Geotechnical Engineering Laboratory

General Test Information		Sample Preparation	
Device:	CSS	**Prepared total weight (kg):**	12.600
Specimen ID:	TX-ACLD	**Prepared dry weight (kg):**	8.690
Test ID:	TXD10	**Prepared height (mm):**	181.6
Date of test:	4/15/2015	**Prepared total density (kg/m3):**	942
Test performed:	Monotonic Shear	**Prepared dry density (kg/m3):**	650
Test material:	MSW	**Pre-compression Stage**	
Sample preparation:	Reconstituted FP specimen with similar pre-compressed density as ACLD1 and ACLD2. Specimen slid significantly.	**Pre-compressed strain (%):**	45.2
		Compressed total density (kg/m3):	1694
		Compressed dry density (kg/m3):	1186
		Secondary compression ratio:	0.00607
		Total weight before shearing (kg):	14.213
		Dry weight before shearing (kg):	9.931

Consolidation Stage		Shear Stage		
Consolidated height (mm):	112.76	**Type of test:**		CV-strain
Vertical stress (kPa):	98.3	**Shear strain rate (%/min):**		0.35
Immediate strain (εimm, %)	45.02	**10% strain**	**Shear stress (kPa)**	26.3
Strain before shearing (εall, %)	45.7		**Tan friction angle (°)**	26.8
Compression index (Cεε)	0.226		**Sin friction angle (°)**	30.4
Constrained modulus	4.44	**30% strain**	**Shear stress (kPa)**	22.4
Consolidated total density	1711		**Tan friction angle (°)**	29.1
Consolidated dry density	1196		**Sin friction angle (°)**	33.8

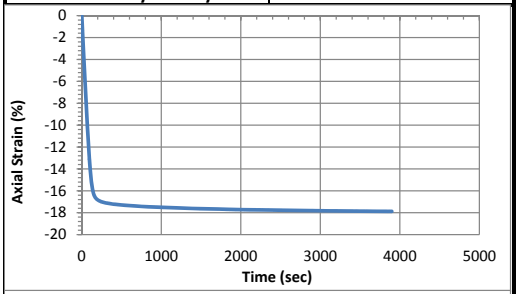

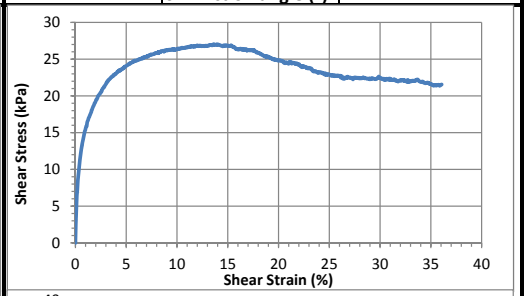

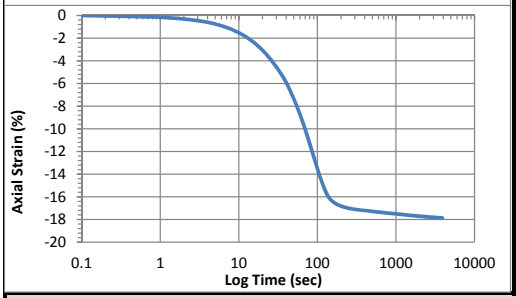

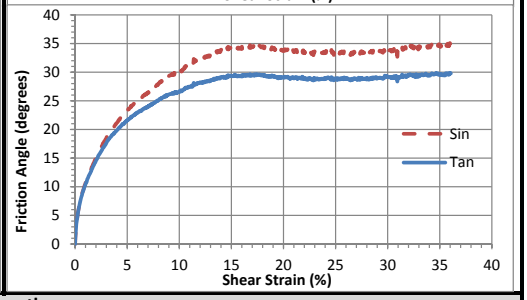

Strength			
τ/σv' at 10% strain	0.51	**τ/σv0' at 10% strain**	0.27
τ/σv' at 30% strain	0.56	**τ/σv0' at 30% strain**	0.23

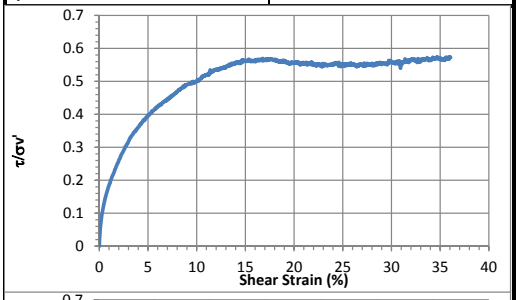

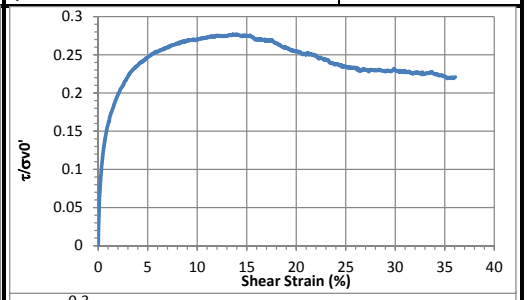

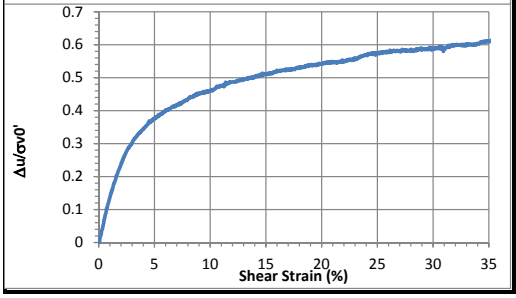

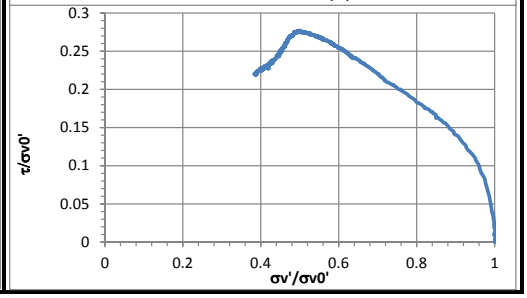

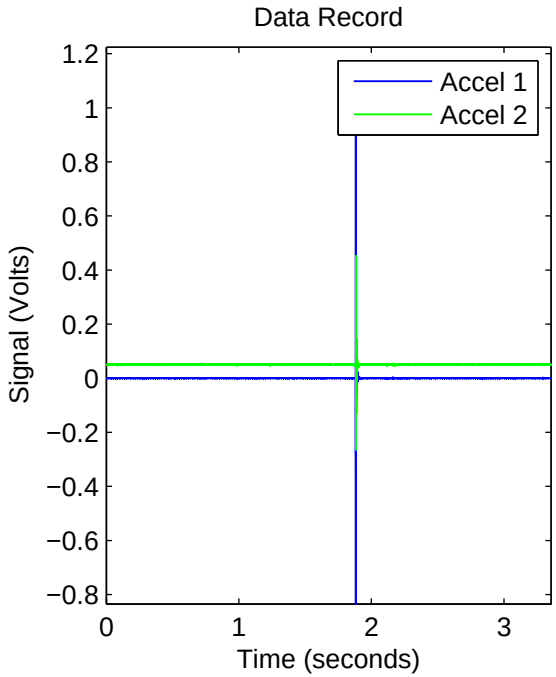
Data Record
Accel 1
Accel 2
Signal (Volts)
Time (seconds)

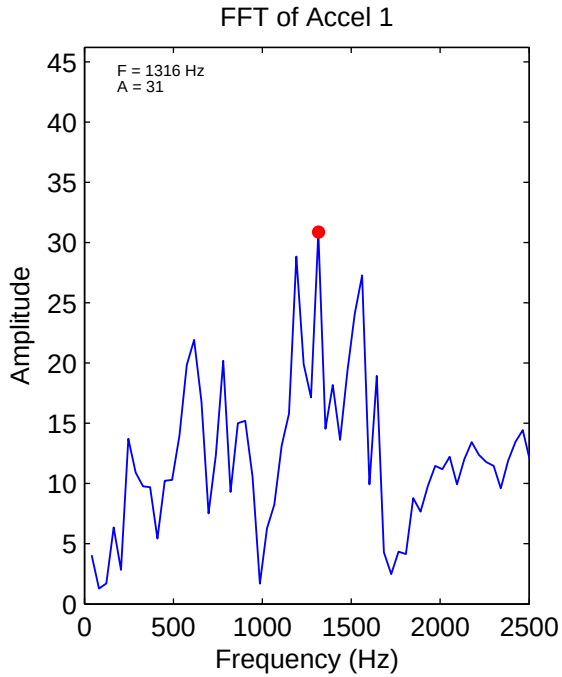
FFT of Accel 1
F = 1316 Hz
A = 31
Amplitude
Frequency (Hz)

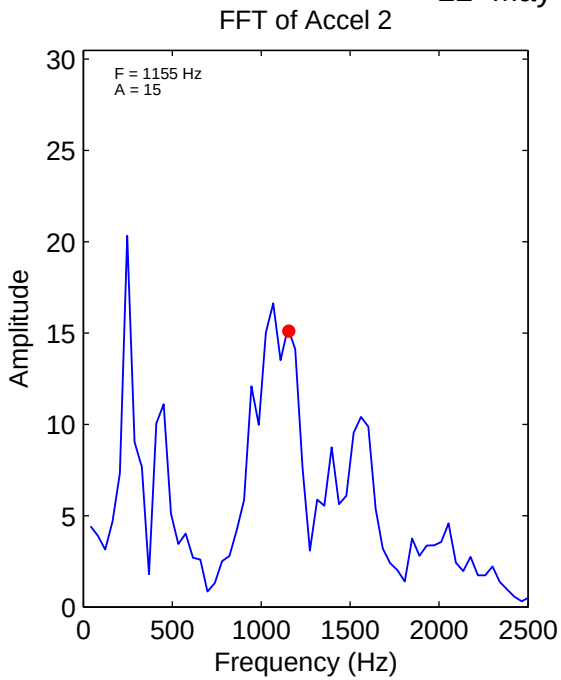
FFT of Accel 2
F = 1155 Hz
A = 15
Amplitude
Frequency (Hz)

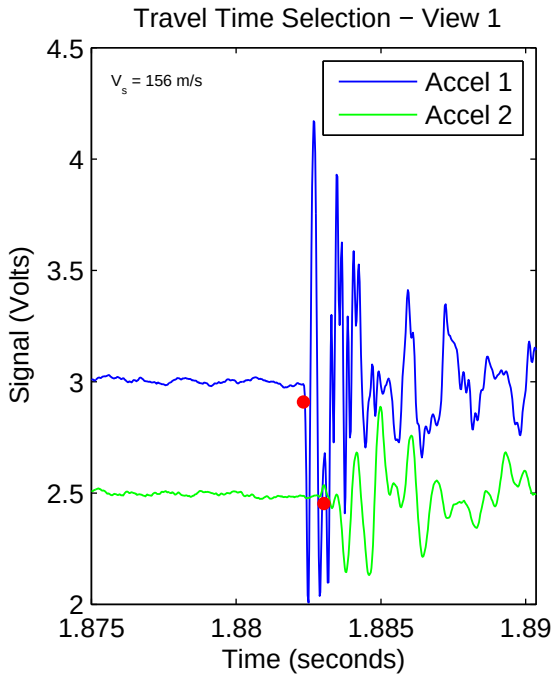
Travel Time Selection − View 1
V_s = 156 m/s
Accel 1
Accel 2
Signal (Volts)
Time (seconds)

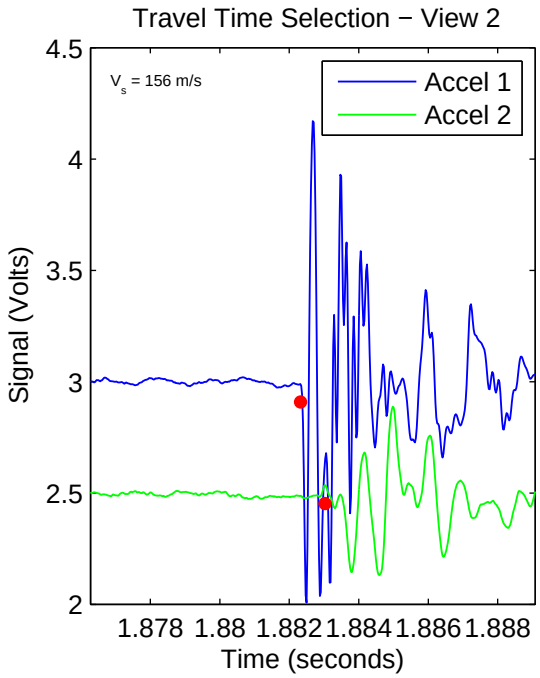
Travel Time Selection − View 2
V_s = 156 m/s
Accel 1
Accel 2
Signal (Volts)
Time (seconds)

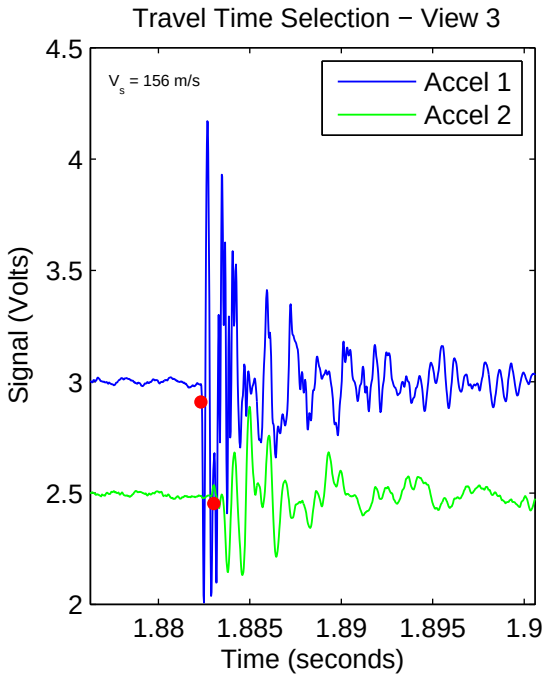
Travel Time Selection − View 3
V_s = 156 m/s
Accel 1
Accel 2
Signal (Volts)
Time (seconds)

CSS Monotonic Shear Test Report

10/28/2013_Version 8.0

Geotechnical Engineering Laboratory

General Test Information		Sample Preparation	
Device:	CSS	Prepared total weight (kg):	15.300
Specimen ID:	TX-ACLD	Prepared dry weight (kg):	10.552
Test ID:	TXD11	Prepared height (mm):	235.0
Date of test:	4/19/2015	Prepared total density (kg/m3):	884
Test performed:	Monotonic Shear	Prepared dry density (kg/m3):	610
Test material:	MSW	**Pre-compression Stage**	
Sample preparation:	Reconstituted FP specimen with similar pre-compressed density as ACLD1 and ACLD2. Bottom ring uplifted.	Pre-compressed strain (%):	48.2
		Compressed total density (kg/m3):	1683
		Compressed dry density (kg/m3):	1178
		Secondary compression ratio:	0.00434
		Total weight before shearing (kg):	15.078
		Dry weight before shearing (kg):	10.552

Consolidation Stage		Shear Stage		
Consolidated height (mm):	120.20	Type of test:		CL-strain
Vertical stress (kPa):	97.5	Shear strain rate (%/min):		0.33
Immediate strain (εimm, %)	48.47	10% strain	Shear stress (kPa)	29.2
Strain before shearing (εall, %)	48.8		Tan friction angle (°)	16.7
Compression index (Cc ε)	0.244		Sin friction angle (°)	17.6
Constrained modulus	4.13	30% strain	Shear stress (kPa)	29.0
Consolidated total density	1703		Tan friction angle (°)	16.7
Consolidated dry density	1192		Sin friction angle (°)	17.5

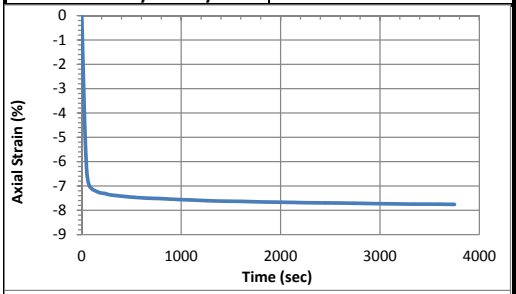

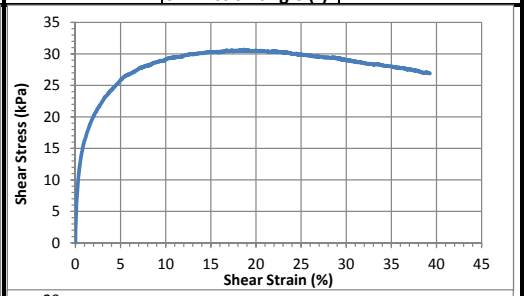

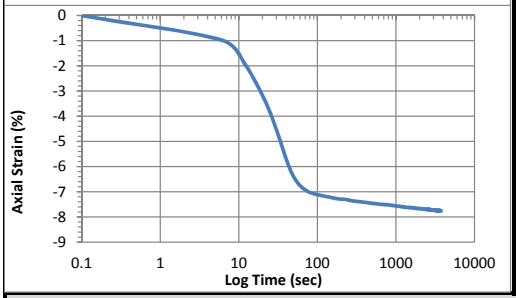

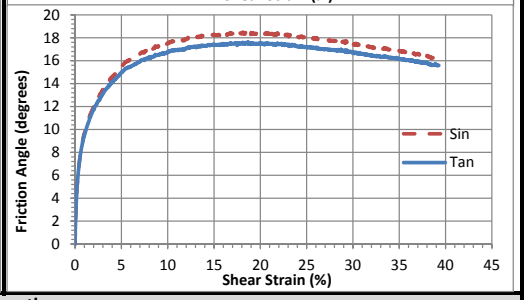

Strength

τ/σv' at 10% strain	0.30	τ/σv0' at 10% strain	0.30
τ/σv' at 30% strain	0.30	τ/σv0' at 30% strain	0.30

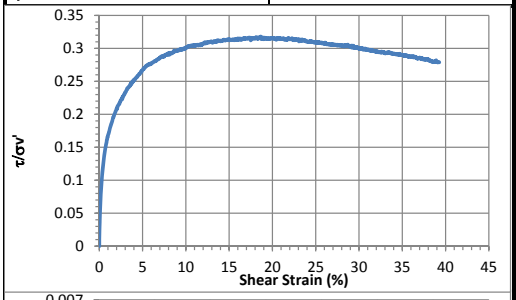

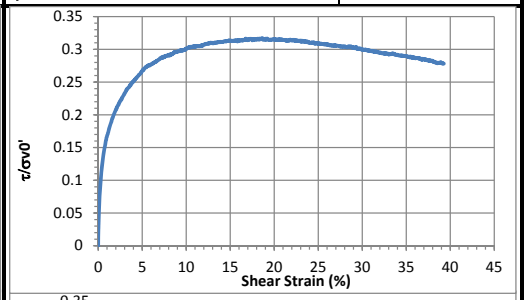

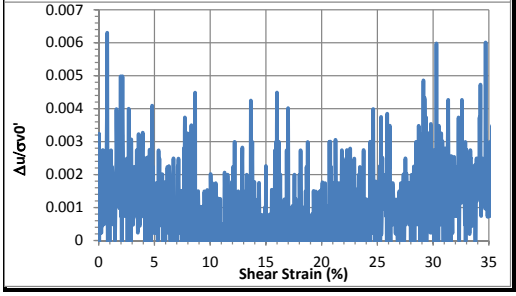

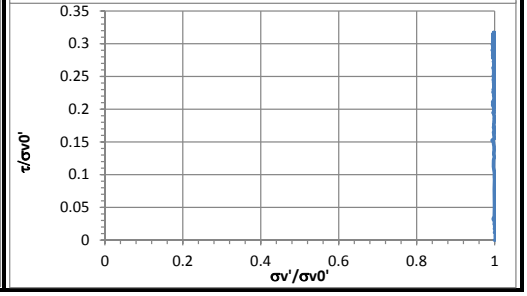

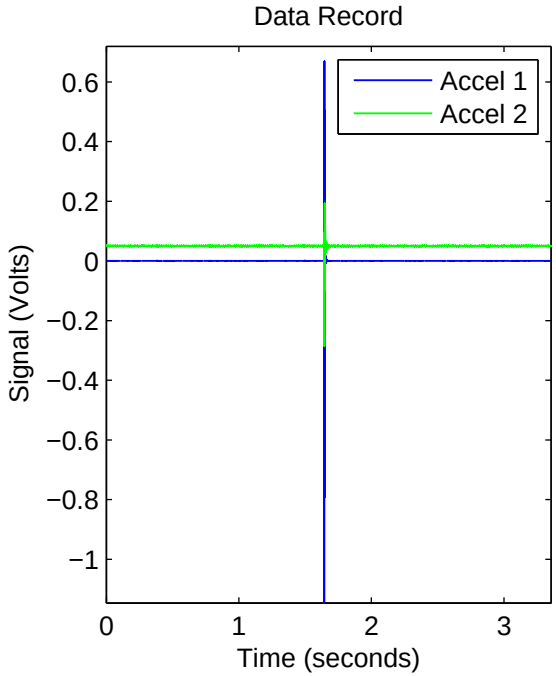
Data Record
Accel 1
Accel 2
Signal (Volts)
Time (seconds)

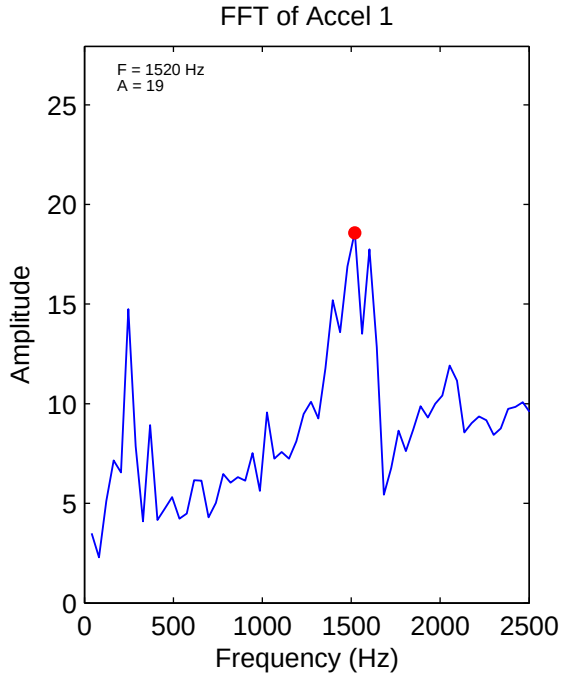
FFT of Accel 1
F = 1520 Hz
A = 19
Amplitude
Frequency (Hz)

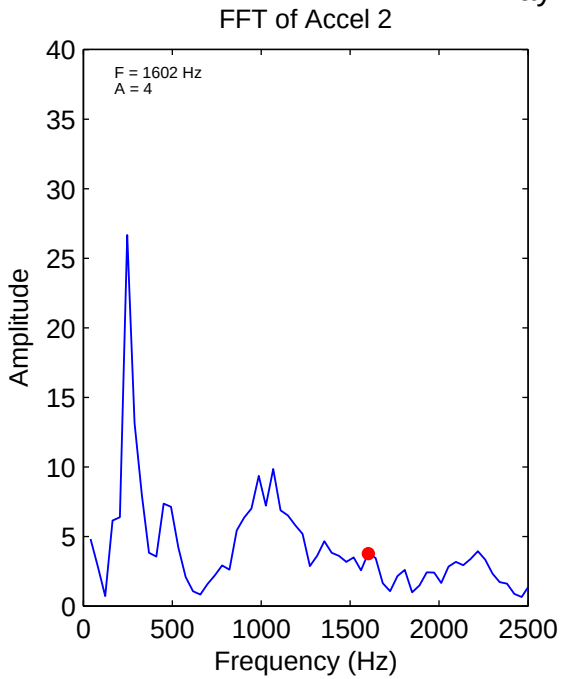
FFT of Accel 2
F = 1602 Hz
A = 4
Amplitude
Frequency (Hz)

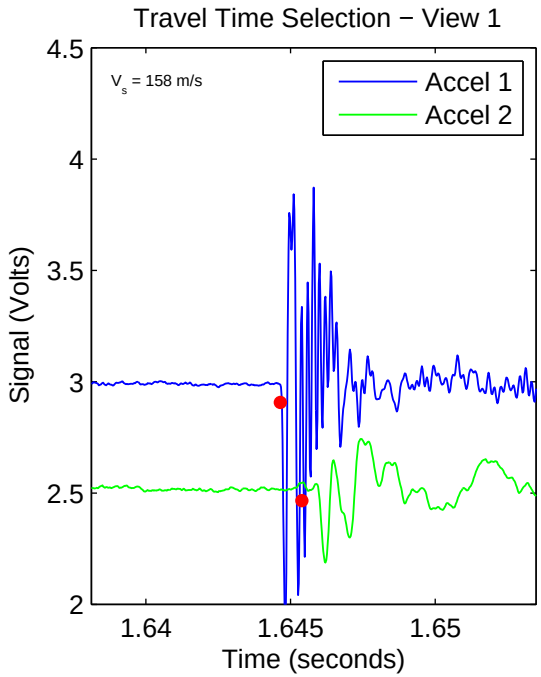
Travel Time Selection − View 1
V_s = 158 m/s
Accel 1
Accel 2
Signal (Volts)
Time (seconds)

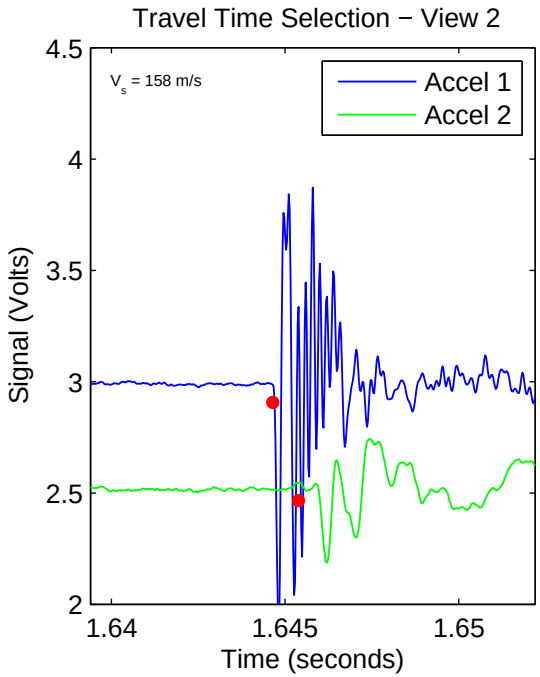
Travel Time Selection − View 2
V_s = 158 m/s
Accel 1
Accel 2
Signal (Volts)
Time (seconds)

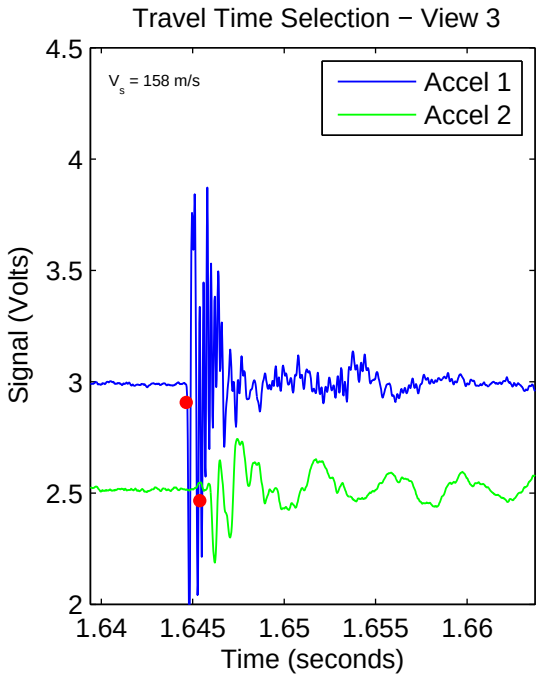
Travel Time Selection − View 3
V_s = 158 m/s
Accel 1
Accel 2
Signal (Volts)
Time (seconds)

CSS Monotonic Shear Test Report

10/28/2013_Version 8.0

Geotechnical Engineering Laboratory

General Test Information and Sample Preparation

Device:	CSS	**Layers prior to shear:**	8.94
Specimen ID:	CA-LCF	**Weight/layer (kg):**	1.33
Test ID:	CAF1	**Height/layer (mm):**	25.4
Date of Test:	9/3/2014	**As-prepared height (mm):**	239.8
Test Performed:	Monotonic Shear	**Soil-only specimen diameter (mm):**	306.2
Test Material:	MSW	**Total weight (kg):**	11.89
Sample Preparation:	The same initial composition and unit weight as Sim. #5. Staged pre-compress for 52 (24) hours, consolidate for 1 hour.	**As-prepared density (kg/m^3):**	697
		Membrane thickness (mm):	0.000635
		Moisture content (%):	23.5
		Saturated (Y/N):	N
		Prepared by:	Fei

Pre-compression Stage

Pre-compressed strain (%):	49.3	**Secondary compression ratio:**	missing
Pre-compressed height (mm):	121.7	**Density (kg/m3):**	1373

Consolidation Stage

Initial height (mm):	137.5
Initial density (kg/m3):	1174
Vertical Stress (kPa):	394.6
Immediate strain (εimm, %)	49.5
Strain before shear (εall, %)	50.2
Compression index (Cεε)	0.191
Constrained modulus	4.0
Consolidated density (kg/m^3):	1400

Shear Stage

Type of test:		CL-strain
Shear strain rate (%/min):		0.35
10% strain	**Shear stress (kPa)**	130.9
	Tan friction angle (°)	18.3
	Sin friction angle (°)	19.2
30% strain	**Shear stress (kPa)**	168.9
	Tan friction angle (°)	23.1
	Sin friction angle (°)	25.3

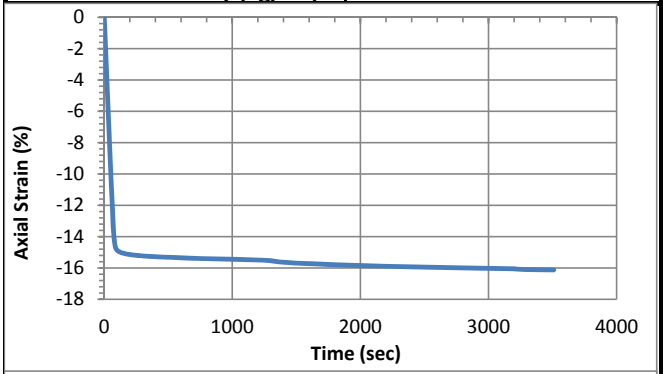

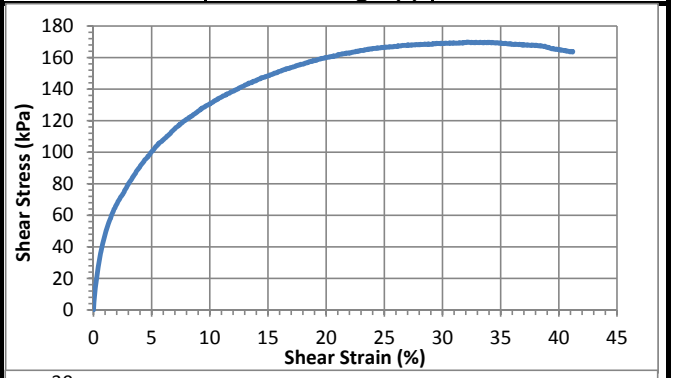

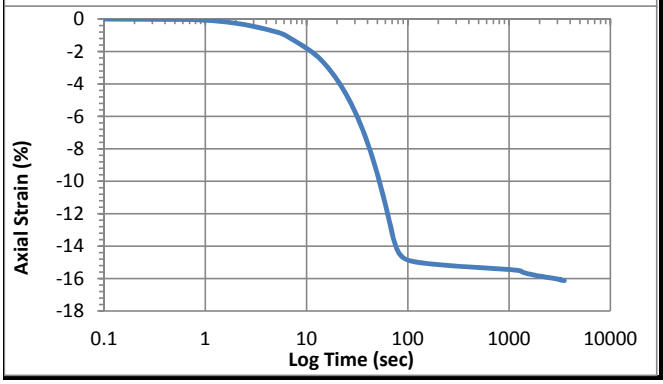

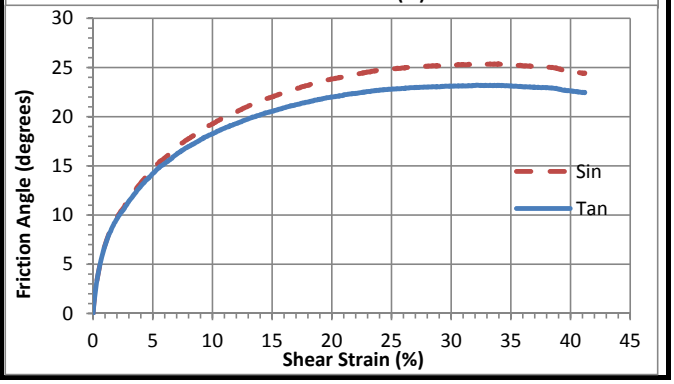

Strength			
τ/σv' at 10% strain	0.33	τ/σv0' at 10% strain	0.33
τ/σv' at 30% strain	0.43	τ/σv0' at 30% strain	0.43

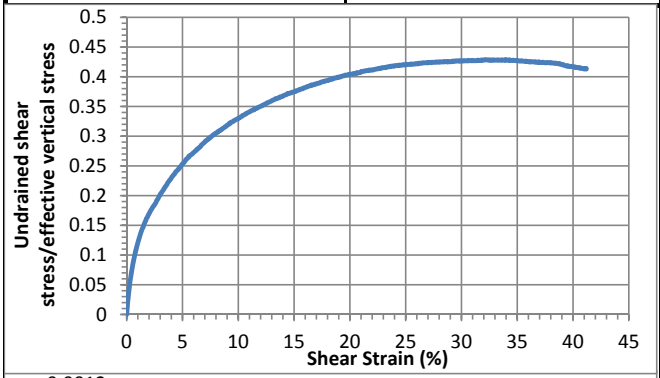

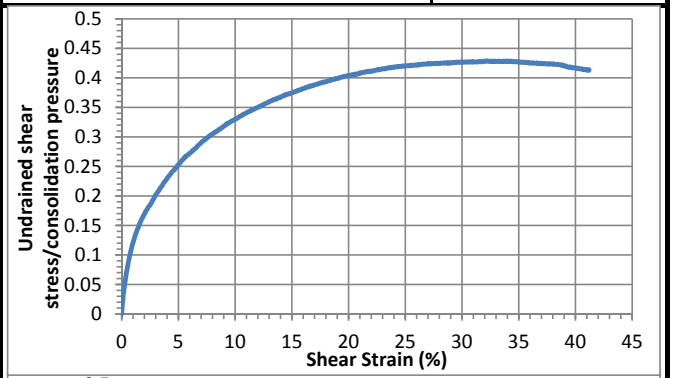

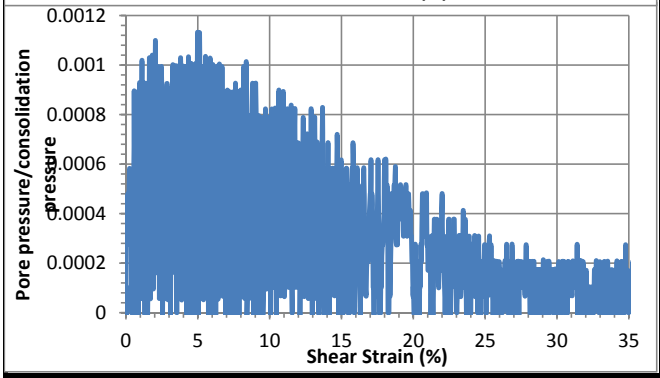

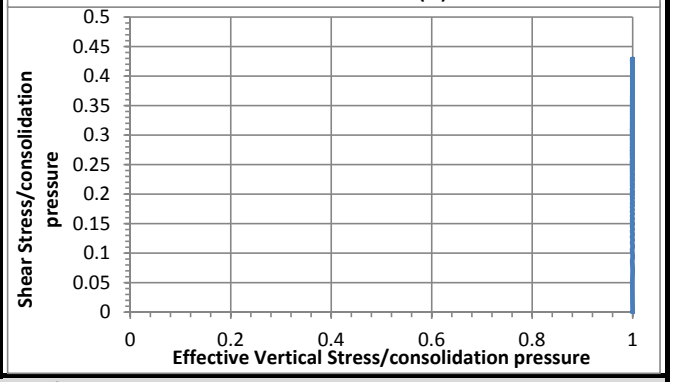

Shear wave velocity				
Signal type	Sinusoidal	First rise	initiation time (ms)	-0.0154
Signal amplitude (Vpp)	90		arrival time (ms)	0.2867
Signal frequency (kHz)	4		Vs (m/s)	353
Sensor spacing (mm)	106.60	First peak	initiation time (ms)	0.0512
R+P average Vs (m/s)	350		arrival time (ms)	0.3584
Stdev. (m/s)	4		Vs (m/s)	347
P+V average Vs (m/s)	347	First valley	initiation time (ms)	0.1792
Stdev. (m/s)	0		arrival time (ms)	0.4864
Wavelength (m)	0.087		Vs (m/s)	347
Spacing/wavelength	1.2			

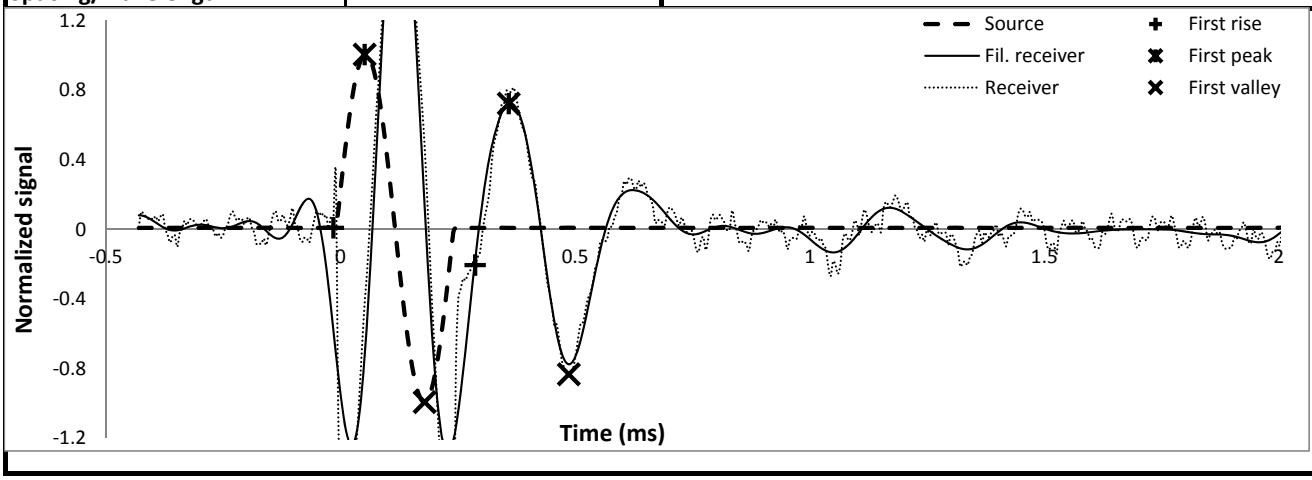

CSS Monotonic Shear Test Report

10/28/2013_Version 8.0

Geotechnical Engineering Laboratory

General Test Information and Sample Preparation			
Device:	CSS	**Layers:**	6.76
Specimen ID:	LCF	**Weight/layer (kg):**	1.33
Test ID:	CAF2	**Height/layer (mm):**	25.4
Date of Test:	9/4/2014	**Total height (mm):**	171.704
Test Performed:	Monotonic Shear	**Soil-Only Specimen Diameter (mm):**	306.2
Test Material:	MSW	**Total weight (kg):**	8.9908
Sample Preparation:	The same initial composition and unit weight as Sim. #5. Staged pre-compress for 23 hours, consolidate for 1 hour.	**Density (kg/m^3):**	711
		Membrane Thickness (mm):	0.000635
		Moisture Content (%):	23.5
		Saturated (Y/N):	N
		Prepared by:	Fei

Pre-compression Stage			
Pre-compression strain:	0.31	**Secondary compression ratio:**	0.00693
Height (mm):	139.8	**Density (kg/m3):**	969

Consolidation Stage		Shear Stage		
Initial height (mm):	137.5	**Type of Test:**		CD-strain
Initial density (kg/m3):	888	**Shear Strain Rate (%/min):**		0.33
Vertical Stress (kPa):	48.6	**10% strain**	**Shear stress (kPa)**	18.7
Immediate strain (εimm, %)	32.0		**Tan friction angle (°)**	20.8
Consolidated Height (mm):	119.8		**Sin friction angle (°)**	22.4
Compression index (Ccε)	0.196	**30% strain**	**Shear stress (kPa)**	24.0
Consolidation modulus	6.0		**Tan friction angle (°)**	26.0
Consolidated density (kg/m^3):	1019		**Sin friction angle (°)**	29.1

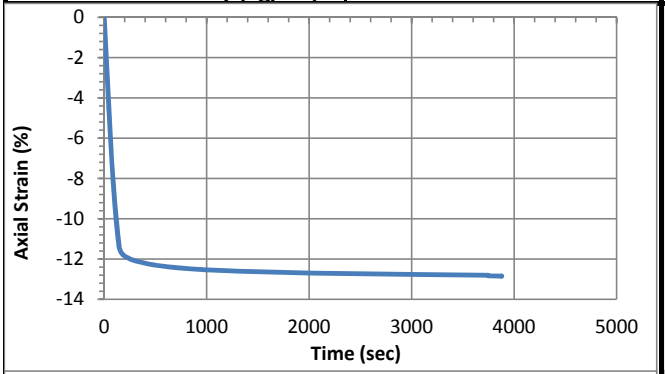

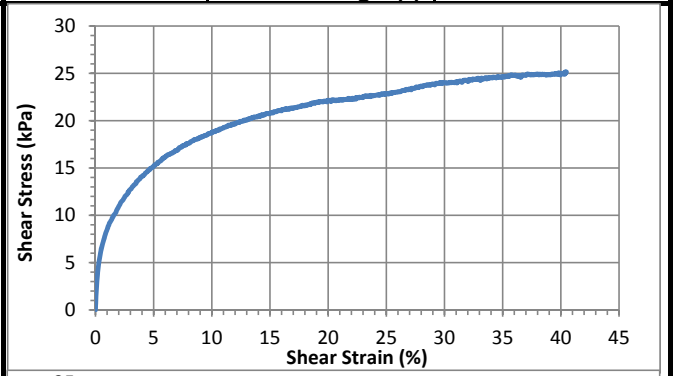

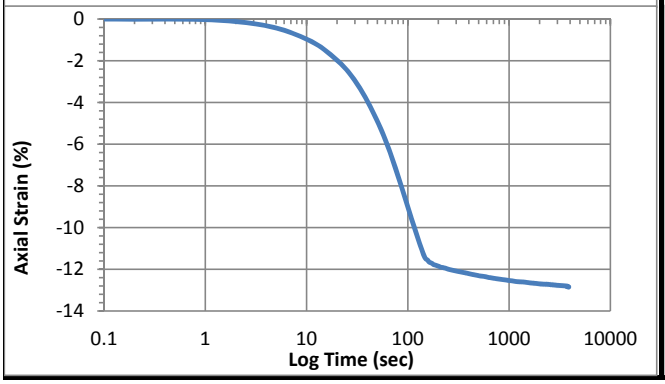

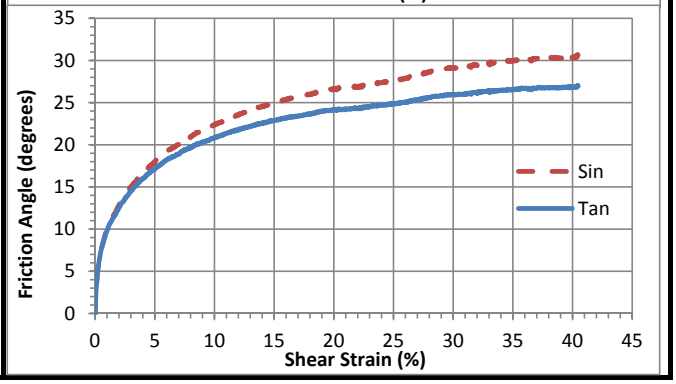

Undrained Strength			
Su/σv' at 10% strain	0.38	Su/σvc' at 10% strain	0.38
Su/σv' at 30% strain	0.49	Su/σvc' at 30% strain	0.49

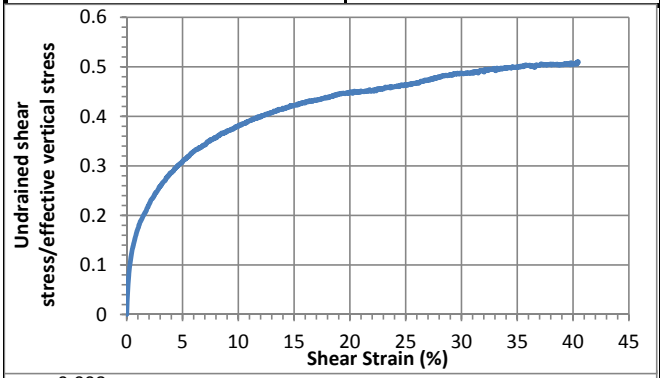

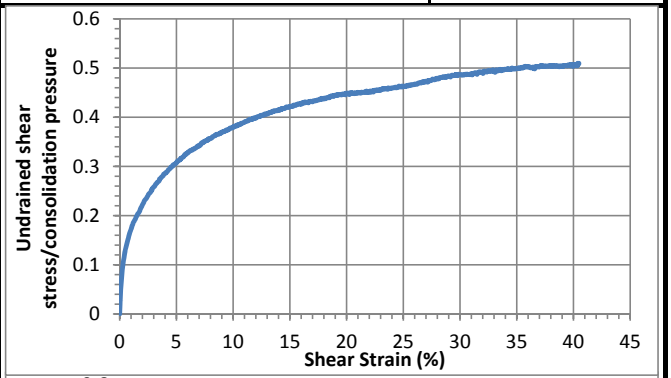

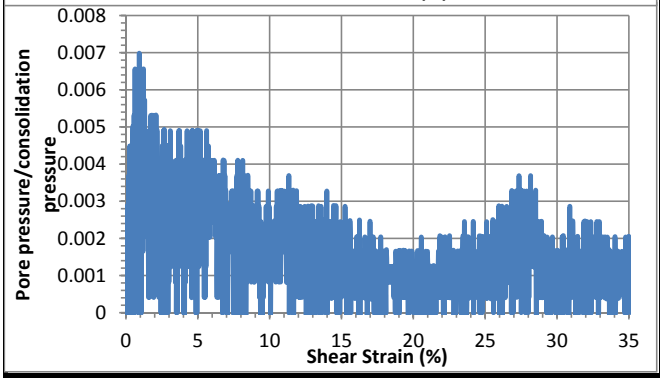

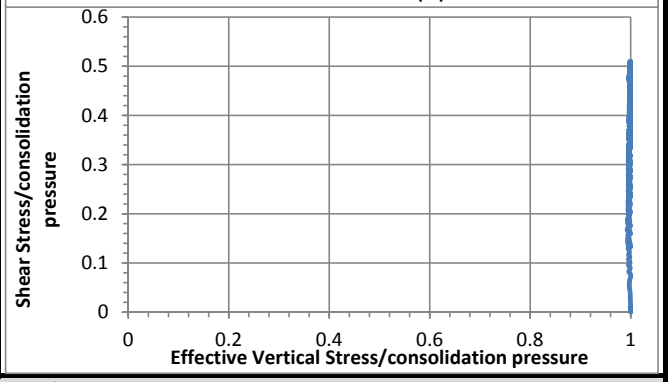

Shear wave velocity				
Signal type	Sinusoidal	First rise	initiation time (ms)	-0.0205
Signal amplitude (Vpp)	90		arrival time (ms)	0.7117
Signal frequency (kHz)	2.5		Vs (m/s)	152
Sensor spacing (mm)	111.04	First peak	initiation time (ms)	0.0819
R+P average Vs (m/s)	148		arrival time (ms)	0.8499
Stdev. (m/s)	5		Vs (m/s)	145
P+V average Vs (m/s)	147	First valley	initiation time (ms)	0.2816
Stdev. (m/s)	4		arrival time (ms)	1.0240
Wavelength (m)	0.059		Vs (m/s)	150
Spacing/wavelength	1.9			

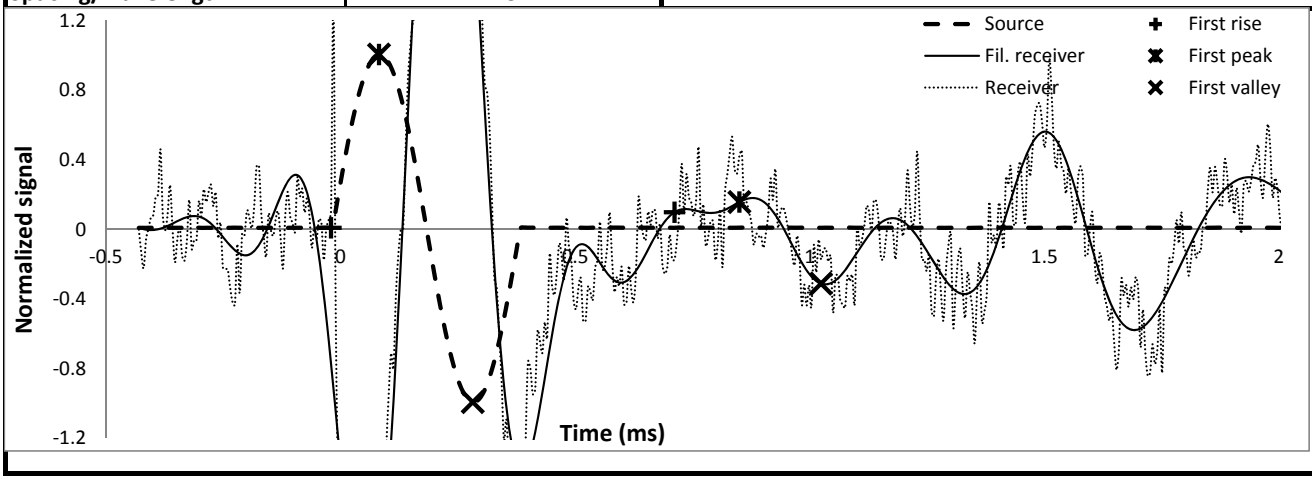

CSS Monotonic Shear Test Report

10/28/2013_Version 8.0

Geotechnical Engineering Laboratory

General Test Information and Sample Preparation			
Device:	CSS	**Layers:**	6.75
Specimen ID:	LCF	**Weight/layer (kg):**	1.33
Test ID:	CAF3	**Height/layer (mm):**	25.4
Date of Test:	9/5/2014	**Total height (mm):**	171.45
Test Performed:	Monotonic Shear	**Soil-Only Specimen Diameter (mm):**	306.2
Test Material:	MSW	**Total weight (kg):**	8.9775
Sample Preparation:	The same initial composition and unit weight as Sim. #5. Staged pre-compress for 23 hours, consolidate for 1 hour.	**Density (kg/m^3):**	711
		Membrane Thickness (mm):	0.000635
		Moisture Content (%):	23.5
		Saturated (Y/N):	N
		Prepared by:	Fei

Pre-compression Stage			
Pre-compression strain:	0.33	**Secondary compression ratio:**	0.01107
Height (mm):	123.1	**Density (kg/m3):**	990

Consolidation Stage		Shear Stage		
Initial height (mm):	135.4	**Type of Test:**		CU-strain
Initial density (kg/m3):	900	**Shear Strain Rate (%/min):**		0.34
Vertical Stress (kPa):	47.7	**10% strain**	**Shear stress (kPa)**	15.2
Immediate strain (εimm, %)	32.0		**Tan friction angle (°)**	26.8
Consolidated Height (mm):	118.3		**Sin friction angle (°)**	30.4
Compression index (Ccε)	0.205	**30% strain**	**Shear stress (kPa)**	15.7
Consolidation modulus	5.8		**Tan friction angle (°)**	32.4
Consolidated density (kg/m^3):	1030		**Sin friction angle (°)**	39.3

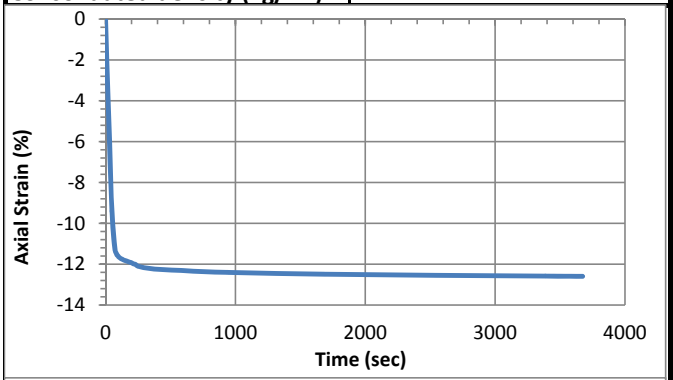

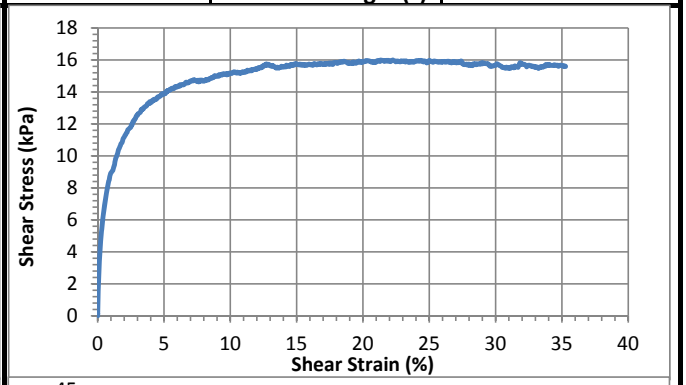

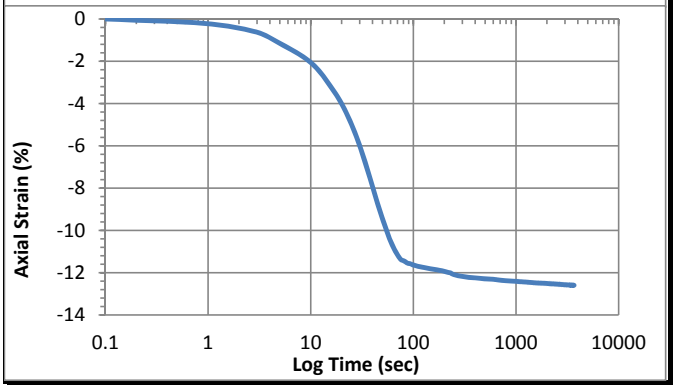

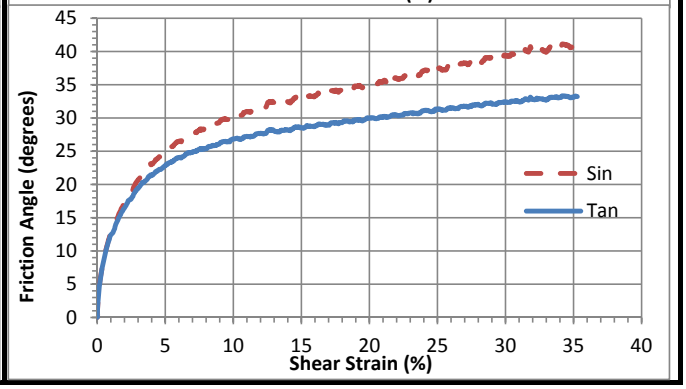

Undrained Strength			
Su/σv' at 10% strain	0.51	Su/σvc' at 10% strain	0.32
Su/σv' at 30% strain	0.63	Su/σvc' at 30% strain	0.33

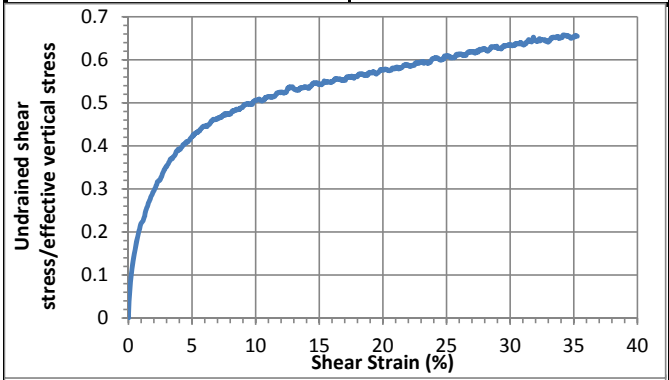

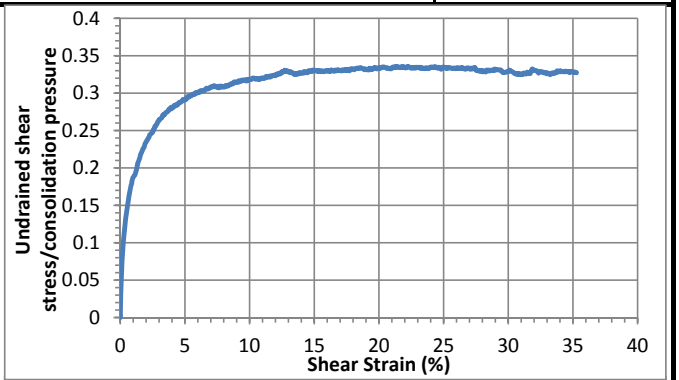

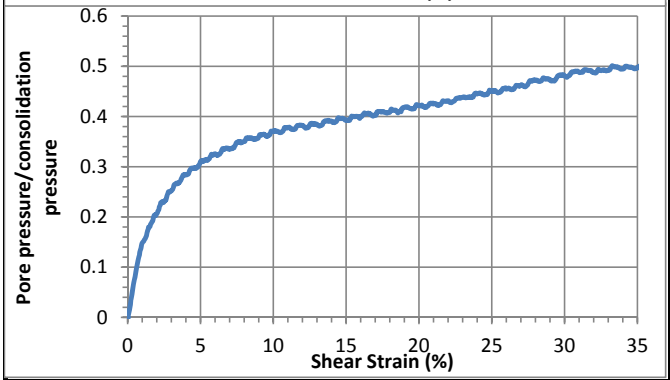

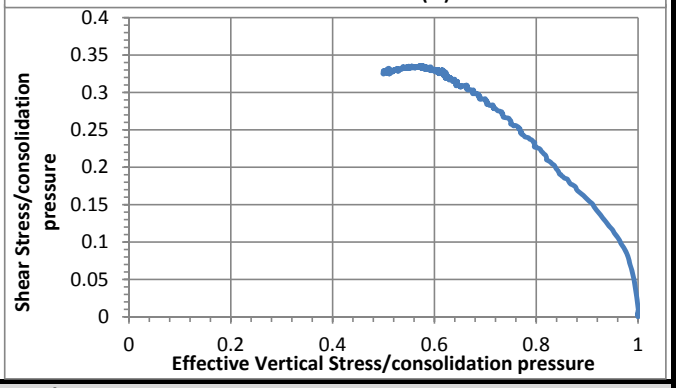

Shear wave velocity				
Signal type	Sinusoidal	First rise	initiation time (ms)	0.6605
Signal amplitude (Vpp)	90		arrival time (ms)	0.0819
Signal frequency (kHz)	2.5		Vs (m/s)	162
Sensor spacing (mm)	109.52	First peak	initiation time (ms)	0.7578
R+P average Vs (m/s)	155		arrival time (ms)	0.2816
Stdev. (m/s)	10		Vs (m/s)	148
P+V average Vs (m/s)	154	First valley	initiation time (ms)	1.0240
Stdev. (m/s)	10		arrival time (ms)	160.8288
Wavelength (m)	0.062		Vs (m/s)	161
Spacing/wavelength	1.8			

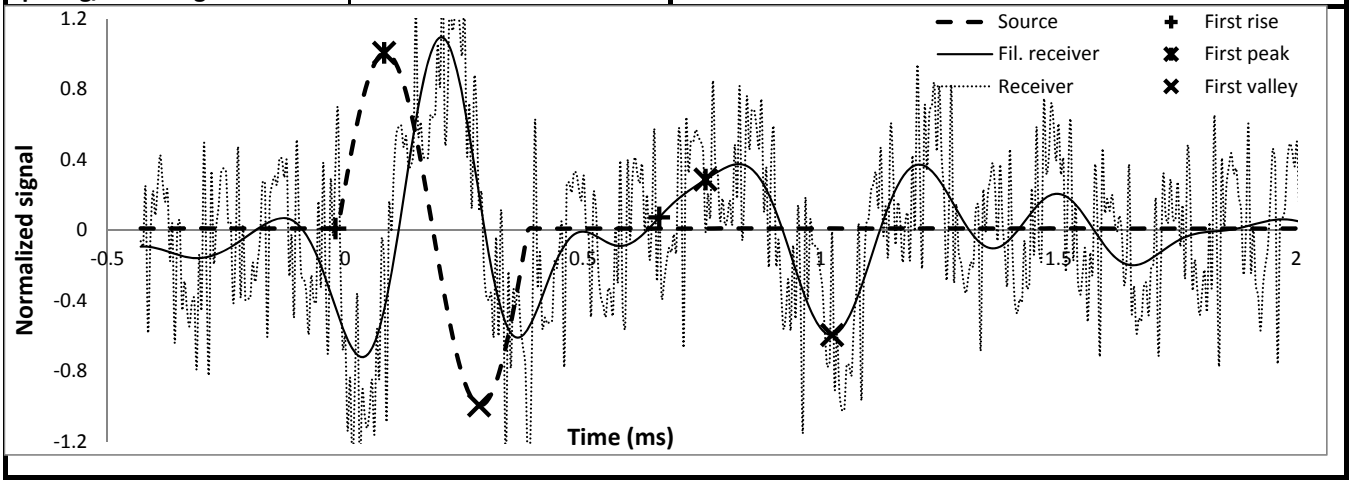

CSS Monotonic Shear Test Report

10/28/2013_Version 8.0

Geotechnical Engineering Laboratory

General Test Information and Sample Preparation			
Device:	CSS	**Layers:**	7.75
Specimen ID:	LCF	**Weight/layer (kg):**	1.33
Test ID:	CAF4	**Height/layer (mm):**	25.4
Date of Test:	9/7/2014	**Total height (mm):**	196.85
Test Performed:	Monotonic Shear	**Soil-Only Specimen Diameter (mm):**	306.2
Test Material:	MSW	**Total weight (kg):**	10.3075
Sample Preparation:	The same initial composition and unit weight as Sim. #5. Staged pre-compress for 23 hours, consolidate for 1 hour.	**Density (kg/m^3):**	711
		Membrane Thickness (mm):	0.000635
		Moisture Content (%):	23.5
		Saturated (Y/N):	N
		Prepared by:	Fei

Pre-compression Stage			
Pre-compression strain:	0.37	**Secondary compression ratio:**	0.01091
Height (mm):	127.8	**Density (kg/m3):**	1095

Consolidation Stage		Shear Stage		
Initial height (mm):	136.1	**Type of Test:**		CD-strain
Initial density (kg/m3):	1028	**Shear Strain Rate (%/min):**		0.33
Vertical Stress (kPa):	97.9	**10% strain**	**Shear stress (kPa)**	36.4
Immediate strain (εimm, %)	36.4		**Tan friction angle (°)**	20.4
Consolidated Height (mm):	122.0		**Sin friction angle (°)**	21.9
Compression index (Ccε)	0.196	**30% strain**	**Shear stress (kPa)**	45.8
Consolidation modulus	5.1		**Tan friction angle (°)**	25.1
Consolidated density (kg/m^3):	1147		**Sin friction angle (°)**	27.9

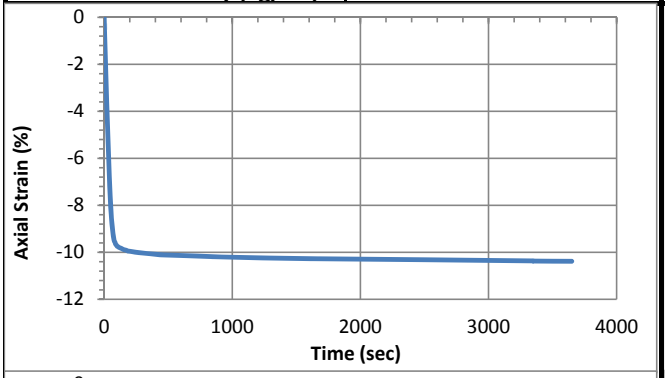

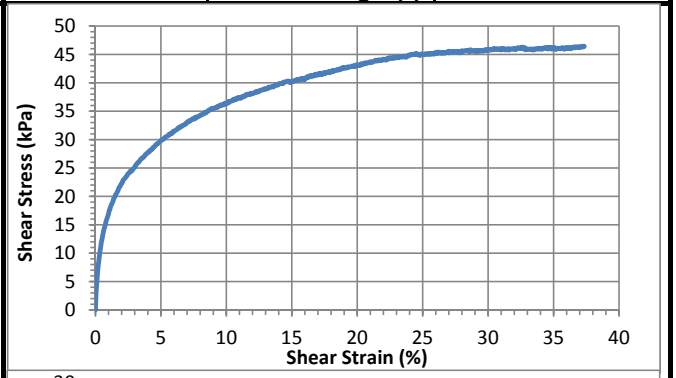

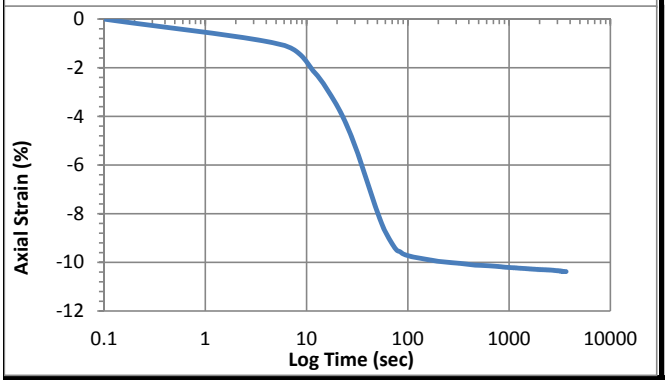

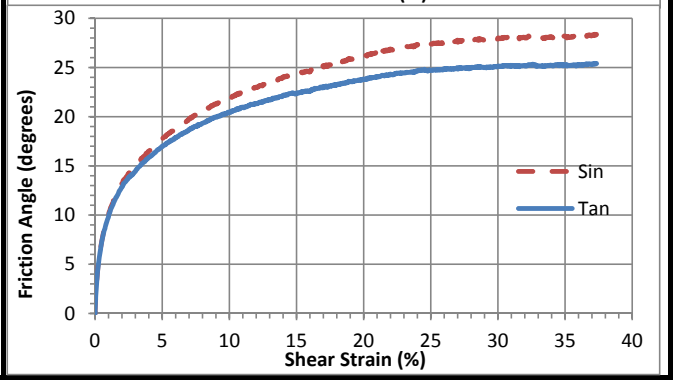

Undrained Strength			
Su/σv' at 10% strain	0.37	Su/σvc' at 10% strain	0.37
Su/σv' at 30% strain	0.47	Su/σvc' at 30% strain	0.47

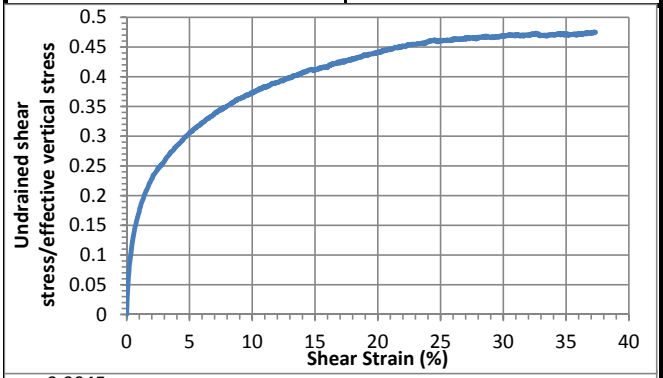

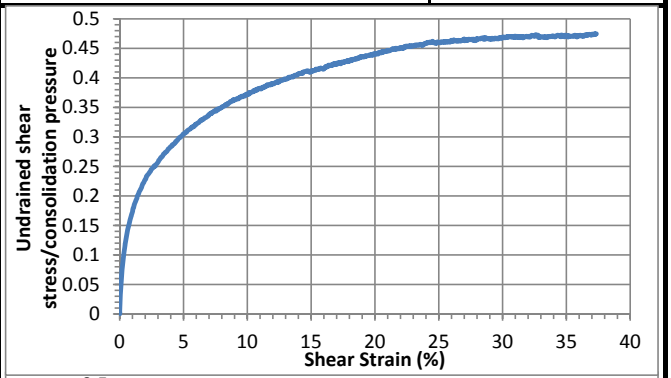

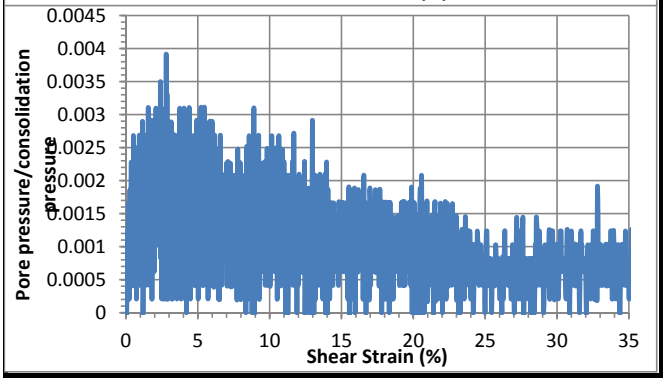

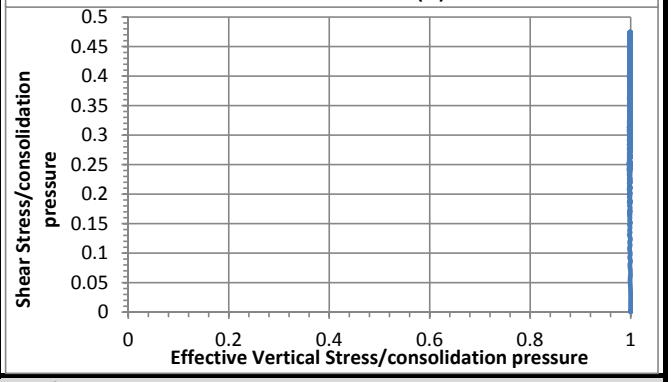

Shear wave velocity				
Signal type	Sinusoidal	First rise	initiation time (ms)	-0.0205
Signal amplitude (Vpp)	90		arrival time (ms)	0.5171
Signal frequency (kHz)	2.5		Vs (m/s)	211
Sensor spacing (mm)	113.21	First peak	initiation time (ms)	0.0870
R+P average Vs (m/s)	211		arrival time (ms)	0.6246
Stdev. (m/s)	0		Vs (m/s)	211
P+V average Vs (m/s)	222	First valley	initiation time (ms)	0.2867
Stdev. (m/s)	16		arrival time (ms)	0.7731
Wavelength (m)	0.089		Vs (m/s)	233
Spacing/wavelength	1.3			

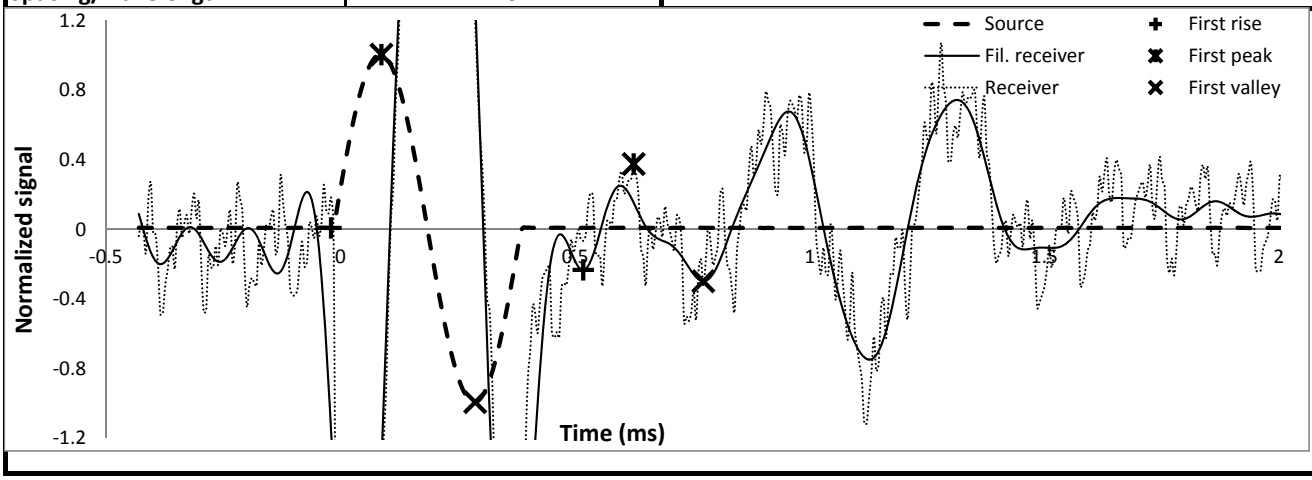

CSS Monotonic Shear Test Report

10/28/2013_Version 8.0

Geotechnical Engineering Laboratory

General Test Information and Sample Preparation			
Device:	CSS	**Layers:**	7.75
Specimen ID:	LCF	**Weight/layer (kg):**	1.33
Test ID:	CAF5	**Height/layer (mm):**	25.4
Date of Test:	9/15/2014	**Total height (mm):**	196.85
Test Performed:	Monotonic Shear	**Soil-Only Specimen Diameter (mm):**	306.2
Test Material:	MSW	**Total weight (kg):**	10.3075
Sample Preparation:	The same initial composition and unit weight as Sim. #5. Staged pre-compress for 23 hours, consolidate for 1 hour.	**Density (kg/m^3):**	711
		Membrane Thickness (mm):	0.000635
		Moisture Content (%):	23.5
		Saturated (Y/N):	N
		Prepared by:	Fei

Pre-compression Stage			
Pre-compression strain:	0.22	**Secondary compression ratio:**	
Height (mm):	184.2	**Density (kg/m3):**	760

Consolidation Stage		Shear Stage		
Initial height (mm):	135.5	**Type of Test:**		CU-strain
Initial density (kg/m3):	1032	**Shear Strain Rate (%/min):**		0.33
Vertical Stress (kPa):	94.3	**10% strain**	**Shear stress (kPa)**	31.5
Immediate strain (εimm, %)	38.8		**Tan friction angle (°)**	26.5
Consolidated Height (mm):	119.6		**Sin friction angle (°)**	29.9
Compression index (Ccε)	0.196	**30% strain**	**Shear stress (kPa)**	33.5
Consolidation modulus	5.2		**Tan friction angle (°)**	30.0
Consolidated density (kg/m^3):	1170		**Sin friction angle (°)**	35.2

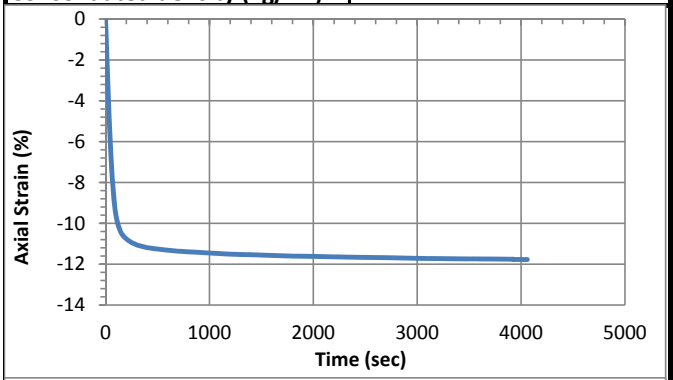

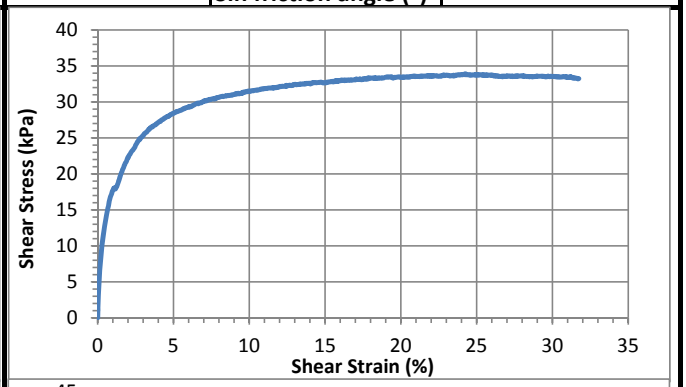

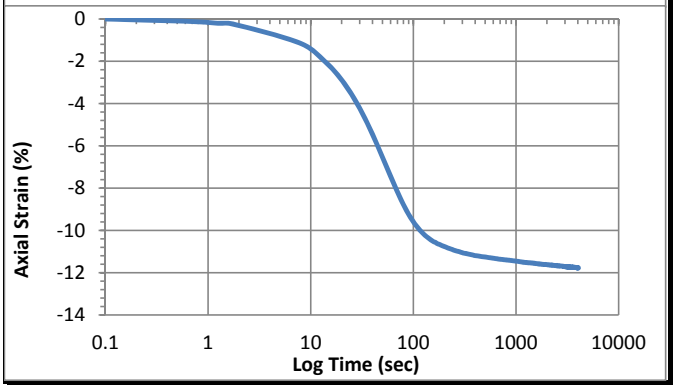

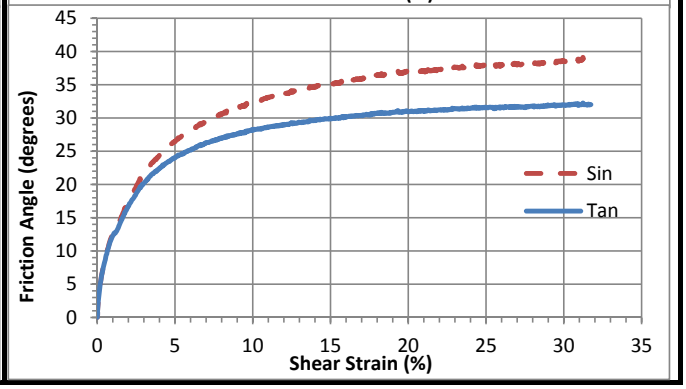

Undrained Strength			
Su/σv' at 10% strain	0.50	Su/σvc' at 10% strain	0.32
Su/σv' at 30% strain	0.58	Su/σvc' at 30% strain	0.34

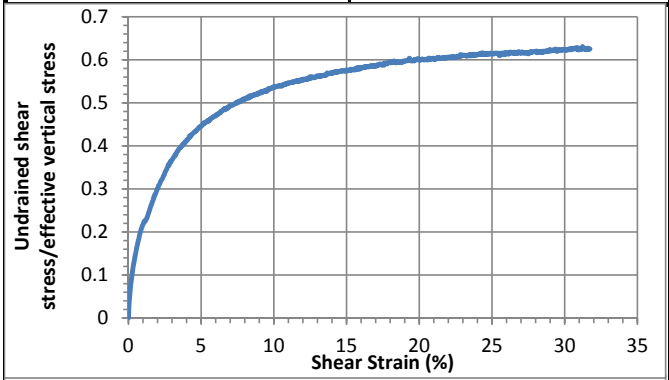

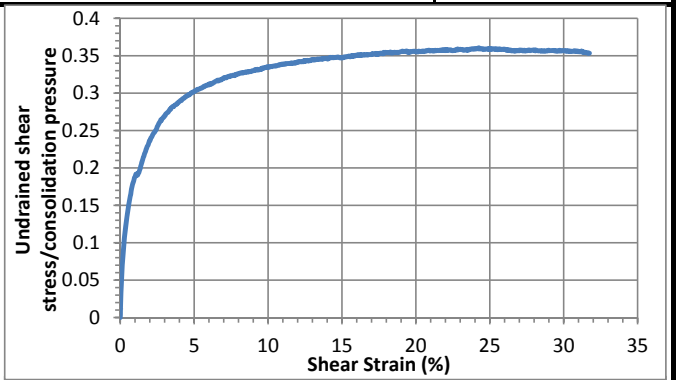

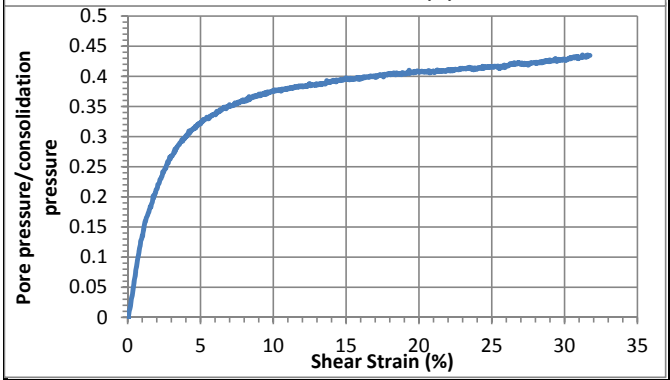

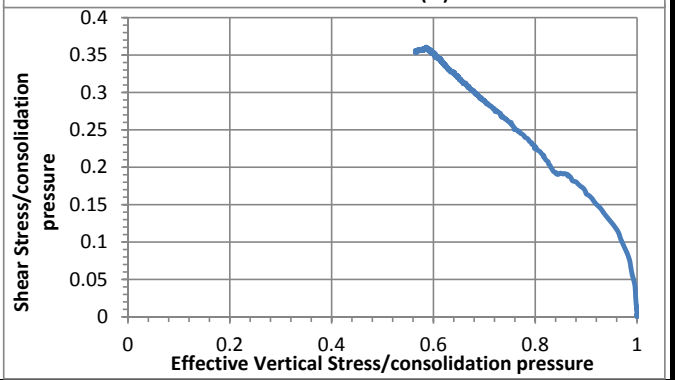

Shear wave velocity				
Signal type	Sinusoidal	First rise	initiation time (ms)	-0.0102
Signal amplitude (Vpp)	90		arrival time (ms)	0.4915
Signal frequency (kHz)	4.0		Vs (m/s)	221
Sensor spacing (mm)	110.84	First peak	initiation time (ms)	0.0563
R+P average Vs (m/s)	221		arrival time (ms)	0.5581
Stdev. (m/s)	0		Vs (m/s)	221
P+V average Vs (m/s)	222	First valley	initiation time (ms)	0.1792
Stdev. (m/s)	2		arrival time (ms)	0.6758
Wavelength (m)	0.056		Vs (m/s)	223
Spacing/wavelength	2.0			

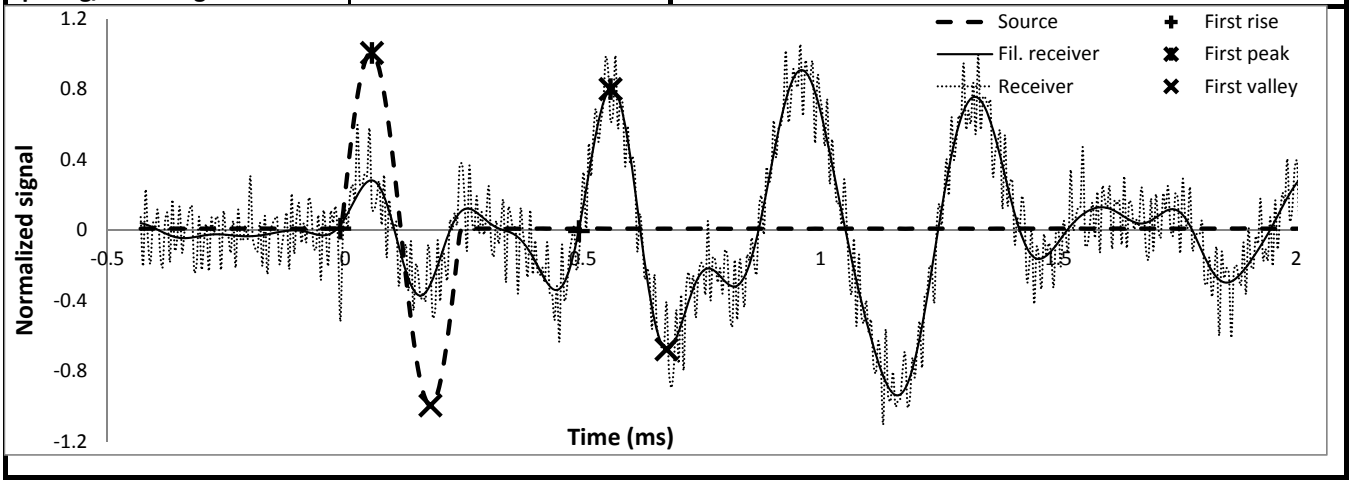

CSS Monotonic Shear Test Report

10/28/2013_Version 8.0

Geotechnical Engineering Laboratory

General Test Information and Sample Preparation			
Device:	CSS	**Layers:**	8.33
Specimen ID:	LCF	**Weight/layer (kg):**	1.33
Test ID:	CAF6	**Height/layer (mm):**	25.4
Date of Test:	9/18/2014	**Total height (mm):**	211.582
Test Performed:	Monotonic Shear	**Soil-Only Specimen Diameter (mm):**	306.2
Test Material:	MSW	**Total weight (kg):**	11.0789
Sample Preparation:	The same initial composition and unit weight as Sim. #5. Staged pre-compress for 23 hours, consolidate for 1 hour.	**Density (kg/m^3):**	711
		Membrane Thickness (mm):	0.000635
		Moisture Content (%):	23.5
		Saturated (Y/N):	N
		Prepared by:	Fei

Pre-compression Stage			
Pre-compression strain:	0.41	**Secondary compression ratio:**	0.00897
Height (mm):	127.9	**Density (kg/m3):**	1236

Consolidation Stage		Shear Stage		
Initial height (mm):	135.5	**Type of Test:**		CD-strain
Initial density (kg/m3):	1110	**Shear Strain Rate (%/min):**		0.35
Vertical Stress (kPa):	194.2	**10% strain**	**Shear stress (kPa)**	67.9
Immediate strain (εimm, %)	40.2		**Tan friction angle (°)**	19.2
Consolidated Height (mm):	115.7		**Sin friction angle (°)**	20.5
Compression index (Ccε)	0.183	**30% strain**	**Shear stress (kPa)**	86.8
Consolidation modulus	4.8		**Tan friction angle (°)**	24.0
Consolidated density (kg/m^3):	1300		**Sin friction angle (°)**	26.5

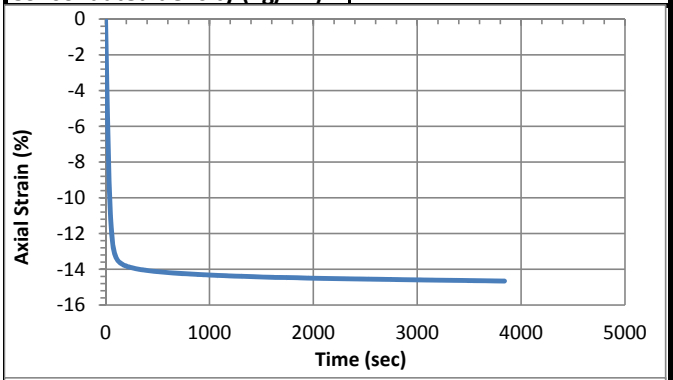

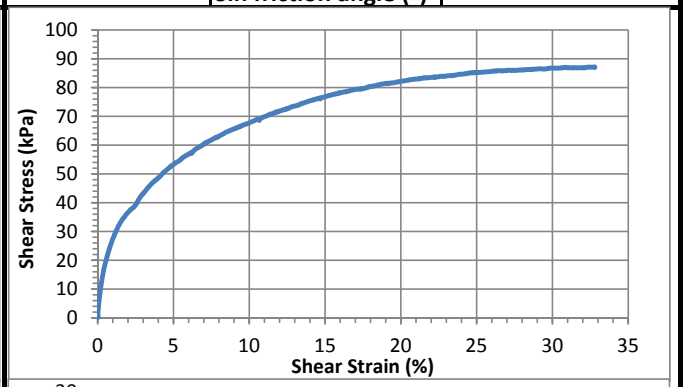

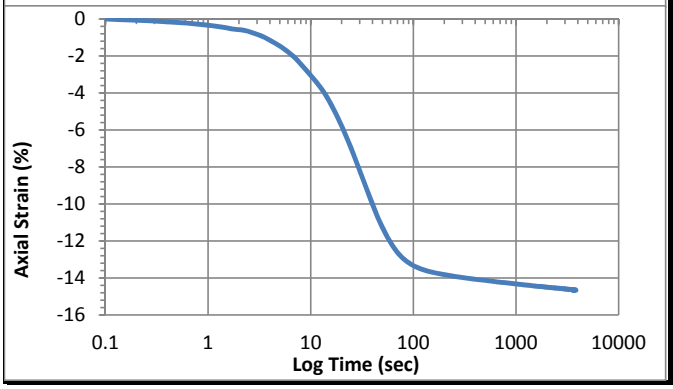

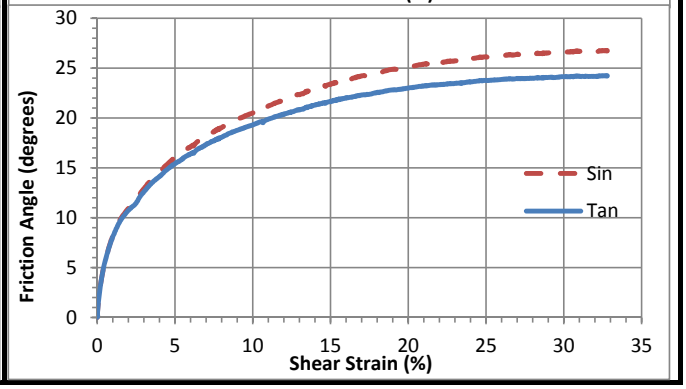

Undrained Strength			
Su/σv' at 10% strain	0.35	Su/σvc' at 10% strain	0.35
Su/σv' at 30% strain	0.45	Su/σvc' at 30% strain	0.45

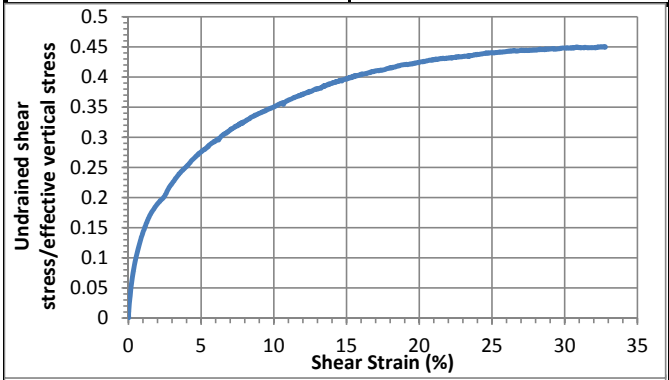

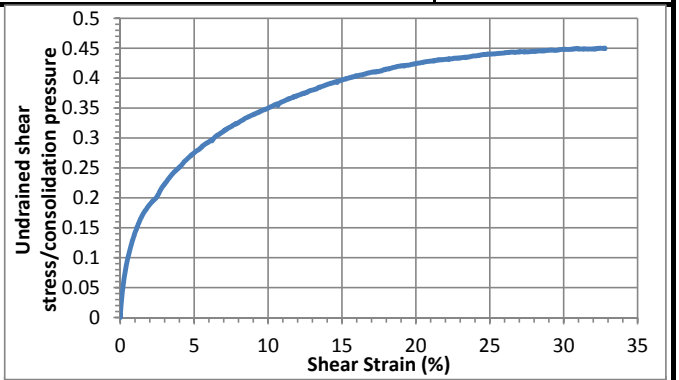

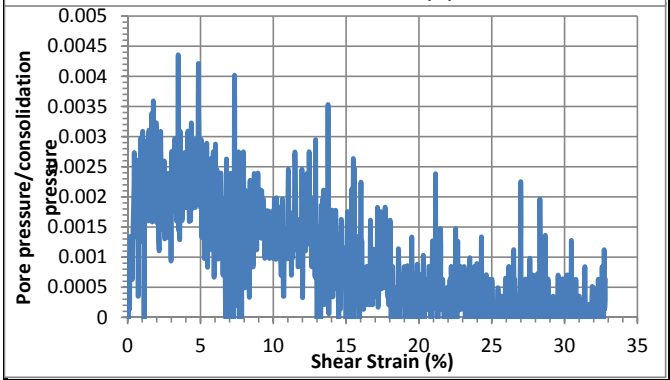

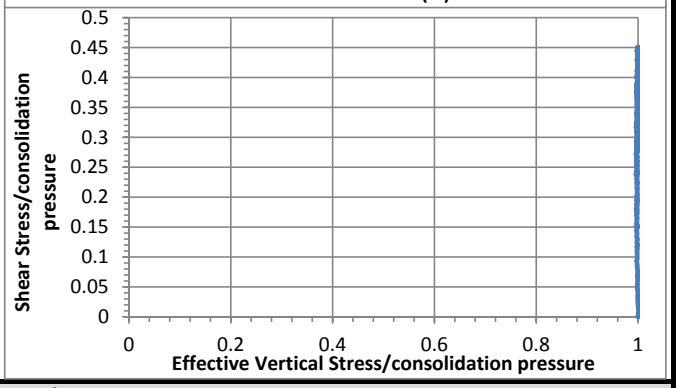

Shear wave velocity				
Signal type	Sinusoidal	First rise	initiation time (ms)	-0.0154
Signal amplitude (Vpp)	90		arrival time (ms)	0.3430
Signal frequency (kHz)	4		Vs (m/s)	298
Sensor spacing (mm)	106.90	First peak	initiation time (ms)	0.0512
R+P average Vs (m/s)	294		arrival time (ms)	0.4198
Stdev. (m/s)	6		Vs (m/s)	290
P+V average Vs (m/s)	299	First valley	initiation time (ms)	0.1792
Stdev. (m/s)	12		arrival time (ms)	0.5274
Wavelength (m)	0.075		Vs (m/s)	307
Spacing/wavelength	1.4			

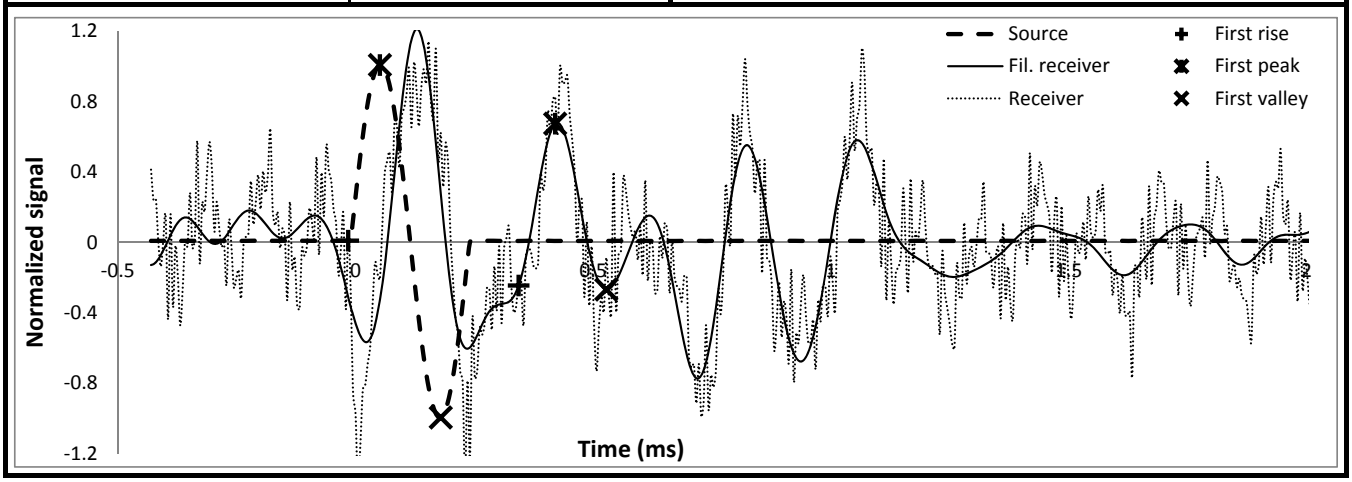

CSS Monotonic Shear Test Report

10/28/2013_Version 8.0

Geotechnical Engineering Laboratory

General Test Information and Sample Preparation			
Device:	CSS	**Layers:**	8.30
Specimen ID:	LCF	**Weight/layer (kg):**	1.33
Test ID:	CAF7	**Height/layer (mm):**	25.4
Date of Test:	9/21/2014	**Total height (mm):**	210.82
Test Performed:	Monotonic Shear	**Soil-Only Specimen Diameter (mm):**	306.2
Test Material:	MSW	**Total weight (kg):**	11.039
Sample Preparation:	The same initial composition and unit weight as Sim. #5. Staged pre-compress for 23 hours, consolidate for 1 hour.	**Density (kg/m^3):**	711
		Membrane Thickness (mm):	0.000635
		Moisture Content (%):	23.5
		Saturated (Y/N):	N
		Prepared by:	Fei

Pre-compression Stage			
Pre-compression strain:	0.42	**Secondary compression ratio:**	0.00818
Height (mm):	121.7	**Density (kg/m3):**	1232

Consolidation Stage		Shear Stage		
Initial height (mm):	135.3	**Type of Test:**		CU-strain
Initial density (kg/m3):	1108	**Shear Strain Rate (%/min):**		0.34
Vertical Stress (kPa):	196.4	**10% strain**	**Shear stress (kPa)**	54.8
Immediate strain (εimm, %)	42.3		**Tan friction angle (°)**	24.7
Consolidated Height (mm):	116.5		**Sin friction angle (°)**	27.3
Compression index (Ccε)	0.192	**30% strain**	**Shear stress (kPa)**	56.0
Consolidation modulus	4.5		**Tan friction angle (°)**	28.8
Consolidated density (kg/m^3):	1287		**Sin friction angle (°)**	33.3

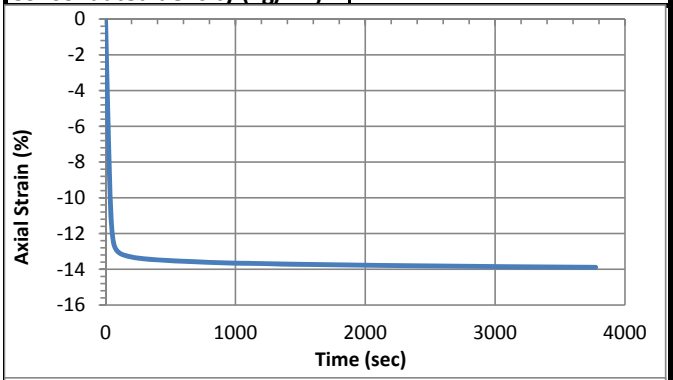

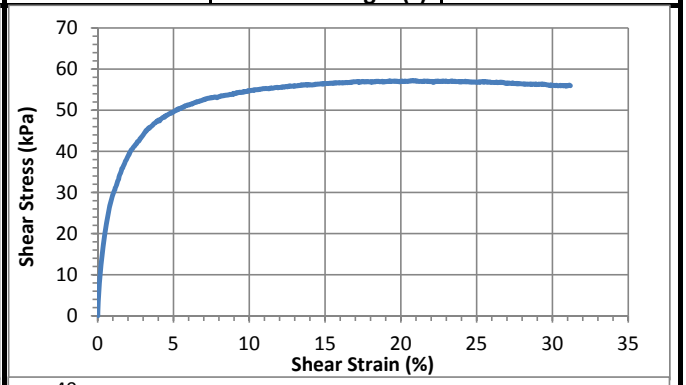

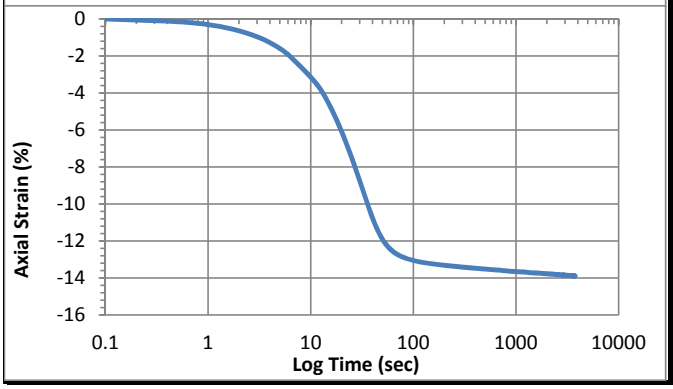

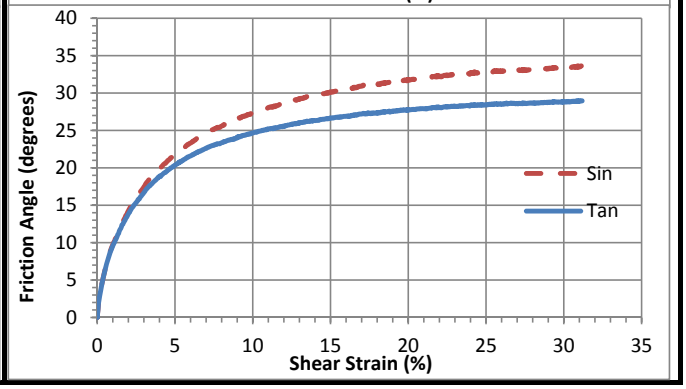

Undrained Strength			
Su/σv' at 10% strain	0.46	Su/σvc' at 10% strain	0.28
Su/σv' at 30% strain	0.55	Su/σvc' at 30% strain	0.29

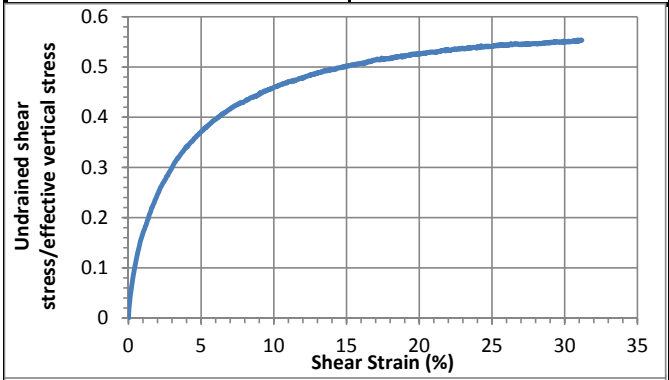

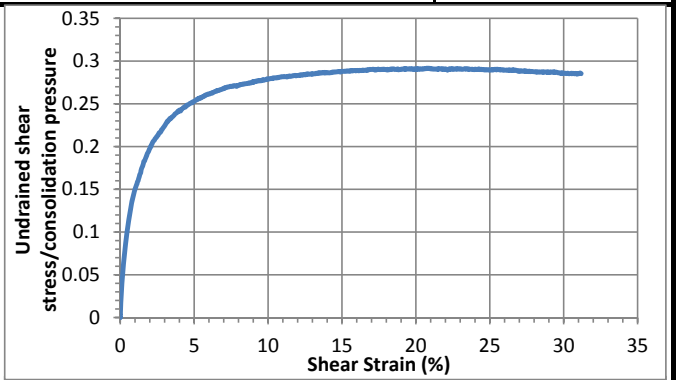

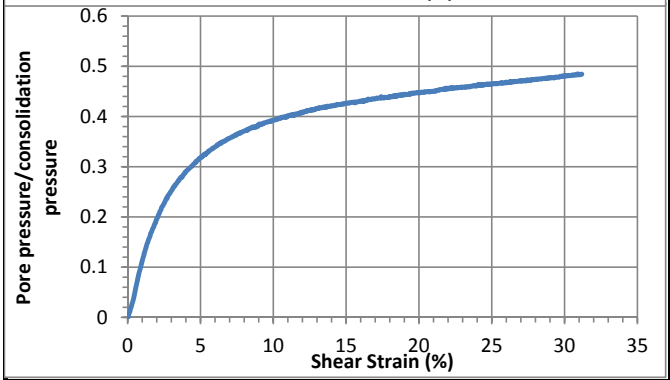

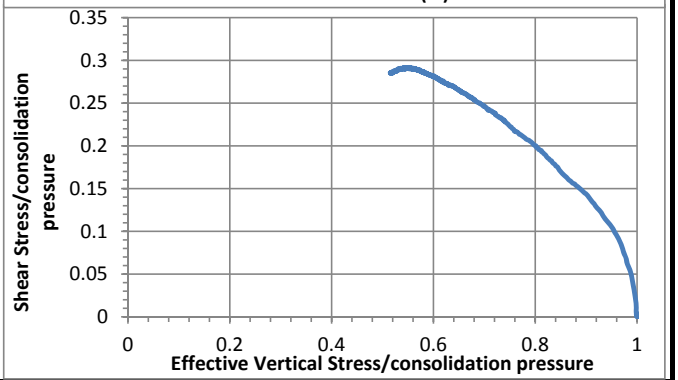

Shear wave velocity				
Signal type	Sinusoidal	First rise	initiation time (ms)	-0.0154
Signal amplitude (Vpp)	90		arrival time (ms)	0.3994
Signal frequency (kHz)	4.0		Vs (m/s)	260
Sensor spacing (mm)	107.68	First peak	initiation time (ms)	0.0512
R+P average Vs (m/s)	257		arrival time (ms)	0.4762
Stdev. (m/s)	4		Vs (m/s)	253
P+V average Vs (m/s)	255	First valley	initiation time (ms)	0.1741
Stdev. (m/s)	2		arrival time (ms)	0.5939
Wavelength (m)	0.064		Vs (m/s)	256
Spacing/wavelength	1.7			

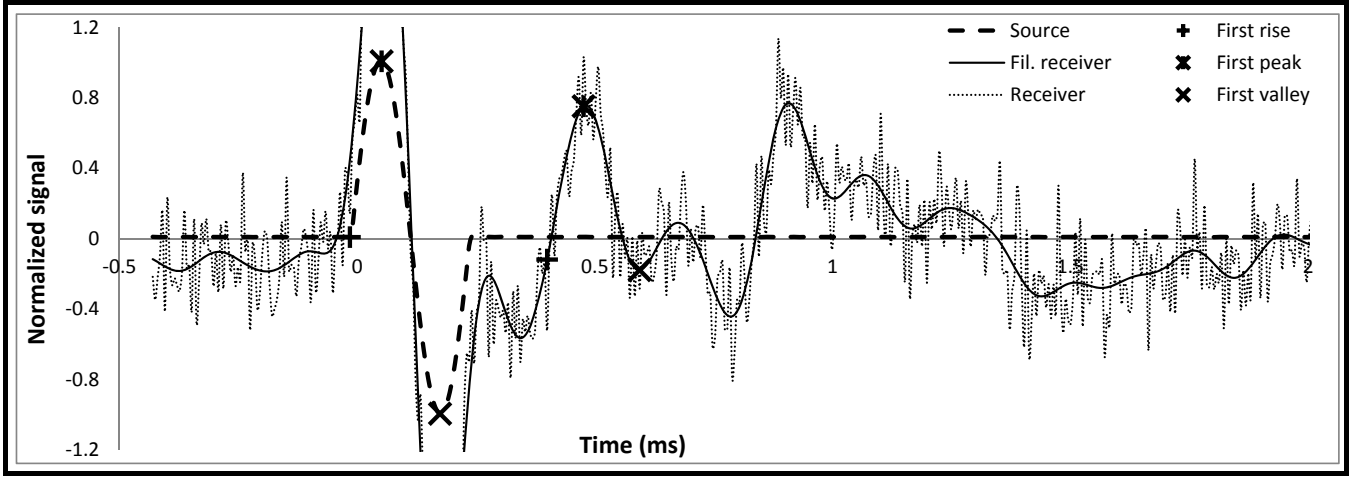

CSS Monotonic Shear Test Report

10/28/2013_Version 8.0

Geotechnical Engineering Laboratory

General Test Information and Sample Preparation			
Device:	CSS	**Layers prior to shear:**	8.80
Specimen ID:	CA-LCF	**Weight/layer (kg):**	1.33
Test ID:	CAF8	**Height/layer (mm):**	25.4
Date of test:	9/24/2014	**As-prepared height (mm):**	220.7
Test performed:	Monotonic Shear	**Soil-only specimen diameter (mm):**	306.2
Test material:	MSW	**Total weight (kg):**	11.70
Sample preparation:	The same initial composition and unit weight as Sim. #5. Staged pre-compress for 23 hours, consolidate for 1 hour.	**As-prepared density (kg/m^3):**	720
		Membrane thickness (mm):	0.000635
		Moisture content (%):	23.5
		Saturated (Y/N):	N
		Prepared by:	Fei

Pre-compression Stage			
Pre-compressed strain (%):	48.7	**Secondary compression ratio:**	0.00736
Pre-compressed height (mm):	113.3	**Pre-compressed density (kg/m3):**	1403

Consolidation Stage		Shear Stage		
Initial height (mm):	132.6	**Type of test:**		CU-strain
Initial density (kg/m3):	1198	**Shear strain rate (%/min):**		0.37
Vertical Stress (kPa):	394.5	**10% strain**	**Shear stress (kPa)**	106.4
Immediate strain (εimm, %)	48.5		**Tan friction angle (°)**	23.8
Strain before shear (εall, %)	50.7		**Sin friction angle (°)**	26.1
Compression index (Ccε)	0.194	**30% strain**	**Shear stress (kPa)**	109.1
Constrained modulus	4.0		**Tan friction angle (°)**	28.1
Consolidated density (kg/m^3):	1459		**Sin friction angle (°)**	32.3

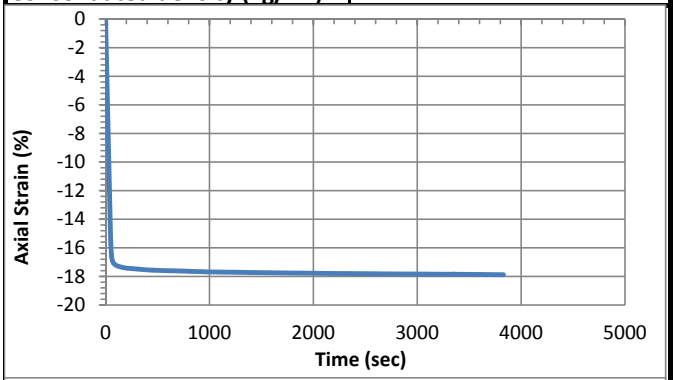

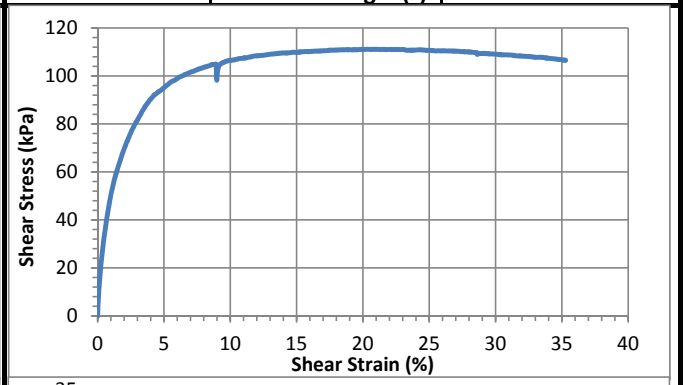

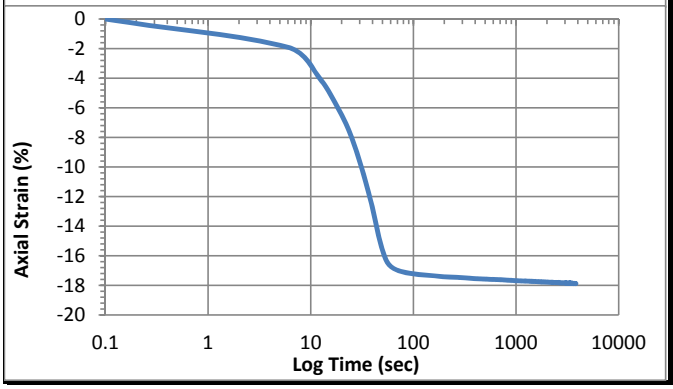

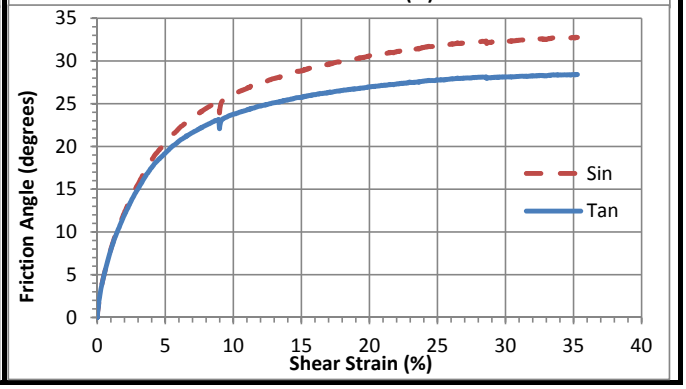

Strength			
τ/σv' at 10% strain	0.44	τ/σv0' at 10% strain	0.27
τ/σv' at 30% strain	0.53	τ/σv0' at 30% strain	0.28

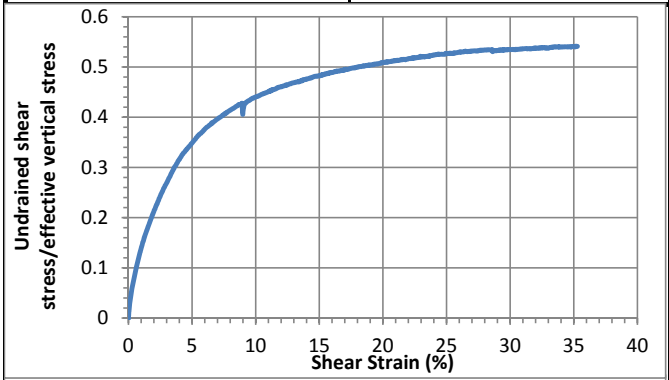

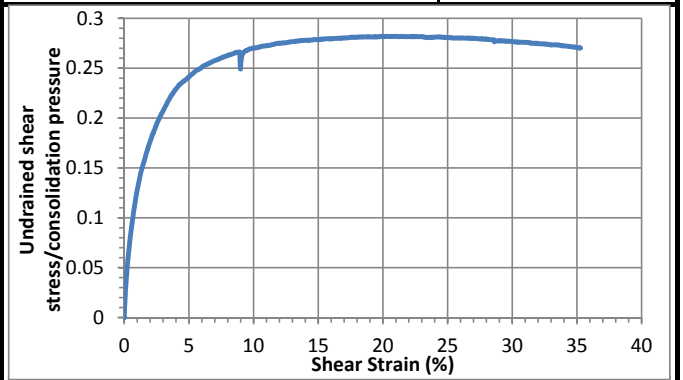

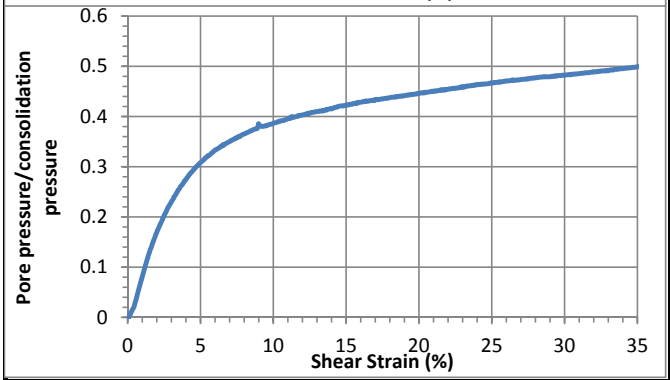

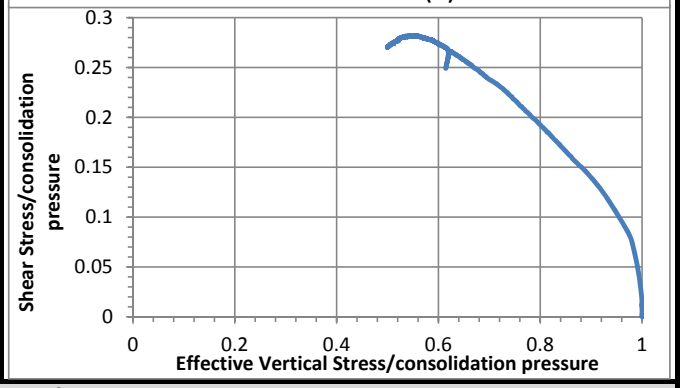

Shear wave velocity				
Signal type	Sinusoidal	First rise	initiation time (ms)	-0.0154
Signal amplitude (Vpp)	90		arrival time (ms)	0.2816
Signal frequency (kHz)	4		Vs (m/s)	337
Sensor spacing (mm)	100.13	First peak	initiation time (ms)	0.0512
R+P average Vs (m/s)	350		arrival time (ms)	0.3277
Stdev. (m/s)	18		Vs (m/s)	362
P+V average Vs (m/s)	359	First valley	initiation time (ms)	0.1741
Stdev. (m/s)	5		arrival time (ms)	0.4557
Wavelength (m)	0.090		Vs (m/s)	356
Spacing/wavelength	1.1			

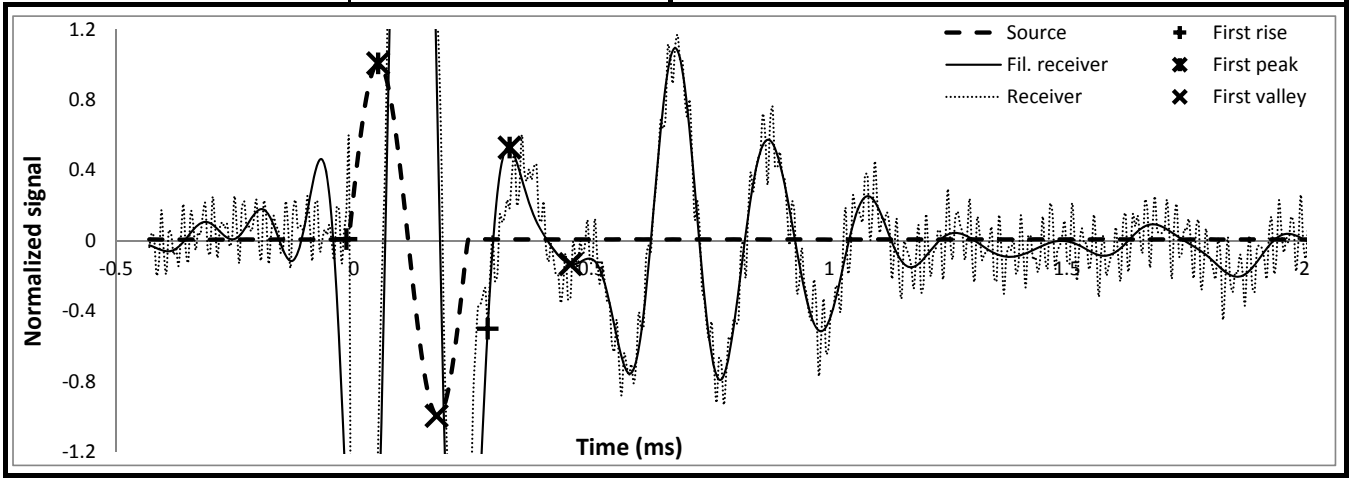

CSS Monotonic Shear Test Report

10/28/2013_Version 8.0

Geotechnical Engineering Laboratory

General Information		Sample Preparation	
Device:	CSS	Layers prior to shear:	8.00
Specimen ID:	CA-LCF	Weight/layer (kg):	1.33
Test ID:	CAF9	Height/layer (mm):	25.4
Date of Test:	12/5/2014	As-prepared height (mm):	125.5
Test Performed:	Monotonic Shear	Soil-only specimen diameter (mm):	306.2
Test Material:	MSW	Total weight (kg):	10.64
Sample Preparation:	The same initial composition as Sim. #5. Compacted. Pre-compress for 23 hours, consolidate for 1 hour.	As-prepared density (kg/m^3):	1007
		Membrane thickness (mm):	0.000635
		Moisture content (%):	23.5
		Saturated (Y/N):	N
		Prepared by:	Fei

Pre-compression Stage			
Pre-compressed strain (%):	22.1	Secondary compression ratio:	0.00629
Pre-compressed height (mm):	97.8	Pre-compressed density (kg/m3):	1292

Consolidation Stage		Shear Stage		
Initial height (mm):	135.4	Type of test:		CL-strain
Initial density (kg/m3):	1067	Shear strain rate (%/min):		0.34
Vertical Stress (kPa):	47.0	10% strain	Shear stress (kPa)	23.9
Immediate strain (εimm, %)	18.8		Tan friction angle (°)	27.4
Strain before shear (εall, %)	19.4		Sin friction angle (°)	31.0
Compression index (Ccε)	0.112	30% strain	Shear stress (kPa)	27.9
Constrained modulus	10.7		Tan friction angle (°)	30.8
Consolidated density (kg/m^3):	1249		Sin friction angle (°)	36.6

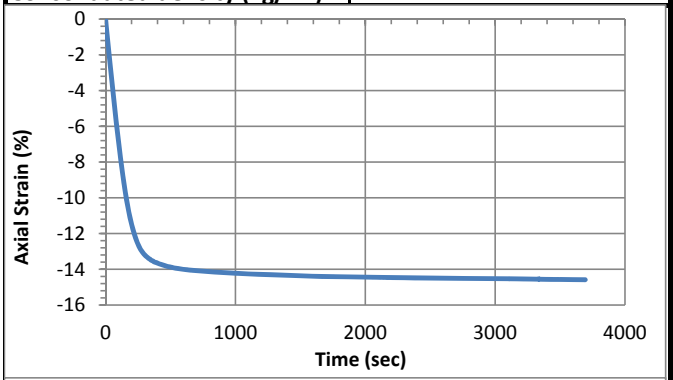

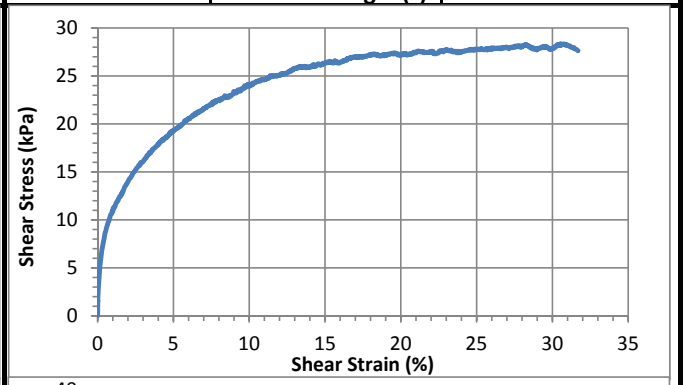

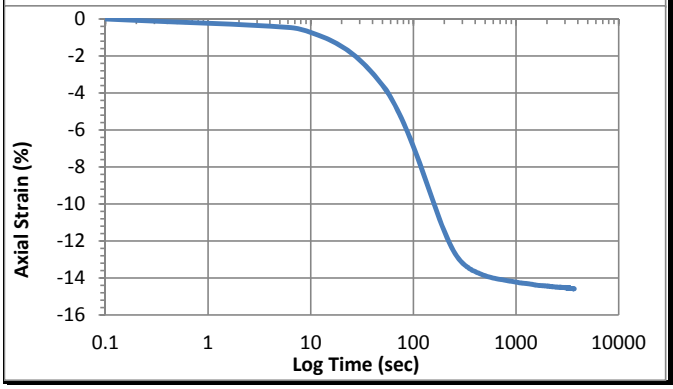

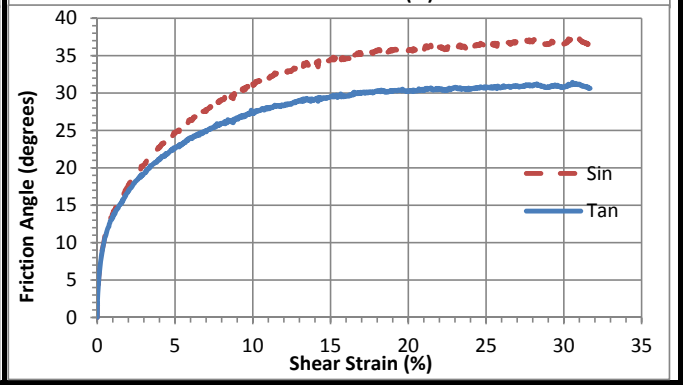

Strength			
τ/σv' at 10% strain	0.51	τ/σv0' at 10% strain	0.51
τ/σv' at 30% strain	0.60	τ/σv0' at 30% strain	0.60

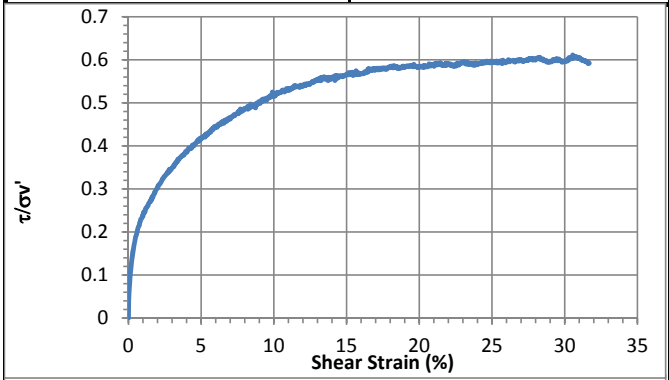

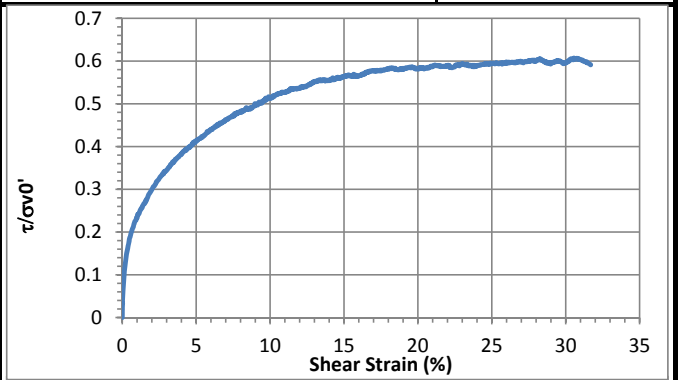

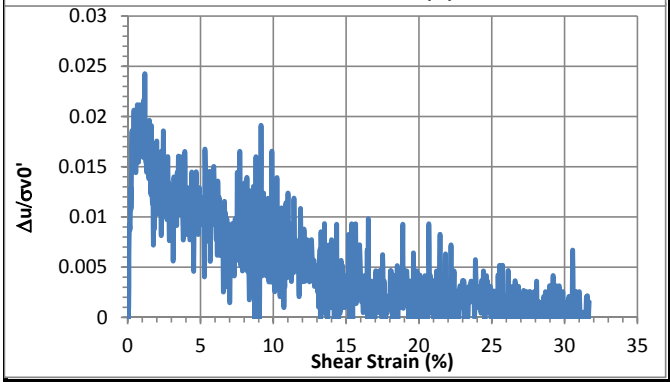

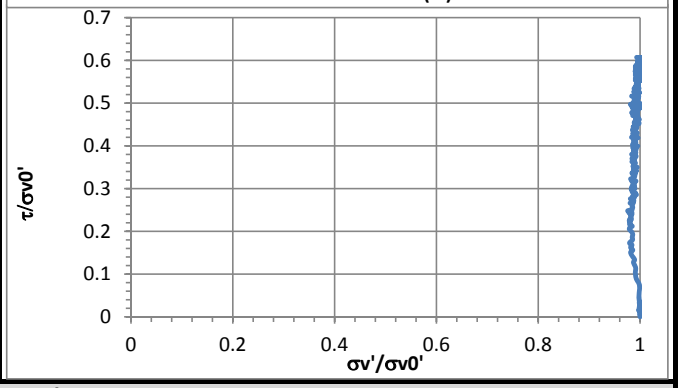

Shear wave velocity				
Signal type	Sinusoidal	First rise	initiation time (ms)	-0.0102
Signal amplitude (Vpp)	90		arrival time (ms)	0.6246
Signal frequency (kHz)	10		Vs (m/s)	168
Sensor spacing (mm)	106.88	First peak	initiation time (ms)	0.0205
R+P average Vs (m/s)	165		arrival time (ms)	0.6810
Stdev. (m/s)	5		Vs (m/s)	162
P+V average Vs (m/s)	162	First valley	initiation time (ms)	0.0717
Stdev. (m/s)	0		arrival time (ms)	0.7322
Wavelength (m)	0.016		Vs (m/s)	162
Spacing/wavelength	6.6			

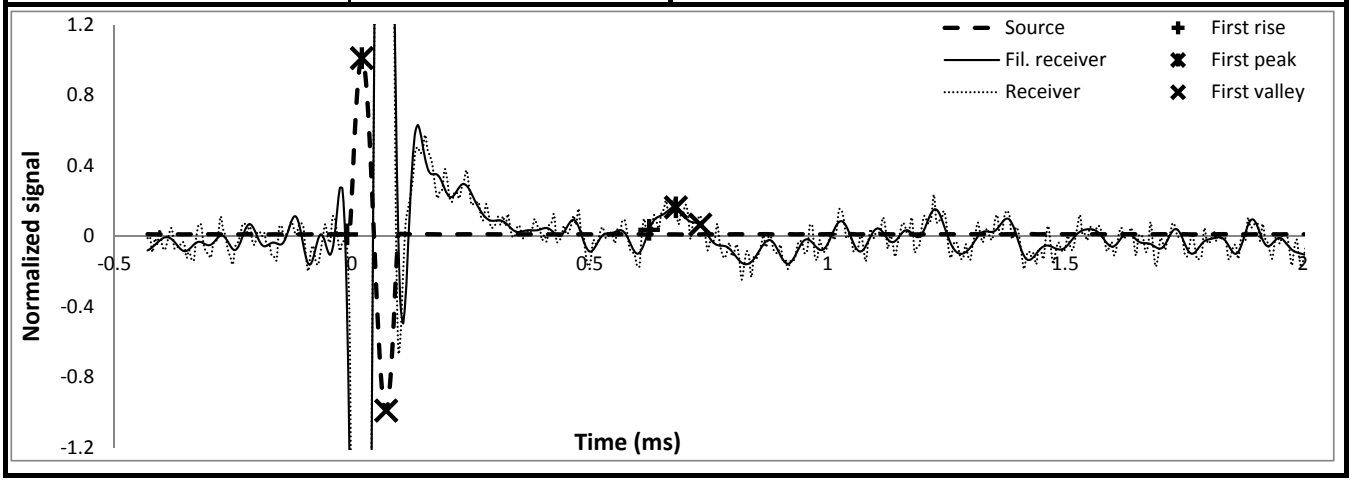

CSS Monotonic Shear Test Report

10/28/2013_Version 8.0

Geotechnical Engineering Laboratory

General Test Information and Sample Preparation

Device:	CSS	**Layers prior to shear:**	9.17
Specimen ID:	CA-LCF	**Weight/layer (kg):**	1.33
Test ID:	CAF11	**Height/layer (mm):**	25.4
Date of Test:	12/19/2014	**As-prepared height (mm):**	171.5
Test Performed:	Monotonic Shear	**Soil-only specimen diameter (mm):**	306.2
Test Material:	MSW	**Total weight (kg):**	12.20
Sample Preparation:	The same initial composition as Sim. #5. Compacted. Pre-compress for 23 hours, consolidate for 1 hour.	**As-prepared density (kg/m^3):**	1053
		Membrane thickness (mm):	0.000635
		Moisture content (%):	60.0
		Saturated (Y/N):	N
		Prepared by:	Fei

Pre-compression Stage

Pre-compressed strain (%):	20.0	**Secondary compression ratio:**	0.00516
Pre-compressed height (mm):	137.2	**Pre-compressed density (kg/m3):**	1316

Consolidation Stage

Initial height (mm):	137.7
Initial density (kg/m3):	1203
Vertical Stress (kPa):	97.5
Immediate strain (εimm, %)	21.1
Strain before shear (εall, %)	21.5
Compression index (Cεε)	0.106
Constrained modulus	9.5
Consolidated density (kg/m^3):	1342

Shear Stage

Type of test:		CL-strain
Shear strain rate (%/min):		0.32
10% strain	**Shear stress (kPa)**	47.5
	Tan friction angle (°)	26.1
	Sin friction angle (°)	29.5
30% strain	**Shear stress (kPa)**	54.6
	Tan friction angle (°)	29.3
	Sin friction angle (°)	34.2

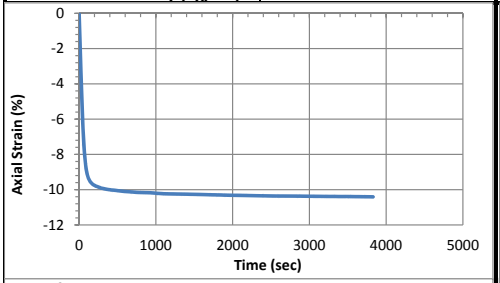

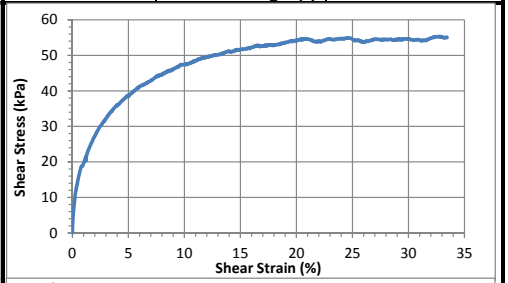

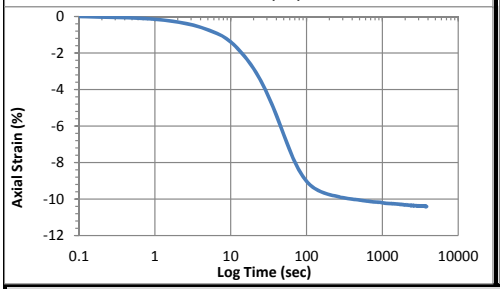

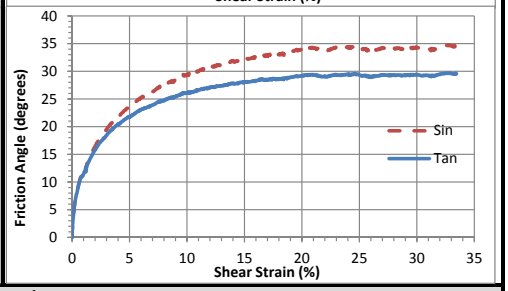

Strength

τ/σv' at 10% strain	0.49	**τ/σv0' at 10% strain**	0.49
τ/σv' at 30% strain	0.56	**τ/σv0' at 30% strain**	0.56

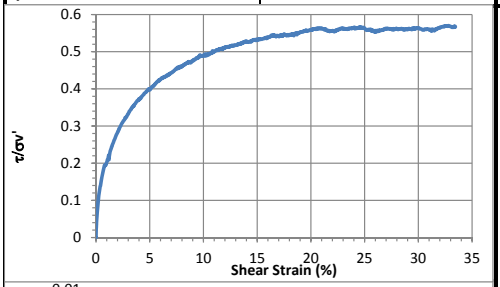

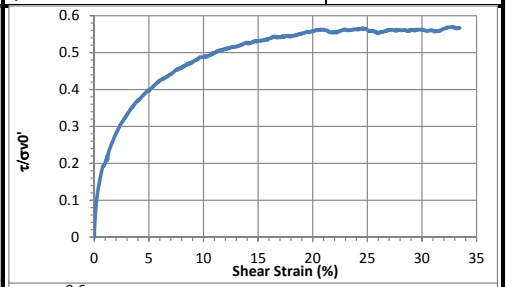

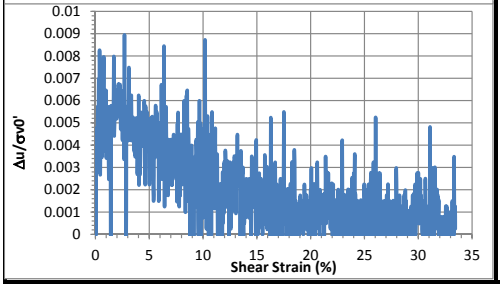

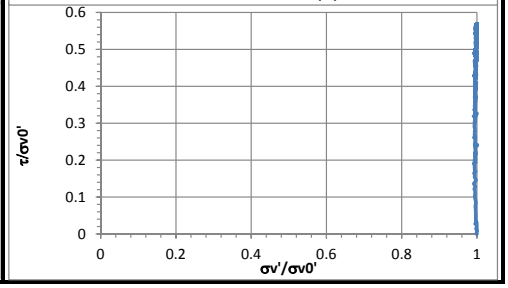

CSS Monotonic Shear Test Report

10/28/2013_Version 8.0

Geotechnical Engineering Laboratory

General Test Information and Sample Preparation			
Device:	CSS	**Layers prior to shear:**	9.36
Specimen ID:	CA-LCF	**Weight/layer (kg):**	1.33
Test ID:	CAF12	**Height/layer (mm):**	25.4
Date of Test:	12/21/2014	**As-prepared height (mm):**	181.6
Test Performed:	Monotonic Shear	**Soil-only specimen diameter (mm):**	306.2
Test Material:	MSW	**Total weight (kg):**	12.45
Sample Preparation:	The same initial composition as Sim. #5. Compacted. Pre-compress for 23 hours, consolidate for 1 hour.	**As-prepared density (kg/m^3):**	994
		Membrane thickness (mm):	0.000635
		Moisture content (%):	60.0
		Saturated (Y/N):	N
		Prepared by:	Fei

Pre-compression Stage			
Pre-compressed strain (%):	27.1	**Secondary compression ratio:**	0.00558
Pre-compressed height (mm):	132.3	**Pre-compressed density (kg/m3):**	1365

Consolidation Stage		Shear Stage		
Initial height (mm):	137.7	**Type of test:**		CL-strain
Initial density (kg/m3):	1227	**Shear strain rate (%/min):**		0.34
Vertical Stress (kPa):	198.1	**10% strain**	**Shear stress (kPa)**	80.8
Immediate strain (εimm, %)	30.2		**Tan friction angle (°)**	22.3
Strain before shear (εall, %)	30.9		**Sin friction angle (°)**	24.1
Compression index (Ccε)	0.131	**30% strain**	**Shear stress (kPa)**	97.6
Constrained modulus	6.6		**Tan friction angle (°)**	26.3
Consolidated density (kg/m^3):	1440		**Sin friction angle (°)**	29.6

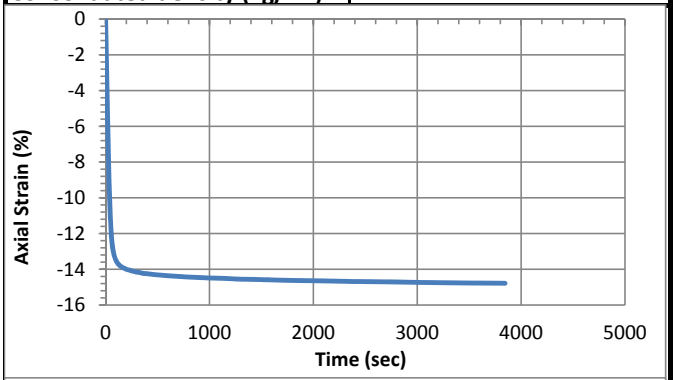

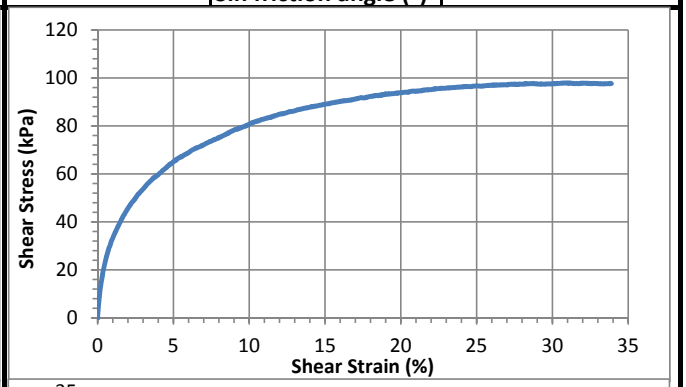

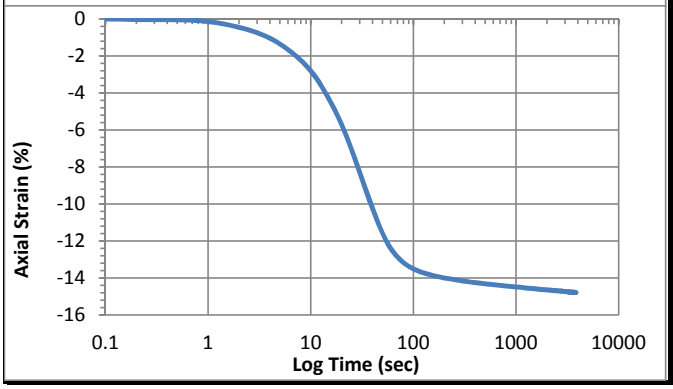

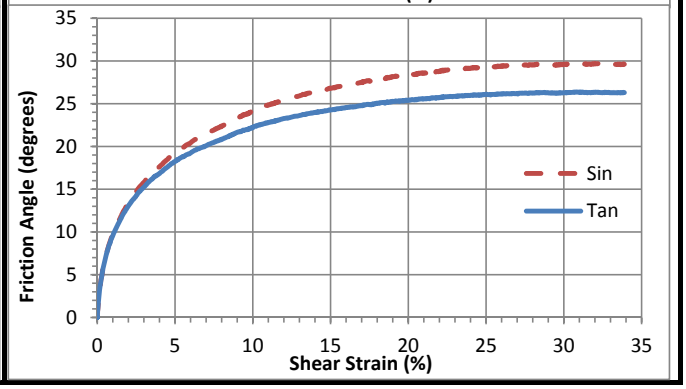

Strength			
τ/σv' at 10% strain	0.41	τ/σv0' at 10% strain	0.41
τ/σv' at 30% strain	0.49	τ/σv0' at 30% strain	0.49

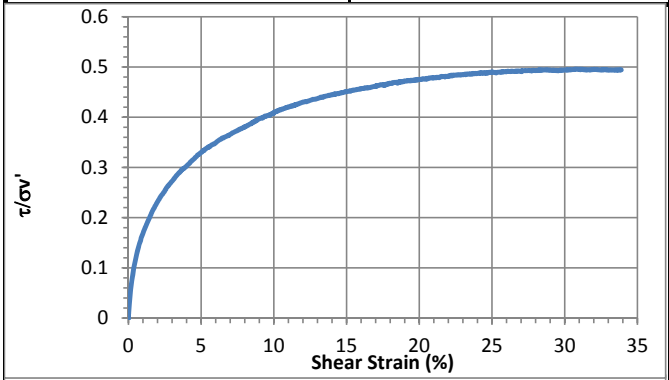

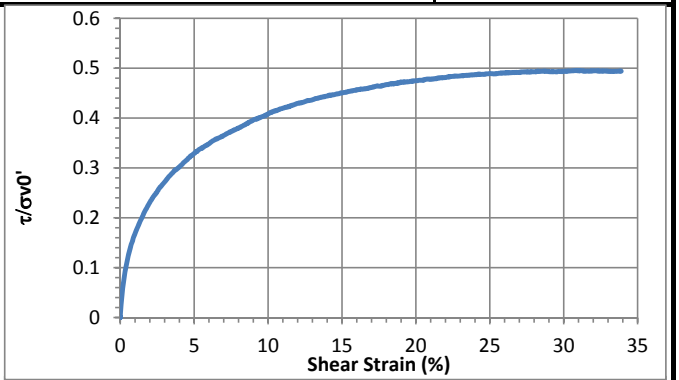

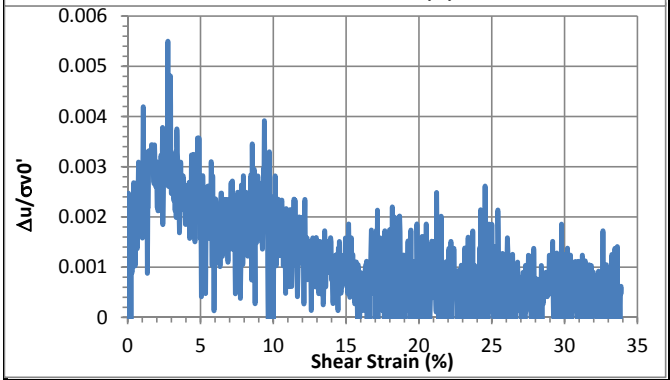

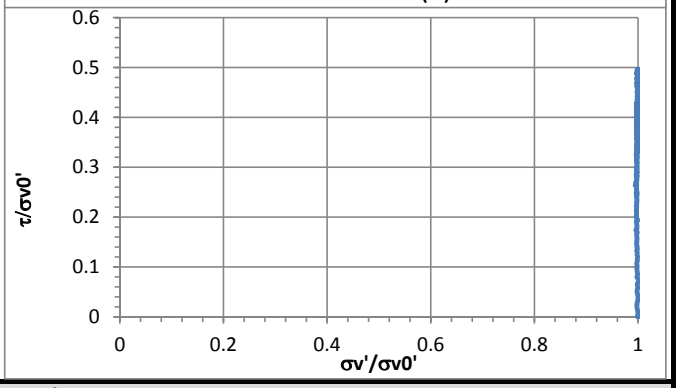

Shear wave velocity				
Signal type	Sinusoidal	First rise	initiation time (ms)	-0.0205
Signal amplitude (Vpp)	90		arrival time (ms)	0.0000
Signal frequency (kHz)	2		Vs (m/s)	5304
Sensor spacing (mm)	108.63	First peak	initiation time (ms)	0.1075
R+P average Vs (m/s)	2776		arrival time (ms)	0.5478
Stdev. (m/s)	3576		Vs (m/s)	247
P+V average Vs (m/s)	-28	First valley	initiation time (ms)	0.3584
Stdev. (m/s)	389		arrival time (ms)	0.0000
Wavelength (m)	-0.014		Vs (m/s)	-303
Spacing/wavelength	-7.7			

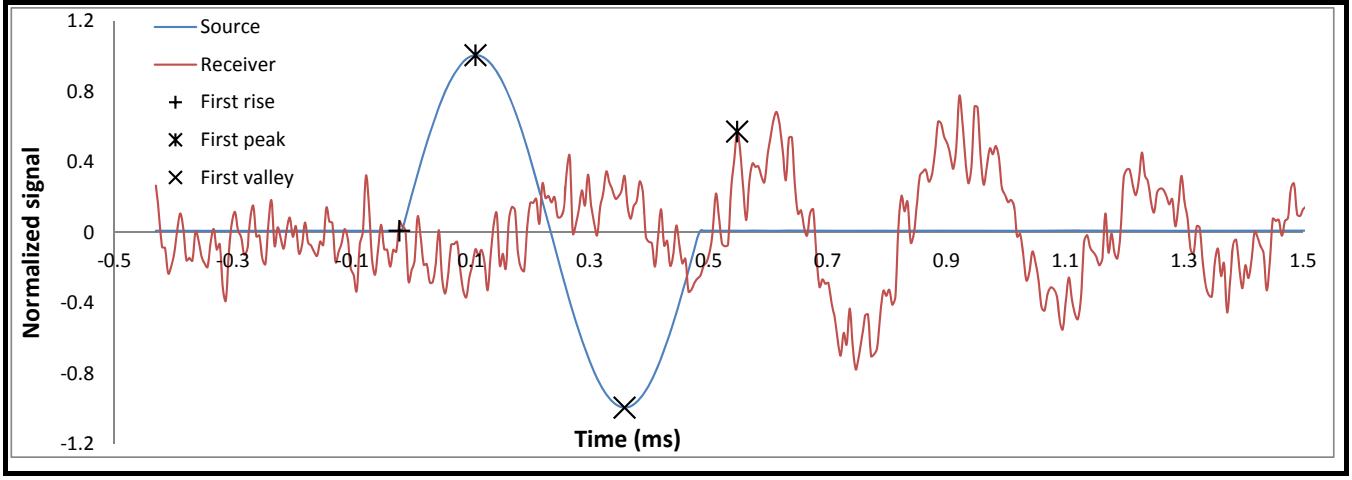

CSS Monotonic Shear Test Report

10/28/2013_Version 8.0

Geotechnical Engineering Laboratory

General Test Information and Sample Preparation			
Device:	CSS	**Layers prior to shear:**	10.20
Specimen ID:	CA-LCF	**Weight/layer (kg):**	1.33
Test ID:	CAF13	**Height/layer (mm):**	25.4
Date of test:	12/23/2014	**As-prepared height (mm):**	179.0
Test performed:	Monotonic Shear	**Soil-only specimen diameter (mm):**	306.2
Test material:	MSW	**Total weight (kg):**	13.57
Sample preparation:	The same initial composition as Sim. #5. Compacted. Pre-compress for 23 hours, consolidate for 1 hour.	**As-prepared density (kg/m^3):**	1029
		Membrane thickness (mm):	0.000635
		Moisture content (%):	60.0
		Saturated (Y/N):	N
		Prepared by:	Fei

Pre-compression Stage			
Pre-compressed strain (%):	32.8	**Secondary compression ratio:**	0.00938
Pre-compressed height (mm):	120.3	**Pre-compressed density (kg/m3):**	1531

Consolidation Stage		Shear Stage		
Initial height (mm):	135.3	**Type of test:**		CL-strain
Initial density (kg/m3):	1362	**Shear strain rate (%/min):**		0.34
Vertical Stress (kPa):	393.8	**10% strain**	**Shear stress (kPa)**	141.5
Immediate strain (εimm, %)	33.4		**Tan friction angle (°)**	19.8
Strain before shear (εall, %)	33.8		**Sin friction angle (°)**	21.1
Compression index (Cc̄ε)	0.129	**30% strain**	**Shear stress (kPa)**	166.4
Constrained modulus	6.0		**Tan friction angle (°)**	22.9
Consolidated density (kg/m^3):	1554		**Sin friction angle (°)**	25.0

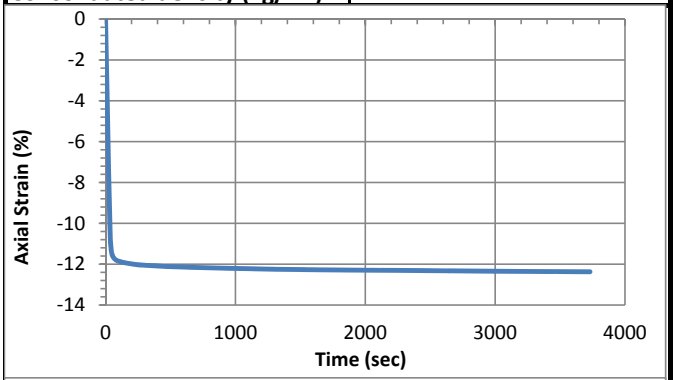

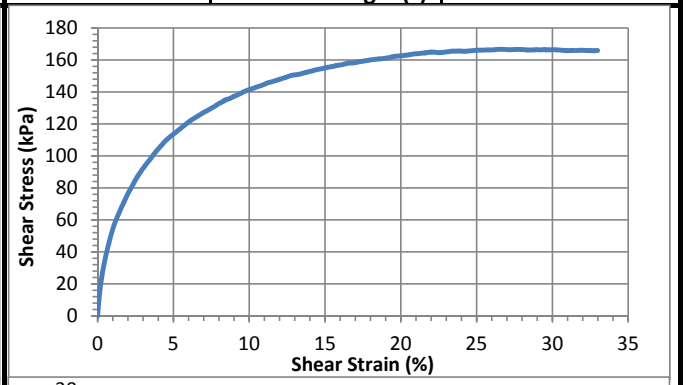

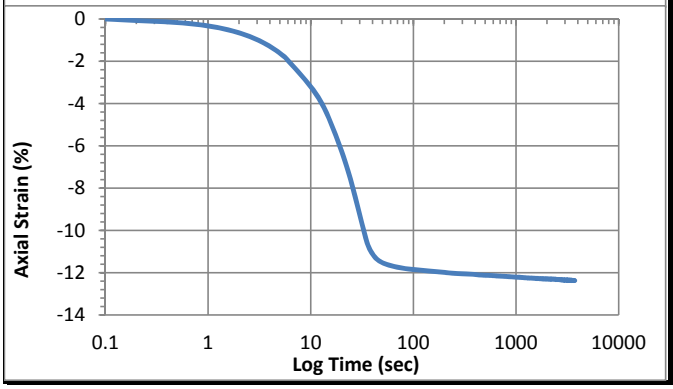

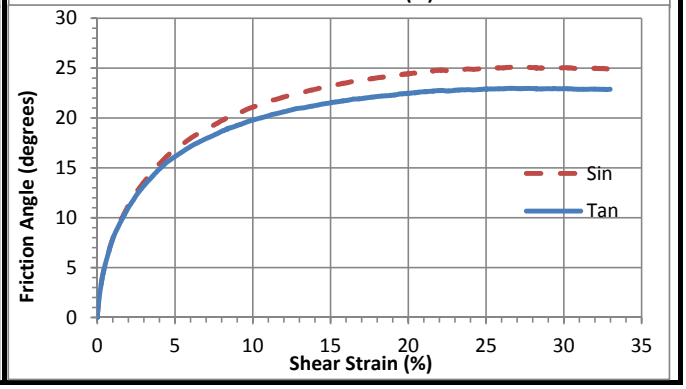

Strength			
τ/σv' at 10% strain	0.36	τ/σv0' at 10% strain	0.36
τ/σv' at 30% strain	0.42	τ/σv0' at 30% strain	0.42

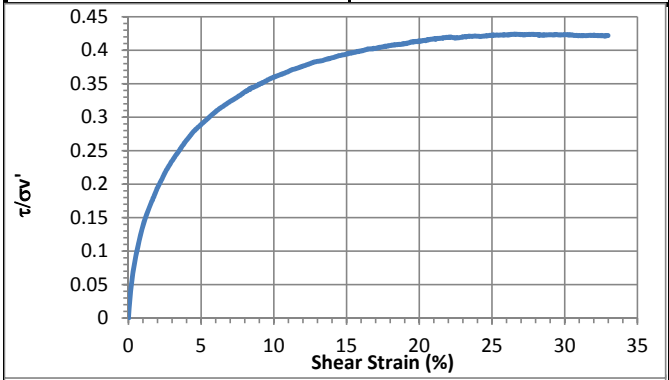

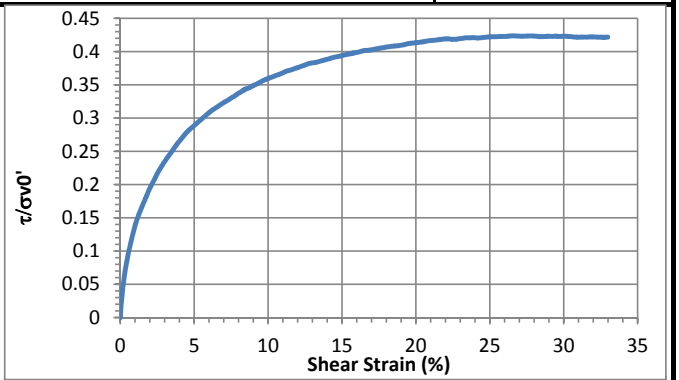

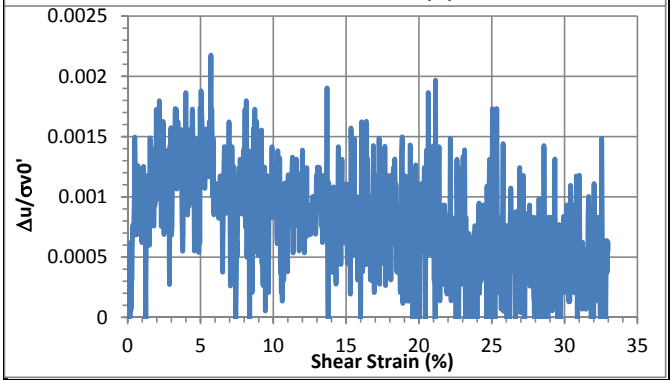

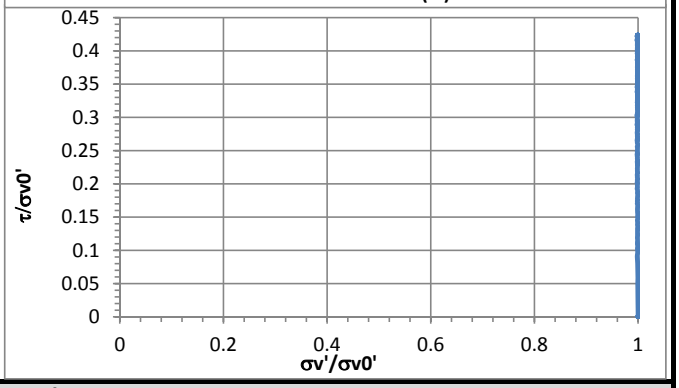

Shear wave velocity				
Signal type	Sinusoidal	First rise	initiation time (ms)	-0.0205
Signal amplitude (Vpp)	90		arrival time (ms)	0.2970
Signal frequency (kHz)	2		Vs (m/s)	373
Sensor spacing (mm)	118.50	First peak	initiation time (ms)	0.1075
R+P average Vs (m/s)	335		arrival time (ms)	0.5069
Stdev. (m/s)	54		Vs (m/s)	297
P+V average Vs (m/s)	321	First valley	initiation time (ms)	0.3584
Stdev. (m/s)	34		arrival time (ms)	0.7014
Wavelength (m)	0.161		Vs (m/s)	345
Spacing/wavelength	0.7			

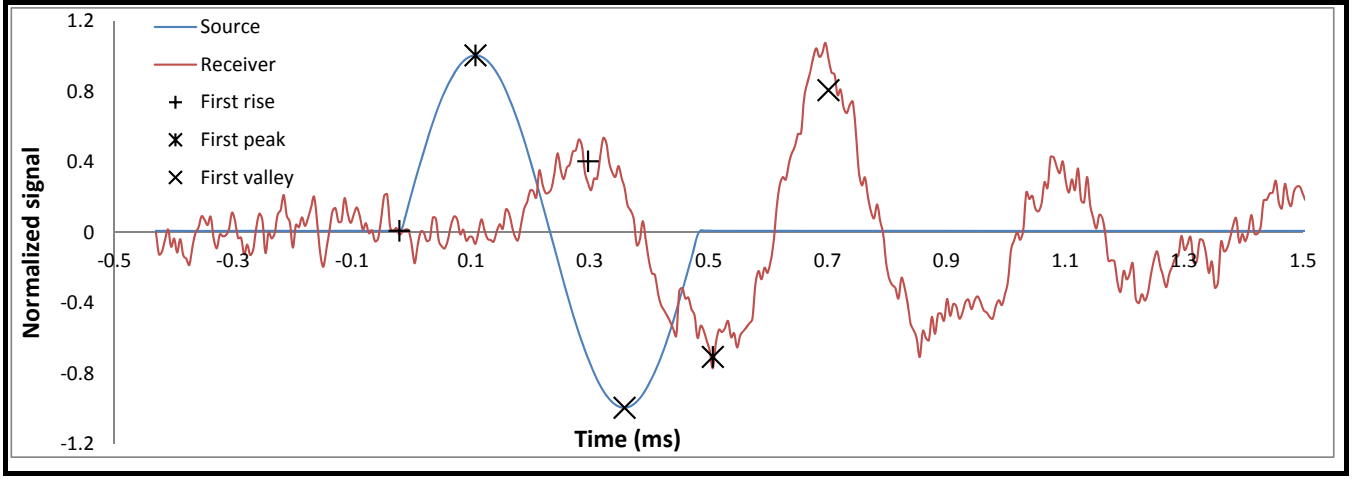

CSS Monotonic Shear Test Report

10/28/2013_Version 8.0

Geotechnical Engineering Laboratory

General Test Information and Sample Preparation

Device:	CSS	**Layers prior to shear:**	9.00
Specimen ID:	CA-LCF	**Weight/layer (kg):**	1.33
Test ID:	CAF14	**Height/layer (mm):**	25.4
Date of test:	1/23/2015	**As-prepared height (mm):**	152.8
Test performed:	Monotonic Shear	**Soil-only specimen diameter (mm):**	306.2
Test material:	MSW	**Total weight (kg):**	11.97
Sample preparation:	The same initial composition as Sim. #5. Compacted. Pre-compress for 23 hours, consolidate for 1 hour.	**As-prepared density (kg/m^3):**	1064
		Membrane thickness (mm):	0.000635
		Moisture content (%):	60.0
		Saturated (Y/N):	N
		Prepared by:	Fei

Pre-compression Stage

Pre-compressed strain (%):	23.7	**Secondary compression ratio:**	0.00534
Pre-compressed height (mm):	116.6	**Pre-compressed density (kg/m3):**	1394

Consolidation Stage

Initial height (mm):	127.7
Initial density (kg/m3):	1272
Vertical Stress (kPa):	96.5
Immediate strain (εimm, %)	22.9
Strain before shear (εall, %)	23.6
Compression index (Cεε)	0.115
Constrained modulus	8.7
Consolidated density (kg/m^3):	1392

Shear Stage

Type of Test:		CV-strain
Shear Strain Rate (%/min):		0.34
10% strain	**Shear stress (kPa)**	41.5
	Tan friction angle (°)	28.7
	Sin friction angle (°)	33.4
30% strain	**Shear stress (kPa)**	40.9
	Tan friction angle (°)	30.4
	Sin friction angle (°)	35.9

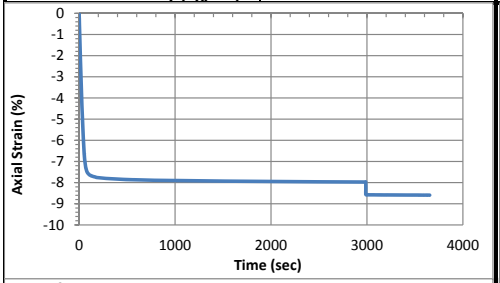

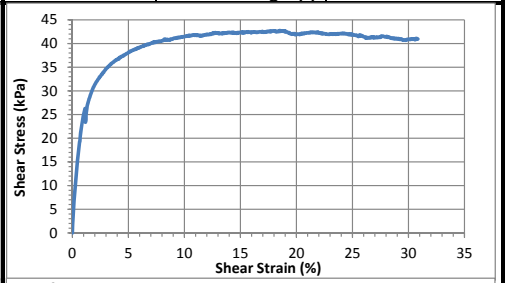

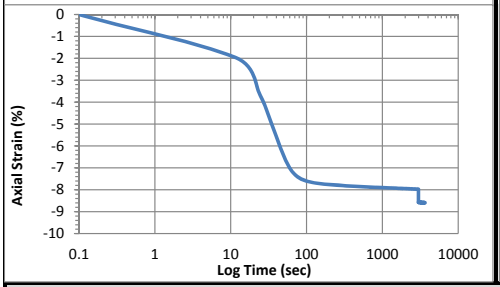

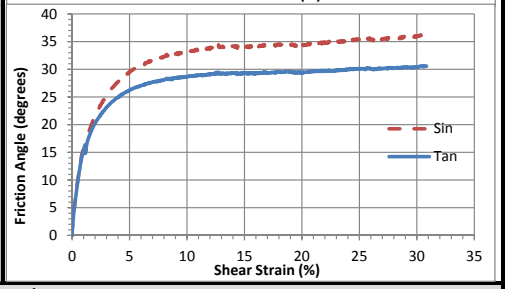

Strength

τ/σv' at 10% strain	0.54	**τ/σv0' at 10% strain**	0.43
τ/σv' at 30% strain	0.59	**τ/σv0' at 30% strain**	0.42

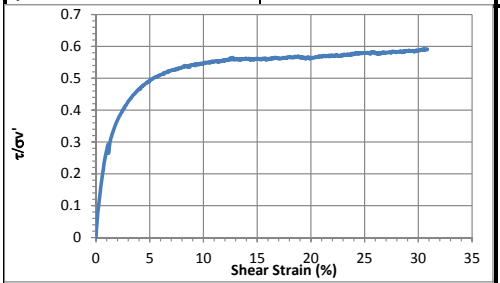

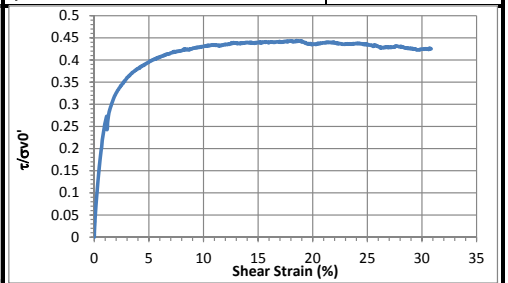

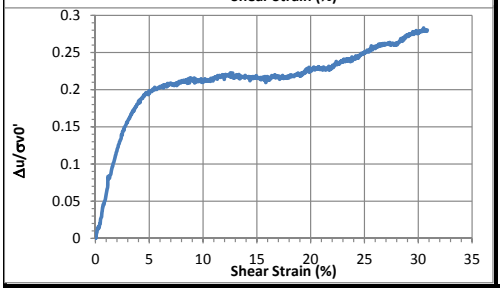

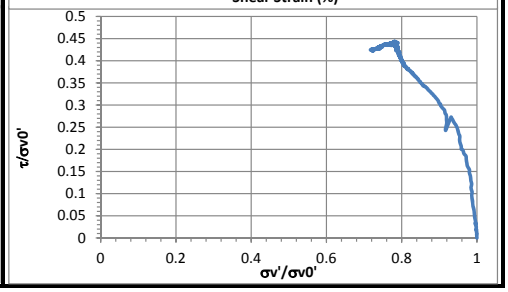

CSS Monotonic Shear Test Report

10/28/2013_Version 8.0

Geotechnical Engineering Laboratory

General Test Information and Sample Preparation

Device:	CSS	**Layers prior to shear:**	10.00
Specimen ID:	CA-LCF	**Weight/layer (kg):**	1.33
Test ID:	CAF15	**Height/layer (mm):**	25.4
Date of test:	1/28/2015	**As-prepared height (mm):**	171.6
Test performed:	Monotonic Shear	**Soil-only specimen diameter (mm):**	306.2
Test material:	MSW	**Total weight (kg):**	13.3
Sample preparation:	The same initial composition as Sim. #5. Compacted. Pre-compress for 23 hours, consolidate for 1 hour.	**As-prepared density (kg/m^3):**	1052
		Membrane thickness (mm):	0.000635
		Moisture content (%):	60.0
		Saturated (Y/N):	N
		Prepared by:	Fei

Pre-compression Stage

Pre-compressed strain (%):	25.4	**Secondary compression ratio:**	0.00713
Pre-compressed height (mm):	128.0	**Pre-compressed density (kg/m3):**	1410

Consolidation Stage

Initial height (mm):	137.8
Initial density (kg/m3):	1311
Vertical Stress (kPa):	197.7
Immediate strain (εimm, %)	26.2
Strain before shear (εall, %)	26.8
Compression index (Cεε)	0.114
Constrained modulus	7.6
Consolidated density (kg/m^3):	1437

Shear Stage

Type of test:		CV-strain
Shear strain rate (%/min):		0.32
10% strain	**Shear stress (kPa)**	61.6
	Tan friction angle (°)	26.1
	Sin friction angle (°)	29.4
30% strain	**Shear stress (kPa)**	62.7
	Tan friction angle (°)	28.5
	Sin friction angle (°)	32.9

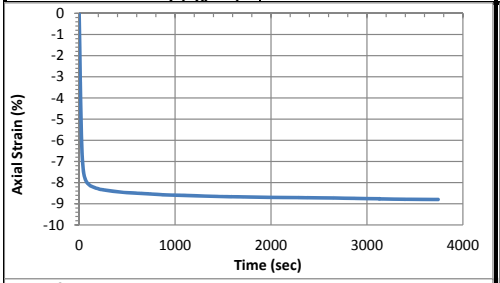

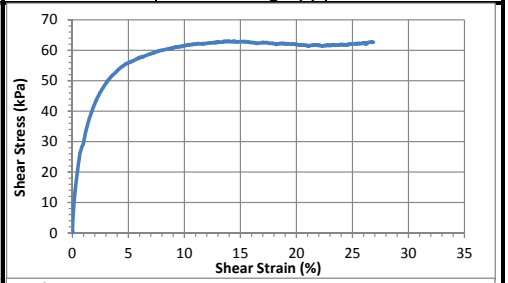

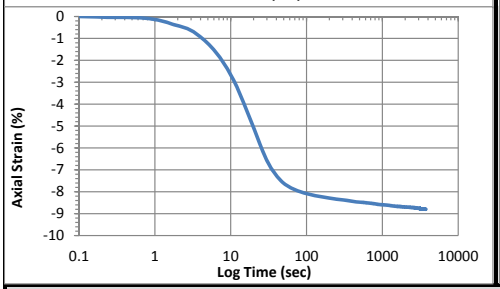

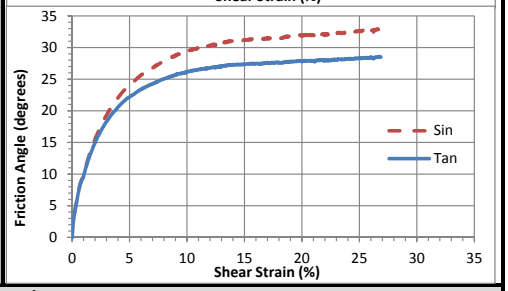

Strength

τ/σv' at 10% strain	0.49	**τ/σv0' at 10% strain**	0.31
τ/σv' at 30% strain	0.54	**τ/σv0' at 30% strain**	0.32

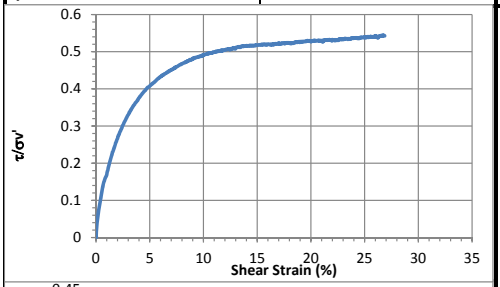

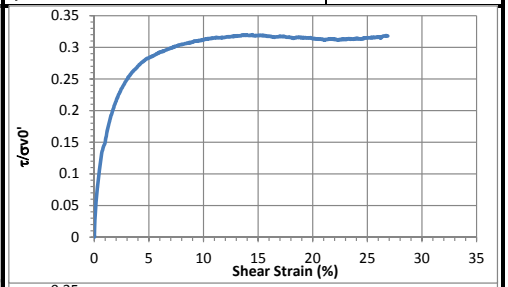

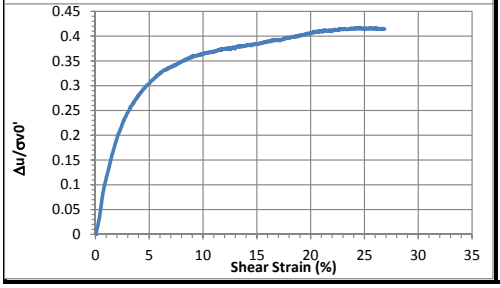

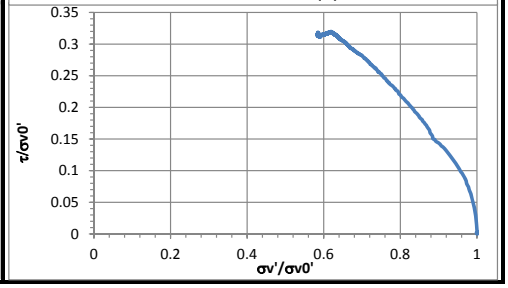

CSS Monotonic Shear Test Report

10/28/2013_Version 8.0

Geotechnical Engineering Laboratory

General Test Information and Sample Preparation			
Device:	CSS	**Layers prior to shear:**	10.14
Specimen ID:	CA-LCF	**Weight/layer (kg):**	1.33
Test ID:	CAF16	**Height/layer (mm):**	25.4
Date of test:	1/30/2015	**As-prepared height (mm):**	179.0
Test performed:	Monotonic Shear	**Soil-only specimen diameter (mm):**	306.2
Test material:	MSW	**Total weight (kg):**	13.49
Sample preparation:	The same initial composition as Sim. #5. Compacted. Pre-compress for 23 hours, consolidate for 1 hour.	**As-prepared density (kg/m^3):**	1023
		Membrane thickness (mm):	0.000635
		Moisture content (%):	60.0
		Saturated (Y/N):	N
		Prepared by:	Fei

Pre-compression Stage			
Pre-compressed strain (%):	32.8	**Secondary compression ratio:**	0.00938
Pre-compressed height (mm):	120.3	**Pre-compressed density (kg/m3):**	1522

Consolidation Stage		Shear Stage		
Initial height (mm):	137.7	**Type of test:**		CV-strain
Initial density (kg/m3):	1329	**Shear strain rate (%/min):**		0.33
Vertical Stress (kPa):	399.4	**10% strain**	**Shear stress (kPa)**	106.3
Immediate strain (εimm, %)	31.7		**Tan friction angle (°)**	20.8
Strain before shear (εall, %)	31.9		**Sin friction angle (°)**	22.3
Compression index (Cεε)	0.122	**30% strain**	**Shear stress (kPa)**	108.1
Constrained modulus	6.3		**Tan friction angle (°)**	22.0
Consolidated density (kg/m^3):	1501		**Sin friction angle (°)**	23.8

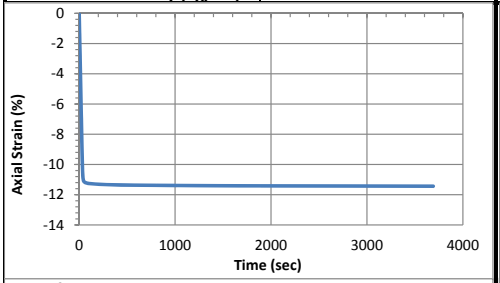

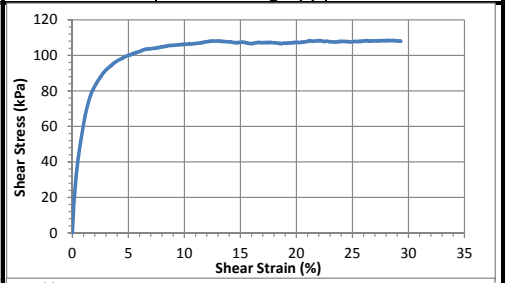

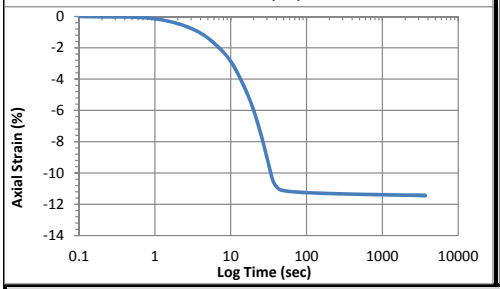

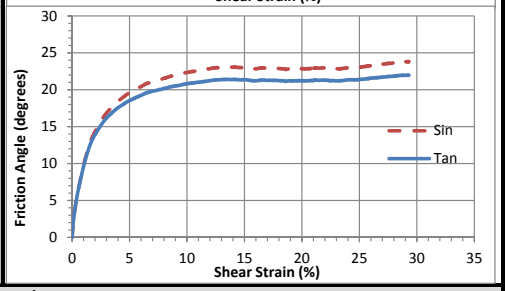

Strength			
τ/σv' at 10% strain	0.38	**τ/σv0' at 10% strain**	0.27
τ/σv' at 30% strain	0.40	**τ/σv0' at 30% strain**	0.27

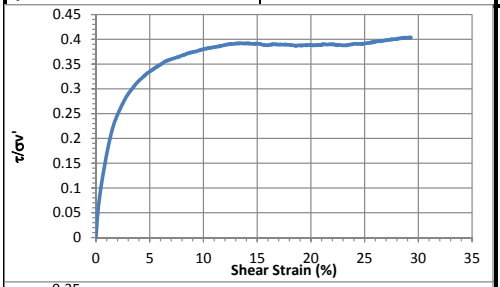

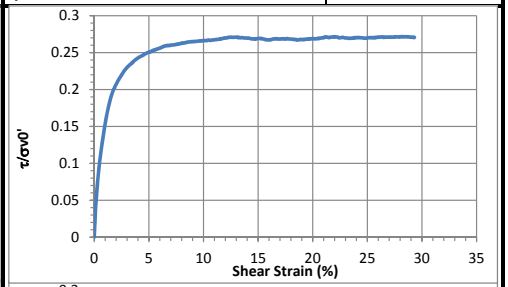

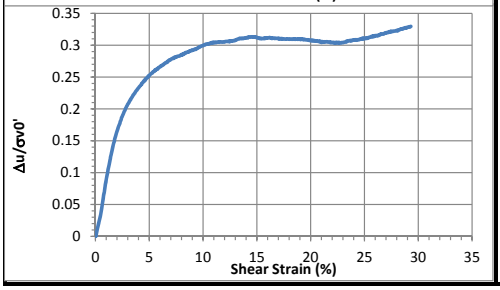

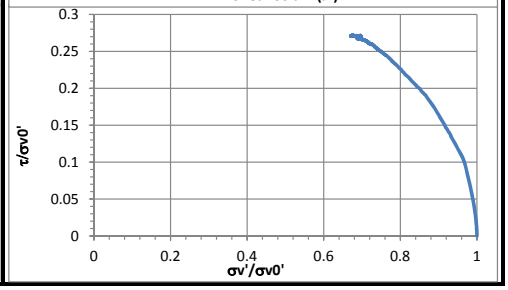

CSS Monotonic Shear Test Report

10/28/2013_Version 8.0

Geotechnical Engineering Laboratory

General Test Information		Sample Preparation	
Device:	CSS	Prepared total weight (kg):	16.000
Specimen ID:	CA-LC	Prepared dry weight (kg):	13.061
Test ID:	CAF18	Prepared height (mm):	139.1
Date of test:	5/7/2015	Prepared total density (kg/m3):	1529
Test performed:	Monotonic Shear	Prepared dry density (kg/m3):	1248
Test material:	MSW	**Pre-compression Stage**	
Sample preparation:	CA-LC fresh FP. wc,dry=22.5%. Partialy slid.	Pre-compressed strain (%):	9.8
		Compressed total density (kg/m3):	1695
		Compressed dry density (kg/m3):	1384
		Secondary compression ratio:	0.00181
		Total weight before shearing (kg):	15.576
		Dry weight before shearing (kg):	12.715

Consolidation Stage		Shear Stage		
Consolidated height (mm):	129.52	Type of test:		CL-strain
Vertical stress (kPa):	98.5	Shear strain rate (%/min):		0.31
Immediate strain (εimm, %)	6.52	10% strain	Shear stress (kPa)	64.9
Strain before shearing (εall, %)	6.9		Tan friction angle (°)	33.0
Compression index (Cεε)	0.033		Sin friction angle (°)	41.4
Constrained modulus	30.68	30% strain	Shear stress (kPa)	74.3
Consolidated total density	1633		Tan friction angle (°)	37.1
Consolidated dry density	1333		Sin friction angle (°)	49.1

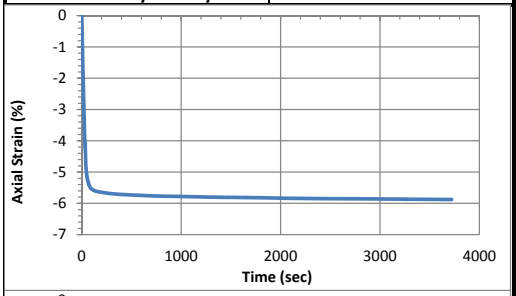

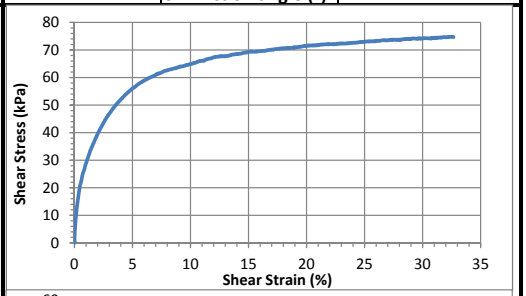

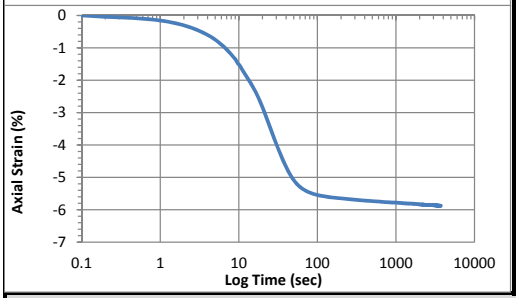

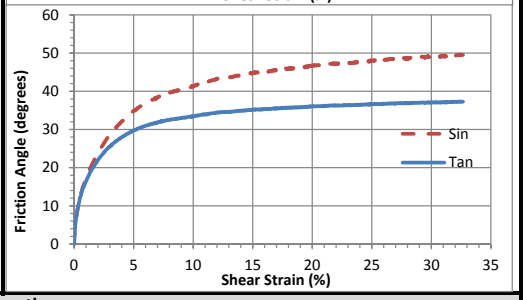

Strength			
τ/σv' at 10% strain	0.66	τ/σv0' at 10% strain	0.66
τ/σv' at 30% strain	0.76	τ/σv0' at 30% strain	0.76

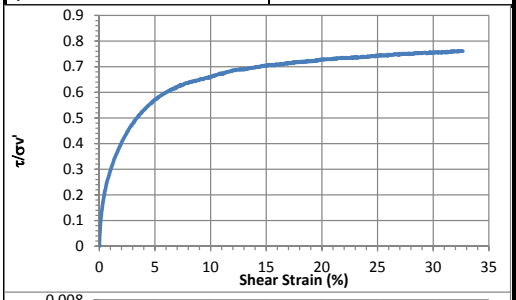

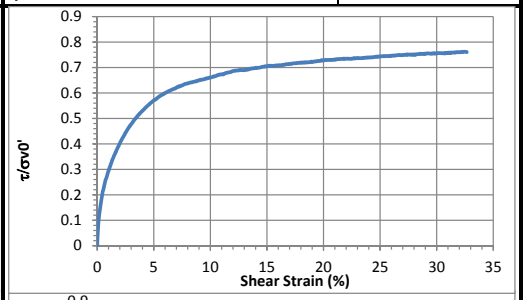

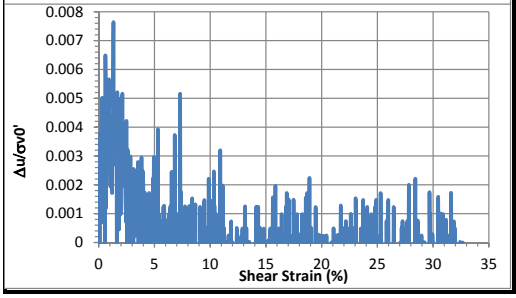

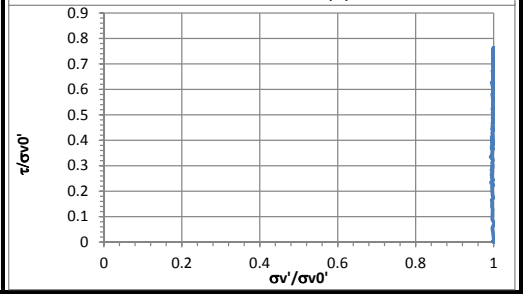

CSS Monotonic Shear Test Report

10/28/2013_Version 8.0

Geotechnical Engineering Laboratory

General Test Information	
Device:	CSS
Specimen ID:	CA-LC
Test ID:	CAF20
Date of test:	5/11/2015
Test performed:	Monotonic Shear
Test material:	MSW
Sample preparation:	CA-LC fresh FP.

Sample Preparation	
Prepared total weight (kg):	16.000
Prepared dry weight (kg):	13.061
Prepared height (mm):	160.7
Prepared total density (kg/m3):	1352
Prepared dry density (kg/m3):	1103
Pre-compression Stage	
Pre-compressed strain (%):	17.0
Compressed total density (kg/m3):	1628
Compressed dry density (kg/m3):	1329
Secondary compression ratio:	0.00139
Total weight before shearing (kg):	15.949
Dry weight before shearing (kg):	13.010

Consolidation Stage	
Consolidated height (mm):	132.27
Vertical stress (kPa):	198.8
Immediate strain (εimm, %)	17.40
Strain before shearing (εall, %)	17.7
Compression index (Cεε)	0.076
Constrained modulus	11.49
Consolidated total density	1637
Consolidated dry density	1335

Shear Stage		
Type of test:		CL-strain
Shear strain rate (%/min):		0.30
10% strain	Shear stress (kPa)	95.2
	Tan friction angle (°)	25.6
	Sin friction angle (°)	28.7
30% strain	Shear stress (kPa)	112.5
	Tan friction angle (°)	29.6
	Sin friction angle (°)	34.5

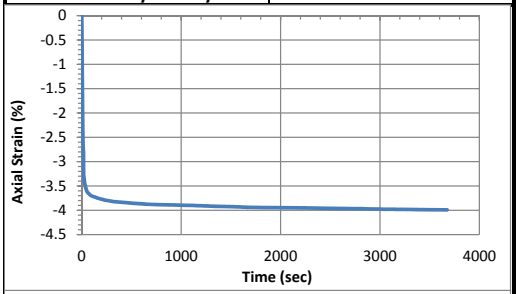

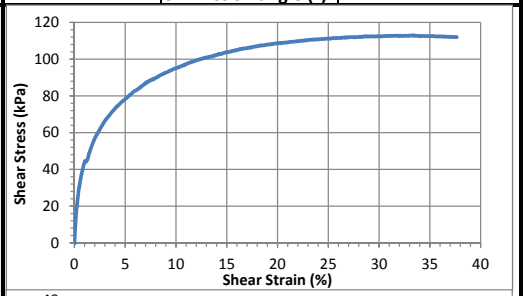

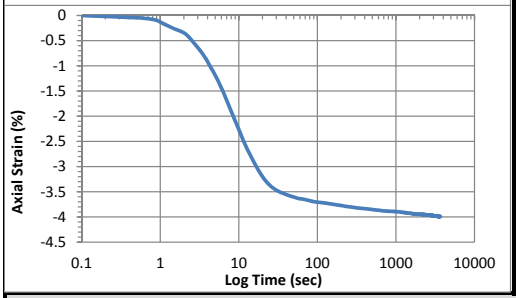

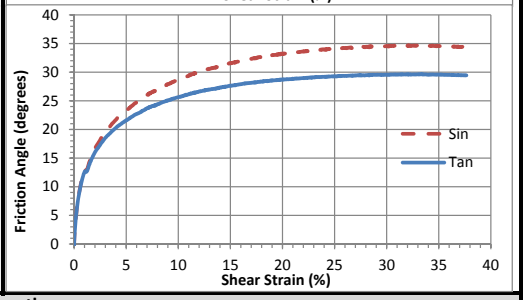

Strength

τ/σv' at 10% strain	0.48	τ/σv0' at 10% strain	0.48
τ/σv' at 30% strain	0.57	τ/σv0' at 30% strain	0.57

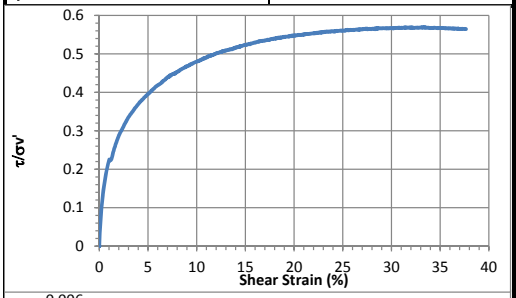

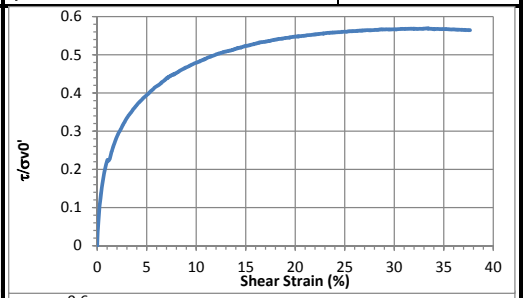

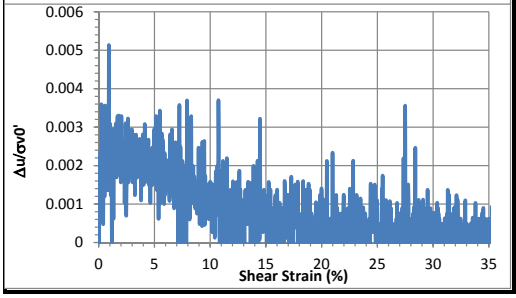

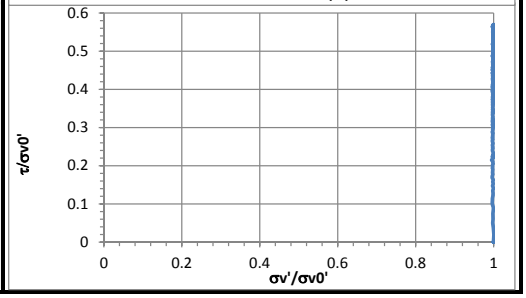

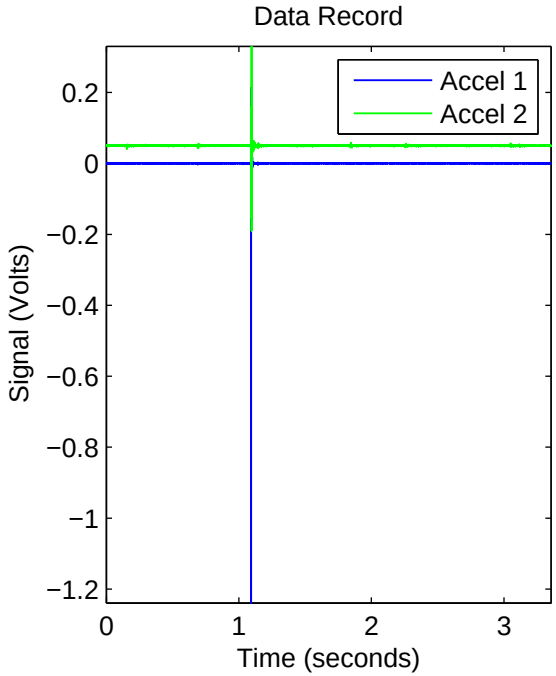
Data Record
Accel 1
Accel 2
Signal (Volts)
Time (seconds)

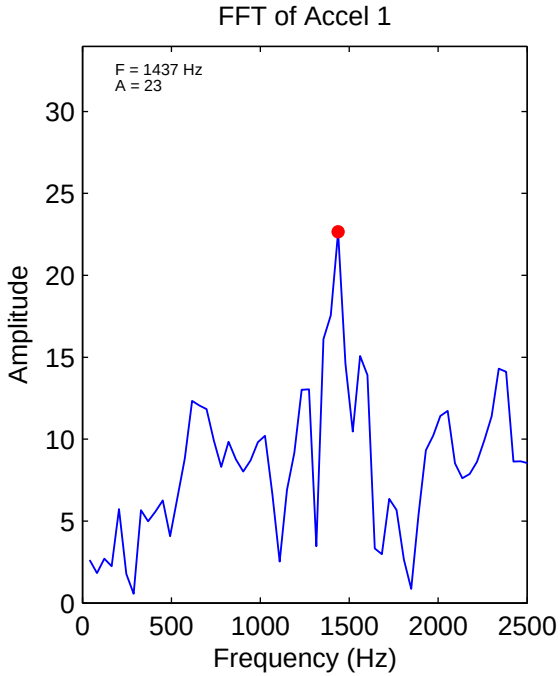
FFT of Accel 1
F = 1437 Hz
A = 23
Amplitude
Frequency (Hz)

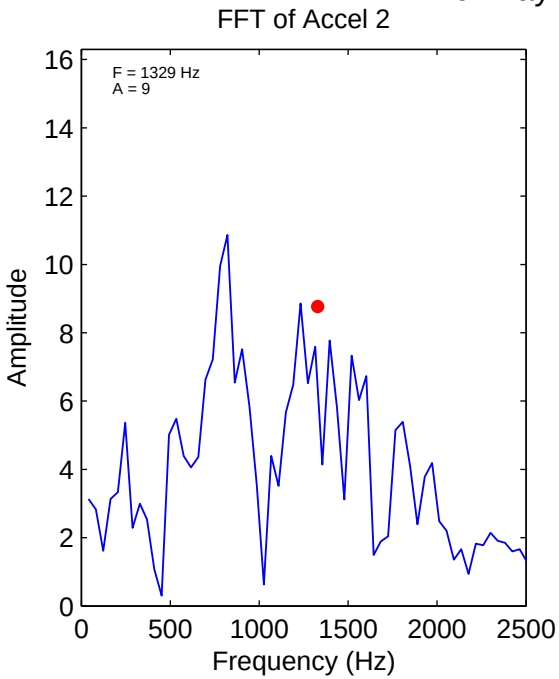
FFT of Accel 2
F = 1329 Hz
A = 9
Amplitude
Frequency (Hz)

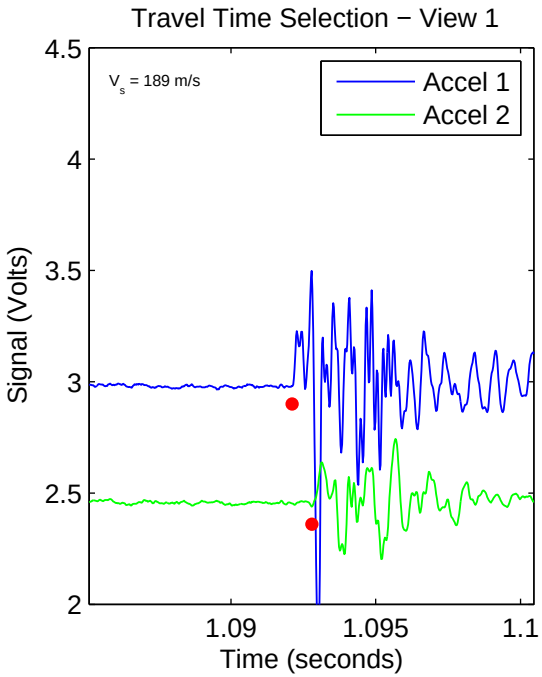
Travel Time Selection − View 1
V_s = 189 m/s
Accel 1
Accel 2
Signal (Volts)
Time (seconds)

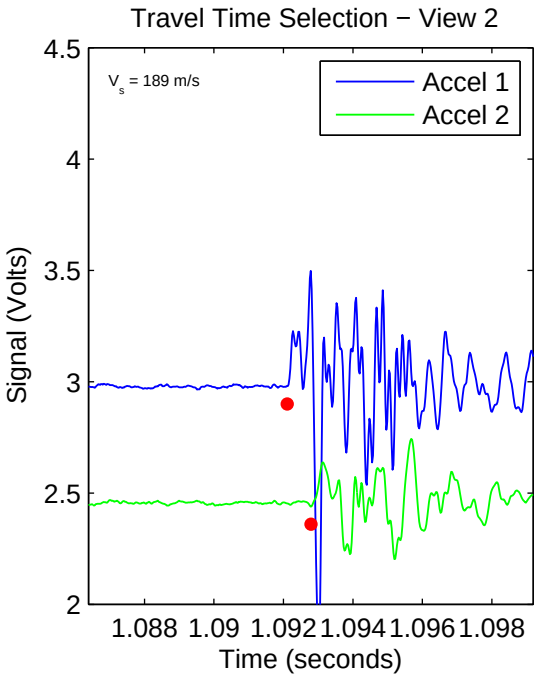
Travel Time Selection − View 2
V_s = 189 m/s
Accel 1
Accel 2
Signal (Volts)
Time (seconds)

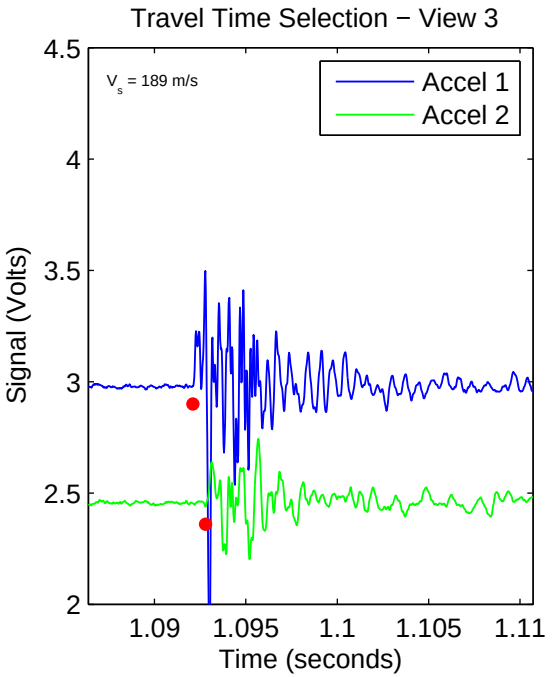
Travel Time Selection − View 3
V_s = 189 m/s
Accel 1
Accel 2
Signal (Volts)
Time (seconds)

CSS Monotonic Shear Test Report

10/28/2013_Version 8.0

Geotechnical Engineering Laboratory

General Test Information	
Device:	CSS
Specimen ID:	CA-LC
Test ID:	CAF21
Date of test:	5/13/2015
Test performed:	Monotonic Shear
Test material:	MSW
Sample preparation:	CA-LC fresh FP. Slid near the end. Only use 24% strain

Sample Preparation	
Prepared total weight (kg):	15.500
Prepared dry weight (kg):	12.653
Prepared height (mm):	136.9
Prepared total density (kg/m3):	1538
Prepared dry density (kg/m3):	1255
Pre-compression Stage	
Pre-compressed strain (%):	10.3
Compressed total density (kg/m3):	1715
Compressed dry density (kg/m3):	1400
Secondary compression ratio:	0.00158
Total weight before shearing (kg):	15.423
Dry weight before shearing (kg):	12.576

Consolidation Stage	
Consolidated height (mm):	124.93
Vertical stress (kPa):	196.6
Immediate strain (εimm, %)	6.47
Strain before shearing (εall, %)	8.7
Compression index (Cεε)	0.028
Constrained modulus	30.93
Consolidated total density	1676
Consolidated dry density	1367

Shear Stage		
Type of test:		CV-strain
Shear strain rate (%/min):		0.32
10% strain	Shear stress (kPa)	87.9
	Tan friction angle (°)	32.4
	Sin friction angle (°)	39.4
30% strain	Shear stress (kPa)	97.2
	Tan friction angle (°)	33.6
	Sin friction angle (°)	41.6

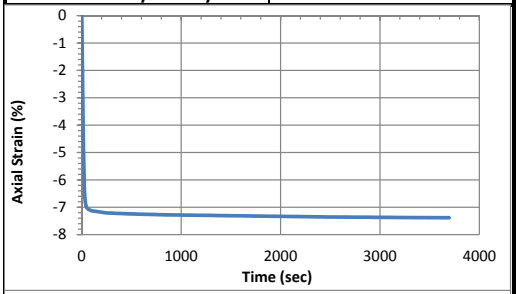

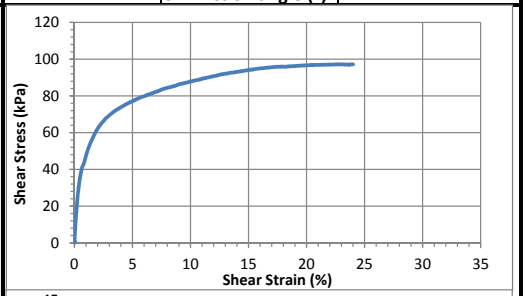

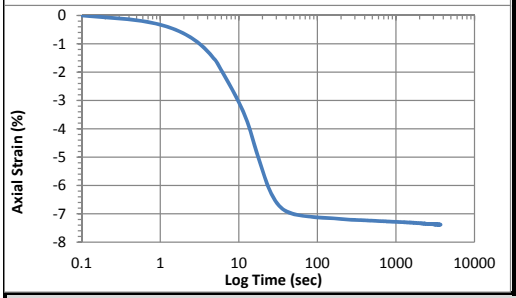

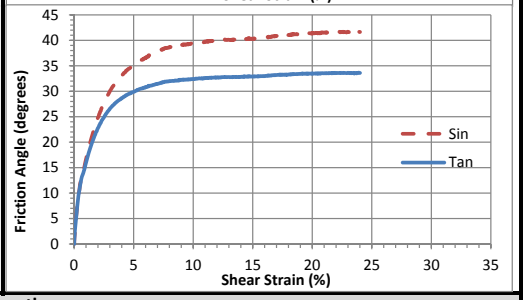

Strength

τ/σv' at 10% strain	0.63	τ/σv0' at 10% strain	0.45
τ/σv' at 30% strain	0.66	τ/σv0' at 30% strain	0.49

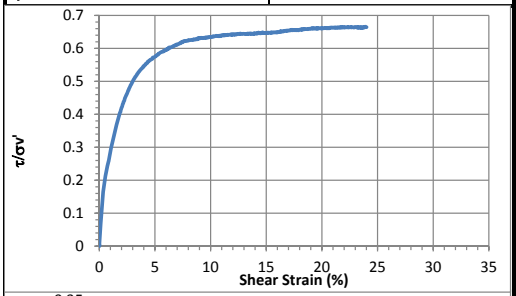

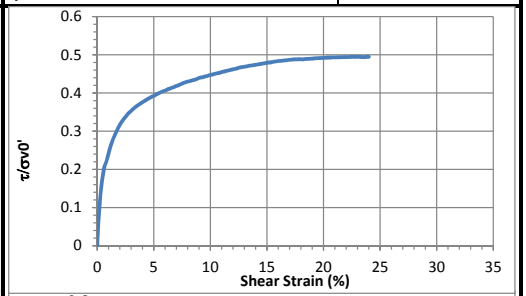

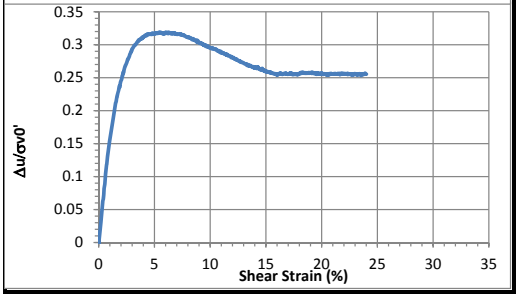

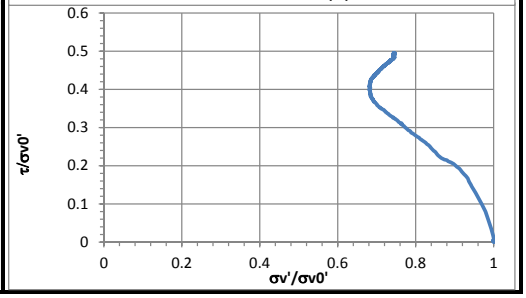

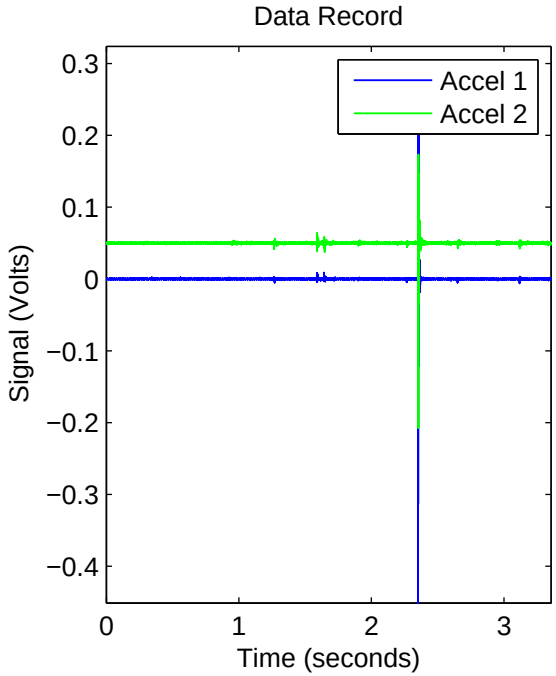
Data Record
Accel 1
Accel 2
Signal (Volts)
Time (seconds)

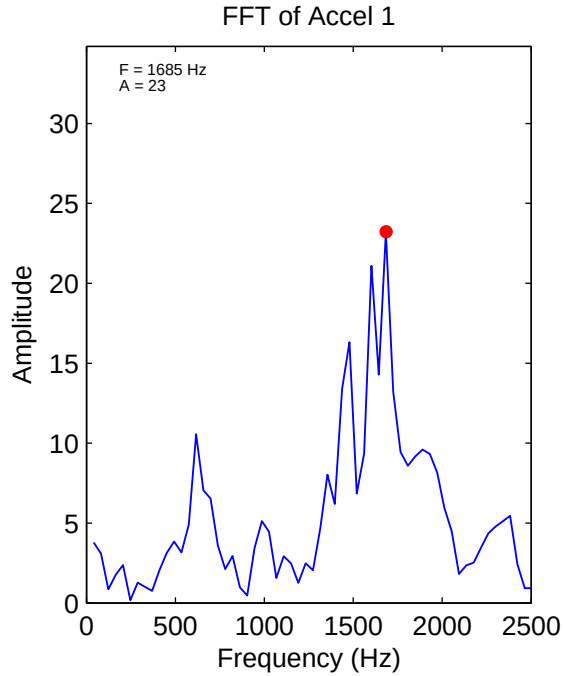
FFT of Accel 1
F = 1685 Hz
A = 23
Amplitude
Frequency (Hz)

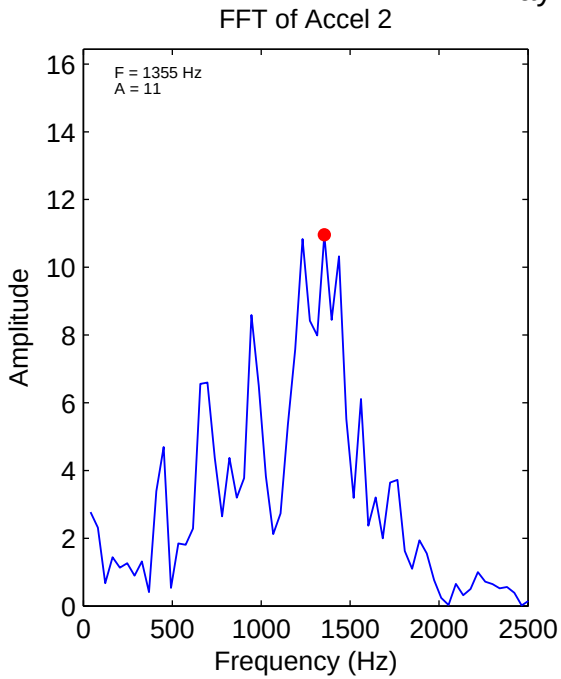
FFT of Accel 2
F = 1355 Hz
A = 11
Amplitude
Frequency (Hz)

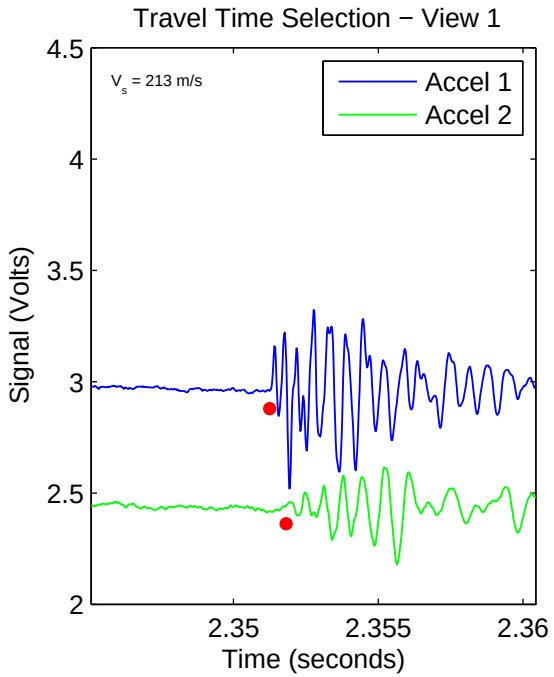
Travel Time Selection − View 1
V_s = 213 m/s
Accel 1
Accel 2
Signal (Volts)
Time (seconds)

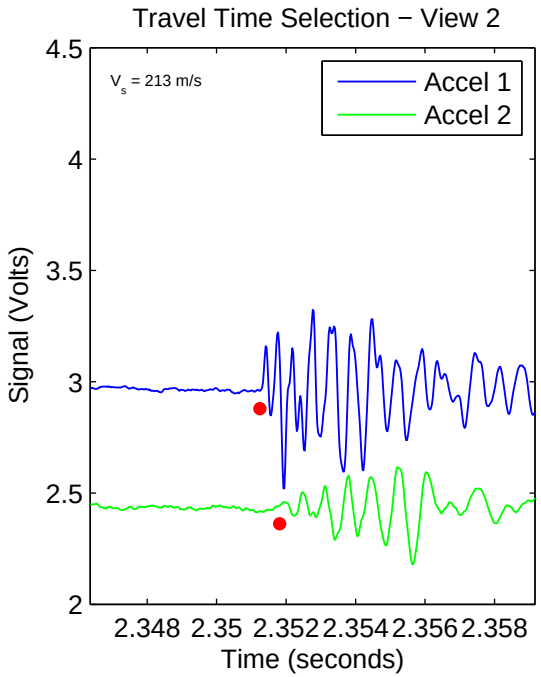
Travel Time Selection − View 2
V_s = 213 m/s
Accel 1
Accel 2
Signal (Volts)
Time (seconds)

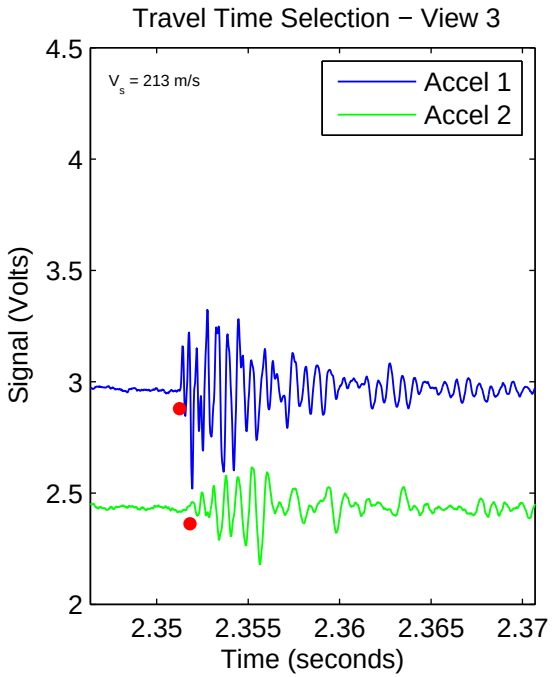
Travel Time Selection − View 3
V_s = 213 m/s
Accel 1
Accel 2
Signal (Volts)
Time (seconds)

CSS Monotonic Shear Test Report

10/28/2013_Version 8.0

Geotechnical Engineering Laboratory

General Test Information		Sample Preparation	
Device:	CSS	**Prepared total weight (kg):**	16.000
Specimen ID:	CA-LC	**Prepared dry weight (kg):**	13.061
Test ID:	CAF22	**Prepared height (mm):**	151.6
Date of test:	5/15/2015	**Prepared total density (kg/m3):**	1433
Test performed:	Monotonic Shear	**Prepared dry density (kg/m3):**	1170
Test material:	MSW	**Pre-compression Stage**	
Sample preparation:	CA-LC fresh FP. Use 2 bars on bottom plate.	**Pre-compressed strain (%):**	22.3
		Compressed total density (kg/m3):	1844
		Compressed dry density (kg/m3):	1506
		Secondary compression ratio:	
		Total weight before shearing (kg):	15.929
		Dry weight before shearing (kg):	12.990

Consolidation Stage		Shear Stage		
Consolidated height (mm):	122.19	**Type of test:**		CV-strain
Vertical stress (kPa):	500.1	**Shear strain rate (%/min):**		0.33
Immediate strain (εimm, %)		**10% strain**	**Shear stress (kPa)**	143.3
Strain before shearing (εall, %)	19.4		**Tan friction angle (°)**	28.4
Compression index (Cc ε)			**Sin friction angle (°)**	32.8
Constrained modulus		**30% strain**	**Shear stress (kPa)**	148.5
Consolidated total density	1770		**Tan friction angle (°)**	32.0
Consolidated dry density	1443		**Sin friction angle (°)**	38.6

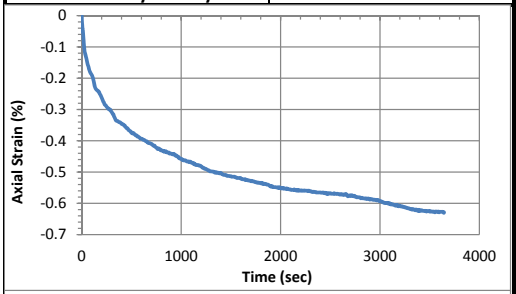

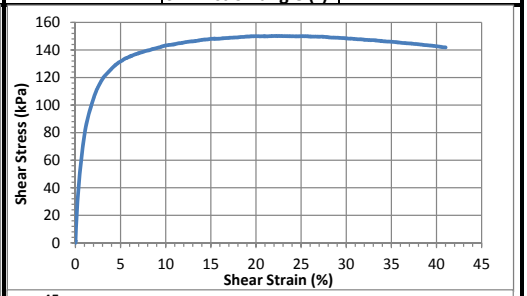

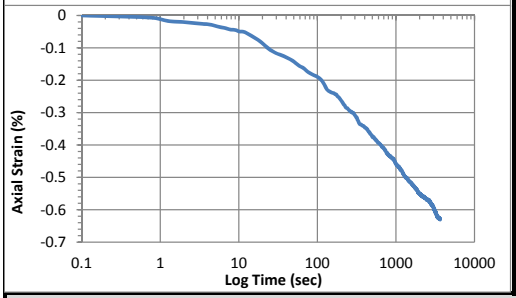

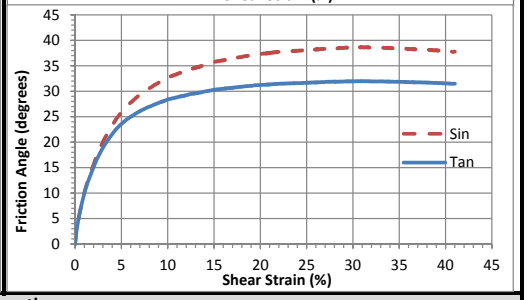

Strength

τ/σv' at 10% strain	0.54	**τ/σv0' at 10% strain**	0.29
τ/σv' at 30% strain	0.62	**τ/σv0' at 30% strain**	0.30

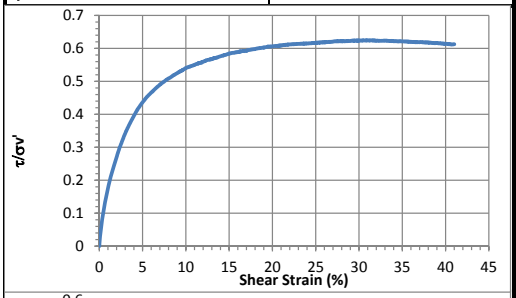

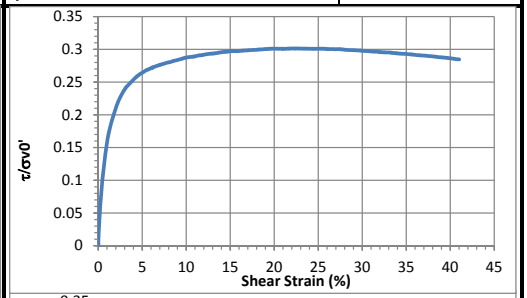

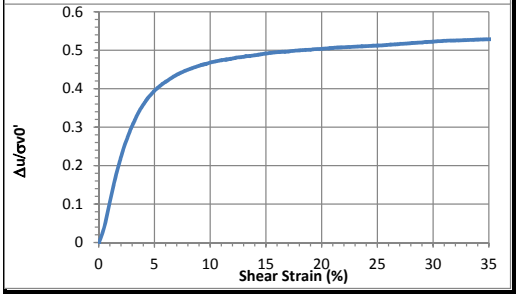

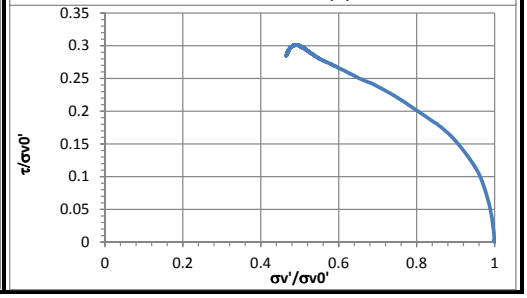

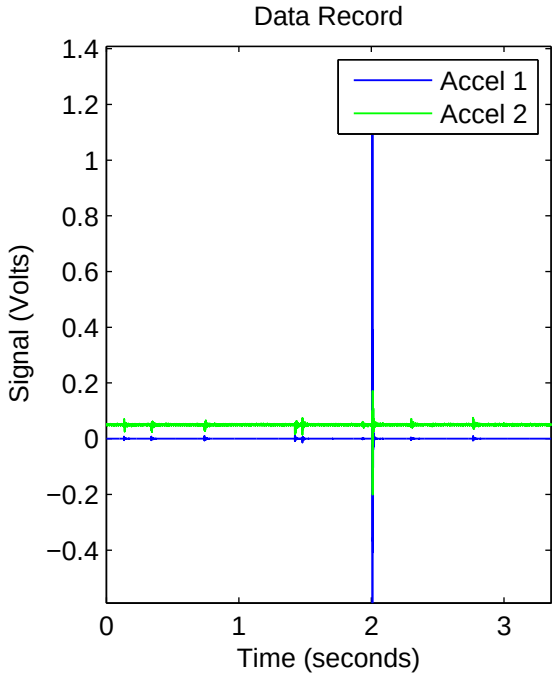
Data Record
Accel 1
Accel 2
Signal (Volts)
Time (seconds)

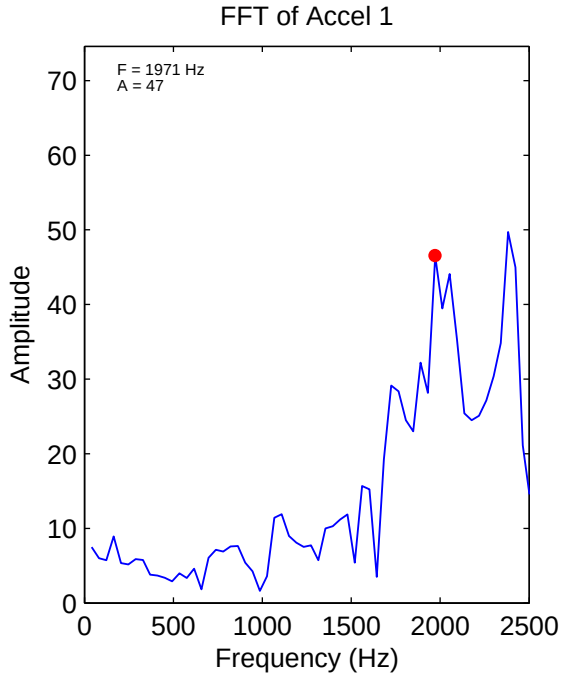
FFT of Accel 1
F = 1971 Hz
A = 47
Amplitude
Frequency (Hz)

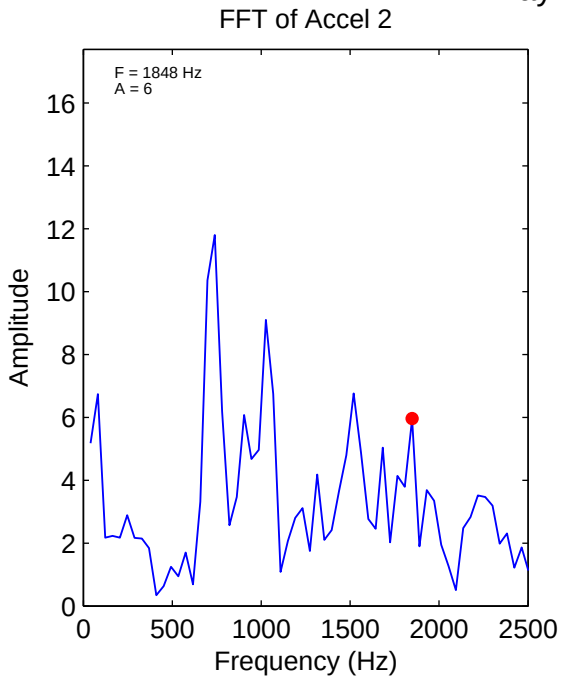
FFT of Accel 2
F = 1848 Hz
A = 6
Amplitude
Frequency (Hz)

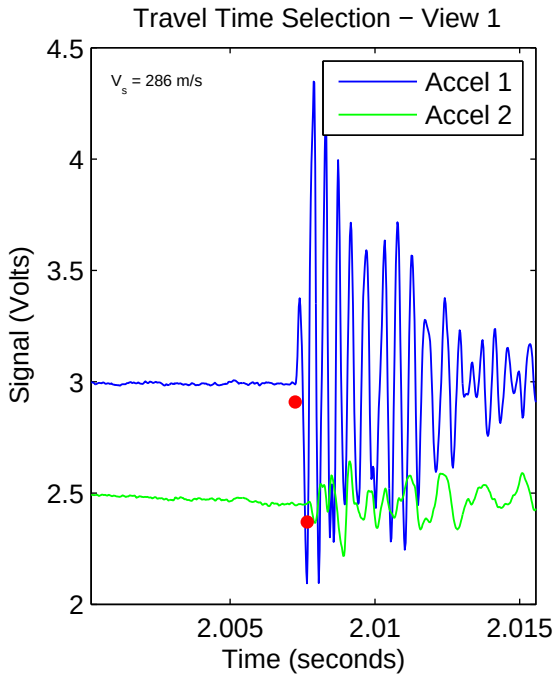
Travel Time Selection − View 1
V_s = 286 m/s
Accel 1
Accel 2
Signal (Volts)
Time (seconds)

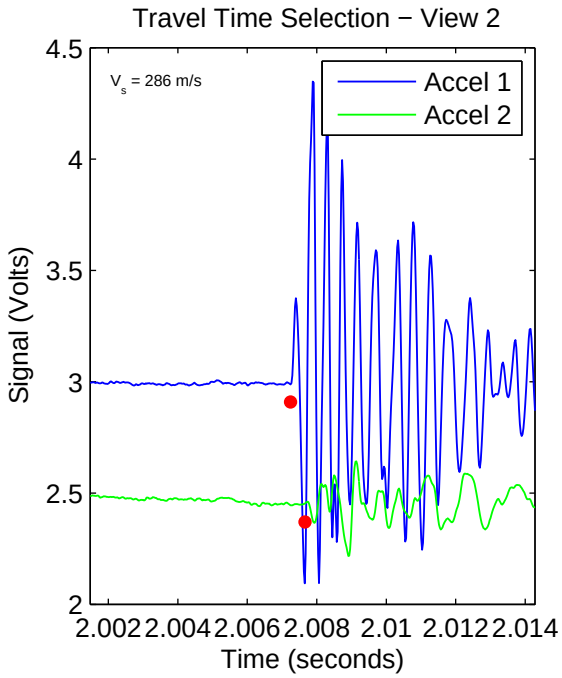
Travel Time Selection − View 2
V_s = 286 m/s
Accel 1
Accel 2
Signal (Volts)
Time (seconds)

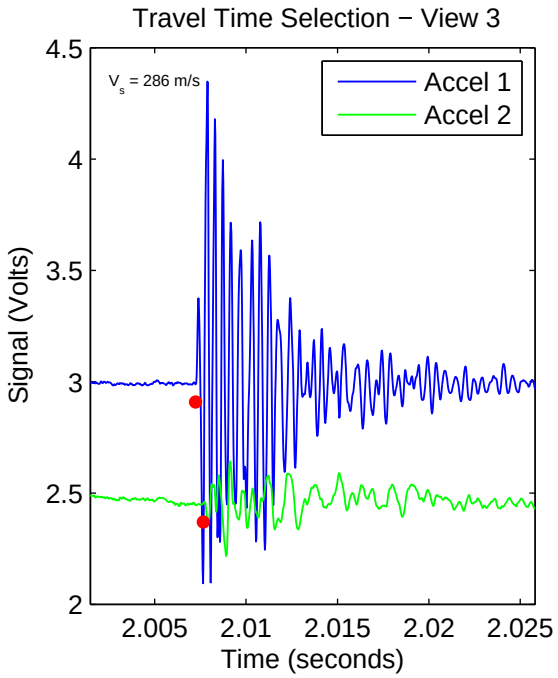
Travel Time Selection − View 3
V_s = 286 m/s
Accel 1
Accel 2
Signal (Volts)
Time (seconds)

CSS Monotonic Shear Test Report

10/28/2013_Version 8.0

Geotechnical Engineering Laboratory

General Test Information		Sample Preparation	
Device:	CSS	**Prepared total weight (kg):**	16.000
Specimen ID:	CA-LC	**Prepared dry weight (kg):**	13.061
Test ID:	CAF23	**Prepared height (mm):**	141.5
Date of test:	5/17/2015	**Prepared total density (kg/m3):**	1536
Test performed:	Monotonic Shear	**Prepared dry density (kg/m3):**	1254
Test material:	MSW	**Pre-compression Stage**	
Sample preparation:	CA-LC fresh FP. Slid slightly near the end.	**Pre-compressed strain (%):**	16.1
		Compressed total density (kg/m3):	1831
		Compressed dry density (kg/m3):	1495
		Secondary compression ratio:	0.00229
		Total weight before shearing (kg):	15.937
		Dry weight before shearing (kg):	12.999

Consolidation Stage		Shear Stage		
Consolidated height (mm):	120.59	**Type of test:**		CL-strain
Vertical stress (kPa):	497.2	**Shear strain rate (%/min):**		0.33
Immediate strain (εimm, %)	14.46	**10% strain**	**Shear stress (kPa)**	182.3
Strain before shearing (εall, %)	14.8		**Tan friction angle (°)**	20.2
Compression index (Cεε)	0.054		**Sin friction angle (°)**	21.6
Constrained modulus	13.83	**30% strain**	**Shear stress (kPa)**	233.8
Consolidated total density	1794		**Tan friction angle (°)**	25.2
Consolidated dry density	1464		**Sin friction angle (°)**	28.1

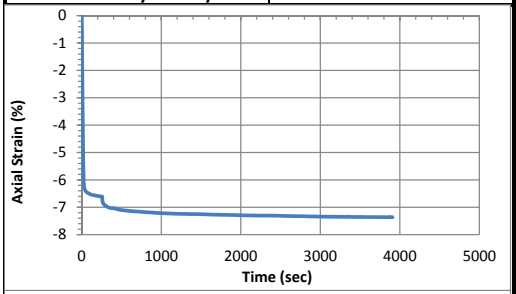

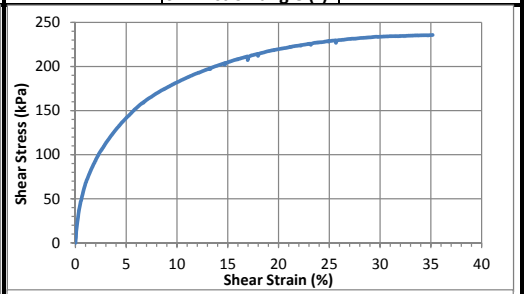

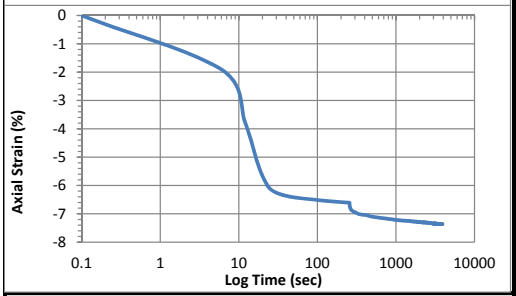

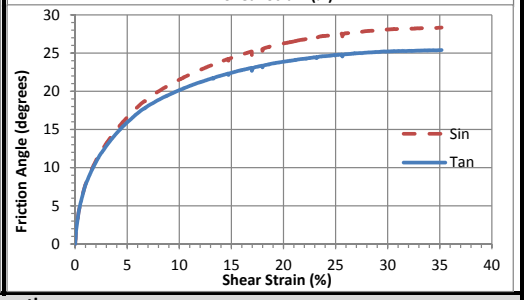

Strength			
τ/σv' at 10% strain	0.37	**τ/σv0' at 10% strain**	0.37
τ/σv' at 30% strain	0.47	**τ/σv0' at 30% strain**	0.47

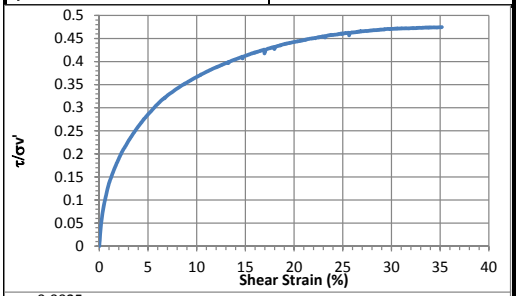

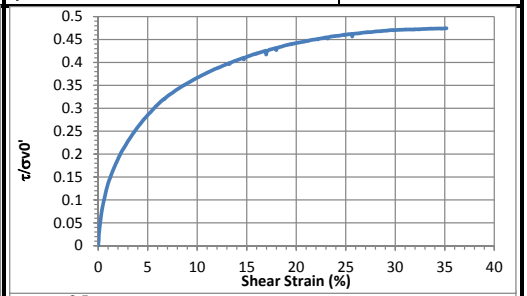

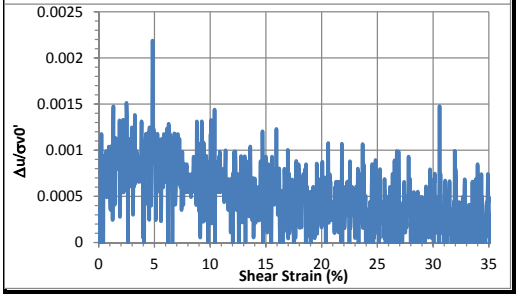

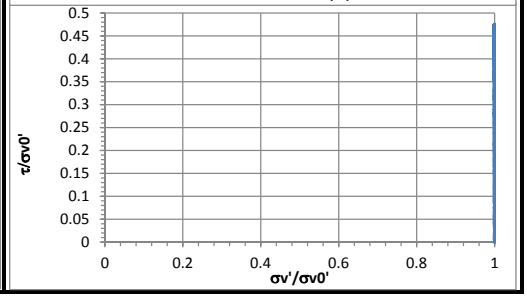

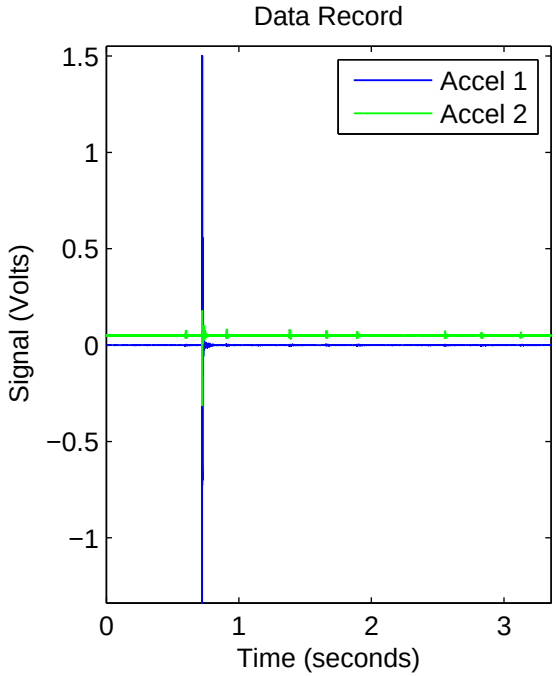
Data Record
Accel 1
Accel 2
Signal (Volts)
Time (seconds)

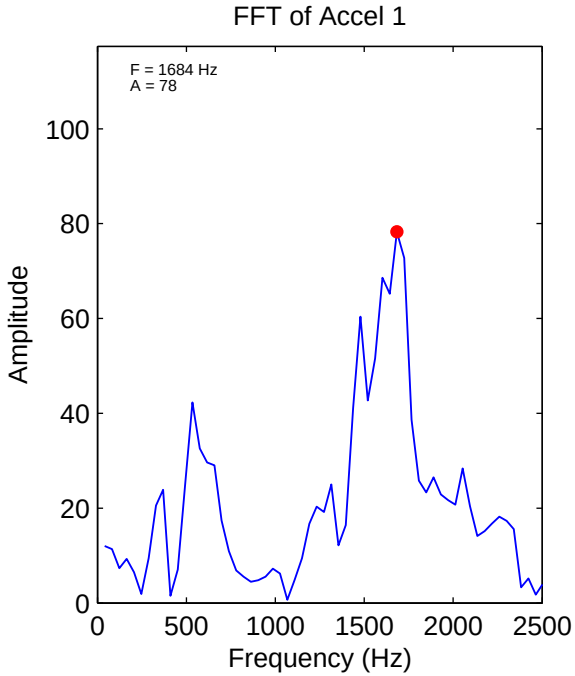
FFT of Accel 1
F = 1684 Hz
A = 78
Amplitude
Frequency (Hz)

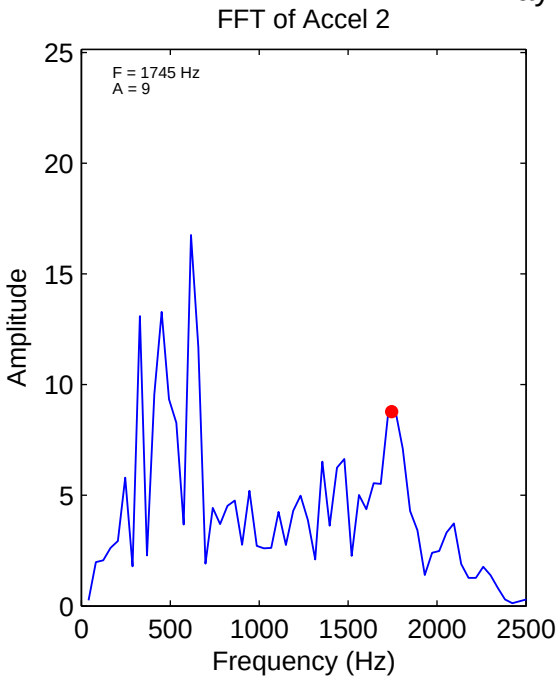
FFT of Accel 2
F = 1745 Hz
A = 9
Amplitude
Frequency (Hz)

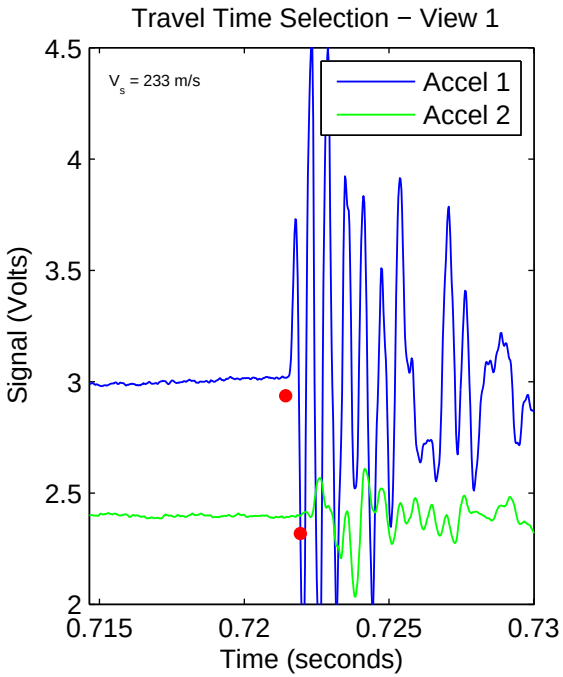
Travel Time Selection − View 1
V_s = 233 m/s
Accel 1
Accel 2
Signal (Volts)
Time (seconds)

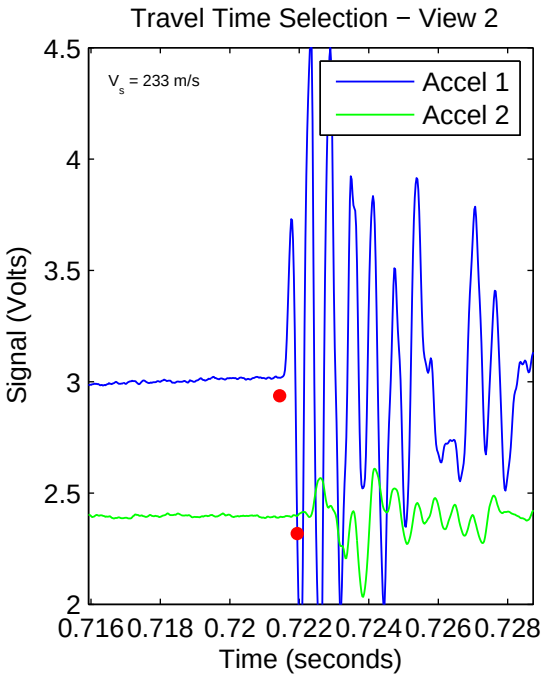
Travel Time Selection − View 2
V_s = 233 m/s
Accel 1
Accel 2
Signal (Volts)
Time (seconds)

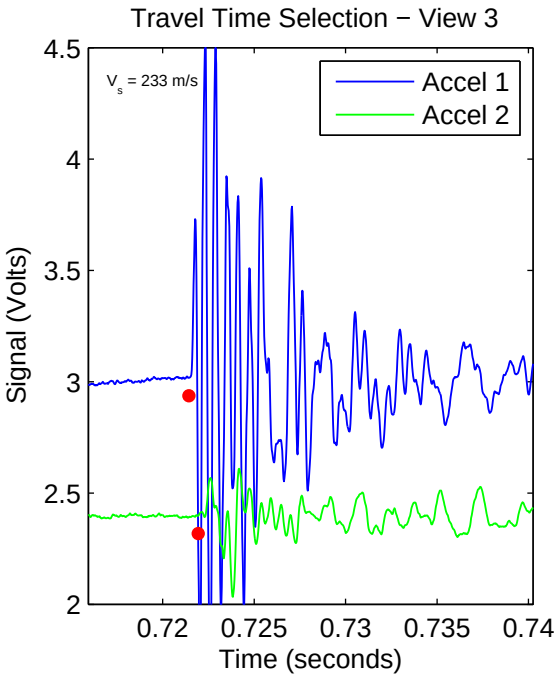
Travel Time Selection − View 3
V_s = 233 m/s
Accel 1
Accel 2
Signal (Volts)
Time (seconds)

CSS Monotonic Shear Test Report

10/28/2013_Version 8.0

Geotechnical Engineering Laboratory

General Test Information		Sample Preparation	
Device:	CSS	**Prepared total weight (kg):**	16.000
Specimen ID:	CA-LC	**Prepared dry weight (kg):**	13.061
Test ID:	CAF24	**Prepared height (mm):**	115.3
Date of test:	5/21/2015	**Prepared total density (kg/m3):**	
Test performed:	Monotonic Direct Shear	**Prepared dry density (kg/m3):**	
Test material:	MSW	**Pre-compression Stage**	
Sample preparation:	CA-LC fresh FP. Direct shear. CL mode. Opening=0.125 in.	**Pre-compressed strain (%):**	10.7
		Compressed total density (kg/m3):	
		Compressed dry density (kg/m3):	
		Secondary compression ratio:	0.00096
		Total weight before shearing (kg):	15.883
		Dry weight before shearing (kg):	12.944

Consolidation Stage		Shear Stage		
Consolidated height (mm):	109.84	**Type of test:**		CL-direct shear
Vertical stress (kPa):	99.3	**Shear strain rate (%/min):**		0.13
Immediate strain (εimm, %)	4.62	**12 mm**	**Shear stress (kPa)**	73.2
Strain before shearing (εall, %)	4.7		**Tan friction angle (°)**	36.5
Compression index (Cεε)	0.023		**Sin friction angle (°)**	
Constrained modulus	43.25	**35 mm**	**Shear stress (kPa)**	82.1
Consolidated total density	1630		**Tan friction angle (°)**	39.7
Consolidated dry density	1328		**Sin friction angle (°)**	

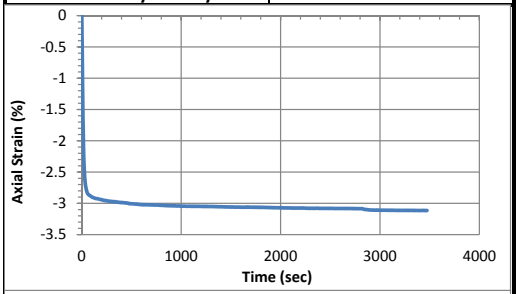

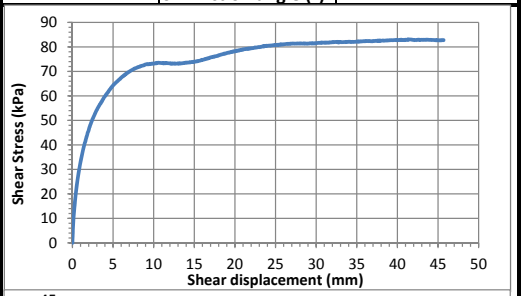

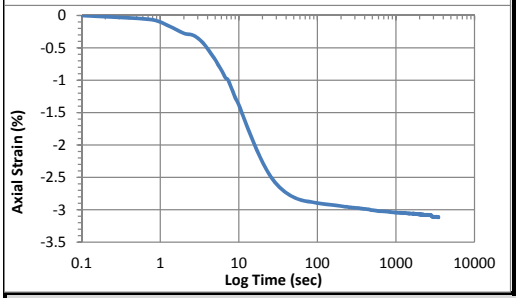

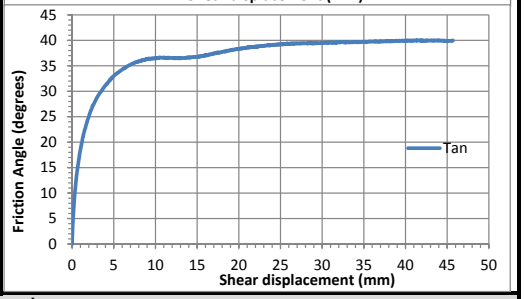

Strength

τ/σv' at 10% strain		**τ/σv0' at 10% strain**	
τ/σv' at 30% strain		**τ/σv0' at 30% strain**	

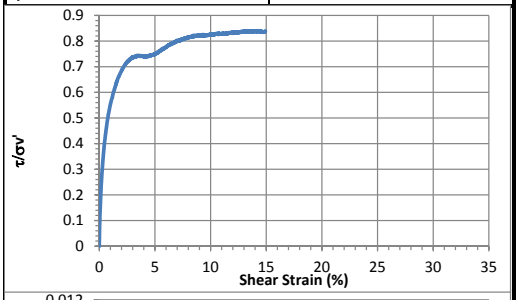

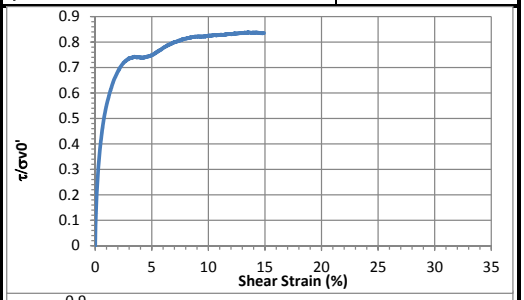

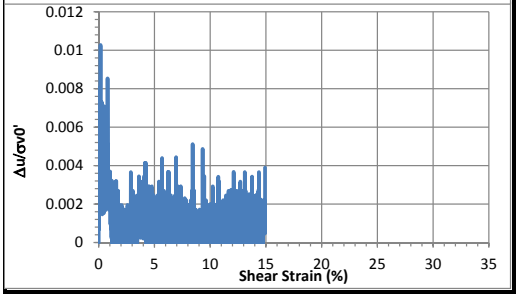

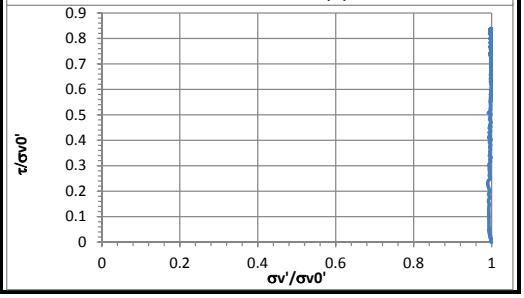

CSS Monotonic Shear Test Report

10/28/2013_Version 8.0

Geotechnical Engineering Laboratory

General Test Information		Sample Preparation	
Device:	CSS	**Prepared total weight (kg):**	18.000
Specimen ID:	CA-LC	**Prepared dry weight (kg):**	14.694
Test ID:	CAF25	**Prepared height (mm):**	130.7
Date of test:	5/23/2015	**Prepared total density (kg/m3):**	
Test performed:	Monotonic Direct Shear	**Prepared dry density (kg/m3):**	
Test material:	MSW	**Pre-compression Stage**	
Sample preparation:	CA-LC fresh FP. Direct shear. CL mode. Opening=0.125 in.	**Pre-compressed strain (%):**	16.1
		Compressed total density (kg/m3):	
		Compressed dry density (kg/m3):	
		Secondary compression ratio:	0.00301
		Total weight before shearing (kg):	16.531
		Dry weight before shearing (kg):	13.495

Consolidation Stage		Shear Stage		
Consolidated height (mm):	105.50	**Type of test:**		CL-direct shear
Vertical stress (kPa):	498.2	**Shear strain rate (%/min):**		0.12
Immediate strain (εimm, %)	11.29	**12 mm**	**Shear stress (kPa)**	196.6
Strain before shearing (εall, %)	11.7		**Tan friction angle (°)**	21.6
Compression index (Cεc)	0.042		**Sin friction angle (°)**	
Constrained modulus	17.71	**35 mm**	**Shear stress (kPa)**	244.2
Consolidated total density	1754		**Tan friction angle (°)**	26.2
Consolidated dry density	1432		**Sin friction angle (°)**	

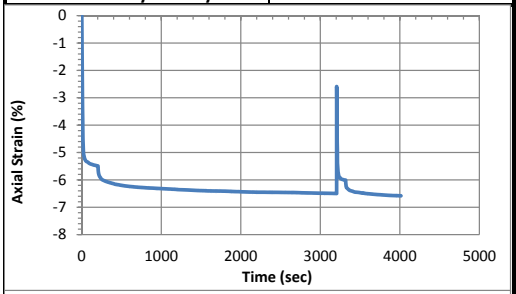

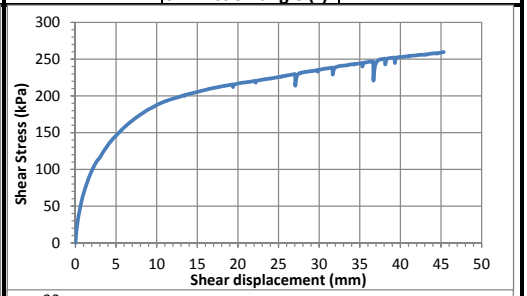

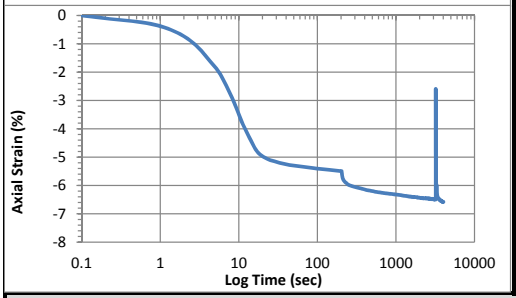

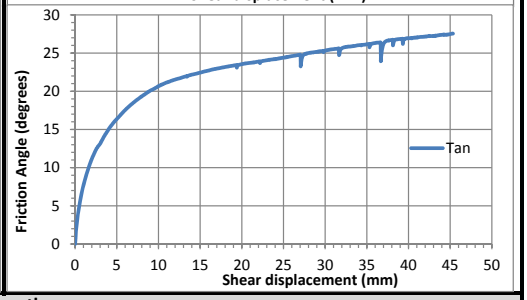

Strength

τ/σv' at 10% strain		**τ/σv0' at 10% strain**	
τ/σv' at 30% strain		**τ/σv0' at 30% strain**	

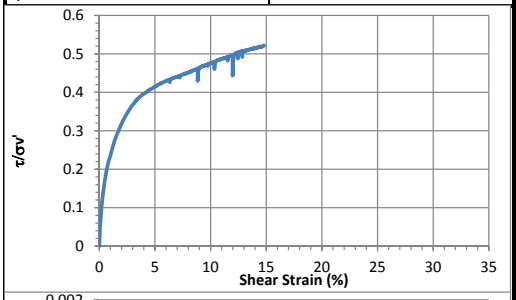

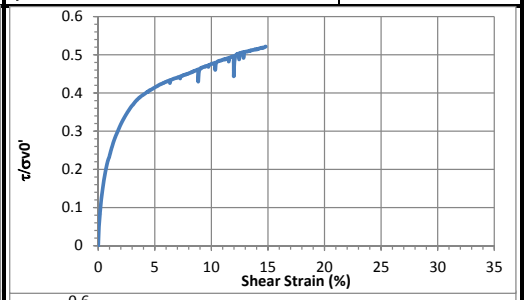

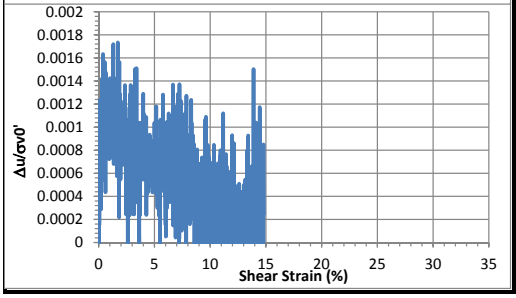

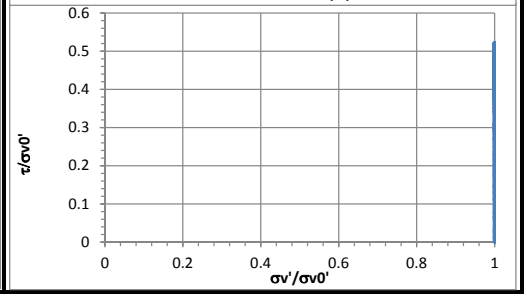

CSS Monotonic Shear Test Report

10/28/2013_Version 8.0

Geotechnical Engineering Laboratory

General Test Information		Sample Preparation	
Device:	CSS	Prepared total weight (kg):	13.300
Specimen ID:	CA-LC	Prepared dry weight (kg):	10.769
Test ID:	CAF26	Prepared height (mm):	137.0
Date of test:	5/25/2015	Prepared total density (kg/m3):	
Test performed:	Monotonic Direct Shear	Prepared dry density (kg/m3):	
Test material:	MSW	**Pre-compression Stage**	
Sample preparation:	CA-LC fresh MSW. Direct shear. CL mode. Opening=0.125 in.	Pre-compressed strain (%):	20.7
		Compressed total density (kg/m3):	
		Compressed dry density (kg/m3):	
		Secondary compression ratio:	0.00372
		Total weight before shearing (kg):	11.908
		Dry weight before shearing (kg):	9.642

Consolidation Stage		Shear Stage		
Consolidated height (mm):	99.14	Type of test:		CL-direct shear
Vertical stress (kPa):	99.2	Shear strain rate (%/min):		
Immediate strain (εimm, %)	19.25	12 mm	Shear stress (kPa)	59.5
Strain before shearing (εall, %)	19.9		Tan friction angle (°)	31.1
Compression index (Cεε)	0.096		Sin friction angle (°)	
Constrained modulus	10.39	35 mm	Shear stress (kPa)	72.7
Consolidated total density	1329		Tan friction angle (°)	36.4
Consolidated dry density	1077		Sin friction angle (°)	

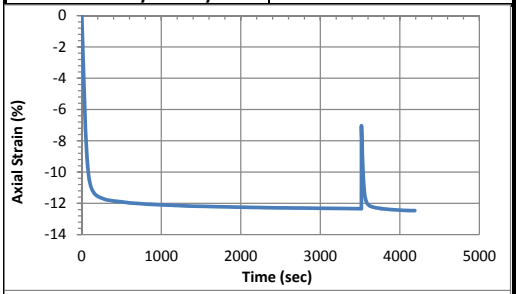

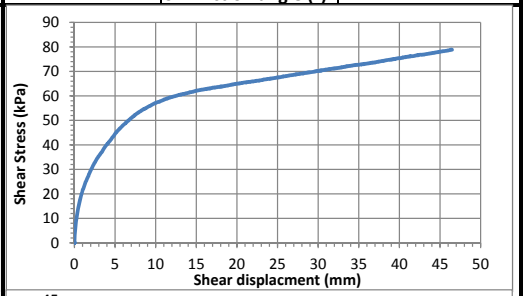

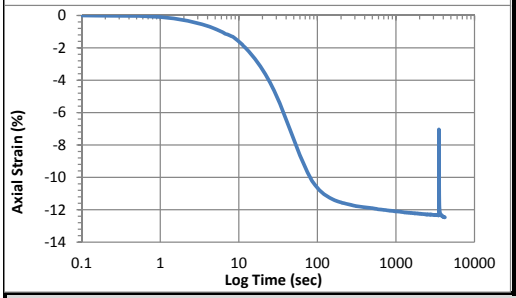

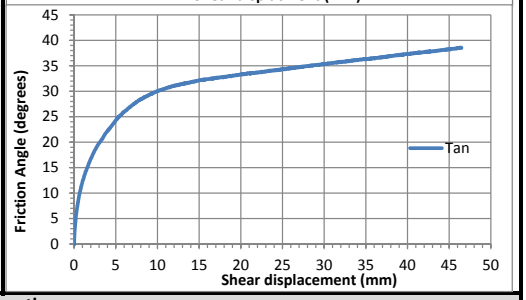

Strength			
τ/σv' at 10% strain	0.58	τ/σv0' at 10% strain	0.58
τ/σv' at 30% strain	0.71	τ/σv0' at 30% strain	0.71

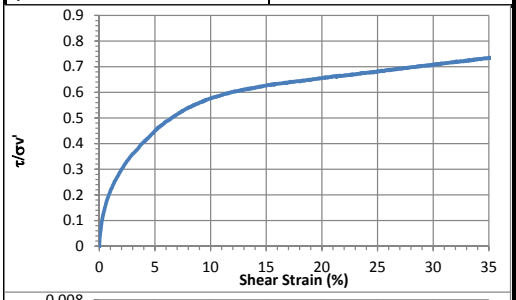

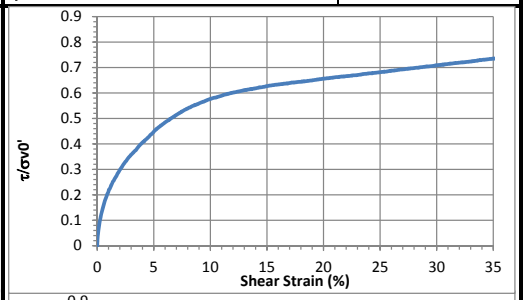

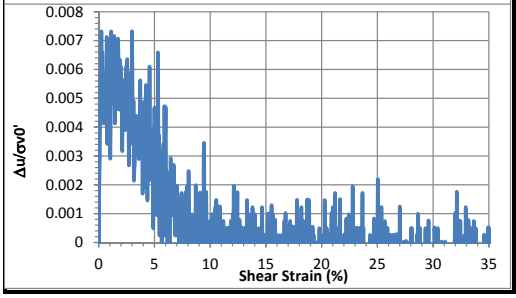

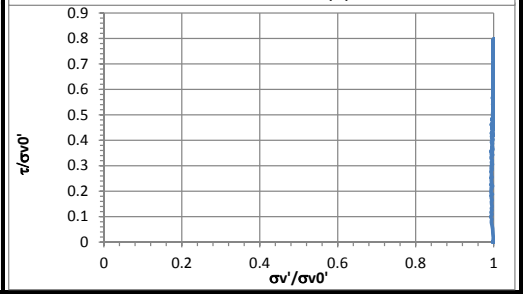

CSS Monotonic Shear Test Report

10/28/2013_Version 8.0

Geotechnical Engineering Laboratory

General Test Information		Sample Preparation	
Device:	CSS	**Prepared total weight (kg):**	13.300
Specimen ID:	CA-LC	**Prepared dry weight (kg):**	10.769
Test ID:	CAF27	**Prepared height (mm):**	138.8
Date of test:	5/27/2015	**Prepared total density (kg/m3):**	
Test performed:	Monotonic Direct Shear	**Prepared dry density (kg/m3):**	
Test material:	MSW	**Pre-compression Stage**	
Sample preparation:	CA-LC fresh MSW. Direct shear. CL mode. Opening=0.125 in.	**Pre-compressed strain (%):**	32.5
		Compressed total density (kg/m3):	
		Compressed dry density (kg/m3):	
		Secondary compression ratio:	0.00215
		Total weight before shearing (kg):	13.218
		Dry weight before shearing (kg):	10.703

Consolidation Stage		Shear Stage		
Consolidated height (mm):	98.83	**Type of test:**		CL-direct shear
Vertical stress (kPa):	496.9	**Shear strain rate (%/min):**		
Immediate strain (εimm, %)	28.98	**12 mm**	**Shear stress (kPa)**	160.6
Strain before shearing (εall, %)	28.8		**Tan friction angle (°)**	17.8
Compression index (Cεε)	0.107		**Sin friction angle (°)**	
Constrained modulus	6.90	**35 mm**	**Shear stress (kPa)**	186.2
Consolidated total density	1480		**Tan friction angle (°)**	20.5
Consolidated dry density	1198		**Sin friction angle (°)**	

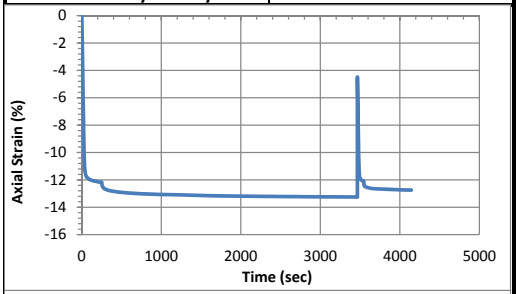

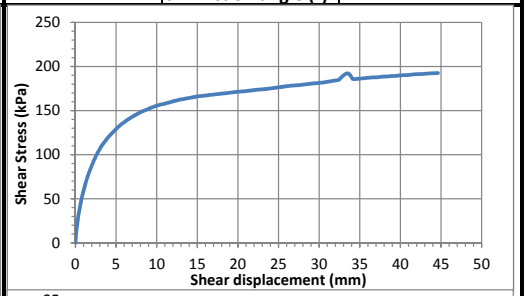

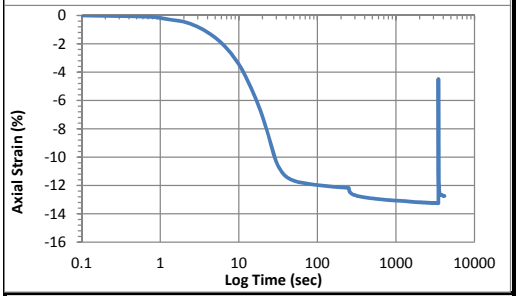

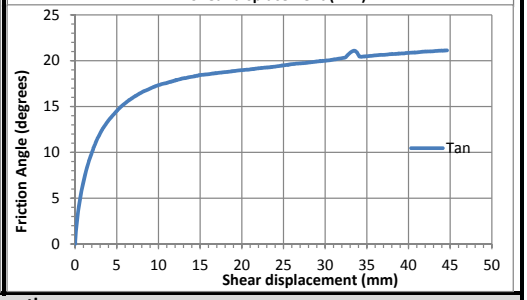

Strength

τ/σv' at 10% strain		**τ/σv0' at 10% strain**	
τ/σv' at 30% strain		**τ/σv0' at 30% strain**	

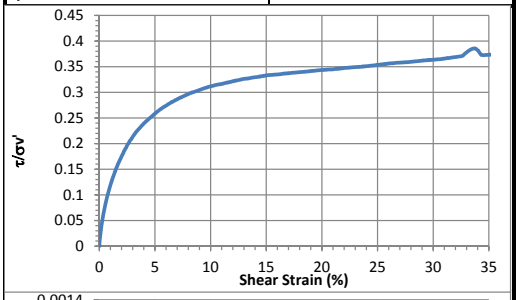

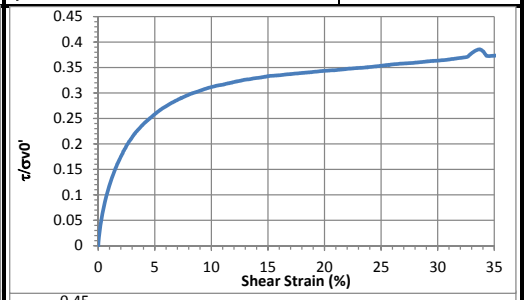

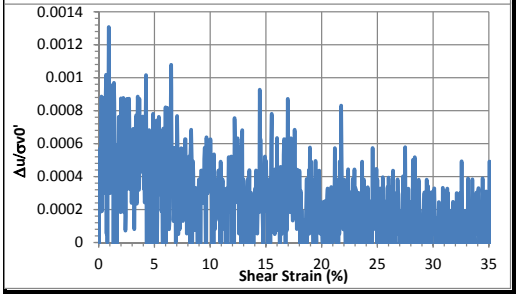

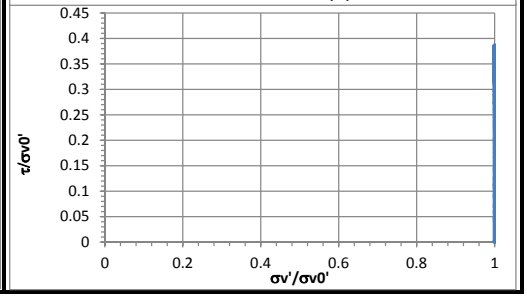

CSS Monotonic Shear Test Report

10/28/2013_Version 8.0

Geotechnical Engineering Laboratory

General Test Information		Sample Preparation	
Device:	CSS	Prepared total weight (kg):	11.970
Specimen ID:	CA-LC	Prepared dry weight (kg):	9.692
Test ID:	CAF28	Prepared height (mm):	120.4
Date of test:	5/29/2015	Prepared total density (kg/m3):	
Test performed:	Monotonic Direct Shear	Prepared dry density (kg/m3):	
Test material:	MSW	**Pre-compression Stage**	
Sample preparation:	CA-LC fresh MSW. Direct shear. CL mode. Larger opening=0.25 in.	Pre-compressed strain (%):	28.1
		Compressed total density (kg/m3):	
		Compressed dry density (kg/m3):	
		Secondary compression ratio:	0.00255
		Total weight before shearing (kg):	11.867
		Dry weight before shearing (kg):	9.609

Consolidation Stage		Shear Stage		
Consolidated height (mm):	94.09	Type of test:		CL-direct shear
Vertical stress (kPa):	195.5	Shear strain rate (%/min):		
Immediate strain (εimm, %)	21.13	12 mm	Shear stress (kPa)	95.6
Strain before shearing (εall, %)	21.8		Tan friction angle (°)	26.2
Compression index (Cεc)	0.092		Sin friction angle (°)	
Constrained modulus	9.46	35 mm	Shear stress (kPa)	114.0
Consolidated total density	1382		Tan friction angle (°)	30.3
Consolidated dry density	1119		Sin friction angle (°)	

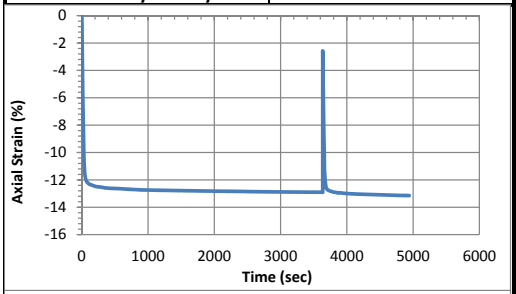

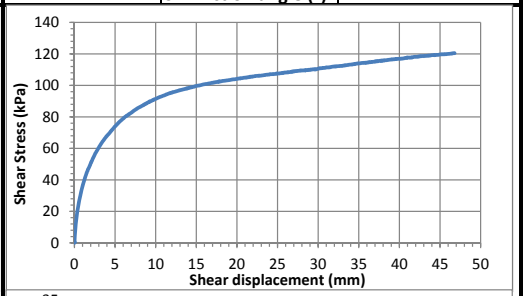

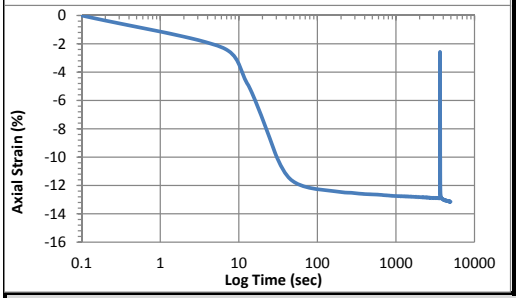

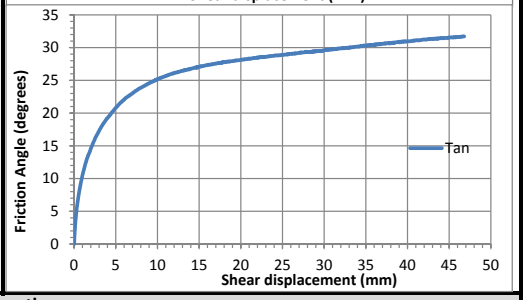

Strength			
τ/σv' at 10% strain	0.46	τ/σv0' at 10% strain	0.46
τ/σv' at 30% strain	0.56	τ/σv0' at 30% strain	0.56

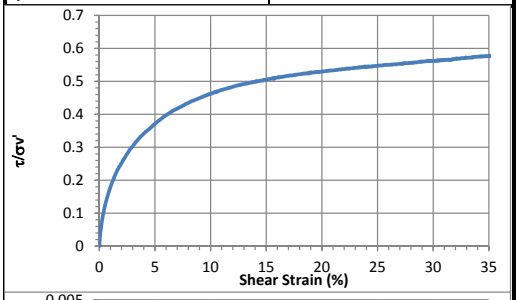

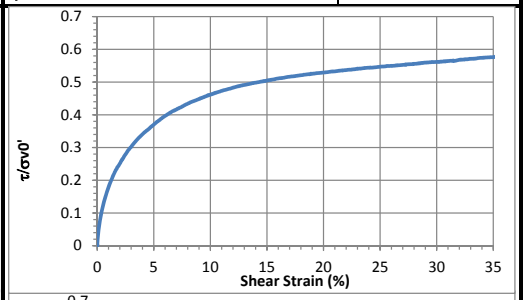

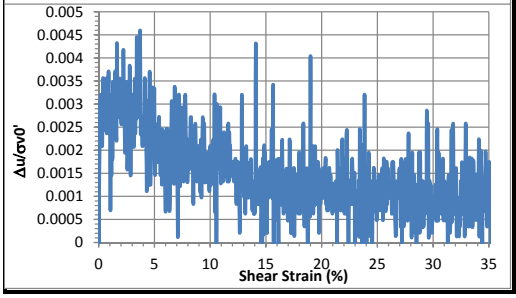

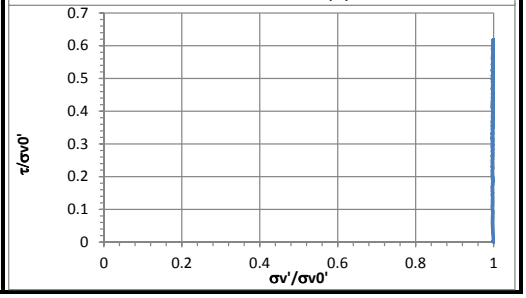

CSS Monotonic Shear Test Report

10/28/2013_Version 8.0

Geotechnical Engineering Laboratory

General Test Information		Sample Preparation	
Device:	CSS	Prepared total weight (kg):	16.725
Specimen ID:	CA-LCFD	Prepared dry weight (kg):	10.385
Test ID:	CAFD1	Prepared height (mm):	231.0
Date of test:	9/25/2015	Prepared total density (kg/m3):	983
Test performed:	Monotonic Shear	Prepared dry density (kg/m3):	611
Test material:	MSW	**Pre-compression Stage**	
Sample preparation:	CA-LC3 degraded undisturbed bottom part. Removed 4.514 kg before shearing.	Pre-compressed strain (%):	33.8
		Compressed total density (kg/m3):	1485
		Compressed dry density (kg/m3):	922
		Secondary compression ratio:	0.00752
		Total weight before shearing (kg):	10.658
		Dry weight before shearing (kg):	7.279

Consolidation Stage		Shear Stage		
Consolidated height (mm):	105.42	Type of test:		CL-strain
Vertical stress (kPa):	199.7	Shear strain rate (%/min):		0.38
Immediate strain (εimm, %)	33.74	10% strain	Shear stress (kPa)	69.7
Strain before shearing (εall, %)	34.9		Tan friction angle (°)	19.4
Compression index (Cc ε)	0.147		Sin friction angle (°)	20.6
Constrained modulus	5.93	peak	Shear stress (kPa)	97.1
Consolidated total density	1373		Tan friction angle (°)	26.0
Consolidated dry density	937		Sin friction angle (°)	29.2

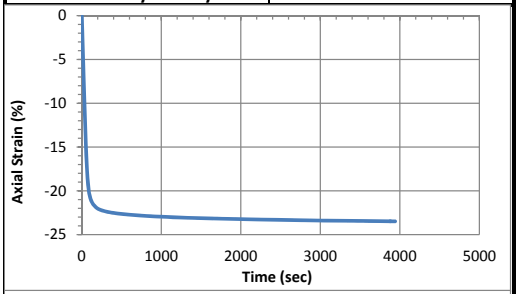

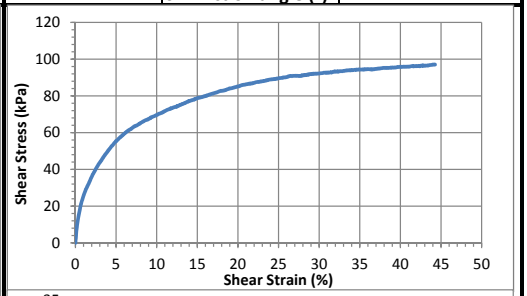

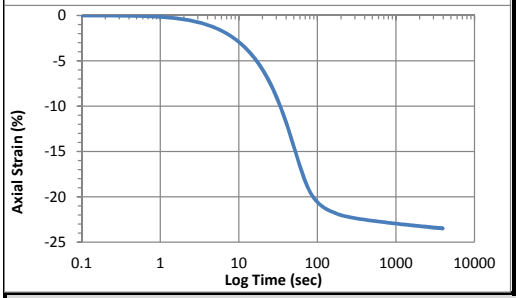

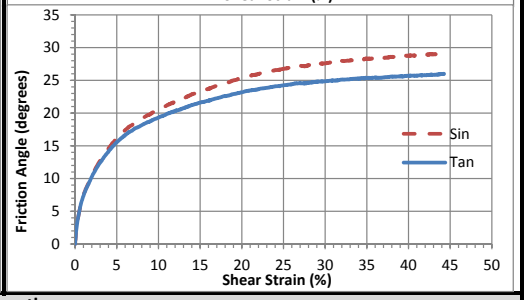

Strength			
τ/σv' at 10% strain	0.35	τ/σv0' at 10% strain	0.35
τ/σv' at peak	0.49	τ/σv0' at peak	0.49

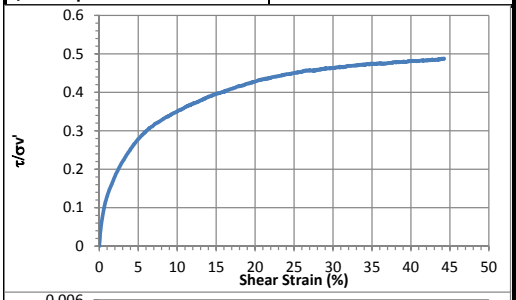

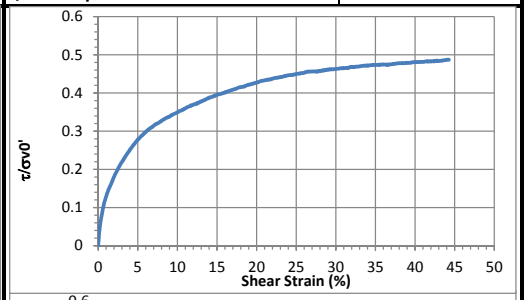

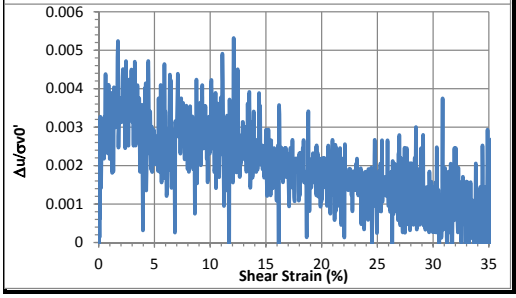

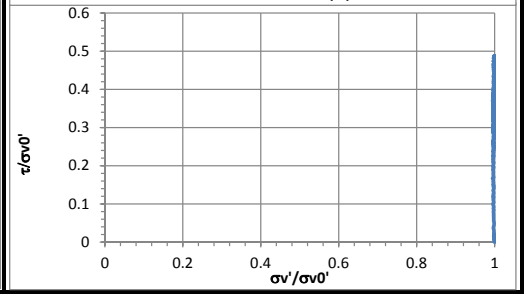

Accelerometer-Based Shear Wave Velocity Datasheet

Specimen ID: 092515-LCFD1-200-X-4
Test Material: LCFD1
Date: 092515
Test Performed by: Fei
Filename: 092515-LCFD1-200-X-4

Vertical Stress: 200kPa
Sensor Spacing: 0.10548 m
V_s(rise) = 161 m/s

Data Record

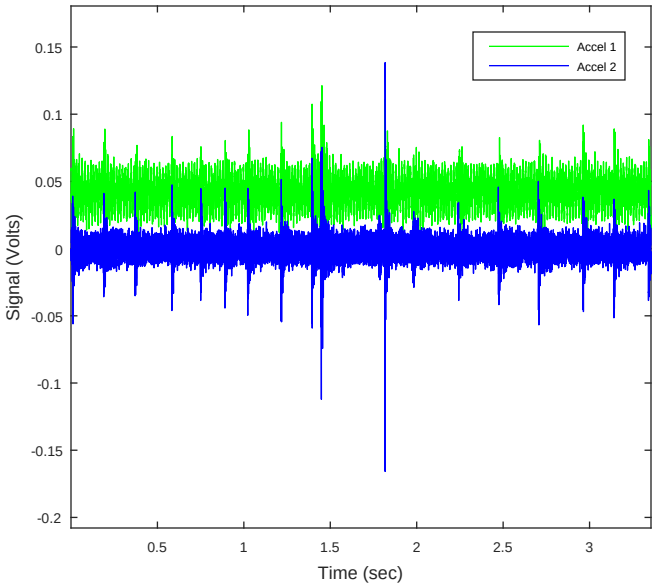

FFT of Accel 1

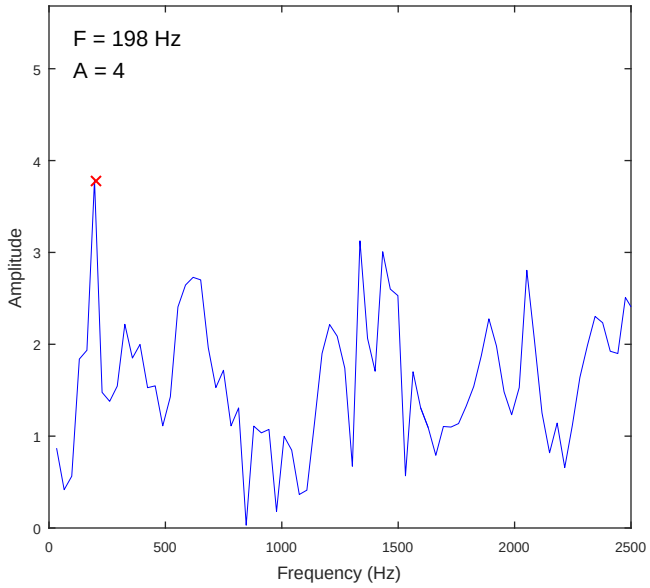

FFT of Accel 2

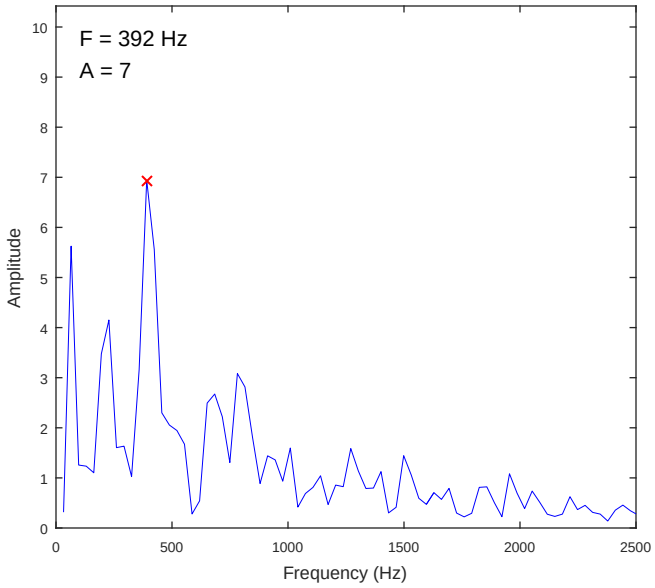

Travel Time Selection - View 1

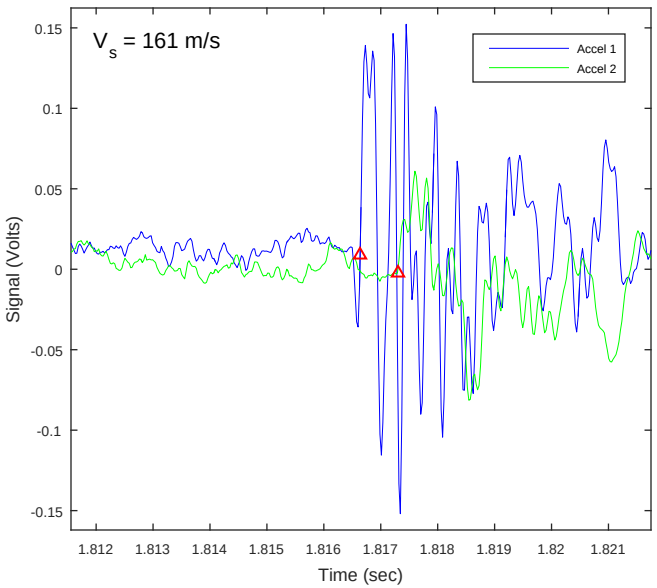

Travel Time Selection - View 2

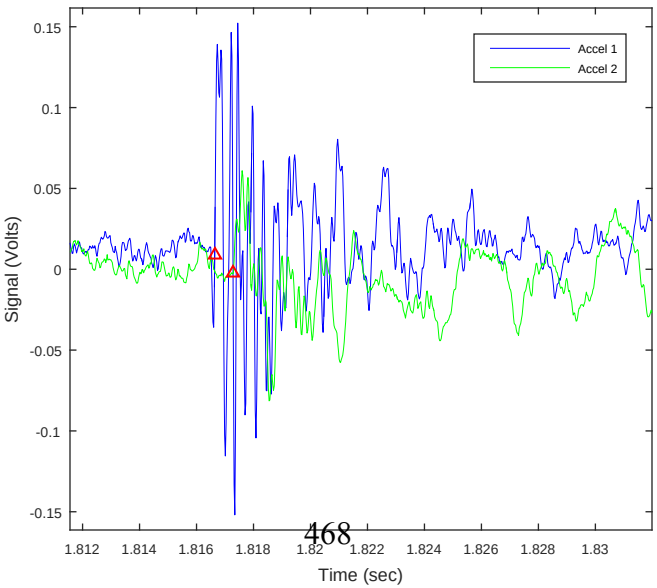

Travel Time Selection - View 3

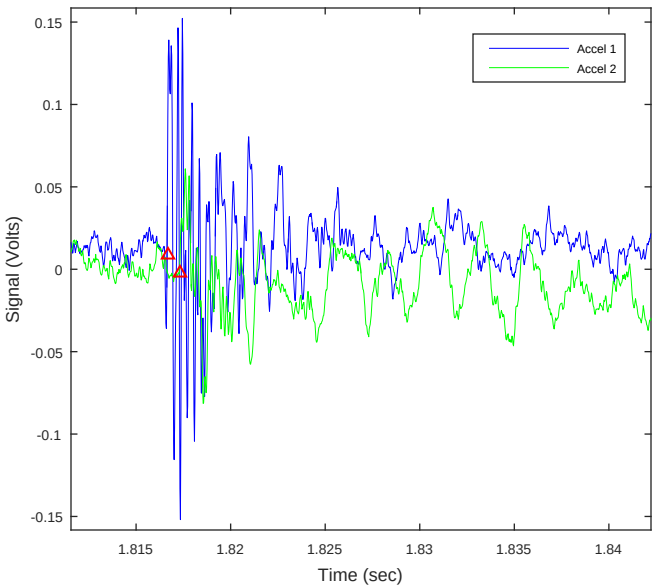

CSS Monotonic Shear Test Report

10/28/2013_Version 8.0

Geotechnical Engineering Laboratory

General Test Information		Sample Preparation	
Device:	CSS	Prepared total weight (kg):	17.618
Specimen ID:	CA-LCFD	Prepared dry weight (kg):	10.797
Test ID:	CAFD2	Prepared height (mm):	246.2
Date of test:	9/29/2015	Prepared total density (kg/m3):	972
Test performed:	Monotonic Shear	Prepared dry density (kg/m3):	595
Test material:	MSW	**Pre-compression Stage**	
Sample preparation:	CA-LC3 degraded undisturbed bottom part. Removed 2.878 kg before shearing. 4 stands on the bottom ring was bent near the end of shearing.	Pre-compressed strain (%):	43.4
		Compressed total density (kg/m3):	1718
		Compressed dry density (kg/m3):	1053
		Secondary compression ratio:	0.00299
		Total weight before shearing (kg):	12.907
		Dry weight before shearing (kg):	8.816

Consolidation Stage		Shear Stage		
Consolidated height (mm):	112.66	Type of test:		CL-strain
Vertical stress (kPa):	398.8	Shear strain rate (%/min):		0.36
Immediate strain (εimm, %)	43.44	10% strain	Shear stress (kPa)	137.6
Strain before shearing (εall, %)	44.0		Tan friction angle (°)	19.0
Compression index (Cεε)	0.167		Sin friction angle (°)	20.2
Constrained modulus	4.60	peak	Shear stress (kPa)	160.5
Consolidated total density	1555		Tan friction angle (°)	21.9
Consolidated dry density	1063		Sin friction angle (°)	23.8

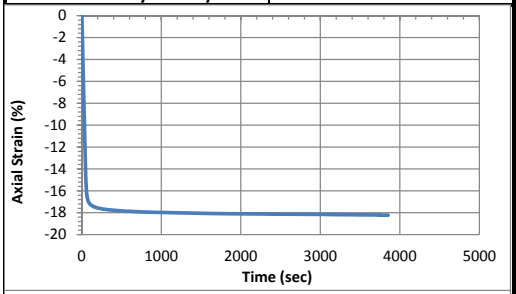

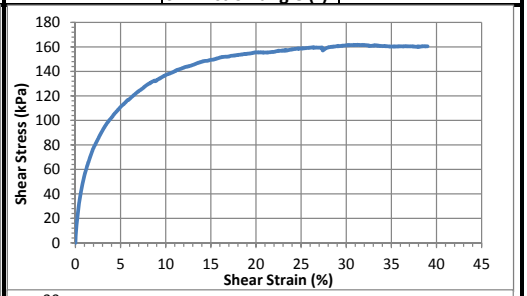

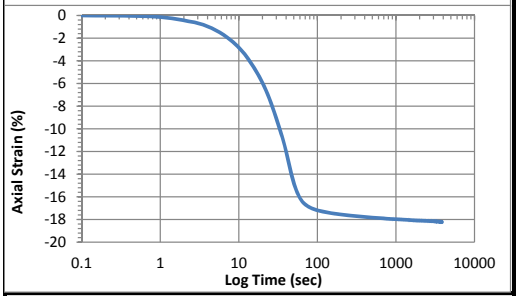

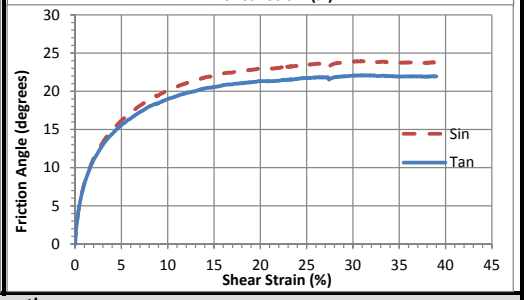

Strength			
τ/σv' at 10% strain	0.34	τ/σv0' at 10% strain	0.34
τ/σv' at peak	0.41	τ/σv0' at peak	0.41

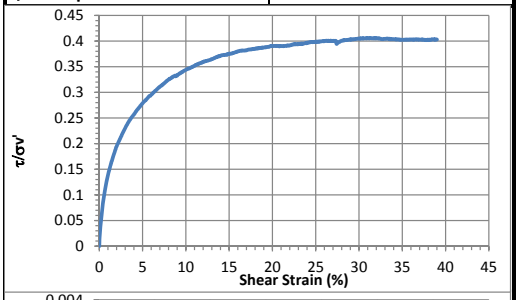

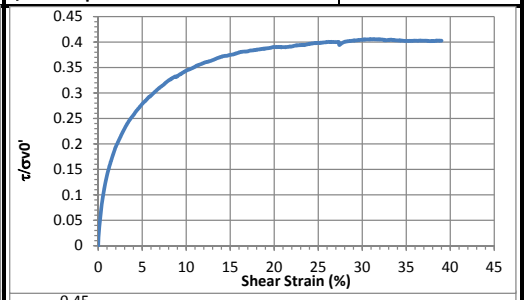

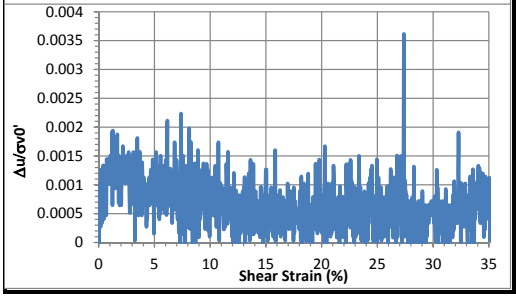

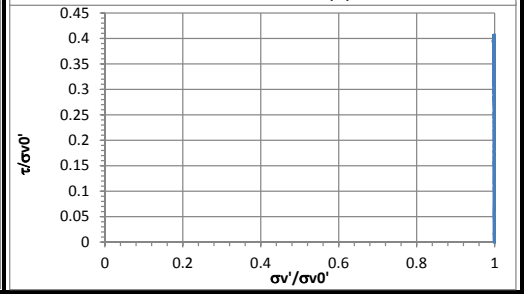

Accelerometer-Based Shear Wave Velocity Datasheet

Specimen ID: 092915-LCFD2-400-X-4
Test Material: LCFD2
Date: 092915
Test Performed by: Fei
Filename: 092915-LCFD2-400-X-4

Vertical Stress: 400kPa
Sensor Spacing: 0.11268 m
V_s(rise) = 294 m/s

Data Record

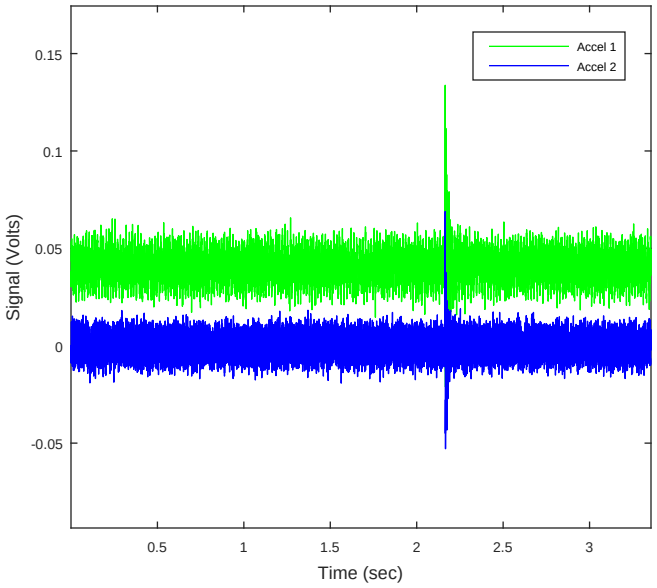

FFT of Accel 1

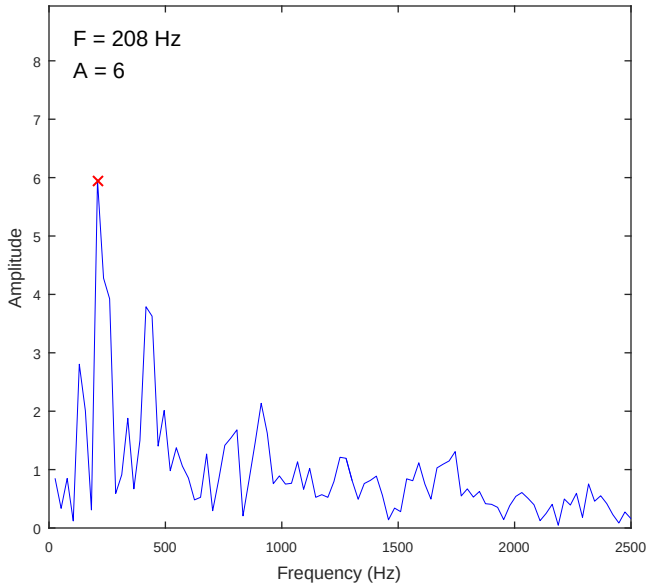

FFT of Accel 2

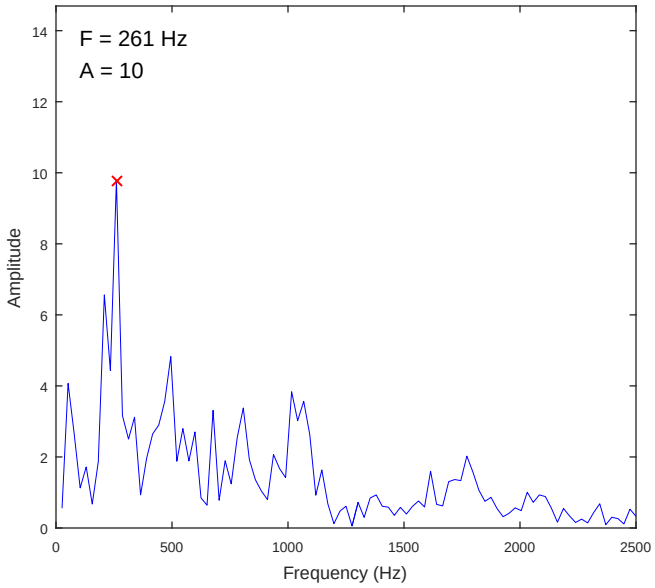

Travel Time Selection - View 1

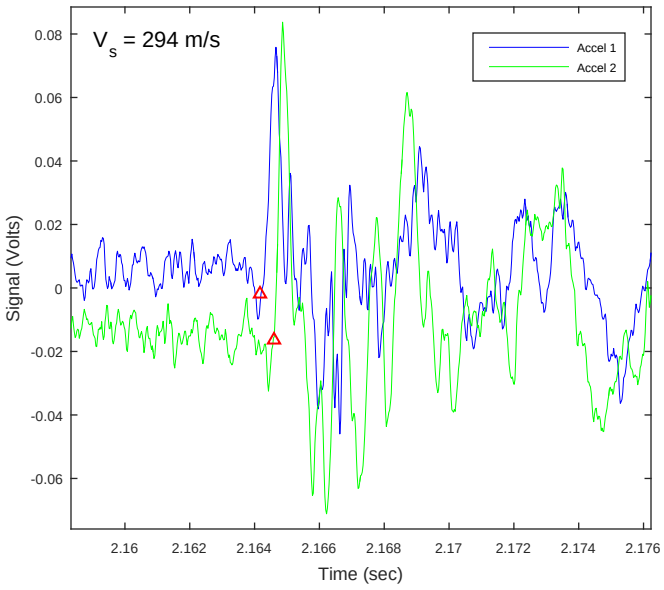

Travel Time Selection - View 2

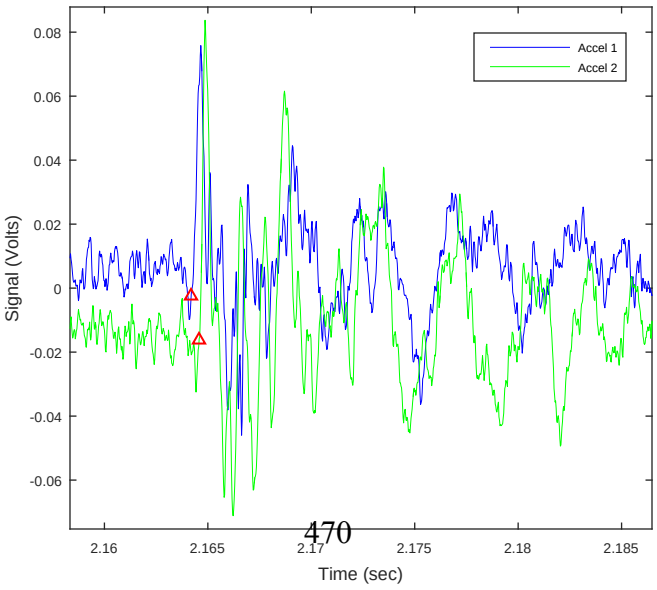

Travel Time Selection - View 3

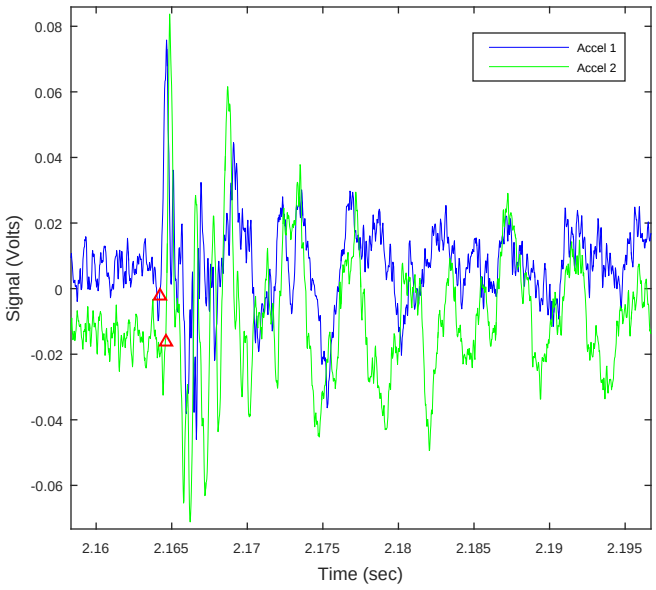

CSS Monotonic Shear Test Report

10/28/2013_Version 8.0

Geotechnical Engineering Laboratory

General Test Information		Sample Preparation	
Device:	CSS	Prepared total weight (kg):	14.400
Specimen ID:	CA-LCFD	Prepared dry weight (kg):	9.206
Test ID:	CAFD3	Prepared height (mm):	204.7
Date of test:	10/6/2015	Prepared total density (kg/m3):	955
Test performed:	Monotonic Shear	Prepared dry density (kg/m3):	611
Test material:	MSW	**Pre-compression Stage**	
Sample preparation:	CA-LCF degraded reconstituted. Removed 1.272 kg before shearing.	Pre-compressed strain (%):	36.2
		Compressed total density (kg/m3):	1498
		Compressed dry density (kg/m3):	0
		Secondary compression ratio:	0.00523
		Total weight before shearing (kg):	12.113
		Dry weight before shearing (kg):	8.331

Consolidation Stage		Shear Stage		
Consolidated height (mm):	118.26	Type of test:		CL-strain
Vertical stress (kPa):	198.5	Shear strain rate (%/min):		0.34
Immediate strain (εimm, %)	35.14	10% strain	Shear stress (kPa)	77.5
Strain before shearing (εall, %)	36.1		Tan friction angle (°)	21.5
Compression index (Cεc)	0.153		Sin friction angle (°)	23.1
Constrained modulus	5.69	peak	Shear stress (kPa)	99.4
Consolidated total density	1391		Tan friction angle (°)	26.7
Consolidated dry density	956		Sin friction angle (°)	30.2

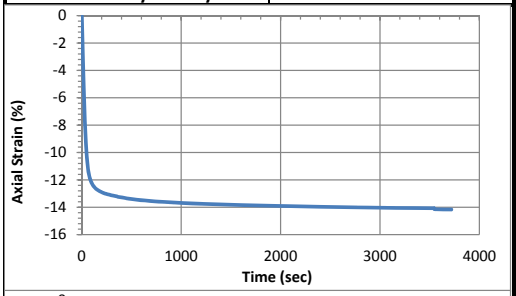

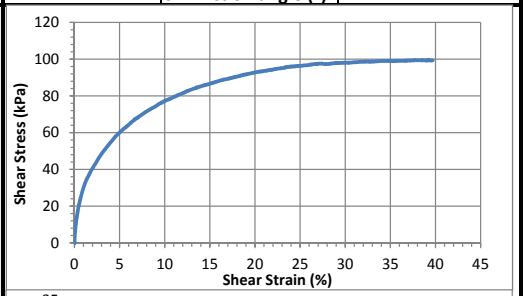

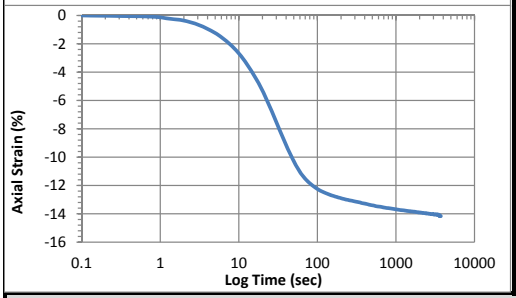

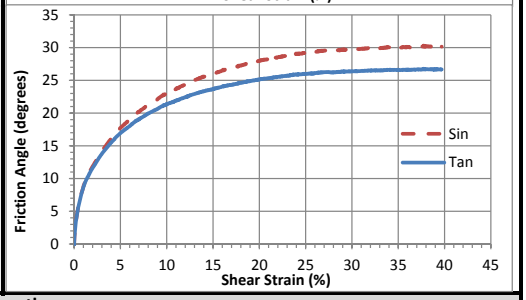

Strength

τ/σv' at 10% strain	0.39	τ/σv0' at 10% strain	0.39
τ/σv' at peak	0.50	τ/σv0' at peak	0.50

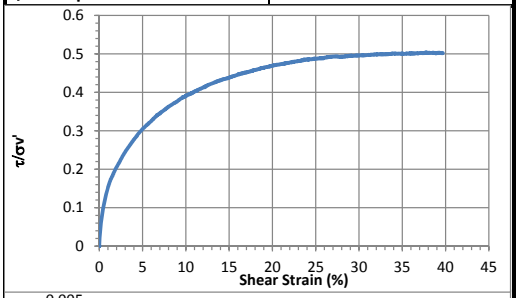

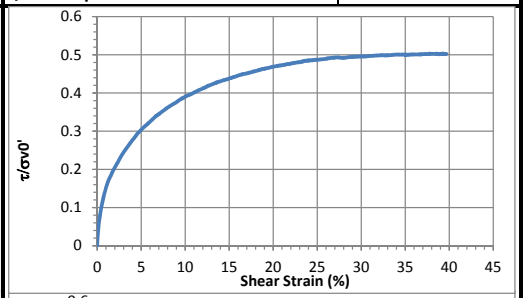

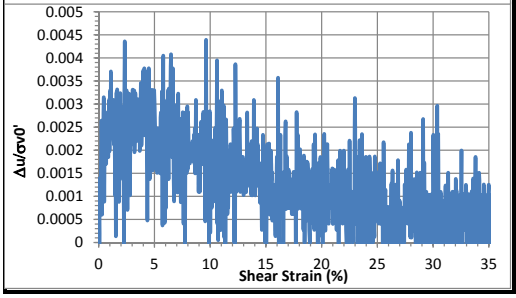

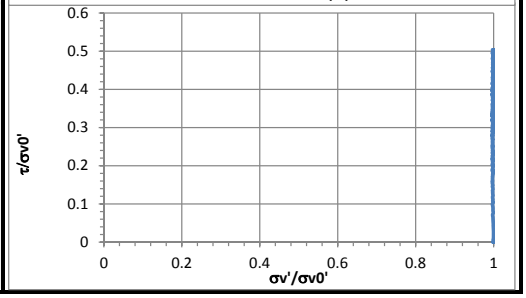

Accelerometer-Based Shear Wave Velocity Datasheet

Specimen ID: 100615-LCFD3-200-X-4
Test Material: LCFD3
Date: 100615
Test Performed by: Fei
Filename: 100615-LCFD3-200-X-4

Vertical Stress: 200kPa
Sensor Spacing: 0.11837 m
V_s(rise) = 167 m/s

Data Record

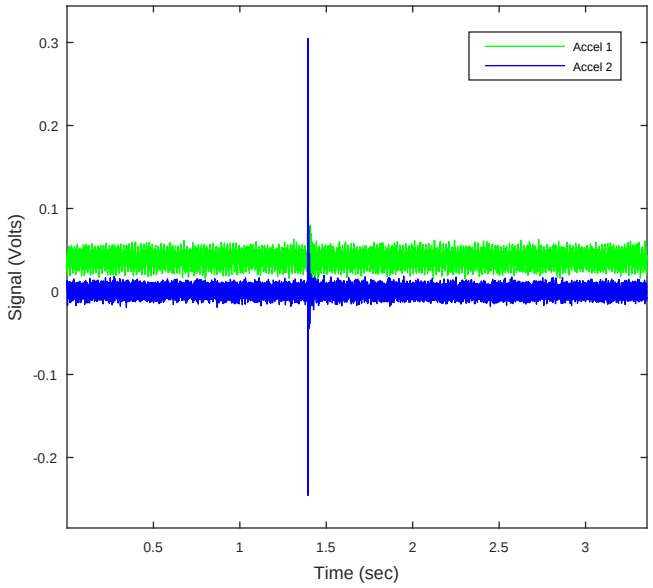

FFT of Accel 1

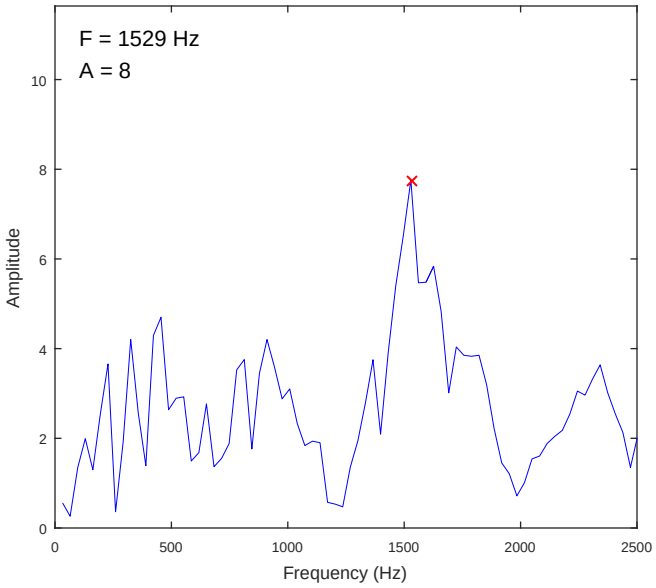

FFT of Accel 2

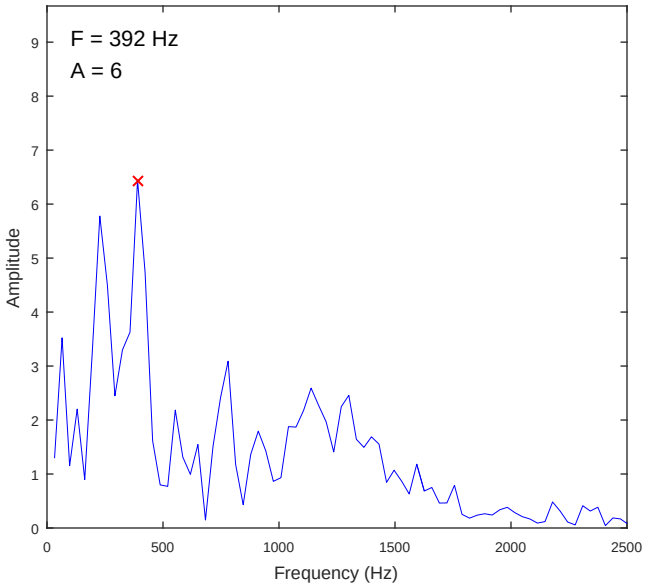

Travel Time Selection - View 1

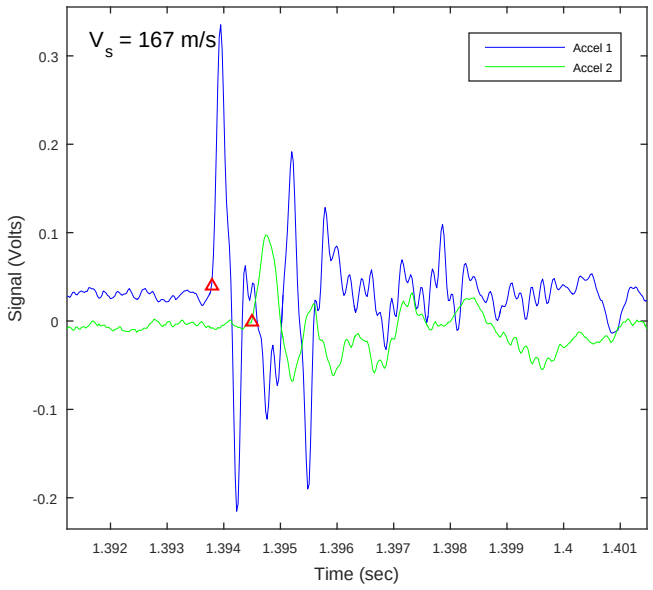

Travel Time Selection - View 2

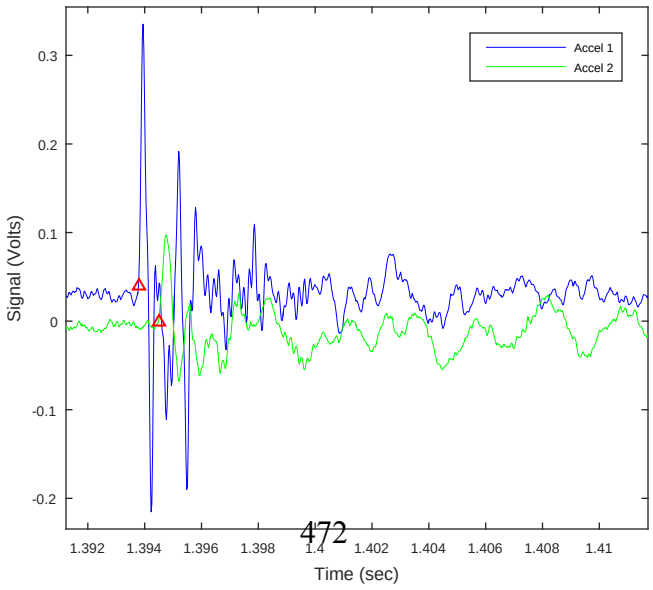

Travel Time Selection - View 3

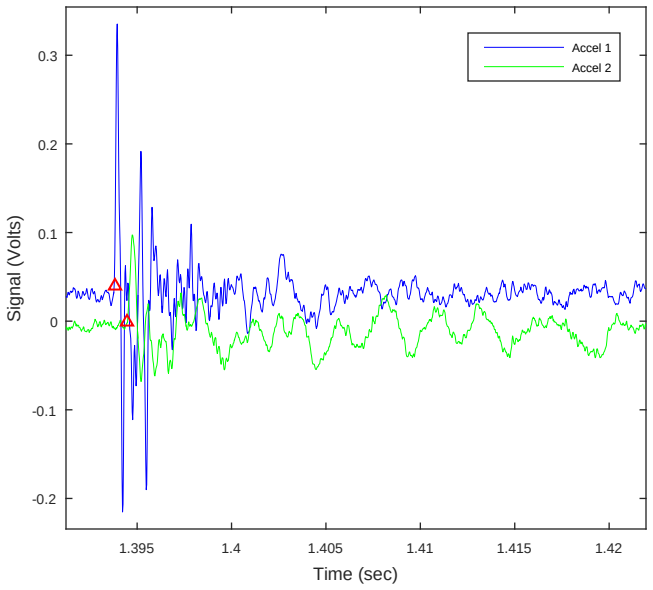

CSS Monotonic Shear Test Report

10/28/2013_Version 8.0

Geotechnical Engineering Laboratory

General Test Information		Sample Preparation	
Device:	CSS	Prepared total weight (kg):	12.600
Specimen ID:	CA-LCFD	Prepared dry weight (kg):	8.055
Test ID:	CAFD4	Prepared height (mm):	218.3
Date of test:	10/9/2015	Prepared total density (kg/m3):	784
Test performed:	Monotonic Shear	Prepared dry density (kg/m3):	501
Test material:	MSW	**Pre-compression Stage**	
Sample preparation:	CA-LCF degraded reconstituted.	Pre-compressed strain (%):	47.4
		Compressed total density (kg/m3):	1489
		Compressed dry density (kg/m3):	952
		Secondary compression ratio:	0.00293
		Total weight before shearing (kg):	11.915
		Dry weight before shearing (kg):	8.055

Consolidation Stage		Shear Stage		
Consolidated height (mm):	109.32	Type of test:		CL-strain
Vertical stress (kPa):	96.3	Shear strain rate (%/min):		0.37
Immediate strain (εimm, %)	49.48	10% strain	Shear stress (kPa)	39.9
Strain before shearing (εall, %)	49.9		Tan friction angle (°)	22.7
Compression index (Cεε)	0.249		Sin friction angle (°)	24.7
Constrained modulus	4.04	peak	Shear stress (kPa)	52.3
Consolidated total density	1480		Tan friction angle (°)	28.7
Consolidated dry density	1000		Sin friction angle (°)	33.1

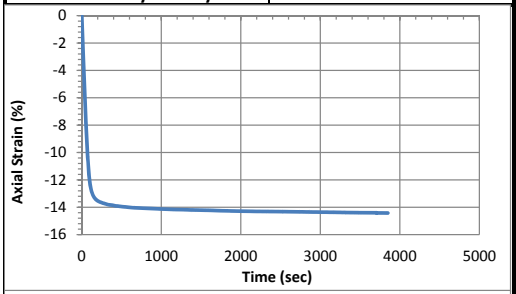

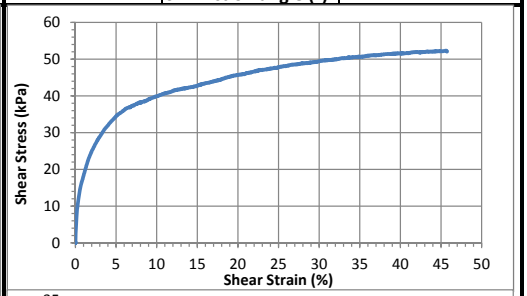

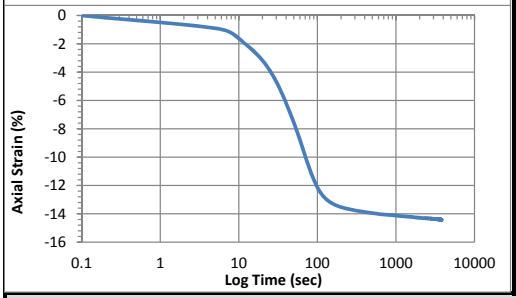

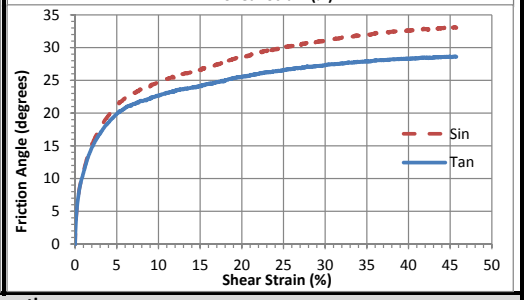

Strength

τ/σv' at 10% strain	0.42	τ/σv0' at 10% strain	0.42
τ/σv' at peak	0.55	τ/σv0' at peak	0.55

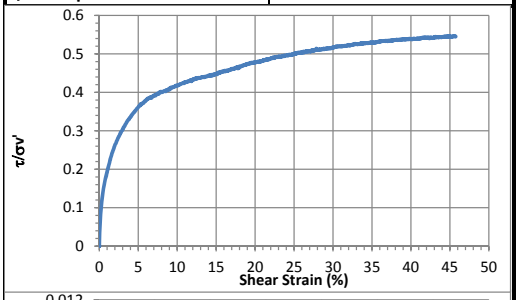

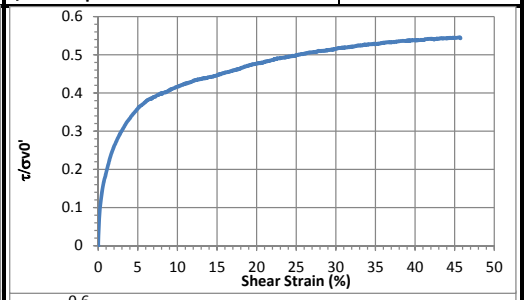

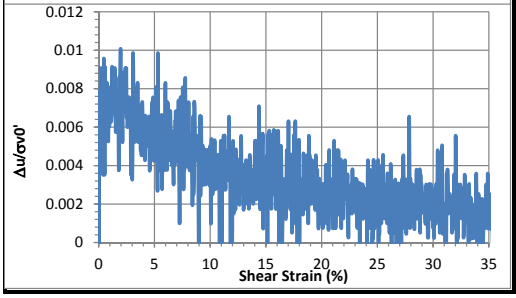

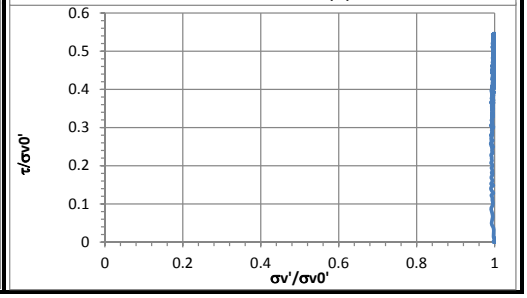

Accelerometer-Based Shear Wave Velocity Datasheet

Specimen ID: 100915-LCFD4-100-X-4
Test Material: LCFD4
Date: 100915
Test Performed by: Fei
Filename: 100915-LCFD4-100-X-4

Vertical Stress: 100kPa
Sensor Spacing: 0.10934 m
V_s(rise) = 144 m/s

Data Record

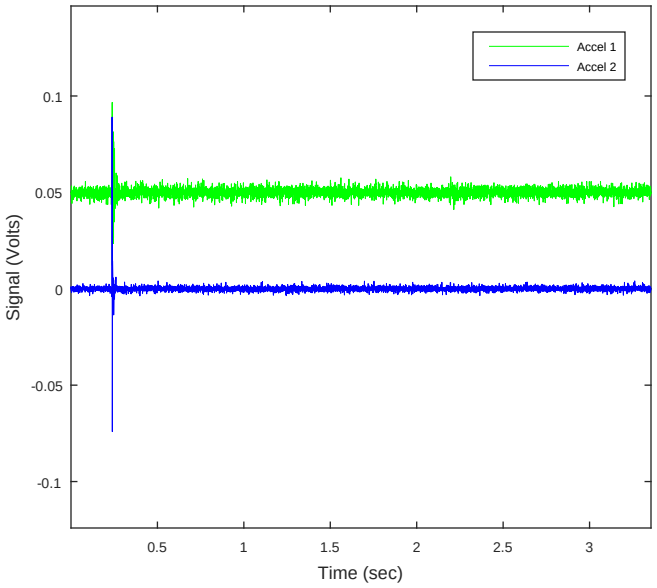

FFT of Accel 1

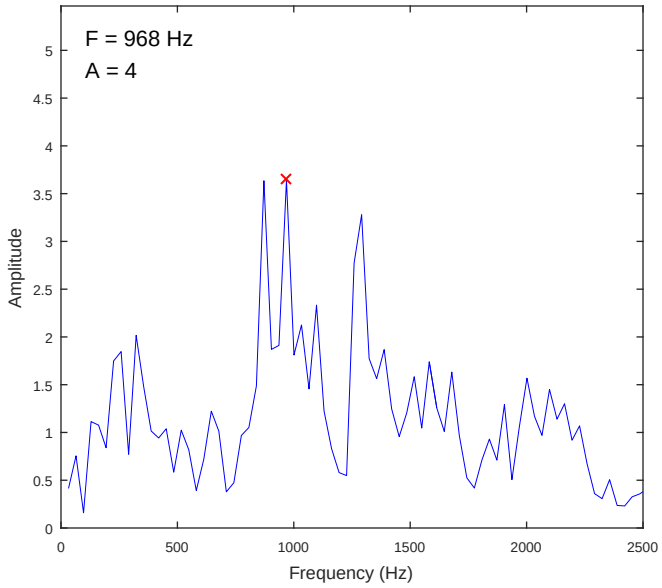

FFT of Accel 2

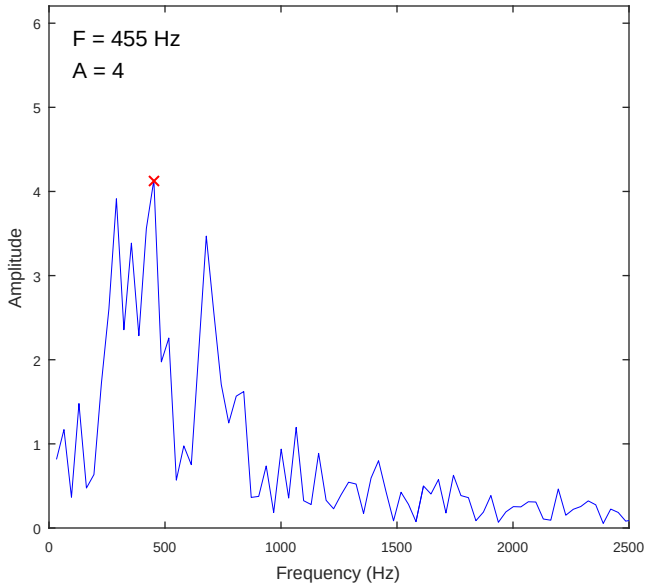

Travel Time Selection - View 1

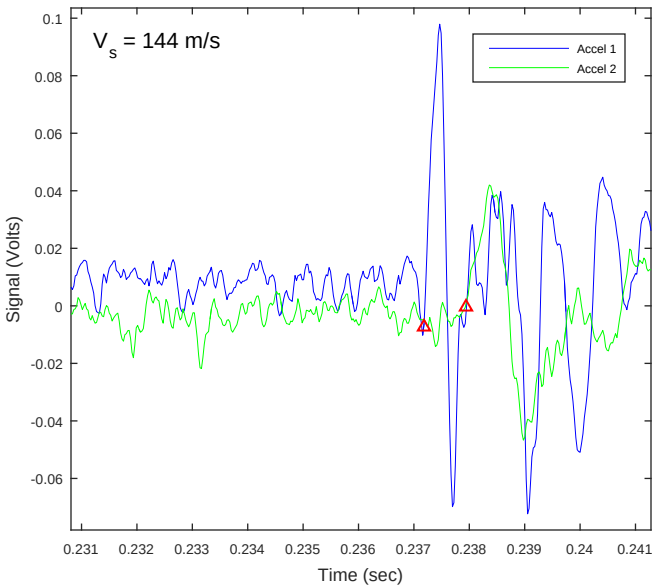

Travel Time Selection - View 2

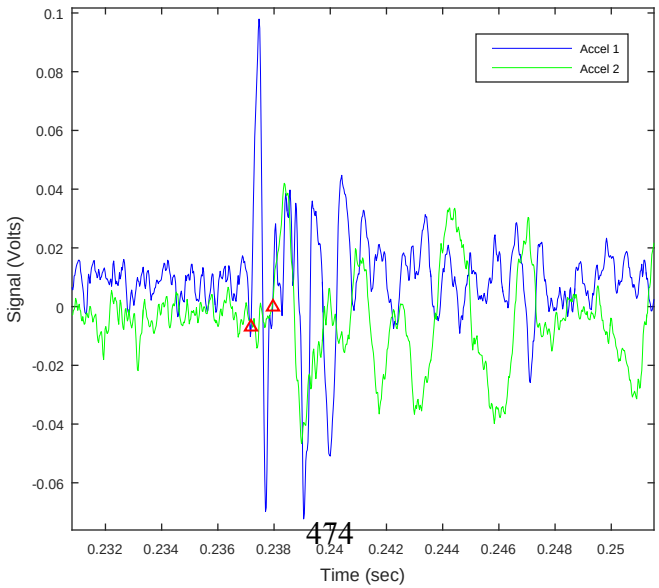

Travel Time Selection - View 3

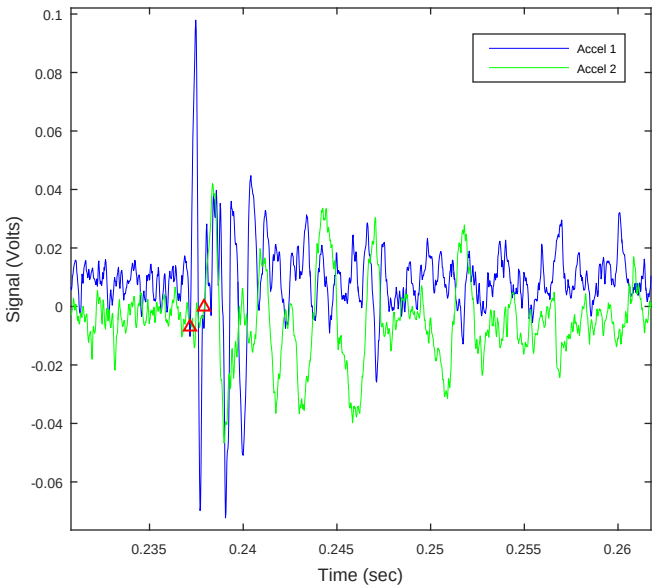

CSS Monotonic Shear Test Report

10/28/2013_Version 8.0

Geotechnical Engineering Laboratory

General Test Information		Sample Preparation	
Device:	CSS	**Prepared total weight (kg):**	14.400
Specimen ID:	CA-LCFD	**Prepared dry weight (kg):**	9.206
Test ID:	CAFD5	**Prepared height (mm):**	213.4
Date of test:	10/13/2015	**Prepared total density (kg/m3):**	916
Test performed:	Monotonic Shear	**Prepared dry density (kg/m3):**	586
Test material:	MSW	**Pre-compression Stage**	
Sample preparation:	CA-LCF degraded reconstituted. Removed 0.514 kg before shearing. 2 stands on the bottom ring was bent near the end of shearing.	**Pre-compressed strain (%):**	45.9
		Compressed total density (kg/m3):	1695
		Compressed dry density (kg/m3):	1083
		Secondary compression ratio:	0.00483
		Total weight before shearing (kg):	12.345
		Dry weight before shearing (kg):	8.823

Consolidation Stage		Shear Stage		
Consolidated height (mm):	112.73	**Type of test:**		CL-strain
Vertical stress (kPa):	394.7	**Shear strain rate (%/min):**		0.36
Immediate strain (εimm, %)	43.99	**10% strain**	**Shear stress (kPa)**	143.6
Strain before shearing (εall, %)	45.0		**Tan friction angle (°)**	19.9
Compression index (Cεε)	0.169		**Sin friction angle (°)**	21.1
Constrained modulus	4.55	**peak**	**Shear stress (kPa)**	179.8
Consolidated total density	1487		**Tan friction angle (°)**	24.4
Consolidated dry density	1063		**Sin friction angle (°)**	26.9

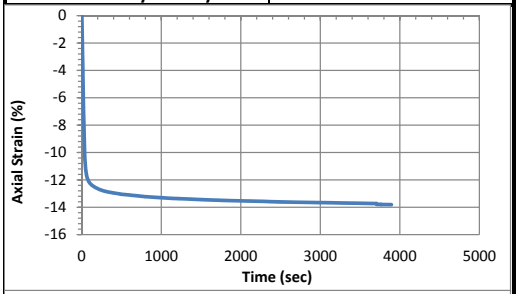

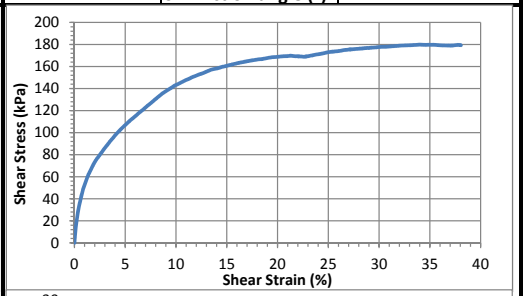

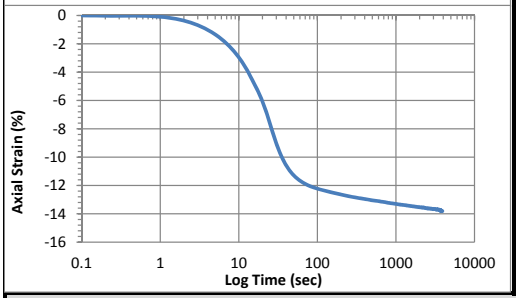

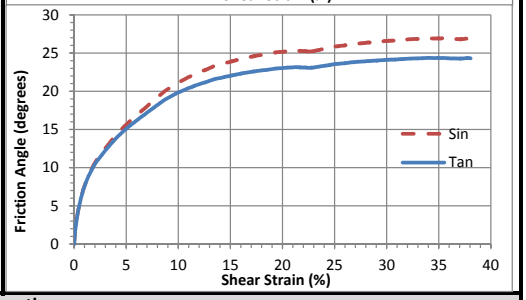

Strength			
τ/σv' at 10% strain	0.36	**τ/σv0' at 10% strain**	0.36
τ/σv' at peak	0.45	**τ/σv0' at peak**	0.45

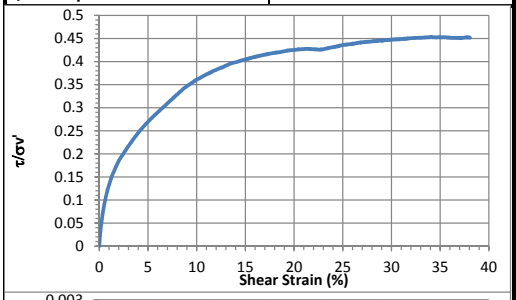

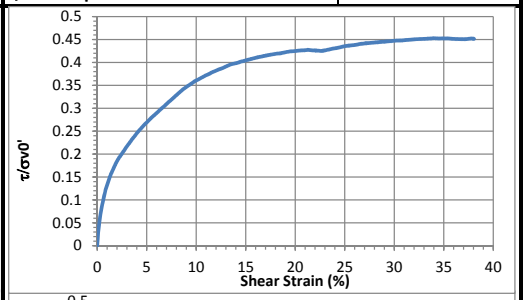

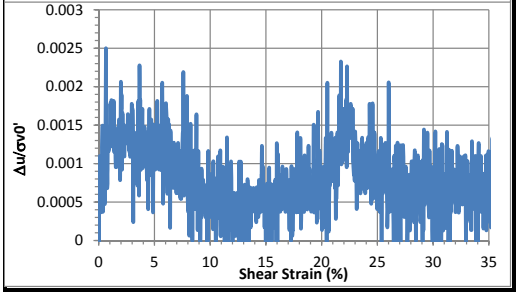

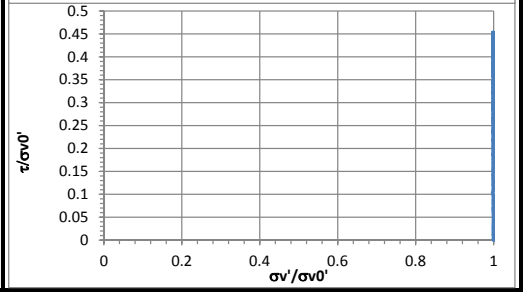

Accelerometer-Based Shear Wave Velocity Datasheet

Specimen ID: 101315-LCFD5-400-X-2
Test Material: LCFD5
Date: 101315
Test Performed by: Fei
Filename: 101315-LCFD5-400-X-2

Vertical Stress: 400kPa
Sensor Spacing: 0.11283 m
V_s(rise) = 162 m/s

Data Record

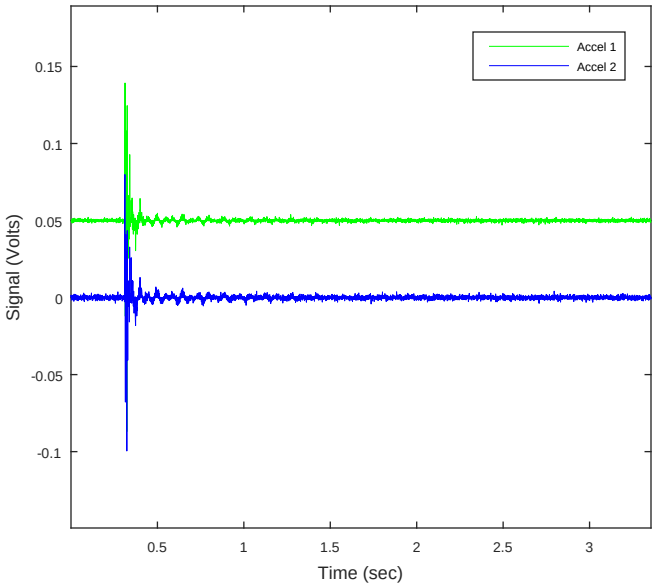

FFT of Accel 1

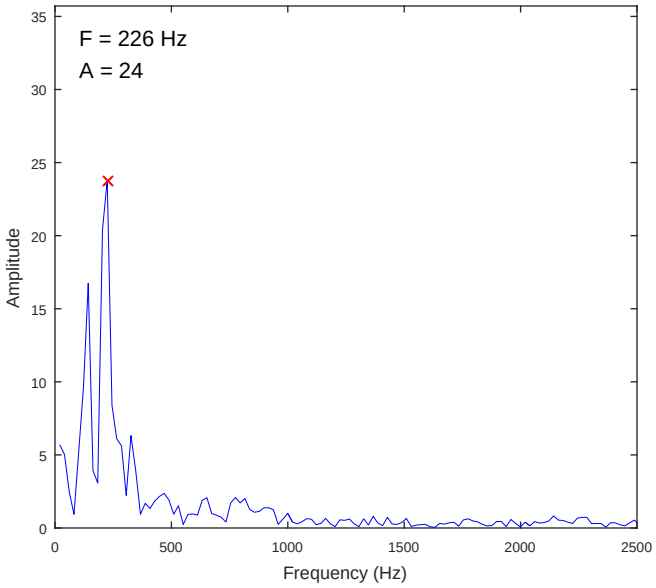

FFT of Accel 2

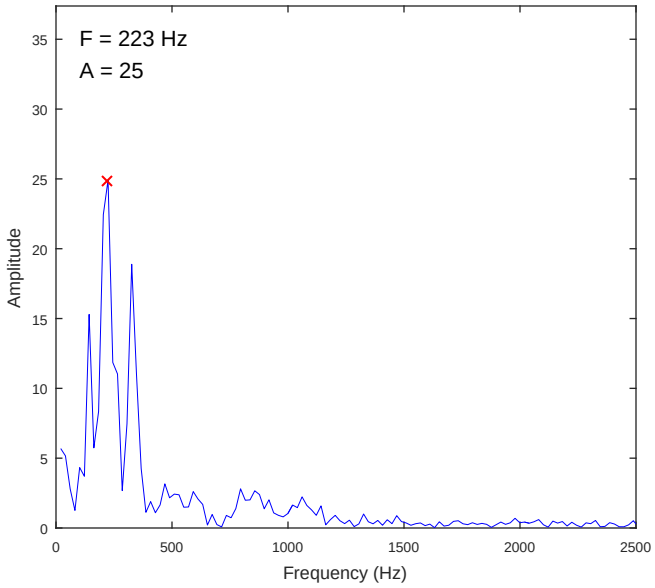

Travel Time Selection - View 1

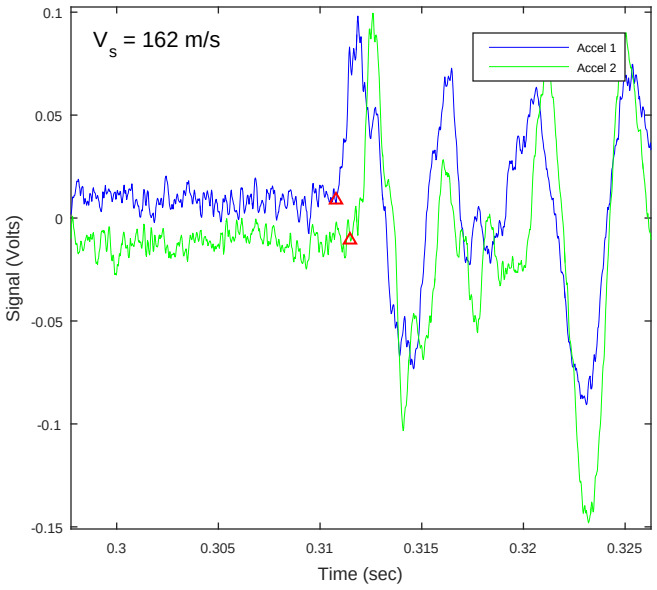

Travel Time Selection - View 2

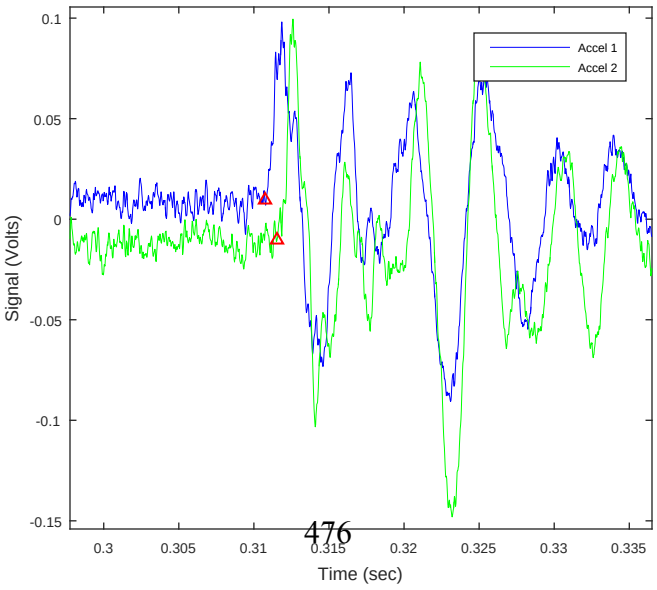

Travel Time Selection - View 3

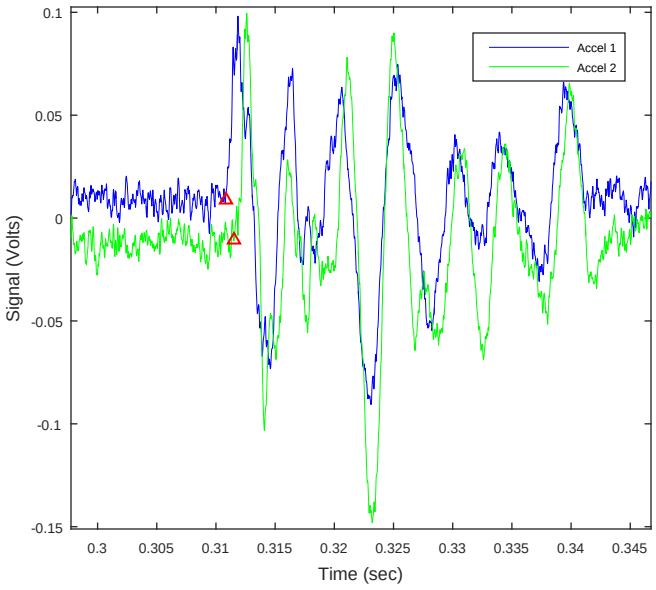

CSS Monotonic Shear Test Report

10/28/2013_Version 8.0

Geotechnical Engineering Laboratory

General Test Information	
Device:	CSS
Specimen ID:	CA-LCFD
Test ID:	CAFD6
Date of test:	10/24/2015
Test performed:	Monotonic Shear
Test material:	MSW
Sample preparation:	CA-LCF degraded compacted. Membrane was lifted up above the pedesatl. Shearing stopped once after 1.5 minutes and resumed.

Sample Preparation	
Prepared total weight (kg):	14.400
Prepared dry weight (kg):	9.206
Prepared height (mm):	165.0
Prepared total density (kg/m3):	1185
Prepared dry density (kg/m3):	757
Pre-compression Stage	
Pre-compressed strain (%):	28.9
Compressed total density (kg/m3):	1667
Compressed dry density (kg/m3):	1066
Secondary compression ratio:	0.00424
Total weight before shearing (kg):	13.052
Dry weight before shearing (kg):	9.206

Consolidation Stage	
Consolidated height (mm):	117.70
Vertical stress (kPa):	197.1
Immediate strain (εimm, %)	27.74
Strain before shearing (εall, %)	28.7
Compression index (Cεε)	0.121
Constrained modulus	7.21
Consolidated total density	1506
Consolidated dry density	1062

Shear Stage		
Type of test:		CL-strain
Shear strain rate (%/min):		0.34
10% strain	Shear stress (kPa)	92.0
	Tan friction angle (°)	25.0
	Sin friction angle (°)	27.9
peak	Shear stress (kPa)	114.9
	Tan friction angle (°)	30.3
	Sin friction angle (°)	35.7

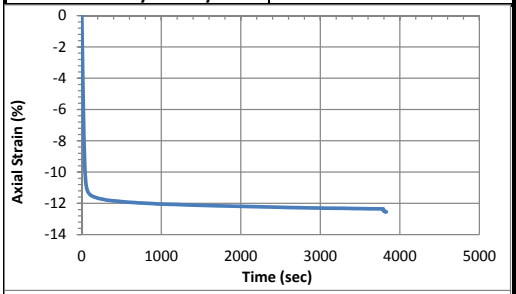

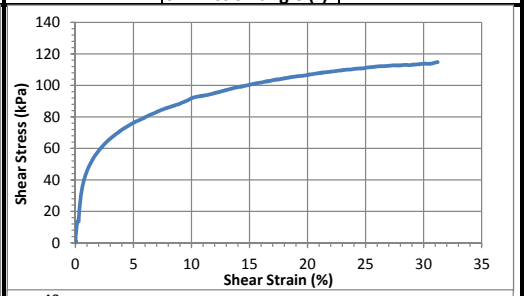

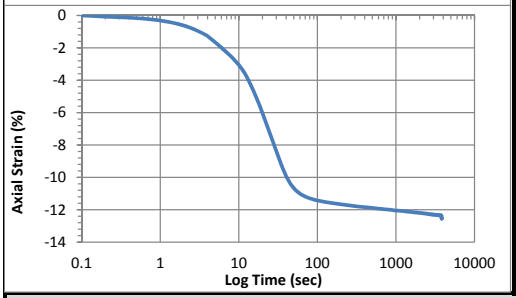

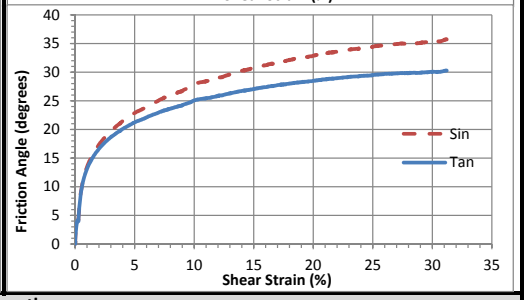

Strength

τ/σv' at 10% strain	0.47	τ/σv0' at 10% strain	0.47
τ/σv' at peak	0.58	τ/σv0' at peak	0.58

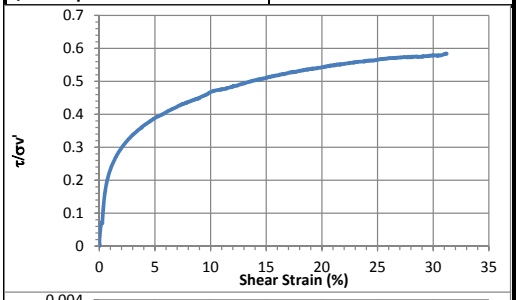

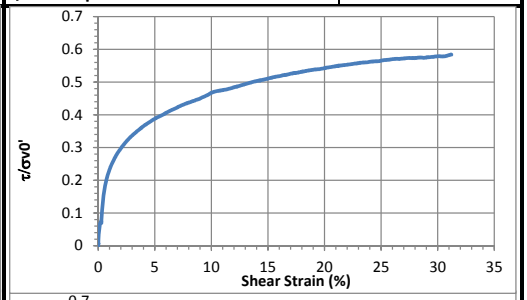

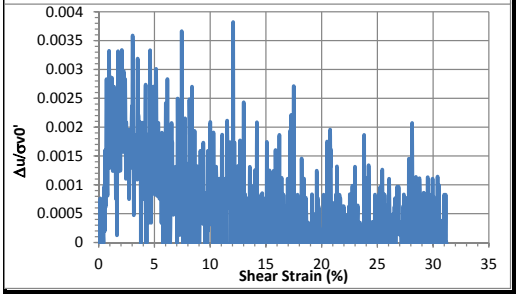

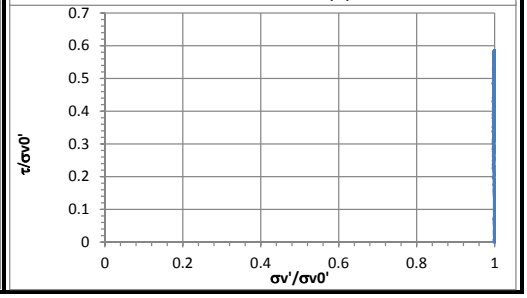

CSS Monotonic Shear Test Report

10/28/2013_Version 8.0

Geotechnical Engineering Laboratory

General Test Information and Sample Preparation

Device:	CSS	**Layers:**	9.50
Specimen ID:	CA-LC3	**Weight/layer (kg):**	0.987
Test ID:	CA31	**Height/layer (mm):**	25.4
Date of Test:	8/16/2014	**Total height (mm):**	241.3
Test Performed:	Monotonic Shear	**Soil-Only Specimen Diameter (mm):**	306.2
Test Material:	MSW	**Total weight (kg):**	9.3765
Sample Preparation:	The same initial composition and unit weight as Sim. #6. Staged pre-compress for 52 (24) hours, consolidate for 2.5 hours.	**Density (kg/m^3):**	528
		Membrane Thickness (mm):	0.000635
		Moisture Content (%):	60.0
		Saturated (Y/N):	N
		Prepared by:	Fei

Pre-compression Stage

Pre-compression strain:	0.50	**Secondary compression ratio:**	
Height (mm):	130.3	**Density (kg/m3):**	1029

Consolidation Stage

Initial height (mm):	137.5
Initial density (kg/m3):	926
Vertical Stress (kPa):	395.3
Immediate strain (εimm, %)	
Consolidated Height (mm):	106.4
Compression index (Cc$_\varepsilon$)	0.214
Consolidation modulus	3.6
Consolidated density (kg/m^3):	1197

Shear Stage

Type of Test:		CD-strain
Shear Strain Rate (%/min):		0.38
10% strain	**Shear stress (kPa)**	121.5
	Tan friction angle (°)	17.1
	Sin friction angle (°)	17.9
30% strain	**Shear stress (kPa)**	151.1
	Tan friction angle (°)	20.9
	Sin friction angle (°)	22.5

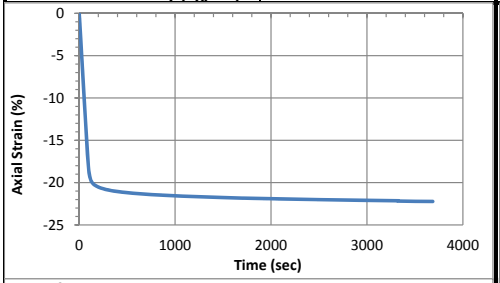

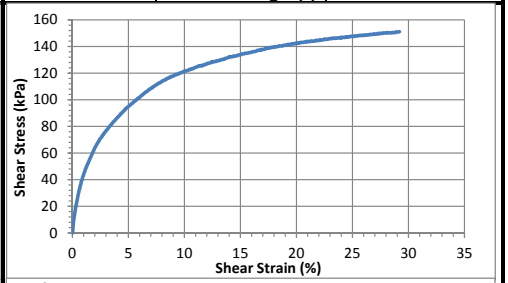

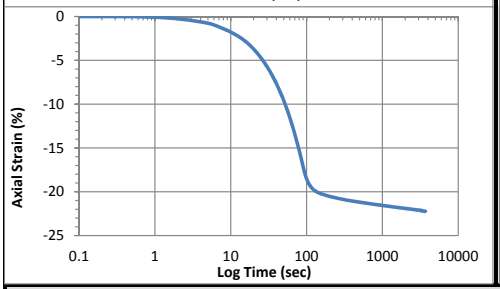

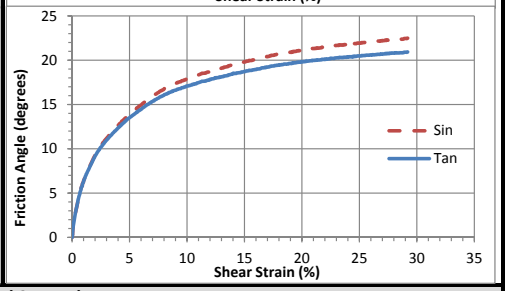

Undrained Strength

Su/σv' at 10% strain	0.31	**Su/σvc' at 10% strain**	0.31
Su/σv' at 30% strain	0.38	**Su/σvc' at 30% strain**	0.38

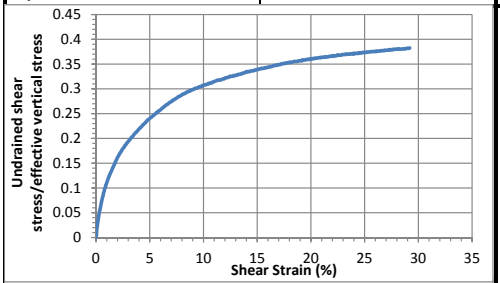

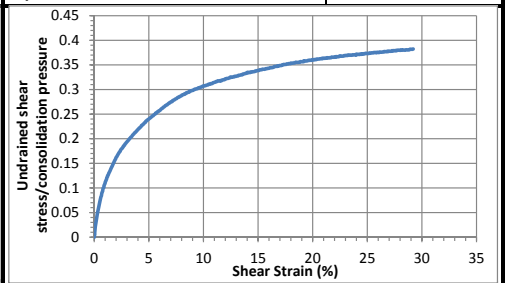

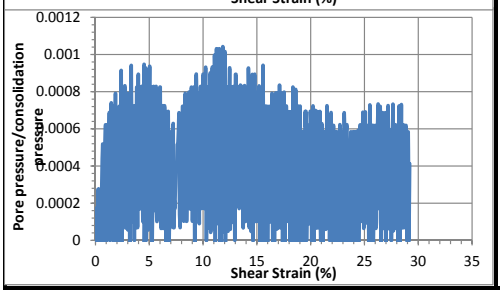

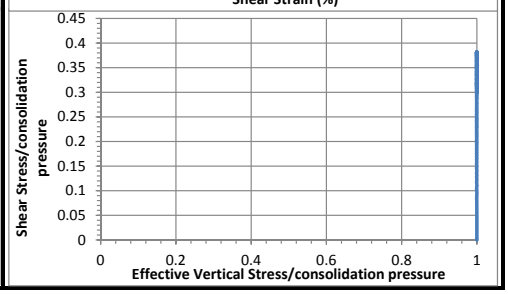

CSS Monotonic Shear Test Report

10/28/2013_Version 8.0

Geotechnical Engineering Laboratory

General Test Information and Sample Preparation			
Device:	CSS	**Layers:**	7.50
Specimen ID:	CA-LC3	**Weight/layer (kg):**	0.987
Test ID:	CA32	**Height/layer (mm):**	25.4
Date of Test:	8/18/2014	**Total height (mm):**	190.5
Test Performed:	Monotonic Shear	**Soil-Only Specimen Diameter (mm):**	306.2
Test Material:	MSW	**Total weight (kg):**	7.4025
Sample Preparation:	The same initial composition and unit weight as Sim. #6. Pre-compress for 23 hours, consolidate for 1 hour.	**Density (kg/m^3):**	528
		Membrane Thickness (mm):	0.000635
		Moisture Content (%):	60.0
		Saturated (Y/N):	N
		Prepared by:	Fei

Pre-compression Stage			
Pre-compression strain:	0.40	**Secondary compression ratio:**	0.00940
Height (mm):	123.4	**Density (kg/m3):**	814

Consolidation Stage		Shear Stage		
Initial height (mm):	137.4	**Type of Test:**		CD-strain
Initial density (kg/m3):	731	**Shear Strain Rate (%/min):**		0.34
Vertical Stress (kPa):	47.8	**10% strain**	**Shear stress (kPa)**	17.4
Immediate strain (εimm, %)	38.5		**Tan friction angle (°)**	20.0
Consolidated Height (mm):	118.2		**Sin friction angle (°)**	21.4
Compression index (Ccε)	0.241	**30% strain**	**Shear stress (kPa)**	19.9
Consolidation modulus	4.9		**Tan friction angle (°)**	22.6
Consolidated density (kg/m^3):	850		**Sin friction angle (°)**	24.7

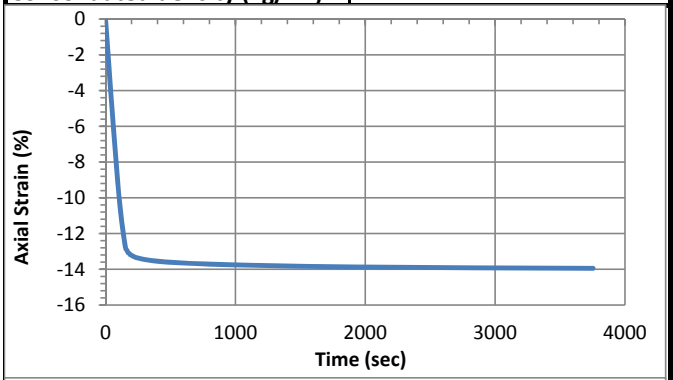

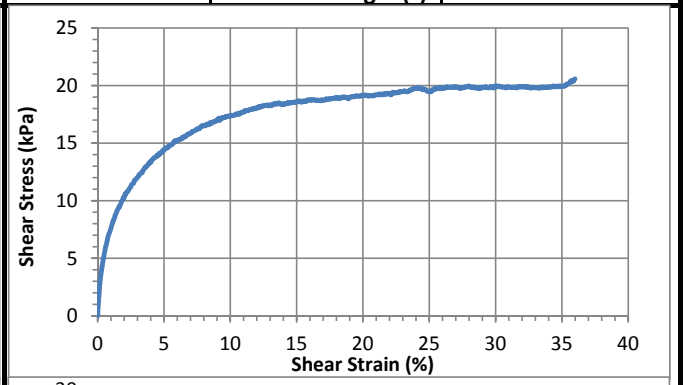

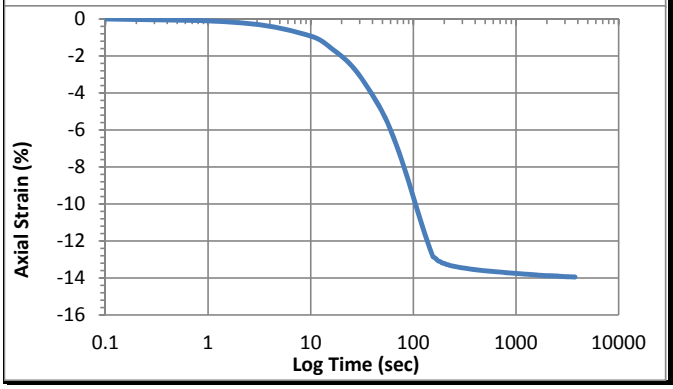

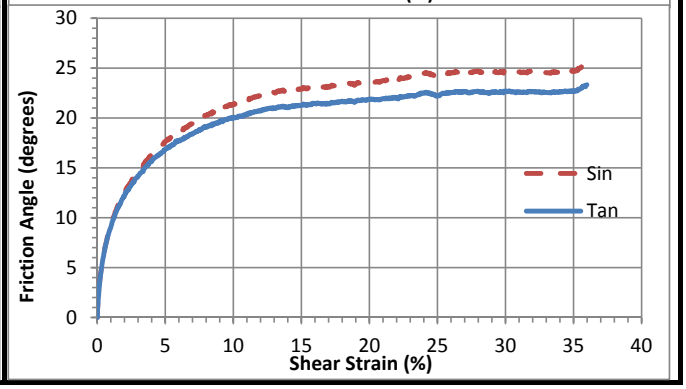

Undrained Strength			
Su/σv' at 10% strain	0.36	Su/σvc' at 10% strain	0.36
Su/σv' at 30% strain	0.42	Su/σvc' at 30% strain	0.42

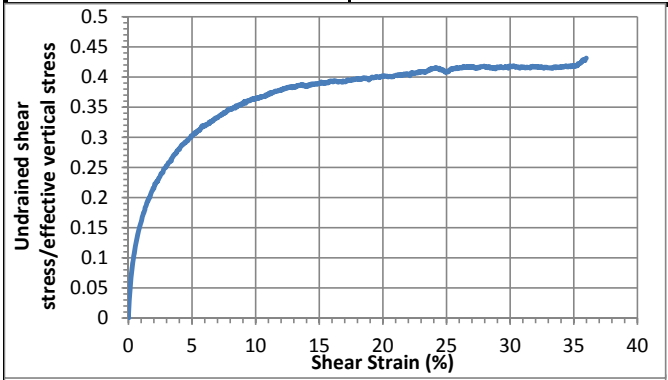

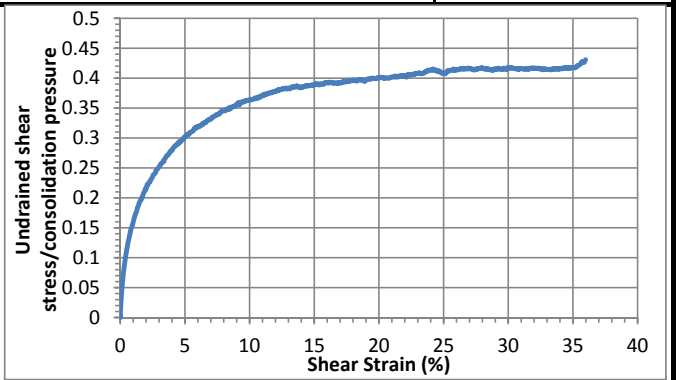

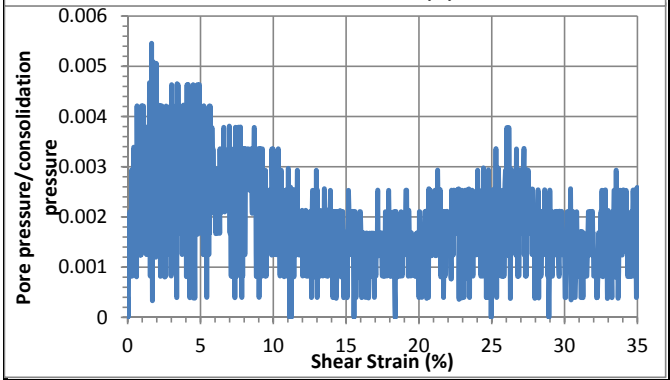

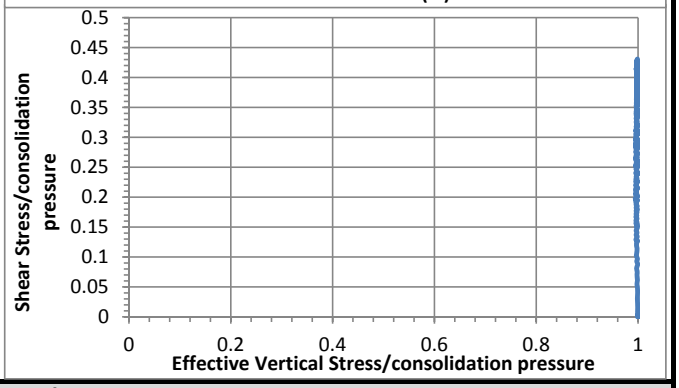

Shear wave velocity				
Signal type	Sinusoidal	First rise	initiation time (ms)	-0.0154
Signal amplitude (Vpp)	90		arrival time (ms)	1.0803
Signal frequency (kHz)	5		Vs (m/s)	100
Sensor spacing (mm)	109.42	First peak	initiation time (ms)	0.0410
R+P average Vs (m/s)	99		arrival time (ms)	1.1571
Stdev. (m/s)	1		Vs (m/s)	98
P+V average Vs (m/s)	95	First valley	initiation time (ms)	0.1382
Stdev. (m/s)	5		arrival time (ms)	1.3363
Wavelength (m)	0.019		Vs (m/s)	91
Spacing/wavelength	5.8			

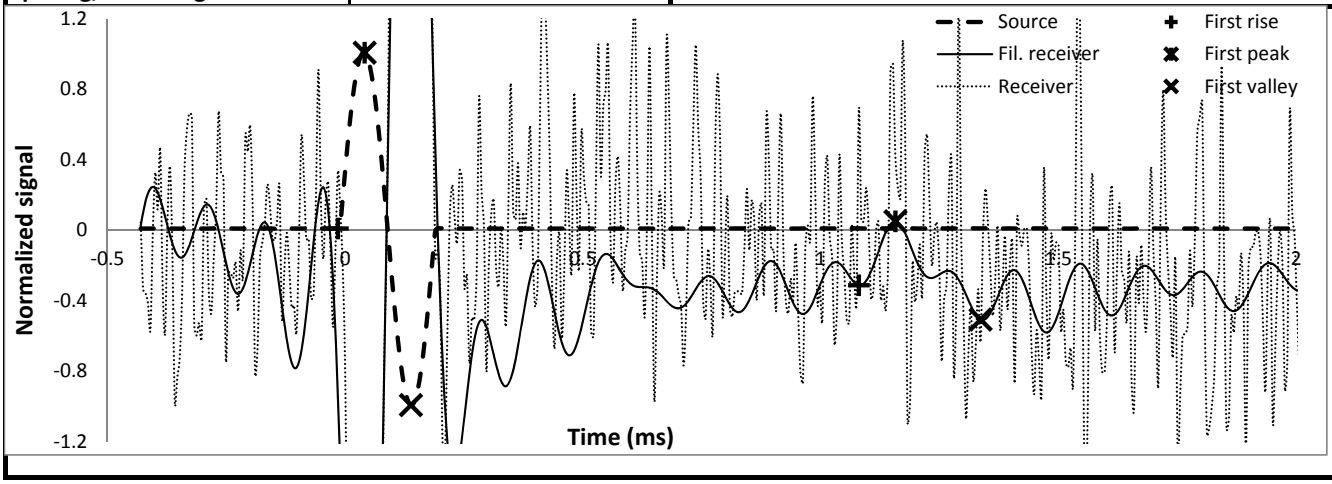

CSS Monotonic Shear Test Report

10/28/2013_Version 8.0

Geotechnical Engineering Laboratory

General Test Information and Sample Preparation			
Device:	CSS	**Layers:**	7.50
Specimen ID:	CA-LC3	**Weight/layer (kg):**	0.987
Test ID:	CA33	**Height/layer (mm):**	25.4
Date of Test:	8/21/2014	**Total height (mm):**	190.5
Test Performed:	Monotonic Shear	**Soil-Only Specimen Diameter (mm):**	306.2
Test Material:	MSW	**Total weight (kg):**	7.4025
Sample Preparation:	The same initial composition and unit weight as Sim. #6. Pre-compress for 23 hours, consolidate for 1 hour. Vertical P=5, I=0.5.	**Density (kg/m^3):**	528
		Membrane Thickness (mm):	0.000635
		Moisture Content (%):	60.0
		Saturated (Y/N):	N
		Prepared by:	Fei

Pre-compression Stage			
Pre-compression strain:	0.38	**Secondary compression ratio:**	0.00934
Height (mm):	126.3	**Density (kg/m3):**	796

Consolidation Stage		Shear Stage		
Initial height (mm):	135.7	**Type of Test:**		CU-strain
Initial density (kg/m3):	741	**Shear Strain Rate (%/min):**		0.34
Vertical Stress (kPa):	47.6	**10% strain**	**Shear stress (kPa)**	15.5
Immediate strain (εimm, %)	37.8		**Tan friction angle (°)**	26.1
Consolidated Height (mm):	119.5		**Sin friction angle (°)**	29.3
Compression index (Ccε)	0.237	**30% strain**	**Shear stress (kPa)**	15.7
Consolidation modulus	5.0		**Tan friction angle (°)**	29.4
Consolidated density (kg/m^3):	841		**Sin friction angle (°)**	34.3

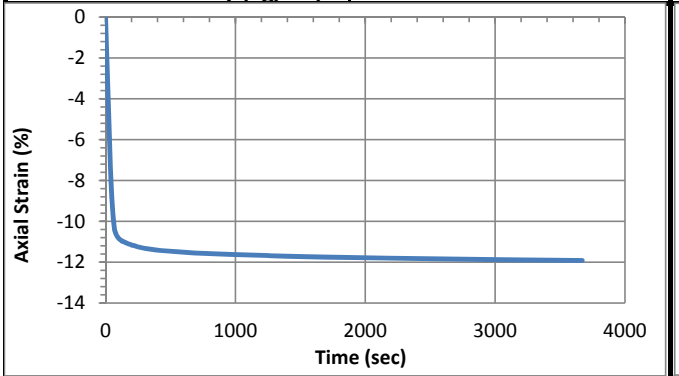

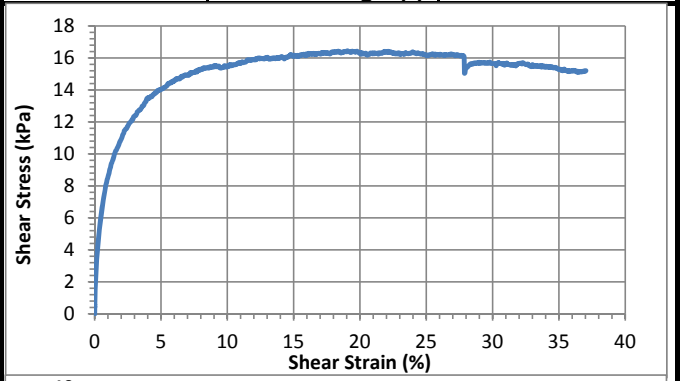

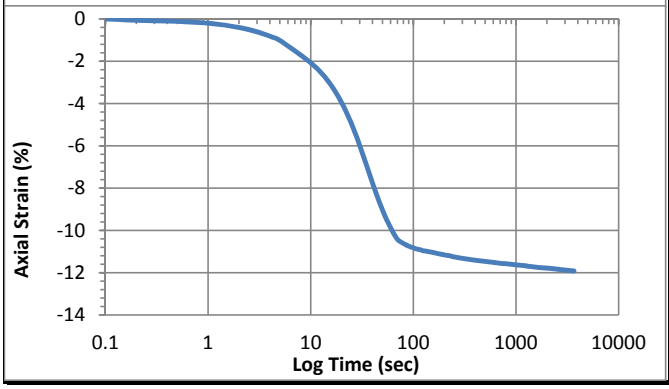

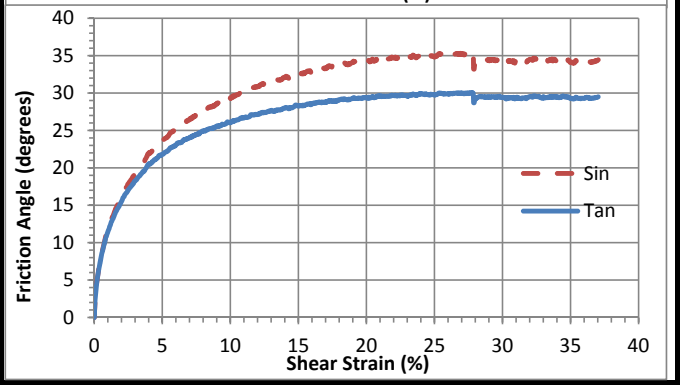

Undrained Strength			
Su/σv' at 10% strain	0.49	Su/σvc' at 10% strain	0.32
Su/σv' at 30% strain	0.56	Su/σvc' at 30% strain	0.33

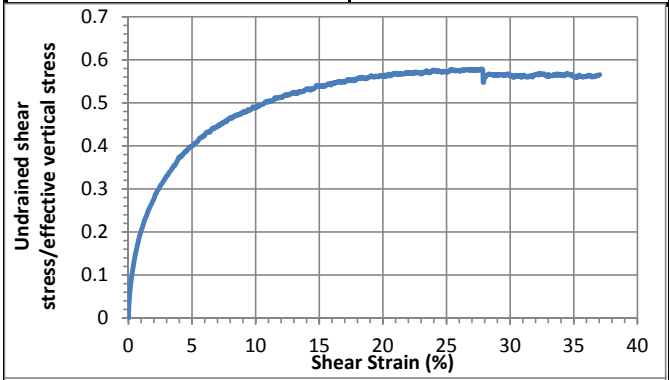

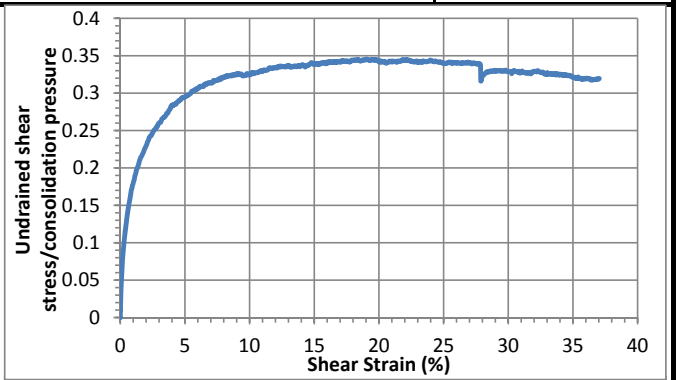

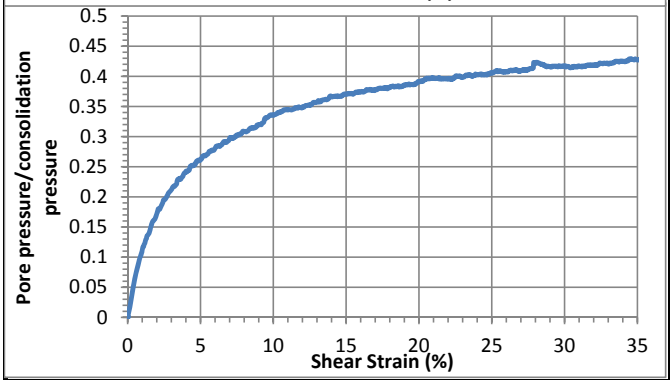

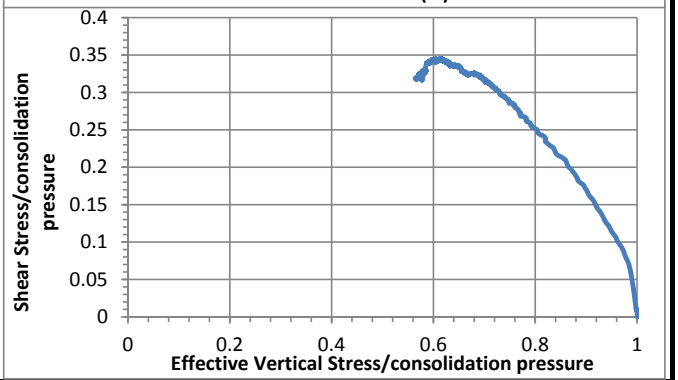

Shear wave velocity				
Signal type	Sinusoidal	First rise	initiation time (ms)	-0.0205
Signal amplitude (Vpp)	90		arrival time (ms)	0.8858
Signal frequency (kHz)	2		Vs (m/s)	122
Sensor spacing (mm)	110.74	First peak	initiation time (ms)	0.1075
R+P average Vs (m/s)	122		arrival time (ms)	1.0240
Stdev. (m/s)	1		Vs (m/s)	121
P+V average Vs (m/s)	120	First valley	initiation time (ms)	0.3584
Stdev. (m/s)	1		arrival time (ms)	1.2851
Wavelength (m)	0.060		Vs (m/s)	119
Spacing/wavelength	1.8			

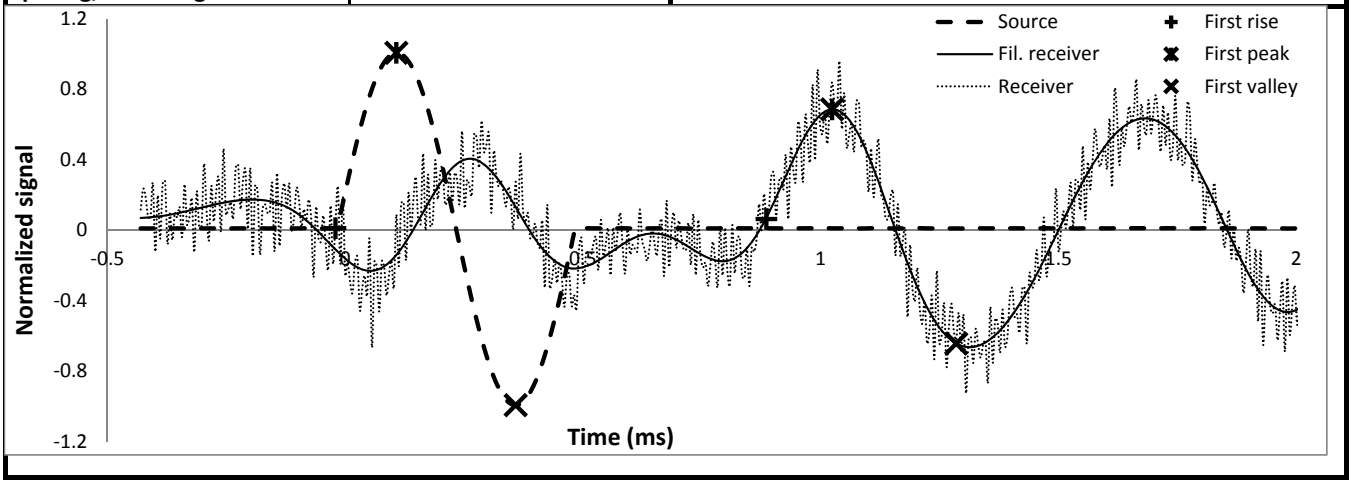

CSS Monotonic Shear Test Report

10/28/2013_Version 8.0

Geotechnical Engineering Laboratory

General Test Information and Sample Preparation			
Device:	CSS	**Layers:**	8.50
Specimen ID:	CA-LC3	**Weight/layer (kg):**	0.987
Test ID:	CA34	**Height/layer (mm):**	25.4
Date of Test:	8/23/2014	**Total height (mm):**	215.9
Test Performed:	Monotonic Shear	**Soil-Only Specimen Diameter (mm):**	306.2
Test Material:	MSW	**Total weight (kg):**	8.3895
Sample Preparation:	The same initial composition and unit weight as Sim. #6. Pre-compress for 23 hours, consolidate for 1 hour.	**Density (kg/m^3):**	528
		Membrane Thickness (mm):	0.000635
		Moisture Content (%):	60.0
		Saturated (Y/N):	N
		Prepared by:	Fei

Pre-compression Stage			
Pre-compression strain:	0.45	**Secondary compression ratio:**	0.00748
Height (mm):	123.5	**Density (kg/m3):**	922

Consolidation Stage		Shear Stage		
Initial height (mm):	136.3	**Type of Test:**		CD-strain
Initial density (kg/m3):	836	**Shear Strain Rate (%/min):**		0.34
Vertical Stress (kPa):	97.1	**10% strain**	**Shear stress (kPa)**	34.5
Immediate strain (εimm, %)	44.6		**Tan friction angle (°)**	19.6
Consolidated Height (mm):	117.6		**Sin friction angle (°)**	20.8
Compression index (Ccε)	0.232	**30% strain**	**Shear stress (kPa)**	43.2
Consolidation modulus	4.3		**Tan friction angle (°)**	24.0
Consolidated density (kg/m^3):	969		**Sin friction angle (°)**	26.5

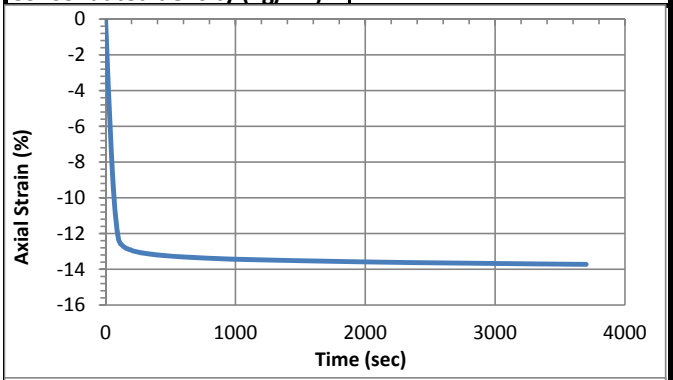

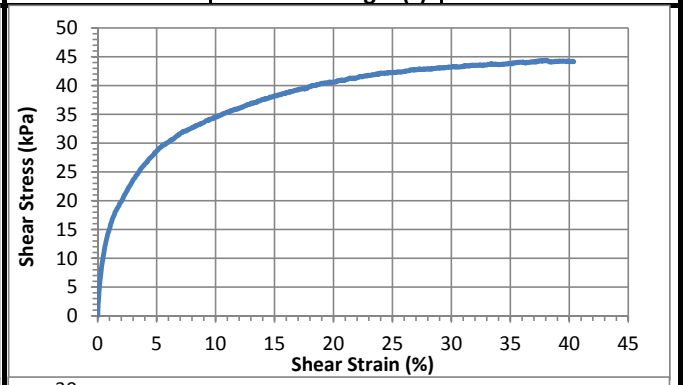

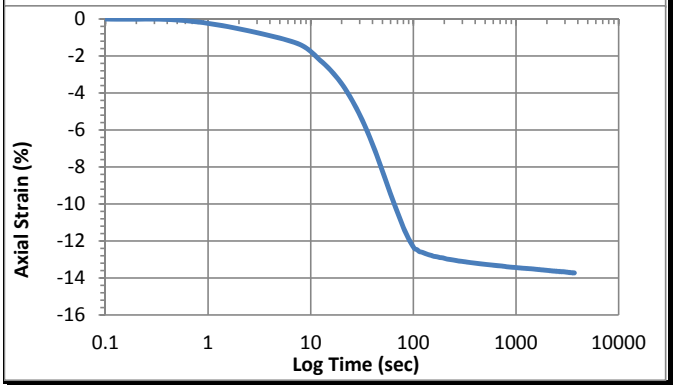

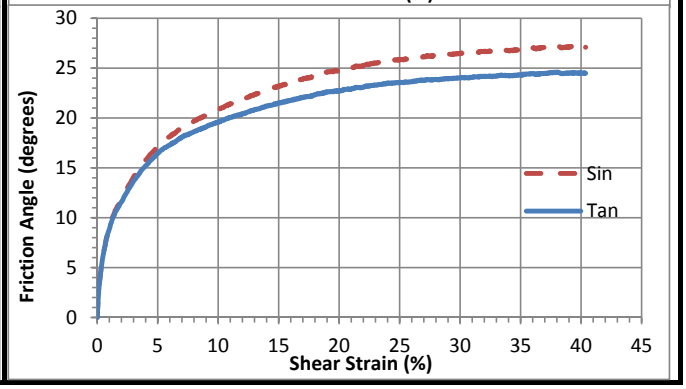

Undrained Strength			
Su/σv' at 10% strain	0.36	Su/σvc' at 10% strain	0.36
Su/σv' at 30% strain	0.45	Su/σvc' at 30% strain	0.45

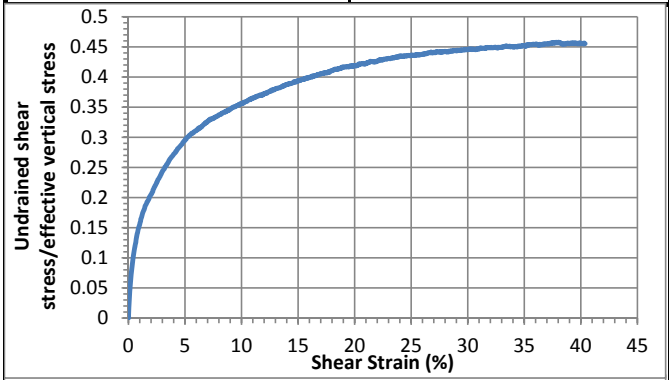

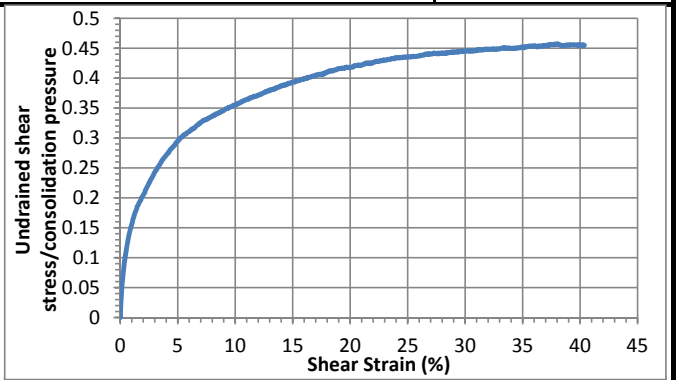

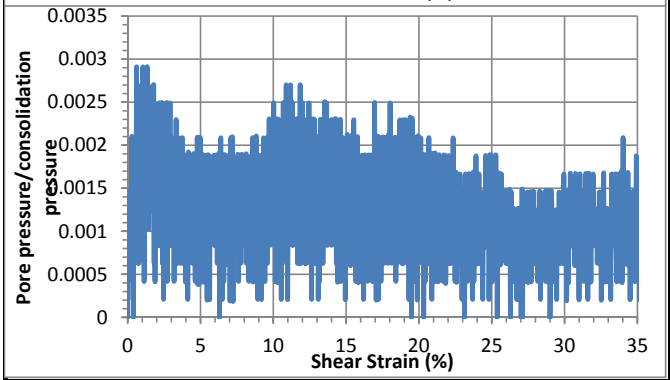

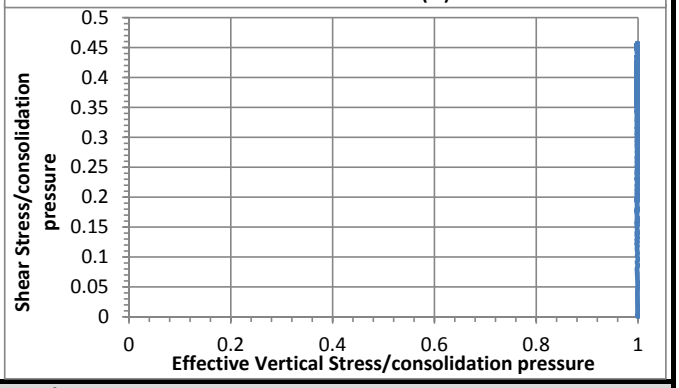

Shear wave velocity				
Signal type	Sinusoidal	First rise	initiation time (ms)	-0.0154
Signal amplitude (Vpp)	90		arrival time (ms)	0.7987
Signal frequency (kHz)	5		Vs (m/s)	134
Sensor spacing (mm)	108.82	First peak	initiation time (ms)	0.0410
R+P average Vs (m/s)	132		arrival time (ms)	0.8755
Stdev. (m/s)	2		Vs (m/s)	130
P+V average Vs (m/s)	129	First valley	initiation time (ms)	0.1382
Stdev. (m/s)	2		arrival time (ms)	0.9882
Wavelength (m)	0.026		Vs (m/s)	128
Spacing/wavelength	4.2			

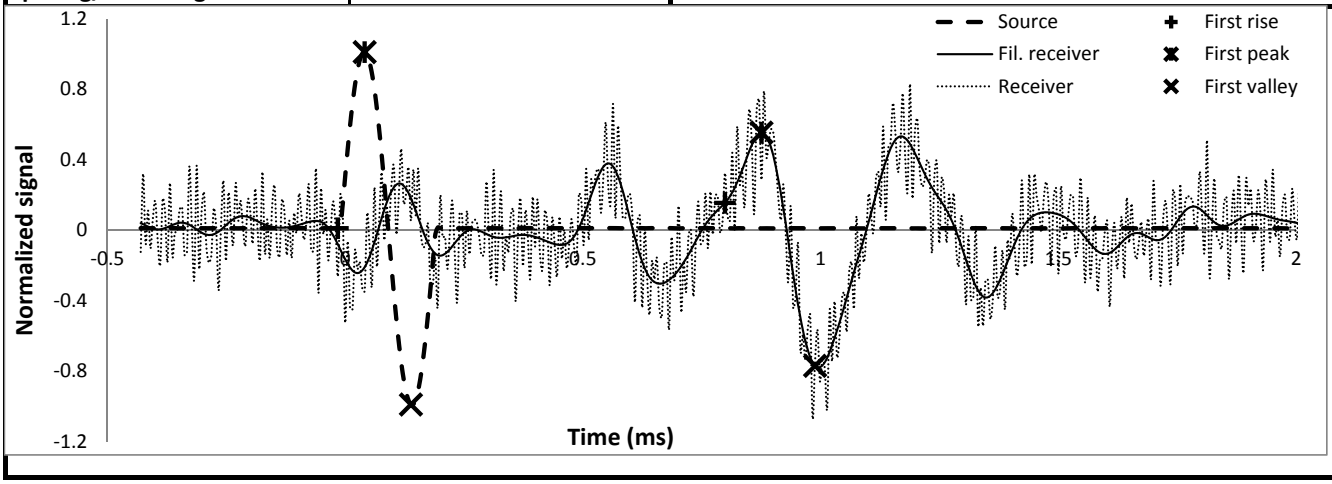

CSS Monotonic Shear Test Report

10/28/2013_Version 8.0

Geotechnical Engineering Laboratory

General Test Information and Sample Preparation			
Device:	CSS	**Layers:**	8.50
Specimen ID:	CA-LC3	**Weight/layer (kg):**	0.987
Test ID:	CA35	**Height/layer (mm):**	25.4
Date of Test:	8/24/2014	**Total height (mm):**	215.9
Test Performed:	Monotonic Shear	**Soil-Only Specimen Diameter (mm):**	306.2
Test Material:	MSW	**Total weight (kg):**	8.3895
Sample Preparation:	The same initial composition and unit weight as Sim. #6. Pre-compress for 23 hours, consolidate for 1 hour. Vertical P=10, I=0.5.	**Density (kg/m^3):**	528
		Membrane Thickness (mm):	0.000635
		Moisture Content (%):	60.0
		Saturated (Y/N):	N
		Prepared by:	Fei

Pre-compression Stage			
Pre-compression strain:	0.42	**Secondary compression ratio:**	0.00824
Height (mm):	125.2	**Density (kg/m3):**	910

Consolidation Stage		Shear Stage		
Initial height (mm):	135.7	**Type of Test:**		CU-strain
Initial density (kg/m3):	839	**Shear Strain Rate (%/min):**		0.34
Vertical Stress (kPa):	97.4	**10% strain**	**Shear stress (kPa)**	28.4
Immediate strain (εimm, %)	41.8		**Tan friction angle (°)**	23.3
Consolidated Height (mm):	118.7		**Sin friction angle (°)**	25.6
Compression index (Ccε)	0.219	**30% strain**	**Shear stress (kPa)**	28.0
Consolidation modulus	4.6		**Tan friction angle (°)**	27.4
Consolidated density (kg/m^3):	960		**Sin friction angle (°)**	31.2

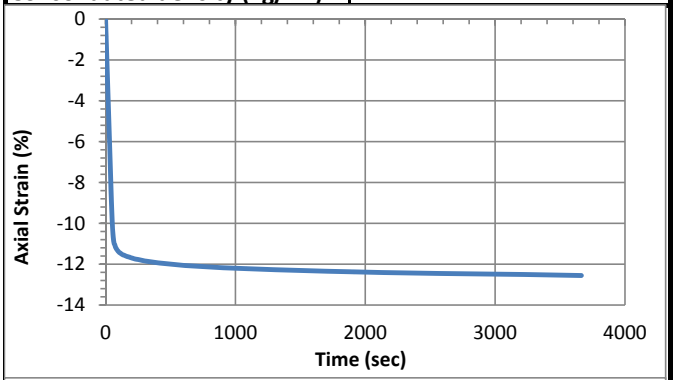

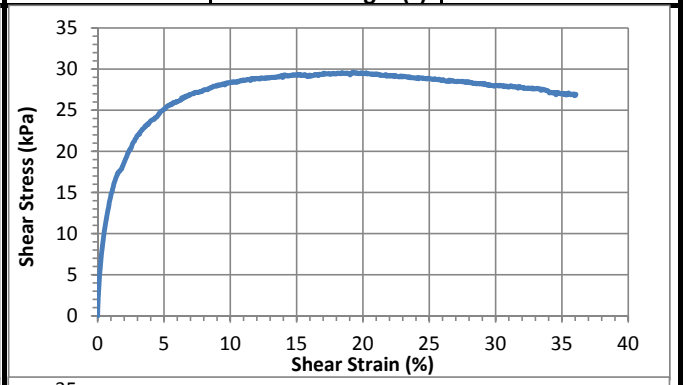

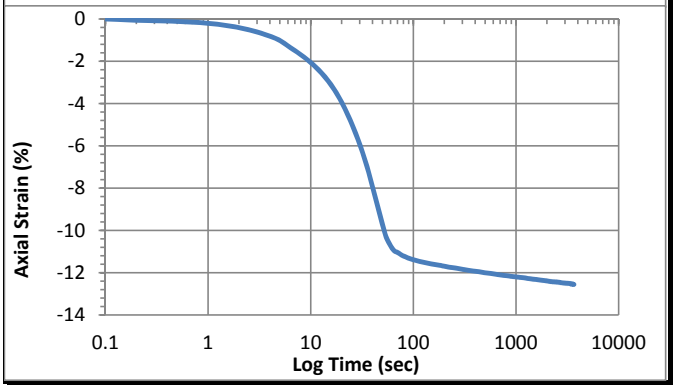

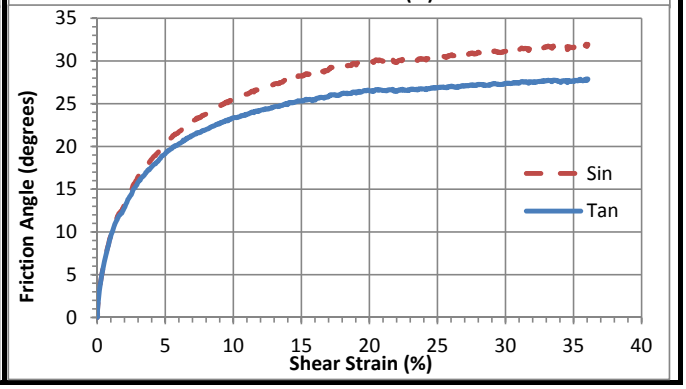

Undrained Strength			
Su/σv' at 10% strain	0.43	Su/σvc' at 10% strain	0.29
Su/σv' at 30% strain	0.52	Su/σvc' at 30% strain	0.29

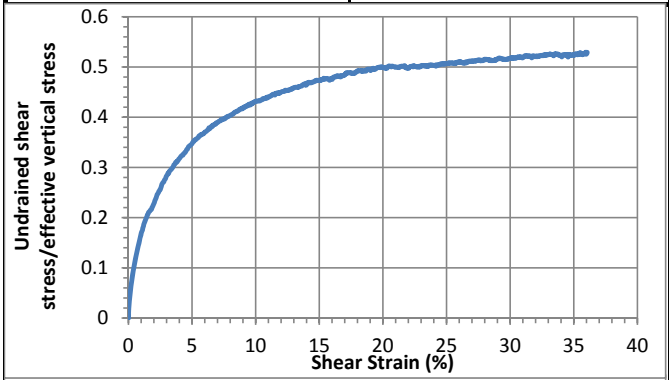

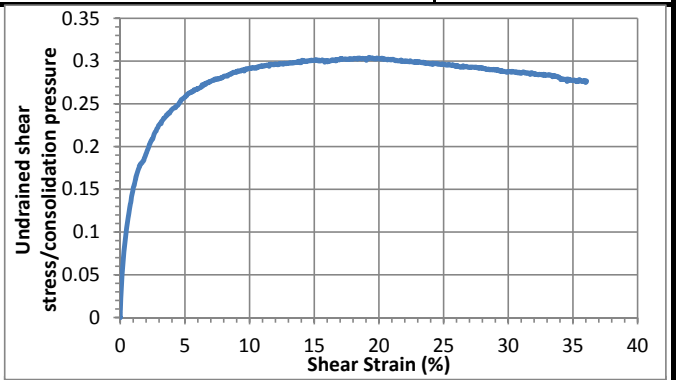

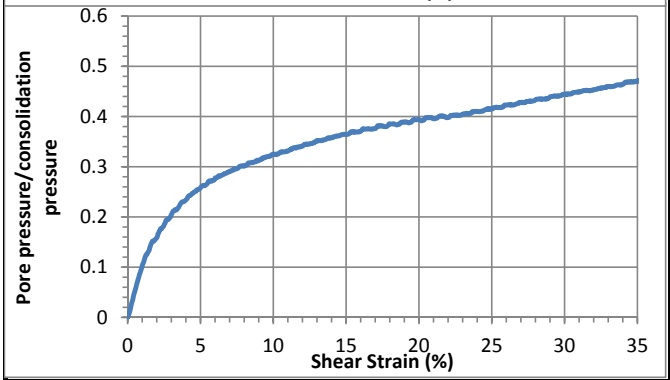

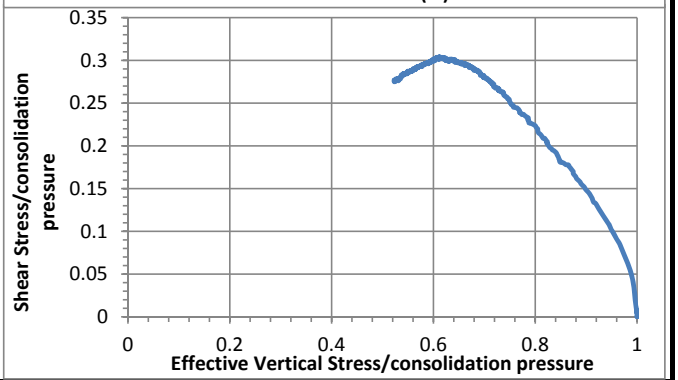

Shear wave velocity				
Signal type	Sinusoidal	First rise	initiation time (ms)	-0.0154
Signal amplitude (Vpp)	90		arrival time (ms)	0.8960
Signal frequency (kHz)	5		Vs (m/s)	121
Sensor spacing (mm)	109.88	First peak	initiation time (ms)	0.0410
R+P average Vs (m/s)	120		arrival time (ms)	0.9677
Stdev. (m/s)	1		Vs (m/s)	119
P+V average Vs (m/s)	119	First valley	initiation time (ms)	0.1382
Stdev. (m/s)	1		arrival time (ms)	1.0547
Wavelength (m)	0.024		Vs (m/s)	120
Spacing/wavelength	4.6			

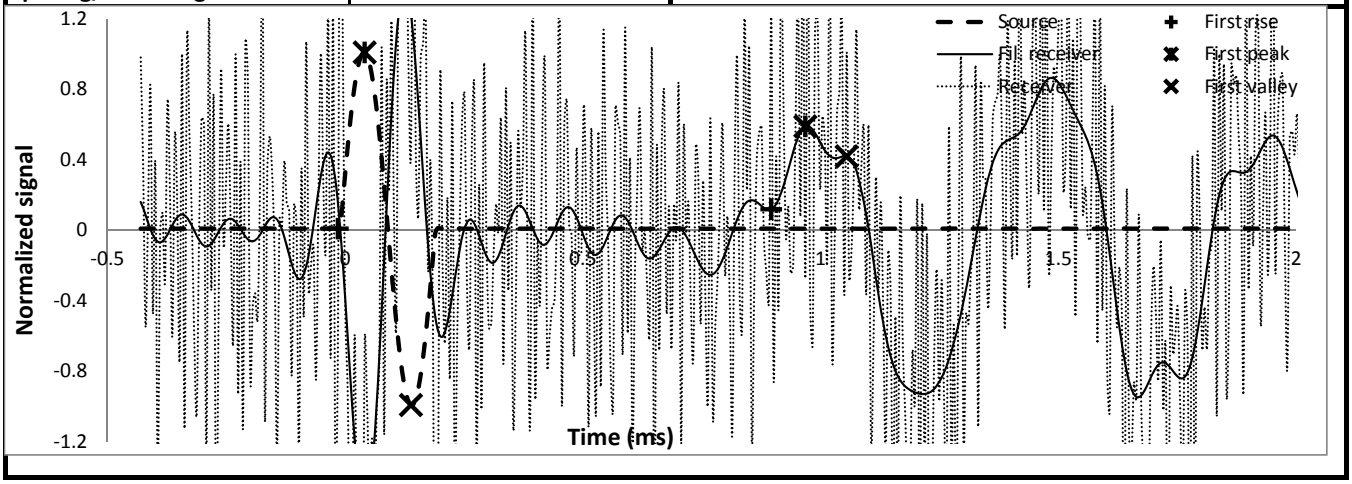

CSS Monotonic Shear Test Report

10/28/2013_Version 8.0

Geotechnical Engineering Laboratory

General Test Information and Sample Preparation			
Device:	CSS	**Layers:**	9.25
Specimen ID:	CA-LC3	**Weight/layer (kg):**	0.987
Test ID:	CA36	**Height/layer (mm):**	25.4
Date of Test:	8/26/2014	**Total height (mm):**	234.95
Test Performed:	Monotonic Shear	**Soil-Only Specimen Diameter (mm):**	306.2
Test Material:	MSW	**Total weight (kg):**	9.12975
Sample Preparation:	The same initial composition and unit weight as Sim. #6. Pre-compress for 23 hours, consolidate for 1 hour.	**Density (kg/m^3):**	528
		Membrane Thickness (mm):	0.000635
		Moisture Content (%):	60.0
		Saturated (Y/N):	N
		Prepared by:	Fei

Pre-compression Stage			
Pre-compression strain:	0.53	**Secondary compression ratio:**	0.00983
Height (mm):	109.1	**Density (kg/m3):**	1137

Consolidation Stage		Shear Stage		
Initial height (mm):	136.8	**Type of Test:**		CD-strain
Initial density (kg/m3):	906	**Shear Strain Rate (%/min):**		0.36
Vertical Stress (kPa):	196.6	**10% strain**	**Shear stress (kPa)**	67.3
Immediate strain (εimm, %)	47.1		**Tan friction angle (°)**	18.9
Consolidated Height (mm):	112.4		**Sin friction angle (°)**	20.0
Compression index (Ccε)	0.215	**30% strain**	**Shear stress (kPa)**	84.0
Consolidation modulus	4.1		**Tan friction angle (°)**	23.2
Consolidated density (kg/m^3):	1103		**Sin friction angle (°)**	25.3

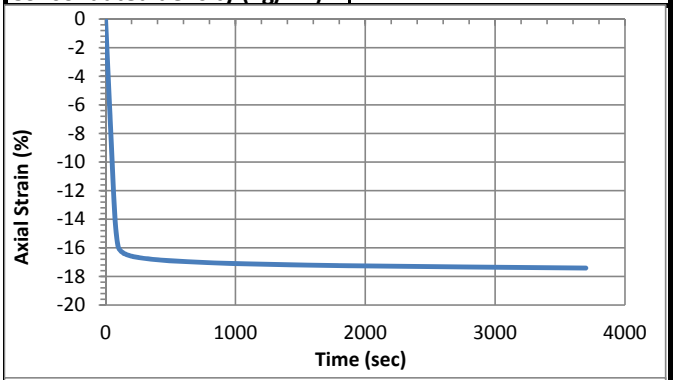

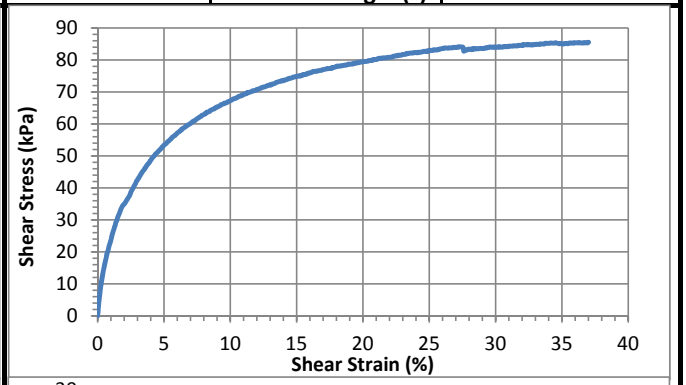

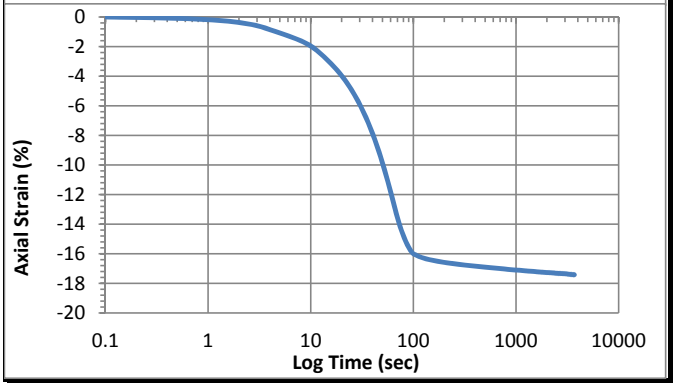

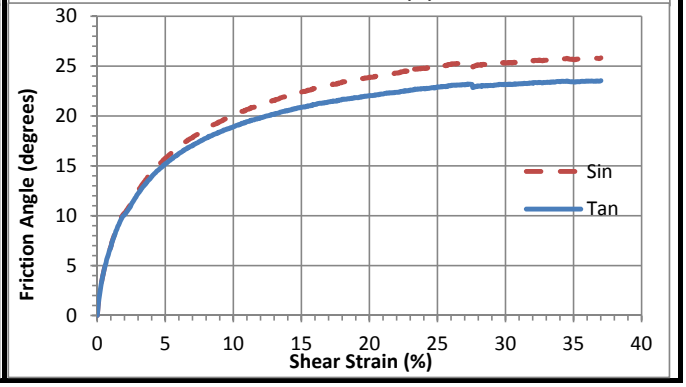

Undrained Strength			
Su/σv' at 10% strain	0.34	Su/σvc' at 10% strain	0.34
Su/σv' at 30% strain	0.43	Su/σvc' at 30% strain	0.43

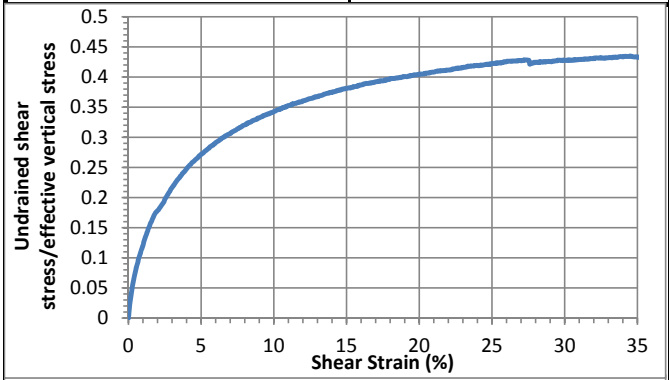

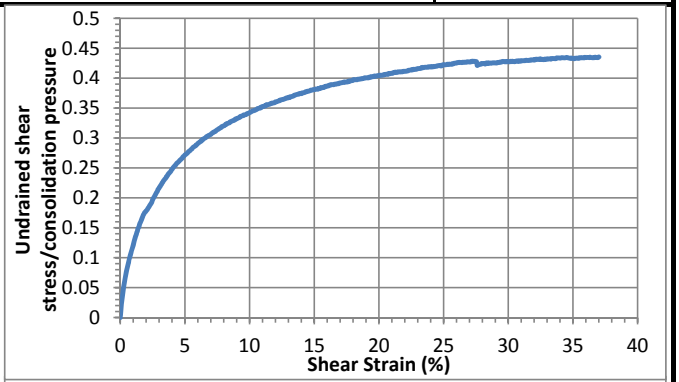

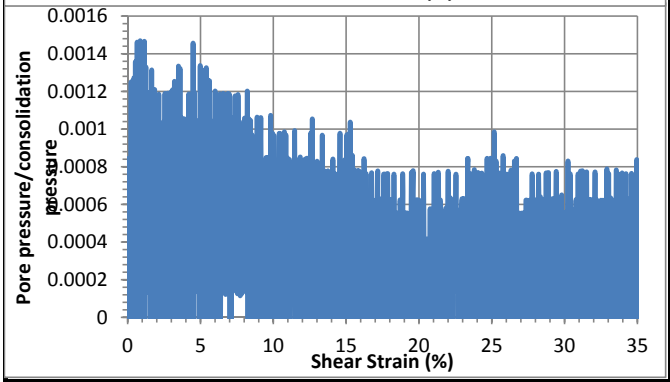

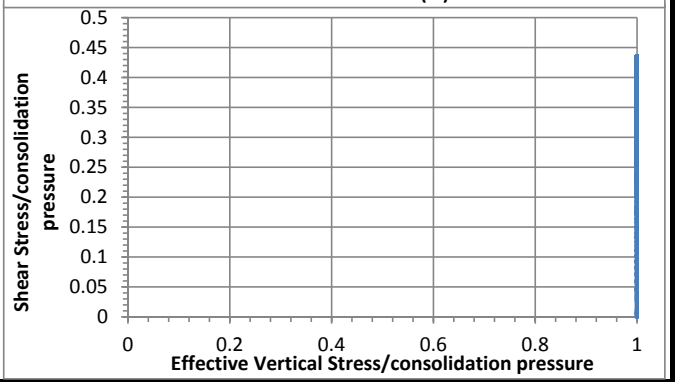

Shear wave velocity				
Signal type	Sinusoidal	First rise	initiation time (ms)	-0.0154
Signal amplitude (Vpp)	90		arrival time (ms)	0.4915
Signal frequency (kHz)	5		Vs (m/s)	200
Sensor spacing (mm)	101.29	First peak	initiation time (ms)	0.0410
R+P average Vs (m/s)	197		arrival time (ms)	0.5632
Stdev. (m/s)	4		Vs (m/s)	194
P+V average Vs (m/s)	194	First valley	initiation time (ms)	0.1382
Stdev. (m/s)	0		arrival time (ms)	0.6605
Wavelength (m)	0.039		Vs (m/s)	194
Spacing/wavelength	2.6			

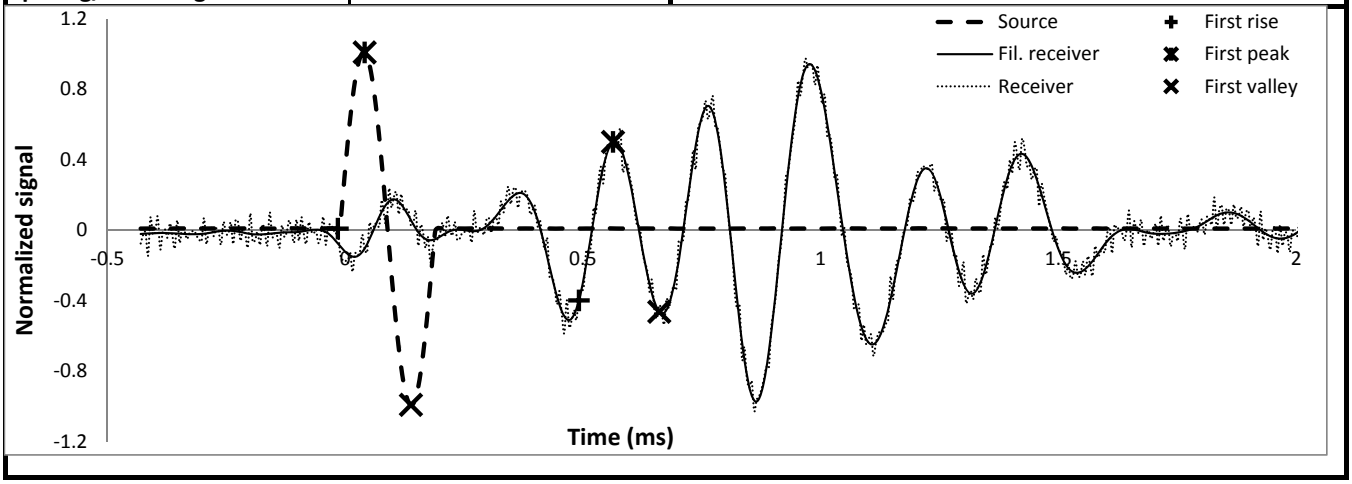

CSS Monotonic Shear Test Report

10/28/2013_Version 8.0

Geotechnical Engineering Laboratory

General Test Information and Sample Preparation			
Device:	CSS	**Layers:**	9.25
Specimen ID:	CA-LC3	**Weight/layer (kg):**	0.987
Test ID:	CA37	**Height/layer (mm):**	25.4
Date of Test:	8/28/2014	**Total height (mm):**	234.95
Test Performed:	Monotonic Shear	**Soil-Only Specimen Diameter (mm):**	306.2
Test Material:	MSW	**Total weight (kg):**	9.12975
Sample Preparation:	The same initial composition and unit weight as Sim. #6. Pre-compress for 23 hours, consolidate for 1 hour. Vertical P=20, I=0.5.	**Density (kg/m^3):**	528
		Membrane Thickness (mm):	0.000635
		Moisture Content (%):	60.0
		Saturated (Y/N):	N
		Prepared by:	Fei

Pre-compression Stage			
Pre-compression strain:	0.49	**Secondary compression ratio:**	0.01105
Height (mm):	123.0	**Density (kg/m3):**	1008

Consolidation Stage		Shear Stage		
Initial height (mm):	135.4	**Type of Test:**		CU-strain
Initial density (kg/m3):	916	**Shear Strain Rate (%/min):**		0.35
Vertical Stress (kPa):	196.9	**10% strain**	**Shear stress (kPa)**	58.1
Immediate strain (εimm, %)	48.2		**Tan friction angle (°)**	23.3
Consolidated Height (mm):	114.4		**Sin friction angle (°)**	25.5
Compression index (Ccε)	0.222	**30% strain**	**Shear stress (kPa)**	61.2
Consolidation modulus	3.9		**Tan friction angle (°)**	27.9
Consolidated density (kg/m^3):	1084		**Sin friction angle (°)**	32.0

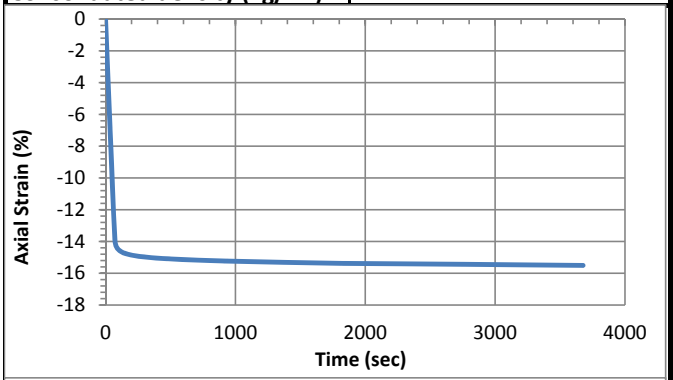

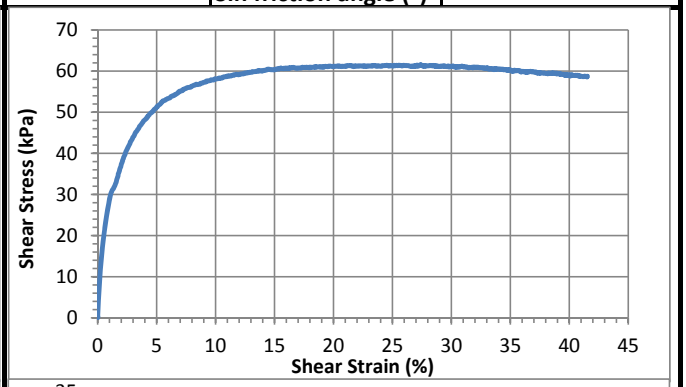

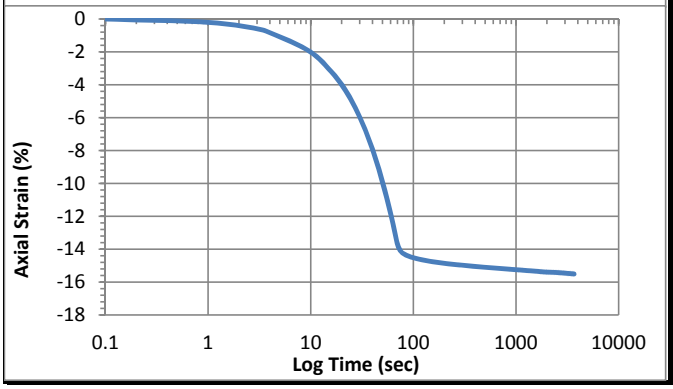

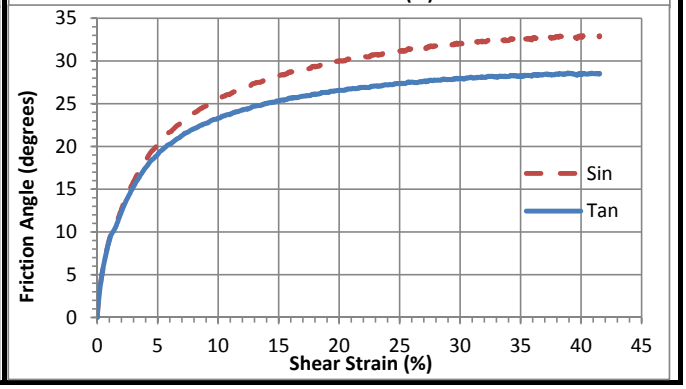

Undrained Strength			
Su/σv' at 10% strain	0.43	Su/σvc' at 10% strain	0.30
Su/σv' at 30% strain	0.53	Su/σvc' at 30% strain	0.31

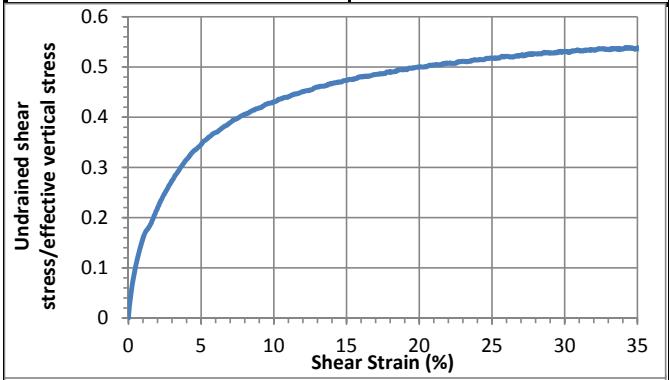

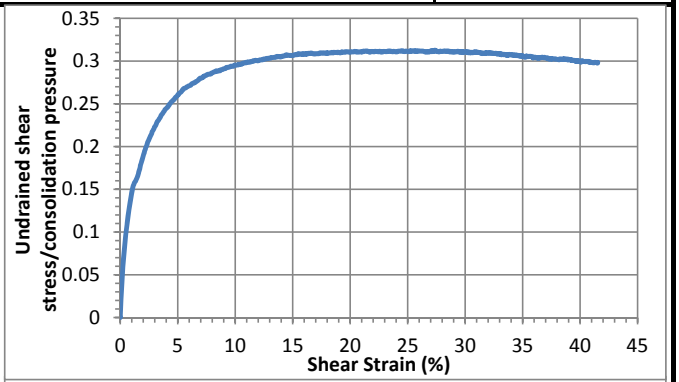

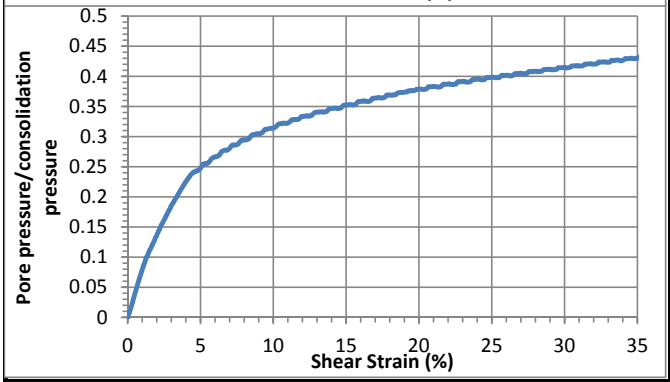

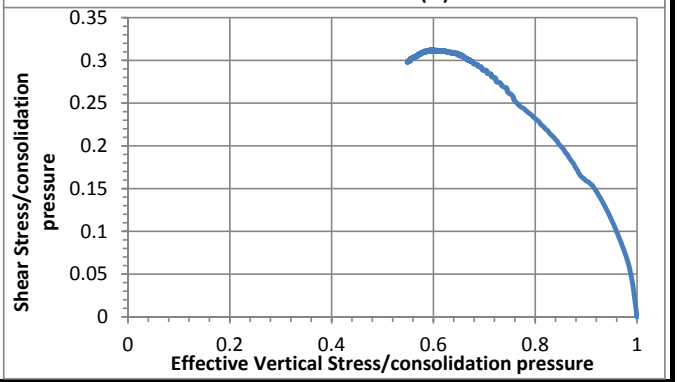

Shear wave velocity				
Signal type	Sinusoidal	First rise	initiation time (ms)	-0.0102
Signal amplitude (Vpp)	90		arrival time (ms)	0.5478
Signal frequency (kHz)	5		Vs (m/s)	189
Sensor spacing (mm)	105.59	First peak	initiation time (ms)	0.0410
R+P average Vs (m/s)	185		arrival time (ms)	0.6246
Stdev. (m/s)	6		Vs (m/s)	181
P+V average Vs (m/s)	183	First valley	initiation time (ms)	0.1434
Stdev. (m/s)	3		arrival time (ms)	0.7117
Wavelength (m)	0.037		Vs (m/s)	186
Spacing/wavelength	2.9			

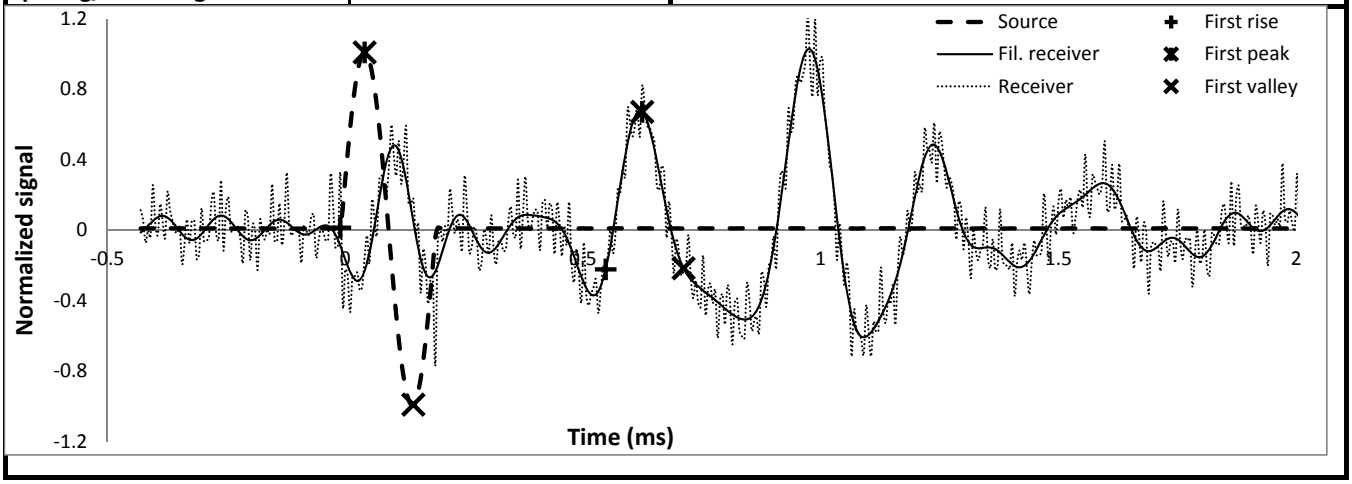

CSS Monotonic Shear Test Report

10/28/2013_Version 8.0

Geotechnical Engineering Laboratory

General Test Information and Sample Preparation			
Device:	CSS	**Layers:**	9.78
Specimen ID:	CA-LC3	**Weight/layer (kg):**	0.987
Test ID:	CA38	**Height/layer (mm):**	25.4
Date of Test:	8/30/2014	**Total height (mm):**	248.412
Test Performed:	Monotonic Shear	**Soil-Only Specimen Diameter (mm):**	306.2
Test Material:	MSW	**Total weight (kg):**	9.65286
Sample Preparation:	The same initial composition and unit weight as Sim. #6. Pre-compress for 23 hours, consolidate for 1 hour. Vertical P=30, I=0.5.	**Density (kg/m^3):**	528
		Membrane Thickness (mm):	0.000635
		Moisture Content (%):	60.0
		Saturated (Y/N):	N
		Prepared by:	Fei

Pre-compression Stage			
Pre-compression strain:	0.53	**Secondary compression ratio:**	0.01091
Height (mm):	112.5	**Density (kg/m3):**	1165

Consolidation Stage		Shear Stage		
Initial height (mm):	135.3	**Type of Test:**		CU-strain
Initial density (kg/m3):	968	**Shear Strain Rate (%/min):**		0.37
Vertical Stress (kPa):	394.5	**10% strain**	**Shear stress (kPa)**	109.1
Immediate strain (εimm, %)	51.0		**Tan friction angle (°)**	22.1
Consolidated Height (mm):	108.5		**Sin friction angle (°)**	23.9
Compression index (Ccε)	0.205	**30% strain**	**Shear stress (kPa)**	110.0
Consolidation modulus	3.8		**Tan friction angle (°)**	27.2
Consolidated density (kg/m^3):	1207		**Sin friction angle (°)**	31.0

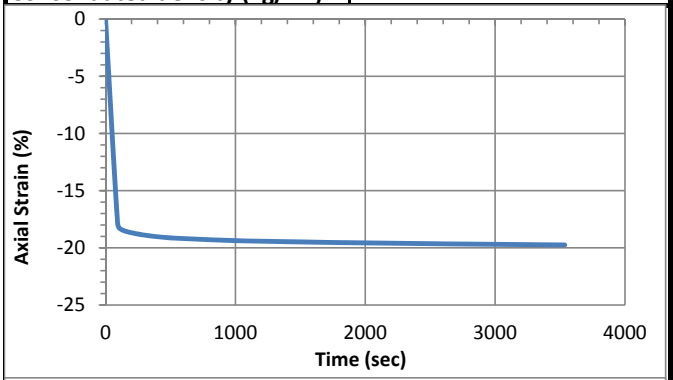

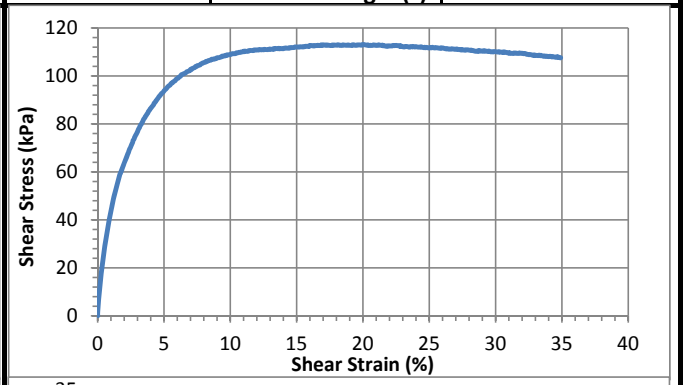

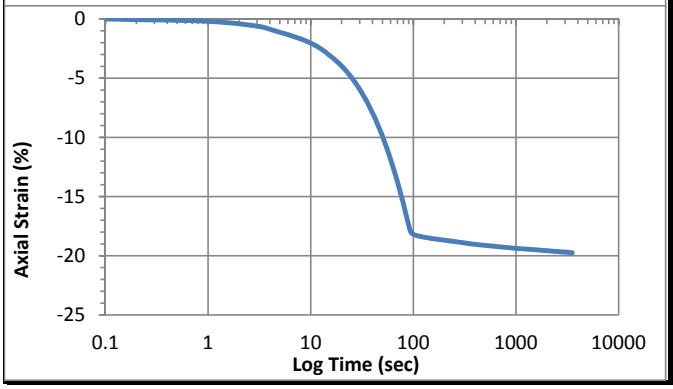

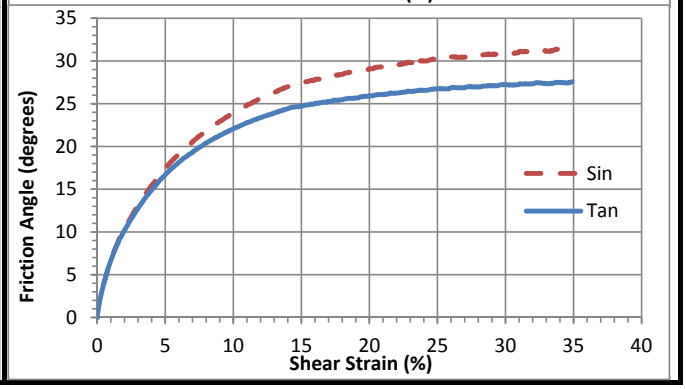

Undrained Strength			
Su/σv' at 10% strain	0.41	Su/σvc' at 10% strain	0.28
Su/σv' at 30% strain	0.51	Su/σvc' at 30% strain	0.28

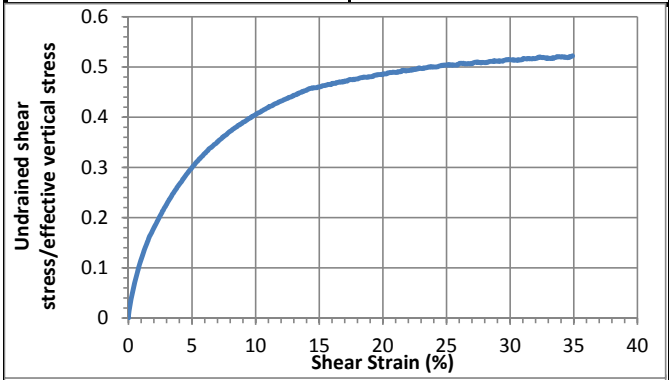

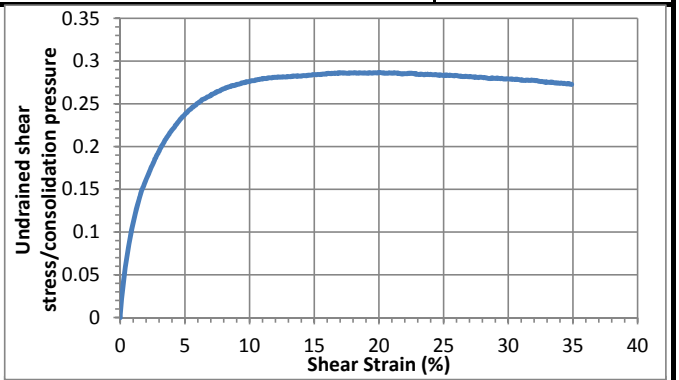

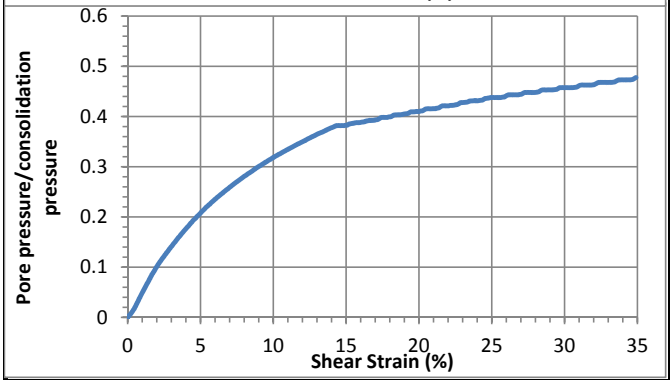

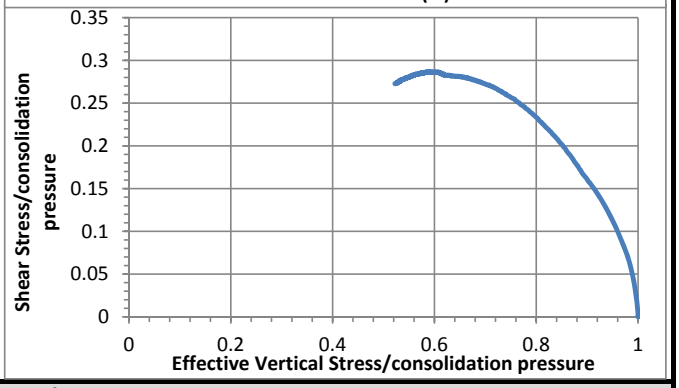

Shear wave velocity				
Signal type	Sinusoidal	First rise	initiation time (ms)	-0.0102
Signal amplitude (Vpp)	90		arrival time (ms)	0.4045
Signal frequency (kHz)	5		Vs (m/s)	243
Sensor spacing (mm)	100.94	First peak	initiation time (ms)	0.0410
R+P average Vs (m/s)	240		arrival time (ms)	0.4659
Stdev. (m/s)	4		Vs (m/s)	238
P+V average Vs (m/s)	242	First valley	initiation time (ms)	0.1434
Stdev. (m/s)	6		arrival time (ms)	0.5530
Wavelength (m)	0.048		Vs (m/s)	246
Spacing/wavelength	2.1			

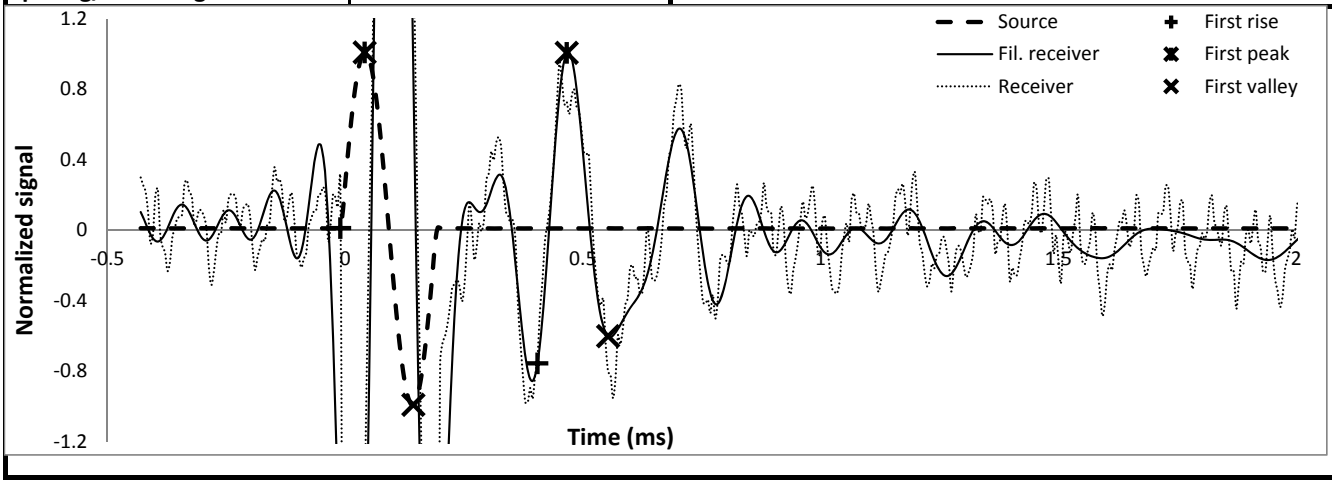

CSS Monotonic Shear Test Report

10/28/2013_Version 8.0

Geotechnical Engineering Laboratory

General Test Information and Sample Preparation			
Device:	CSS	**Layers:**	9.25
Specimen ID:	AZ-LR	**Weight/layer (kg):**	1.014
Test ID:	AZ1	**Height/layer (mm):**	25.4
Date of Test:	9/29/2014	**Total height (mm):**	234.95
Test Performed:	Monotonic Shear	**Soil-Only Specimen Diameter (mm):**	306.2
Test Material:	MSW	**Total weight (kg):**	9.3795
Sample Preparation:	The same initial composition and unit weight as Sim. #4. Staged pre-compress for 24 hours, consolidate for 1 hour.	**Density (kg/m^3):**	542
		Membrane Thickness (mm):	0.000635
		Moisture Content (%):	60.0
		Saturated (Y/N):	N
		Prepared by:	Fei

Pre-compression Stage			
Pre-compression strain:	0.55	**Secondary compression ratio:**	
Height (mm):	107.5	**Density (kg/m3):**	1185

Consolidation Stage		Shear Stage		
Initial height (mm):	132.7	**Type of Test:**		CD-strain
Initial density (kg/m3):	960	**Shear Strain Rate (%/min):**		0.39
Vertical Stress (kPa):	393.2	**10% strain**	**Shear stress (kPa)**	104.8
Immediate strain (εimm, %)	55.9		**Tan friction angle (°)**	14.9
Consolidated Height (mm):	103.0		**Sin friction angle (°)**	15.5
Compression index (Ccε)	0.216	**30% strain**	**Shear stress (kPa)**	128.9
Consolidation modulus	3.6		**Tan friction angle (°)**	18.2
Consolidated density (kg/m^3):	1236		**Sin friction angle (°)**	19.2

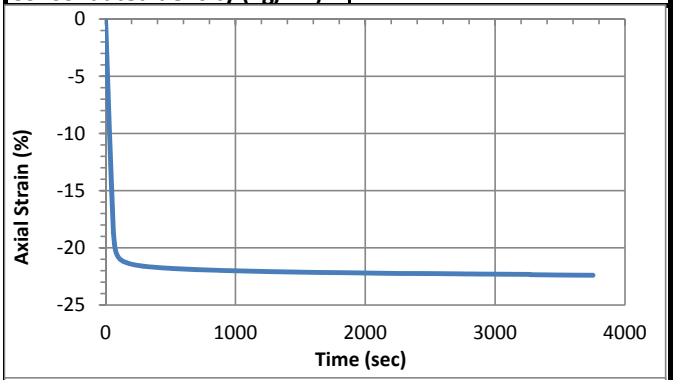

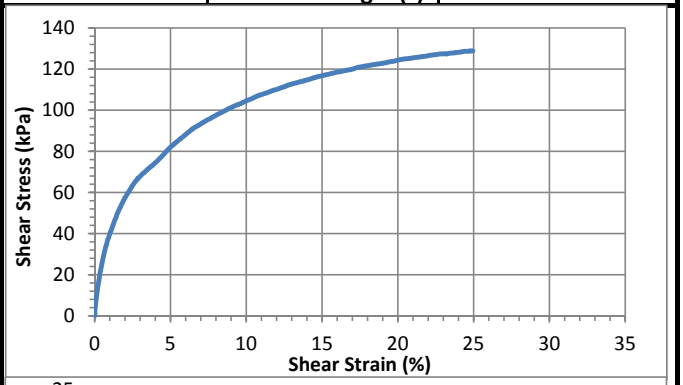

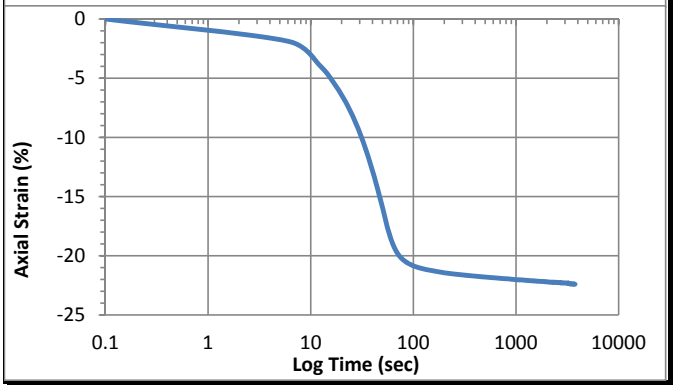

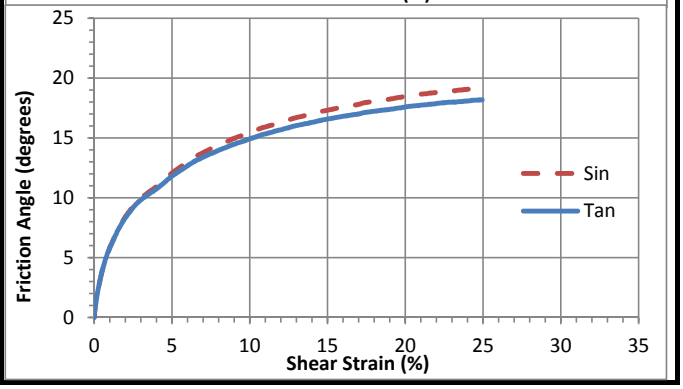

Undrained Strength

Su/σv' at 10% strain	0.27	Su/σvc' at 10% strain	0.27
Su/σv' at 30% strain	0.33	Su/σvc' at 30% strain	0.33

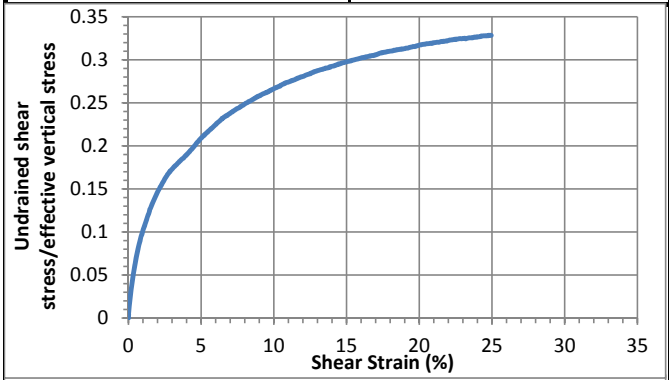

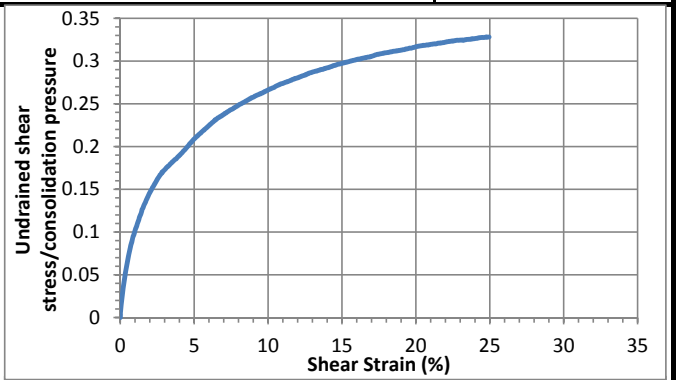

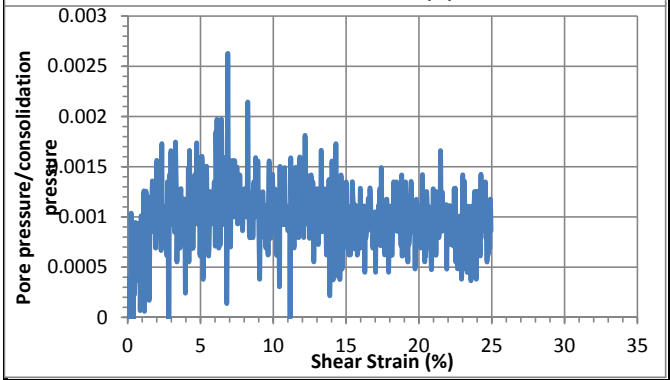

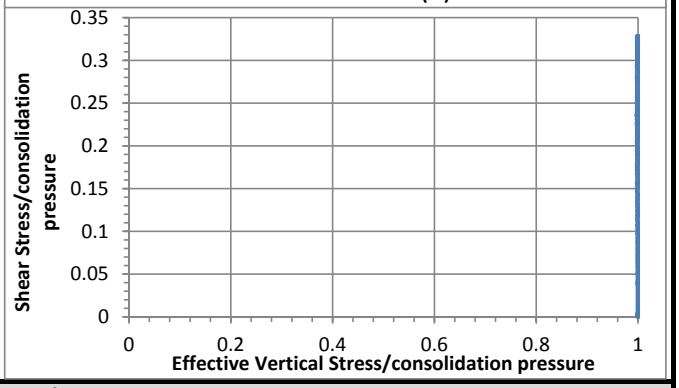

Shear wave velocity

Signal type	Sinusoidal	First rise	initiation time (ms)	-0.0154
Signal amplitude (Vpp)	90		arrival time (ms)	0.0000
Signal frequency (kHz)	4		Vs (m/s)	6572
Sensor spacing (mm)	100.94	First peak	initiation time (ms)	0.0512
R+P average Vs (m/s)	3445		arrival time (ms)	0.3686
Stdev. (m/s)	4422		Vs (m/s)	318
P+V average Vs (m/s)	-131	First valley	initiation time (ms)	0.1741
Stdev. (m/s)	635		arrival time (ms)	0.0000
Wavelength (m)	-0.033		Vs (m/s)	-580
Spacing/wavelength	-3.1			

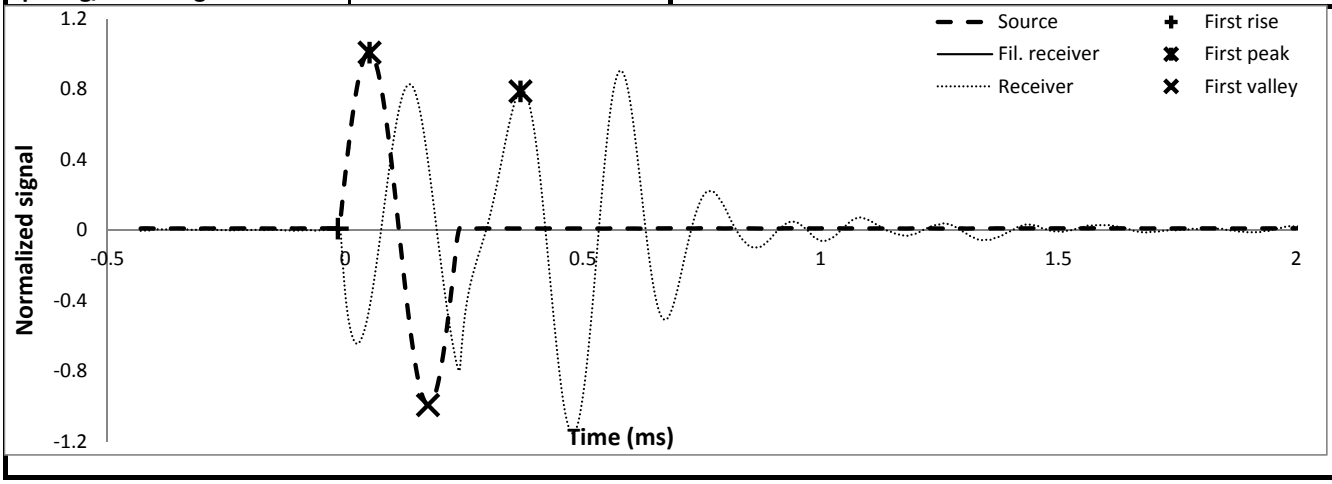

CSS Monotonic Shear Test Report

10/28/2013_Version 8.0

Geotechnical Engineering Laboratory

General Test Information and Sample Preparation			
Device:	CSS	**Layers:**	8.00
Specimen ID:	AZ-LR	**Weight/layer (kg):**	1.014
Test ID:	AZ1	**Height/layer (mm):**	25.4
Date of Test:	10/1/2014	**Total height (mm):**	203.2
Test Performed:	Monotonic Shear	**Soil-Only Specimen Diameter (mm):**	306.2
Test Material:	MSW	**Total weight (kg):**	8.112
Sample Preparation:	The same initial composition and unit weight as Sim. #4. Staged pre-compress for 24 hours, consolidate for 1 hour.	**Density (kg/m^3):**	542
		Membrane Thickness (mm):	0.000635
		Moisture Content (%):	60.0
		Saturated (Y/N):	N
		Prepared by:	Fei

Pre-compression Stage			
Pre-compression strain:	0.42	**Secondary compression ratio:**	0.01058
Height (mm):	127.9	**Density (kg/m3):**	861

Consolidation Stage		Shear Stage		
Initial height (mm):	136.6	**Type of Test:**		CD-strain
Initial density (kg/m3):	806	**Shear Strain Rate (%/min):**		0.33
Vertical Stress (kPa):	48.5	**10% strain**	**Shear stress (kPa)**	15.9
Immediate strain (εimm, %)	41.0		**Tan friction angle (°)**	18.4
Consolidated Height (mm):	122.4		**Sin friction angle (°)**	19.5
Compression index (Ccε)	0.259	**30% strain**	**Shear stress (kPa)**	19.6
Consolidation modulus	4.6		**Tan friction angle (°)**	22.2
Consolidated density (kg/m^3):	899		**Sin friction angle (°)**	24.1

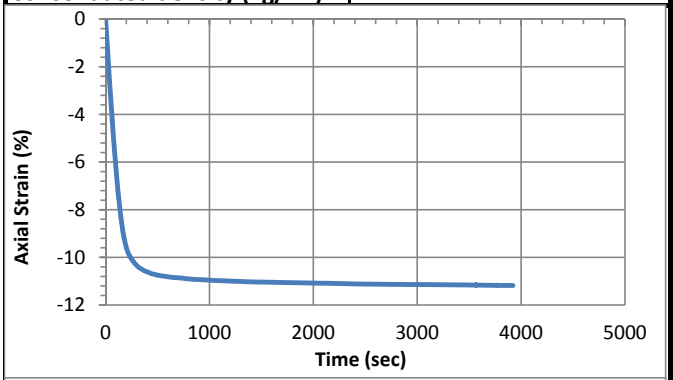

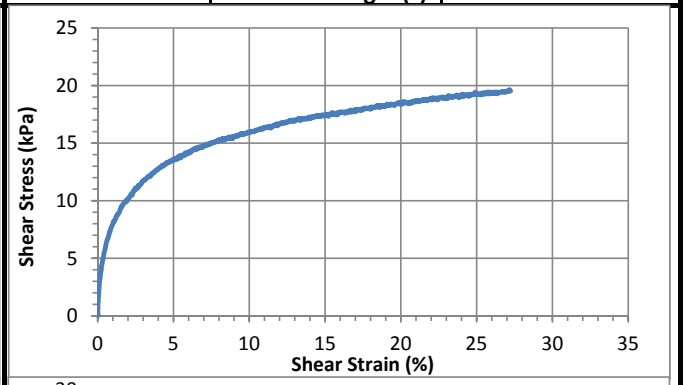

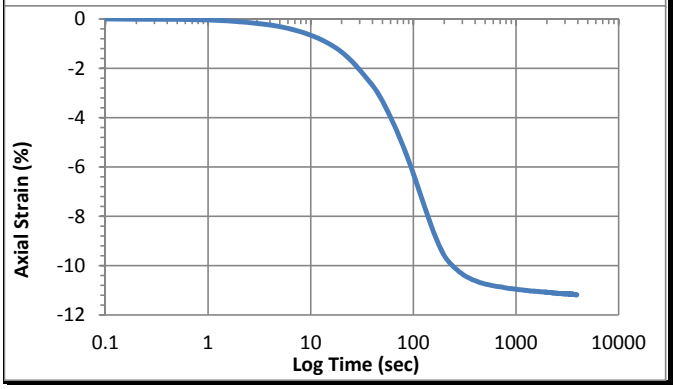

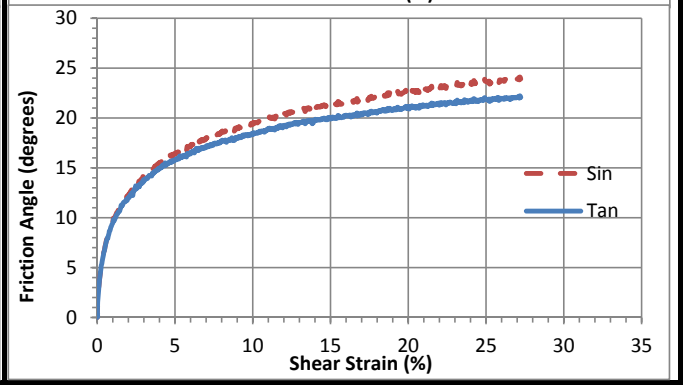

Undrained Strength			
Su/σv' at 10% strain	0.33	Su/σvc' at 10% strain	0.33
Su/σv' at 30% strain	0.41	Su/σvc' at 30% strain	0.41

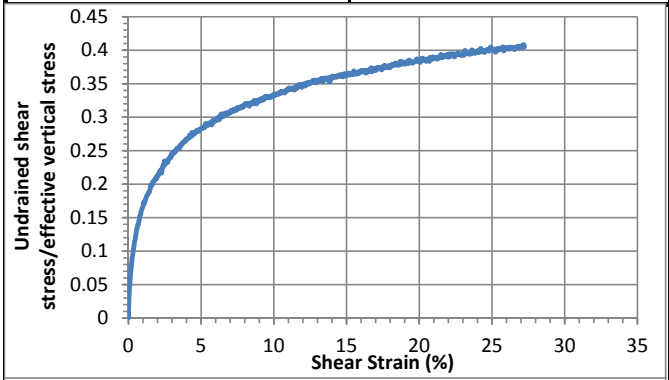

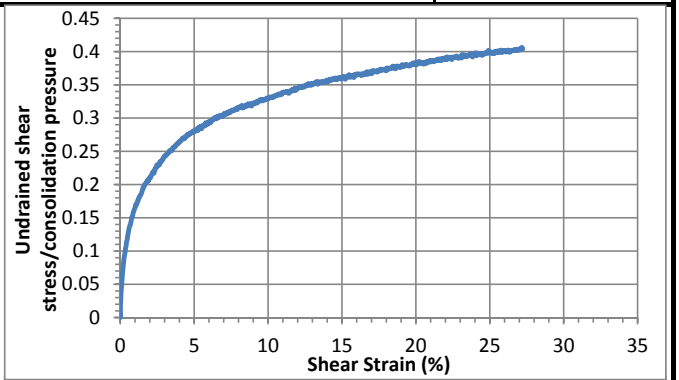

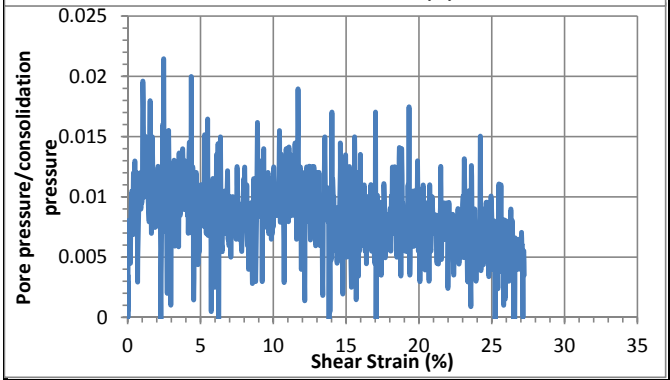

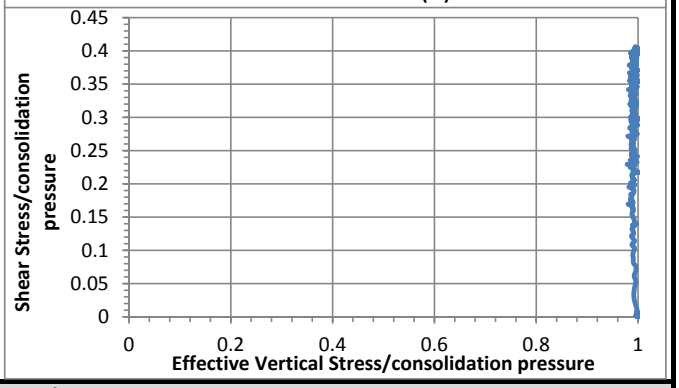

Shear wave velocity				
Signal type	Sinusoidal	First rise	initiation time (ms)	-0.0205
Signal amplitude (Vpp)	90		arrival time (ms)	0.6963
Signal frequency (kHz)	2.5		Vs (m/s)	159
Sensor spacing (mm)	113.68	First peak	initiation time (ms)	0.0819
R+P average Vs (m/s)	158		arrival time (ms)	0.8038
Stdev. (m/s)	1		Vs (m/s)	157
P+V average Vs (m/s)	157	First valley	initiation time (ms)	0.2816
Stdev. (m/s)	1		arrival time (ms)	1.0086
Wavelength (m)	0.063		Vs (m/s)	156
Spacing/wavelength	1.8			

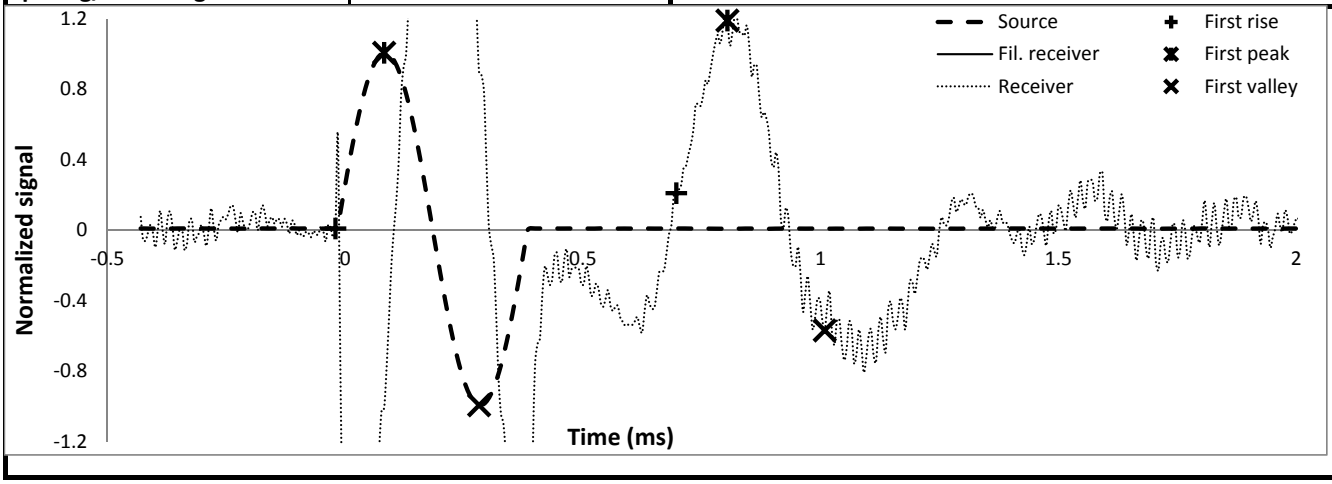

CSS Monotonic Shear Test Report

10/28/2013_Version 8.0

Geotechnical Engineering Laboratory

General Test Information and Sample Preparation			
Device:	CSS	**Layers:**	8.00
Specimen ID:	AZ-LR	**Weight/layer (kg):**	1.014
Test ID:	AZ3	**Height/layer (mm):**	25.4
Date of Test:	10/3/2014	**Total height (mm):**	203.2
Test Performed:	Monotonic Shear	**Soil-Only Specimen Diameter (mm):**	306.2
Test Material:	MSW	**Total weight (kg):**	8.112
Sample Preparation:	The same initial composition and unit weight as Sim. #4. Staged pre-compress for 23 hours, consolidate for 1 hour.	**Density (kg/m^3):**	542
		Membrane Thickness (mm):	0.000635
		Moisture Content (%):	60.0
		Saturated (Y/N):	N
		Prepared by:	Fei

Pre-compression Stage			
Pre-compression strain:	0.41	**Secondary compression ratio:**	0.00970
Height (mm):	128.2	**Density (kg/m3):**	859

Consolidation Stage		Shear Stage		
Initial height (mm):	137.7	**Type of Test:**		CU-strain
Initial density (kg/m3):	800	**Shear Strain Rate (%/min):**		0.33
Vertical Stress (kPa):	49.9	**10% strain**	**Shear stress (kPa)**	14.7
Immediate strain (εimm, %)	40.7		**Tan friction angle (°)**	22.7
Consolidated Height (mm):	122.1		**Sin friction angle (°)**	24.6
Compression index (Ccε)	0.250	**30% strain**	**Shear stress (kPa)**	16.0
Consolidation modulus	4.7		**Tan friction angle (°)**	26.7
Consolidated density (kg/m^3):	902		**Sin friction angle (°)**	30.2

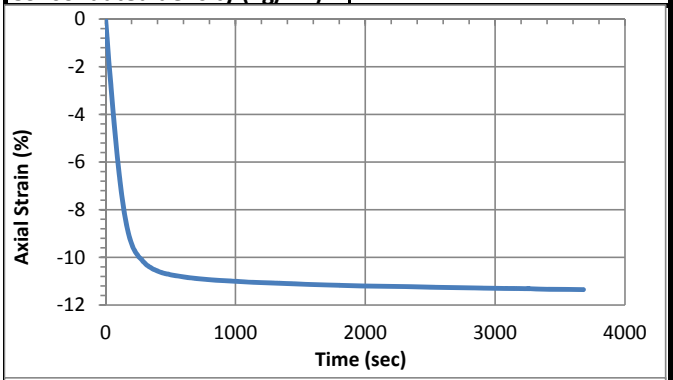

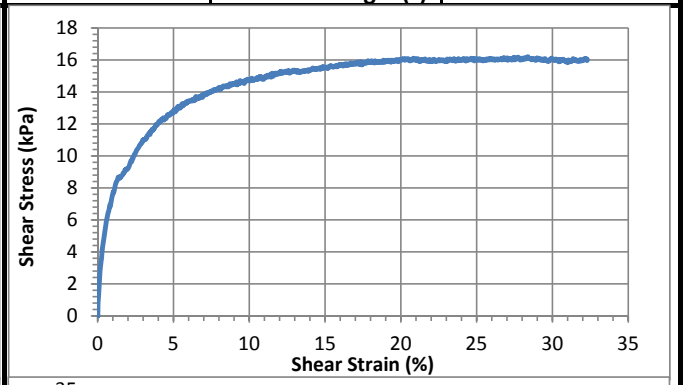

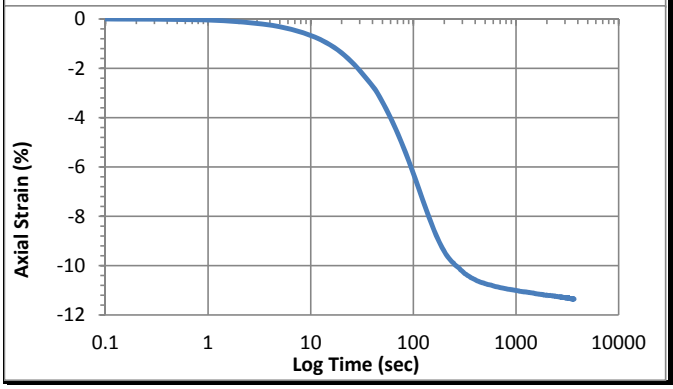

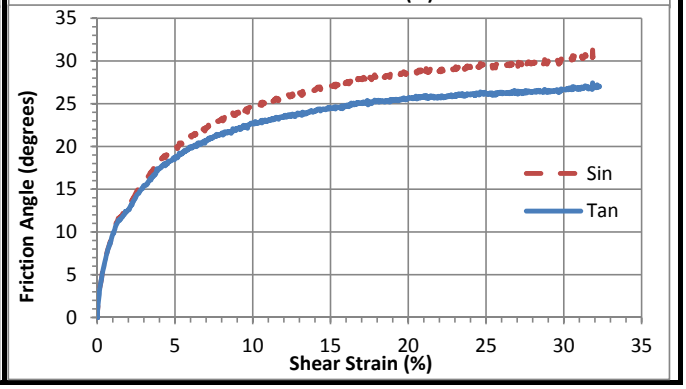

Undrained Strength			
Su/σv' at 10% strain	0.42	Su/σvc' at 10% strain	0.30
Su/σv' at 30% strain	0.50	Su/σvc' at 30% strain	0.32

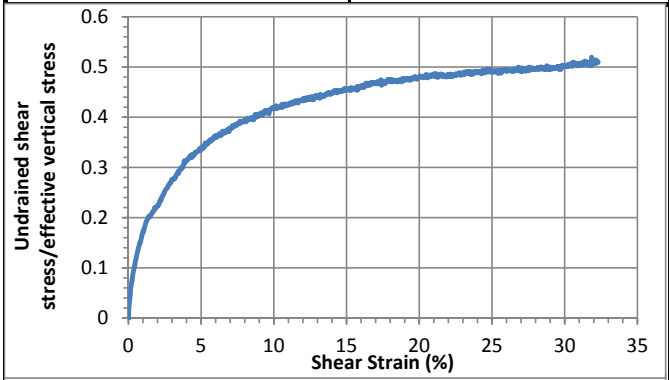

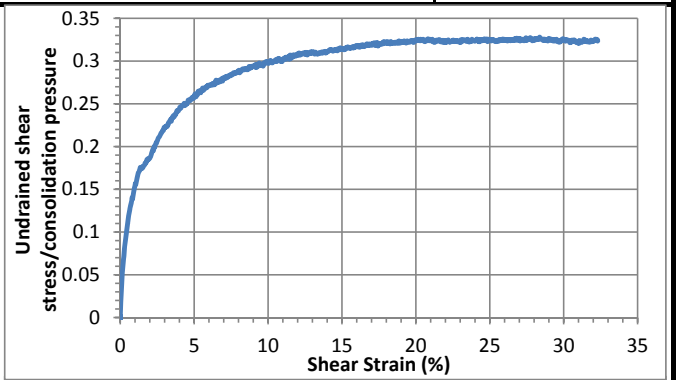

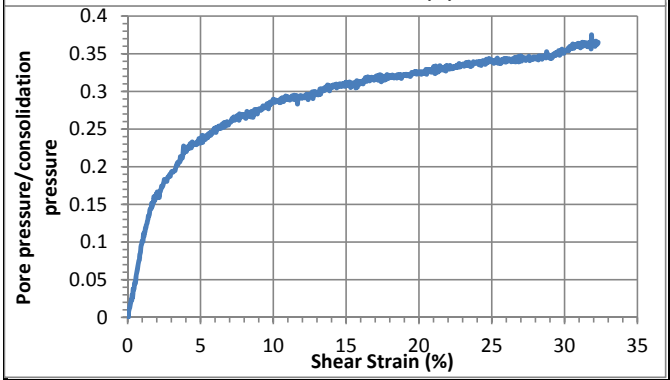

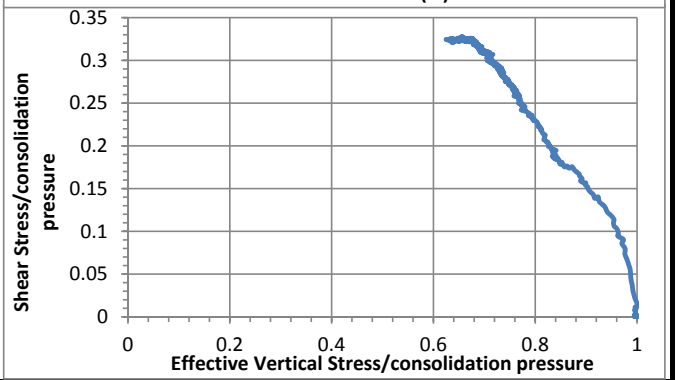

Shear wave velocity				
Signal type	Sinusoidal	First rise	initiation time (ms)	-0.0205
Signal amplitude (Vpp)	90		arrival time (ms)	0.5325
Signal frequency (kHz)	2.5		Vs (m/s)	205
Sensor spacing (mm)	113.34	First peak	initiation time (ms)	0.0870
R+P average Vs (m/s)	200		arrival time (ms)	0.6707
Stdev. (m/s)	8		Vs (m/s)	194
P+V average Vs (m/s)	200	First valley	initiation time (ms)	0.2867
Stdev. (m/s)	8		arrival time (ms)	0.8397
Wavelength (m)	0.080		Vs (m/s)	205
Spacing/wavelength	1.4			

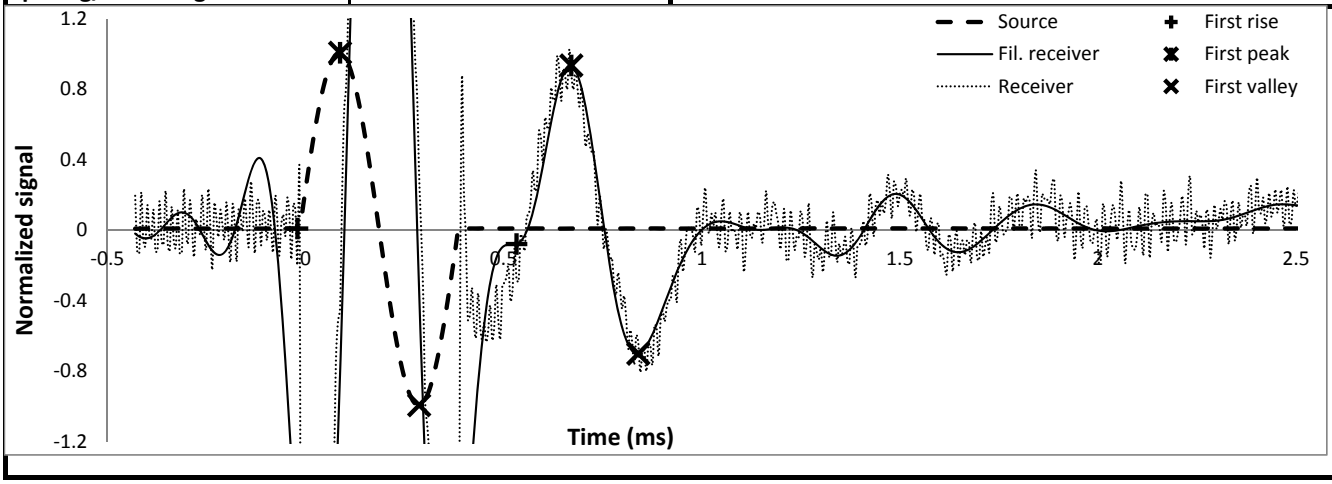

CSS Monotonic Shear Test Report

10/28/2013_Version 8.0

Geotechnical Engineering Laboratory

General Test Information and Sample Preparation			
Device:	CSS	**Layers:**	8.30
Specimen ID:	AZ-LR	**Weight/layer (kg):**	1.014
Test ID:	AZ4	**Height/layer (mm):**	25.4
Date of Test:	10/5/2014	**Total height (mm):**	210.82
Test Performed:	Monotonic Shear	**Soil-Only Specimen Diameter (mm):**	306.2
Test Material:	MSW	**Total weight (kg):**	8.4162
Sample Preparation:	The same initial composition and unit weight as Sim. #4. Staged pre-compress for 24 hours, consolidate for 1 hour.	**Density (kg/m^3):**	542
		Membrane Thickness (mm):	0.000635
		Moisture Content (%):	60.0
		Saturated (Y/N):	N
		Prepared by:	Fei

Pre-compression Stage			
Pre-compression strain:	0.46	**Secondary compression ratio:**	0.00806
Height (mm):	121.1	**Density (kg/m3):**	944

Consolidation Stage		Shear Stage		
Initial height (mm):	137.7	**Type of Test:**		CD-strain
Initial density (kg/m3):	830	**Shear Strain Rate (%/min):**		0.34
Vertical Stress (kPa):	98.2	**10% strain**	**Shear stress (kPa)**	28.0
Immediate strain (εimm, %)	44.7		**Tan friction angle (°)**	17.2
Consolidated Height (mm):	118.1		**Sin friction angle (°)**	18.0
Compression index (Ccε)	0.231	**30% strain**	**Shear stress (kPa)**	35.2
Consolidation modulus	4.3		**Tan friction angle (°)**	21.2
Consolidated density (kg/m^3):	968		**Sin friction angle (°)**	22.8

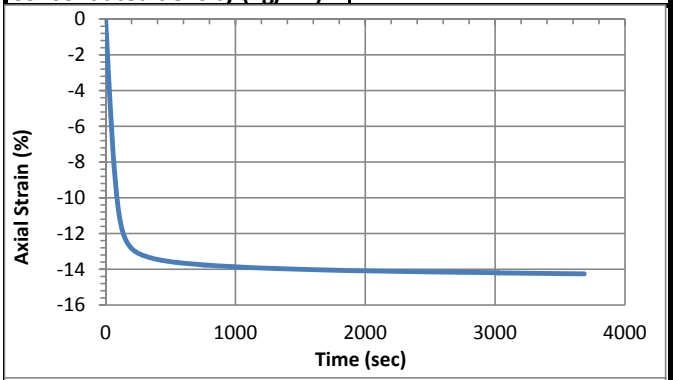

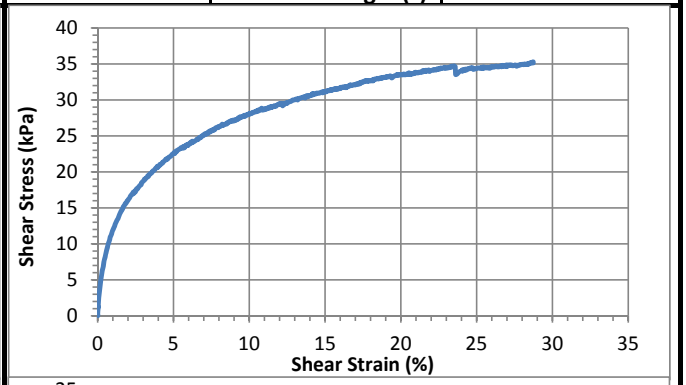

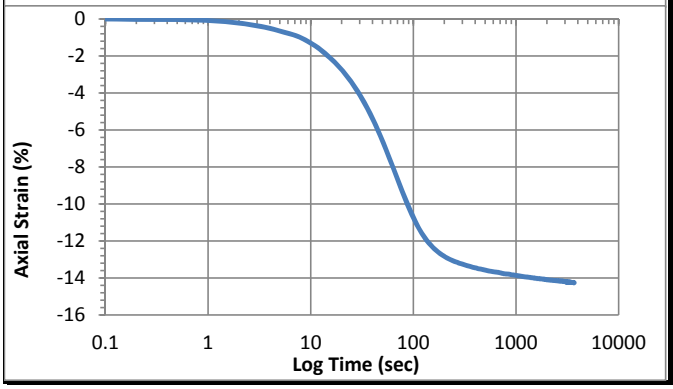

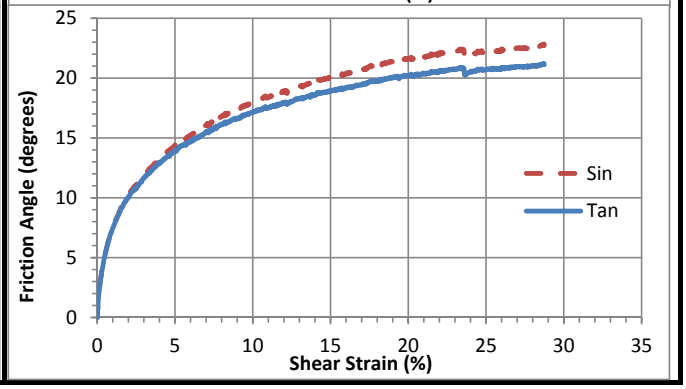

Undrained Strength			
Su/σv' at 10% strain	0.31	Su/σvc' at 10% strain	0.31
Su/σv' at 30% strain	0.39	Su/σvc' at 30% strain	0.39

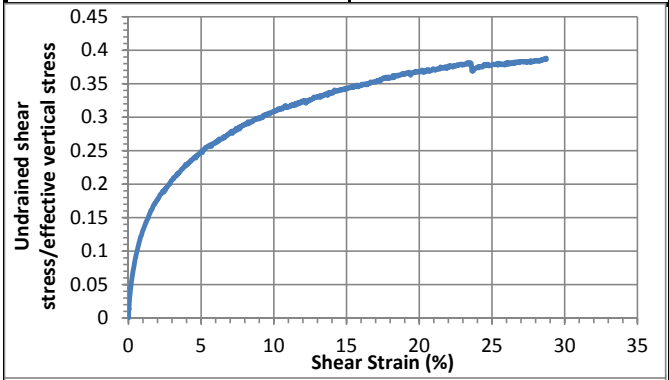

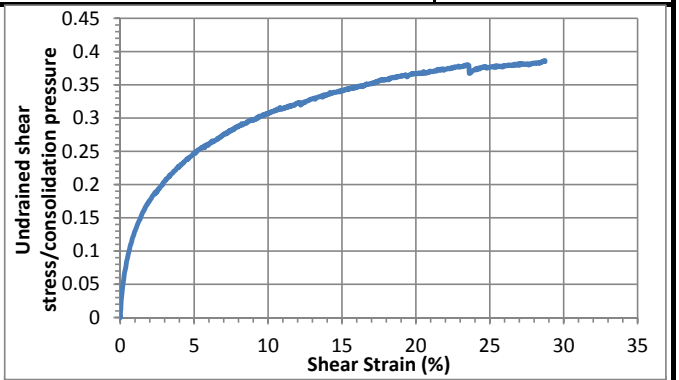

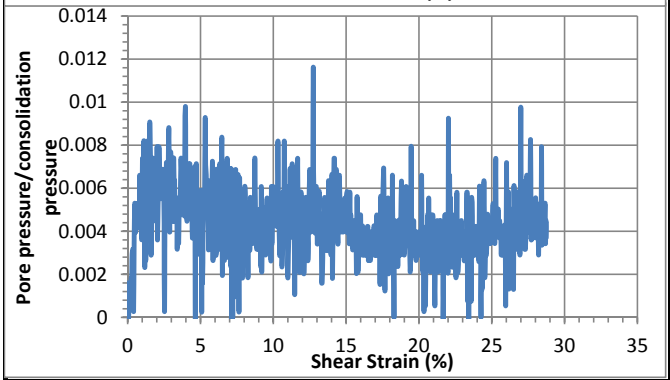

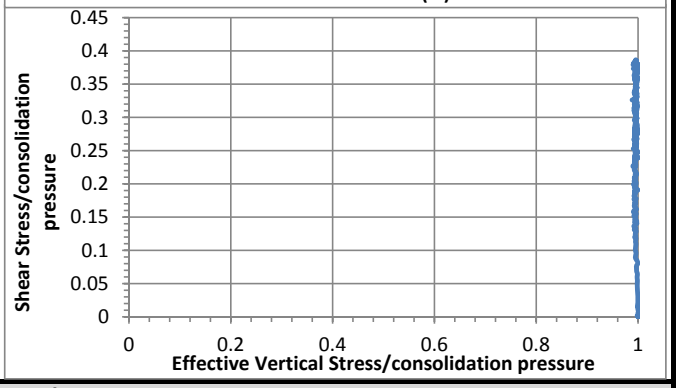

Shear wave velocity				
Signal type	Sinusoidal	First rise	initiation time (ms)	-0.0154
Signal amplitude (Vpp)	90		arrival time (ms)	0.4966
Signal frequency (kHz)	4		Vs (m/s)	214
Sensor spacing (mm)	109.37	First peak	initiation time (ms)	0.0512
R+P average Vs (m/s)	214		arrival time (ms)	0.5632
Stdev. (m/s)	0		Vs (m/s)	214
P+V average Vs (m/s)	213	First valley	initiation time (ms)	0.1792
Stdev. (m/s)	1		arrival time (ms)	0.6963
Wavelength (m)	0.053		Vs (m/s)	212
Spacing/wavelength	2.1			

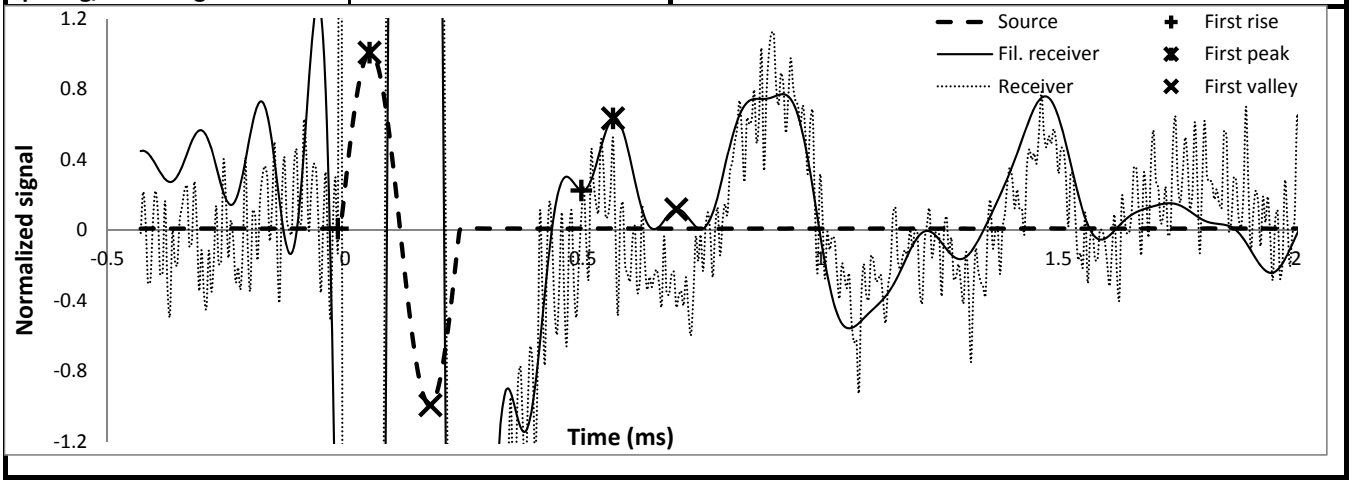

CSS Monotonic Shear Test Report

10/28/2013_Version 8.0

Geotechnical Engineering Laboratory

General Test Information and Sample Preparation			
Device:	CSS	**Layers:**	8.30
Specimen ID:	AZ-LR	**Weight/layer (kg):**	1.014
Test ID:	AZ5	**Height/layer (mm):**	25.4
Date of Test:	10/7/2014	**Total height (mm):**	210.82
Test Performed:	Monotonic Shear	**Soil-Only Specimen Diameter (mm):**	306.2
Test Material:	MSW	**Total weight (kg):**	8.4162
Sample Preparation:	The same initial composition and unit weight as Sim. #4. Staged pre-compress for 24 hours, consolidate for 1 hour.	**Density (kg/m^3):**	542
		Membrane Thickness (mm):	0.000635
		Moisture Content (%):	60.0
		Saturated (Y/N):	N
		Prepared by:	Fei

Pre-compression Stage			
Pre-compression strain:	0.47	**Secondary compression ratio:**	0.01013
Height (mm):	116.9	**Density (kg/m3):**	978

Consolidation Stage		Shear Stage		
Initial height (mm):	131.5	**Type of Test:**		CU-strain
Initial density (kg/m3):	869	**Shear Strain Rate (%/min):**		0.36
Vertical Stress (kPa):	95.7	**10% strain**	**Shear stress (kPa)**	28.0
Immediate strain (εimm, %)	46.1		**Tan friction angle (°)**	23.1
Consolidated Height (mm):	111.2		**Sin friction angle (°)**	25.3
Compression index (Ccε)	0.244	**30% strain**	**Shear stress (kPa)**	30.4
Consolidation modulus	4.1		**Tan friction angle (°)**	27.4
Consolidated density (kg/m^3):	1028		**Sin friction angle (°)**	31.3

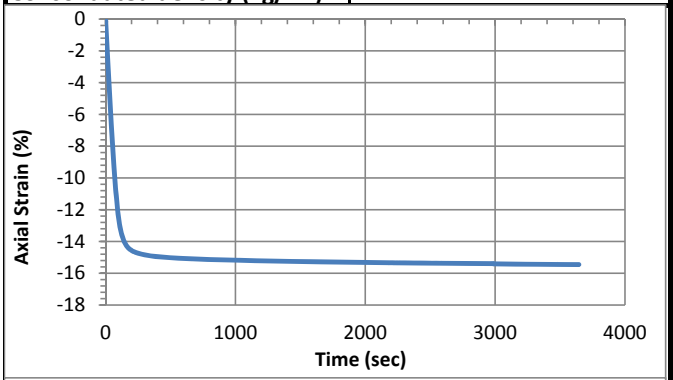

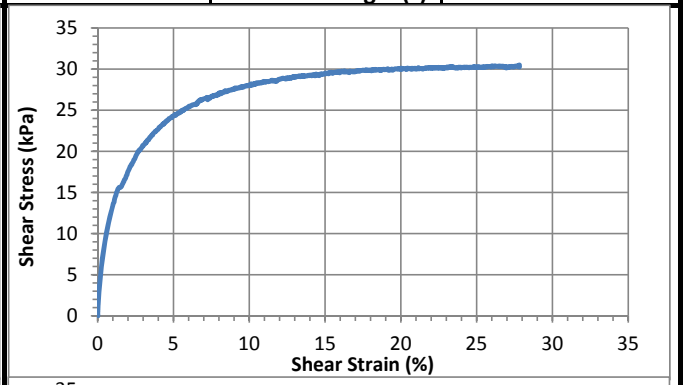

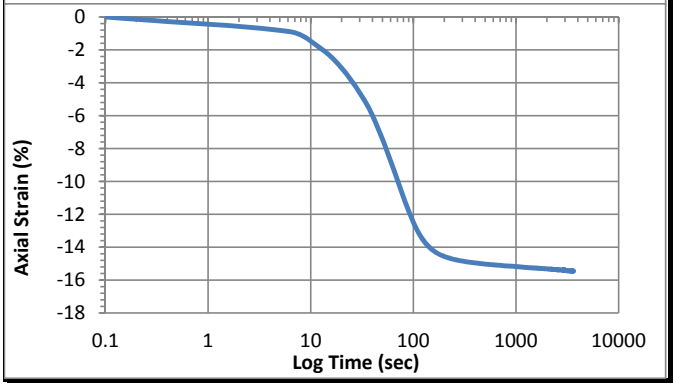

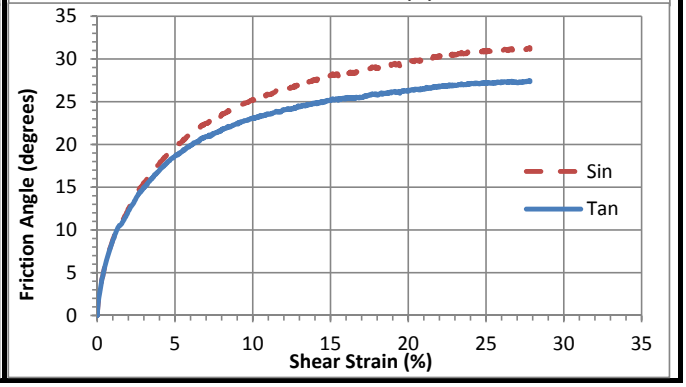

Undrained Strength			
Su/σv' at 10% strain	0.43	Su/σvc' at 10% strain	0.29
Su/σv' at 30% strain	0.52	Su/σvc' at 30% strain	0.32

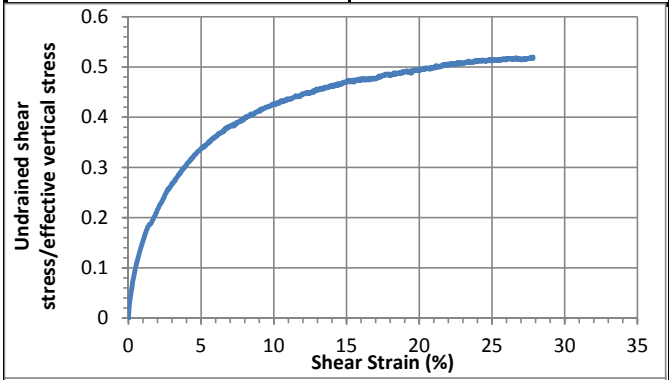

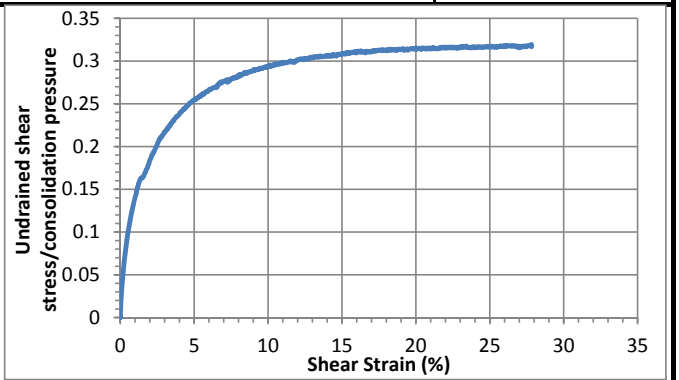

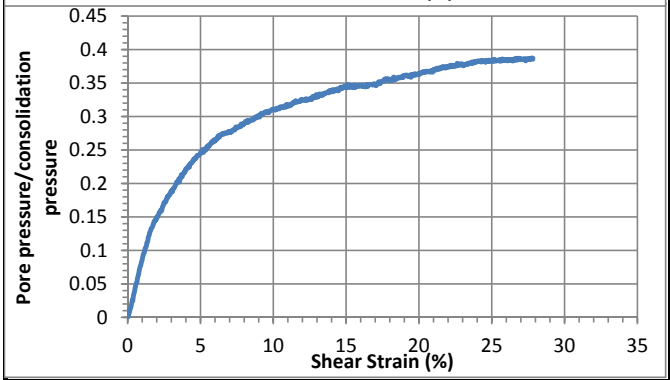

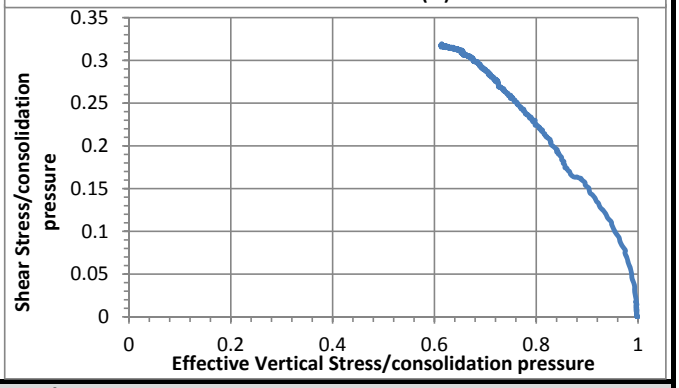

Shear wave velocity				
Signal type	Sinusoidal	First rise	initiation time (ms)	-0.0154
Signal amplitude (Vpp)	90		arrival time (ms)	0.5632
Signal frequency (kHz)	4		Vs (m/s)	177
Sensor spacing (mm)	102.48	First peak	initiation time (ms)	0.0512
R+P average Vs (m/s)	176		arrival time (ms)	0.6400
Stdev. (m/s)	2		Vs (m/s)	174
P+V average Vs (m/s)	173	First valley	initiation time (ms)	0.1792
Stdev. (m/s)	1		arrival time (ms)	0.7731
Wavelength (m)	0.043		Vs (m/s)	173
Spacing/wavelength	2.4			

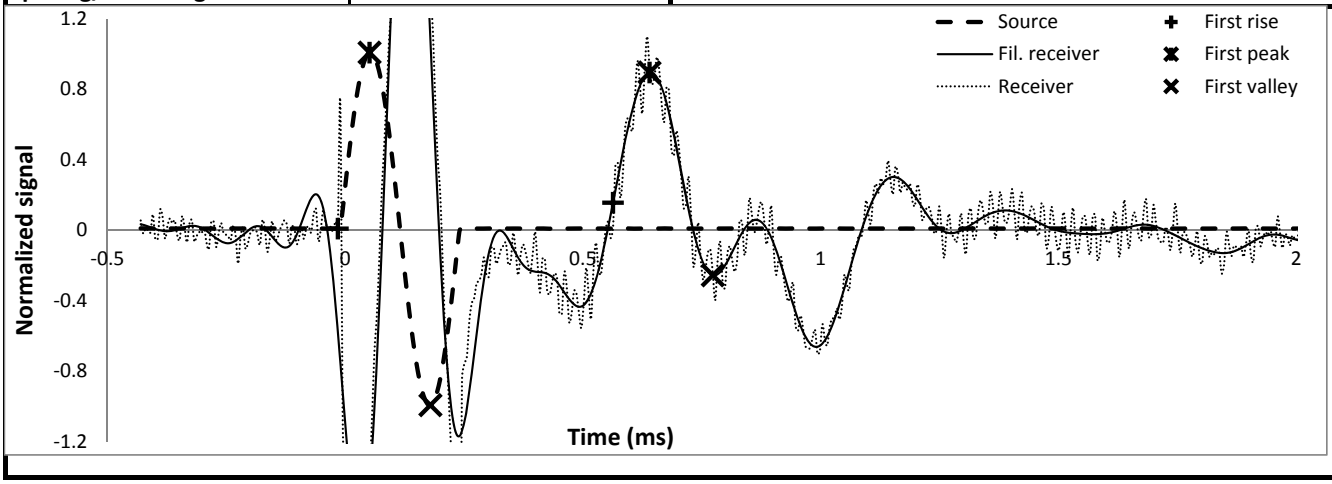

CSS Monotonic Shear Test Report

10/28/2013_Version 8.0

Geotechnical Engineering Laboratory

General Test Information and Sample Preparation			
Device:	CSS	**Layers:**	9.00
Specimen ID:	AZ-LR	**Weight/layer (kg):**	1.014
Test ID:	AZ6	**Height/layer (mm):**	25.4
Date of Test:	10/10/2014	**Total height (mm):**	228.6
Test Performed:	Monotonic Shear	**Soil-Only Specimen Diameter (mm):**	306.2
Test Material:	MSW	**Total weight (kg):**	9.126
Sample Preparation:	The same initial composition and unit weight as Sim. #4. Staged pre-compress for 23 hours, consolidate for 1 hour.	**Density (kg/m^3):**	542
		Membrane Thickness (mm):	0.000635
		Moisture Content (%):	60.0
		Saturated (Y/N):	N
		Prepared by:	Fei

Pre-compression Stage			
Pre-compression strain:	0.54	**Secondary compression ratio:**	0.01227
Height (mm):	110.4	**Density (kg/m3):**	1123

Consolidation Stage		Shear Stage		
Initial height (mm):	132.7	**Type of Test:**		CD-strain
Initial density (kg/m3):	933	**Shear Strain Rate (%/min):**		0.37
Vertical Stress (kPa):	194.2	**10% strain**	**Shear stress (kPa)**	61.6
Immediate strain (εimm, %)	55.4		**Tan friction angle (°)**	17.6
Consolidated Height (mm):	107.3		**Sin friction angle (°)**	18.6
Compression index (Ccε)	0.254	**30% strain**	**Shear stress (kPa)**	77.0
Consolidation modulus	3.4		**Tan friction angle (°)**	21.7
Consolidated density (kg/m^3):	1155		**Sin friction angle (°)**	23.5

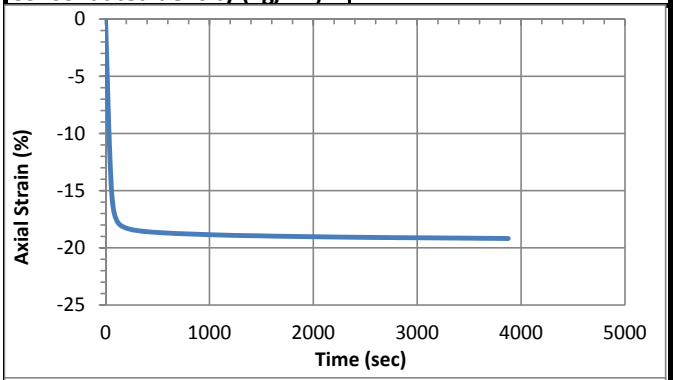

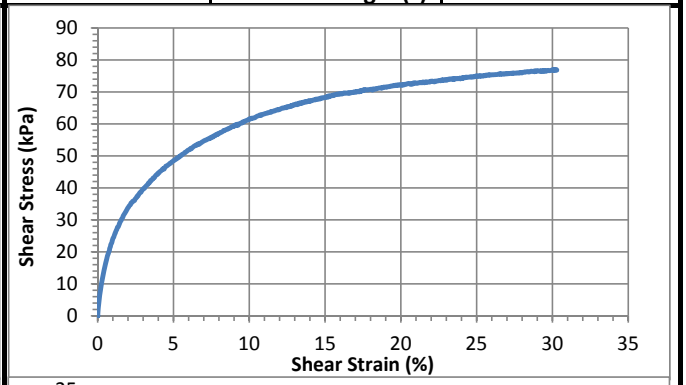

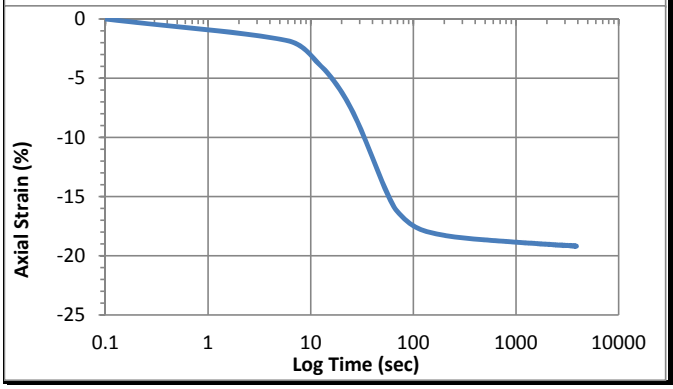

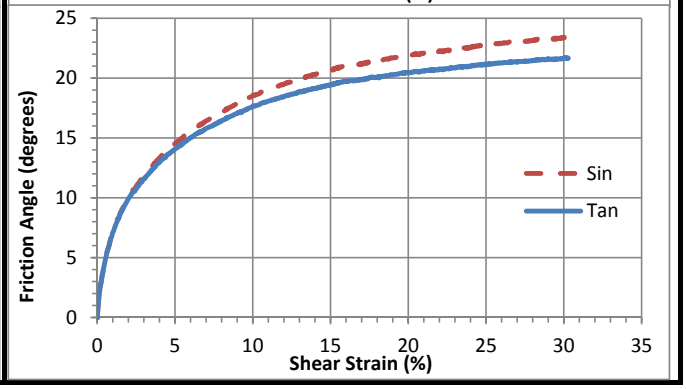

Undrained Strength			
Su/σv' at 10% strain	0.32	Su/σvc' at 10% strain	0.32
Su/σv' at 30% strain	0.40	Su/σvc' at 30% strain	0.40

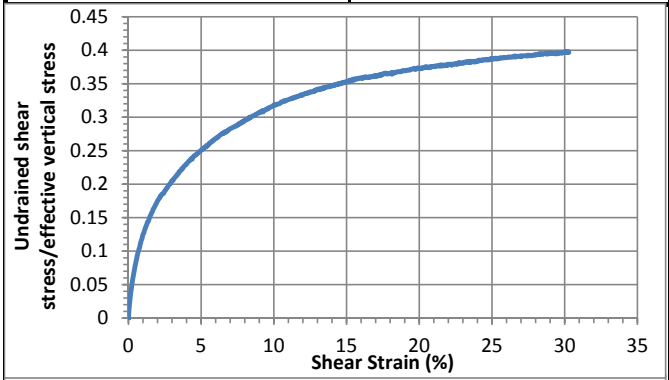

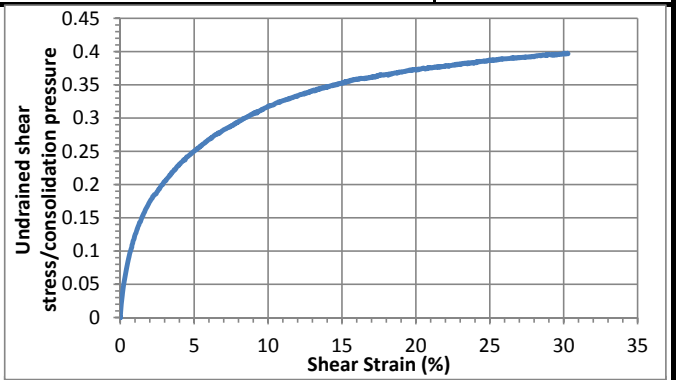

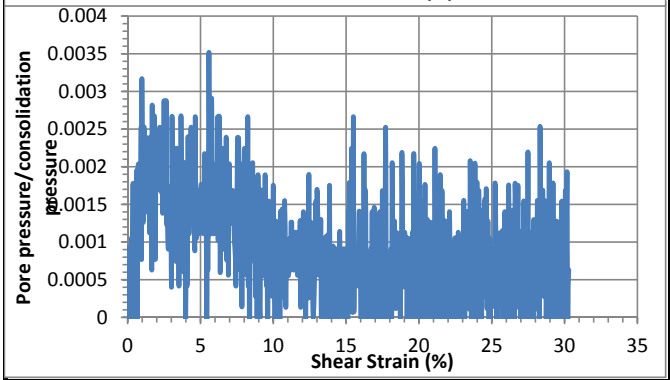

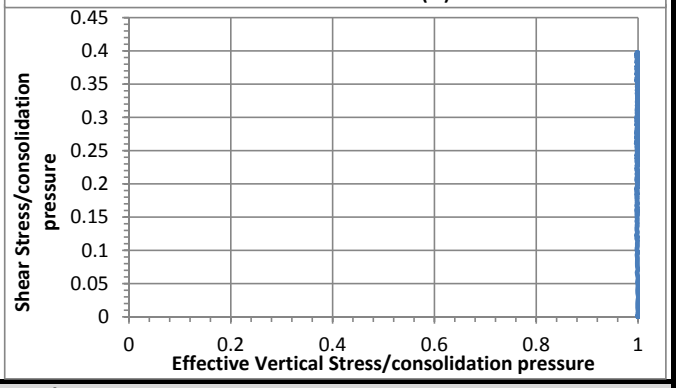

Shear wave velocity				
Signal type	Sinusoidal	First rise	initiation time (ms)	-0.0154
Signal amplitude (Vpp)	90		arrival time (ms)	0.3994
Signal frequency (kHz)	4		Vs (m/s)	238
Sensor spacing (mm)	98.54	First peak	initiation time (ms)	0.0512
R+P average Vs (m/s)	233		arrival time (ms)	0.4813
Stdev. (m/s)	6		Vs (m/s)	229
P+V average Vs (m/s)	226	First valley	initiation time (ms)	0.1792
Stdev. (m/s)	4		arrival time (ms)	0.6195
Wavelength (m)	0.057		Vs (m/s)	224
Spacing/wavelength	1.7			

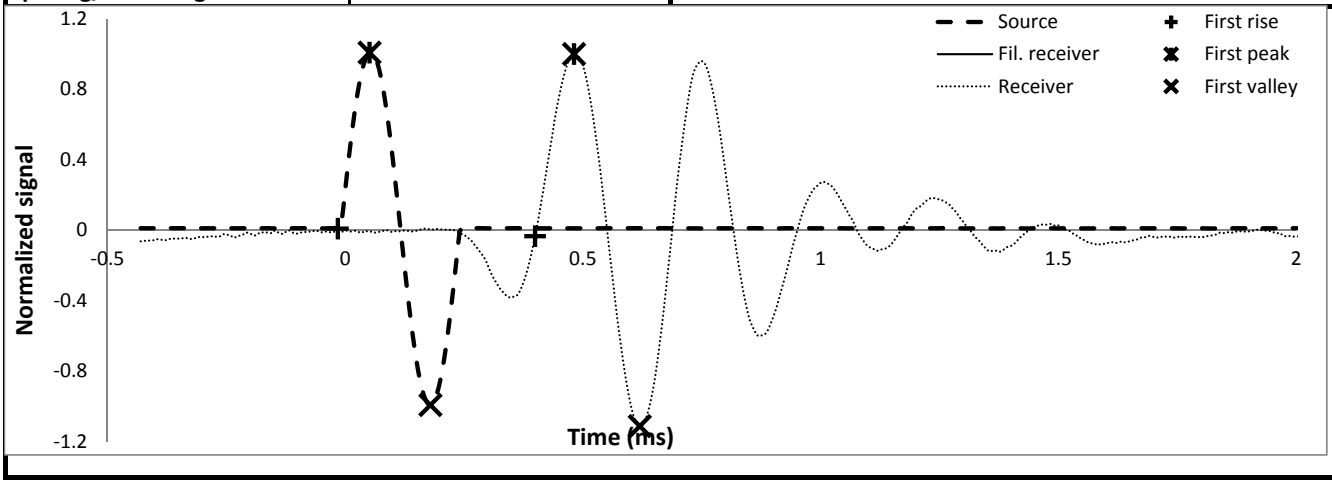

CSS Monotonic Shear Test Report

10/28/2013_Version 8.0

Geotechnical Engineering Laboratory

General Test Information and Sample Preparation			
Device:	CSS	**Layers:**	9.00
Specimen ID:	AZ-LR	**Weight/layer (kg):**	1.014
Test ID:	AZ7	**Height/layer (mm):**	25.4
Date of Test:	10/17/2014	**Total height (mm):**	228.6
Test Performed:	Monotonic Shear	**Soil-Only Specimen Diameter (mm):**	306.2
Test Material:	MSW	**Total weight (kg):**	9.126
Sample Preparation:	The same initial composition and unit weight as Sim. #4. Staged pre-compress for 25 hours, consolidate for 1 hour.	**Density (kg/m^3):**	542
		Membrane Thickness (mm):	0.000635
		Moisture Content (%):	60.0
		Saturated (Y/N):	N
		Prepared by:	Fei

Pre-compression Stage			
Pre-compression strain:	0.53	**Secondary compression ratio:**	0.00888
Height (mm):	107.7	**Density (kg/m3):**	1151

Consolidation Stage		Shear Stage		
Initial height (mm):	127.7	**Type of Test:**		CU-strain
Initial density (kg/m3):	970	**Shear Strain Rate (%/min):**		0.38
Vertical Stress (kPa):	193.9	**10% strain**	**Shear stress (kPa)**	54.0
Immediate strain (εimm, %)	50.6		**Tan friction angle (°)**	22.0
Consolidated Height (mm):	105.9		**Sin friction angle (°)**	23.7
Compression index (Ccε)	0.230	**30% strain**	**Shear stress (kPa)**	57.9
Consolidation modulus	3.8		**Tan friction angle (°)**	26.1
Consolidated density (kg/m^3):	1170		**Sin friction angle (°)**	29.4

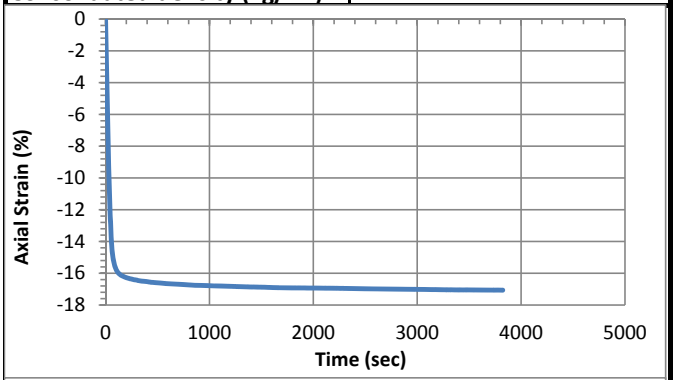

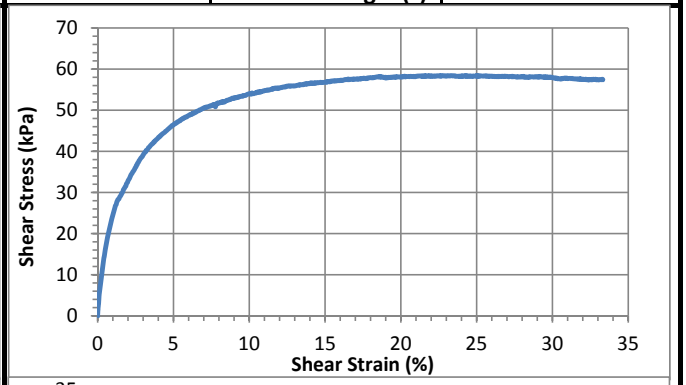

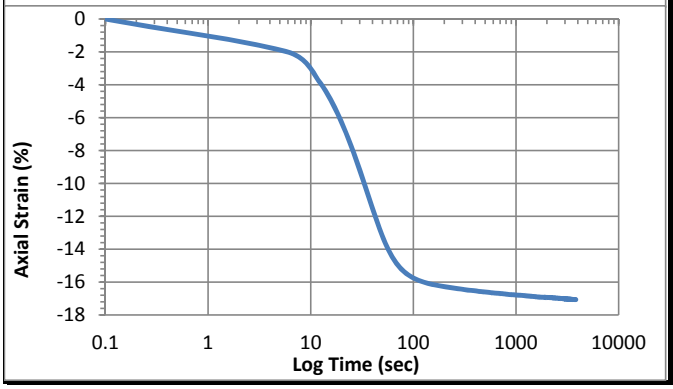

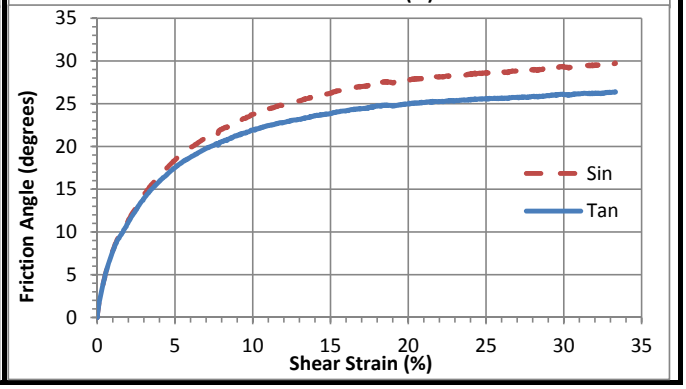

Undrained Strength			
Su/σv' at 10% strain	0.40	Su/σvc' at 10% strain	0.28
Su/σv' at 30% strain	0.49	Su/σvc' at 30% strain	0.30

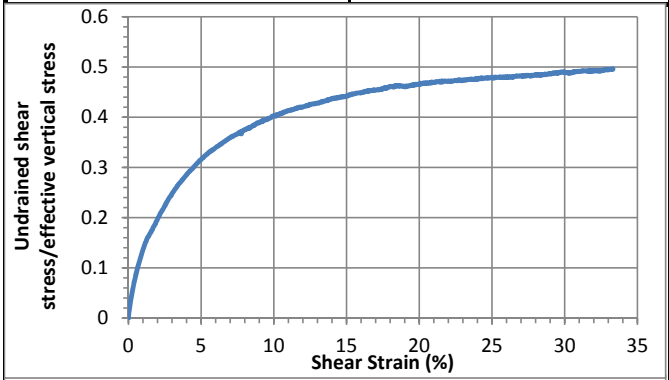

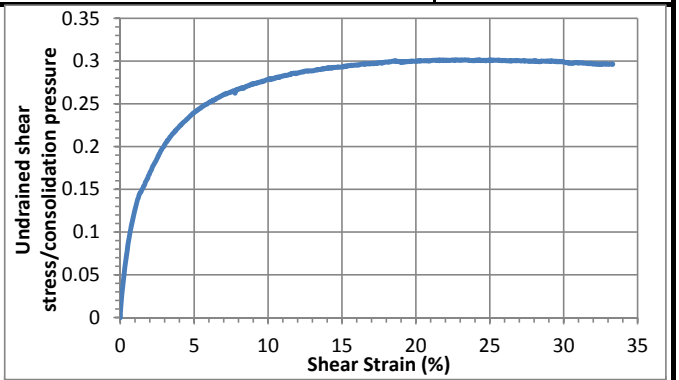

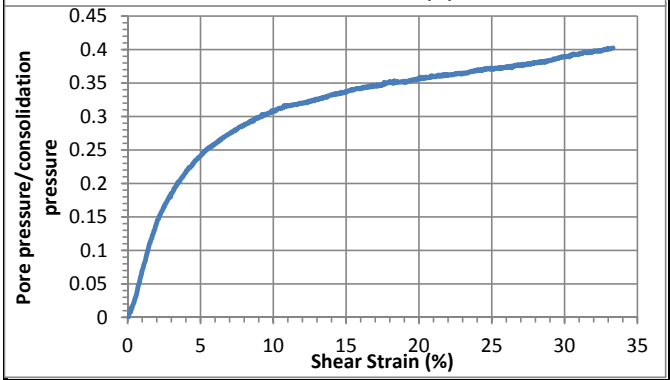

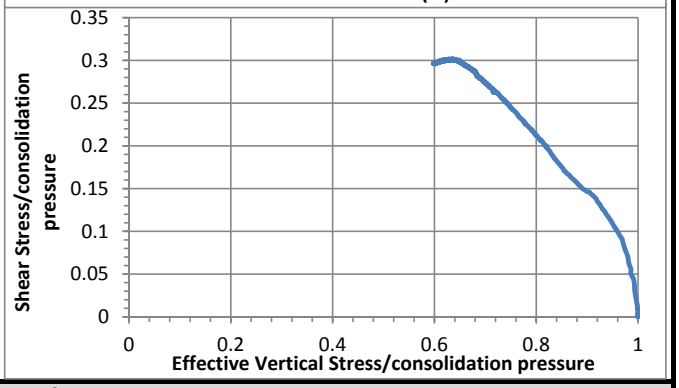

Shear wave velocity				
Signal type	Sinusoidal	First rise	initiation time (ms)	-0.0154
Signal amplitude (Vpp)	90		arrival time (ms)	0.3635
Signal frequency (kHz)	4		Vs (m/s)	257
Sensor spacing (mm)	97.30	First peak	initiation time (ms)	0.0512
R+P average Vs (m/s)	255		arrival time (ms)	0.4352
Stdev. (m/s)	2		Vs (m/s)	253
P+V average Vs (m/s)	252	First valley	initiation time (ms)	0.1741
Stdev. (m/s)	2		arrival time (ms)	0.5632
Wavelength (m)	0.063		Vs (m/s)	250
Spacing/wavelength	1.5			

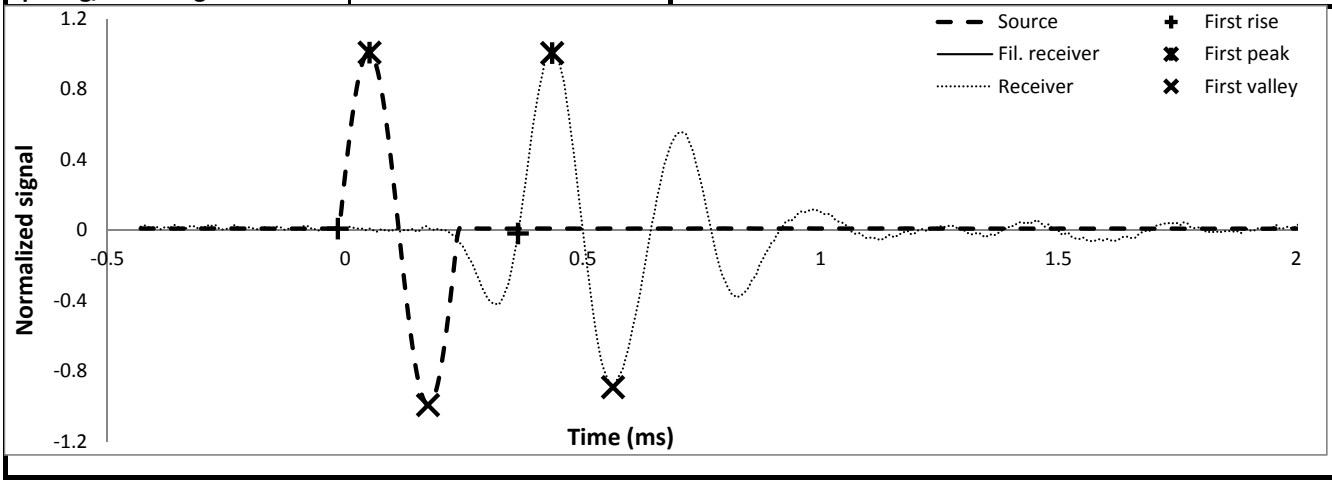

CSS Monotonic Shear Test Report

10/28/2013_Version 8.0

Geotechnical Engineering Laboratory

General Test Information and Sample Preparation			
Device:	CSS	**Layers:**	9.75
Specimen ID:	AZ-LR	**Weight/layer (kg):**	1.014
Test ID:	AZ8	**Height/layer (mm):**	25.4
Date of Test:	10/21/2014	**Total height (mm):**	247.65
Test Performed:	Monotonic Shear	**Soil-Only Specimen Diameter (mm):**	306.2
Test Material:	MSW	**Total weight (kg):**	9.8865
Sample Preparation:	The same initial composition and unit weight as Sim. #4. Staged pre-compress for 23 hours, consolidate for 1 hour.	**Density (kg/m^3):**	542
		Membrane Thickness (mm):	0.000635
		Moisture Content (%):	60.0
		Saturated (Y/N):	N
		Prepared by:	Fei

Pre-compression Stage			
Pre-compression strain:	0.57	**Secondary compression ratio:**	0.01003
Height (mm):	97.9	**Density (kg/m3):**	1300

Consolidation Stage		Shear Stage		
Initial height (mm):	125.5	**Type of Test:**		CU-strain
Initial density (kg/m3):	1070	**Shear Strain Rate (%/min):**		0.41
Vertical Stress (kPa):	393.7	**10% strain**	**Shear stress (kPa)**	98.7
Immediate strain (εimm, %)	56.1		**Tan friction angle (°)**	20.8
Consolidated Height (mm):	98.4		**Sin friction angle (°)**	22.3
Compression index (Ccε)	0.224	**30% strain**	**Shear stress (kPa)**	109.3
Consolidation modulus	3.4		**Tan friction angle (°)**	25.7
Consolidated density (kg/m^3):	1364		**Sin friction angle (°)**	28.7

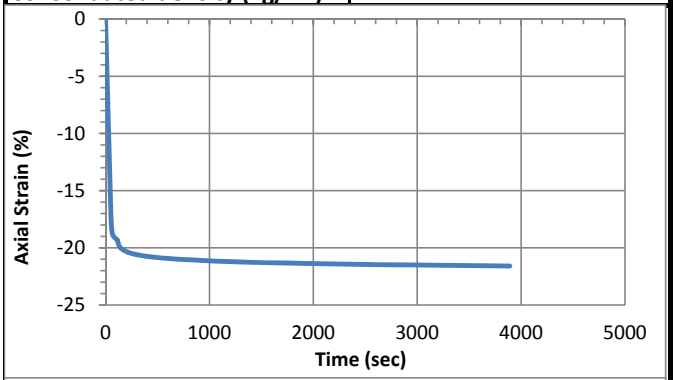

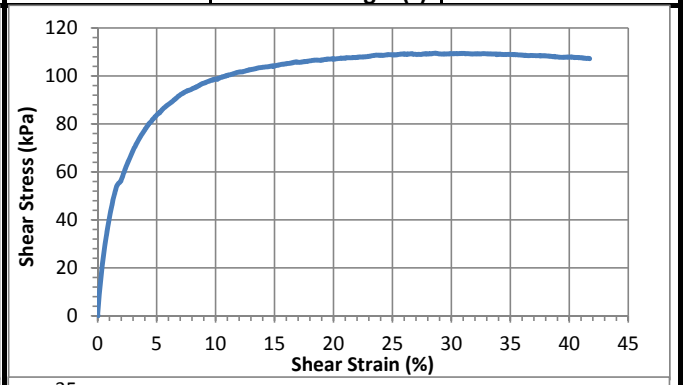

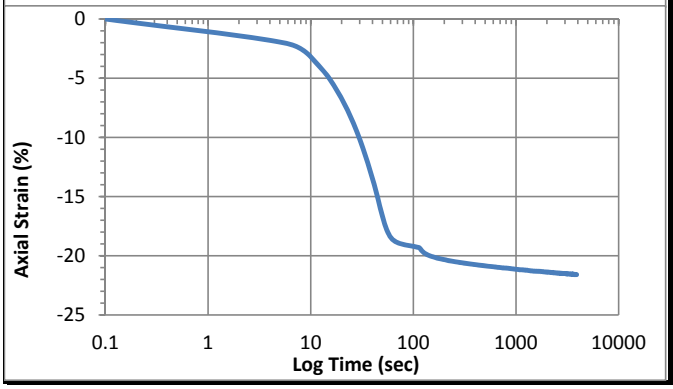

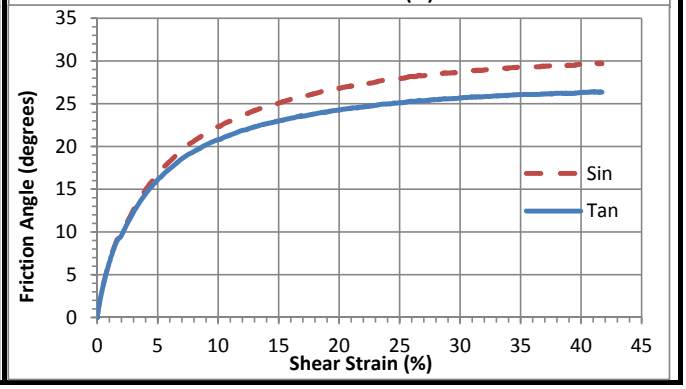

Undrained Strength			
Su/σv' at 10% strain	0.38	Su/σvc' at 10% strain	0.25
Su/σv' at 30% strain	0.48	Su/σvc' at 30% strain	0.28

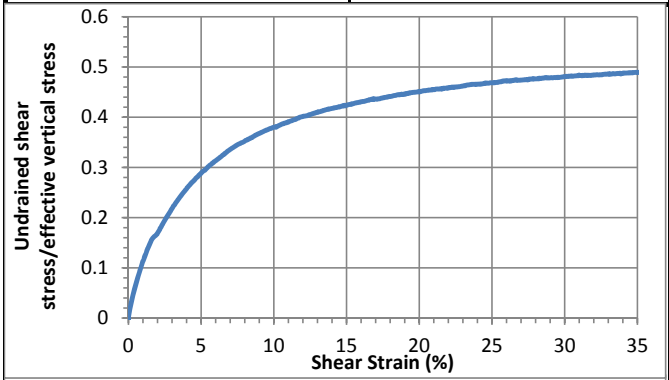

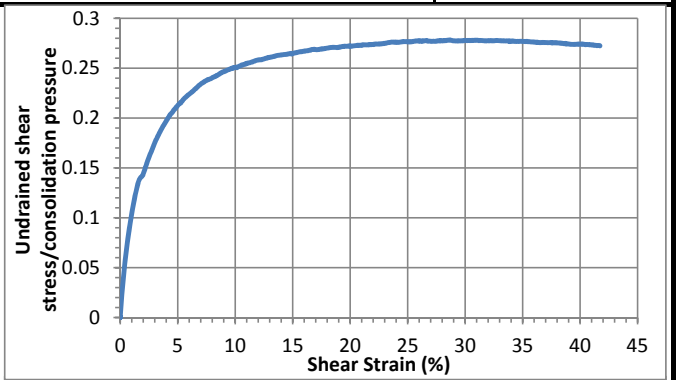

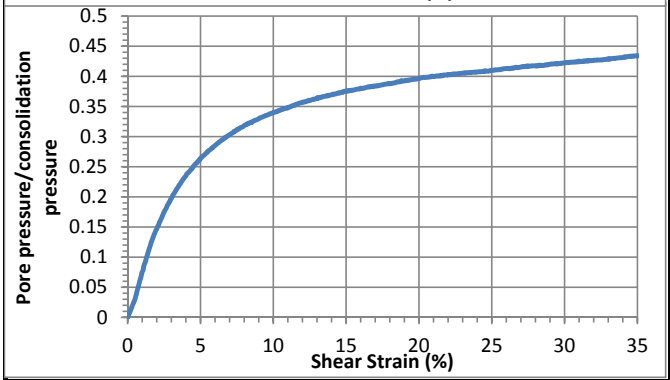

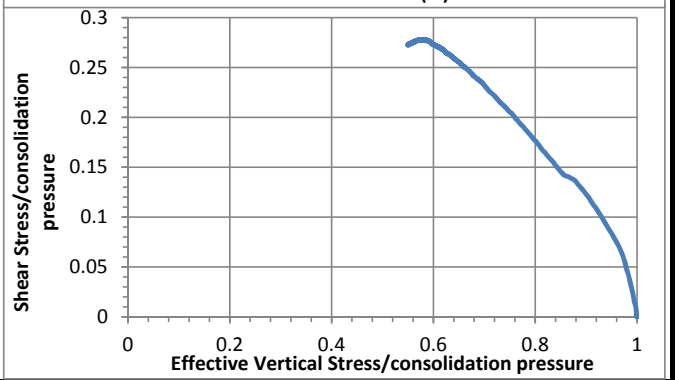

Shear wave velocity				
Signal type	Sinusoidal	First rise	initiation time (ms)	-0.0154
Signal amplitude (Vpp)	90		arrival time (ms)	0.2970
Signal frequency (kHz)	4		Vs (m/s)	294
Sensor spacing (mm)	91.74	First peak	initiation time (ms)	0.0512
R+P average Vs (m/s)	294		arrival time (ms)	0.3635
Stdev. (m/s)	0		Vs (m/s)	294
P+V average Vs (m/s)	291	First valley	initiation time (ms)	0.1741
Stdev. (m/s)	3		arrival time (ms)	0.4915
Wavelength (m)	0.073		Vs (m/s)	289
Spacing/wavelength	1.3			

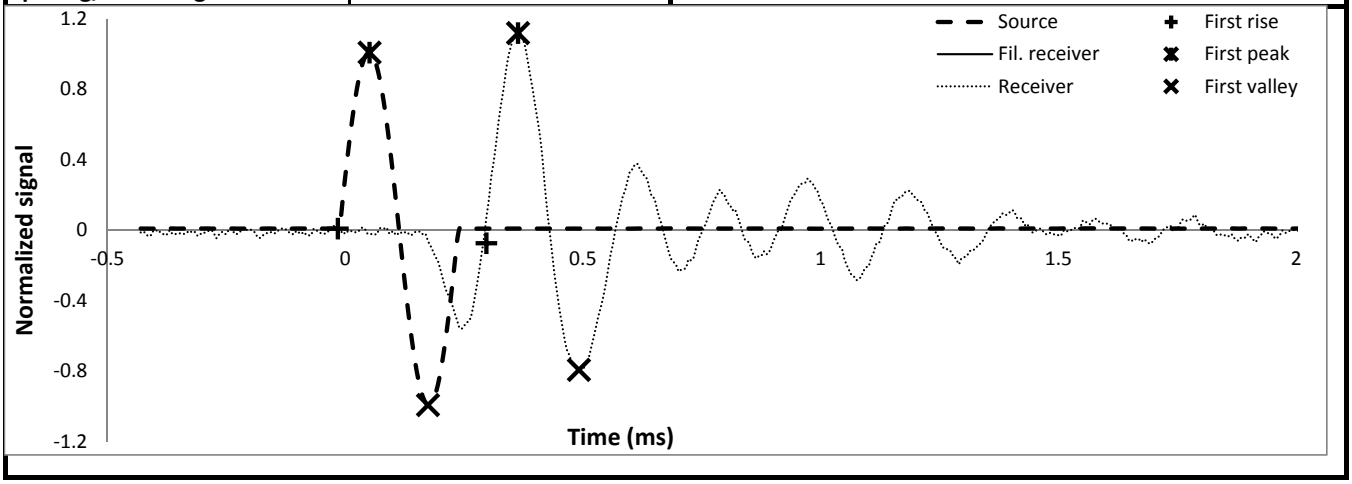

CSS Monotonic Shear Test Report

10/28/2013_Version 8.0

Geotechnical Engineering Laboratory

General Test Information		Sample Preparation	
Device:	CSS	Prepared total weight (kg):	19.418
Specimen ID:	AZ-LRD	Prepared dry weight (kg):	11.783
Test ID:	AZD1	Prepared height (mm):	304.8
Date of test:	10/30/2015	Prepared total density (kg/m3):	865
Test performed:	Monotonic Shear	Prepared dry density (kg/m3):	525
Test material:	MSW	**Pre-compression Stage**	
Sample preparation:	AZ degraded undisturbed specimen. Removed 2.066 kg before consolidation. Vertical stress from 200 to 400 kPa.	Pre-compressed strain (%):	52.2
		Compressed total density (kg/m3):	1808
		Compressed dry density (kg/m3):	1097
		Secondary compression ratio:	0.00790
		Total weight before shearing (kg):	13.283
		Dry weight before shearing (kg):	10.197

Consolidation Stage		Shear Stage		
Consolidated height (mm):	108.01	Type of test:		CL-strain
Vertical stress (kPa):	397.4	Shear strain rate (%/min):		0.37
Immediate strain (εimm, %)	58.26	10% strain	Shear stress (kPa)	111.1
Strain before shearing (εall, %)	59.0		Tan friction angle (°)	15.7
Compression index (Cεε)	0.224		Sin friction angle (°)	16.3
Constrained modulus	3.43	peak or 30% strain	Shear stress (kPa)	137.8
Consolidated total density	1670		Tan friction angle (°)	19.2
Consolidated dry density	1282		Sin friction angle (°)	20.3

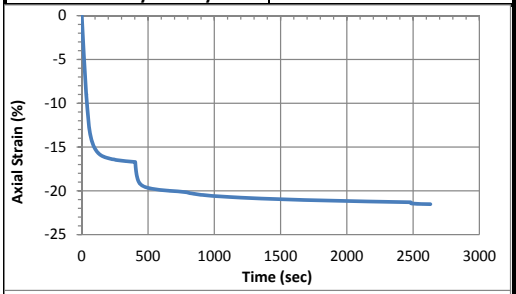

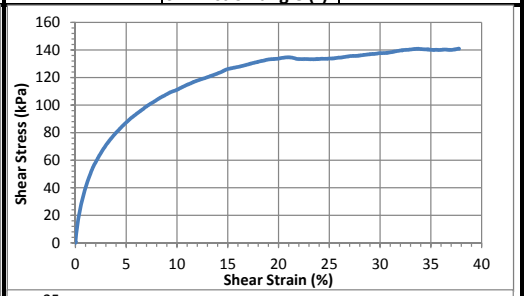

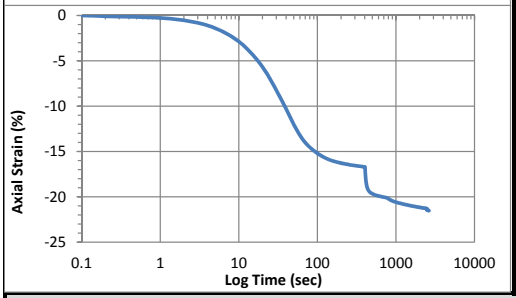

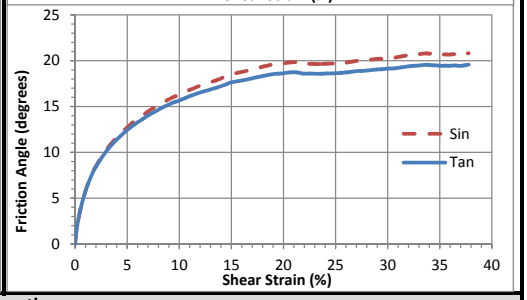

Strength			
τ/σv' at 10% strain	0.28	τ/σv0' at 10% strain	0.28
τ/σv' at peak or 30% strain	0.35	τ/σv0' at peak or 30% strain	0.35

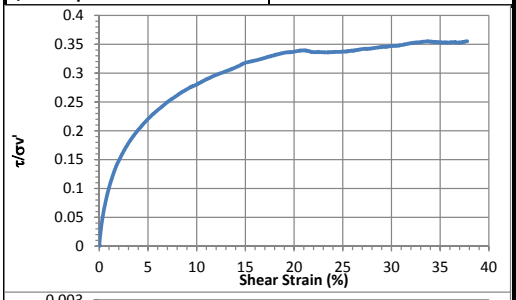

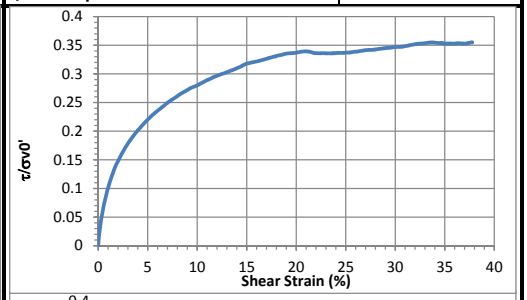

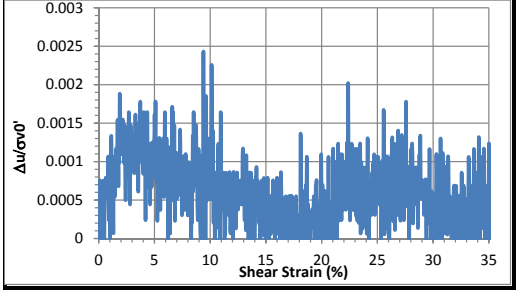

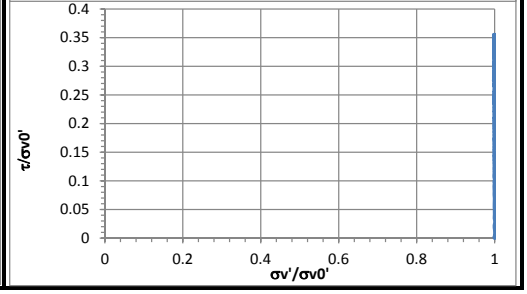

REFERENCES

Abbassi-Guendouz, A., Brockmann, D., Trably, E., Dumas, C., Delgenes, J. P., Steyer, J. P., and Escudie, R. (2012). "Total solids content drives high solid anaerobic digestion via mass transfer limitation." *Bioresource Technology*, 111, 55-61.

Abichou, T., Barlaz, M. A., Green, R., and Hater, G. (2013). "Liquid balance monitoring inside conventional, retrofit, and bio-reactor landfill cells." *Waste Management*, 33(10), 2006-2014.

Abuashour, J., Joy, D. M., Lee, H., Whiteley, H. R., and Zelin, S. (1994). "Transport of microorganisms through soil." *Water Air Soil Pollut.*, 75(1-2), 141-158.

Agostini, F., Sundberg, C., and Navia, R. (2012). "Is biodegradable waste a porous environment? A review." *Waste Manage. Res.*, 30(10), 1001-1015.

Airey, D. W., Budhu, M., and Woods, D. M. (1985). "Some aspects of the behavior of soils in simple shear." *Proc., Developments in Soil Mechanics and Foundation Engineering*, Elsevier.

Altschul, S. F., Gish, W., Miller, W., Myers, E. W., and Lipman, D. J. (1990). "Basic local alignment search tool." *Journal of Molecular Biology*, 215(3), 403-410.

Amini, H. R., Reinhart, D. R., and Mackie, K. R. (2012). "Determination of first-order landfill gas modeling parameters and uncertainties." *Waste Management*, 32(2), 305-316.

Amini, H. R., Reinhart, D. R., and Niskanen, A. (2013). "Comparison of first-order-decay modeled and actual field measured municipal solid waste landfill methane data." *Waste Management*, 33(12), 2720-2728.

APHA (2005). Standard methods for the examination of water and wastewater. American Public Health Association, Washington, DC.

Appels, L., Lauwers, J., Degreve, J., Helsen, L., Lievens, B., Willems, K., Van Impe, J., and Dewil, R. (2011). "Anaerobic digestion in global bio-energy production: Potential and research challenges." *Renew. Sust. Energ. Rev.*, 15(9), 4295-4301.

ASCE (2014). "2013 report card for america's infrastructure - solid waste." American Society of Civil Engineers, http://www.infrastructurereportcard.org/a/#p/solid-waste/overview.

ASTM (2007). "D6528-07 standard test method for consolidated undrained direct simple shear testing of cohesive soils." ASTM International, West Conshohocken, PA, USA.

ASTM (2011). "D3080-11 standard test method for direct shear test of soils under consolidated drained conditions." ASTM International, West Conshohocken, PA, USA.

Athanasopoulos, G. A. (2011a). "Laboratory testing of municipal solid waste." *Geotechnical characterization, field measurement, and laboratory testing of municipal solid waste: Proceedings of the 2008 international symposium on waste mechanics*, D. Zekkos, ed., ASCE, Geo-Institute, Reston VA.

Athanasopoulos, G. A. (2011b). "Laboratory testing of municipal solid waste." *Geotechnical characterization, field measurement, and laboratory testing of municipal solid waste*, 195-205.

Augenstein, D., Yazdani, R., Moore, R., Dahl, K., and Soc Waste Assoc, N. A. (1997). "Yolo county controlled landfill demonstration project." *Proceedings from Swana's 20th Annual Landfill Gas Symposium*, 43-87.

Bareither, C., Benson, C., and Edil, T. (2012a). "Compression behavior of municipal solid waste: Immediate compression." *Journal of Geotechnical and Geoenvironmental Engineering*, 138(9), 1047-1062.
Bareither, C. A. (2010). "Compression behavior of solid waste." Ph.D., The University of Wisconsin - Madison, Madison, WI, USA.
Bareither, C. A., Benson, C. H., Barlaz, M. A., Edil, T. B., and Tolaymat, T. M. (2010). "Performance of north american bioreactor landfills. I: Leachate hydrology and waste settlement." *J. Environ. Eng.-ASCE*, 136(8), 824-838.
Bareither, C. A., Benson, C. H., and Edil, T. B. (2012b). "Compression behavior of municipal solid waste: Immediate compression " *Journal of Geotechnical and Geoenvironmental Engineering*, 138(9), 1047-1062.
Bareither, C. A., Benson, C. H., and Edil, T. B. (2012c). "Effects of waste composition and decomposition on the shear strength of municipal solid waste." *Journal of Geotechnical and Geoenvironmental Engineering*, 138(10), 1161-1174.
Bareither, C. A., Benson, C. H., Edil, T. B., and Barlaz, M. A. (2012d). "Abiotic and biotic compression of municipal solid waste " *Journal of Geotechnical and Geoenvironmental Engineering*, 138(8), 877-888.
Bareither, C. A., Breitmeyer, R. J., Benson, C. H., Barlaz, M. A., and Edil, T. B. (2012e). "Deer track bioreactor experiment: Field-scale evaluation of municipal solid waste bioreactor performance." *Journal of Geotechnical and Geoenvironmental Engineering*, 138(6), 658-670.
Bareither, C. A., Benson, C. H., and Edil, T. B. (2013a). "Compression of municipal solid waste in bioreactor landfills: Mechanical creep and biocompression." *Journal of Geotechnical and Geoenvironmental Engineering*, 139(7), 1007-1021.
Bareither, C. A., Wolfe, G. L., McMahon, K. D., and Benson, C. H. (2013b). "Microbial diversity and dynamics during methane production from municipal solid waste." *Waste Management*, 33(10), 1982-1992.
Barlaz, M. A., Ham, R. K., and Schaefer, D. M. (1989a). "Mass balance analysis of anaerobically decomposed refuse." *J. Environ. Eng.-ASCE*, 115(6), 1088-1102.
Barlaz, M. A., Schaefer, D. M., and Ham, R. K. (1989b). "Bacterial population development and chemical characteristics of refuse decomposition in a simulated sanitary landfill." *Appl. Environ. Microbiol.*, 55(1), 55-65.
Barlaz, M. A., Ham, R. K., and Schaefer, D. M. (1992). "Microbial, chemical and methane production characteristics of anaerobically decomposed refuse with and without leachate recycling." *Waste Manage. Res.*, 10(3), 257-267.
Barlaz, M. A., Rooker, A. P., Kjeldsen, P., Gabr, M. A., and Borden, R. C. (2002). "Critical evaluation of factors required to terminate the postclosure monitoring period at solid waste landfills." *Environmental Science & Technology*, 36(16), 3457-3464.
Barlaz, M. A. (2006). "Forest products decomposition in municipal solid waste landfills." *Waste Management*, 26(4), 321-333.
Barlaz, M. A., Bareither, C. A., Hossain, A., Saquing, J., Mezzari, I., Benson, C. H., Tolaymat, T. M., and Yazdani, R. (2010a). "Performance of north american bioreactor landfills. Ii: Chemical and biological characteristics." *J. Environ. Eng.-ASCE*, 136(8), 839-853.
Barlaz, M. A., Staley, B. F., and de los Reyes, F. L. (2010b). "Anaerobic biodegradation of solid waste." *Environ. Microbiol.*, R. Mitchell, and J. Gu, eds., Wiley-Blackwell, Hoboken, NJ, 281-299.

Batstone, D. J., J. Keller, I. Angelidaki, S. V. Kalyuzhnyi, S. G. Pavlosthathis, A. Rozzi, W. T. M. Sanders, H. Siegrist, and V. A. Vavilin (2002). "Anaerobic digestion model no. 1." *IWA Publishing, Scientific and Technical Report No. 13.* Cornwall, UK.

Beaven, R. P. (2008). "Review of responses to a landfill modelling challenge." *Proceedings of the ICE - Waste and Resource Management*, 161(4), 155-166.

Benbelkacem, H., Bayard, R., Abdelhay, A., Zhang, Y., and Gourdon, R. (2010). "Effect of leachate injection modes on municipal solid waste degradation in anaerobic bioreactor." *Bioresource Technology*, 101(14), 5206-5212.

Bengtsson, L., Bendz, D., Hogland, W., Rosqvist, H., and Akesson, M. (1994). "Water-balance for landfills of different age." *J. Hydrol.*, 158(3-4), 203-217.

Benson, C. H., Barlaz, M. A., Lane, D. T., and Rawe, J. M. (2007). "Practice review of five bioreactor/recirculation landfills." *Waste Management*, 27(1), 13-29.

Bentley, H. W., Smith, S. J., and Schrauf, T. (2005). "Baro-pneumatic estimation of landfill gas generation rates at four operating landfills." *Proc., SWANA 10th Annual Landfill Gas Symposium and Solid Waste Management*.

Bioreactor.org (2011). "Bioreactors around the world." *http://www.bioreactor.org/world.html*.

Bjarngard, A., and Edgers, L. (1990). "Settlement of municipal solid waste landfills." *Proc., 13th Annual Madison Waste Conference: Municipal & Industrial Waste*, 192-205.

Bjerrum, L., and Landva, A. (1966). "Direct simple-shear tests on a norwegian quick clay." *Geotechnique*, 1-20.

Bogner, J., and Matthews, E. (2003). "Global methane emissions from landfills: New methodology and annual estimates 1980-1996." *Glob. Biogeochem. Cycle*, 17(2).

Boni, M. R., Chiavola, A., and Sbaffoni, S. (2006). "Pretreated waste landfilling: Relation between leachate characteristics and mechanical behaviour." *Waste Management*, 26(10), 1156-1165.

Borglin, S. E., Hazen, T. C., Oldenburg, C. M., and Zawislanski, P. T. (2004). "Comparison of aerobic and anaerobic biotreatment of municipal solid waste." *Journal of the Air & Waste Management Association*, 54(7), 815-822.

Bray, J. D., Zekkos, D., Kavazanjian, E., Jr., Athanasopoulos, G. A., and Riemer, M. F. (2009). "Shear strength of municipal solid waste." *Journal of Geotechnical and Geoenvironmental Engineering*, 135(6), 709-722.

Breitmeyer, R. J. (2011). "Hydraulic characterization of municpal solid waste." Ph.D., The University of Wisconsin - Madison.

Breitmeyer, R. J., and Benson, C. H. (2011). "Measurement of unsaturated hydraulic properties of municipal solid waste." *Proc., Geofrontiers 2011*, ASCE.

Breitmeyer, R. J., and Benson, C. H. (2014). "Evaluation of parameterization techniques for unsaturated hydraulic conductivity functions for municipal solid waste." *Geotech. Test. J.*, 37(4).

Budhu, M. (1984). "Nonuniformities imposed by simple shear apparatus." *Can. Geotech. J.*, 21(1), 125-137.

Budka, A., Aniel, D., Puglierin, L., and Stoppioni, E. (2007). "Bioreactor and conventional landfill: Lfg modeling after three management years of two compared cells in sonzay, france." *Proc., Eleventh International Waste Management and Landfill Symposium*.

Burrell, P. C., O'Sullivan, C., Song, H., Clarke, W. P., and Blackall, L. L. (2004). "Identification, detection, and spatial resolution of clostridium populations responsible for cellulose

degradation in a methanogenic landfill leachate bioreactor." *Appl. Environ. Microbiol.*, 70(4), 2414-2419.
Caicedo, B., Yamin, L., Giraldo, E., and Coronado, O. (2002). "Geomechanical properties of municipal solid waste in dona juana sanitary landfill." *Proc., 4th International Congress on Environmental Geotechnics*, 177-182.
Calli, B., Durmaz, S., and Mertoglu, B. (2006). "Identification of prevalent microbial communities in a municipal solid waste landfill." *Water Sci. Technol.*, 53(8), 139-147.
Capelo, J., and de Castro, M. A. H. (2007). "Measuring transient water flow in unsaturated municipal solid waste - a new experimental approach." *Waste Management*, 27(6), 811-819.
CensusBureau (2010). "Population profile of the united states." *http://www.census.gov/population/www/pop-profile/natproj.html*.
Chen, A. C., Ueda, K., Sekiguchi, Y., Ohashi, A., and Harada, H. (2003). "Molecular detection and direct enumeration of methanogenic archaea and methanotrophic bacteria in domestic solid waste landfill soils." *Biotechnol. Lett.*, 25(18), 1563-1569.
Chen, J. D., Shi, J. Y., and Hu, Y. D. (2008). "One-dimensional compression modified method of settlement of landfills and verification of degradation of organic content in solid waste." *Rock and Soil Mechanics*, 29(7), 1797-1801 (in Chinese).
Chen, Q. H. (2009). "Simulation study of leachate recirculation semi-aerobic landfills." M.S., Southwest Jiaotong University, Chendu, China (in Chinese).
Chen, Q. H., Yang, Q. Y., Huang, Y. F., and Lin, N. (2010a). "Study on settlement characteristics of simulating semi-aerobic landfill with leachate recirculation (in chinese)." *Journal of Safety and Environment*, 10(2), No. 14.
Chen, T. H., and Chynoweth, D. P. (1995). "Hydraulic conductivity of compacted municipal solid waste." *Bioresource Technology*, 51(2-3), 205-212.
Chen, Y. M., Zhan, T. L. T., Wei, H. Y., and Ke, H. (2009). "Aging and compressibility of municipal solid wastes." *Waste Management*, 29(1), 86-95.
Chen, Y. M., Ke, H., Fredlund, D. G., Zhan, L. T., and Xie, Y. (2010b). "Secondary compression of municipal solid wastes and a compression model for predicting settlement of municipal solid waste landfills." *Journal of Geotechnical and Geoenvironmental Engineering*, 136(5), 706-717.
Chiao, T.-H., Clancy, T. M., Pinto, A., Xi, C., and Raskin, L. (2014). "Differential resistance of drinking water bacterial populations to monochloramine disinfection." *Environmental Science & Technology*.
Cho, H. S., Moon, H. S., and Kim, J. Y. (2012). "Effect of quantity and composition of waste on the prediction of annual methane potential from landfills." *Bioresource Technology*, 109, 86-92.
Colberg, P. J. (1988). "Anaerobic microbial degradation of cellulose, lignin, oligolignols, and monoaromatic lignin derivatives." *Biology of anaerobic microorganisms*, A. J. B. Zehnder, ed., Wiley-Liss, New York, 333-372.
Cooke, A. J., Rowe, R. K., Rittmann, B. E., VanGulck, J., and Millward, S. (2001). "Biofilm growth and mineral precipitation in synthetic leachate columns." *Journal of Geotechnical and Geoenvironmental Engineering*, 127(10), 849-856.
Cooke, A. J., Rowe, R. K., VanGulck, J., and Rittmann, B. E. (2005). "Application of the bioclog model for landfill leachate clogging of gravel-packed columns." *Can. Geotech. J.*, 42(6), 1600-1614.

Copty, N. K., Ergene, D., and Onay, T. T. (2004). "Stochastic model for landfill gas transport and energy recovery." *Journal of Environmental Engineering-Asce*, 130(9), 1042-1049.
Daliri, F., and Basu, D. H. (2013). "Monotonic simple shear response of fine grained silts under different saturation condition." *Multiphysical testing of soils and shales*, L. Laloui, and A. Ferrari, eds., Springer Berlin Heidelberg, 93-98.
de Abreu, R. C. (2003). "Facultative bioreactor landfill: An environmental and geotechnical study." Ph.D., University of New Orleans, New Orleans, LA.
de Abreu, R. C., McManis, K. L., and Boutwell, G. P. (2005). "A new model for immediate settlement predictions in landfills." *Proc., Proceedings of the 16th International Conference on Soil Mechanics and Geotechnical Engineering*, Millpress Science Publishers, 2233-2236.
De la Cruz, F. B., and Barlaz, M. A. (2010). "Estimation of waste component-specific landfill decay rates using laboratory-scale decomposition data." *Environmental Science & Technology*, 44(12), 4722-4728.
Dearman, B., and Bentham, R. H. (2007). "Anaerobic digestion of food waste: Comparing leachate exchange rates in sequential batch systems digesting food waste and biosolids." *Waste Management*, 27(12), 1792-1799.
DeGroot, D. J., Ladd, C. C., and Germaine, J. T. (1992). "Direct simple shear testing of cohesive soils."
Dixon, N., and Jones, D. R. V. (2005). "Engineering properties of municipal solid waste." *Geotext. Geomembr.*, 23(3), 205-233.
Dixon, N., Whittle, R. W., Jones, D. R. V., and Ng'Ambi, S. (2006). "Pressuremeter tests in municipal solid waste: Measurement of shear stiffness." *Geotechnique*, 56(3), 211-222.
Dixon, N., Langer, U., and Gotteland, P. (2008). "Classification and mechanical behavior relationships for municipal solid waste: Study using synthetic wastes." *Journal of Geotechnical and Geoenvironmental Engineering*, 134(1), 79-90.
Donnelly, F. A., and Scarpino, P. V. (1984). "Isolation, characterization and identification of microorganisms from laboratory and full scale landfills." *EPA Project summary. EPA 600/S2-84-119*, U.S. Environmental Protection Agency, Cincinnati, OH.
Duncan, J. M., and Dunlop, P. (1969). "Behavior of soils in simple shear tests." *Proc., the 7th International Conference on Soil Mechanics and Foundation*, 101-109.
Dyvik, R., Berre, T., Lacasse, S., and Raadim, B. (1987). "Comparison of truly undrained and constant volume direct simple shear tests." *Geotechnique*, 3-10.
Edgers, L., Noble, J. J., and Williams, E. (1992). A biologic model for long-term settlement in landfills. Balkema, Rotterdam.
Edil, T. B., Ranguette, V. J., and Wuellner, W. W. (1990). Settlement of municipal refuse. Amer Soc Testing and Materials, Philadelphia.
Eid, H. T., Stark, T. D., Evans, W. D., and Sherry, P. E. (2000). "Municipal solid waste slope failure. I: Waste and foundation soil properties." *Journal of Geotechnical and Geoenvironmental Engineering*, 126(5), 397-407.
El-Fadel, M., Findikakis, A. N., and Leckie, J. O. (1996a). "Numerical modelling of generation and transport of gas and heat in sanitary landfills. 2. Model application." *Waste Manage. Res.*, 14(6), 537-551.
El-Fadel, M., Findikakis, A. N., and Leckie, J. O. (1996b). "Numerical modelling of generation and transport of gas and heat in landfills. 1. Model formulation." *Waste Manage. Res.*, 14(5), 483-504.

El-Fadel, M., Findikakis, A. N., and Leckie, J. O. (1997). "Modeling leachate generation and transport in solid waste landfills." *Environ. Technol.*, 18(7), 669-686.
El-Fadel, M., Shazbak, S., Saliby, E., and Leckie, J. (1999). "Comparative assessment of settlement models for municipal solid waste landfill applications." *Waste Manage. Res.*, 17(5), 347-368.
El-Fadel, M., and Khoury, R. (2000). "Modeling settlement in msw landfills: A critical review." *Crit. Rev. Environ. Sci. Technol.*, 30(3), 327-361.
Elagroudy, S. A., Abdel-Razik, M. H., Warith, M. A., and Ghobrial, F. H. (2008). "Waste settlement in bioreactor landfill models." *Waste Management*, 28(11), 2366-2374.
Eleazer, W. E., Odle, W. S., Wang, Y. S., and Barlaz, M. A. (1997). "Biodegradability of municipal solid waste components in laboratory-scale landfills." *Environmental Science & Technology*, 31(3), 911-917.
EPA (1976). Resource conservation and recovery act. United States Environmental Protection Agency. Washington, DC, USA. http://www.epa.gov/epawaste/inforesources/online/index.htm.
EPA (1996). "Standards of performance for new stationary sources and guidelines for control of existing sources: Municipal solid waste landfills. 40 cfp parts 51, 52 and 60." 61(49), 9905-9944.
EPA (2000). "Final project agreement for the yolo county accelerated anaerobic & aerobic composting (bioreactor) project." R. Yazdani, D. Augenstein, and J. G. Pacey, eds., County of Yolo, Planning and Public Works Department, Divisoin of Integrated Waste Management, Woodland, CA.
EPA (2005). "Landfill gas emissions model (landgem), version 3.02." *http://www.epa.gov/ttn/catc/dir1/landgem-v302-guide.pdf*.
EPA (2006a). "Landfill bioreactor performance, second interim report, outer loop recycling & disposal facility, louisville, kentucky." *EPA/600/R-07/060, September 2006*, National Risk Management Research Laboratory, Office of Research and Development, U. S. Environmental Protection Agency, Cincinnati, Ohio 45268.
EPA (2006b). "Solid waste management and greenhouse gases: A life-cycle assessment of emissions and risks, www.Epa.Gov/climatechange/wycd/waste/swmghgreport.Html."U.S. Environmental Protection Agency Office of Solid Waste, Washington, D. C.
EPA (2010a). "Wastes - non-hazardous waste - municipal solid waste." *http://www.epa.gov/wastes/nonhaz/municipal/*.
EPA (2010b). "Wastes - non-hazardous waste - municipal solid waste - bioreactors." <http://www.epa.gov/osw/nonhaz/municipal/landfill/bioreactors.htm>.
EPA (2010c). "Green power from landfill gas - helping build a sustainable energy future while improving the environment." *EPA's Landfill Methane Outreach Program, December 2010*.
EPA (2011). "Municipal solid waste generation, recycling, and disposal in the united states: Facts and figures for 2010." *United States Environmental Protection Agency Solid Waste and Emergency Response (5306P)*, <www.epa.gov/osw/nonhaz/municipal/pubs/msw_2010_rev_factsheet.pdf>. (Sept. 13, 2013).
EPA (2014a). "Municipal solid waste generation, recycling, and disposal in the united states: Facts and figures for 2012." *United States Environmental Protection Agency Solid Waste and Emergency Response (5306P)*, <www.epa.gov/osw/nonhaz/municipal/pubs/msw_2010_rev_factsheet.pdf>. (Sept. 13, 2013).

EPA (2014b). "Inventory of u.S. Greenhouse gas emissions and sinks - 1990-2012." United States Environmental Protection Agency, Washington, DC.
Erses, A. S., Onay, T. T., and Yenigun, O. (2008). "Comparison of aerobic and anaerobic degradation of municipal solid waste in bioreactor landfills." *Bioresource Technology*, 99(13), 5418-5426.
Fang, Y. F. (2005). "Organic substance degradation and deformation of municipal solid waste." M.S., Hohai University, Nanjing, China (in Chinese).
Faour, A. A., Reinhart, D. R., and You, H. X. (2007). "First-order kinetic gas generation model parameters for wet landfills." *Waste Management*, 27(7), 946-953.
Fei, X., and Zekkos, D. (2012). "Settlement due to anaerobic biodegradation from large-scale laboratory landfill simulators." *Proc., GeoCongress 2012*, 4242-4251.
Fei, X., and Zekkos, D. (2013). "Factors influencing long-term settlement of municipal solid waste in laboratory bioreactor landfill simulators." *Journal of Hazardous, Toxic, and Radioactive Waste*, 17(4), 25-271.
Fei, X., Zekkos, D., and Raskin, L. (2013). "A laboratory landfill simulator for physical, geotechnical, chemical and microbial characterization of solid waste biodegradation processes." *Proc., Coupled Phenomena in Environmental Geotechnics*, Taylor & Francis Group, London, 321-327.
Fei, X., Zekkos, D., and Raskin, L. (2014a). "An experimental setup for simultaneous physical, geotechnical and biochemical characterization of municipal solid waste undergoing biodegradation in the laboratory." *Geotech. Test. J.*, 37(1).
Fei, X., Zekkos, D., and Raskin, L. (2014b). "Relationships between composition of municipal solid waste and generation rate and potential generation capacity of methane in laboratory batch and simulator tests." *Proc., GeoShanghai 2014*, GSP241: 100-109.
Fei, X., and Zekkos, D. (2015). "Large-size controlled degradation experiment and constant load simple shear testing on michigan municipal solid waste." *Proc., XVI European Conference on Soil Mechanics and Geotechnical Engineering*, ISSMGE.
Fei, X., Zekkos, D., and Raskin, L. (2015a). "Archaeal community structure in leachate and municipal solid waste is correlated to the methane generation and volume reduction during biodegradation of municipal solid waste." *Waste Management*, 36, 184-190.
Fei, X., Zekkos, D., and Raskin, L. (2015b). "Quantification of parameters influencing methane generation from biodegradation of municipal solid waste in landfills and laboratory experiments." *Waste Management*, (in press).
Fei, X., and Zekkos, D. (2016). "Impacts of initial composition, moisture content and overburden pressure of landfilled municipal solid waste on its degradation process." *Journal of Geotechnical and Geoenvironmental Engineering*, (under review).
Fei, X., Zekkos, D., and Raskin, L. (2016). "Experimental assessment of physico-biochemical-hydro-mechanical characteristics of municipal solid waste undergoing degradation." *Journal of Geotechnical and Geoenvironmental Engineering*, (under review).
Fellner, J., and Brunner, P. H. (2010). "Modeling of leachate generation from msw landfills by a 2-dimensional 2-domain approach." *Waste Management*, 30(11), 2084-2095.
Feng, J. H. (2009). "In site accelerated elimination of contaminants in landfill leachate by embeded permeable reactive barrier bioreactor." M.S., Shanghai Jiaotong University, Shanghai, China (in Chinese).

Feng, J. H., Zhu, N. W., Lin, K. M., and Lou, Z. Y. (2009). "Study on inhibitory effects toward leachate at the initial stage of loading barrier landfill method for domestic waste (in chinese)." *Chinese Journal of Environmental Engineering*, 3(5), 849-853.

Fleming, I. R., Rowe, R. K., and Cullimore, D. R. (1999). "Field observations of clogging in a landfill leachate collection system." *Can. Geotech. J.*, 36(4), 685-707.

Fleming, I. R., and Rowe, R. K. (2004). "Laboratory studies of clogging of landfill leachate collection and drainage systems." *Can. Geotech. J.*, 41(1), 134-153.

Forney, L. J., Zhou, X., and Brown, C. J. (2004). "Molecular microbial ecology: Land of the one-eyed king." *Curr. Opin. Microbiol.*, 7(3), 210-220.

Francois, V., Feuillade, G., Skhiri, N., Lagier, T., and Matejka, G. (2006). "Indicating the parameters of the state of degradation of municipal solid waste." *J. Hazard. Mater.*, 137(2), 1008-1015.

Gabr, M. A., Hossain, M. S., and Barlaz, M. A. (2007). "Shear strength parameters of municipal solid waste with leachate recirculation." *Journal of Geotechnical and Geoenvironmental Engineering*, 133(4), 478-484.

Gallagher, E. M. (1998). "Biological clogging of geocomposites exposed to raw landfill leachate over an extended period." *Waste Manage. Res.*, 16(5), 421-429.

Garg, A., and Achari, G. (2010). "A comprehensive numerical model simulating gas, heat, and moisture transport in sanitary landfills and methane oxidation in final covers." *Environmental Modeling & Assessment*, 15(5), 397-410.

Gawande, N. A., Reinhart, D. R., and Yeh, G. T. (2010). "Modeling microbiological and chemical processes in municipal solid waste bioreactor, part i: Development of a three-phase numerical model biokemod-3p." *Waste Management*, 30(2), 202-210.

Gotteland, P., Gourc, J. P., Aboura, A., and Thomas, S. (2000). "On site determination of geomechanical characteristics of waste." *Proc., International Conference on Geotechnical and Geological Engineering 2000*, 19-24.

Gourc, J. P., Olivier, F., Thomas, S., Chatelet, L., Denecheau, P., and Munoz, M. L. (2001). "Monitoring of waste settlements on five landfills: Comparison of the efficiency of different devices." *Proc., Sardinia 2001, Eighth International Waste Management and Landfill Symposium*, 515-524.

Gourc, J. P., Staub, M. J., and Conte, M. (2010). "Decoupling msw settlement into mechanical and biochemical processes - modelling and validation on large-scale setups." *Waste Management*, 30(8-9), 1556-1568.

Grainger, J. M., Jones, K. L., and Hotten, P. M. (1984). "Estimation and control of microbial activity in landfill." *Microbiological methods for environmental biotechnology. The society for applied bacteriology technical series no. 9*, J. M. Grainger, and J. M. Lynch, eds., Academic Press, Inc., Orlando, FL.

Grellier, S., Reddy, K. R., Gangathulasi, J., R., A., and Peters, C. (2007). "Us msw and its biodegradation in a bioreactor landfill." *Proc., 11th International Waste Management and Landfill Symposium*, CISA Publisher, Padova, Italy.

Griffin, M. E., McMahon, K. D., Mackie, R. I., and Raskin, L. (1998). "Methanogenic population dynamics during start-up of anaerobic digesters treating municipal solid waste and biosolids." *Biotechnol. Bioeng.*, 57(3), 342-355.

Grisolia, M., Napoleoni, Q., and Tancredi, G. (1992). "Considerazioni sulla compressibilita dei rifiuti solidi urbani." *Proc., 1st Italian-Brazilian symposium on sanitary and environmental engineering*.

Grisolia, M., Napoleoni, Q., and Tangredi, G. (1995). "The use of triaxial tests for the mechanical characterization of municipal solid waste." *Proc., 5th International Landfill Symposium - Sardinia*, CISA, 761-767.
Halvadakis, C., Robertson, A., and Leckie, J. O. (1983). "Landfill methanogenesis." *Technical Report No. 271*, Dept. of Civil Engineering, Stanford University, Palo Alto CA.
Han, B. H., Scicchitano, V., and Imhoff, P. T. (2011). "Measuring fluid flow properties of waste and assessing alternative conceptual models of pore structure." *Waste Management*, 31(3), 445-456.
Handy, R. L. (2002). "First-order rate equations in geotechnical engineering." *Journal of Geotechnical and Geoenvironmental Engineering*, 128(5), 416-425.
Hansen, T. L., Svard, A., Angelidaki, I., Schmidt, J. E., Jansen, J., and Christensen, T. H. (2003). "Chemical characteristics and methane potentials of source-separated and pre-treated organic municipal solid waste." *Water Sci. Technol.*, 48(4), 205-208.
Hanson, J. L., Yesiller, N., Von Stockhausen, S. A., and Wong, W. W. (2010). "Compaction characteristics of municipal solid waste." *Journal of Geotechnical and Geoenvironmental Engineering*, 136(8), 1095-1102.
Harris, J. M., Shafer, A. L., DeGroff, W., Hater, G. R., Gabr, M., and Barlaz, M. A. (2006). "Shear strength of degraded reconstituted municipal solid waste." *Geotech. Test. J.*, 29(2), 141-148.
Hartmann, H., Angelidaki, I., and Ahring, B. K. (2000). "Increase of anaerobic degradation of particulate organic matter in full-scale biogas plants by mechanical maceration." *Water Sci. Technol.*, 41(3), 145-153.
Hashemi, M., Kavak, H. I., Tsotsis, T. T., and Sahimi, M. (2002). "Computer simulation of gas generation and transport in landfills - i: Quasi-steady-state condition." *Chem. Eng. Sci.*, 57(13), 2475-2501.
He, P. J., Shao, L. M., Qu, X., Li, G. J., and Lee, D. J. (2005). "Effects of feed solutions on refuse hydrolysis and landfill leachate characteristics." *Chemosphere*, 59(6), 837-844.
Head, I. M., Saunders, J. R., and Pickup, R. W. (1998). "Microbial evolution, diversity, and ecology: A decade of ribosomal rna analysis of uncultivated microorganisms." *Microb. Ecol.*, 35(1), 1-21.
Hendron, D. M., Fernandez, G., Prommer, P. J., Giroud, J. P., and Orozco, L. F. (1999). "Investigation of 27th september 1997 slope failure at the dona juana landfill." *Proc., Sardinia 1999, Seventh International Waste Management and Landfill Symposium*, 545-554.
Holtz, R. D., and Kovacs, W. D. (1981). An introduction to geotechnical engineering. Prentice Hall, Englewood Cliffs, NJ.
Hossain, M. S., Gabr, M. A., and Barlaz, M. A. (2003). "Relationship of compressibility parameters to municipal solid waste decomposition." *Journal of Geotechnical and Geoenvironmental Engineering*, 129(12), 1151-1158.
Hossain, M. S., and Gabr, M. A. (2005). "Prediction of municipal solid waste landfill settlement with leachate recirculation." *Proc., Geo-Frontiers 2005 Congress*.
Hossain, M. S., Gabr, M. A., and Asce, F. (2009). "The effect of shredding and test apparatus size on compressibility and strength parameters of degraded municipal solid waste." *Waste Management*, 29(9), 2417-2424.
Hossain, M. S., and Haque, M. A. (2012). "Effects of intermixed soils and decomposition on hydraulic conductivity of municipal solid waste in bioreactor landfills." *J. Mater. Civ. Eng.*, 24(10), 1337-1342.

Houston, W. N., Houston, S. L., Liu, J. W., Elsayed, A., and Sanders, C. O. (1995). "In situ testing methods for dynamic properties of msw landfills." *Earthquake design and performance of solid waste landfills*, ASCE Geotechnical Special Publication No. 54, 73-82.
Huang, F. S., Hung, J. M., and Lu, C. J. (2012). "Enhanced leachate recirculation and stabilization in a pilot landfill bioreactor in taiwan." *Waste Manage. Res.*, 30(8), 849-858.
Huang, L. N., Zhou, H., Zhu, S., and Qu, L. H. (2004). "Phylogenetic diversity of bacteria in the leachate of a full-scale recirculating landfill." *FEMS Microbiol. Ecol.*, 50(3), 175-183.
Huang, L. N., Zhu, S., Zhou, H., and Qu, L. H. (2005). "Molecular phylogenetic diversity of bacteria associated with the leachate of a closed municipal solid waste landfill." *FEMS Microbiol. Lett.*, 242(2), 297-303.
Hudson, A. P., Beaven, R. P., and Powrie, W. (2009). "Assessment of vertical and horizontal hydraulic conductivities of household waste in a large scale compression cell." *Proc., 12th Waste Management and Landfill Symposium Sardinia 2009*.
Huvaj-Sarihan, N., and Stark, T. D. (2008). "Back-analyses of landfill slope failures." 6th International Conference on Case Histories in Geotechnical Engineering, Arlington, VA, August 11-16, 2008, Paper # 2.34 (in CD proceedings).
Ishigaki, T., Sugano, W., Nakanishi, A., Tateda, M., Ike, M., and Fujita, M. (2004). "The degradability of biodegradable plastics in aerobic and anaerobic waste landfill model reactors." *Chemosphere*, 54(3), 225-233.
Ivanova, L. K., Richards, D. J., and Smallman, D. J. (2008a). "Assessment of the anaerobic biodegradation potential of msw." *Proceedings of the ICE - Waste and Resource Management*, 167-180.
Ivanova, L. K., Richards, D. J., and Smallman, D. J. (2008b). "The long-term settlement of landfill waste." *Waste and Resource Management*, 161(WR3), 121-133.
Jafari, N. H., Stark, T. D., and Merry, S. (2013). "The july 10 2000 payatas landfill slope failure." *International Journal of Geoengineering Case Histories*, 2(3), 208-228.
Jessberger, H. L., and Kockel, R. (1993). "Determination and assessment of the mechanical properties of waste." *Proc., Waste disposal by landfill - Green*, Rotterdam- Balkema, 313-322.
Jiang, J., Yang, Y., Yang, S., Ye, B., and Zhang, C. (2010). "Effects of leachate accumulation on landfill stability in humid regions of china." *Waste Management*, 30(5), 848-855.
Jin, H. (2005). "Decomposition of high organic and moisture content municipal soild waste in bioreactor landfills." M.S., Ryerson University, Toronto, Canada.
Jones, D. R. V., and Dixon, N. (2005). "Landfill lining stability and integrity: The role of waste settlement." *Geotext. Geomembr.*, 23(1), 27-53.
Karimpour-Fard, M., Machado, S. L., Shariatmadari, N., and Noorzad, A. (2011). "A laboratory study on the msw mechanical behavior in triaxial apparatus." *Waste Management*, 31(8), 1807-1819.
Kavazanjian, E., Jr., Matasovic, N., and Bachus, R. C. (1999). "Large diameter static and cyclic laboratory testing of municipal solid waste." *Proc., 7th International Waste Management and Landfill Symposium*, 437-444.
Kavazanjian, E., Jr. (2001). "Mechanical properties of municipal solid waste." *Proc., Sardinia 2001, Eighth International Waste Management and Landfill Symposium*, 415-424.
Kavazanjian, E., Jr. (2006). "Waste mechanics: Recent findings and unanswered questions." *Keynote Address, GeoShanghai*.

Kavazanjian, E., Jr., Matasovic, N., and Bachus, R. C. (2013). "11th peck lecture: Predesign geotechnical investigation for the oii superfund site landfill." *Journal of Geotechnical and Geoenvironmental Engineering*, 139(11), 1849-1863.

Kayen, R., Moss, R. E. S., Thompson, E. M., Seed, R. B., Cetin, K. O., Kiureghian, A. D., Tanaka, Y., and Tokimatsu, K. (2013). "Shear-wave velocity-based probabilistic and deterministic assessment of seismic soil liquefaction potential." *Journal of Geotechnical and Geoenvironmental Engineering*, 139(3), 407-419.

Kelly, R. J., Shearer, B. D., Kim, J., Goldsmith, C. D., Hater, G. R., and Novak, J. T. (2006). "Relationships between analytical methods utilized as tools in the evaluation of landfill waste stability." *Waste Management*, 26(12), 1349-1356.

Kim, H., Jang, Y. C., and Townsend, T. (2011). "The behavior and long-term fate of metals in simulated landfill bioreactors under aerobic and anaerobic conditions." *J. Hazard. Mater.*, 194, 369-377.

Kim, H. D. (2005). "Comparative studies of aerobic and anaerobic landfills using simulated landfill lysimeters." Ph.D., University of Florida, Gainesville, FL, USA.

Kim, J., and Pohland, F. G. (2003). "Process enhancement in anaerobic bioreactor landfills." *Water Sci. Technol.*, 48(4), 29-36.

Kjeldsen, P., Barlaz, M. A., Rooker, A. P., Baun, A., Ledin, A., and Christensen, T. H. (2002). "Present and long-term composition of msw landfill leachate: A review." *Crit. Rev. Environ. Sci. Technol.*, 32(4), 297-336.

Kjellman, W. (1951). "Testing the shear strength of clay in sweden." *Geotechnique*, 225-232.

Klindworth, A., Pruesse, E., Schweer, T., Peplies, J., Quast, C., Horn, M., and Glockner, F. O. (2013). "Evaluation of general 16s ribosomal rna gene pcr primers for classical and next-generation sequencing-based diversity studies." *Nucleic Acids Research*, 41(1), 11.

Koelsch, F., Fricke, K., Mahler, C., and Damanhuri, E. (2005). "Stability of landfills - the bandung dumpsite disaster." *Proc., 10th International Waste Management and Landfill Symposium*.

Koerner, R. M., and Soong, T. Y. (2000). "Stability assessment of ten large landfill failures " *Advances in Transportation and Geoenvironmental Systems Using Geosynthetics, Proceedings of Sessions of Geo Denver 2000*, 1-38.

Kong, X. J., Sun, X. L., Zou, D. G., and Lou, S. L. (2006). "Study on relationship between volume reduction of municipal solid waste due to biodegradation and time (english abstract)." *Chinese Journal of Geotechnical Engineering*, 28(12), 2060-2065.

Kramer, S. L. (1996). Geotechnical earthquake engineering. Prentice Hall.

Kulhawy, F. H., and Mayne, P. W. (1990). "Manual on estimating soil properties for foundation design." Electric Power Research Inst., Palo Alto, CA (USA.

La Rochelle, P. (1981). "Limitations of direct simple shear test devices." *Laboratory shear strength of soil*, ASTM, 653-658.

Laloui-Carpentier, W., Li, T., Vigneron, V., Mazeas, L., and Bouchez, T. (2006). "Methanogenic diversity and activity in municipal solid waste landfill leachates." *Antonie Van Leeuwenhoek*, 89(3-4), 423-434.

Lamborn, J. (2012). "Observations from using models to fit the gas production of varying volume test cells and landfills." *Waste Management*, 32(12), 2353-2363.

Landva, A. O., and Clark, J. I. (1990). "Geotechnics of waste fill." *Geotechnics of waste fills - theory and practice*, A. Landva, and G. D. Knowles, eds., Amer Soc Testing and Materials, Philadelphia, 86-103.

Landva, A. O., Pelkey, S. G., and Valsangkar, A. J. (1998). "Coefficient of permeability of municipal refuse." *Proc., 3rd International Congress on Environmental Geotechnics*, 163-167.
Landva, A. O., Valsangkar, A. J., and Pelkey, S. G. (2000). "Lateral earth pressure at rest and compressibility of municipal solid waste." *Can. Geotech. J.*, 37(6), 1157-1165.
Leckie, J. O., Pacey, J. G., and Halvadakis, C. (1979). "Landfill management with moisture control." *Journal of the Environmental Engineering Division-Asce*, 105(2), 337-355.
Lee, J. J. (2007). "Dynamic characteristics of municipal solid waste (msw) in the linear and nonlinear strain ranges." Ph.D., University of Texas at Austion, Austin, TX.
Lee, J. S., and Santamarina, J. C. (2005). "Bender elements: Performance and signal interpretation." *Journal of Geotechnical and Geoenvironmental Engineering*, 131(9), 1063-1070.
Legendre, P., and Legendre, L. (2012). Numerical ecology 3rd edition. Elsevier, Amsterdam, The Netherlands.
Liao, Z. Q. (2006). "Degradation of sanitary landfilled waste and settlement mechanisms study." Ph.D., Hohai University, Nanjing, China (in Chinese).
Liao, Z. Q. (2007). "Experimental study and mechanism analysis of transient modulus changing law of msw (english abstract)." *Rock and Soil Mechanics*, 28(3), No. 5.
Ling, H. I., Leshchinsky, D., Mohri, Y., and Kawabata, T. (1998). "Estimation of municipal solid waste landfill settlement." *Journal of Geotechnical and Geoenvironmental Engineering*, 124(1), 21-28.
Liu, J. L., Ke, H., Zhan, L. T., and Chen, Y. M. (2009). "Simulation tests of biodegradation and compression of municipal solid waste." *Proc., the International Symposium on Geoenvironmental Engineering in Hangzhou, China. September 8-10, 2009.*, Springer, 521-524.
Liu, J. L. (2010). "Municipal solid waste compression tests and model study on landfill settlement." M.S., Zhejiang University, Hangzhou, China (in Chinese).
Liu, R., Shi, J. Y., and Peng, G. X. (2005). "Experimental studies on mechanical behavior of refuse samples (english abstract)." *Rock and Soil Mechanics*, 26(1), 108-112.
Lobo, A., Herrero Lantaron, J., Montero Fernandez, O., Tejero Monzon, I., and Fantelli Lamia, M. (2002). "Modelling for environmental assessment of municipal solid waste landfills (part ii: Biodegradation)." *Waste Manage. Res.*, 20(6), 514-528.
Lockhart, R. J., Van Dyke, M. I., Beadle, I. R., Humphreys, P., and McCarthy, A. J. (2006). "Molecular biological detection of anaerobic gut fungi (neocallimastigales) from landfill sites." *Appl. Environ. Microbiol.*, 72(8), 5659-5661.
Lozecznik, S., Sparling, R., Oleszkiewicz, J. A., Clark, S., and VanGulck, J. F. (2010). "Leachate treatment before injection into a bioreactor landfill: Clogging potential reduction and benefits of using methanogenesis." *Waste Management*, 30(11), 2030-2036.
Luton, P. E., Wayne, J. M., Sharp, R. J., and Riley, P. W. (2002). "The mcra gene as an alternative to 16s rrna in the phylogenetic analysis of methanogen populations in landfill." *Microbiology-(UK)*, 148, 3521-3530.
Machado, S. L., Carvalho, M. F., Gourc, J. P., Vilar, O. M., and do Nascimento, J. C. F. (2009). "Methane generation in tropical landfills: Simplified methods and field results." *Waste Management*, 29(1), 153-161.
Madigan, M. T., Martinko, J. M., Stahl, D. A., and Clark, D. P. (2010). Brock biology of microorganisms 13th ed. Benjamin Cummings, San Francisco, CA.

Mahar, R. B., Liu, J. G., Li, H., and Nie, Y. F. (2009). "Bio-pretreatment of municipal solid waste prior to landfilling and its kinetics." *Biodegradation*, 20(3), 319-330.
Mali, S. T., Khare, K. C., and Biradar, A. H. (2012). "Enhancement of methane production and bio-stabilisation of municipal solid waste in anaerobic bioreactor landfill." *Bioresource Technology*, 110, 10-17.
Mazzucato, N., Simonini, P., and Colombo, S. (1999). "Analysis of block slide in a msw landfill." *Proc., 7th International Waste Management and Landfill Symposium*, 537-544.
McDonald, J. E., Lockhart, R. J., Cox, M. J., Allison, H. E., and McCarthy, A. J. (2008). "Detection of novel fibrobacter populations in landfill sites and determination of their relative abundance via quantitative pcr." *Environ. Microbiol.*, 10(5), 1310-1319.
McDonald, J. E., Allison, H. E., and McCarthy, A. J. (2010). "Composition of the landfill microbial community as determined by application of domain- and group-specific 16s and 18s rrna-targeted oligonucleotide probes." *Appl. Environ. Microbiol.*, 76(4), 1301-1306.
McDougall, J. (2007). "A hydro-bio-mechanical model for settlement and other behaviour in landfilled waste." *Comput. Geotech.*, 34(4), 229-246.
McDougall, J. (2011). "Settlement: The short and the long of it." *Geotechnical characterization, field measurement, and laboratory testing of municipal solid waste: Proceedings of the 2008 international symposium on waste mechanics*, D. Zekkos, ed., ASCE, Geo-Institute, Reston, Va, 76-111.
McDougall, J. R., and Pyrah, I. C. (2004). "Phase relations for decomposable soils." *Geotechnique*, 54(7), 487-493.
McDougall, J. R., Pyrah, I. C., Yuen, S. T. S., Monteiro, V. E. D., Melo, M. C., and Juca, J. F. T. (2004). "Decomposition and settlement in landfilled waste and other soil-like materials." *Geotechnique*, 54(9), 605-609.
McIsaac, R., and Rowe, R. K. (2008). "Clogging of unsaturated gravel permeated with landfill leachate." *Can. Geotech. J.*, 45(8), 1045-1063.
McLsaac, R., and Rowe, R. K. (2007). "Clogging of gravel drainage layers permeated with landfill leachate." *Journal of Geotechnical and Geoenvironmental Engineering*, 133(8), 1026-1039.
McMahon, K. D., Stroot, P. G., Mackie, R. I., and Raskin, L. (2001). "Anaerobic codigestion of municipal solid waste and biosolids under various mixing conditions - ii: Microbial population dynamics." *Water Res.*, 35(7), 1817-1827.
McMahon, K. D., Zheng, D. D., Stams, A. J. M., Mackie, R. I., and Raskin, L. (2004). "Microbial population dynamics during start-up and overload conditions of anaerobic digesters treating municipal solid waste and sewage sludge." *Biotechnol. Bioeng.*, 87(7), 823-834.
Mehta, R., Barlaz, M. A., Yazdani, R., Augenstein, D., Bryars, M., and Sinderson, L. (2002). "Refuse decomposition in the presence and absence of leachate recirculation." *J. Environ. Eng.-ASCE*, 128(3), 228-236.
Meima, J. A., Naranjo, N. M., and Haarstrick, A. (2008). "Sensitivity analysis and literature review of parameters controlling local biodegradation processes in municipal solid waste landfills." *Waste Management*, 28(5), 904-918.
Mellendorf, M., Huber-Humer, M., Gamperling, O., Huber, P., Gerzabek, M. H., and Watzinger, A. (2010). "Characterisation of microbial communities in relation to physical-chemical parameters during in situ aeration of waste material." *Waste Management*, 30(11), 2177-2184.

Merry, S. M., Fritz, W. U., Budhu, M., and Jesionek, K. (2006). "Effect of gas on pore pressures in wet landfills." *Journal of Geotechnical and Geoenvironmental Engineering*, 132(5), 553-561.
Mersiowsky, I., Weller, M., and Ejlertsson, J. (2001). "Fate of plasticised pvc products under landfill conditions: A laboratory-scale landfill simulation reactor study." *Water Res.*, 35(13), 3063-3070.
Mitchell, J. K., and Soga, K. (2005). Fundamentals of soil behavior. John Wiley & Sons, Hoboken, NJ.
Morel, F. M. M., and Hering, J. G. (1993). Principles and applications of aquatic chemistry. Wiley, New York.
Morris, J. W. F., Vasuki, N. C., Baker, J. A., and Pendleton, C. H. (2003). "Findings from long-term monitoring studies at msw landfill facilities with leachate recirculation." *Waste Management*, 23(7), 653-666.
Nayak, B. S., Levine, A. D., Cardoso, A., and Harwood, V. J. (2009). "Microbial population dynamics in laboratory-scale solid waste bioreactors in the presence or absence of biosolids." *J. Appl. Microbiol.*, 107(4), 1330-1339.
Olivier, F., and Gourc, J. P. (2007). "Hydro-mechanical behavior of municipal solid waste subject to leachate recirculation in a large-scale compression reactor cell." *Waste Management*, 27(1), 44-58.
Oonk, H., van Zomeren, A., Rees-White, T. C., Beaven, R. P., Hoekstra, N., Luning, L., Hannen, M., Hermkes, H., and Woelders, H. (2013). "Enhanced biodegradation at the landgraaf bioreactor test-cell." *Waste Management*, 33(10), 2048-2060.
Oweis, I. S., and Khera, R. (1986). "Criteria for geotechnical construction on sanitary landfills." *Proc., International Symposium on Environmental Geotechnology*, Lehigh University Press, Bethlehem PA, 205-222.
Oweis, I. S. (2006). "Estimate of landfill settlements due to mechanical and decompositional processes." *Journal of Geotechnical and Geoenvironmental Engineering*, 132(5), 644-650.
Palmeira, E. M., Remigio, A. F. N., Ramos, M. L. G., and Bernardes, R. S. (2008). "A study on biological clogging of nonwoven geotextiles under leachate flow." *Geotext. Geomembr.*, 26(3), 205-219.
Palmisano, A. C., and Barlaz, M. A. (1996). Microbiology of solid waste. CRC Press, Boca Raton, FL.
Park, H. I., and Lee, S. R. (2002). "Long-term settlement behaviour of msw landfills with various fill ages." *Waste Manage. Res.*, 20(3), 259-268.
Pelkey, S. A., Valsangkar, A. J., and Landva, A. (2001). "Shear displacement dependent strength of municipal solid waste and its major constituent." *Geotech. Test. J.*, 24(4), 381-390.
Peng, G. X. (2004). "Municipal solid waste settlement and deformation." Ph.D., HoHai University, Nanjing, China (in Chinese).
Pietramellara, G., Ascher, J., Borgogni, F., Ceccherini, M. T., Guerri, G., and Nannipieri, P. (2009). "Extracellular DNA in soil and sediment: Fate and ecological relevance." *Biol. Fertil. Soils*, 45(3), 219-235.
Pinto, A. J., and Raskin, L. (2012). "Pcr biases distort bacterial and archaeal community structure in pyrosequencing datasets." *PLoS ONE*, 7(8).
Pohland, F. G. (1975). "Sanitary landfill stabilization with leachate recycle and residual treatment." U. S. E. P. A. EPA-600/2-75-043, ed.Cincinnati, Ohio 45268, 1057-1069.

Pohland, F. G., and Harper, S. R. (1986). "Critical review and summary of leachate and gas production from landfills." U. S. E. P. A. EPA/600/2-86/073, ed.Cincinnati, Ohio 45268.
Pohland, F. G., and Alyousfi, B. (1994). "Design and operation of landfills for optimum stabilization and biogas production." *Water Sci. Technol.*, 30(12), 117-124.
Pohland, F. G., and Kim, J. C. (2000). "Microbially mediated attenuation potential of landfill bioreactor systems." *Water Sci. Technol.*, 41(3), 247-254.
Pommier, S., Chenu, D., Quintard, M., and Lefebvre, X. (2007). "A logistic model for the prediction of the influence of water on the solid waste methanization in landfills." *Biotechnol. Bioeng.*, 97(3), 473-482.
Pommier, S., Llamas, A. M., and Lefebvre, X. (2010). "Analysis of the outcome of shredding pretreatment on the anaerobic biodegradability of paper and cardboard materials." *Bioresource Technology*, 101(2), 463-468.
Pourcher, A. M., Sutra, L., Hebe, I., Moguedet, G., Bollet, C., Simoneau, P., and Gardan, L. (2001). "Enumeration and characterization of cellulolytic bacteria from refuse of a landfill." *FEMS Microbiol. Ecol.*, 34(3), 229-241.
Powrie, W., and Beaven, R. P. (1999). "Hydraulic properties of household waste and implications for landfills." *Proceedings of the ICE - Waste and Resource Management*, 137(4), 235-247.
Prevost, J. H., and Høeg, K. (1976). "Reanalysis of simple shear soil testing." *Can. Geotech. J.*, 13(4), 418-429.
Qian, X., Koerner, R. M., and Gray, D. H. (2002). Geotechnical aspects of landfill design and construction. Prentice Hall.
Qu, X., Mazeas, L., Vavilin, V. A., Epissard, J., Lemunier, M., Mouchel, J. M., He, P. J., and Bouchez, T. (2009a). "Combined monitoring of changes in delta(13)ch(4) and archaeal community structure during mesophilic methanization of municipal solid waste." *FEMS Microbiol. Ecol.*, 68(2), 236-245.
Qu, X., Vavilin, V. A., Mazeas, L., Lemunier, M., Duquennoi, C., He, P. J., and Bouchez, T. (2009b). "Anaerobic biodegradation of cellulosic material: Batch experiments and modelling based on isotopic data and focusing on aceticlastic and non-aceticlastic methanogenesis." *Waste Management*, 29(6), 1828-1837.
Rafizul, I. M., Howlader, M. K., and Alamgir, M. (2012). "Construction and evaluation of simulated pilot scale landfill lysimeter in bangladesh." *Waste Management*, 32(11), 2068-2079.
Ramaiah, B., Ramana, G., and Kavazanjian, E. (2014). "Undrained response of municipal solid waste collected from a waste site in delhi, india." *Geoenvironmental engineering*, 130-139.
Raskin, L., Capman, W. C., Sharp, R., Poulsen, L. K., and Stahl, D. A. (1997). "Molecular ecology of gastrointestinal ecosystems." *Gastrointestinal microbiology, volume 2: Gastrointestinal microbes and host interactions*, R. I. Mackie, B. A. White, and R. E. Isaacson, eds., Chapman & Hall, New York.
Reddy, K. R., Hettiarachchi, H., Parakalla, N., Gangathulasi, J., Bogner, J., and Lagier, T. (2009a). "Hydraulic conductivity of msw in landfills." *Journal of Environmental Engineering-Asce*, 135(8), 677-683.
Reddy, K. R., Hettiarachchi, H., Parakalla, N. S., Gangathulasi, J., and Bogner, J. E. (2009b). "Geotechnical properties of fresh municipal solid waste at orchard hills landfill, USA." *Waste Management*, 29(2), 952-959.

Reddy, K. R., Hettiarachchi, H., Gangathulasi, J., and Bogner, J. E. (2011). "Geotechnical properties of municipal solid waste at different phases of biodegradation." *Waste Management*, 31(11), 2275-2286.
Reinhart, D. R., and Townsend, T. G. (1998). Landfill bioreactor design and operation. Lewis Publishers, Boca Raton, FL.
Reinhart, D. R., McCreanor, P. T., and Townsend, T. (2002). "The bioreactor landfill: Its status and future." *Waste Manage. Res.*, 20(2), 172-186.
Rich, C., Gronow, J., and Voulvoulis, N. (2008). "The potential for aeration of msw landfills to accelerate completion." *Waste Management*, 28(6), 1039-1048.
Richardson, G., and Reynolds, D. (1991). "Geosynthetic considerations in a landfill on compressible clays." *Proc., Geosynthetics*, Industrial Fabrics Association International.
Rittmann, B. E., Banaszak, J. E., Cooke, A., and Rowe, R. K. (2003). "Biogeochemical evaluation of mechanisms controlling caco3(s) precipitation in landfill leachate-collection systems." *Journal of Environmental Engineering-Asce*, 129(8), 723-730.
Rittmann, B. E., Hausner, M., Loffler, F., Love, N. G., Muyzer, G., Okabe, S., Oerther, D. B., Peccia, J., Raskin, L., and Wagner, M. (2006). "A vista for microbial ecology and environmental biotechnology." *Environmental Science & Technology*, 40(4), 1096-1103.
Roscoe, K. H. (1953). "An apparatus for the application of simple shear to soil samples." *Proc., the 3rd International Conference on Soil Mechanics and Foundation Engineering*, 186-191.
Rosqvist, H., and Bendz, D. (1999). "An experimental evaluation of the solute transport volume in biodegraded municipal solid waste." *Hydrology and Earth System Sciences*, 3(3), 429-438.
Rosqvist, N. H., Dollar, L. H., and Fourie, A. B. (2005). "Preferential flow in municipal solid waste and implications for long-term leachate quality: Valuation of laboratory-scale experiments." *Waste Manage. Res.*, 23(4), 367-380.
Rowe, R. K., Armstrong, M. D., and Cullimore, D. R. (2000a). "Particle size and clogging of granular media permeated with leachate." *Journal of Geotechnical and Geoenvironmental Engineering*, 126(9), 775-786.
Rowe, R. K., Armstrong, M. D., and Cullimore, D. R. (2000b). "Mass loading and the rate of clogging due to municipal solid waste leachate." *Can. Geotech. J.*, 37(2), 355-370.
Rowe, R. K. (2012). "Short- and long-term leakage through composite liners." *Can. Geotech. J.*, 49(2), 141-169.
Sahadewa, A., Zekkos, D., Fei, X., Li, J., and Zhao, X. (2014a). "Recurring shear wave velocity measurements at smith's creek bioreactor landfill." *Geocongress 2014*, American Society of Civil Engineers, Reston, VA, U.S., Atlanta, GA, 2072-2081.
Sahadewa, A., Zekkos, D., Woods, R. D., Stokoe, K. H., II, and Matasovic, N. (2014b). "In-situ assessment of the dynamic properties of msw at a landfill in texas." *Earthquake Engineering and Soil Dynamics Journal* submitted.
Sawamura, H., Yamada, M., Endo, K., Soda, S., Ishigaki, T., and Ike, M. (2010). "Characterization of microorganisms at different landfill depths using carbon-utilization patterns and 16s rrna gene based t-rflp." *J. Biosci. Bioeng.*, 109(2), 130-137.
Schink, B., and Stams, A. J. M. (2006). "Syntrophism among prokaryotes." *The prokaryotes, volume 1: Symbiotic associations, biotechnology, applied microbiology*, M. Dworkin, S. Falkow, E. Rosenberg, K. H. Schleifer, and E. Stackebrant, eds., Springer Verlag, New York.
Schloss, P. D., Westcott, S. L., Ryabin, T., Hall, J. R., Hartmann, M., Hollister, E. B., Lesniewski, R. A., Oakley, B. B., Parks, D. H., Robinson, C. J., Sahl, J. W., Stres, B., Thallinger, G. G., Van Horn, D. J., and Weber, C. F. (2009). "Introducing mothur: Open-

source, platform-independent, community-supported software for describing and comparing microbial communities." *Appl. Environ. Microbiol.*, 75(23), 7537-7541.
Shariatmadari, N., Machado, S. L., Noorzad, A., and Karimpour-Fard, M. (2009). "Municipal solid waste effective stress analysis." *Waste Management*, 29(12), 2918-2930.
Sharma, H. D., and Reddy, K. R. (2004). Geoenvironmental engineering - site remediation, waste containment, and emerging waste management technoloies. Wiley.
Sharma, H. D., and De, A. (2007). "Municipal solid waste landfill settlement: Postclosure perspectives." *Journal of Geotechnical and Geoenvironmental Engineering*, 133(6), 619-629.
Sheridan, S. (2003). "Modeling solid waste settlement as a function of mass loss." M.S., University of Florida, Gainesville, FL, USA.
Singh, M. K., Sharma, J. S., and Fleming, I. R. (2009). "Shear strength testing of intact and recompacted samples of municipal solid waste." *Can. Geotech. J.*, 46(10), 1133-1145.
Sivathayalan, S. (1994). "Static, cyclic and post liquefaction simple shear response of sands." Ph.D., The University of British Columbia, Vancouver, B.C., Canada.
Sleat, R., Harries, C., Viney, I., and Rees, J. F. (1987). "Activities and distribution of key microbial groups in landfill." *Proc., ISWA Symposium on process, technology and environmental impact of sanitary landfills*, 11-14.
Smith, A. L., Skerlos, S. J., and Raskin, L. (2013). "Psychrophilic anaerobic membrane bioreactor treatment of domestic wastewater." *Water Res.*, 47(4), 1655-1665.
Solomon, S., Qin, D., Manning, M., Chen, Z., Marquis, M., Averyt, K. B., Tignor, M., and Miller, H. L. (2007). Contribution of working group i to the fourth assessment report of the intergovernmental panel on climate change, 2007. Cambridge University Press, Cambridge, U.K. and New York, NY, U.S.
Soong, T. Y., Zhao, X., Liu, W. L., Subbarayan, M., and Williams, M. (2009). "Full size septage bioreactor landfill - a rd&d project update." WASTECON. Long Beach, CA.
Sormunen, K., Laurila, T., and Rintala, J. (2013). "Determination of waste decay rate for a large finnish landfill by calibrating methane generation models on the basis of methane recovery and emissions." *Waste Manage. Res.*, 31(10), 979-985.
Sowers, G. F. (1968). "Foundation problems in sanitary landfills." *Journal of the Sanitary Engineering, ASCE*, 94(SA1), 103-116.
Sowers, G. F. (1973). "Settlement of waste disposal landfills." *Proc., 8th International Conference on Soil Mechanics and Foundation Engineering*, 207-210.
Spikula, D. R. (1997). "Subsidence performance of landfills." *Geotext. Geomembr.*, 15(4–6), 395-402.
Spokas, K., Bogner, J., Chanton, J. P., Morcet, M., Aran, C., Graff, C., Moreau-Le Golvan, Y., and Hebe, I. (2006). "Methane mass balance at three landfill sites: What is the efficiency of capture by gas collection systems?" *Waste Management*, 26(5), 516-525.
Staley, B. F., and Barlaz, M. A. (2009). "Composition of municipal solid waste in the united states and implications for carbon sequestration and methane yield." *Journal of Environmental Engineering*, 135(10), 901-909.
Staley, B. F., de los Reyes, F. L., and Barlaz, M. A. (2011a). "Effect of spatial differences in microbial activity, ph, and substrate levels on methanogenesis initiation in refuse." *Appl. Environ. Microbiol.*, 77(7), 2381-2391.
Staley, B. F., Saikaly, P. E., de los Reyes, F. L., and Barlaz, M. A. (2011b). "Critical evaluation of solid waste sample processing for DNA-based microbial community analysis." *Biodegradation*, 22(1), 189-204.

Staley, B. F., de los Reyes, F. L., and Barlaz, M. A. (2012). "Comparison of bacteria and archaea communities in municipal solid waste, individual refuse components, and leachate." *FEMS Microbiol. Ecol.*, 79(2), 465-473.
Stams, A. J. M. (1994). "Metabolic interactions between anaerobic-bacteria in methanogenic environments." *Antonie Van Leeuwenhoek*, 66(1-3), 271-294.
Stark, T. D., Eid, H. T., Evans, W. D., and Sherry, P. E. (2000). "Municipal solid waste slope failure. Ii. Stability analyses." *Journal of Geotechnical and Geoenvironmental Engineering*, 126(5), 408-419.
Staub, M. J., Gourc, J. P., Laurent, J. P., Kintzuger, C., Oxarango, L., Benbelkacem, H., Bayard, R., and Morra, C. (2010). "Long-term moisture measurements in large-scale bioreactor cells using tdr and neutron probes." *J. Hazard. Mater.*, 180(1-3), 165-172.
Staub, M. J., Gourc, J. P., Drut, N., Stoltz, G., and Mansour, A. A. (2013). "Large-scale bioreactor pilots for monitoring the long-term hydromechanics of msw." *Journal of Hazardous, Toxic, and Radioactive Waste*, 17(4), 285-294.
Stessel, R. I., and Murphy, R. J. (1992). "A lysimeter study of the aerobic landfill concept." *Waste Management & Research*, 10(6), 485-503.
Stoltz, G., Gourc, J. P., and Oxarango, L. (2010a). "Liquid and gas permeabilities of unsaturated municipal solid waste under compression." *J. Contam. Hydrol.*, 118(1-2), 27-42.
Stoltz, G., Gourc, J. P., and Oxarango, L. (2010b). "Characterisation of the physico-mechanical parameters of msw." *Waste Management*, 30(8-9), 1439-1449.
Stoltz, G., Tinet, A. J., Staub, M. J., Oxarango, L., and Gourc, J. P. (2012). "Moisture retention properties of municipal solid waste in relation to compression." *Journal of Geotechnical and Geoenvironmental Engineering*, 138(4), 535-543.
Stroot, P. G., McMahon, K. D., Mackie, R. I., and Raskin, L. (2001). "Anaerobic codigestion of municipal solid waste and biosolids under various mixing conditions - i. Digester performance." *Water Res.*, 35(7), 1804-1816.
Stulgis, R. P., Soydemir, C., and Telgener, R. J. (1995). Predicting landfill settlement.
Sun, X. L. (2007). "Municipal solid waste strain and strength properties study." Ph.D., Dalian University of Technology, Dalian, China (in Chinese).
Sun, Y. J., Sun, X. J., and Zhao, Y. C. (2011). "Comparison of semi-aerobic and anaerobic degradation of refuse with recirculation after leachate treatment by aged refuse bioreactor." *Waste Management*, 31(6), 1202-1209.
Swati, M., and Joseph, K. (2008). "Settlement analysis of fresh and partially stabilised municipal solid waste in simulated controlled dumps and bioreactor landfills." *Waste Management*, 28(8), 1355-1363.
Tang, P., Zhao, Y. C., and Liu, D. (2008). "A laboratory study on stabilization criteria of semi-aerobic landfill." *Waste Manage. Res.*, 26(6), 566-572.
Tchobanoglous, G., Burton, F. L., and Stensel, D. H. (2002). Wastewater engineering: Treatment and reuse 2nd ed. McGraw-Hill, New York, NY.
Tchobanoglous, G., and Kreith, F. (2002). Handbook of solid waste management 2nd ed. McGraw-Hill, New York.
Thauer, R. K., Kaster, A. K., Seedorf, H., Buckel, W., and Hedderich, R. (2008). "Methanogenic archaea: Ecologically relevant differences in energy conservation." *Nat. Rev. Microbiol.*, 6(8), 579-591.
Themelis, N. J., and Ulloa, P. A. (2007). "Methane generation in landfills." *Renewable Energy*, 32(7), 1243-1257.

Thompson, S., Sawyer, J., Bonam, R., and Valdivia, J. E. (2009). "Building a better methane generation model: Validating models with methane recovery rates from 35 canadian landfills." *Waste Management*, 29(7), 2085-2091.

Tinet, A. J., Oxarango, L., Bayard, R., Benbelkacem, H., Stoltz, G., Staub, M. J., and Gourc, J. P. (2011). "Experimental and theoretical assessment of the multi-domain flow behaviour in a waste body during leachate infiltration." *Waste Management*, 31(8), 1797-1806.

Tolaymat, T. M., Green, R. B., Hater, G. R., Barlaz, M. A., Black, P., Bronson, D., and Powell, J. (2010). "Evaluation of landfill gas decay constant for municipal solid waste landfills operated as bioreactors." *Journal of the Air & Waste Management Association*, 60(1), 91-97.

Urakawa, H., Martens-Habbena, W., and Stahl, D. A. (2010). "High abundance of ammonia-oxidizing archaea in coastal waters, determined using a modified DNA extraction method." *Appl. Environ. Microbiol.*, 76(7), 2129-2135.

Uz, I., Rasche, M. E., Townsend, T., Ogram, A. V., and Lindner, A. S. (2003). "Characterization of methanogenic and methanotrophic assemblages in landfill samples." *Proc. R. Soc. Lond. Ser. B-Biol. Sci.*, 270, S202-S205.

Valencia, R., van der Zon, W., Woelders, H., Lubberding, H. J., and Gijzen, H. J. (2009a). "The effect of hydraulic conditions on waste stabilisation in bioreactor landfill simulators." *Bioresource Technology*, 100(5), 1754-1761.

Valencia, R., van der Zon, W., Woelders, H., Lubberding, H. J., and Gijzen, H. J. (2009b). "Achieving "final storage quality" of municipal solid waste in pilot scale bioreactor landfills." *Waste Management*, 29(1), 78-85.

Van Dyke, M. I., and McCarthy, A. J. (2002). "Molecular biological detection and characterization of clostridium populations in municipal landfill sites." *Appl. Environ. Microbiol.*, 68(4), 2049-2053.

van Haaren, R., Themelis, N. J., and Goldstein, N. (2010). "The state of garbage in america." *Biocycle*, October 2010.

VanGulck, J. F., and Rowe, R. K. (2004a). "Influence of landfill leachate suspended solids on clog (biorock) formation." *Waste Management*, 24(7), 723-738.

VanGulck, J. F., and Rowe, R. K. (2004b). "Evolution of clog formation with time in columns permeated with synthetic landfill leachate." *J. Contam. Hydrol.*, 75(1-2), 115-139.

VanGulck, J. F., and Rowe, R. K. (2008). "Parameter estimation for modelling clogging of granular medium permeated with leachate." *Can. Geotech. J.*, 45(6), 812-823.

Vavilin, V. A., Rytov, S. V., Lokshina, J. Y., Pavlostathis, S. G., and Barlaz, M. A. (2003). "Distributed model of solid waste anaerobic digestion - effects of leachate recirculation and ph adjustment." *Biotechnol. Bioeng.*, 81(1), 66-73.

Vavilin, V. A., Lokshina, L. Y., Jokela, J. P. Y., and Rintala, J. A. (2004). "Modeling solid waste decomposition." *Bioresource Technology*, 94(1), 69-81.

Vavilin, V. A., and Angelidaki, I. (2005). "Anaerobic degradation of solid material: Importance of initiation centers for methanogenesis, mixing intensity, and 2d distributed model." *Biotechnol. Bioeng.*, 89(1), 113-122.

Vavilin, V. A., Jonsson, S., Ejlertsson, J., and Svensson, B. H. (2006). "Modelling msw decomposition under landfill conditions considering hydrolytic and methanogenic inhibition." *Biodegradation*, 17(5), 389-402.

Vavilin, V. A., Fernandez, B., Palatsi, J., and Flotats, X. (2008). "Hydrolysis kinetics in anaerobic degradation of particulate organic material: An overview." *Waste management*, 28(6), 939-951.

Viggiani, G., and Atkinson, J. H. (1995). "Interpretation of bender element tests." *Geotechnique*, 45(1), 149-154.
Wall, D. K., and Zeiss, C. (1995). "Municipal landfill biodegradation and settlement." *Journal of Environmental Engineering-Asce*, 121(3), 214-224.
Wang, J. L. (2007). "Characteristic study on municipal solid waste bioreactor landfill." M.S., Chinese Agriculture University, Beijing, China (in Chinese).
Wang, X., Padgett, J. M., De la Cruz, F. B., and Barlaz, M. A. (2011a). "Wood biodegradation in laboratory-scale landfills." *Environmental Science & Technology*, In press.
Wang, X., Padgett, J. M., De la Cruz, F. B., and Barlaz, M. A. (2011b). "Wood biodegradation in laboratory-scale landfills." *Environmental Science & Technology*, 45(16), 6864-6871.
Wang, X., Nagpure, A. S., DeCarolis, J. F., and Barlaz, M. A. (2013). "Using observed data to improve estimated methane collection from select u.S. Landfills." *Environmental Science & Technology*, 47(7), 3251-3257.
Wang, X., Nagpure, A. S., DeCarolis, J. F., and Barlaz, M. A. (2015). "Characterization of uncertainty in estimation of methane collection from select us landfills." *Environmental Science & Technology*, 49(3), 1545-1551.
Wang, Y. S., Byrd, C. S., and Barlaz, M. A. (1994). "Anaerobic biodegradability of cellulose and hemicellulose in excavated refuse samples using a biochemical methane potential assay." *J. Indust. Microbiol.*, 13(3), 147-153.
Wang, Y. S., Odle, W. S., Eleazer, W. E., and Barlaz, M. A. (1997). "Methane potential of food waste and anaerobic toxicity of leachate produced during food waste decomposition." *Waste Manage. Res.*, 15(2), 149-167.
Westlake, K., Archer, D. B., and Boone, D. R. (1995). "Diversity of cellulolytic bacteria in landfill." *J. Appl. Bacteriol.*, 79(1), 73-78.
White, J. K., Beaven, R. P., Powrie, W., and Knox, K. (2011). "Leachate recirculation in a landfill: Some insights obtained from the development of a simple 1-d model." *Waste Management*, 31(6), 1210-1221.
White, J. K., Nayagum, D., and Beaven, R. P. (2014). "A multi-component two-phase flow algorithm for use in landfill processes modelling." *Waste Management*, 34(9), 1644-1656.
Willumsen, H. (2007). "Cdm - landfill gas projects." *Proc., World Bank Workshop*, http://siteresources.worldbank.org/INTUSWM/Resources/463617-1185383612643/Willumsen.pdf.
Woodman, N. D., Siddiqui, A. A., Powrie, W., Stringfellow, A., Beaven, R. P., and Richards, D. J. (2013). "Quantifying the effect of settlement and gas on solute flow and transport through treated municipal solid waste." *J. Contam. Hydrol.*, 153, 106-121.
Woodman, N. D., Rees-White, T. C., Stringfellow, A. M., Beaven, R. P., and Hudson, A. P. (2014). "Investigating the effect of compression on solute transport through degrading municipal solid waste." *Waste Management*, 34(11), 2196-2208.
Xie, M. L., Aldenkortt, D., Wagner, J. F., and Rettenberger, G. (2006). "Effect of plastic fragments on hydraulic characteristics of pretreated municipal solid waste." *Can. Geotech. J.*, 43(12), 1333-1343.
Xu, X. B., Zhan, T. L. T., Chen, Y. M., and Guo, Q. G. (2015). "Parameter determination of a compression model for landfilled municipal solid waste: An experimental study." *Waste Manage. Res.*, 33(2), 199-210.

Yazdani, R., Mostafid, M. E., Han, B., Imhoff, P. T., Chiu, P., Augenstein, D., Kayhanian, M., and Tchobanoglous, G. (2010). "Quantifying factors limiting aerobic degradation during aerobic bioreactor landfilling." *Environmental Science & Technology*, 44(16), 6215-6220.
Yazdani, R., Barlaz, M. A., Augenstein, D., Kayhanian, M., and Tchobanoglous, G. (2012). "Performance evaluation of an anaerobic/aerobic landfill-based digester using yard waste for energy and compost production." *Waste Management*, 32(5), 912-919.
Yochim, A., Zytner, R. G., McBean, E. A., and Endres, A. L. (2013). "Estimating water content in an active landfill with the aid of gpr." *Waste Management*, 33(10), 2015-2028.
Yu, L., Batlle, F., and Carrera, J. (2011). "Variations of waste unit weight during mechanical and degradation processes at landfills." *Waste Manage. Res.*, 29(12), 1303-1315.
Yuan, P., Kavazanjian, E., Jr., Chen, W., and Seo, B. (2011). "Compositional effects on the dynamic properties of municipal solid waste." *Waste Management*, 31(12), 2380-2390.
Yuen, S. T. S., and McDougall, J. (2003). "Effect of enhanced biodegradation on settlement of municipal solid waste landfills." *Australian Geomechanics*, 38(2), 17-28.
Zacharof, A. I., and Butler, A. P. (2004). "Stochastic modelling of landfill processes incorporating waste heterogeneity and data uncertainty." *Waste Management*, 24(3), 241-250.
Zehnder, A. J. B., and Stumm, W. (1988). "Geochemistry and biogeochemistry of anaerobic habitats." *Biology of anaerobic microorganisms*, A. J. B. Zehnder, ed., Wiley, New York, 1-38.
Zekkos, D., Bray, J. D., Kavazanjian, E., Jr., Matasovic, N., Rathje, E. M., Riemer, M. F., and Stokoe, K. H., II (2006). "Unit weight of municipal solid waste." *Journal of Geotechnical and Geoenvironmental Engineering*, 132(10), 1250-1261.
Zekkos, D., Bray, J. D., and Riemer, M. F. (2008). "Shear modulus and material damping of municipal solid waste based on large-scale cyclic triaxial testing." *Can. Geotech. J.*, 45(1), 45-58.
Zekkos, D., Athanasopoulos, G. A., Bray, J. D., Grizi, A., and Theodoratos, A. (2010a). "Large-scale direct shear testing of municipal solid waste." *Waste Management*, 30(8-9), 1544-1555.
Zekkos, D., Kavazanjian, E., Bray, J. D., Matasovic, N., and Riemer, M. F. (2010b). "Physical characterization of municipal solid waste for geotechnical purposes." *Journal of Geotechnical and Geoenvironmental Engineering*, 136(9), 1231-1241.
Zekkos, D., Bray, J. D., and Riemer, M. F. (2012). "Drained response of municipal solid waste in large-scale triaxial shear testing." *Waste Management*, 32(10), 1873-1885.
Zekkos, D. (2013). "Experimental evidence of anisotropy in municipal solid waste." *Proc., Coupled Phenomena in Environmental Geotechnics*, Taylor & Francis Group, London, 69-77.
Zekkos, D., Grizi, A., and Athanasopoulos, G. (2013a). "Experimental investigation of the effect of fibrous reinforcement on shear resistance of soil-waste mixtures." *Geotech. Test. J.*, 36(6), 867-881.
Zekkos, D., Sahadewa, A., Woods, R. D., Stokoe, K. H., II, and Matasovic, N. (2013b). "In situ assessment of the nonlinear shear modulus of municipal solid waste." *Proc., 18th International Conference on Soil Mechanics and Geotechnical Engineering*.
Zekkos, D., Vlachakis, V. S., and Athanasopoulos, G. A. (2013c). "The 2010 xerolakka landfill slope instability." *Environmental Geotechnics*, 1(1), 56-65.
Zekkos, D., Sahadewa, A., Woods, R., and Stokoe, K. (2014). "Development of model for shear-wave velocity of municipal solid waste." *Journal of Geotechnical and Geoenvironmental Engineering*, 140(3), 04013030.

Zekkos, D., and Fei, X. (2016). "Comparison of constant load and constant volume simple shear response of municipal solid waste." *Can. Geotech. J.*, in press.
Zekkos, D., Fei, X., Grizi, A., and Athanasopoulos, G. (2016). "Response of municipal solid waste to mechanical compression." *Journal of Geotechnical and Geoenvironmental Engineering*, (under review).
Zhan, T. L. T., Chen, Y. M., and Ling, W. A. (2008). "Shear strength characterization of municipal solid waste at the suzhou landfill, china." *Engineering Geology*, 97(3–4), 97-111.
Zhan, T. L. T., Xu, X. B., Chen, Y. M., Ma, X. F., and Lan, J. W. (2015). "Dependence of gas collection efficiency on leachate level at wet municipal solid waste landfills and its improvement methods in china." *Journal of Geotechnical and Geoenvironmental Engineering*, 141(4).
Zhang, B., Dixon, N., and El-Hamalawi, A. (2010). "Development and evaluation of a phase relationship for msw." *Waste and Resource Management*, 163(WR2), 67-75.
Zhang, Y., and Banks, C. J. (2013). "Impact of different particle size distributions on anaerobic digestion of the organic fraction of municipal solid waste." *Waste Management*, 33(2), 297-307.
Zhao, X., Soong, T. Y., Subbarayan, M., and Williams, M. (2013a). "Full-scale field research and demonstration of septage bioreactor landfill technology." *Journal of Hazardous, Toxic, and Radioactive Waste*, 17(4), 295-306.
Zhao, X. D., Soong, T. Y., Subbarayan, M., and Williams, M. B. (2013b). "Full scale field research and demonstration of septage bioreactor landfill technology." *Journal of Hazardous, Toxic, and Radioactive Waste*, in press.
Zhao, Y. C., Chen, Z. G., Shi, Q. G., and Huang, R. H. (2001). "Monitoring and long-term prediction of refuse compositions and settlement in large-scale landfill." *Waste Manage. Res.*, 19(2), 160-168.
Zheng, B., Richards, D. J., Smallman, D. J., and Beaven, R. P. (2007). "Assessing msw degradation by bmp and fibre analysis." *Waste and Resource Management*, 160(4), 133-139.
Zinder, S. H. (1993). "Physiological ecology of methanogens." *Methanogenesis: Ecology, physiology, biochemistry, and genetics*, J. G. Ferry, ed., Chapman & Hall, New York, 128-206.
Zornberg, J. G., Jernigan, B. L., Sanglerat, T. R., and Cooley, B. H. (1999). "Retention of free liquids in landfills undergoing vertical expansion." *Journal of Geotechnical and Geoenvironmental Engineering*, 125(7), 583-594.